Distribution Agreement

In presenting this thesis or dissertation as a partial fulfillment of the requirements for an advanced degree from Emory University, I hereby grant to Emory University and its agents the non-exclusive license to archive, make accessible, and display my thesis or dissertation in whole or in part in all forms of media, now or hereafter known, including display on the world wide web. I understand that I may select some access restrictions as part of the online submission of this thesis or dissertation. I retain all ownership rights to the copyright of the thesis or dissertation. I also retain the right to use in future works (such as articles or books) all or part of this thesis or dissertation.

Signature:

_____ _____

Colleen E. Keohane Date

Promysalin and CD437: Compounds Investigating New Antibacterial Mechanisms

By

Colleen E. Keohane

Doctor of Philosophy

Chemistry

_____

William, M. Wuest, Ph.D.
Advisor

_____

Dennis C. Liotta, Ph.D.
Committee Member

_____

David G. Lynn, Ph.D.
Committee Member

Accepted:

_____

Lisa A. Tedesco, Ph.D.
Dean of the James T. Laney School of Graduate Studies

_____
Date

Promysalin and CD437: Compounds Investigating New Antibacterial Mechanisms

By

Colleen E. Keohane

B.S., Florida State University, 2013

Advisor: William M. Wuest, Ph.D.

An abstract of

A dissertation submitted to the Faculty of the

James T. Laney School of Graduate Studies of Emory University

in partial fulfillment of the requirements for the degree of

Doctor of Philosophy in Chemistry

2019

Abstract

Promysalin and CD437: Compounds Investigating New Antibacterial Mechanisms

By Colleen E. Keohane

The growing crisis surrounding antibiotic resistance continues to provide scientists with exciting and impactful research opportunities. The work reported herein will encompass two different approaches at investigating this monumental problem. Promysalin investigates the problem from a narrow-spectrum approach, wherein selectively killing one bacterial species instead of the entire community holds promise for dampening the rate of resistance. Alternatively, CD437 acts via a new mechanism wherein we can hopefully reestablish bioactivity by incorporating new approaches. Promysalin is a natural product isolated from the rhizosphere, a microbiome housing a wealth of microbial diversity, produced by a common plant beneficial bacteria, *Pseudomonas putida*. Our interest lies in the highly specific activity of the natural product wherein it solely has inhibitory activity against the Gram-negative pathogen *Pseudomonas aeruginosa.* We have spent the past five years working to understand the mechanism of inhibition and in doing so have completed the first total synthesis of the natural product, allowing for the determination of the natural stereochemistry; carried out a structure-activity relationship investigation which lead to the synthesis of a probe compound and used the probe to putatively determine the target. During this time, a second compound was investigated for antibacterial activity, CD437. CD437 was identified in a high-throughput screen by the Mylonakis Lab (Brown University) to have activity against Methicillin Resistant *Staphylococcus aureus* (MRSA) persister cells. This activity is attributed to a new mechanism of membrane permeabilization and a library of analogs was synthesized to support this discovery. The entirety of the work highlights the ability to use synthetic organic chemistry as a means to investigate biological problems.

Promysalin and CD437: Compounds Investigating New Antibacterial Mechanisms

By

Colleen E. Keohane

B.S., Florida State University, 2013

Advisor: William M. Wuest, Ph.D.

A dissertation submitted to the Faculty of the
James T. Laney School of Graduate Studies of Emory University
in partial fulfillment of the requirements for the degree of
Doctor of Philosophy in Chemistry
2019

Acknowledgements:

The past five years would not have been possible without the support of my advisor, family, and colleagues. First and foremost, I would like to thank my advisor, Professor William Wuest for the opportunity to work in his research lab. His guidance, mentorship, and support has been constant throughout my graduate career and for that I am extremely grateful. Bill challenged me to always do better and encouraged my future goals and aspirations. I am appreciative for all the time spent helping me become the scientist I am today and for providing opportunities (Gordon conferences, Germany, ACS Meetings, etc) that contributed to my overall success. I feel lucky to have been a part of Bill's group and have had such a pleasant graduate experience because of it and for that I am truly thankful.

I would like to thank my family for their continual love and support. Graduate school is not always the easiest of experiences but through it all they have been there encouraging me on this journey. Thank you to my parents for instilling values of hard-work and dedication throughout my life, these traits have provided me the ability to succeed in this environment. My brothers, Liam and Kevin, have never neglected to remind me how proud they are of me every time the topic of graduate school comes up.

I would like to acknowledge my collaborators – Professor Stefan Sieber and Professor Elefteris Mylonakis. I feel very fortunate to have been able to work with both of you and your talented students and post-docs. It has been a pleasure learning new skills and contributing to exciting science under your mentorship.

I would like to acknowledge my colleagues. Thank you to the entire Wuest Lab, past and present. I have been fortunate enough to constantly be surrounded by extraordinarily talented and genuine people. A special thank you to team promysalin, Dr. Andrew Steele and Kyle Knouse, not only for being incredibly supportive and helpful but for your friendship. Working with you both was quite the enjoyable experience and for that I am very grateful. Amy Solinski and Erika Csatary were the best lab mates, roommates, and friends – moving would not have been bearable without the two of you (and the best friends tab). Thank

you to all of my graduate school friends, near and far. Graduate school has provided me the opportunity to meet wonderful people with whom I will remain friends. I could not have gotten through without you: Dr. Brenden Derstein, Evan Samples, Dr. Brandon Kelley, Derek Wozniak, Dr. Megan Jennings, Dr. Rich Brzozowski and Alex Koval. I am especially thankful for Dr. Christiana Teijaro for great times and endless support. To the fifth-floor post-docs in the Liotta Lab: Dr. Robert Wilson, Dr. Leon Jacobs, Dr. Eric Miller, Dr. Nicole Pribut, Dr. Tom Kaiser, Dr. Edgars Jecs and Zack Dentmon, thank you for being our first friends at Emory and for the countless fun times and memories; our transition would not have been as enjoyable without you all! I am blessed to have had such wonderful times to make the experience one to remember.

Lastly, I would like to thank Aaron Bedermann for his patience, love, encouragement and support. I am lucky to have had someone who understands the frustrations of graduate school be there to listen and help in times of struggle. I am so thankful for you.

Table of Contents

List of Figures:

Chapter 1:

Chapter 2:

Chapter 3:

Chapter 4:

Chapter 5:

List of Schemes:

Chapter 2:

List of Tables:

Chapter 2:

Abbreviations:

ABC-transporter – ATP-binding cassette transporter

AfBPP – affinity-based protein profiling

AHL – N-acyl homoserine lactone

BINOL – 1,1'-Bi-2-naphthol

CAS – chrome azurol S

c-di-GMP – cyclic di-GMP

CF – Cystic Fibrosis

CFTR – Cystic fibrosis transmembrane conductance regulator

CSA – camphorsulfonic acid

CuAAC – copper(I)-catalyzed alkyne-azide cycloaddition

DCM – dichloromethane

DMAP – 4-dimethylaminopyridine

DMP – Dess-Martin periodinane

DMPU – N,N’-Dimethylpropyleneurea

DMSO – dimethyl sulfoxide

DNA – deoxyribonucleic acid

DTS – diverted total synthesis

ED pathway – Entner-Doudoroff pathway

EDC – 1-Ethyl-3-(3-dimethylaminopropyl)carbodiimide

EDTA – ethylenediaminetetraacetic acid

EMP pathway – Embden-Meyerhof-Parnas pathway

FDR – false discovery rate

H_2O_2 – hydrogen peroxide

HATU – (1-[Bis(dimethylamino)methylene]-1H-1,2,3-triazolo[4,5-b]pyridinium 3-oxid hexafluorophosphate

HTS – high throughput screen

IC_{50} – inhibitory concentration, 50%

KEGG – Kyoto Encyclopedia of Genes and Genomes

LC-MS/MS – liquid chromatography tandem mass spectrometry

LiOH – lithium hydroxide

MDR – multidrug resistance

MEM – 2-methoxyethoxymethyl

MNBA – 2-methyl-6-nitrobenzoic anhydride

MOA – mechanism of action

MOM – methoxymethyl acetal

mRNA – messenger ribonucleic acid

MRSA – methicillin resistant *Staphylococcus aureus*

NMR – nuclear magnetic resonance

NRPS – nonribosomal peptide-synthetase

PA – *Pseudomonas aeruginosa*

PBP – penicillin binding protein

PP – *Pseudomonas putida*

PP pathway – pentose phosphate pathway

RNA – ribonucleic acid

RNAP – ribonucleic acid polymerase

RNA-seq – RNA sequencing

rRNA – ribosomal ribonucleic acid

SAR – structure activity relationship

SCV – small colony variant

Sdh – succinate dehydrogenase

SEM – 2-(trimethylsilyl)ethoxymethyl chloride

SNP – single nucleotide polymorphism

TASF – tris(dimethylamino)sulfonium difluorotrimethylsilicate

TBAF – tetrabutyl-n-ammonium fluoride

TBSCl – tert-butyldimethylsilyl chloride

TBT – TonB dependent transporter

TCA – tricarboxylic acid

THF – tetrahydrofuran

TSB – tryptic soy broth

WGS – whole genome sequencing

Chapter 1 Introduction

1.1 Antibiotics

Undoubtedly, the most impactful breakthrough for human health was the discovery of penicillin. Discovered from mold by Sir. Alexander Fleming in 1927, this discovery certainly marked the beginning of the "Golden Age" of antibiotics.[2] Resistance to penicillin however, was in existence, as a now well characterized mechanism, prior to its first clinical use as an antibiotic.[3] Today, this topic is of critical importance as we are no longer in the golden-age and have found ourselves in desperate need of new antibiotics, solely as a result of antibiotic resistance. Interestingly, Fleming's serendipitous discovery came accompanied by his initial warning about the importance of selective pressures and the subsequent development of resistance.[4] An overview of key findings and their resistant timeframes is shown in Figure 1.1.

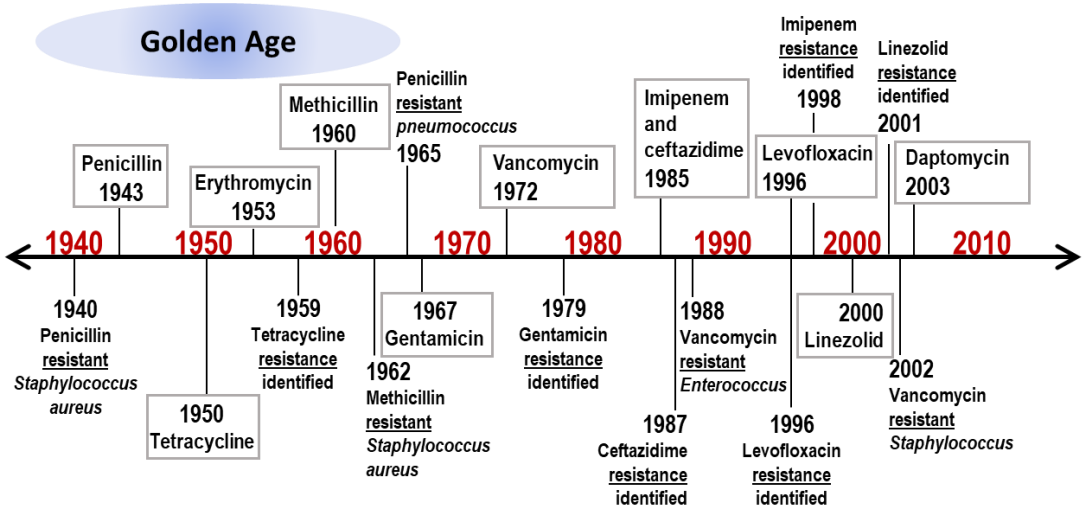

Figure 1.1 *Timeline of key antibiotic discoveries and their resistance*

Nevertheless, this initial discovery prompted a surge of discoveries, leading to a multitude of antibiotics with well-known mechanisms of action and now well-known mechanisms of resistance.[5] Over the last decade, this problem has worsened, providing for the selection of "super-bugs", bacterial strains possessing

resistance to antibiotics of last resort.[6] A survey of common antibiotic scaffolds is shown in Figure 1.2. While this overview will discuss both the mechanism of action and resistance of the classical antibiotics, it should be noted their development was ***greatly*** impactful and saved countless lives. It stands to *represent a current need in the field*, for the discovery of new antibiotics with novel mechanisms and novel structure.[7]

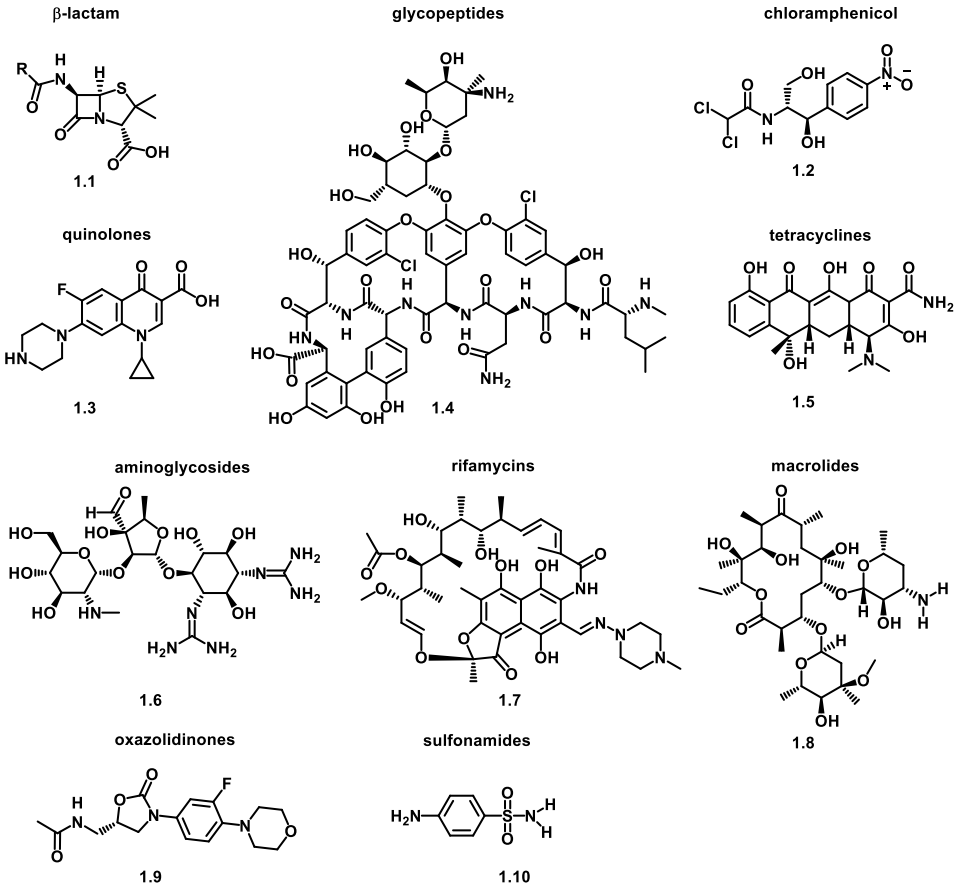

Figure 1.2 *Overview of antibiotic classes and structures*

1.1.1 Mechanism of inhibition

Amidst the golden-age of antibiotics came the mechanistic understanding of how the life-changing antibiotics were able to inhibit bacterial growth. The most prominent and well understood will be discussed herein.

1.1.1.1 Cell wall biosynthesis

The first and most well-known mechanism attacks an aspect crucial to the survival of bacteria, the integrity (and existence) of their cell wall. A key component is peptidoglycan, a cross-linked polymer and outermost layer, functioning to protect the cell.[8] Without peptidoglycan, the cell cannot survive. Composition requires the functioning of penicillin binding proteins (PBP), or transpeptidases, to assemble peptidoglycan units.[9] Two distinct mechanisms exist for the successful targeting of cell-wall biosynthesis, both interfering with PBP's crosslinking ability.[10] To appropriately explain the difference, it is necessary to briefly explain the exact role of the enzyme. The final step of peptidoglycan synthesis is the transpeptidation (or crosslinking) of pentapeptide precursors. Specifically, PBP will bind to the D-Ala-D-Ala terminus, releasing a D-alanine; next, an amide from the prospective peptidoglycan polymer will displace the enzyme, crosslinking the stands, freeing PBP (Figure 1.3).[9] Therefore, the two mechanisms for inhibition are: (1) β-lactams (penicillin and cephalosporins) disable PBPs, the enzyme will attack the β-lactam ring instead of the D-Ala-D-Ala terminus (suicide inhibition) preventing both the construction of peptidoglycan and the ability of the enzyme to turnover.[11] Alternatively, (2) vancomycin (glycopeptide antibiotics) act by directly binding

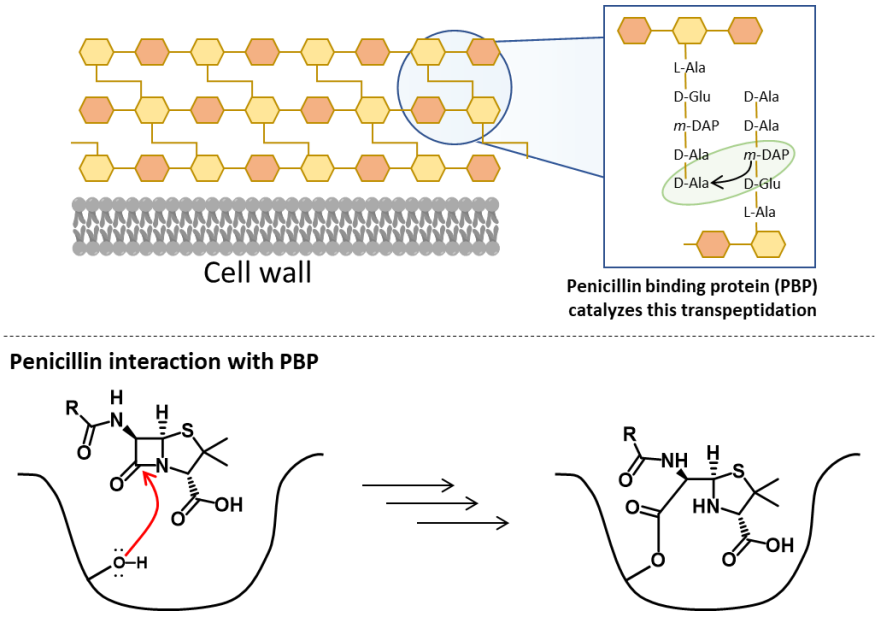

Figure 1.3 *Cell wall biosynthesis inhibition*

to the D-Ala-D-Ala terminus, prior to transpeptidase activity by PBPs, inhibiting their ability to crosslink, yet leaving the enzyme unaffected.[12]

1.1.1.2 DNA replication

A second class of antibiotics targets DNA replication. These compounds are quinolines and target topoisomerases. Topoisomerases are enzymes that exist to alleviate strain caused by tangles and supercoils of DNA. DNA gyrase (topoisomerase II) and topoisomerase IV induce breaks (double stranded) in the DNA, once broken innate cellular machinery goes to the break to repair it. Quinolones bind to the topoisomerase/DNA complex, locking it in place and inhibiting the ability of DNA to be repaired.[13] Specifically, inhibition is a consequence of the inaccessibility of the cut DNA because the topoisomerase/DNA/quinolone complex will remain intact, with quinolones acting to hold it together. This process results in rapid cell death as DNA is unable to be replicated (Figure 1.4).

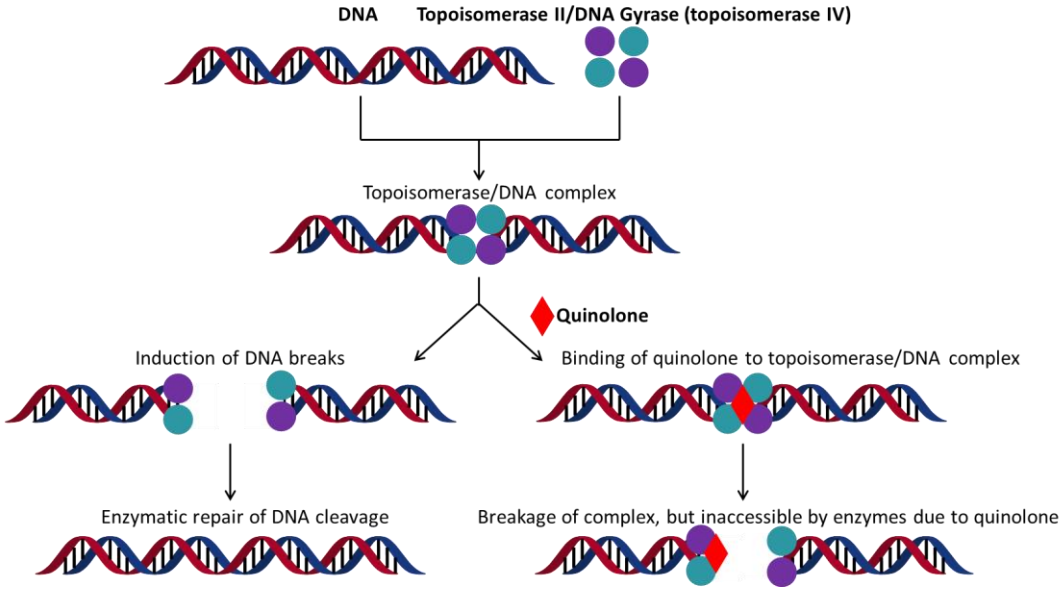

Figure 1.4 *Mechanism of quinolone-mediated cell death*

1.1.1.3 RNA synthesis

RNA synthesis is another target of inhibition by antibiotics. The rifamycin class of antibiotics contains both naturally occurring and semi-synthetic compounds that act via the inhibition of DNA-dependent RNA polymerase.[14] The compounds inhibit by sterically blocking the "exit" channel of the DNA/RNA polymerase complex and subsequently inhibiting the elongation of the RNA chain.[15] This interaction leads to rapid cell death, permitting RNA synthesis is still in the initiation phase (Figure 1.5).

1.1.1.4 Protein Synthesis

The final major class of antibiotic targets is that of protein synthesis. The three steps in protein synthesis include: initiation, elongation, and termination. These processes are catalyzed by the ribosome and its associated factors. Protein synthesis initiates as a result of the complexation of mRNA with the smaller, 30S, subunit of the ribosome. Before the initiation step is complete, the larger, 50S, subunit will associate with the 30S/mRNA complex and elongation will commence.[16] As such, inhibition of protein synthesis is accomplished by drugs targeting ***either*** the 30S or 50S subunit.[17] Classes of drugs targeting the 30S subunit are tetracyclines and aminocyclitols (spectinomycin and aminoglycosides). Tetracyclines inhibit via binding to the 30S subunit, preventing aminoacyl-tRNA attachment – an event that would initiate elongation.[18] Similarly, aminocyclitols bind to a specific component of the 30S subunit, the 16S rRNA, resulting in the inability to begin elongation (as with tetracycline); alternatively, this can lead to mismatching and mistranslation.[11] The drug classes targeting the 50S subunit are macrolides, lincosamides, amphenicols, and oxazolidinones. Classical inhibition requires binding to the 50S subunit in a manner such that either initiation or elongation is prevented (Figure 1.5).[16, 19]

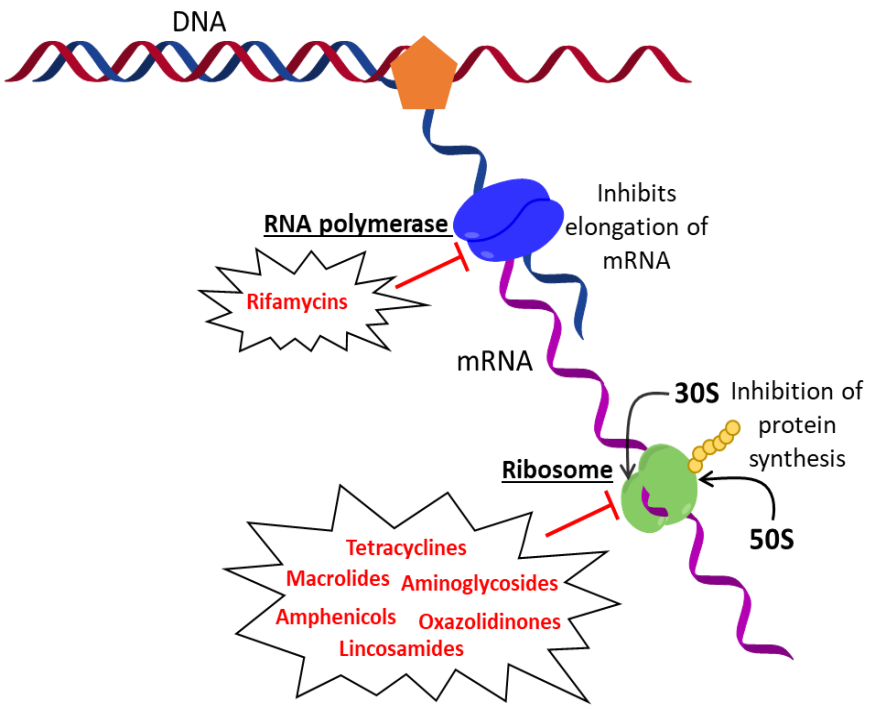

Figure 1.5 *Inhibition of RNA synthesis and protein synthesis*

1.1.2 Mechanism of resistance

Classical mechanisms conferring antibiotic resistance have become well characterized as their prevalence continually increases. Crucial to the process is the ability of bacteria to transfer genes via horizontal gene transfer.[20] Horizontal gene transfer permits the direct incorporation of resistant genes to various species, which are then replicated, passed on to the next generation, and begin to be characteristic of the entire population. A contributor facilitating this process is the over-use and mis-use of antibiotics, wherein selective pressure has facilitated the selection of resistant strains. Selection often permits "survival of the fittest", where the fittest may possess evolutionary advantages allowing them to survive.[4] Another prominent area where resistance developed has been used in agriculture.[21]. The most common mechanisms fall into three major categories; drug efflux, bacterial target modification (or access prevention), and drug metabolism (inactivation), all of which will be discussed (shown in Figure 1.6).

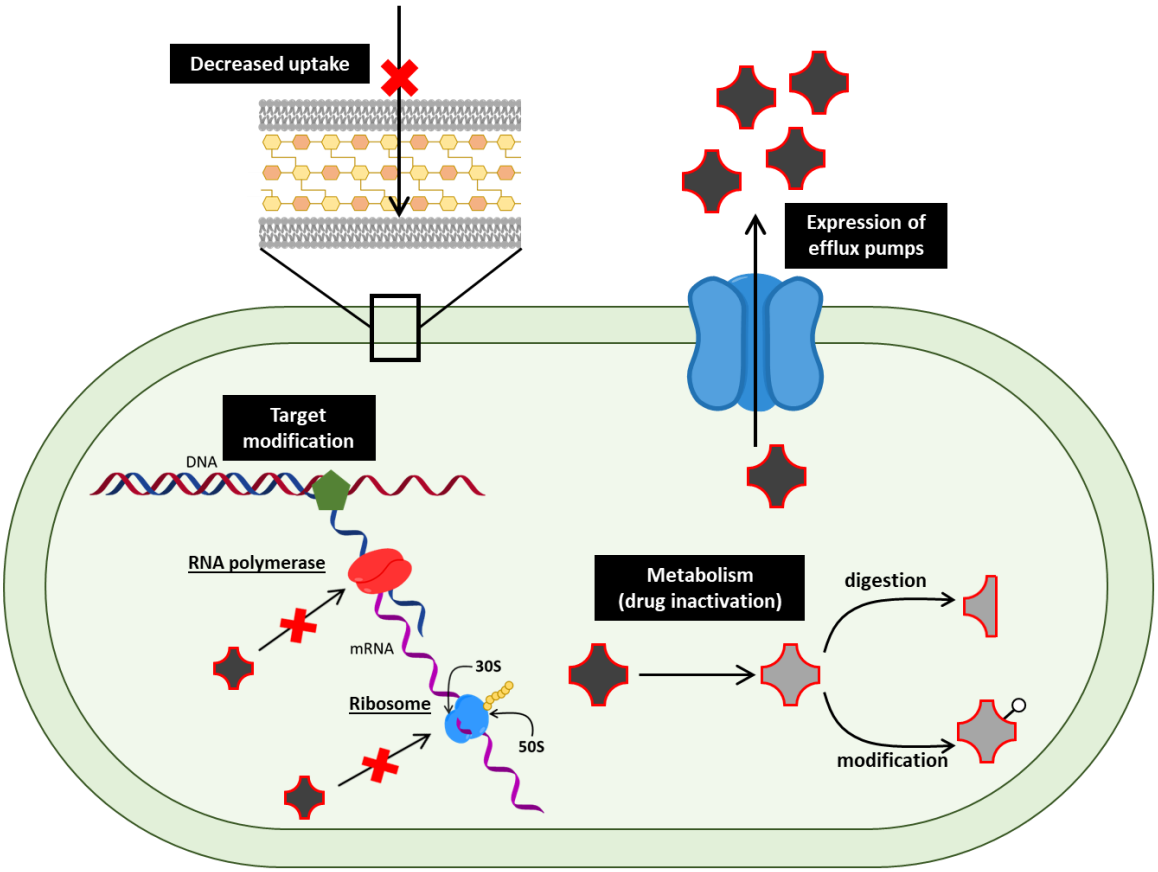

Figure 1.6 *Classical drug resistance mechanisms*

1.1.2.1 Efflux

Perhaps the conceptually simplest way to evade inhibition by antibiotics is simply to extrude the compound from the cell, a process that occurs by the expression of efflux pumps. Mechanistically similar, would be the inability to enter the cell, a mechanism that becomes relevant when considering the differences between the two major classes of bacterial species, Gram-negative and Gram-positive, composed cell membranes of markedly different composition (*vide infra*). To date, five unique classes of efflux pumps have been identified.[22] A large number of pumps fall into the category of multidrug resistance (MDR) efflux pumps, wherein they are capable of transporting drugs of varying structure (nonspecific).[23] This comes as a great concern, as it makes predicting the likelihood of substrate efflux complicated. One class that foregoes the broad range of substrates are tetracycline specific efflux pumps. Despite the necessity for substrate specificity, tetracycline efflux pumps are extremely effective at lowering the overall concentration of drug within the cell and exist for a wide range of bacterial species, including both Gram-negative and Gram-positive.[18]

1.1.2.2 Target modification

Target modification is another significant contributor to bacterial resistance. This can be characterized by a decreased affinity for the drug/target interaction. Several examples of this mechanism exist and will be explained relative to their class of antibiotic.

(1) Perhaps the most well-known cell-wall biosynthesis resistance mechanism is the transcription of β-lactamases (*vide infra*). However, there has also been the selection for β-lactam sensitive penicillin binding proteins, in particular, PBP2a, possessing lower affinity for β-lactams. This decreased affinity permits the construction of the cell wall, even in the presence of β-lactams.[24]

(2) DNA replication inhibitors consist of quinolones. Quinolone resistance arises from strategic mutations near the active site of either DNA gyrase or topoisomerase IV.[25] Subtle amino acid modifications to larger amino acid derivatives disrupt the structure significantly enough to confer resistance.[22] Often,

additional mutations, or mutations increasing the structural differences, will occur to increase the effectiveness.

(3) RNA synthesis inhibitors are of the rifamycin family. Rifampicin resistance has been confirmed a result of mutated RNA polymerase (RNAP). This was initially confirmed upon investigation of RNAP isolated from a resistant strain and its altered migration, compared to wild type with gel electrophoresis.[26] Mutated enzymes do not bind rifamycin's, rendering their use ineffective.

(4) Protein synthesis inhibitors fall in a variety of structural classes, each with a unique target modification mechanism. In contrast to an expressed mutation of the target, macrolide targets are modified enzymatically. Erm enzymes methylate a key amino acid, facilitating both steric and electronic blocks for inhibitors of various structure.[22] Additionally, linezolid target genes exist in multiple, identical copies. One of which will have a mutation that will proliferate upon treatment with the drug, conferring resistance.[23] Finally, tetracycline resistance is the result of Tet(M) and Tet(O), two ribosomal protection proteins. Tet(M) and Tet(O) act to protect RNA synthesis by dislodging tetracycline from its binding site as a result of their interaction with the complex.[27]

1.1.2.3 Metabolism

Drug inactivation is the final common method to confer resistance. Perhaps the most studied mechanism of this type is related to β-lactams. Enzymes of the β-lactamase class were first identified in 1940, prior to the first clinical use of penicillin as an antibiotic. These enzymes exist to "disarm" the antibiotic by hydrolysis of the β-lactam ring.[22] β-lactams, however, are not the only antibiotic that is met with drug altering mechanisms. Another type of inactivation is in the form of modification, observed as phosphorylation, acylation, or adenylation of aminoglycosides.[24, 28] The modification, in all cases, increases steric bulk and decreases activity as a direct result. Similarly, the piperazine ring of fluoroquinolones is often acetylated by attack from an acetyltransferase, AAC(6')-Ib-cr, again rendering the drug inactive.[29] Interestingly, the acetyltransferase responsible for acetylating fluoroquinolones differs by ***only two*** amino

acids from the acetyltransferase able to acetylate certain aminoglycosides, highlighting the ability of bacteria to tailor their enzymes to overcome inhibition of various mechanisms.[29]

Understanding the mechanisms by which bacteria are essentially able to disarm antibiotics brings the field to a common solution: new bacterial targets. Of course, alternatives exist, co-therapies have made a significant contribution. For example, the antibiotic Augmentin is a β-lactam co-dosed with a β-lactamase inhibitor, successfully aiding the effectiveness of β-lactam antibiotics. Continual research in this area will certainly contribute to alleviating some of the pressures associated with combatting super-bugs; however, investigating alternative mechanisms wherein we are subjecting the bacteria to treatment it has never experienced before will, be the solution we need. Take for example Augmentin, while, we are able to treat infections, we are still exposing bacteria to the selective pressure forcing the transcription of β-lactamases, a trait able to inheritable to the next generation.

Novel areas such as targeting virulence, bacterial biofilms, or siderophores may provide new mechanisms and potentially a lessened, dampened rate of resistance. These targets aim to eliminate the pathogenicity of the bacteria, not necessarily promote cell death. Virulence is the ability for bacteria to become pathogenic. Often bacteria are told to "turn on" mechanisms which upregulate the transcription of virulence factors via communication with small molecules, targeting the synthesis or reception of these signals may inhibit the ability to communicate. Biofilms are bacterial "safe zones", in their mature form they are a 3-D structure of tightly packed and protected bacterial cells. This is often established to protect the population. Biofilm formation occurs in a stepwise manner and inhibiting any of the stages may aid in eliminating pathogenicity. Lastly, siderophores are small molecules which bind iron. Iron is essential to all forms of life and to ensure they have enough, bacteria secrete scavengers to steal or solubilize iron. Targeting the synthesis of these molecules would disarm the bacteria making them weaker and potentially more susceptible to antibiotic treatment.

An area that could be of particular interest in investigating the above targets, as well as novel natural product scaffolds will be discussed in the next section.

1.2 Rhizosphere microbiome

The combination of microbial diversity and evolutionary pressure has incentivized bacteria to create natural products with extraordinary selectivity and bioactivity.[30] These scaffolds serve with distinction as antibacterial agents as an estimated 70% of marketed antibiotics are derived from natural products. One specific example exists within the rhizosphere where evolution of microorganisms required the utilization of chemical warfare to both colonize the environment and defend themselves.[31-32] The ability to survive within this environment raises the question: What can we learn from interspecies-interactions? More specifically, can we take advantage of the tactics utilized by the microorganisms as methods towards combatting them? The following section will explain the complexity of the rhizosphere with respect to the chemical diversity and antibacterial advantages.

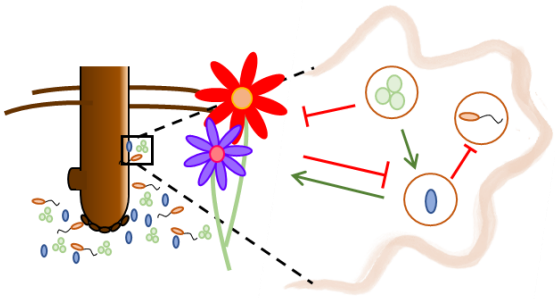

Figure 1.7 *Representative example of microbial interactions in the rhizosphere*

1.2.1 Diverse microbiome

Exquisitely explained in Martin Blaser's 'Missing Microbes', humans possess a diverse microbiome, residing in our gut, the equilibrium of which serves to protect us. This environment and protective relationship that results from the cohabitation of human cells and microorganisms can be directly translated to the rhizosphere, wherein the host is now a plant. The rhizosphere is the area in the soil directly surrounding the root of plants, the role of which is largely in crop protection. Understanding the differences in bacterial interactions, can be beneficial in understanding mechanisms by which bacteria can be inhibited, aside from classical antibiotic mechanisms. The predominant players in the rhizosphere are nematodes,

fungi/oomycetes, protozoa, arthropods, algae, bacteria, archaea, and viruses and an array of key compounds that will be discussed below.[33]

1.2.2 Types of metabolites found in the rhizosphere

The type of microbes commonly found in the rhizosphere fall into three major categories referred to by Mendes et al. with the most accurate description, "the good, the bad, and the ugly".[33] These labels correspond to the more canonical terms: plant beneficial (or symbionts), plant pathogenic (or pathovars), and human pathogenic, respectively.[31] A variety of metabolites facilitate the interactions that establish the competitive environment. These vary in structural complexity and function, allowing for microbes to "steal" resources, inhibit one another, or promote growth of the plant.[32, 34] Two key classes the compounds loosely fall into are signaling molecules and antimicrobials.

The first major class of compounds are signaling molecules. Arguably the largest of this class are flavonoids, small molecules exuded by roots. Flavonoids are composed of a "flavone" backbone, or derivative thereof and are related to a variety of tasks. Of particular importance is the ability to alter nutrient composition in the soil, exemplified by acting as antioxidants and metal chelators.[1] A survey of common derivatives of the key scaffolds are shown in Figure 1.8 When secreted by the host, flavonoids are responsible for the expression of *nod* genes, producing Nod factors, which facilitate the symbiotic relationship between the plant and other organisms.[35] Recently there has been increasing evidence supporting a connection of flavonoids and quorum sensing, specifically, its regulation (*vide infra*).[36]

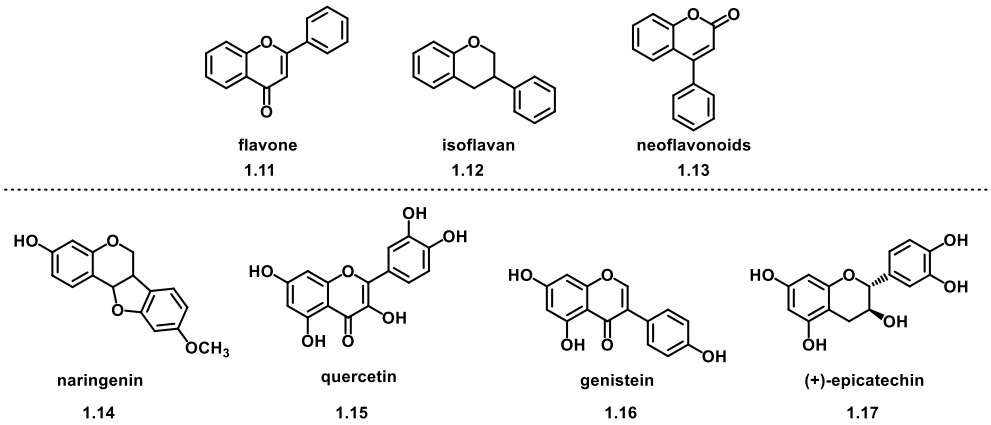

Figure 1.8 *Flavonoids with different functions in the rhizosphere*[1]

Another class of signaling molecules prevalent in the rhizosphere are strigalactones. The core structure typically consists of 4 rings, derivatives of which are outlined in Figure 1.9. This structurally diverse class of compounds functions dually as both signaling molecules and plant hormones. The first identified of the class was strigol, found exuded by the roots of cotton and identified as a germination stimulant.[37] A particularly prominent relationship facilitated by strigalactones, specifically, 5-deoxystrigol, consists of the symbiosis between rhizobacteria and fungi, accomplished by nutrient exchange between the two.[35, 38] This interaction is primarily positive, however, they have also been shown to promote the growth of parasitic species in cases such as sorgolactone and sorgomol.[39]

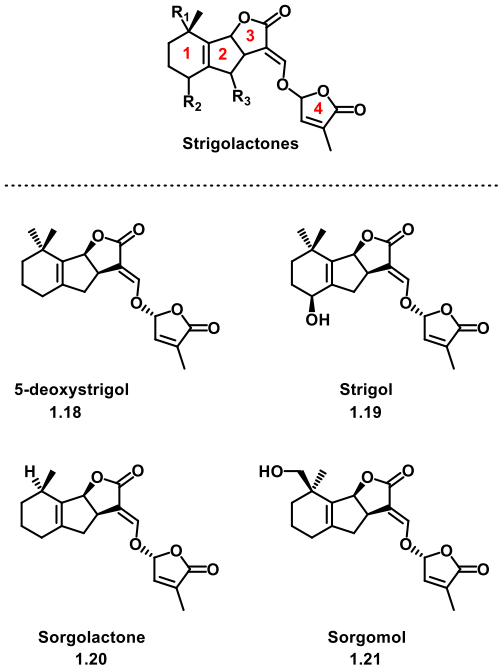

Figure 1.9 *Structure of strigalactones and well-known examples*

Another class of signaling molecule found in the rhizosphere regulates quorum sensing. Quorum sensing is the ability of bacteria to communicate with one another by means of small molecules, triggered by increased cell density (a "quorum" being met). This communication permits the ability to produce defense mechanisms or weapons, when a threat is imminent, allowing for increased community fitness.[40]

The most prominent small molecule class regulating quorum sensing is acyl homoserine lactones (AHLs). AHLs are structurally comprised of an alkyl chain of 4-18 carbons providing a wide range of diversity. AHLs bind to receptors, triggering virulence mechanisms such as biofilm formation and siderophore biosynthesis. The biggest challenge associated with these molecules is that no two species produce an identical AHL, making their inhibition challenging and increasing their impact.[41] However, while none are synthetically identical, Figure 1.10 highlights the structural similarities of the most common AHLs. These similarities allow for bacterial receptors to interpret signals from multiple species allowing larger populations to become virulent, an act that underscores the importance of inhibiting small molecule communication.

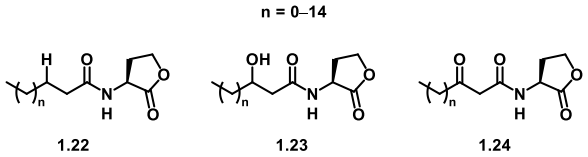

Figure 1.10 *Common AHL scaffolds and their diversity*

In addition to signaling molecules aiding in protection or pathogenicity, several antimicrobial compounds are also present in the rhizosphere. These compounds aid in pathogenicity for both beneficial and pathogenic bacteria, in all cases promoting self-survival within the 'war-zone'.[31] Functioning via membrane disruption, followed by lysis, lipopeptides are commonly secreted by rhizobacteria to defend against their predators.[42] For example, masselotide A (Figure 1.11, top) is a metabolite made by *Pseudomonas fluorescens* that has been proven to protect colonized tomato plants from pathogens and disease.[43]

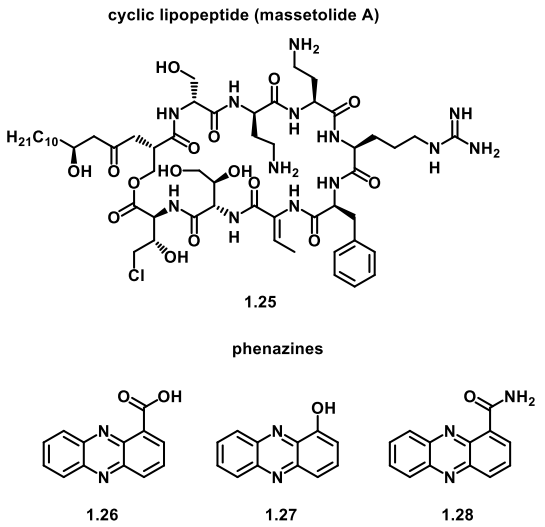

Figure 1.11 *Antimicrobials found in the rhizosphere*

Even more threatening, *Pseudomonads* are able to utilize certain lipopeptides to dismantle select mature bacterial biofilms, increasing their pathogenicity.[44] Phenazines represent an additional class of antibiotics found in the rhizosphere. They induce cell death by means of oxygen radical formation.[44] Additionally, they have been shown to induce defense pathways in plants, serving to cause the upregulation of broad-spectrum resistance mechanisms.[45] A third use for phenazines takes advantage of the redox potential in ferric (3+) iron acquisition, leading into a third class of molecules prevalent in the rhizosphere.

Iron is essential to all forms of life and required for many biological processes. However, abundantly available iron typically exists as Fe^{3+}, which is insoluble in water, yielding environmental iron unavailable in the rhizosphere (at physiological pH).[31] Solubilizing Fe^{3+} can be accomplished with the aid of secreted bacterial metabolites called siderophores. As Fe^{3+} remains insoluble when unbound, once sequestered by siderophores, it can be transferred across cellular membranes with designated transporter proteins.[46] Siderophores in the rhizosphere have evolved as a mechanism of self-preservation, wherein they are able to secure iron for themselves, while also starving out the competitors. In addition to the ability to secure iron, siderophores have been proven to promote plant growth in a variety of rhizobacteria.[47] Amongst one of the most well characterized siderophores is pyoverdine (Figure 1.12), native to *Pseudomonads*,

pyoverdine has a unique structure in all of its producing strains.[48] The common iron chelating moieties (highlighted in red, Figure 1.12) can be found, to some extent, in most siderophores. Often, iron is needed to promote biofilm formation, making inhibiting acquisition another mechanism to disarm bacterial pathogenicity.

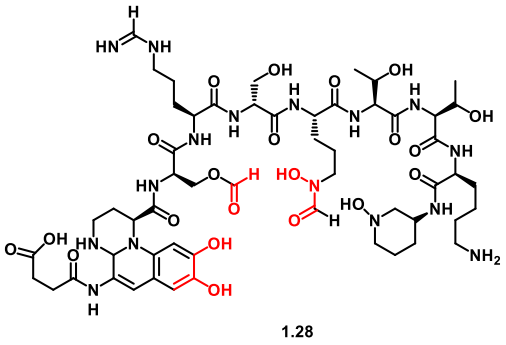

1.28

Figure 1.12 *Structure of pyoverdine*

The rhizosphere represents an area rich for investigation as pursing non-conventional methods towards combatting superbugs. As represented in the previous section, the microbiome encompasses compounds with varying levels of structural complexity. This variation is accompanied by a wide range of biological activities permitting the unearthing of novel mechanisms and structures. Each of the previously mentioned interactions has been extensively studied to have a notable impact, the more we learn of these, the more we will develop creative methods towards generating new inhibitory mechanisms.

1.3 References

1. Hassan, S.; Mathesius, U., The role of flavonoids in root-rhizosphere signalling: opportunities and challenges for improving plant-microbe interactions. *J Exp Bot* **2012,** *63* (9), 3429-44.
2. Davies, J., Where Have All the Antibiotics Gone? *Can J Infect Dis Med Microbiol.* **2006,** *17* (5), 287-290.
3. Davies, J.; Davies, D., Origins and evolution of antibiotic resistance. *Microbiol Mol Biol Rev* **2010,** *74* (3), 417-33.
4. Ventola, C. L., The Antibiotic Crisis: part 1: causes and threats. *P T* **2015,** *40* (4), 277-283.
5. Neu, H. C., The Crisis in Antibiotic Resistance. *Science* **1992,** *257*, 1064-1073.
6. Wright, G. D., Resisting resistance: new chemical strategies for battling superbugs. *Chemistry & biology* **2000,** *7* (6), R127-R132.

7. Aminov, R. I., A brief history of the antibiotic era: lessons learned and challenges for the future. *Front Microbiol* **2010,** *1*, 134.
8. Vollmer, W.; Blanot, D.; de Pedro, M. A., Peptidoglycan structure and architecture. *FEMS Microbiol Rev* **2008,** *32* (2), 149-67.
9. Blumberg, P. M.; Strominger, J. L., Interaction of Penicillin with the Bacterial Cell: Penicillin-Binding Proteins and Penicillin-Sensitive Enzymes. *Bacteriology Reviews* **1974,** *38* (8), 291-335.
10. Sauvage, E.; Kerff, F.; Terrak, M.; Ayala, J. A.; Charlier, P., The penicillin-binding proteins: structure and role in peptidoglycan biosynthesis. *FEMS Microbiol Rev* **2008,** *32* (2), 234-58.
11. Kohanski, M. A.; Dwyer, D. J.; Collins, J. J., How antibiotics kill bacteria: from targets to networks. *Nat Rev Microbiol* **2010,** *8* (6), 423-35.
12. Kahne, D.; Leimkuhler, C.; Lu, W.; Walsh, C., Glycopeptide and lipoglycopeptide antibiotics. *Chem Rev* **2005,** *105* (2), 425-48.
13. Drlica, K.; Malik, M.; Kerns, R. J.; Zhao, X., Quinolone-mediated bacterial death. *Antimicrob Agents Chemother* **2008,** *52* (2), 385-92.
14. Hatmann, G.; Honikel, K. O.; Knusel, F.; Nuesch, J., The specific inhibition of the DNA-directed RNA synthesis by rifamycin. *Biochem Biophys Acta* **1967,** *145*, 843-844.
15. Floss, H. G.; Yu, T. W., Rifamycin-mode of action, resistance, and biosynthesis. *Chem Rev* **2005,** *105* (2), 621-32.
16. Mukhtar, T. A.; Wright, G. D., Streptogramins, oxazolidinones, and other inhibitors of bacterial protein synthesis. *Chem Rev* **2005,** *105* (2), 529-42.
17. Weisblum, B.; Davies, J., Antibiotic inhibitors of the bacterial ribosome. *Bacteriological Reviews* **1968,** *32* (4), 493-528.
18. Chopra, I.; Roberts, M., Tetracycline antibiotics: mode of action, applications, molecular biology, and epidemiology of bacterial resistance. *Microbiol Mol Biol Rev* **2001,** *65* (2), 232-60 ; second page, table of contents.
19. Katz, L.; Ashley, G. W., Translation and protein synthesis: macrolides. *Chem Rev* **2005,** *105* (2), 499-528.
20. Ochman, H.; Lawrence, J. G.; Groisman, E. A., Lateral gene transfer and the nature of bacterial innovation. *Nature* **2000,** *405* (6784), 299-304.
21. Venter, H.; Henningsen, M. L.; Begg, S. L., Antimicrobial resistance in healthcare, agriculture and the environment: the biochemistry behind the headlines. *Essays Biochem* **2017,** *61* (1), 1-10.
22. Wright, G. D., Molecular mechanisms of antibiotic resistance. *Chem Commun (Camb)* **2011,** *47* (14), 4055-61.
23. Blair, J. M.; Webber, M. A.; Baylay, A. J.; Ogbolu, D. O.; Piddock, L. J., Molecular mechanisms of antibiotic resistance. *Nat Rev Microbiol* **2015,** *13* (1), 42-51.
24. Munita, J. M.; Arias, C. A., Mechanisms of Antibiotic Resistance. *Microbiology Spectrum* **2016,** *4* (2).
25. Piddock, L. J., Mechanisms of fluoroquinolone resistance: an update 1994-1998. *Drugs* **1999,** *58 Suppl 2*, 11-8.
26. Goldstein, B. P., Resistance to rifampicin: a review. *J Antibiot (Tokyo)* **2014,** *67* (9), 625-30.
27. Connell, S. R.; Tracz, D. M.; Nierhaus, K. H.; Taylor, D. E., Ribosomal Protection Proteins and Their Mechanism of Tetracycline Resistance. *Antimicrob Agents Chemother* **2003,** *47* (12), 3675-3681.
28. Mingeot-Leclercq, M.-P.; Glupczynski, Y.; Tulkens, P. M., Aminoglycosides: Activity and Resistance. *Antimicrobial Agents and Chemotherapy* **1999,** *43* (4), 727-737.
29. Jacoby, G. A.; Gacharna, N.; Black, T. A.; Miller, G. H.; Hooper, D. C., Temporal appearance of plasmid-mediated quinolone resistance genes. *Antimicrob Agents Chemother* **2009,** *53* (4), 1665-6.
30. Rossiter, S. E.; Fletcher, M. H.; Wuest, W. M., Natural Products as Platforms To Overcome Antibiotic Resistance. *Chem Rev* **2017,** *117* (19), 12415-12474.

31. Keohane, C. E.; Steele, A. D.; Wuest, W. M., The Rhizosphere Microbiome: A Playground for Natural Product Chemists. *Synlett* **2015,** *26* (20), 2739-2744.
32. Philippot, L.; Raaijmakers, J. M.; Lemanceau, P.; van der Putten, W. H., Going back to the roots: the microbial ecology of the rhizosphere. *Nat Rev Microbiol* **2013,** *11* (11), 789-99.
33. Mendes, R.; Garbeva, P.; Raaijmakers, J. M., The rhizosphere microbiome: significance of plant beneficial, plant pathogenic, and human pathogenic microorganisms. *FEMS Microbiol Rev* **2013,** *37* (5), 634-63.
34. Nihorimbere, V.; Ongena, M.; Smargiassi, M.; Thonart, P., *Beneficial effect of the rhizosphere microbial community for plant growth and health*. 2011; Vol. 15, p 327-337.
35. Zhang, Y.; Ruyter-Spira, C.; Bouwmeester, H. J., Engineering the plant rhizosphere. *Curr Opin Biotechnol* **2015,** *32*, 136-142.
36. Perez-Montano, F.; Guasch-Vidal, B.; Gonzalez-Barroso, S.; Lopez-Baena, F. J.; Cubo, T.; Ollero, F. J.; Gil-Serrano, A. M.; Rodriguez-Carvajal, M. A.; Bellogin, R. A.; Espuny, M. R., Nodulation-gene-inducing flavonoids increase overall production of autoinducers and expression of N-acyl homoserine lactone synthesis genes in rhizobia. *Res Microbiol* **2011,** *162* (7), 715-23.
37. Xie, X., Structural diversity of strigolactones and their distribution in the plant kingdom. *J Pestic Sci* **2016,** *41* (4), 175-180.
38. Ruyter-Spira, C.; Al-Babili, S.; van der Krol, S.; Bouwmeester, H., The biology of strigolactones. *Trends Plant Sci* **2013,** *18* (2), 72-83.
39. Xie, X.; Yoneyama, K.; Kusumoto, D.; Yamada, Y.; Takeuchi, Y.; Sugimoto, Y.; Yoneyama, K., Sorgomol, germination stimulant for root parasitic plants, produced by Sorghum bicolor. *Tetrahedron Letters* **2008,** *49* (13), 2066-2068.
40. Phelan, V. V.; Liu, W. T.; Pogliano, K.; Dorrestein, P. C., Microbial metabolic exchange--the chemotype-to-phenotype link. *Nat Chem Biol* **2011,** *8* (1), 26-35.
41. Schuster, M.; Sexton, D. J.; Diggle, S. P.; Greenberg, E. P., Acyl-homoserine lactone quorum sensing: from evolution to application. *Annu Rev Microbiol* **2013,** *67*, 43-63.
42. Raaijmakers, J. M.; de Bruijn, I.; de Kock, M. J., Cyclic lipopeptide production by plant-associated Pseudomonas spp.: diversity, activity, biosynthesis, and regulation. *Mol Plant Microbe Interact* **2006,** *19* (7), 699-710.
43. Tran, H.; Ficke, A.; Asiimwe, T.; Hofte, M.; Raaijmakers, J. M., Role of the cyclic lipopeptide massetolide A in biological control of Phytophthora infestans and in colonization of tomato plants by Pseudomonas fluorescens. *New Phytol* **2007,** *175* (4), 731-42.
44. Raaijmakers, J. M.; Mazzola, M., Diversity and natural functions of antibiotics produced by beneficial and plant pathogenic bacteria. *Annu Rev Phytopathol* **2012,** *50*, 403-24.
45. Pierson, L. S., 3rd; Pierson, E. A., Metabolism and function of phenazines in bacteria: impacts on the behavior of bacteria in the environment and biotechnological processes. *Appl Microbiol Biotechnol* **2010,** *86* (6), 1659-70.
46. Miethke, M.; Marahiel, M. A., Siderophore-based iron acquisition and pathogen control. *Microbiol Mol Biol Rev* **2007,** *71* (3), 413-51.
47. Leong, J., Siderophores: Their biochemistry and possible role in the biocontrol of plant pathogens. **1986,** *34*.
48. Hohnadel, D.; Meyer, J.-M., Specificity of Pyoverdine-Mediated Iron Uptake among Fluorescent Pseudomonas Strains. *Journal of Bacteriology* **1988,** *170* (10), 4865-4873.

Chapter 2 Promysalin

Sections 2.1, 2.2, 2.3, 2.4 have been adapted with permission from (Steele, A. D.; Knouse, K. W.; Keohane, C. E.; Wuest, W. M., Total Synthesis and Biological Investigation of (−)-Promysalin. *Journal of the American Chemical Society* **2015**, *137* (23), 7314-7317. DOI: 10.1021/jacs.5b04767). **Copyright © 2015 American Chemical Society**
(https://pubs.acs.org/articlesonrequest/AOR-GZM4GhTpI3cX8sf88S5U)

Sections 2.4, 2.5 have been adapted with permission from (Steele, A. D.; Keohane, C. E.; Knouse, K. W.; Rossiter, S. E.; Williams, S. J.; Wuest, W. M., Diverted Total Synthesis of Promysalin Analogs Demonstrates That an Iron-Binding Motif Is Responsible for Its Narrow-Spectrum Antibacterial Activity. *Journal of the American Chemical Society* **2016**, *138* (18), 5833-5836. DOI: 10.1021/jacs.6b03373). **Copyright © 2016 American Chemical Society**
(https://pubs.acs.org/articlesonrequest/AOR-b3jTwUMXrMjXGwbHjA8X)

Sections 2.6, 2.7, 2.8 have been adapted with permission from (Keohane, C. E.; Steele, A. D.; Fetzer, C.; Khowsathit, J.; Van Tyne, D.; Moynié, L.; Gilmore, M. S.; Karanicolas, J.; Sieber, S. A.; Wuest, W. M., Promysalin Elicits Species-Selective Inhibition of Pseudomonas aeruginosa by Targeting Succinate Dehydrogenase. *Journal of the American Chemical Society* **2018**, *140* (5), 1774-1782 DOI: 10.1021/jacs.7b11212.). **Copyright © 2018 American Chemical Society**
(https://pubs.acs.org/articlesonrequest/AOR-n65xDt3tBgiimZmCrN42)

Section 2.10 has been adapted with permission from (Giglio, K. M.[#]; Keohane, C. E.[#]; Stodghill, P. V.; Steele, A. D.; Fetzer, C.; Sieber, S. A.; Filiatrault, M. J.; Wuest, W. M., Transcriptomic Profiling Suggests That Promysalin Alters the Metabolic Flux, Motility, and Iron Regulation in Pseudomonas putida KT2440. *ACS Infectious Diseases* **2018**, *4* (8), 1179-1187.). **Copyright © 2018 American Chemical Society**
(https://pubs.acs.org/articlesonrequest/AOR-rHT4YTGFuBMcp3rSUZ4a)

This work was completed with the help of collaborators (indicated with their contribution). Synthetic work for the synthesis and analogs was done while working with Andrew Steele, PhD and side chains with Savannah Post.

2.1 Introduction

2.1.1 Narrow-spectrum antibiotics and Gram-negative pathogens

The continued rise of antibiotic resistant bacterial infections warrants the development of novel treatments with *unique modes of action*. To date, there is a general lack of diversity amongst cellular targets of approved antibiotics with recent reports estimating that fewer than twenty-five targets are represented.[1] Most of these compounds are non-discriminatory (broad-spectrum), and target essential pathways (see chapter one).[2] Although some "narrow-spectrum" therapies are available, they target large subsets of

bacteria (for example anaerobes vs. aerobes, Gram-positive vs. Gram-negative) instead of focusing on particular pathogenic species. The latter method of treatment would be preferred to reduce adverse side effects to the host and microbiome communities and to minimize the development of resistance. However, both financial and technical limitations have thwarted such efforts to date.[3] Furthermore, the identification of either 1) unique targets that would permit selective killing or 2) compounds that discriminate species is not trivial; this presents a clear unmet need that is ripe for discovery.

Of particular health interest is the bacterial species *Pseudomonas aeruginosa* (PA), an opportunistic environmental pathogen inherently resistant to many antibiotics yet rarely infective to healthy individuals.[4] However, those with compromised immune systems are especially susceptible to a fatal infection. One of the primary scenarios are cystic fibrosis patients. Cystic fibrosis is an autoimmune disease resulting from a mutation in the CFTR transmembrane protein. Mutation of such transporter disallows the efflux of chloride ions out of cells, resulting in mucus build up on the surface of the lungs (Figure 2.1). This mucus will trap bacteria (PA being a primary colonizer) and cause an infection on the lungs, frequently leading to lung failure and inevitably death.[5-6] To this end, targeting the primary cause of infection could prove highly effective, increasing the importance of identifying compounds able to inhibit the growth of PA. In 2013, the Centers for Disease Control listed multi-drug resistant PA one of the top fifteen urgent/serious microbial threats facing society, and the following year they increased its priority to the highest level, "critical", demonstrating a pressing need to develop new therapeutics which target this pathogen of interest.[7]

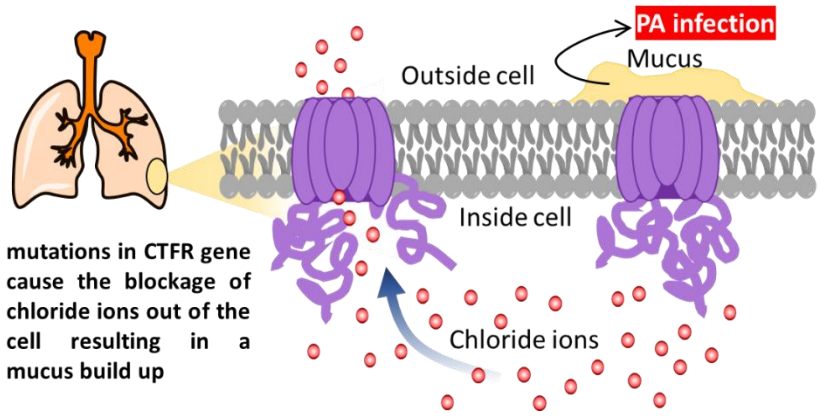

Figure 2.1 *CF mechanism*

An increased challenge associated with targeting PA is the bacterial 'sub-category' it falls into: Gram-negative. Nearly all bacterial species fall into two discrete categories guided solely by membrane composition. This was originally discovered in 1884 by Christian Gram through 'an accident' that is now a well-established method termed Gram-staining.[8] This finding identified the difference to be the presence of either a double or single cell membrane (Figure 2.2). This difference drastically increases the challenge associated with seeking narrow-spectrum drugs because compounds with activity against Gram-positive bacteria are often unable to permeate the double cell membrane of their Gram-negative counterparts.[9] Furthermore, the evolution of numerous mechanisms available to evade the effect of antibiotics renders many Gram-negative pathogens multi-drug resistant.

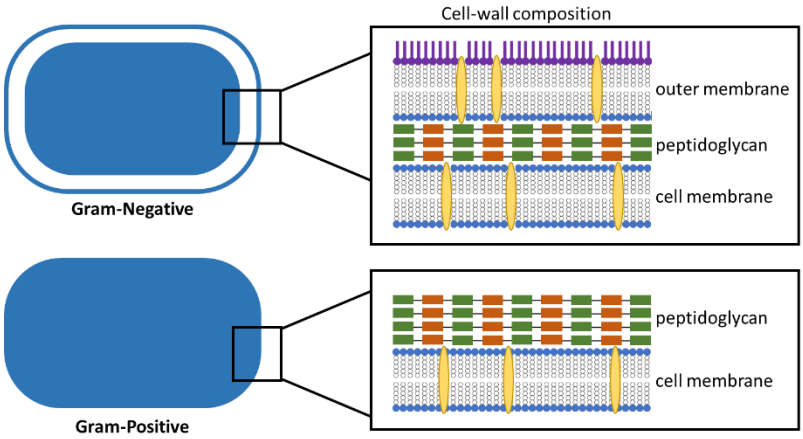

Figure 2.2 *Difference in composition of cell membrane of Gram-positive and Gram-negative bacteria*

The challenges associated with Gram-negative resistance, particularly PA, is of high concern and has become the focus of a great deal of research.[10-11] Highlighting this notion, recent work by the Hergenrother Lab has identified specific guidelines for designing molecules with activity against Gram-negative pathogens. This work not only provides insight towards the composition of new compounds but suggests modifications to drugs currently active against only Gram-positive bacteria.[12-13] In light of recent efforts to render compounds active against all pathogens, research also focuses on **specifically targeting one pathogen**, a theme underlying the research contained in this chapter. To this end, recent efforts by both

the De Mot[14] and Muller[15] labs have focused on this call by targeting untapped resources within the soil, which are rich in diversity. Work by both groups has revealed natural products with complex chemical architecture and unique bioactivity providing inspiration for organic chemists as platforms for further discovery.

2.1.2 Promysalin isolation

In 2011, De Mot and co-workers isolated a novel metabolite, promysalin (**2.1**), from *Pseudomonas putida* RW10S1, which resides in the rhizosphere of rice plants (Figure 2.3).[16] The natural product showed unique species-specific bioactivity, most notably against *Pseudomonas aeruginosa*, inhibiting growth at low-micromolar concentrations. Promysalin selectively inhibits certain PA strains and other Gram-negative bacteria but shows no activity against their Gram-positive counterparts. In contrast, the compound was also shown to promote swarming of the producing organism, hinting at two discrete modes of action. The original report characterized the biosynthetic gene cluster and proposed a biosynthesis via annotation and the characterization of shunt products. The authors elucidated the structure of promysalin through spectroscopic methods; however, no absolute or relative stereochemical assignments were made. Considering the significance of PA in clinical settings (cystic fibrosis, immunocompromised patients) and in agriculture, promysalin could serve as an attractive alternative to current therapies.[4] The unique bioactivity, unknown mode of action, and structural ambiguity are what prompted the synthesis reported herein. Before initiating our synthetic investigation, we sought to reannotate the biosynthetic gene cluster using AntiSMASH (**Figure 2.4**).[17] We postulated that this computational work would aid in determining

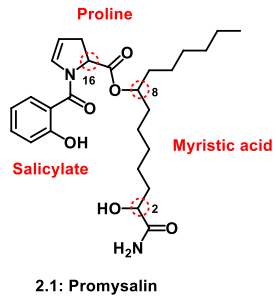

Figure 2.3 *Promysalin structure*

the absolute stereochemistry of dehydroproline, thus limiting the synthesis to one enantiomeric series. This study confirmed that ppgJ encodes for a truncated nonribosomal peptide synthetase (NRPS) module containing both adenylation (A) and thiolation domains but lacking a condensation domain, reminiscent of sylC found in Pseudomonas syringae.[18] Upon closer inspection, we were unable to identify any putative epimerase or thioesterase domains contained in either the characterized gene cluster or the flanking regions. Bioinformatic investigation of the ppgJ A domain revealed the Stachelhaus code, DVQFVAHV, corresponding to the selective activation of L-proline as previously hypothesized by De Mot.[19] This exercise led us to the conclusion that the absolute configuration of the C16 stereocenter should be assigned as (*S*). Based on these results, we reevaluated the proposed biosynthesis of promysalin, which is depicted in Figure 2.4. With this information in hand, we began our campaign to synthesize the four diastereomers generated from the two unresolved stereocenters (C2 and C8).

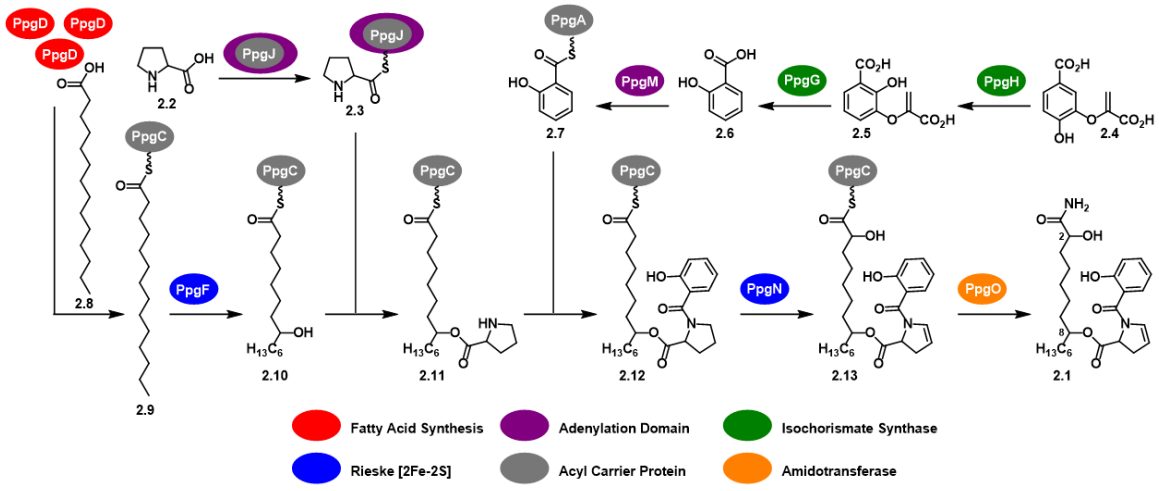

Figure 2.4 *Proposed biosynthesis of Promysalin*

2.2 Synthesis of promysalin diastereomers

2.2.1 Synthetic strategy

Our retrosynthetic strategy is outlined in Scheme 2.1. The strategy entailed a late-stage esterification of key acid intermediate **2.13** with all four possible diastereomer side chains (**2.16**). To further the convergent strategy, the side chain (**2.16**) would be assembled via a cross metathesis wherein each unknown stereocenter would be on an independent fragment allowing either configuration to be set from an asymmetric oxidation (**2.17**) or asymmetric allylation (**2.18**). Key acid intermediate **2.13** can be obtained from an amidation of a protected salicylic acid derivate (**2.14**) and trans hydroxy proline (**2.15**).

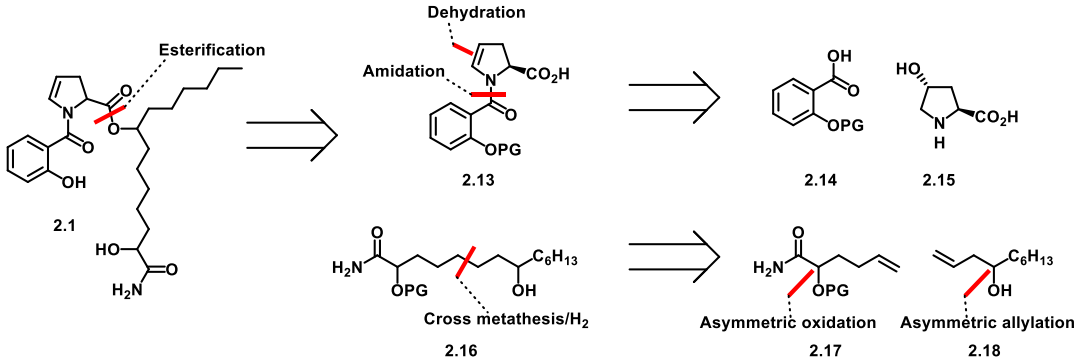

Scheme 2.1 *Retrosynthetic design*

2.2.2 Side chain synthesis

The synthesis of the side chain (Scheme 2.2) began with installation of the phenylaniline-derived Evans oxazolidinone, **(+)-2.20** or **(−)-2.20**, onto 5-hexenoic acid, **2.19**. This produced the known intermediate, **2.21**, which underwent diastereoselective oxidation using the Davis oxaziridine, (±)**2.22**. The free alcohol is subject to silyl protection furnishing compound **(+)-2.24** and **(−)2.24** in good yield. Homoallylic alcohols **(+)-2.27** or **(−)-2.27** are synthesized from heptanal and (*R*) or (*S*) BINOL. Cross metathesis with the known enantiomerically pure homoallylic alcohol **(+)-2.27** or **(−)-2.27** in the presence of modified Grubb's catalyst, C711, **2.28**, assembles the side chain (diastereomers **2.29a-d**). Subsequent hydrogenation, and ammonolysis provided diastereomers **2.31a-d**. This route provided concise access to

all four diastereomers in enantiomerically pure form (45−54% yield over five steps). Following the completion of the synthesis this reaction required optimization to permit gram-scale synthesis of the natural product. I undertook this task and was able to establish work-up and purification conditions wherein the product could be isolated in multi-gram scale in near quantitative yields with high purity.

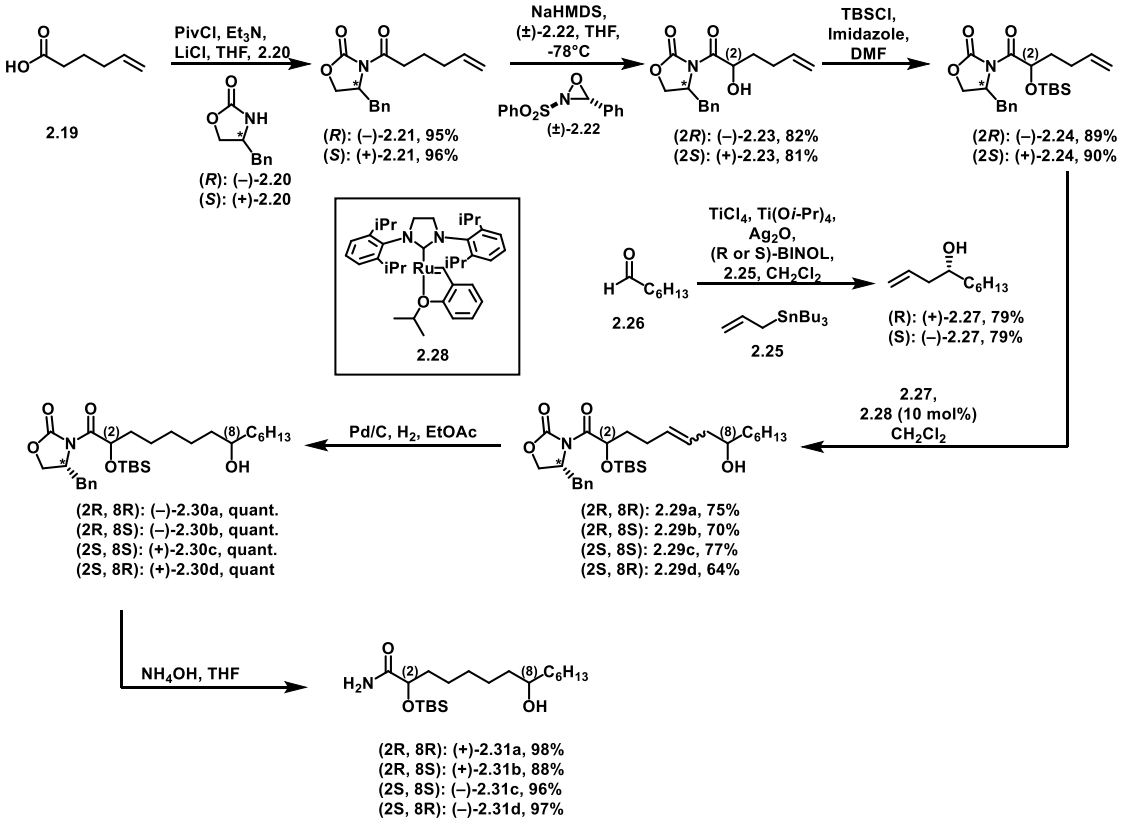

Scheme 2.2 *Synthesis of amide alcohol side chain fragment*

2.2.3 Acid synthesis

The synthesis of the proline−salicylate fragment (Scheme 2.3) commenced with SEM protection of methyl salicylate, **2.32**. Ester hydrolysis of SEM-protected methyl salicylate, **2.33**, needed to be promptly amidated with trans-4-L-hydroxyproline methyl ester, **2.35**, as the acid intermediate, **2.34**, is prone to ortho-SEM migration yielding the free phenol. Subsequent Dess−Martin oxidation provided intermediate **(+)-2.37**. At this stage, we sought to develop a method for the regioselective dehydration of **(+)-2.37** to give

the delicate enamide functionality. To this end, we treated the ketone with triflic anhydride and 2,6-lutidine to provide the desired enol triflate, **(−)-2.38**. We then cleanly reduced the enol triflate using a modified Stille reaction to furnish the corresponding enamide, **(−)-2.39** with the desired regiochemistry found in the natural product. Base hydrolysis of the methyl ester ultimately led to the key coupling fragment **(−)-2.40** in six steps and an overall yield of 56%.

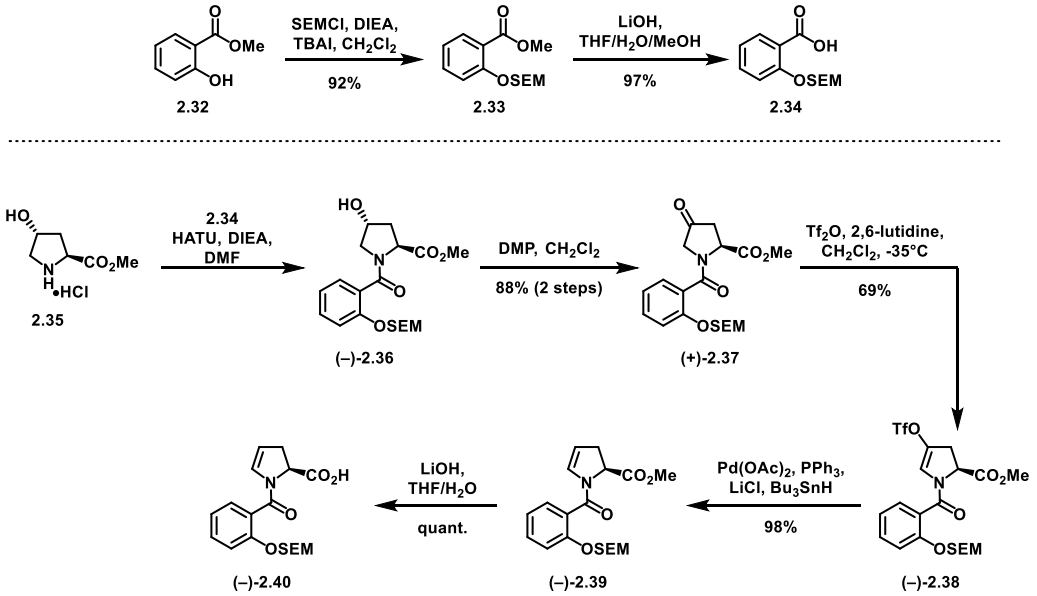

Scheme 2.3 *Synthesis of acid fragment*

2.2.4 End Game

The synthesis was completed (Scheme 2.4) with an EDC-mediated esterification of alcohols **2.31a−d** with **(−)-2.40** which proceeded smoothly to give all four diastereomers of fully protected promysalin **2.41a-d**. As is the case in many total syntheses, the final global deprotection proved to be nontrivial. Most literature methods for SEM deprotection call for either Brønsted or Lewis acidic conditions or fluoride (TBAF or TASF) at elevated temperatures. Unfortunately, the substrate was unstable to both prolonged heat and/or acid, providing only trace amounts of the desired product. As a solution, we sought milder deprotection conditions. After much experimentation, we found that 1 M TBAF in THF with DMPU

as a cosolvent cleanly removed both silyl protecting groups in a single operation, providing diastereomers **2.1a-d** (Scheme 2.4).[20]

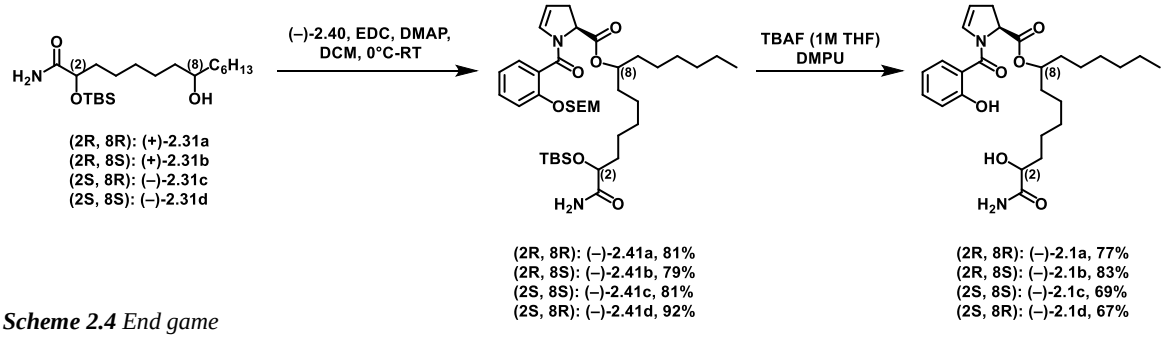

Scheme 2.4 *End game*

Our method of SEM deprotection provides a straightforward alternative to previously published precedent, as it is performed at ambient temperature using commercially available TBAF/THF solution and short reaction times (30−60 min). Despite the discovery of successful global deprotection conditions, an unwanted partially deprotected reaction intermediate, **2.42a-d**, was identified (Scheme 2.5). We observed the appearance of this intermediate when trace amounts of water are present in the TBAF, resulting in the deprotection halting at the hemi-acetal **2.42a-d**. In order to avoid this pathway, both TBAF and DMPU need to be dried over activated 3Å molecular sieves for a minimum of 24 hours.

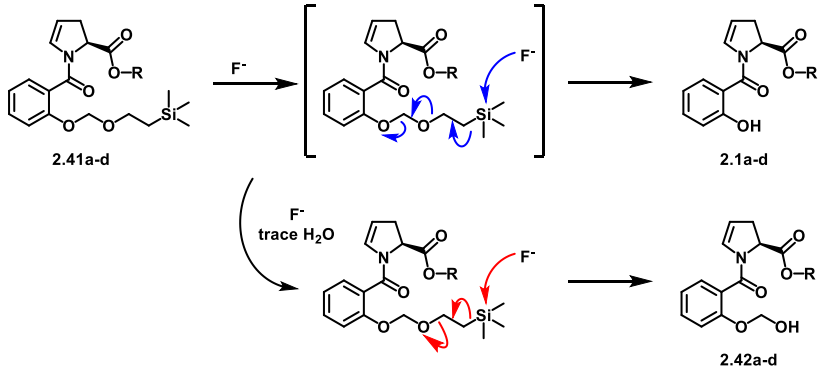

Scheme 2.5 *Partial deprotection mechanism*

2.3 Structure elucidation

2.3.1 NMR analysis

With the four diastereomers in hand, we set out to unequivocally define the relative and absolute stereochemistries through both NMR spectral comparison and biological assays. Upon careful examination of the chemical shift differences in the ^{1}H and ^{13}C NMR spectra of compounds **2.1a–d**, we identified distinct features that were used to assess the correct configurations at C2 and C8. As shown in Table 2.1, the spectral data of compound **2.1a** best correlate to those of the isolated material compared with the other diastereomers.

	ΔδH					**ΔδC**				
	Promysalin	**2.1a**	**2.1b**	**2.1c**	**2.1d**	**Promysalin**	**2.1a**	**2.1b**	**2.1c**	**2.1d**
C1	-	-	-	-	-	177.1	-0.2	-0.3	0	0
C2	4.10	0.00	0.00	-0.02	-0.01	71.1	0.1	**0.4**	**0.4**	**0.4**
C3A	1.80	0.00	-0.03	-0.04	0.04	34	0	-0.1	-0.2	0
C3B	1.65	-0.02	0.00	**-0.13**	**-0.06**	-	-	-	-	-
C4	1.43	0.00	-0.05	**-0.08**	0.01	24.4	0	0.1	0.1	0.1
C5	1.27	-0.01	-0.01	-0.01	-0.01	28.1	0.1	**0.6**	**0.6**	0.3
C6A	1.43	0.01	-0.05	**-0.08**	0.01	24.7	0	0.1	0.1	0
C6B	1.27	-0.01	-0.01	-0.01	-0.01	-	-	-	-	-
C7	1.60	-0.02	**-0.07**	**-0.08**	-0.02	34.1	0	0	-0.1	0.1
C8	5.00	0.00	-0.04	-0.05	0.01	75.8	0	0	0.1	0.2
C9	1.60	-0.02	**-0.07**	**-0.08**	-0.02	34.4	0	-0.1	-0.1	-0.1
C10A	1.43	0.00	-0.05	-0.05	0.01	25.4	0	-0.3	-0.3	-0.1
C10B	1.27	-0.01	-0.01	-0.02	-0.01	-	-	-	-	-
C11	1.27	-0.01	-0.01	-0.02	-0.01	29.1	0	0	-0.1	0
C12	1.27	-0.01	-0.01	-0.02	-0.01	31.7	0	0	0	0
C13	1.27	-0.01	-0.01	-0.02	-0.01	22.5	0	0	0	0
C14	0.87	0.00	0.01	0.00	0.00	14.1	-0.1	-0.1	-0.1	-0.1
C15	-	-	-	-	-	171.2	-0.1	**-0.4**	**-0.4**	-0.1
C16	5.01	0.00	0.00	-0.01	0.00	59.1	0.1	**0.6**	**0.5**	0.1
C17A	3.14	0.00	0.00	-0.01	0.00	33.5	0	0.1	0.1	0
C17B	2.70	0.00	0.01	0.00	0.00	-	-	-	-	-
C18	5.29	0.00	0.01	0.00	0.00	111	-0.1	-0.1	-0.2	-0.1
C19	6.71	0.01	**0.10**	**0.07**	0.01	130.7	0	0.1	0	0
C20	-	-	-	-	-	167.2	0	0.1	0.1	0
C21	-	-	-	-	-	117.6	0	**-0.7**	**-0.6**	0
C22	-	-	-	-	-	157.7	0.1	**1.2**	**1**	0.2
C23	6.99	0.00	0.02	0.01	0.01	117.8	0	0.1	0.1	0.1
C24	7.38	0.00	-0.01	-0.01	-0.02	133.3	0	0.2	0.1	0
C25	6.91	0.00	-0.01	0.00	0.00	119.3	-0.3	-0.3	-0.1	-0.1

Table 2.1 *NMR comparison of synthesized diastereomers and isolated promysalin*

Key chemical shifts of protons located on C3, C7, C9, and C19 strongly indicate the (2*R*,8*R*,16*S*) as the proper stereochemical assignment. Unfortunately, with neither an optical rotation value or authentic sample, we hoped to confirm the assignment with replication of the biological assays presented in the isolation report.

2.3.2 Biological confirmation

In De Mot's initial report, they surveyed the biological activities of >100 bacterial strains through halo diffusion assays with cotreatment of the producing organism, noting qualitative inhibition.[16, 21] More specifically, they quantified the IC_{50} value for PA14, providing a strain with which we could directly compare. In accordance with their findings, compound **(−)-2.1a** possessed the most potent biological activity of the four compounds, with an IC_{50} value of 0.067 nM against PA14 (1.8 μM reported) and 4.1 μM against PAO1 (not reported). Compounds **2.1b−d** were each ∼10−100 times less effective against both strains (Table 2.2). This data nicely supported the NMR analysis presented in the previous section and led us to assign the natural stereochemistry as 2*R*,8*R*,16*S*.

	PAO1 IC_{50} **(μM)**	**PA14** IC_{50} **(μM)**
2.1a **2*R*,8*R***	4.1	0.067
2.1b **2*R*,8*S***	46	6.6
2.1c **2*S*,8*S***	90	22
2.1d **2*S*,8*R***	33	4.3

Table 2.2 *Biological activity of synthesized promysalin diastereomers against PA strains PAO1 and PA14*

2.3.3 Investigation of swarming phenotype

In addition to the inhibitory activity against PA, promysalin was also shown to induce swarming in the *Pseudomonas putida* (PP) producing strain, RW10S1. While performing our biological assays in the lab of Dr. Bettina Buttaro at Temple University, we had access to a variety of other PP strains which we utilized to explore whether promysalin was able to elicit a similar response. The strains tested were PP KT2440, a fluorescent pseudomonad, PP WCS358, PP OUS82, and a *P. fluorescens* strain WCS365. It was at this time we observed promysalin is indeed able to induce a similar swarming phenotype, seen both with the producing strain and in a variety of related strains. (Figure 2.5).

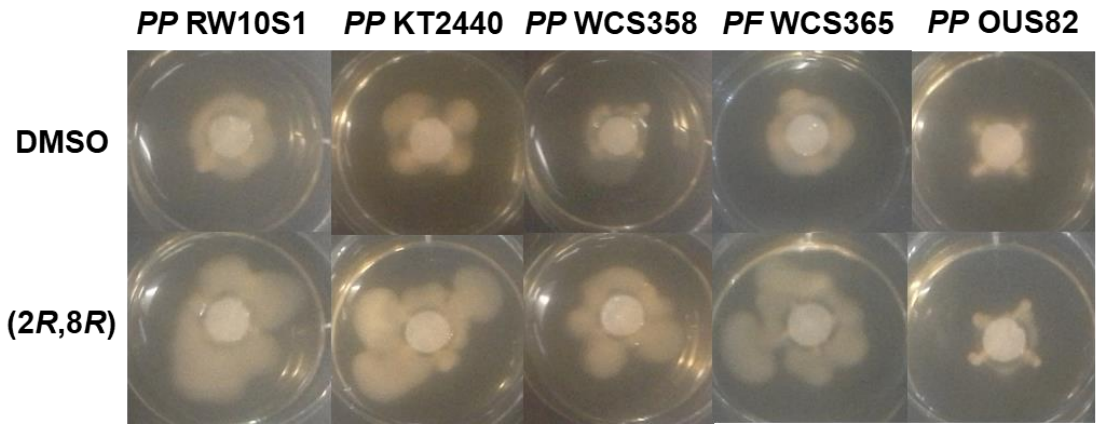

Figure 2.5 *Swarm plates 24 hours after treatment with 2.1a relative to the DMSO control*

One strain, however, did not display the swarming phenotype. This particular strain, PPOUS82, was isolated from oil contaminated soil and is characterized by its ability to degrade hydrocarbons. Considering the native environment of the strain and the alkyl chain on promysalin, we attributed this phenotype to promysalin digestion by the bacterial species.

Upon further analysis of the swarm plates we identified two previously unreported phenotypes for promysalin, discussed in the next section.

2.4 Discovery of new phenotypes

2.4.1 Fluorescent phenotype

While exploring the possibility of promysalin to elicit the swarming phenotype in other strains we serendipitously uncovered two new phenotypes. Two days following completion of the swarming assay, we observed one set of the plates had turned green, interestingly, the green pigment was not present in the wells that had been treated with **2.1a**. Intrigued by this we examined the plates with strain KT2440, the fluorescent strain, under UV light and observed that all wells were fluorescing except the ones treated with **2.1a** (Figure 2.6). Pyoverdine is a siderophore produced by a wide-range of Pseudomonads and is responsible for their fluorescent properties.[21] Furthermore, it has been shown that pyoverdine deficient mutants of P. syringae pv tabaci 6605 exhibit reduced virulence in host tobacco infection.[22] Recent reports have shown that strains deficient in pyoverdine have increased swarming and biosurfactant phenotypes, in accordance with observations reported herein.[23] While still unknown, the loss of green pigment observed for WCS358 may be indicating a similar mechanism. It has been characterized that the siderophore native to the strain PP WCS358 is pseudobactin 358 and is characterized by a green/yellow pigment.[24] Taken together, these results suggest that promysalin either directly or indirectly affects siderophore biosynthesis and/or transport in related strains.

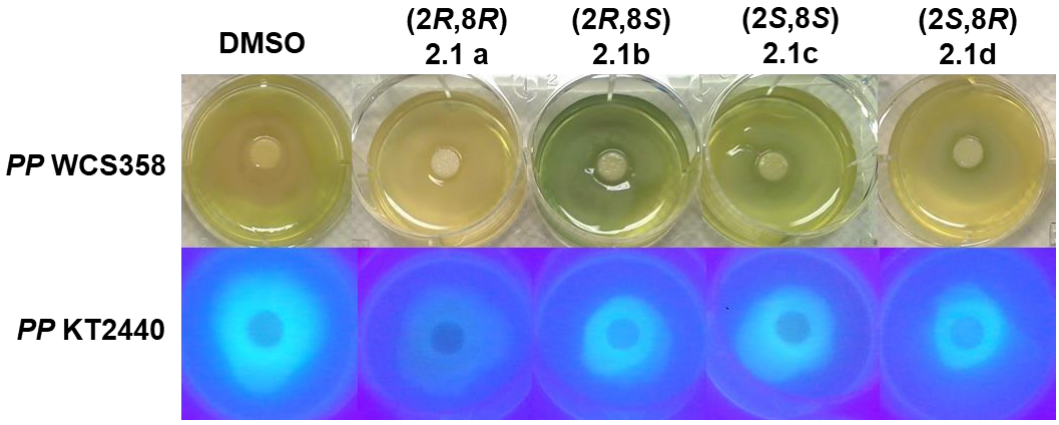

Figure 2.6 *Discovery of new phenotypes elicited by promysalin*

2.4.2 CAS Assay

In effort to support the previous findings that promysalin may be involved in siderophore biosynthesis or uptake mechanisms, we sought to determine if promysalin was able to chelate iron. A simple CAS assay, wherein any compound able to chelate iron will take the blue pigment out of the media, leaving an orange halo, allowed us to qualitatively determine any chelation ability. As shown in Figure 2.7, promysalin tested positive for Fe^{3+} chelation on CAS agar at concentrations ranging from 6 to 100 µM, albeit with reduced affinity when compared to the known iron chelator EDTA. Furthermore, Fe^{3+} chelation was confirmed down to 1 µM using the solution-based CAS assay (Figure 2.7, middle).[25]

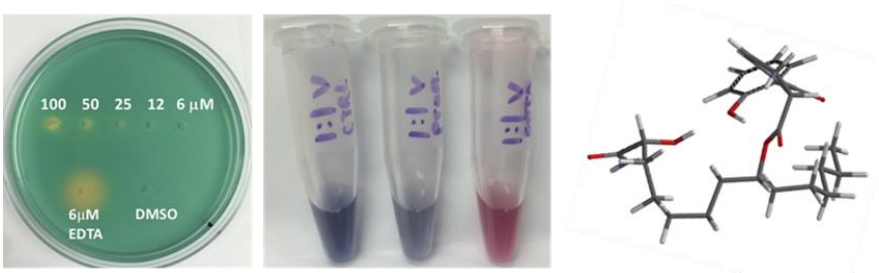

Figure 2.7 *(L) solid CAS assay. Promysalin is able to chelate iron on solid agar (Mid) Liquid CAS assay with (L-R) DMSO, Promysalin, and EDTA, (R) minimum energy confirmation of promysalin, computed*

With the CAS results in hand, we turned to the hypothesis that the highly selective biological activity could be a result of promysalin's ability to chelate iron. The result of the minimum energy conformation suggests an intermolecular hydrogen bond network, holding the molecule in a macrocyclic conformation, providing further evidence supporting this hypothesis (Figure 2.7, right). Taken in sum, these results would serve to support our future SAR investigation.

2.4.3 Conclusions

In conclusion, we reported the first stereo-controlled synthesis of the four diastereomers of the L-proline series of the natural product. This culminated in compound **(−)-2.1a**, which is identical to the isolated material as determined by ^{1}H NMR, ^{13}C NMR, and HRMS analyses, as the proposed structure of

promysalin. Furthermore, biological investigations support that the synthesized diastereomer is that of the natural product. Finally, we successfully confirmed initial reports that promysalin is able to induce swarming in the producing strain and demonstrate similar effects in related pseudomonas we well. The potential of promysalin to have activity related to iron is enticing, as it could provide a novel method to combat virulence both in agricultural and human health. The route presented allows the preparation of gram quantities of the natural product and a variety of structural analogs to better understand the specific target of promysalin, results of which will be discussed in the following section.

2.5 SAR investigation

2.5.1 Design of SAR study

Our synthetic strategy was designed such that not only would be have access to all four diastereomers in a highly convergent manner, but we would also have access to a wide variety of differentially functionalized structural analogs. At the onset of this endeavor, we sought answers to four key questions (Figure 2.9).

(1) Do biologically relevant (often acidic) conditions have a significance? Enamines are quite susceptible to acid hydrolysis, and we were curious about the stability of promysalin in low pH environments. This would encompass (a) Somewhat surprisingly, we (and others) noticed the instability of promysalin under mildly acidic conditions, which we were able to attribute to the formation of cyclized products **2.43a/b** (Scheme 2.6).[26] We wondered if this cyclization event was biologically relevant, whereby the compound would be dispensed by PP and would undergo cyclization in the known acidic environment present around PA.[27] (b) the potential for promysalin to be a "prodrug", whereby either the acid or diol

moiety is the active species; due to the acid labile ester linkage between the two - activated by either an enzyme (i.e., an esterase) unique to PA or the physical environment surrounding PA itself.

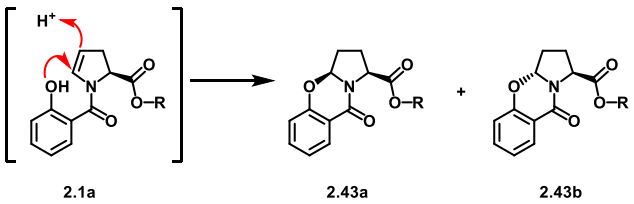

Scheme 2.6 *Acid sensitivity of promysalin*

(2) Is activity related to the ability to chelate iron? As mentioned earlier, Pseudomonads are well-known to produce a variety of siderophores in the rhizosphere. A cursory look at the literature reveals two specific siderophores with known salicylamide iron-binding motifs, reminiscent of promysalin: pyochelin and pseudomonine (Figure 2.8).[28-32] Additionally, ferrocin, another Pseudomonad siderophore, bearing a fatty acid moiety, has been shown to possess antimicrobial activity specifically against Gram-negative bacteria, and in particular PA.[33] Based on these findings, and in light of our bioactivity and modeling results, we speculated that promysalin might be capable of binding iron. This hypothesis was reinforced by earlier findings demonstrating that promysalin is capable of promoting swarming in PP and inhibiting pyoverdine production. One possible mechanism of action of promysalin is through the inhibition of siderophore transport pathways thereby severely limiting or inhibiting the organism's ability to acquire iron. This mechanism is especially intriguing when considering the specific activity of promysalin against PA14 as PA14 differs greatly from PAO1 in its acquisition of iron. Supporting our hypothesis, Rahme and co-workers have recently shown that ybtQ, a yersiniabactin ABC-transporter (yersiniabactin is a phenolate-thiazoline siderophore that shares structural features with pyochelin), is found in PA14 and is primarily responsible for its virulence.[34-35] Additionally, chemists, the Miller group in particular, have exploited siderophore transport pathways with great success using "sideromimetic" compounds in which antibiotic moieties are tethered to known siderophores for uptake.[36-37] Conversely, there are only a few reports of iron-binding natural products

which also possess antibacterial activity, though none of these have been conclusively shown to inhibit siderophore transport systems. However, it seems likely that this type of process is indeed taking place in the rhizosphere, resulting in narrow spectrum Gram-negative agents.

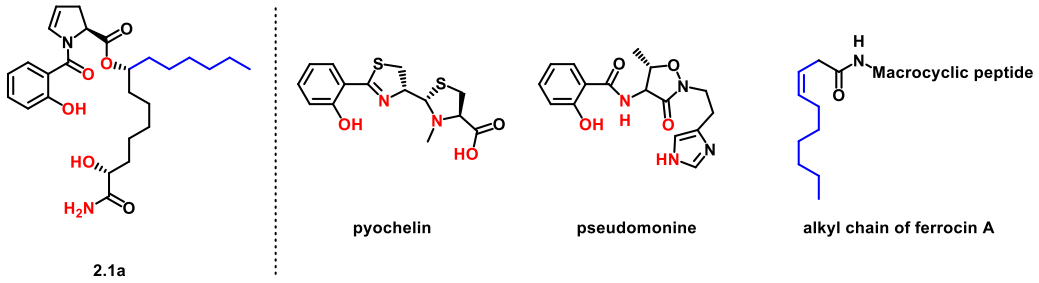

Figure 2.8 *Pseudomonad siderophores and amphiphilic antimicrobials*

(3) Are we able to simplify our synthetic route? Significant structural simplification is independently rationalized when considering each building block of the molecule. As such, each of these will be discussed in the following sections with each class of analog.

(4) Is promysalin's structure amenable to the addition of the diazirine-alkyne minimalist probe? At the onset of this project, we had the long-term goal of target identification investigations facilitated by AfBPP. However, use of promysalin as a probe necessitated the identification of which functional group on the molecule would be tolerant to modification, details of which will be discussed in the next section.

Our earlier synthetic studies hinted that the exact three-dimensional shape of the molecule was key to its biological activity, as we observed a 100−200-fold decrease in activity by altering either stereocenter on the alkyl fragment. To address these questions, we constructed a library of hypothesis-driven analogs via diverted total synthesis (DTS)[38] to build a structure−activity relationship (SAR) profile. DTS has proven useful in previous natural product mechanistic studies and, in some cases, has provided therapeutically useful analogs, exemplified by the development of fludelone.[39-40] It should be noted that the analogs accessed from DTS presented here are inaccessible by enzymatic or chemical manipulation of the natural product directly, thus showcasing the power of organic synthesis.

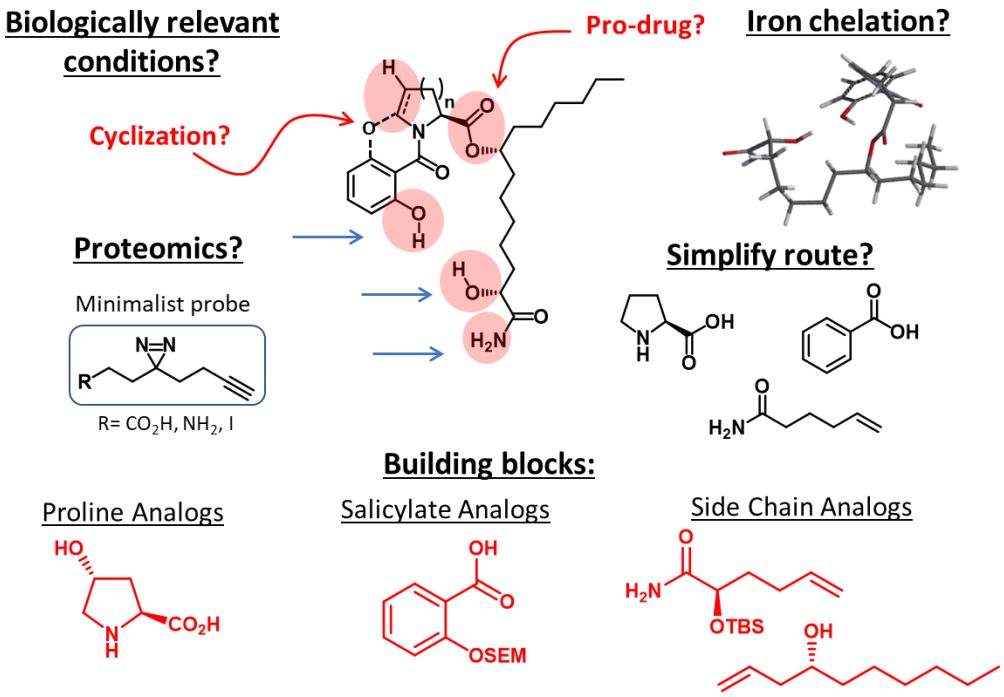

Figure 2.9 *Key questions surrounding the SAR investigation*

2.5.2 Proline analogs

Due to its lack of prevalence in natural products, we speculated the enamide moiety of promysalin was relevant for the bioactivity wherein it could covalently interact with its biological target; therefore, we postulated that any modification would render the molecule inactive. The first analog was the hydroxy proline derivative (Scheme 2.8). Starting from intermediate **(−)-2.36**, we protected the free alcohol with TBSCl, providing proline methyl ester **(−)-2.44**. Following TBS protection, the methyl ester was hydrolyzed to the corresponding acid. Acid, **(−)-2.45** was subject to EDC esterification and deprotection in accordance to our published route, which provided hydroxy proline analog, **(−)-2.47**.

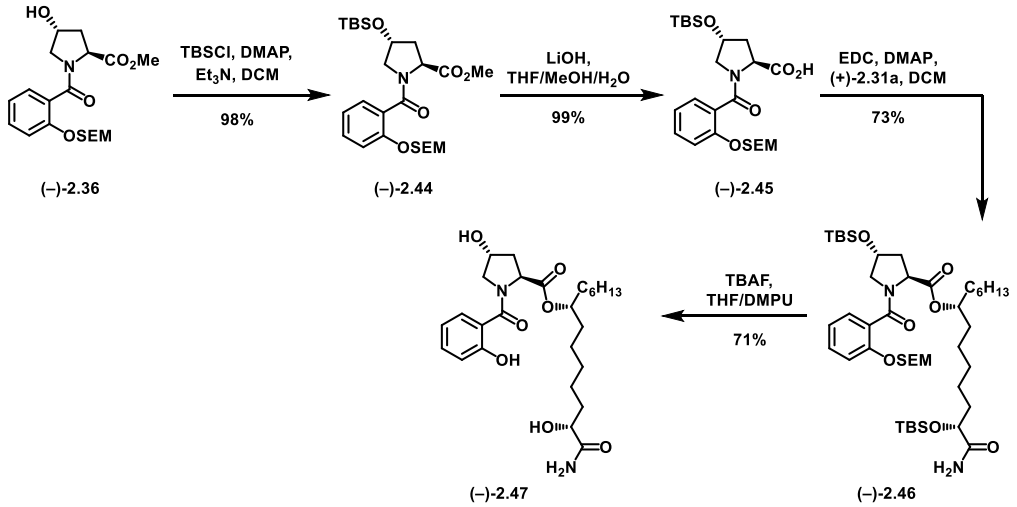

Scheme 2.8 *Hydroxy-proline analog*

We next exploited the inherent reactivity of our triflate intermediate via Pd-mediated coupling reactions to provide access to two functionalized enamide analogs. First, starting from enol-triflate intermediate, **(−)-2.38**, we performed a Suzuki cross-coupling with methylboronic acid. Hydrolysis of the methyl ester **(−)-2.48**, furnished acid **(−)-2.49**, which was esterified using EDC and deprotected following our general procedure affording methyldehydroproline analog, **(−)-2.51** (Scheme 2.7).

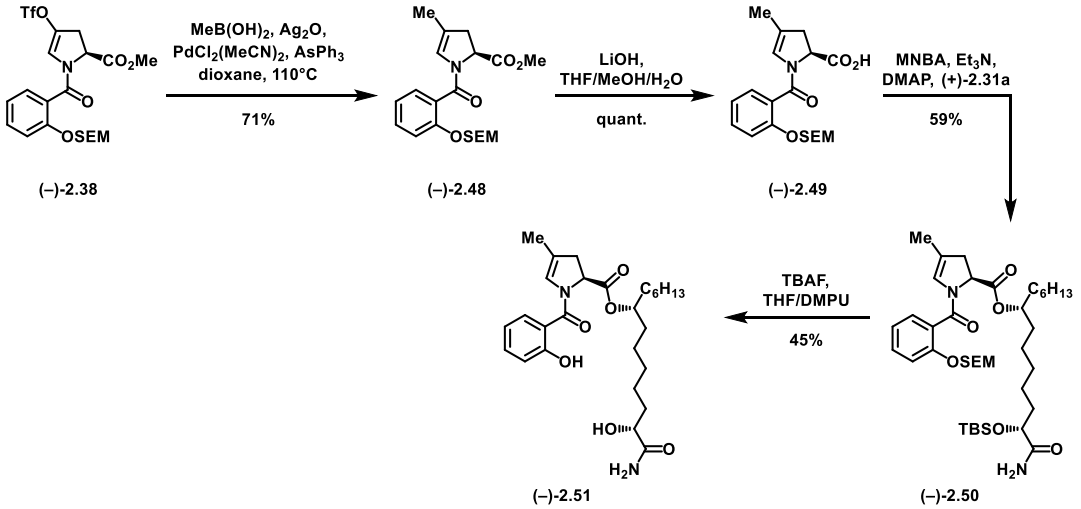

Scheme 2.7 *Synthesis of 4-methyldehydroproline analog*

Next, further taking advantage of our triflate intermediate, **(−)-2.38**, we synthesized stannane **(−)-2.52**. Following stannylation, treatment with selectfluor provided 4-flurorodehydroproline methyl ester **(−)-2.54**. Hydrolysis, esterification with intermediate **(+)-2.31a**, and deprotection with TBAF/DMPU as previously described furnished fluro-analog, **(+)-2.56** (Scheme 2.9).

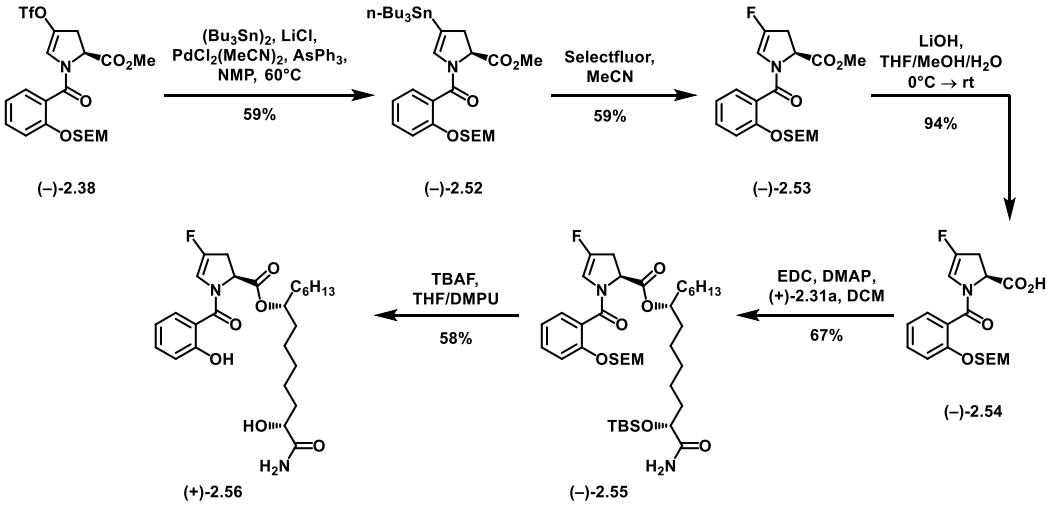

Scheme 2.9 *Synthesis of 4-flurordehydroproline analog*

The final two proline analogs were prepared in an identical fashion, starting from the methyl ester of proline (**(−)-2.57**) or piperidine (**(−)-2.58**) as shown in Scheme 2.10. Amidation with MOM-protected acid, **2.59** and HATU provided amides **(−)-2.60** and **(−)-2.61**. Subsequent hydrolysis and esterification yielded the protected analogs **(−)-2.64** and **(−)-2.65**, which were deprotected upon treatment with acetyl chloride. Deprotection of analogs **(−)-2.66** and **(−)-2.67** were much simpler as both analogs lack the delicate enamide functionality, allowing acid-catalyzed deprotection conditions.

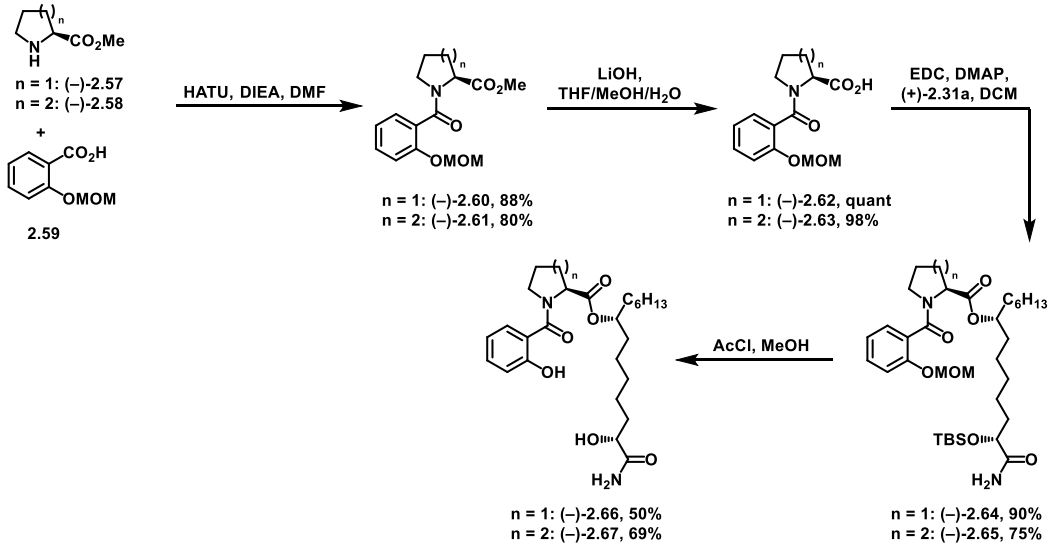

Scheme 2.10 *Synthesis of proline and piperidine analogs*

In summary, we utilized DTS to access five specific dehydroproline derivatives (Figure 2.10). The synthesis of the proline, piperidine, and hydroxyproline analogs was straightforward using standard coupling reactions and protecting group manipulations whereas we were able to take advantage of our triflate intermediate for the fluro- and methyl analogs. Three of the analogs (proline (**(−)-2.66**), piperidine (**(−)-2.67**), and hydroxyproline (**(−)-2.47**)) contain route simplification – whereas we alleviate the installation of the enamide, lowering the overall step count and eliminating the formation of hemiacetal intermediate **(−)-2.42**.

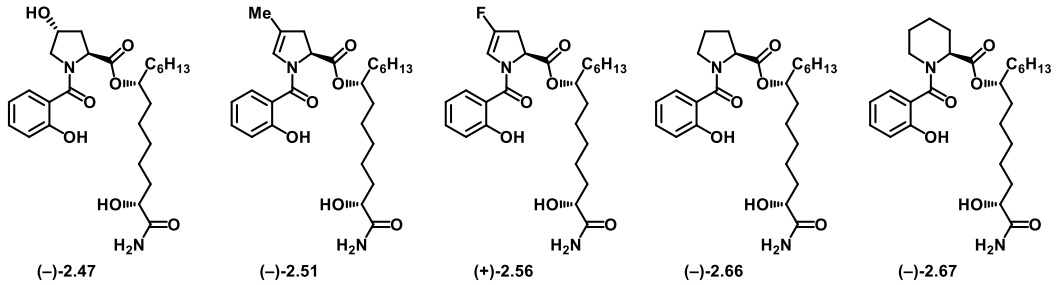

Figure 2.10 *Structure of all dehydroproline analogs*

2.5.3 Salicylate analogs

Preliminary computational models of promysalin highlighted an intricate intramolecular hydrogen-bonding network resulting in a rigidified molecular framework. We hypothesized that this network, composed of the phenol, hydroxyl, and ester moieties, were therefore critical for activity. To test this hypothesis, we designed analogs varying these key functionalities. The salicylate fragment was systematically altered in three specific ways: (1) the position and presence of the phenol; (2) the substitution of the phenol; or (3) by increasing the electron density within the ring.

This effort began with SEM protection of two regioisomers of methyl salicylate **2.68** and **2.69** (Scheme 2.11). Following hydrolysis of the methyl esters, the unstable acids were used immediately in the subsequent HATU mediated amidation. The rest of the sequence followed our published route, including oxidation, formation of the enol triflate, reduction of the triflate, hydrolysis, esterification, and deprotection forming analogs **(−)-2.84** and **(−)-2.85**. It should be noted, at this point many of the esterifications used

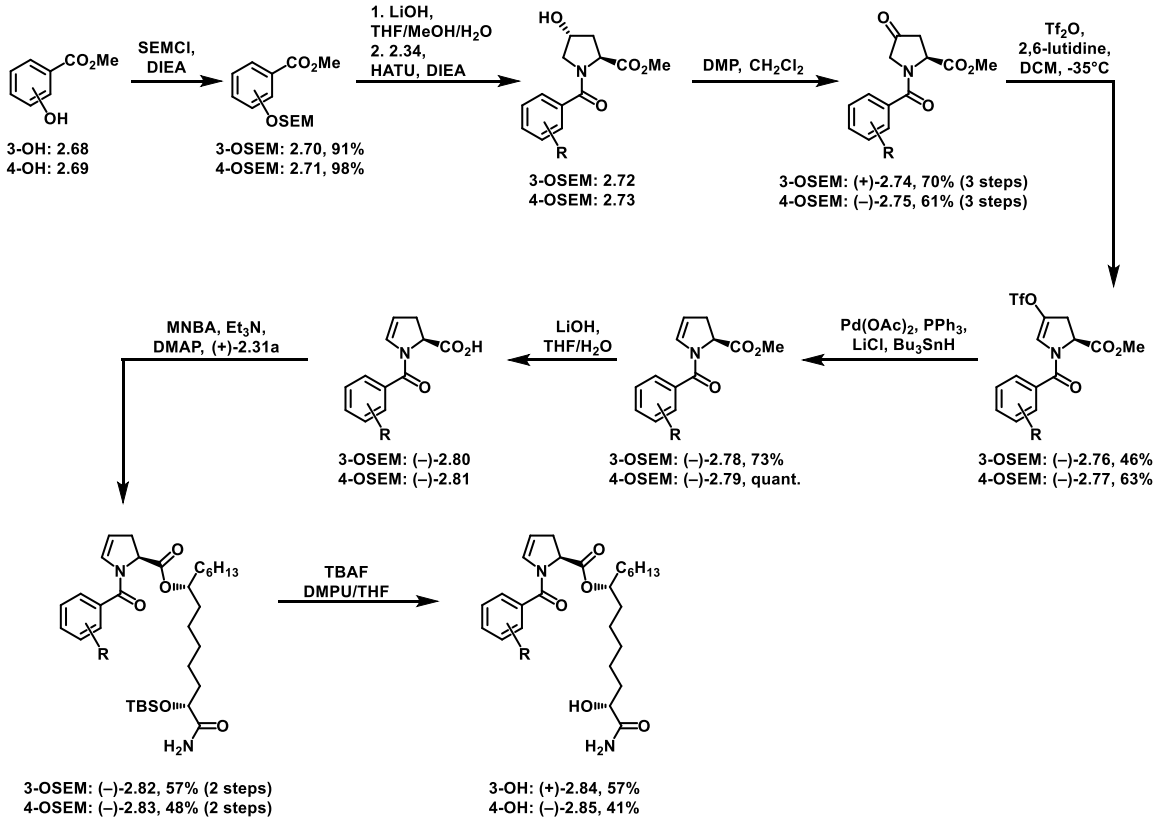

Scheme 2.11 *Synthesis of salicylate regioisomers.*

Shiina reagent, (methyl nitro benzoic anhydride, MNBA) instead of EDC, as our EDC yields were inexplicably low.

Next, we tackled three analogs that investigated the presence of a phenol, as well as the substitution. These analogs would eliminate the necessity of a protecting group on the phenol, allowing for a shorter synthesis and removal of deprotection issues. Starting with Scheme 2.12, intermediate **2.86** is a known compound formed from the amidation of tri-methoxy substituted acid chloride. Once oxidized, intermediate **(+)-2.87** was carried through analogously to our synthetic route. However, in this case, ester **(−)-2.91** could be deprotected with TBAF, without DMPU as a cosolvent due to the absent SEM-ether, yielding analog **(−)-2.92**.

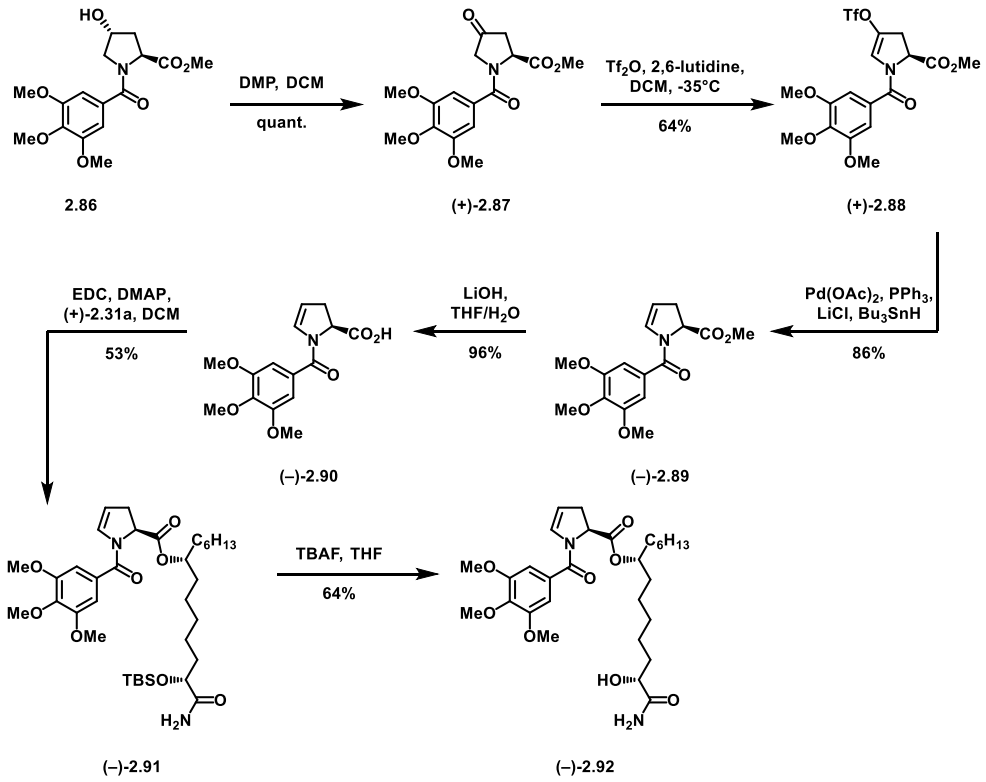

Scheme 2.12 *Synthesis of tri-methoxy analog*

Next, analog **(−)-2.98** was synthesized in an analogous fashion, starting again from an acid chloride (full details in Scheme 2.13). Finally, analog **(−)-2.103**, the methyl ether derivative, was synthesized by a premature deprotection of the SEM ether (Scheme 2.14. Intermediate **(−)-2.99** could be treated with TMS-diazomethane to afford the methyl capped **(−)-2.100**. Following installation of the methyl, the remainder of the synthesis is as previously disclosed, with the final step again eliminating DMPU as a co-solvent and any side products formed during deprotection.

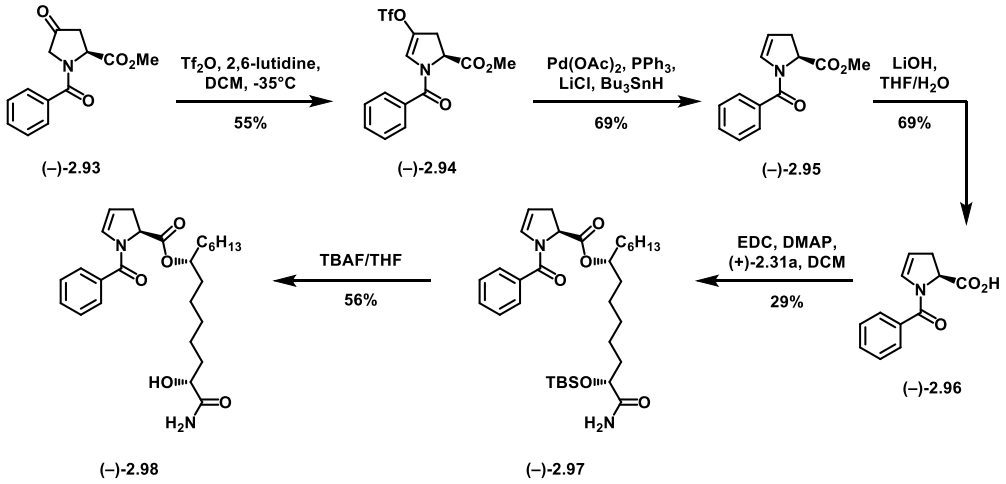

Scheme 2.13 *Synthesis of benzyl analog*

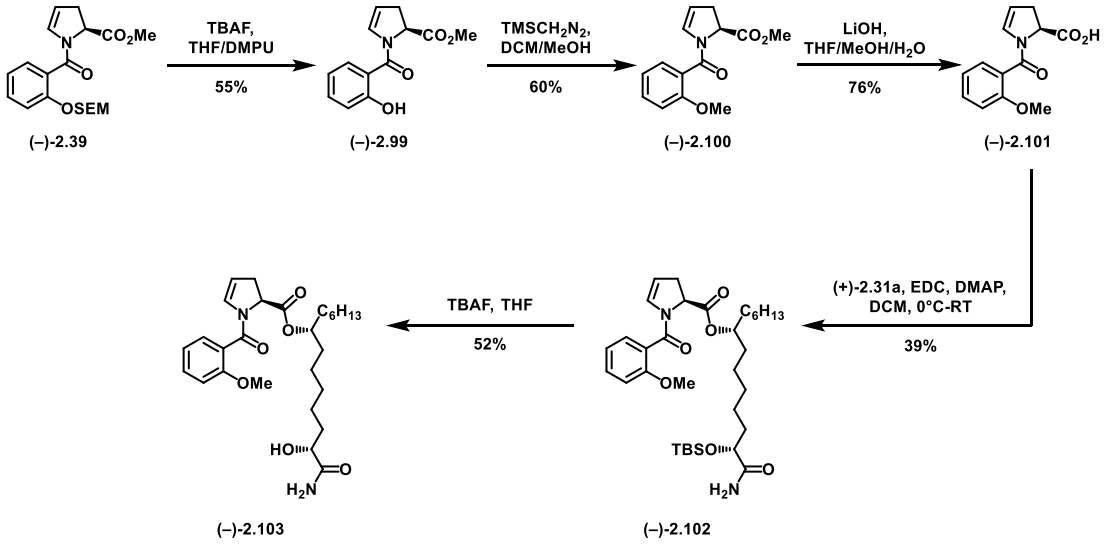

Scheme 2.14 *Synthesis of phenol methyl ether*

Unfortunately, analog **(−)-2.114** was not our originally intended product, we had hoped to synthesize the 2,6-bisphenol however synthesis was not as straightforward as we had originally intended. Starting from bisphenol **2.104** we were able to obtain ester **(−)-2.111** without any issues. However, when treated with TBAF and THF/DMPU, we only successfully removed one of the SEM ethers and TBS. Alternative conditions such as $MgBr_2$ led to recovery of starting material or decomposition. In efforts to salvage this analog, we capped the deprotected phenol with a methyl ether using TMS-diazomethane (**(−)-2.113**). Following installation of the methyl, we subjected the material to an additional round of TBAF and

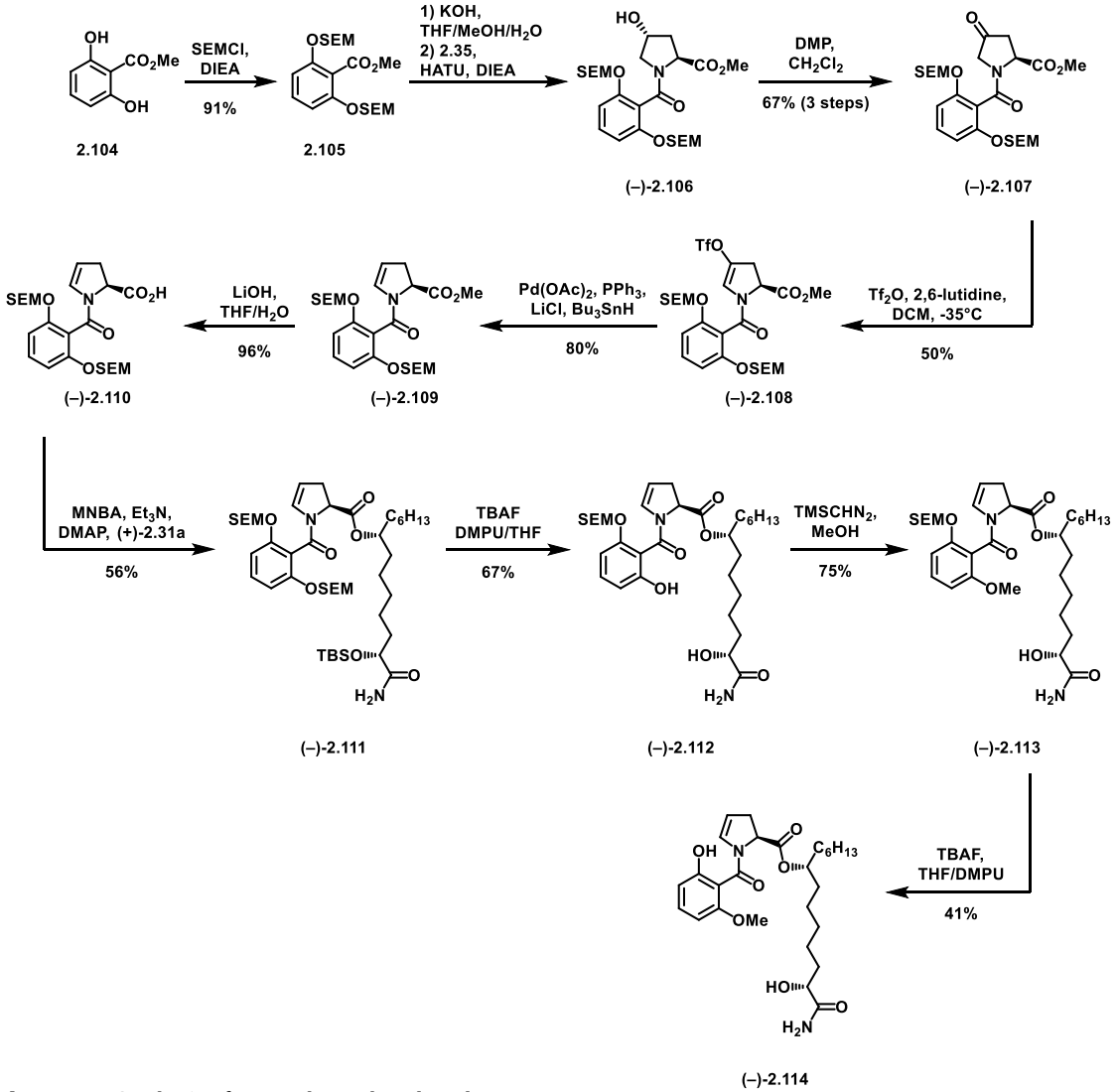

Scheme 2.15 *Synthesis of 2,6-methoxy phenol analog*

THF/DMPU, this time removing the second SEM ether and furnishing analog **(−)-2.114**. Full synthetic details can be found in Scheme 2.15.

The final salicylate analog was unable to be synthesized following our established route. Analog **(−)-2.122**, Scheme 2.16, started with the amidation of 2-nitrobenzoyl chloride (**2.116**) and TBS protected pyrrolidone derivative (**2.115**). Amide, **(−)-2.117**, was treated with Comins' reagent to form the triflate and subsequently reduced to form intermediate **(−)-2.118**. Treatment with CSA removed the silyl protecting group to the free primary alcohol, **(−)-2.121**, which was subjected to oxidation, yielding acid **(−)-2.122**. Shiina esterification provided the protected analog, **(−)-2.121** which was treated with acetyl chloride to furnish analog **(−)-2.122**.

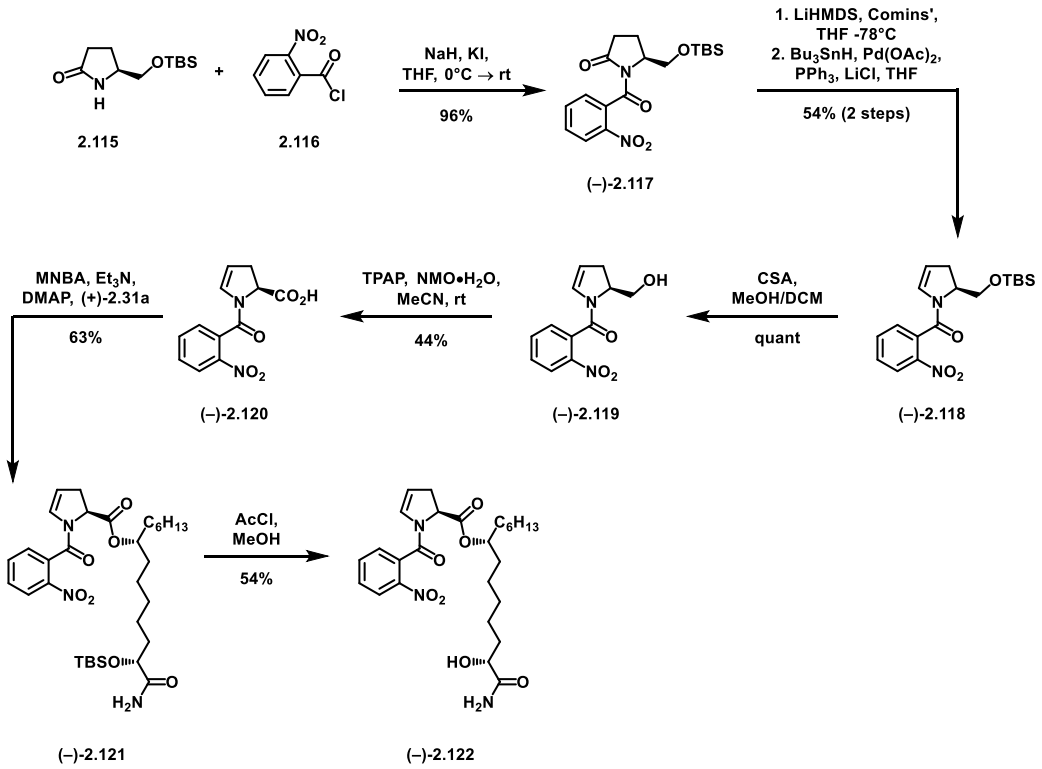

Scheme 2.16 *Synthesis of nitro analog*

The full list of salicylate analogs is shown in Figure 2.11.

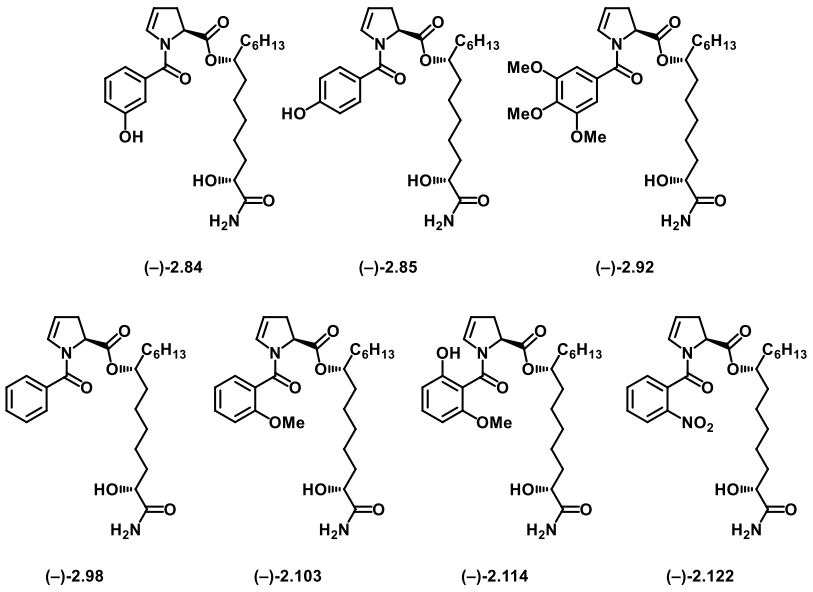

Figure 2.11 *Salicylate analogs*

2.5.4 Side chain analogs

As our side chain bears minimal structural complexity, our SAR-space was limited. Nevertheless, we were able to synthesize an analog from each intermediate in our forward synthetic route We began by investigating the importance of the side chain alcohol. Not only would we remove several steps, as this has to be made in an asymmetric fashion, but it is integral to the proposed intramolecular hydrogen bond network. Synthesis of **(−)-2.127** was relatively straightforward and began with hexenoic acid, **2.19**. In lieu of installation of Evan's chiral oxazolidinone, we treated the acid with isobutyl chloroformate and ammonium hydroxide and obtain amide **2.123**. Following amidation, we reacted the corresponding product with alcohol, **(+)-2.27** in the presence of modified Grubb's catalyst, **C711**, to form alkene **(−)-2.124**. The alkene was then carried through as previously disclosed to obtain deoxy analog **(−)-2.127**, shown in Scheme 2.17.

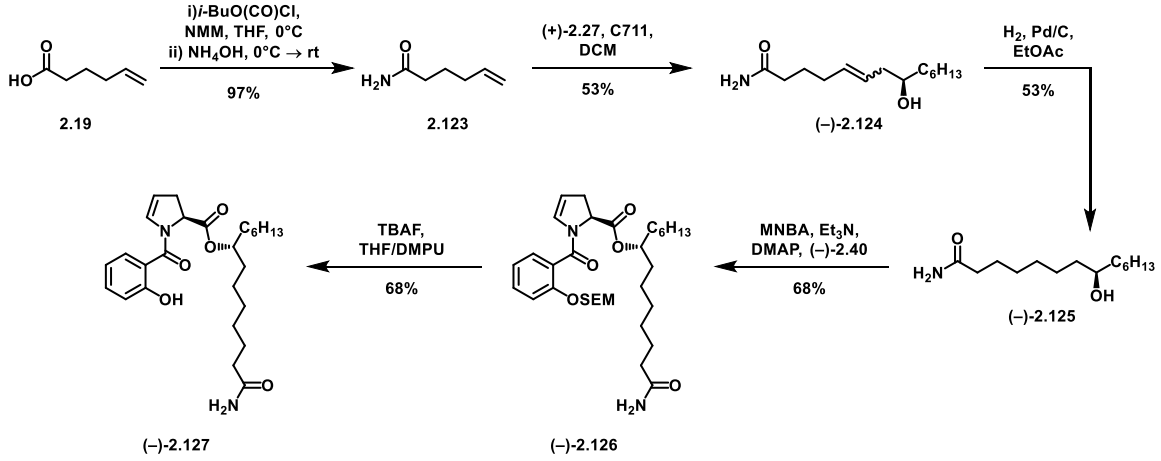

Scheme 2.17 *Synthesis of deoxy analog*

Alternatively, following installation of the chiral auxiliary, intermediate **(−)-2.23** was capped as the methyl ether, **(−)-2.128**, by treatment with Meerwein's reagent and Proton Sponge (Scheme 2.18). From here each the remainder of the synthesis of the analog followed our published route, yielding methyl ether analog, **(−)-2.133**.

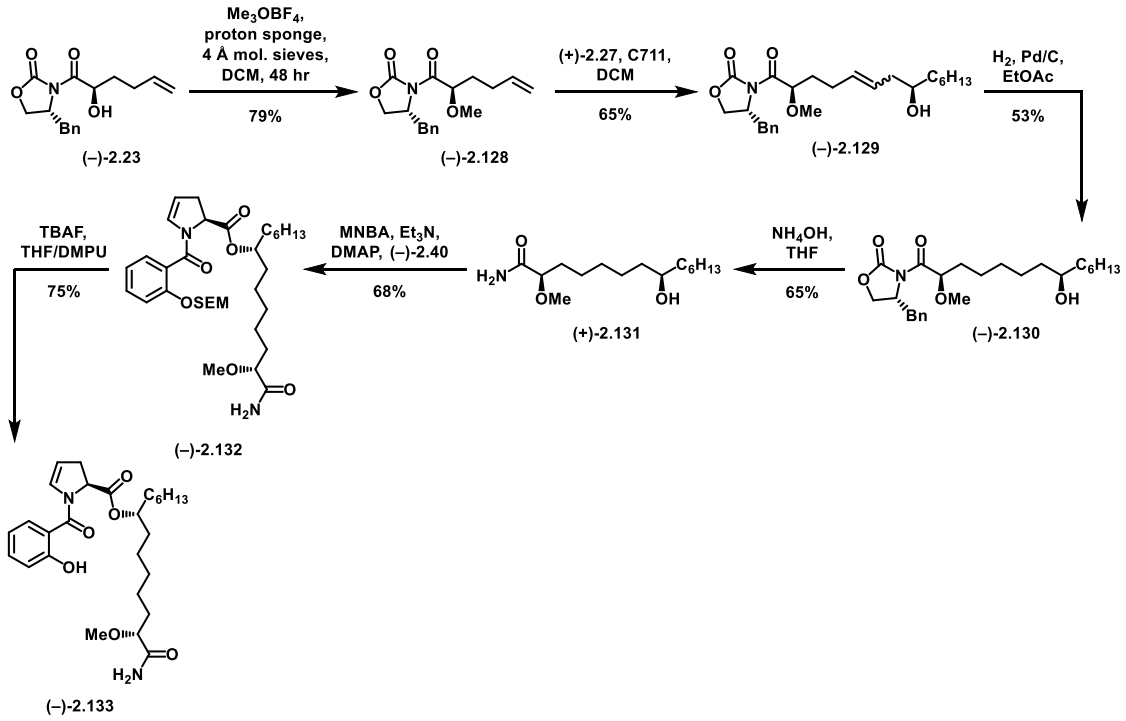

Scheme 2.18 *Synthesis of side chain methyl ether analog*

In efforts to investigate the potential instability of the ester linkage, we sought installation of a non-hydrolysable amide linker in its place (Scheme 2.19). Starting from the (2*R*,8*S*) alkene intermediate, **2.29**, a Mitsunobu reactiod provided azide **(−)-2.134**. Following installation of the azide, hydrogenation of both the alkene and azide gave access to intermediate **(−)-2.135**. Subsequent ammonolysis, amidation, and deprotection yielded amide analog, **(−)-2.138**.

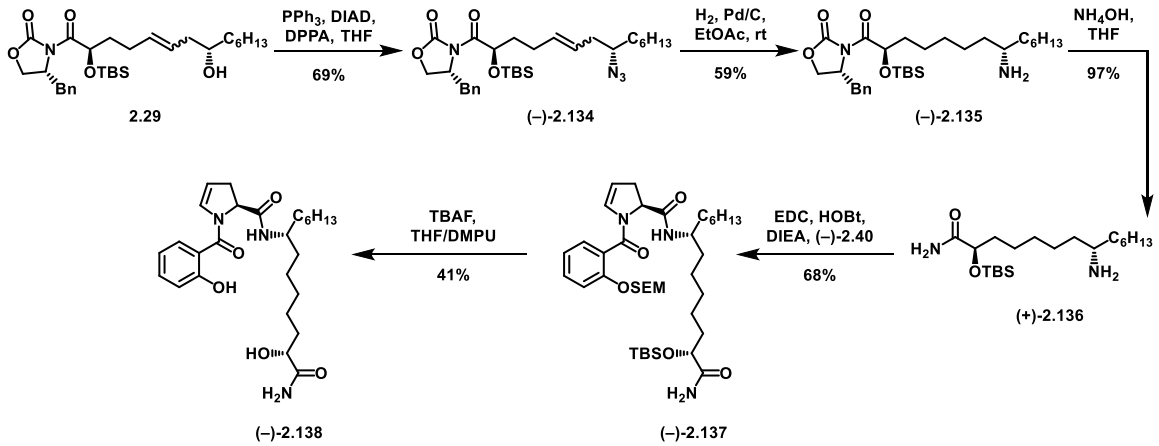

Scheme 2.19 *Synthesis of amide analog*

An analog designed to increase rigidity of the side chain and potentially stabilize the active conformation, retains the alkene installed from cross metathesis. Analog **(−)-2.141** was synthesized in an identical manner as the natural product, with the exception of the hydrogenation step (Scheme 2.20).

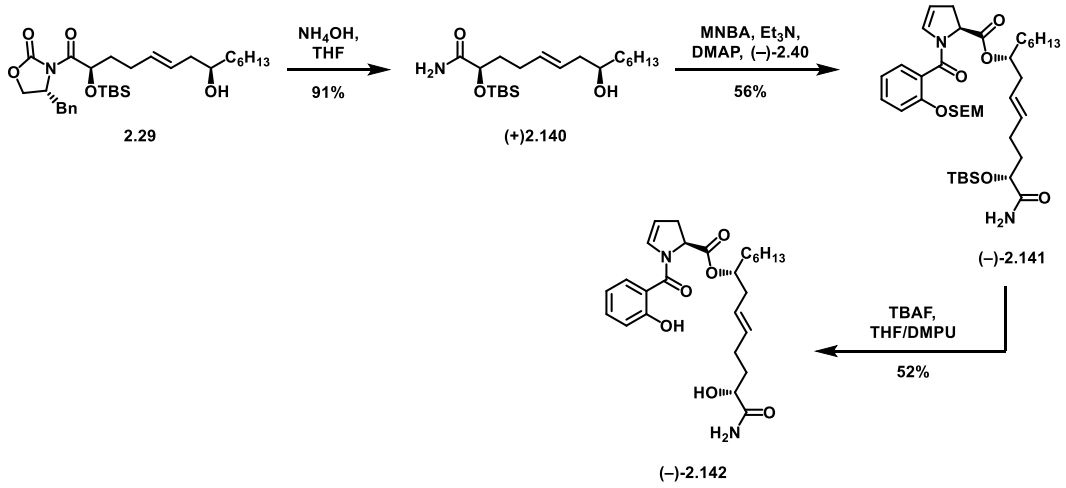

Scheme 2.20 *Synthesis of alkene analog*

A final analog was hypothesized such that we could explore the effect on activity from alkylating the amide (Scheme 2.21). Starting from intermediate **2.30** we displaced Evan's oxazolidinone with propargyl amine. Intermediate **(+)-2.142** was esterified with Shiina reagent to afford ester **(−)-2.143**. The ester was promptly deprotected with TBAF and THF/DMPU yielding analog **(−)-2.144**.

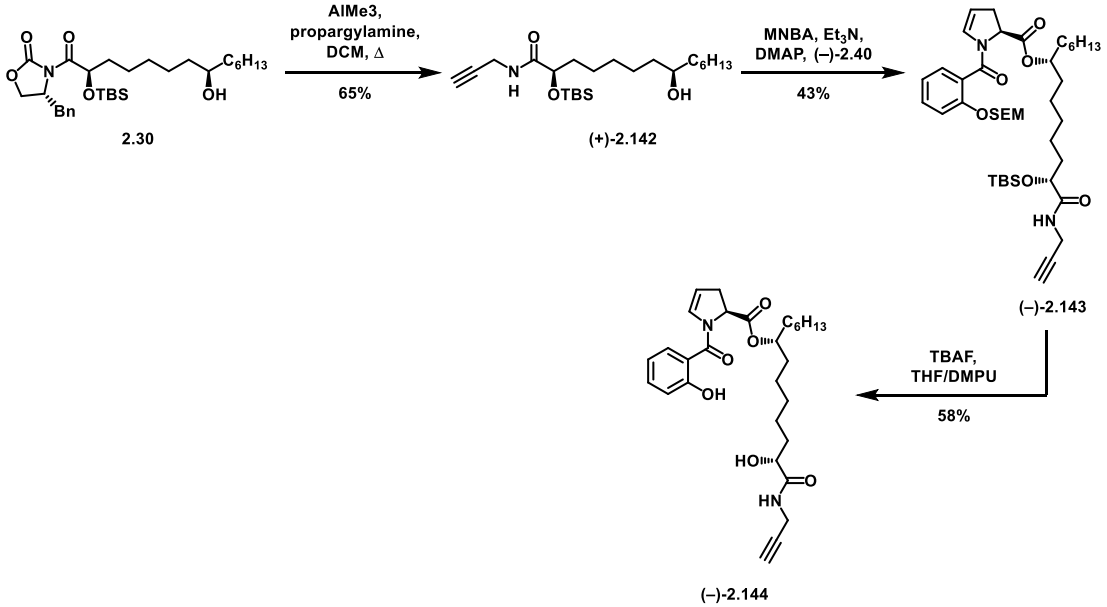

Scheme 2.21 *Synthesis of propargyl analog*

All side chain analogs are shown in Figure 2.12.

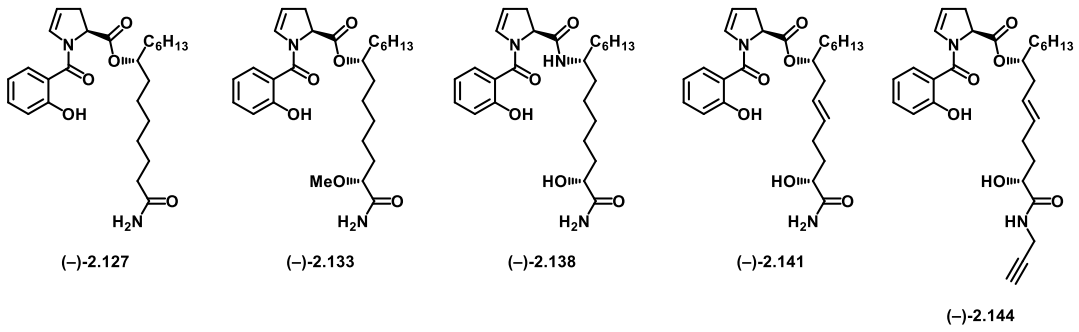

Figure 2.12 *Side chain analogs*

2.5.5 Biologically relevant analogs

In addition to the analogs stemming from each of the three building blocks, we also synthesized analogs that could have been affected by biological conditions. It is well-known that bacteria possess enzymes capable of hydrolyzing esters. Therefore, we questioned if the hydrolyzed fragments **(−)-2.99 and (+)-2.145** would be active, attributing the activity to a pro-drug like mechanism. We synthesized methyl ester **(−)-2.99** in lieu of the acid, for cell permeability purposes. Additionally, it was mentioned previously that we observed cyclization of the natural product under acidic conditions, we wondered if this cyclization event was biologically relevant, whereby the compound would be dispensed by PP and would undergo cyclization in the known acidic environment present around PA.[27]. Shown in Scheme 2.22 are the four compounds synthesized for investigation.

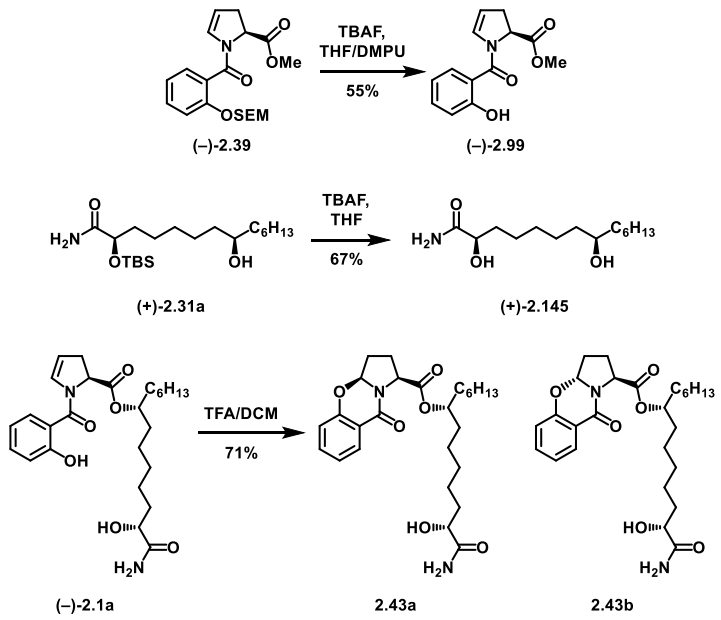

Scheme 2.22 *Analogs investigating the effect of biological conditions*

2.5.6 Biological Results

With a library of 17 analogs in hand (Figure 2.13), we evaluated all of the compounds for inhibitory activity against *P. aeruginosa* strains PAO1 and PA14. The data for the active analogs (IC_{50} < 250 μM) are shown in Table 2.3 along with the inhibitory data for the less potent diastereomers of promysalin (for numbering, see Figure 2.13). The inhibition data supported our initial hypothesis that the conformation of promysalin is exquisitely linked to its inhibition of PA. Of our modifications to the proline structure, fluorination (**(+)-2.56**) - being the smallest steric perturbation - was the only compound with equipotency to that of promysalin. Methylation (**(–)-2.51**) was slightly tolerated, while the hydroxyproline (**(–)-2.47**) and piperidine (**(–)-2.67**) derivatives were inactive. To our surprise, proline derivative **(–)-2.66** retained modest activity, which may hint at an inhibitory mechanism that involves both structural recognition and covalent binding. The structure of the salicylate moiety was largely unforgiving in terms of the position (**(–)-2.84** and **(–)-2.85**), substitution (**(–)-2.122**), or exclusion of the phenol (**(–)-2.98**). In addition, adding

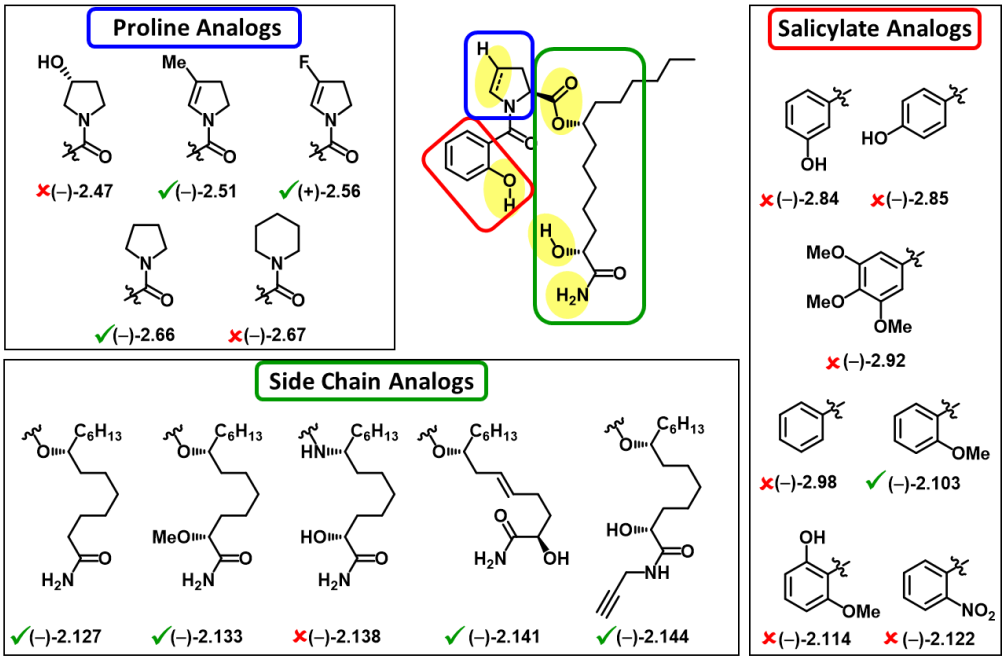

Figure 2.13 *Library of analogs – inactive analogs are marked with red x*

	PA14	PAO1
2.1a (2*R*, 8*R*)	0.067	4.1
2.1a (2*R*, 8*R*)	6.6	46
2.1a (2*R*, 8*R*)	22	90
2.1a (2*R*, 8*R*)	4.3	33
2.66	28	111
2.56	0.019	7.7
2.51	12	32
2.103	6.7	57
2.127	0.035	5.8
2.133	11	38
2.141	0.067	8.3
2.144	0.222	N.D.

Table 2.3 *IC_{50} values for active analogs. All values in μM.*

methoxy substituents in the presence (**(–)-2.114**) or absence (**(–)-2.92**) of the o-phenol was not tolerated. The only active salicylate analog was the methyl ether (**(–)-2.103**), albeit with an order of magnitude less potency. In contrast, the side chain analogs all retained some, if not all, activity, with the one exception being the amide (**(–)-2.138**). Methylation of the hydroxyl group (**(–)-2.133**) resulted in a decrease in potency on par with the methylated phenol (**(–)-2.103**). Rigidifying the side chain by including the alkene (**(–)-2.141**) led to an equipotent analog. However, when the secondary alcohol was removed, providing compound **(–)-2.127**, biological activity was fully retained. At first this result was particularly surprising, as we postulated that the alcohol was integral to the hydrogen-bonding network, as evidenced by the difference in activity between **2.1a** and **2.1b/c** (a 10−100-fold decrease in potency). However, when considering our proposed macrocyclic structure (shown to the right of Table 2.3) the implications of epimerization at a hydroxyl group can lead to drastic bond angle changes; in contrast, **(–)-2.127** can adopt a similar conformation simply by substituting the amide carbonyl as a Lewis base in place of the alcohol. Methyl ester **2.99** and diol **2.146** were both inactive up to concentrations of 250 μM, as were both cyclized derivatives **2.43a/b**. Additionally, we have also recently shown that appending the acid fragment of promysalin to another myristate-derived natural product, lyngbic acid, yielded compounds devoid of activity against PA.[41] Taken in sum, it appears that the cyclization and hydrolysis reactions are synthetic artifacts and not biologically relevant.

In reference to our original questions, we have gained insight towards how promysalin is able to elicit such specific activity. First, as previously mentioned, there is no pro-drug mechanism facilitating activity. Second, as far as iron chelating mechanism, we have demonstrated that the macrocyclic confirmation can be supported by our SAR results and future work (*vide infra*) will further interrogate this possibility. Third, for salicylate and proline we are unable to simplify our synthetic route and retain sufficient biological activity. However, for our side chain, we surprisingly observe retention of activity with removal of the alcohol (**2.127**) requiring two less overall steps. Additionally, it is more atom-economical than that of promysalin, as the use of a protecting group and chiral auxiliary is avoided. Finally, our SAR was able to indicate appropriate probe placement, which will be discussed in detail in section 2.7.

2.5.7 Conclusions

In conclusion, we have leveraged the power of DTS to access a 16-membered library of rationally designed synthetic promysalin analogs. This structural diversity, which is inaccessible by semi synthesis, has shed light on the key structural features responsible for bioactivity and highlights the importance of the key functionalities within the hydrogen-bonding network (which are presumably also critical for binding iron). The next section(s) will be focused on the unequivocal identification of its biological target.

2.6 Investigation of iron relevance to activity

Previous reports have demonstrated that the inhibitory activity of sideromycins is correlated to iron-concentration as they rely on a chelation strategy to penetrate bacterial cells.[42] In an elegant display of chemical creativity, the Miller group used these molecules as inspiration and developed a second-generation of synthetic sideromycins, whereby established antibiotics were covalently tethered to known siderophores

effectively creating a “Trojan Horse” strategy that was remarkably successful.[43-44] This approach is best exemplified by BAL30072, a novel siderophore-sulfactam conjugate that entered Phase 1 clinical trials.[45]

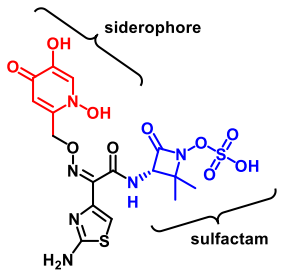

BAL30072

Figure 2.14 *Sideromycin BAL30072*

Similarly, these molecules also rely on iron-concentration and their activity can be enhanced by either the introduction of strong iron-chelators or prior removal of iron from the media. Based on this knowledge we sought to probe the bioactivity of promysalin against PA strains PAO1 and PA14 over a range of iron concentrations. Under iron-limited conditions, we expected transcriptional up-regulation of iron transport systems would facilitate the diffusion of promysalin into the cell and consequently increase its potency akin to sideromycins. However, our studies revealed that there was no identifiable effect of the available iron on efficacy as indicated by IC_{50} values, suggesting that iron chelation is coincidental and separate from antibiotic activity.

Previous work investigating the mechanism of action of BAL30072 identified the iron receptor PiuA as the active transporter responsible for the uptake of the molecule into PA.[46] PiuA is a member of the TonB dependent transporter (TBT) family, which are membrane-bound proteins responsible for the active transport of siderophores by means of the proton motive force.[47] Transcription of such systems is up-regulated in response to stress and conversely down-regulated when an equilibrium is met, as excess iron is toxic.[48] Previous findings have shown that TBTs regulate pyoverdine production and also vary widely between *Pseudomonads*, which could potentially explain our prior results. Initially, we investigated the

ability of promysalin to form an Fe^{3+}-bound complex with a variety of iron sources ($Fe(acac)_3$, $(NH_4)_5[Fe(C_6H_4O_7)_2]$, and $FeCl_3$) by UV-Visible spectroscopy. In all instances, we did not observe the characteristic Fe^{3+}-siderophore complex at ~500 nm seen in other systems like enterobactin (representative depiction, $Fe(acac)_3$ shown in Figure 2.15). Recently, the lab of our collaborator solved the crystal structure of PiuA and revealed the putative binding site of BAL30072.[49] To further confirm that promysalin was not interacting via the PiuA system our collaborators utilized isothermal microcalorimetry titration experiments to determine the extent at which the natural product binds. However, these studies again refuted our earlier hypothesis as no appreciable interaction was observed (data not shown). Taken in sum, these findings demonstrate that although promysalin is capable of binding iron, it does not appear to be acting as a viable siderophore and/or using siderophore transport channels to elicit its response. (Assays run by Lucielle Moynie)

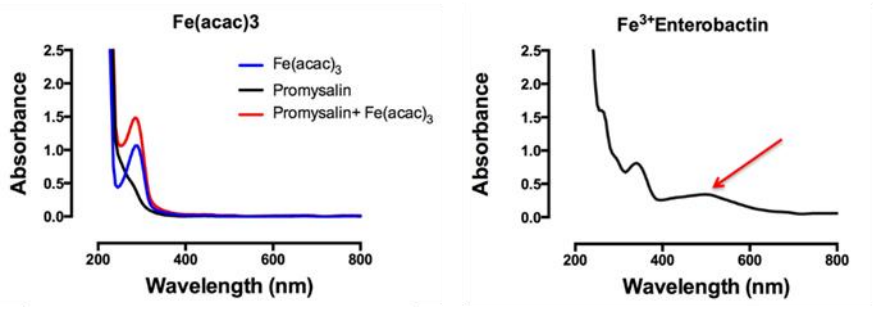

Figure 2.15 *UV-Vis spectra of attempts to complex promysalin with Fe^{3+}. Enterobactin shown for comparison*

With our initial siderophore-based hypothesis disproven, we next planned to implement affinity-based protein profiling (AfBPP) to identify likely candidates.

2.7 Affinity-based protein profiling

2.7.1 Intro

Affinity-based protein profiling (AfBPP) is a technique that has been utilized for about a decade for studying the proteome. We sought this technique for its use in target identification of natural products

and small molecules. Foundationally, AfBPP relies on active-site directed covalent target engagement which allows for subsequent identification of a bound protein. This serves as an alternative to historically successful drug design methodologies (i.e. target based screens), because chemical proteomics requires use of the molecule of interest as a probe, allowing for its innate activity to shed light on its target/mechanism. This is demonstrated pictorially in Figure 2.16 where (from left to right) we have the proteome of interest being treated with the small molecule or natural product that will engage its target. This interaction is the foundational step of AfBPP as the assay is activity driven. Following interaction with the target, various analytical techniques will allow for the identification of the engaged target.

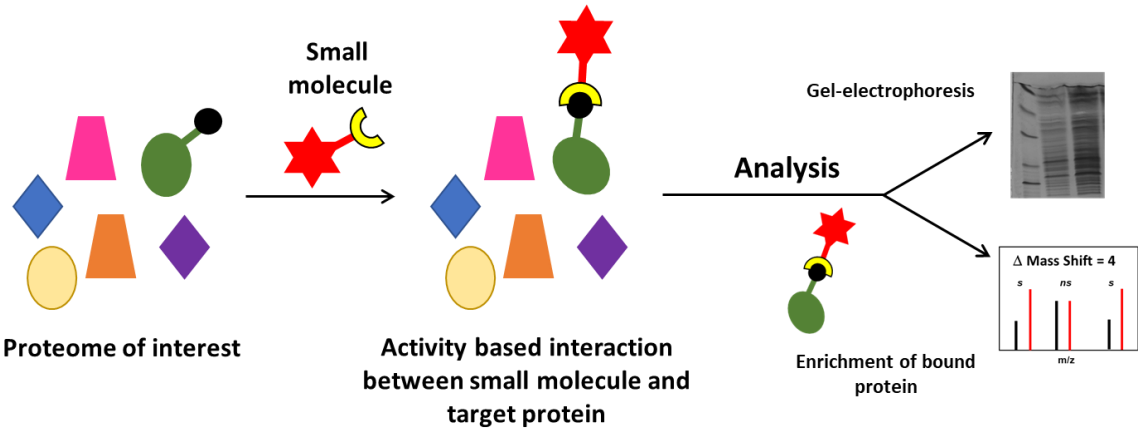

Figure 2.16 *General overview of ABPP*

Often, two key modifications (or incorporations) to the structure must be made for direct use of the small molecule as a probe. First, AfBPP requires covalent crosslinking to the target in order to analyze results. This crosslinking is occasionally inherent to the MOA, however, to ensure a covalent interaction, installation of a photoreactive group is often necessary. Various functionalities are able to be employed, with the most common shown in Figure 2.17.

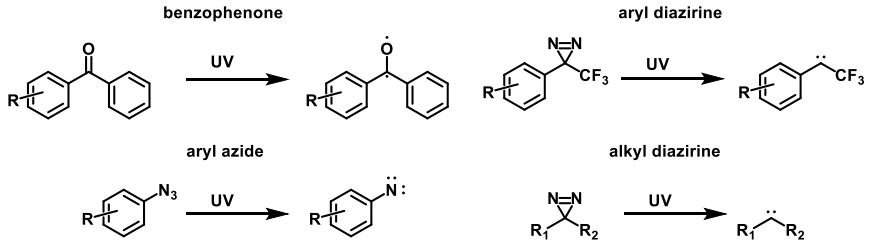

Figure 2.17 *Photoreactive groups used to ensure covalent crosslinking*

The second structural modification is the incorporation of functionality permitting target enrichment or visualization. Classical analysis strategies utilize biotin/streptavidin or visualization with SDS page via the incorporation of a fluorophore; neither of which would be minimally invasive to the chemical structure. However, the field of biorthogonal chemistry has alleviated this obstacle. Therefore, the most common enrichment strategy utilizes the Copper-catalyzed azide alkyne cycloaddition (CuAAc) or "click reaction" to append a fluorophore or affinity label. Use of CuAAc requires the minimal installation of an alkyne to the molecule; then, following incubation, azide linked to the affinity label can be added and the protein of interest can be enriched with avidin or visualized with gel electrophoresis (Figure 2.18).

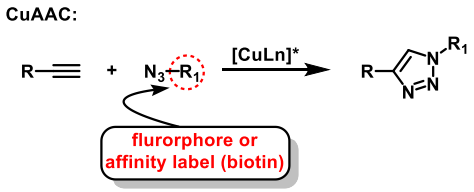

Figure 2.18 *Copper-catalyzed azide alkyne cycloaddition, "click" reaction*

While AfBPP can be highly useful, the significant drawback is the requirement for the incorporation of not one, but two new functionalities (photoreactive group and azide/alkyne) ***while*** retaining biological activity. The Yao lab has designed a 'minimalist' probe, wherein both photoreactive group and alkyne handle are on the same fragment, with the hope that modification of the structure can be minimal,

and incorporation can be late stage (Figure 2.19).[50] In addition, the probe can be differentially functionalized such that multiple structural features can be modified (acids, amides, alcohols).

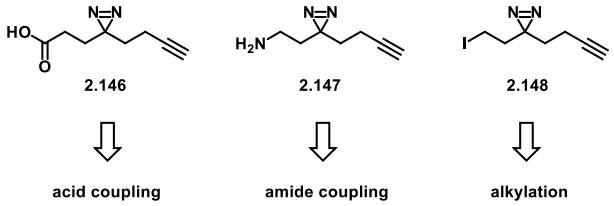

Figure 2.19 *Photoaffinity probe with three possible likers*

A common problem with such methodology however, is the enrichment of a significant number of proteins, often including false positives. Multiple experiments can be performed aiming to decrease the number of falsely enriched proteins which will be discussed *vide infra*.

2.7.2 Synthesis of probe

At the onset of this project it was unclear if promysalin covalently modified its target; we therefore decided to install a photoaffinity probe to ensure capture of the biological moiety. Initially, we envisioned installing the diazirine photoprobe to one of three locations on the natural product - the phenol, side chain alcohol, or on the amide (Figure 2.20, left). From our SAR we observed loss of activity with addition of a much smaller methyl group on both the phenol and side chain alcohol, allowing us to focus our efforts on the alkylation of the amide nitrogen.[51] For preliminary screening, we appended a propargyl moiety to the amide nitrogen (**2.144**), which was approximately three-fold less active than the natural product (218 nM vs. 67 nM in PA14), thus permitting our strategy to synthesize the amide probe, **2.147**.

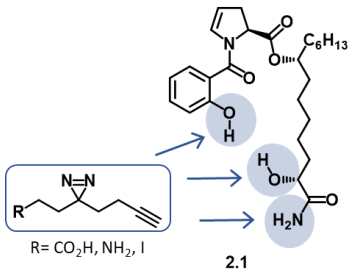

Figure 2.20 *Locations on the natural product we proposed probe installation*

We had originally hoped that in a similar fashion to the synthesis of the propargyl analog, **(–)-2.144**, we could displace the auxiliary with our amine, however, in preparation of analog **(–)-2.144** successful displacement required greater than 10 equivalents of amine. While this was feasible for that analog, synthesis of the probe amine is a 9-step sequence and using significant excess would not be ideal. As such, we sought an alternative approach. Classic displacement of Evans' to the acid requires LiOH and H_2O_2 however, under these conditions we observed rapid TBS protecting group cleavage. To circumvent the basic hydrolytic conditions, we displaced the auxiliary with benzyl alcohol, giving intermediate **(+)-2.149**. Following displacement, we hydrogenated the benzyl ester, yielding the acid and leaving our protecting group untouched. This intermediate was unstable (rapid TBS cleavage upon standing), so it was reacted immediately with amine, **(–)-2.147**, and HATU to form **(+)-2.149**. Following successful incorporation of the probe, we esterified with EDC and deprotected as with the natural product, yielding the natural product probe, **(–)-2.152** (Scheme 2.23).

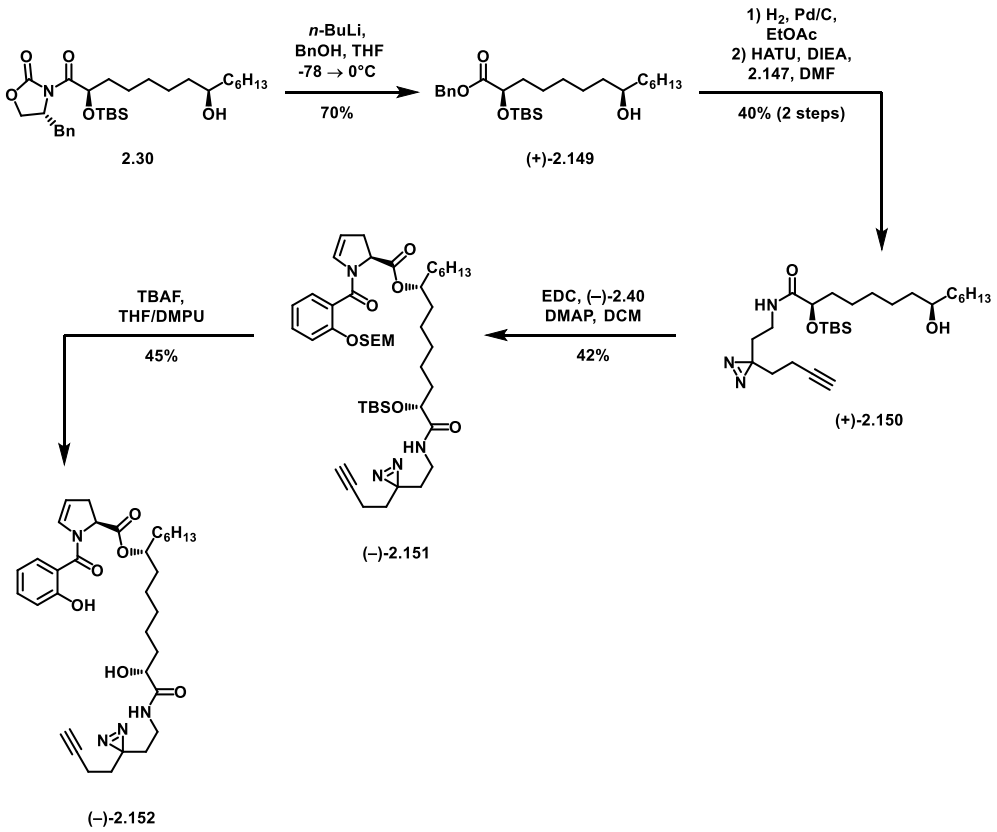

Scheme 2.23 *Synthesis of promysalin photoaffinity probe*

As a control, we also synthesized a negative probe (**(–)-2.154**) wherein we coupled the diazirine-alkyne amine to inactive analog, **(–)-2.98**. The negative probe was constructed in an analogous manner as the natural product probe, **(–)-2.152**, using acid **(–)-2.96** (Scheme 2.24).

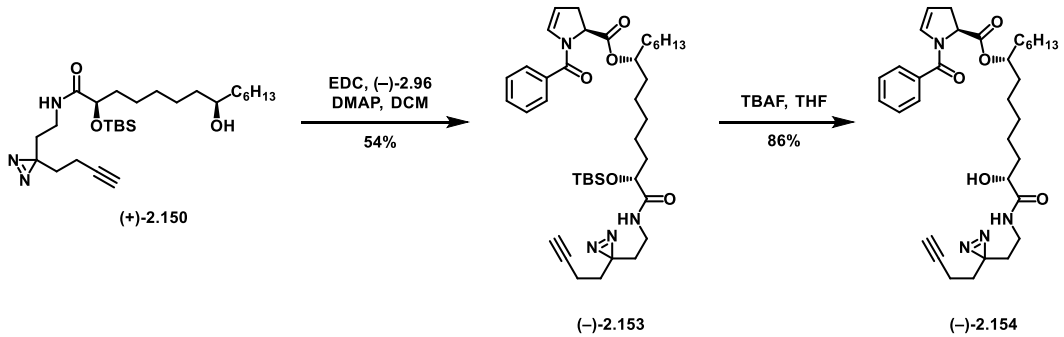

Scheme 2.24 *Synthesis of negative probe*

Activity of the probe was confirmed, with an IC_{50} value of 1.7 μM (in PA14), supporting its use for proteomic studies.

2.7.3 Outline of experiments

With the probe in hand we turned to AfBPP to elucidate the protein targets of promysalin. General workflow starts with incubation and UV irradiation of bacteria in the presence of the probe molecule allowing for target engagement. Following incubation, crosslinked cells are subjected to CuAAC conditions. Upon attachment of either fluorophore or affinity label, results are analyzed vis SDS-page or cell lysis followed by tryptic digestion for mass spectrometry analysis.

For each experiment, three different sample types were prepared for gel-free *in situ* proteomic analysis. Cultures of *P. aeruginosa* PAO1 and PA14 were grown to log phase and incubated with either 1) promysalin photoprobe, **(–)-2.152**, 2) promysalin **(–)-2.1** followed by promysalin photoprobe **(–)-2.152** (competitive inhibitor), or 3) inactive promysalin photoprobe, **(–)-2.154**; experiments 2 and 3 serve to identify and eliminate any false positives (Figure 2.21). After UV irradiation, cells were lysed, reacted *in situ* with biotin-azide, and enriched on avidin beads. Enriched proteins were subjected to a trypsin-digest and labeled with light, medium or heavy isotopes via dimethyl-isotope labeling.[52] Isotope labels were switched throughout biological replicates and samples with corresponding labels were pooled prior to LC-MS/MS measurement.

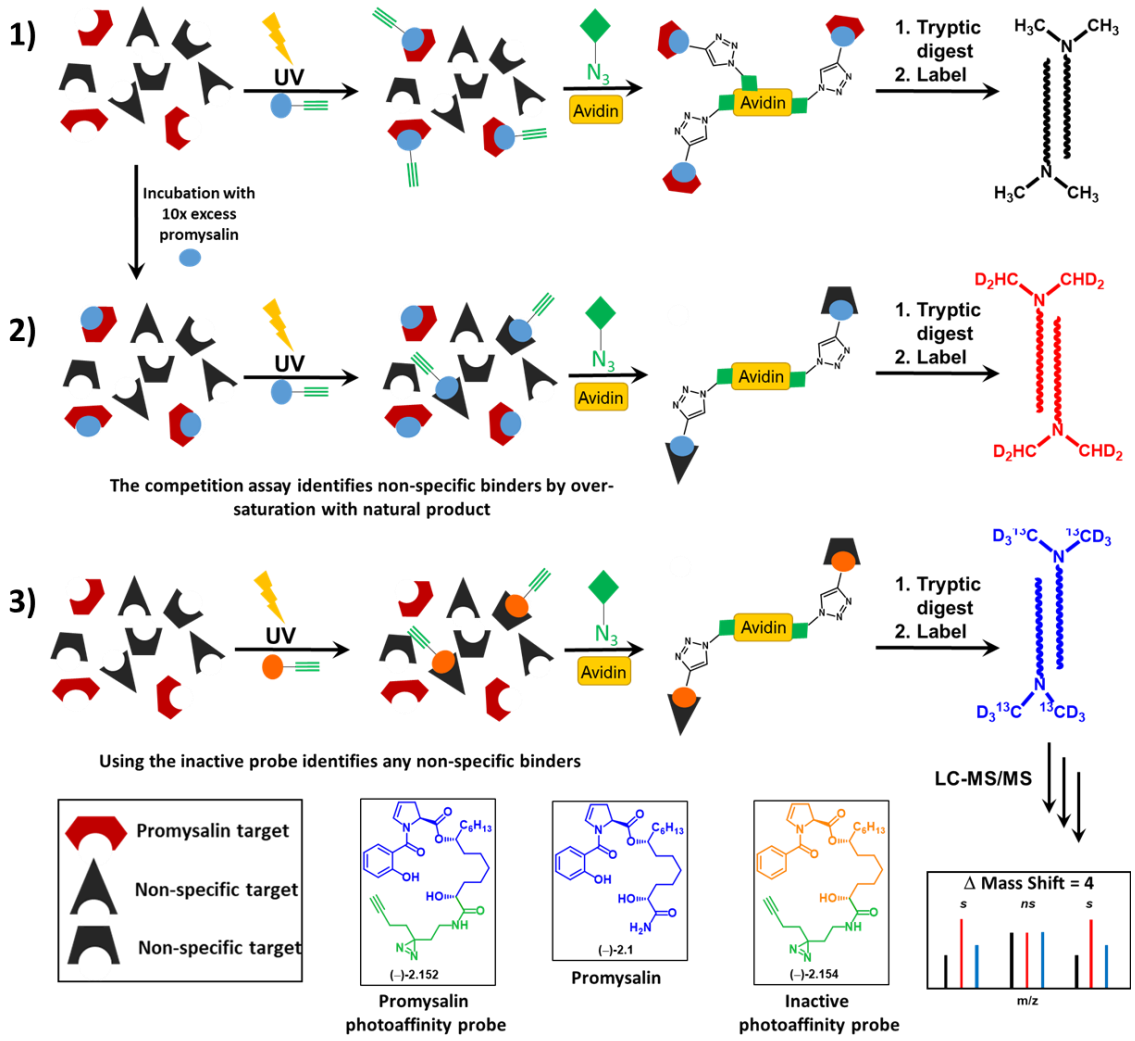

Figure 2.21 *Outline of each of the three experiments preformed*

2.7.4 Results

Statistical analysis revealed only a small number of significantly (p-value ≤ 0.05; log2-ratio ≥ 1) enriched proteins (Figure 2.22). The most prominent hit in both PA strains (PAO1 and PA14) as visualized by the volcano plots was the succinate dehydrogenase C-subunit (SdhC); furthermore, the enrichment could be outcompeted by promysalin thereby providing preliminary validation of SdhC as the biological target.

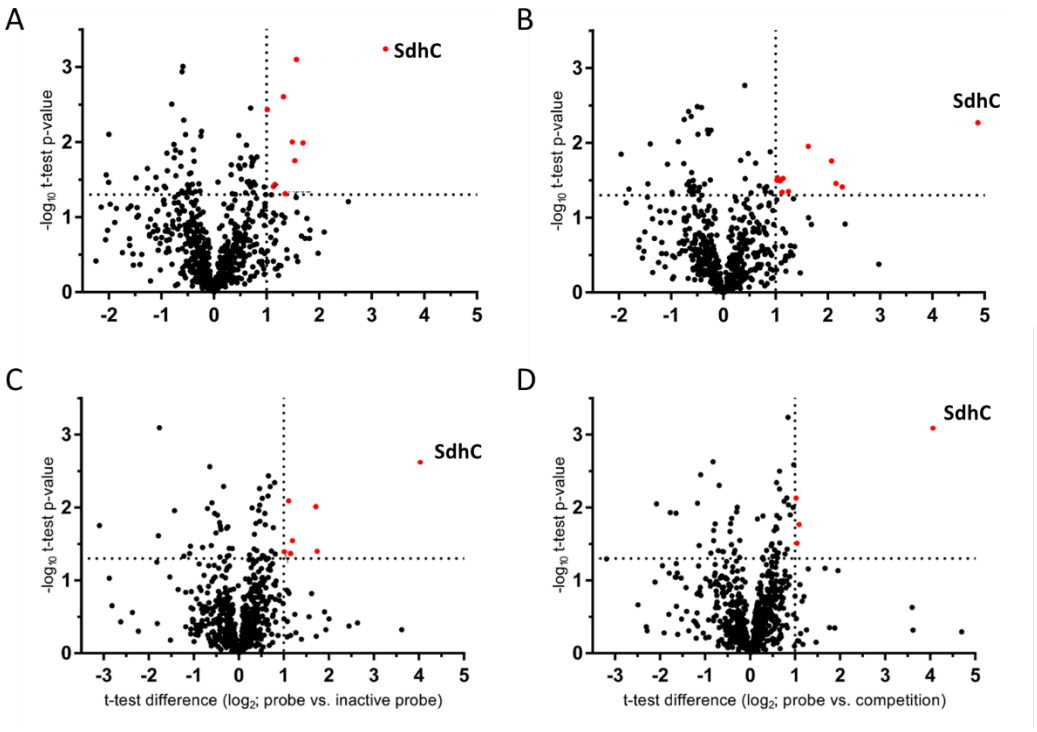

Figure 2.22 *Volcano plots from AfBPP experiments. A) PA14 probe vs inactive, B) PA14 probe vs competition C) PAO1 probe vs inactive, D) PAO1 probe vs competition*

2.8 Investigation of primary metabolism as target

Following our pull down assay, we turned to support the notion that promysalin could be targeting a difference in primary metabolism between species of *Pseudomonads*.[53] This initially seemed counterintuitive: one would not expect that an essential enzyme, critical to nearly all life, could be the target of a narrow-spectrum agent. Nonetheless, the following section will support the surprising finding that the target of promysalin is succinate dehydrogenase (Sdh), a conserved enzyme that plays a key role in both in the tricarboxylic acid cycle (TCA) and in respiration.

2.8.1 In vitro inhibition of SdhC

In efforts to initially confirm our proteomic studies we sought to determine an *in vitro* IC_{50} against Sdh itself. While previous reports mention isolating Sdh from PA membranes, we leveraged a commercially available colorimetric mitochondrial Sdh assay. This would both give us confidence in Sdh as the target (as

bacterial and mammalian enzymes are homologous) and provide information regarding selectivity between the two kingdoms. We observed complete inhibition of complex II at 200 µM and an IC_{50} of 2.5 µM (Figure 2.23). It should be noted that the ~50-fold difference in activity between the *in vitro* mammalian assay and our *in vivo* bacterial studies suggests that promysalin preferentially targets bacteria.

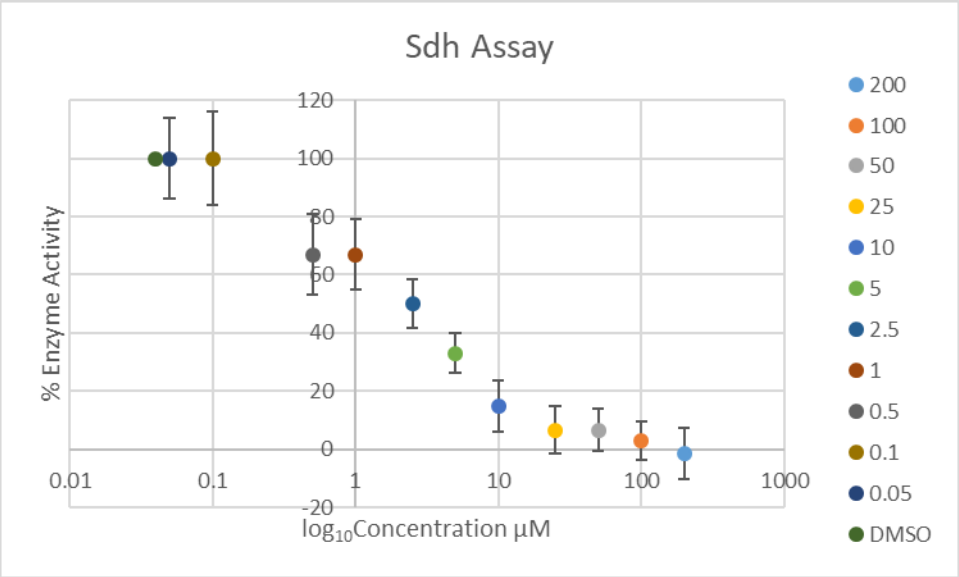

Figure 2.23 *IC_{50} curve with mammalian Sdh, all concentration in µM*

2.8.2 Docking studies

With consistent proteomic data and *in vitro* inhibitory activity in hand we sought to identify a putative binding site with computational modeling. Ideally, we would have preferred to co-crystallize promysalin with Sdh; however, the *Pseudomonas* protein has not yet been crystallized. The homologous enzyme in *E. coli* has been structurally characterized, and thus this served as a starting point for modeling the *Pseudomonas* enzyme.[54] Small molecule inhibitors of the enzyme typically inhibit via the ubiquinone binding site and based on shared structural features of these compounds we anticipated that promysalin would bind at the analogous site (Figure 2.24).[55]

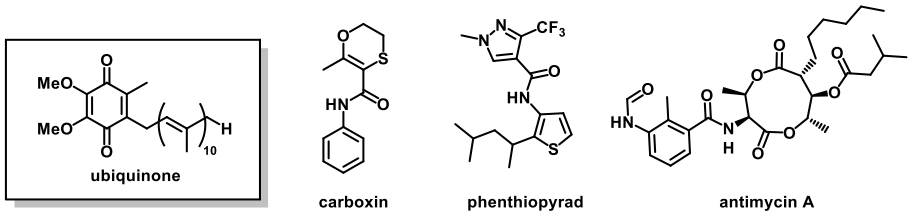

Figure 2.24 *Ligand of SdhC and inhibitors*

Our collaborators at the Fox Chase Cancer Center aligned each of these known inhibitors onto the *Pseudomonas* enzyme then used these compounds as the basis for pharmacophoric matching using a broad range of possible promysalin three-dimensional conformations. Upon energy minimization, these yielded many bound poses with comparable predicted energetics; thus, we leveraged our existing structure-activity relationship (SAR) data to narrow down the possible models.[51] To our satisfaction, we found that the SAR was fully consistent with only one of these very diverse models: this points to the stringency of the constraints that arise from our thorough SAR characterization and provides confidence in the final model. There are three key observations that allowed us to reject all possible models but this one, Figure 2.25. First, we previously reported that the replacement of the ester linker with an amide abolished activity: in

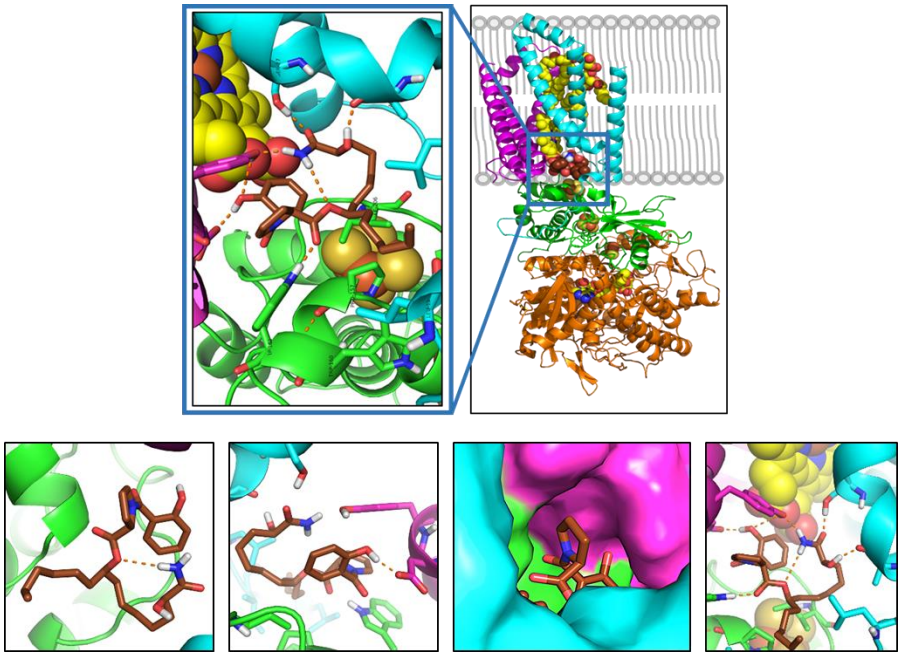

Figure 2.25 *Docked model of promysalin in ubiquinone binding site. (Bottom) Left to right; key interactions – amide and ester hydrogen bond; phenol interaction; proline space filling; side chain alcohol interaction*

the docked model the ester adopts a conformation where the oxygen is engaged in intramolecular hydrogen bonding, whereas an amide substitution here would abolish this favorable interaction. Second, replacing the salicylate hydroxyl group with a methoxy group greatly reduced activity: in the docked model this hydroxyl group engages in hydrogen bonding with a nearby aspartate and tyrosine; alkylating the oxygen would render these interactions impossible. Finally, adding a methyl group to the dehydroproline heterocycle resulted in a compound with moderate activity; in the docked model this position points outward from the binding pocket, explaining how incorporation of an extra substituent is tolerated.

This model is additionally consistent with information that was not part of the SAR used in its selection. The model includes a hydrogen bond between a backbone carbonyl of SdhC and the alcohol side chain on the myristate region: the modeled position and orientation of the side chain alcohol explains why its stereochemistry was important for activity (changing this stereochemistry would lead to a steric clash), and yet its removal was also tolerated. Separately, we note that promysalin must bind in a manner that can accommodate the diazirine photoprobe with only minimal effects on bioactivity (~10x less active): the terminal amide in this model engages in two hydrogen bonds with the enzyme, and still would allow the alkyne moiety of the photoprobe to project toward the hydrophobic groove occupied by the fatty acid side chain.

Another key consequence of this model relates to the strain-specific activity of promysalin. We mapped the sequences for each Sdh subunit for PAO1, PA14, and KT2440 back onto this model of binding: notably, there was not a single sequence difference among the three at this site. The model therefore implies that the observed differential activity is not based on binding preferences of promysalin for Sdh, but rather upon some other factor that distinguishes these strains.

2.8.3 Resistance selection

There is precedent that bacteria and fungi can generate resistance to Sdh inhibitors. For example, carboxin resistance is of major concern in the agriculture industry and a number of Sdh mutations have been disclosed which render the compound inactive.[56-57] In an effort to validate both our proteomic results and our proposed docking model we sought to select for a promysalin-resistant mutant in PA14. Toward this end, bacteria were subjected to sub-lethal concentrations of promysalin daily for a 24-day period. After the course of treatment, two morphologically-distinct mutant strains were obtained (Figure 2.26). Strain O5, which had a similar morphology to that of the parent strain was >60-fold more resistant to promysalin. The mutant contained a non-synonymous single nucleotide polymorphism (SNP) in SdhB, which resulted in an I206V mutation within the ubiquinone binding site at the interface of SdhB and SdhC. This subtle mutation is unique to promysalin as it has not been identified in carboxin-resistant strains and is likely attributed to a greater loss of hydrophobic contact with promysalin when compared to ubiquinone. A second resistant strain (N5) was also identified and based on its "abnormal" morphology was suspected of having distinct mutations. Whole genome sequencing (WGS) of this strain revealed the same SNP in Sdh and a second mutation in YfiR, a regulator of intracellular c-di-GMP levels.[58-59] YfiR mutants have been shown

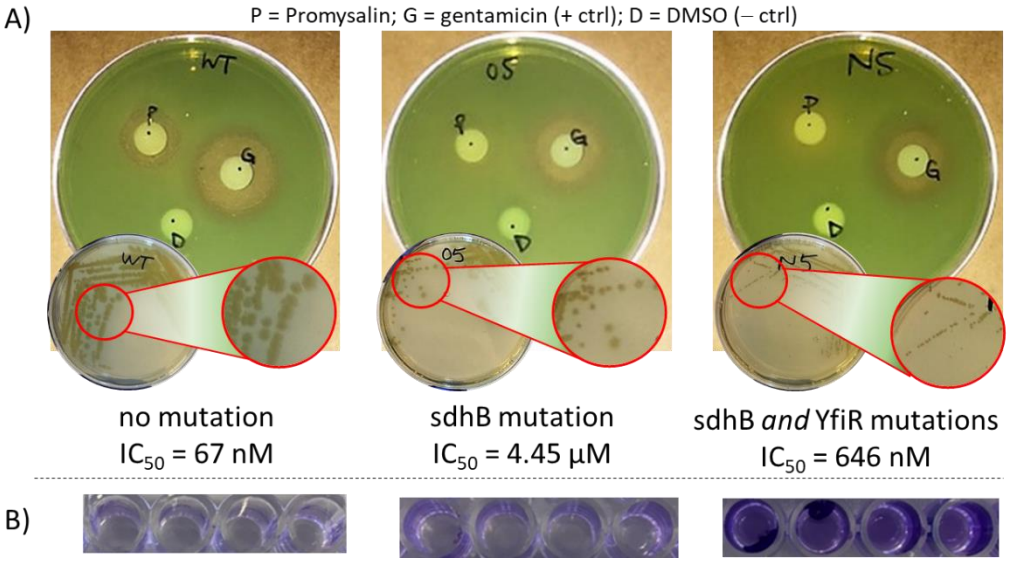

Figure 2.26 *Resistant strains resulting from 24-day serial passage assay. (A) disc diffusion shows decreased inhibition, inlet highlights altered morphology. (B) crystal violet staining shows increased biofilm formation for N5 strain*

to form small colony variants (SCVs) thereby explaining the altered morphology.[60] The abnormal morphology of the single colonies, containing the YfiR mutation, is consistent with YfiR knockouts, which were first discovered in PA CF sputum isolates. YfiR acts as the regulator in the YfiBNR system closely regulating YfiN, which functions as a diguanylate cyclase, producing c-di-GMP. In wild-type strains, YfiN is repressed by YfiR, however in YfiR mutants the de-repression of YfiN leads to an increased production of c-di-GMP.[60] Adaptations of this mutation increase the number of persister cells and also form more robust biofilms.[61] Presumably, the initial YfiR mutation in PA arose in a similar manner, that is from the sublethal treatment of antibiotic. It will be interesting to see if the mutation of YfiR is a common defense mechanism utilized by PA to resist antibiotic treatment in these anaerobic environments. Strain N5 displayed a 10-fold increase in resistance to promysalin (IC_{50} = 646 nM) and a significant increase in biofilm formation, in line with previous studies of this mutation. Taken in sum, the WGS data further validates our proteomic, in vitro and docking model confirming succinate dehydrogenase as the biological target of promysalin in PA14.

Further analysis of the mutation with respect to the original model supports the decreased activity when treated with promysalin while unaffecting the affinity for the natural ligand, ubiquinone. This can be highlighted with the space filling representation as shown in Figure 2.27.

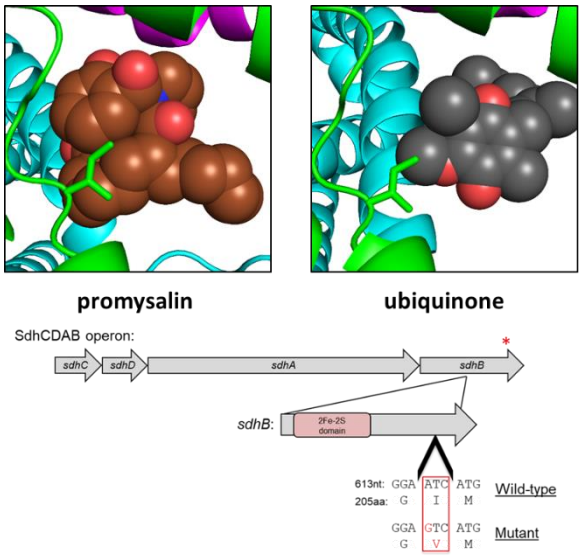

Figure 2.27 *Space filling representation of promysalin and ubiquinone. Mutated amino acid is shown*

2.8.4 Feeding experiments

In order to gain insight in regard to the selectivity we looked more into the enzyme itself and the role it plays. The Tricarboxylic Acid (TCA) cycle is an essential pathway in primary metabolism and facilitates the release of stored energy through a series of eight reactions.[60] Succinate dehydrogenase is an enzyme that is part of both the TCA cycle and the electron transport chain (housed in membrane).[62] Its specific function within the process is to catalyze the oxidation of succinate to fumarate with simultaneous reduction of the cofactor ubiquinone (CoQ10) to ubiquinol (Figure 2.28). Under stress, however, alternative pathways can be employed. The glyoxylate shunt pathway is one such alternative which circumvents four of the eight steps in the TCA cycle, one of which involves Sdh, for specific metabolic uses.[63] In the glyoxylate pathway, isocitrate is converted to glyoxylate and sequentially converted to malate, thereby bypassing several transformations including the oxidation of succinate. Alternatively, isocitrate can also be directly converted to succinate. However, in this pathway, the succinate produced is often released for

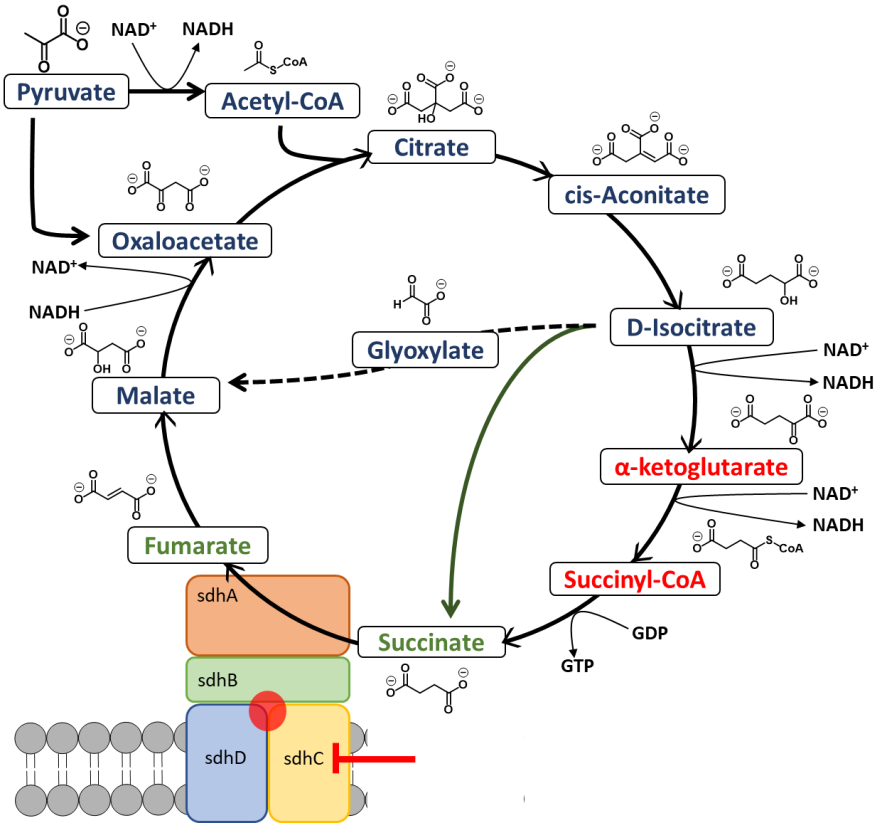

Figure 2.28 *Closer examination of the role SdhC plays in primary metabolism*

energy production and biosynthesis, suggesting metabolism and subsequent cellular function can persist without Sdh.

Based on this understanding of the TCA cycle, we postulated that we could rationalize the species-selectivity of promysalin on differences in metabolism which would become clear through microbiological growth assays in defined media. Toward this end, we first attempted, albeit unsuccessfully, to rescue growth of PA through media supplementation with fumarate. These results were not surprising based on the dual modality of Sdh, as this enzyme not only converts succinate to fumarate but also facilitates electron transport. Although the supplementation assay would rescue the former deficiency, it would not address the latter. We next hypothesized that through purposefully selected feeding studies we could potentially override any inherent species-specific preferences in primary metabolism. To begin, we grew each strain (PA14, PAO1, PP KT2440, and PP RW10S1) in TSB or M9 minimal media supplemented with either succinate or glucose. As expected, promysalin was active only against PA and not PP in TSB and M9 media supplemented with glucose as these carbon sources allowed the bacteria to utilize either the full TCA cycle or the shunt pathway in a fully aerobic process. Conversely, a clear zone of inhibition is present in both PP strains (gentamicin shown as a control) as can be seen in Figure 2.29, including the producing organism,

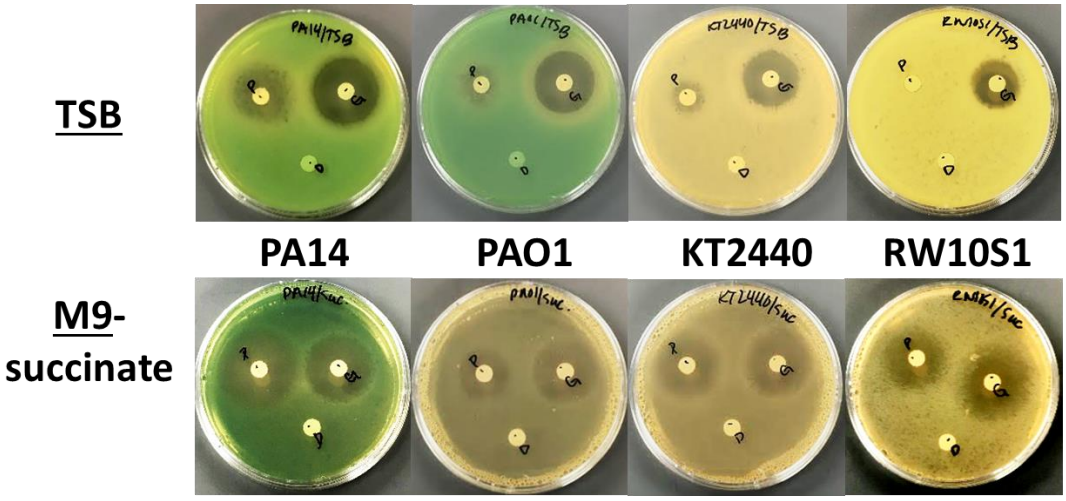

Figure 2.29 *Feeding experiments with PA14, PAO1, KT2440, and RW10S1 in nutrient rich media (top) and minimal media with succinate supplementation (bottom)*

demonstrating that promysalin is capable of inhibiting the growth of PP in presumably non-environmental circumstances.

While inhibition of the producing organism is surprising it is not unprecedented as bacteria can develop modes of self-resistance to their own antibiotics. Toward this end we sought to explain this finding by revisiting the isolation paper where the genome of the producing strain was fully sequenced.[16] In that report, no transporter or resistance genes were disclosed; however, the gene cluster encoding the biosynthesis of the natural product is found immediately adjacent to the TCA genes and presumably under the control of the same promoter. This would allow the bacteria to modify its metabolism accordingly whenever antibiotic production was activated. Taken in sum, these results shed light on how promysalin can elicit is species-selectivity through the inhibition of Sdh.

2.8.5 Conclusions

Based on the narrow-spectrum activity of the natural product, we expected to either identify a target unique to PA or a transporter specific to the natural product. Instead, we uncovered succinate dehydrogenase, an enzyme involved in primary metabolism, as the biological target. Computational modeling, in vitro assays, and whole genome sequencing of resistant mutants further validated these findings. Previous studies have shown that other rhizosphere natural products, like siccanin, a fungal natural product, also target Sdh. This small molecule was "rediscovered" through an initial screen for PA membrane inhibitors but was later shown to be species-selective preferentially targeting PA, but not *E. col*i or *Corynebacterium glutamicum*.[64] When considering promysalin and siccanin, recent studies investigating the effect of growth conditions on essential functions of PA confirm SdhABCD as essential, regardless of growth media. These findings complement the siccanin data, as SdhABCD has been found to be non-essential in corresponding E. coli investigations.[65] This difference in activity can be understood via the dual roles that Sdh serves both in metabolism by means of the TCA cycle and in respiration through the electron transport chain (ETC). While PA is able, under specific conditions, to grow and survive via fermentation, respiration is almost solely responsible for ATP production (via oxidative phosphorylation following the

ETC); consequently, unless in the proper environment, PA requires the ETC to generate ATP and survive.[65-66] This facultative anaerobic behavior is a critical difference between PA and PP as PP possesses a highly versatile aerobic metabolism, often favoring the Entner-Doudoroff pathway.[67] Furthermore, recent work by the Collins lab has demonstrated that metabolic flux in PA greatly varies between growth conditions (i.e. carbon sources), and that by targeting specific enzymes within the TCA cycle, one can potentiate antibiotic activity.[53] These findings may help to explain the differential activity between PAO1 and PA14, though they cannot fully rationalize the inactivity in PP.[53] In a separate study looking at systems-level metabolic pathways, it has been postulated that PP may be able to interchangeably utilize the glyoxylate shunt pathway in lieu of the TCA cycle without sacrificing overall growth.[68] Future work in our laboratory will seek to confirm these computational findings via transcriptomic studies.

Taken together, we have identified the target of a species-selective antibiotic via proteomic studies. The success of these studies hinged on our previous analog findings thereby allowing for the chemical synthesis of a diazirine photoprobe which retained activity. Succinate dehydrogenase was identified using AfBPP and was further validated with in vitro assays, feeding studies, and whole genome sequencing of resistant mutants. Computational molecular docking was used to predict the putative binding pose within the ubiquinone pocket, and additionally provided insight into the basis for the observed I206V resistance mutation. Furthermore, we showed that under specific media conditions, that the species-selective nature of promysalin was abolished to the extent that it is capable of inhibiting growth of its producing strain. Our findings add to the emerging discoveries focusing on the targeting of the TCA cycle both to potentiate existing antibiotics and develop narrow-spectrum therapies, which will undoubtedly find utility both in drug discovery and in deconvoluting multi-species microbiomes.

2.9 Side chain analogs

With a target identified and a model on hand to rationalize activity, we sought exploration of an additional set of structural analogs. We were interested in understanding the space we have in the hydrophobic side chain pocket with regards to rigidity and length. Towards this end we synthesized 14 analogs with variation in the alkyl chain. The variation was rationalized for two reasons, first - solubility. Solubility is a problem often encountered with known inhibitors of Sdh, we encountered this first hand in attempting to test their efficacy against our bacterial strains. We speculated increasing the alkyl chain could have a negative effect on solubility, despite the space that appeared available in the docking studies, Figure 2.30. Additionally, we sought investigation of alkyl chain on efficacy with respect to specificity. Bacteria construct metabolites with extreme precision, rendering each structural component strategic. Often, bacteria communicate via signaling molecules, an effort relevant to virulence, and more specifically quorum sensing. One such classification is acyl-homoserine lactones (AHLs), molecules that are tailored to each individual species of bacteria. As promysalin contains a biologically relevant myristic acid derived alkyl chain, we wondered how relevant this was not only to activity but perhaps specificity.

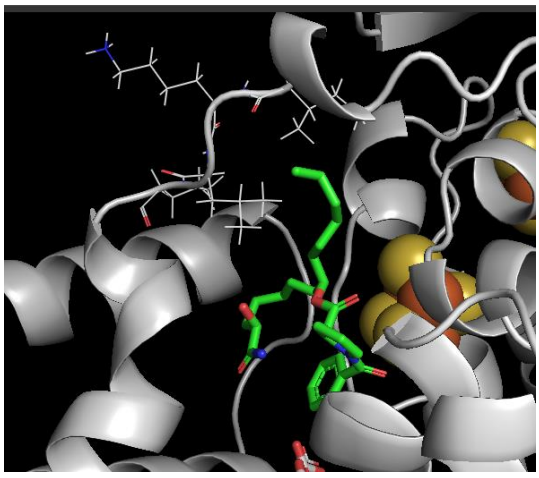

Figure 2.30 *Docked promysalin showing space at end of binding pocket*

2.9.1 Synthesis of side chain analogs

Synthetic efforts utilized the route published for our total synthesis. Originally, we had hoped to truncate the alkyl chain down to one carbon and extend to 10. Unfortunately, we had synthetic challenges with the shorter chains – in both the early and late stage steps. In setting the stereocenter for the free alcohol, we utilize an asymmetric allylation. Therefore, each analog was synthesized from a different aldehyde. What we observed, as well as others, is the volatility of the product from both propanal and butanal starting materials. Despite these challenges, we were able to push through material. The final analog arising from the butanal allylation successfully synthesized, unfortunately, that from propanal was not. Stability issues were encountered at each step and we observed decomposition of the ester within hours of purification every time. Therefore, the compounds will begin with Scheme 2.25 and the isopropyl analog.

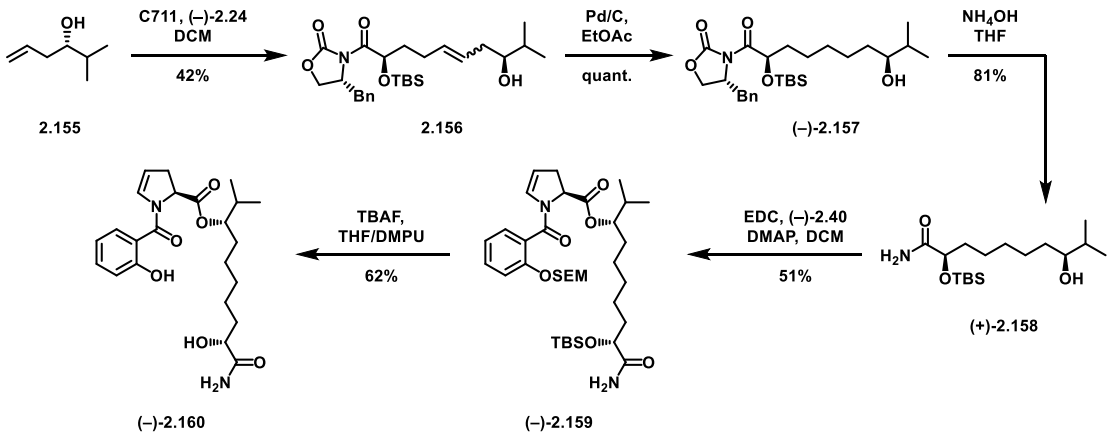

Scheme 2.25 *Synthesis of isopropyl analog,* ***(–)-2.159****.*

In this case, we hoped to determine the effect of increasing steric bulk. Starting with known allylation product, a result of the allyl-tributyl stannane allylation with isobutyraldehyde, **(–)-2.155**, we subjected the homoallylic alcohol to cross metathesis with TBS-protected intermediate (–**)-2.24**. Following assembly of the side chain, the remainder of the synthesis is as previously reported, including hydrogenation, ammonolysis, esterification, and deprotection, yielding analog **(–)-2.160**.

The next series of analogs are the final containing a truncated chain, shown in Scheme 2.26. In an analogous fashion, analogs (**–)-2.176,** (**–)-2.177, and** (**–)-2.178** were synthesized from butanal, pentanal, and hexanal, respectively.

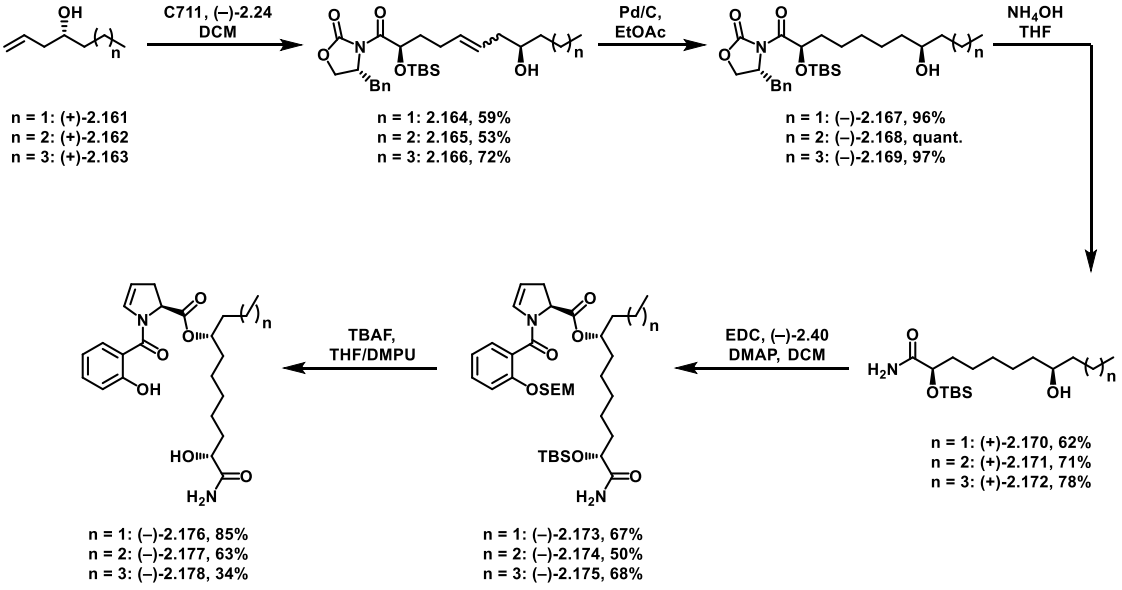

Scheme 2.26 *Synthesis of remainder of truncated side chain analogs.*

The next three analogs comprise the lengthened alkyl chain derivatives. (**–)-2.194**, (**–)-2.195**, and (**–)-2.196** were synthesized from their corresponding aldehydes, octanal, nonanal, and decanal (Scheme 2.27). While the synthesis followed the normal route, we encountered an issue with the greasier compounds not previously observed. The hydrogenation step took multiple resubmissions to completely hydrogenate the alkene. Typical conditions utilized for promysalin require the use of ethyl acetate as previous attempts with methanol often lead to deprotection of the TBS, necessitating milder reaction conditions. Even with the

analogs requiring multiple subjections, the addition of methanol did not increase the conversion. Despite the challenges, in all cases the alkene is successfully hydrogenated.

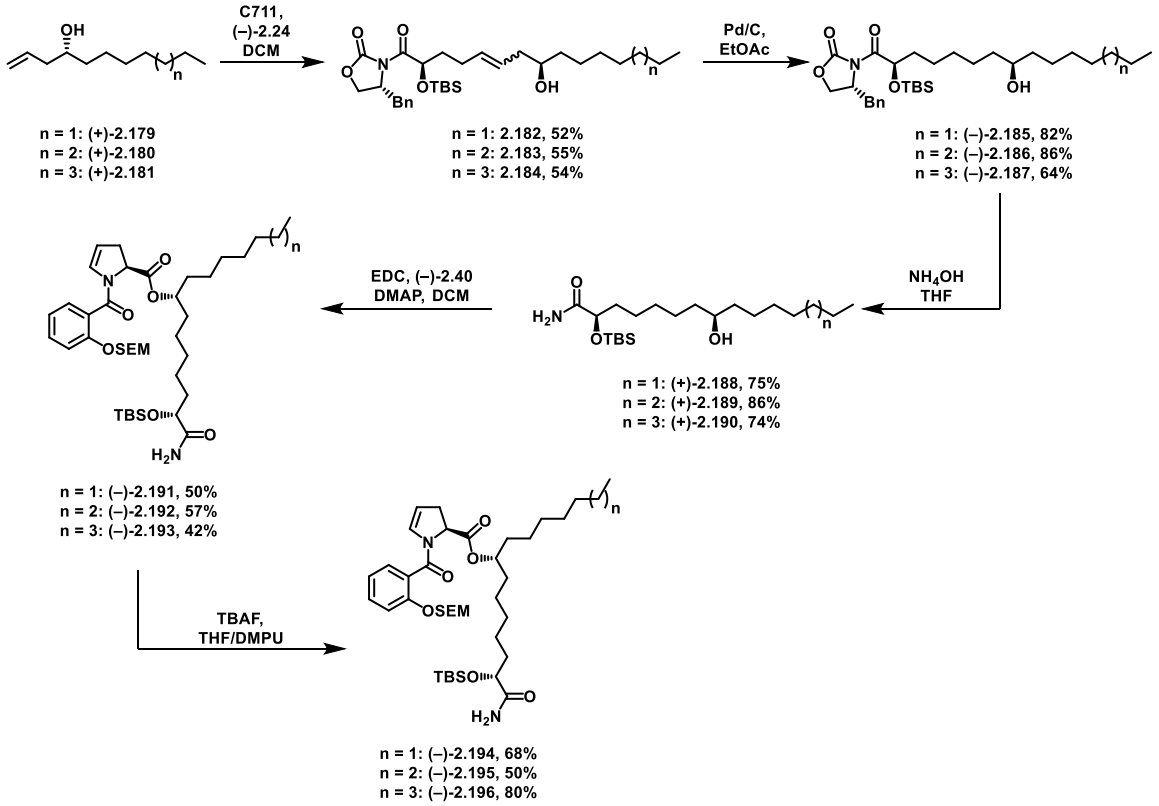

Scheme 2.27 *Longer alkyl chain analogs*

Next, we explored the effects of installing an aryl moiety in place of our alkyl chain. We hypothesized increasing rigidity could increase affinity. Additionally, the aryl moiety could be utilized for future analogs (with use of 3-bromo derivative) via cross-coupling chemistry, should it show any activity. Starting from the known allylation product from 3-bromobenzaldehyde we obtain allylic alcohol **(+)-2.197** (Scheme 2.28). In an analogous fashion as the previous analogs, the aryl derivative, **(–)-2.202** was obtained.

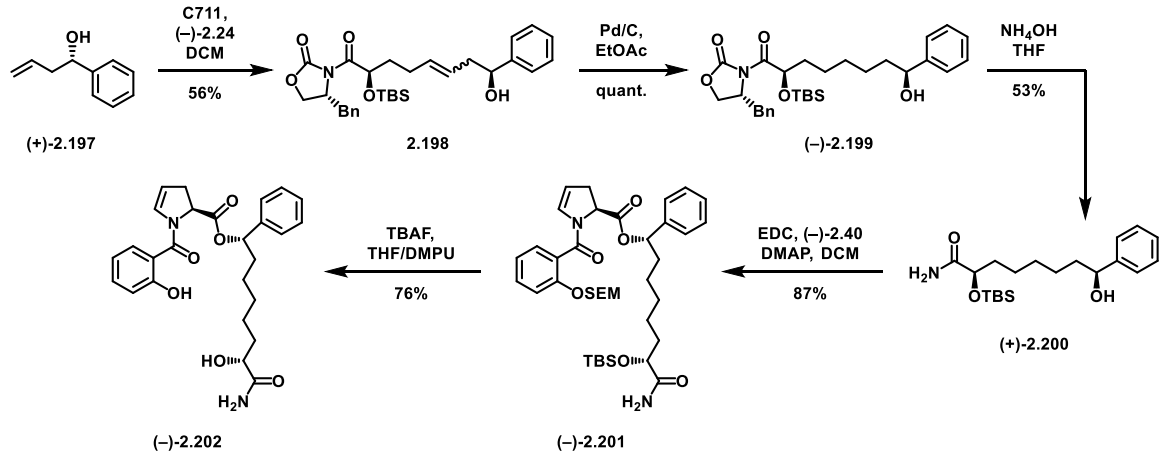

Scheme 2.28 *Synthesis of aryl analog*

Two analogs were synthesized such that the myristic acid derived aspect is conserved, keeping the total carbon count to 14, but the length of alkyl chain is altered. To this end, analogs **(–)-2.211** and **(–)-2.220** were synthesized (Scheme 2.29 and Scheme 2.30, respectively). Initiating with pentenoic acid, **2.203** or heptenoic acid, **2.2212**, installation of Evans' chiral auxiliary, Davis oxidation, and TBS-protection

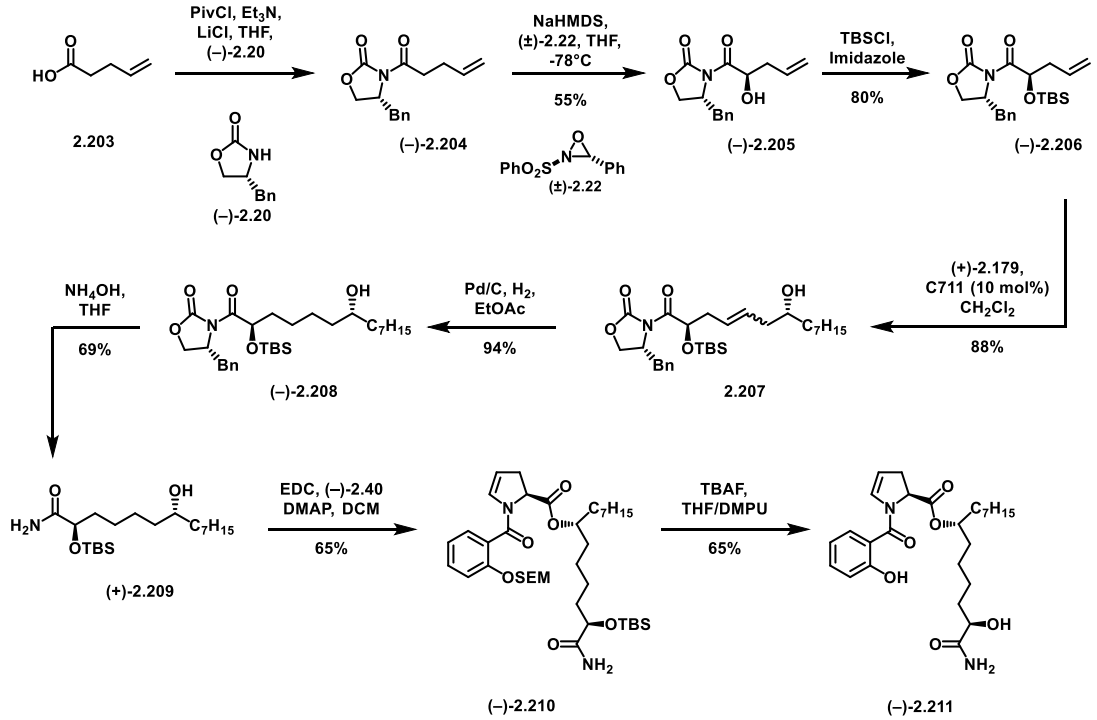

Scheme 2.29 *Synthesis of pentxoct analog*

proceeded as previously disclosed. Cross-metathesis partners were chosen such that the total number of carbons was conserved, therefore the octanal allylation product (**2.179**) was crossed with **2.206** and the hexanal allylation product (**2.163**) was crossed with **2.215**. Subsequent hydrogenation, ammonolysis, esterification, and deprotection provided final compounds **(–)-2.211** and **(–)-2.220**.

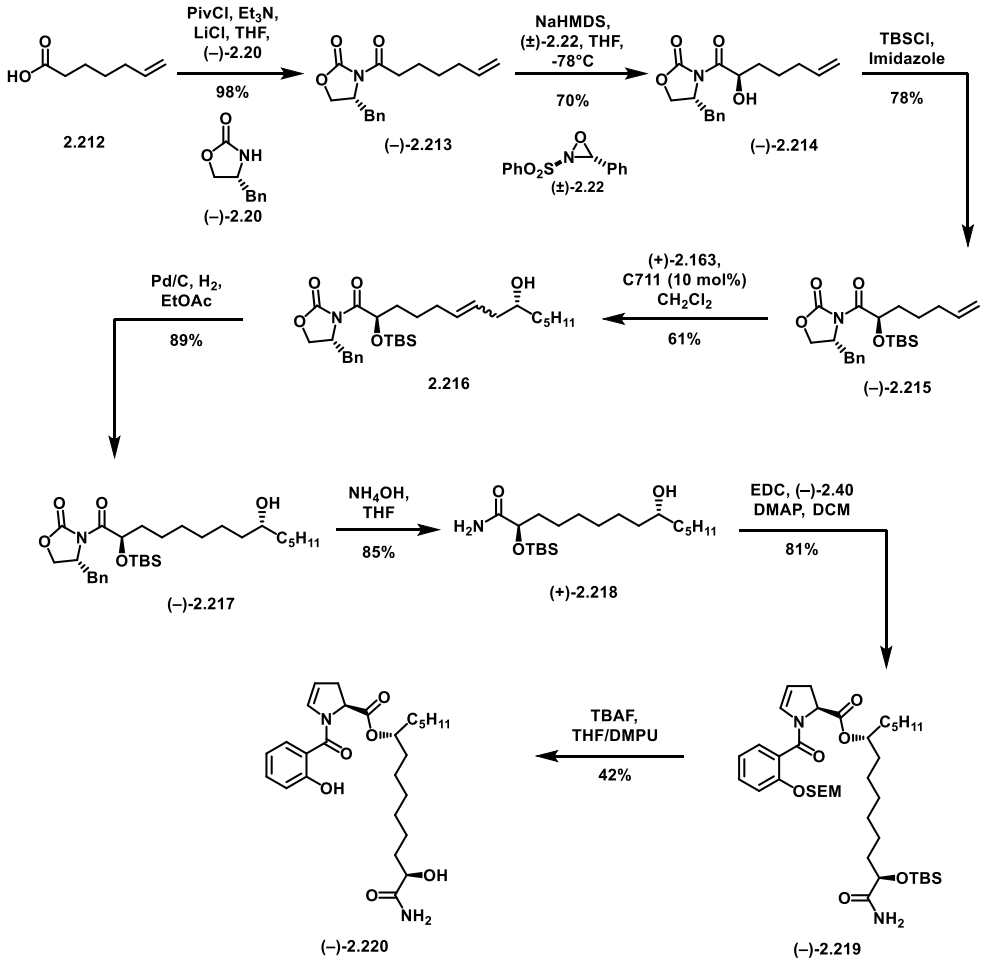

Scheme 2.30 *Synthesis of heptxhex analog*

2.9.2 Biological results

Biological testing commenced with inhibition assays of all strains against PA (PA14, PAO1, and the mutant strain, O5). For comparison purposes, promysalin (**(–)-2.1a**), has 6 carbons in its alkyl region, and accordingly the number of carbons comprising the alkyl chain are indicated in Table 2.3. Isobutyl, **(–)-2.159** and benzyl **(–)-2.198**, had the highest drop in potency, with the isobutyl analog being essentially

inactive. Interestingly, we decrease the number of carbons from 6 the activity decreases stepwise, with an approximate 2-fold decrease every time. However, increasing the carbons to 7 or 8 retain all activity and even show a mild increase in activity (within one dilution). There does reach a point, with 9 carbons, that the activity takes a turn and becomes less active. The trend can be visualized graphically in Figure 2.31.

	14	O5
2.160 (ISO)	130	>250
2.176 (3)	9.3	76
2.177 (4)	5.7	49
2.178 (5)	2.5	16
2.194 (7)	0.026	3.7
2.195 (8)	0.035	1.7
2.196 (9)	0.146	1.8
2.202 (BN)	38	>250
2.211 (PO)	3.1	15
2.220 (HH)	5.7	40

Table 2.4 *Activity of side chain analogs*

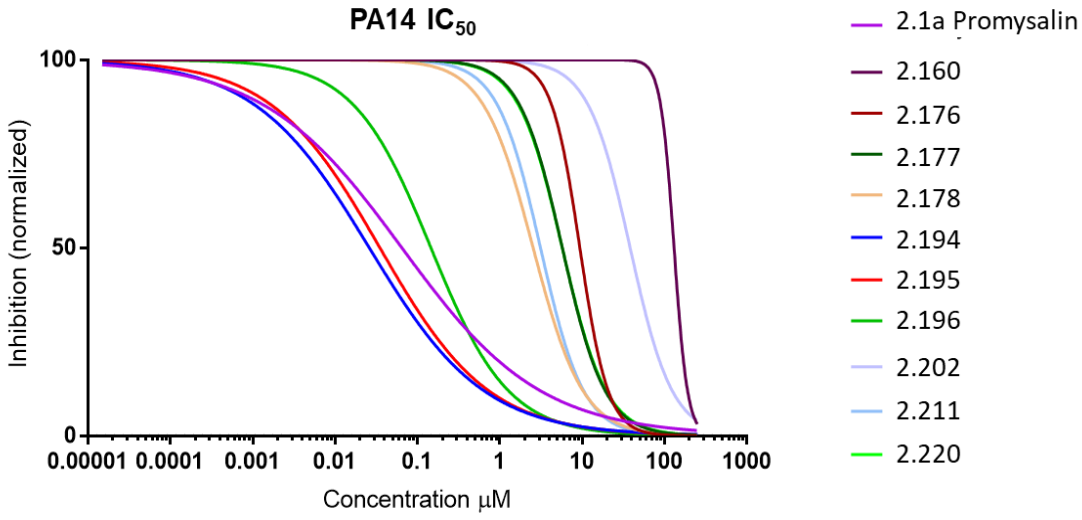

Figure 2.31 *Graphical depiction of side chain analogs*

This trend is observed for all strains tested and would be supported with docking studies, work that is currently underway in the Wuest Lab in collaboration with John Karanicolas at the Fox Chase Cancer Center.

2.9.3 Future directions

Future directions for this project, synthetically, would require extremely close examination of the model and understanding of known inhibitors. I believe with the knowledge acquired over the past five years it could be possible to overcome any type of resistance, however, due to the number of known inhibitors and the prevalence of resistance, thorough understanding of the computational models and known inhibition will be necessary.

2.10 Transcriptomics

(Work done in collaboration with Melanie Filiatrault, Ph.D. MF ran experiments/collected data, analyses were done in collaboration)

We initially focused on implementing proteomic methods for target identification. Affinity-based protein profiling (AfBPP) was used to determine proteomic targets of small molecules by covalent modification. Previously discussed efforts utilized a promysalin derivative bearing a photoaffinity probe (**(–)-2.152**) to identify Sdh as the biological target in *P. aeruginosa* (PAO1 and PA14).[69] Based on these initial successes, we sought to leverage the same chemical probe in AfBPP studies with PP_KT2440. Three samples were prepared and, in all cases, the promysalin photoaffinity probe (**(–)-2.152**) was incubated with PP_KT2440 and irradiated to thereby covalently attach the probe to the nearest protein. Following crosslinking, the cells were lysed, reacted with biotin-azide, and enriched on avidin beads. Trypsin digest and dimethyl-isotope labeling permitted analysis of enriched proteins via LC-MS/MS (Figure 2.32).

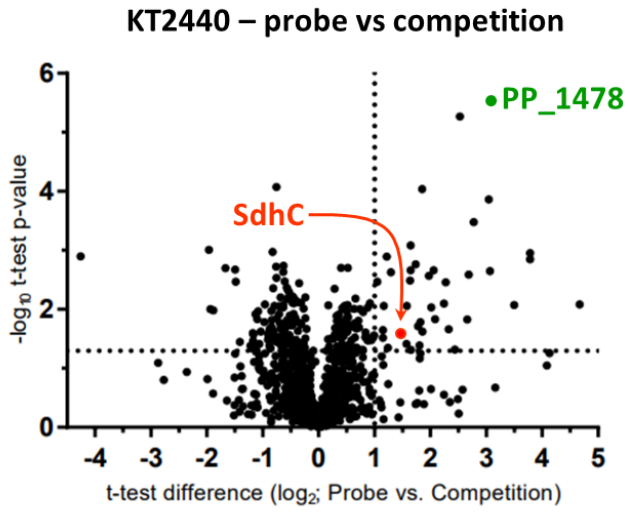

Figure 2.32 *Results of AfBPP probe vs competition experiment in Pseudomonas aeruginosa*

After proteomic analysis, whereby two controls were used to eliminate non-specific binders (see section on AfBPP for further details), 45 enriched proteins were identified. This contrasted with our previous experiments in PAO1 and PA14 where SdhC was the only statistically significant hit.

Locus	Gene	Protein	-Log t-test p-value	t-test Difference
PP_0133	*algB*	Alginate biosynthesis transcriptional regulatory protein AlgB	1.17	1.81
PP_0310	*dgcA*	Putative dimethylglycine dehydrogenase subunit (EC 1.5.8.-)	2.85	3.78
PP_0325	*soxA*	Sarcosine oxidase subunit alpha (EC 1.5.3.1)	3.86	3.04
PP_0328	*fdhA*	Formaldehyde dehydrogenase (EC 1.2.1.46)	2.08	4.67
PP_0395	*ycgB*	Putative type IV piliation protein	2.76	1.74
PP_0397	*yeaG*	Protein kinase (EC 2.7.11.1)	2.57	1.97
PP_0412	PP_0412	Polyamine ABC transporter, periplasmic polyamine-binding protein	2.49	1.63
PP_0614	PP_0614	Putative N-carbamoyl-beta-alanine amidohydrolase/allantoine amidohydrolase 1 (EC 3.5.1.6) (EC 3.5.3.9)	1.26	4.13
PP_0658	PP_0658	Homocysteine S-methyltransferase family protein	1.06	1.16
PP_0743	*yfcH*	Conserved protein with NAD(P)-binding Rossmann-fold domain	1.32	2.44
PP_0766	*PP_0766*	Uncharacterized protein	2.03	2.02
PP_0901	*colR*	DNA-binding response regulator	1.05	4.08
PP_0940	*tldD*	Putative protease involved in Microcin B17 maturation and in sensitivity to the DNA gyrase inhibitor LetD	2.47	1.05
PP_1141	*livK*	Branched-chain amino acids ABC transporter-periplasmic leucine binding subunit	3.08	1.65
PP_1291	PP_1291	PhoH family protein	2.46	2.27
PP_1478	PP_1478	Putative Xenobiotic reductase	5.55	3.09
PP_1502	PP_1502	OmpA family protein	1.83	2.09
PP_1743	*actP-I*	Acetate permease	2.95	3.78
PP_2112	*acnA-I*	Aconitate hydratase (Aconitase) (EC 4.2.1.3)	2.63	1.29
PP_2215	PP_2215	Acetyl-CoA acetyltransferase (EC 2.3.1.9)	1.41	1.57
PP_2335	*prpC*	Citrate synthase	2.07	3.50
PP_2364	PP_2364	Uncharacterized protein	2.06	1.16
PP_3668	*katG*	Catalase-peroxidase (CP) (EC 1.11.1.21) (Peroxidase/catalase)	2.89	1.22
PP_4011	*icd*	Isocitrate dehydrogenase [NADP] (EC 1.1.1.42)	1.66	2.32
PP_4034	*hyuC*	N-carbamoyl-beta-alanine amidohydrolase/allantoine amidohydrolase 2 (EC 3.5.1.6) (EC 3.5.3.9)	5.27	2.53

PP_4036	*pydB*	D-hydantoinase/dihydropyrimidinase (EC 3.5.2.2)	2.50	2.68
PP_4038	*pydA*	NADP-dependent dihydropyrimidine dehydrogenase subunit PreA (EC 1.3.1.2)	2.66	1.65
PP_4064	*ivd*	Isovaleryl-CoA dehydrogenase (EC 1.3.8.4)	1.62	1.85
PP_4065	*mccB*	Methylcrotonyl-CoA carboxylase biotin-containing subunit beta (EC 6.4.1.4)	1.31	1.65
PP_4067	*mccA*	Methylcrotonyl-CoA carboxylase biotin-containing subunit alpha (EC 6.4.1.4)	1.25	1.82
PP_4116	*aceA*	Isocitrate lyase (EC 4.1.3.1)	2.66	2.06
PP_4193	*sdhC*	Succinate dehydrogenase membrane b-556 subunit (EC 1.3.5.1)	1.60	1.45
PP_4279	*xdhB*	Xanthine dehydrogenase subunit XdhB (EC 1.17.1.4)	1.71	1.78
PP_4299	*glxR*	Tartronate semialdehyde reductase (EC 1.1.1.60)	2.10	2.24
PP_4402	*bkdAB*	Branched-chain alpha-keto acid dehydrogenase complex, beta subunit (EC 1.2.1.25) (EC 1.2.4.4)	4.04	1.85
PP_4487	*acsA1*	Acetyl-coenzyme A synthetase 1 (AcCoA synthetase 1) (Acs 1) (EC 6.2.1.1) (Acetate--CoA ligase 1) (Acyl-activating enzyme 1)	3.48	2.77
PP_4591	*rnd*	Ribonuclease D (RNase D) (EC 3.1.13.5)	1.20	1.13
PP_4620	*hmgB*	Fumarylacetoacetase (EC 3.7.1.2)	2.06	1.58
PP_4621	*hmgA*	Homogentisate 1,2-dioxygenase (HGDO) (EC 1.13.11.5) (Homogentisate oxygenase) (Homogentisic acid oxidase) (Homogentisicase)	1.39	1.80
PP_4666	*mmsB*	3-hydroxyisobutyrate dehydrogenase (HIBADH) (EC 1.1.1.31)	2.65	3.06
PP_4667	*mmsA-II*	Methylmalonate-semialdehyde dehydrogenase (EC 1.2.1.27)	1.83	2.66
PP_4702	*acsA2 acsB*	Acetyl-coenzyme A synthetase 2 (AcCoA synthetase 2) (Acs 2) (EC 6.2.1.1) (Acetate--CoA ligase 2) (Acyl-activating enzyme 2)	1.78	1.82
PP_4945	*rlmJ*	Ribosomal RNA large subunit methyltransferase J (EC 2.1.1.266) (23S rRNA (adenine(2030)-N6)-methyltransferase) (23S rRNA m6A2030 methyltransferase)	1.52	1.15
PP_5165	*plpB*	NLPA lipoprotein	1.35	1.24
PP_5186	*argE*	Acetylornithine deacetylase (EC 3.-.-.-) (EC 3.5.1.-) (EC 3.5.1.16)	1.65	1.15

Table 2.5 *All proteins that were enriched in pull-down assay*

Although SdhC was identified in this assay, many other potential targets were also found including the most prominent hit, a xenobiotic reductase, PP_1478 (Table 2.5). As promysalin is not toxic to PP_KT2440 but elicits a multitude of biological effects, we speculated that the molecule could elicit an antibiotic resistance response whereby it is either altered or expelled via efflux.

RNA-Sequencing has provided useful insights into the mechanisms of antibiotic susceptibility and resistance as well as insights into the putative mode of action of molecules.[70-71] Therefore, we (MF) performed a global transcriptome analysis (RNA-Seq) on bacterial cells that were treated with promysalin or DMSO as the control to better understand how promysalin is affecting cellular processes. Since phenotypic differences can be seen at 24 hours on swarming medium between cells treated with promysalin and those with the DMSO control, it was chosen to evaluate transcriptional changes at this physiologically relevant time point. A total of 109,540,045 reads were acquired for the three promysalin treated samples and 151,278,351 total reads for control samples (Table 2.6).

Sequence read type[a]	Promysalin treated[b]	Control[c]
Total reads	109,540,045	151,278,351
Aligned 0 times	3,488,427	12,422,474
Aligned >1 time	2,522,000	3,054,800
Uniquely aligned	103,539,618	135,801,077

Table 2.6 *(a) reads mapped to Pp KT2440 genome; (b) quantity of reads when Pp KT2440 cells were treated with 50μM promysalin; (c) quantity of reads when Pp KT2440 cells were treated with DMSO*

DESeq2 was used to identify those genes differentially expressed between the two conditions. Analysis of the RNA-Seq data revealed 455 genes were differentially expressed between the promysalin treated and control samples using an FDR of 0.05 and a fold change cutoff of 1.5-fold (433 down-regulated, 22 up-regulated). The list of up regulated proteins is shown in Table 2.7.

Our previous studies suggested that promysalin enhanced surface motility, even when used with agar concentrations that typically inhibit swarming (>0.5%).[16, 72] Swarming motility typically requires flagella and biosurfactant, therefore, we were surprised to find that nine genes were down-regulated that encode proteins involved in flagella-dependent motility. We hypothesized that decreased expression of genes involved in flagella assembly would result in reduced swimming in the presence of promysalin. To determine if promysalin influenced flagella, we evaluated swimming motility with 0.3% agar media. In contrast to the swarming phenotype observed when PP_KT2440 is treated with 100 μM promysalin, we see reduced swimming as compared to DMSO at the same concentration, suggesting that flagella production or function is inhibited in the presence of promysalin. To determine if flagella production was influenced by the presence of promysalin a Western blot was performed using cells that were grown in the presence or absence of promysalin. No observable differences in FliC could be detected. It is possible that the slight differences observed in the transcriptional profiles (2-fold) do not equate to differences at the protein level.

Swarming motility can be influenced by the availability of iron. We recently confirmed that promysalin binds iron, albeit quite weakly, and questioned its ability to act as a siderophore.[51] We found that promysalin had a widespread effect on expression of genes predicted to be involved with iron binding or homeostasis, influencing the expression of 15 genes in this category (Table 2.7). Bacterioferritins are proteins that oxidize Fe^{2+} to Fe^{3+} for storage of Fe^{3+} when excess iron is available.[73] In the current study, expression of all three *bfr* genes decreased in promysalin treated cells, suggesting the cells are experiencing iron-limiting conditions even though they are being grown in iron-rich media. Under iron-limited conditions, many

Locus	Gene	Protein	Log2 Fold Change	Fold change	P-value
PP_0372	aruC	Acetylornithine aminotransferase 2	1.73	3.31	7.80E-05
PP_1266	PP_1266	Putative Fusaric acid resistance protein	1.28	2.42	0.0119
PP_1413	ung	Uracil-DNA glycosylase	0.94	1.91	0.0473
PP_1418	PP_1418	Putative Tricarboxylate transport protein TctC	0.94	1.92	0.0031
PP_2061	PP_2061	Uncharacterized protein	1.12	2.18	0.0272
PP_2404	PP_2404	Uncharacterized protein	1.02	2.03	0.0228
PP_2418	PP_2418	Putative cobalamin ABC transporter, periplasmic	0.97	1.96	0.0088
PP_2429	PP_2429	Putative Membrane protein	1.10	2.14	0.0090
PP_2430	PP_2430	Transcriptional regulator, AraC family	1.42	2.68	0.0099
PP_2543	gabP-II	Gamma-aminobutyrate permease	1.55	2.92	0.0053
PP_2651	PP_2651	Major facilitator family transporter	1.15	2.23	0.0094
PP_2776	PP_2776	Homocysteine S-methyltransferase family protein	1.13	2.19	0.0050
PP_2778	PP_2778	3-oxoacyl-(Acyl-carrier-protein) synthase II	1.01	2.01	1.37E-06
PP_2779	PP_2779	Putative Beta-ketoacyl synthase	1.19	2.29	0.0066
PP_3022	PP_3022	Transcriptional regulator, AraC family	1.12	2.18	0.0492
PP_3159	benR	BenABC operon transcriptional activator	0.97	1.96	7.06E-06
PP_3219	PP_3219	Putative Alkansulfonate monooxygenase	1.09	2.14	0.0031
PP_3273	PP_3273	Uncharacterized protein	1.25	2.38	0.0335
PP_3481	PP_3481	Uncharacterized protein	1.24	2.36	0.0409
PP_3520	PP_3520	Uncharacterized protein	1.10	2.14	0.0456
PP_3553	PP_3553	Fatty-acyl-coA synthase	1.35	2.55	3.77E-07
PP_5530	PP_5530	Uncharacterized protein	1.01	2.01	0.0374

Table 2.7 *Upregulated proteins*

proteins that use iron as a cofactor, such as cytochromes involved in electron transport, are often down-regulated due to the lack of iron availability needed for protein function.[74-75] Our RNA-Seq data showed 11 genes predicted to encode iron-binding proteins were down-regulated in response to promysalin (Table 2.8). Two of these encode part of the cytochrome C maturation (*ccm*) system that is involved with heme transport and cytochrome C biosynthesis.[76-77] The remaining genes in this category are annotated as cytochrome subunits or cytochrome-type proteins involved in electron transport. Taken together, these findings suggest that promysalin treated cells are experiencing an iron deficient environment. While it is tempting to speculate that the iron-binding properties of promysalin allow it to sequester iron and plunge the cells into iron-limited conditions, it must be noted that we did not observe increased expression of genes involved in biosynthesis of siderophores—a hallmark of bacteria that are exposed to iron-limiting conditions. In fact, previous studies from our lab have shown that pyoverdine production is inhibited by promysalin in PP_KT2440 specifically.

Locus	Gene	Protein	Fold Change	P-value (adj)
PP_0160	PP_0160	Putative ferrioxamine receptor	-2.45	6.66E-03
PP_0481	*katA*	Catalase	-3.68	2.86E-05
PP_0482	*bfr-I*	Bacterioferritin	-4.03	6.64E-04
PP_0489	*fdoG*	Formate dehydrogenase-O major subunit	-2.00	1.28E-03
PP_1082	*bfr-II*	Bacterioferritin	-7.01	1.32E-04
PP_3332	PP_3332	Putative cytochrome c-type protein	-4.38	1.16E-02
PP_3823	PP_3823	Cytochrome c-type protein	-2.66	1.16E-03
PP_4251	*ccoO-I*	Cytochrome c oxidase subunit, cbb3-type	-3.34	2.21E-03
PP_4253	*ccoP-I*	Cbb3-type cytochrome c oxidase subunit	-2.23	1.82E-04
PP_4324	*ccmD*	Heme exporter protein D	-3.10	1.83E-03
PP_4325	*ccmC*	Protoheme IX reservoir complex subunit	-3.25	2.56E-02
PP_4839	PP_4839	Putative iron-regulated membrane protein	-2.99	8.46E-03
PP_4856	PP_4856	Ferritin, Dps family protein	-3.36	5.61E-04

Table 2.8 *Quantitative RT-PCR*

Based on our inconclusive proteomic results we postulated that promysalin might be removed by efflux from the bacteria before it can properly engage its target. Seven of the genes that are up-regulated in

response to promysalin encode putative transporters, four of which are efflux transporters and three are predicted to be involved in uptake of nutrients. Although changes in gene expression do not always correlate with phenotypic differences, the up-regulation of genes encoding proteins involved in multidrug resistance suggests a mechanism for resistance to promysalin via export.

The iron regulatory network is one of the central control mechanisms of cell metabolism. We identified Sdh as the biological target in PAO1 and PA14. Based on the high levels of homology of the enzyme between PA and PP_KT2440 we suspected that differences in metabolic capacity or preference for TCA intermediates may account for the insusceptibility. It is known that in PP_KT2440, the primary catabolic pathway for conversion of glucose to pyruvate is the Entner-Doudoroff (ED) pathway, rather than the more common Embden-Meyerhof-Parnas (EMP) pathway, due to a lack of the 6-phosphofructokinase enzyme. In rich media such as TSB, the ED pathway is the central metabolic pathway for catabolism of glucose.

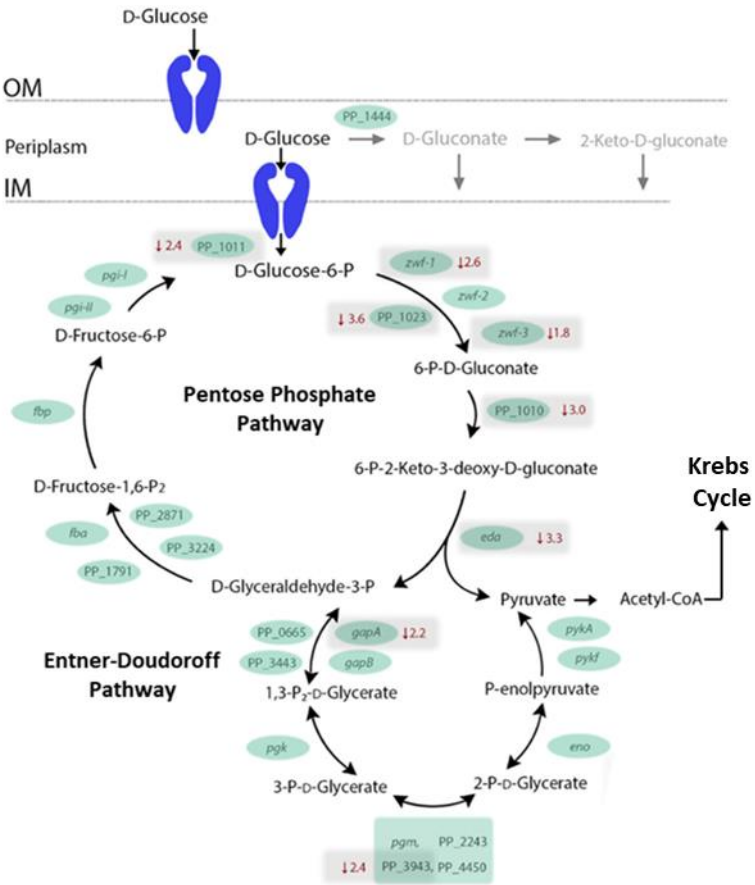

Figure 2.33 *Putida metabolism and genes involved and their response to promysalin*

Metabolites produced in the pathway are precursors for both the pentose phosphate pathway (PPP) and the TCA cycle, where the PA target is located. Our RNA-seq data revealed that expression of genes involved in several steps in the ED pathway are down-regulated (Figure 2.33). This suggests that *P. putida* cells exposed to promysalin are using alternative metabolic pathways. This is additionally supported both by the up-regulation of transporters involved in the uptake of nutrients (PP_1418, PP_2418, and PP_2543 (*gabp-II*)) and our previous finding that promysalin is toxic to PP_KT2440 when grown in succinate-supplemented minimal media.[11]

Expression of *aruC*, a gene involved in arginine metabolism, PP_1418 (*tctC*), a tricarboxylate transporter, and *benR*, a transcriptional regulator that activates transcription of genes involved with benzoate metabolism, were also up-regulated upon promysalin exposure, lending evidence to activation of alternative metabolic pathways (Figure 2.34). In related bacteria, TctC is induced during catabolite repression, and has been implicated in citrate and isocitrate import, indicating the switch to alternative routes of metabolism during promysalin treatment.[78-79] PP_3159 (*benR*) encodes a protein with similarity to the XylS family of transcriptional regulators and there are several orthologs with this group. This family

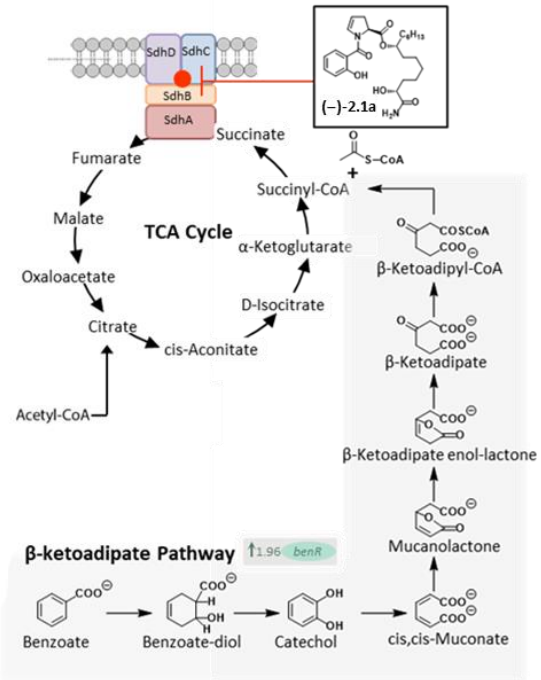

Figure 2.34 *Peripheral aromatic degradation pathway upregulated in PP upon promysalin treatment*

of transcriptional activators regulates genes involved in carbon metabolism via the β-ketoadipate pathway, stress response and pathogenesis[80]. Increased expression of *benR* suggests an increase in utilization of the β-ketoadipate pathway. It is intriguing to postulate that PP_KT2440 is able to digest promysalin by down-regulating genes en route to the TCA cycle and up-regulating the peripheral pathways to avoid toxicity, as these pathways are commonly used to catabolize xenobiotics. In a similar fashion, PP_KT2440 has been shown to combat the toxicity of trinitrotoluene (TNT), a nitroaromatic compound, by up-regulating genes encoding a xenobiotic reductase pathway, XenR, in addition to the up-regulation of efflux pumps.[81] This finding, in particular, is relevant as the major hit in our initial proteomic assay was PP_1478, a putative Xenobiotic reductase, lending credence that it might be the preferred target within PP_KT2440. While it certainly may not be the only aspect at play, modifications in metabolism indicate other bacteria may identify promysalin as a xenobiotic and as such modify their functions for its removal.

PP_2430 and PP_3022 belong to the AraC family of transcriptional regulators. These proteins are widespread among bacteria, and regulate transcription of genes having a myriad of functions including carbon metabolism and stress response.[82-83] Additionally, AraC regulators also function as negative regulators which could play a regulatory role in the down-regulation of genes in promysalin-treated cells.[84]

Our findings add to the discoveries of others who have reported on transcriptional changes of PP_KT2440 to various small molecule stressors. Dominguez-Cuevas et al. reported that when PP_KT2440 is exposed to toluene (a stress) they redirect priorities of the cell to more vital tasks.[29] For example, upon exposure PP_KT2440 increases expression of several genes that encode chaperones and genes involved in general metabolism. Flagella and chemotaxis genes were shown to be repressed under this type of stress.[29] Similarly, upon exposure to promysalin we observed differences in expression for genes related to heat shock, motility, metabolism, and iron acquisition. However, these systems are down-regulated in the presence of promysalin, suggesting the bacteria are not experiencing a stressful condition. We did however observe decreased expression of genes related to motility, iron homeostasis, and repression of genes involved in primary metabolism, which is consistent with a strategy to redirect resources to save energy.[29]

In natural environments, competition between bacteria for resources can lead to production of compounds designed to promote the survivability of the producing species, and/or inhibit growth of competing species. Often, these natural products are secondary metabolites with a very narrow distribution among species, and have a variety of functions including cell signaling, inter-species or even inter-kingdom communication, chemotaxis, and antimicrobial activity.[30] In the rhizosphere, bacteria experience extreme competition for the limited resources in the soil, and an array of biologically active compounds have been isolated from the bacteria that reside in this niche that can inhibit growth of (bacteriostatic), or kill (bactericidal) other non-producing species of bacteria.[5, 31]

Taken together, our results suggest that PP_KT2440 is able to tolerate promysalin exposure by taking a two-prong approach. First, it up-regulates efflux and nutrient transporter genes, presumably minimizing promysalin exposure while simultaneously compensating for metabolic changes. Evaluating the expression of efflux transporters in *P. aeruginosa* or expressing efflux transporters from *P. putida* in *P. aeruginosa* may provide insight into other possible resistance mechanisms. Second, it redistributes metabolic flux to avoid Sdh, which in turn triggers a localized "iron-limited" response. However, this effect is quite surprising, as no difference in gene expression was observed for siderophore biosynthesis genes (and, pyoverdine) between cells exposed to promysalin or left untreated, which one would expect for such a response. It is possible that the metabolic rerouting that occurs to avoid Sdh deemphasizes the importance of Fe^{3+} which in turn limits pyoverdine production in an effort to maximize resources and is ultimately responsible for this localized response. These findings complement our earlier work and add credence to the hypothesis that promysalin elicits its narrow-spectrum activity via targeting primary metabolism in *Pseudomonas spp.*

2.11 References

1. Fair, R. J.; Tor, Y., Antibiotics and bacterial resistance in the 21st century. *Perspect Medicin Chem* **2014,** *6*, 25-64.
2. Walsh, C., Molecular mechanisms that confer antibacterial drug resistance. *Nature* **2000,** *406* (6797), 775-81.
3. Maxson, T.; Mitchell, D. A., Targeted Treatment for Bacterial Infections: Prospects for Pathogen-Specific Antibiotics Coupled with Rapid Diagnostics. *Tetrahedron* **2016,** *72* (25), 3609-3624.
4. Gellatly, S. L.; Hancock, R. E., Pseudomonas aeruginosa: new insights into pathogenesis and host defenses. *Pathog Dis* **2013,** *67* (3), 159-73.
5. Cutting, G. R., Cystic fibrosis genetics: from molecular understanding to clinical application. *Nat Rev Genet* **2015,** *16* (1), 45-56.
6. Govan, J. R. W.; Deretic, V., Microbial Pathogenesis in Cystic Fibrosis: Mucoid Pseudomonas aeruginosa and Burkholderia cepacia. *Microbiological Reviews* **1996,** *60* (3), 539-574.
7. CDC Biggest Threats and Data.
8. Bartholomew, J. W.; Mittwer, T., The Gram Stain. *Bacteriology Reviews* **1952,** *19*, 1-29.
9. Delcour, A. H., Outer membrane permeability and antibiotic resistance. *Biochim Biophys Acta* **2009,** *1794* (5), 808-16.
10. Vasoo, S.; Barreto, J. N.; Tosh, P. K., Emerging issues in gram-negative bacterial resistance: an update for the practicing clinician. *Mayo Clin Proc* **2015,** *90* (3), 395-403.
11. Peleg, A. Y.; Hooper, D. C., Hospital-acquired infections due to gram-negative bacteria. *N Engl J Med* **2010,** *362* (19), 1804-13.
12. Richter, M. F.; Drown, B. S.; Riley, A. P.; Garcia, A.; Shirai, T.; Svec, R. L.; Hergenrother, P. J., Predictive compound accumulation rules yield a broad-spectrum antibiotic. *Nature* **2017,** *545* (7654), 299-304.
13. Richter, M. F.; Hergenrother, P. J., The challenge of converting Gram-positive-only compounds into broad-spectrum antibiotics. *Ann N Y Acad Sci* **2018**.
14. Vlassak, K.; Vanholm, L.; Duchateau, L.; Vanderleyden, J.; Demot, R., Isolation and Characterization of Fluorescent Pseudomonas Associated with the Roots of Rice and Banana Grown in Sri-Lanka. *Plant and Soil* **1992,** *145* (1), 51-63.
15. Herrmann, J.; Fayad, A. A.; Muller, R., Natural products from myxobacteria: novel metabolites and bioactivities. *Nat Prod Rep* **2017,** *34* (2), 135-160.
16. Li, W.; Estrada-de los Santos, P.; Matthijs, S.; Xie, G. L.; Busson, R.; Cornelis, P.; Rozenski, J.; De Mot, R., Promysalin, a salicylate-containing Pseudomonas putida antibiotic, promotes surface colonization and selectively targets other Pseudomonas. *Chem Biol* **2011,** *18* (10), 1320-30.
17. Blin, K.; Medema, M. H.; Kazempour, D.; Fischbach, M. A.; Breitling, R.; Takano, E.; Weber, T., antiSMASH 2.0--a versatile platform for genome mining of secondary metabolite producers. *Nucleic Acids Res* **2013,** *41* (Web Server issue), W204-12.
18. Imker, H. J.; Walsh, C. T.; Wuest, W. M., SylC catalyzes ureido-bond formation during biosynthesis of the proteasome inhibitor syringolin A. *J Am Chem Soc* **2009,** *131* (51), 18263-5.
19. Stachelhaus, T.; Mootz, H. D.; Marahiel, M. A., The specificity-conferring code of adenylation domains in nonribosomal peptide synthetases. *Chemistry & Biology* **1999,** *6* (8), 493-505.
20. An, C.; Hoye, A. T.; Smith, A. B., 3rd, Total synthesis of (-)-irciniastatin B and structural confirmation via chemical conversion to (+)-irciniastatin A (psymberin). *Organic letters* **2012,** *14* (17), 4350-4353.
21. Ravel, J.; Cornelis, P., Genomics of pyoverdine-mediated iron uptake in pseudomonads. *Trends in Microbiology* **2003,** *11* (5), 195-200.
22. Taguchi, F.; Suzuki, T.; Inagaki, Y.; Toyoda, K.; Shiraishi, T.; Ichinose, Y., The siderophore pyoverdine of Pseudomonas syringae pv. tabaci 6605 is an intrinsic virulence factor in host tobacco infection. *J Bacteriol* **2010,** *192* (1), 117-26.

23. Johnstone, T. C.; Nolan, E. M., Beyond iron: non-classical biological functions of bacterial siderophores. *Dalton Trans* **2015,** *44* (14), 6320-39.
24. Marugg, J. D.; van Spanje, M.; Hoekstra, W. P. M.; Schippers, B.; Weisbeek, P. J., Isolation and Analysis of Genes Involved in Siderophore

Biosynthesis in Plant-Growth-Stimulating Pseudomonas

putida WCS358. *Journal of Bacteriology* **1985,** *164* (2), 563-570.
25. Schwyn, B.; Neilands, J. B., Universal chemical assay for the detection and determination of siderophores. *Analytical Biochemistry* **1987,** *160* (1), 47-56.
26. Kaduskar, R. D.; Dhavan, A. A.; Dallavalle, S.; Scaglioni, L.; Musso, L., Total synthesis of the salicyldehydroproline-containing antibiotic promysalin. *Tetrahedron* **2016,** *72* (16), 2034-2041.
27. Hunter, R. C.; Beveridge, T. J., Application of a pH-sensitive fluoroprobe (C-SNARF-4) for pH microenvironment analysis in Pseudomonas aeruginosa biofilms. *Appl Environ Microbiol* **2005,** *71* (5), 2501-10.
28. Cox, C. D.; Rinehart, K. L.; Moore, M. L.; Cook, J. C., Pyochelin: novel structure of an iron-chelating growth promoter for Pseudomonas aeruginosa. *Proceedings of the National Academy of Sciences* **1981,** *78* (7), 4256-4260.
29. Schlegel, K.; Lex, J.; Taraz, K.; Budzikiewicz, H., The X-Ray Structure of the Pyochelin Fe3+ Complex. *Z. Naturforsch. C* **2006,** *61*, 263-266.
30. Anthoni, U.; Christophersen, C.; Nielsen, P. H.; Gram, L.; Petersen, B. O., Pseudomonine, an Isoxazolidone with Siderophoric Activity from Pseudomonas fluorescens AH2 Isolated from Lake Victorian Nile Perch. *Journal of Natural Products* **1995,** *58* (11), 1786-1789.
31. Sattely, E. S.; Walsh, C. T., A latent oxazoline electrophile for N-O-C bond formation in pseudomonine biosynthesis. *J Am Chem Soc* **2008,** *130* (37), 12282-4.
32. Wuest, W. M.; Sattely, E. S.; Walsh, C. T., Three siderophores from one bacterial enzymatic assembly line. *J Am Chem Soc* **2009,** *131* (14), 5056-7.
33. Katayama, N.; Nozaki, Y.; Okonogi, K.; Harada, S.; Ono, H., Ferrocins, new iron-containing peptide antibiotics produced by bacteria. Taxonomy, fermentation and biological activity. *The Journal of Antibiotics* **1993,** *46* (1), 65-70.
34. Haag, H.; Hantke, K.; Drechsel, H.; Stojiljkovic, I.; Jung, G.; Zahner, H., Purification of yersiniabactin: a siderophore and possible virulence factor of Yersinia enterocolitica. *J Gen Microbiol* **1993,** *139* (9), 2159-65.
35. Choi, J. Y.; Sifri, C. D.; Goumnerov, B. C.; Rahme, L. G.; Ausubel, F. M.; Calderwood, S. B., Identification of Virulence Genes in a Pathogenic Strain of Pseudomonas aeruginosa by Representational Difference Analysis. *Journal of Bacteriology* **2002,** *184* (4), 952-961.
36. Wencewicz, T. A.; Mollmann, U.; Long, T. E.; Miller, M. J., Is drug release necessary for antimicrobial activity of siderophore-drug conjugates? Syntheses and biological studies of the naturally occurring salmycin "Trojan Horse" antibiotics and synthetic desferridanoxamine-antibiotic conjugates. *Biometals* **2009,** *22* (4), 633-48.
37. Starr, J.; Brown, M. F.; Aschenbrenner, L.; Caspers, N.; Che, Y.; Gerstenberger, B. S.; Huband, M.; Knafels, J. D.; Lemmon, M. M.; Li, C.; McCurdy, S. P.; McElroy, E.; Rauckhorst, M. R.; Tomaras, A. P.; Young, J. A.; Zaniewski, R. P.; Shanmugasundaram, V.; Han, S., Siderophore receptor-mediated uptake of lactivicin analogues in gram-negative bacteria. *J Med Chem* **2014,** *57* (9), 3845-55.
38. Wilson, R. M.; Danishefsky, S. J., Small molecule natural products in the discovery of therapeutic agents: the synthesis connection. *J Org Chem* **2006,** *71* (22), 8329-51.
39. Szpilman, A. M.; Carreira, E. M., Probing the biology of natural products: molecular editing by diverted total synthesis. *Angew Chem Int Ed Engl* **2010,** *49* (50), 9592-628.
40. Rivkin, A.; Chou, T. C.; Danishefsky, S. J., On the remarkable antitumor properties of fludelone: how we got there. *Angew Chem Int Ed Engl* **2005,** *44* (19), 2838-50.

41. Knouse, K. W.; Wuest, W. M., The enantioselective synthesis and biological evaluation of chimeric promysalin analogs facilitated by diverted total synthesis. *J Antibiot (Tokyo)* **2016,** *69* (4), 337-9.
42. Braun, V.; Pramanik, A.; Gwinner, T.; Koberle, M.; Bohn, E., Sideromycins: tools and antibiotics. *Biometals* **2009,** *22* (1), 3-13.
43. Wencewicz, T. A.; Miller, M. J., Biscatecholate-monohydroxamate mixed ligand siderophore-carbacephalosporin conjugates are selective sideromycin antibiotics that target Acinetobacter baumannii. *J Med Chem* **2013,** *56* (10), 4044-52.
44. de Carvalho, C. C.; Fernandes, P., Siderophores as "Trojan Horses": tackling multidrug resistance? *Front Microbiol* **2014,** *5*, 290.
45. Butler, M. S.; Blaskovich, M. A.; Cooper, M. A., Antibiotics in the clinical pipeline at the end of 2015. *J Antibiot (Tokyo)* **2017,** *70* (1), 3-24.
46. van Delden, C.; Page, M. G.; Kohler, T., Involvement of Fe uptake systems and AmpC beta-lactamase in susceptibility to the siderophore monosulfactam BAL30072 in Pseudomonas aeruginosa. *Antimicrob Agents Chemother* **2013,** *57* (5), 2095-102.
47. Moynie, L.; Luscher, A.; Rolo, D.; Pletzer, D.; Tortajada, A.; Weingart, H.; Braun, Y.; Page, M. G.; Naismith, J. H.; Kohler, T., Structure and Function of the PiuA and PirA Siderophore-Drug Receptors from Pseudomonas aeruginosa and Acinetobacter baumannii. *Antimicrob Agents Chemother* **2017,** *61* (4).
48. Noinaj, N.; Guillier, M.; Barnard, T. J.; Buchanan, S. K., TonB-dependent transporters: regulation, structure, and function. *Annu Rev Microbiol* **2010,** *64*, 43-60.
49. Luscher, A.; Moynie, L.; Auguste, P. S.; Bumann, D.; Mazza, L.; Pletzer, D.; Naismith, J. H.; Kohler, T., TonB-Dependent Receptor Repertoire of Pseudomonas aeruginosa for Uptake of Siderophore-Drug Conjugates. *Antimicrob Agents Chemother* **2018,** *62* (6).
50. Li, Z.; Hao, P.; Li, L.; Tan, C. Y.; Cheng, X.; Chen, G. Y.; Sze, S. K.; Shen, H. M.; Yao, S. Q., Design and synthesis of minimalist terminal alkyne-containing diazirine photo-crosslinkers and their incorporation into kinase inhibitors for cell- and tissue-based proteome profiling. *Angew Chem Int Ed Engl* **2013,** *52* (33), 8551-6.
51. Steele, A. D.; Keohane, C. E.; Knouse, K. W.; Rossiter, S. E.; Williams, S. J.; Wuest, W. M., Diverted Total Synthesis of Promysalin Analogs Demonstrates That an Iron-Binding Motif Is Responsible for Its Narrow-Spectrum Antibacterial Activity. *J Am Chem Soc* **2016,** *138* (18), 5833-6.
52. Boersema, P. J.; Raijmakers, R.; Lemeer, S.; Mohammed, S.; Heck, A. J., Multiplex peptide stable isotope dimethyl labeling for quantitative proteomics. *Nat Protoc* **2009,** *4* (4), 484-94.
53. Meylan, S.; Porter, C. B.; Yang, J. H.; Belenky, P.; Gutierrez, A.; Lobritz, M. A.; Park, J.; Kim, S. H.; Moskowitz, S. M.; Collins, J. J., Carbon Sources Tune Antibiotic Susceptibility in Pseudomonas aeruginosa via Tricarboxylic Acid Cycle Control. *Cell Chem Biol* **2017,** *24* (2), 195-206.
54. Yankovskaya, V.; Horsefield, R.; Tornroth, S.; Luna-Chavez, C.; Miyoshi, H.; Leger, C.; Byrne, B.; Cecchini, G.; Iwata, S., Architecture of succinate dehydrogenase and reactive oxygen species generation. *Science* **2003,** *299* (5607), 700-4.
55. Sierotzki, H.; Scalliet, G., A review of current knowledge of resistance aspects for the next-generation succinate dehydrogenase inhibitor fungicides. *Phytopathology* **2013,** *103* (9), 880-7.
56. Shima, Y.; Ito, Y.; Hatabayashi, H.; Koma, A.; Yabe, K., Five Carboxin-Resistant Mutants Exhibited Various Responses to Carboxin and Related Fungicides. *Bioscience, Biotechnology, and Biochemistry* **2014,** *75* (1), 181-184.
57. Ito, Y.; Muraguchi, H.; Seshime, Y.; Oita, S.; Yanagi, S. O., Flutolanil and carboxin resistance in Coprinus cinereus conferred by a mutation in the cytochrome b560 subunit of succinate dehydrogenase complex (Complex II). *Mol Genet Genomics* **2004,** *272* (3), 328-35.
58. Li, S.; Li, T.; Xu, Y.; Zhang, Q.; Zhang, W.; Che, S.; Liu, R.; Wang, Y.; Bartlam, M., Structural insights into YfiR sequestering by YfiB in Pseudomonas aeruginosa PAO1. *Sci Rep* **2015,** *5*, 16915.
59. Malone, J. G.; Jaeger, T.; Spangler, C.; Ritz, D.; Spang, A.; Arrieumerlou, C.; Kaever, V.; Landmann, R.; Jenal, U., YfiBNR mediates cyclic di-GMP dependent small colony variant formation and persistence in Pseudomonas aeruginosa. *PLoS Pathog* **2010,** *6* (3), e1000804.

60. Akram, M., Citric acid cycle and role of its intermediates in metabolism. *Cell Biochem Biophys* **2014,** *68* (3), 475-8.
61. Malone, J. G.; Jaeger, T.; Manfredi, P.; Dotsch, A.; Blanka, A.; Bos, R.; Cornelis, G. R.; Haussler, S.; Jenal, U., The YfiBNR signal transduction mechanism reveals novel targets for the evolution of persistent Pseudomonas aeruginosa in cystic fibrosis airways. *PLoS Pathog* **2012,** *8* (6), e1002760.
62. Hederstedt, L.; Rutberg, L., Succinate Dehydrogenase - a Comparative Review. *Microbiological Reviews* **1981,** *45* (4), 542-555.
63. Kornberg, H. L., The role and control of the glyoxylate cycle inEscherichia coli. *Biochemical Journal* **1966,** *99* (1), 1-11.
64. Mogi, T.; Kawakami, T.; Arai, H.; Igarashi, Y.; Matsushita, K.; Mori, M.; Shiomi, K.; Omura, S.; Harada, S.; Kita, K., Siccanin rediscovered as a species-selective succinate dehydrogenase inhibitor. *J Biochem* **2009,** *146* (3), 383-7.
65. Lee, S. A.; Gallagher, L. A.; Thongdee, M.; Staudinger, B. J.; Lippman, S.; Singh, P. K.; Manoil, C., General and condition-specific essential functions of Pseudomonas aeruginosa. *Proc Natl Acad Sci U S A* **2015,** *112* (16), 5189-94.
66. Wu, M.; Guina, T.; Brittnacher, M.; Nguyen, H.; Eng, J.; Miller, S. I., The Pseudomonas aeruginosa proteome during anaerobic growth. *J Bacteriol* **2005,** *187* (23), 8185-90.
67. Chavarria, M.; Nikel, P. I.; Perez-Pantoja, D.; de Lorenzo, V., The Entner-Doudoroff pathway empowers Pseudomonas putida KT2440 with a high tolerance to oxidative stress. *Environ Microbiol* **2013,** *15* (6), 1772-85.
68. Fahnoe, K. C.; Flanagan, M. E.; Gibson, G.; Shanmugasundaram, V.; Che, Y.; Tomaras, A. P., Non-traditional antibacterial screening approaches for the identification of novel inhibitors of the glyoxylate shunt in gram-negative pathogens. *PLoS One* **2012,** *7* (12), e51732.
69. Keohane, C. E.; Steele, A. D.; Fetzer, C.; Khowsathit, J.; Van Tyne, D.; Moynie, L.; Gilmore, M. S.; Karanicolas, J.; Sieber, S. A.; Wuest, W. M., Promysalin Elicits Species-Selective Inhibition of Pseudomonas aeruginosa by Targeting Succinate Dehydrogenase. *J Am Chem Soc* **2017,** *Accepted*, DOI: 10.1021/ja-2017-112122
70. Heo, A.; Jang, H. J.; Sung, J. S.; Park, W., Global transcriptome and physiological responses of Acinetobacter oleivorans DR1 exposed to distinct classes of antibiotics. *PLoS One* **2014,** *9* (10), e110215.
71. Slager, J.; Kjos, M.; Attaiech, L.; Veening, J. W., Antibiotic-induced replication stress triggers bacterial competence by increasing gene dosage near the origin. *Cell* **2014,** *157* (2), 395-406.
72. Steele, A. D.; Knouse, K. W.; Keohane, C. E.; Wuest, W. M., Total synthesis and biological investigation of (-)-promysalin. *J Am Chem Soc* **2015,** *137* (23), 7314-7.
73. Rivera, M., Bacterioferritin: Structure, Dynamics, and Protein-Protein Interactions at Play in Iron Storage and Mobilization. *Acc Chem Res* **2017,** *50* (2), 331-340.
74. Gao, T.; O'Brian, M. R., Iron-dependent cytochrome c1 expression is mediated by the status of heme in Bradyrhizobium japonicum. *J Bacteriol* **2005,** *187* (15), 5084-9.
75. Lim, C. K.; Hassan, K. A.; Tetu, S. G.; Loper, J. E.; Paulsen, I. T., The effect of iron limitation on the transcriptome and proteome of Pseudomonas fluorescens Pf-5. *PLoS One* **2012,** *7* (6), e39139.
76. Goddard, A. D.; Stevens, J. M.; Rao, F.; Mavridou, D. A.; Chan, W.; Richardson, D. J.; Allen, J. W.; Ferguson, S. J., c-Type cytochrome biogenesis can occur via a natural Ccm system lacking CcmH, CcmG, and the heme-binding histidine of CcmE. *J Biol Chem* **2010,** *285* (30), 22882-9.
77. Stevens, J. M.; Mavridou, D. A.; Hamer, R.; Kritsiligkou, P.; Goddard, A. D.; Ferguson, S. J., Cytochrome c biogenesis System I. *FEBS J* **2011,** *278* (22), 4170-8.
78. Brocker, M.; Schaffer, S.; Mack, C.; Bott, M., Citrate utilization by Corynebacterium glutamicum is controlled by the CitAB two-component system through positive regulation of the citrate transport genes citH and tctCBA. *J Bacteriol* **2009,** *191* (12), 3869-80.
79. Widenhorn, K. A.; Somers, J. M.; Kay, W. W., Genetic regulation of the tricarboxylate transport operon (tctI) of Salmonella typhimurium. *J Bacteriol* **1989,** *171* (8), 4436-41.

80. Gallegos, M. T.; Williams, P. A.; Ramos, J. L., Transcriptional control of the multiple catabolic pathways encoded on the TOL plasmid pWW53 of Pseudomonas putida MT53. *J Bacteriol* **1997,** *179* (16), 5024-9.
81. Fernandez, M.; Duque, E.; Pizarro-Tobias, P.; Van Dillewijn, P.; Wittich, R. M.; Ramos, J. L., Microbial responses to xenobiotic compounds. Identification of genes that allow Pseudomonas putida KT2440 to cope with 2,4,6-trinitrotoluene. *Microb Biotechnol* **2009,** *2* (2), 287-94.
82. Frota, C. C.; Papavinasasundaram, K. G.; Davis, E. O.; Colston, M. J., The AraC family transcriptional regulator Rv1931c plays a role in the virulence of Mycobacterium tuberculosis. *Infect Immun* **2004,** *72* (9), 5483-6.
83. Khoroshkin, M. S.; Leyn, S. A.; Van Sinderen, D.; Rodionov, D. A., Transcriptional Regulation of Carbohydrate Utilization Pathways in the Bifidobacterium Genus. *Front Microbiol* **2016,** *7*, 120.
84. Rowe, S. E.; Campbell, C.; Lowry, C.; O'Donnell, S. T.; Olson, M. E.; Lindgren, J. K.; Waters, E. M.; Fey, P. D.; O'Gara, J. P., AraC-Type Regulator Rbf Controls the Staphylococcus epidermidis Biofilm Phenotype by Negatively Regulating the icaADBC Repressor SarR. *J Bacteriol* **2016,** *198* (21), 2914-2924.

Chapter 3 CD437

3.1 Introduction

3.1.1 *Staphylococcus aureus*

Staphylococcus aureus is Gram-positive pathogen responsible for a variety of infections. Most prominent in skin and tissue infections, *S. aureus* can also be the cause of pneumonia, endocarditis, and many others.[1] The dramatically high mortality rate was revolutionized by the discovery of penicillin, able to effectively kill *S. aureus*. Soon after, the appearance of resistance was identified, necessitating optimized therapeutics.[2] The mechanism of resistance, now extremely well characterized, occurs through the expression of β-lactamases (originally, penicillinase) via the hydrolysis of the β-lactam ring (Figure 3.1).[3]

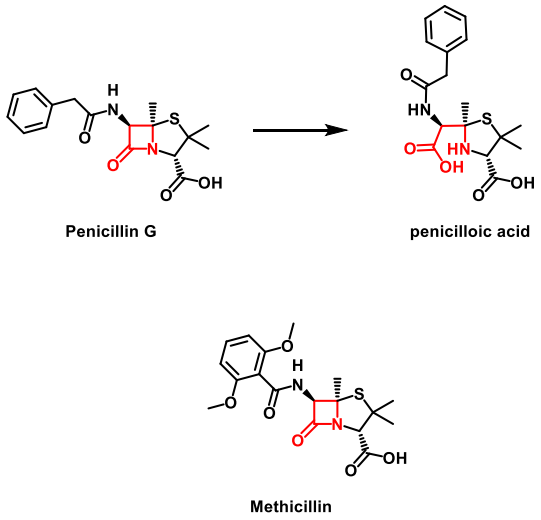

Figure 3.1 *Penicillin and methicillin*

Revolutionary, for a time, was methicillin - a semi-synthetic penicillin derivative designed to withstand degradation by β-lactamases. Unfortunately, resistance to methicillin was rapid and the emergence of Methicillin-resistant *Staphylococcus aureus* (MRSA) began.[1] Today MRSA continues to present a monumental challenge, particularly in hospitals, as it has been shown to convey resistance to all known β-lactam antibiotics.[4]

Furthering the challenges faced by researchers towards *S. aureus* and MRSA infections is the emergence of persister cells. First identified in 1944 by Joseph Bigger, persister cells were found to be a very small subset of the bacterial population that lay dormant (non-dividing) and did not display resistant phenotypes to antibiotic, yet survived antibiotic treatment. [5] This subset of bacteria now represents an additional threat posed by MRSA and its continual effect on society.

3.1.2 Persister cells

Persister cells have been identified for a variety of bacterial species based on their ability to tolerate antibiotic treatment.[6] The precise mechanism towards obtaining a tolerant state is a result of random events – rendering detailed studies challenging, especially considering persister cells of various species are quite different.[7] What is understood is that persister cells are phenotypically different than the normal population and once antibiotic treatment is complete, the original population may re-infect. A key difference between this population and a resistant population is that the newly infected population is still susceptible to antibiotics, as it is ***not*** a resistant mutant.[8-9] Unfortunately, this does not mean that the particular population could not become resistant to a given antibiotic. The differences between susceptible, resistant, and persistent bacteria can be visualized in Figure 3.2. Recent work has demonstrated that classical aminoglycoside antibiotics can be potentiated with cotreatment of metabolites to effectively kill persister cells.[10] The concept of potentiation was discussed in Chapter 1 with respect to Amoxicillin and is accomplished by co-dosing with an adjuvant. The Collins Lab accomplished utilized synergy by generation of the proton motive force (PMF), typically not in effect in dormant, persister cells. This work highlighted the ability to facilitate the entry of aminoglycosides across persister cell membranes, an additional method will be discussed in the remainder of this chapter.[11]

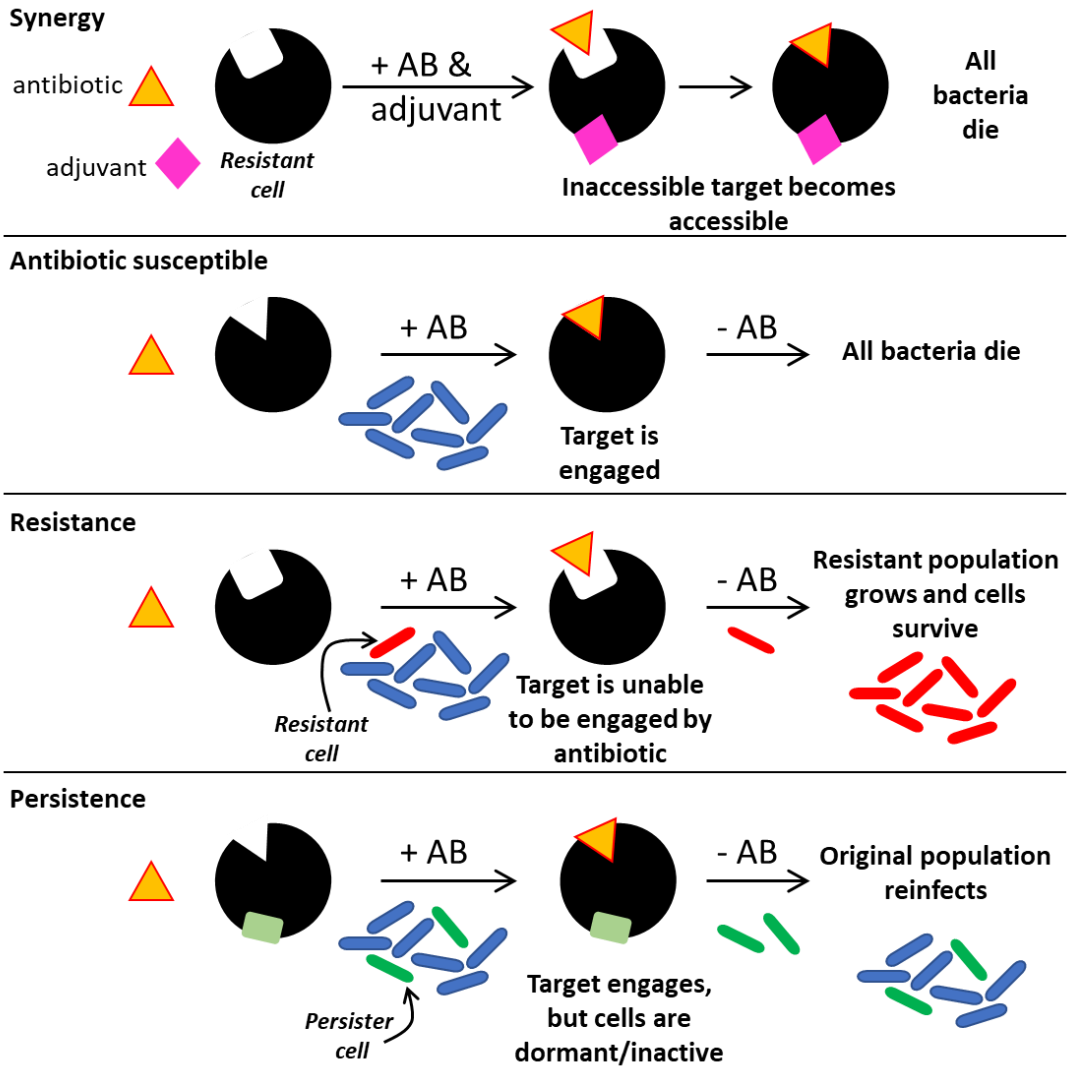

Figure 3.2 *Difference between susceptibility, resistance, and persistence*

3.2 CD437

Biological assays were completed by the Mylonakis lab (Wooseong Kim) and synthetic compounds were synthesized by Colleen Keohane and Andrew Steele, Wuest Lab. Analysis of results was done collaboratively.

3.2.1 *C. Elegans* high throughput screen identifies CD437

Our collaborators in the Mylonakis Lab at Brown University developed a HTS (high throughput screen) wherein they are able to simultaneously observe killing of MRSA as well as toxicity of the compounds on the host, *C. elegans*.[12] In the assay, SYTOX Orange is employed, as it specifically stains *dead* worms. This allows for visualization of dead worms as a result of either MRSA or toxicity of the screened compounds. Shown in Figure 3.3 is the result of a HTS wherein two compounds (**3.1** and **3.2**) were identified to have activity against MRSA persister cells relative to DMSO and vancomycin. CD437 (**3.1**) and CD5130 (**3.2**) are vitamin A analogs investigated previously for activity[13], adarotene (**3.3**) is a potential cancer drug, and adapalene (**3.4**) is a skin care additive. As indicated in Figure 3.3, Adapalene (**3.4)** was unable to prevent death of the worms, while CD437 (**3.1)**, CD1530 (**3.2**) and Adarotene (**3.3**) were.

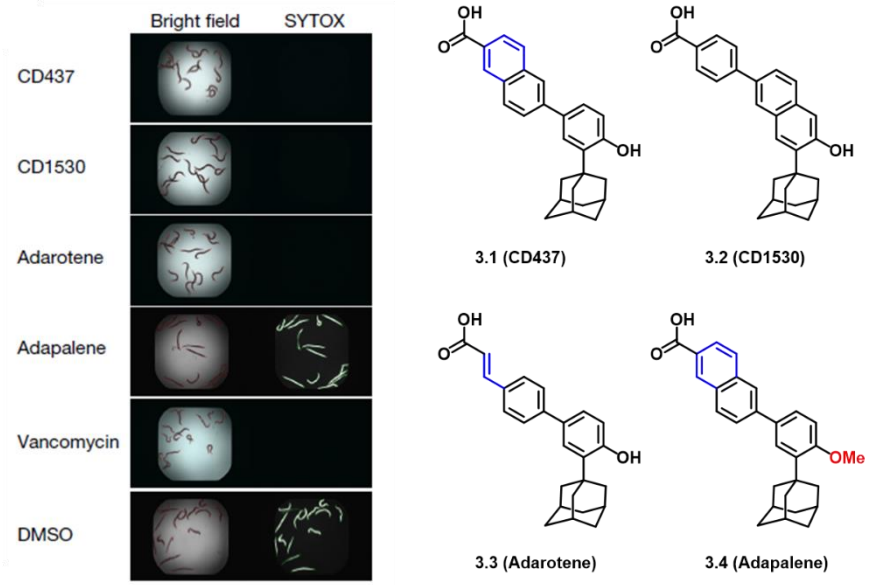

Figure 3.3 *Results of HTS against C. elegans infection.*

Further investigation provided MIC values (against *S aureus* MW2) of 1 µg/mL for CD437 and CD1530 and 2 µg/mL for adarotene with minimal resistance to all three after 100 days in comparison to ciprofloxacin and daptomycin.[11] The serial passage assay identified mutations in three genes important for membrane composition, suggesting these compounds were acting on the cell membrane. As a result of the serial passage assays, further investigation necessitated membrane integrity-based assays. SYTOX green assays show CD437, CD15230, and adarotene (all except adapalene) to exhibit membrane permeabilization of *S. aureus*, however, only CD437 and CD1530 influence membrane permeabilization of MRSA-persister cells. It was this distinct result that led to the further investigation of the mechanism of action of these retinoid compounds.

3.2.2 Proposed mechanism

Thorough mechanistic investigation was carried out by our collaborators wherein molecular dynamic simulations were conducted, the results of which are schematically depicted in Figure 3.4.

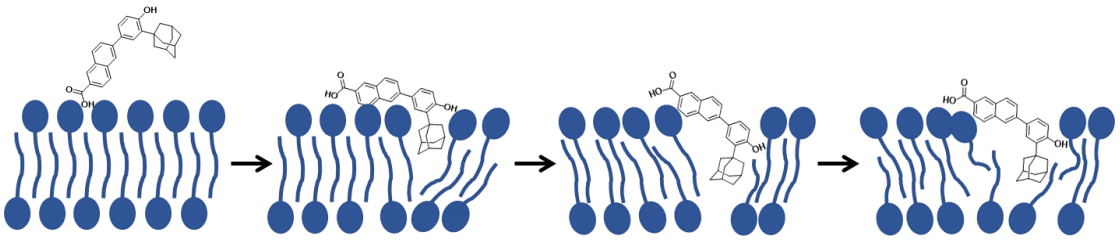

Figure 3.4 *Proposed mechanism of CD437*

Starting from an initial attachment of the polar headgroup to the lipid bilayer, a subsequent attachment of the phenol anchors the molecule from both ends, facilitating the intercalation of the greasy adamantyl moiety into the membrane. Over time, this will cause several disruptions to the membrane until the final conformation is achieved wherein the phenol and acid continue to anchor to the membrane and the adamantly resides orthogonal to the membrane.

Following the proposal of the mechanism, it was discovered that CD437 and CD1530 display synergy with gentamicin against ***both*** growing and persister MRSA cells. This observation was presumably a result of the compromised membrane, facilitating passive diffusion of gentamicin into the cell. Synthetic analogs of CD437 were required to further support the molecular dynamic simulations and will be discussed in the next section.

3.3 Synthesis of CD437 Analogs

3.3.1 First series of analogs

The first series of analogs sought to probe two key components of the proposed mechanism; the anchoring of the molecules to the membrane via acid and phenol moieties. In doing so, we imagined a series of functional group interconversions from commercially available adapalene would facilitate this investigation (Figure 3.5).

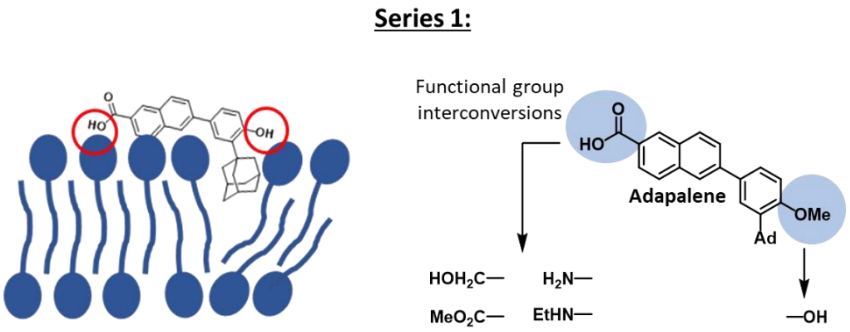

Figure 3.5 *Series one strategy*

As adapalene contains the acid moiety and a methyl ether, we envisioned first modifying the acid, in one of four ways: installation of the ethyl or primary amide (**3.5** or **3.7**), reduction to the primary alcohol (**3.9**), or formation of the methyl ester (**3.11**). Each of the first transformations would be a testable analog (containing ***neither*** an acid or phenol). Following modification of the acid, we sought to unmask each methyl ether to the phenol, providing the second set of four analogs (**3.6**, **3.8**, **3.10**, **3.11**), shown in **Error! Reference source not found.**

In the forward sense, analog **3.5** was synthesized from treatment of adapalene, **3.4**, with ethylammonium chloride, HATU, and diisopropylethylamine. Further treatment of analog **3.5** with BBr_3 in dichloromethane, provided the phenol analog, **3.6** (Scheme 3.1). In a similar fashion, adapalene, **3.4**, could be transformed to the acid chloride using oxalyl chloride and subsequently amidated with ammonium hydroxide yielding analog **3.7**. Again, treatment with BBr_3 provides access to an additional analog containing the free phenol, **3.8**.

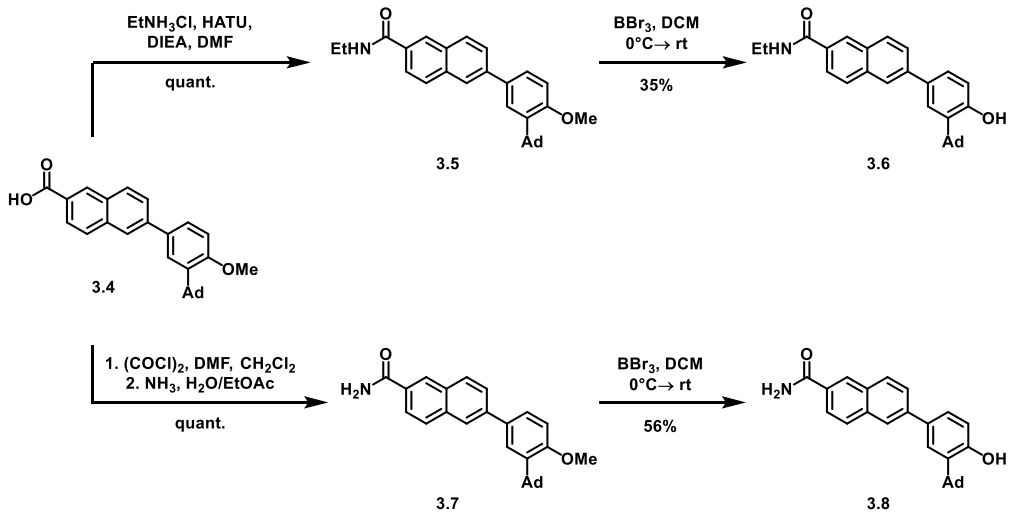

Scheme 3.1 *Synthesis of amide analogs*

The next two transformations of adapalene (**3.4**) are reduction with lithium aluminum hydride, providing primary alcohol **3.9** or treatment of **3.4** with TMS-diazomethane to install the methyl ester, **3.11** (Scheme 3.2).

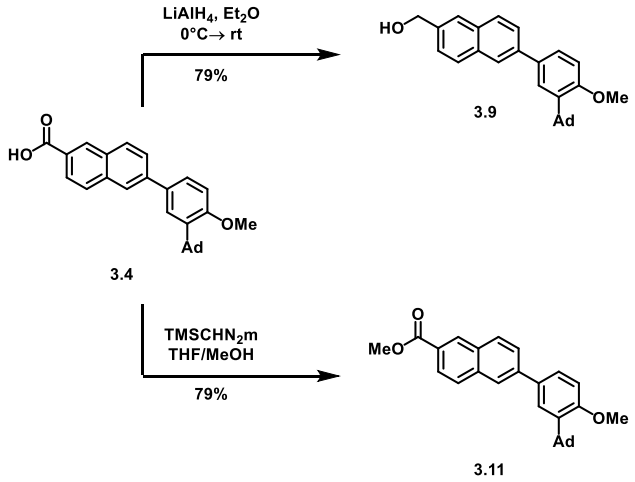

Scheme 3.2 *Synthesis of reduced and methylated analogs*

Unfortunately, analogs **3.9** and **3.11** were unable to be subsequently treated with BBr_3 and therefore synthesis of the analogous phenol derivatives (**3.10** and **3.12**) required an initial transformation of adapalene, **3.4**, to CD437, **3.1**, with BBr_3 (Scheme 3.3). Following successful removal of the methyl ether, CD347 was treated with lithium aluminum hydride to provide the primary alcohol phenol analog, **3.10**. Alternatively, CD437, **3.1**, was treated with thionyl chloride in methanol to generate the methyl ester phenol analog, **3.12** (Scheme 3.3).

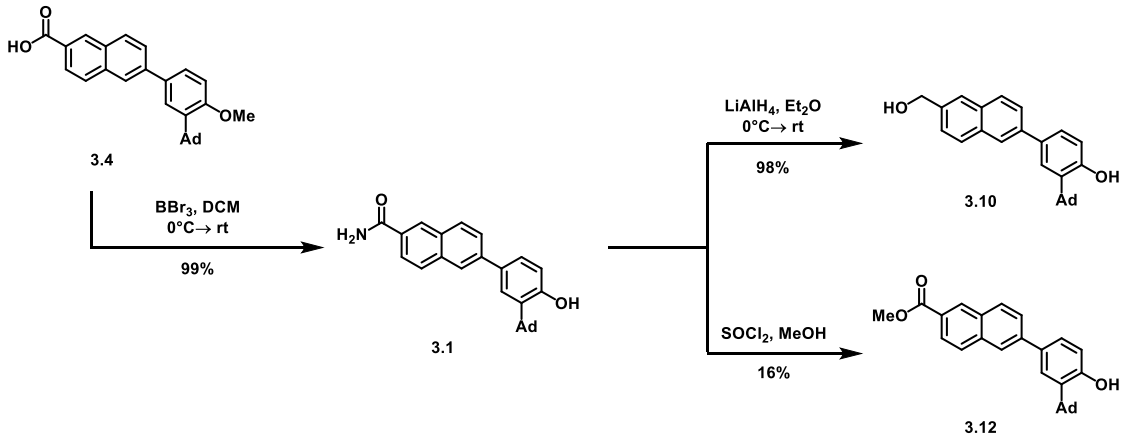

Scheme 3.3 *Synthesis of reduced and methylated* ***phenol*** *analogs*

The first eight analogs were sent to our collaborators for biological testing in one week, the results of which will be discussed in section 3.4.

3.3.2 Rationale for second series of analogs

A second series of eight potential analogs would require scaffold modifications. While CD437 was fairly active (1 μg/mL), it exhibited moderate toxicity to human cell lines. As such, we sought optimization of activity and toxicity. Towards this end, we hoped to utilize a late stage Suzuki cross-coupling, permitting derivation of both the phenol and naphthalene fragments This would provide a variety of coupling partners allowing for increased diversity (Figure 3.6). Boronic acid phenol derivatives would be designed such that one building block would represent the native fragment, a second will contain a benzyl in place of adamantane for increased flexibility within the membrane, and a third will alter the projection of adamantane into the membrane with movement of the hydroxyl group para to adamantane. The goal for the naphthalene fragments was to add hydroxyl groups, increasing the number of polar contacts, facilitating the initial attachment. To investigate which modifications (if any) effected activity or toxicity – the ‘naked’ naphthalene fragment would also be used as a coupling partner for all constructed boronic acids.

Unfortunately, efforts towards increasing functionality were not as straightforward as initially intended and will be discussed in the upcoming sections.

3.3.3 Boronic acid fragments

Synthesis of boronic acids commence with the native phenol building block. Selective installation of adamantane on 4-bromo phenol (Scheme 3.4), yields known intermediate **3.13**.[14] Following adamantylation, the phenol was protected as the MEM ether, **3.14**, and the subsequent boronic acid was

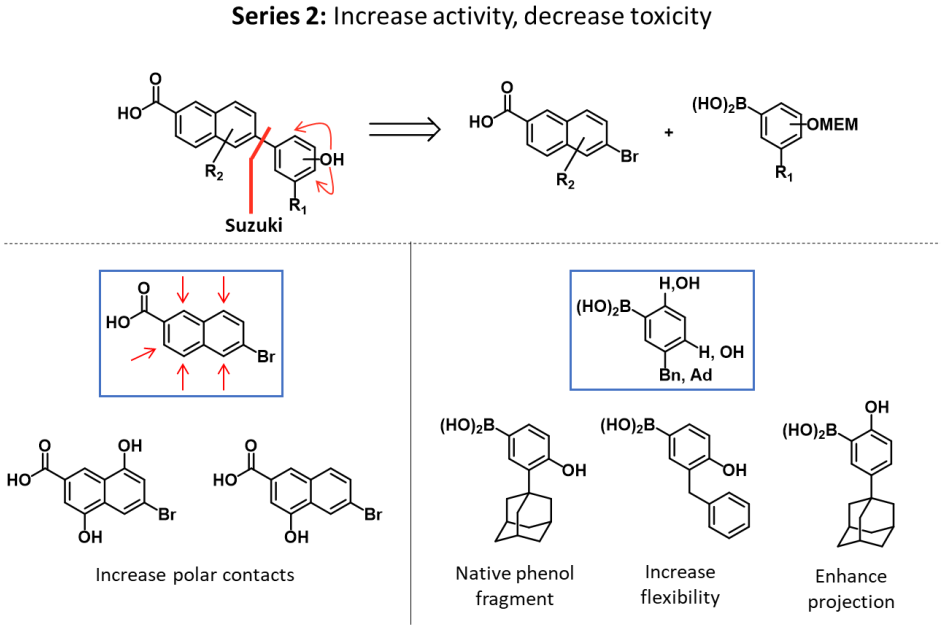

Figure 3.6 *Rationale for second series of analogs*

formed upon treatment with trimethyl borate and acidic workup conditions. Boronic acid **3.15** was isolated as a mixture with oligomers, as such the mixture was carried into the cross-couplings and yield reported over 2 steps.

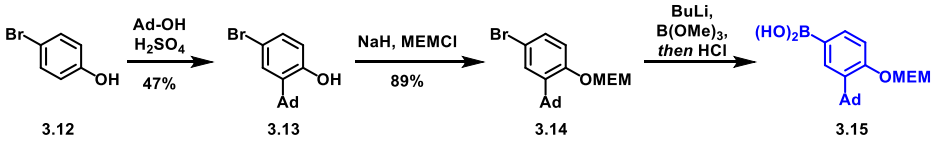

Scheme 3.4 *Synthesis of native phenol boronic acid*

Boronic acid **3.19** can be synthesized in an analogous manner starting from 2-bromo phenol (Scheme 3.5).

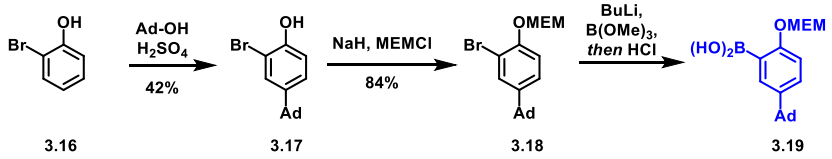

Scheme 3.5 *Synthesis of hydroxyl regioisomer boronic acid*

The final boronic acid building block **3.23** is synthesized in a similar fashion (Scheme 3.6). Starting from 2-benzylphenol, treatment with tetrabutylammonium bromide selectively installs a bromine para to the hydroxyl group, **3.21**. Protection of the free phenol as the MEM ether (**3.22**) and treatment with trimethyl borate provides boronic acid **3.23**.

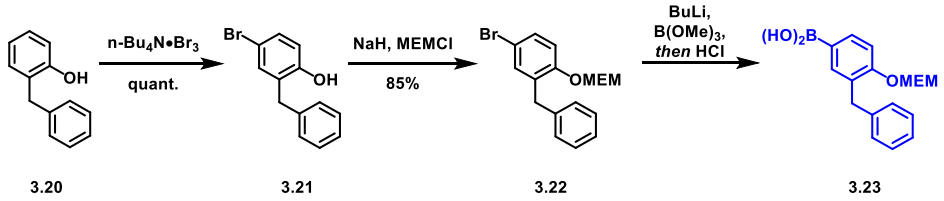

Scheme 3.6 *synthesis of benzyl boronic acid*

3.3.4 Cyclization – first strategy

At the onset of this project, we were aware of the minimal precedent for functionalizing bromonaphthalene in the manner with which we desired. Nevertheless, initial efforts of forming building blocks sought to leverage the construction of known compound **3.27** (Figure 3.7).[15] Literature precedent condenses dimethyl succinate (**3.25**) with 4-bromo benzaldehyde in the presence of potassium *tert*-butoxide to afford intermediate **3.26**. Following condensation and hydrolysis, the diacid can be subject to acid mediated intramolecular Friedel-Crafts cyclization. We sought to increase and differentially functionalize the napthalenes by starting with various methoxy substituted bromo benzaldehydes. Following an identical synthetic route would allow for the generation of four additional building blocks as we would have access to mixed hydroxy/methoxy bromonaphthalene (**3.28** and **3.30**) and dihydroxy bromonaphthalene (**3.29** and **3.31**) with treatment of BBr_3.

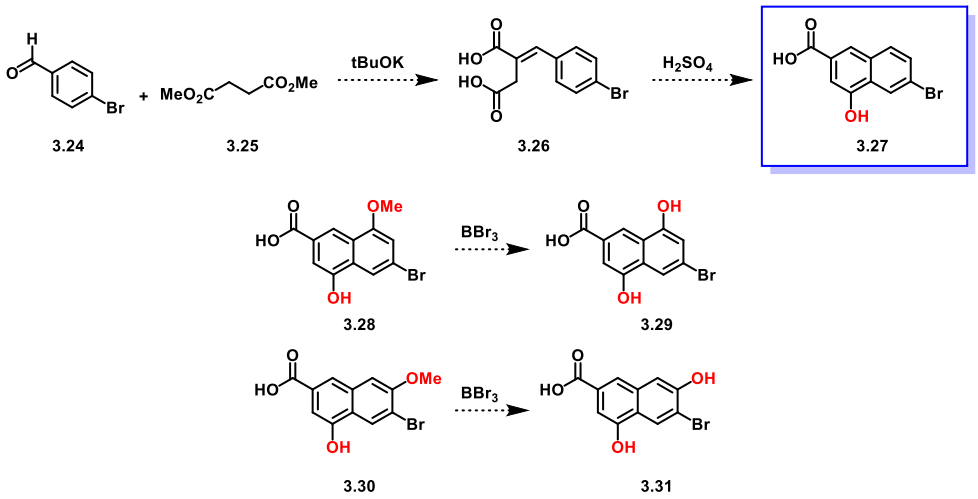

Figure 3.7 *Proposed synthetic plan of series two analogs*

Unfortunately, in our hands, the known cyclized product **3.27** was never constructed and only starting material recovered. Reaction conditions require stirring in concentrated sulfuric acid for 48 hours; increasing reaction time and temperature had no effect on product formation. Due to time restrictions (the previously submitted publication had a short window to address reviewer concerns), alternative attempts

had begun to make the minimally precedented bromonaphthalenes. However, in retrospect, the most probable rationale for recovery of starting material in all cases is outlined in Figure 3.8. The presumed intermediate, **3.32**, can react following the red arrow, proceeding to the right, yielding the desired product, **3.27**. Alternatively, trace water present in the 'concentrated' sulfuric acid would allow for an alternate pathway wherein the cyclic anhydride opens back up to the starting material, **3.26**.

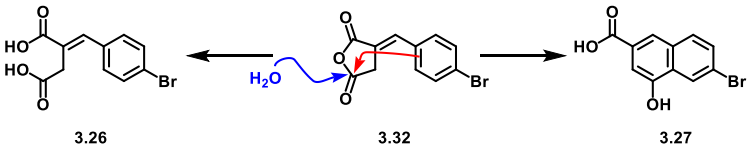

Figure 3.8 *Proposed explanation for failed cyclization attempt 1.*

3.3.5 Cyclization – second strategy

A second attempt was made to construct the bromonaphthalene building blocks, this time taking advantage of known chemistry used by the Kozlowski Lab (Scheme 3.7).[16] Starting from 4-methoxyphenylacetic acid (**3.33**), selective bromination will provide intermediate **3.34**. Treatment with thionyl chloride will generate the acid chloride intermediate that will be condensed with dimethyl malonate (**3.35**), providing Friedel-Crafts precursor **3.36**. In contrast to the failed acid mediated cyclization attempted previously, cyclization was attempted on the diacid with acetic anhydride and pyridine, successfully providing cyclized adduct **3.37**.

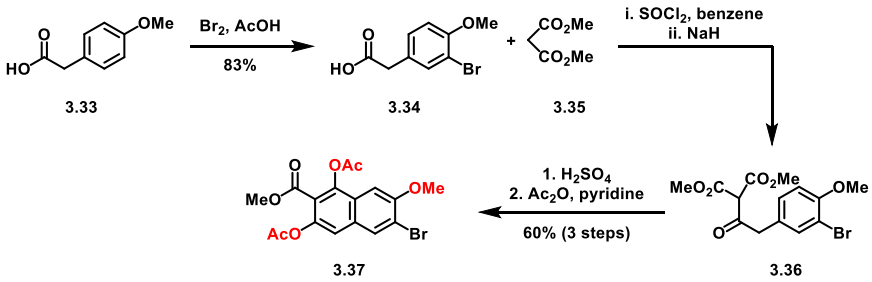

Scheme 3.7 *Kozlowski method at constructing bromo naphthalene*

With our functionalized bromonaphthalene building block in hand, we successfully coupled each boronic acid yielding intermediates **3.38**, **3.39**, **3.40** (Scheme 3.8). The initial design permitted various deprotection conditions allowing for different functionality around the naphthalene (methoxy or hydroxy). Unfortunately, upon deprotection, each proton NMR lacked one aromatic proton. Upon closer examination, removal of the acetate groups generates a reactive position on the molecules, indicated by multiple resonance structures (Scheme 3.8, bottom). We speculate the analogs dimerized following deprotection due to the reactivity at the indicated position. This doesn't come as too much of a surprise, as the Kozlowski Lab synthesized naphthalene monomers with the intent of dimerization. Unfortunately, the dimerization didn't happen spontaneously as in our case – nevertheless, we sought additional methods towards functionalizing the naphthalene ring.

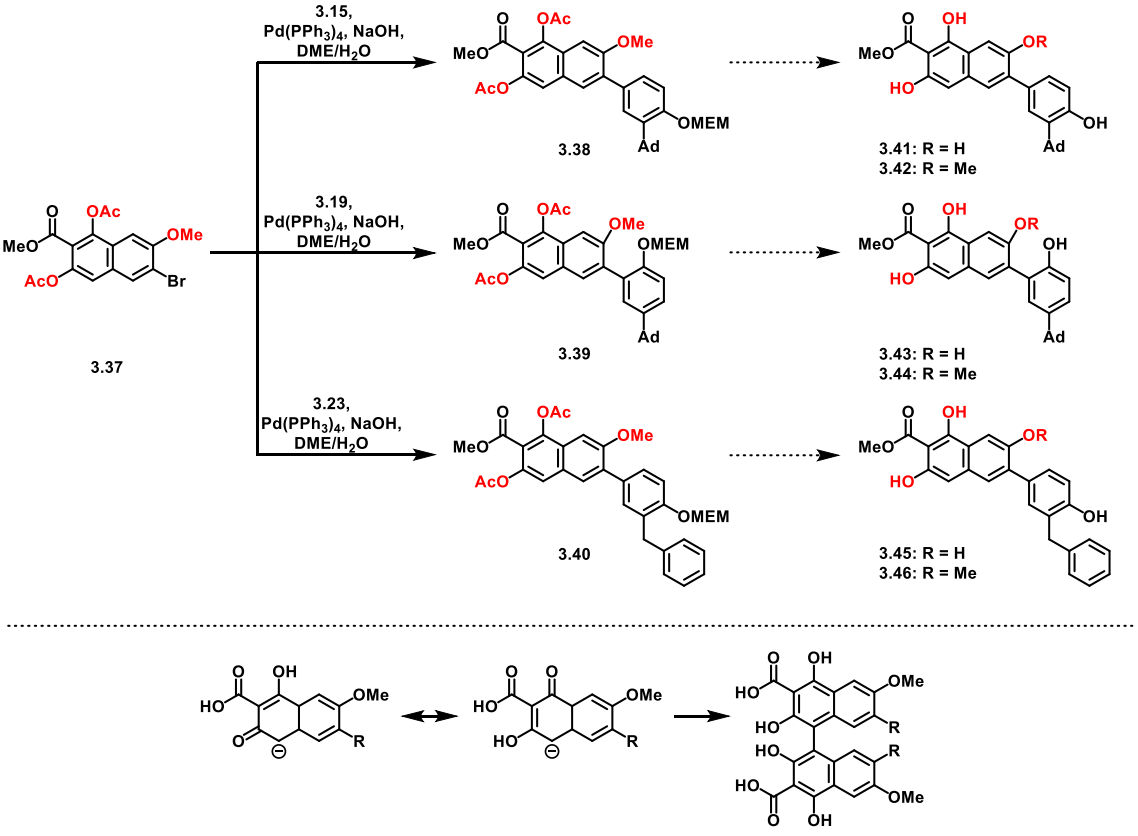

Scheme 3.8 *Deprotection of second series*

3.3.6 Final cyclization and assembly

A third, and final, assembly of the functionalized naphthalene cores utilizes phosphonate **3.48** for a Horner-Wadsworth Emmons reaction generating olefins **3.51** and **3.53**.[17] In a similar vein to previous attempts, we sought implementation of this method with two commercially available starting materials, **3.49** and **3.52**, which would provide for increased diversity (Figure 3.10). Following formation of alkenes **3.50** and **3.53**, selective hydrolysis of the *tert*-butyl ester followed by treatment with acetic anhydride and sodium acetate afforded the Friedel-Crafts cyclized products, **3.51** and **3.54**.

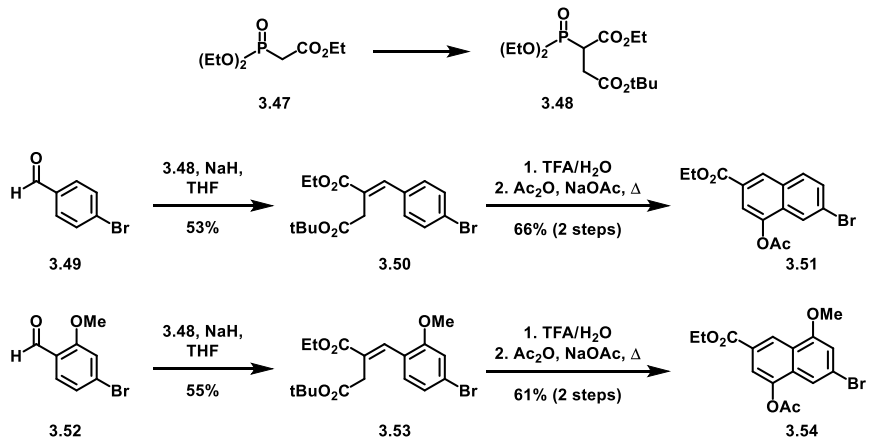

Scheme 3.9 *Final cyclization attempt*

Following successful cyclization, each bromonaphthalene was cross coupled and deprotected, this time without any obstacles. Starting with the series shown in Scheme 3.10, bromonaphthalene, **3.51**, was subject to Suzuki conditions to afford protected analogs **3.55**, **3.57**, and **3.59**. Deprotection of the acetate group was observed all three cases following the cross-coupling, leaving deprotection of the MEM ether and hydrolysis of the ethyl ester. Treatment with HCl/dioxane and subsequent saponification provides analogs **3.56**, **3.58**, **3.60**.

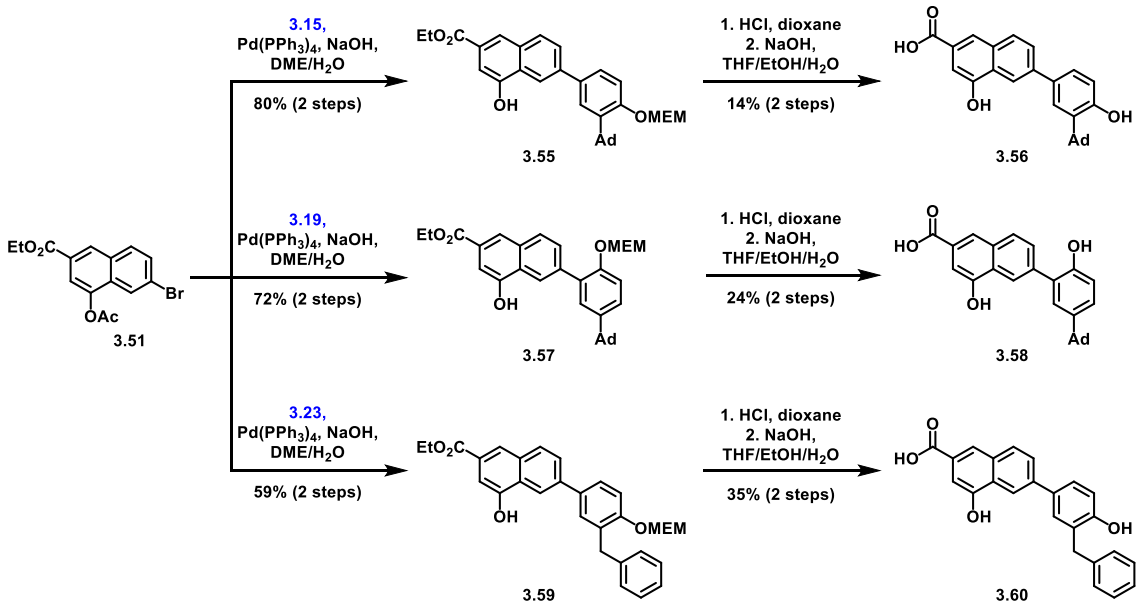

Scheme 3.10 *Hydroxy naphthalene derivatives*

In an analogous fashion, a second set of analogs was constructed from bromonaphthalene **3.54** (Scheme 3.12). When subject to Suzuki conditions with each of the three boronic acids intermediates **3.61**, **3.63**, and **3.65** were isolated. Like the previous three analogs, the acetates were removed in the cross-coupling step for **3.63** and **3.65**, however for **3.61** the acetate remained. It should be noted, the removal of the acetates during the coupling was serendipitous, however it happened in nearly all cases. Regardless of the presence (or absence) of the acetates, all three intermediates were fully deprotected (saponification, acetate removal, MEM and methyl ether deprotection) upon treatment with BBr_3 providing analogs **3.62**, **3.64**, and **3.66**. Overall yields for this step was much lower than we would have hoped, however, we initially prioritized sending of the compounds to our collaborators over optimization of yield; a task that would have come second if the compounds showed increased activity relative to CD437.

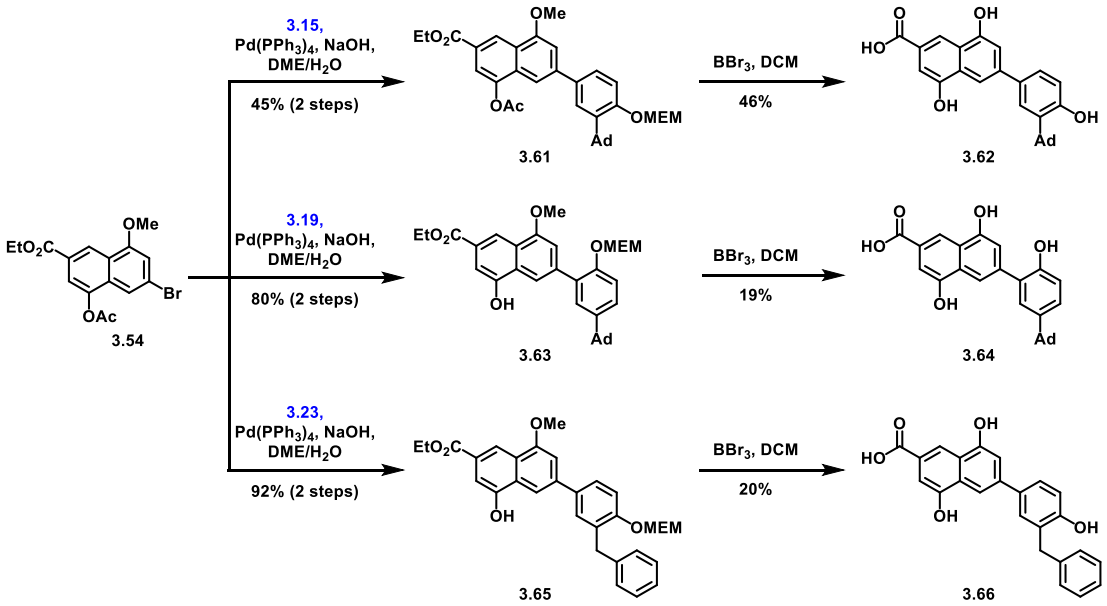

Scheme 3.12 *Bis-hydroxy derivatives*

Lastly, we sought a series of analogs using the modified phenol fragment, with an unfunctionalized bromonaphthalene (Scheme 3.11). We found the chemistry more robust when using methyl ester **3.67** in comparison to the acid derivative. Suzuki cross-couplings provided intermediates **3.68** and **3.70**. Finally, treatment with HCl/dioxane for deprotection of the MEM ether and subsequent saponification led to the final two analogs, **3.69** and **3.71**.

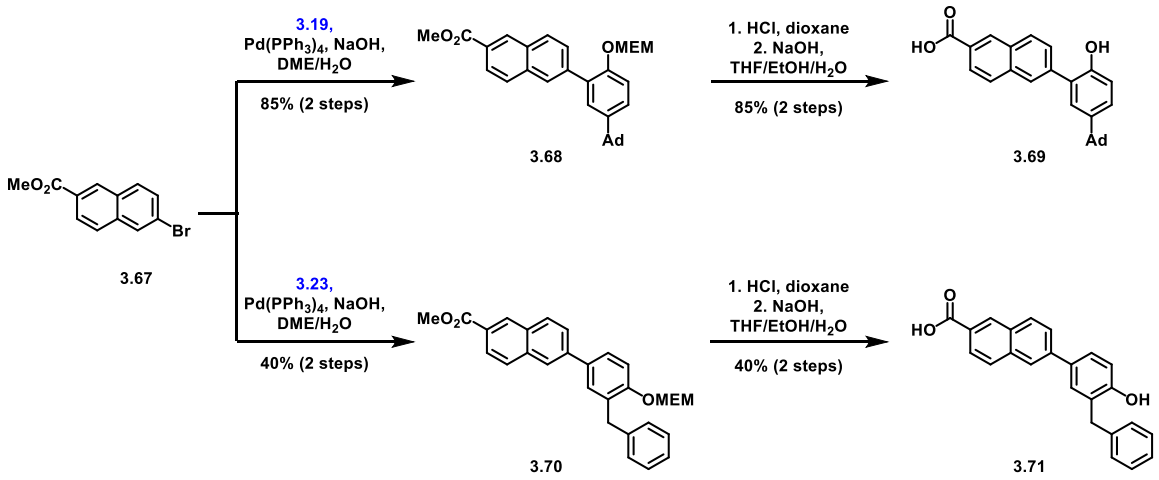

Scheme 3.11 *Naphthyl derivatives*

The second series of eight analogs were sent to our collaborators and tested for activity and toxicity, results of which will be discussed in the next section.

3.4 Biological data

Analysis of all 16 analogs initiated with inhibitory activity. Analogs active below 64 μg/mL are shown in Figure 3.9. None of the analogs had increased activity relative to CD437 (**3.1**); however, two were within one dilution, at 2 μg/mL.

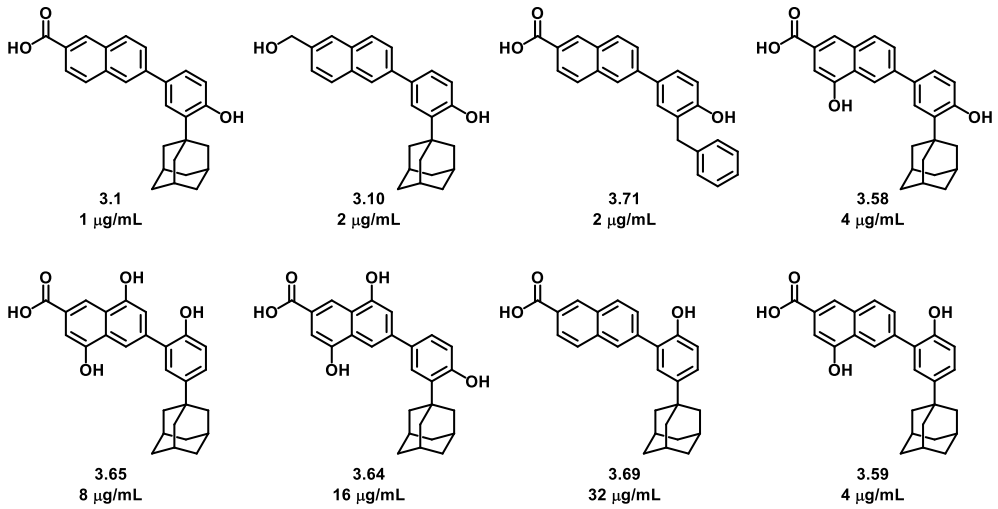

Figure 3.9 *analogs with activity*

Analyses that were initially drawn from this data supported the proposed mechanism wherein the acid and phenol were crucial for attachment to the membrane. None of the methyl ether derivatives displayed any activity and neither did either amide or methyl ester. Interestingly, the primary alcohol, **3.10**, was within one dilution of CD437 and was subject to further investigation. To our surprise, none of the analogs with additional hydroxy groups around the naphthalene showed increased activity relative to CD437. The other analog with modest activity was **3.71**, which differs from CD437 by replacing the adamantly group with a benzyl group.

Upon closer examination of the two most active analogs, **3.10** and **3.71**, we observe minimal structural changes. The activity of the two however, displays a rather significant difference (Figure 3.10). In comparison to Triton-X100, **3.10** is not lytic to red blood cells, whereas lytic behavior is observed at 16 µg/mL for analog **3.71**. Additionally, when tested against rat hepatocytes, a marked decrease of toxicity was observed for analog **3.10** over **3.71**.

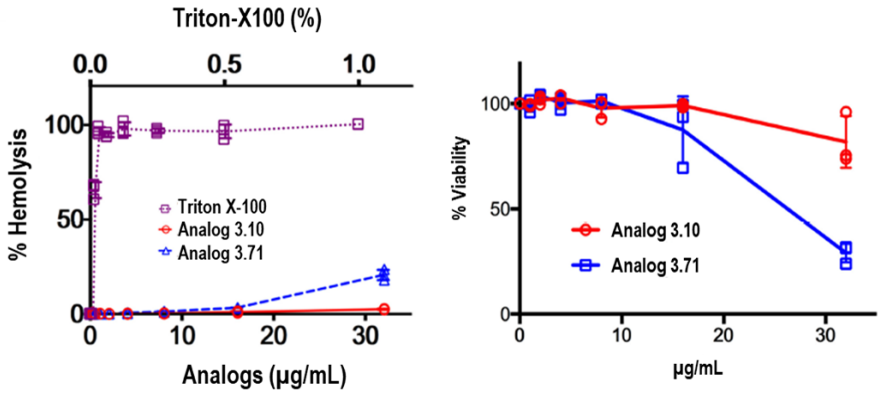

Figure 3.10 *Comparison of most active analogs*

While analog **3.10** appeared a more promising candidate to continue investigating, we still analyzed the ability of **3.71** to inhibit MRSA persisters. As shown in Figure 3.11, analog **3.71** was only able to inhibit MRSA persisters at 16 µg/mL, the same concentration at which its activity is lytic, suggesting this analogs

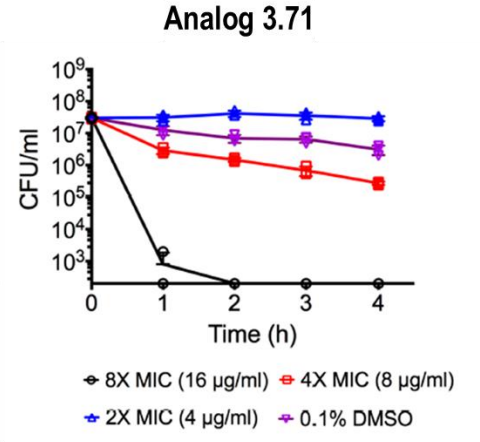

Figure 3.11 *Persister activity of* ***3.68***

activity is due to cell lysis, not membrane permeabilization. Considering this finding, it seemed more beneficial to pursue investigation of analog **3.10**.

Of the most exciting results was the activity of analog **3.10**, containing the less polar primary alcohol in place of the acid, and its significant reduction of toxicity relative to CD437 is highlighted in Figure 3.12 (top). In addition to being markedly less toxic, **3.10** retains activity against MRSA persister cells and shows synergy with gentamicin (bottom).

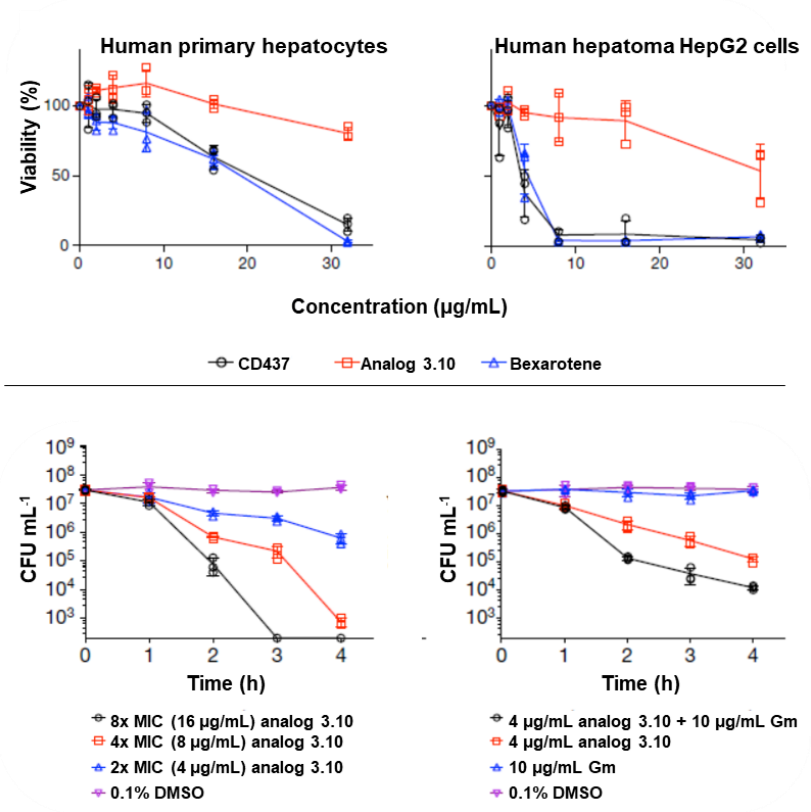

Figure 3.12 *Biological analysis of lead compound*

Pleased by these results, we synthesized approximately 500mg of analog **3.10** to send to the NIH for animal testing. At this time, it was determined that **3.10** is tolerable in considerably large quantities in mice, a promising result – unfortunately, it was also determined to bind soluble proteins.

3.5 Conclusions

This project represents an area in the antibacterial realm that has been looked at less intensely over the years. While the scientific community heavily focuses on resistance and its development, specifically targeting persister cells is less common. Furthermore, we have disclosed a previously unknown mechanism effective against persisters - membrane permeabilization. Over the course of this project we were able to provide synthetic support for molecular dynamic simulations allowing for the characterization of the new mechanism. While we were successfully able to synthesize a compound with similar inhibitory activity and significantly decreased toxicity, our analog has serum protein binding, requiring further optimization. This project is currently continuing in the Wuest Lab. Ana Cheng, another graduate student, is looking to optimize activity/toxicity via implementation of phenol bioisosteres, results of which will be reported in due course.

3.6 References

1. Peacock, S. J.; Paterson, G. K., Mechanisms of Methicillin Resistance in Staphylococcus aureus. *Annu Rev Biochem* **2015,** *84*, 577-601.
2. Rammelkamp, C. H.; Maxon, T., Resistance of *Staphylococcus aureus* to the action of penicillin. *Exp. Biol. Med.* **1942,** *51*, 386-389.
3. Lowy, F. D., Antimicrobial resistance: the example of *Staphylococcus aureus*. *J Clin Invest* **2003,** *111*, 1265-1273.
4. Grundmann, H.; Aires-de-Sousa, M.; Boyce, J.; Tiemersma, E., Emergence and resurgence of meticillin-resistant *Staphylococcus aureus* as a public-health threat. *Lancet* **2006,** *368*, 874-885.
5. Bigger, J. W., Treatment of Staphylococcal infections with penicillin. *Lancet* **1944**, 497-500.
6. Lewis, K., Persister cells, dormancy and infectious disease. *Nat Rev Microbiol* **2007,** *5* (1), 48-56.
7. Dawson, C. C.; Intapa, C.; Jabra-Rizk, M. A., "Persisters": survival at the cellular level. *PLoS Pathog* **2011,** *7* (7), e1002121.
8. Brauner, A.; Fridman, O.; Gefen, O.; Balaban, N. Q., Distinguishing between resistance, tolerance and persistence to antibiotic treatment. *Nat Rev Microbiol* **2016,** *14* (5), 320-30.
9. Cohen, N. R.; Lobritz, M. A.; Collins, J. J., Microbial persistence and the road to drug resistance. *Cell Host Microbe* **2013,** *13* (6), 632-42.
10. Allison, K. R.; Brynildsen, M. P.; Collins, J. J., Metabolite-enabled eradication of bacterial persisters by aminoglycosides. *Nature* **2011,** *473* (7346), 216-20.

11. Kim, W.; Zhu, W.; Hendricks, G. L.; Van Tyne, D.; Steele, A. D.; Keohane, C. E.; Fricke, N.; Conery, A. L.; Shen, S.; Pan, W.; Lee, K.; Rajamuthiah, R.; Fuchs, B. B.; Vlahovska, P. M.; Wuest, W. M.; Gilmore, M. S.; Gao, H.; Ausubel, F. M.; Mylonakis, E., A new class of synthetic retinoid antibiotics effective against bacterial persisters. *Nature* **2018,** *556,* 103.
12. Rajamuthiah, R.; Fuchs, B. B.; Jayamani, E.; Kim, Y.; Larkins-Ford, J.; Conery, A.; Ausubel, F. M.; Mylonakis, E., Whole animal automated platform for drug discovery against multi-drug resistant Staphylococcus aureus. *PLoS One* **2014,** *9* (2), e89189.
13. Altucci, L.; Leibowitz, M. D.; Ogilvie, K. M.; de Lera, A. R.; Gronemeyer, H., RAR and RXR modulation in cancer and metabolic disease. *Nat Rev Drug Discov* **2007,** *6* (10), 793-810.
14. Cincinelli, R.; Dallavalle, S.; Nannei, R.; Carella, S.; De Zani, D.; Merlini, L.; Penco, S.; Garattini, E.; Giannini, G.; Pisano, C.; Vesci, L.; Carminati, P.; Zuco, V.; Zanchi, C.; Zunino, F., Synthesis and structure-activity relationships of a new series of retinoid-related biphenyl-4-ylacrylic acids endowed with antiproliferative and proapoptotic activity. *J Med Chem* **2005,** *48* (15), 4931-46.
15. Liang, J. L.; Javed, U.; Lee, S. H.; Park, J. G.; Jahng, Y., Synthesis of 6-deoxymollugins and their inhibitory activities on tyrosinase. *Arch Pharm Res* **2014,** *37* (7), 862-72.
16. Morgan, B. J.; Mulrooney, C. A.; O'Brien, E. M.; Kozlowski, M. C., Perylenequinone natural products: total syntheses of the diastereomers (+)-phleichrome and (+)-calphostin D by assembly of centrochiral and axial chiral fragments. *J Org Chem* **2010,** *75* (1), 30-43.
17. Boger, D. L.; Han, N.; Tarby, C. M.; Boyce, C. W.; Cai, H.; Jin, Q.; Kitos, P. A., Synthesis, Chemical Properties, and Preliminary Evaluation of Substituted CBI Analogs of CC-1065 and the Duocarmycins Incorporating the 7-Cyano-1,2,9,9a-tetrahydrocyclopropa[c]benz[e]indol-4-one Alkylation Subunit: Hammett Quantitation of the Magnitude of Electronic Effects on Functional Reactivity. *J Org Chem* **1996,** *61* (15), 4894-4912.

Chapter 4 Conclusion

In conclusion, we have been able to demonstrate the potential of alternative inhibitory mechanisms towards the combat of antibiotic resistance.[1-2] Conceptually, we hope to take advantage of current antibiotic deficiencies through accounting for differences inherent between bacterial species. The rhizosphere represents an ideal environment towards studying and understanding these differences, as a wide variety of microbial diversity exists within the microbiome.[3-5] It is important to acknowledge the breadth of interspecies interactions that occur, wherein it may facilitate not only the investigation of relationships resulting in inhibition but also commensal and mutually beneficial interactions.[6-7] Understanding intricate bacterial differences may serve to facilitate the deliberate targeting of individual species.

Two of the deficiencies discussed within this dissertation account for broad bacterial differences, such as membrane composition and metabolic activity. Membrane composition can be classified as Gram-negative and Gram-positive wherein Gram-negative species have posed an increased challenge with the existence of an additional cellular membrane.[8] Clinically, Gram-negative pathogens are of high concern as they represent an increased threat to immunocompromised patients. Metabolically inactive bacterial cells, also known as persister cells, lie dormant permitting them to withstand antibiotic treatment and subsequently the ability to reinfect following the completion of treatment.[9] There currently exists few methods towards combatting these classes of bacteria and therefore researching them holds the potential for high-impact.

Investigating promysalin, a natural product shown to have selective inhibitory activity against Gram-negative pathogen, *Pseudomonas aeruginosa*, has permitted the identification of succinate dehydrogenase as the target.[1] Moreover, this work represents a case-study wherein targeting a highly conserved enzyme resulted in selectivity between bacterial species. This finding allows for the demonstration that unique process and cellular targets may not be necessary for narrow-spectrum therapeutics but, understanding and taking advantage of differences such as utility of metabolic pathways

can in fact allow for selective killing.[10] To support this concept, we have provided rationalization for the lack of inhibition of *Pseudomonas putida* with transcriptomic analysis.[11] In this investigation we observe the upregulation of peripheral metabolic pathways capable of degradation of catechols and benzoates with a corresponding down regulation of enzymes required for glycolysis. We hope this finding will serve as a platform moving forward when addressing antibiotic deficiencies. Additionally, the results we have obtained will hopefully allow the further investigation and optimization of binding affinity and overcome the inherent propensity to mutate.

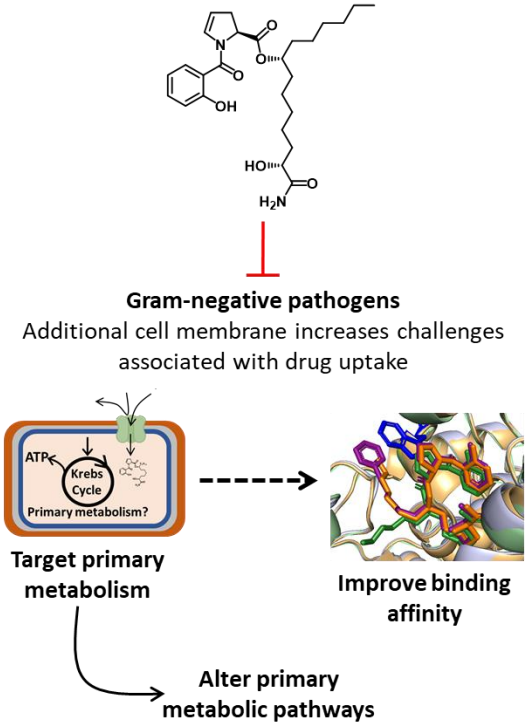

Figure 4.1 *Promysalin overview.*

Our collaboration with the Mylonakis Lab allowed for the investigation of MRSA persister cell inhibitors. Our synthetic data in collaboration with molecular dynamic simulations, and a wide range of bacterial assays, allowed the disclosure of a previously unknown mechanism of membrane permeabilization.[2] This activity is exemplified by synergy with gentamicin and can be rationalized by the newfound ability of aminoglycosides to now permeate the cell membrane of persister cells (generally

impenetrable). As a result of this uptake, aminoglycosides are now able to kill the bacteria. Our synthetic work sought to rationalize the proposed mechanism while also addressing inherent toxicity issues of the active scaffold. Throughout this investigation we uncovered a new lead compound, with increased therapeutic index, which unfortunately does require further optimization and is currently underway in the lab – results of which will be reported in due course.

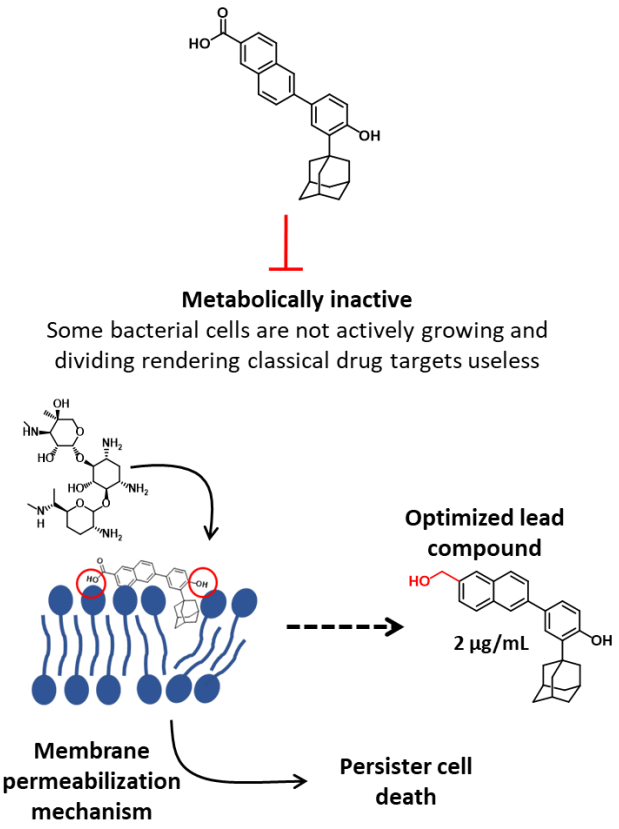

Figure 4.2 *CD437 overview.*

I feel as though these research projects, while targeting vastly different species, serve to highlight two of the many different bacterial classifications and provide evidence that accounting for these differences may provide alternatives to classical antibiotic targets. Our continual interest (and that of many others) in this area will hopefully provide insight further supporting this concept. This support will not only come from investigating alternative mechanisms but also from studying interspecies interactions and collectively this data will allow for a breadth of future discoveries!

1. Keohane, C. E.; Steele, A. D.; Fetzer, C.; Khowsathit, J.; Van Tyne, D.; Moynié, L.; Gilmore, M. S.; Karanicolas, J.; Sieber, S. A.; Wuest, W. M., Promysalin Elicits Species-Selective Inhibition of Pseudomonas aeruginosa by Targeting Succinate Dehydrogenase. *Journal of the American Chemical Society* **2018,** *140* (5), 1774-1782.
2. Kim, W.; Zhu, W.; Hendricks, G. L.; Van Tyne, D.; Steele, A. D.; Keohane, C. E.; Fricke, N.; Conery, A. L.; Shen, S.; Pan, W.; Lee, K.; Rajamuthiah, R.; Fuchs, B. B.; Vlahovska, P. M.; Wuest, W. M.; Gilmore, M. S.; Gao, H.; Ausubel, F. M.; Mylonakis, E., A new class of synthetic retinoid antibiotics effective against bacterial persisters. *Nature* **2018,** *556*, 103.
3. Keohane, C. E.; Steele, A. D.; Wuest, W. M., The Rhizosphere Microbiome: A Playground for Natural Product Chemists. *Synlett* **2015,** *26* (20), 2739-2744.
4. Mendes, R.; Garbeva, P.; Raaijmakers, J. M., The rhizosphere microbiome: significance of plant beneficial, plant pathogenic, and human pathogenic microorganisms. *FEMS Microbiol Rev* **2013,** *37* (5), 634-63.
5. Philippot, L.; Raaijmakers, J. M.; Lemanceau, P.; van der Putten, W. H., Going back to the roots: the microbial ecology of the rhizosphere. *Nat Rev Microbiol* **2013,** *11* (11), 789-99.
6. Miles, J.; Handelsman, J.; Holt, J. F., Allies and Adversaries: Roles of the Microbiome in Infectious Disease. *Microbe Magazine* **2015,** *10* (9), 370-374.
7. Shade, A.; Peter, H.; Allison, S. D.; Baho, D. L.; Berga, M.; Burgmann, H.; Huber, D. H.; Langenheder, S.; Lennon, J. T.; Martiny, J. B.; Matulich, K. L.; Schmidt, T. M.; Handelsman, J., Fundamentals of microbial community resistance and resilience. *Front Microbiol* **2012,** *3*, 417.
8. Delcour, A. H., Outer membrane permeability and antibiotic resistance. *Biochim Biophys Acta* **2009,** *1794* (5), 808-16.
9. Lewis, K., Persister cells, dormancy and infectious disease. *Nat Rev Microbiol* **2007,** *5* (1), 48-56.
10. Shapiro, J. A.; Kaplan, A. R.; Wuest, W. M., From General to Specific: Can Pseudomonas Primary Metabolism Be Exploited for Narrow-Spectrum Antibiotics? *Chembiochem* **2019,** *20* (1), 34-39.
11. Giglio, K. M.; Keohane, C. E.; Stodghill, P. V.; Steele, A. D.; Fetzer, C.; Sieber, S. A.; Filiatrault, M. J.; Wuest, W. M., Transcriptomic Profiling Suggests That Promysalin Alters the Metabolic Flux, Motility, and Iron Regulation in Pseudomonas putida KT2440. *ACS Infectious Diseases* **2018,** *4* (8), 1179-1187.

Chapter 5 Experimental Details

5.1 Biology: General notes

Bacterial Strains and Culture Conditions

Pseudomonas putida KT2440, OUS82, and WCS385, *P. fluorescens* WCS365, *P. aeruginosa* PA01, and PA14 were gifts from Prof. George O'Toole (Dartmouth Medical School) and P. putida RW10S1 from Prof. René De Mot (KU Leuven). Bacterial cultures were grown from freezer stocks overnight (16-24 hr) with shaking at 37°C in Tryptic Soy Broth (TSB) media (10 mL). Growth curves were obtained for PA01 and PA14 to determine the OD of each strain in exponential growth; OD readings at 595 nm were taken every 10 mins for 10 hours using a SPEC at 37°C with shaking and repeated six times. (Figure 5.1 and Figure 5.2)

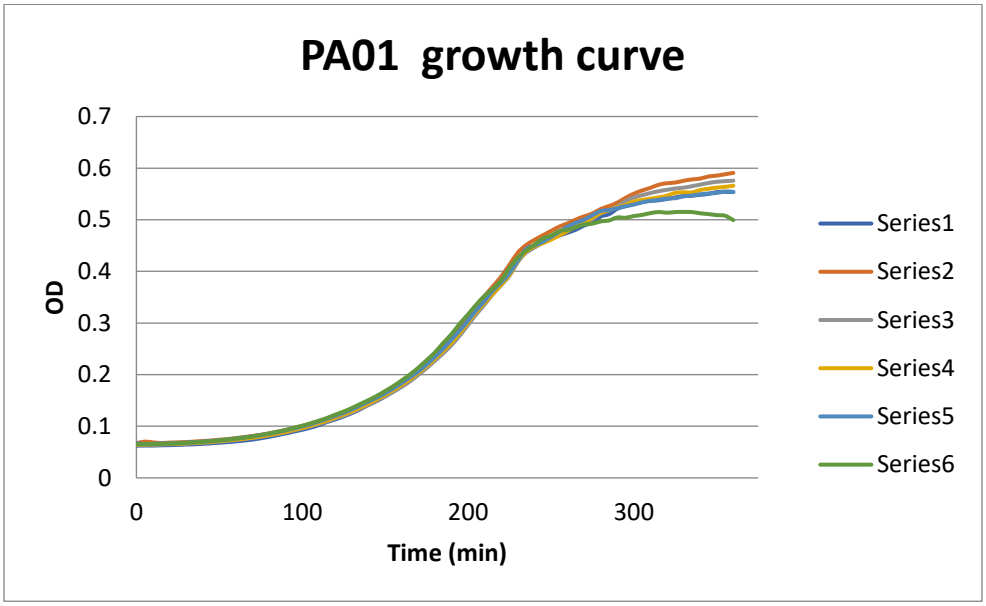

Figure 5.1*PAO1 growth curve*

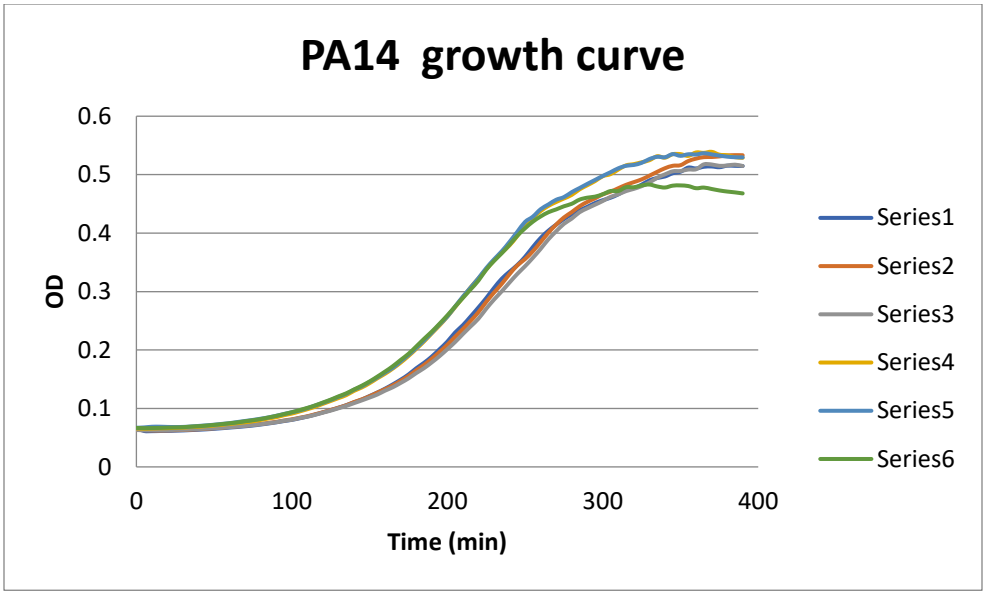

Figure 5.2 *PA14 growth curve*

5.2 Biology: Procedures and supplemental information

IC_{50} Assay

Compounds were serially diluted in sterile DI water from a stock solution (10% DMSO/H_2O) yielding 24 test concentrations. Bacteria were diluted to a final concentration of 0.004 from regrown overnight culture according to the following equation:

(xμL bacterial culture)(OD reading) = (0.004)(total volume needed) and 100 μL was inoculated into each well of a flat-bottom 96-well plate (Corning 3370) containing 100 μL of compound solution. Plates were incubated statically at 37°C for 20 hours upon which time OD at 595 nm was measured using a plate reader (SpectraMax 190 or SpectraMax iD3). IC_{50} values were calculated using OD values and concentrations with a 4-parameter logistic model. Control experiments used a 10%DMSO/H_2O stock serially diluted to the same 24 concentrations. Compounds were tested in triplicate from three independent single colonies.

Swarming/Motility Assay

Hot TSB agar of the indicated concentration was poured into 6 well plates (~5 mL/well) and allowed to set open in a laminar flow hood for an hour after the surface became gelatinous (typically within 5 minutes). After the set time, a small cross was cut into the surface of the agar, and 5 µL of overnight bacterial culture was inoculated into the cross. Compound stock solution (30 µL) of the indicated concentration was absorbed into discs and allowed to dry. Then the discs were carefully placed on top of the site of inoculation in the 6-well plate. The plates were statically incubated at 30°C, and the swarming phenotype was visualized after 20 hours. UV irradiation/visualization was performed after 48 hours of incubation.

CAS Assay

CAS agar was prepared as described by Cordero et al (Cordero, O. X.; Ventouras, L.; DeLong, E. F.; Polz, M. F., *PNAS*, **2012**, *109*, 49, 29059). 10µL of compound was dosed on plates and pictures taken after 24 hours. Stock solutions were made in 10%DMSO/H_2O.

Affinity-Based Protein Profiling (AfBPP):

Preparation of samples: 100 mL of TSB-Medium were inoculated 1:100 from an overnight culture of *P. aeruginosa* PAO1, *P. aeruginosa* PA14 or *P. putida* KT2440 and incubated (*P. aeruginosa* 37 °C; *P. putida* 30 °C; 200 rpm) until OD_{600} = 1.0. The cultures were centrifuged (5 min, 6000 g), washed with 0.5 volumes PBS and resuspended in the same amount of PBS. Per sample 20 mL of washed culture were incubated (*P. aeruginosa* 37 °C; *P. putida* 30 °C; 30 min, 200 rpm) with either promysalin probe (3 µM), inactive promysalin probe (3 µM) or for competition experiments with promysalin (30 µM; 10 min pre-incubation) and promysalin probe (3 µM). The samples were poured in petri dishes (90 mm) and irradiated for 20 min (365 nm; Philips TL-D BLB 18W) without lids. The cultures were centrifuged (10 min, 6000 g) and washed with the same amount of PBS. The pellets were resuspended in 1 mL PBS, transferred to a 1.5 mL tube, centrifuged again and stored at -80 °C.

Click-Chemistry: Pellets were resuspended in 150 µL lysis buffer with EDTA-free protease inhibitors (PBS with 0.5% SDS and 1% Triton 100) and lysed using sonication (2 × 15 s, 60% intensity) with cooling on ice. Protein concentration was adjusted to 1 mg/mL using BCA assay. 500 µL of each sample were used for CuAAC reaction. All reagents for the click reaction were premixed and added to the samples at the indicated final concentrations: 100 µM biotin-azide (10 mM stock in DMSO), 1 mM $CuSO_4$ (50 mM stock in ddH_2O), 1 mM TCEP (50 mM stock in ddH_2O) and 100 µM TBTA (10 mM stock in DMSO). Samples were incubated at r.t. for one hour. 10 µL of EDTA (500 mM) were added and the whole sample was then transferred in a 15 mL tube containing 3 mL cold acetone (-80 °C). Proteins were allowed to precipitate overnight at -80 °C.

Pulldown and Digestion: The precipitate was centrifuged (10 min, 18,000 g) and washed twice with 1 mL cold methanol (-80 °C) with resuspension (5 s ultrasonic bath) and centrifugation steps (10 min, 18,000 g) in between. All pellets were air-dried for 30 min at r.t. The washed pellets were resuspended in 500 µL PBS (containing 0.2% SDS and 1 mM DTT), centrifuged (20 min, 17,000 g), the supernatant transferred in low-bind tubes containing 50 µL washed avidin agarose beads and incubated (2 h, r.t.) with gentle rotation. Avidin beads were washed before five times with 700 µL PBS (containing 0.2% SDS). After incubation beads were washed (2 × 200 µL PBS + 0.2% SDS; 3 × 200 µL 4 M Urea in PBS; 3 × 200 µL 50 mM TEAB) reconstituted in 50 µL 50 mM TEAB and 2 µL 250 mM DTT were added followed by incubation on a shaker (30 min, 55 °C, 600 rpm). Beads were washed with 50 mM TEAB followed by addition of 50 µL TEAB and 2 µL 500 mM iodoacetamide with incubation on a shaker in the dark (30 min, 25 °C, 600 rpm). After two more washed with TEAB beads were reconstituted in 50 µL 50 mM TEAB and 2 µL trypsin (0.5 µg/µL in 50 mM acetic acid) and incubated overnight (37 °C and 750 rpm).

Desalt and dimethyl label: The beads were centrifuged, the supernatant transferred in a new low-bind tube and digestion was stopped by addition of 0.7 µL formic acid (FA). Beads were washed two more times with 50 µL 0.1% FA in 50 mM TEAB and supernatants were combined. Desalting of the samples was conducted on 50 mg SepPak C18 columns (Waters). Columns were equilibrated with 1 mL acetonitrile (ACN), 1 mL

elution buffer (80% ACN, 0.5% FA) and 3 mL aqueous 0.5% FA solution. The acidified samples were loaded by gravity flow, washed five times with 1 mL 0.5% FA and then labeled with five times 1 mL of the respective dimethyl labeling agents (light (L): 30 mM $NaBH_3CN$, 0.2 % CH_2O, 45 mM sodium phosphate buffer, pH 7.5; medium (M): 30 mM $NaBH_3CN$, 0.2 % CD_2O, 45 mM sodium phosphate buffer, pH 7.5; heavy (H): 30 mM $NaBD_3CN$, 0.2 % $^{13}CD_2O$, 45 mM sodium phosphate buffer, pH 7.5). Column bound peptides were washed two more times with 1 mL 0.5% FA and then eluted with two times 250 µL elution buffer. 900 µL of each sample were combined in a 15 mL tube, frozen in liquid nitrogen and lyophilized. Prior to LC-MS/MS measurement samples were dissolved in 40 µL 1% FA and filtered with 0.22 µm ultrafree centrifugal filters (Merck) equilibrated with 300 µL 1% FA. The filtrate was transferred into MS vials and queued for LC-MS/MS measurement.

LC/MS Data analysis: 4 µL of each sample were injected into the LC-MS/MS system. Samples were analyzed via HPLC-MS/MS using an UltiMate 3000 nano HPLC system (Dionex, Sunnyvale, California, USA) equipped with an Acclaim C18 PepMap100 75 µm ID x 2 cm trap and an Acclaim Pepmap RSLC C18 separation column (75 µm ID x 50 cm) in an EASY-spray setting coupled to a Thermo Fischer LTQ Orbitrap Fusion (Thermo Fisher Scientific Inc., Waltham, Massachusetts, USA). Samples were loaded on the trap and washed with 0.1 % TFA (at 5 µL/min), then transferred to the analytical column and separated using a non-linear 115 min gradient from 5 % A to 32 % B, then in 10 min to 90% B followed by another 10 min at 90 % B (at 300 nL/min flow rate) (buffer A: H_2O with 0.1% FA, buffer B: MeCN with 0.1% FA). LTQ Orbitrap Fusion was operated in a 3 second top speed data dependent mode. Full scan acquisition was performed in the orbitrap at a resolution of 120000 and an AGC target of 2e5 in a scan range of 300-1500 m/z. Monoisotopic precursor selection as well as dynamic exclusion for 60 s were enabled. Precursors with charge states of 2-7 and intensities greater than 5e3 were selected for fragmentation. Isolation was performed in the quadrupole using a window of 1.6 m/z. Precursors were collected to an AGC target of 1e4 for a maximum injection time of 50 ms with “inject ions for all available parallelizable time” enabled. Fragments were generated using higher-energy collisional dissociation (HCD, normalized collision energy:

30%) and detected in the ion trap at a rapid scan rate. Internal calibration was performed using the ion signal of fluoranthene cations (EASY-IC).

Raw files were analysed using MaxQuant software (version 1.5.3.8) with the Andromeda search engine. The search included carbamidomethylation of cysteines as a fixed modification and oxidation of methionines and acetylation of protein N-termini as variable modifications. Light, medium and heavy labels (of lys and N-term) was set according to the samples, number of max. labeled AAs was set to 4. Trypsin was specified as the proteolytic enzyme with N-terminal cleavage to proline and two missed cleavages allowed. Precursor mass tolerance was set to 4.5 ppm (main search) and fragment mass tolerance to 0.5 Da. Searches were performed against the Uniprot database for either *Pseudomonas aeruginosa* PAO1 (taxon identifier: 208964, including isoforms), *Pseudomonas aeruginosa* PA14 (taxon identifier: 208963, including isoforms) or *Pseudomonas putida* KT2440 (taxon identifier: 160488, including isoforms). The second peptide identification option was enabled. False discovery rate determination was carried out using a decoy database and thresholds were set to 1% FDR both at peptide-spectrum match and at protein levels. "I = L", "requantification" and "match between runs" (0.7 min match and 20 min alignment time windows) options were enabled.

Statistical analysis was performed with Perseus software (version 1.5.2.6). Putative contaminants, reverse sequences and only identified by site hits were filtered out. Ratios were logarithmized (log_2) and z-score normalized (within one replicate). Statistical evaluation was performed using "One-sample t-test" (both-sided; Benjamini-Hochberg FDR 0.05).

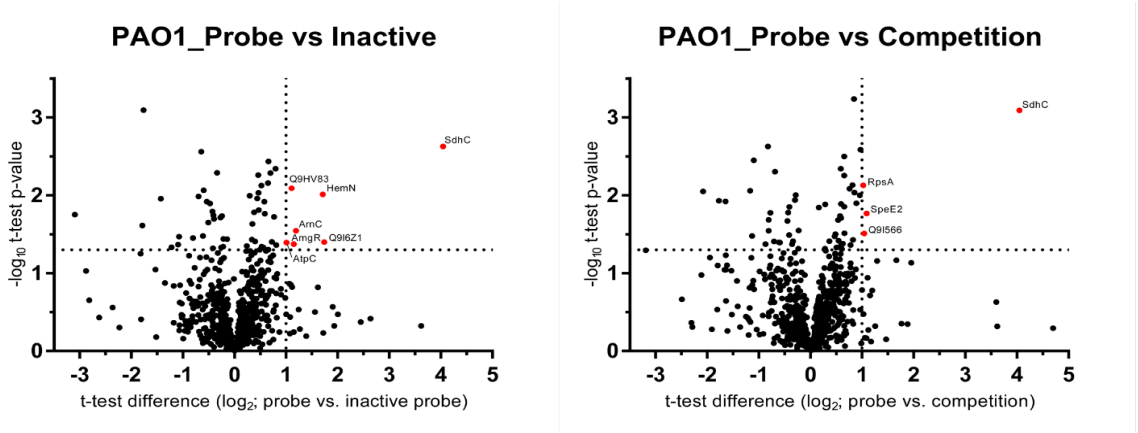

Supplementary Figure 3
ABPP volcano plots for PAO1

Succinate Dehydrogenase *in vitro* assay

All reagents (except inhibitors) were provided with commercially available kit, MitoCheck® Complex II Activity Assay Kit (item # 700940). Readings were obtained using SpedctraMax iD3 microplate reader at 600nM. Assay was run in triplicate.

Resistance Assay:

Bacteria were grown overnight from single colonies in TSB media at 37 ºC with shaking. Cultures were treated with a concentration gradient of compound, 0.25xMIC, 0.5xMIC, MIC, and 2xMIC. Due to lack of clear-to turbid differentiation at these concentrations we tested the compounds at lower concentrations for increased growth development (63µM, 31 µM, 16 µM, 7.8 µM, 3.9 µM, 1.9 µM and 250µM (MIC) as positive control) and each day the highest concentration with full growth, relative to 10%DMSO/H_2O was inoculated into fresh media containing compound at the same 6 concentrations (adjusted to match resistance development). This was repeated for 24 days. After 24 days, the bacteria were streaked out, single colonies chosen (6 for each phenotype), and freezer stocks made. The bacteria were tested for inhibitory activity and

two colonies from two unique strains from both mutant types, and wild type, were sent for whole genome sequencing.

Zone of inhibition:

100µL overnight culture was added to TSB or M9 agar plates and bacterial lawns were 'created' using Roll & Grow Plating Beads. Compound stock solution 20µL of a 250µM solution, 10µL of a 10mg/mL gentamicin solution, and 20µL of a 250µM DMSO control (stock = 10%DMSO/H_2O) was absorbed into discs and allowed to dry. Discs were placed on the plates and incubated at 37°C for 24 hours. Assay was run in triplicate from separate overnight cultures.

Biofilm Assay:

Bacteria were grown overnight at 37ºC. The next day, overnight cultures were diluted 1:1000 in fresh TSB media. Once in exponential growth, bacteria were diluted to a final concentration of 0.004 according to the following equation:

(xµL bacterial culture)(OD reading) = (0.004)(total volume needed) and 100 µL was inoculated into each well of a flat-bottom 96-well plate (Corning 3370) containing 100 µL of water. Plates were incubated statically at 37°C for 24 hours upon which time OD at 595 nm was measured using a plate reader (SpectraMax 190 or SpectraMax iD3). Plates were inverted, emptied, and rinsed 2x with DI water and allowed to dry in incubator overnight. The next day, plates were incubated for 10min at room with 200µL of 1% w/v crystal violet (5% ethanol in H2O). Excess crystal violet was removed and wells were rinsed with 200µL DI water, 3x. Plates were then inverted and dried at room temperature. Crystal violet was redissolved with 200µL of 95% ethanol or 200µL 30% AcOH, 100µL of which was then transferred to a fresh flat-bottom 96-well plate for absorbance measurements at 595nm. DMSO controls corresponding to each test concentration were performed. Three biological replicates were performed.

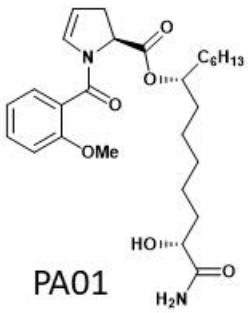

PA01

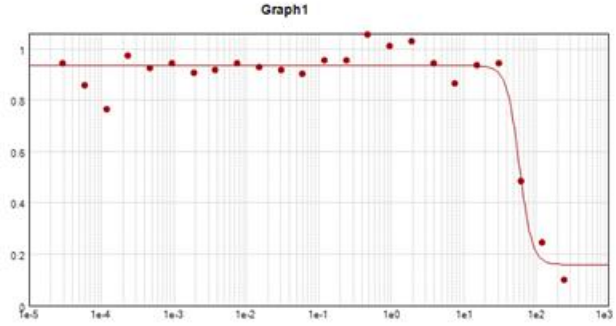

Curve Fit : 4-Parameter $y = D + \frac{A - D}{1 + \left(\frac{x}{C}\right)^B}$

	Parameter	Estimated Value
Plot1 R^2 = 0.934 EC50 = 59.28	A	0.934
	B	4.979
	C	59.28
	D	0.159

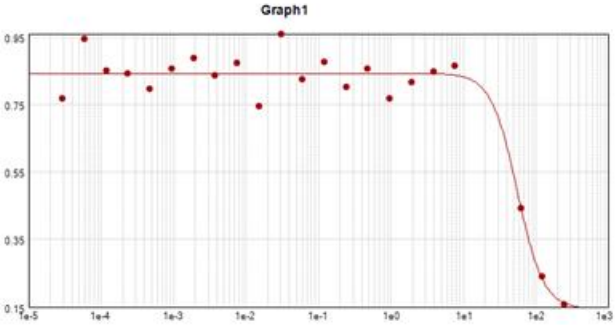

Curve Fit : 4-Parameter $y = D + \frac{A - D}{1 + \left(\frac{x}{C}\right)^B}$

	Parameter	Estimated Value
Plot1 R^2 = 0.941 EC50 = 55.73	A	0.843
	B	2.421
	C	55.73
	D	0.144

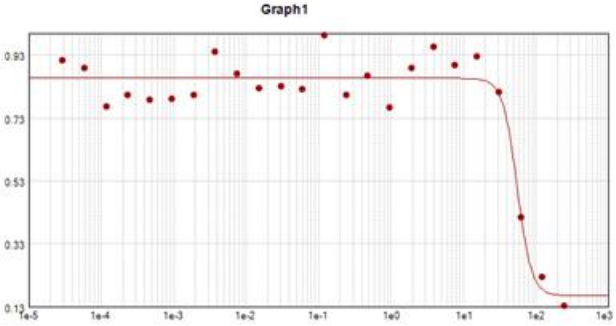

Curve Fit : 4-Parameter $y = D + \frac{A - D}{1 + \left(\frac{x}{C}\right)^B}$

	Parameter	Estimated Value
Plot1 R^2 = 0.916 EC50 = 55.49	A	0.856
	B	4.403
	C	55.49
	D	0.165

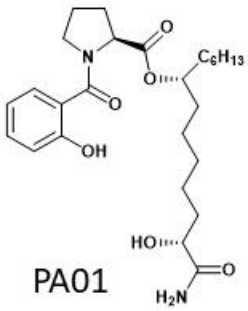

PA01

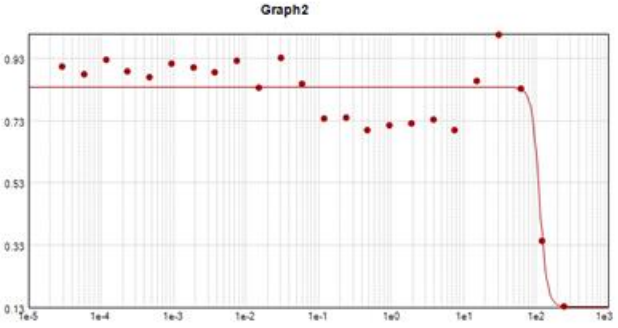

Curve Fit : 4-Parameter $y = D + \frac{A - D}{1 + \left(\frac{x}{C}\right)^B}$

	Parameter	Estimated Value
Plot1 R^2 = 0.799 EC50 = 112.6	A	0.838
	B	8.189
	C	112.6
	D	0.132

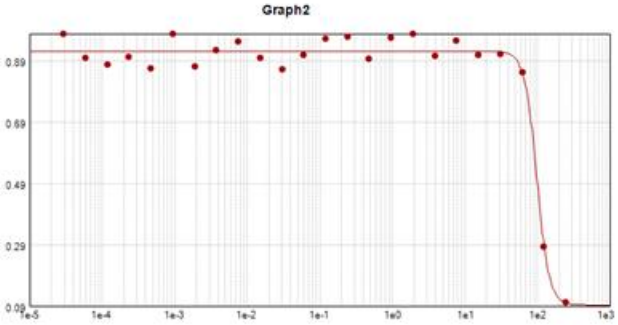

Curve Fit : 4-Parameter $y = D + \frac{A - D}{1 + \left(\frac{x}{C}\right)^B}$

	Parameter	Estimated Value
Plot1 R^2 = 0.969 EC50 = 98.88	A	0.923
	B	5.141
	C	98.88
	D	0.093

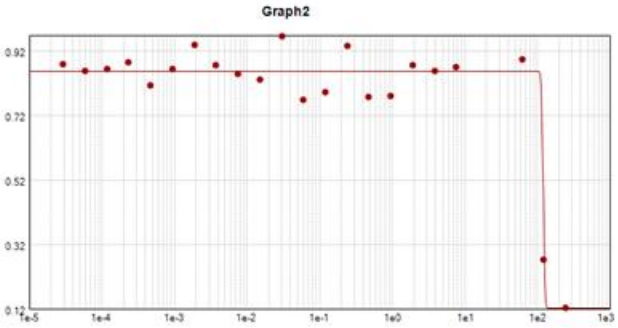

Curve Fit : 4-Parameter $y = D + \frac{A - D}{1 + \left(\frac{x}{C}\right)^B}$

	Parameter	Estimated Value
Plot1 R^2 = 0.936 EC50 = 121.1	A	0.859
	B	43.60
	C	121.1
	D	0.122

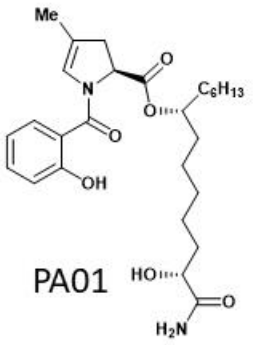

PA01

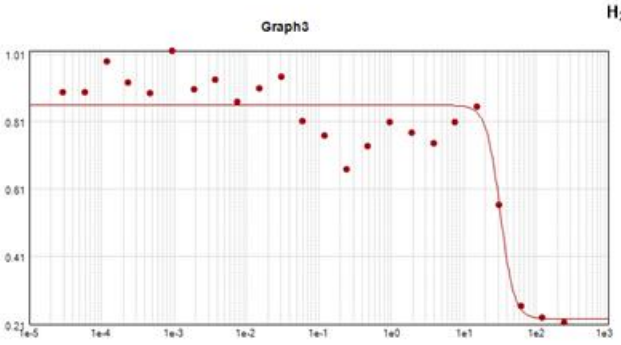

Curve Fit : 4-Parameter $y = D + \frac{A - D}{1 + \left(\frac{x}{C}\right)^B}$

	Parameter	Estimated Value
Plot1 R^2 = 0.872 EC50 = 32.26	A	0.858
	B	4.585
	C	32.26
	D	0.226

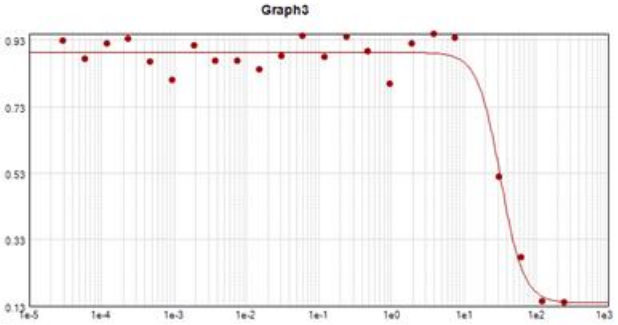

Curve Fit : 4-Parameter $y = D + \frac{A - D}{1 + \left(\frac{x}{C}\right)^B}$

	Parameter	Estimated Value
Plot1 R^2 = 0.973 EC50 = 32.53	A	0.893
	B	2.744
	C	32.53
	D	0.139

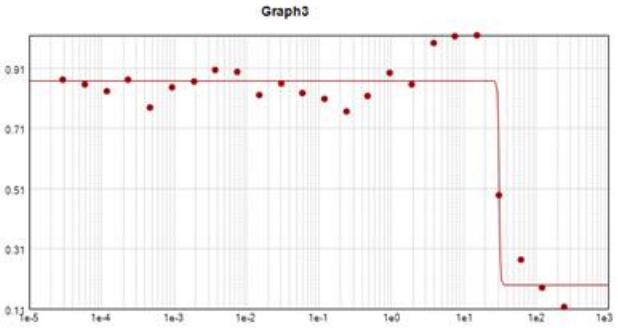

Curve Fit : 4-Parameter $y = D + \frac{A - D}{1 + \left(\frac{x}{C}\right)^B}$

	Parameter	Estimated Value
Plot1 R^2 = 0.923 EC50 = 31.07	A	0.869
	B	42.63
	C	31.07
	D	0.189

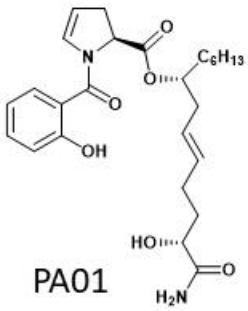

PA01

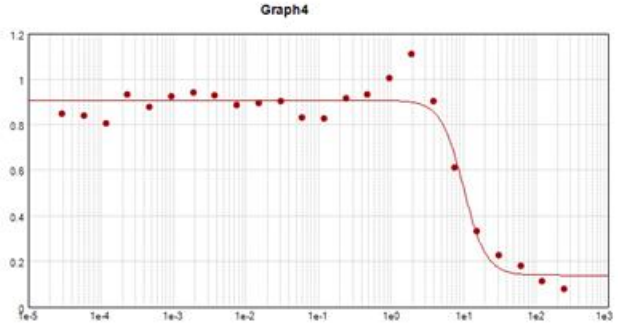

Curve Fit : 4-Parameter $y = D + \frac{A - D}{1 + \left(\frac{x}{C}\right)^B}$

	Parameter	Estimated Value
Plot1 R^2 = 0.953 EC50 = 10.13	A	0.907
	B	2.789
	C	10.13
	D	0.139

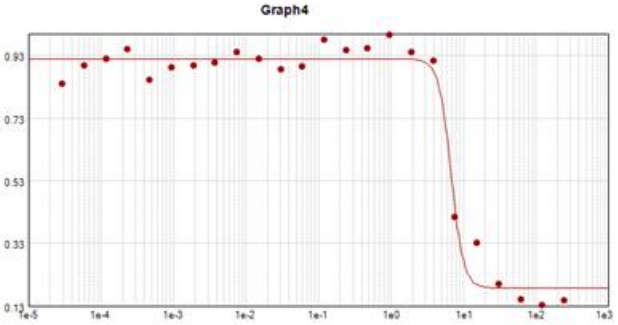

Curve Fit : 4-Parameter $y = D + \frac{A - D}{1 + \left(\frac{x}{C}\right)^B}$

	Parameter	Estimated Value
Plot1 R^2 = 0.976 EC50 = 6.814	A	0.920
	B	5.080
	C	6.814
	D	0.187

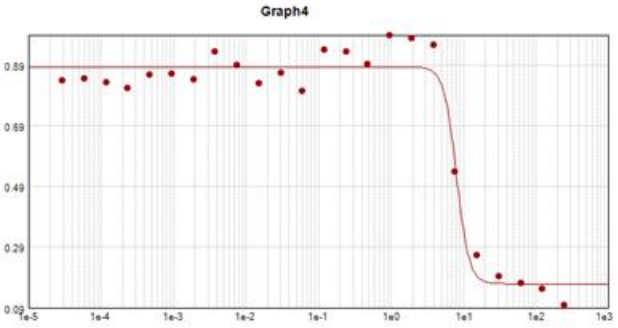

Curve Fit : 4-Parameter $y = D + \frac{A - D}{1 + \left(\frac{x}{C}\right)^B}$

	Parameter	Estimated Value
Plot1 R^2 = 0.966 EC50 = 8.071	A	0.885
	B	5.052
	C	8.071
	D	0.169

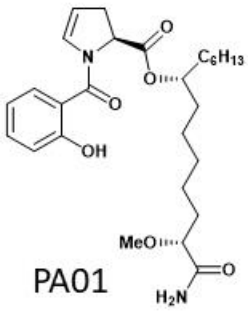

PA01

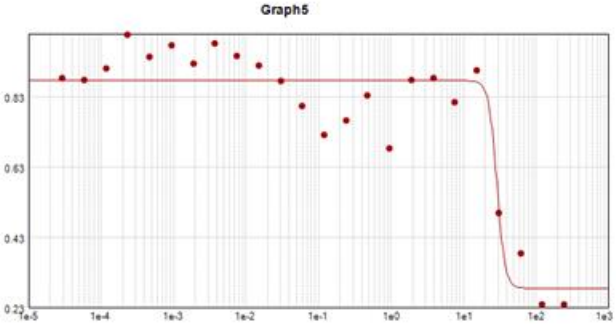

Curve Fit : 4-Parameter $y = D + \frac{A - D}{1 + \left(\frac{x}{C}\right)^B}$

	Parameter	Estimated Value
Plot1 R^2 = 0.866 EC50 = 29.15	A	0.876
	B	7.872
	C	29.15
	D	0.284

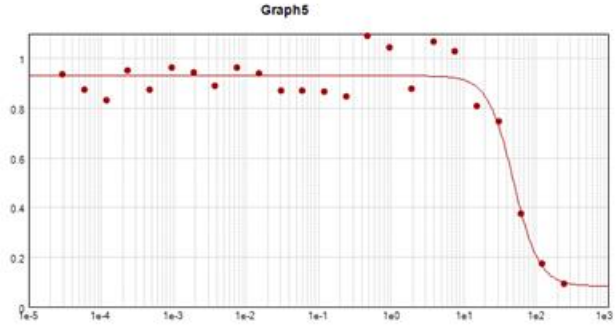

Curve Fit : 4-Parameter $y = D + \frac{A - D}{1 + \left(\frac{x}{C}\right)^B}$

	Parameter	Estimated Value
Plot1 R^2 = 0.922 EC50 = 49.29	A	0.931
	B	2.476
	C	49.29
	D	0.083

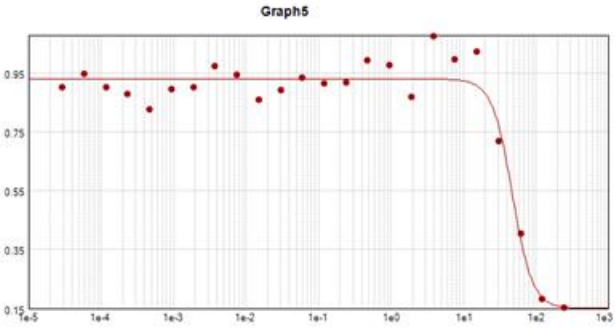

Curve Fit : 4-Parameter $y = D + \frac{A - D}{1 + \left(\frac{x}{C}\right)^B}$

	Parameter	Estimated Value
Plot1 R^2 = 0.942 EC50 = 47.56	A	0.931
	B	3.146
	C	47.56
	D	0.151

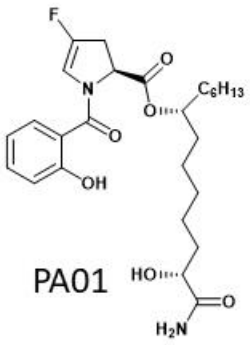

PA01

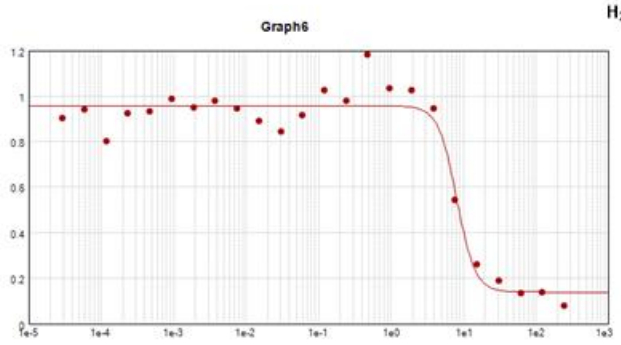

Curve Fit : 4-Parameter $y = D + \frac{A - D}{1 + \left(\frac{x}{C}\right)^B}$

	Parameter	Estimated Value
Plot1 R^2 = 0.952 EC50 = 8.114	A	0.957
	B	3.429
	C	8.114
	D	0.139

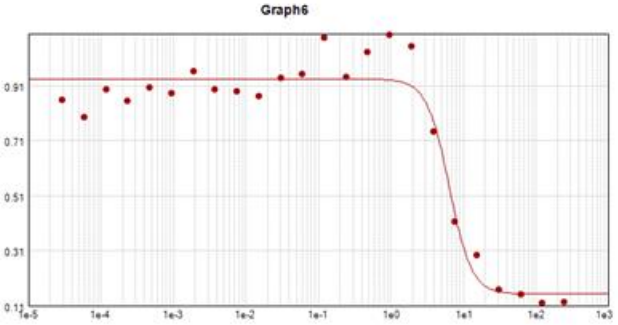

Curve Fit : 4-Parameter $y = D + \frac{A - D}{1 + \left(\frac{x}{C}\right)^B}$

	Parameter	Estimated Value
Plot1 R^2 = 0.945 EC50 = 6.410	A	0.935
	B	2.825
	C	6.410
	D	0.152

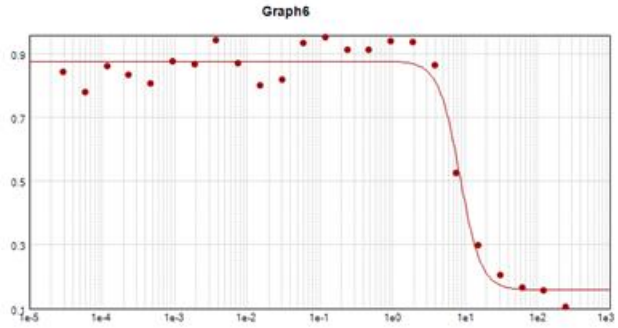

Curve Fit : 4-Parameter $y = D + \frac{A - D}{1 + \left(\frac{x}{C}\right)^B}$

	Parameter	Estimated Value
Plot1 R^2 = 0.969 EC50 = 8.567	A	0.878
	B	2.987
	C	8.567
	D	0.159

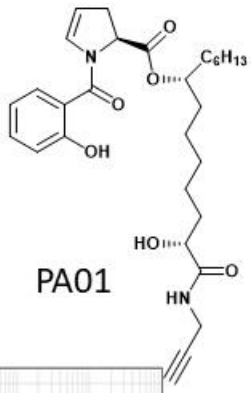

PA01

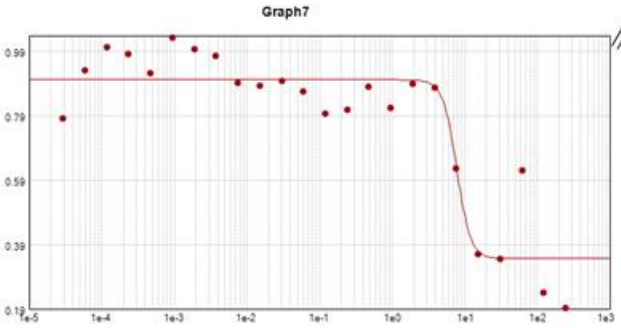

Curve Fit : 4-Parameter $y = D + \frac{A - D}{1 + \left(\frac{x}{C}\right)^B}$

	Parameter	Estimated Value
Plot1 R^2 = 0.856 EC50 = 7.806	A	0.902
	B	4.598
	C	7.806
	D	0.346

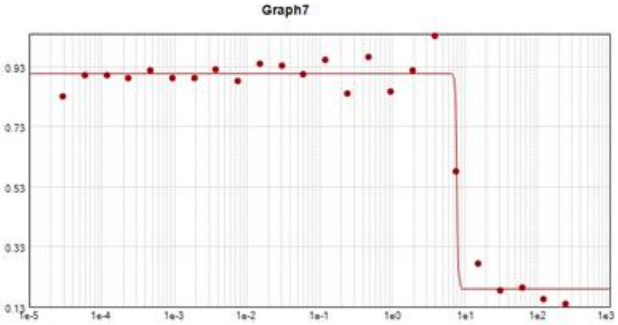

Curve Fit : 4-Parameter $y = D + \frac{A - D}{1 + \left(\frac{x}{C}\right)^B}$

	Parameter	Estimated Value
Plot1 R^2 = 0.977 EC50 = 7.847	A	0.908
	B	38.73
	C	7.847
	D	0.188

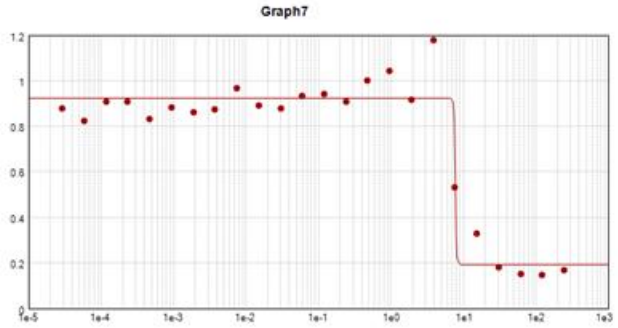

Curve Fit : 4-Parameter $y = D + \frac{A - D}{1 + \left(\frac{x}{C}\right)^B}$

	Parameter	Estimated Value
Plot1 R^2 = 0.937 EC50 = 7.786	A	0.922
	B	45.79
	C	7.786
	D	0.194

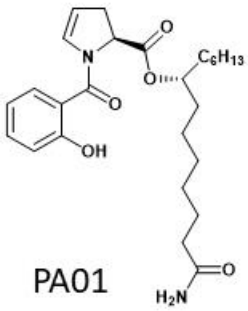

PA01

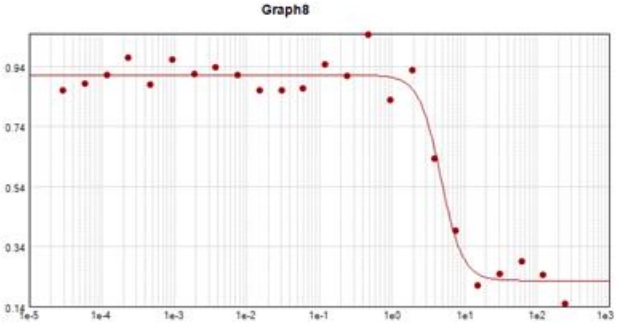

Curve Fit : 4-Parameter $y = D + \frac{A - D}{1 + \left(\frac{x}{C}\right)^B}$

	Parameter	Estimated Value
Plot1 R^2 = 0.968 EC50 = 4.783	A	0.911
	B	2.885
	C	4.783
	D	0.226

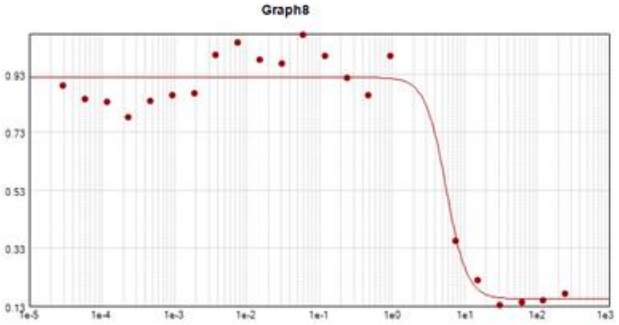

Curve Fit : 4-Parameter $y = D + \frac{A - D}{1 + \left(\frac{x}{C}\right)^B}$

	Parameter	Estimated Value
Plot1 R^2 = 0.954 EC50 = 5.639	A	0.919
	B	3.052
	C	5.639
	D	0.154

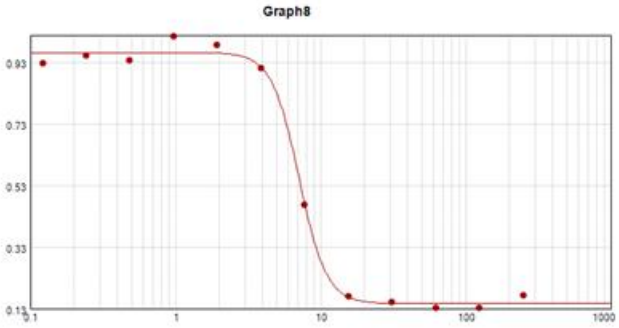

Curve Fit : 4-Parameter $y = D + \frac{A - D}{1 + \left(\frac{x}{C}\right)^B}$

	Parameter	Estimated Value
Plot1 R^2 = 0.996 EC50 = 7.117	A	0.963
	B	4.608
	C	7.117
	D	0.146

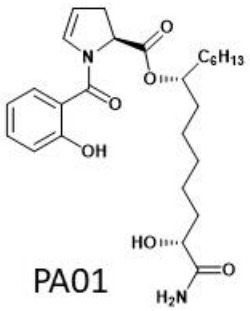

PA01

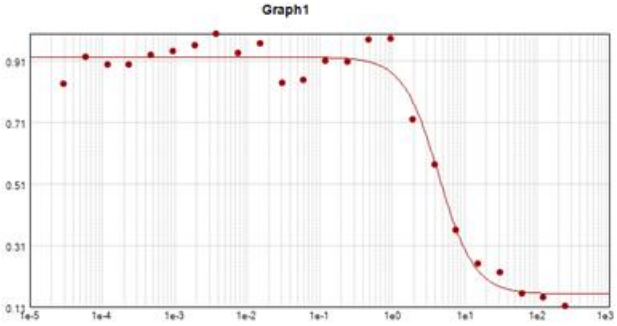

Curve Fit : 4-Parameter $y = D + \frac{A - D}{1 + \left(\frac{x}{C}\right)^B}$

	Parameter	Estimated Value
Plot1 R^2 = 0.976 EC50 = 4.437	A	0.923
	B	1.769
	C	4.437
	D	0.151

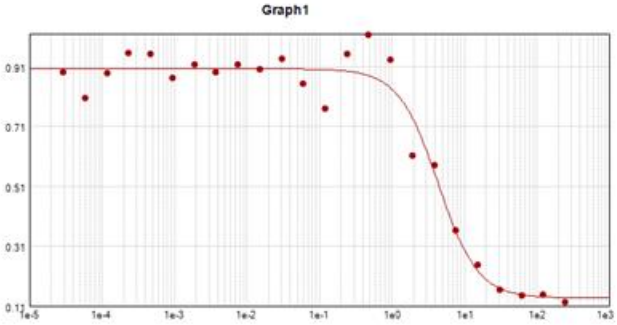

Curve Fit : 4-Parameter $y = D + \frac{A - D}{1 + \left(\frac{x}{C}\right)^B}$

	Parameter	Estimated Value
Plot1 R^2 = 0.963 EC50 = 4.370	A	0.902
	B	1.592
	C	4.370
	D	0.136

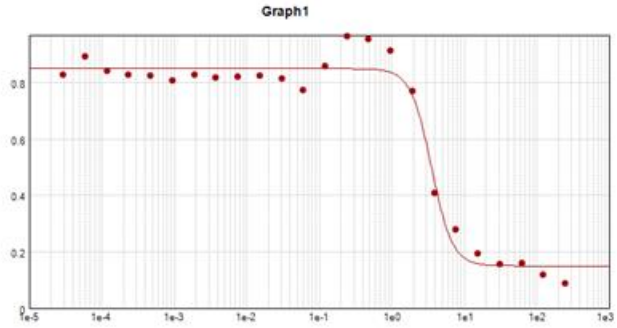

Curve Fit : 4-Parameter $y = D + \frac{A - D}{1 + \left(\frac{x}{C}\right)^B}$

	Parameter	Estimated Value
Plot1 R^2 = 0.973 EC50 = 3.544	A	0.851
	B	3.040
	C	3.544
	D	0.150

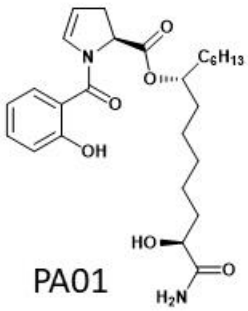

PA01

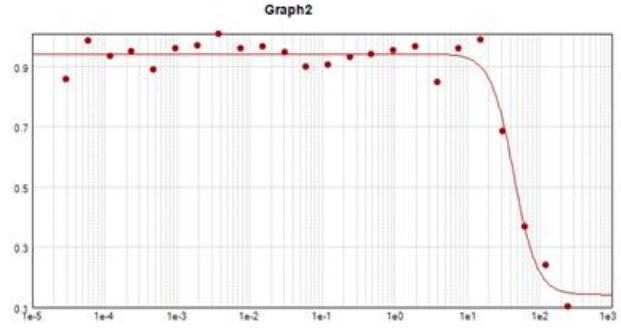

Curve Fit : 4-Parameter $y = D + \frac{A - D}{1 + \left(\frac{x}{C}\right)^B}$

	Parameter	Estimated Value
Plot1 R^2 = 0.967 EC50 = 44.44	A	0.943
	B	2.739
	C	44.44
	D	0.141

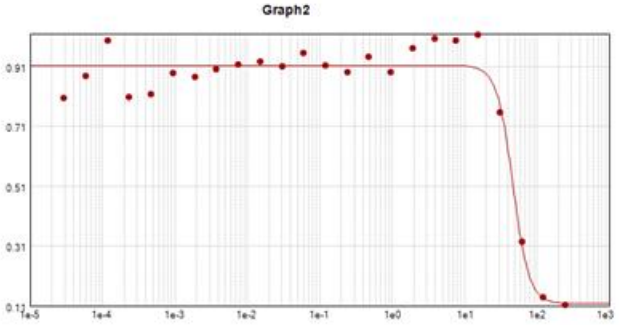

Curve Fit : 4-Parameter $y = D + \frac{A - D}{1 + \left(\frac{x}{C}\right)^B}$

	Parameter	Estimated Value
Plot1 R^2 = 0.947 EC50 = 46.88	A	0.914
	B	3.886
	C	46.88
	D	0.117

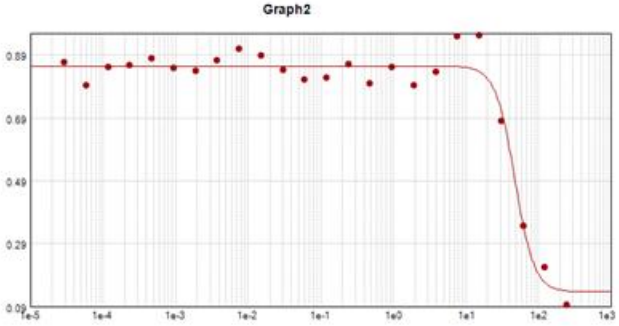

Curve Fit : 4-Parameter $y = D + \frac{A - D}{1 + \left(\frac{x}{C}\right)^B}$

	Parameter	Estimated Value
Plot1 R^2 = 0.958 EC50 = 47.67	A	0.855
	B	3.266
	C	47.67
	D	0.136

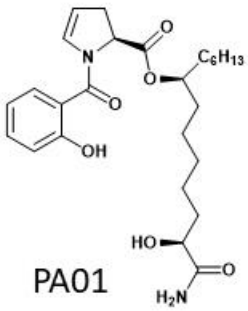

PA01

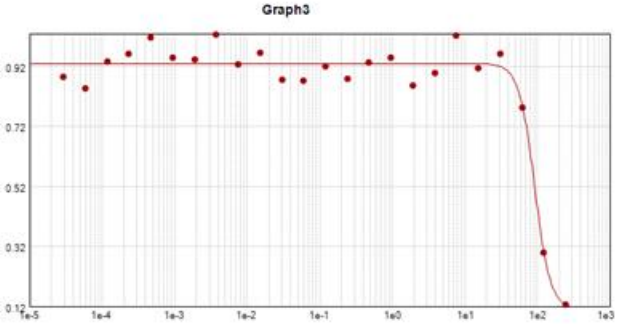

Curve Fit : 4-Parameter $y = D + \frac{A - D}{1 + \left(\frac{x}{C}\right)^B}$

	Parameter	Estimated Value
Plot1 R^2 = 0.946 EC50 = 92.05	A	0.930
	B	4.046
	C	92.05
	D	0.111

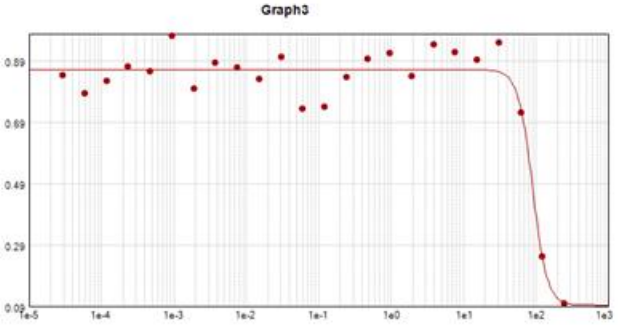

Curve Fit : 4-Parameter $y = D + \frac{A - D}{1 + \left(\frac{x}{C}\right)^B}$

	Parameter	Estimated Value
Plot1 R^2 = 0.913 EC50 = 90.36	A	0.863
	B	4.355
	C	90.36
	D	0.093

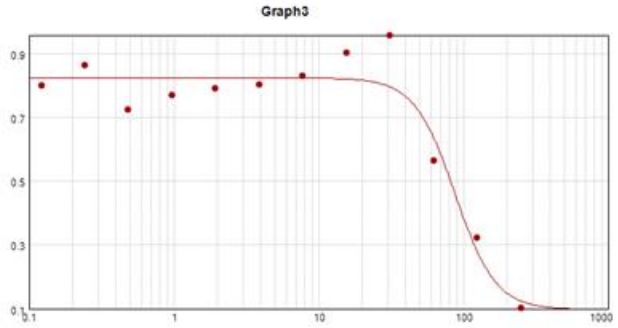

Curve Fit : 4-Parameter $y = D + \frac{A - D}{1 + \left(\frac{x}{C}\right)^B}$

	Parameter	Estimated Value
Plot1 R^2 = 0.919 EC50 = 87.58	A	0.826
	B	3.109
	C	87.58
	D	0.097

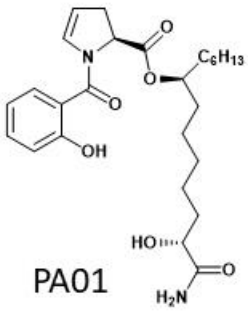

PA01

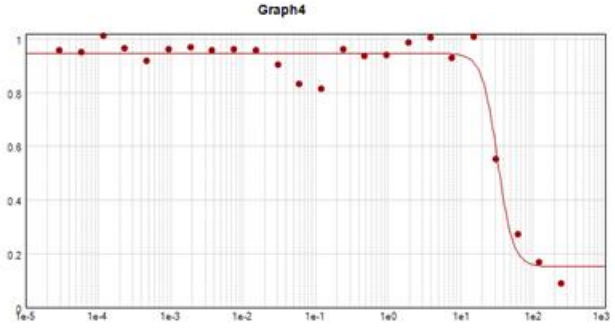

Curve Fit : 4-Parameter $y = D + \frac{A - D}{1 + \left(\frac{x}{C}\right)^B}$

	Parameter	Estimated Value
Plot1 R^2 = 0.962 EC50 = 32.72	A	0.947
	B	4.089
	C	32.72
	D	0.151

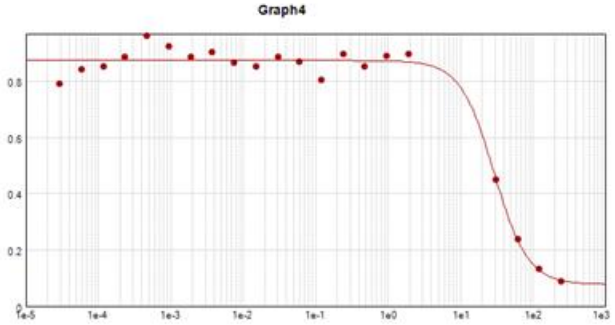

Curve Fit : 4-Parameter $y = D + \frac{A - D}{1 + \left(\frac{x}{C}\right)^B}$

	Parameter	Estimated Value
Plot1 R^2 = 0.981 EC50 = 29.25	A	0.875
	B	1.869
	C	29.25
	D	0.077

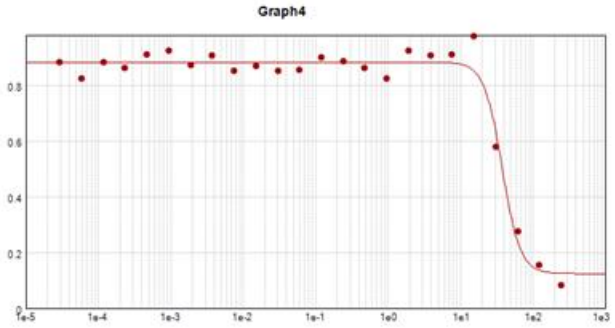

Curve Fit : 4-Parameter $y = D + \frac{A - D}{1 + \left(\frac{x}{C}\right)^B}$

	Parameter	Estimated Value
Plot1 R^2 = 0.972 EC50 = 37.85	A	0.883
	B	3.505
	C	37.85
	D	0.124

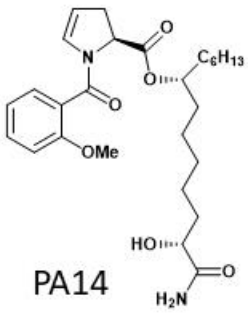

PA14

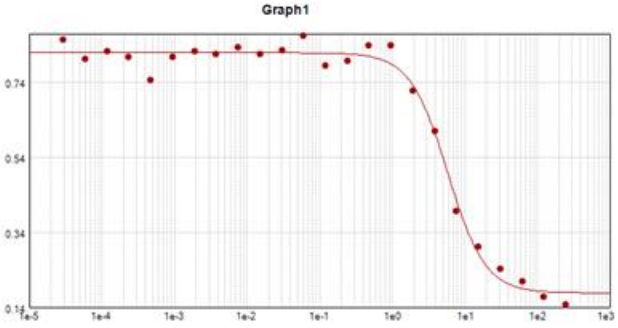

Curve Fit : 4-Parameter $y = D + \frac{A - D}{1 + \left(\frac{x}{C}\right)^B}$

	Parameter	Estimated Value
Plot1 R^2 = 0.988 EC50 = 5.860	A	0.819
	B	1.680
	C	5.860
	D	0.178

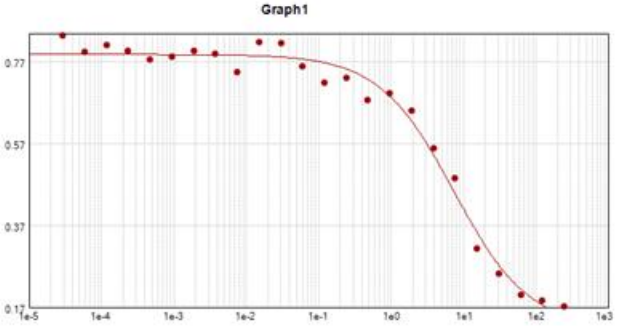

Curve Fit : 4-Parameter $y = D + \frac{A - D}{1 + \left(\frac{x}{C}\right)^B}$

	Parameter	Estimated Value
Plot1 R^2 = 0.985 EC50 = 7.388	A	0.788
	B	0.845
	C	7.388
	D	0.119

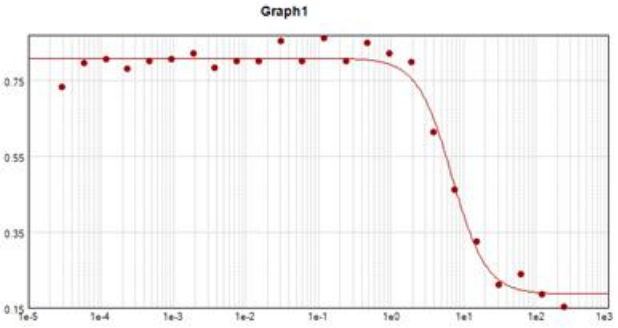

Curve Fit : 4-Parameter $y = D + \frac{A - D}{1 + \left(\frac{x}{C}\right)^B}$

	Parameter	Estimated Value
Plot1 R^2 = 0.984 EC50 = 6.978	A	0.809
	B	1.833
	C	6.978
	D	0.186

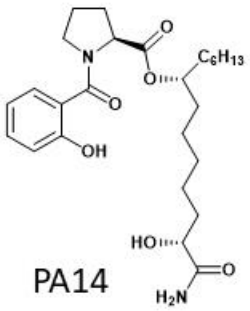

PA14

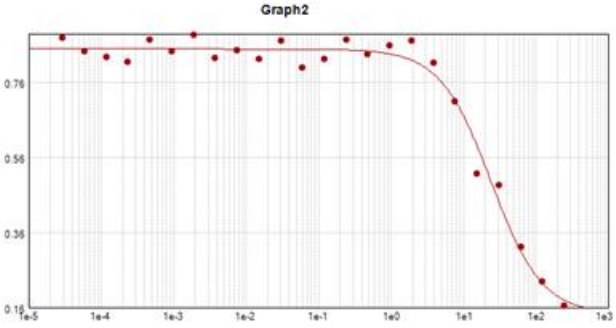

Curve Fit : 4-Parameter $y = D + \frac{A - D}{1 + \left(\frac{x}{C}\right)^B}$

	Parameter	Estimated Value
Plot1 R^2 = 0.980 EC50 = 24.28	A	0.849
	B	1.238
	C	24.28
	D	0.142

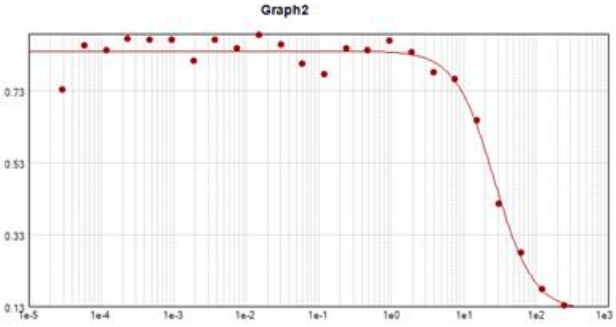

Curve Fit : 4-Parameter $y = D + \frac{A - D}{1 + \left(\frac{x}{C}\right)^B}$

	Parameter	Estimated Value
Plot1 R^2 = 0.977 EC50 = 27.05	A	0.842
	B	1.620
	C	27.05
	D	0.118

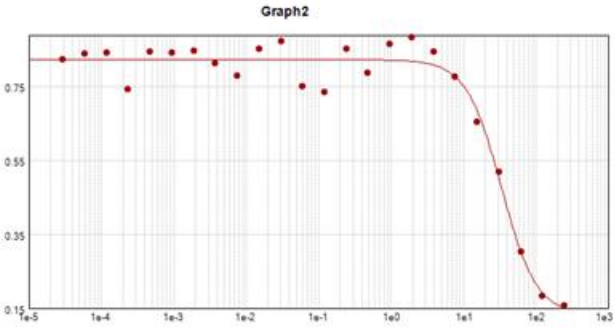

Curve Fit : 4-Parameter $y = D + \frac{A - D}{1 + \left(\frac{x}{C}\right)^B}$

	Parameter	Estimated Value
Plot1 R^2 = 0.965 EC50 = 33.66	A	0.823
	B	1.798
	C	33.66
	D	0.132

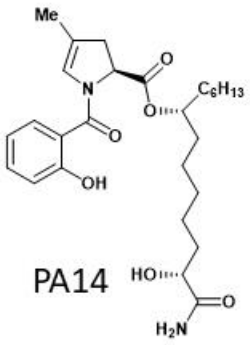

PA14

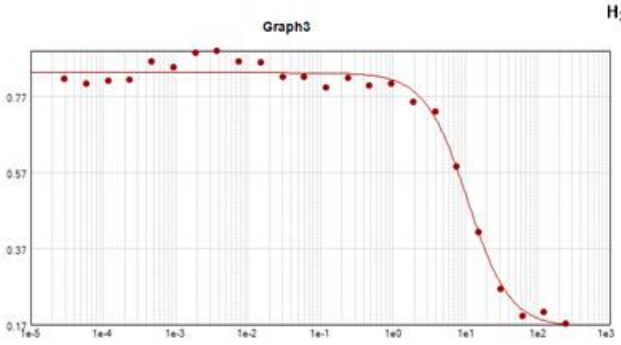

Curve Fit : 4-Parameter $y = D + \frac{A - D}{1 + \left(\frac{x}{C}\right)^B}$

	Parameter	Estimated Value
Plot1 R^2 = 0.989 EC50 = 10.83	A	0.832
	B	1.493
	C	10.83
	D	0.163

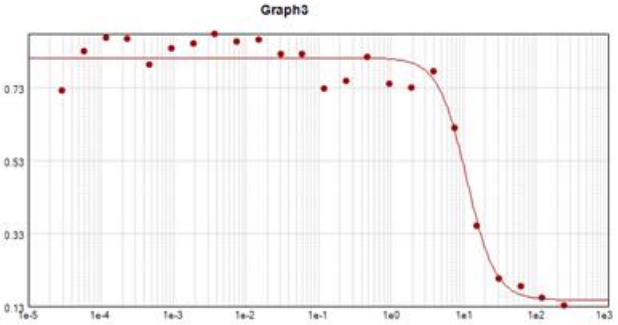

Curve Fit : 4-Parameter $y = D + \frac{A - D}{1 + \left(\frac{x}{C}\right)^B}$

	Parameter	Estimated Value
Plot1 R^2 = 0.969 EC50 = 11.18	A	0.814
	B	2.213
	C	11.18
	D	0.147

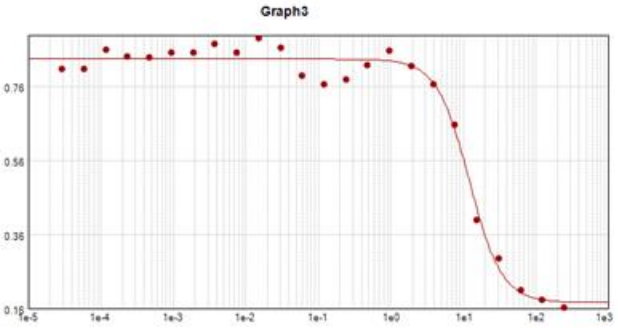

Curve Fit : 4-Parameter $y = D + \frac{A - D}{1 + \left(\frac{x}{C}\right)^B}$

	Parameter	Estimated Value
Plot1 R^2 = 0.984 EC50 = 12.18	A	0.835
	B	1.936
	C	12.18
	D	0.176

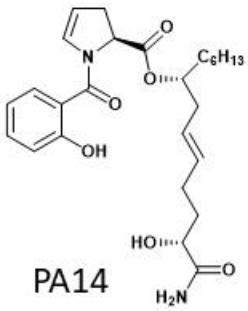

PA14

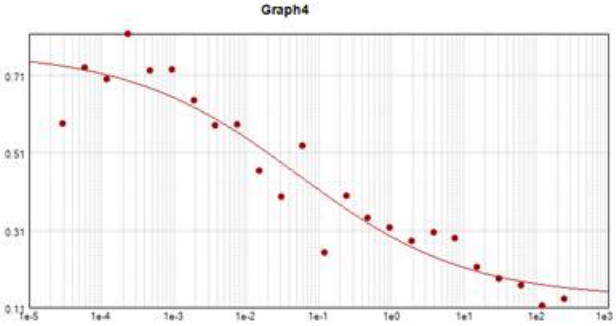

Curve Fit : 4-Parameter $y = D + \frac{A - D}{1 + \left(\frac{x}{C}\right)^B}$

	Parameter	Estimated Value
Plot1 R^2 = 0.907 EC50 = 0.052	A	0.773
	B	0.373
	C	0.052
	D	0.135

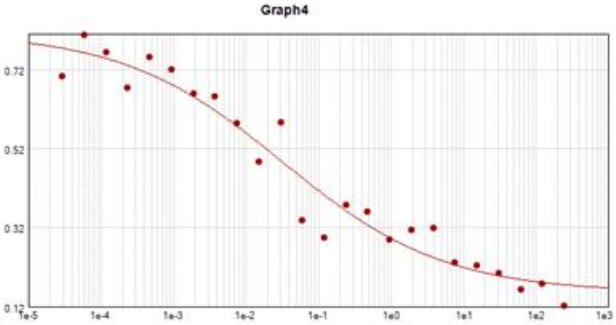

Curve Fit : 4-Parameter $y = D + \frac{A - D}{1 + \left(\frac{x}{C}\right)^B}$

	Parameter	Estimated Value
Plot1 R^2 = 0.945 EC50 = 0.033	A	0.813
	B	0.391
	C	0.033
	D	0.156

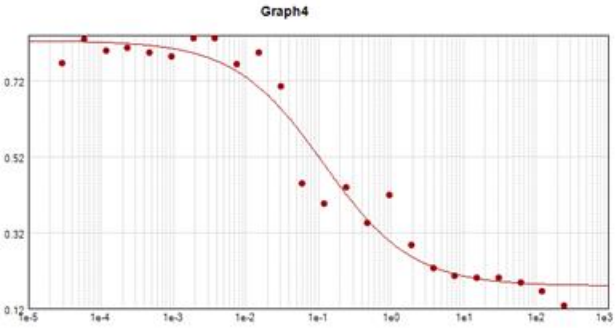

Curve Fit : 4-Parameter $y = D + \frac{A - D}{1 + \left(\frac{x}{C}\right)^B}$

	Parameter	Estimated Value
Plot1 R^2 = 0.961 EC50 = 0.118	A	0.825
	B	0.712
	C	0.118
	D	0.179

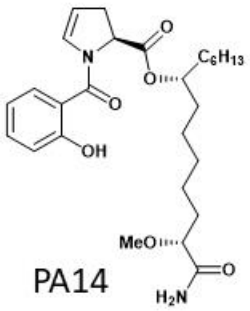

PA14

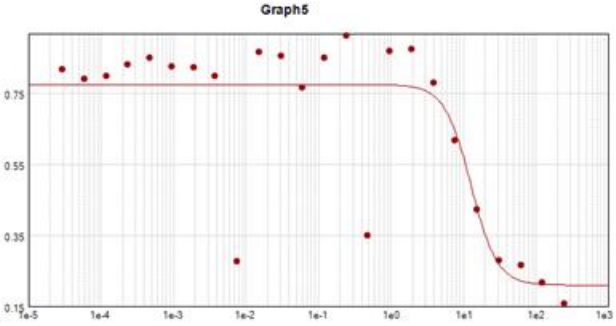

Curve Fit : 4-Parameter $y = D + \frac{A - D}{1 + \left(\frac{x}{C}\right)^B}$

	Parameter	Estimated Value
Plot1 R^2 = 0.669 EC50 = 12.78	A	0.776
	B	2.395
	C	12.78
	D	0.209

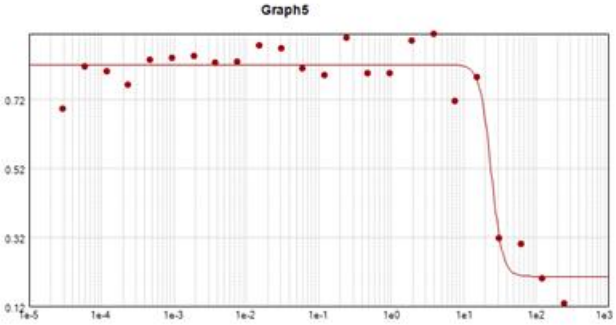

Curve Fit : 4-Parameter $y = D + \frac{A - D}{1 + \left(\frac{x}{C}\right)^B}$

	Parameter	Estimated Value
Plot1 R^2 = 0.939 EC50 = 24.21	A	0.820
	B	5.682
	C	24.21
	D	0.206

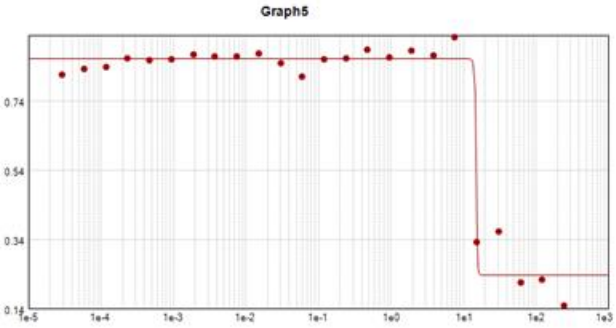

Curve Fit : 4-Parameter $y = D + \frac{A - D}{1 + \left(\frac{x}{C}\right)^B}$

	Parameter	Estimated Value
Plot1 R^2 = 0.976 EC50 = 15.03	A	0.861
	B	44.45
	C	15.03
	D	0.236

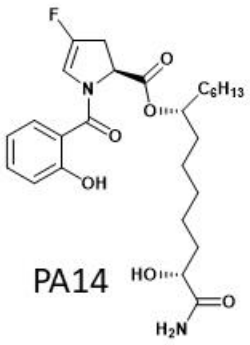

PA14

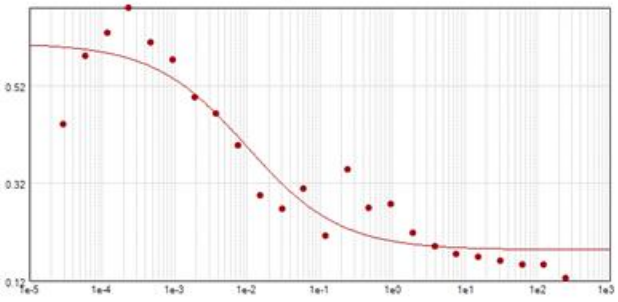

Curve Fit : 4-Parameter $y = D + \frac{A - D}{1 + \left(\frac{x}{C}\right)^B}$

	Parameter	Estimated Value
Plot1 R^2 = 0.884 EC50 = 0.010	A	0.607
	B	0.676
	C	0.010
	D	0.183

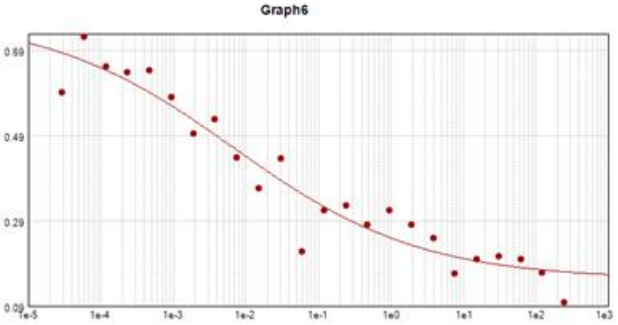

Curve Fit : 4-Parameter $y = D + \frac{A - D}{1 + \left(\frac{x}{C}\right)^B}$

	Parameter	Estimated Value
Plot1 R^2 = 0.927 EC50 = 0.007	A	0.770
	B	0.337
	C	0.007
	D	0.153

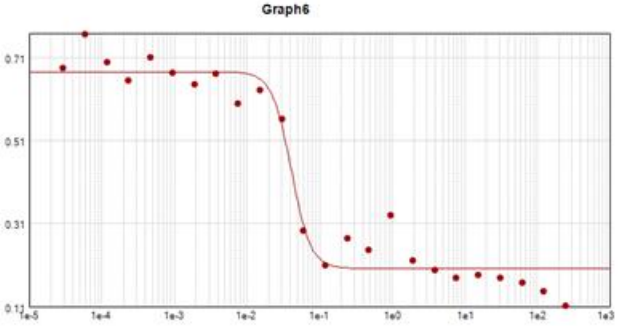

Curve Fit : 4-Parameter $y = D + \frac{A - D}{1 + \left(\frac{x}{C}\right)^B}$

	Parameter	Estimated Value
Plot1 R^2 = 0.957 EC50 = 0.041	A	0.677
	B	3.269
	C	0.041
	D	0.202

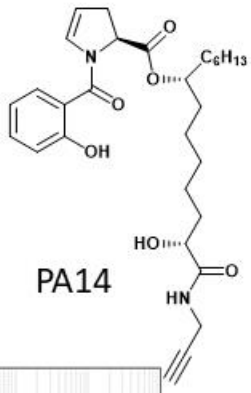

PA14

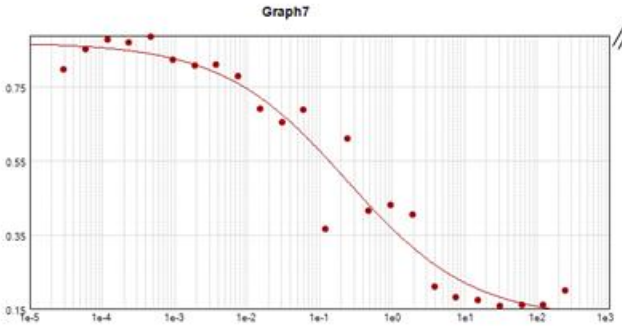

Curve Fit : 4-Parameter $y = D + \frac{A - D}{1 + \left(\frac{x}{C}\right)^B}$

	Parameter	Estimated Value
Plot1 R^2 = 0.953 EC50 = 0.241	A	0.871
	B	0.505
	C	0.241
	D	0.122

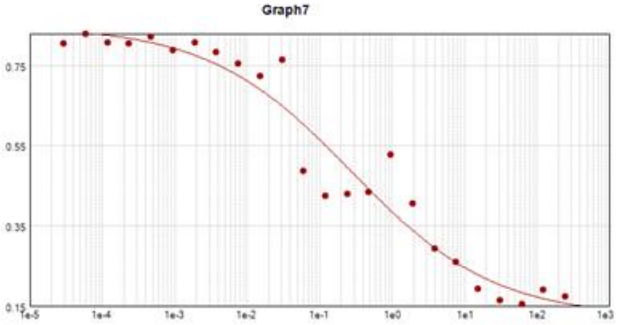

Curve Fit : 4-Parameter $y = D + \frac{A - D}{1 + \left(\frac{x}{C}\right)^B}$

	Parameter	Estimated Value
Plot1 R^2 = 0.948 EC50 = 0.277	A	0.849
	B	0.440
	C	0.277
	D	0.122

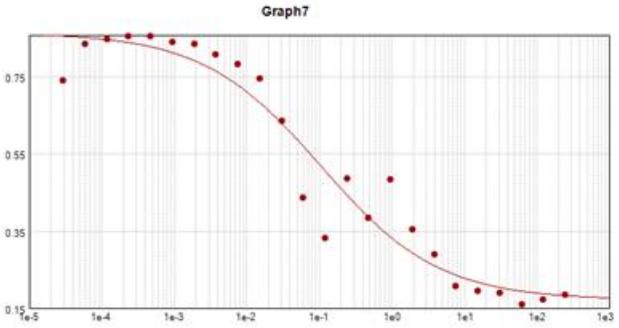

Curve Fit : 4-Parameter $y = D + \frac{A - D}{1 + \left(\frac{x}{C}\right)^B}$

	Parameter	Estimated Value
Plot1 R^2 = 0.939 EC50 = 0.106	A	0.866
	B	0.533
	C	0.106
	D	0.171

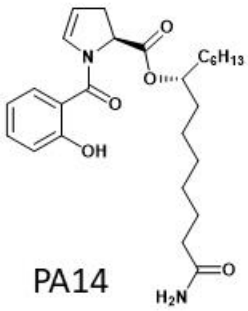

PA14

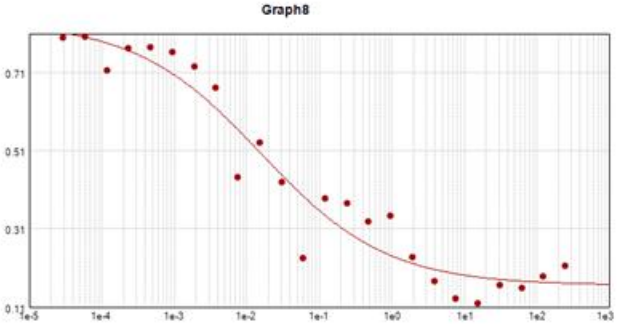

Curve Fit : 4-Parameter $y = D + \frac{A - D}{1 + \left(\frac{x}{C}\right)^B}$

	Parameter	Estimated Value
Plot1 R^2 = 0.938 EC50 = 0.016	A	0.839
	B	0.500
	C	0.016
	D	0.166

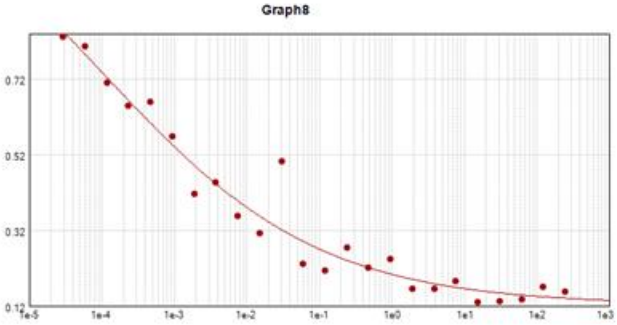

Curve Fit : 4-Parameter $y = D + \frac{A - D}{1 + \left(\frac{x}{C}\right)^B}$

	Parameter	Estimated Value
Plot1 R^2 = 0.951 EC50 = 1.03e-4	A	1.350
	B	0.289
	C	1.03e-4
	D	0.123

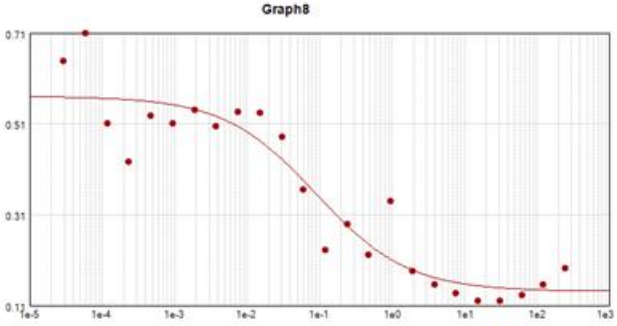

Curve Fit : 4-Parameter $y = D + \frac{A - D}{1 + \left(\frac{x}{C}\right)^B}$

	Parameter	Estimated Value
Plot1 R^2 = 0.887 EC50 = 0.090	A	0.570
	B	0.685
	C	0.090
	D	0.141

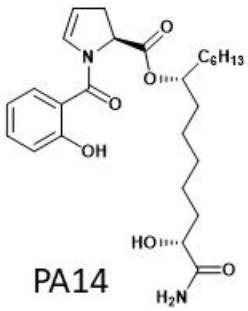

PA14

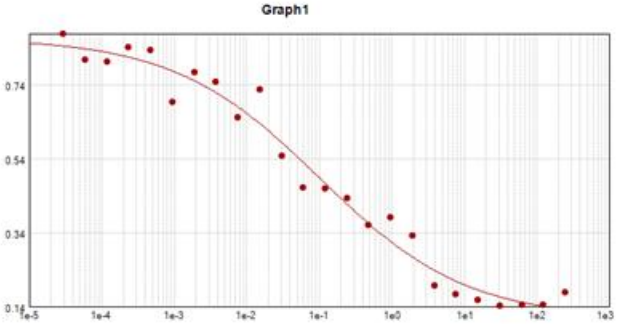

Curve Fit : 4-Parameter $y = D + \frac{A - D}{1 + \left(\frac{x}{C}\right)^B}$

	Parameter	Estimated Value
Plot1 R^2 = 0.975 EC50 = 0.103	A	0.868
	B	0.430
	C	0.103
	D	0.106

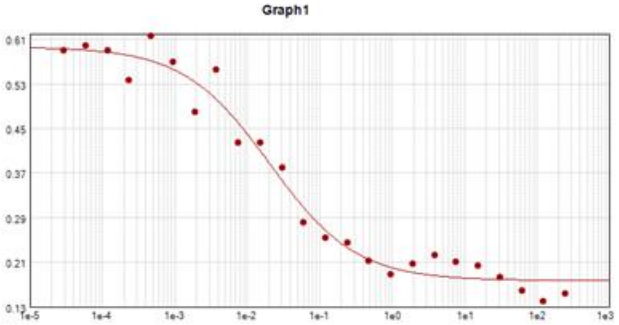

Curve Fit : 4-Parameter $y = D + \frac{A - D}{1 + \left(\frac{x}{C}\right)^B}$

	Parameter	Estimated Value
Plot1 R^2 = 0.974 EC50 = 0.021	A	0.596
	B	0.730
	C	0.021
	D	0.177

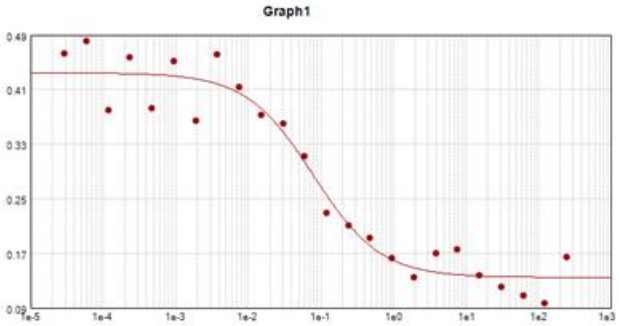

Curve Fit : 4-Parameter $y = D + \frac{A - D}{1 + \left(\frac{x}{C}\right)^B}$

	Parameter	Estimated Value
Plot1 R^2 = 0.948 EC50 = 0.079	A	0.435
	B	0.940
	C	0.079
	D	0.135

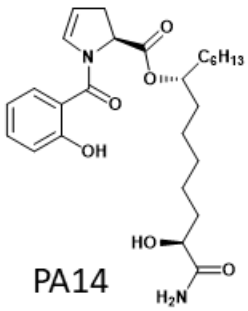

PA14

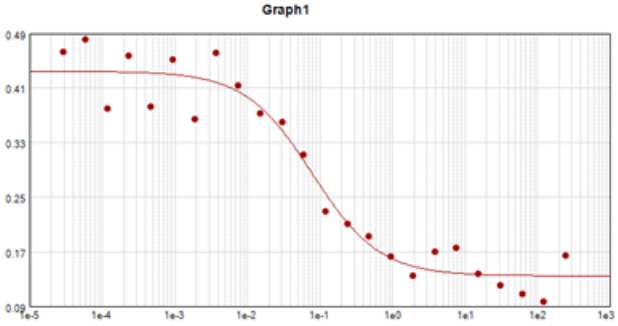

Curve Fit : 4-Parameter $y = D + \frac{A - D}{1 + \left(\frac{x}{C}\right)^B}$

	Parameter	Estimated Value
Plot1 R^2 = 0.948 EC50 = 0.079	A	0.435
	B	0.940
	C	0.079
	D	0.135

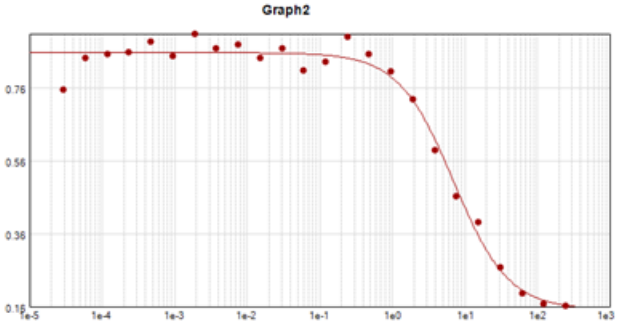

Curve Fit : 4-Parameter $y = D + \frac{A - D}{1 + \left(\frac{x}{C}\right)^B}$

	Parameter	Estimated Value
Plot1 R^2 = 0.984 EC50 = 7.017	A	0.858
	B	1.147
	C	7.017
	D	0.152

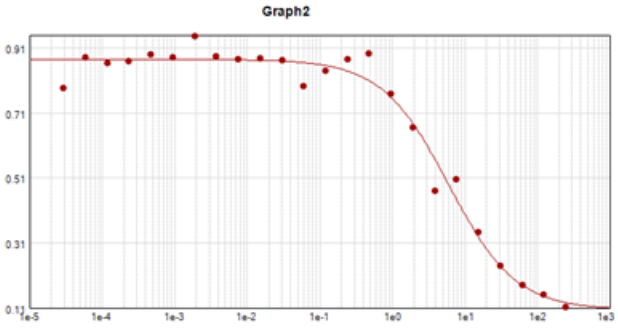

Curve Fit : 4-Parameter $y = D + \frac{A - D}{1 + \left(\frac{x}{C}\right)^B}$

	Parameter	Estimated Value
Plot1 R^2 = 0.977 EC50 = 6.013	A	0.875
	B	0.943
	C	6.013
	D	0.104

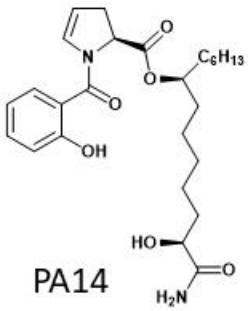

PA14

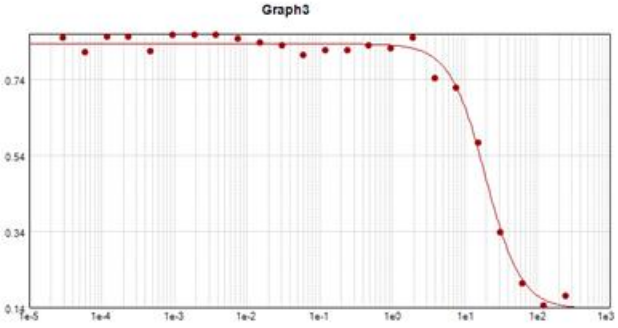

Curve Fit : 4-Parameter $y = D + \frac{A - D}{1 + \left(\frac{x}{C}\right)^B}$

	Parameter	Estimated Value
Plot1 R^2 = 0.992	A	0.833
EC50 = 19.44	B	1.777
	C	19.44
	D	0.135

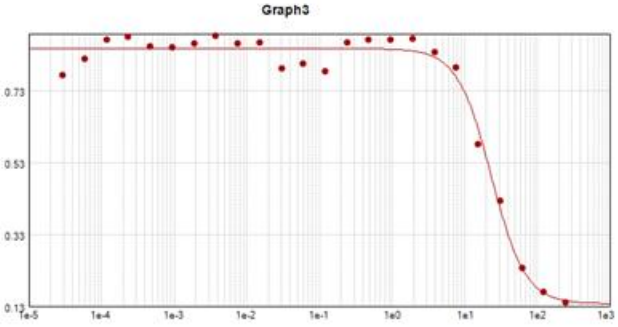

Curve Fit : 4-Parameter $y = D + \frac{A - D}{1 + \left(\frac{x}{C}\right)^B}$

	Parameter	Estimated Value
Plot1 R^2 = 0.981	A	0.849
EC50 = 23.45	B	1.865
	C	23.45
	D	0.137

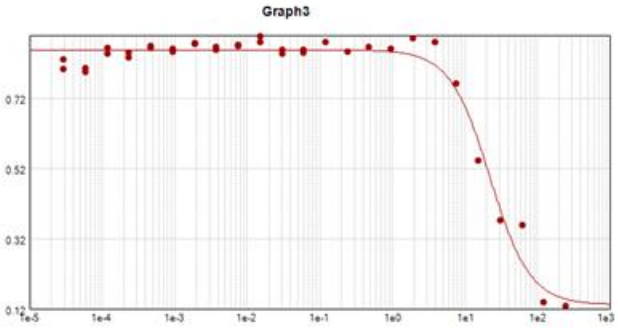

Curve Fit : 4-Parameter $y = D + \frac{A - D}{1 + \left(\frac{x}{C}\right)^B}$

	Parameter	Estimated Value
Plot1 R^2 = 0.973	A	0.858
EC50 = 22.31	B	1.575
	C	22.31
	D	0.132

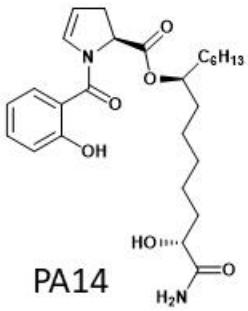

PA14

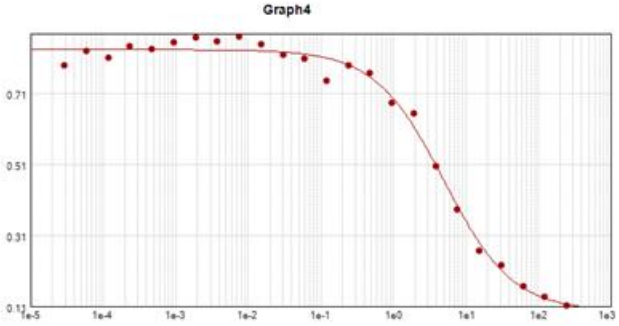

Curve Fit : 4-Parameter $y = D + \frac{A - D}{1 + \left(\frac{x}{C}\right)^B}$

	Parameter	Estimated Value
Plot1 R^2 = 0.992 EC50 = 5.010	A	0.834
	B	0.918
	C	5.010
	D	0.096

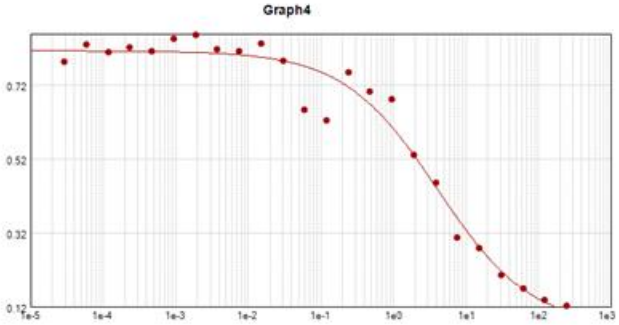

Curve Fit : 4-Parameter $y = D + \frac{A - D}{1 + \left(\frac{x}{C}\right)^B}$

	Parameter	Estimated Value
Plot1 R^2 = 0.970 EC50 = 4.082	A	0.814
	B	0.673
	C	4.082
	D	0.064

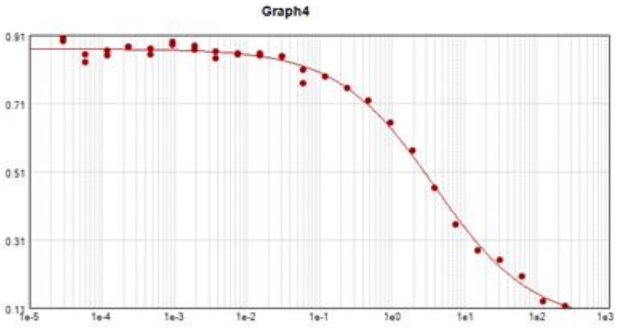

Curve Fit : 4-Parameter $y = D + \frac{A - D}{1 + \left(\frac{x}{C}\right)^B}$

	Parameter	Estimated Value
Plot1 R^2 = 0.995 EC50 = 3.877	A	0.869
	B	0.649
	C	3.877
	D	0.065

5.3 Chemistry: General notes

NMR spectra were recorded using the following spectrometers: Bruker Advance 500 (500/125 MHz) or Bruker Advance 400 (400/100 MHz). Chemical shifts are quoted in ppm relative to tetramethylsilane and with the indicated solvent as an internal reference. The following abbreviations are used to describe signal multiplicities: s (singlet), d (doublet), t (triplet), q (quartet), m (multiplet), br (broad), dd (doublet of doublets), dt (doublet of triplets), etc. Accurate mass spectra were recorded on an Agilent 6520 Accurate-Mass Q-TOF LC/MS, infrared spectra were obtained using a Thermo Nicolet Nexus 670 FTIR spectrophotometer and specific rotation measurements were made with a 1 dm path length using a Perkin Elmer 341 Polarimeter.

Non-aqueous reactions were performed under an atmosphere of argon, in flame- dried glassware, with HPLC-grade solvents dried by passage through activated alumina. 2,6-lutidine, triethylamine, and diisopropylethylamine were freshly distilled from CaH2 prior to use. Brine refers to a saturated aqueous solution of sodium chloride, sat. NaHCO3 refers to a saturated aqueous solution of sodium bicarbonate, sat. NH4Cl refers to a saturated aqueous solution of ammonium chloride, etc. 3 Å molecular sieves were activated in a round-bottom flask under vacuum heating at 120°C in an oil bath overnight. “Column chromatography”, unless otherwise indicated, refers to purification in a gradient of increasing EtOAc concentration in hexanes on a Biotage® flash chromatography purification system. Metathesis catalysts were obtained as generous gifts from Materia, Inc. All other chemicals were used as received from Oakwood, TCI America, Sigma-Aldrich, Alfa Aesar, or AK Scientific.

5.4 Chemistry: Procedures and characterization

Chapter 2:

General procedure A: Cross metathesis. Homoallylic alcohol (5 eq) was combined with **TBS protected alkene (1 eq)** in CH_2Cl_2 (**0.02M**). The flask was charged with catalyst C711 (Materia, CAS [635679-242]) (**10 mol%**) and stirred under a static argon atmosphere for 24 hours. The solution was loaded directly onto a silica gel column and subjected to chromatography.

General procedure B: Hydrogenation of alkenes. Alkene (1 eq) was dissolved in EtOAc (**.05 M**) and 10% Pd/C (**5 mol%**) then the reaction flask was vacuum and backfilled with H_2 5x and stirred under a H_2 balloon overnight. The reaction was filtered through celite and concentrated.

General procedure C: Removal of Evans oxazolidinone. Alcohol (1 eq) was dissolved in THF (**0.03 M**) and ammonium hydroxide (**concentration**) was added. The flask was tightly sealed and the biphasic mixture was stirred for 48 hours. The reaction was carefully vented, concentrated, and azeotroped with methanol 3x. The crude reaction was purified with column chromatography (20% Et_2O/DCM → 30% Et_2O/DCM → 5%MeOH/30%Et_2O/65% DCM).

General procedure D: SEM protection of methyl hydroxybenzoates. To a methyl hydroxybenzoate (1 eq) dissolved in CH_2Cl_2 (2 M) was added SEMCl (2 eq) and then cooled to 0 °C. Diisopropylethylamine (4 eq) was added dropwise and the solution was allowed to warm to room temperature while stirring overnight. The following day, the mixture was poured into water and extracted with Et_2O 3x. The combined organic layers were washed with brine, dried over $MgSO_4$, filtered, concentrated, and purified by column chromatography.

General procedure E: Hydrolysis of methyl esters. Methyl ester (1.0 eq) was dissolved in 3:1:1 THF:MeOH:H_2O (1 M) and LiOH•H_2O (5 eq) was added as a solution in a minimal volume of water. The

reaction was monitored by TLC and upon completion was carefully acidified by addition of 1M HCl or 5% AcOH (pH 5-6). The solution was extracted with CH_2Cl_2 3x, washed with brine, dried over $MgSO_4$, filtered, and concentrated.

General procedure F: HATU-mediated amide coupling of SEM-benzoic acids and hydroxyproline methyl ester. Acid (1.0 eq) was dissolved in DMF (0.2 M) with HATU (1.2 eq) to which a solution of amine hydrochloride (1.2 eq) and diisopropylethylamine (1.5 eq) in an equal volume of DMF was added. Another portion of diisopropylethylamine (3 eq) was added and the reaction was allowed to stir overnight, then was poured into water and extracted with EtOAc 3x. The combined organic layers were washed with sat. NH_4Cl, sat. $NaHCO_3$, water 2x and brine 2x, then dried over $MgSO_4$, filtered, concentrated, and purified by column chromatography (0 → 50% EtOAc/CH_2Cl_2).

General procedure G: DMP oxidation. An acylated trans-L-hydroxyproline derivative (1 eq) was dissolved in dry CH_2Cl_2 (0.05 M), and to the resulting solution was added $NaHCO_3$ (20 eq) and Dess-Martin periodinane (2 eq), and the reaction was allowed to stir overnight. The next day, the reaction was quenched with 2:1:1 H_2O:sat. $NaHCO_3$:sat. $Na_2S_2O_3$ and allowed to stir for an hour. The mixture was then extracted with CH2Cl2 3x and the combined organic layers were washed with sat. $Na_2S_2O_3$, sat. $NaHCO_3$, water, and brine, then dried over $MgSO_4$, filtered, concentrated, and purified by column chromatography.

General procedure H: Synthesis of enol triflates from ketones. Ketone (1 eq) was dissolved in CH_2Cl_2 (0.1 M) and cooled to -50 °C. 2,6-Lutidine (4 eq) was added, and trifluoromethanesulfonic anhydride (2 eq) was added dropwise. The reaction was allowed to warm to -35 °C. After 30 minutes the reaction was quenched with sat. $NaHCO_3$ and extracted with CH_2Cl_2 3x. The combined organic layers were washed with sat. $NaHCO_3$, brine, dried over $MgSO_4$, concentrated, and purified by column chromatography (0 → 5% EtOAc/hexanes held at 5% until 2,6-lutidine finished eluting, then 5 → 20% EtOAc/hexanes).

General procedure I: Reductive cleavage of enol triflates. To a solution of enol triflate (1 eq) dissolved in THF (0.1 M) was added PPh_3 (0.3 eq), $Pd(OAc)_2$ (0.1 eq), and flame-dried LiCl (1.5 eq). Tributyltin hydride (1 eq) was then added dropwise. The reactions turned orange or brown upon completion, then were quenched with a solution of KF (1M) and extracted with Et_2O 3x. The combined organic layers were washed with 1M KF, water, and brine, dried over Na_2SO_4, filtered, concentrated, and purified by column chromatography (0 → 30% EtOAc/hexanes, load in CH_2Cl_2).

General procedure J: EDC Esterification. An acid (1.3 eq) was dissolved in DCM (0.2 M), cooled to 0°C and EDC (2 eq) was added. A solution of alcohol (1 eq) and DMAP (0.5 eq) were dissolved in an equal volume of DCM and added to the first solution. The reaction was allowed to warm to room temperature and stir overnight. The resulting mixture was poured into water and extracted with DCM 3x. The combined organic layers were washed with brine, dried over $MgSO_4$, concentrated, and purified by column chromatography (0 → 30% EtOAc/DCM).

General procedure K: Shiina esterification. To a solution of acid (1.4 eq) dissolved in CH_2Cl_2 (0.2 M) was added MNBA (2.6 eq) and Et_3N (3.3 eq), and the solution was stirred for 10 minutes. Then alcohol (1 eq) and DMAP (0.1 eq) dissolved in an equal volume of CH_2Cl_2 as above was added, and the reaction was stirred overnight. The reaction was poured into sat. NH_4Cl, extracted with CH_2Cl_2 3x, washed with brine, dried over $MgSO_4$, filtered, concentrated, and purified by column chromatography (0 → 30% Et_2O/CH_2Cl_2).

General procedure L: Global Deprotection. The protected ester was dissolved in DMPU (1:1 v/v TBAF, dried over 3Å molecular sieves). Tetrabutylammonium fluoride (20 eq, 1M solution in THF, dried over 3Å molecular sieves for 1 - 2 days) was added dropwise. The reaction was quenched with sat. NH_4Cl after 30 minutes. The mixture was extracted with Et_2O (5 times, TLC analysis of aqueous layer to confirm full extraction), and the combined organic layers were washed with sat'd NH_4Cl 5x followed by brine. The

solution was dried over Na_2SO_4, concentrated, and purified by column chromatography (0 → 5% MeOH/CH_2Cl_2).

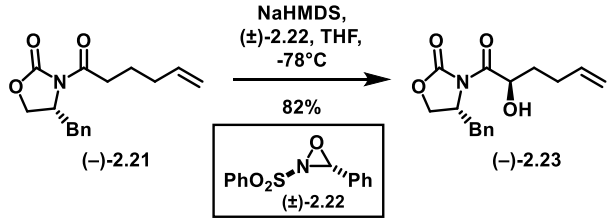

(4R)-4-benzyl-3-[(2R)-2-hydroxyhex-5-enoyl]-1,3-oxazolidin-2-one ((-)-2.23). NaHMDS (16.2 mL, 1M soln. in THF, 16.2 mmol) was diluted with anhydrous THF (100 mL) and cooled to -78°C. **(-)-2.21** (3.7 g, 13.53 mmol) was dissolved in THF (20 mL), cooled to -78°C, and slowly added to the NaHMDS solution via cannula. The resulting solution was stirred for an hour at -78°C. Davis oxaziridine (**(±)-2.22**, 5.3 g, 20.3 mmol) was dissolved in THF (20 mL) and added via syringe pump to the reaction over a 25 minute period. The reaction was stirred for an additional hour at -78°C. (±)-Camphorsulfonic acid (CSA) (15.7 g, 67.8 mmol) dissolved in THF (135 mL) was added, and the reaction was warmed up to room temperature. H2O was added, and the solution was extracted 3x EtOAc. The combined organic layers were washed with brine, dried (MgSO4), filtered, concentrated, and purified by column chromatography (0→10% EtOAc in hexanes) to yield **(-)-2.23** as a yellow oil (3.2 g, 82%). $\mathbf{R_f}$ (2:1 hexanes:EtOAc) = 0.36; **^{1}H NMR** (400 MHz, CDCl3) δ = 7.37 – 7.26 (m, 3H), 7.23 – 7.19 (m, 2H), 5.84 (ddt, J = 17.0, 10.2, 6.7 Hz, 1H), 5.08 (ddd, J = 17.1, 3.5, 1.6 Hz, 1H), 5.03 – 4.96 (m, 2H), 4.67 (ddt, J = 9.5, 6.9, 3.2 Hz, 1H), 4.31 – 4.22 (m, 2H), 3.52 (d, J = 7.8 Hz, 1H), 3.31 (dd, J = 13.5, 3.2 Hz, 1H), 2.84 (dd, J = 13.5, 9.3 Hz, 1H), 2.38 – 2.18 (m, 2H), 1.92 (dddd, J = 13.8, 9.1, 7.1, 3.5 Hz, 1H), 1.69 (dtd, J = 14.3, 8.5, 5.9 Hz, 1H); **^{13}C NMR** (125 MHz, CDCl3) δ = 174.9, 153.3, 137.6, 134.9, 129.6, 129.1, 127.6, 115.4, 70.3, 67.1, 55.6, 37.6, 33.3, 29.5; $\mathbf{[\alpha]^{25}_D}$ -59.1 (c = 1.75 in CHCl3); **IR** (film) 3502 (br O-H) 2925, 1778 (C=O), 1695 (C=O), 1497, 1455, 1397, 1351, 1289, 1210, 1197, 1109, 1074, 1051, 980, 914, 751, 701; **HRMS** Accurate mass (ES^+): Found 290.1393 (-0.6 ppm), $C_{16}H_{19}NO_4$ ($M+H^+$) requires 290.1387.

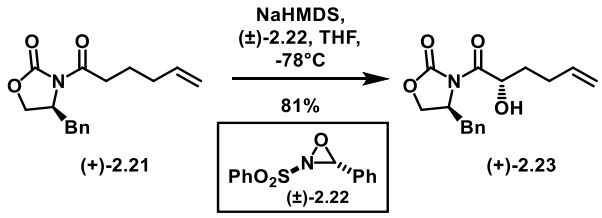

(4S)-4-benzyl-3-[(2S)-2-hydroxyhex-5-enoyl]-1,3-oxazolidin-2-one ((+)-**2.23).** Following the same procedure as (–)-**2.23**; NaHMDS (6.218 mL, 1M soln. in THF, 6.218 mmol), diluted with THF (35 mL), compound **(+)-2.21** (1.4162g, 5.1813 mmol) dissolved in THF (10 mL), Davis oxaziridine (2.031g, 7.7720 mmol) dissolved in THF (10 mL), and CSA (6.018g, 25.907 mmol) dissolved in THF (50 mL) yielded **(+)-2.23** as a yellow oil (1.211g, 81%) **^{1}H NMR** (500 MHz, $CDCl_3$) δ = 7.35 (tt, J = 8.1, 1.7 Hz, 2H), 7.31 – 7.27 (m, 1H), 7.23 – 7.19 (m, 2H), 5.84 (ddt, J = 17.0, 10.2, 6.7 Hz, 1H), 5.08 (ddd, J = 17.1, 3.5, 1.6 Hz, 1H), 5.03 – 4.96 (m, 2H), 4.73 – 4.62 (m, 1H), 4.32 – 4.22 (m, 2H), 3.50 (d, J = 7.8 Hz, 1H), 3.31 (dd, J = 13.5, 3.3 Hz, 1H), 2.85 (dd, J = 13.5, 9.4 Hz, 1H), 2.35 – 2.22 (m, 2H), 1.92 (dddd, J = 13.8, 9.1, 7.0, 3.5 Hz, 1H), 1.70 (dtd, J = 14.2, 8.6, 5.7 Hz, 1H); **^{13}C NMR** (100 MHz, $CDCl_3$) δ = 174.9, 153.4, 137.7, 134.9, 129.6, 129.2, 127.7, 115.5, 70.4, 67.1, 55.7, 37.6, 33.4, 29.5; **$[\alpha]^{25}_{D}$** +62.1 (c = 1.47 in $CHCl_3$); **IR** (film) 3502 (br O-H), 2922 (C-H), 1778 (C=O), 1695 (C=O), 1640, 1498, 1387, 1351, 1288, 1255, 1211, 1197, 1109, 1074, 1051, 980, 913, 814, 752, 733, 701, 634, 592; **HRMS** Accurate mass (ES^+): Found 290.1385 (-0.2 ppm), $C_{16}H_{19}NO_4$ ($M+H^+$) requires 290.1387.

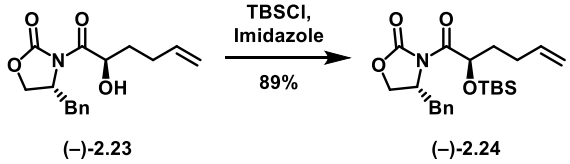

(4R)-4-benzyl-3-[(2R)-2-hydroxyhex-5-enoyl]-1,3-oxazolidin-2-one ((-)-2.24). To a solution of **(-)-2.23** (3.16g, 10.92 mmol) in DMF (60 mL) at 0°C was added tert-Butyldimethylsilyl chloride (2.47g, 16.38 mmol) and imidazole (966 mg, 14.19 mmol). The solution was then allowed to warm to room temperature and stirred overnight. The following day, the reaction was poured into H_2O (60 mL) and extracted with 1:1

EtOAc:hexanes (4x50 mL). The combined organic layers were washed sequentially with H_2O and brine, dried (Na_2SO_4), filtered, concentrated, and purified by column chromatography to give **(-)-2.24** as a clear oil (3.90 g, 89%). $\mathbf{R_f}$ (2:1 hexanes:EtOAc) = 0.78 ; **^{1}H NMR** (400 MHz, $CDCl_3$) δ 7.37 – 7.27 (m, 3H), 7.26 – 7.21 (m, 2H), 5.83 (ddt, J = 16.9, 10.2, 6.6 Hz, 1H), 5.39 (dd, J = 8.2, 3.5 Hz, 1H), 5.04 (ddd, J = 17.1, 3.3, 1.7 Hz, 1H), 4.98 (dd, J = 10.2, 1.6 Hz, 1H), 4.62 (ddt, J = 9.9, 6.5, 3.4 Hz, 1H), 4.28 – 4.12 (m, 2H), 3.41 (dd, J = 13.3, 3.3 Hz, 1H), 2.70 (dd, J = 13.2, 10.2 Hz, 1H), 2.34 – 2.13 (m, 2H), 1.85 – 1.66 (m, 2H), 0.96 – 0.93 (m, 9H), 0.11 (s, 3H), 0.09 (s, 3H); **^{13}C NMR** (100 MHz, $CDCl_3$) δ = 174.4, 153.2, 137.9, 135.4, 129.6, 129.2, 127.5, 115.2, 71.0, 66.7, 55.8, 37.8, 34.7, 29.8, 26.0, 18.5, -4.5, -4.9; **$[\alpha]^{25}_D$** -5.8 (c = 1.10 in $CHCl_3$) ; **IR** (film) 2953, 2929, 2857, 1779 (C=O), 1713 (C=O), 1456, 1472, 1387, 1348, 1250, 1209, 1196, 1142, 1106, 1050, 1011, 983, 913, 814, 777, 700; **HRMS** Accurate mass (ES^+): Found 404.2262 (+1.0 ppm), $C_{22}H_{33}NO_4Si$ ($M+H^+$) requires 404.2252.

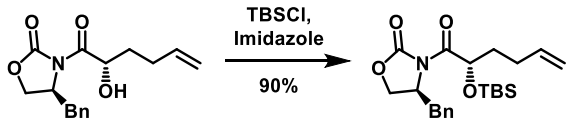

(+)-2.23 (+)-2.24

(4S)-4-benzyl-3-[(2S)-2-[(tert-butyldimethylsilyl)oxy]hex-5-enoyl]-1,3-oxazolidin-2-one ((+)-2.24). Following the same procedure as **(-)-2.24**; compound **(+)-2.23** (599 mg, 2.069 mmol) in DMF (12 mL), tertbutyldimethylsilyl chloride (525.9 mg, 3.489 mmol), and imidazole (206 mg, 3.024 mmol), yielded **(+)-2.24** as a clear oil (751 mg, 90%). **^{1}H NMR** (500 MHz, $CDCl_3$) δ = 7.36 – 7.31 (m, 2H), 7.30 – 7.26 (m, 1H), 7.26 – 7.23 (m, 2H), 5.83 (ddt, J = 17.0, 10.2, 6.6 Hz, 1H), 5.39 (dd, J = 8.3, 3.4 Hz, 1H), 5.04 (ddd, J = 17.1, 3.5, 1.6 Hz, 1H), 4.98 (ddd, J = 10.2, 3.2, 1.3 Hz, 1H), 4.62 (ddt, J = 10.1, 6.6, 3.3 Hz, 1H), 4.24 – 4.16 (m, 2H), 3.41 (dd, J = 13.3, 3.2 Hz, 1H), 2.70 (dd, J = 13.3, 10.2 Hz, 1H), 2.31 – 2.16 (m, 2H), 1.85 – 1.68 (m, 2H), 0.94 (s, 9H), 0.11 (s, 3H), 0.09 (s, 3H); **^{13}C NMR** (100 MHz, $CDCl_3$) δ = 174.4, 153.2, 137.9, 135.4, 129.6, 129.1, 127.5, 115.2, 71.0, 66.7, 55.8, 37.8, 34.7, 29.8, 26.0, 18.5, -4.5, -4.9; **$[\alpha]^{25}_D$** +9.12 (c = 1.25 in $CHCl_3$); **IR** (film) 2953, 2928, 2856, 1779 (C=O), 1711 (C=O), 1455, 1387, 1348, 1250, 1209,

1195, 1143, 1106, 982, 913, 814, 777, 700; **HRMS** Accurate mass (ES^+): Found 404.2272 (+2.0 ppm), $C_{22}H_{33}NO_4Si$ ($M+H^+$) requires 404.2252.

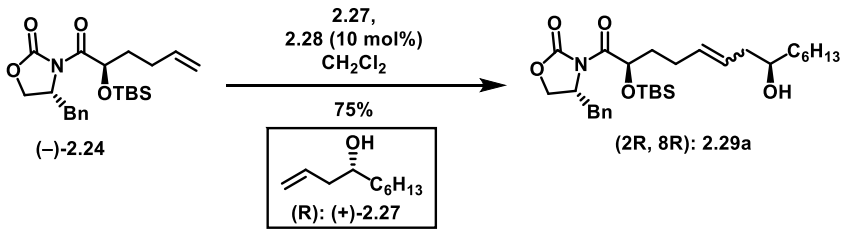

(4R)-4-benzyl-3-[(2R,8R)-2-[(tert-butyldimethylsilyl)oxy]-8-hydroxytetradec-5-enoyl]-1,3-oxazolidin-2-one (2.29a). Following general procedure A; homoallylic alcohol **(+)-2.27** (52 mg, 0.128 mmol) and oxazolidinone **(–)-2.24** (99 mg, 0.644 mmol) yielded **2.29a** as a brown oil (66 mg, 75%). $\mathbf{R_f}$ (9:1 DCM:EtOAc) = 0.73; **^{1}H NMR** (Mixture of *E*/*Z* isomers) (400 MHz, $CDCl_3$, mixture of *E*/*Z* isomers) δ = 7.37 – 7.27 (m, 3H), 7.26 – 7.22 (m, 2H), 5.64 – 5.41 (m, 2H), 5.37 (dd, J = 8.3, 3.4 Hz, 1H), 4.62 (ddt, J = 10.1, 6.5, 3.2 Hz, 1H), 4.24 – 4.16 (m, 2H), 3.59 (br s, 1H), 3.41 (dd, J = 13.2, 3.3 Hz, 1H), 2.68 (dd, J = 13.3, 10.2 Hz, 1H), 2.28 – 2.17 (m, 3H), 2.10 – 1.97 (m, 1H), 1.82 – 1.67 (m, 3H), 1.48 – 1.39 (m, 3H), 1.34 – 1.26 (m, 6H), 0.94 (s, 9H), 0.88 (t, J = 6.8 Hz, 3H), 0.12 (s, 0.44H), 0.11 (s, 2.24H), 0.10 (s, 0.64H), 0.09 (s, 2.29H); **^{13}C NMR** (100 MHz, $CDCl_3$) δ = 174.5, 153.3, 135.4, 133.1, 129.6, 129.2, 127.6, 127.4, 71.0, 70.8, 66.7, 55.8, 53.6, 40.9, 37.9, 37.0, 35.2, 32.0, 29.5, 28.6, 26.0, 25.8, 22.8, 18.5, 14.3, -4.4, - 4.9; **IR** (film) 3545 (br O-H), 2927, 2856, 1780 (C=O), 1714 (C=O), 1471, 1387, 1348, 1249, 1210, 1196, 1111, 1012 ,971, 814, 777, 700; **HRMS** Accurate mass (ES^+): Found 532.3438 (-1.5 ppm), $C_{30}H_{49}NO_5Si$ ($M+H^+$) requires 532.3453.

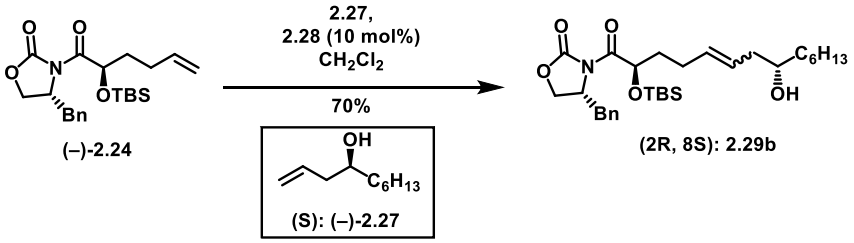

(4R)-4-benzyl-3-[(2R,8S)-2-[(tert-butyldimethylsilyl)oxy]-8-hydroxytetradec-5-enoyl]-1,3-oxazolidin-2-one (2.29b). Following general procedure A; homoallylic alcohol **(–)-2.27** (100 mg, 0.247 mmol) and oxazolidinone **(–)-2.24** (173 mg, 1.23 mmol) yielded **2.29b** as a brown oil (92 mg, 70%). **^{1}H NMR** (400 MHz, $CDCl_3$, mixture of *E*/*Z* isomers) δ = 7.37 – 7.27 (m, 3H), 7.26 – 7.22 (m, 2H), 5.51 (tdd, J = 22.0, 15.2, 6.6 Hz, 2H), 5.37 (dd, J = 8.3, 3.3 Hz, 1H), 4.62 (qd, J = 6.6, 3.1 Hz, 1H), 4.23 – 4.15 (m, 2H), 3.58 (br s, 1H), 3.41 (dd, J = 13.0, 3.1 Hz, 1H), 2.68 (dd, J = 13.2, 10.2 Hz, 1H), 2.30 – 2.15 (m, 3H), 1.85 – 1.66 (m, 3H), 1.49 – 1.38 (m, 3H), 1.33 – 1.24 (m, 8H), 0.94 (s, 9H), 0.88 (t, J = 6.8 Hz, 3H), 0.11 (s, 3H), 0.09 (s, 3H).; **^{13}C NMR** (125 MHz, $CDCl_3$) δ 174.5, 153.2, 135.4, 133.1, 129.6, 129.1, 127.5, 127.4, 71.1, 70.8, 66.7, 55.7, 40.9, 37.8, 37.0, 35.2, 32.0, 29.8, 29.5, 28.6, 26.0, 25.8, 22.8, 18.5, 14.2, -4.4, -4.9; **IR** (film) 3545 (br O-H), 2927, 2855, 1780 (C=O), 1713 (C=O), 1455, 1388, 1348, 1249, 1210, 1196, 1111, 1012, 971, 814, 777, 700; **HRMS** Accurate mass (ES^+): Found 532.3438 (-1.5 ppm), $C_{30}H_{49}NO_5Si$ ($M+H^+$) requires 532.3453.

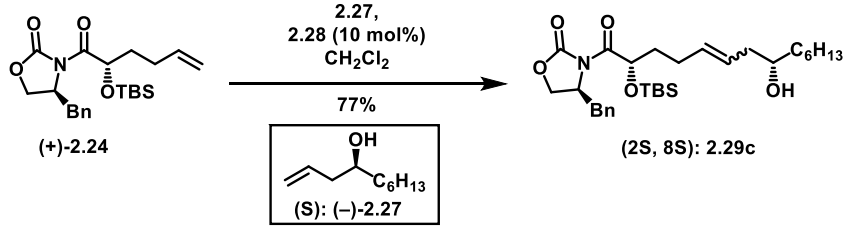

(4S)-4-benzyl-3-[(2S,8S)-2-[(tert-butyldimethylsilyl)oxy]-8-hydroxytetradec-5-enoyl]-1,3-oxazolidin-2-one (2.29c). Following general procedure A; homoallylic alcohol **(–)-2.27** (207 mg, 0.512 mmol) and oxazolidinone **(+)-2.24** (400 mg, 2.56 mmol) yielded **2.29c** as a brown oil (210 mg, 77%). **^{1}H NMR** (400 MHz, $CDCl_3$, mixture of *E*/*Z* isomers) δ = 7.37 – 7.27 (m, 3H), 7.26 – 7.22 (m, 2H), 5.61 – 5.42 (m, 2H), 5.37 (dd, J = 8.3, 3.4 Hz, 1H), 4.62 (ddt, J = 10.2, 6.6, 3.3 Hz, 1H), 4.24 – 4.15 (m, 2H), 3.65 – 3.54 (m,

1H), 3.41 (dd, J = 13.3, 3.1 Hz, 1H), 2.70 (dt, J = 13.2, 9.1 Hz, 1H), 2.32 – 2.13 (m, 3H), 1.83 – 1.66 (m, 3H), 1.50 – 1.37 (m, 3H), 1.36 – 1.20 (m, 8H), 0.94 (s, J = 5.0 Hz, 9H), 0.88 (t, J = 6.7 Hz, 3H), 0.12 (s, 0.44H), 0.11 (s, 2.19H), 0.10 (s, 0.67H), 0.09 (s, J = 3.8 Hz, 2.43H); **^{13}C NMR** (125 MHz, $CDCl_3$) δ = 174.4, 153.2, 135.3, 132.9, 129.5, 129.1, 127.5, 127.3, 66.7, 55.7, 40.8, 37.8, 36.9, 35.2, 31.9, 29.5, 28.5, 25.9, 25.9, 22.7, 18.4, 14.2, -4.5, -4.9. ; **IR** (film) 3545 (br O-H) 2927, 2856, 1779 (C=O), 1712 (C=O), 1456, 1387, 1348, 1249, 1210, 1195, 111, 1012, 971, 814, 777, 700; **HRMS** Accurate mass (ES^+): Found 532.3443 (-1.0 ppm), $C_{30}H_{49}NO_5Si$ ($M+H^+$) requires 532.3453

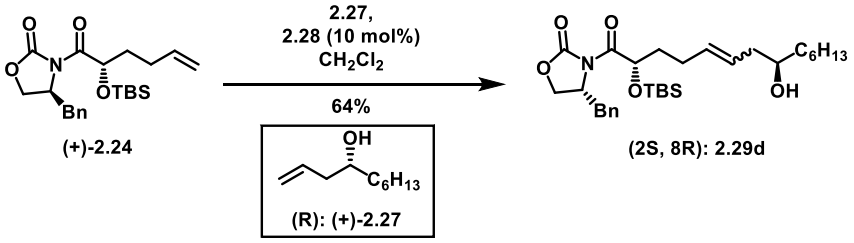

(4S)-4-benzyl-3-[(2S,8R)-2-[(tert-butyldimethylsilyl)oxy]-8-hydroxytetradec-5-enoyl]-1,3-oxazolidin-2- one. (2.29d). Following general procedure A; homoallylic alcohol **(+)-2.27** (89 mg, 0.221 mmol) and oxazolidinone **(+)-2.24** (154 mg, 0.996 mmol) yielded **2.29d** as a brown oil (75 mg, 64%). . **^{1}H NMR** (500 MHz, $CDCl_3$) δ = 7.36 – 7.31 (m, 2H), 7.31 – 7.26 (m, 1H), 7.25 – 7.22 (m, 2H), 5.58 – 5.43 (m, 2H), 5.37 (dd, J = 8.4, 3.3 Hz, 1H), 4.61 (qd, J = 6.5, 3.1 Hz, 1H), 4.22 – 4.15 (m, 2H), 3.62 – 3.53 (m, 1H), 3.41 (dd, J = 13.2, 3.2 Hz, 1H), 2.72 – 2.62 (m, 1H), 2.29 – 2.16 (m, 3H), 2.08 – 2.01 (m, 1H), 1.79 – 1.66 (m, 2H), 1.48 – 1.37 (m, 3H), 1.33 – 1.25 (m, 6H), 0.94 (s, 9H), 0.88 (t, J = 6.9 Hz, 3H), 0.10 (s, 3H), 0.09 (s, 3H); **^{13}C NMR** (125 MHz, $CDCl_3$) δ = 174.4, 153.2, 135.4, 133.1, 129.6, 129.1, 127.5, 127.4, 71.0, 70.8, 66.7, 55.7, 40.9, 37.8, 37.0, 35.2, 32.0, 29.5, 28.6, 26.0, 25.8, 22.8, 18.5, 14.2, -4.4, -4.9; **IR** (film) 3526 (br O-H), 2954, 2927, 2856, 1779 (C=O), 1711 (C=O), 1455, 1387, 1348, 1289, 1249, 1210, 1111, 971, 836, 777, 701; **HRMS** Accurate mass (ES^+): Found 532.3472 (+1.9 ppm), $C_{30}H_{49}NO_5Si$ ($M+H^+$) requires 532.3453.

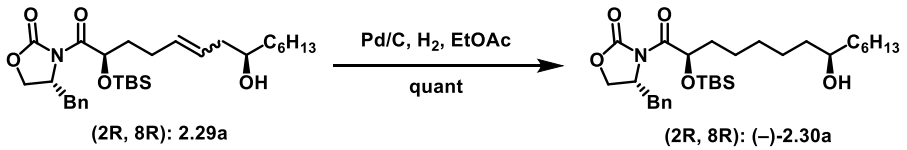

(4R)-4-benzyl-3-[(2R,8R)-2-[(tert-butyldimethylsilyl)oxy]-8-hydroxytetradecanoyl]-1,3-oxazolidin-2-one ((–)-2.30a). Following general procedure B; alcohol **2.29a** (139 mg, 0.260 mmol) yielded **(–)-2.30a** as a clear oil (136 mg, quant.). **^{1}H NMR** (500 MHz, $CDCl_3$) δ = 7.36 – 7.31 (m, 2H), 7.31 – 7.26 (m, 1H), 7.25 – 7.23 (m, 2H), 5.37 (dd, J = 8.4, 3.3 Hz, 1H), 4.62 (ddt, J = 6.9, 6.3, 3.0 Hz, 1H), 4.25 – 4.14 (m, 2H), 3.58 (br s, 1H), 3.41 (dd, J = 13.2, 3.1 Hz, 1H), 2.69 (dd, J = 13.3, 10.2 Hz, 1H), 1.74 – 1.58 (m, 2H), 1.53 – 1.22 (m, 19H), 0.94 (s, 9H), 0.88 (t, J = 7.0 Hz, 3H), 0.11 (s, 3H), 0.09 (s, 3H); **^{13}C NMR** (125 MHz, $CDCl_3$) δ = 174.6, 153.3, 135.4, 129.6, 129.2, 127.5, 77.2, 72.0, 71.4, 66.7, 55.8, 37.9, 37.6, 37.5, 35.2, 32.0, 29.5, 29.2, 26.0, 25.8, 25.6, 25.5, 22.8, 18.5, 14.2, -4.5, -4.9.; **$[\alpha]^{25}_{D}$** -2.5 (c = 0.72 in $CHCl_3$) ; **IR** (film) 3545 (br O-H), 2927, 2856, 1780 (C=O), 1714 (C=O), 1456, 1472, 1387, 1348, 1289, 1249, 1210, 1195, 1106, 1012, 975, 836, 777, 701; **HRMS** Accurate mass (ES^+): Found 534.3616 (+0.7 ppm), $C_{30}H_{51}NO_5Si$ ($M+H^+$) requires 534.3609.

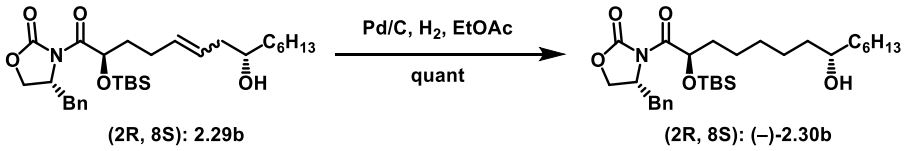

(4R)-4-benzyl-3-[(2R,8S)-2-[(tert-butyldimethylsilyl)oxy]-8-hydroxytetradecanoyl]-1,3-oxazolidin-2-one ((–)-2.30b). Following general procedure B; **2.29b** (105 mg, 0.197 mmol) yielded **(–)-2.30b** as a clear oil (105 mg, quant.). **^{1}H NMR** (400 MHz, $CDCl_3$) δ 7.37 – 7.31 (m, 2H), 7.31 – 7.27 (m, 1H), 7.26 – 7.22 (m, 2H), 5.36 (dd, J = 8.3, 3.4 Hz, 1H), 4.62 (qd, J = 6.6, 3.2 Hz, 1H), 4.26 – 4.16 (m, 2H), 3.58 (br s, 1H), 3.41 (dd, J = 13.2, 3.2 Hz, 1H), 2.69 (dd, J = 13.2, 10.2 Hz, 1H), 1.76 – 1.60 (m, 2H), 1.53 – 1.24 (m, 19H), 0.94 (s, J = 2.9 Hz, 9H), 0.88 (t, J = 6.8 Hz, 3H), 0.11 (s, J = 3.1 Hz, 3H), 0.09 (s, J = 7.8 Hz, 3H); **^{13}C NMR** (100 MHz, $CDCl_3$) δ = 174.6, 153.3, 135.4, 129.6, 129.2, 127.5, 71.9, 71.4, 66.7, 55.8, 37.9, 37.7, 37.5, 35.2, 32.0, 29.5, 29.2, 26.0, 25.8, 25.6, 25.5, 22.8, 18.5, 14.2, -4.5, -5.0; **$[\alpha]^{25}_{D}$** -9.5 (c = 0.21 in $CHCl_3$)

; **IR** (film) 3545 (br O-H), 2927, 2856, 1781 (C=O), 1712 (C=O), 1456, 1387, 1348, 1249, 1210, 1195, 1106, 1051, 1012, 975, 834, 777, 700; **HRMS** Accurate mass (ES^+): Found 534.3598 (-1.1 ppm), $C_{30}H_{51}NO_5Si$ ($M+H^+$) requires 534.3609.

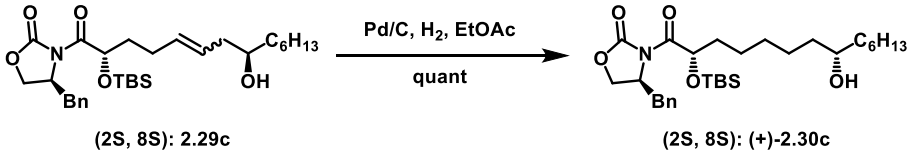

(4S)-4-benzyl-3-[(2S,8S)-2-[(tert-butyldimethylsilyl)oxy]-8-hydroxytetradecanoyl]-1,3-oxazolidin-2-one ((+)-2.30c). Following general procedure B; **2.29c** (198 mg, 0.371 mmol) yielded (+)-**S6** as a clear oil (198 mg, quant.) **^{1}H NMR** (400 MHz, $CDCl_3$) δ = 7.37 – 7.31 (m, 2H), 7.31 – 7.27 (m, 1H), 7.26 – 7.22 (m, 2H), 5.36 (dd, J = 8.3, 3.4 Hz, 1H), 4.62 (ddd, J = 10.2, 6.8, 3.3 Hz, 1H), 4.24 – 4.15 (m, 2H), 3.57 (br s, 1H), 3.40 (dd, J = 13.1, 3.1 Hz, 1H), 2.70 (dd, J = 13.2, 10.2 Hz, 1H), 1.77 – 1.59 (m, 2H), 1.53 – 1.34 (m, 8H), 1.34 – 1.19 (m, 11H), 0.94 (s, J = 2.6 Hz, 9H), 0.90 – 0.86 (m, 3H), 0.11 (s, 3H), 0.09 (s, 3H); **^{13}C NMR** (100 MHz, $CDCl_3$) δ = 174.6, 153.3, 135.4, 129.6, 129.1, 127.5, 72.1, 71.5, 66.6, 55.7, 37.8, 37.7, 37.5, 35.3, 32.0, 29.5, 29.3, 25.9, 25.7, 25.6, 25.6, 22.8, 18.5, 14.2, -4.5, -5.0; **$[\alpha]^{25}_D$** +4.96 (c = 1.6 in $CHCl_3$); **IR** (film) 3545 (br O-H), 2928, 2856, 1780 (C=O), 1712 (C=O), 1456, 1387, 1348, 1249, 1210, 1195, 1106,1051, 1012, 975, 939, 836, 776, 753, 700; **HRMS** Accurate mass (ES^+): Found 534.3625 (+1.6 ppm), $C_{30}H_{51}NO_5Si$ ($M+H^+$) requires 534.3609.

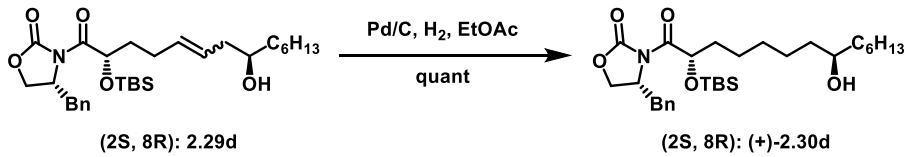

(4S)-4-benzyl-3-[(2S,8R)-2-[(tert-butyldimethylsilyl)oxy]-8-hydroxytetradecanoyl]-1,3-oxazolidin-2-one ((+)-2.30d). Following general procedure B; **2.29d** (302 mg, 0.569 mmol) yielded **(+)-2.30d** as a clear oil (310 mg, quant.). **^{1}H NMR** (500 MHz, $CDCl_3$) δ = 7.36 – 7.31 (m, 2H), 7.30 – 7.27 (m, 1H), 7.26 – 7.22 (m, 2H), 5.36 (dt, J = 6.6, 3.2 Hz, 1H), 4.62 (qd, J = 6.4, 2.9 Hz, 1H), 4.27 – 4.13 (m, 2H), 3.58 (br s, 1H), 3.40 (dd, J = 13.2, 3.0 Hz, 1H), 2.70 (dd, J = 13.2, 10.2 Hz, 1H), 1.74 – 1.20 (m, 19H), 0.94 (s, 9H), 0.90 –

0.86 (m, 3H), 0.11 (s, 3H), 0.09 (s, 3H); **^{13}C NMR** (125 MHz, $CDCl_3$) δ = 174.6, 153.3, 135.4, 129.6, 129.1, 127.5, 71.9, 71.4, 66.7, 55.7, 37.8, 37.61, 37.4, 35.2, 32.0, 29.5, 29.2, 25.9, 25.8, 25.5, 25.5, 22.8, 18.5, 14.2, -4.5, -5.0; **$[\alpha]^{25}_D$** +3.6 (c = 1.03 in $CHCl_3$); **IR** (film) 3545 (br O-H), 2929, 2857, 1781 (C=O), 1712 (C=O), 1456, 1387, 1349, 1214, 1195, 1108, 1014, 975, 939, 836, 776, 753, 701, 667; **HRMS** Accurate mass (ES^+): Found 534.3609, $C_{30}H_{51}NO_5Si$ ($M+H^+$) requires 534.3609.

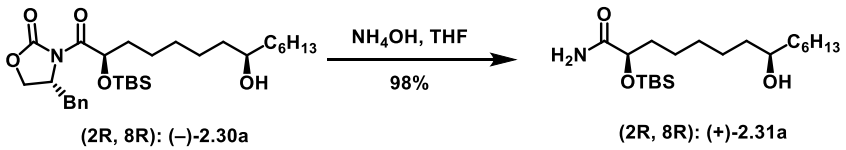

(2R,8R)-2-[(tert-butyldimethylsilyl)oxy]-8-hydroxytetradecanamide ((+)-2.31a). Following modified general procedure C; **(–)-2.30a** (136 mg, 0.255 mmol) dissolved in THF (6 mL) was added ammonium hydroxide solution (30% NH_3, 3 mL). The biphasic mixture was vigorously stirred for 48 hours. The reaction was carefully vented, concentrated, and co-evaporated with methanol 3 times to remove residual water. To the residue was added hexanes, the solution was cooled in a freezer, and then filtered to remove precipitated oxazolidinone. The process was repeated (typically 3x) until white solids no longer appeared. Concentration of the filtrate yielded crude **(+)-2.31a** as a clear oil (95 mg, contains *ca.* 11 % w/w oxazolidinone by NMR analysis, 98% yield). The crude mixture could be carried through to the next step directly without purification. An analytically pure sample was prepared by purification with column chromatography (0→30% Et_2O/DCM→5%MeOH/30%Et_2O/65% DCM). **Rf** (2:1 DCM:Et_2O) = 0.23; **^{1}H NMR** (500 MHz, $CDCl_3$) δ = 6.52 (d, J = 3.4 Hz, 1H), 5.74 (d, J = 3.0 Hz, 1H), 4.13 (t, J = 5.1 Hz, 1H), 3.57 (br s, 1H), 1.76 (ddd, J = 16.2, 10.9, 5.5 Hz, 1H), 1.67 (ddd, J = 14.6, 10.1, 4.9 Hz, 2H), 1.50 – 1.13 (m, 19H), 0.92 (s, 9H), 0.90 – 0.82 (m, 3H), 0.10 (s, 3H), 0.08 (s, 3H); **^{13}C NMR** (125 MHz, $CDCl_3$) δ = 177.2, 73.6, 72.0, 37.6, 37.5, 35.2, 32.0, 29.8, 29.7, 29.5, 25.9, 25.8, 25.6, 24.3, 22.8, 18.2, 14.2, -4.7, -5.1; **$[\alpha]^{25}_D$** +12.1 (c = 1.36 in $CHCl_3$) ; **IR** (film) 3480 (N-H), 3297 (br O-H), 2927, 2856, 1693 (C=O), 1558, 1463, 1389, 1362, 1339, 1253, 1098, 836, 778, 723, 668; **HRMS** Accurate mass (ES^+): Found 374.3091 (+0.6 ppm), $C_{20}H_{43}NO_3Si$ ($M+H^+$) requires 374.3085.

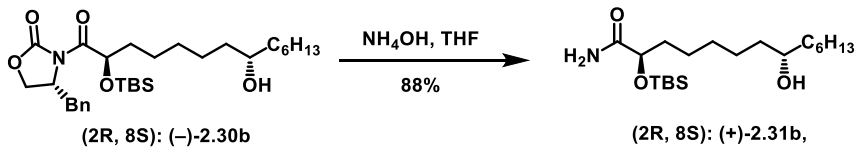

(2R, 8S): (–)-2.30b (2R, 8S): (+)-2.31b,

(2R,8S)-2-[(tert-butyldimethylsilyl)oxy]-8-hydroxytetradecanamide ((+)-2.31b). Following the same procedure as **(+)-2.31a**; compound **(–)-2.30b** (154 mg, 0.289 mmol), THF (6 mL), and NH_4OH (3 mL) yielded **(+)-2.31b** as a clear oil (107 mg, contains *ca.* 7 % w/w oxazolidinone, 88% yield). **^{1}H NMR** (500 MHz, $CDCl_3$) δ = 6.52 (br s, 1H), 5.90 (br s, 1H), 4.13 (t, J = 5.0 Hz, 1H), 3.56 (br s, 1H), 1.80 – 1.71 (m, 1H), 1.71 – 1.61 (m, 1H), 1.50 – 1.15 (m, 19H), 0.92 (s, 9H), 0.87 (t, J = 5.8 Hz, 3H), 0.09 (s, 3H), 0.08 (s, 3H); **^{13}C NMR** (100 MHz, $CDCl_3$) δ = 177.3, 73.6, 72.0, 37.6, 37.5, 35.2, 32.0, 29.8, 29.7, 29.5, 25.9, 25.8, 25.7, 24.2, 22.8, 18.1, 14.2, -4.7, -5.1; **$[\alpha]^{25}_D$** +14.9 (c = 0.96 in $CHCl_3$); **IR** (film) 3480 (N-H), 3297 (br O-H), 2927, 2856, 1683 (C=O), 1577, 1436, 1253, 1099, 836, 778, 730, 668, 599; **HRMS** Accurate mass (ES^+): Found 374.3084 (-0.1 ppm), $C_{20}H_{43}NO_3Si$ ($M+H^+$) requires 374.3085.

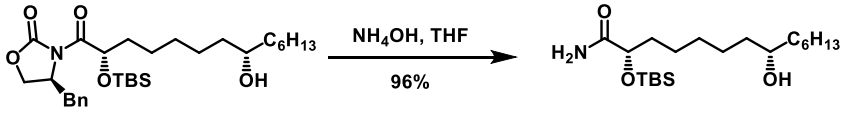

(2S, 8S): (+)-2.30c (2S, 8S): (–)-2.31c

(2S,8S)-2-[(tert-butyldimethylsilyl)oxy]-8-hydroxytetradecanamide ((–)-2.31c). Following the same procedure as **(+)-2.31a**; compound **(+)-2.30c** (100 mg, 0.1866 mmol), THF (3 mL), and NH_4OH (2 mL) yielded **(–)-2.31c** as a clear oil (76 mg, contains *ca.* 9 % w/w oxazolidinone, 96% yield). **^{1}H NMR** (400 MHz, $CDCl_3$) δ = 6.50 (br s, 1H), 6.41 (br s, 1H), 4.09 (t, J = 4.8 Hz, 1H), 3.53 (br s, 1H), 1.71 (dd, J = 10.2, 4.8 Hz, 1H), 1.69 – 1.57 (m, 1H), 1.47 – 1.16 (m, 19H), 0.89 (s, 9H), 0.85 (t, J = 6.4 Hz, 3H), 0.07 (s, 3H), 0.06 (s, 3H); **^{13}C NMR** (100 MHz, $CDCl_3$) δ = 177.5, 73.4, 71.9, 37.5, 37.4, 35.1, 31.9, 29.7, 29.5, 25.8, 25.7, 25.6, 24.2, 22.7, 18.1, 14.2, -4.8, - 5.2; **$[\alpha]^{25}_D$** -14.4 (c = 1.12 in $CHCl_3$); **IR** (film) 3480 (N-H), 3292 (br O-H), 2927, 2856, 1683 (C=O), 1582, 1463, 1389, 1361, 1339, 1253, 1098, 1005, 938, 835, 778, 755, 667, 577; **HRMS** Accurate mass (ES^+): Found 374.3078 (-0.7 ppm), $C_{20}H_{43}NO_3Si$ ($M+H^+$) requires 374.3085.

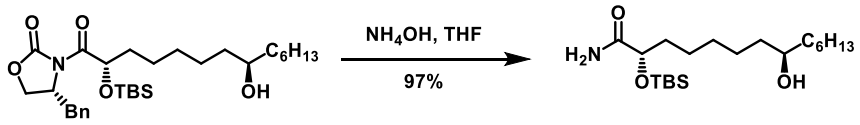

(2S, 8R): (+)-2.30d (2S, 8R): (–)-2.31d

(2S,8R)-2-[(tert-butyldimethylsilyl)oxy]-8-hydroxytetradecanamide ((–)-2.31d). Following the same procedure as **(+)-2.31a**; compound **(+)-2.30d** (97 mg, 0.182 mmol), THF (3 mL), and NH_4OH (3 mL) yielded **(–)-2.31d** as a clear oil (76 mg, contains *ca.* 13 % w/w oxazolidinone, 97% yield). **^{1}H NMR** (500 MHz, $CDCl_3$) δ = 6.53 (br s, 1H), 5.37 (br s, 1H), 4.14 (t, J = 5.1 Hz, 1H), 3.57 (br s, 1H), 1.81 – 1.73 (m, 1H), 1.71 – 1.64 (m, 1H), 1.47 – 1.26 (m, 19H), 0.93 (s, 9H), 0.88 (t, J = 6.9 Hz, 3H), 0.11 (s, 3H), 0.09 (s, 3H).; **^{13}C NMR** (125 MHz, $CDCl_3$) δ = 177.4, 73.5, 71.9, 37.6, 37.4, 35.1, 31.9, 29.7, 29.5, 25.8, 25.7, 25.6, 24.2, 22.7, 18.1, 14.2, -4.7, -5.2; **$[\alpha]^{25}_D$** -14.8 (c = 1.05 in $CHCl_3$) ; **IR** (film) 3480 (N-H), 3292 (br O-H), 2927, 2856, 1683 (C=O), 1584, 1463, 1389, 1361, 1339, 1253, 1098, 1005, 938, 835, 778, 724, 668, 591; **HRMS** Accurate mass (ES^+): Found 374.3078 (+0.7 ppm), $C_{20}H_{43}NO_3Si$ ($M+H^+$) requires 374.3085.

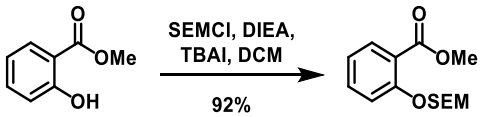

2.32 2.33

Methyl 2-{[2-(trimethylsilyl)ethoxy]methoxy}benzoate (2.33). Prepared as previously described[4]. To a solution of methyl salicylate (0.510 mL, 3.94 mmol) in DCM (10 mL) was added SEMCl (1.40 mL, 7.89 mmol) and TBAI (146 mg, 0.400 mmol) at room temperature. The mixture was cooled to 0°C and diisopropylethylamine was slowly added (2.80 mL, 15.77 mmol), after which the reaction was warmed to room temperature and stirred for 16 hours. The color of the reaction went from pink to orange to a burgundy red. The reaction was poured into H_2O and extracted with DCM 3x. The combined organics were washed with brine, dried ($MgSO_4$), filtered, concentrated and purified by column chromatography to yield compound **2.33** as a clear oil (1.023g, 92%). **R_f** (9:1 hex:EtOAc) = 0.34; **^{1}H NMR** (500 MHz, $CDCl_3$) δ = 7.77 (dd, J = 7.8, 1.7 Hz, 1H), 7.43 (ddd, J = 8.4, 7.3, 1.8 Hz, 1H), 7.22 (dd, J = 8.4, 0.9 Hz, 1H), 7.02 (td, J = 7.7, 1.0 Hz, 1H), 5.30 (s, 2H), 3.88 (s, 3H), 3.83 – 3.78 (m, 2H), 0.99 – 0.91 (m, 2H), -0.01 (s, 9H); **^{13}C**

NMR (125 MHz, $CDCl_3$) δ = 166.8, 157.0, 133.4, 131.5, 121.5, 121.4, 116.5, 93.7, 66.7, 52.1, 18.2, 1.3; **IR** film 2952, 1731 (C=O), 1601, 1583, 1489, 1454, 1297, 1247, 1188, 1048, 985, 938, 755, 694, 659; **HRMS** Accurate mass (ES^+): Found 305.1183 (+0.3 ppm), $C_{14}H_{22}O_4SiNa$ ($M+Na^+$) requires 305.1180.

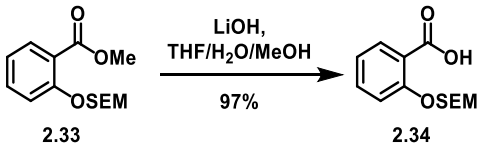

2.33 2.34

2-{[2-(trimethylsilyl)ethoxy]methoxy}benzoic acid (2.34). Following general procedure E; methoxy benzoate **2.33** (2.217g, 7.849 mmol) dissolved in 3:1:1 THF:MeOH:H2O (80 mL) was added LiOH·H2O (1.180g, 28.124 mmol) yielded **2.34** as a yellow oil (2.036g, 97%). **^{1}H NMR** (500 MHz, $CDCl_3$) δ = 10.82 (br s, 1H), 8.19 (dd, J = 7.9, 1.8 Hz, 1H), 7.55 (ddd, J = 8.4, 7.3, 1.9 Hz, 1H), 7.30 (dd, J = 8.4, 0.8 Hz, 1H), 7.17 (ddd, J = 7.9, 7.4, 1.0 Hz, 1H), 5.47 (s, 2H), 3.85 – 3.77 (m, 2H), 1.03 – 0.93 (m, 2H), 0.01 (s, 9H); **^{13}C NMR** (500 MHz, $CDCl_3$) δ = 165.5, 156.4, 135.1, 133.8, 123.1, 118.3, 115.2, 94.6, 68.1, 18.2, 1.3; **IR** (film) 3300 (br O-H), 2953, 2870, 1738, 1694, 1602, 1581, 1486, 1458, 1411, 1381, 1301, 1248, 1232, 1154, 1083, 938, 856, 833, 755, 692, 650; **HRMS** Accurate mass (ES^+): Found 291.1037 (+1.4 ppm), $C_{13}H_{20}O_4SiNa$ ($M+Na^+$) requires 291.1023.

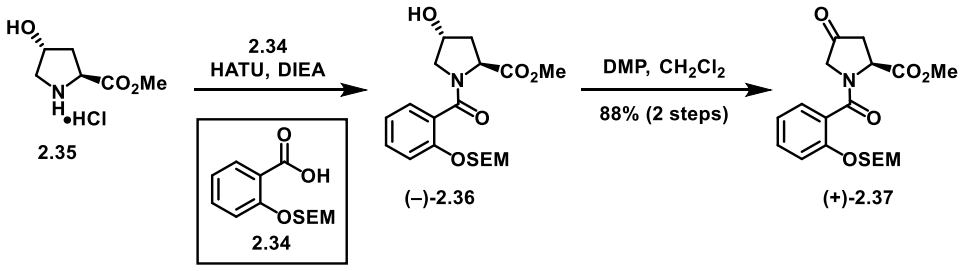

Methyl (2S)-4-oxo-1-(2-{[2-(trimethylsilyl)ethoxy]methoxy}benzoyl)pyrrolidine-2-carboxylate ((+)-2.37). To a solution of **2.34** (660 mg, 2.4598 mmol) in DMF (12 mL) was added HATU (1.122 g, 2.952 mmol). In a separate vessel, L-4-hydroxyproline methyl ester hydrochloride (**2.35**) (574 mg, 2.952 mmol) was dissolved in DMF (12 mL) and diisopropylethylamine (0.64 mL, 3.69 mmol) was added. The amine solution was then added to the acid/HATU solution via syringe, followed by diisopropylethylamine (1.30

mL, 7.38 mmol). The resulting yellow solution was stirred for 16 hours, and upon completion turned orange. The reaction was diluted with EtOAc and saturated aqueous NH_4Cl solution and H2O until the solids dissolved then extracted 3x with EtOAc. The combined organics were washed with H2O, 5% LiCl solution (x2), and brine then dried ($MgSO_4$), filtered, concentrated, and purified by column chromatography $\mathbf{R_f}$ (5% MeOH/EtOAc) = 0.71. The amide intermediate (orange oil, 1.184g) was not of sufficient purity for characterization. The intermediate was dissolved in DCM (50 mL), to which $NaHCO_3$ (4.133g, 49.196 mmol) was added, forming a slurry. DMP (2.087g, 4.920 mmol) was then added in one portion. After 16 hours, H_2O (44 μL, 2.46 mmol) was added to the vigorously stirring bright yellow solution very slowly over 20 minutes. After 1 additional hour of reaction time, the starting material was consumed by TLC. 2:1:1 H_2O:sat. $Na_2S_2O_3$:sat. $NaHCO_3$ (60 mL) was added and stirred for 16 hours. The mixture was filtered and extracted 3x with DCM, the combined organics were washed with sat. $Na_2S_2O_3$, sat. $NaHCO_3$, water, and brine; then dried (Na_2SO_4), filtered, concentrated, and purified by column chromatography yielding (+)-**2.37** as a yellow oil (851 mg, 88% over 2 steps). $\mathbf{R_f}$ (1:1 hexanes:EtOAc) = 0.46 ; **^{1}H NMR** (500 MHz, $CDCl_3$, mixture of conformers) δ = 7.40 – 7.30 (m, 1.75H), 7.25 – 7.24 (m, 0.25H), 7.19 (d, J = 8.4 Hz, 1H), 7.08 – 7.03 (m, 1H), 5.29 – 5.22 (m, 2.56H), 4.67 (d, J = 9.1 Hz, 0.30H), 4.38 (d, J = 19.8 Hz, 0.30H), 3.98 (dd, J = 35.3, 19.2 Hz, 1H), 3.81 (s, J = 4.6 Hz, 2.51H), 3.79 – 3.69 (m, 2.49H), 3.61 (s, 0.76H), 2.99 (dd, J = 19.1, 10.7 Hz, 0.83H), 2.93 (d, J = 10.1 Hz, 0.17H), 2.69 (dd, J = 19.0, 2.7 Hz, 0.70H), 2.61 (d, J = 18.3 Hz, 0.31H), 0.97 – 0.90 (m, 2H), -0.00 (s, 2.47H), -0.01 (s, 6.18H); **^{13}C NMR** (125 MHz, $CDCl_3$) δ = 207.4, 207.3, 171.4, 171.2, 168.4, 153.1, 131.3, 131.3, 128.6, 128.1, 126.1, 125.0, 122.2, 115.3, 115.1, 66.7, 57.4, 55.0, 53.7, 53.5, 52.6, 52.6, 52.0, 41.7, 40.2, 17.9, -1.5; $\mathbf{[\alpha]^{25}_D}$ +1.53 (c = 1.43 in $CHCl_3$); **IR** (film) 2953, 1764 (C=O), 1747 (C=O), 1646, 1601, 1488, 1455, 1406, 1359, 1228, 1177, 1142, 1086, 1033, 981, 937, 918, 834, 753, 694, 657; **HRMS** Accurate mass (ES^+): Found 416.1503 (+0.3 ppm), $C_{19}H_{27}NO_6SiNa$ ($M+Na^+$) requires 416.1500.

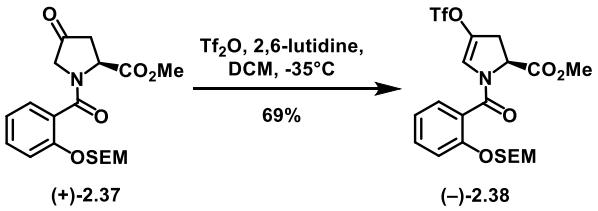

(+)-2.37 (–)-2.38

Methyl (2S)-4-(trifluoromethanesulfonyloxy)-1-(2-{[2-(trimethylsilyl)ethoxy]methoxy} benzoyl)-2,3-dihydro-1H-pyrrole-2-carboxylate ((–)-2.38). Following general procedure H; ketone **(+)-2.37** (293 mg, 0.745 mmol) yielded **(–)-2.38** as an orange oil (269 mg, 69%). $\mathbf{R_f}$ (3:1 hexanes:EtOAc) = 0.54; **^{1}H NMR** (400 MHz, $CDCl_3$) δ = 7.45 – 7.33 (m, 2H), 7.26 – 7.15 (m, 1H), 7.11 – 6.99 (m, 1H), 6.43 (t, J = 1.9 Hz, 1H), 5.26 – 5.21 (m, 2H), 5.09 (dd, J = 11.9, 4.8 Hz, 1H), 3.83 (s, 3H), 3.81 – 3.69 (m, 2H), 3.41 (ddd, J = 16.4, 11.9, 2.3 Hz, 1H), 2.95 (ddd, J = 16.4, 4.8, 1.6 Hz, 1H), 0.98 – 0.88 (m, 2H), -0.01 (s, J = 3.2 Hz, 9H).; **^{13}C NMR** (100 MHz, $CDCl_3$) δ = 169.7, 165.7, 154.0, 134.1, 132.3, 129.4, 124.1, 123.5, 122.3, 115.5, 93.6, 66.9, 57.1, 53.0, 33.4, 18.1, -1.3; $\mathbf{[\alpha]^{25}_D}$ -51.6 (c = 1.13 in $CHCl_3$); **IR** (film) 2955, 1751 (C=O), 1652 (C=O), 1601, 1488, 1456, 1407, 1306, 1218, 1136, 1088, 1029, 981, 936, 910, 834, 754, 665, 604; **HRMS** Accurate mass (ES^+): Found 548.1001 (+0.8 ppm), $C_{20}H_{26}F_3NO_8SSiNa$ ($M+Na^+$) requires 548.0993.

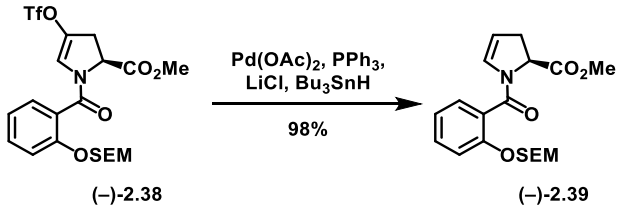

(–)-2.38 (–)-2.39

Methyl (2S)-1-(2-{[2-(trimethylsilyl)ethoxy]methoxy}benzoyl)-2,3-dihydro-1H-pyrrole-2-carboxylate ((–)-2.39). Following general procedure I; enol triflate **(–)-2.38** (931 mg, 1.771 mmol) yielded **(–)-2.39** as an orange oil (658 mg, 98%). $\mathbf{R_f}$ (3:1 hexanes:EtOAc) = 0.26; **^{1}H NMR** (500 MHz, $CDCl_3$) δ = 7.39 – 7.34 (m, 2H), 7.19 (dd, J = 8.9, 0.9 Hz, 1H), 7.05 (td, J = 7.5, 1.0 Hz, 1H), 6.17 (dt, J = 4.4, 2.2 Hz, 1H), 5.27 – 5.19 (m, 2H), 5.07 – 4.99 (m, 2H), 3.81 (s, 3H), 3.78 – 3.73 (m, 2H), 3.52 – 3.44 (m, 1H), 3.11 (ddt, J = 16.6, 11.6, 2.4 Hz, 1H), 2.71 (dddd, J = 17.0, 4.8, 2.7, 2.0 Hz, 1H), 0.96 – 0.92 (m, 2H), -0.01 (s, 9H); **^{13}C NMR** (125 MHz, $CDCl_3$) δ = 171.3, 164.9, 153.6, 131.1, 130.8, 128.8, 125.7, 121.8, 115.0, 108.3,

93.1, 66.4, 57.7, 52.3, 34.0, 17.9, -1.5; **[α]$^{25}_{D}$** - 91.3 (c = 1.12 in $CHCl_3$); **IR** (film) 2952, 1750 (C=O), 1650 (C=O), 1618, 1600, 1487, 1405, 1363, 1290, 1248, 1229, 1200, 1179, 1151, 1016, 1006, 983, 940, 857 755, 696, 656, 613; **HRMS** Accurate mass (ES^+): Found 400.1543 (-0.8 ppm), $C_{19}H_{27}NO_5Si$ ($M+Na^+$) requires 400.1551.

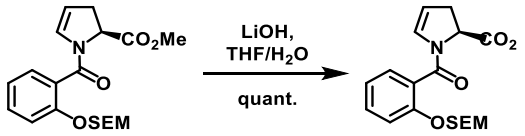

(–)-2.39 (–)-2.40

(2S)-1-(2-{[2-(trimethylsilyl)ethoxy]methoxy}benzoyl)-2,3-dihydro-1H-pyrrole-2-carboxylic acid ((–)-2.40). To a solution of **(–)-2.39** (255 mg, 0.675 mmol) in 4:1 THF:H2O (5 mL) was added LiOH·H2O (283 mg, 6.750 mmol). After 4 hours the mixture was acidified (pH 5) with 5% aqueous AcOH and extracted 3x DCM. The combined organics were washed with brine, dried (Na2SO4), filtered, and concentrated to yield **(–)-2.40** as a yellow oil (260 mg, quant.). **^{1}H NMR** (400 MHz, $CDCl_3$) δ = 7.45 – 7.34 (m, 2H), 7.23 (d, J = 8.4 Hz, 1H), 7.08 (t, J = 7.5 Hz, 1H), 6.07 (dt, J = 4.4, 2.3 Hz, 1H), 5.26 (dd, J = 4.2, 1.8 Hz, 1H), 5.23 (d, J = 1.5 Hz, 2H), 5.17 (dd, J = 10.9, 4.1 Hz, 1H), 3.76 – 3.69 (m, 2H), 3.38 – 3.28 (m, 1H), 3.01 (ddd, J = 14.8, 10.9, 2.5 Hz, 1H), 0.98 – 0.89 (m, 2H), -0.01 (s, 9H); **^{13}C NMR** (100 MHz, $CDCl_3$) δ = 173.2, 167.2, 153.8, 131.9, 130.0, 129.0, 124.7, 122.0, 115.1, 111.1, 93.3, 66.77, 58.9, 33.2, 18.1, -1.3; **[α]$^{25}_{D}$** -69.5 (c = 1.13 in $CHCl_3$); **IR** (film) 2952, 1748 (C=O), 1599 (C=O), 1456, 1410, 1230, 1152, 1086, 984, 834, 752, 729, 650, 613; **HRMS** Accurate mass (ES^+): Found 386.1401 (+0.7 ppm), $C_{18}H_{25}NO_5Si$ ($M+Na^+$) requires 386.1394.

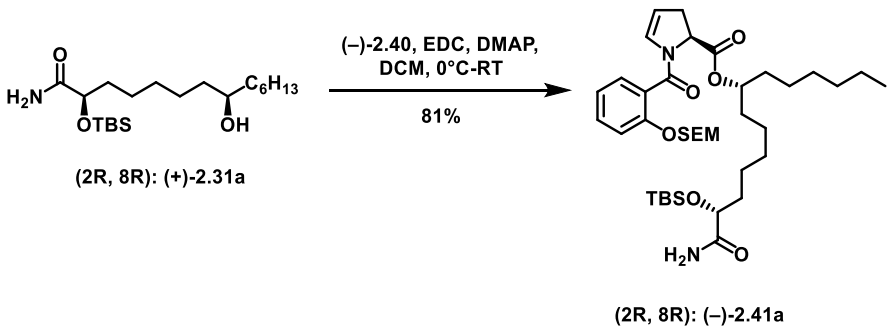

(1R,7R)-1-[(tert-butyldimethylsilyl)oxy]-1-carbamoyltridecan-7-yl(2S)-1-(2-{[2-(trimethylsilyl)ethoxy]methoxy}benzoyl)-2,3-dihydro-1H-pyrrole-2-carboxylate ((–)-2.41a). Following general procedure J; acid **(–)-2.40** (105 mg, 0.288 mmol) and amide alcohol **(+)-2.31a** (74 mg containing 11% w/w oxazolidinone, corrected mass = 66 mg, 0.176 mmol) yielded **(–)-2.41a** as a yellow oil (102 mg, 81%). $\mathbf{R_f}$ (1:1 hexanes:EtOAc) = 0.39; **^{1}H NMR** (500 MHz, $CDCl_3$, mixture of conformers) δ 7.40 – 7.28 (m, 2H), 7.23 – 7.12 (m, 1H), 7.07 – 6.94 (m, 1H), 6.51 (br s, 1H), 6.15 (br s, 1H), 5.74 (br s, 1H), 5.22 (dd, J = 16.8, 7.0 Hz, 2H), 5.05 – 4.93 (m, 2H), 4.17 – 4.07 (m, 1H), 3.73 (t, J = 8.3 Hz, 2H), 3.16 – 3.07 (m, 1H), 2.66 (d, J = 17.0 Hz, 1H), 1.82 – 1.70 (m, 1H), 1.70 – 1.60 (m, 1H), 1.60 – 1.47 (m, 5H), 1.41 – 1.15 (m, 14H), 0.97 – 0.91 (m, 11H), 0.87 – 0.83 (m, 3H), 0.08 (s, 3H), 0.07 (s, 3H), -0.02 (s, 9H); **^{13}C NMR** (100 MHz, $CDCl_3$) δ = 176.9, 170.8, 165.0, 153.9, 131.2, 131.1, 129.0, 126.0, 122.0, 115.2, 108.4, 93.4, 75.5, 73.6, 66.6, 58.2, 35.1, 34.4, 34.1, 31.9, 29.5, 29.3, 25.9, 25.3, 25.1, 24.1, 22.7, 18.2, 14.2, -1.3, -4.7, -5.1; $\mathbf{[\alpha]^{25}_D}$ -17.7 (c = 0.78 in $CHCl_3$); **IR** (film) 3481 (N-H), 2927, 2857, 1739 (C=O), 1690 (C=O), 1651 (C=O), 1620, 1601, 1488, 1455, 1406, 1249, 1230, 1194, 1151, 1087, 990, 939, 824, 778, 754, 697, 666, 613; **HRMS** Accurate mass (ES^+): Found 719.4503 (+2.2 ppm), $C_{38}H_{66}N_2O_7Si_2$ ($M+H^+$) requires 719.4481.

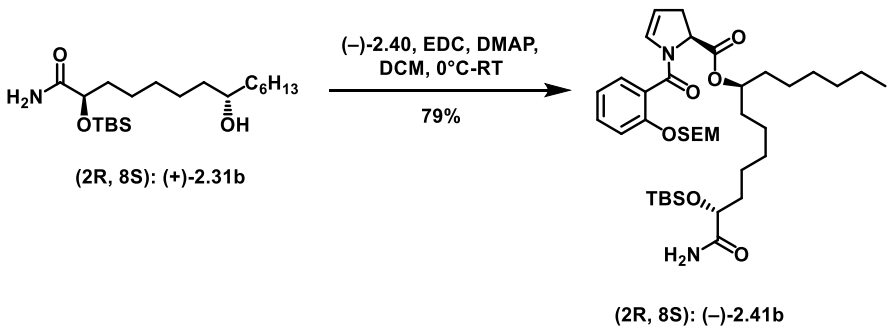

(1R,7S)-1-[(tert-butyldimethylsilyl)oxy]-1-carbamoyltridecan-7-yl(2S)-1-[1-(2-{[2-(trimethylsilyl)ethoxy]methoxy}phenyl)ethenyl]-2,3-dihydro-1H-pyrrole-2-carboxylate ((–)-2.41b). Following general procedure J; acid **(–)-2.40** (105 mg, 0.288 mmol) and amide alcohol **(+)-2.31b** (68 mg, containing 7% w/w oxazolidinone, corrected mass = 63 mg, 0.169 mmol) yielded **(–)-2.41b** (85 mg, 79%) as a yellow oil. **^{1}H NMR** (400 MHz, $CDCl_3$) δ = 7.39 – 7.27 (m, 2H), 7.22 – 7.12 (m, 1H), 7.07 – 6.95 (m, 1H), 6.52 (d, J = 3.9 Hz, 1H), 6.16 (br s, 1H), 5.63 (br s, 1H), 5.22 (q, J = 7.1 Hz, 2H), 5.05 – 4.90 (m, 3H), 4.12 (t, J = 5.0 Hz, 1H), 3.79 – 3.69 (m, 2H), 3.19 – 3.05 (m, 1H), 2.73 – 2.61 (m, 1H), 1.82 – 1.70 (m, 1H), 1.70 – 1.62 (s, 1H), 1.62 – 1.50 (m, 5H), 1.34 – 1.03 (m, 14H), 0.96 – 0.89 (m, 11H), 0.89 – 0.83 (m, 3H), 0.09 (s, 3H), 0.08 (s, 3H), -0.02 (s, 9H); **^{13}C NMR** (100 MHz, $CDCl_3$) δ = 177.0, 170.8, 165.0, 153.8, 131.2, 131.0, 129.0, 126.0, 122.0, 115.2, 108.3, 93.3, 75.5, 73.5, 66.6, 58.2, 35.2, 34.4, 34.1, 34.0, 31.8, 29.5, 29.3, 25.8, 25.2, 24.1, 22.7, 18.1, 14.2, -1.3, -4.7, -5.1; **$[\alpha]^{25}_{D}$** -28.9 (c = 1.0 in $CHCl_3$); **IR** (film) 3481 (N-H), 2927, 2857, 1744 (C=O), 1690 (C=O), 1652 (C=O), 1620, 1601, 1488, 1455, 1406, 1249, 1230, 1194, 1151, 1087, 990, 939, 824, 778, 754, 697, 666, 613; **HRMS** Accurate mass (ES^+): Found 719.4478 (-0.3 ppm), $C_{38}H_{66}N_2O_7Si_2$ ($M+H^+$) requires 719.4481.

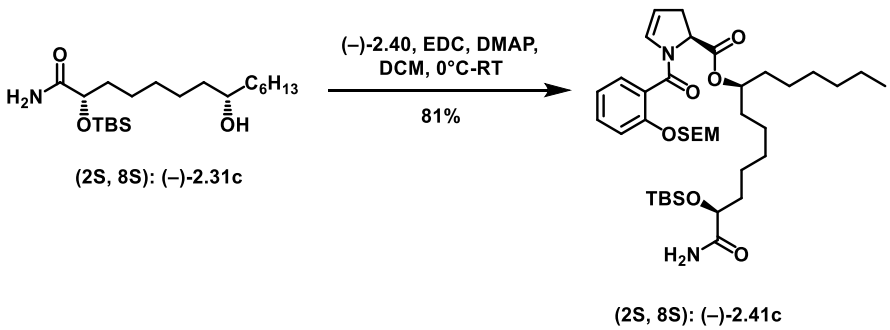

(1S,7S)-1-[(tert-butyldimethylsilyl)oxy]-1-carbamoyltridecan-7-yl(2S)-1-(2-{[2-(trimethylsilyl)ethoxy]methoxy}benzoyl)-2,3-dihydro-1H-pyrrole-2-carboxylate ((–)-2.41c). Following general procedure J; acid **(–)-2.40** (75 mg, 0.206 mmol) and amide alcohol **(–)-2.31c** (70 mg, containing 9% w/w oxazolidinone, corrected mass = 64 mg, 0.171 mmol) yielded **(–)-2.41c** (100 mg, 81%) as a yellow oil. **^{1}H NMR** (500 MHz, $CDCl_3$) δ = 7.40 – 7.29 (m, 2H), 7.23 – 7.15 (m, 1H), 7.08 – 6.98 (m, 1H), 6.52 (br s, 1H), 6.19 – 6.14 (m, 1H), 5.34 – 5.28 (m, 1H), 5.27 – 5.19 (m, 2H), 5.04 – 4.92 (m, 2H), 4.17 – 4.07 (m, 1H), 3.78 – 3.71 (m, 2H), 3.16 – 3.08 (m, 1H), 2.71 – 2.62 (m, 1H), 1.80 – 1.71 (m, 1H), 1.71 – 1.61 (m, 1H), 1.61 – 1.50 (m, 5H), 1.43 – 1.15 (m, 14H), 0.97 – 0.89 (m, 11H), 0.86 (t, J = 6.9 Hz, 3H), 0.09 (s, 3H), 0.09 (s, 3H), -0.01 (s, 9H); **^{13}C NMR** (125 MHz, $CDCl_3$) δ = 177.0, 170.8, 165.0, 153.8, 131.2, 131.0, 129.0, 126.0, 122.0, 115.2, 108.3, 93.3, 75.4, 73.5, 66.6, 58.2, 35.2, 34.4, 34.2, 34.1, 31.8, 29.5, 29.3, 25.8, 25.3, 25.2, 24.2, 22.7, 18.1, 18.1, 14.2, -1.3, -4.7, -5.1; **$[\alpha]^{25}_{D}$** -42.6 (c = 0.98 in CHCl3); **IR** (film) 3481 (N-H), 2928, 2857, 1734 (C=O), 1689 (C=O), 1652 (C=O), 1620, 1601, 1488, 1455, 1406, 1249, 1230, 1194, 1151, 1087, 990, 939, 824, 778, 753, 697, 676, 606 ; **HRMS** Accurate mass (ES^+): Found 719.4503 (+2.2 ppm), $C_{38}H_{66}N_2O_7Si_2$ ($M+H^+$) requires 719.4481.

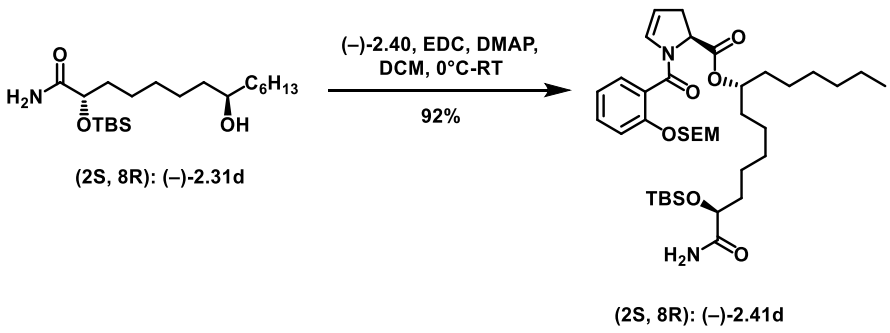

(1S,7R)-1-[(tert-butyldimethylsilyl)oxy]-1-carbamoyltridecan-7-yl(2S)-1-(2-{[2-(trimethylsilyl)ethoxy]methoxy}benzoyl)-2,3-dihydro-1H-pyrrole-2-carboxylate ((–)-2.41d). Following general procedure J; acid **(–)-2.40** (138 mg, 0.378 mmol) and amide alcohol **(–)-2.41d** (63 mg, 0.168 mmol) yielding **(–)-2.41d** as a yellow oil (111 mg, 92%). **^{1}H NMR** (500 MHz, $CDCl_3$) δ = 7.39 – 7.30 (m, 2H), 7.23 – 7.15 (m, 1H), 7.07 – 7.00 (m, 1H), 6.53 (d, J = 4.8 Hz, 1H), 6.16 (dt, J = 4.3, 2.1 Hz, 1H), 5.38 – 5.29 (m, 1H), 5.27 – 5.18 (m, 2H), 5.05 – 4.90 (m, 2H), 4.17 – 4.09 (m, 1H), 3.78 – 3.70 (m, 1H), 3.18 – 3.06 (m, 1H), 2.74 – 2.63 (m, 1H), 1.81 – 1.71 (m, 1H), 1.69 – 1.63 (m, 1H), 1.62 – 1.51 (m, 5H), 1.42 – 1.18 (m, 14H), 0.96 – 0.93 (m, 2H), 0.91 (s, 9H), 0.86 (t, J = 6.8 Hz, 3H), 0.09 (s, 3H), 0.07 (s, 3H), -0.01 (s, 9H); **^{13}C NMR** (125 MHz, $CDCl_3$) δ = 177.0, 170.8, 165.0, 153.8, 131.2, 131.1, 129.0, 126.0, 122.0, 115.2, 108.3, 93.4, 75.5, 73.6, 66.6, 58.2, 35.2, 34.4, 34.1, 34.1, 31.9, 29.5, 29.3, 25.9, 25.3, 25.1, 24.1, 22.7, 18.2, 18.1, 14.2, -1.3, -4.7, -5.1; **$[\alpha]^{25}_{D}$** -44.0 (c = 1.21 in $CHCl_3$); **IR** (film) 3481 (N-H), 2927, 2857, 1739 (C=O), 1690 (C=O), 1651 (C=O), 1620, 1601, 1488, 1455, 1406, 1249, 1230, 1194, 1151, 1087, 990, 939, 824, 778, 754, 697, 666, 613; **HRMS** Accurate mass (ES^+): Found 719.4492 (+1.1 ppm), $C_{38}H_{66}N_2O_7Si_2$ ($M+H^+$) requires 719.4481.

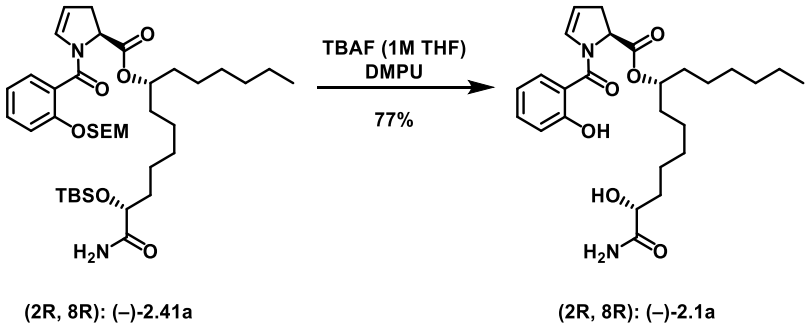

(1R,7R)-1-carbamoyl-1-hydroxytridecan-7-yl(2S)-1-(2-hydroxybenzoyl)-2,3-dihydro-1H-pyrrole-2-carboxylate ((–)-2.1a). To a solution of compound **(–)-2.41a** (25 mg, 0.035 mmol) dissolved in DMPU (0.7 mL, dried over 3Å molecular sieves for at least 24 hours prior to use) was added TBAF (0.7 mL 1M solution in THF, 0.70 mmol, 20 equiv., dried over 3Å molecular sieves for at least 24 hours prior to use) dropwise. The reaction was stirred at room temperature until LC-MS analysis (non-polar phase 95% acetonitrile/5% water/0.1% formic acid, 15 minute gradient 40→90% non-polar phase, product retention time = 5.6 minutes, SEM-protected/TBS-deprotected intermediate retention time = 12.6 minutes) indicated consumption of the mono-protected SEM ether intermediate (TBS deprotection occurred in <1 minute by TLC analysis), which was typically complete in 30 minutes. After completion, the reaction was quenched with saturated ammonium chloride solution (6 mL) and water (6 mL), and extracted with Et2O (12 mL). The organic layer was separated and washed 5x with 1M ammonium chloride solution (10 mL), water, and brine. The organic layer was then dried (Na_2SO_4), filtered, concentrated, and purified by column chromatography (0→3% MeOH/DCM) to yield **(–)-2.1a** as a white translucent oil (13 mg, 77% yield). $\mathbf{R_f}$ (19:1 EtOAc:MeOH) = 0.44; **^{1}H NMR** (500 MHz, $CDCl_3$) δ = 9.53 (s, 1H), 7.47 – 7.31 (m, 2H), 6.98 (d, J = 8.1 Hz, 1H), 6.90 (t, J = 7.5 Hz, 1H), 6.71 (s, 1H), 6.62 (s, 1H), 5.46 (s, 1H), 5.35 – 5.24 (m, 1H), 5.01 (dd, J = 11.1, 4.6 Hz, 2H), 4.09 (s, 1H), 3.48 (s, 1H), 3.21 – 3.08 (m, 1H), 2.69 (d, J = 17.0 Hz, 1H), 1.80 (m, 1H), 1.76 – 1.48 (m, 6H), 1.48 – 1.33 (m, 5H), 1.32 – 1.17 (m, 21H), 0.87 (t, J = 6.9 Hz, 3H); **^{13}C NMR** (100 MHz, $CDCl_3$) δ = 177.0, 171.3, 167.4, 158.0, 133.5, 130.8, 128.3, 119.4, 118.0, 117.8, 111.1, 76.0, 71.4, 59.3, 34.5, 34.3, 34.2, 33.7, 31.8, 29.2, 28.3, 25.5, 24.8, 24.6, 22.7, 14.2; $\mathbf{[\alpha]^{25}_D}$ -32.2 (c = 1.06 in $CHCl_3$); **IR** (film) 3338 (br O-H), 2926, 2857, 1733 (C=O), 1667 (C=O), 1592 (C=O), 1457, 1429, 1376,

1294, 1252, 1197, 1152, 1098, 1017, 945, 859, 817, 761, 665, 614; **HRMS** Accurate mass (ES^+): Found 475.2806 (+0.3 ppm), $C_{26}H_{38}N_2O_6$ ($M+H^+$) requires 475.2803.

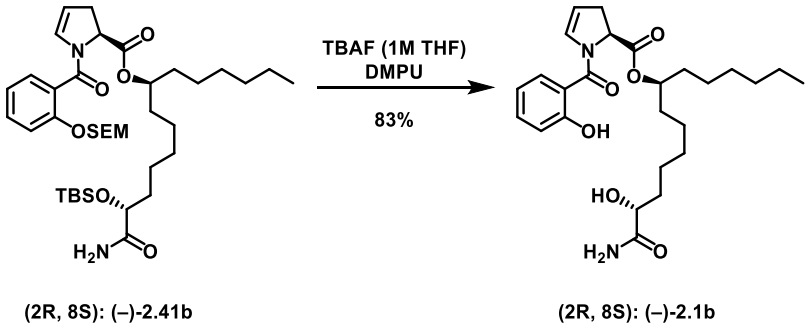

1R,7S)-1-carbamoyl-1-hydroxytridecan-7-yl(2S)-1-(2-hydroxybenzoyl)-2,3-dihydro-1H-pyrrole-2-carboxylate ((–)-2.1b). Following the same procedure as **(–)-2.1a**, **(–)-2.41b** (16 mg, 0.023 mmol), DMPU (0.46 mL), and TBAF (0.46 mL 1M solution in THF, 0.46 mmol) yielded **(–)-2.1b** as a white translucent oil (9 mg, 83% yield). **^{1}H NMR** (500 MHz, $CDCl_3$) δ = 9.94 (s, 1H), 7.45 – 7.33 (m, 2H), 7.00 (d, J = 8.0 Hz, 1H), 6.90 (t, J = 7.5 Hz, 1H), 6.80 (s, 1H), 6.53 (s, 1H), 5.54 (s, 1H), 5.29 (d, J = 4.1 Hz, 1H), 5.05 – 4.99 (m, 1H), 4.99 – 4.90 (m, 1H), 4.09 (d, J = 4.5 Hz, 1H), 3.18 – 3.09 (m, 1H), 3.06 (s, 1H), 2.70 (d, J = 17.1 Hz, 1H), 1.81 – 1.72 (m, 1H), 1.68 – 1.46 (m, 9H), 1.37 (s, 4H), 1.35 – 1.17 (m, 18H), 0.87 (t, J = 6.9 Hz, 3H); **^{13}C NMR** (125 MHz, $CDCl_3$) δ = 177.0, 170.9, 167.5, 159.0, 133.7, 130.9, 128.5, 119.2, 118.1, 117.0, 111.0, 76.0, 71.7, 59.8, 34.5, 34.3, 34.0, 33.8, 31.8, 29.2, 28.8, 25.2, 25.0, 24.7, 22.7, 14.2; **$[\alpha]^{20}_D$** -29.1 (c = 1.00 in CHCl3); **IR** (film) 3339 (br O-H), 2927, 2857, 1733 (C=O), 1667 (C=O), 1592 (C=O), 1457, 1429, 1376, 1294, 1252, 1197, 1152, 1098, 1017, 945, 859, 817, 761, 665, 614; **HRMS** Accurate mass (ES^+): Found 475.2806 (+0.3 ppm), $C_{26}H_{38}N_2O_6$ ($M+H^+$) requires 475.2803.

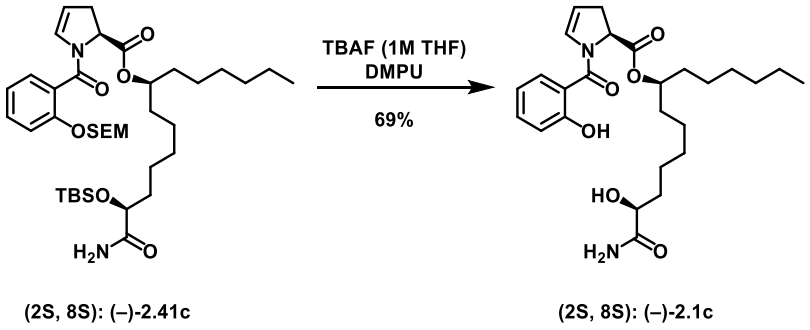

(1S,7S)-1-carbamoyl-1-hydroxytridecan-7-yl(2S)-1-(2-hydroxybenzoyl)-2,3-dihydro-1H-pyrrole-2-carboxylate ((–)-2.1c). Following the same procedure as **(–)-2.1a**, **(–)-2.41c** (63 mg, 0.087 mmol), DMPU (1.74 mL), and TBAF (1.74 mL 1M solution in THF, 1.74 mmol) yielded **(–)-2.1c** as a white translucent oil (28 mg, 69% yield). **^{1}H NMR** (500 MHz, $CDCl_3$) δ = 9.87 (s, 1H), 7.44 – 7.33 (m, 2H), 6.99 (d, J = 8.2 Hz, 1H), 6.89 (t, J = 7.5 Hz, 1H), 6.77 (s, 1H), 6.65 (s, 1H), 5.79 (s, 1H), 5.32 – 5.20 (m, 1H), 4.99 (dd, J = 11.2, 4.8 Hz, 1H), 4.94 (s, 1H), 4.07 (d, J = 4.1 Hz, 1H), 3.43 (s, 1H), 3.21 – 3.04 (m, 1H), 2.69 (d, J = 17.1 Hz, 1H), 1.80 – 1.69 (m, 1H), 1.64 – 1.43 (m, 6H), 1.43 – 1.09 (m, 17H), 0.86 (t, J = 6.8 Hz, 3H); **^{13}C NMR** (125 MHz, $CDCl_3$) δ = 177.2, 170.9, 167.5, 158.9, 133.6, 130.9, 128.5, 119.2, 118.0, 117.2, 111.0, 76.0, 71.6, 59.8, 34.5, 34.2, 33.9, 33.8, 31.8, 29.2, 28.8, 25.2, 25.0, 24.7, 22.7, 14.2. **$[\alpha]^{20}_{D}$** -41.5 (c = 0.26 in $CHCl_3$); **IR** (film) 3339 (br O-H), 2927, 2857, 1733 (C=O), 1667 (C=O), 1592 (C=O), 1457, 1429, 1376, 1294, 1252, 1197, 1152, 1098, 1017, 945, 859, 817, 761, 665, 614 ; **HRMS** Accurate mass (ES^+): Found 475.2815 (+1.2 ppm), $C_{26}H_{38}N_2O_6$ ($M+H^+$) requires 475.2803.

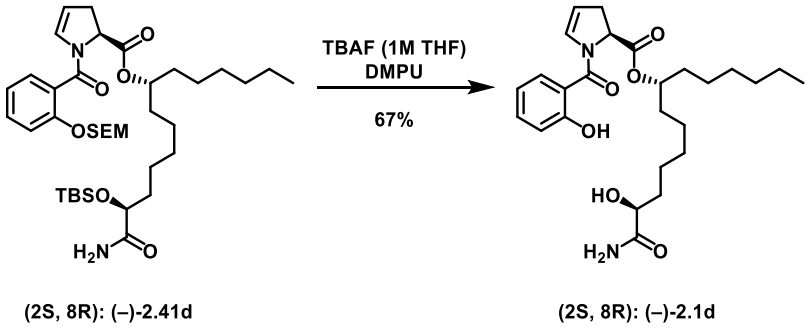

(1S,7R)-1-carbamoyl-1-hydroxytridecan-7-yl(2S)-1-(2-hydroxybenzoyl)-2,3-dihydro-1H-pyrrole-2-carboxylate ((–)-2.1d). Following the same procedure as **(–)-2.1a**, **(–)-2.41d** (11 mg, 0.0152 mmol), DMPU (0.61 mL), and TBAF (0.30 mL 1M solution in THF, 0.30 mmol) yielded **(–)-2.1d** as a white translucent oil (5 mg, 67% yield). **^{1}H NMR** (500 MHz, $CDCl_3$) δ = 9.54 (s, 1H), 7.37 (dd, J = 16.8, 7.7 Hz, 1H), 6.98 (d, J = 8.2 Hz, 1H), 6.90 (t, J = 7.5 Hz, 1H), 6.71 (s, 1H), 6.61 (s, 1H), 5.61 (s, 1H), 5.30 – 5.24 (m, 1H), 5.00 (dd, J = 11.2, 4.6 Hz, 1H), 4.08 (d, J = 4.2 Hz, 1H), 3.54 – 3.33 (m, 1H), 3.19 – 3.08 (m, 1H), 2.69 (d, J = 17.0 Hz, 1H), 1.89 – 1.72 (m, 1H), 1.69 – 1.49 (m, 6H), 1.47 – 1.16 (m, 18H), 0.86 (t, J = 7.0 Hz, 1H); **^{13}C NMR** (100 MHz, $CDCl_3$) δ = 177.3, 171.3, 167.4, 158.1, 133.5, 130.9, 128.4, 119.4, 118.0, 117.8, 111.0, 76.2, 71.7, 59.4, 34.5, 34.3, 34.2, 33.7, 31.8, 29.2, 28.6, 25.5, 24.8, 24.7, 22.7, 14.2; **$[\alpha]^{20}_{D}$** -65.1 (c = 1.29 in $CHCl_3$); **IR** (film) 3339 (br O-H), 2927, 2857, 1733 (C=O), 1667 (C=O), 1592 (C=O), 1457, 1429, 1376, 1294, 1252, 1197, 1152, 1098, 1017, 945, 859, 817, 761, 665, 614; **HRMS** Accurate mass (ES^+): Found 475.2806 (+0.3 ppm), $C_{26}H_{38}N_2O_6$ ($M+H^+$) requires 475.2803.

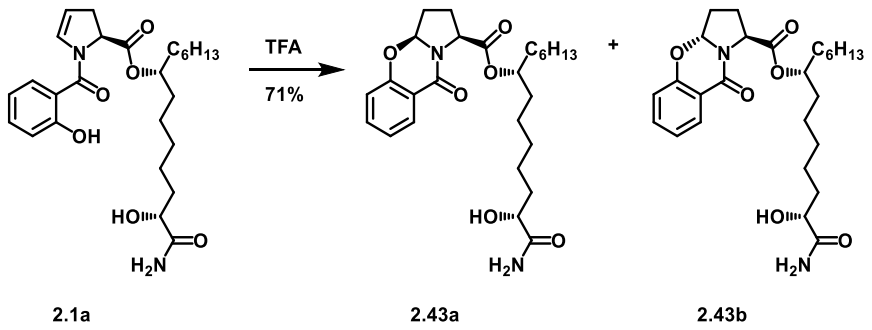

(7R,13R)-14-amino-13-hydroxy-14-oxotetradecan-7-yl (1S,3aS)-9-oxo-1,2,3,3a-tetrahydro- 9H-benzo[e]pyrrolo[2,1-b][1,3]oxazine-1-carboxylate (2.43a), **(7R,13R)-14-amino-13-hydroxy- 14-oxotetradecan-7-yl (1S,3aR)-9-oxo-1,2,3,3a-tetrahydro-9H-benzo[e]pyrrolo[2,1- b][1,3]oxazine-1-carboxylate (2.43b).** To a solution of **(–)-2.1a** (12 mg, 0.025 mmol) dissolved in CH_2Cl_2 (1 mL) was added trifluoroacetic acid (1 mL), and the reaction was stirred for 30 minutes at room temperature. The reaction was slowly quenched with sat. Na_2CO_3 solution until the pH was greater than 8, then extracted with CH_2Cl_2 3x, washed with brine, dried over $MgSO_4$, filtered, concentrated, and purified by preparative TLC (2% MeOH/EtOAc), yielding diastereomeric compounds **2.43a** and **2.43b** (configurations were not assigned). *Less polar isomer* (5.0 mg, 42% yield): **^{1}H NMR** (500 MHz, $CDCl_3$) δ 7.88 – 7.81 (m, 1H), 7.49 – 7.43 (m, 1H), 7.12 (td, J = 7.7, 0.9 Hz, 1H), 7.01 – 6.70 (m, 2H), 5.78 – 5.73 (m, 1H), 5.42 (s, 1H), 5.04 – 4.97 (m, 1H), 4.82 – 4.71 (m, 1H), 4.28 – 4.17 (m, 2H), 2.59 – 2.46 (m, 2H), 2.36 – 2.27 (m, 1H), 2.03 – 1.96 (m, 1H), 1.95 – 1.87 (m, 1H), 1.80 – 1.70 (m, 1H), 1.68 – 1.43 (m, 7H), 1.42 – 1.20 (m, 12H), 0.88 (t, J = 6.9 Hz, 3H); **^{13}C NMR** (125 MHz, $CDCl_3$) δ 177.48, 171.59, 171.49, 161.36, 157.42, 134.64, 128.18, 128.04, 123.12, 119.04, 116.94, 88.82, 75.73, 71.17, 58.31, 34.64, 33.98, 33.86, 31.87, 30.96, 29.84, 29.22, 27.73, 26.36, 25.56, 24.62, 24.28, 22.70, 14.21; **$[\alpha]^{25}_D$** +63.8 (c = 0.13 in $CHCl_3$) **IR** (film) 3326 (br, O-H), 2928, 2858, 2360, 1733 (C=O), 1660 (C=O), 1597, 1507, 1468, 1431, 1351, 1197, 1166, 1099, 1019, 959, 860, 822, 788, 758, 651, 608, 585; **HRMS** Accurate mass (ES^+): Found 475.2781 (-5.7 ppm), $C_{26}H_{39}N_2O_6$ ($M+H^+$) requires 475.2808; **R_f** (2% MeOH/EtOAc) = 0.37 *More polar isomer* (3.5 mg, 29% yield)*:* **^{1}H NMR** (500 MHz, $CDCl_3$) δ 7.91 – 7.79 (m, 1H), 7.49 – 7.44 (m, 1H), 7.12 (td, J = 7.7, 1.0 Hz, 1H), 7.01 (dd, J = 8.2, 4.2 Hz, 1H), 6.94 – 6.73 (m, 1H), 5.58 (dt, J = 9.8, 4.9 Hz, 1H), 5.39 (s, 1H), 5.05 – 4.94 (m,

1H), 4.68 – 4.59 (m, 1H), 4.28 (d, J = 17.5 Hz, 1H), 4.17 – 4.09 (m, 1H), 2.53 – 2.47 (m, 1H), 2.44 – 2.25 (m, 2H), 2.19 (dd, J = 13.4, 7.8 Hz, 1H), 1.87 – 1.79 (m, 1H), 1.77 – 1.68 (m, 1H), 1.59 – 1.35 (m, 7H), 1.30 – 1.20 (m, 12H), 0.87 (t, J = 7.0 Hz, 3H); **^{13}C NMR** (100 MHz, $CDCl_3$) δ 177.36, 170.73, 161.68, 158.00, 134.67, 127.96, 123.01, 119.04, 117.12, 88.70, 75.62, 71.05, 57.27, 34.68, 33.93, 33.71, 31.85, 30.33, 29.84, 29.21, 27.61, 26.19, 25.57, 24.60, 24.05, 22.69, 14.22; **$[\alpha]^{25}_D$** –28.1 (c = 0.11 in $CHCl_3$) **IR** (film) 3326 (br, O-H), 2927, 2856, 2360, 1734 (C=O), 1659 (C=O), 1613, 1578, 1469, 1432, 1351, 1225, 1196, 1079, 1024, 954, 907, 856, 785, 759, 732, 700, 652, 606, 584; **HRMS** Accurate mass (ES^+): Found 475.2783 (-5.3 ppm), $C_{26}H_{39}N_2O_6$ ($M+H^+$) requires 475.2808; **R_f** (2% MeOH/EtOAc) = 0.29.

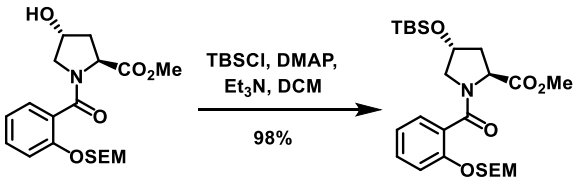

(–)-2.36 **(–)-2.44**

Methyl (2S,4R)-4-[(tert-butyldimethylsilyl)oxy]-1-(2-{[2-(trimethylsilyl)ethoxy]methoxy}benzoyl)pyrrolidine-2-carboxylate (–)-2.44. To a solution of compound **(–)-2.36** (64 mg, 0.162 mmol) in CH_2Cl_2 (1 mL) was added imidazole (22 mg, 0.324 mmol) followed by TBSCl (49 mg, 0.324 mmol), and the reaction was stirred for 24 hours, after which time TLC analysis indicated the reaction was incomplete. Another portion of imidazole (22 mg, 0.324 mmol) and TBSCl (49 mg, 0.324) were added, and the reaction was stirred at room temperature for an additional 24 hours, after which time TLC analysis indicated the consumption of starting material. The reaction was quenched with water and extracted with CH_2Cl_2 3x. The combined organic layers were washed with water and brine, dried over $MgSO_4$, filtered, concentrated and purified by column chromatography, yielding the title compound as a clear oil (80 mg, 98% yield). **^{1}H NMR** (500 MHz, $CDCl_3$, mixture of rotamers/conformers) δ 7.36 – 7.27 (m, 1.36H), 7.20 – 7.17 (m, 1.31H), 7.03 (td, J = 7.5, 1.0 Hz, 0.68H), 6.98 (td, J = 7.5, 0.9 Hz, 0.33H), 5.25 – 5.19 (m, 2H), 4.75 (t, J = 7.8 Hz, 0.67H), 4.52 – 4.44 (m, 0.59H), 4.43 – 4.38 (m, 0.69H), 3.82 – 3.72 (m, 4.53H), 3.59 (dd, J = 10.9, 4.5 Hz, 0.68H), 3.37 (s, 0.89H), 3.18

(dd, J = 11.0, 1.7 Hz, 0.68H), 2.28 – 2.19 (m, 1H), 2.14 – 2.05 (m, 1H), 0.95 (td, J = 8.3, 2.5 Hz, 2H), 0.90 (s, J = 2.9 Hz, 2.84H), 0.82 (s, J = 2.9 Hz, 6H), 0.10 (s, J = 3.1 Hz, 0.85H), 0.09 (s, J = 3.0 Hz, 0.86H), 0.02 (s, J = 2.8 Hz, 1.79H), 0.00 – -0.01 (m, 8.25H), -0.04 (s, 2H); **^{13}C NMR** (125 MHz, $CDCl_3$) δ 172.74, 168.16, 153.74, 130.77, 130.73, 128.24, 127.33, 122.04, 121.71, 115.89, 93.86, 93.47, 70.45, 69.40, 66.47, 57.47, 56.28, 54.78, 52.26, 51.98, 40.39, 38.58, 25.78, 25.65, 18.12, 18.02, 17.87, -1.32, -1.36, -4.81, -4.92; **$[\alpha]^{25}_D$** –65.9 (c = 0.72 in $CHCl_3$); **IR** (film) 2952, 2924, 2893, 2856, 1746 (C=O), 1644 (C=O), 1601 (C=O), 1489, 1455, 1412, 1359, 1317, 1249, 1227, 1197, 1175, 1144, 1086, 1023, 986, 920, 833, 775, 753, 693, 653; **HRMS** Accurate mass (ES^+): Found 532.2485 (-7.9 ppm), $C_{25}H_{43}NO_6Si_2Na$ ($M+Na^+$) requires 532.2527.

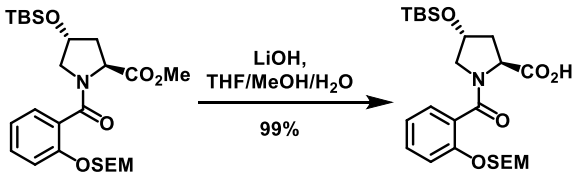

(–)-2.44 (–)-2.45

(2S,4R)-4-[(tert-butyldimethylsilyl)oxy]-1-(2-{[2-(trimethylsilyl)ethoxy]methoxy}benzoyl)pyrrolidine-2-carboxylic acid (–)-2.45. Using general procedure E, methyl ester **(–)-2.44** (166 mg, 0.325 mmol) yielded the title compound as a clear oil (160 mg, 99% yield). **^{1}H NMR** (400 MHz, $CDCl_3$) δ 7.57 (br s, 1H), 7.38 (t, J = 7.9 Hz, 1H), 7.30 (d, J = 7.5 Hz, 1H), 7.22 (d, J = 8.4 Hz, 1H), 7.16 (d, J = 8.5 Hz, 1H), 7.05 (t, J = 7.5 Hz, 1H), 6.99 – 6.93 (m, 1H), 5.26 – 5.18 (m, 2H), 4.87 (t, J = 7.7 Hz, 1H), 4.36 (s, 1H), 3.49 (dd, J = 11.2, 4.1 Hz, 1H), 3.20 (t, J = 17.9 Hz, 1H), 2.53 – 2.44 (m, 1H), 2.25 – 2.12 (m, 1H), 0.98 – 0.87 (m, 3H), 0.82 (s, 9H), 0.03 (s, 3H), -0.01 (s, 9H), -0.06 (s, 3H); **^{13}C NMR** (125 MHz, $CDCl_3$) δ 172.72, 171.48, 153.73, 131.57, 128.02, 125.78, 122.12, 115.57, 93.64, 69.84, 66.80, 58.79, 57.12, 37.22, 25.72, 18.10, 17.95, -1.27, -4.73, -4.89; **$[\alpha]^{25}_D$** –86.6 (c = 1.75 in $CHCl_3$); **IR** (film) 2952, 2856, 2359, 2341, 1743 (C=O), 1595 (C=O), 1489, 1462, 1434, 1361, 1249, 1024, 988, 921, 754, 693, 667, 611; **HRMS** Accurate mass (ES^+): Found 518.2330 (-7.7 ppm), $C_{24}H_{41}NO_6Si_2Na$ ($M+Na^+$) requires 518.2370.

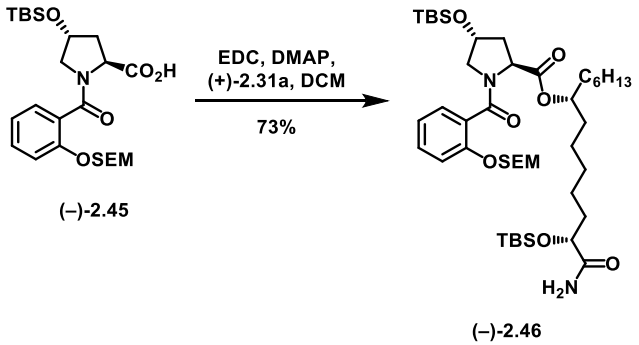

(1R,7R)-1-[(tert-butyldimethylsilyl)oxy]-1-carbamoyltridecan-7-yl (2S,4R)-4-[(tert-butyldimethylsilyl)oxy]-1-(2-{[2-(trimethylsilyl)ethoxy]methoxy}benzoyl)pyrrolidine-2-carboxylate (–)-2.46. Using modified general procedure J; (1.5 eq acid, 2 eq EDC, 0.1 eq DMAP), acid **(–)-2.45** (125 mg, 0.252 mmol) yielded the title compound as a clear oil (103 mg, 73% yield). **^{1}H NMR** (500 MHz, $CDCl_3$, mixture of rotamers/conformers) δ 7.34 – 7.27 (m, 1.35H), 7.25 – 7.17 (m, 1.35H), 7.14 (d, J = 8.1 Hz, 0.33H), 7.02 (td, J = 7.5, 0.9 Hz, 0.65H), 6.93 (td, J = 7.5, 0.9 Hz, 0.32H), 6.60 – 6.48 (m, 1H), 5.73 (s, 0.40H), 5.68 (s, 0.60H), 5.24 – 5.19 (m, 2H), 4.97 – 4.90 (m, 0.63H), 4.72 (t, J = 7.6 Hz, 0.63H), 4.60 – 4.54 (m, 0.32H), 4.50 – 4.45 (m, 0.32H), 4.45 – 4.37 (m, 1H), 4.13 (dt, J = 13.1, 5.2 Hz, 1H), 3.87 – 3.69 (m, 2.72H), 3.57 (dd, J = 10.7, 4.3 Hz, 0.63H), 3.16 (dd, J = 10.9, 2.7 Hz, 0.63H), 2.24 (ddd, J = 12.8, 8.2, 4.7 Hz, 1H), 2.14 – 2.03 (m, 1H), 1.81 – 1.70 (m, 1H), 1.70 – 1.46 (m, 4H), 1.46 – 1.09 (m, 16H), 0.95 – 0.93 (m, 4H), 0.91 – 0.89 (m, 8.54H), 0.83 – 0.81 (m, 5.72H), 0.12 – 0.06 (m, 8.34H), 0.01 – -0.02 (m, 10.78H), -0.05 (s, 1.77H); **^{13}C NMR** (125 MHz, $CDCl_3$) δ 177.18, 171.97, 168.48, 168.01, 153.83, 130.67, 128.29, 127.45, 126.67, 122.04, 121.88, 115.88, 93.92, 93.43, 75.48, 75.11, 73.49, 70.42, 69.34, 66.48, 58.74, 57.83, 56.18, 54.35, 40.40, 38.72, 35.25, 35.12, 34.09, 33.74, 33.69, 31.82, 31.75, 29.55, 29.49, 29.24, 29.13, 25.82, 25.71, 25.31, 25.24, 25.10, 24.79, 24.08, 22.66, 22.61, 18.20, 18.08, 17.93, 14.15, -1.27, -4.76, -4.80, -4.90, -5.19; **$[\alpha]^{25}_{D}$** –20.8 (c = 0.86 in $CHCl_3$); **IR** (film) 3480 (N-H), 2927, 2856, 1739 (C=O), 1691 (C=O), 1644 (C=O), 1455, 1412, 1250, 1189, 1088, 991, 937, 897, 834, 754, 574; **HRMS** Accurate mass (ES^+): Found 873.5226 (-5.8 ppm), $C_{44}H_{82}N_2O_8Si_3Na$ ($M+Na^+$) requires 873.5277.

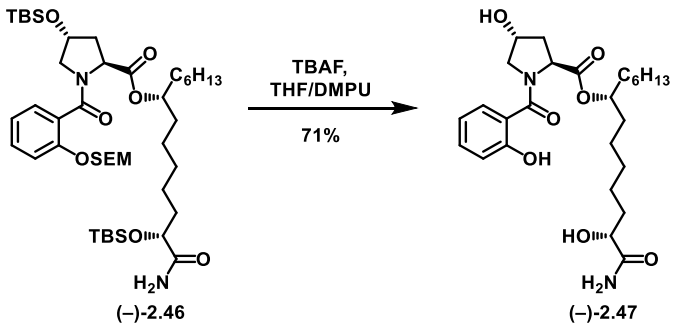

(1R,7R)-1-carbamoyl-1-hydroxytridecan-7-yl (2S,4R)-4-hydroxy-1-(2- hydroxybenzoyl)pyrrolidine-2-carboxylate (–)-2.47. Using modified general procedure L; (25 eq. TBAF, 0.040M DMPU), silyl ether **(–)-2.46** (25 mg, 0.029 mmol) with column chromatography eluting in 0 → 5% MeOH/CH_2Cl_2 yielded the title compound as a clear oil (10 mg, 71% yield). **^{1}H NMR** (500 MHz, $CDCl_3$) δ 10.50 (br s, 1H), 7.41 (d, J = 7.2 Hz, 1H), 7.32 (t, J = 7.7 Hz, 1H), 6.93 (d, J = 8.3 Hz, 1H), 6.86 (t, J = 7.5 Hz, 1H), 6.74 (br s, 1H), 5.69 (br s, 1H), 4.97 (br s, 1H), 4.81 (t, J = 8.2 Hz, 1H), 4.53 (s, 1H), 4.05 (dd, J = 7.7, 3.4 Hz, 1H), 3.95 (d, J = 8.7 Hz, 1H), 3.82 – 3.61 (m, 2H), 3.15 (br s, 1H), 2.43 – 2.30 (m, 1H), 2.09 (ddd, J = 13.0, 8.7, 4.4 Hz, 1H), 1.85 – 1.72 (m, 1H), 1.65 – 1.32 (m, 9H), 1.30 – 1.12 (m, 10H), 0.86 (t, J = 7.1 Hz, 3H); **^{13}C NMR** (125 MHz, $CDCl_3$) δ 177.57, 172.31, 170.88, 158.86, 133.28, 128.30, 118.98, 117.88, 75.73, 71.58, 70.44, 59.12, 58.36, 37.40, 34.48, 34.17, 34.04, 31.84, 29.23, 28.42, 25.46, 24.70, 24.50, 22.69, 14.21; **$[\alpha]^{25}_D$** – 43.4 (c = 0.71 in $CHCl_3$); **IR** (film) 3303 (br O-H), 2928, 2857, 1732 (C=O), 1666 (C=O), 1586 (C=O), 1434, 1376, 1298, 1193, 1082, 1001, 958, 911, 878, 754, 728, 651, 609; **HRMS** Accurate mass (ES^+): Found 515.2691 (-8.2 ppm), $C_{26}H_{40}N_2O_7Na$ ($M+Na^+$) requires 515.2733; **R_f** (9:1 CH_2Cl_2:MeOH) = 0.34.

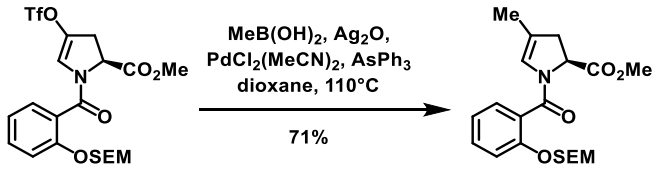

(–)-2.38 (–)-2.48

Methyl (S)-4-methyl-1-(2-((2-(trimethylsilyl)ethoxy)methoxy)benzoyl)-2,3-dihydro-1H-pyrrole-2-carboxylate (–)-2.48. Triflate **(–)-2.38** (75 mg, 0.143 mmol) was dissolved in dioxane (1.5 mL), and triphenylarsine (18 mg, 0.057 mmol), methylboronic acid (30 mg, 0.501 mmol), silver oxide (133 mg, 0.572 mmol) and K_3PO_4 (182 mg, 0.858 mmol) were added, and the reaction flask was covered in foil. The flask was vacuumed and back-filled with argon 3x, then $PdCl_2(MeCN)_2$ (4 mg, 0.014 mmol) was added, and the reaction was heated to 110°C. Upon heating, the reaction turned from green to dark red, and TLC analysis indicated the starting material was consumed. The reaction was filtered through Celite, concentrated, and purified by column chromatography, yielding the title compound as an orange oil (39 mg, 71% yield). **^{1}H NMR** (400 MHz, $CDCl_3$, mixture of rotamers/conformers) δ 7.39 – 7.28 (m, 2H), 7.20 (d, J = 8.1 Hz, 0.91H), 7.15 (d, J = 7.9 Hz, 0.15H), 7.04 (td, J = 7.5, 1.0 Hz, 0.92H), 6.99 (td, J = 7.5, 1.0 Hz, 0.14H), 5.88 (dd, J = 3.5, 1.7 Hz, 1H), 5.26 – 5.19 (m, 2H), 5.01 (dd, J = 11.6, 4.9 Hz, 1H), 3.80 (s, 3H), 3.78 – 3.71 (m, 2H), 3.06 – 2.96 (m, 1H), 2.61 – 2.53 (m, 1H), 1.64 (d, J = 1.4 Hz, 3H), 0.98 – 0.89 (m, 2H), 0.01 – -0.03 (m, 9H); **^{13}C NMR** (100 MHz, $CDCl_3$) δ 171.70, 164.44, 153.83, 131.11, 128.90, 126.23, 125.30, 122.04, 119.42, 115.48, 93.48, 66.58, 58.32, 52.59, 38.23, 18.16, 13.54, -1.27; **$[\alpha]^{25}_D$** –18.5 (c = 0.43 in $CHCl_3$); **IR** (film) 2951, 2919, 2850, 2102, 1747 (C=O), 1670 (C=O), 1600, 1486, 1454, 1409, 1345, 1247, 1230, 1144, 1088, 1052, 976, 916, 857, 834, 755, 694, 664, 605; **HRMS** Accurate mass (ES^+): Found 414.1684 (-7.0 ppm), $C_{20}H_{29}NO_5SiNa$ ($M+Na^+$) requires 414.1713.

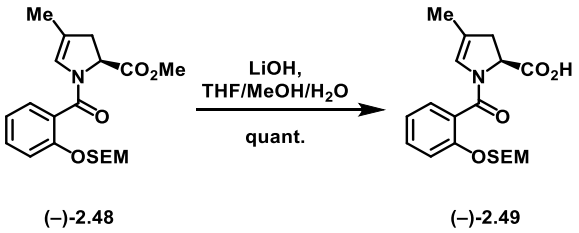

(–)-2.48 (–)-2.49

(S)-4-methyl-1-(2-((2-(trimethylsilyl)ethoxy)methoxy)benzoyl)-2,3-dihydro-1H-pyrrole-2- carboxylic acid (–)-2.49. Using general procedure E, methyl ester **(–)-2.48** (19 mg, 0.049 mmol) yielded the title compound as a clear oil (20 mg, quant. yield). **^{1}H NMR** (500 MHz, $CDCl_3$) δ 7.41 (t, J = 7.7 Hz, 1H), 7.33 (d, J = 6.5 Hz, 1H), 7.23 (d, J = 8.3 Hz, 1H), 7.07 (t, J = 7.5 Hz, 1H), 5.78 (s, 1H), 5.22 (s, 2H), 5.20 – 5.11 (m, 1H), 3.75 – 3.69 (m, 2H), 3.22 (d, J = 16.4 Hz, 1H), 2.97 – 2.85 (m, 1H), 1.70 (s, 3H), 0.99 – 0.87 (m, 2H), -0.01 (s, 9H); **^{13}C NMR** (100 MHz, $CDCl_3$) δ 170.97, 167.90, 153.86, 132.11, 124.43, 124.15, 123.55, 122.09, 115.25, 93.38, 66.87, 60.45, 36.19, 18.17, 13.61, -1.27; **$[\alpha]^{25}_D$** –80.6 (c = 0.70 in $CHCl_3$); **IR** (film) 2954, 2921, 2857, 1743, 1598, 1489, 1457, 1427, 1378, 1303, 1232, 1143, 1086, 1043, 983, 916, 856, 834, 754, 694, 658; **HRMS** Accurate mass (ES^+): Found 400.1573 (+4.2 ppm), $C_{19}H_{27}NO_5SiNa$ ($M+Na^+$) requires 400.1556.

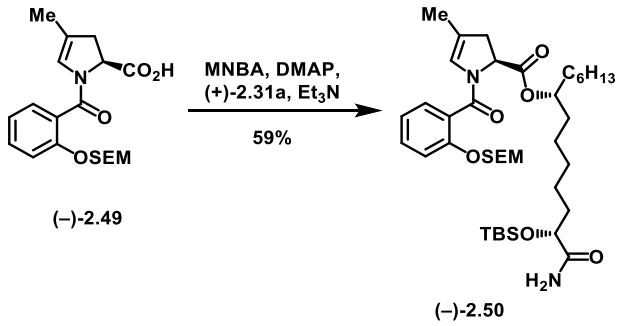

(–)-2.49 (–)-2.50

(7R,13R)-14-amino-13-((tert-butyldimethylsilyl)oxy)-14-oxotetradecan-7-yl (S)-4-methyl-1- (2-((2-(trimethylsilyl)ethoxy)methoxy)benzoyl)-2,3-dihydro-1H-pyrrole-2-carboxylate (–)-2.50. Using modified general procedure K; (1.2 eq acid, 1.2 eq MNBA, 1.0 eq alcohol, 0.1 eq DMAP), acid **(–)-2.49** (25 mg, 0.066 mmol) after purification by column chromatography eluting in 0 → 30% Et_2O/CH_2Cl_2, yielded the title compound as a yellow oil (24 mg, 59% yield). **^{1}H NMR** (500 MHz, $CDCl_3$) δ 7.37 – 7.31

(m, 2H), 7.19 (t, J = 9.5 Hz, 1H), 7.03 (td, J = 7.5, 0.9 Hz, 1H), 6.53 (t, J = 8.5 Hz, 1H), 5.87 (d, J = 1.6 Hz, 1H), 5.58 – 5.46 (m, 1H), 5.22 (dd, J = 17.5, 7.1 Hz, 2H), 5.03 – 4.91 (m, 2H), 4.16 – 4.09 (m, 1H), 3.79 – 3.70 (m, 2H), 3.08 – 2.96 (m, 1H), 2.51 (dd, J = 16.7, 4.8 Hz, 1H), 1.79 – 1.66 (m, 3H), 1.64 (s, 3H), 1.60 – 1.51 (m, 4H), 1.41 – 1.19 (m, 18H), 0.96 – 0.89 (m, 12H), 0.88 – 0.84 (m, 3H), 0.09 – 0.05 (m, 6H), 0.01 – -0.03 (m, 9H); **^{13}C NMR** (100 MHz, $CDCl_3$) δ 176.96, 170.93, 164.26, 153.87, 131.01, 128.89, 126.36, 125.41, 121.99, 119.19, 115.47, 93.48, 75.41, 73.57, 66.56, 58.63, 38.46, 35.12, 34.08, 31.87, 29.52, 29.32, 25.88, 25.34, 25.05, 24.12, 22.73, 18.17, 14.22, 13.58, -1.26, -4.69, -5.13; **$[\alpha]^{25}_{D}$** – 18.3 (c = 0.69 in $CHCl_3$); **IR** (film) 2927, 2856, 2359, 2341, 1733 (C=O), 1683 (C=O), 1645 (C=O), 1601, 1506, 1488, 1456, 1419, 1377, 1248, 1188, 1141, 1086, 989, 834, 778, 754, 692, 667, 561; **HRMS** Accurate mass (ES^+): Found 733.4666 (+3.1 ppm), $C_{39}H_{69}N_2O_7Si_2$ ($M+H^+$) requires 733.4643.

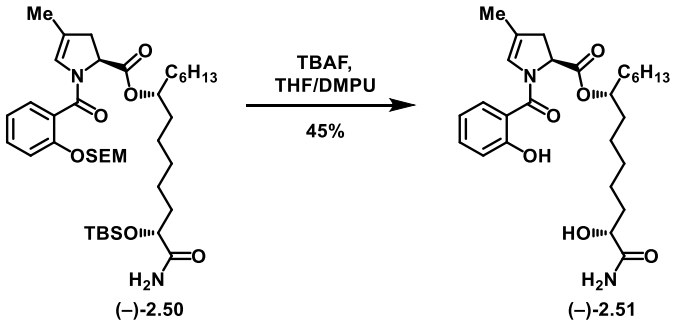

(7R,13R)-14-amino-13-hydroxy-14-oxotetradecan-7-yl (S)-1-(2-hydroxybenzoyl)-4-methyl- 2,3-dihydro-1H-pyrrole-2-carboxylate (–)-2.51. Using general procedure L, silyl ether **(–)-2.50** (10.7 mg, 0.0146 mmol) yielded the title compound as a clear oil (3.2 mg, 45% yield). **^{1}H NMR** (500 MHz, $CDCl_3$) δ 9.53 (s, 1H), 7.44 – 7.32 (m, 2H), 7.01 – 6.96 (m, 1H), 6.90 (t, J = 7.4 Hz, 1H), 6.61 (s, 0.68H), 6.55 (s, 0.46H), 6.44 (s, 1H), 5.32 (s, 1H), 5.05 – 4.94 (m, 2H), 4.13 – 4.05 (m, 1H), 3.47 (s, 1H), 3.09 – 3.00 (m, 1H), 2.59 – 2.51 (m, 1H), 1.84 – 1.77 (m, 1H), 1.75 (s, J = 8.0 Hz, 3H), 1.68 – 1.49 (m, 12H), 1.48 – 1.36 (m, 4H), 1.36 – 1.22 (m, 12H), 0.87 (t, J = 7.0 Hz, 3H); **^{13}C NMR** (125 MHz, $CDCl_3$) δ 176.97, 171.46, 166.42, 157.88, 133.25, 128.21, 125.19, 122.31, 119.35, 117.98, 117.92, 75.91, 71.33, 59.76, 56.13, 37.72, 34.59, 34.27, 34.20, 31.84, 29.85, 29.22, 28.26, 25.53, 24.81, 24.54, 22.69, 14.20, 13.70; **$[\alpha]^{25}_{D}$** –21.8 (c = 0.27 in $CHCl_3$); **IR** (film) 3306 (br O-H), 2921, 2855, 2493, 2361, 2159, 2031, 1978, 1734 (C=O), 1669

(C=O), 1591 (C=O), 1457, 1378, 1298, 1202, 1157, 1096, 1020, 867, 806, 756, 667; **HRMS** Accurate mass (ES^+): Found 489.2937 (-5.7 ppm), $C_{27}H_{41}N_2O_6$ ($M+H^+$) requires 489.2965.

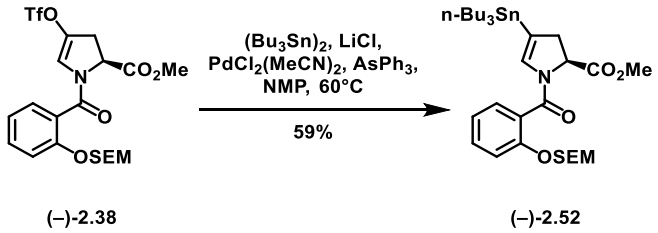

(–)-2.38 (–)-2.52

Methyl (S)-4-(tributylstannyl)-1-(2-((2-(trimethylsilyl)ethoxy)methoxy)benzoyl)-2,3-dihydro- 1H-pyrrole-2-carboxylate (–)-S14. To a solution of triflate **(–)-2.52** (559 mg, 1.064 mmol) in NMP (6 mL) was added $PdCl_2(MeCN)_2$ (14 mg, 0.053 mmol), $AsPh_3$ (65 mg, 0.213 mmol), LiCl (135 mg, 3.191 mmol), and bis(tributyltin) (0.56 mL, 1.117 mmol). The solution was heated to 60 °C for 1 hour, after which time the reaction turned from orange to brown/black. The reaction was cooled to room temperature, quenched with 1M aq. KF, and extracted 2x with Et_2O. The combined organic layers were washed with 1M aq. KF, and brine 2x, then dried over $MgSO_4$, filtered, concentrated and purified by column chromatography, yielding the title compound as a yellow oil (416 mg, 59% yield). **^{1}H NMR** (400 MHz, $CDCl_3$) δ 7.41 – 7.35 (m, 2H), 7.22 (dd, J = 8.8, 0.9 Hz, 1H), 7.09 – 7.03 (m, 1H), 5.97 (t, J = 2.1 Hz, 1H), 5.26 – 5.19 (m, 2H), 4.96 (dd, J = 11.4, 5.0 Hz, 1H), 3.84 – 3.72 (m, 5H), 3.15 (ddd, J = 16.8, 11.3, 2.3 Hz, 1H), 2.76 (ddd, J = 16.8, 5.0, 1.9 Hz, 1H), 1.52 – 1.38 (m, 6H), 1.33 – 1.20 (m, 8H), 0.98 – 0.82 (m, 18H), 0.00 (s, 9H); **^{13}C NMR** (125 MHz, $CDCl_3$) δ 171.83, 164.19, 154.01, 135.61, 131.09, 128.90, 126.25, 121.93, 118.43, 93.64, 66.39, 58.29, 52.28, 40.55, 29.08, 29.00, 27.24, 27.16, 17.92, 13.67, 13.63, 9.52 (J = 309 Hz, ^{13}C-^{117}Sn; J = 355 Hz, ^{13}C-^{119}Sn), -1.36; **$[\alpha]^{25}_D$** –41.5 (c = 1.63 in $CHCl_3$); **IR** (film) 2953, 2923, 2869, 2852, 1754 (C=O), 1651 (C=O), 1584, 1488, 1454, 1399, 1283, 1247, 1228, 1198, 1176, 1152, 1087, 1019, 989, 917, 856, 834, 753, 731, 692, 658, 599, 561; **HRMS** Accurate mass (ES^+): Found 668.2798 (+0.7 ppm), $C_{31}H_{54}NO_5SiSn$ ($M+H^+$) requires 668.2793.

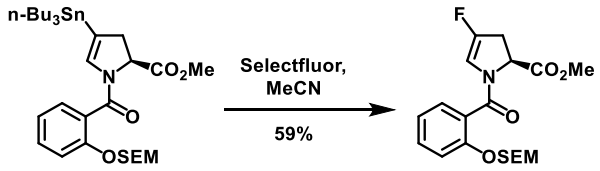

(–)-2.52 (–)-2.53

Methyl (S)-4-fluoro-1-(2-((2-(trimethylsilyl)ethoxy)methoxy)benzoyl)-2,3-dihydro-1H-pyrrole-2-carboxylate (–)-2.53. To a solution of stannane **(–)-2.52** (400 mg, 0.6001 mmol) in acetonitrile (5 mL) was added Selectfluor® (234 mg, 0.6601 mmol). After 5 minutes, solids crashed out and the solution was filtered into water. The layers were separated and the aqueous layer was extracted with CH_2Cl_2 2x. The combined organic layers were washed with brine, dried over $MgSO_4$, filtered, concentrated, and purified by column chromatography, yielding the title compound as a clear oil (140 mg, 59%). **^{1}H NMR** (500 MHz, $CDCl_3$) δ 7.40 – 7.34 (m, 2H), 7.21 (t, J = 7.2 Hz, 1H), 7.05 (td, J = 7.5, 0.9 Hz, 1H), 6.06 (dd, J = 4.1, 2.2 Hz, 1H), 5.24 (q, J = 7.1 Hz, 2H), 5.05 (dd, J = 11.7, 4.7 Hz, 1H), 3.83 (s, 3H), 3.79 – 3.73 (m, 2H), 3.32 (dddd, J = 16.4, 11.8, 4.3, 2.3 Hz, 1H), 2.89 – 2.83 (m, 1H), 0.99 – 0.91 (m, 2H), -0.01 (s, 9H); **^{13}C NMR** (125 MHz, $CDCl_3$) δ 170.10, 165.21, 153.60, 151.05, 148.92, 131.45, 128.93, 124.94, 121.95, 115.07, 111.54 (d, J = 30 Hz 13C-19F), 93.20, 66.66, 56.30, 56.26, 52.70, 32.07, 31.91, 18.04, -1.47; **$[\alpha]^{25}_D$** –56.1 (c = 1.08 in $CHCl_3$; **IR** (film) 2953, 2924, 1749 (C=O), 1644 (C=O), 1600, 1488, 1456, 1417, 1356, 1229, 1306, 1247, 1231, 1201, 1179, 1144, 1086, 1028, 982, 934, 914, 857, 834, 754, 693, 658, 577; **HRMS** Accurate mass (ES^+): Found 418.1427 (- 8.4 ppm), $C_{19}H_{26}FNO_5SiNa$ ($M+Na^+$) requires 418.1462.

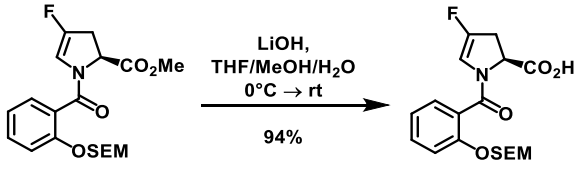

(–)-2.53 (–)-2.54

(S)-4-fluoro-1-(2-((2-(trimethylsilyl)ethoxy)methoxy)benzoyl)-2,3-dihydro-1H-pyrrole-2- carboxylic acid (–)-2.54. To a solution of methyl ester **(–)-2.53** (128 mg, 0.3236 mmol) in 3:1:1 THF:MeOH:H_2O (3 mL) was added LiOH•H_2O (14 mg) dissolved in water (0.5 mL) at 0 °C. The reaction was stirred for 15

minutes then warmed to room temperature and stirred for 2 hours. The reaction was acidified (pH ~ 5-6) with 5% aq. AcOH and extracted with CH_2Cl_2 3x. The combined organic layers were washed with brine, dried over $MgSO_4$, filtered, concentrated and purified by column chromatography (0 → 5% MeOH/0.1% AcOH/CH_2Cl_2), yielding the title compound as a clear oil (116 mg, 94% yield). *Note:* While the acids in this study prepared by ester hydrolysis generally did not require chromatography, this one in particular required purification for acceptable yields in the next step. **^{1}H NMR** (400 MHz, $CDCl_3$) δ 7.47 – 7.42 (m, 1H), 7.36 (dd, J = 7.5, 1.5 Hz, 1H), 7.24 (d, J = 8.5 Hz, 1H), 7.09 (td, J = 7.5, 0.7 Hz, 1H), 5.96 (d, J = 1.9 Hz, 1H), 5.28 – 5.20 (m, 3H), 3.76 – 3.70 (m, 2H), 3.62 – 3.54 (m, 1H), 3.27 – 3.14 (m, 1H), 0.97 – 0.91 (m, 2H), 0.00 (s, 9H); **^{13}C NMR** (100 MHz, $CDCl_3$) δ 171.19, 167.47, 153.70, 153.26, 150.58, 132.17, 129.05, 123.85, 122.08, 115.05, 110.80 (d, J = 31 Hz, 13C-19F), 93.26, 66.93, 57.71, 18.13, -1.39; **$[\alpha]^{25}_D$** – 62.7 (c = 0.72 in $CHCl_3$); **IR** (film) 2954, 2923, 2853, 1742 (C=O), 1600 (C=O), 1458, 1425, 1354, 1315, 1248, 1231, 1144, 1086, 983, 916, 857, 834, 753, 693, 658 **HRMS** Accurate mass (ES^+): Found 404.1291 (-3.5 ppm), $C_{18}H_{24}FNO_5SiNa$ ($M+Na^+$) requires 404.1305; **R_f** (10% MeOH/0.1% AcOH/CH_2Cl_2) = 0.29.

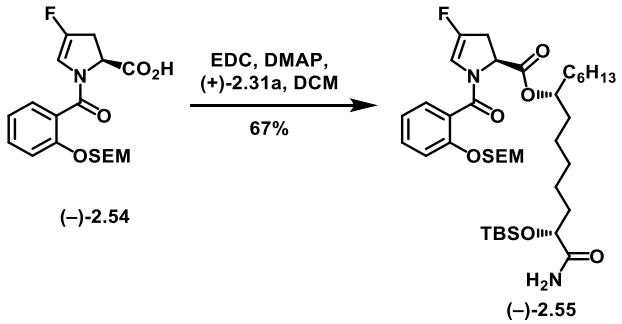

(–)-2.54

(–)-2.55

(7R,13R)-14-amino-13-((tert-butyldimethylsilyl)oxy)-14-oxotetradecan-7-yl (S)-4-fluoro-1-(2-((2-(trimethylsilyl)ethoxy)methoxy)benzoyl)-2,3-dihydro-1H-pyrrole-2-carboxylate (–)-2.55. Using general procedure J, acid **(–)-2.54** (39 mg, 0.102 mmol) yielded the title compound as a clear oil (36 mg, 67% yield). **^{1}H NMR** (400 MHz, $CDCl_3$) δ 7.40 – 7.30 (m, 2H), 7.20 (d, J = 8.2 Hz, 1H), 7.04 (t, J = 7.1 Hz, 1H), 6.57 – 6.48 (m, 1H), 6.05 (d, J = 1.8 Hz, 1H), 5.57 – 5.43 (m, 1H), 5.24 (q, J = 7.1 Hz, 2H), 5.08 – 4.91 (m, 2H), 4.13 (t, J = 5.1 Hz, 1H), 3.80 – 3.71 (m, 2H), 3.38 – 3.27 (m, 1H), 2.85 – 2.75 (m, 1H), 1.82 – 1.70 (m, 1H), 1.69 – 1.50 (m, 6H), 1.41 – 1.19 (m, 20H), 0.97 – 0.89 (m, 12H), 0.89 – 0.85 (m, 3H), 0.13

– 0.06 (m, 6H), -0.01 (s, 9H); **^{13}C NMR** (125 MHz, $CDCl_3$) δ 177.10, 169.48, 165.13, 153.75, 151.09, 148.97, 131.45, 129.02, 125.18, 122.02, 115.20, 111.72 (d, J = 31 Hz, 13C-19F), 93.33, 76.00, 73.52, 66.76, 56.71, 35.16, 35.06, 34.00, 33.95, 32.39, 32.23, 31.81, 29.80, 29.44, 29.27, 25.84, 25.31, 25.19, 25.00, 24.14, 24.07, 22.68, 18.17, 18.11, 14.16, -1.30, -1.35, -4.74, -5.16; **$[\alpha]^{25}_D$** –12.5 (c = 1.18 in $CHCl_3$) **IR** (film) 3480, 2951, 2927, 2856, 2242, 1742 (C=O), 1688 (C=O), 1645 (C=O), 1601, 1488, 1456, 1419, 1353, 1249, 1189, 1142, 1088, 988, 916, 835, 778, 754, 730, 659, 577; **HRMS** Accurate mass (ES^+): Found 759.4182 (-4.0 ppm), $C_{38}H_{65}FN_2O_7Si_2Na$ ($M+Na^+$) requires 759.4212; **R_f** (2:1 CH_2Cl_2:Et_2O) = 0.60.

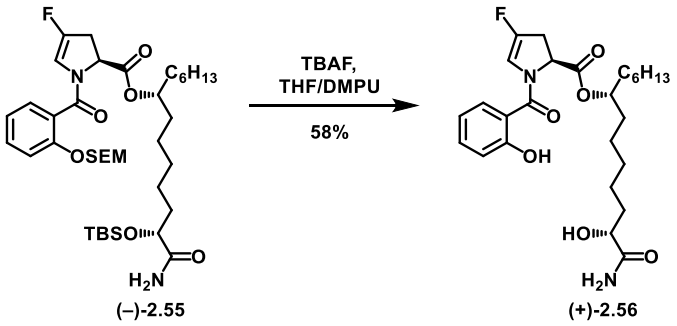

(7R,13R)-14-amino-13-hydroxy-14-oxotetradecan-7-yl (S)-4-fluoro-1-(2-hydroxybenzoyl)- 2,3-dihydro-1H-pyrrole-2-carboxylate (+)-2.56. Using general procedure L, silyl ether **(–)-2.55** (21 mg, 0.029 mmol) yielded the title compound as a clear oil (8.1 mg, 58% yield). **^{1}H NMR** (500 MHz, $CDCl_3$) δ 9.67 (br d, 1H), 7.41 – 7.33 (m, 2H), 7.02 – 6.96 (m, 1H), 6.91 (t, J = 7.6 Hz, 1H), 6.70 (d, J = 38.0 Hz, 1H), 6.55 (d, J = 28.6 Hz, 1H), 5.49 (d, J = 44.7 Hz, 1H), 5.07 – 4.92 (m, 2H), 4.09 (dd, J = 7.9, 3.5 Hz, 1H), 3.35 (t, J = 14.0 Hz, 1H), 3.03 (br s, 1H), 2.88 – 2.80 (m, 1H), 1.84 – 1.72 (m, 1H), 1.72 – 1.50 (m, 6H), 1.50 – 1.18 (m, 14H), 0.87 (t, J = 7.0 Hz, 3H); **^{13}C NMR** (125 MHz, $CDCl_3$) δ 176.96, 176.73, 169.87, 169.56, 167.43, 159.01, 158.10, 152.93, 152.82, 150.67, 133.80, 133.63, 127.97, 119.49, 119.28, 118.22, 118.13, 117.08, 116.43, 112.12, 111.87, 76.58, 71.68, 71.48, 58.34, 57.83, 34.53, 34.45, 34.37, 34.14, 33.86, 31.82, 29.21, 28.81, 28.43, 25.52, 25.27, 24.95, 24.84, 24.61, 22.68, 14.19; **$[\alpha]^{25}_D$** +12.0 (c = 0.45 in $CHCl_3$); **IR** (film) 3308 (br, O-H), 2929, 2858, 1734 (C=O), 1669 (C=O), 1653, 1623, 1594, 1521, 1457, 1436, 1354, 1337, 1300, 1192, 1142, 1097, 1037, 1004, 919, 859, 804, 755, 655; **HRMS** Accurate mass (ES^+): Found 493.2738 (+4.9 ppm), $C_{26}H_{38}FN_2O_6$ ($M+H^+$) requires 493.2714.

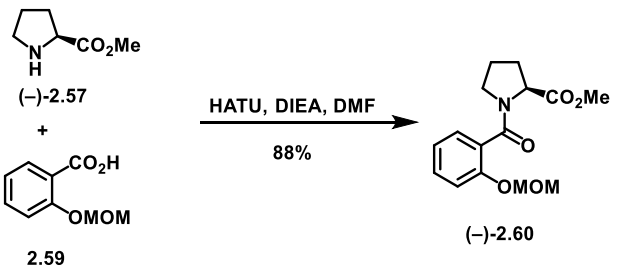

Methyl (2S)-1-[2-(methoxymethoxy)benzoyl]pyrrolidine-2-carboxylate (–)-2.60. Using general procedure F, 2-methoxymethyloxybenzoic acid **2.59** (248 mg, 1.364 mmol) and proline methyl ester hydrochloride **(–)-2.57** (271 mg, 1.636 mmol) yielded the title compound as a clear oil (352 mg, 88% yield). **^{1}H NMR** (400 MHz, MeOD, mixture of rotamers/conformers) δ 7.43 – 7.34 (m, 1H), 7.28 (dd, J = 7.5, 1.7 Hz, 0.73H), 7.23 (d, J = 8.4 Hz, 0.71H), 7.20 (d, J = 8.3 Hz, 0.30H), 7.15 (d, J = 7.6 Hz, 0.26H), 7.09 (td, J = 7.5, 0.9 Hz, 0.74H), 7.04 (dd, J = 11.2, 3.8 Hz, 0.29H), 5.26 – 5.20 (m, 2H), 4.59 (dd, J = 8.7, 4.7 Hz, 0.72H), 4.30 (dd, J = 8.6, 2.8 Hz, 0.28H), 3.77 (s, 1.52H), 3.75 – 3.69 (m, 0.54H), 3.48 (s, 0.63H), 3.47 (s, 1.88H), 3.46 (s, 1.18H), 3.41 (dt, J = 17.4, 5.3 Hz, 1.40H), 3.35 (s, 1.28H), 2.44 – 2.25 (m, 1H), 2.09 – 1.86 (m, 3H); **^{13}C NMR** (100 MHz, MeOD) δ 173.83, 170.08, 169.82, 154.26, 131.97, 129.18, 128.65, 128.30, 127.93, 123.08, 122.81, 116.41, 116.07, 95.98, 61.55, 59.94, 56.67, 52.73, 49.54, 47.42, 31.87, 30.48, 25.55, 23.76; **$[\alpha]^{25}_{D}$** –18.3 (c = 0.66 in $CHCl_3$) **IR** (film) 2054, 2359, 1741 (C=O), 1625 (C=O), 1601, 1489, 1455, 1418, 1362, 1281, 1234, 1198, 1152, 1107, 1078, 1041, 989, 922, 844, 747, 666; **HRMS** Accurate mass (ES^+): Found 316.1134 (-8.6 ppm), $C_{15}H_{19}NO_5Na$ ($M+Na^+$) requires 316.1161.

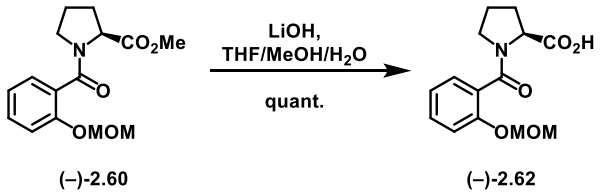

(2S)-1-[2-(methoxymethoxy)benzoyl]pyrrolidine-2-carboxylic acid (–)-2.62. Using general procedure E, methyl ester (–)-**2.60** (117 mg, 0.399 mmol) yielded the title compound as a clear oil (115 mg, quant. yield). **^{1}H NMR** (400 MHz, MeOD, mixture of rotamers/conformers) δ 7.91 (s, 0.55H), 7.43 – 7.34 (m, 1.06H), 7.31 (dd, J = 7.5, 1.6 Hz, 0.66H), 7.26 – 7.18 (m, 1.29H), 7.09 (td, J = 7.5, 0.9 Hz, 0.64H), 7.03 (t,

J = 7.5 Hz, 0.31H), 5.26 – 5.19 (m, 2H), 4.57 (dd, J = 8.5, 4.5 Hz, 0.60H), 4.23 (d, J = 6.6 Hz, 0.31H), 3.80 – 3.67 (m, 0.66H), 3.47 (s, 3H), 3.45 – 3.35 (m, 1H), 2.44 – 2.22 (m, 1H), 2.14 – 1.84 (m, 3H); **^{13}C NMR** (100 MHz, MeOD) δ 175.57, 170.59, 170.23, 154.43, 132.01, 128.76, 128.55, 123.19, 122.97, 116.54, 116.05, 96.13, 96.01, 79.48, 56.66, 49.74, 47.41, 32.11, 30.81, 25.64, 23.78; **$[\alpha]^{25}_{D}$** –71.4 (c = 1.28 in $CHCl_3$); **IR** (film) 2956, 2359, 1733 (C=O), 1592 (C=O), 1490, 1456, 1234, 1198, 1152, 1107, 1078, 1042, 979, 921, 845, 748, 665; **HRMS** Accurate mass (ES^+): Found 302.1012 (+2.6 ppm), $C_{14}H_{17}NO_5$ ($M+Na^+$) requires 302.1004.

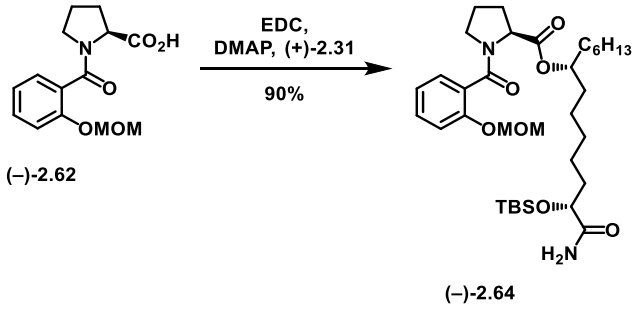

(1R,7R)-1-[(tert-butyldimethylsilyl)oxy]-1-carbamoyltridecan-7-yl (2S)-1-[2-(methoxymethoxy)benzoyl]pyrrolidine-2-carboxylate (–)-2.64. Using modified general procedure J (2 eq acid, 2 eq EDC, 1 eq alcohol, 0.1 eq DMAP), acid (–)-**2.62** (43 mg, 0.154 mmol) yielded the title compound as a clear oil (43 mg, 90% yield). **^{1}H NMR** (500 MHz, $CDCl_3$, mixture of rotamers/conformers) δ 7.29 (tdd, J = 9.8, 8.2, 1.4 Hz, 1.36H), 7.25 – 7.20 (m, 0.86H), 7.14 (d, J = 8.2 Hz, 0.69H), 7.08 (d, J = 8.4 Hz, 0.41H), 7.03 (t, J = 7.4 Hz, 0.68H), 6.94 (t, J = 7.5 Hz, 0.39H), 6.53 (dd, J = 10.1, 4.3 Hz, 1H), 5.77 (s, 0.39H), 5.74 (s, 0.58H), 5.21 – 5.14 (m, 2H), 4.92 (dt, J = 12.2, 6.2 Hz, 0.62H), 4.69 – 4.60 (m, 1H), 4.27 – 4.21 (m, 0.34H), 4.12 (dt, J = 10.4, 5.0 Hz, 1H), 3.81 – 3.73 (m, 0.63H), 3.50 – 3.38 (m, 3.66H), 3.33 (dt, J = 10.6, 6.7 Hz, 1H), 2.34 – 2.17 (m, 1H), 2.06 – 1.79 (m, 4H), 1.79 – 1.47 (m, 5H), 1.42 – 1.16 (m, 18H), 0.94 – 0.88 (m, 9H), 0.85 (t, J = 6.8 Hz, 3H), 0.10 (d, J = 5.6 Hz, 1.78H), 0.06 (d, J = 6.1 Hz, 3.81H); **^{13}C NMR** (125 MHz, $CDCl_3$) δ 177.06, 172.01, 167.68, 153.19, 130.57, 128.16, 127.98, 122.31, 115.60, 95.22, 95.09, 75.56, 75.15, 73.54, 60.47, 58.90, 56.36, 48.31, 46.18, 35.23, 35.11, 34.10, 33.98, 33.77, 31.85, 31.78, 31.43, 29.92, 29.49, 29.29, 29.18, 25.85, 25.31, 25.11, 24.86, 24.10, 22.89, 22.69,

22.64, 18.12, 14.17, -4.73, -5.16; **[α]$^{25}_{D}$** –21.4 (c = 0.95 in $CHCl_3$); **IR** (film) 3477 (N-H), 3307 (br O-H); 2927, 2856, 1738 (C=O), 1683 (C=O), 1626, 1601, 1558, 1489, 1456, 1417, 1338, 1281, 1235, 1194, 1153, 1079, 1042, 989, 922, 837, 755, 652; **HRMS** Accurate mass (ES^+): Found 635.4109 (+2.7 ppm), $C_{34}H_{59}N_2O_7Si$ ($M+H^+$) requires 635.4092.

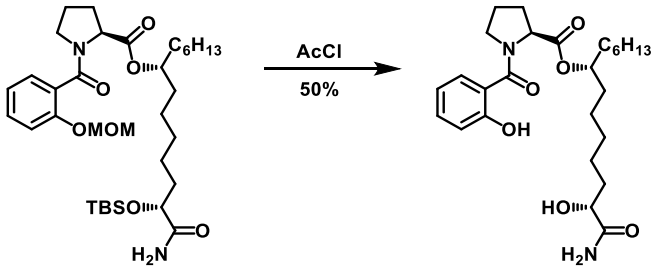

(1R,7R)-1-carbamoyl-1-hydroxytridecan-7-yl (2S)-1-(2-hydroxybenzoyl)pyrrolidine-2- carboxylate (□)-6. To a solution of protected ester **(□)-S5** (43 mg, 0.068 mmol) in MeOH (1 mL) was added acetyl chloride (*ca.* 1 μL, 1 drop) at room temperature. After 1 hour, the reaction was quenched with sat. NaHCO3 and extracted with CH2Cl2 3x. The combined organic layers were washed with water, dried over Na2SO4, filtered, concentrated, and purified by column chromatography (0 → 10% MeOH/CH2Cl2), yielding the title compound as a clear oil (16 mg, 50% yield). **1H NMR** (500 MHz, CDCl3) δ 10.64 (s, 1H), 7.49 (d, J = 6.9 Hz, 1H), 7.33 (t, J = 7.6 Hz, 1H), 6.96 (t, J = 8.6 Hz, 1H), 6.86 (t, J = 7.3 Hz, 1H), 6.66 (s, 1H), 5.52 (s, 1H), 4.98 (s, 1H), 4.71 – 4.60 (m, 1H), 4.08 (s, J = 19.6 Hz, 1H), 3.93 – 3.83 (m, 1H), 3.83 – 3.73 (m, 1H), 3.66 (s, 1H), 2.40 – 2.28 (m, 1H), 2.15 – 2.05 (m, 1H), 2.05 – 1.90 (m, 2H), 1.87 – 1.76 (m, 3H), 1.68 – 1.48 (m, 5H), 1.48 – 1.33 (m, 6H), 1.33 – 1.16 (m, 11H), 0.86 (t, J = 7.0 Hz, 3H); **13C NMR** (125 MHz, CDCl3) δ 177.22, 172.37, 170.30, 159.04, 133.20, 128.10, 118.83, 117.85, 117.73, 75.42, 71.48, 60.56, 50.78, 34.58, 34.39, 34.29, 31.84, 29.21, 28.52, 25.82, 25.49, 24.87, 24.65, 22.67, 14.19; **[α]25D** –28.0 (c = 1.51 in CHCl3); **IR** (film) 3189 (br O-H), 2928, 2857, 2360, 1736 (C=O), 1667 (C=O), 1583 (C=O), 1434, 1374, 1186, 1089, 1025, 877, 754, 651, 609, 563; **HRMS** Accurate mass (ES+): Found 477.2935 (-6.3 ppm), C26H41N2O6 ($M+H^+$) requires 477.2965.

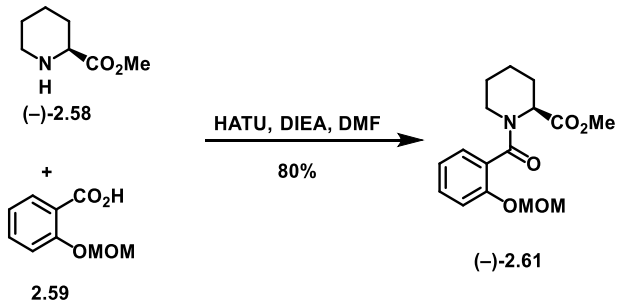

Methyl (2S)-1-[2-(methoxymethoxy)benzoyl]piperidine-2-carboxylate (–)-2.61. Using general procedure F, 2-methoxymethyloxybenzoic acid **(2.59)** (200 mg, 1.101 mmol) and methyl 2-piperidinecarboxylate hydrochloride **(–)-2.58** (237 mg, 1.321 mmol) yielded the title compound as a clear oil (248 mg, 80% yield). **^{1}H NMR** (500 MHz, $CDCl_3$, mixture of rotamers/conformers) δ 7.42 – 7.26 (m, 2.67H), 7.25 – 7.17 (m, 1.16H), 7.14 – 7.03 (m, 1.23H), 5.67 (s, 0.73H), 5.27 (dt, J = 11.7, 6.9 Hz, 2H), 5.15 (dd, J = 39.3, 6.6 Hz, 0.32H), 4.81 (d, J = 13.7 Hz, 0.31H), 4.43 (d, J = 5.1 Hz, 0.08H), 4.36 (d, J = 4.3 Hz, 0.22H), 3.85 (s, 2.22H), 3.76 (s, J = 4.4 Hz, 1.08H), 3.59 – 3.46 (m, 4.22H), 3.41 – 3.33 (m, 0.55H), 3.18 (td, J = 13.0, 2.4 Hz, 0.57H), 2.92 – 2.84 (m, 0.23H), 2.41 (t, J = 13.5 Hz, 0.75H), 2.28 (d, J = 12.8 Hz, 0.32H), 1.87 – 1.73 (m, 2.52H), 1.68 – 1.51 (m, 2.08H), 1.51 – 1.35 (m, 1.49H); **^{13}C NMR** (125 MHz, $CDCl_3$) δ 171.53, 171.34, 171.26, 168.93, 168.85, 168.72, 153.19, 152.82, 152.62, 130.27, 130.24, 127.98, 127.81, 127.42, 126.70, 126.65, 126.53, 122.28, 122.11, 122.05, 115.15, 114.77, 114.72, 94.85, 94.78, 94.70, 77.36, 60.27, 57.86, 56.17, 56.11, 52.28, 52.24, 52.07, 51.82, 51.60, 45.34, 44.53, 39.40, 39.05, 27.38, 26.87, 26.59, 25.49, 25.33, 24.64, 21.16, 21.10, 20.95, 14.12; **$[\alpha]^{25}_{D}$** –28.6 (c = 2.15 in $CHCl_3$); **IR** (film) 1076, 2945, 1737 (C=O), 1633 (C=O), 1599, 1488, 1452, 1422, 1339, 1286, 1232, 1199, 1143, 985, 921, 756, 645; **HRMS** Accurate mass (ES^+): Found 308.1502 (+1.3 ppm), $C_{16}H_{21}NO_5Na$ ($M+Na^+$) requires 308.1498.

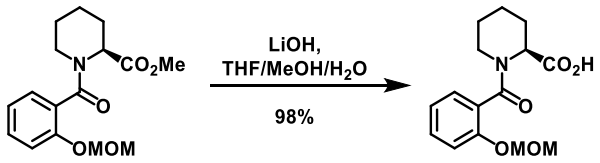

(–)-2.61 (–)-2.63

(2S)-1-[2-(methoxymethoxy)benzoyl]piperidine-2-carboxylic acid (–)-2.63. Using general procedure E, methyl ester **(–)-2.61** (215 mg, 0.700 mmol) yielded the title compound as a clear oil (200 mg, 98% yield). **^{1}H NMR** (500 MHz, $CDCl_3$, mixture of rotamers/conformers) δ 9.53 (br s, 1H), 7.36 – 7.23 (m, 2.16H), 7.16 (dt, J = 18.2, 8.0 Hz, 1.56H), 7.04 (t, J = 7.3 Hz, 0.91H), 6.99 (t, J = 7.6 Hz, 0.37H), 5.64 – 5.56 (m, 0.75H), 5.18 (ddd, J = 14.8, 13.8, 7.3 Hz, 2H), 5.06 (dd, J = 40.1, 6.7 Hz, 0.40H), 4.72 (d, J = 10.5 Hz, 0.31H), 4.35 (d, J = 4.9 Hz, 0.09H), 4.27 (d, J = 4.0 Hz, 0.20H), 3.76 (t, J = 6.0 Hz, 0.60H), 3.49 – 3.40 (m, 3.74H), 3.32 – 3.22 (m, 0.61H), 3.12 (t, J = 12.0 Hz, 0.57H), 2.86 – 2.77 (m, 0.28H), 2.37 (d, J = 13.2 Hz, 0.77H), 2.19 (d, J = 13.3 Hz, 0.26H), 2.07 (d, J = 11.4 Hz, 0.12H), 1.89 – 1.82 (m, 0.62H), 1.82 – 1.63 (m, 2.67H), 1.56 (dd, J = 32.8, 13.9 Hz, 1.35H), 1.51 – 1.32 (m, 2.57H); **^{13}C NMR** (125 MHz, $CDCl_3$) δ 175.19, 174.99, 174.14, 169.79, 169.58, 169.27, 153.31, 152.97, 152.77, 130.68, 130.58, 128.22, 128.01, 127.59, 126.13, 122.40, 122.18, 115.15, 114.79, 94.92, 94.78, 67.95, 57.89, 56.29, 56.26, 52.02, 51.92, 45.59, 44.84, 39.64, 27.51, 26.73, 26.55, 25.61, 25.53, 25.36, 24.75, 21.17; **$[\alpha]^{25}_{D}$** –59.8 (c = 0.85 in $CHCl_3$); **IR** (film) 2941, 1731 (C=O), 1587 (C=O), 1442, 1286, 1233, 1199, 1151, 1077, 1041, 983, 921, 864, 755, 732, 700, 641; **HRMS** Accurate mass (ES^+): Found 316.1173 (+3.8 ppm), $C_{15}H_{19}NO_5Na$ ($M+Na^+$) requires 316.1161.

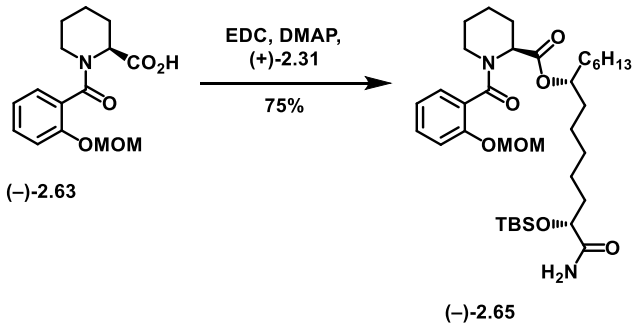

(1R,7R)-1-[(tert-butyldimethylsilyl)oxy]-1-carbamoyltridecan-7-yl (2S)-1-[2-(methoxymethoxy)benzoyl]piperidine-2-carboxylate (–)-2.65. Using modified general procedure J (1.5 eq acid, 1.7 eq EDC, 0.5 eq DMAP, 1.0 eq alcohol); acid **(–)-2.63** (85 mg, 0.291 mmol) yielded the title compound as a clear oil (94 mg, 75% yield). **^{1}H NMR** (500 MHz, $CDCl_3$, mixture of rotamers/conformers) δ 7.34 – 7.27 (m, 1.42H), 7.25 – 7.10 (m, 2.47H), 7.04 (t, J = 7.5 Hz, 0.82H), 6.96 (t, J = 6.9 Hz, 0.45H), 6.52 (s, 1.13H), 5.56 (s, 0.88H), 5.49 – 5.33 (m, 1.49H), 5.25 – 5.16 (m, 2.13H), 4.94 (s, 0.77H), 4.75 (d, J = 13.9 Hz, 0.71H), 4.16 – 4.07 (m, 1.93H), 3.48 (d, J = 3.8 Hz, 3H), 3.45 – 3.37 (m, 1.45H), 3.12 (t, J = 12.7 Hz, 0.59H), 2.90 – 2.80 (m, 0.48H), 2.39 – 2.29 (m, 0.81H), 2.23 – 2.15 (m, 0.51H), 1.82 – 1.68 (m, 4.11H), 1.60 – 1.45 (m, 9.21H), 1.45 – 1.11 (m, 17.89H), 0.93 (d, J = 6.7 Hz, 9.57H), 0.87 (t, J = 7.0 Hz, 4.95H), 0.11 – 0.06 (m, 6H); **^{13}C NMR** (100 MHz, $CDCl_3$) δ 176.93, 170.95, 170.77, 168.84, 153.37, 152.84, 130.34, 128.13, 127.04, 125.65, 122.31, 114.92, 94.96, 75.69, 73.53, 58.07, 56.43, 56.32, 52.06, 45.55, 35.20, 34.05, 31.83, 30.43, 29.55, 29.31, 25.86, 25.43, 25.32, 24.19, 22.70, 21.39, 18.14, 14.20, -4.71, -5.12; **$[\alpha]^{25}_{D}$** +13.9 (c = 2.42 in $CHCl_3$); **IR** (film) 3480, 2928, 2857, 1732 (C=O), 1687 (C=O), 1634 (C=O), 1600, 1489, 1455, 1424, 1286, 1251, 1233, 1198, 1153, 1096, 1078, 1042, 991, 922, 836, 778, 755, 730, 668, 645; **HRMS** Accurate mass (ES+): Found 649.4264 (+2.3 ppm), $C_{35}H_{61}N_2O_7Si$ ($M+H^+$) requires 649.4249.

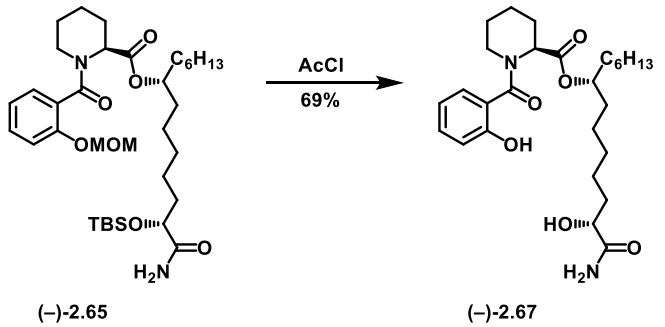

(1R,7R)-1-carbamoyl-1-hydroxytridecan-7-yl (2S)-1-(2-hydroxybenzoyl)piperidine-2- carboxylate (–)-2.67. To a solution of protected ester **(–)-2.65** (25 mg, 0.038 mmol) dissolved in MeOH (1 mL) was added acetyl chloride (5 μL, 0.006 mmol) at 0°C. The reaction was stirred at this temperature for 45 minutes then warmed to room temperature and stirred for 2 hours. The reaction was quenched with sat. $NaHCO_3$, and extracted with CH_2Cl_2 3x. The combined organic layers were washed with brine, dried over $MgSO_4$, filtered, concentrated, and purified by preparative TLC (100% EtOAc), yielding the title compound as a clear oil (12 mg, 69% yield). *Note: High temperature ^{1}H NMR was possible, but extended heating times caused decomposition.* **^{1}H NMR** (500 MHz, $CDCl_3$, 328K) δ 8.67 (br s, 0.39H), 8.54 (br s, 0.47H), 7.37 – 7.27 (m, 1H), 6.99 (d, J = 8.1 Hz, 1H), 6.87 (s, 1H), 5.21 (d, J = 34.3 Hz, 1H), 5.05 – 4.96 (m, 1H), 4.16 – 3.98 (m, 2H), 3.36 – 3.22 (m, 1H), 2.39 – 2.26 (m, 1H), 1.80 (d, J = 11.5 Hz, 3H), 1.60 (s, 10H), 1.30 (s, 15H), 0.90 (t, J = 6.6 Hz, 3H); **^{13}C NMR** (125 MHz, $CDCl_3$, room temp) δ 171.55, 171.12, 157.86, 132.52, 132.41, 130.70, 128.11, 128.03, 119.41, 119.26, 118.08, 118.01, 60.41, 34.83, 34.56, 34.46, 34.23, 34.10, 31.88, 29.86, 29.29, 29.24, 29.03, 28.80, 26.95, 26.79, 25.58, 25.54, 25.36, 25.21, 25.14, 24.80, 22.66, 21.38, 21.24, 14.33, 14.03; **$[\alpha]^{25}_D$** +21.5 (c = 1.3 in $CHCl_3$); **IR** (film) 3291 (br O-H), 2928, 2857, 1731 (C=O), 1692 (C=O), 1624 (C=O), 1454, 1373, 1207, 1142, 1007, 935, 911, 847, 827, 753, 645, 602; **HRMS** Accurate mass (ES^+): Found 491.3097 (-4.9 ppm) $C_{27}H_{43}N_2O_6$ ($M+H^+$) requires 491.3121.

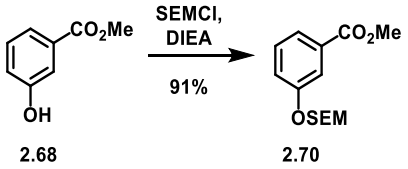

Methyl 3-((2-(trimethylsilyl)ethoxy)methoxy)benzoate 2.70. Using general procedure D, methyl 3-hydroxybenzoate **(2.68)** (250 mg, 1.640 mmol) yielded the title compound as a clear oil (421 mg, 91% yield). **^{1}H NMR** (500 MHz, $CDCl_3$) δ 7.71 – 7.66 (m, 2H), 7.34 (dd, J = 11.9, 4.2 Hz, 1H), 7.23 (ddd, J = 8.2, 2.6, 1.1 Hz, 1H), 5.26 (s, 2H), 3.91 (s, J = 2.9 Hz, 3H), 3.80 – 3.73 (m, 2H), 0.98 – 0.93 (m, 2H), -0.01 (s, J = 3.3 Hz, 9H); **^{13}C NMR** (125 MHz, $CDCl_3$) δ 166.58, 157.34, 131.42, 129.27, 122.79, 120.89, 116.93, 92.73, 77.16, 66.22, 51.93, 17.91, -1.51; **IR** (film) 2952, 2897, 1723 (C=O), 1586, 1488, 1447, 1380, 1274, 1248, 1211, 1153, 1106, 1083, 1009, 994, 918, 857, 833, 783, 755, 683; **HRMS** Accurate mass (ES^+): Found 305.1195 (+3.3 ppm), $C_{14}H_{22}O_4SiNa$ ($M+Na^+$) requires 305.1185.

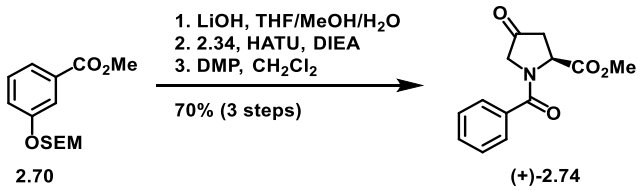

Methyl (S)-4-oxo-1-(3-((2-(trimethylsilyl)ethoxy)methoxy)benzoyl)pyrrolidine-2- carboxylate (+)-2.74. Using general procedure E, methyl ester **2.70** (264 mg, 0.934 mmol) yielded the corresponding acid, which was used directly in the next step. Using general procedure F, the acid yielded the corresponding acylhydroxyproline methyl ester compound, whose purity made it unsuitable for characterization. Using general procedure G, the alcohol intermediate yielded the title compound as a yellow oil (254 mg, 70% over 3 steps). **^{1}H NMR** (500 MHz, $CDCl_3$) δ 7.37 – 7.32 (m, 1H), 7.19 – 7.11 (m, 3H), 5.37 – 5.27 (m, 1H), 5.24 (s, 2H), 3.85 – 3.70 (m, 5H), 2.97 (dd, J = 18.8, 10.6 Hz, 1H), 2.70 (d, J = 20.3 Hz, 1H), 0.98 – 0.91 (m, 2H), -0.00 (s, J = 3.4 Hz, 9H); **^{13}C NMR** (100 MHz, $CDCl_3$) δ 207.21, 171.60, 170.18, 157.50, 136.18, 129.90, 120.19, 118.61, 114.92, 92.81, 66.44, 55.37, 52.90, 40.02, 18.04, -1.39; **$[\alpha]^{25}_{D}$** +25.3 (c = 0.91 in $CHCl_3$); **IR** (film) 2950, 2395, 2342, 1757 (C=O), 1635 (C=O), 1575 (C=O), 1445, 1393, 1296, 1264, 1250,

1228, 1186, 1151, 1122, 1078, 1030, 1008, 990, 950, 862, 833, 817, 774, 753, 694, 600, 562; **HRMS** Accurate mass (ES^+): Found 394.1700 (+3.6 ppm), $C_{19}H_{28}NO_6Si$ ($M+H^+$) requires 394.1686.

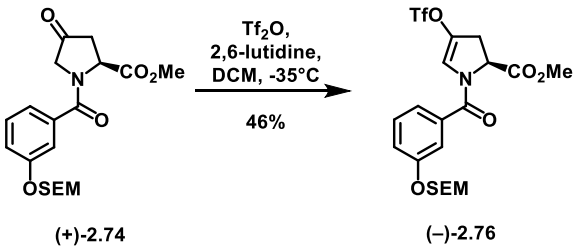

Methyl (S)-4-(((trifluoromethyl)sulfonyl)oxy)-1-(3-((2- (trimethylsilyl)ethoxy)methoxy) benzoyl)-2,3-dihydro-1H-pyrrole-2-carboxylate (–)-2.76. Using general procedure H, ketone **(+)-2.74** (150 mg, 0.388 mmol) yielded the title compound as an orange oil (95 mg, 46% yield). **^{1}H NMR** (500 MHz, $CDCl_3$) δ 7.37 (t, J = 7.9 Hz, 1H), 7.18 (dt, J = 24.8, 8.2 Hz, 3H), 6.81 (s, 1H), 5.24 (s, 2H), 5.08 (d, J = 6.5 Hz, 1H), 3.83 (s, 3H), 3.78 – 3.72 (m, 2H), 3.46 – 3.36 (m, 1H), 2.97 (ddd, J = 16.4, 4.8, 1.5 Hz, 1H), 0.99 – 0.92 (m, 2H), 0.00 (s, 9H); **^{13}C NMR** (125 MHz, $CDCl_3$) δ 169.70, 167.12, 159.69, 157.65, 144.29, 137.47, 134.65, 134.45, 130.04, 124.14, 123.29, 123.07, 120.90, 119.79, 119.45, 117.23, 115.61, 92.84, 66.56, 58.33, 57.60, 53.02, 33.18, 24.36, 18.09, -1.42; **$[\alpha]^{25}_D$** –56.4 (c = 0.45 in $CHCl_3$); **IR** (film) 2954, 2359, 2341, 1749 (C=O), 1652 (C=O), 1581 (C=O), 1488, 1427, 1398, 1207, 1137, 1086, 1005, 990, 917, 857, 832, 744, 693, 667, 605; **HRMS** Accurate mass (ES^+): Found 548.1028 (+5.5 ppm), $C_{20}H_{26}NO_8SSiNa$ ($M+Na^+$) requires 548.0998.

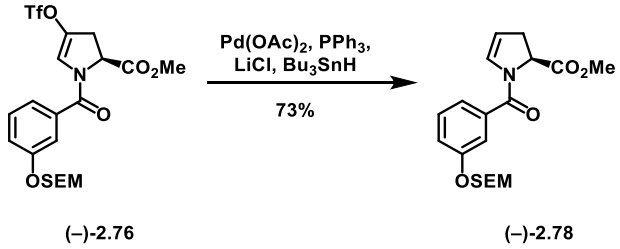

Methyl (S)-1-(3-((2-(trimethylsilyl)ethoxy)methoxy)benzoyl)-2,3-dihydro-1H-pyrrole-2- carboxylate (–)-2.78. Using general procedure I, triflate **(–)-2.76** (90 mg, 0.171 mmol) yielded the title compound as a yellow oil (47 mg, 73% yield). **^{1}H NMR** (500 MHz, $CDCl_3$) δ 7.33 (t, J = 7.9 Hz, 1H), 7.23 (s, 1H), 7.18

(d, J = 7.6 Hz, 1H), 7.14 (d, J = 8.4 Hz, 1H), 6.58 – 6.52 (m, 1H), 5.23 (s, 2H), 5.11 (d, J = 5.1 Hz, 1H), 5.01 (dd, J = 11.6, 5.0 Hz, 1H), 3.80 (s, 3H), 3.77 – 3.72 (m, 2H), 3.15 – 3.06 (m, 1H), 2.76 – 2.67 (m, 1H), 0.98 – 0.93 (m, 2H), 0.00 (s, 9H); **^{13}C NMR** (100 MHz, $CDCl_3$) δ 171.56, 166.75, 157.46, 136.25, 130.97, 129.71, 121.15, 118.65, 115.86, 109.05, 92.95, 66.49, 58.51, 52.64, 33.87, 18.14, -1.31; **$[\alpha]^{25}_D$** –44.0 (c = 0.31 in $CHCl_3$); **IR** (film) 2953, 2359, 2341, 1749 (C=O), 1646, 1617, 1488, 1446, 1398, 1362, 1317, 1086, 1005, 989, 858, 834, 694, 668; **HRMS** Accurate mass (ES^+): Found 378.1706 (-8.2 ppm), $C_{19}H_{28}NO_5Si$ ($M+H^+$) requires 378.1737.

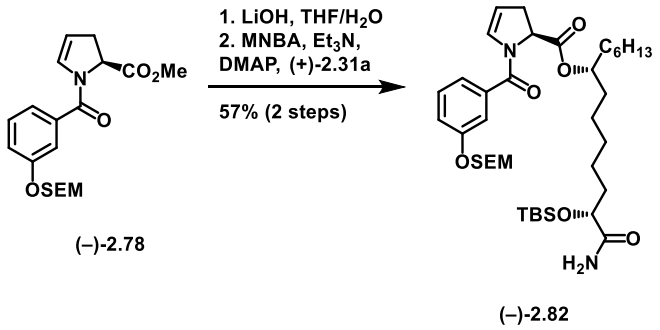

(7R,13R)-14-amino-13-((tert-butyldimethylsilyl)oxy)-14-oxotetradecan-7-yl (S)-1-(3-((2-(trimethylsilyl)ethoxy)methoxy)benzoyl)-2,3-dihydro-1H-pyrrole-2-carboxylate (–)-2.82. Using general procedure E, methyl ester **(–)-2.78** (26 mg, 0.069 mmol) yielded the acid intermediate as a yellow oil. This compound was not of sufficient purity for characterization. Next, using modified general procedure K (1.2 eq acid and MNBA), acid intermediate (25 mg, 0.069 mmol) yielded the title compound as a yellow oil (24 mg, 57% yield, 2 steps). **^{1}H NMR** (500 MHz, $CDCl_3$) δ 7.32 (q, J = 7.8 Hz, 1H), 7.20 (s, J = 11.1 Hz, 1H), 7.15 (dd, J = 15.5, 7.9 Hz, 2H), 6.52 (s, 2H), 5.54 – 5.44 (m, 1H), 5.23 (s, 2H), 5.08 (d, J = 1.9 Hz, 1H), 5.01 – 4.90 (m, 2H), 4.17 – 4.08 (m, 1H), 3.80 – 3.67 (m, 2H), 3.15 – 3.06 (m, 1H), 2.67 (d, J = 16.9 Hz, 1H), 1.81 – 1.70 (m, 1H), 1.69 – 1.47 (m, 7H), 1.26 (dd, J = 14.1, 6.9 Hz, 17H), 0.97 – 0.89 (m, 12H), 0.85 (t, J = 6.9 Hz, 3H), 0.10 – 0.06 (m, 6H), -0.01 (s, J = 3.2 Hz, 9H); **^{13}C NMR** (100 MHz, $CDCl_3$) δ 176.94, 170.86, 166.62, 157.49, 136.52, 131.08, 129.70, 121.13, 118.46, 115.85, 108.87, 92.97, 75.62, 73.60, 66.51, 58.80, 35.13, 34.05, 31.85, 29.85, 29.51, 29.32, 25.89, 25.31, 25.08, 24.11, 22.72, 18.17, 14.22, -1.28, -4.68, -5.12; **$[\alpha]^{25}_D$** –16.1 (c = 1.18 in $CHCl_3$); **IR (**film) 3480, 2927, 2867, 1739 (C=O), 1689

(C=O), 1651 (C=O), 1618, 1579, 1488, 1446, 1397, 1248, 1192, 1088, 1029, 1005, 991, 938, 857, 834, 778, 745, 694, 668; **HRMS** Accurate mass (ES^+): Found 719.4445 (-5.8 ppm), $C_{38}H_{67}N_2O_7Si_2$ ($M+H^+$) requires 719.4487.

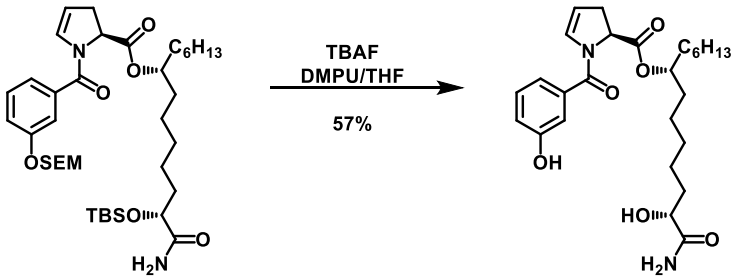

(7R,13R)-14-amino-13-hydroxy-14-oxotetradecan-7-yl (S)-1-(3-hydroxybenzoyl)-2,3- dihydro-1H-pyrrole-2-carboxylate (+)-2.84. Using general procedure L, silyl ether **(–)-2.82** (24 mg, 0.033 mmol) yielded the title compound as a clear oil (9 mg, 57% yield) after purification by column chromatography (50 → 100% EtOAc/hexanes). **^{1}H NMR** (400 MHz, $CDCl_3$) δ 7.22 (d, J = 7.8 Hz, 1H), 7.05 – 6.87 (m, 5H), 6.57 (s, 1H), 5.91 (s, 1H), 5.16 (s, 1H), 5.09 – 5.01 (m, 1H), 4.93 (dd, J = 11.4, 5.1 Hz, 1H), 4.12 – 4.02 (m, 1H), 3.18 – 3.07 (m, 1H), 2.67 (d, J = 17.3 Hz, 1H), 1.87 – 1.76 (m, 1H), 1.61 – 1.23 (m, 27H) 0.88 (t, J = 5.6 Hz, 3H); **^{13}C NMR** (100 MHz, $CDCl_3$) δ 178.78, 171.03, 167.83, 167.38, 157.46, 157.32, 135.46, 130.94, 129.78, 118.82, 115.06, 110.10, 75.42, 71.04, 58.70, 34.90, 34.43, 33.97, 33.75, 31.85, 29.84, 29.24, 27.91, 25.63, 24.83, 24.60, 22.70, 14.21; **$[\alpha]^{25}_D$** +14.4 (c = 0.90 in $CHCl_3$); **IR** (film) 3195 (br, O-H), 2925, 2856, 1732 (C=O), 1662 (C=O), 1579, 1416, 1273, 1196, 998, 880, 746; **HRMS** Accurate mass (ES^+): Found 475.2838 (+6.3 ppm), $C_{26}H_{39}N_2O_6$ ($M+H^+$) requires 475.2808

Methyl 4-((2-(trimethylsilyl)ethoxy)methoxy)benzoate 2.71. Using general procedure D, methyl 4-hydroxybenzoate **(2.69)** (250 mg, 1.640 mmol) yielded the title compound as a clear oil (454 mg, 98%

yield). **^{1}H NMR** (500 MHz, $CDCl_3$) δ 7.99 (dd, J = 8.9, 1.9 Hz, 2H), 7.05 (dd, J = 8.8, 1.9 Hz, 2H), 5.27 (s, J = 1.8 Hz, 2H), 3.89 (s, 3H), 3.78 – 3.73 (m, 2H), 0.95 (s, 2H), -0.01 (s, 9H); **^{13}C NMR** (125 MHz, $CDCl_3$) δ 166.96, 161.32, 131.63, 123.55, 115.75, 92.71, 66.73, 52.02, 18.17, -1.28, -1.31; **IR** (film) 2952, 2896, 1717 (C=O), 1605, 1580, 1510, 1435, 1381, 1315, 1276, 1234, 1191, 1168, 1090, 1013, 986, 938, 917, 851, 834, 770, 696, 668, 610; **HRMS** Accurate mass (ES^+): Found 283.1373 (+2.5 ppm), $C_{14}H_{23}O_4Si$ ($M+H^+$) requires 283.1366.

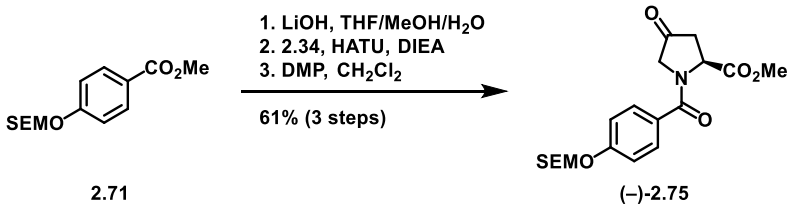

2.71 (–)-2.75

Methyl (2S)-4-oxo-1-(4-{[2-(trimethylsilyl)ethoxy]methoxy}benzoyl)pyrrolidine-2- carboxylate (–)-2.75. Using general procedure E, methyl ester **2.71** (445 mg, 1.577 mmol) yielded the corresponding acid, which was used directly in the next step. Using general procedure F, the acid yielded the corresponding acylhydroxyproline methyl ester compound, whose purity made it unsuitable for characterization. Using general procedure G, the alcohol intermediate yielded the title compound as a yellow oil (394 mg, 61% over 3 steps). **^{1}H NMR** (500 MHz, $CDCl_3$) δ 7.49 (br s, J = 12.1 Hz, 2H), 7.12 – 7.06 (m, 2H), 5.25 (s, 2H), 3.83 – 3.72 (m, 5H), 2.96 (dd, J = 18.8, 10.5 Hz, 1H), 2.69 (dd, J = 18.8, 2.2 Hz, 1H), 1.03 – 0.91 (m, 2H), - 0.00 (s, J = 3.3 Hz, 9H); **^{13}C NMR** (100 MHz, $CDCl_3$) δ 207.52, 207.36, 171.78, 171.05, 170.65, 159.54, 129.46, 129.22, 127.41, 125.35, 116.02, 115.53, 92.59, 66.57, 65.02, 52.91, 18.00, - 1.42; **$[\alpha]^{25}_D$** –24.2 (c = 1.39 in $CHCl_3$); **IR** (film) 2953, 1764 (C=O), 1745 (C=O), 1606 (C=O), 1513, 1404, 1230, 1168, 1090, 1025, 986, 918, 834, 764, 692, 612; **HRMS** Accurate mass (ES^+): Found 394.1698 (+3.0 ppm), $C_{19}H_{28}NO_6Si$ ($M+H^+$) requires 394.1686.

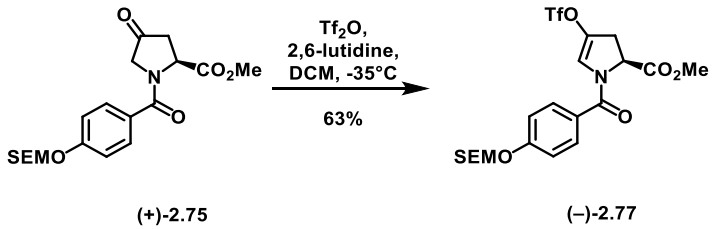

Methyl (2S)-4-(trifluoromethanesulfonyloxy)-1-(4-{[2- (trimethylsilyl)ethoxy]methoxy} benzoyl)-2,3-dihydro-1H-pyrrole-2-carboxylate (–)-2.77. Using general procedure H, ketone **(+)-2.75** (100 mg, 0.254 mmol) yielded the title compound as a yellow oil (85 mg, 63% yield). **^{1}H NMR** (400 MHz, $CDCl_3$) δ 7.52 (d, J = 8.7 Hz, 2H), 7.10 (d, J = 8.7 Hz, 2H), 6.87 (s, 1H), 5.27 (s, 2H), 5.08 (dd, J = 11.6, 5.1 Hz, 1H), 3.82 (s, 3H), 3.80 – 3.72 (m, 2H), 3.44 – 3.35 (m, 1H), 2.97 (ddd, J = 16.4, 5.1, 1.6 Hz, 1H), 1.00 – 0.91 (m, 2H), 0.00 (s, 9H); **^{13}C NMR** (125 MHz, $CDCl_3$) δ 169.86, 167.25, 160.10, 134.28, 129.89, 126.40, 123.58, 119.82, 117.26, 116.24, 92.72, 66.71, 57.83, 53.01, 33.25, 29.79, 18.12, -1.36; **$[\alpha]^{25}_{D}$** – 18.5 (c = 0.20 in 2:1 $CHCl_3$/MeOH); **IR** (film) 2954, 2899, 1750 (C=O), 1644, 1606, 1512, 1424, 1398, 1306, 1280, 1208, 1170, 1136, 1091, 1027, 987, 935, 910, 833, 759, 694, 644, 607; **HRMS** Accurate mass (ES^+): Found 526.1148 (-5.9 ppm), $C_{20}H_{27}F_3NO_8SSi$ ($M+H^+$) requires 526.1179.

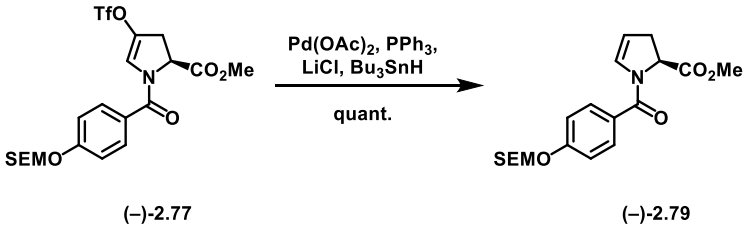

Methyl (2S)-1-(4-{[2-(trimethylsilyl)ethoxy]methoxy}benzoyl)-2,3-dihydro-1H-pyrrole-2-carboxylate (–)-2.79. Using general procedure I, triflate **(–)-2.77** (62 mg, 0.117 mmol) yielded the title compound as a yellow oil (47 mg, quant. yield). **^{1}H NMR** (400 MHz, $CDCl_3$) δ 7.53 (d, J = 8.5 Hz, 2H), 7.08 – 7.03 (m, 2H), 6.60 (s, 1H), 5.25 (s, 2H), 5.11 (s, 1H), 5.04 – 4.95 (m, 1H), 3.84 – 3.71 (m, 5H), 3.17 – 3.03 (m, 1H), 2.77 – 2.66 (m, 1H), 0.97 – 0.90 (m, 2H), -0.01 (s, J = 3.3 Hz, 9H); **^{13}C NMR** (125 MHz, $CDCl_3$) δ 171.72, 166.83, 159.49, 131.22, 129.91, 128.10, 115.94, 108.69, 92.76, 66.60, 58.70, 52.59, 33.82, 18.16, -1.31; **$[\alpha]^{25}_{D}$** –60.2 (c = 1.22 in MeOH); **IR** (film) 2952, 2924, 2872, 1749 (C=O), 1644 (C=O),

1606, 1574, 1511, 1396, 1362, 1291, 1231, 1201, 1170, 1089, 1023, 985, 917, 834, 759, 694, 582; **HRMS** Accurate mass (ES^+): Found 378.1710 (-7.1 ppm), $C_{19}H_{28}NO_5Si$ ($M+H^+$) requires 378.1737; $\mathbf{R_f}$ (3:1 hexanes:EtOAc) = 0.20.

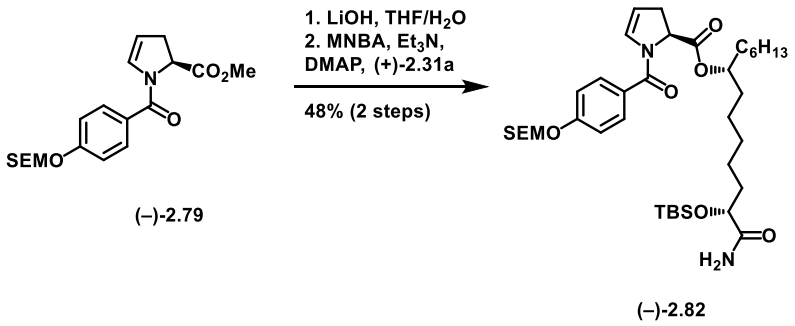

(1R,7R)-1-[(tert-butyldimethylsilyl)oxy]-1-carbamoyltridecan-7-yl (2S)-1-(4-{[2-(trimethylsilyl)ethoxy]methoxy}benzoyl)-2,3-dihydro-1H-pyrrole-2-carboxylate (–)-2.82. Using general procedure E, methyl ester **(–)-2.79** (22 mg, 0.055 mmol) was converted to the corresponding acid, which was not of sufficient purity for characterization. Next, using modified general procedure K (1.2 eq acid, 1.2 eq MNBA), the acid intermediate yielded the title compound as a yellow oil (19 mg, 48% yield). **^{1}H NMR** (500 MHz, $CDCl_3$) δ 7.52 (d, J = 8.6 Hz, 2H), 7.05 (d, J = 8.6 Hz, 2H), 6.60 – 6.51 (m, 2H), 5.45 (m, 2H), 5.25 (s, 2H), 5.09 (s, 1H), 5.01 – 4.89 (m, 2H), 4.88 – 4.81 (m, 1H), 4.15 – 4.12 (m, 2H), 3.78 – 3.72 (m, 2H), 3.14 – 3.06 (m, 1H), 2.71 – 2.64 (m, 1H), 1.80 – 1.70 (m, 1H), 1.69 – 1.65 (m, 1H), 1.61 – 1.47 (m, 7H), 1.40 – 1.17 (m, 27H), 0.91 (s, 9H), 0.86 (t, J = 8.0 Hz, 3H), 0.08 (d, J = 6.0 Hz, 6H), -0.00 (s, 9H); **^{13}C NMR** (125 MHz, $CDCl_3$) δ 176.97, 171.07, 166.70, 159.41, 131.32, 129.85, 128.40, 115.93, 108.50, 92.80, 75.56, 74.45, 73.60, 66.61, 58.98, 35.20, 35.15, 34.26, 34.18, 34.02, 31.84, 29.56, 29.51, 29.32, 25.88, 25.40, 25.33, 25.28, 25.07, 24.18, 24.12, 22.71, 21.42, 18.18, 14.20, -1.30, -4.69, -5.12; $\mathbf{[\alpha]^{25}_D}$ –16.8 (c = 0.95 in $CHCl_3$); **IR** (film) 2926, 2856, 1733 (C=O), 1688 (C=O), 1645 (C=O), 1607, 1510, 1463, 1396, 1248, 1195, 1169, 1089, 991, 939, 760, 713, 580; **HRMS** Accurate mass (ES^+): Found 719.4447 (-5.6 ppm), $C_{38}H_{67}N_2O_7Si_2$ ($M+H^+$) requires 719.4487.

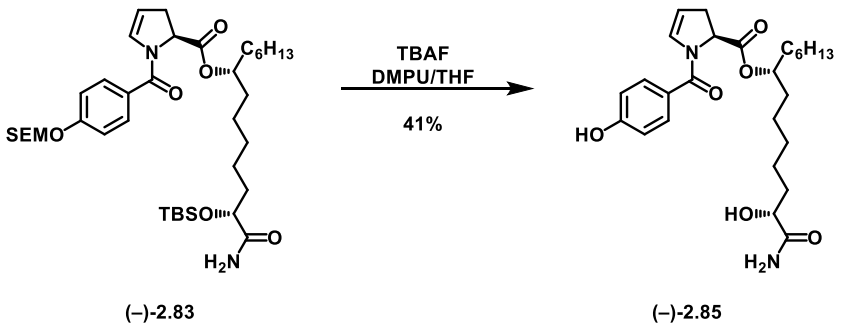

(1R,7R)-1-carbamoyl-1-hydroxytridecan-7-yl (2S)-1-(4-hydroxybenzoyl)-2,3-dihydro-1H-pyrrole-2-carboxylate (–)-2.85. Using general procedure L, silyl ether **(–)-2.83** (18.9 mg, 0.026 mmol) yielded the title compound as a clear oil (5.3 mg, 41% yield). **^{1}H NMR** (500 MHz, $CDCl_3$) δ 8.11 (s, 1H), 7.38 (d, J = 7.9 Hz, 2H), 6.94 (s, 1H), 6.79 (d, J = 8.1 Hz, 2H), 6.53 (d, J = 45.0 Hz, 1H), 5.63 (s, 1H), 5.17 (s, 1H), 4.96 (s, 2H), 4.03 (s, 2H), 3.18 – 3.09 (m, 1H), 2.69 (d, J = 16.8 Hz, 1H), 1.77 – 1.12 (m, 37H), 0.87 (t, J = 6.8 Hz, 3H); **^{13}C NMR** (125 MHz, $CDCl_3$) δ 171.12, 168.20, 159.37, 131.12, 129.98, 115.68, 109.85, 74.51, 70.77, 60.57, 58.82, 34.80, 34.27, 34.21, 34.06, 31.85, 29.85, 29.32, 29.25, 28.97, 27.62, 25.60, 25.45, 25.23, 24.78, 24.32, 22.70, 21.47, 14.34, 14.21; **$[\alpha]^{25}_D$** +17.9 (c = 0.24 in $CHCl_3$); **IR** (film) 3300 (br O-H), 2956, 2923, 2853, 2361, 2341, 2159, 2028, 1976, 1733, 1669, 1653, 1609, 1558, 1516, 1507, 1467, 1436, 1378, 1260, 1198, 1165, 1093, 1021, 948, 847, 798, 761, 721, 667; **HRMS** Accurate mass (ES^+): Found 475.2804 (-0.8 ppm), $C_{26}H_{39}N_2O_6$ ($M+H^+$) requires 475.2808.

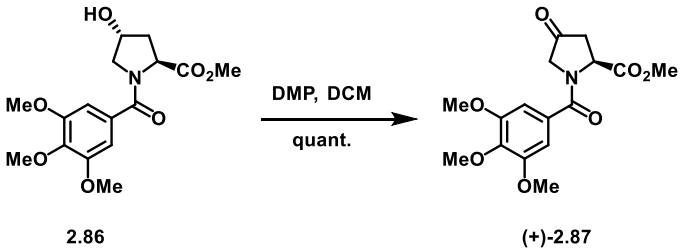

Methyl (2S)-4-oxo-1-(3,4,5-trimethoxybenzoyl)pyrrolidine-2-carboxylate (+)-2.87. Using general procedure G, alcohol **2.86** (1.340g, 3.950 mmol) yielded the title compound as a white foam (1.33g, quant. yield). **^{1}H NMR** (400 MHz, $CDCl_3$) δ 6.66 (s, 2H), 5.19 (br s, 1H), 3.97 (br s, 1H), 3.83 – 3.67 (m, 12H), 2.91 (dd, J = 18.8, 10.5 Hz, 1H), 2.59 (d, J = 18.6 Hz, 1H); **^{13}C NMR** (100 MHz, $CDCl_3$) δ 207.11, 171.59,

170.16, 153.24, 139.94, 129.95, 104.43, 77.36, 60.80, 56.19, 52.80; **[α]$^{25}_{D}$** +4.4 (c = 0.45 in 2:1 $CHCl_3$/MeOH); **IR** (film) 3451, 2953, 2360, 1728 (C=O), 1633 (C=O), 1580, 1506, 1448, 1414, 1324, 1238, 1179, 1119, 998, 922, 879, 840, 763, 723, 691, 603; **HRMS** Accurate mass (ES^+): Found 360.1072 (+3.6 ppm), $C_{16}H_{19}NO_7Na$ ($M+Na^+$) requires 360.1059.

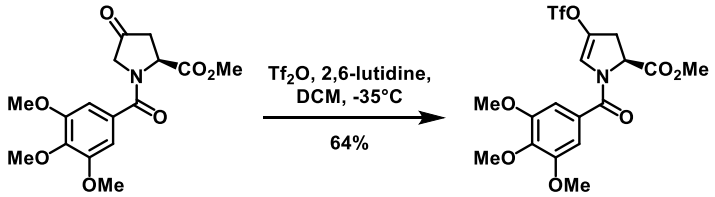

(+)-2.87 (+)-2.88

Methyl (2S)-4-(trifluoromethanesulfonyloxy)-1-(3,4,5-trimethoxybenzoyl)-2,3-dihydro-1H-pyrrole-2-carboxylate (+)-2.88. Using general procedure H, ketone **(+)-2.87** (145 mg, 0.431 mmol) yielded the title compound as an orange oil (129 mg, 64% yield). **^{1}H NMR** (500 MHz, $CDCl_3$) δ 6.90 (s, 1H), 6.75 (s, 2H), 5.10 – 5.00 (m, 1H), 3.88 – 3.78 (m, 12H), 3.40 (dd, J = 15.2, 13.1 Hz, 1H), 3.00 – 2.90 (m, 1H); **^{13}C NMR** (125 MHz, $CDCl_3$) δ 169.72, 167.22, 153.49, 140.84, 134.51, 128.35, 123.32, 105.35, 61.03, 56.37, 53.10; **[α]$^{25}_{D}$** +7.3 (c = 0.26 in $CHCl_3$); **IR** (film) 2953, 2359, 1745 (C=O), 1636 (C=O), 1582, 1413, 1326, 1234, 1120, 999, 924, 819, 760, 725, 637, 605; **HRMS** Accurate mass (ES^+): Found 470.0756 (+4.9 ppm), $C_{17}H_{19}F_3NO_9S$ ($M+H^+$) requires 470.0733.

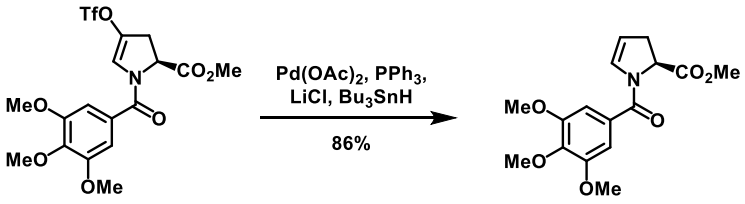

(+)-2.88 (–)-2.89

Methyl (2S)-1-(3,4,5-trimethoxybenzoyl)-2,3-dihydro-1H-pyrrole-2-carboxylate (–)-2.89. Using general procedure I, triflate **(+)-2.88** (110 mg, 0.234 mmol) yielded the title compound as a yellow oil (61 mg, 86% yield). **^{1}H NMR** (500 MHz, $CDCl_3$) δ 6.78 (s, 2H), 6.60 (s, 1H), 5.13 (s, 1H), 4.98 (dd, J = 11.2, 4.6 Hz, 1H), 3.91 – 3.76 (m, 12H), 3.16 – 3.07 (m, 1H), 2.71 (ddd, J = 17.0, 4.7, 2.3 Hz, 1H); **[α]$^{25}_{D}$** –48.3

(c = 0.40 in $CHCl_3$); **^{13}C NMR** (125 MHz, $CDCl_3$) δ 171.56, 166.79, 153.30, 140.20, 131.00, 130.21, 109.13, 105.39, 61.02, 58.61, 56.43, 52.65, 33.81; **IR** (film) 2997, 2950, 2832, 1751 (C=O), 1642 (C=O), 1619, 1582, 1506, 1462, 1404, 1361, 1315, 1235, 1196, 1177, 1143, 1119, 1000, 964, 895, 850, 810, 754, 734, 675, 570; **HRMS** Accurate mass (ES^+): Found 344.1087(-6.7 ppm), $C_{16}H_{19}NO_6Na$ ($M+Na^+$) requires 344.1110.

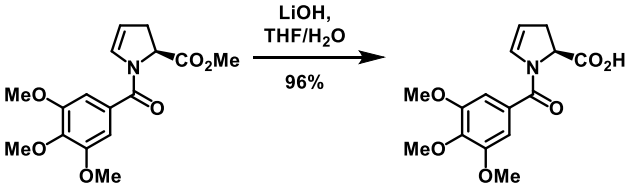

(–)-2.89 (–)-2.90

(2S)-1-(3,4,5-trimethoxybenzoyl)-2,3-dihydro-1H-pyrrole-2-carboxylic acid (–)-2.90. Using general procedure E, methyl ester **(–)-2.89** (55 mg, 0.180 mmol) yielded the title compound as a yellow oil (50 mg, 96% yield). **^{1}H NMR** (400 MHz, $CDCl_3$) δ 6.83 – 6.76 (m, 2H), 6.55 (s, 1H), 5.28 (d, J = 11.1 Hz, 1H), 5.06 (d, J = 6.1 Hz, 1H), 3.92 – 3.83 (m, 12H), 3.14 – 3.00 (m, 2H); **^{13}C NMR (**100 MHz, $CDCl_3$) δ 173.49, 167.90, 153.29, 140.45, 132.30, 132.20, 130.28, 129.39, 128.76, 128.64, 110.99, 105.54, 68.02, 61.02, 59.25, 56.42; **$[\alpha]^{25}_D$** –104.3 (c = 0.29 in $CHCl_3$); **IR** (film) 3269, 2954, 2899, 1747 (C=O), 1631 (C=O), 1605, 1467, 1425, 1363, 1311, 1208, 1136, 1028, 912, 833, 755, 693, 665, 605; **HRMS** Accurate mass (ES^+): Found 308.1148 (+4.5 ppm), $C_{15}H_{18}NO_6$ ($M+H^+$) requires 308.1134.

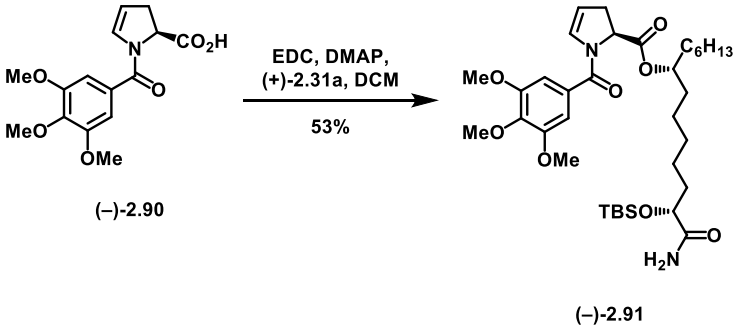

(–)-2.90 (–)-2.91

(1R,7R)-1-[(tert-butyldimethylsilyl)oxy]-1-carbamoyltridecan-7-yl (2S)-1-(3,4,5-trimethoxybenzoyl)-2,3-dihydro-1H-pyrrole-2-carboxylate (–)-2.91. Using general procedure J, acid **(–**

)-2.90 (26 mg, 0.085 mmol) yielded the title compound as a yellow oil (21 mg, 53% yield). **^{1}H NMR** (500 MHz, $CDCl_3$) δ 6.78 (s, 2H), 6.58 (s, 1H), 6.53 (d, J = 4.1 Hz, 1H), 5.47 (d, J = 4.1 Hz, 1H), 5.12 (s, 1H), 5.01 – 4.91 (m, 2H), 4.13 (t, J = 5.1 Hz, 1H), 3.87 (s, 9H), 3.16 – 3.06 (m, 1H), 2.68 (d, J = 16.5 Hz, 1H), 1.80 – 1.71 (m, 1H), 1.68 – 1.46 (m, 10H), 1.39 – 1.16 (m, 20H), 0.91 (s, J = 6.5 Hz, 9H), 0.86 (t, J = 7.0 Hz, 3H), 0.08 (d, J = 5.8 Hz, 6H); **^{13}C NMR** (100 MHz, $CDCl_3$) δ 177.02, 170.84, 166.66, 153.28, 140.01, 131.08, 130.50, 129.10, 108.95, 105.25, 75.67, 73.52, 61.03, 58.84, 56.39, 35.10, 34.01, 31.83, 29.49, 29.31, 25.85, 25.30, 25.03, 24.06, 22.69, 18.13, 14.18, -4.72, -5.15; **$[\alpha]^{25}_{D}$** –34.7 (c = 0.86 in $CHCl_3$); **IR** (film) 3480, 2927, 2856, 1738 (C=O), 1687 (C=O), 1645 (C=O), 1616, 1582, 1506, 1456, 1414, 1358, 1236, 1192, 1126, 1004, 951, 836, 810, 778, 720, 671; **HRMS** Accurate mass (ES^+): Found 663.4066 (+3.8 ppm), $C_{35}H_{59}N_2O_8Si$ ($M+H^+$) requires 663.4041.

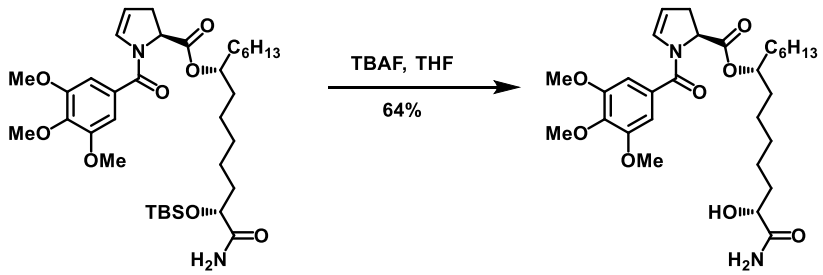

(–)-2.91 (–)-2.92

(1R,7R)-1-carbamoyl-1-hydroxytridecan-7-yl (2S)-1-(3,4,5-trimethoxybenzoyl)-2,3-dihydro- 1H-pyrrole-2-carboxylate (–)-2.92. To a solution of silyl ether **(–)-2.91** (12.5 mg, 0.0189 mmol) dissolved in THF (0.5 mL) was added TBAF (0.094 mL, 1M in THF, 0.094 mmol). After 20 minutes, the reaction was diluted with Et_2O, and washed with sat. NH_4Cl 4x, dried over Na_2SO_4, filtered, concentrated, and purified by preparative TLC (100% EtOAc), yielding the title compound as a clear oil (6.7 mg, 64% yield). **^{1}H NMR** (500 MHz, $CDCl_3$) δ 6.96 – 6.66 (t, J = 14.9 Hz, 2H), 6.57 (s, 1H), 5.20 (dd, J = 64.4, 27.8 Hz, 2H), 5.11 – 4.96 (m, 1H), 4.96 – 4.85 (m, 1H), 4.28 (d, J = 25.3 Hz, 1H), 4.05 (d, J = 39.2 Hz, 1H), 3.87 (s, J = 6.2 Hz, 9H), 3.13 (s, 1H), 2.69 (d, J = 16.0 Hz, 1H), 1.82 (s, 1H), 1.75 – 1.40 (m, 12H), 1.35 – 1.16 (m, 10H), 0.87 (s, J = 6.3 Hz, 3H); **^{13}C NMR** (125 MHz, $CDCl_3$) δ 177.45, 170.66, 167.47, 153.39, 140.28, 130.92, 129.85, 110.16, 109.95, 105.18, 75.30, 70.81, 61.09, 58.71, 56.48, 34.77, 34.04, 33.98, 33.81,

31.85, 29.25, 27.53, 25.59, 24.67, 24.28, 22.69, 14.20; **[α]$^{25}_{D}$** –32.4 (c = 0.67 in $CHCl_3$); **IR** (film) 3337 (br O-H), 2927, 2856, 1733 (C=O), 1668 (C=O), 1614 (C=O), 1581, 1506, 1414, 1318, 1236,1194, 1124, 1002, 951, 853, 810, 756, 722, 674**; HRMS** Accurate mass (ES^+): Found 549.3152 (-4.4 ppm), $C_{29}H_{45}N_2O_8$ ($M+H^+$) requires 283.1366.

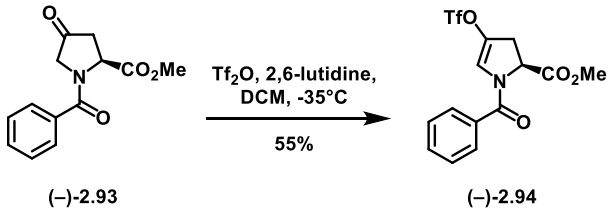

(–)-2.93 (–)-2.94

Methyl (2S)-1-benzoyl-4-(trifluoromethanesulfonyloxy)-2,3-dihydro-1H-pyrrole-2- carboxylate (–)-2.94. Using general procedure H, ketone **(–)-2.93**[2] (50 mg, 0.202 mmol) yielded the title compound as an orange oil (44 mg, 55% yield). **^{1}H NMR** (500 MHz, $CDCl_3$) δ 7.59 – 7.43 (m, 5H), 6.79 (s, 1H), 5.16 – 5.05 (m, 1H), 3.83 (s, 3H), 3.45 – 3.37 (m, 1H), 2.98 (ddd, J = 16.5, 4.9, 1.6 Hz, 1H); **^{13}C NMR** (100 MHz, $CDCl_3$) δ 169.78, 167.56, 134.52, 133.50, 131.67, 128.95, 127.93, 123.31, 120.14, 116.95, 77.16, 57.65, 53.12, 33.26; **[α]$^{25}_{D}$** –47.6 (c = 1.49 in $CHCl_3$); **IR** (film) 2957, 2921, 2851, 2361, 2160, 2031, 1979, 1749 (C=O), 1648 (C=O), 1578, 1495, 1448, 1426, 1404, 1306, 1208, 1135, 1029, 937, 909, 843, 752, 721, 702, 669; **HRMS** Accurate mass (ES^+): Found 402.0244 (+2.2 ppm), $C_{14}H_{12}F_3NO_6SNa$ ($M+Na^+$) requires 402.0235.

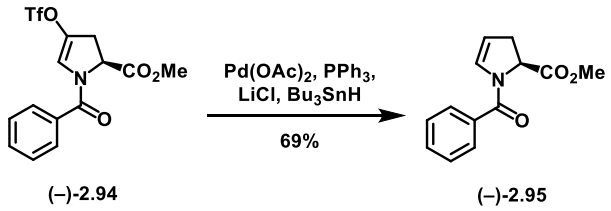

(–)-2.94 (–)-2.95

Methyl (2S)-1-benzoyl-2,3-dihydro-1H-pyrrole-2-carboxylate (–)-2.95. Using general procedure I, triflate **(–)-2.94** (100 mg, 0.252 mmol) yielded the title compound as a yellow oil (40 mg, 69% yield). **^{1}H NMR** (500 MHz, $CDCl_3$) δ 7.57 (d, J = 7.3 Hz, 2H), 7.50 – 7.37 (m, 3H), 6.53 (s, 1H), 5.12 (s, 1H), 5.02 (dd, J = 11.5, 5.0 Hz, 1H), 3.81 (s, 3H), 3.15 – 3.07 (m, 1H), 2.72 (d, J = 16.9 Hz, 1H); **^{13}C NMR** (125

MHz, $CDCl_3$) δ 171.6, 167.2, 135.1, 131.0, 130.9, 128.6, 128.0, 109.1, 58.5, 52.7, 33.9; **[α]$^{25}_D$** –110.8 (c = 1.00 in $CHCl_3$); **IR** (film) 2953, 2923, 2160, 2029, 1979, 1747 (C=O), 1641, 1615, 1576, 1496, 1447, 1403, 1362, 1290, 1201, 1179, 1106, 1016, 936, 841, 790, 724, 700, 662; **HRMS** Accurate mass (ES^+): Found 254.0813 (+7.9 ppm), $C_{13}H_{13}NO_3Na$ ($M+Na^+$) requires 254.0793.

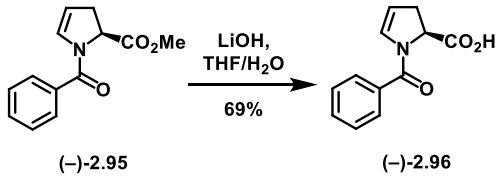

(2S)-1-benzoyl-2,3-dihydro-1H-pyrrole-2-carboxylic acid (–)-2.96. Using general procedure E, methyl ester **(–)-2.95** (37 mg, 0.160 mmol) yielded the title compound as a yellow oil (24 mg, 69% yield). **^{1}H NMR** (500 MHz, $CDCl_3$) δ 7.61 – 7.43 (m, 5H), 6.47 (s, 1H), 5.30 (s, 1H), 5.12 (d, J = 7.5 Hz, 1H), 3.19 (d, J = 17.1 Hz, 1H), 3.10 – 3.02 (m, 1H); **^{13}C NMR** (100 MHz, $CDCl_3$) δ 173.24, 168.67, 131.41, 130.06, 128.71, 128.56, 128.23, 111.50, 59.52, 32.97, 29.83; **[α]$^{25}_D$** –85.3 (c = 1.20 in $CHCl_3$); **IR** (film) 3061 (br, CO_2-H), 2953, 2924, 2918, 1716 (C=O), 1596 (C=O), 1573, 1497, 1448, 1408, 1352, 1315, 1289, 1195, 1106, 1017, 941, 846, 787, 753, 719, 700, 660; **HRMS** Accurate mass (ES^+): Found 218.0825 (+3.2 ppm), $C_{12}H_{12}NO_3$ ($M+H^+$) requires 218.0818.

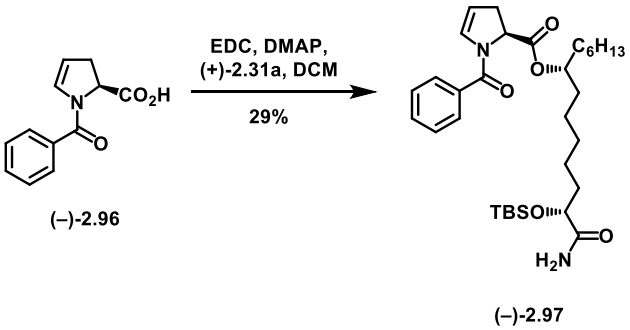

(1R,7R)-1-[(tert-butyldimethylsilyl)oxy]-1-carbamoyltridecan-7-yl (2S)-1-benzoyl-2,3- dihydro-1H-pyrrole-2-carboxylate (–)-2.97. Using modified general procedure J (1.2 eq acid, 1.5 eq EDC, 1.0 eq alcohol, 0.5 eq DMAP), acid **(–)-2.96** (24 mg, 0.111 mmol) after purification by preparative TLC (2:1 CH_2Cl_2:Et_2O), yielded the title compound as a clear oil (15 mg, 29% yield). **^{1}H NMR** (500 MHz, $CDCl_3$)

δ 7.57 (d, J = 7.5 Hz, 2H), 7.45 (dt, J = 14.5, 7.1 Hz, 3H), 6.53 (s, 2H), 5.58 (s, 1H), 5.02 (dd, J = 11.5, 4.7 Hz, 1H), 4.98 – 4.94 (m, 1H), 3.18 – 3.08 (m, 1H), 2.70 (d, J = 17.1 Hz, 1H), 1.85 – 1.16 (m, 10H), 0.92 (s, 9H), 0.87 (t, J = 6.6 Hz, 3H), 0.10 (s, 3H), 0.09 (s, 3H); **^{13}C NMR** (100 MHz, $CDCl_3$) δ 177.0, 170.9, 167.0, 135.3, 131.1, 130.7, 128.6, 127.9, 108.9, 75.6, 73.6, 58.8, 35.1, 34.0, 31.8, 29.8, 29.5, 29.3, 25.9, 25.3, 25.1, 24.1, 22.7, 18.2, 14.2, -4.7, -5.1; **$[\alpha]^{25}_{D}$** –38.6 (c = 1.43 in $CHCl_3$); **IR** (film) 3480, 2927, 2856, 1738 (C=O), 1688 (C=O), 1645 (C=O), 1618, 1577, 1463, 1495, 1402, 1360, 1253, 1195, 1100, 1004, 940, 836, 779, 723, 699, 666; **HRMS** Accurate mass (ES^+): Found 573.3695 (-5.1 ppm), $C_{32}H_{53}N_2O_5Si$ ($M+H^+$) requires 573.3724; **R_f** (2:1 CH_2Cl_2:Et_2O) = 0.70.

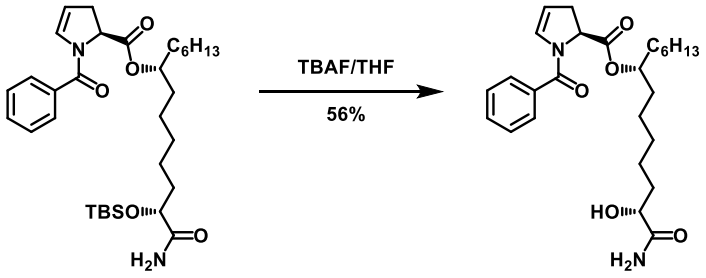

(1R,7R)-1-carbamoyl-1-hydroxytridecan-7-yl (2S)-1-benzoyl-2,3-dihydro-1H-pyrrole-2- carboxylate (–)-14. To a solution of silyl ether **(–)-S38** (14 mg, 0.025 mmol) dissolved in THF (0.5 mL) was added TBAF (0.25 mL, 1M in THF, 0.250 mmol) at room temperature. After 5 minutes, the reaction was quenched with 1M aq. NH4Cl and extracted with Et2O 3x. The combined organic layers were washed with brine, dried over Na2SO4, filtered, concentrated, and purified by preparative TLC (2% MeOH/EtOAc), yielding the title compound as a clear oil (6.4 mg, 56% yield). **1H NMR** (500 MHz, CDCl3) δ 7.61 – 7.36 (m, 5H), 6.95 (s, 0.16H), 6.91 (s, 0.45H), 6.83 (s, 0.67H), 6.52 – 6.47 (m, 1H), 5.47 (s, 0.37H), 5.27 (s, 1H), 5.16 (d, J = 4.0 Hz, 1H), 5.08 – 5.02 (m, 1H), 5.02 – 4.94 (m, 1H), 4.35 (s, 0.55H), 4.14 – 3.99 (m, 1H), 3.18 – 3.08 (m, 1H), 2.76 – 2.66 (m, 1H), 1.87 – 1.79 (m, 1H), 1.77 – 1.48 (m, 11H), 1.48 – 1.16 (m, 22H), 0.87 (t, J = 6.8 Hz, 3H); **13C NMR** (125 MHz, CDCl3) δ 177.59, 170.92, 170.62, 167.88, 167.49, 134.93, 134.69, 131.09, 130.80, 128.81, 128.76, 127.78, 127.69, 110.01, 109.84, 75.54, 75.24, 70.64, 59.14, 58.60, 34.84, 34.53, 34.39, 34.15, 34.02, 33.78, 33.61, 31.85, 29.84, 29.25, 27.73, 27.49, 25.60, 25.31, 24.68, 24.50,

24.24, 24.00, 22.70, 14.20; **[α]25D** –5.3 (c = 0.62 in CHCl3); **IR** (film) 3325 (br, O-H), 2925, 2856, 2360, 1733 (C=O), 1668 (C=O), 1615 (C=O), 1576, 1496, 1448, 1406, 1197, 1153, 1082, 1017, 1001, 944, 844, 788, 724, 699, 660; **HRMS** Accurate mass (ES+): Found 481.2650 (-5.8 ppm), C26H38N2O5Na (M+Na+) requires 481.2678; **Rf** (2% MeOH/EtOAc) = 0.50.

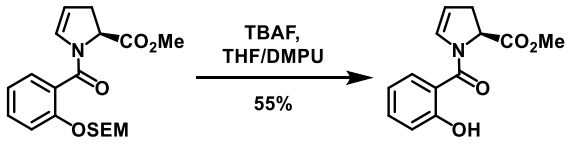

(–)-2.39 (–)-2.99

Methyl (2S)-1-(2-hydroxybenzoyl)-2,3-dihydro-1H-pyrrole-2-carboxylate (–)-2.99. Using modified procedure L (10 eq TBAF, 0.10 M DMPU), SEM-ether **(–)-2.39** (23 mg, 0.061 mmol) yielded the title compound as a clear oil (8.2 mg, 55% yield). **^{1}H NMR** (500 MHz, $CDCl_3$) δ 9.80 (s, 1H), 7.43 (dd, J = 7.8, 1.5 Hz, 1H), 7.41 – 7.35 (m, 1H), 7.01 (dd, J = 8.3, 0.8 Hz, 1H), 6.89 (td, J = 7.8, 1.1 Hz, 1H), 6.83 (s, 1H), 5.28 (dt, J = 4.4, 2.7 Hz, 1H), 5.04 (dd, J = 11.3, 5.2 Hz, 1H), 3.80 (s, 3H), 3.11 (ddt, J = 16.4, 11.3, 2.4 Hz, 1H), 2.73 (ddt, J = 17.1, 5.0, 2.5 Hz, 1H); **^{13}C NMR** (100 MHz, $CDCl_3$) δ 171.45, 167.75, 159.36, 133.70, 130.99, 128.49, 118.98, 118.15, 110.85, 77.16, 59.29, 52.85, 33.49, 29.83. **$[\alpha]^{25}_{D}$** –104.5 (c = 1.00 in $CHCl_3$); **IR** (film) 3119 (br, O-H), 2954, 2918, 2850, 2360, 2341, 2160, 2031, 1979, 1746 (C=O), 1616, 1590 (C=O), 1487, 1434, 1362, 1295, 1250, 1202, 1179, 1153, 1098, 1017, 984, 944, 855, 817, 757, 721, 667; **HRMS** Accurate mass (ES^+): Found 270.0751 (+3.3 ppm), $C_{13}H_{13}NO_4Na$ ($M+Na^+$) requires 270.0742.

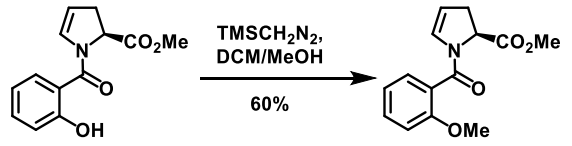

(–)-2.99 (–)-2.100

Methyl (2S)-1-(2-methoxybenzoyl)-2,3-dihydro-1H-pyrrole-2-carboxylate (–)-S21. To a solution of phenol **(–)-2.99** (45 mg, 0.182 mmol) in 3:1 CH_2Cl_2:MeOH (2 mL) was added $TMSCHN_2$ (0.46 mL, 2M in hexanes, 0.920 mmol), and the reaction went from a clear to yellow color, with effervescence. After 2 hours, TLC analysis indicated remaining starting material, and more MeOH (0.5 mL) was added, after

another 30 minutes the starting material was consumed. The reaction was concentrated and purified by column chromatography, yielding the title compound as a yellow oil (28 mg, 60% yield). **^{1}H NMR** (500 MHz, $CDCl_3$) δ 7.41 – 7.34 (m, 2H), 7.00 (t, J = 7.5 Hz, 1H), 6.94 (d, J = 8.3 Hz, 1H), 6.17 – 6.13 (m, 1H), 5.07 – 5.00 (m, 2H), 3.84 (s, 3H), 3.81 (s, 3H), 3.16 – 3.07 (m, 1H), 2.75 – 2.67 (m, 1H); **^{13}C NMR** (100 MHz, $CDCl_3$) δ 171.61, 165.22, 155.94, 131.42, 130.91, 129.11, 124.94, 120.92, 111.44, 108.60, 57.88, 55.90, 52.59, 34.17; **$[\alpha]^{25}_{D}$** –85.9 (c = 1.27 in $CHCl_3$); **IR** (film) 2951, 2923, 2851, 2160, 2032, 1979, 1746 (C=O), 1643 (C=O), 1618, 1600, 1491, 1461, 1436, 1406, 1363, 1280, 1249, 1201, 1179, 1103, 1046, 1016, 843, 754, 654; **HRMS** Accurate mass (ES^+): Found 284.0875 (-8.4 ppm), $C_{14}H_{15}NO_4Na$ ($M+Na^+$) requires 284.0899.

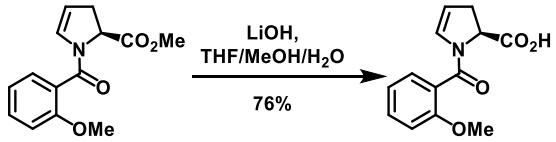

(–)-2.100 (–)-2.101

(2S)-1-(2-methoxybenzoyl)-2,3-dihydro-1H-pyrrole-2-carboxylic acid (–)-2.100. Using general procedure B, methyl ester **(–)-2.101** (27 mg, 0.103 mmol) yielded the title compound as a yellow oil (19 mg, 76% yield). **^{1}H NMR** (500 MHz, $CDCl_3$) δ 8.03 (s, 1H), 7.46 – 7.41 (m, 1H), 7.38 (d, J = 7.5 Hz, 1H), 7.03 (t, J = 7.5 Hz, 1H), 6.96 (d, J = 8.4 Hz, 1H), 6.06 (dt, J = 4.3, 2.2 Hz, 1H), 5.23 (dd, J = 4.3, 2.4 Hz, 1H), 5.13 (dd, J = 11.0, 4.2 Hz, 1H), 3.84 (s, 3H), 3.19 (d, J = 17.1 Hz, 1H), 3.09 – 3.00 (m, 1H); **^{13}C NMR** (125 MHz, $CDCl_3$) δ 172.39, 167.64, 155.96, 132.16, 129.76, 129.23, 123.82, 121.07, 111.58, 111.51, 59.25, 55.89, 32.89, 29.82; **$[\alpha]^{25}_{D}$** –82.1 (c = 1.80 in $CHCl_3$); **IR** (film) 3444 (br, CO_2-H), 2930, 1738 (C=O), 1598 (C=O), 1492, 1464, 1437, 1412, 1356, 1282, 1249, 1185, 1163, 1104, 1047, 1018, 941, 848, 754, 723, 652; **HRMS** Accurate mass (ES^+): Found 270.0721 (-7.8 ppm), $C_{13}H_{13}NO_4Na$ ($M+Na^+$) requires 270.0742.

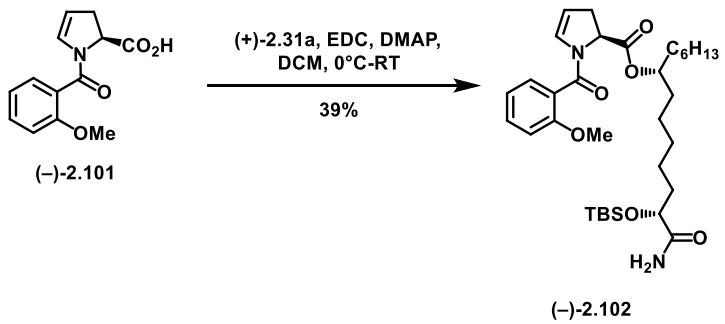

(1R,7R)-1-[(tert-butyldimethylsilyl)oxy]-1-carbamoyltridecan-7-yl (2S)-1-(2- methoxybenzoyl)-2,3-dihydro-1H-pyrrole-2-carboxylate (–)-2.102. Using modified general procedure J (1.2 eq acid, 1.5 eq EDC, 1.0 eq alcohol, 0.1 eq DMAP), acid **(–)-2.101** (18 mg, 0.073 mmol), after purification by column chromatography eluting with 0 → 2% MeOH/CH_2Cl_2, yielded the title compound as a clear oil (14 mg, 39% yield). **^{1}H NMR** (500 MHz, $CDCl_3$) δ 7.40 – 7.31 (m, 2H), 7.17 (d, J = 7.2 Hz, 1H), 6.99 (s, 1H), 6.93 (d, J = 8.2 Hz, 1H), 6.54 (s, 1H), 6.14 (dd, J = 4.1, 1.9 Hz, 1H), 5.71 – 5.59 (m, 1H), 5.05 – 4.95 (m, 2H), 4.17 – 4.06 (m, 2H), 3.83 (s, 3H), 3.12 (ddd, J = 14.1, 11.6, 2.0 Hz, 1H), 2.91 – 2.85 (m, 1H), 2.66 (ddd, J = 17.1, 4.3, 2.1 Hz, 1H), 1.76 – 1.54 (m, 6H), 1.39 – 1.19 (m, 20H), 0.91 (s, 9H), 0.89 – 0.83 (m, 3H), 0.08 (d, J = 6.2 Hz, 6H); **^{13}C NMR** (100 MHz, $CDCl_3$) δ 177.11, 170.92, 165.02, 155.98, 131.32, 131.01, 129.17, 129.11, 127.43, 125.11, 120.89, 111.42, 108.46, 75.50, 73.55, 69.78, 58.23, 55.86, 53.93, 41.65, 35.11, 34.39, 34.08, 34.02, 31.85, 29.83, 29.51, 29.33, 25.87, 25.31, 25.05, 24.11, 22.72, 18.15, 14.21, -4.70, -5.13; **$[\alpha]^{25}_D$** –27.2 (c = 1.11 in $CHCl_3$); **IR** (film) 3481, 2927, 2856, 1745, 1683, 1646, 1619, 1601, 1491, 1463, 1437, 1406, 1360, 1280, 1251, 1194, 1101, 1048, 1019, 939, 837, 778, 754, 701, 655; **HRMS** Accurate mass (ES^+): Found 603.3802 (-4.5 ppm), $C_{33}H_{55}N_2O_6Si$ ($M+H^+$) requires 603.3829; **R_f** (2:1 CH_2Cl_2:Et_2O) = 0.60.

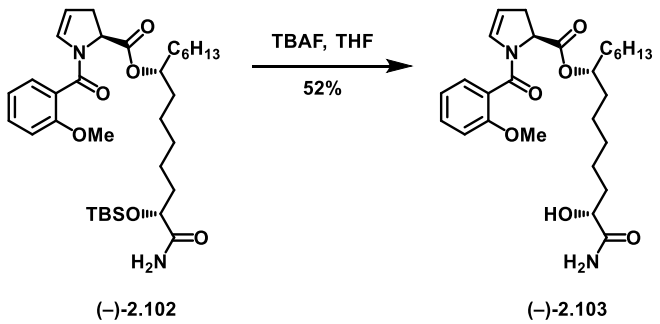

(1R,7R)-1-carbamoyl-1-hydroxytridecan-7-yl (2S)-1-(2-methoxybenzoyl)-2,3-dihydro-1H-pyrrole-2-carboxylate (–)-2.103. To a solution of protected ester **(–)-2.102** (11 mg, 0.018 mmol) dissolved in THF (0.5 mL) was added TBAF (0.18 mL, 1M in THF, 0.180 mmol). After 5 minutes the reaction was poured into 1M aq. NH_4Cl and extracted with Et_2O 3x. The combined organic layers were washed with brine, dried over Na_2SO_4, filtered, concentrated and purified by preparative TLC (2% MeOH/EtOAc), yielding the title compound as a clear oil (4.6 mg, 52% yield). **^{1}H NMR** (500 MHz, $CDCl_3$) δ 7.43 – 7.38 (m, 1H), 7.33 (d, J = 7.3 Hz, 1H), 7.00 (t, J = 7.5 Hz, 1H), 6.97 – 6.91 (m, 2H), 6.19 – 6.12 (m, 1H), 5.15 – 5.02 (m, 3H), 4.95 (dd, J = 11.6, 4.8 Hz, 1H), 4.43 (s, 1H), 4.06 (d, J = 4.4 Hz, 1H), 3.83 (s, 3H), 3.18 – 3.09 (m, 1H), 2.68 (ddd, J = 14.7, 4.5, 2.2 Hz, 1H), 1.87 – 1.77 (m, 1H), 1.69 – 1.35 (m, 17H), 1.35 – 1.16 (m, 21H), 0.88 (t, J = 6.8 Hz, 4H); **^{13}C NMR** (100 MHz, $CDCl_3$) δ 177.75, 170.61, 165.90, 155.96, 131.80, 130.74, 128.96, 124.24, 120.99, 111.52, 109.73, 74.99, 70.35, 58.07, 55.92, 34.99, 34.27, 33.52, 31.86, 29.85, 29.26, 27.29, 25.65, 24.65, 24.22, 22.71, 14.22; **$[\alpha]^{25}_D$** –8.9 (c = 0.45 in $CHCl_3$); **IR** (film) 2920, 2850, 1740 (C=O), 1668 (C=O), 1618 (C=O), 1492, 1463, 1439, 1412, 1377, 1280, 1253, 1196, 1102, 1047, 1021, 847, 803, 755, 720; **HRMS** Accurate mass (ES^+): Found 489.2941 (- 4.9 ppm), $C_{27}H_{41}N_2O_6$ ($M+H^+$) requires 489.2965; **R_f** (2% MeOH/EtOAc) = 0.45.

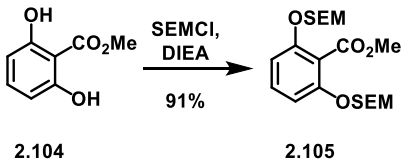

2.104 2.105

Methyl 2,6-bis((2-(trimethylsilyl)ethoxy)methoxy)benzoate 2.105. Using modified general procedure D (double equivalents of SEMCl and DIEA, and 0.1 eq tetrabutylammonium iodide), 2,6-dihydroxy methyl benzoate (563 mg, 3.348 mmol) yielded the title compound as a yellow oil (1.308g, 91% yield). **^{1}H NMR** (500 MHz, $CDCl_3$) δ 7.24 (t, J = 8.4 Hz, 1H), 6.82 (d, J = 8.4 Hz, 2H), 5.21 (s, 4H), 3.90 (s, J = 2.6 Hz, 3H), 3.76 – 3.71 (m, 4H), 0.96 – 0.92 (m, 4H), 0.01 – -0.02 (m, 18H); **^{13}C NMR** (125 MHz, $CDCl_3$) δ 166.89, 155.07, 130.98, 115.47, 108.36, 93.22, 66.55, 52.41, 18.12, -1.30; **IR** (film) 2951, 2897, 2359, 2341, 1738 (C=O), 1599, 1469, 1272, 1245, 1145, 1111, 1038, 936, 917, 895, 856, 831, 757, 692, 667, 609**;** **HRMS** Accurate mass (ES^+): Found 451.1915 (-7.3 ppm), $C_{20}H_{36}O_6Si_2Na$ ($M+Na^+$) requires 451.1948; **R_f** (7:1 hexanes:EtOAc) = 0.34.

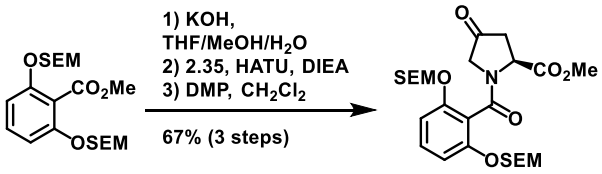

2.105 (–)-2.106

Methyl (S)-1-(2,6-bis((2-(trimethylsilyl)ethoxy)methoxy)benzoyl)-4-oxopyrrolidine-2- carboxylate (–)-2.106. Methyl ester **2.105** (1.283g, 2.993 mmol) was dissolved in 9:1:1 MeOH:THF:H_2O (11 mL), and KOH (1.914g, 34.117 mmol) was added as a solid. The reaction was heated to reflux (80 °C) overnight. The following day, the reaction was cooled to room temperature, acidified (pH 5-6) with 5% aq. AcOH, and extracted with CH_2Cl_2 3x. The combined organic layers were washed with brine, dried over $MgSO_4$, filtered and concentrated. The crude acid was unstable and used directly in the next step. Using general procedure F, the acid yielded the corresponding acylhydroxyproline methyl ester compound, whose purity made it unsuitable for characterization. Using general procedure G, the alcohol intermediate yielded the title compound as a yellow oil (1.075g, 67% over 3 steps). **^{1}H NMR** (500 MHz, $CDCl_3$, mixture of

rotamers/conformers) δ 7.29 – 7.24 (m, 1H), 6.86 (tt, J = 7.4, 4.3 Hz, 2H), 5.32 – 5.15 (m, 4.56H), 5.11 (t, J = 5.8 Hz, 0.35H), 4.64 – 4.59 (m, 0.33H), 4.43 (d, J = 19.7 Hz, 0.34H), 4.07 – 4.03 (m, 0.18H), 4.03 – 3.99 (m, 0.16), 3.93 – 3.90 (m, 0.30), 3.90 – 3.86 (m, 0.41H), 3.82 – 3.66 (m, 6.48H), 3.63 – 3.59 (m, 0.83H), 3.03 – 2.93 (m, 0.73H), 2.90 – 2.82 (m, 0.38H), 2.72 – 2.62 (m, 0.73H), 2.57 (d, J = 18.1 Hz, 0.35H), 0.98 – 0.88 (m, 4H), 0.05 – -0.06 (m, 18H); **^{13}C NMR** (125 MHz, $CDCl_3$) δ 207.70, 170.94, 165.99, 154.92, 154.16, 131.50, 131.17, 116.27, 109.11, 108.75, 108.54, 108.23, 93.81, 93.63, 93.47, 93.31, 66.84, 66.73, 66.68, 57.33, 54.73, 52.69, 52.55, 51.82, 41.95, 40.69, 18.10, 14.31, -1.27, -1.30, -1.31; **$[\alpha]^{25}_D$** –1.8 (c = 1.41 in CHCl3); **IR** (film) 2952, 2896, 1765 (C=O), 1747 (C=O), 1658 (C=O), 1596, 1467, 1404, 1245, 1177, 1142, 1094, 1035, 918, 893, 856, 832, 790, 751, 693, 664; **HRMS** Accurate mass (ES^+): Found 562.2232 (-6.4 ppm), $C_{25}H_{41}NO_8Si_2Na$ ($M+Na^+$) requires 562.2268; **R_f** (3:1 hexanes:EtOAc) = 0.25.

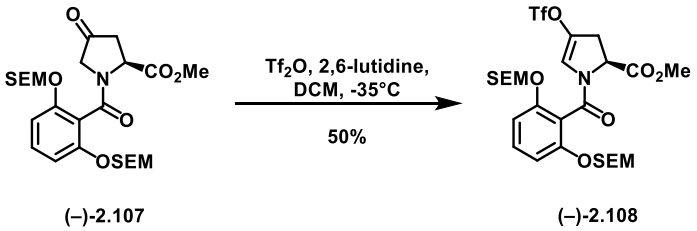

(–)-2.107 (–)-2.108

Methyl (S)-1-(2,6-bis((2-(trimethylsilyl)ethoxy)methoxy)benzoyl)-4-(((trifluoromethyl)sulfonyl)oxy)-2,3-dihydro-1H-pyrrole-2-carboxylate (–)-2.108. Using general procedure I, ketone **(–)-2.107** (238 mg, 0.440 mmol) yielded the title compound as an orange oil (149 mg, 50% yield). **^{1}H NMR** (400 MHz, $CDCl_3$) δ 7.37 – 7.28 (m, 1H), 6.87 (t, J = 8.2 Hz, 2H), 6.35 (s, 1H), 5.28 – 5.16 (m, 4H), 5.10 (dd, J = 11.8, 5.0 Hz, 1H), 3.82 (s, 3H), 3.74 (dt, J = 21.8, 8.0 Hz, 4H), 3.45 – 3.34 (m, 1H), 2.95 (dd, J = 16.5, 4.9 Hz, 1H), 0.93 (dd, J = 16.0, 7.7 Hz, 4H), -0.01 (s, J = 7.4 Hz, 18H); **^{13}C NMR** (125 MHz, $CDCl_3$) δ 169.52, 163.25, 155.19, 133.94, 131.84, 123.14, 114.23, 108.67, 108.37, 93.48, 93.16, 66.69, 66.64, 56.77, 52.81, 33.66, 18.04, -1.34, -1.38; **$[\alpha]^{25}_D$** –41.3 (c = 1.04 in $CHCl_3$); **IR** (film) 3269, 2954, 2899, 1747 (C=O), 1605 (C=O), 1425, 1363, 1311, 1208, 1136, 1028, 912, 833, 755, 693, 605; **HRMS** Accurate mass (ES^+): Found 694.1727 (-4.9 ppm), $C_{26}H_{40}F_3NO_{10}SSi_2Na$ (M+Na+) requires 694.1761; **R_f** (3:1 hexanes:EtOAc) = 0.48.

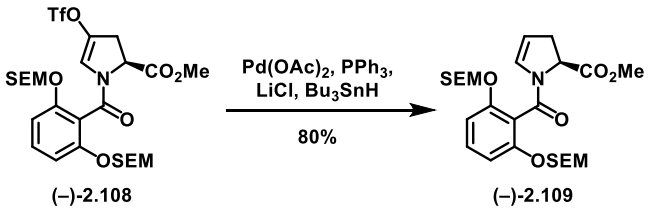

Methyl (S)-1-(2,6-bis((2-(trimethylsilyl)ethoxy)methoxy)benzoyl)-2,3-dihydro-1H-pyrrole-2-carboxylate (–)-2.109. Using general procedure I, triflate **(–)-2.108** (130 mg, 0.194 mmol) yielded the title compound as a yellow oil (82 mg, 80% yield). **^{1}H NMR** (500 MHz, $CDCl_3$) δ 7.25 – 7.20 (m, 1H), 6.83 (dt, J = 12.5, 6.2 Hz, 2H), 6.11 (dt, J = 4.4, 2.2 Hz, 1H), 5.29 (d, J = 7.1 Hz, 1H), 5.24 – 5.13 (m, 3H), 5.01 (ddd, J = 8.3, 6.9, 3.8 Hz, 2H), 3.86 – 3.64 (m, 7H), 3.12 (ddt, J = 16.7, 11.6, 2.3 Hz, 1H), 2.74 – 2.68 (m, 1H), 0.99 – 0.87 (m, 4H), 0.02 – -0.06 (m, 18H); **^{13}C NMR** (100 MHz, $CDCl_3$) δ 171.27, 162.64, 154.96, 154.81, 130.92, 130.58, 115.96, 108.57, 108.29, 108.10, 93.02, 92.96, 66.43, 57.50, 52.35, 34.42, 18.05, -1.36; **$[\alpha]^{25}_D$** –55.9 (c = 1.49 in $CHCl_3$); **IR** (film) 2952, 2921, 2899, 1744 (C=O), 1656 (C=O), 1620, 1596, 1468, 1404, 1245, 1199, 1178, 1151, 1094, 1038, 917, 895, 857, 832, 741, 694, 608; **HRMS** Accurate mass (ES^+): Found 546.2288 (-5.7 ppm), $C_{25}H_{41}NO_7Si_2Na$ ($M+Na^+$) requires 546.2319.

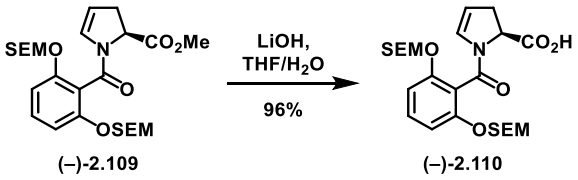

(S)-1-(2,6-bis((2-(trimethylsilyl)ethoxy)methoxy)benzoyl)-2,3-dihydro-1H-pyrrole-2- carboxylic acid (–)-2.110. Using general procedure E, methyl ester **(–)-2.109** (73 mg, 0.139 mmol) yielded the title compound as a yellow oil (68 mg, 96% yield). **^{1}H NMR** (400 MHz, $CDCl_3$) δ 7.31 (t, J = 8.4 Hz, 1H), 6.85 (dd, J = 8.5, 0.8 Hz, 2H), 6.02 (dt, J = 4.4, 2.2 Hz, 1H), 5.28 – 5.16 (m, 6H), 3.74 – 3.67 (m, 4H), 3.48 – 3.40 (m, 1H), 2.98 (ddt, J = 17.4, 11.0, 2.5 Hz, 1H), 0.95 – 0.89 (m, 4H), -0.01 (d, J = 1.7 Hz, 18H); **^{13}C NMR** (100 MHz, $CDCl_3$) δ 171.36, 166.43, 154.97, 154.62, 131.84, 129.07, 114.45, 112.17, 108.27, 107.97, 93.08, 92.94, 77.36, 66.75, 66.67, 59.24, 32.64, 30.43, 29.81, 18.10, -1.30, -1.33; **$[\alpha]^{25}_D$** –66.4 (c = 1.38 in $CHCl_3$); **IR** (film) 2952, 2924, 2896, 1748 (C=O), 1652 (C=O), 1619, 1595, 1468, 1405, 1245,

1183, 1150, 1093, 1039, 832, 738, 693, 664; **HRMS** Accurate mass (ES^+): Found 532.2130 (-6.2 ppm), $C_{24}H_{39}NO_7Si_2Na$ ($M+Na^+$) requires 532.2163.

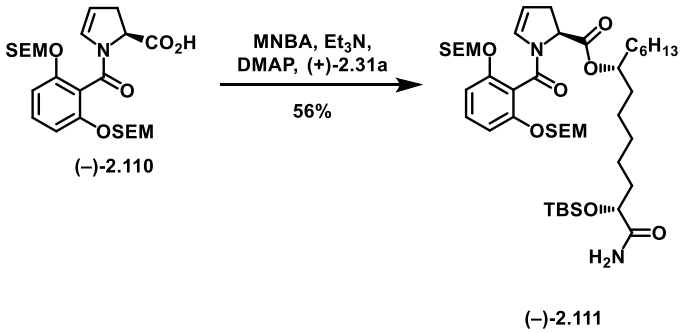

(7R,13R)-14-amino-13-((tert-butyldimethylsilyl)oxy)-14-oxotetradecan-7-yl (S)-1-(2,6- bis((2-(trimethylsilyl)ethoxy)methoxy)benzoyl)-2,3-dihydro-1H-pyrrole-2-carboxylate (–)- 2.111. Using general procedure K, acid **(–)-2.110** (81 mg, 0.158 mmol) yielded the title compound as a yellow oil (55 mg, 56% yield). **^{1}H NMR** (500 MHz, $CDCl_3$) δ 7.23 (d, J = 8.4 Hz, 1H), 6.92 – 6.75 (m, 2H), 6.57 – 6.48 (m, 1H), 6.10 (dt, J = 4.2, 2.0 Hz, 1H), 5.46 – 5.35 (m, 1H), 5.30 – 5.12 (m, 5H), 4.98 (dt, J = 8.7, 5.3 Hz, 2H), 4.13 (t, J = 5.1 Hz, 1H), 3.83 – 3.64 (m, 4H), 3.17 – 3.07 (m, 1H), 2.70 – 2.62 (m, 1H), 1.81 – 1.70 (m, 1H), 1.70 – 1.62 (m, 1H), 1.43 – 1.17 (m, 16H), 0.98 – 0.89 (m, 12H), 0.87 (t, J = 6.3 Hz, 3H), 0.14 – 0.04 (m, 6H), 0.03 – -0.06 (m, 18H); **^{13}C NMR** (125 MHz, $CDCl_3$) δ 177.02, 170.41, 162.48, 155.04, 154.97, 130.87, 130.79, 116.20, 108.76, 108.22, 108.10, 93.11, 93.03, 75.01, 73.54, 66.43, 57.85, 35.10, 34.67, 34.07, 34.02, 31.85, 29.48, 29.30, 25.85, 25.28, 25.06, 24.11, 22.68, 18.16, 18.10, 14.17, -1.30, -4.73, -5.15; **$[\alpha]^{25}_D$** –25.4 (c = 1.27 in $CHCl_3$); **IR** (film) 2927, 2857, 1749 (C=O), 1689 (C=O), 1657 (C=O), 1621, 1596, 1467, 1404, 1247, 1188, 1151, 1095, 1040, 937, 896, 833, 778, 751, 694, 665, 580, 554; **HRMS** Accurate mass (ES^+): Found 865.5290 (+4.6 ppm), $C_{44}H_{81}N_2O_9Si_3$ ($M+H^+$) requires 865.5250; **R_f** (4:1 CH_2Cl_2:Et_2O) = 0.67.

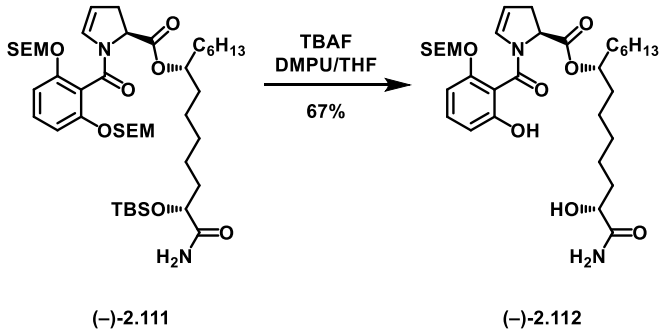

(–)-2.111 (–)-2.112

(7R,13R)-14-amino-13-hydroxy-14-oxotetradecan-7-yl (S)-1-(2-hydroxy-6-((2-(trimethylsilyl)ethoxy)methoxy)benzoyl)-2,3-dihydro-1H-pyrrole-2-carboxylate (–)-2.112. Using general procedure L, compound **(–)-2.111** (37 mg, 0.043 mmol) yielded the title compound, after purification by preparative TLC (4% MeOH/EtOAc), as a yellow oil (18 mg, 67% yield). **^{1}H NMR** (400 MHz, $CDCl_3$) δ 8.13 – 7.89 (m, 1H), 7.22 (t, J = 8.3 Hz, 1H), 6.81 (s, 1H), 6.71 (t, J = 7.2 Hz, 1H), 6.62 (d, J = 8.3 Hz, 1H), 6.31 – 6.25 (m, 1H), 5.33 – 5.02 (m, 6H), 4.14 – 3.99 (m, 2H), 3.77 – 3.68 (m, 2H), 3.23 – 3.10 (m, 1H), 2.70 (d, J = 17.5 Hz, 1H), 1.86 – 1.74 (m, 1H), 1.73 – 1.15 (m, 22H), 0.99 – 0.81 (m, 5H), -0.01 (d, J = 2.9 Hz, 9H); **^{13}C NMR** (125 MHz, $CDCl_3$) δ 177.79, 172.11, 164.33, 155.46, 154.76, 132.20, 130.96, 130.57, 111.63, 110.73, 110.27, 106.20, 93.42, 76.45, 70.80, 66.78, 58.28, 34.75, 34.29, 34.13, 33.84, 31.81, 29.17, 27.77, 25.59, 24.78, 24.40, 22.66, 18.13, 14.18, -1.29; **$[\alpha]^{25}_{D}$** –1.7 (c = 0.93 in $CHCl_3$); **IR** (film) 3338 (br, O-H), 2927, 2858, 1748 (C=O), 1661, 1616, 1601, 1466, 1432, 1378, 1292, 1247, 1193, 1153, 1102, 1038, 941, 835, 792, 721; **HRMS** Accurate mass (ES^+): Found 643.3417 (+4.0 ppm), $C_{32}H_{52}N_2O_8SiNa$ ($M+Na^+$) requires 643.3391.

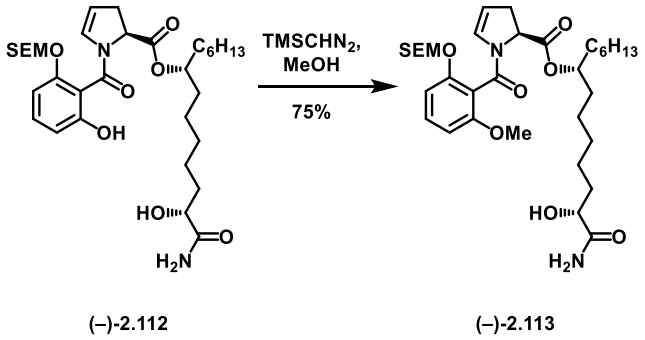

(–)-2.112 (–)-2.113

(7R,13R)-14-amino-13-hydroxy-14-oxotetradecan-7-yl (S)-1-(2-methoxy-6-((2-(trimethylsilyl)ethoxy)methoxy)benzoyl)-2,3-dihydro-1H-pyrrole-2-carboxylate (–)-2.113. To a solution of compound **(–)-2.112** (19 mg, 0.031 mmol) in MeOH (1 mL) was added $TMSCHN_2$ (0.070 mL, 2M in hexanes, 0.140 mmol). The reaction was stirred overnight at room temperature, over which time the reaction turned from yellow to clear. The reaction was concentrated and purified by preparative TLC (5% MeOH/EtOAc), yielding the title compound as a yellow oil (15 mg, 75% yield). **^{1}H NMR** (500 MHz, $CDCl_3$, mixture of rotamers/conformers) δ 8.00 (dd, J = 8.3, 1.3 Hz, 1H), 7.61 – 7.56 (m, 0.39H), 7.45 (t, J = 7.8 Hz, 1H), 7.28 (td, J = 8.0, 1.9 Hz, 1H), 6.97 (d, J = 26.7 Hz, 1H), 6.78 (dd, J = 8.2, 6.7 Hz, 1H), 6.58 (dd, J = 8.3, 2.7 Hz, 1H), 6.43 (s, 0.37H), 6.10 (ddq, J = 12.7, 6.4, 2.2 Hz, 1H), 5.32 – 5.03 (m, 5H), 4.98 – 4.88 (m, 2H), 4.26 (dd, J = 7.0, 3.2 Hz, 0.38H), 4.16 – 4.11 (m, 0.42H), 4.06 (d, J = 6.6 Hz, 0.62H), 3.84 – 3.80 (m, 1.84H), 3.80 – 3.76 (m, 2.25H), 3.75 – 3.66 (m, 1.59H), 3.18 – 3.08 (m, 1H), 2.74 – 2.63 (m, 1H), 1.89 – 1.68 (m, 2H), 1.68 – 1.37 (m, 12H), 1.36 – 1.14 (m, 24H), 0.98 – 0.77 (m, 9H), -0.02 (d, J = 5.9 Hz, 9H); **^{13}C NMR** (100 MHz, $CDCl_3$) δ 178.21, 178.09, 170.41, 170.07, 165.15, 163.64, 157.65, 157.10, 155.01, 154.80, 133.70, 131.56, 131.47, 130.53, 129.95, 128.63, 113.96, 113.59, 109.58, 107.87, 107.12, 104.95, 104.55, 101.07, 93.07, 92.78, 82.51, 79.60, 77.16, 74.43, 74.34, 70.81, 70.12, 69.95, 66.72, 66.65, 63.15, 57.71, 56.30, 56.06, 35.11, 34.57, 34.35, 33.50, 32.06, 31.87, 29.84, 29.50, 29.29, 27.22, 27.04, 26.15, 25.66, 24.80, 24.63, 24.23, 24.15, 22.83, 22.71, 18.15, 18.10, 14.22, -1.28; **$[\alpha]^{25}_D$** –19.8 (c = 1.72 in $CHCl_3$); **IR** (film) 3329 (br, O-H), 2924, 2854, 1721, 1658, 1619, 1595, 1472, 1409, 1379, 1291, 1247, 1190, 1107, 1073, 1002, 951, 898, 858, 835, 789, 716; 668, 604; **HRMS** Accurate mass (ES^+): Found 657.3570 (+3.5 ppm), $C_{33}H_{54}N_2O_8SiNa$ ($M+Na^+$) requires 657.3547.

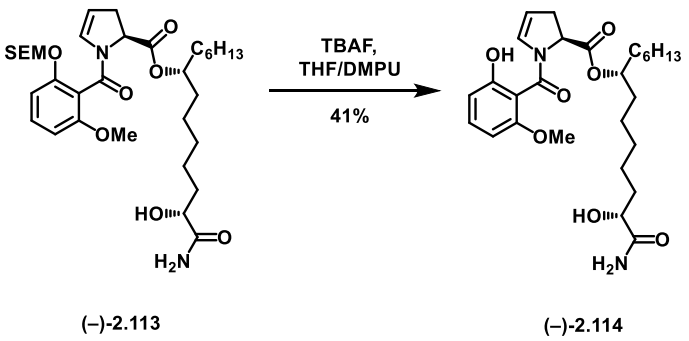

(–)-2.113 (–)-2.114

(7R,13R)-14-amino-13-hydroxy-14-oxotetradecan-7-yl (S)-1-(2-hydroxy-6- methoxybenzoyl)-2,3-dihydro-1H-pyrrole-2-carboxylate (–)-2.114. Using modified general procedure L (10 eq TBAF, 0.1M DMPU), silyl ether **(–)-2.113** (17 mg, 0.027 mmol) after purification by column chromatography (0 → 3% MeOH/CH_2Cl_2), yielded the title compound as a clear oil (5.6 mg, 41% yield). **^{1}H NMR** (500 MHz, $CDCl_3$) δ 7.98 (s, 1H), 7.28 – 7.23 (m, 1H), 6.83 (s, 1H), 6.60 (dd, J = 8.3, 4.8 Hz, 1H), 6.47 (t, J = 8.7 Hz, 1H), 6.25 (dt, J = 4.4, 2.2 Hz, 1H), 5.19 (dt, J = 4.6, 2.4 Hz, 1H), 5.14 – 5.04 (m, 2H), 4.60 (d, J = 5.9 Hz, 1H), 4.08 – 4.00 (m, 1H), 3.83 – 3.79 (m, 3H), 3.21 – 3.12 (m, 1H), 2.69 (d, J = 18.6 Hz, 1H), 1.84 – 1.74 (m, 1H), 1.71 – 1.19 (m, 22H), 0.88 (t, J = 6.9 Hz, 3H); **^{13}C NMR** (125 MHz, $CDCl_3$) δ 177.47, 176.57, 172.39, 172.24, 164.48, 164.39, 157.00, 155.68, 132.38, 130.55, 110.52, 110.44, 110.14, 110.10, 102.72, 102.63, 76.66, 76.46, 70.77, 70.70, 64.51, 58.37, 58.33, 56.07, 56.02, 34.79, 34.35, 34.21, 34.07, 33.81, 33.58, 31.83, 29.84, 29.18, 27.72, 27.53, 25.63, 24.75, 24.69, 24.33, 24.14, 22.68, 14.20; **$[\alpha]^{25}_D$** –10.5 (c = 0.56 in $CHCl_3$); **IR** (film) 3307 (br, O-H), 2926, 2856, 1733 (C=O), 1653, 1592, 1470, 1435, 1250, 1194, 1088, 1016, 947, 847, 791, 720, 601; **HRMS** Accurate mass (ES^+): Found 527.2751 (+3.4 ppm), $C_{27}H_{40}N_2O_7Na$ ($M+Na^+$) requires 527.2733.

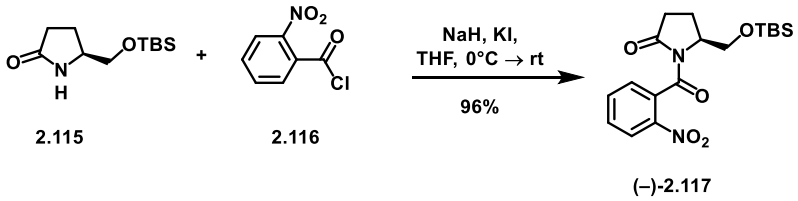

2.115 2.116 (–)-2.117

(S)-5-(((tert-butyldimethylsilyl)oxy)methyl)-1-(2-nitrobenzoyl)pyrrolidin-2-one (–)-2.117. To a suspension of NaH (60% in mineral oil, 74 mg, 1.852 mmol) and KI (307 mg, 1.852 mmol) in THF (4 mL)

at 0°C was added a solution of (S)-5-(((tert-butyldimethylsilyl)oxy)methyl)pyrrolidin- 2-one **(2.115)** (386 mg, 1.683 mmol) dropwise in THF (2 mL). The solution was allowed to warm to room temperature and stir for 90 minutes. Then 2-nitrobenzoyl chloride **(2.116)** (0.27 mL, 2.020 mmol) was added as a solution in THF (2 mL). After 10 minutes, the reaction was quenched with sat. NH_4Cl (10 mL) and extracted 3x with EtOAc. The combined organic layers were washed 2x with sat. Na_2CO_3, water, and brine, dried over $MgSO_4$, filtered, concentrated, and filtered through a plug of silica gel, which was washed with 3:1 hexanes:EtOAc. The filtrate was concentrated then triturated with MeOH, yielding the title compound as a white solid (609 mg, 96% yield). **^{1}H NMR** (500 MHz, $CDCl_3$) δ 8.23 (dd, J = 8.3, 0.9 Hz, 1H), 7.71 (td, J = 7.5, 1.2 Hz, 1H), 7.58 (ddd, J = 8.3, 7.5, 1.4 Hz, 1H), 7.32 (dt, J = 6.7, 3.4 Hz, 1H), 4.69 – 4.62 (m, 1H), 4.14 (dd, J = 10.4, 3.7 Hz, 1H), 3.85 (d, J = 10.6 Hz, 1H), 2.75 (dt, J = 17.8, 10.3 Hz, 1H), 2.36 (ddd, J = 17.8, 9.8, 2.0 Hz, 1H), 2.21 (ddd, J = 34.5, 22.6, 11.4 Hz, 2H), 0.90 (s, 9H), 0.11 (s, 3H), 0.11 (s, 3H); **^{13}C NMR** (125 MHz, $CDCl_3$) δ 175.70, 166.50, 145.21, 134.37, 133.47, 129.94, 127.72, 124.17, 63.52, 58.18, 32.27, 25.94, 21.33, 18.29, -5.39, -5.50; **$[\alpha]^{25}_D$** –76.1 (c = 0.77 in $CHCl^3$); **IR** (film) 2925, 2891, 2853, 1743 (C=O), 1668 (C=O), 1533, 1471, 1353, 1319, 1264, 1226, 1193, 1104, 1087, 1028, 1005, 986, 967, 872, 837, 776, 744, 703, 640, 560;; **HRMS** Accurate mass (ES^+): Found 401.1536 (+6.7 ppm), $C_{18}H_{26}N2O_5SiNa$ ($M+Na^+$) requires 401.1509; **MP** 121.5 – 124.0°C.

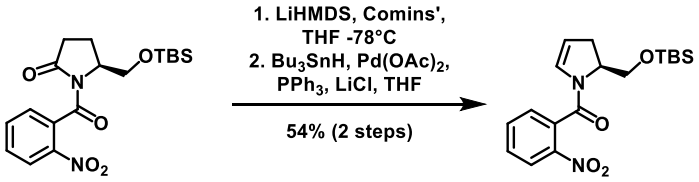

(–)-2.117 (–)-2.118

(S)-(2-(((tert-butyldimethylsilyl)oxy)methyl)-2,3-dihydro-1H-pyrrol-1-yl)(2- nitrophenyl)methanone (–)-2.118. LiHMDS (1M in THF, 2.83 mL, 2.83 mmol) was diluted with THF (12 mL) and cooled to -78°C. A solution of compound **(–)-2.117** (713 mg, 1.884 mmol) was added dropwise as a solution in THF (6 mL), and the reaction turned a deep purple color. After 1 hour, Comins' reagent (1.849g, 4.710 mmol) was added dropwise as a solution in THF (5 mL), and the reaction was stirred for 2 hours at -78°C, quenched with sat.

NH_4Cl, warmed to room temperature, and extracted 3x with EtOAc. The combined organic layers were washed with sat $NaHCO_3$ and brine, then purified by column chromatography [triflate R_f (4:1 hexanes:EtOAc) = 0.49], which yielded the triflate intermediate as a yellow oil, which was highly unstable (decomposed overnight in a freezer). The triflate was immediately taken up in THF (15 mL) and to the resulting solution was added LiCl (240 mg, 5.651 mmol), $Pd(OAc)_2$ (42 mg, 0.188 mmol), PPh_3 (148 mg, 0.565 mmol), and Bu_3SnH (0.40 mL, 1.484 mmol) dropwise; during addition of the stannane the solution turned from a yellow suspension to a clear orange/brown solution. After 10 minutes, the reaction was quenched with aqueous 1M KF and extracted 3x with EtOAc. The combined organic layers were washed with aqueous 1M KF, water, and brine, dried over $MgSO_4$, filtered, concentrated, and purified by column chromatography, yielding the title compound as a yellow solid (366 mg, 54% over two steps). **^{1}H NMR** (500 MHz, $CDCl_3$) δ 8.20 (dd, J = 8.3, 1.0 Hz, 1H), 7.72 (td, J = 7.5, 1.2 Hz, 1H), 7.63 – 7.57 (m, 1H), 7.45 (dd, J = 7.6, 1.4 Hz, 1H), 5.87 – 5.83 (m, 1H), 5.15 – 5.10 (m, 1H), 4.70 (qd, J = 7.1, 3.7 Hz, 1H), 4.09 – 3.95 (m, 1H), 3.90 – 3.80 (m, 1H), 2.86 (ddt, J = 12.3, 9.9, 2.6 Hz, 1H), 2.73 (ddd, J = 17.0, 5.0, 3.3 Hz, 1H), 0.91 (s, J = 2.8 Hz, 9H), 0.11 (s, 3H), 0.10 (s, 3H); **^{13}C NMR** (125 MHz, $CDCl_3$) δ 163.35, 145.47, 134.47, 132.51, 130.27, 128.78, 128.71, 124.75, 112.36, 58.64, 32.34, 25.86, 18.23, -5.31, -5.32; **$[\alpha]^{25}_D$** – 144.6 (c = 0.81 in $CHCl_3$); **IR** (film) 2952, 2929, 2856, 1633 (C=O), 1615, 1571, 1528, 1480, 1471, 1422, 1388, 1345, 1286, 1248, 1205, 1179, 1104, 1077, 1060, 1006, 969,941, 832, 775, 763, 740, 723, 701, 687, 666, 642, 607; **HRMS** Accurate mass (ES^+): Found 363.1754 (+3.9 ppm), $C_{18}H_{27}N_2O_4Si$ ($M+H^+$) requires 363.1740. **MP** 90.1 – 94.7°C.

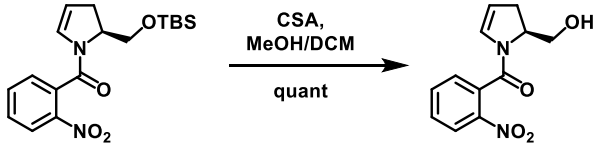

(–)-2.118 (–)-2.119

(S)-(2-(hydroxymethyl)-2,3-dihydro-1H-pyrrol-1-yl)(2-nitrophenyl)methanone (–)-2.119. To a solution of compound **(–)-2.118** (285 mg, 0.786 mmol) in 1:1 MeOH:CH_2Cl_2 (8 mL) was added CSA (183 mg, 0.7862 mmol). The reaction was stirred for 1 hour at rt then quenched with sat. $NaHCO_3$ and extracted

3x with CH_2Cl_2. The combined organic layers were washed with water and brine, dried over $MgSO_4$, filtered, concentrated, and purified by column chromatography, yielding the title compound as a yellow oil (209 mg, quant. yield). **^{1}H NMR** (500 MHz, $CDCl_3$) δ 8.24 (dd, J = 8.3, 0.9 Hz, 1H), 7.77 (td, J = 7.5, 1.1 Hz, 1H), 7.67 – 7.62 (m, 1H), 7.52 – 7.49 (m, 1H), 5.88 (dt, J = 4.4, 2.2 Hz, 1H), 5.18 (dt, J = 4.4, 2.7 Hz, 1H), 4.78 (td, J = 10.0, 4.9 Hz, 1H), 3.92 (d, J = 4.5 Hz, 2H), 3.01 (ddt, J = 17.1, 10.5, 2.5 Hz, 1H), 2.44 (d, J = 16.8 Hz, 1H); **^{13}C NMR** (100 MHz, $CDCl_3$) δ 165.39, 145.33, 134.82, 132.02, 130.72, 128.81, 128.69, 124.98, 113.00, 66.05, 61.30, 33.25; **$[\alpha]^{25}_D$** –105.2 (c = 1.23 in $CHCl_3$); **IR** (film) 3392 (br O-H), 2928, 2359, 2341, 1610 (C=O), 1574, 1526, 1482, 1418, 1343, 1240, 1046, 967, 789, 761, 687, 668, 643; **HRMS** Accurate mass (ES^+): Found 271.0715 (+7.4 ppm), $C_{12}H_{12}N_2O_4Na$ ($M+Na^+$) requires 271.0695.

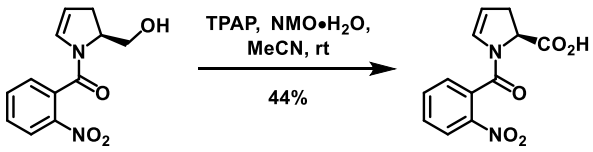

(–)-2.119 **(–)-2.120**

(S)-1-(2-nitrobenzoyl)-2,3-dihydro-1H-pyrrole-2-carboxylic acid (–)-2.120. To a solution of compound **(–)-2.119** (52 mg, 0.210 mmol) in MeCN (2 mL) was added NMO•H_2O (294 mg, 2.096 mmol), and the solution was stirred until complete dissolution. Then TPAP (7 mg, 0.021 mmol) was added, and the reaction was stirred for 1 hour, quenched with IPA, concentrated, and filtered over a plug of silica gel, which was washed with 1% AcOH/MeCN. The filtrate was concentrated and purified by column chromatography, eluting with 0 → 3% MeOH/0.1% AcOH/ CH_2Cl_2, yielding the title compound as a brown residue (24 mg, 44% yield). **^{1}H NMR** (400 MHz, $CDCl_3$) δ 8.15 (d, J = 8.1 Hz, 1H), 7.73 (t, J = 7.0 Hz, 1H), 7.64 – 7.55 (m, 2H), 5.92 (s, 1H), 5.17 (s, 1H), 5.02 (s, 1H), 3.17 – 3.01 (m, 1H), 2.97 – 2.85 (m, 1H); **^{13}C NMR** (100 MHz, $CDCl_3$) δ 174.39, 164.60, 145.33, 134.98, 131.34, 130.80, 129.52, 128.51, 124.76, 112.48, 99.77, 59.21, 53.58, 33.98; **$[\alpha]^{25}_D$** –127.8 (c = 0.94 in $CHCl_3$); **IR** (film) 3446, 3098, 2921, 2851, 1733 (C=O), 1615 (C=O), 1526, 1485, 1417, 1344, 1200, 1119, 1080, 1018, 941, 860, 840, 790, 762, 737, 704, 642; **HRMS** Accurate mass (ES^+): Found 263.683 (+5.7 ppm), $C_{12}H_{11}N_2O_5$ ($M+H^+$) requires 263.0668.

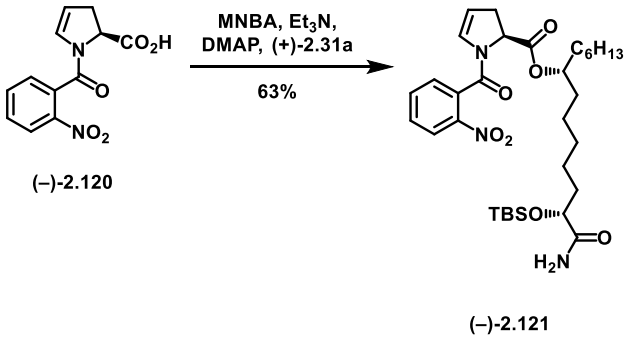

(7R,13R)-14-amino-13-((tert-butyldimethylsilyl)oxy)-14-oxotetradecan-7-yl (S)-1-(2- nitrobenzoyl)-2,3-dihydro-1H-pyrrole-2-carboxylate (–)-2.121. Using general procedure K, acid **(–)-2.120** (19 mg, 0.073 mmol), after purification by preparative TLC (2:1 CH_2Cl_2: Et_2O) yielded the title compound as a clear oil (24 mg, 63% yield). **^{1}H NMR** (500 MHz, $CDCl_3$) δ 8.20 (d, J = 8.2 Hz, 1H), 7.74 (td, J = 7.5, 1.0 Hz, 1H), 7.64 – 7.55 (m, 2H), 6.52 (d, J = 3.9 Hz, 1H), 6.01 (dt, J = 4.2, 2.1 Hz, 1H), 5.49 (s, 1H), 5.14 – 5.11 (m, 1H), 5.07 (dd, J = 11.7, 5.0 Hz, 1H), 5.02 – 4.95 (m, 1H), 4.14 – 4.09 (m, 1H), 3.23 – 3.15 (m, 1H), 2.72 (ddd, J = 19.5, 4.8, 2.4 Hz, 1H), 1.74 (dd, J = 14.9, 9.5 Hz, 1H), 1.69 – 1.51 (m, 6H), 1.37 – 1.21 (m, 16H), 0.90 (s, J = 3.0 Hz, 9H), 0.87 (t, J = 6.8 Hz, 3H), 0.12 – 0.04 (m, 9H); **^{13}C NMR** (125 MHz, $CDCl_3$) δ 177.07, 170.65, 163.28, 145.61, 134.56, 131.99, 130.59, 129.38, 129.26, 124.80, 110.35, 75.99, 73.59, 58.19, 35.15, 34.45, 34.14, 34.09, 31.86, 29.48, 29.29, 25.87, 25.41, 25.08, 24.11, 22.71, 18.14, 14.20, -4.70, -5.14; **$[\alpha]^{25}_D$** –71.1 (c = 1.21 in $CHCl_3$); **IR** (film) 3480, 2927, 2856, 1739 (C=O), 1658 (C=O), 1622 (C=O), 1574, 1531, 1463, 1413, 1347, 1252, 1198, 1098, 1005, 940, 836, 779, 739, 705, 669, 642, 582; **HRMS** Accurate mass (ES^+): Found 618.3548 (-4.4 ppm), $C_{32}H_{52}N_3O_7Si$ ($M+H^+$) requires 618.3575.

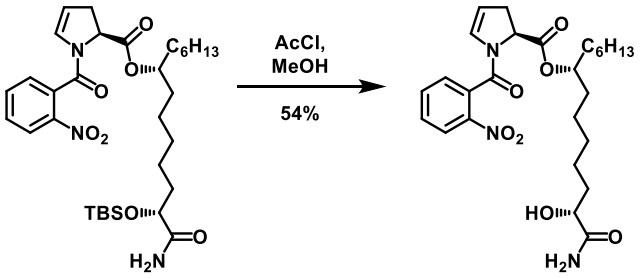

(–)-2.121 (–)-2.122

(7R,13R)-14-amino-13-hydroxy-14-oxotetradecan-7-yl (S)-1-(2-nitrobenzoyl)-2,3-dihydro- 1H-pyrrole-2-carboxylate (–)-2.122. To a solution of silyl ether **(–)-2.121** (13 mg, 0.021 mmol) dissolved in MeOH (0.5 mL) was added acetyl chloride (ca. 1 μL, 1 drop). After 10 minutes, the reaction was diluted with EtOAc and quenched with sat. $NaHCO_3$, then extracted with EtOAc 3x. The combined organic layers were washed with water and brine, dried over $MgSO_4$, filtered, concentrated, and purified by preparative TLC (10% MeOH/CH_2Cl_2), yielding the title compound as a yellow oil (7.0 mg, 54% yield). **^{1}H NMR** (500 MHz, $CDCl_3$) δ 8.21 (dd, J = 8.3, 0.9 Hz, 1H), 7.76 (tt, J = 4.0, 2.0 Hz, 1H), 7.67 – 7.60 (m, 2H), 6.64 (s, 1H), 6.03 (dt, J = 4.4, 2.2 Hz, 1H), 5.26 – 5.21 (m, 1H), 5.20 – 5.17 (m, 1H), 5.11 – 5.02 (m, 2H), 4.04 – 3.99 (m, 1H), 3.90 (t, J = 7.0 Hz, 1H), 3.21 (ddt, J = 16.8, 11.7, 2.4 Hz, 1H), 2.76 – 2.69 (m, 1H), 1.85 – 1.76 (m, 1H), 1.68 – 1.36 (m, 16H), 1.36 – 1.20 (m, 14H), 0.88 (t, J = 7.0 Hz, 3H); **$[\alpha]^{25}_D$** –64.6 (c = 0.22 in $CHCl_3$); **^{13}C NMR** (125 MHz, $CDCl_3$) δ 177.43, 170.48, 166.04, 145.51, 134.79, 131.33, 130.99, 129.33, 129.09, 124.94, 111.34, 75.58, 70.85, 58.13, 35.78, 34.34, 34.12, 33.82, 31.86, 29.84, 29.24, 27.60, 25.65, 25.66, 24.66, 24.33, 22.71, 14.22; **IR** (film) 3350 (br, O-H), 2926, 2856, 1733 (C=O), 1652 (C=O), 1621, 1530, 1483, 1417, 1346. 1197, 1079, 840, 791, 763, 740, 705; **HRMS** Accurate mass (ES^+): Found 526.2540 (+2.1 ppm), $C_{26}H_{37}N_3O_7Na$ ($M+Na^+$) requires 526.2529.

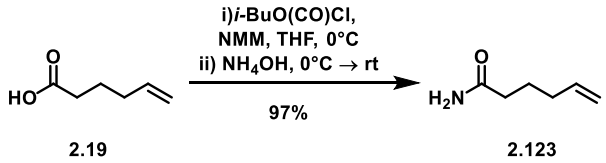

Hex-5-enamide 2.123. To a solution of 5-hexenoic acid **(2.19)** (0.44 mL, 3.701 mmol) dissolved in THF (5 mL) was added N-methylmorpholine (0.45 mL, 4.071 mmol) and the solution was cooled to 0 °C. Isobutyl chloroformate (0.53 mL, 4.071 mmol) was added dropwise and the reaction was stirred at 0 °C for 30 minutes, then ammonium hydroxide (28% NH_3 in H_2O, 0.64 mL) was added and the reaction was allowed to warm to room temperature and stir overnight. The reaction was quenched with sat. NH_4Cl and extracted with EtOAc 3x. The combined organic layers were washed with 1M HCl and brine, dried over $MgSO_4$, filtered and concentrated, yielding the title compound as a white solid (407 mg, 97% yield). **^{1}H NMR** (400 MHz, $CDCl_3$) δ 5.79 (ddt, J = 17.0, 10.2, 6.7 Hz, 1H), 5.34 (br s, 2H), 5.10 – 4.95 (m, 2H), 2.28 – 2.21 (m, 1H), 2.12 (dd, J = 14.2, 7.1 Hz, 2H), 1.82 – 1.70 (m, 1H); **^{13}C NMR** (101 MHz, $CDCl_3$) δ 175.73, 137.90, 115.51, 35.16, 33.16, 24.57; **IR** (film) 3361 (br N-H), 3184 (br N-H), 2944, 2359, 2342, 1633 (C=O), 1415, 1229, 1135, 1077, 991, 908, 775, 667; **HRMS** Accurate mass (ES^+): Found 114.0917 (-1.8 ppm), $C_6H_{12}NO$ ($M+H^+$) requires 114.0919; **MP** 70.0 – 75.1°C.

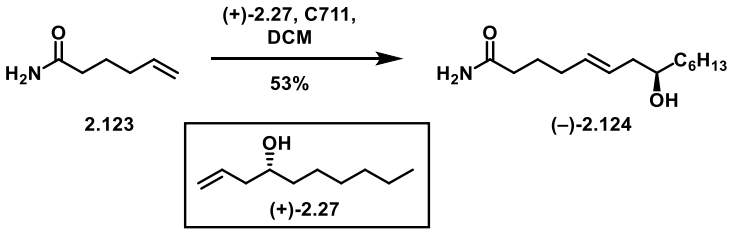

(R,E)-8-hydroxytetradec-5-enamide (–)-2.124. To a solution of **2.123** (41 mg, 0.362 mmol) and alcohol **(+)-2.27** (283 mg, 1.812 mmol) in CH_2Cl_2 (1 mL) was added catalyst C711 (13 mg, 0.018 mmol, CAS #635679-24-2). The reaction was stirred for overnight at room temperature, concentrated and purified by column chromatography (0 → 5% MeOH/CH_2Cl_2) yielding the title compound as a tan solid (46 mg, 53% yield). **^{1}H NMR** (400 MHz, $CDCl_3$) δ 5.52 – 5.44 (m, 2H), 5.30 (br s, 1H), 3.59 (br s, 1H), 2.23 (dd, J = 13.6, 6.1 Hz, 2H), 2.08 (dt, J = 14.3, 6.8 Hz, 2H), 1.74 (dt, J = 14.3, 7.2 Hz, 2H), 1.66 – 1.54 (m, 3H), 1.50

– 1.38 (m, 3H), 1.29 (t, J = 15.3 Hz, 7H), 0.93 – 0.84 (m, 10H); **^{13}C NMR** (100 MHz, $CDCl_3$) δ 176.13, 132.67, 127.69, 71.13, 40.68, 37.00, 35.02, 31.95, 31.90, 29.41, 25.83, 25.76, 24.93, 22.67, 14.15; **$[\alpha]^{25}_D$** – 1.8 (c = 1.69 in $CHCl_3$); **IR** (film) 3361, 3183,2954, 2921, 2850, 2359, 1650 (C=O), 1416, 1349, 1268, 1202, 1126, 1068, 1040, 1008, 966, 940, 863, 647, 598, 559; **HRMS** Accurate mass (ES^+): Found 264.1950 (+3.8 ppm), $C_{14}H_{27}NO_2Na$ ($M+Na^+$) requires 264.1940; **MP** 54.6 - 56.8°C; **R_f** (5% $MeOH/CH_2Cl_2$) = 0.23.

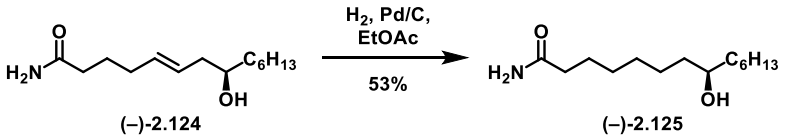

(R)-8-hydroxytetradecanamide (–)-2.124. Following general procedure B; alkene **(–)-2.125** (89 mg, 0.168 mmol) yielded the title compound as a white solid (91 mg, quant. yield). **^{1}H NMR (**400 MHz, $CDCl_3$) δ 5.24 (br d, 2H), 3.58 (br s, 1H), 2.38 (td, J = 7.4, 4.2 Hz, 1H), 2.27 – 2.16 (m, 2H), 1.69 – 1.60 (m, 2H), 1.48 – 1.21 (m, 18H), 0.90 – 0.85 (m, 3H); **^{13}C NMR** (100 MHz, $CDCl_3$) δ 175.89, 72.02, 37.65, 37.46, 35.99, 35.87, 31.96, 29.49, 29.45, 29.27, 25.75, 25.56, 22.74, 14.22; **$[\alpha]^{25}_D$** +7.0 (c = 1.34 in $CHCl_3$); **IR** (film) 3207 (br O-H), 2922, 2849, 1651 (C=O), 1614, 1467, 1413, 1129, 1066, 1012, 913, 850, 793, 720, 655; **HRMS** Accurate mass (ES^+): Found 266.2102 (+2.3 ppm), $C_{14}H_{29}NO_2Na$ ($M+Na^+$) requires 266.2096; **MP** 95.4 - 98.7 °C.

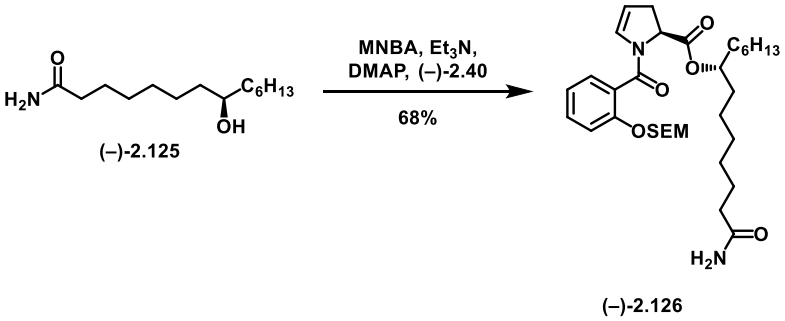

(R)-14-amino-14-oxotetradecan-7-yl (S)-1-(2-((2-(trimethylsilyl)ethoxy)methoxy)benzoyl)- 2,3-dihydro-1H-pyrrole-2-carboxylate (–)-2.126. Using modified general procedure K (1.2 eq acid, 1.2 eq MNBA), acid **(–)-2.125** (18 mg, 0.050 mmol) and alcohol **(–)-S61** (9.7 mg, 0.040 mmol) yielded the title compound as a yellow oil (16 mg, 68% yield). **^{1}H NMR** (500 MHz, $CDCl_3$) δ 7.40 – 7.28 (m, 2H), 7.19 (t,

J = 8.0 Hz, 1H), 7.04 (td, J = 7.5, 0.8 Hz, 1H), 6.31 (s, 1H), 6.19 – 6.12 (m, 1H), 5.22 (ddd, J = 16.3, 7.1, 2.9 Hz, 2H), 5.11 (s, 1H), 5.04 (td, J = 5.4, 2.9 Hz, 1H), 5.03 – 4.93 (m, 2H), 3.79 – 3.69 (m, 2H), 3.19 – 3.10 (m, 1H), 2.72 – 2.64 (m, 1H), 2.23 – 2.11 (m, 1H), 1.66 – 1.52 (m, 6H), 1.45 – 1.16 (m, 16H), 0.97 – 0.90 (m, 2H), 0.90 – 0.83 (m, 3H), 0.03 – -0.05 (m, 9H); **^{13}C NMR** (125 MHz, $CDCl_3$) δ 170.73, 165.29, 153.74, 131.43, 130.96, 128.89, 125.67, 122.05, 115.33, 108.77, 93.34, 75.35, 66.70, 58.08, 35.99, 34.60, 34.37, 31.85, 29.27, 28.83, 28.55, 25.48, 25.09, 24.70, 22.70, 18.15, 14.19, -1.28; **$[\alpha]^{25}_D$** –27.2 (c = 0.79 in $CHCl_3$); **IR** (film) 2925, 2856, 1738 (C=O), 1645 (C=O), 1618 (C=O), 1600, 1487, 1455, 1406, 1355, 1277, 1229, 1193, 1150, 1085, 1043, 987, 938, 917, 857, 834, 754, 696, 655; **HRMS** Accurate mass (ES^+): Found 611.3533 (+6.7 ppm), $C_{32}H_{52}N_2O_6SiNa$ ($M+Na^+$) requires 611.3492.

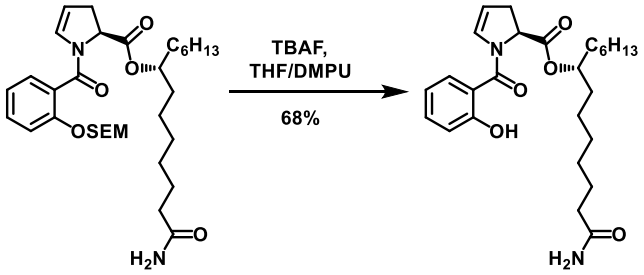

(–)-2.126 (–)-2.127

(R)-14-amino-14-oxotetradecan-7-yl (S)-1-(2-hydroxybenzoyl)-2,3-dihydro-1H-pyrrole-2-carboxylate (–)-2.127. Using modified general procedure L (10 eq TBAF, 0.1M DMPU), SEM ether **(–)-2.126** (7.5 mg, 0.013 mmol) yielded the title compound as a clear oil (4.1 mg, 68% yield) **^{1}H NMR** (500 MHz, $CDCl_3$) δ 9.83 (d, J = 46.9 Hz, 1H), 7.44 – 7.34 (m, 2H), 6.99 (dd, J = 7.4, 3.5 Hz, 1H), 6.89 (t, J = 7.8 Hz, 1H), 6.79 (s, 1H), 5.60 (br d, 1H), 5.29 (d, J = 10.2 Hz, 2H), 5.05 – 4.90 (m, 2H), 3.17 – 3.08 (m, 1H), 2.70 (d, J = 18.0 Hz, 1H), 2.23 – 2.16 (m, 2H), 1.66 – 1.48 (m, 8H), 1.39 – 1.16 (m, 15H), 0.86 (t, J = 7.0 Hz, 3H); **^{13}C NMR** (125 MHz, $CDCl_3$) δ 175.77, 171.03, 167.50, 159.30, 158.93, 133.56, 131.00, 128.41, 119.11, 118.06, 110.79, 75.99, 74.40, 59.54, 36.00, 35.90, 34.33, 34.19, 31.82, 29.25, 29.08, 29.02, 28.91, 25.41, 25.24, 24.90, 22.69, 14.20; **$[\alpha]^{25}_D$** –20.8 (c = 0.24 in $CHCl_3$); **IR** (film) 3190 (br O-H), 2926, 2856, 1733 (C=O), 1660 (C=O), 1593, 1456, 1414, 1294, 1252, 1194, 1152, 1098, 1016, 945, 912, 859,

816, 755, 723, 654, 617, 567; **HRMS** Accurate mass (ES^+): Found 481.2700 (+4.6 ppm), $C_{26}H_{38}N_2O_5Na$ ($M+Na^+$) requires 481.2678.

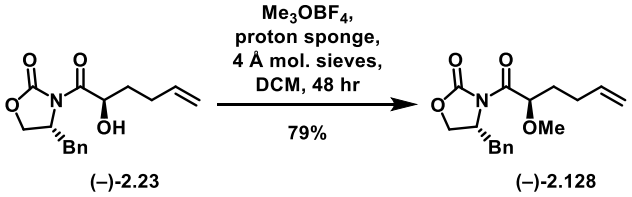

(R)-4-benzyl-3-((R)-2-methoxyhex-5-enoyl)oxazolidin-2-one (–)-2.128. 4 Å molecular sieves were flame-dried in a round-bottom flask, and alcohol **(–)-2.23** (121 mg, 0.418 mmol) was added to the flask as a solution in CH_2Cl_2 (2 mL) followed by trimethyloxonium tetrafluoroborate (493 mg, 3.333 mmol) and 1,8-Bis(dimethylamino)naphthalene (714 mg, 3.333 mmol). The reaction was stirred at room temperature for 48 hours, then quenched with isopropanol and filtered. The solution was diluted with Et_2O and washed with 1M HCl, sat. $NaHCO_3$, and brine, dried over Na_2SO_4, filtered, concentrated, and purified by column chromatography (4:1 hexanes:EtOAc) yielding the title compound as a yellow oil. **^{1}H NMR** (400 MHz, $CDCl_3$) δ 7.38 – 7.27 (m, 3H), 7.25 – 7.20 (m, 2H), 5.82 (ddt, J = 16.9, 10.1, 6.7 Hz, 1H), 5.09 – 4.97 (m, 2H), 4.91 (dd, J = 8.3, 3.5 Hz, 1H), 4.68 (ddt, J = 10.1, 6.7, 3.3 Hz, 1H), 4.28 – 4.21 (m, 2H), 3.42 (s, 3H), 3.36 (dd, J = 13.3, 3.1 Hz, 1H), 2.87 – 2.80 (m, 1H), 2.26 (dt, J = 14.0, 6.9 Hz, 2H), 1.88 – 1.68 (m, 2H); **^{13}C NMR** (100 MHz, $CDCl_3$) δ 173.15, 153.22, 137.59, 135.13, 129.54, 129.11, 127.57, 115.42, 79.27, 66.87, 58.17, 55.61, 37.93, 32.13, 29.67; **$[\alpha]^{25}_D$** –6.0 (c = 0.63 in $CHCl_3$); **IR** (film) 2923, 2854, 1723 (C=O), 1583, 1452, 1376, 1313, 1271, 1109, 1070, 1028, 967, 817, 743, 710; **HRMS** Accurate mass (ES^+): Found 326.1381 (+4.0 ppm), $C_{17}H_{21}NO_4Na$ ($M+Na^+$) requires 326.1368.

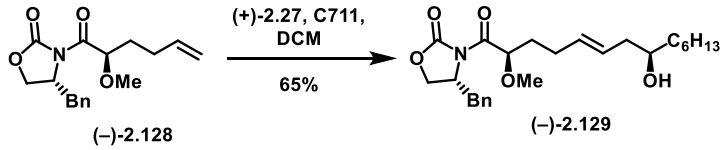

(R)-4-benzyl-3-((2R,8R,E)-8-hydroxy-2-methoxytetradec-5-enoyl)oxazolidin-2-one (–)-2.129. Catalyst C711 (13 mg, 0.017 mmol - CAS #635679-24-2) was added to a solution of alcohol **(+)- 2.27** (258

mg, 1.651 mmol) and methyl ether **(–)-2.128** (100 mg, 0.330 mmol) dissolved in CH_2Cl_2 (2 mL) and stirred at room temperature overnight. The reaction was concentrated and purified by column chromatography (4:1 hexanes:EtOAc), yielding the title compound as a yellow oil (95 mg, 65% yield). **^{1}H NMR** (400 MHz, $CDCl_3$) δ 7.37 – 7.27 (m, 3H), 7.23 (d, J = 6.9 Hz, 2H), 5.52 (dt, J = 13.2, 8.3 Hz, 3H), 4.91 (dd, J = 8.1, 3.6 Hz, 1H), 4.73 – 4.65 (m, 1H), 4.27 – 4.20 (m, 2H), 3.60 (br s, 2H), 3.41 (s, J = 3.4 Hz, 3H), 3.39 – 3.33 (m, 1H), 2.87 – 2.78 (m, 1H), 2.32 – 2.20 (m, 3H), 2.14 – 2.07 (m, 1H), 1.85 – 1.70 (m, 2H), 1.64 – 1.56 (m, 2H), 1.51 – 1.39 (m, 6H), 1.34 – 1.24 (m, 14H), 0.88 (t, J = 6.4 Hz, 3H); **^{13}C NMR** (100 MHz, $CDCl_3$) δ 173.25, 153.23, 135.11, 132.69, 130.09, 129.53, 129.11, 127.56, 79.13, 70.95, 70.84, 66.91, 58.18, 55.61, 40.85, 40.72, 37.94, 37.03, 36.86, 32.68, 31.93, 29.44, 28.51, 25.80, 25.76, 22.72, 14.19; **$[\alpha]^{25}_D$** –17.5 (c = 0.83 in $CHCl_3$); **IR** (film) 3500 (br, O-H), 2925, 2854, 1778 (C=O), 1705 (C=O), 1455, 1387, 1349, 1290, 1252, 1211, 1113, 1073, 1049, 971, 814, 761, 732, 700; **HRMS** Accurate mass (ES^+): Found 454.2585 (+3.5 ppm), $C_{25}H_{37}NO_5Na$ ($M+Na^+$) requires 454.2569.

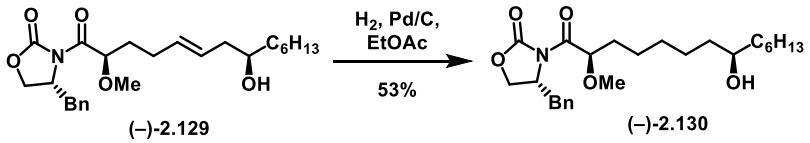

(R)-4-benzyl-3-((2R,8R)-8-hydroxy-2-methoxytetradecanoyl)oxazolidin-2-one (–)-2.130. Following general procedure B; alkene **(–)-2.129** (95 mg, 0.220 mmol) yielded the title compound as a clear oil (89 mg, 93% yield). **^{1}H NMR** (400 MHz, $CDCl_3$) δ 7.36 – 7.27 (m, 3H), 7.24 – 7.20 (m, 2H), 4.90 (dd, J = 7.9, 3.5 Hz, 1H), 4.72 – 4.66 (m, 1H), 4.28 – 4.22 (m, 2H), 3.59 (br s, 2H), 3.41 (s, 3H), 3.34 (dd, J = 7.3, 4.2 Hz, 1H), 2.83 (dd, J = 13.4, 9.5 Hz, 1H), 2.39 (dt, J = 10.8, 7.4 Hz, 1H), 1.70 – 1.59 (m, 2H), 1.50 – 1.37 (m, 10H), 1.32 – 1.23 (m, 12H), 0.88 – 0.85 (m, 3H); **^{13}C NMR** (100 MHz, $CDCl_3$) δ 173.14, 153.17, 135.05, 129.43, 128.97, 127.42, 79.81, 71.80, 71.69, 66.76, 58.04, 55.46, 37.80, 37.52, 37.47, 37.35, 37.31, 32.79, 31.85, 29.39, 29.24, 25.62, 25.39, 22.62, 14.10; **$[\alpha]^{25}_D$** –12.0 (c = 0.93 in $CHCl_3$); **IR** (film) 2924, 2855, 1781 (C=O), 1705, 1456, 1387, 1349, 1211, 1107, 1019, 814, 754, 700, 667; **HRMS** Accurate mass (ES^+): Found 434.2911 (+1.2 ppm), $C_{25}H_{40}NO_5$ ($M+H^+$) requires 434.2906.

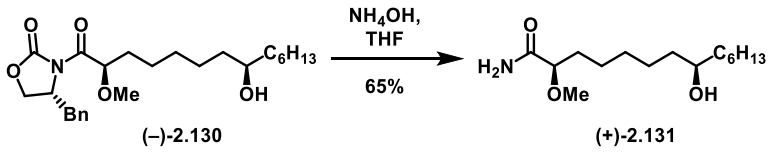

(2R,8R)-8-hydroxy-2-methoxytetradecanamide (+)-2.131. To a solution of oxazolidinone **(–)-2.130** (88 mg, 0.203 mmol) in THF (3 mL) was added ammonium hydroxide (28% NH_3 in H_2O, 2 mL), and the reaction was tightly sealed and stirred for 48 hours. The reaction was diluted with MeOH and concentrated, and this process was repeated 2x. Purification by column chromatography (0 → 8% MeOH/CH_2Cl_2) yielded the title compound as a white solid (36 mg, 65% yield). **^{1}H NMR** (500 MHz, $CDCl_3$) δ 6.46 (br s, 1H), 5.57 (br s, 1H), 3.62 (dd, J = 6.9, 4.4 Hz, 1H), 3.57 (br s, 1H), 3.41 (s, 3H), 1.82 – 1.74 (m, 1H), 1.73 – 1.63 (m, 2H), 1.47 – 1.35 (m, 9H), 1.35 – 1.22 (m, 10H), 0.88 (t, J = 6.9 Hz, 3H); **^{13}C NMR** (100 MHz, $CDCl_3$) δ 175.75, 99.78, 82.49, 72.06, 58.47, 37.62, 37.47, 32.44, 31.99, 29.58, 29.51, 25.76, 25.59, 24.85, 22.76, 14.24; **$[\alpha]^{25}_D$** +21.0 (c = 0.67 in $CHCl_3$); **IR** (film) 3366 (br, N-H), 3189 (br, N-H), 2916, 2852, 1636 (C=O), 1532, 1462, 1431, 1340, 1221, 1207, 1133, 1112, 1067, 1050, 1001, 926, 859, 806, 726, 682, 617; **HRMS** Accurate mass (ES^+): Found 274.2385 (+1.1 ppm), $C_{15}H_{32}NO_3$ ($M+H^+$) requires 274.2382; **MP** 106 – 110°C, **R_f** (8% MeOH/CH_2Cl_2) = 0.36.

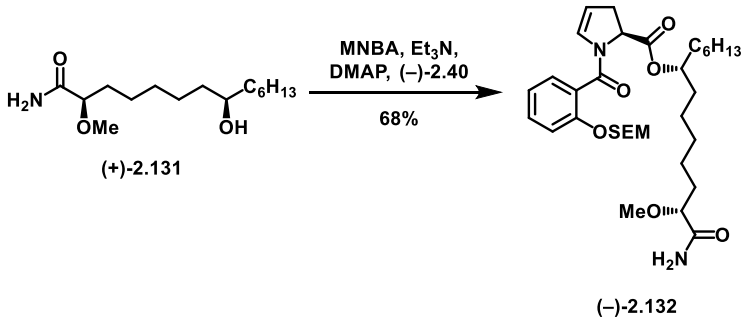

(7R,13R)-14-amino-13-methoxy-14-oxotetradecan-7-yl (S)-1-(2-((2-(trimethylsilyl)ethoxy)methoxy)benzoyl)-2,3-dihydro-1H-pyrrole-2-carboxylate (–)-2.132. Using general procedure K, alcohol **(+)-2.131** (9 mg, 0.033 mmol) and acid **(–)-2.40** (17 mg, 0.047 mmol) yielded the title compound as a yellow oil (19 mg, 95% yield). **^{1}H NMR** (400 MHz, $CDCl_3$) δ 7.40 – 7.28 (m, 2H), 7.21 – 7.16 (m, 1H), 7.03 (td, J = 7.5, 0.8 Hz, 1H), 6.52 (br s, 1H), 6.20 – 6.11 (m, 1H), 5.60 (br s, 1H),

5.25 – 5.18 (m, 1H), 5.04 – 5.00 (m, 1H), 5.01 – 4.93 (m, 2H), 3.74 (dd, J = 16.0, 7.6 Hz, 2H), 3.60 (dd, J = 6.8, 4.5 Hz, 1H), 3.37 (s, 3H), 3.12 (ddd, J = 14.2, 10.4, 5.8 Hz, 1H), 2.70 – 2.62 (m, 1H), 1.77 – 1.64 (m, 2H), 1.62 – 1.48 (m, 4H), 1.41 – 1.17 (m, 17H), 0.93 (dd, J = 10.6, 6.2 Hz, 2H), 0.85 (t, J = 5.8 Hz, 3H), -0.02 (s, 9H); **^{13}C NMR** (100 MHz, $CDCl_3$) δ 175.79, 170.79, 165.03, 153.82, 131.26, 131.02, 129.01, 125.91, 121.98, 115.24, 108.45, 99.74, 93.34, 82.37, 75.46, 66.63, 58.33, 58.16, 34.40, 34.18, 34.09, 32.33, 31.85, 29.30, 25.35, 25.01, 24.68, 22.71, 18.15, 14.20, -1.28; **$[\alpha]^{25}_D$** –10.0 (c = 0.24 in $CHCl_3$); **IR** (film) 2927, 2858, 1733 (C=O), 1652 (C=O), 1619, 1601, 1488, 1456, 1278, 1407, 1248, 1230, 1194, 1153, 1087, 988, 836, 754, 697, 656, 609; **HRMS** Accurate mass (ES^+): Found 641.3621 (+3.6 ppm), $C_{33}H_{54}N_2O_7SiNa$ ($M+Na^+$) requires 641.3598.

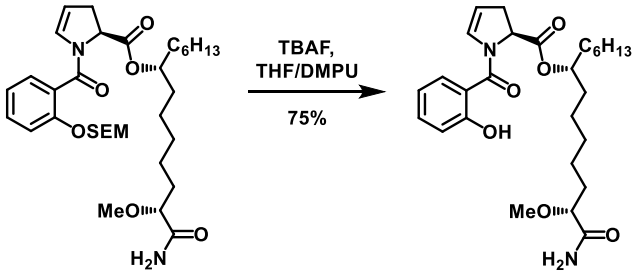

(–)-2.132 (–)-2.133

(7R,13R)-14-amino-13-methoxy-14-oxotetradecan-7-yl (S)-1-(2-hydroxybenzoyl)-2,3- dihydro-1H-pyrrole-2-carboxylate (–)-2.133. Using modified general procedure L (10 eq TBAF, 0.1M DMPU), SEM-ether **(–)-2.132** (13.7 mg, 0.022 mmol) yielded the title compound as a clear oil (8.1 mg, 75% yield). **^{1}H NMR** (400 MHz, $CDCl_3$) δ 9.87 (s, 1H), 7.42 (dd, J = 7.8, 1.4 Hz, 1H), 7.39 – 7.34 (m, 1H), 6.99 (dd, J = 8.3, 0.9 Hz, 1H), 6.93 – 6.86 (m, 1H), 6.81 (br s, 1H), 6.47 (br s, 1H), 5.40 (br s, 1H), 5.27 (d, J = 4.2 Hz, 1H), 5.06 – 4.91 (m, 2H), 3.61 (dd, J = 6.7, 4.5 Hz, 1H), 3.38 (s, 3H), 3.18 – 3.07 (m, 1H), 2.70 (d, J = 17.0 Hz, 1H), 1.79 – 1.62 (m, 2H), 1.61 – 1.46 (m, 5H), 1.43 – 1.17 (m, 15H), 0.85 (t, J = 6.9 Hz, 3H); **^{13}C NMR** (100 MHz, $CDCl_3$) δ 175.68, 170.88, 167.53, 159.28, 133.54, 131.05, 128.48, 118.96, 118.09, 117.03, 110.68, 82.44, 75.98, 59.61, 58.39, 34.16, 34.09, 33.66, 32.34, 31.82, 29.27, 25.35, 25.05, 24.71, 22.69, 14.21; **$[\alpha]^{25}_D$** –21.3 (c = 0.39 in $CHCl_3$); **IR** (film) 3386 (N-H), 3348 (N-H), 3144 (br, O-H), 2927, 2858, 1719 (C=O), 1688 (C=O), 1672, 1619, 1567, 1487, 1445, 1431, 1355, 1303, 1281, 1252, 1230, 1191, 1147,

1120, 1095, 1070, 1039, 1020, 1003, 992, 954, 943, 905, 857, 822, 796, 759, 730, 699, 667, 643; **HRMS** Accurate mass (ES^+): Found 489.2979 (+2.9 ppm), $C_{27}H_{41}N_2O_6$ ($M+H^+$) requires 308.1498.

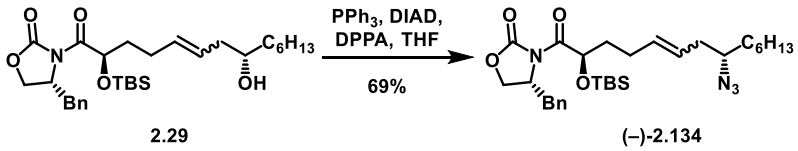

2.29 (–)-2.134

(R)-3-((2R,8R,E)-8-azido-2-((tert-butyldimethylsilyl)oxy)tetradec-5-enoyl)-4- benzyloxazolidin-2-one (–)-2.134. To a solution of compound **2.29** (153 mg, 0.288 mmol) in THF (2 mL) was added PPh_3 (302 mg, 1.153 mmol), diisopropyl azodicarboxylate (DIAD) (0.23 mL, 1.153 mmol), and diphenylphosphoryl azide (DPPA) (0.25 mL, 1.153 mmol). After 30 minutes, the reaction was concentrated and purified by prep TLC (neat CH_2Cl_2), yielding the title compound as a yellow oil (111 mg, 69% yield). **^{1}H NMR** (400 MHz, $CDCl_3$) δ 7.26 – 7.16 (m, 3H), 7.15 – 7.11 (m, 2H), 5.48 – 5.29 (m, 2H), 5.27 (dd, J = 8.2, 3.4 Hz, 1H), 4.55 – 4.47 (m, 1H), 4.12 – 4.04 (m, 2H), 3.30 (dd, J = 13.3, 3.0 Hz, 1H), 2.58 (dd, J = 13.2, 10.2 Hz, 1H), 2.19 – 2.01 (m, 2H), 1.72 – 1.52 (m, 2H), 1.42 – 1.26 (m, 3H), 1.26 – 1.10 (m, 8H), 0.86 – 0.82 (m, 9H), 0.77 (t, J = 6.7 Hz, 3H), 0.02 – -0.03 (m, 6H); **^{13}C NMR** (125 MHz, $CDCl_3$) δ 174.33, 153.18, 135.34, 132.97, 129.56, 129.11, 127.51, 126.26, 71.01, 66.62, 62.84, 55.71, 37.79, 35.00, 33.98, 31.82, 29.17, 28.68, 26.15, 25.93, 22.69, 18.44, 14.18, 1.13, -4.49, -4.95; **$[\alpha]^{25}_D$** – 5.0 (c = 0.42 in $CHCl_3$); **IR** (film) 2927, 2856, 2097, 1780 (C=O), 1712 (C=O), 1455, 1386, 1347, 1249, 1209, 1194, 1106, 1012, 969, 835, 777, 749, 700, 663, 593; **HRMS** Accurate mass (ES^+): Found 579.3367 (+4.1 ppm), $C_{30}H_{48}N_4O_4SiNa$ ($M+Na^+$) requires 579.3343.

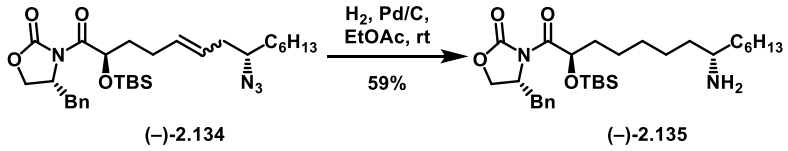

(–)-2.134 (–)-2.135

(R)-3-((2R,8R)-8-amino-2-((tert-butyldimethylsilyl)oxy)tetradecanoyl)-4-benzyloxazolidin- 2-one (–)-2.135. To a solution of compound **(–)-1.134** (111 mg, 0.199 mmol) in EtOAc (10 mL) was added Pd/C (10% by wt., 100 mg), and stirred for 16 hours under a balloon of H_2. The reaction was filtered through

Celite and purified by column chromatography, eluting in 50% → 0% hexanes/CH_2Cl_2 then 0 → 20% MeOH/CH_2Cl_2, yielding the title compound as a clear oil (63 mg, 59% yield). **^{1}H NMR** (400 MHz, $CDCl_3$) δ 7.36 – 7.29 (m, 3H), 7.25 – 7.22 (m, 2H), 5.40 – 5.34 (m, 1H), 4.70 – 4.59 (m, 1H), 4.32 – 4.24 (m, 1H), 4.15 (dd, J = 9.0, 2.2 Hz, 1H), 3.42 – 3.35 (m, 1H), 3.15 – 3.07 (m, 1H), 2.70 (dd, J = 13.3, 10.1 Hz, 1H), 1.74 – 1.57 (m, 10H), 1.52 – 1.19 (m, 20H), 0.93 (s, 9H), 0.86 (t, J = 6.1 Hz, 3H), 0.10 (s, 3H), 0.08 (s, 3H); **^{13}C NMR** (125 MHz, $CDCl_3$) δ 174.56, 153.26, 135.40, 129.58, 129.12, 127.51, 71.45, 66.64, 55.72, 37.83, 35.33, 31.98, 29.58, 29.48, 26.15, 26.04, 25.95, 25.63, 22.77, 18.48, 14.22, -4.50, -4.95; **$[\alpha]^{25}_D$** –9.3 (c = 0.45 in $CHCl_3$); **IR** (film) 2927, 2856, 1779 (C=O), 1711 (C=O), 1605, 1519, 1455, 1387, 1348, 1248, 1210, 1145, 1109, 1051, 1007, 977, 939, 835, 776, 762, 700, 663, 593; **HRMS** Accurate mass (ES^+): Found 533.3745 (-5.6 ppm), $C_{30}H_{53}N_2O_4Si$ ($M+H^+$) requires 533.3775; **R_f** (9:1 CH_2Cl_2:MeOH) = 0.18, stains brown in ninhydrin).

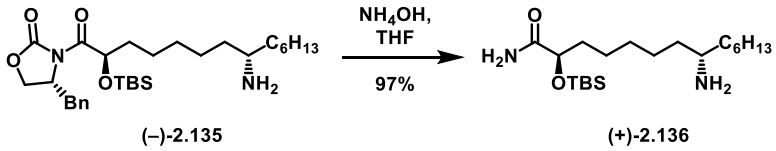

(–)-2.135 (+)-2.136

(2R,8R)-8-amino-2-((tert-butyldimethylsilyl)oxy)tetradecanamide (+)-2.136. Following modified general procedure C; oxazolidinone **(–)- 2.135** (44 mg, 0.083 mmol) yielded the title compound as a clear oil (29 mg, 97% yield) (purified by column chromatography, eluting in 0 → 15% MeOH/0.1% NH_4OH/CH_2Cl_2,). **^{1}H NMR** (500 MHz, $CDCl_3$) δ 6.64 – 6.50 (m, 2H), 4.15 – 4.09 (m, 1H), 3.12 (dt, J = 14.7, 7.4 Hz, 2H), 1.79 (ddd, J = 15.1, 10.2, 4.9 Hz, 1H), 1.75 – 1.57 (m, 6H), 1.45 – 1.23 (m, 22H), 0.91 (s, 9H), 0.86 (t, J = 6.6 Hz, 3H), 0.09 (s, 3H), 0.08 (s, 3H); **^{13}C NMR** (125 MHz, $CDCl_3$) δ 177.56, 73.20, 52.12, 34.60, 33.25, 32.94, 31.71, 29.78, 29.20, 29.04, 25.84, 25.40, 24.94, 23.51, 22.68, 18.11, 14.16, -4.73, -5.16; **$[\alpha]^{25}_D$** +5.8 (c = 1.47 in $CHCl_3$); **IR** (film) 3477, 2925, 2854, 1672 (C=O), 1557, 1462, 1388, 1361, 1337, 1252, 1101, 1005, 938, 836, 778, 721, 668, 588; **HRMS** Accurate mass (ES^+): Found 373.3264 (+3.8 ppm), $C_{20}H_{45}N_2O_2Si$ ($M+H^+$) requires 373.3250; **R_f** (0.1% NH_4OH/10% MeOH/90% CH_2Cl_2) = 0.18.

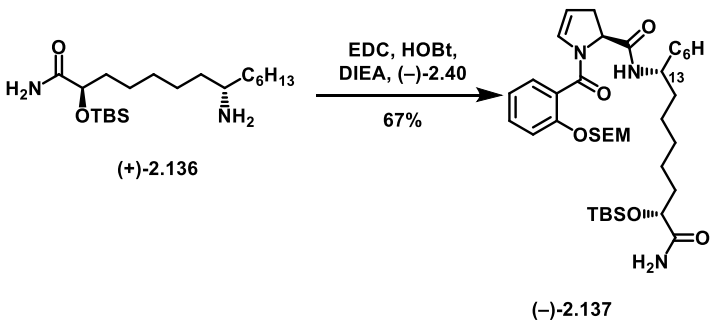

(S)-N-((7R,13R)-14-amino-13-((tert-butyldimethylsilyl)oxy)-14-oxotetradecan-7-yl)-1-(2-((2-(trimethylsilyl)ethoxy)methoxy)benzoyl)-2,3-dihydro-1H-pyrrole-2-carboxamide (–)-2.137. To a solution of acid **(–)-2.40** (19 mg, 0.053 mmol) dissolved in CH_2Cl_2 (1 mL), was added EDC (9 mg, 0.056 mmol), HOBt•H_2O (9 mg, 0.056 mmol), DIEA (0.02 mL, 0.113 mmol), and amine **(+)-2.136** (14 mg, 0.038 mmol) dissolved in CH_2Cl_2 (1 mL). The reaction was stirred overnight, then poured into water, extracted 3x with CH_2Cl_2, washed with water and brine, dried over $MgSO_4$ and purified by column chromatography, eluting in 0 → 20% Et_2O/CH_2Cl_2, yielding the title compound as a yellow oil (18 mg, 67% yield). **^{1}H NMR** (500 MHz, $CDCl_3$) δ 7.41 – 7.36 (m, 1H), 7.25 (d, J = 8.5 Hz, 1H), 7.07 (t, J = 7.5 Hz, 1H), 6.98 (s, 1H), 6.52 (d, J = 4.3 Hz, 1H), 6.11 – 6.02 (m, 1H), 5.52 (s, 1H), 5.23 (t, J = 7.2 Hz, 2H), 5.19 – 5.14 (m, 1H), 5.09 (dd, J = 15.0, 5.4 Hz, 1H), 4.18 – 4.08 (m, 1H), 3.93 (s, 1H), 3.77 – 3.69 (m, 2H), 3.18 – 2.89 (m, 2H), 1.80 – 1.45 (m, 6H), 1.40 – 1.17 (m, 22H), 0.96 – 0.89 (m, 12H), 0.88 – 0.81 (m, 3H), 0.08 (s, 3H), 0.08 (s, 3H), -0.01 (s, 9H); **^{13}C NMR** (100 MHz, $CDCl_3$) δ 176.95, 169.89, 153.58, 131.57, 129.66, 128.59, 125.53, 122.27, 114.83, 111.81, 93.28, 73.55, 66.95, 59.47, 56.12, 49.30, 35.34, 35.07, 31.87, 29.84, 29.58, 29.36, 25.87, 24.17, 22.74, 18.22, 18.15, 14.21, 1.16, -1.25, -4.69, -5.12; **$[\alpha]^{25}_D$** –46.4 (c = 0.74 in $CHCl_3$); **IR** (film) 3480, 3295, 2926, 2855, 1662, 1618, 1551, 1487, 1455, 1404, 1249, 1228, 1087, 985, 938, 778, 754, 730, 667, 506; **HRMS** Accurate mass (ES^+): Found 740.4447 (-2.6 ppm), $C_{38}H_{67}N_3O_6Si_2Na$ ($M+Na^+$) requires 740.4466; **R_f** (1:1 Et_2O:CH_2Cl_2) = 0.51.

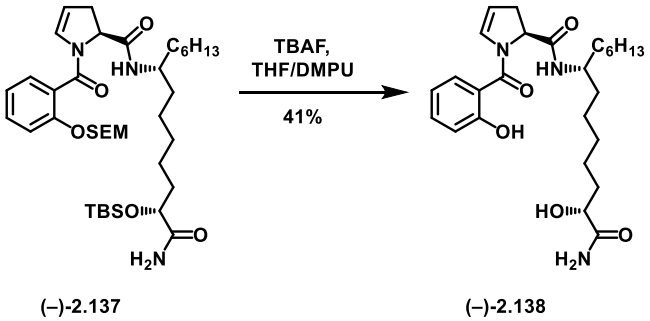

(S)-N-((7R,13R)-14-amino-13-hydroxy-14-oxotetradecan-7-yl)-1-(2-hydroxybenzoyl)-2,3- dihydro-1H-pyrrole-2-carboxamide (–)-2.138. Using general procedure L, silyl ether **(–)-2.137** (15 mg, 0.021 mmol) yielded the title compound as translucent oil (7.6 mg, 76% yield). **^{1}H NMR** (500 MHz, $CDCl_3$) δ 9.68 (s, 1H), 7.33 (t, J = 7.2 Hz, 2H), 6.97 (d, J = 8.2 Hz, 1H), 6.89 (t, J = 7.3 Hz, 1H), 6.82 (s, 1H), 6.61 (s, 1H), 6.45 (s, 1H), 5.74 (s, 1H), 5.26 (s, 1H), 5.08 – 4.99 (m, 1H), 4.14 (s, 1H), 4.03 (s, 1H), 3.92 (s, 1H), 3.07 – 2.96 (m, 1H), 2.90 (d, J = 15.2 Hz, 1H), 1.81 (d, J = 69.1 Hz, 2H), 1.64 – 1.11 (m, 22H), 0.86 (t, J = 6.5 Hz, 3H); **^{13}C NMR** (100 MHz, $CDCl_3$) δ 177.87, 170.68, 167.49, 156.12, 132.93, 130.44, 128.40, 119.71, 117.58, 112.13, 71.27, 60.12, 49.71, 35.65, 34.89, 33.89, 31.89, 29.32, 28.13, 26.13, 25.18, 24.29, 22.73, 14.22; **$[\alpha]^{25}_D$** –57.5 (c = 0.76 in $CHCl_3$); **IR** (film) 3287 (br, O-H), 2927, 2856, 1653 (C=O), 1616 (C=O), 1558, 1540, 1507, 1489, 1457, 1398, 1295, 1235, 1155, 1096, 1016, 944, 855, 817, 754, 723, 653, 620, 566; **HRMS** Accurate mass (ES^+): Found 496.2817 (+6.0 ppm), $C_{26}H_{39}N_3O_5Na$ ($M+Na^+$) requires 496.2787; **R_f** (5% MeOH/ 95% CH_2Cl_2) = 0.23.

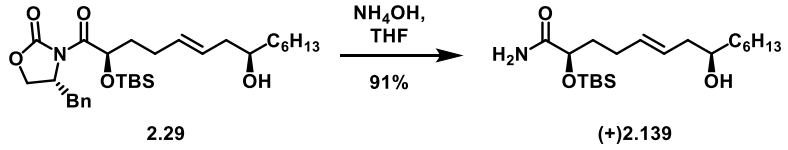

(2R,8R,E)-2-((tert-butyldimethylsilyl)oxy)-8-hydroxytetradec-5-enamide (+)-2.139. Following general procedure C; oxazolidinone **2.29** (50 mg, 0.094 mmol) yielded the title compound as a yellow oil (32 mg, 91% yield). **^{1}H NMR (**400 MHz, $CDCl_3$) δ 6.63 – 6.46 (m, 1H), 5.60 – 5.40 (m, 3H), 4.21 – 4.12 (m, 1H), 3.55 (d, J = 16.1 Hz, 1H), 2.28 – 1.99 (m, 4H), 1.95 – 1.80 (m, 1H), 1.80 – 1.71 (m, 3H), 1.47 – 1.39 (m, 2H), 1.33 – 1.23 (m, 6H), 0.93 (s, J = 2.9 Hz, 9H), 0.88 (t, J = 6.7 Hz, 3H), 0.13 – 0.07 (m, 6H);

^{13}C NMR (100 MHz, $CDCl_3$) δ 177.15, 133.16, 126.95, 72.95, 71.03, 56.05, 40.79, 36.87, 34.91, 31.92, 29.44, 27.36, 25.82, 22.70, 18.09, 14.18, -4.73, -5.15; **$[\alpha]^{25}_D$** +9.3 (c = 1.64 in $CHCl_3$); **IR** (film) 3479, 2954, 2927, 2855, 1682 (C=O), 1556, 1463, 1388, 1361, 1253, 1101, 1005, 967, 912, 836, 778, 722, 669, 578; **HRMS** Accurate mass (ES^+): Found 394.2757 (+1.0 ppm), $C_{20}H_{41}NO_3SiNa$ ($M+Na^+$) requires 394.2753; **R_f** (2:1 CH_2Cl_2:Et_2O) = 0.25.

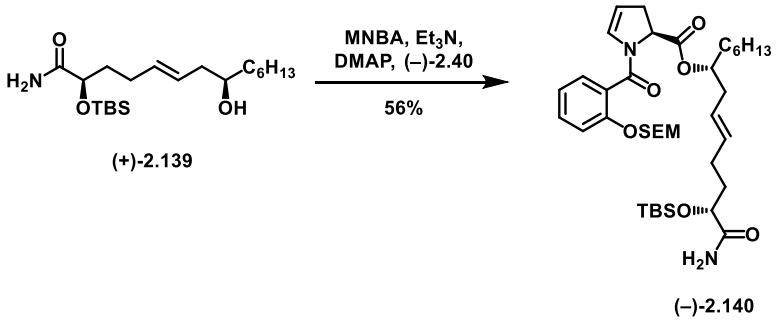

(7R,13R,E)-14-amino-13-((tert-butyldimethylsilyl)oxy)-14-oxotetradec-9-en-7-yl (S)-1-(2-((2-(trimethylsilyl)ethoxy)methoxy)benzoyl)-2,3-dihydro-1H-pyrrole-2-carboxylate (–)-2.140. Using general procedure K, acid **(–)-2.40** (22 mg, 0.060 mmol) and alcohol **(+)-2.139** (16 mg, 0.043 mmol) yielded the title compound as a yellow oil (24 mg, 77% yield). **^{1}H NMR** (500 MHz, $CDCl_3$) δ 7.38 – 7.31 (m, 2H), 7.20 (d, J = 8.2 Hz, 1H), 7.03 (td, J = 7.5, 0.8 Hz, 1H), 7.00 – 6.92 (m, 1H), 6.53 (d, J = 4.2 Hz, 1H), 6.15 (dd, J = 4.2, 2.1 Hz, 1H), 5.70 (s, 1H), 5.44 (dtd, J = 22.1, 15.3, 6.6 Hz, 2H), 5.27 – 5.19 (m, 2H), 5.06 – 4.90 (m, 3H), 4.19 – 4.09 (m, 1H), 3.79 – 3.69 (m, 2H), 3.16 – 3.06 (m, 1H), 2.70 – 2.63 (m, 1H), 2.33 – 2.26 (m, 2H), 2.14 – 2.02 (m, 3H), 1.89 – 1.78 (m, 2H), 1.77 – 1.68 (m, 2H), 1.61 – 1.51 (m, 3H), 1.35 – 1.17 (m, 12H), 0.96 – 0.89 (m, 9H), 0.86 (t, J = 6.9 Hz, 3H), 0.11 – 0.06 (m, 6H), -0.02 (s, 9H); **^{13}C NMR** (100 MHz, $CDCl_3$) δ 176.80, 170.68, 164.99, 153.84, 132.90, 131.25, 131.00, 128.99, 125.92, 125.52, 121.97, 115.21, 108.43, 93.33, 74.91, 73.13, 66.63, 58.24, 37.36, 34.89, 34.39, 33.45, 31.84, 30.43, 29.82, 29.26, 27.44, 25.86, 25.28, 22.70, 18.15, 14.19, -1.28, -4.70, -5.12; **$[\alpha]^{25}_D$** –19.8 (c = 1.20 in $CHCl_3$); **IR** (film) 3479, 2952, 2926, 2856, 1736 (C=O), 1689, 1650, 1619, 1600, 1488, 1455, 1406, 1359, 1249, 1230, 1191, 1151, 1087, 1043, 988, 917, 778, 754; **HRMS** Accurate mass (ES^+): Found 717.4299 (-4.3 ppm), $C_{38}H_{65}N_2O_7Si_2$ ($M+H^+$) requires 717.4330; **R_f** (2:1 CH_2Cl_2:Et_2O) = 0.76.

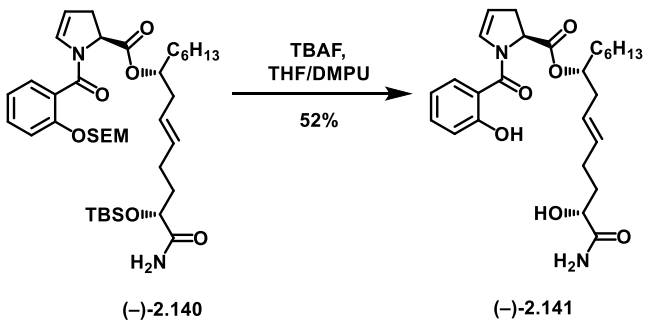

(7R,13R,E)-14-amino-13-hydroxy-14-oxotetradec-9-en-7-yl (S)-1-(2-hydroxybenzoyl)-2,3- dihydro-1H-pyrrole-2-carboxylate (–)-2.141. Using general procedure L, silyl ether **(–)-2.140** (24 mg, 0.034 mmol) yielded the title compound as a clear oil (8.3 mg, 52% yield). **^{1}H NMR** (500 MHz, $CDCl_3$) δ 9.06 (s, 1H), 7.42 – 7.34 (m, 2H), 7.03 – 6.95 (m, 1H), 6.95 – 6.87 (m, 1H), 6.62 (d, J = 17.8 Hz, 2H), 5.52 (s, 2H), 5.35 – 5.29 (m, 1H), 5.29 – 5.23 (m, 1H), 5.03 (dd, J = 11.5, 4.6 Hz, 2H), 4.08 – 4.00 (m, 1H), 3.90 (s, 1H), 3.20 – 3.08 (m, 1H), 2.70 (d, J = 17.2 Hz, 1H), 2.34 – 2.11 (m, 2H), 1.96 – 1.87 (m, 1H), 1.72 – 1.49 (m, 5H), 1.34 – 1.18 (m, 10H), 0.87 (t, J = 7.0 Hz, 3H); **^{13}C NMR** (100 MHz, $CDCl_3$) δ 177.53, 171.32, 167.40, 157.36, 133.41, 132.37, 130.76, 128.36, 126.87, 119.55, 118.26, 118.03, 111.07, 70.14, 59.13, 37.82, 34.65, 33.75, 33.34, 31.79, 29.16, 27.87, 25.45, 22.66, 14.20; **$[\alpha]^{25}_D$** –40.3 (c = 0.83 in $CHCl_3$); **IR** (film) 3200 (br, O-H), 2926, 2855, 1733 (C=O), 1662 (C=O), 1592, 1487, 1430,1194, 1152, 1097, 1017, 969, 860, 755; **HRMS** Accurate mass (ES^+): Found 473.2689 (+7.8 ppm), $C_{26}H_{37}N_2O_6$ ($M+H^+$) requires 473.2652.

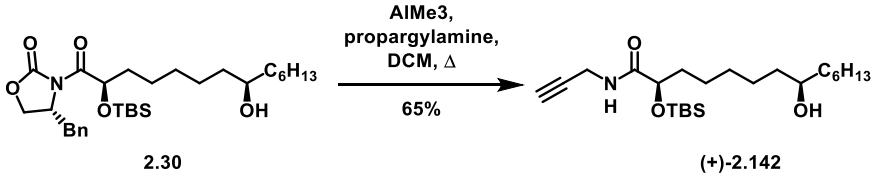

(2R,8R)-2-((tert-butyldimethylsilyl)oxy)-8-hydroxy-N-(prop-2-yn-1-yl)tetradecanamide (+)-2.142. To a solution of propargylamine (0.020 mL, 0.310 mmol) dissolved in CH_2Cl_2 (1 mL) at 0°C was added trimethylaluminum (2M in CH_2Cl_2, 0.155 mL, 0.310 mmol), and the solution was allowed to warm to room temperature. Oxazolidinone **(–)-2.30** (33 mg, 0.062 mmol) was added as a solution in CH_2Cl_2 (1 mL) and

the reaction was heated to reflux overnight. The reaction was then quenched with water and filtered through Celite. The layers were separated and the aqueous was extracted further (2x) with CH_2Cl_2. The combined organic layers were washed with water and brine, dried over $MgSO_4$, filtered, concentrated, and purified by column chromatography, yielding the title compound as a clear oil (17 mg, 65% yield). **^{1}H NMR** (500 MHz, $CDCl_3$) δ 6.74 (t, J = 5.2 Hz, 1H), 4.17 – 4.08 (m, 2H), 3.97 (ddd, J = 17.6, 4.8, 2.5 Hz, 1H), 3.61 – 3.50 (m, 1H), 2.22 (t, J = 2.5 Hz, 1H), 1.74 – 1.65 (m, 2H), 1.46 – 1.16 (m, 28H), 0.93 (s, 9H), 0.87 (t, J = 6.8 Hz, 3H), 0.09 (s, J = 2.9 Hz, 3H), 0.08 (s, 3H); **^{13}C NMR** (101 MHz, $CDCl_3$) δ 173.73, 125.65, 79.37, 73.59, 72.02, 71.73, 37.61, 37.47, 35.25, 31.97, 30.44, 29.66, 29.50, 28.76, 25.89, 25.75, 25.60, 24.28, 22.75, 18.17, 14.23, -4.68, -5.13; **$[\alpha]^{25}_D$** +21.8 (c = 1.00 in $CHCl_3$); **HRMS** Accurate mass (ES^+): Found 434.3085 (+4.4 ppm), $C_{23}H_{45}NO_3SiNa$ ($M+Na^+$) requires 434.3066; **R_f** (2:1 hexanes:EtOAc) = 0.44.

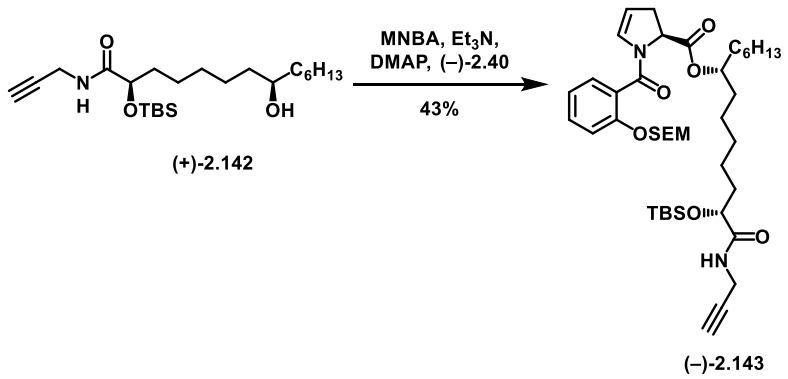

(7R,13R)-13-((tert-butyldimethylsilyl)oxy)-14-oxo-14-(prop-2-yn-1-ylamino)tetradecan-7-yl (S)-1-(2-((2-(trimethylsilyl)ethoxy)methoxy)benzoyl)-2,3-dihydro-1H-pyrrole-2-carboxylate (–)-2.143. Following general procedure K; acid **(–)-2.40** (25 mg, 0.068 mmol) and alcohol **(+)-2.142** (20 mg, 0.049 mmol) yielded the title compound as a yellow oil (16 mg, 43% yield). **^{1}H NMR** (500 MHz, $CDCl_3$) δ 7.36 (dd, J = 12.2, 4.6 Hz, 2H), 7.20 (d, J = 8.0 Hz, 1H), 7.07 – 7.00 (m, 1H), 6.74 (t, J = 5.4 Hz, 1H), 6.16 (dt, J = 4.2, 2.1 Hz, 1H), 5.22 (dd, J = 17.4, 7.1 Hz, 2H), 5.02 (dt, J = 4.8, 2.5 Hz, 1H), 4.99 – 4.91 (m, 2H), 4.16 – 4.08 (m, 2H), 3.97 (tt, J = 4.9, 3.5 Hz, 1H), 3.75 (dd, J = 16.5, 8.1 Hz, 2H), 3.11 (ddt, J = 16.7, 11.6, 2.3 Hz, 1H), 2.69 – 2.63 (m, 1H), 2.23 (t, J = 2.6 Hz, 1H), 1.76 – 1.48 (m, 7H), 1.41 – 1.19 (m, 17H), 0.96 – 0.90 (m, 11H), 0.86 (t, J = 6.8 Hz, 3H), 0.09 – 0.05 (m, 6H), -0.01 (s, 9H); **^{13}C NMR** (101 MHz, $CDCl_3$)

δ 173.69, 170.79, 164.95, 153.85, 131.22, 131.06, 129.03, 125.96, 121.97, 115.21, 108.31, 93.34, 79.42, 75.50, 73.59, 71.72, 66.62, 58.19, 35.29, 34.41, 34.10, 31.86, 29.56, 29.33, 28.71, 25.90, 25.31, 25.13, 24.16, 22.72, 18.17, 14.21, -1.27, -4.68, -5.15; **[α]$^{25}_{D}$** –17.7 (c = 1.00 in $CHCl_3$); **HRMS** Accurate mass (ES^+): Found 757.4687 (+5.8 ppm), $C_{41}H_{69}N_2O_7Si_2$ ($M+H^+$) requires 757.4643.

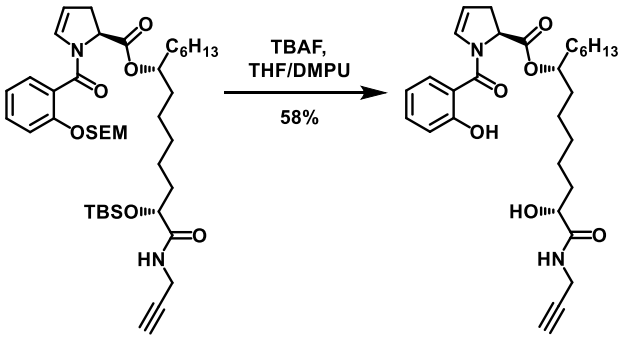

(–)-2.143 (–)-2.144

(7R,13R)-13-hydroxy-14-oxo-14-(prop-2-yn-1-ylamino)tetradecan-7-yl (S)-1-(2-hydroxybenzoyl)-2,3-dihydro-1H-pyrrole-2-carboxylate (–)-2.144. Following general procedure L; silyl ether **(–)-2.143** (14.9 mg, 0.0197 mmol) yielded the title compound as a clear oil (5.9 mg, 58% yield). **^{1}H NMR** (500 MHz, $CDCl_3$) δ 9.53 (br s, 1H), 7.44 – 7.35 (m, 2H), 7.03 – 6.98 (m, 1H), 6.94 – 6.87 (m, 1H), 6.73 (s, 1H), 5.33 – 5.25 (m, 1H), 5.01 (dd, J = 11.3, 4.6 Hz, 2H), 4.13 – 3.94 (m, 3H), 3.35 (br s, 1H), 3.19 – 3.08 (m, 1H), 2.70 (d, J = 17.3 Hz, 1H), 2.19 (t, J = 2.5 Hz, 1H), 1.87 – 1.76 (m, 1H), 1.71 – 1.48 (m, 6H), 1.32 (ddd, J = 28.0, 17.2, 10.1 Hz, 15H), 0.87 (t, J = 7.0 Hz, 3H); **^{13}C NMR** (126 MHz, CDCl3) δ 173.87, 171.31, 167.45, 158.09, 133.52, 130.86, 128.33, 119.42, 118.06, 117.70, 111.12, 79.64, 75.98, 71.62, 71.53, 59.39, 34.54, 34.31, 34.11, 31.83, 29.22, 28.86, 28.27, 25.52, 24.84, 24.56, 22.68, 14.20; **[α]$^{25}_{D}$** –32.4 (c = 0.38 in $CHCl_3$); **HRMS** Accurate mass (ES^+): Found 513.2991 (+5.3 ppm), $C_{29}H_{41}N_2O_6$ ($M+H^+$) requires 513.2964; **R_f** (3:1 EtOAc:hexanes) = 0.20.

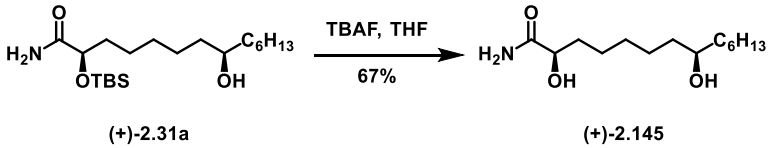

(2R,8R)-2,8-dihydroxytetradecanamide (+)-2.145. To a solution of silyl ether **(+)-2.31a** (25 mg, 0.069 mmol) in THF (0.5 mL) was added TBAF (1M in THF, 0.34 mL, 0.34 mmol), and the reaction was stirred for 30 minutes, poured into sat. NH_4Cl, and extracted with Et_2O 3x. The combined organic layers were washed with 1M NH_4Cl 5x, dried over $MgSO_4$, filtered, concentrated, and purified by column chromatography (2:1 CH_2Cl_2:Et_2O) yielding the title compound as a white solid (12 mg, 67% yield). **^{1}H NMR** (500 MHz, MeOD) δ 3.98 (dd, J = 7.9, 3.9 Hz, 1H), 3.53 – 3.46 (m, 1H), 1.80 – 1.72 (m, 1H), 1.64 – 1.55 (m, 1H), 1.50 – 1.26 (m, 18H), 0.91 (t, J = 7.0 Hz, 3H); **^{13}C NMR** (125 MHz, MeOD) δ 180.66, 72.68, 72.42, 38.47, 38.36, 35.64, 33.07, 30.63, 30.57, 26.80, 26.72, 26.13, 23.71, 14.43; **$[\alpha]^{25}_D$** +14.8 (c = 0.59 in MeOH); **IR** (film) 3232 (br, O-H), 2953, 2922, 2852, 2545, 2410, 2361, 2342, 2159, 2027, 1978, 1734, 1622 (C=O), 1591, 1558, 1465, 1452, 1436, 1378, 1363, 1345, 1227, 1169, 1133, 1090, 1065, 1024, 957, 923, 906, 857, 803, 721, 668, 609; **HRMS** Accurate mass (ES^+): Found 282.2041 (-1.4 ppm), $C_{14}H_{29}NO_3Na$ ($M+Na^+$) requires 282.2045; **MP** 99.2 - 101.7 °C.

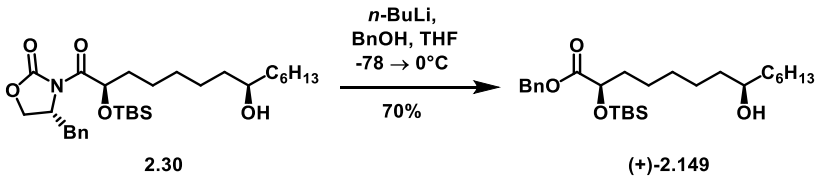

Benzyl (2R,8R)-2-((tert-butyldimethylsilyl)oxy)-8-hydroxytetradecanoate (+)-2.149. To a solution of benzyl alcohol (0.040 mL, 0.388 mmol) dissolved in THF (3 mL) at -78 °C was added *n*-BuLi (2.25 M in hexanes, 0.140 mL, 0.323 mmol) dropwise. After 5 minutes, a solution of oxazolidinone **(–)-2.30** (69 mg, 0.129 mmol) was added dropwise to the reaction. The reaction was warmed to 0 °C, after which time TLC indicated the consumption of starting material. The reaction was quenched with sat. NH_4Cl, extracted with EtOAc 3x, and the combined organic layers were washed with brine, dried over $MgSO_4$, filtered, concentrated, and purified by column chromatography, yielding the title compound as a clear oil (42 mg,

70% yield). **^{1}H NMR** (500 MHz, $CDCl_3$) δ 7.37 – 7.30 (m, 5H), 5.15 (dd, J = 27.9, 12.2 Hz, 2H), 4.22 (dd, J = 6.7, 5.5 Hz, 1H), 3.56 (s, 1H), 1.74 – 1.67 (m, 2H), 1.46 – 1.22 (m, 22H), 0.88 (s, J = 9H), 0.03 (s, 3H), 0.02 (s, 3H); **^{13}C NMR** (125 MHz, $CDCl_3$) δ 173.85, 135.86, 128.63, 128.54, 128.41, 72.38, 72.03, 66.54, 37.62, 37.46, 35.23, 31.97, 29.50, 25.83, 25.73, 25.60, 25.20, 22.75, 18.41, 14.22, -4.80, -5.24; **$[\alpha]^{25}_D$** +20.3 (c = 1.00 in $CHCl_3$); **HRMS** Accurate mass (ES^+): Found 465.3413 (2.8 ppm), $C_{27}H_{49}O_4Si$ ($M+H^+$) requires 465.3400.

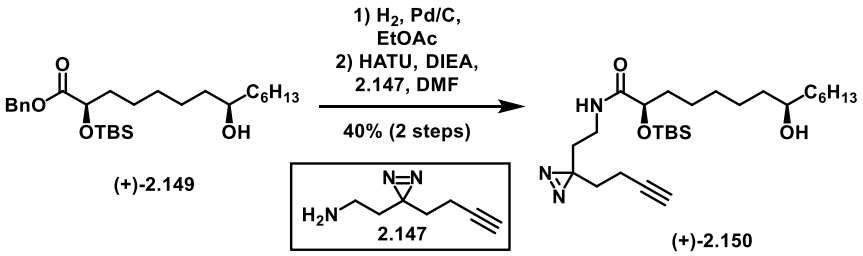

(2R,8R)-N-(2-(3-(but-3-yn-1-yl)-3H-diazirin-3-yl)ethyl)-2-((tert-butyldimethylsilyl)oxy)-8-hydroxytetradecanamide (+)-2.150. To a solution of benzyl ester **(+)-2.149** (43 mg, 0.093 mmol) dissolved in EtOAc (2 mL) was added 10% Pd/C (20 mg), and the reaction flask was vacuumed and backfilled 5x with a balloon of H_2. The reaction was closely monitored by TLC, and after 2 hours, the starting material was consumed. The reaction was filtered over Celite and concentrated (*the acid intermediate, in particular the silyl ether moiety, was highly unstable, and cleavage was observed in as little as an hour)* and immediately used in the next step. The acid was dissolved in DMF (1 mL), and HATU (42 mg, 0.112 mmol) was added as a solid, followed by a solution of amine **2.147** (14 mg, 0.102 mmol) dissolved in DMF (1 mL), then DIEA (0.05 mL, 0.279 mmol) was added, and the reaction was stirred at room temperature overnight. The following day, the reaction was poured into water and EtOAc, and the layers were separated. The aqueous layer was extracted 2x more with EtOAc and the combined organic layers were washed with water and brine, concentrated, and purified by column chromatography, yielding the title compound as a yellow oil (18 mg, 40% over 2 steps). **^{1}H NMR** (500 MHz, $CDCl_3$) δ 6.63 (t, J = 5.5 Hz, 1H), 4.15 – 4.09 (m, 1H), 3.56 (s, 1H), 3.16 – 3.06 (m, 2H), 2.06 – 1.95 (m, 3H), 1.79 – 1.61 (m, 6H), 1.47 – 1.21 (m, 19H), 0.94 (s, 9H), 0.88 (t, J = 6.7 Hz, 3H), 0.10 (d, J = 7.0 Hz, 6H); **$[\alpha]^{25}_D$** +12.2 (c

= 0.81 in $CHCl_3$); **^{13}C NMR** (100 MHz, $CDCl_3$) δ 173.99, 82.62, 73.48, 72.00, 69.49, 37.60, 37.48, 35.18, 33.80, 32.79, 32.35, 31.96, 29.70, 29.49, 26.84, 25.90, 25.74, 25.60, 24.13, 22.74, 18.16, 14.21, 13.38, -4.66, -5.04; **HRMS** Accurate mass (ES^+): Found 494.3801 (+4.7 ppm), $C_{27}H_{52}N_3O_3Si$ ($M+H^+$) requires 494.3778.

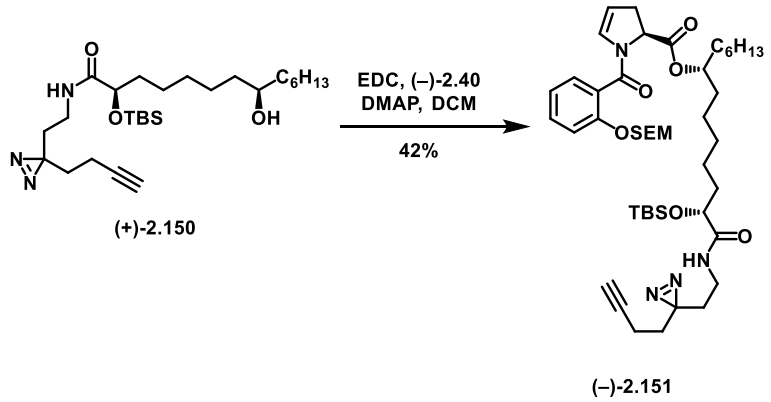

(–)-2.151

(7R,13R)-14-((2-(3-(but-3-yn-1-yl)-3H-diazirin-3-yl)ethyl)amino)-13-((tert-butyldimethylsilyl)oxy)-14-oxotetradecan-7-yl (S)-1-(2-((2-methoxyethoxy)methoxy)benzoyl)-2,3-dihydro-1H-pyrrole-2-carboxylate (–)-2.151. Following modified general procedure J; acid **(–)-2.40** (33 mg, 0.091 mmol), alcohol **(+)-2.150** (28 mg, 0.057 mmol), EDC (20 mg, 0.114 mmol) and DMAP (3 mg, 0.029 mmol) yielded the title compound as a yellow oil (20 mg, 42% yield). **^{1}H NMR** (500 MHz, $CDCl_3$) δ 7.37 – 7.32 (m, 2H), 7.19 (d, J = 8.0 Hz, 1H), 7.03 (t, J = 7.5 Hz, 1H), 6.64 (t, J = 5.9 Hz, 1H), 6.16 (dt, J = 4.2, 2.0 Hz, 1H), 5.22 (dd, J = 18.2, 7.1 Hz, 2H), 5.01 (dt, J = 4.7, 2.5 Hz, 1H), 4.99 – 4.91 (m, 2H), 4.12 (t, J = 5.0 Hz, 1H), 3.76 – 3.70 (m, 2H), 3.18 – 3.02 (m, 3H), 2.70 – 2.61 (m, 1H), 2.02 – 1.96 (m, 3H), 1.78 – 1.16 (m, 26H), 0.92 (s, 9H), 0.86 (t, J = 6.7 Hz, 3H), 0.08 (s, 3H), 0.07 (s, 3H), -0.02 (s, J = 9H); **^{13}C NMR** (126 MHz, CDCl3) δ 173.95, 170.78, 164.95, 153.86, 131.22, 131.08, 129.03, 126.02, 121.98, 115.25, 108.29, 93.37, 82.64, 75.50, 73.55, 69.49, 66.62, 58.22, 35.26, 34.42, 34.11, 33.82, 32.83, 32.35, 31.86, 29.82, 29.62, 29.33, 26.84, 25.93, 25.32, 25.14, 24.09, 22.72, 18.17, 14.20, 13.39, -1.27, -4.64, -5.03; **$[\alpha]^{25}_D$** −16.3 (c = 1.00 in $CHCl_3$); **HRMS** Accurate mass (ES^+): Found 839.5166 (-1.0 ppm), $C_{45}H_{76}N_4O_7Si_2$ ($M+H^+$) requires 839.5174.

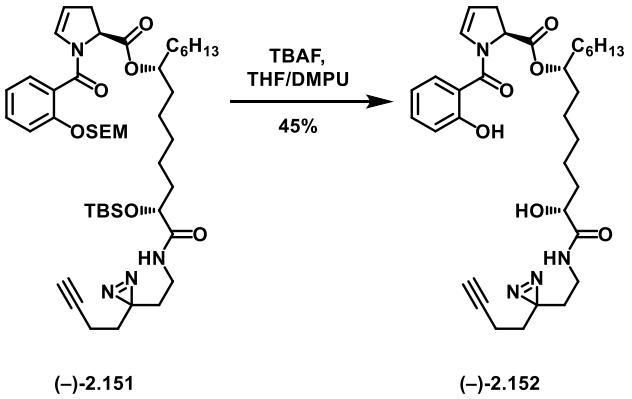

(–)-2.151 (–)-2.152

(7R,13R)-14-((2-(3-(but-3-yn-1-yl)-3H-diazirin-3-yl)ethyl)amino)-13-hydroxy-14-oxotetradecan-7-yl (S)-1-(2-hydroxybenzoyl)-2,3-dihydro-1H-pyrrole-2-carboxylate (–)-2.152. Following general procedure L; silyl ether **(–)-2.159** (13 mg, 0.015 mmol) yielded the title compound as a clear oil (4.0 mg, 45% yield). **^{1}H NMR** (500 MHz, $CDCl_3$) δ 9.54 (br s, 1H), 7.43 – 7.35 (m, 2H), 6.98 (t, J = 10.1 Hz, 1H), 6.91 (t, J = 7.5 Hz, 1H), 6.73 (s, 1H), 5.31 – 5.25 (m, 1H), 5.01 (dd, J = 11.2, 4.4 Hz, 1H), 4.07 (dd, J = 8.0, 3.4 Hz, 1H), 3.30 (br s, 1H), 3.18 – 3.03 (m, 3H), 2.70 (d, J = 17.0 Hz, 1H), 2.02 – 1.94 (m, 3H), 1.80 (s, 1H), 1.71 – 1.11 (m, 25H), 0.87 (t, J = 6.9 Hz, 3H); **^{13}C NMR** (100 MHz, $CDCl_3$) δ 174.21, 171.24, 167.42, 158.14, 133.54, 130.86, 128.34, 119.41, 118.03, 117.65, 111.14, 82.80, 75.98, 71.60, 69.49, 59.39, 34.52, 34.33, 34.09, 32.77, 32.21, 31.83, 29.84, 29.22, 28.30, 26.89, 25.51, 24.84, 24.57, 22.69, 14.21, 13.38; **$[\alpha]^{25}_{D}$** −28.4 (c = 0.52 in $CHCl_3$); **HRMS** Accurate mass (ES^+): Found 595.3523 (+4.5 ppm), $C_{33}H_{47}N_4O_6$ ($M+H^+$) requires 595.3496.

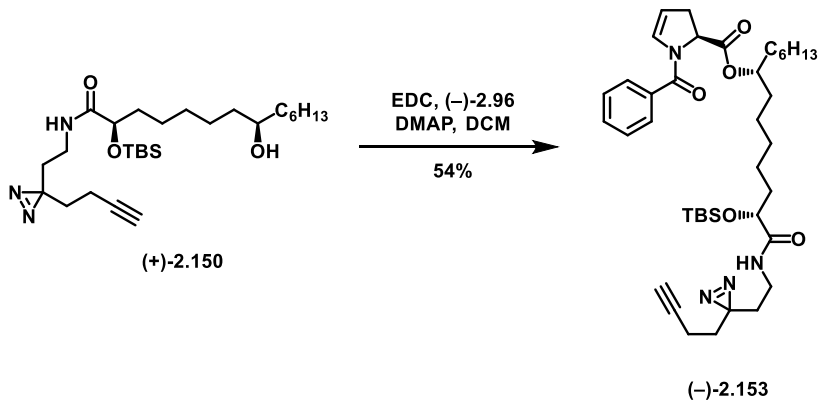

(7R,13R)-14-((2-(3-(but-3-yn-1-yl)-3H-diazirin-3-yl)ethyl)amino)-13-((tert-butyldimethylsilyl)oxy)-14-oxotetradecan-7-yl (S)-1-benzoyl-2,3-dihydro-1H-pyrrole-2-carboxylate (–)-2.153. Following modified general procedure J; acid **(–)-2.96** (22 mg, 0.101 mmol), alcohol **(+)-S7** (25 mg, 0.051 mmol), EDC (19 mg, 0.101 mmol) and DMAP (3 mg, 0.026 mmol), yielded the title compound as a yellow oil (19 mg, 54% yield). **^{1}H NMR** (500 MHz, $CDCl_3$) δ 7.55 (d, J = 6.9 Hz, 2H), 7.48 – 7.39 (m, 3H), 6.65 (t, J = 6.0 Hz, 1H), 6.51 (s, 1H), 5.10 (s, 1H), 5.02 – 4.90 (m, 1H), 4.12 (t, J = 4.9 Hz, 1H), 3.17 – 3.02 (m, 3H), 2.75 – 2.63 (m, 1H), 2.04 – 1.96 (m, 2H), 1.74 – 1.50 (m, 12H), 1.41 – 1.15 (m, 14H), 0.93 (s, 9H), 0.85 (t, J = 6.8 Hz, 3H), 0.08 (d, J = 5.8 Hz, 6H); **^{13}C NMR** (125 MHz, $CDCl_3$) δ 173.97, 170.88, 166.96, 135.27, 131.05, 130.72, 128.55, 127.93, 108.84, 82.63, 75.64, 73.53, 69.49, 58.80, 35.23, 34.07, 33.81, 32.81, 32.33, 31.83, 29.60, 29.30, 26.84, 25.92, 25.27, 25.13, 24.07, 22.69, 18.17, 14.19, 13.39, -4.65, -5.04; **$[\alpha]^{25}_{D}$** –26.6 (c = 1.36 in $CHCl_3$); **HRMS** Accurate mass (ES^+): Found 693.4409 (-0.3 ppm), $C_{39}H_{61}N_4O_5Si$ ($M+H^+$) requires 693.4411; **R_f** (9:1 CH_2Cl_2:Et_2O) = 0.50.

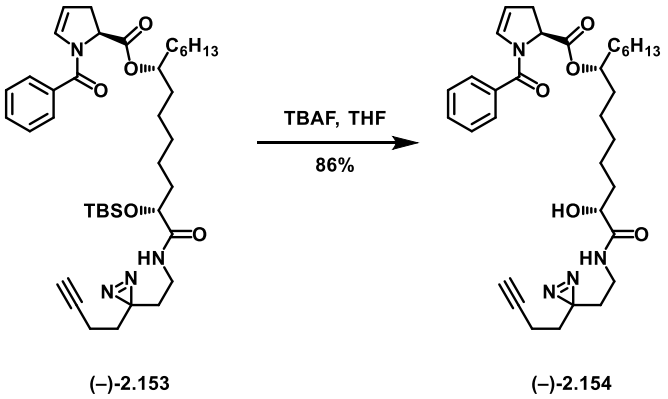

(–)-2.153 (–)-2.154

(7R,13R)-14-((2-(3-(but-3-yn-1-yl)-3H-diazirin-3-yl)ethyl)amino)-13-hydroxy-14-oxotetradecan-7-yl (S)-1-benzoyl-2,3-dihydro-1H-pyrrole-2-carboxylate (–)-2.154. To a solution of silyl ether **(–)-2.153** (18 mg, 0.026 mmol) in THF (1 mL) was added TBAF (1M in THF, 0.03 mL, 0.03 mmol). After 15 minutes the reaction was quenched with sat. NH_4Cl, and the mixture was extracted with EtOAc 3x, washed with brine, dried over Na_2SO_4, filtered, concentrated, and purified by column chromatography, yielding the title compound as a clear oil (13 mg, 86% yield). **^{1}H NMR** (500 MHz, $CDCl_3$) δ 7.56 – 7.42 (m, 5H), 6.89 (t, J = 5.9 Hz, 1H), 6.50 (dt, J = 4.3, 2.1 Hz, 1H), 5.18 – 5.14 (m, 1H), 5.04 (qd, J = 8.4, 4.2 Hz, 1H), 4.96 (dd, J = 11.6, 5.0 Hz, 1H), 4.02 (dd, J = 8.5, 3.3 Hz, 1H), 3.14 (ddt, J = 16.7, 11.6, 2.4 Hz, 2H), 2.92 (dd, J = 13.3, 7.1 Hz, 2H), 2.73 – 2.64 (m, 1H), 1.99 – 1.94 (m, 3H), 1.86 – 1.77 (m, 1H), 1.68 – 1.38 (m, 16H), 1.34 – 1.19 (m, 8H), 0.87 (t, J = 7.0 Hz, 3H); **^{13}C NMR** (125 MHz, $CDCl_3$) δ 174.74, 170.53, 167.80, 134.73, 131.12, 130.81, 128.78, 127.83, 125.66, 110.03, 82.77, 75.19, 70.85, 69.42, 58.61, 34.77, 34.00, 33.91, 33.67, 32.79, 32.20, 31.84, 30.44, 29.25, 27.50, 26.82, 25.59, 24.67, 24.26, 22.69, 14.20, 13.37; **$[\alpha]^{25}_D$** –25.1 (c = 0.49 in $CHCl_3$); **HRMS** Accurate mass (ES^+): Found 579.3558 (+2.1 ppm), $C_{33}H_{47}N_4O_5$ ($M+H^+$) requires 579.3546.

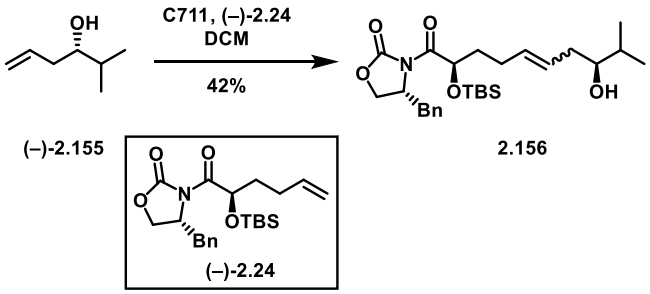

(R)-4-benzyl-3-((2R,8S,E)-2-((tert-butyldimethylsilyl)oxy)-8-hydroxy-9-methyldec-5-enoyl)oxazolidin-2-one (2.156). Following general procedure A, homoallylic alcohol **(–)-2.155** (0.546 g, 01.35 mmol) yielded the title compound as a brown oil (0.278 g, 42% yield). **^{1}H NMR** (500 MHz, $CDCl_3$ mixture of *E*/*Z* isomers) δ 7.36 – 7.31 (m, 2H), 7.31 – 7.27 (m, 1H), 7.25 – 7.22 (m, 2H), 5.63 – 5.52 (m, 1H), 5.51 – 5.43 (m, 1H), 5.37 (dd, *J* = 8.4, 3.3 Hz, 1H), 4.66 – 4.58 (m, 1H), 4.24 – 4.14 (m, 2H), 3.43 – 3.31 (m, 2H), 2.74 – 2.65 (m, 1H), 2.29 – 2.14 (m, 3H), 2.08 – 2.00 (m, 1H), 1.82 – 1.61 (m, 4H), 0.94 (d, *J* = 1.6 Hz, 9H), 0.92 (dd, *J* = 9.7, 6.8 Hz, 6H), 0.11 (d, *J* = 3.6 Hz, 3H), 0.09 (d, *J* = 3.6 Hz, 3H).; **^{13}C NMR** (126 MHz, $CDCl_3$) δ 174.44, 153.24, 135.35, 132.89, 129.58, 129.13, 127.74, 127.53, 75.64, 70.86, 66.69, 55.75, 55.74, 37.84, 37.72, 35.27, 33.16, 28.56, 25.95, 18.88, 18.45, 17.81, -4.44, -4.92.; **IR** (film) 3538 (br O-H), 2955, 2928, 2856, 1778 (C=O), 1710 (C=O), 1471, 1387, 1348, 1249, 1210, 1196, 1109, 1006 ,972, 836, 777, 701; **HRMS** Accurate mass (ES^+): Found 490.2989, $C_{27}H_{44}NO_5Si$ (M+H) requires 490.2989.

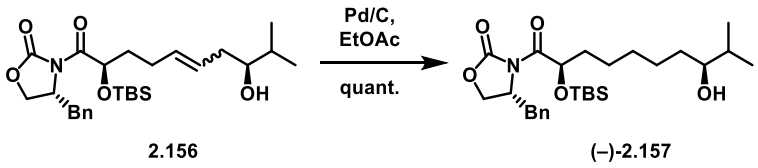

(R)-4-benzyl-3-((2R,8S)-2-((tert-butyldimethylsilyl)oxy)-8-hydroxy-9-methyldecanoyl)oxazolidin-2-one (–)-2.157. Following general procedure B, alkene **2.156** (278 mg, 0.568 mmol) yielded the title compound as a clear oil (281 mg, quant.). **^{1}H NMR** (500 MHz, $CDCl_3$) δ 7.36 – 7.32 (m, 2H), 7.30 – 7.27 (m, 1H), 7.25 – 7.23 (m, 2H), 5.36 (dd, *J* = 8.3, 3.3 Hz, 1H), 4.62 (qd, *J* = 6.3, 3.0 Hz, 1H), 4.24 – 4.14 (m, 2H), 3.40 (dd, *J* = 13.3, 3.2 Hz, 1H), 3.34 (ddd, *J* = 8.3, 5.0, 3.1 Hz, 1H), 2.70 (dd, *J* = 13.3, 10.1 Hz, 1H),

1.72 – 1.59 (m, 3H), 1.56 – 1.42 (m, 5H), 1.41 – 1.27 (m, *J* = 18.1, 14.4, 8.0, 4.1 Hz, 4H), 0.94 (s, 9H), 0.90 (t, *J* = 6.5 Hz, 6H), 0.11 (s, 3H), 0.09 (s, 3H).; **^{13}C NMR** (126 MHz, $CDCl_3$) δ 174.53, 153.24, 135.37, 129.55, 129.10, 127.49, 71.44, 66.63, 55.72, 37.83, 35.26, 34.14, 33.60, 29.35, 25.94, 25.92, 25.57, 18.97, 18.46, 17.20, -4.50, -4.96.; **$[\alpha]^{25}_D$** -2.7 (c = 0.51 in $CHCl_3$);**IR** (film) 3522 (br O-H), 2928, 2856, 1779 (C=O), 1710 (C=O), 1462, 1387, 1348, 1249, 1210, 1195, 1107, 1007, 976, 835, 777, 701; **HRMS** Accurate mass (ES^+): Found 492.3135, $C_{27}H_{46}NO_5Si$ (M+H) requires 492.3145.

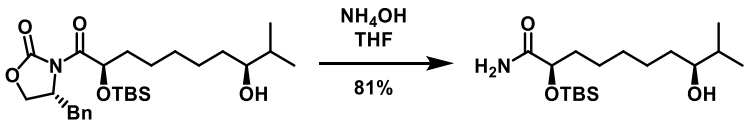

(–)-2.157 (+)-2.158

(2R,8S)-2-((tert-butyldimethylsilyl)oxy)-8-hydroxy-9-methyldecanamide (+)-2.158. Following general procedure C, oxazolidinone **(–)-2.157** (84 mg, 0.171 mmol) yielded the title compound as a clear oil (46 mg, 81% yield). **^{1}H NMR** (500 MHz, $CDCl_3$) δ 6.52 (d, *J* = 4.6 Hz, 1H), 5.94 (d, *J* = 4.5 Hz, 1H), 4.15 – 4.10 (m, 1H), 3.36 – 3.30 (m, 1H), 1.81 – 1.71 (m, 1H), 1.70 – 1.58 (m, 2H), 1.49 – 1.40 (m, 3H), 1.40 – 1.26 (m, 6H), 0.91 (d, *J* = 0.8 Hz, 9H), 0.89 (dd, *J* = 6.8, 5.5 Hz, 6H), 0.09 (s, 3H), 0.08 (s, 3H).; **^{13}C NMR** (126 MHz, $cdcl_3$) δ 177.24, 76.75, 73.57, 35.23, 34.16, 33.58, 29.73, 25.99, 25.86, 24.27, 18.99, 18.14, 17.21, -4.71, -5.12.; **$[\alpha]^{25}_D$** +2.3 (c = 0.85 in $CHCl_3$); **IR** (film) 3478 (N-H), 3350 (br O-H), 2928, 2857, 1680 (C=O), 1583, 1463, 1388, 1361, 1253, 1101, 1005, 835, 777, 669; **HRMS** Accurate mass (ES^+): Found 332.2615, $C_{17}H_{38}NO_3Si$ (M+H) requires 332.2621.

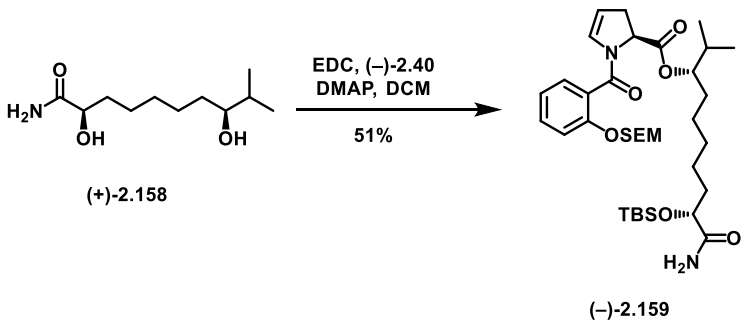

(3S,9R)-10-amino-9-((tert-butyldimethylsilyl)oxy)-2-methyl-10-oxodecan-3-yl (S)-1-(2-((2-(trimethylsilyl)ethoxy)methoxy)benzoyl)-2,3-dihydro-1H-pyrrole-2-carboxylate (–)-2.159. Following general procedure J, alcohol **(+)-2.158** (34 mg, 0.102 mmol) yielded the title compound as a clear oil (35 mg, 51% yield). **^{1}H NMR** (500 MHz, $CDCl_3$) δ 7.37 – 7.33 (m, 2H), 7.20 (dd, *J* = 8.9, 1.0 Hz, 1H), 7.03 (td, *J* = 7.5, 1.0 Hz, 1H), 6.52 (d, *J* = 4.6 Hz, 1H), 6.18 – 6.14 (m, 1H), 5.62 (d, *J* = 4.6 Hz, 1H), 5.26 – 5.18 (m, 2H), 5.05 – 4.99 (m, 2H), 4.86 – 4.81 (m, 1H), 4.11 (t, *J* = 5.1 Hz, 1H), 3.76 – 3.71 (m, 2H), 3.17 – 3.08 (m, 1H), 2.73 – 2.65 (m, 1H), 1.91 – 1.83 (m, 1H), 1.76 – 1.70 (m, 1H), 1.69 – 1.61 (m, 1H), 1.59 – 1.49 (m, 2H), 1.44 – 1.22 (m, 7H), 0.95 – 0.92 (m, 6H), 0.91 (s, 9H), 0.78 (dd, *J* = 14.2, 6.8 Hz, 1H), 0.08 (s, 3H), 0.07 (s, 3H), -0.01 (s, 9H).; **^{13}C NMR** (126 MHz, $CDCl_3$) δ 176.97, 170.96, 164.96, 153.92, 131.24, 131.07, 129.03, 125.98, 121.98, 115.27, 110.14, 108.34, 93.38, 79.59, 73.62, 66.63, 58.33, 35.16, 34.53, 31.40, 31.03, 29.54, 25.88, 25.24, 24.15, 18.69, 18.18, 17.70, -1.27, -4.71, -5.13.; **$[\alpha]^{25}_{D}$** -3.5 (c = 1.30 in $CHCl_3$); **IR** (film) 3481 (N-H), 2929, 2857, 1734 (C=O), 1688 (C=O), 1649 (C=O), 1455, 1406, 1249, 1195, 1087, 988, 835, 778, 755, 731, 696; **HRMS** Accurate mass (ES^+): Found 677.4009, $C_{35}H_{61}N_2O_7Si_2$ (M+H) requires 677.4017.

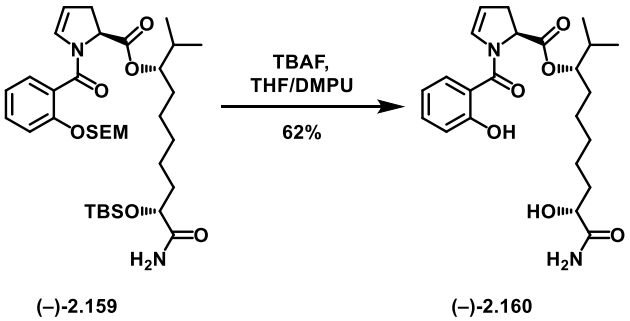

(3S,9R)-10-amino-9-hydroxy-2-methyl-10-oxodecan-3-yl (S)-1-(2-hydroxybenzoyl)-2,3-dihydro-1H-pyrrole-2-carboxylate (–)-2.160. Following general procedure L, silyl ether **(–)-2.159** (18 mg, 0.026 mmol) yielded the title compound as a clear oil (7 mg, 62% yield). **^{1}H NMR** (600 MHz, $CDCl_3$) δ 9.48 (s, 1H), 7.41 – 7.34 (m, 2H), 6.99 (d, *J* = 7.6 Hz, 1H), 6.91 (t, *J* = 7.1 Hz, 1H), 6.71 (s, 1H), 6.61 (s, 1H), 5.40 (s, 1H), 5.32 – 5.24 (m, 1H), 5.04 (dd, *J* = 11.3, 4.7 Hz, 1H), 4.88 (s, 1H), 4.13 – 4.06 (m, 1H), 3.44 (s, 1H), 3.19 – 3.11 (m, 1H), 2.72 (d, *J* = 17.1 Hz, 1H), 1.89 – 1.76 (m, 2H), 1.71 – 1.61 (m, 4H), 1.52 – 1.37 (m, 5H), 0.91 (d, *J* = 6.7 Hz, 6H).; **^{13}C NMR** (151 MHz, $CDCl_3$) δ 177.03, 171.42, 167.41, 157.89, 133.50, 130.86, 128.31, 119.48, 118.03, 117.85, 111.11, 80.29, 71.35, 59.34, 34.26, 31.97, 31.30, 29.84, 28.38, 25.08, 24.60, 18.84, 17.86.; **[α]$^{25}_D$** -50.7 (c = 0.71 in $CHCl_3$); **IR** (film) 3338 (br O-H), 2927, 2859, 1729 (C=O), 1664 (C=O), 1594 (C=O), 1459, 1428, 1377, 1294, 1198, 1153, 1110, 1015, 945, 859, 817, 755, 727, 653, 617; **HRMS** Accurate mass (ES$^+$): Found 433.2330, $C_{23}H_{33}N_2O_6$ (M+H) requires 433.2339.

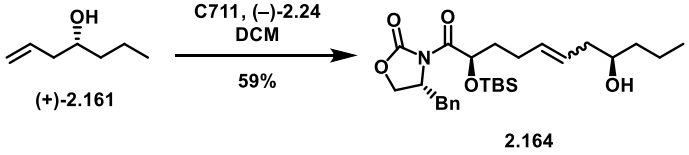

(R)-4-benzyl-3-((2R,8R)-2-((tert-butyldimethylsilyl)oxy)-8-hydroxyundec-5-enoyl)oxazolidin-2-one (2.164). Following general procedure A, homoallylic alcohol **(+)-2.161** (460 mg, 3.85 mmol) yielded the title compound as a brown oil (222 mg, 59% yield). **^{1}H NMR** (400 MHz, $CDCl_3$, mixture of E/Z isomers) δ 7.37 – 7.30 (m, *J* = 7.5 Hz, 3H), 7.25 – 7.20 (m, *J* = 6.8 Hz, 3H), 5.63 – 5.40 (m, *J* = 20.5 Hz, 2H), 5.37 (dd, *J* = 8.3, 3.4 Hz, 1H), 4.70 – 4.54 (m, *J* = 3.1 Hz, 1H), 4.25 – 4.13 (m, 2H), 3.60 (s, 1H), 3.39 (dd, *J* = 13.2, 3.1 Hz, 1H), 2.68 (dd, *J* = 13.2, 10.2 Hz, 1H), 2.22 (s, 3H), 2.11 – 1.99 (m, 1H), 1.87 – 1.66 (m, 3H),

1.48 – 1.36 (m, 4H), 0.94 (s, 9H), 0.91 (s, 3H), 0.10 (s, 3H), 0.09 (s, 3H); **^{13}C NMR** (100 MHz, $CDCl_3$) δ 174.41, 153.20, 135.27, 132.93, 129.54, 129.08, 127.48, 127.24, 70.79, 70.58, 66.65, 55.68, 40.82, 39.00, 37.75, 35.17, 28.53, 25.91, 19.02, 18.42, 14.23, -4.48, -4.96; **IR** (film) 3514 (br O-H), 2954, 2856, 1778 (C=O), 1710 (C=O), 1388, 1348, 1249, 1209, 1108, 1011 ,971, 835, 776, 700; **HRMS** Accurate mass (ES^+): Found 490.2985, $C_{27}H_{44}NO_5Si$ (M+H) requires 490.2989.

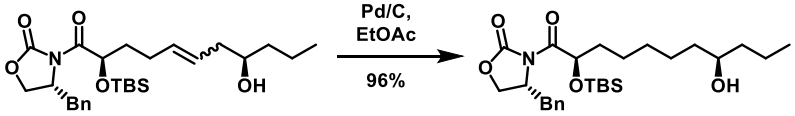

(R)-4-benzyl-3-((2R,8R)-2-((tert-butyldimethylsilyl)oxy)-8-hydroxyundecanoyl)oxazolidin-2-one (–)-2.167. Following general procedure B, alkene **2.164** (80 mg, 0.16 mmol) yielded the title compound as a clear oil (76 mg, 96% yield). **^{1}H NMR** (400 MHz, $CDCl_3$) δ 7.41 – 7.20 (m, 6H), 5.40 – 5.32 (m, 1H), 4.62 (ddt, *J* = 10.1, 6.6, 3.1 Hz, 1H), 4.25 – 4.14 (m, 2H), 3.59 (d, *J* = 4.2 Hz, 1H), 3.40 (dd, *J* = 13.2, 3.2 Hz, 1H), 2.69 (dd, *J* = 13.2, 10.2 Hz, 1H), 1.82 – 1.18 (m, 16H), 0.94 (s, 7H), 0.93 – 0.88 (m, 3H), 0.11 (s, 2H), 0.09 (s, 2H); **^{13}C NMR** (100 MHz, $CDCl_3$) δ 174.51, 153.22, 135.31, 129.53, 129.06, 127.46, 71.71, 71.39, 66.60, 55.67, 39.76, 37.76, 37.43, 35.21, 29.29, 25.90, 25.55, 25.50, 18.91, 18.43, 14.23, -4.54, -5.00; **$[\alpha]^{25}_D$** -1.7 (c = 0.59 in $CHCl_3$); **IR** (film) 3572 (br O-H), 2928, 2856, 1778 (C=O), 1710 (C=O), 1389, 1348, 1248, 1210, 1195, 1105, 1006, 976, 835, 776, 700; **HRMS** Accurate mass (ES^+): Found 492.3145, $C_{27}H_{46}NO_5Si$ (M+H) requires 492.3145.

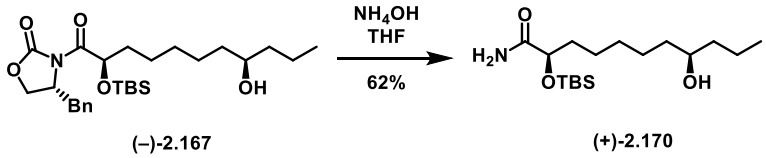

(2R,8R)-2-((tert-butyldimethylsilyl)oxy)-8-hydroxyundecanamide (+)-2.170. Following general procedure C, oxazolidinone **(–)-2.167** (70 mg, 0.14 mmol) yielded the title compound as a clear oil (29 mg, 62% yield). **^{1}H NMR** (600 MHz, $CDCl_3$) δ 6.51 (d, *J* = 4.6 Hz, 1H), 5.96 (d, *J* = 5.1 Hz, 1H), 4.12 (dd, *J* = 5.7, 4.6 Hz, 1H), 3.60 – 3.54 (m, 1H), 1.79 – 1.71 (m, 1H), 1.69 – 1.62 (m, 1H), 1.46 – 1.35 (m, 7H), 1.36

– 1.26 (m, 5H), 0.91 (s, 9H), 0.91 (t, *J* = 6.6 Hz, 3H), 0.09 (s, 3H), 0.07 (s, 3H).; **^{13}C NMR** (151 MHz, $CDCl_3$) δ 177.29, 73.54, 71.69, 39.78, 37.49, 35.18, 29.67, 25.85, 25.58, 24.23, 18.95, 18.13, 14.24, -4.71, -5.13.**; [α]$^{25}_{D}$** +57.8 (c = 0.45 in $CHCl_3$); **IR** (film) 3479 (N-H), 3300 (br O-H), 2928, 2857, 1680 (C=O), 1582, 1463, 1389, 1361, 1339, 1253, 1096, 1005, 835, 777, 668; **HRMS** Accurate mass (ES^+): Found 332.2613, $C_{17}H_{38}NO_3Si$ (M+H) requires 332.2621.

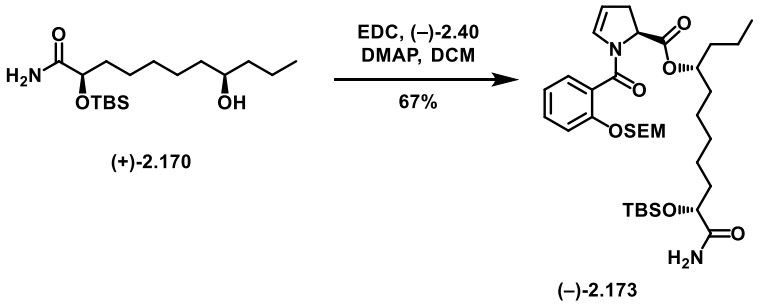

(4R,10R)-11-amino-10-((tert-butyldimethylsilyl)oxy)-11-oxoundecan-4-yl (S)-1-(2-((2-(trimethylsilyl)ethoxy)methoxy)benzoyl)-2,3-dihydro-1H-pyrrole-2-carboxylate (–)-2.173. Following general procedure J, alcohol **(+)-2.170** (34 mg, 0.103 mmol) yielded the title compound as a clear oil (30 mg, 67% yield). **^{1}H NMR** (600 MHz, $CDCl_3$) δ 7.37 – 7.31 (m, 2H), 7.19 (d, *J* = 8.3 Hz, 1H), 7.04 (t, *J* = 7.4 Hz, 1H), 6.53 (dd, *J* = 15.8, 4.6 Hz, 1H), 6.18 – 6.13 (m, 1H), 5.55 (s, 1H), 5.23 (q, 2H), 5.04 – 4.93 (m, 3H), 4.12 (t, *J* = 5.3 Hz, 1H), 3.74 (t, *J* = 8.3 Hz, 2H), 3.17 – 3.06 (m, 2H), 2.71 – 2.61 (m, 1H), 1.79 – 1.62 (m, 3H), 1.61 – 1.54 (m, 3H), 1.54 – 1.46 (m, 1H), 1.43 – 1.27 (m, 7H), 1.24 – 1.10 (m, 1H), 0.96 – 0.92 (m, 2H), 0.93 – 0.88 (m, 11H), 0.08 (s, 3H), 0.07 (s, 3H), -0.01 (s, 9H).; **^{13}C NMR** (151 MHz, $CDCl_3$) δ 176.97, 170.81, 165.00, 153.87, 131.23, 131.06, 129.00, 126.01, 122.00, 115.28, 108.37, 93.38, 75.23, 73.60, 66.64, 58.24, 36.30, 35.14, 34.44, 34.11, 29.50, 25.88, 25.07, 24.13, 18.66, 18.19, 18.15, 14.14, -1.27, -4.69, -5.12.; **[α]$^{25}_{D}$** -29.5 (c = 0.39 in $CHCl_3$); **IR** (film) 3480 (N-H), 2928, 2857, 1738 (C=O), 1687 (C=O), 1649 (C=O), 1454, 1407, 1249, 1194, 1087, 988, 834, 778, 754, 696; **HRMS** Accurate mass (ES^+): Found 677.4020, $C_{35}H_{61}N_2O_7Si_2$ (M+H) requires 677.4017.

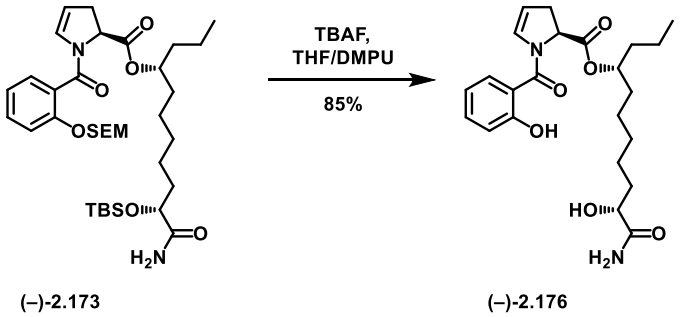

(–)-2.173 (–)-2.176

(4R,10R)-11-amino-10-hydroxy-11-oxoundecan-4-yl (S)-1-(2-hydroxybenzoyl)-2,3-dihydro-1H-pyrrole-2-carboxylate (–)-2.176. Following general procedure L, silyl ether **(–)-2.173** (17 mg, 0.025 mmol) yielded the title compound as a clear oil (9.2 mg, 85% yield). **^{1}H NMR** (400 MHz, $CDCl_3$) δ 9.51 (s, 1H), 7.42 – 7.33 (m, 2H), 6.99 (d, *J* = 8.2 Hz, 1H), 6.94 – 6.87 (m, 1H), 6.71 (s, 1H), 6.61 (s, 1H), 5.41 (s, 1H), 5.30 – 5.26 (m, 1H), 5.09 – 4.97 (m, 2H), 4.14 – 4.05 (m, 1H), 3.46 (s, 1H), 3.20 – 3.07 (m, 1H), 2.70 (d, *J* = 16.9 Hz, 1H), 1.86 – 1.75 (m, 1H), 1.71 – 1.65 (m, 2H), 1.64 – 1.55 (m, 3H), 1.51 – 1.38 (m, 5H), 1.36 – 1.27 (m, 3H), 0.90 (t, *J* = 7.3 Hz, 3H).; **^{13}C NMR** (151 MHz, $CDCl_3$) δ 176.97, 171.32, 167.42, 158.02, 133.49, 130.86, 128.32, 119.42, 118.02, 117.78, 111.08, 75.76, 71.42, 64.53, 59.34, 36.70, 34.33, 34.21, 28.35, 24.83, 24.57, 18.85, 14.03.; **$[\alpha]^{25}_D$** -72.8 (c = 0.32 in $CHCl_3$); **IR** (film) 3338 (br O-H), 2927, 2859, 1729 (C=O), 1664 (C=O), 1594 (C=O), 1459, 1428, 1377, 1294, 1198, 1153, 1110, 1015, 945, 859, 817, 755, 727, 653, 617; **HRMS** Accurate mass (ES^+): Found 433.2329, $C_{23}H_{33}N_2O_6$ (M+H) requires 433.2339.

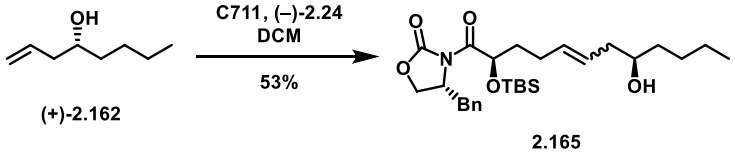

(+)-2.162 2.165

(R)-4-benzyl-3-((2R,8R,E)-2-((tert-butyldimethylsilyl)oxy)-8-hydroxydodec-5-enoyl)oxazolidin-2-one (2.165). Following general procedure A, homoallylic alcohol **(+)2.162** (385 mg, 3.0 mmol) yielded the title compound as a brown oil (161 mg, 53% yield). **^{1}H NMR** (400 MHz, $CDCl_3$, mixture of E/Z isomers) 7.33 (d, *J* = 7.5 Hz, 2H), 7.31 – 7.27 (m, 1H), 7.23 (s, 2H). 5.64 – 5.41 (m, *J* = 22.6, 15.4, 6.9 Hz, 2H), 5.37 (dd, *J* = 8.3, 3.4 Hz, 1H), 4.68 – 4.56 (m, 1H), 4.24 – 4.13 (m, 2H), 3.59 (s, 1H), 3.40 (dd, *J* = 13.2, 2.9 Hz,

1H), 2.68 (dd, *J* = 13.2, 10.2 Hz, 1H), 2.32 – 2.13 (m, *J* = 19.7, 12.2 Hz, 3H), 2.11 – 2.00 (m, 1H), 1.77 – 1.64 (m, 2H), 1.49 – 1.40 (m, *J* = 3.9, 2.3 Hz, 3H), 1.38 – 1.24 (m, 5H), 0.94 (s, *J* = 1.5 Hz, 9H), 0.92 – 0.87 (m, *J* = 9.5, 5.2 Hz, 3H), 0.11 (s, 3H), 0.09 (s, 3H); **^{13}C NMR** (101 MHz, $CDCl_3$) δ 174.35, 153.14, 135.21, 132.79, 129.48, 129.01, 127.42, 127.22, 70.80, 70.72, 66.59, 55.61, 40.75, 37.68, 36.47, 35.12, 28.47, 27.96, 25.85, 22.79, 18.35, 14.16, -4.54, -5.01; **IR** (film) 3514 (br O-H), 2954, 2856, 1778 (C=O), 1710 (C=O), 1389, 1348, 1249, 1209, 1110, 1007 ,971, 836, 777, 700; **HRMS** Accurate mass (ES^+): Found 504.31431 (+0.43 ppm), $C_{28}H_{46}NO_5Si$ ($M+H^+$) requires 504.314527.

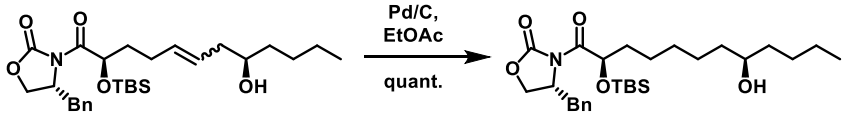

2.165 (–)-2.168

(R)-4-benzyl-3-((2R,8R)-2-((tert-butyldimethylsilyl)oxy)-8-hydroxydodecanoyl)oxazolidin-2-one (–)-2.168. Following general procedure B, alkene **2.165** (155 mg, 0.31 mmol) yielded the title compound as a clear oil (155 mg, quant.). **^{1}H NMR** (400 MHz, cdcl$_3$) δ 7.42 – 7.19 (m, 5H), 5.36 (dd, *J* = 8.3, 3.4 Hz, 1H), 4.62 (qd, *J* = 6.5, 3.1 Hz, 1H), 4.26 – 4.15 (m, 2H), 3.58 (s, 1H), 3.45 – 3.36 (m, 1H), 2.69 (dd, *J* = 13.2, 10.2 Hz, 1H), 1.75 – 1.59 (m, 2H), 1.55 – 1.19 (m, 15H), 0.97 – 0.92 (m, 9H), 0.90 (ddd, *J* = 9.6, 4.1, 2.1 Hz, 3H), 0.10 (s, 3H), 0.09 (s, 3H); **^{13}C NMR** (100 MHz, cdcl$_3$) δ 174.40, 153.12, 135.23, 129.43, 128.95, 127.35, 71.78, 71.30, 66.50, 55.56, 37.64, 37.31, 37.18, 35.11, 29.20, 27.83, 25.82, 25.46, 25.42, 22.77, 18.33, 14.11, -4.63, -5.09; **[α]$^{25}_D$** -2.3 (c = 0.7 in $CHCl_3$); **IR** (film) 3572 (br O-H), 2927, 2856, 1779 (C=O), 1710 (C=O), 1389, 1348, 1249, 1210, 1195, 1106, 1012, 976, 836, 777, 701; **HRMS** Accurate mass (ES^+): Found 506.33011 (+0.13 ppm), $C_{28}H_{48}NO_5Si$ ($M+H^+$) requires 506.330177.

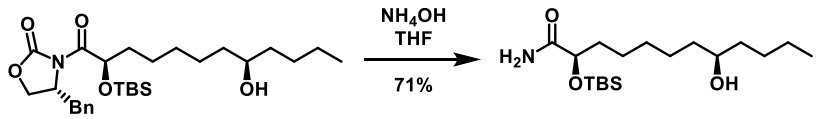

(–)-2.168 (+)-2.171

(2R,8R)-2-((tert-butyldimethylsilyl)oxy)-8-hydroxydodecanamide (+)-2.171. Following general procedure C, oxazolidinone **(–)-2.168** (134 mg, 0.26 mmol) yielded the title compound as a clear oil (65

mg, 71% yield). **^{1}H NMR** (400 MHz, $CDCl_3$) δ 6.50 (s, 1H), 6.38 (s, 1H), 4.09 (t, *J* = 5.0 Hz, 1H), 3.53 (dd, *J* = 6.8, 4.2 Hz, 1H), 1.91 – 1.56 (m, 3H), 1.50 – 1.21 (m, 17H), 0.89 (s, 8H), 0.86 (d, *J* = 10.6 Hz, 3H), 0.07 (s, 3H), 0.06 (s, 2H); **^{13}C NMR** (100 MHz, $CDCl_3$) δ 177.47, 73.47, 71.86, 37.43, 37.23, 35.13, 29.66, 27.93, 25.81, 25.57, 24.20, 22.85, 18.09, 14.18, -4.76, -5.17; **$[\alpha]^{25}_D$** +49 (c = 0.49 in $CHCl_3$); **IR** (film) 3479 (N-H), 3290 (br O-H), 2928, 2857, 1681 (C=O), 1581, 1463, 1389, 1361, 1339, 1253, 1097, 1005, 836, 778, 669; **HRMS** Accurate mass (ES^+): Found 346.27731 (+1.27 ppm), $C_{18}H_{40}NO_3Si$ ($M+H^+$) requires 346.277747.

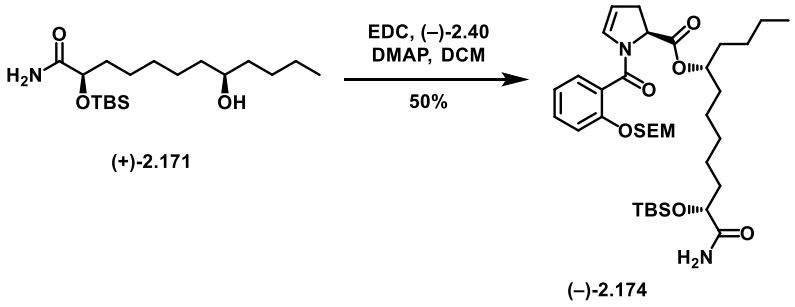

(5R,11R)-12-amino-11-((tert-butyldimethylsilyl)oxy)-12-oxododecan-5-yl (S)-1-(2-((2-(trimethylsilyl)ethoxy)methoxy)benzoyl)-2,3-dihydro-1H-pyrrole-2-carboxylate (–)-2.174. Following general procedure J, alcohol **(+)-2.171** (19 mg, 0.05 mmol) yielded the title compound as a clear oil (19 mg, 50% yield). **^{1}H NMR** (600 MHz, $CDCl_3$) δ 7.35 (dd, *J* = 12.3, 4.6 Hz, 2H), 7.19 (dd, *J* = 10.5, 4.9 Hz, 1H), 7.03 (td, *J* = 7.5, 0.8 Hz, 1H), 6.52 (d, *J* = 4.0 Hz, 1H), 6.16 (dd, *J* = 5.3, 3.1 Hz, 1H), 5.53 (d, *J* = 3.8 Hz, 1H), 5.28 – 5.17 (m, 2H), 5.04 – 4.91 (m, 3H), 4.12 (t, *J* = 5.1 Hz, 1H), 3.77 – 3.71 (m, 2H), 3.11 (ddt, *J* = 16.6, 11.6, 2.3 Hz, 1H), 2.71 – 2.62 (m, 1H), 1.78 – 1.73 (m, *J* = 15.5, 10.3, 5.1 Hz, 1H), 1.70 (s, 2H), 1.68 – 1.62 (m, *J* = 19.3, 9.8, 5.0 Hz, 1H), 1.61 – 1.52 (m, 3H), 1.44 – 1.21 (m, 11H), 0.96 – 0.89 (m, 11H), 0.88 (t, *J* = 9.0, 4.3 Hz, 3H), 0.09 – 0.06 (m, 6H), -0.00 – -0.03 (m, 9H); **^{13}C NMR** (151 MHz, $CDCl_3$) δ 176.98, 170.81, 165.02, 153.87, 131.24, 131.07, 129.02, 126.01, 122.00, 115.28, 108.38, 93.39, 75.47, 73.60, 66.64, 58.23, 35.13, 34.43, 34.05, 33.78, 29.50, 27.51, 25.88, 25.06, 24.11, 22.71, 18.18, 18.16, 14.13, -1.27, -4.70, -5.12; **$[\alpha]^{25}_D$** -24.4 (c = 1.6 in $CHCl_3$); **IR** (film) 3481 (N-H), 2928, 2858, 1737 (C=O),

1689 (C=O), 1650 (C=O), 1455, 1249, 1194, 1087, 987, 834, 778, 754, 696; **HRMS** Accurate mass (ES^+): Found 713.39935, $C_{36}H_{62}N_2O_7Si_2Na$ ($M+Na^+$) requires 713.399329.

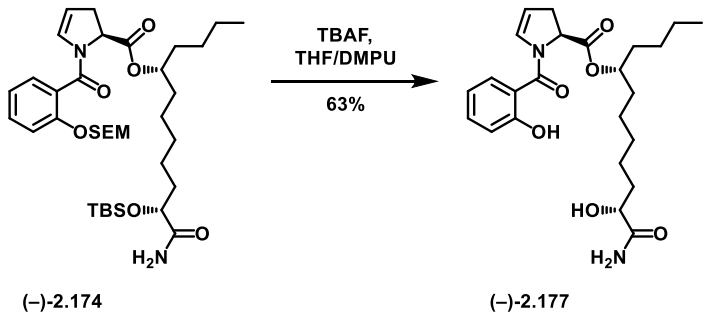

(–)-2.174 (–)-2.177

(5R,11R)-12-amino-11-hydroxy-12-oxododecan-5-yl (S)-1-(2-hydroxybenzoyl)-2,3-dihydro-1H-pyrrole-2-carboxylate (–)-2.177. Following general procedure L; silyl ether **(–)-2.174** (12 mg, 0.017 mmol) yielded the title compound as a clear oil (5 mg, 63% yield). **^{1}H NMR** (600 MHz, $cdcl_3$) δ 7.35 (dd, *J* = 12.3, 4.6 Hz, 2H), 7.19 (dd, *J* = 10.5, 4.9 Hz, 1H), 7.03 (td, *J* = 7.5, 0.8 Hz, 1H), 6.52 (d, *J* = 4.0 Hz, 1H), 6.16 (dd, *J* = 5.3, 3.1 Hz, 1H), 5.53 (d, *J* = 3.8 Hz, 1H), 5.28 – 5.17 (m, 2H), 5.04 – 4.91 (m, 3H), 4.12 (t, *J* = 5.1 Hz, 1H), 3.77 – 3.71 (m, 2H), 3.11 (ddt, *J* = 16.6, 11.6, 2.3 Hz, 1H), 2.71 – 2.62 (m, 1H), 1.78 – 1.73 (m, *J* = 15.5, 10.3, 5.1 Hz, 1H), 1.70 (s, 2H), 1.68 – 1.62 (m, *J* = 19.3, 9.8, 5.0 Hz, 1H), 1.61 – 1.52 (m, 3H), 1.44 – 1.21 (m, 11H), 0.96 – 0.89 (m, 11H), 0.88 (t, *J* = 9.0, 4.3 Hz, 3H), 0.09 – 0.06 (m, 6H), -0.00 – -0.03 (m, 9H); **^{13}C NMR** (151 MHz, $cdcl_3$) δ 176.98, 170.81, 165.02, 153.87, 131.24, 131.07, 129.02, 126.01, 122.00, 115.28, 108.38, 93.39, 75.47, 73.60, 66.64, 58.23, 35.13, 34.43, 34.05, 33.78, 29.50, 27.51, 25.88, 25.06, 24.11, 22.71, 18.18, 18.16, 14.13, -1.27, -4.70, -5.12; **$[\alpha]^{25}_D$** -44.9 (c = 0.35 in $CHCl_3$); **IR** (film) 3338 (br O-H), 2922, 2853, 1731 (C=O), 1665 (C=O), 1592 (C=O), 1460, 1430, 1378, 1294, 1196, 1153, 1110, 1017, 946, 857, 817, 755, 721, 656, 617, 500; **HRMS** Accurate mass (ES^+): Found 447.24936 (+0.34 ppm), $C_{24}H_{35}N_2O_6$ ($M+H^+$) requires 447.24951.

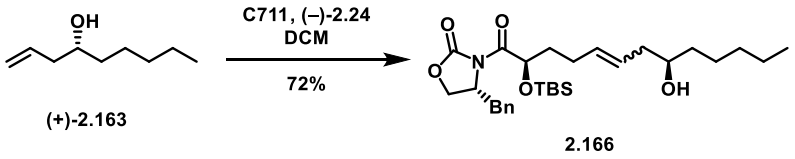

(R)-4-benzyl-3-((2R,8R)-2-((tert-butyldimethylsilyl)oxy)-8-hydroxytridec-5-enoyl)oxazolidin-2-one (2.166). Following general procedure A; homoallylic alcohol **(+)-2.163** (245 mg, 1.7 mmol) yielded the title compound as a brown oil (126 mg, 72% yield). **^{1}H NMR** (500 MHz, $CDCl_3$, mixture of E/Z isomers) δ 7.36 – 7.31 (m, 2H), 7.30 – 7.27 (m, 1H), 7.25 – 7.22 (m, 2H), 5.60 – 5.43 (m, 2H), 5.37 (dd, *J* = 8.4, 3.4 Hz, 1H), 4.66 – 4.59 (m, 1H), 4.24 – 4.15 (m, 2H), 3.63 – 3.55 (m, 1H), 3.43 – 3.35 (m, 1H), 2.69 (dd, *J* = 13.3, 10.1 Hz, 1H), 2.31 – 2.15 (m, 3H), 2.10 – 1.99 (m, 1H), 1.82 – 1.67 (m, 3H), 1.49 – 1.39 (m, 3H), 1.38 – 1.23 (m, 6H), 0.94 (s, 9H), 0.89 (t, *J* = 7.0 Hz, 3H), 0.11 (s, 3H), 0.09 (s, 3H); **^{13}C NMR** (126 MHz, $CDCl_3$) δ 174.46, 153.24, 135.35, 133.04, 129.59, 129.14, 127.55, 127.30, 70.94, 70.85, 66.70, 55.74, 40.87, 37.83, 36.89, 35.24, 32.04, 28.57, 25.95, 25.56, 22.79, 18.46, 14.20, -4.44, -4.91; **IR** (film) 3510 (br O-H), 2928, 2857, 1778 (C=O), 1711 (C=O), 1387, 1348, 1250, 1210, 1109, 1015 ,973, 908, 836, 729, 701; **HRMS** Accurate mass (ES^+): Found 540.3120, $C_{29}H_{47}NO_5SiNa$ (M+Na) requires 540.3121.

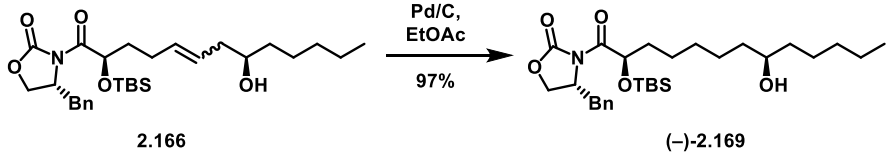

(R)-4-benzyl-3-((2R,8R)-2-((tert-butyldimethylsilyl)oxy)-8-hydroxytridecanoyl)oxazolidin-2-one (–)-2.169. Following general procedure B; alkene **2.166** (126 mg, 0.243 mmol) yielded the title compound as a clear oil (122 mg, 97% yield). **^{1}H NMR** (500 MHz, $CDCl_3$) δ 7.25 – 7.21 (m, 2H), 7.19 – 7.16 (m, 1H), 7.13 (d, 2H), 5.25 (dd, *J* = 8.3, 3.3 Hz, 1H), 4.54 – 4.48 (m, 1H), 4.12 – 4.05 (m, 2H), 3.46 (s, 1H), 3.29 (dd, *J* = 13.3, 3.3 Hz, 1H), 2.59 (dd, *J* = 13.3, 10.1 Hz, 1H), 1.62 – 1.49 (m, 2H), 1.45 – 1.24 (m, 9H), 1.24 – 1.16 (m, 8H), 0.83 (s, 9H), 0.80 – 0.75 (m, 3H), 0.00 (s, 3H), -0.02 (s, 3H).; **^{13}C NMR** (126 MHz, $CDCl_3$) δ 174.59, 153.28, 135.40, 129.60, 129.14, 127.54, 72.11, 71.49, 71.47, 66.65, 55.74, 37.84, 37.63, 37.50, 35.27, 32.05, 29.35, 25.95, 25.61, 25.58, 25.46, 22.79, 18.49, 14.20, -4.49, -4.95.; **$[\alpha]^{25}_D$** -7.5 (c = 0.65 in

$CHCl_3$); **IR** (film) 3390 (br O-H), 2927, 2856, 1779 (C=O), 1711 (C=O), 1388, 1348, 1250, 1210, 1196, 1107, 1012, 974, 910, 836, 776, 731, 701; **HRMS** Accurate mass (ES^+): Found 520.3470, $C_{29}H_{50}NO_5Si$ (M+H) requires 520.3458.

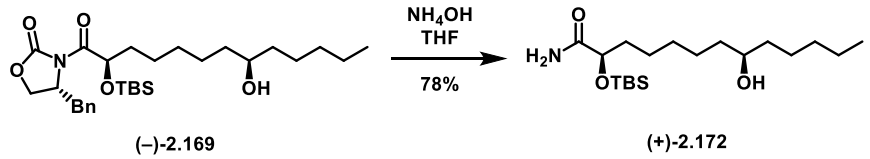

(2R,8R)-2-((tert-butyldimethylsilyl)oxy)-8-hydroxytridecanamide (+)-2.172. Following general procedure C; oxazolidinone **(–)-2.169** (77 mg, 0.14 mmol) yielded the title compound as a clear oil (42 mg, 78% yield). **^{1}H NMR** (400 MHz, $CDCl_3$) δ 6.52 (d, *J* = 3.5 Hz, 1H), 6.01 (s, 1H), 4.11 (t, *J* = 5.1 Hz, 1H), 3.55 (s, 1H), 1.97 (s, 1H), 1.82 – 1.51 (m, 3H), 1.49 – 1.19 (m, 17H), 0.91 (s, 9H), 0.87 (t, *J* = 6.8 Hz, 3H), 0.09 (s, 3H), 0.07 (s, 3H); **^{13}C NMR** (100 MHz, $CDCl_3$) δ 177.31, 73.50, 71.98, 37.54, 37.45, 35.16, 32.03, 29.67, 25.85, 25.59, 25.45, 24.23, 22.77, 18.13, 14.18, -4.71, -5.13; **$[\alpha]^{25}_D$** +28 (c = 2.0 in $CHCl_3$); **IR** (film) 3479 (N-H), 3297 (br O-H), 2928, 2857, 1681 (C=O), 1583, 1463, 1389, 1361, 1339, 1253, 1097, 1005, 835, 778, 669; **HRMS** Accurate mass (ES^+): Found 360.2953, $C_{19}H_{42}NO_3Si$ (M+H) requires 360.2934.

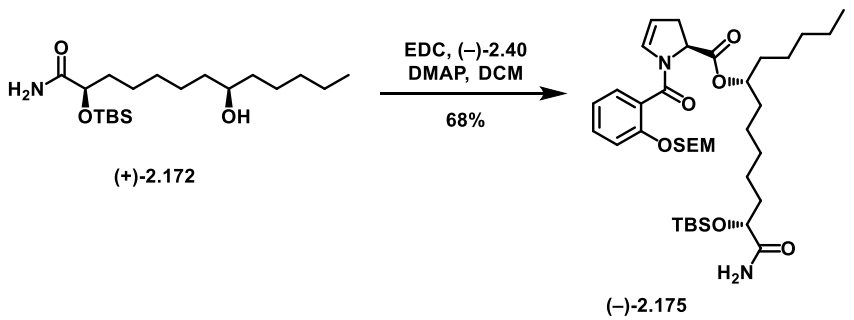

(6R,12R)-13-amino-12-((tert-butyldimethylsilyl)oxy)-13-oxotridecan-6-yl (S)-1-(2-((2-(trimethylsilyl)ethoxy)methoxy)benzoyl)-2,3-dihydro-1H-pyrrole-2-carboxylate (–)-2.175. Following general procedure J; alcohol **(+)-2.172** (25 mg, 0.07 mmol) yielded the title compound as a clear oil (33 mg, 68% yield). **^{1}H NMR** (600 MHz, $CDCl_3$) δ 7.35 (t, *J* = 7.6 Hz, 2H), 7.20 (d, *J* = 8.6 Hz, 1H), 7.04 (t, *J* = 7.5 Hz, 1H), 6.52 (d, *J* = 4.7 Hz, 1H), 6.18 – 6.14 (m, 1H), 5.50 (d, *J* = 23.8 Hz, 1H), 5.26 – 5.19 (m, 2H),

5.04 – 4.93 (m, 2H), 4.12 (t, *J* = 5.1 Hz, 1H), 3.74 (t, *J* = 8.3 Hz, 2H), 3.15 – 3.08 (m, 1H), 2.70 – 2.63 (m, 1H), 1.79 – 1.72 (m, 1H), 1.69 – 1.61 (m, 2H), 1.60 – 1.51 (m, 4H), 1.44 – 1.26 (m, 12H), 0.96 – 0.93 (m, 2H), 0.91 (s, 9H), 0.87 (t, *J* = 6.6 Hz, 3H), 0.09 (s, 3H), 0.07 (s, 3H), -0.01 (s, 9H).; **^{13}C NMR** (151 MHz, $CDCl_3$) δ 176.96, 170.80, 165.00, 153.88, 131.23, 131.08, 129.04, 126.04, 122.00, 115.29, 108.34, 93.39, 75.48, 73.61, 66.64, 58.23, 35.15, 34.43, 34.07, 31.84, 29.52, 25.89, 25.08, 25.04, 24.13, 22.67, 18.19, 18.16, 14.15, -1.26, -4.68, -5.11.; **$[\alpha]^{25}_D$** -38.8 (c = 0.75 in $CHCl_3$); **IR** (film) 3480 (N-H), 2928, 2857, 1734 (C=O), 1683 (C=O), 1463, 1389, 1251, 1189, 1089, 989, 909, 836, 778, 731; **HRMS** Accurate mass (ES^+): Found 705.4357, $C_{37}H_{65}N_2O_7Si_2$ (M+H) requires 705.4330.

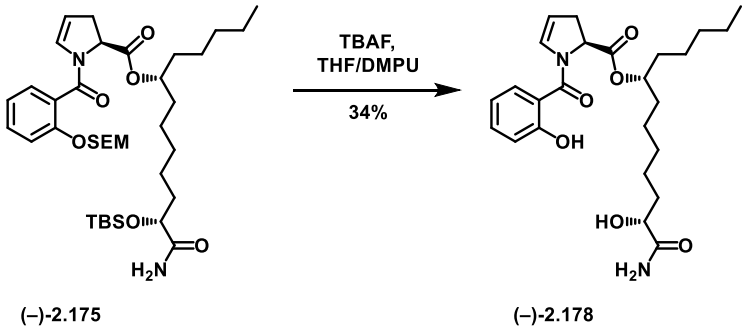

(–)-2.175 (–)-2.178

(6R,12R)-13-amino-12-hydroxy-13-oxotridecan-6-yl (S)-1-(2-hydroxybenzoyl)-2,3-dihydro-1H-pyrrole-2-carboxylate (–)-2.178. Following general procedure L; silyl ether **(–)-2.175** (18 mg, 0.026 mmol) yielded the title compound as a clear oil (4 mg, 34% yield). **^{1}H NMR** (600 MHz, $CDCl_3$) δ 9.52 (s, 1H), 7.42 – 7.35 (m, 2H), 6.99 (d, *J* = 8.3 Hz, 1H), 6.91 (t, *J* = 7.6 Hz, 1H), 6.72 (s, 1H), 6.57 (s, 1H), 5.28 (s, 1H), 5.01 (dd, *J* = 11.5, 4.8 Hz, 2H), 4.11 (d, *J* = 3.7 Hz, 1H), 3.31 (s, 1H), 3.14 (dd, *J* = 17.1, 11.5 Hz, 1H), 2.70 (d, *J* = 17.1 Hz, 1H), 1.85 – 1.78 (m, 1H), 1.70 – 1.51 (m, 9H), 1.48 – 1.40 (m, 4H), 1.33 – 1.27 (m, 5H), 0.87 (t, *J* = 6.5 Hz, 4H).; **^{13}C NMR** (151 MHz, $CDCl_3$) δ 176.85, 171.33, 167.45, 158.08, 133.52, 130.88, 128.32, 119.42, 118.04, 117.74, 111.09, 76.02, 71.42, 59.37, 34.51, 34.34, 34.18, 31.71, 29.85, 28.33, 25.22, 24.84, 24.56, 22.63, 14.10.; **$[\alpha]^{25}_D$** -49.7 (c = 0.41 in $CHCl_3$); **IR** (film) 3339 (br O-H), 2923, 2853, 1730 (C=O), 1665 (C=O), 1594 (C=O), 1461, 1428, 1377, 1294, 1196, 1153, 1111, 1017, 945, 857, 817, 756, 720, 658, 617; **HRMS** Accurate mass (ES^+): Found 461.26471, $C_{25}H_{37}N_2O_6$ (M+H) requires 461.26516.

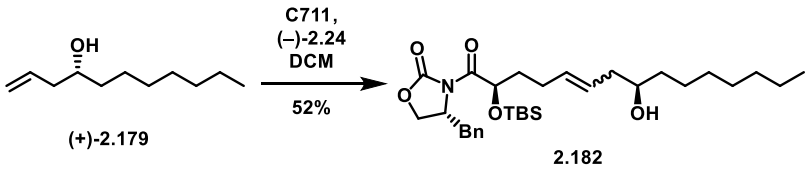

(R)-4-benzyl-3-((2R,8R)-2-((tert-butyldimethylsilyl)oxy)-8-hydroxypentadec-5-enoyl)oxazolidin-2-one (2.182). Following general procedure A; homoallylic alcohol **(+)-2.179** (527 mg, 3.1 mmol) yielded the title compound as a brown oil (175 mg, 52% yield). **^{1}H NMR** (500 MHz, $CDCl_3$, mixture of E/Z isomers) δ 7.34 (t, *J* = 7.2 Hz, 2H), 7.29 (d, *J* = 7.2 Hz, 1H), 7.24 (d, *J* = 7.0 Hz, 2H), 5.59 – 5.43 (m, 2H), 5.40 – 5.35 (m, 1H), 4.66 – 4.59 (m, 1H), 4.24 – 4.15 (m, 2H), 3.63 – 3.55 (m, 1H), 3.44 – 3.37 (m, 1H), 2.74 – 2.64 (m, *J* = 13.3, 10.2 Hz, 1H), 2.28 – 2.15 (m, 3H), 2.12 – 1.99 (m, 1H), 1.88 – 1.60 (m, 3H), 1.45 (s, 3H), 1.28 (s, 10H), 0.94 (s, 9H), 0.88 (t, *J* = 6.8 Hz, 3H), 0.11 (s, 3H), 0.09 (s, 3H); **^{13}C NMR** (126 MHz, $CDCl_3$) δ 174.46, 153.24, 135.34, 133.03, 129.58, 129.14, 127.54, 127.29, 70.93, 70.84, 66.69, 55.73, 40.86, 37.82, 36.92, 35.23, 31.97, 29.79, 29.43, 28.56, 25.95, 25.88, 22.79, 18.46, 14.24, -4.45, -4.92; **IR** (film) 3510 (br O-H), 2928, 2855, 1778 (C=O), 1711 (C=O), 1387, 1348, 1250, 1210, 1112, 1012 ,971, 909, 836, 731, 701; **HRMS** Accurate mass (ES^+): Found 546.3617, $C_{31}H_{52}NO_5Si$ (M+H) requires 546.3615.

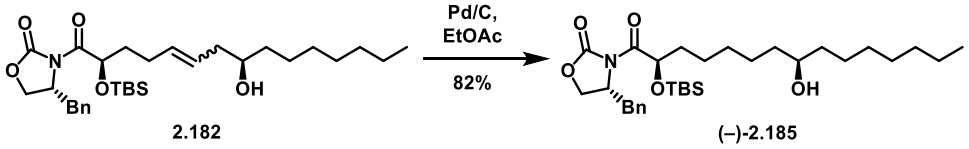

(R)-4-benzyl-3-((2R,8R)-2-((tert-butyldimethylsilyl)oxy)-8-hydroxypentadecanoyl)oxazolidin-2-one (–)-2.185. Following general procedure B; alkene **2.182** (175 mg, 0.32 mmol) yielded the title compound as a clear oil (144 mg, 82% yield). **^{1}H NMR** (500 MHz, $CDCl_3$) δ 7.37 – 7.31 (m, 2H), 7.31 – 7.27 (m, 1H), 7.25 – 7.22 (m, 2H), 5.36 (dd, *J* = 8.4, 3.3 Hz, 1H), 4.62 (qd, *J* = 6.3, 3.1 Hz, 1H), 4.24 – 4.14 (m, 2H), 3.57 (s, 1H), 3.41 (dd, *J* = 13.2, 3.2 Hz, 1H), 2.70 (dd, *J* = 13.3, 10.2 Hz, 1H), 1.74 – 1.59 (m, 2H), 1.49 – 1.35 (m, 8H), 1.34 – 1.22 (m, *J* = 16.2, 13.2 Hz, 14H), 0.94 (s, 9H), 0.90 – 0.85 (m, 3H), 0.11 (s, 3H), 0.09 (s, 3H); **^{13}C NMR** (126 MHz, $CDCl_3$) δ 174.58, 153.27, 135.40, 129.60, 129.14, 127.54, 72.12, 71.47, 66.66, 55.75, 37.85, 37.68, 37.51, 35.28, 31.98, 29.82, 29.45, 29.37, 25.96, 25.80, 25.62, 25.60, 22.81, 18.50,

14.26, -4.48, -4.94.; **[α]$^{25}_{D}$** -7.4 (c = 0.96 in $CHCl_3$); **IR** (film) 3400 (br O-H), 2926, 2855, 1781 (C=O), 1711 (C=O), 1388, 1348, 1249, 1210, 1195, 1106, 1012, 976, 836, 777, 732, 701; **HRMS** Accurate mass (ES^+): Found 570.3602, $C_{31}H_{53}NO_5SiNa$ (M+Na) requires 570.3791.

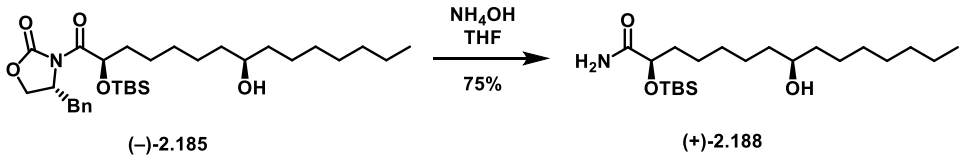

(2R,8R)-2-((tert-butyldimethylsilyl)oxy)-8-hydroxypentadecanamide (+)-2.185. Following general procedure C; oxazolidinone **(–)-2.188** (144 mg, 0.26 mmol) yielded the title compound as a clear oil (77 mg, 75% yield). **^{1}H NMR** (400 MHz, $CDCl_3$) δ 6.52 (d, *J* = 4.1 Hz, 1H), 5.99 (d, *J* = 3.9 Hz, 1H), 4.12 (s, 1H), 3.55 (s, 1H), 1.73 (s, 4H), 1.33 (d, *J* = 58.3 Hz, 19H), 0.91 (s, 9H), 0.86 (s, 3H), 0.09 (s, 3H), 0.07 (s, 3H); ^{13}C NMR (126 MHz, cdcl$_3$) δ 177.27, 73.55, 71.99, 37.61, 37.49, 35.20, 31.95, 29.80, 29.69, 29.41, 25.86, 25.79, 25.60, 24.26, 22.77, 18.13, 14.21, -4.71, -5.12.; **[α]$^{25}_{D}$** +10.8 (c = 0.84 in $CHCl_3$); **IR** (film) 3479 (N-H), 3001 (br O-H), 2926, 2855, 1682 (C=O), 1583, 1463, 1389, 1361, 1339, 1253, 1098, 1005, 835, 778, 772, 668; **HRMS** Accurate mass (ES^+): Found 388.3261, $C_{21}H_{46}NO_3Si$ (M+H) requires 388.3247.

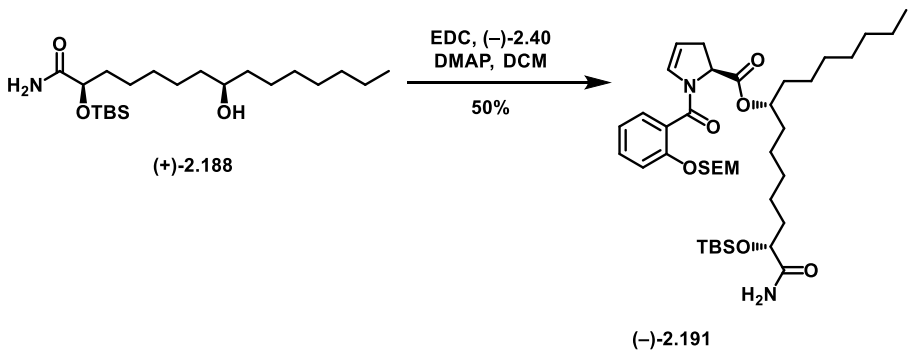

(2R,8R)-1-amino-2-((tert-butyldimethylsilyl)oxy)-1-oxopentadecan-8-yl (S)-1-(2-((2-(trimethylsilyl)ethoxy)methoxy)benzoyl)-2,3-dihydro-1H-pyrrole-2-carboxylate (–)-2.191. Following general procedure J; alcohol **(+)-2.188** (18 mg, 0.046 mmol) yielded the title compound as a clear oil (17 mg, 50% yield). **^{1}H NMR** (400 MHz, $CDCl_3$) δ 7.39 – 7.32 (m, 2H), 7.22 – 7.17 (m, 1H), 7.03 (td, *J* = 7.5, 0.8 Hz, 1H), 6.53 (d, *J* = 4.3 Hz, 1H), 6.14 (t, *J* = 4.2 Hz, 1H), 5.55 (d, *J* = 4.2 Hz, 1H), 5.22 (q, *J* = 7.1 Hz,

2H), 5.05 – 4.91 (m, 3H), 4.12 (t, *J* = 5.1 Hz, 1H), 3.78 – 3.71 (m, 2H), 3.12 (ddt, *J* = 16.6, 11.6, 2.3 Hz, 1H), 2.71 – 2.62 (m, 1H), 1.80 – 1.70 (m, *J* = 18.4, 9.1, 4.2 Hz, 1H), 1.72 – 1.45 (m, *J* = 49.8 Hz, 7H), 1.39 – 1.19 (m, 20H), 0.91 (m, 12H), 0.86 (t, 3H), 0.08 (d, *J* = 4.7 Hz, 6H), -0.02 (s, 9H); **^{13}C NMR** (151 MHz, $CDCl_3$) δ 176.95, 170.80, 164.99, 153.88, 131.23, 131.09, 129.04, 126.04, 122.00, 115.29, 108.33, 93.40, 75.49, 73.61, 66.64, 58.23, 35.15, 34.43, 34.12, 34.06, 31.94, 29.84, 29.63, 29.52, 29.33, 25.89, 25.39, 25.07, 24.13, 22.77, 18.19, 18.16, 14.23, -1.26, -4.68, -5.12; **[α]$^{25}_{D}$** -8.3 (c = 0.30 in $CHCl_3$); **IR** (film) 3343 (N-H), 2927, 2857, 1734 (C=O), 1645 (C=O), 1489, 1455, 1409, 1249, 1162, 1089, 983, 914, 834, 755, 731, 602; **HRMS** Accurate mass (ES^+): Found 755.4483, $C_{39}H_{68}N_2O_7Si_2Na$ (M+Na) requires 744.4463.

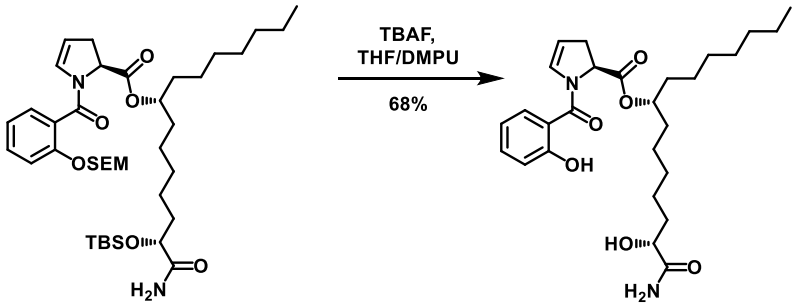

(–)-2.191 (–)-2.194

(2R,8R)-1-amino-2-hydroxy-1-oxopentadecan-8-yl (S)-1-(2-hydroxybenzoyl)-2,3-dihydro-1H-pyrrole-2-carboxylate (–)-2.194. Following general procedure L; silyl ether **(–)-2.191** (18 mg, 0.024 mmol) yielded the title compound as a clear oil (8 mg, 68% yield). **^{1}H NMR** (400 MHz, $CDCl_3$) δ 9.52 (s, 1H), 7.42 – 7.32 (m, 2H), 6.98 (d, *J* = 8.2 Hz, 1H), 6.90 (t, *J* = 7.5 Hz, 1H), 6.71 (s, 1H), 6.62 (s, 1H), 5.42 (s, 1H), 5.30 – 5.26 (m, 1H), 5.01 (dd, *J* = 11.4, 4.8 Hz, 2H), 4.13 – 4.05 (m, 1H), 3.48 (q, *J* = 7.0 Hz, 1H), 3.20 – 3.07 (m, 1H), 2.69 (d, *J* = 16.9 Hz, 1H), 1.85 – 1.75 (m, 1H), 1.73 – 1.65 (m, 2H), 1.62 – 1.52 (m, 3H), 1.49 – 1.36 (m, 4H), 1.32 – 1.21 (m, 12H), 0.87 (t, *J* = 6.8 Hz, 3H).; **^{13}C NMR** (151 MHz, $CDCl_3$) δ 176.98, 171.29, 167.42, 158.04, 133.48, 130.86, 128.31, 119.40, 118.02, 117.76, 111.05, 76.02, 71.42, 59.36, 34.54, 34.34, 34.18, 31.89, 29.84, 29.52, 29.29, 28.37, 25.56, 24.86, 24.59, 22.76, 14.23.; **[α]$^{25}_{D}$** -47.3 (c = 0.82 in $CHCl_3$); **IR** (film) 3326 (br O-H), 2921, 2859, 1741 (C=O), 1665 (C=O), 1597 (C=O),

1459, 1437, 1201, 1105, 1098, 754, 722, 619; **HRMS** Accurate mass (ES^+): Found 489.2959, $C_{27}H_{41}N_2O_6$ (M+H) requires 489.2964.

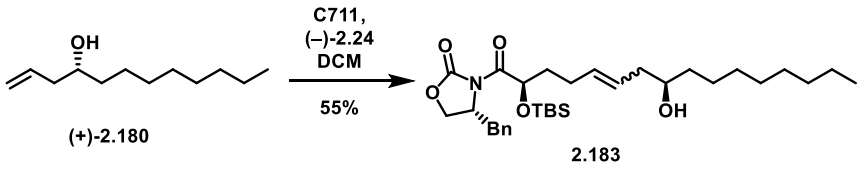

(R)-4-benzyl-3-((2R,8R,E)-2-((tert-butyldimethylsilyl)oxy)-8-hydroxyhexadec-5-enoyl)oxazolidin-2-one (2.183). Following general procedure A, homoallylic alcohol **(+)-2.180** (500 mg, 2.7 mmol) yielded the title compound as a brown oil (167 mg, 55% yield). **^{1}H NMR** (400 MHz, $CDCl_3$, mixture of E/Z isomers) δ 7.37 – 7.27 (m, 3H), 7.22 (d, *J* = 9.1 Hz, 2H), 5.51 (ddd, *J* = 21.2, 15.1, 8.5 Hz, 2H), 5.37 (dd, *J* = 8.2, 3.4 Hz, 1H), 4.67 – 4.57 (m, 1H), 4.24 – 4.13 (m, 2H), 3.59 (d, *J* = 3.9 Hz, 1H), 3.40 (dd, *J* = 13.3, 3.1 Hz, 1H), 2.68 (dd, *J* = 13.3, 10.2 Hz, 1H), 2.28 – 2.17 (m, 3H), 2.10 – 1.98 (m, 1H), 1.69 (ddd, *J* = 29.0, 14.8, 8.0 Hz, 5H), 1.43 (s, 3H), 1.33 – 1.21 (m, 13H), 0.96 – 0.93 (m, 9H), 0.88 (dd, *J* = 12.0, 5.5 Hz, 3H), 0.11 (s, 3H), 0.09 (s, 3H); **^{13}C NMR** (126 MHz, $CDCl_3$) δ 174.46, 153.24, 135.35, 133.04, 129.59, 129.14, 127.55, 127.30, 70.94, 70.85, 66.70, 55.74, 40.87, 37.83, 36.94, 35.24, 32.03, 29.85, 29.74, 29.43, 28.57, 25.96, 25.89, 22.82, 18.46, 14.26, -4.44, -4.91; **IR** (film) 3510 (br O-H), 2926, 2854, 1779 (C=O), 1711 (C=O), 1388, 1348, 1250, 1210, 1113, 1010 ,971, 908, 777, 701; **HRMS** Accurate mass (ES^+): Found 560.3800, $C_{32}H_{54}NO_5Si$ ($M+H^+$) requires 560.3797.

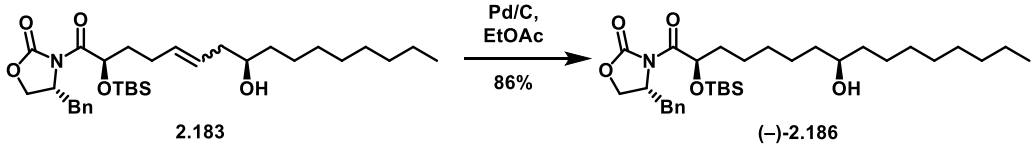

(R)-4-benzyl-3-((2R,8R)-2-((tert-butyldimethylsilyl)oxy)-8-hydroxyhexadecanoyl)oxazolidin-2-one (–)-2.186. Following general procedure B, alkene **2.183** (166 mg, 0.30 mmol) yielded the title compound as a clear oil (145 mg, 86% yield). **^{1}H NMR** 500 MHz, $CDCl_3$) δ 7.37 – 7.31 (m, 2H), 7.30 – 7.27 (m, 1H), 7.25 – 7.21 (m, 2H), 5.36 (dd, *J* = 8.3, 3.3 Hz, 1H), 4.62 (qd, *J* = 6.5, 3.1 Hz, 1H), 4.25 – 4.14 (m, 2H), 3.57 (s, 1H), 3.40 (dd, *J* = 13.3, 3.2 Hz, 1H), 2.73 – 2.67 (m, 1H), 1.76 – 1.57 (m, 3H), 1.54 – 1.35 (m, 8H), 1.35

– 1.23 (m, *J* = 20.4, 13.9 Hz, 14H), 0.94 – 0.92 (m, 9H), 0.88 (t, *J* = 6.9 Hz, 3H), 0.11 (s, *J* = 2.7 Hz, 3H), 0.09 (s, *J* = 2.1 Hz, 3H); **^{13}C NMR** (126 MHz, $CDCl_3$) δ 174.58, 153.27, 135.39, 129.59, 129.14, 127.53, 72.11, 71.46, 66.65, 55.74, 37.84, 37.68, 37.51, 35.28, 32.03, 29.86, 29.74, 29.43, 29.36, 25.96, 25.80, 25.61, 25.59, 22.82, 18.49, 14.26, -4.49, -4.95; **$[\alpha]^{25}_D$** -8.1 (c = 1.1 in $CHCl_3$); **IR** (film) 3390 (br O-H), 2926, 2855, 1779 (C=O), 1711 (C=O), 1388, 1348, 1249, 1210, 1196, 1107, 1012, 909, 836, 777, 731, 701; **HRMS** Accurate mass (ES^+): Found 584.3755, $C_{32}H_{55}NO_5SiNa$ ($M+Na^+$) requires 584.3747.

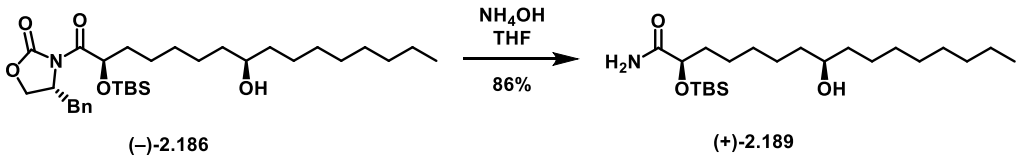

(2R,8R)-2-((tert-butyldimethylsilyl)oxy)-8-hydroxyhexadecanamide (+)-2.189. Following general procedure C, oxazolidinone **(–)-2.186** (93 mg, 0.17 mmol) yielded the title compound as a clear oil (57 mg, 86% yield). **^{1}H NMR** (400 MHz, $CDCl_3$) δ 6.55 (s, 1H), 5.57 (s, 1H), 4.13 (t, *J* = 12.1, 6.6 Hz, 1H), 3.57 (s, 1H), 1.83 – 1.63 (m, 4H), 1.50 – 1.18 (m, 20H), 0.93 – 0.92 (m, 9H), 0.88 (t, *J* = 6.8 Hz, 3H), 0.10 (s, 3H), 0.09 (s, 3H); **^{13}C NMR** (100 MHz, $CDCl_3$) δ 177.40, 73.46, 71.95, 37.58, 37.45, 35.15, 31.99, 29.83, 29.71, 29.68, 29.40, 25.83, 25.78, 25.60, 24.23, 22.78, 18.11, 14.24, -4.73, -5.14; **$[\alpha]^{25}_D$** +18.7 (c = 1.1 in $CHCl_3$); **IR** (film) 3479 (N-H), 3295 (br O-H), 2926, 2855, 1681 (C=O), 1463, 1389, 1251, 1079, 1005, 835, 778, 668; **HRMS** Accurate mass (ES^+): Found 402.3414, $C_{22}H_{48}NO_3Si$ ($M+H^+$) requires 402.3403.

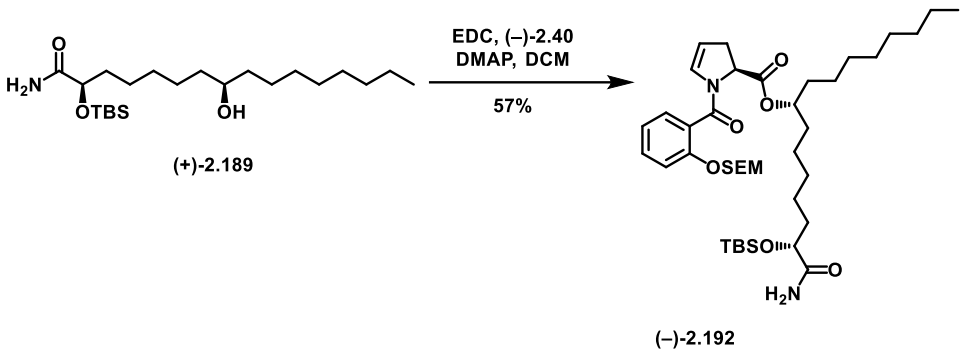

(2R,8R)-1-amino-2-((tert-butyldimethylsilyl)oxy)-1-oxohexadecan-8-yl (S)-1-(2-((2-(trimethylsilyl)ethoxy)methoxy)benzoyl)-2,3-dihydro-1H-pyrrole-2-carboxylate (–)-2.192. Following general procedure J, alcohol **(+)-2.189** (30 mg, 0.07 mmol) yielded the title compound as a clear oil (32 mg, 57% yield). **^{1}H NMR** (600 MHz, $CDCl_3$) δ 7.35 (dd, *J* = 12.1, 4.6 Hz, 2H), 7.21 – 7.18 (m, 1H), 7.03 (td, *J* = 7.5, 0.9 Hz, 1H), 6.51 (d, *J* = 4.3 Hz, 1H), 6.16 (dt, *J* = 4.2, 2.1 Hz, 1H), 5.57 (s, 1H), 5.25 – 5.19 (m, 2H), 5.03 – 4.93 (m, 3H), 4.12 (t, *J* = 5.1 Hz, 1H), 3.76 – 3.72 (m, 2H), 3.11 (ddt, *J* = 16.6, 11.6, 2.3 Hz, 1H), 2.70 – 2.62 (m, 1H), 1.79 – 1.71 (m, 3H), 1.69 – 1.61 (m, 1H), 1.61 – 1.49 (m, 4H), 1.44 – 1.17 (m, *J* = 81.1 Hz, 19H), 0.95 – 0.90 (m, 11H), 0.86 (t, *J* = 7.0 Hz, 3H), 0.08 (s, 2H), 0.07 (s, 2H), -0.02 (s, 6H); **^{13}C NMR** (151 MHz, $CDCl_3$) δ 176.99, 170.79, 165.00, 153.86, 131.23, 131.07, 129.03, 126.01, 121.99, 115.28, 108.35, 93.38, 75.49, 73.60, 66.63, 58.22, 35.13, 34.41, 34.11, 34.05, 31.98, 29.66, 29.62, 29.50, 29.37, 25.88, 25.37, 25.06, 24.12, 22.78, 18.17, 18.15, 14.23, -1.27, -4.70, -5.13; **$[\alpha]^{25}_{D}$** -32.7 (c = 1.57 in $CHCl_3$); **IR** (film) 3481 (N-H), 2927, 2856, 1741 (C=O), 1689 (C=O), 1455, 1406, 1250, 1194, 1087, 989, 835, 777, 731; **HRMS** Accurate mass (ES^+): Found 747.4781, $C_{40}H_{71}N_2O_7Si_2$ ($M+H^+$) requires 747.4800.

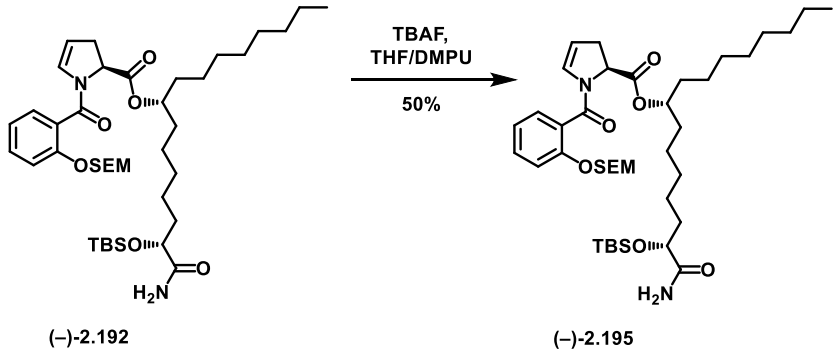

(2R,8R)-1-amino-2-hydroxy-1-oxohexadecan-8-yl (S)-1-(2-hydroxybenzoyl)-2,3-dihydro-1H-pyrrole-2-carboxylate (–)-2.195. Following general procedure L; silyl ether **(–)-2.192** (16 mg, 0.020 mmol) yielded the title compound as a clear oil (5 mg, 50% yield). **^{1}H NMR** (400 MHz, $CDCl_3$) δ 9.52 (s, 1H), 7.38 (t, *J* = 9.0 Hz, 2H), 6.99 (d, *J* = 8.1 Hz, 1H), 6.91 (t, *J* = 7.5 Hz, 1H), 6.72 (s, 1H), 6.60 (s, 1H), 5.36 (s, 1H), 5.28 (d, *J* = 4.0 Hz, 1H), 5.01 (dd, *J* = 11.3, 4.7 Hz, 2H), 4.10 (s, 1H), 3.40 (s, 1H), 3.19 – 3.08 (m, 1H), 2.75 – 2.64 (m, *J* = 16.9 Hz, 1H), 1.86 – 1.74 (m, 1H), 1.72 – 1.50 (m, 10H), 1.42 (s, 5H), 1.30 – 1.19 (m, *J* = 3.2 Hz, 19H), 0.87 (t, *J* = 6.8 Hz, 3H); **^{13}C NMR** (151 MHz, $CDCl_3$) δ 176.89, 171.32, 167.43, 158.04, 133.50, 130.86, 128.31, 119.42, 118.04, 117.75, 111.08, 76.04, 71.42, 59.37, 34.56, 34.34, 34.19, 31.98, 29.84, 29.59, 29.56, 29.34, 28.34, 25.57, 24.85, 24.57, 22.80, 14.25; **$[\alpha]^{25}_D$** -30.6 (c = 0.32 in $CHCl_3$); **IR** (film) 3339 (br O-H), 2923, 2854, 1737 (C=O), 1664 (C=O), 1592 (C=O), 1459, 1430, 1376, 1294, 1196, 1153, 1098, 1017, 945, 858, 817, 755, 721, 654, 616; **HRMS** Accurate mass (ES^+): Found 503.3134, $C_{28}H_{43}N_2O_6$ ($M+H^+$) requires 503.3121.

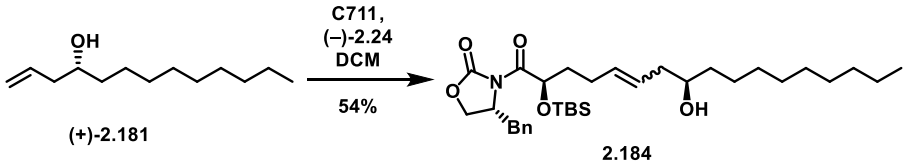

(R)-4-benzyl-3-((2R,8R)-2-((tert-butyldimethylsilyl)oxy)-8-hydroxyheptadec-5-enoyl)oxazolidin-2-one (2.184). Following general procedure A; homoallylic alcohol **(+)-2.181** (713 mg, 3.6 mmol) yielded the title compound as a brown oil (222 mg, 54% yield). **^{1}H NMR** (500 MHz, $CDCl_3$, mixture of E/Z isomers) δ 7.34 (dd, *J* = 9.9, 4.5 Hz, 2H), 7.30 – 7.27 (m, *J* = 7.9, 1.9 Hz, 1H), 7.25 – 7.22 (m, 2H), 5.61 – 5.41 (m,

2H), 5.37 (dt, *J* = 12.4, 4.8 Hz, 1H), 4.65 – 4.58 (m, 1H), 4.25 – 4.15 (m, 2H), 3.64 – 3.54 (m, 1H), 3.40 (dt, *J* = 13.2, 3.5 Hz, 1H), 2.74 – 2.63 (m, 1H), 2.30 – 2.14 (m, 3H), 2.08 – 2.01 (m, 1H), 1.80-1.64 (m, 3H), 1.47 – 1.39 (m, *J* = 15.9 Hz, 3H), 1.33 – 1.22 (m, 13H), 0.94 (s, *J* = 2.9 Hz, 9H), 0.87 (t, *J* = 7.0 Hz, 3H), 0.11 (s, 3H), 0.09 (s, 3H); **^{13}C NMR** (126 MHz, $CDCl_3$) δ 174.45, 153.23, 135.34, 133.01, 129.58, 129.13, 127.53, 127.30, 70.93, 70.84, 66.68, 55.73, 40.85, 37.82, 36.93, 35.23, 32.03, 29.83, 29.77, 29.71, 29.46, 28.56, 25.94, 25.88, 22.81, 18.45, 14.25, -4.45, -4.92; **IR** (film) 3510 (br O-H), 2925, 2854, 1779 (C=O), 1711 (C=O), 1388, 1348, 1250, 1210, 1115, 971, 908, 836, 777, 700; **HRMS** Accurate mass (ES^+): Found 596.3749, $C_{33}H_{55}NO_5SiNa$ ($M+Na^+$) requires 596.3747.

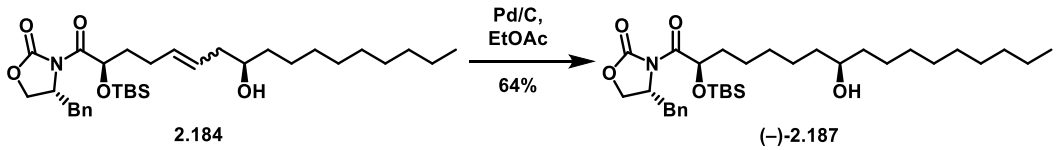

2.184 (–)-2.187

(R)-4-benzyl-3-((2R,8R)-2-((tert-butyldimethylsilyl)oxy)-8-hydroxyheptadecanoyl)oxazolidin-2-one (–)-2.187. Following general procedure B; alkene **2.184** (220 mg, 0.38 mmol) yielded the title compound as a brown oil (140 mg, 64% yield). **^{1}H NMR** (500 MHz, $CDCl_3$) δ 7.36 – 7.31 (m, 2H), 7.30 – 7.27 (m, 1H), 7.25 – 7.22 (m, 2H), 5.39 – 5.33 (m, 1H), 4.62 (qd, *J* = 6.3, 3.0 Hz, 1H), 4.24 – 4.14 (m, 2H), 3.60 – 3.54 (m, 1H), 3.40 (dd, *J* = 13.3, 3.2 Hz, 1H), 2.70 (dd, *J* = 13.3, 10.1 Hz, 1H), 1.74 – 1.58 (m, 3H), 1.53 – 1.35 (m, 9H), 1.33 – 1.23 (m, *J* = 19.3, 12.0 Hz, 17H), 0.93 (s, 7H), 0.87 (t, *J* = 7.0 Hz, 3H), 0.11 (s, *J* = 3.2 Hz, 3H), 0.09 (s, *J* = 6.9 Hz, 3H); **^{13}C NMR** (126 MHz, $CDCl_3$) δ 174.56, 153.25, 135.37, 129.57, 129.11, 127.50, 72.07, 71.44, 66.63, 55.72, 37.81, 37.65, 37.47, 35.25, 32.02, 29.84, 29.77, 29.70, 29.45, 29.34, 25.94, 25.78, 25.59, 25.56, 22.80, 18.46, 14.25, -4.51, -4.97; **$[\alpha]^{25}_D$** -4.2 (c = 1.1 in $CHCl_3$); **IR** (film) 3390 (br O-H), 2926, 2854, 1780 (C=O), 1711 (C=O), 1388, 1348, 1249, 1210, 1195, 1106, 1012, 976, 909, 836, 776, 731, 701; **HRMS** Accurate mass (ES^+): Found 598.3904, $C_{33}H_{57}NO_5SiNa$ ($M+Na^+$) requires 598.3909.

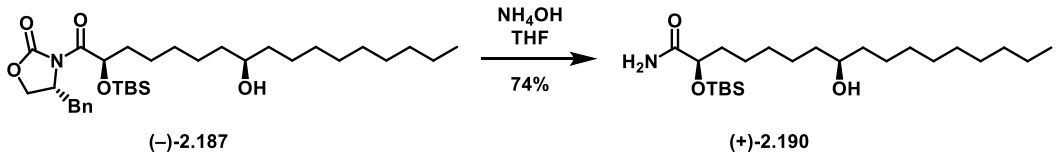

(2R,8R)-2-((tert-butyldimethylsilyl)oxy)-8-hydroxyheptadecanamide (+)-2.190. Following general procedure C; oxazolidinone **(–)-2.187** (140 mg, 0.24 mmol) yielded the title compound as a clear oil (74 mg, 74% yield). **^{1}H NMR** (400 MHz, $CDCl_3$) δ 6.56 – 6.45 (m, *J* = 4.1 Hz, 1H), 6.31 (d, *J* = 3.8 Hz, 1H), 4.09 (t, *J* = 5.1 Hz, 1H), 3.53 (d, *J* = 2.9 Hz, 1H), 1.79 – 1.55 (m, 4H), 1.46 – 1.32 (m, 9H), 1.32 – 1.19 (m, 17H), 0.90 (s, 9H), 0.85 (t, *J* = 6.8 Hz, 3H), 0.07 (s, 3H), 0.06 (s, 3H); **^{13}C NMR** (100 MHz, $CDCl_3$) δ 177.45, 73.46, 71.90, 37.56, 37.43, 35.13, 31.99, 29.82, 29.74, 29.67, 29.42, 25.82, 25.77, 25.57, 24.21, 22.77, 18.09, 14.21, -4.75, -5.16.; **$[\alpha]^{25}_D$** +13.6 (c = 0.56 in $CHCl_3$); **IR** (film) 3479 (N-H), 3300 (br O-H), 2953, 2854, 1682 (C=O), 1583, 1463, 1389, 1361, 1253, 1100, 1005, 836, 778, 667; **HRMS** Accurate mass (ES^+): Found 416.3552, $C_{23}H_{50}NO_3Si$ ($M+H^+$) requires 416.3560.

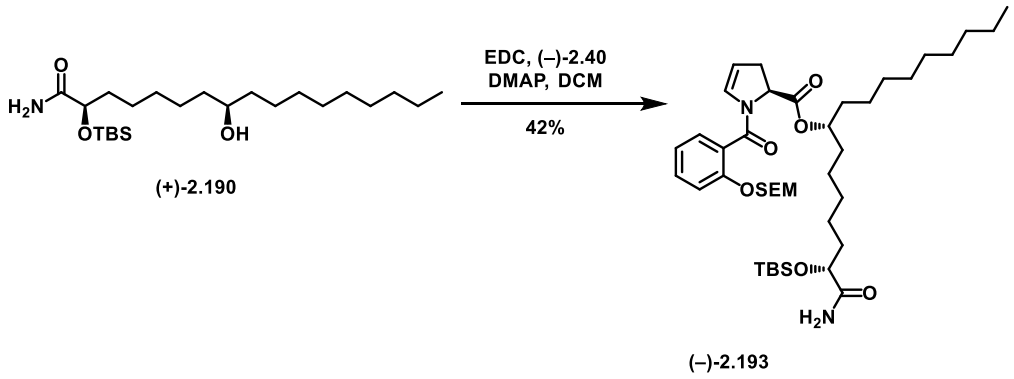

(2R,8R)-1-amino-2-((tert-butyldimethylsilyl)oxy)-1-oxoheptadecan-8-yl (S)-1-(2-((2-(trimethylsilyl)ethoxy)methoxy)benzoyl)-2,3-dihydro-1H-pyrrole-2-carboxylate (–)-2.193. Following general procedure J; alcohol **(+)-2.190** (36 mg, 0.09 mmol) yielded the title compound as a clear oil (29 mg, 42% yield). **^{1}H NMR** (400 MHz, $CDCl_3$)) δ 7.35 (t, *J* = 7.4 Hz, 2H), 7.19 (d, *J* = 8.9 Hz, 1H), 7.03 (t, *J* = 7.5 Hz, 1H), 6.53 (d, *J* = 4.3 Hz, 1H), 6.16 (d, *J* = 4.3 Hz, 1H), 5.57 (s, 1H), 5.22 (q, *J* = 7.1 Hz, 2H), 5.06 – 4.89 (m, 3H), 4.12 (t, *J* = 5.0 Hz, 1H), 3.79 – 3.68 (m, 2H), 3.19 – 3.06 (m, 1H), 2.72 – 2.61 (m, 1H), 1.73 (m, 4H), 1.65 (m, 1H), 1.55 (m, 4H), 1.24 (m, 22H), 0.91 (s, 12H), 0.86 (t, *J* = 6.8 Hz, 3H), 0.08

(s, 3H), 0.07 (s, 3H), 0.00 – -0.03 (m, 9H) ; **^{13}C NMR** (100 MHz, $CDCl_3$) δ 177.05, 170.77, 164.99, 153.82, 131.22, 131.03, 129.00, 125.94, 121.97, 115.22, 108.39, 93.34, 75.49, 73.55, 66.62, 58.20, 35.11, 34.41, 34.10, 34.04, 32.01, 29.66, 29.49, 29.42, 25.87, 25.37, 25.05, 24.11, 22.80, 18.16, 14.24, -1.27, -4.70, -5.14; **$[\alpha]^{25}_D$** -31.0 (c = 1.3 in $CHCl_3$); **IR** (film) 3480 (N-H), 2926, 2855, 1738 (C=O), 1690 (C=O), 1455, 1406, 1249, 1194, 1087, 988, 939, 835, 778, 754, 697; **HRMS** Accurate mass (ES^+): Found 761.4991, $C_{41}H_{73}N_2O_7Si_2$ ($M+H^+$) requires 761.4956.

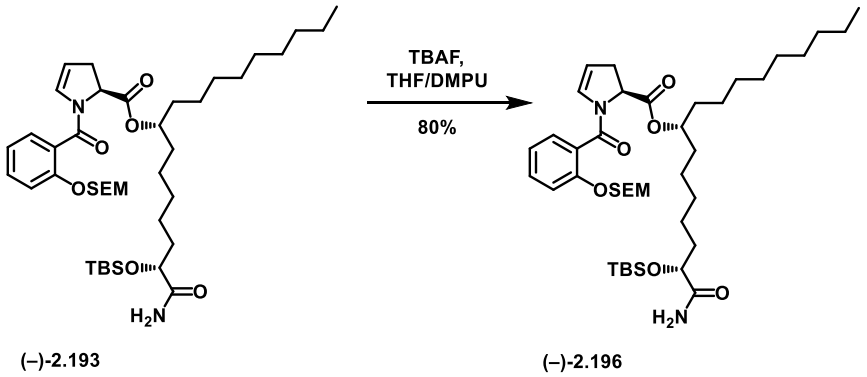

(2R,8R)-1-amino-2-hydroxy-1-oxoheptadecan-8-yl (S)-1-(2-hydroxybenzoyl)-2,3-dihydro-1H-pyrrole-2-carboxylate (–)-2.196. Following general procedure L; silyl ether **(–)-2.193** (13 mg, 0.017 mmol) yielded the title compound as a clear oil (7 mg, 80% yield). **^{1}H NMR** (400 MHz, $CDCl_3$) δ 7.41 – 7.34 (m, 1H), 6.99 (d, *J* = 8.1 Hz, 1H), 6.91 (t, *J* = 7.5 Hz, 1H), 6.71 (s, 1H), 6.63 (s, 1H), 5.53 (s, 1H), 5.30 – 5.26 (m, 1H), 5.01 (dd, *J* = 11.3, 4.7 Hz, 2H), 4.10 (dd, *J* = 7.9, 3.6 Hz, 1H), 3.19 – 3.08 (m, 1H), 2.70 (d, *J* = 17.3 Hz, 1H), 1.86 – 1.75 (m, 1H), 1.68 – 1.52 (m, 6H), 1.48 – 1.38 (m, 5H), 1.31 – 1.19 (m, *J* = 3.7 Hz, 22H), 0.88 (t, *J* = 6.8 Hz, 3H); **^{13}C NMR** (151 MHz, $CDCl_3$) δ 177.02, 171.16, 167.27, 157.83, 133.32, 130.73, 128.19, 119.27, 117.87, 117.70, 110.89, 75.90, 71.29, 59.21, 34.40, 34.18, 34.04, 33.56, 31.88, 29.70, 29.50, 29.42, 29.28, 28.24, 25.42, 24.72, 24.46, 22.67, 14.11; **$[\alpha]^{25}_D$** -28.1 (c = 0.32 in $CHCl_3$); **IR** (film) 3338 (br O-H), 2922, 2853, 1734 (C=O), 1662 (C=O), 1593 (C=O), 1458, 1431, 1376, 1294, 1196, 1153, 1098, 1017, 945, 858, 817, 756, 721, 654, 616; **HRMS** Accurate mass (ES^+): Found 517.3276, $C_{29}H_{45}N_2O_6$ ($M+H^+$) requires 517.3277.

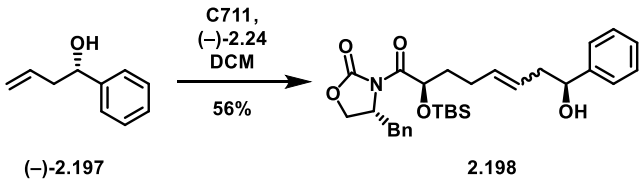

(R)-4-benzyl-3-((2R,8S)-2-((tert-butyldimethylsilyl)oxy)-8-hydroxy-8-phenyloct-5-enoyl)oxazolidin-2-one (2.198). Following general procedure A; homoallylic alcohol **(–)-2.197** (500 mg, 3.42 mmol) yielded the title compound as a brown oil (200 mg, 56% yield). **^{1}H NMR** (500 MHz, $CDCl_3$, mixture of E/Z isomers) δ 7.37 – 7.32 (m, 6H), 7.31 – 7.27 (m, 2H), 7.26 – 7.22 (m, 2H), 5.67 – 5.43 (m, 2H), 5.40 – 5.33 (m, 1H), 4.72 – 4.68 (m, 1H), 4.67 – 4.58 (m, *J* = 12.0, 8.0, 3.8 Hz, 1H), 4.24 – 4.15 (m, 2H), 3.43 – 3.39 (m, 1H), 2.73 – 2.65 (m, 1H), 2.51 – 2.35 (m, 2H), 2.31 – 2.15 (m, 3H), 1.82 – 1.66 (m, 2H), 0.94 (s, 9H), 0.11 (s, 3H), 0.08 (s, 3H); **^{13}C NMR** (126 MHz, $CDCl_3$) δ 174.30, 153.13, 144.11, 135.21, 133.52, 129.47, 129.02, 128.35, 127.43, 127.34, 126.76, 125.79, 73.26, 70.76, 66.59, 55.62, 42.95, 37.71, 35.08, 28.45, 25.83, 18.33, -4.57, -5.04; **IR** (film) 3400 (br O-H), 2928, 2856, 1777 (C=O), 1710 (C=O), 1388, 1349, 1250, 1210, 1127, 1050 ,971, 909, 835, 777, 700; **HRMS** Accurate mass (ES^+): Found 546.2653, $C_{30}H_{41}NO_5SiNa$ (M+Na) requires 546.2652.

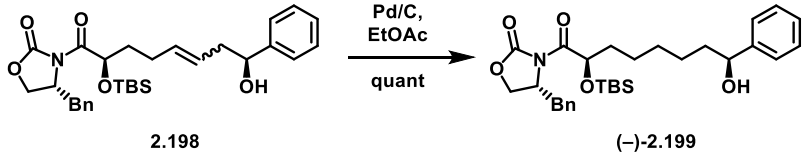

(R)-4-benzyl-3-((2R,8S)-2-((tert-butyldimethylsilyl)oxy)-8-hydroxy-8-phenyloctanoyl)oxazolidin-2-one (–)-2.199. Following general procedure B; alkene **2.198** (260 mg, 0.5 mmol) yielded the title compound as a clear oil (262 mg, quant.). **^{1}H NMR** (500 MHz, $CDCl_3$) δ 7.37 – 7.32 (m, 4H), 7.30 – 7.26 (m, 2H), 7.24 (d, *J* = 8.4 Hz, 2H), 7.17 (d, *J* = 6.7 Hz, 2H), 5.36 (td, *J* = 7.9, 3.4 Hz, 1H), 4.68 – 4.59 (m, 2H), 4.22 – 4.15 (m, 2H), 3.40 (dt, *J* = 13.3, 2.7 Hz, 1H), 2.69 (ddd, *J* = 13.3, 10.1, 1.9 Hz, 1H), 2.62 – 2.57 (m, 1H), 1.84 – 1.75 (m, 1H), 1.73 – 1.57 (m, 4H), 1.45 (s, 2H), 1.33 (s, 3H), 0.93 (d, *J* = 3.8 Hz, 9H), 0.11 (d, *J* = 3.4 Hz, 3H), 0.08 (d, *J* = 4.9 Hz, 3H).; **^{13}C NMR** (126 MHz, $CDCl_3$) δ 174.53, 153.24, 145.02, 142.98, 135.39, 129.59, 129.14, 128.58, 128.53, 128.35, 127.63, 127.53, 126.02, 125.68, 77.41, 77.16, 76.91, 74.75,

71.47, 71.45, 66.64, 55.74, 39.15, 37.84, 36.05, 35.39, 35.25, 31.51, 29.27, 29.22, 25.96, 25.77, 25.53, 18.49, -4.49, -4.94.; **[α]$^{25}_{D}$** -11.5 (c = 1.0 in $CHCl_3$); **IR** (film) 3500 (br O-H), 2928, 2856, 1779 (C=O), 1711 (C=O), 1454, 1387, 1348, 1249, 1210, 1195, 1105, 1121, 1010, 977, 835, 777, 699; **HRMS** Accurate mass (ES^+): Found 526.2998, $C_{30}H_{44}NO_5Si$ (M+H) requires 526.2989.

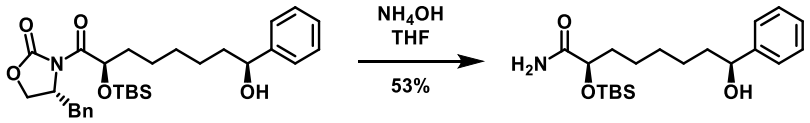

(2R,8S)-2-((tert-butyldimethylsilyl)oxy)-8-hydroxy-8-phenyloctanamide (+)-2.200. Following general procedure C; oxazolidinone **(–)-2.199** (197 mg, 0.375 mmol) yielded the title compound as a clear oil (72 mg, 53% yield). **^{1}H NMR** (500 MHz, $CDCl_3$) δ 7.29 – 7.24 (m, 4H), 7.22 – 7.17 (m, 1H), 6.43 (d, *J* = 3.7 Hz, 1H), 5.73 – 5.65 (m, 1H), 4.58 (t, *J* = 5.9 Hz, 1H), 4.04 (t, *J* = 5.1 Hz, 1H), 2.00 (s, 1H), 1.76 – 1.52 (m, 4H), 1.39 – 1.15 (m, 6H), 0.85 (s, 9H), 0.02 (s, 3H), 0.01 (s, 3H).; **^{13}C NMR** (126 MHz, $cdcl_3$) δ 177.12, 145.05, 128.55, 127.59, 126.02, 74.67, 73.55, 39.13, 35.17, 29.53, 25.87, 25.77, 24.17, 18.14, -4.70, -5.12.; **[α]$^{25}_{D}$** +3.2 (c = 1.1 in $CHCl_3$); **IR** (film) 3475 (N-H), 3300 (br O-H), 2928, 2856, 1780, 1681 (C=O), 1582, 1463, 1389, 1361, 1253, 1005, 909, 836, 778, 730, 700; **HRMS** Accurate mass (ES^+): Found 366.2465, $C_{20}H_{36}NO_3Si$ (M+H) requires 366.2464.

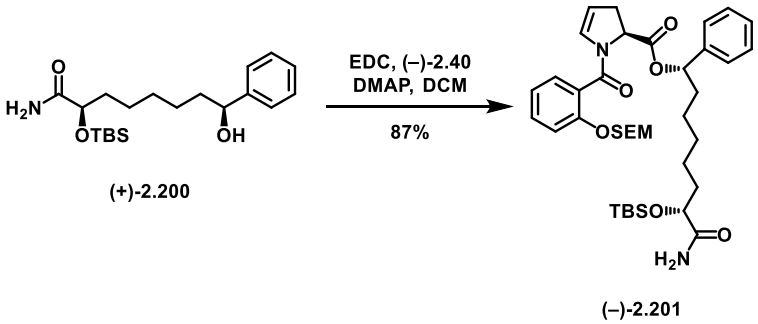

(1S,7R)-8-amino-7-((tert-butyldimethylsilyl)oxy)-8-oxo-1-phenyloctyl (S)-1-(2-((2-(trimethylsilyl)ethoxy)methoxy)benzoyl)-2,3-dihydro-1H-pyrrole-2-carboxylate (–)-2.201. Following general procedure J; alcohol **(+)-2.200** (30 mg, 0.082 mmol) yielded the title compound as a clear oil (51

mg, 87% yield). **^{1}H NMR** (300 MHz, $CDCl_3$) δ 7.36 – 7.26 (m, 7H), 7.18 (d, *J* = 8.3 Hz, 1H), 7.01 (t, *J* = 7.5 Hz, 1H), 6.51 (d, *J* = 4.6 Hz, 1H), 6.16 – 6.09 (m, 1H), 5.87 – 5.70 (m, 2H), 5.25 – 5.17 (m, 2H), 5.05 (dd, *J* = 11.6, 4.6 Hz, 1H), 4.99 – 4.92 (m, 1H), 4.10 (t, *J* = 5.0 Hz, 1H), 3.79 – 3.65 (m, 2H), 3.15 – 2.98 (m, 1H), 2.61 – 2.47 (m, 1H), 2.05 – 1.90 (m, 1H), 1.82 – 1.54 (m, 3H), 1.38 – 1.21 (m, 9H), 0.90 (s, 9H), 0.07 (d, *J* = 1.8 Hz, 6H), -0.03 (s, 6H).; **^{13}C NMR** (126 MHz, $CDCl_3$) δ 176.94, 170.07, 165.10, 153.81, 140.52, 131.22, 130.94, 129.04, 128.55, 127.99, 126.65, 121.97, 115.22, 108.40, 93.34, 77.25, 73.53, 66.61, 57.92, 36.22, 35.10, 33.90, 29.81, 29.35, 25.86, 25.30, 24.05, 18.16, 18.13, -1.29, -4.71, -5.14.; **$[\alpha]^{25}_D$** -21.3 (c = 1.10 in $CHCl_3$); **IR** (film) 3500 (N-H), 2925, 2854, 2362, 1735 (C=O), 1653 (C=O), 1601 (C=O), 1456, 1398, 1249, 1193, 1086, 986, 830, 756; **HRMS** Accurate mass (ES^+): Found 711.3856, $C_{38}H_{59}N_2O_7Si_2$ (M+H) requires 711.3861.

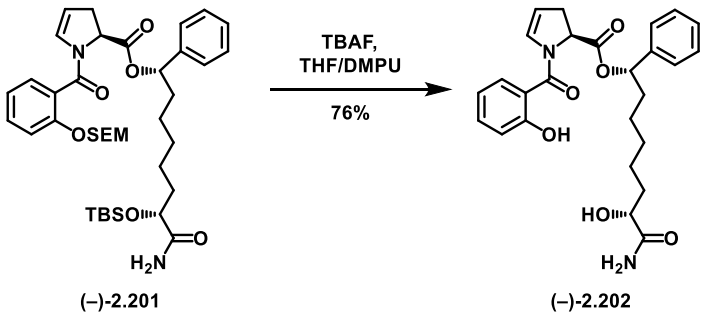

(–)-2.201 (–)-2.202

(1S,7R)-8-amino-7-hydroxy-8-oxo-1-phenyloctyl (S)-1-(2-hydroxybenzoyl)-2,3-dihydro-1H-pyrrole-2-carboxylate (–)-2.202. Following general procedure L; silyl ether **(–)-2.201** (18 mg, 0.025 mmol) yielded the title compound as a clear oil (9 mg, 76% yield). **^{1}H NMR** (600 MHz, $CDCl_3$) δ 9.55 (s, 1H), 7.41 – 7.37 (m, 2H), 7.35 – 7.29 (m, 5H), 6.99 (dd, *J* = 8.3, 1.1 Hz, 1H), 6.90 (t, *J* = 7.5 Hz, 1H), 6.72 (s, 1H), 6.55 (s, 1H), 5.89 (s, 1H), 5.47 (s, 1H), 5.23 – 5.18 (m, 1H), 5.07 (dd, *J* = 11.4, 4.7 Hz, 1H), 4.11 (dd, *J* = 8.0, 3.7 Hz, 1H), 3.12 – 3.03 (m, 1H), 2.57 (d, *J* = 17.1 Hz, 1H), 2.04 – 1.96 (m, 1H), 1.86 – 1.78 (m, 2H), 1.70 – 1.61 (m, 3H), 1.50 – 1.40 (m, 4H), 1.36 – 1.30 (m, 2H).; **^{13}C NMR** (151 MHz, $CDCl_3$) δ 176.95, 170.52, 167.53, 158.34, 140.26, 133.56, 130.80, 128.70, 128.62, 128.24, 126.54, 119.33, 118.05, 117.52, 111.06, 77.29, 71.50, 59.20, 36.24, 34.47, 29.84, 28.36, 25.22, 24.68.; **$[\alpha]^{25}_D$** -63.5 (c = x0.49 in $CHCl_3$); **IR** (film) 3326 (br O-H), 2930, 2859, 1738 (C=O), 1663 (C=O), 1586 (C=O), 1456, 1428, 1354, 1294, 1190, 1153,

1097, 908, 856, 817, 755, 727, 669; **HRMS** Accurate mass (ES^+): Found 489.2019, $C_{26}H_{30}N_2O_6Na$ (M+Na) requires 489.2002.

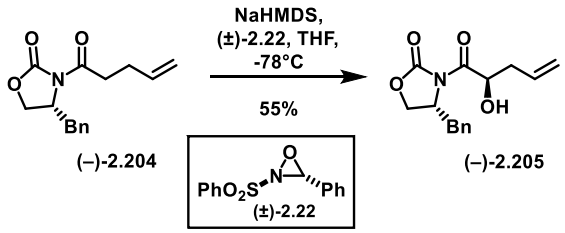

(R)-4-benzyl-3-((R)-2-hydroxypent-4-enoyl)oxazolidin-2-one (–)-2.205. NaHMDS (6.6 mL, 1M soln. in THF, 6.6 mmol) was diluted with anhydrous THF (42 mL) and cooled to -78°C. **(-)-2.204** (1.47 g, 5.7 mmol) was dissolved in THF (8.5 mL), cooled to -78°C, and slowly added to the NaHMDS solution via cannula. The resulting solution was stirred for an hour at -78°C. Davis oxaziridine (**(±)-2.22**, 1.58 g, 6.04 mmol) was dissolved in THF (8.5 mL) and added via syringe pump to the reaction over a 25-minute period. The reaction was stirred for an additional hour at -78°C. (±)-Camphorsulfonic acid (CSA) (6.4 g, 27.5 mmol) dissolved in THF (53 mL) was added, and the reaction was warmed up to room temperature. H_2O was added, and the solution was extracted 3x EtOAc. The combined organic layers were washed with brine, dried ($MgSO_4$), filtered, concentrated, and purified by column chromatography (0→10% EtOAc in hexanes) to yield **(-)-2.205** as a yellow oil (0.853 g, 55%). **^{1}H NMR** (399 MHz, $CDCl_3$) δ 7.38 – 7.32 (m, 2H), 7.32 – 7.27 (m, *J* = 7.5, 3.6, 1.5 Hz, 1H), 7.24 – 7.20 (m, 2H), 5.87 (ddt, *J* = 17.2, 10.2, 7.1 Hz, 1H), 5.23 – 5.07 (m, 3H), 4.66 (ddt, *J* = 9.8, 6.6, 3.4 Hz, 1H), 4.32 – 4.22 (m, 2H), 3.32 (dd, *J* = 13.5, 3.3 Hz, 1H), 2.84 (dd, *J* = 13.5, 9.4 Hz, 1H), 2.62 (dddd, *J* = 6.9, 4.7, 4.1, 1.2 Hz, 1H), 2.45 (dt, *J* = 14.2, 7.1 Hz, 1H.; **^{13}C NMR** (100 MHz, $CDCl_3$) δ 174.09, 153.38, 134.87, 132.96, 129.59, 129.19, 127.68, 118.76, 70.42, 67.13, 55.70, 38.43, 37.64.; **$[\alpha]^{25}_D$** -57.3 (c = 0.77 in $CHCl_3$); **IR** (film) 3496 (br O-H), 3069, 3030, 2977, 2920, 1774 (C=O), 1698 (C=O), 1389, 1350, 1291, 1212, 1117, 763, 704; **HRMS** Accurate mass (ES^+): Found 298.1053, $C_{15}H_{17}NO_4Na$ (M+H) requires 298.1055.

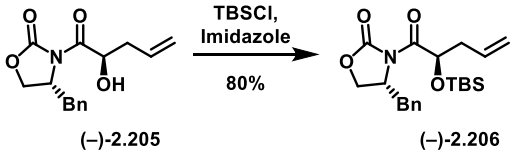

(R)-4-benzyl-3-((R)-2-((tert-butyldimethylsilyl)oxy)pent-4-enoyl)oxazolidin-2-one (–)-2.206. To a solutin of **(–)-2.205** (0.336 g, 1.22 mmol) in DMF (6 mL) at 0°C was added tert-butyldimethylsilyl chloride (0.276 g, 1.83 mmol) and imidiazole (0.108 g, 1.59 mmol). The reaction was allowed to warm to room temperature and stirred for 16 hours. The nexr day, the reaction was poured over H_2O (10 mL) and extracted with 1:1 EtOAc:hexanes (3x50mL). The combined organic layers were washed with water then brine, dried over Na_2SO_4, filtered and concentrated. The product was purified by column chromatography to give **(–)-2.206** as a clear oil (0.379 g, 80%). **^{1}H NMR** (399 MHz, $CDCl_3$) δ 7.37 – 7.31 (m, *J* = 7.8, 6.4 Hz, 2H), 7.28 (t, *J* = 5.1 Hz, 1H), 7.25 – 7.21 (m, 2H), 5.88 (ddt, *J* = 17.1, 10.0, 7.1 Hz, 1H), 5.47 (dd, *J* = 7.2, 4.5 Hz, 1H), 5.16 – 5.05 (m, *J* = 13.6, 7.5 Hz, 2H), 4.62 (dt, *J* = 9.9, 4.4 Hz, 1H), 4.19 (d, *J* = 4.5 Hz, 2H), 3.39 (dd, *J* = 13.3, 3.3 Hz, 1H), 2.76 – 2.68 (m, *J* = 13.3, 10.1 Hz, 1H), 2.57 – 2.35 (m, 2H), 0.94 – 0.91 (m, 9H), 0.11 (s, 3H), 0.09 (s, 3H).**^{13}C NMR** (100 MHz, $CDCl_3$173.59, 153.26, 135.29, 133.59, 129.55, 129.09, 127.50, 118.27, 71.10, 66.69, 55.69, 40.00, 37.80, 25.89, 18.46, -4.58, -4.90.; **$[\alpha]^{25}_D$** -23.6 (c = 0.95 in $CHCl_3$); **IR** (film) 3075, 2960, 2926, 2856, 1777 (C=O), 1712 (C=O), 1386, 1347, 1257, 1209, 1144, 1105, 984, 920, 838, 777, 706; **HRMS** Accurate mass (ES^+): Found 390.2099, $C_{21}H_{32}NO_4Si$ (M+H) requires 390.2101.

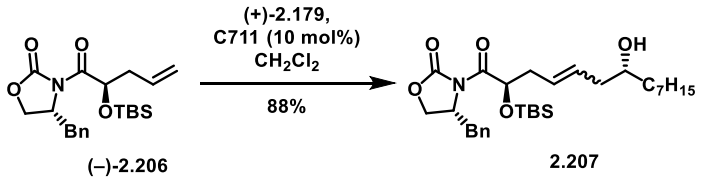

(R)-4-benzyl-3-((2R,7R)-2-((tert-butyldimethylsilyl)oxy)-7-hydroxytetradec-4-enoyl)oxazolidin-2-one (2.207). Following general procedure A, homoallylic alcohol **(+)-2.179** (833 mg, 4.9 mmol) yielded the title compound as a brown oil (54 mg, 61% yield). **^{1}H NMR** (600 MHz, $CDCl_3$, mixture of E/Z isomers) δ 7.35 (t, *J* = 7.6 Hz, 2H), 7.30 (d, *J* = 7.3 Hz, 1H), 7.25 (d, *J* = 7.1 Hz, 2H), 5.77 – 5.54 (m, 2H), 5.53 –

5.49 (m, 1H), 4.68 – 4.61 (m, 1H), 4.28 – 4.16 (m, 2H), 3.59 (s, 1H), 3.39 (dd, *J* = 13.3, 3.3 Hz, 1H), 1.79 (d, *J* = 43.0 Hz, 1H), 1.50 – 1.41 (m, 3H), 1.38 – 1.23 (m, 9H), 0.95 (d, *J* = 2.2 Hz, 9H), 0.92 – 0.88 (m, 3H), 0.14 (d, *J* = 7.5 Hz, 3H), 0.11 (d, *J* = 5.4 Hz, 3H).; **^{13}C NMR** (126 MHz, $CDCl_3$) δ 173.49, 153.19, 135.19, 130.61, 129.49, 129.01, 128.15, 127.43, 77.29, 77.04, 76.78, 70.93, 70.67, 66.60, 55.57, 40.74, 38.44, 37.68, 36.86, 31.85, 29.66, 29.31, 25.83, 25.80, 22.68, 18.33, 14.12, -4.70, -5.02.; **IR** (film) 3510 (br O-H), 2926, 2855, 1781 (C=O), 1712 (C=O), 1388, 1348, 1250, 1210, 1109, 1007, 975, 938, 836, 778, 732, 701; **HRMS** Accurate mass (ES^+): Found 532.3457, $C_{30}H_{50}NO_5Si$ (M+H) requires 532.3458.

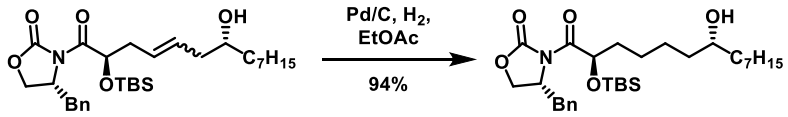

2.207 **(–)-2.208**

(R)-4-benzyl-3-((2R,7R)-2-((tert-butyldimethylsilyl)oxy)-7-hydroxytetradecanoyl)oxazolidin-2-one (–)-2.208. Following general procedure B; alkene **2.207** (456 mg, 0.85 mmol) yielded the title compound as a clear oil (430 mg, 94% yield). **^{1}H NMR** (400 MHz, $CDCl_3$) δ 7.37 – 7.27 (m, 3H), 7.26 – 7.22 (m, 2H), 5.37 (dd, *J* = 8.1, 3.4 Hz, 1H), 4.66 – 4.59 (m, 1H), 4.24 – 4.15 (m, 2H), 3.58 (s, 1H), 3.40 (dd, *J* = 13.2, 3.4 Hz, 1H), 2.70 (dd, *J* = 13.2, 10.2 Hz, 1H), 1.76 – 1.59 (m, 2H), 1.52 – 1.35 (m, 8H), 1.33 – 1.23 (m, 11H), 0.94 (s, 9H), 0.90 – 0.85 (m, 3H), 0.11 (s, 3H), 0.09 (s, 3H).; **^{13}C NMR** (126 MHz, $CDCl_3$) δ 174.44, 153.17, 135.30, 129.50, 129.03, 127.43, 71.30, 66.58, 55.64, 37.72, 37.48, 37.28, 35.18, 31.90, 29.73, 29.37, 25.87, 25.74, 25.53, 25.15, 22.72, 18.39, 14.17, -4.58, -5.03.; **$[\alpha]^{25}_D$** -4.5 (c = 0.83 in $CHCl_3$); **IR** (film) 3390 (br O-H), 2925, 2855, 1781 (C=O), 1711 (C=O), 1388, 1349, 1249, 1210, 1196, 1107, 1051, 1011, 977, 835, 777, 701; **HRMS** Accurate mass (ES^+): Found 534.3622, $C_{30}H_{52}NO_5Si$ (M+H) requires 534.3615.

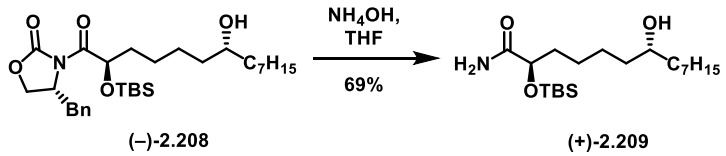

(2R,7R)-2-((tert-butyldimethylsilyl)oxy)-7-hydroxytetradecanamide (+)-2.209. Following general procedure C; oxazolidinone **(–)-2.208** (430 mg, 0.8 mmol) yielded the title compound as a clear oil (208 mg, 69% yield). **^{1}H NMR** (500 MHz, $CDCl_3$) δ 6.53 (d, *J* = 4.0 Hz, 1H), 5.71 (d, *J* = 3.7 Hz, 1H), 4.17 – 4.09 (m, 1H), 3.56 (s, 1H), 1.83 – 1.64 (m, 3H), 1.49 – 1.35 (m, 10H), 1.33 – 1.22 (m, 11H), 0.92 (s, 9H), 0.87 (t, *J* = 7.0 Hz, 3H), 0.10 (s, 3H), 0.08 (s, 3H); **^{13}C NMR** (126 MHz, $CDCl_3$) δ 177.20, 73.46, 71.88, 37.62, 37.39, 35.20, 31.95, 29.79, 29.42, 25.86, 25.78, 25.63, 24.24, 22.78, 18.13, 14.23, -4.71, -5.13; **$[\alpha]^{25}_D$** +8.9 (c = 0.85 in $CHCl_3$); **IR** (film) 3480 (N-H), 3300 (br O-H), 2927, 2856, 1682 (C=O), 1582, 1463, 1361, 1253, 1096, 1005, 835, 778, 731, 669; **HRMS** Accurate mass (ES^+): Found 374.3098, $C_{20}H_{44}NO_3Si$ (M+H) requires 374.3090.

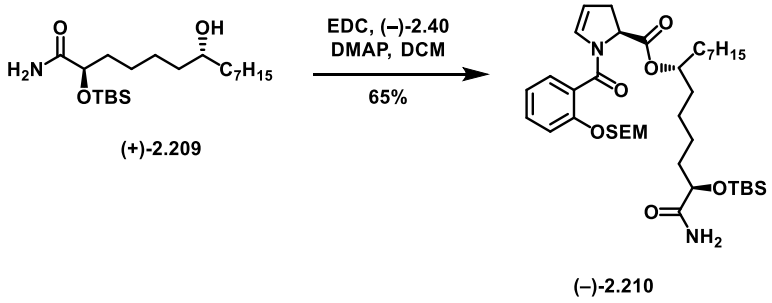

(2R,7R)-1-amino-2-((tert-butyldimethylsilyl)oxy)-1-oxotetradecan-7-yl (S)-1-(2-((2-(trimethylsilyl)ethoxy)methoxy)benzoyl)-2,3-dihydro-1H-pyrrole-2-carboxylate (–)-2.210. Following general procedure J; alcohol **(+)-2.209** (24 mg, 0.064 mmol) yielded the title compound as a clear oil (30 mg, 65% yield). **^{1}H NMR** (600 MHz, $CDCl_3$) δ 7.37 – 7.33 (m, 2H), 7.20 (dd, *J* = 8.9, 1.0 Hz, 1H), 7.04 (td, *J* = 7.5, 1.0 Hz, 1H), 6.54 (d, *J* = 4.5 Hz, 1H), 6.17 – 6.15 (m, 1H), 5.55 (d, *J* = 4.5 Hz, 1H), 5.25 – 5.20 (m, 1H), 5.03 – 4.98 (m, 2H), 4.97 – 4.92 (m, 1H), 4.14 (t, *J* = 5.1 Hz, 1H), 3.74 (t, *J* = 8.3 Hz, 2H), 3.16 – 3.08 (m, 1H), 2.70 – 2.63 (m, 1H), 1.82 – 1.74 (m, 1H), 1.71 – 1.62 (m, 3H), 1.62 – 1.51 (m, 4H), 1.43 – 1.36 (m, 3H), 1.31 – 1.20 (m, 11H), 0.91 (s, 9H), 0.86 (t, *J* = 7.0 Hz, 3H), 0.09 (s, 3H), 0.08 (s, 3H), -0.01

(s, 9H).; **^{13}C NMR** (151 MHz, $CDCl_3$) δ 176.90, 170.76, 165.04, 153.87, 131.25, 131.07, 129.05, 126.00, 122.00, 115.28, 108.41, 93.39, 75.51, 73.45, 66.65, 58.21, 34.97, 34.41, 34.20, 34.03, 31.93, 29.63, 29.33, 25.90, 25.37, 25.16, 24.08, 22.77, 18.19, 18.17, 14.23, -1.26, -4.68, -5.11.; **$[\alpha]^{25}_D$** -27.3 (c = 0.97 in $CHCl_3$); **IR** (film) 3480 (N-H), 2928, 2857, 1740 (C=O), 1683 (C=O), 1456, 1406, 1250, 1195, 1087, 988, 915, 835, 779, 730; **HRMS** Accurate mass (ES^+): Found 719.4514, $C_{38}H_{67}N_2O_7Si_2$ (M+H) requires 719.4487.

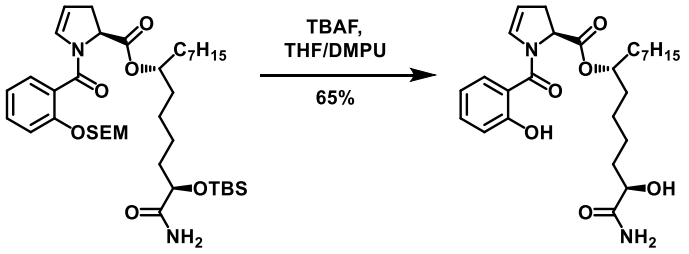

(–)-2.210 (–)-2.211

(2R,7R)-1-amino-2-hydroxy-1-oxotetradecan-7-yl (S)-1-(2-hydroxybenzoyl)-2,3-dihydro-1H-pyrrole-2-carboxylate (–)-2.211. Following general procedure L; silyl ether **(–)-2.210** (19 mg, 0.026 mmol) yielded the title compound as a clear oil (8 mg, 65% yield). **^{1}H NMR** (600 MHz, $CDCl_3$) δ 9.28 (s, 1H), 7.41 – 7.34 (m, 2H), 6.99 (d, *J* = 8.2 Hz, 1H), 6.90 (t, *J* = 7.5 Hz, 1H), 6.71 (s, 1H), 6.62 (s, 1H), 5.28 (s, 1H), 5.02 (dd, *J* = 11.4, 4.9 Hz, 2H), 4.10 (d, *J* = 5.2 Hz, 1H), 3.18 – 3.08 (m, 1H), 2.70 (d, *J* = 17.4 Hz, 1H), 1.90 – 1.80 (m, 1H), 1.73 – 1.56 (m, 9H), 1.55 – 1.37 (m, 8H), 0.87 (t, *J* = 7.1 Hz, 6H).; **^{13}C NMR** (151 MHz, $CDCl_3$) δ 177.11, 171.33, 167.44, 157.99, 133.52, 130.88, 128.38, 119.43, 118.07, 117.83, 111.07, 77.37, 77.16, 76.10, 71.52, 59.32, 34.66, 33.98, 32.07, 31.88, 29.84, 29.51, 29.29, 25.55, 24.83, 24.56, 22.76, 14.22.; **$[\alpha]^{25}_D$** -27.8 (c = 0.83 in $CHCl_3$); **IR** (film) 3334 (br O-H), 2926, 2859, 1738 (C=O), 1665 (C=O), 1600 (C=O), 1459, 1431, 1370, 1198, 1153, 1099, 1035, 1015, 948, 861, 816, 757, 726, 619, 532.; **HRMS** Accurate mass (ES^+): Found 497.2645, $C_{26}H_{38}N_2O_6Na$ (M+Na) requires 497.2628.

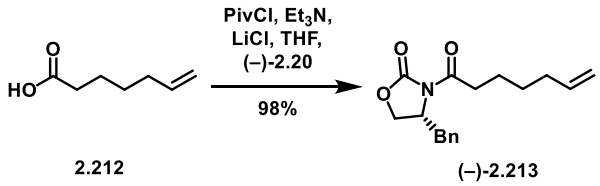

2.212 (–)-2.213

(R)-4-benzyl-3-(hept-6-enoyl)oxazolidin-2-one (–)-2.213. Based on the procedure by Kaliappan, et. al.[1]: To a solution of 6-heptenoic acid (1.05 mL, 7.8 mmol) and triethylamine (2.9 mL, 20.4 mmol) in THF (40 mL) at - 10°C was added pivaloyl chloride (0.961 mL, 7.8 mmol) dropwise, and stirred at this temperature for an hour. Then, LiCl (0.362 g, 8.54 mmol) and (R)-4-(Phenylmethyl)-2-oxazolidinone (1.32 g, 7.43 mmol) were each quickly added in one portion, and reaction was allowed to warm to room temperature, and stirred for 16 hours. Reaction was quenched with saturated $NaHCO_3$ and extracted with EtOAc 3x. The combined organic layers were washed with brine, dried (Na_2SO_4), concentrated, and purified by column chromatography, yielding **(–)-2.213** as a clear oil (2.1 g, 98%). **^{1}H NMR** (400 MHz, $CDCl_3$) δ 7.34 – 7.27 (m, 2H), 7.25 – 7.21 (m, 1H), 7.18 (d, *J* = 7.0 Hz, 2H), 5.79 (ddt, *J* = 16.9, 10.2, 6.7 Hz, 1H), 5.04 – 4.91 (m, 1H), 4.64 (ddd, *J* = 13.0, 6.9, 3.3 Hz, 1H), 4.19 – 4.10 (m, 2H), 3.26 (dd, *J* = 13.4, 3.3 Hz, 1H), 3.00 – 2.82 (m, 2H), 2.75 (dd, *J* = 13.3, 9.6 Hz, 1H), 2.08 (dd, *J* = 14.3, 7.1 Hz, 1H), 1.74 – 1.64 (m, 2H), 1.51 – 1.41 (m, 2H); **^{13}C NMR** (101 MHz, $CDCl_3$) δ 173.22, 153.48, 138.45, 135.34, 129.45, 128.95, 127.34, 114.75, 66.19, 55.14, 37.90, 35.39, 33.51, 28.31, 23.72; **$[\alpha]^{25}_D$** -50.8 (c = 0.59 in $CHCl_3$); **IR** (film) 2923, 2859, 1775 (C=O), 1696 (C=O), 1454, 1384, 1350, 1249, 1197, 1050, 992, 911, 748, 701; **HRMS** Accurate mass (ES^+): Found 288.1592, $C_{17}H_{22}NO_3$ ($M+H^+$) requires 288.1600.

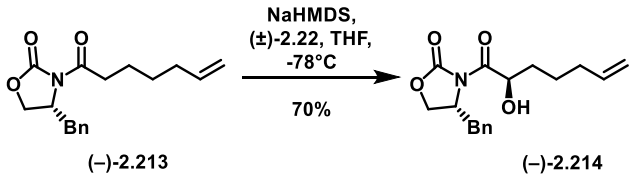

(–)-2.213 (–)-2.214

(R)-4-benzyl-3-((R)-2-hydroxyhept-6-enoyl)oxazolidin-2-one (–)-2.214. NaHMDS (0.44 mL, 1M soln. in THF, 0.44 mmol) was diluted with anhydrous THF (3 mL) and cooled to -78°C. **(-)-2.213** (3.7 g, 13.53 mmol) was dissolved in THF (20 mL), cooled to -78°C, and slowly added to the NaHMDS solution via

cannula. The resulting solution was stirred for an hour at -78°C. Davis oxaziridine (**(±)-2.22**, 0.138 g, 0.44 mmol) was dissolved in THF (1 mL) and added via syringe pump to the reaction over a 25 minute period. The reaction was stirred for an additional hour at -78°C. (±)-Camphorsulfonic acid (CSA) (0.430 g, 1.85 mmol) dissolved in THF (3.5 mL) was added, and the reaction was warmed up to room temperature. H_2O was added, and the solution was extracted 3x EtOAc. The combined organic layers were washed with brine, dried (MgSO4), filtered, concentrated, and purified by column chromatography (0→10% EtOAc in hexanes) to yield **(-)-2.214** as a yellow oil (0.078 g, 70%). **^{1}H NMR** (400 MHz, $CDCl_3$) δ 7.38 – 7.32 (m, *J* = 7.9, 1.9 Hz, 2H), 7.32 – 7.27 (m, *J* = 7.4, 3.7, 1.5 Hz, 1H), 7.24 – 7.19 (m, 2H), 5.81 (ddt, *J* = 16.9, 10.2, 6.6 Hz, 1H), 5.08 – 4.92 (m, 3H), 4.67 (ddt, *J* = 10.3, 7.1, 3.1 Hz, 1H), 4.33 – 4.22 (m, *J* = 9.2, 5.0 Hz, 2H), 3.31 (dd, *J* = 13.5, 3.2 Hz, 1H), 2.84 (dd, *J* = 13.5, 9.4 Hz, 1H), 2.20 – 2.05 (m, 1H), 1.87 – 1.76 (m, 1H), 1.69 – 1.55 (m, 3H); **^{13}C NMR** (100 MHz, cdcl$_3$) δ 174.98, 153.27, 138.40, 134.86, 129.51, 129.09, 127.57, 114.89, 70.75, 66.99, 55.57, 37.51, 33.75, 33.35, 24.60; **[α]$^{25}_D$** -46.3 (c = 0.71 in $CHCl_3$); **IR** (film) 3490 (br O-H), 2923, 2861, 1777 (C=O), 1692 (C=O), 1454, 1387, 1351, 1293, 1210, 1197, 1109, 982, 912, 837, 752, 701; **HRMS** Accurate mass (ES$^+$): Found 304.1540, $C_{17}H_{22}NO_4$ (M+H$^+$) requires 304.1549.

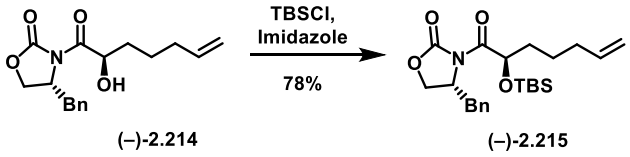

(–)-2.214 (–)-2.215

(R)-4-benzyl-3-((R)-2-((tert-butyldimethylsilyl)oxy)hept-6-enoyl)oxazolidin-2-one (–)-2.215. To a solution of **(-)-2.214** (0.074g, 0.24 mmol) in DMF (1.2 mL) at 0°C was added tert-Butyldimethylsilyl chloride (0.056g, 0.37 mmol) and imidazole (0.021g, 0.31 mmol). The solution was then allowed to warm to room temperature and stirred overnight. The following day, the reaction was poured into H_2O (2 mL) and extracted with 1:1 EtOAc:hexanes (4x20 mL). The combined organic layers were washed sequentially with H_2O and brine, dried (Na_2SO_4), filtered, concentrated, and purified by column chromatography to give **(-)-2.215** as a clear oil (0.078 g, 78%). **^{1}H NMR** (600 MHz, $CDCl_3$) δ 7.36 – 7.32 (m, 2H), 7.28 (ddd, *J* = 6.4, 3.9, 1.2 Hz, 1H), 7.25 – 7.23 (m, 2H), 5.79 (ddt, *J* = 16.9, 10.2, 6.6 Hz, 1H), 5.38 (dd, *J* = 8.1, 3.4 Hz,

1H), 5.05 – 4.91 (m, 2H), 4.67 – 4.59 (m, 1H), 4.19 (qd, *J* = 9.1, 1.7 Hz, 2H), 3.41 (dd, *J* = 13.3, 3.3 Hz, 1H), 2.70 (dd, *J* = 13.3, 10.2 Hz, 1H), 2.17 – 2.02 (m, 2H), 1.73 – 1.59 (m, 3H), 0.97 – 0.91 (m, 9H), 0.14 – 0.07 (m, 6H); **^{13}C NMR** (151 MHz, $CDCl_3$) δ 174.50, 153.26, 138.59, 135.41, 129.60, 129.15, 127.54, 114.85, 71.37, 66.67, 55.76, 37.86, 34.87, 33.42, 25.96, 24.90, 18.49, -4.49, -4.94; **[α]$^{25}_D$** -10.7 (c = 0.75 in $CHCl_3$); **IR** (film) 2928, 2856, 1778 (C=O), 1711 (C=O), 1453, 1386, 1348, 1247, 1209, 1194, 1106, 1006, 972, 835, 776, 700; **HRMS** Accurate mass (ES^+): Found 418.2408, $C_{23}H_{36}NO_4Si$ ($M+H^+$) requires 418.2413.

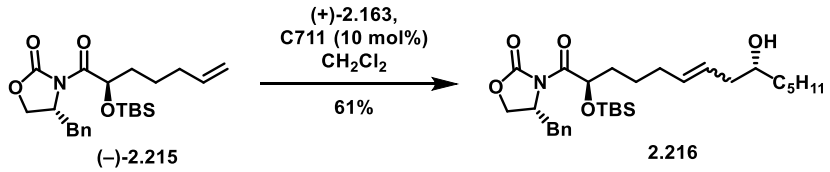

(R)-4-benzyl-3-((2R,9R)-2-((tert-butyldimethylsilyl)oxy)-9-hydroxytetradec-6-enoyl)oxazolidin-2-one (2.216). Following general procedure A, homoallylic alcohol **(+)-2.163** (119 mg, 0.84 mmol) and oxazolidinone **(–)-2.215** (70 mg, 0.168 mmol) yielded the title compound as a brown oil (54 mg, 61% yield). **^{1}H NMR** (400 MHz, $CDCl_3$, mixture of E/Z isomers) δ 7.37 – 7.31 (m, *J* = 7.2 Hz, 2H), 7.31 – 7.27 (m, *J* = 5.0 Hz, 1H), 7.25 – 7.22 (m, 2H), 5.56 – 5.39 (m, 2H), 5.36 (dd, *J* = 8.0, 3.3 Hz, 1H), 4.62 (qd, *J* = 6.5, 3.1 Hz, 1H), 4.25 – 4.15 (m, 1H), 3.63 – 3.51 (m, *J* = 22.2 Hz, 1H), 3.40 (dd, *J* = 13.2, 3.2 Hz, 1H), 2.69 (dd, *J* = 13.2, 10.2 Hz, 1H), 2.21 (dt, *J* = 11.9, 5.8 Hz, 1H), 2.14 – 1.99 (m, 3H), 1.76 – 1.51 (m, 4H), 1.47 – 1.39 (m, *J* = 2.0 Hz, 3H), 1.37 – 1.22 (m, 6H), 0.93 (s, 9H), 0.88 (t, *J* = 6.8 Hz, 3H), 0.11 (s, 3H), 0.09 (s, 3H); **^{13}C NMR** (100 MHz, $cdcl_3$) δ 174.44, 153.25, 135.33, 133.86, 129.54, 129.09, 127.49, 126.62, 71.30, 71.11, 66.64, 55.70, 40.82, 37.78, 36.81, 34.74, 32.18, 31.99, 25.93, 25.48, 25.36, 22.75, 18.45, 14.18, -4.52, -4.98; **IR** (film) 3377 (br O-H), 2928, 2857, 1781 (C=O), 1712 (C=O), 1456, 1388, 1348, 1249, 1210, 1195, 1110, 1013, 970, 836, 777, 701; **HRMS** Accurate mass (ES^+): Found 554.3281, $C_{30}H_{49}NO_5SiNa$ ($M+Na^+$) requires 554.3278.

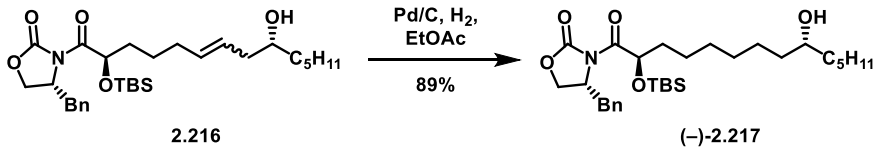

2.216 (–)-2.217

(R)-4-benzyl-3-((2R,9R)-2-((tert-butyldimethylsilyl)oxy)-9-hydroxytetradecanoyl)oxazolidin-2-one (–)-2.217. Following general procedure B; alkene **2.216** (54 mg, 0.10 mmol) yielded the title compound as a clear oil (48 mg, 89% yield). **^{1}H NMR** (399 MHz, cdcl$_3$) δ 7.37 – 7.27 (m, 3H), 7.26 – 7.22 (m, 2H), 5.36 (dd, *J* = 8.2, 3.4 Hz, 1H), 4.67 – 4.57 (m, *J* = 10.1, 6.7, 3.4 Hz, 1H), 4.24 – 4.15 (m, 2H), 3.58 (s, 1H), 3.40 (dd, *J* = 13.3, 3.2 Hz, 1H), 2.69 (dd, *J* = 13.2, 10.2 Hz, 1H), 1.72 – 1.55 (m, 9H), 1.43 (dd, *J* = 24.1, 11.7 Hz, 7H), 1.36 – 1.23 (m, 11H), 0.93 (s, 9H), 0.89 (t, *J* = 6.9 Hz, 3H), 0.11 (s, 3H), 0.09 (s, 3H); **^{13}C NMR** (100 MHz, cdcl$_3$) δ 174.55, 153.22, 135.33, 129.54, 129.07, 127.47, 71.99, 71.41, 66.61, 55.69, 37.78, 37.51, 35.27, 32.02, 29.53, 29.22, 25.92, 25.61, 25.52, 25.43, 22.76, 18.45, 14.17, -4.53, -4.99; **[α]$^{25}_{D}$** -6.6 (c = 1.5 in CHCl$_3$); **IR** (film) 3400 (br O-H), 2926, 2855, 1781 (C=O), 1712 (C=O), 1455, 1388, 1348, 1249, 1210, 1195, 1106, 1011, 976, 835, 777, 700, 593; **HRMS** Accurate mass (ES$^+$): Found 556.3446, $C_{30}H_{51}NO_5SiNa$(M+H$^+$) requires 556.3434.

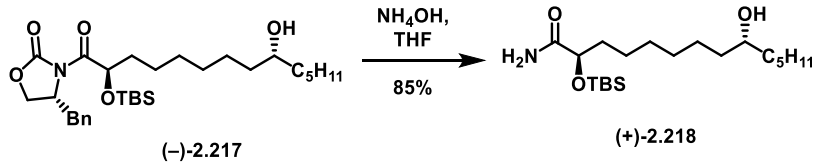

(–)-2.217 (+)-2.218

(2R,9R)-2-((tert-butyldimethylsilyl)oxy)-9-hydroxytetradecanamide (+)-2.218. Following general procedeure C; oxazolidinone **(–)-2.217** (48 mg, 0.09 mmol) yielded the title compound as a clear oil (29 mg, 85% yield). **^{1}H NMR** (300 MHz, CDCl$_3$) δ 6.52 (s, 1H), 5.81 (s, 1H), 4.12 (t, *J* = 5.0 Hz, 1H), 3.56 (s, 1H), 1.90 – 1.56 (m, *J* = 22.9, 18.5, 14.0 Hz, 4H), 1.50 – 1.22 (m, 22H), 0.95 – 0.83 (m, 12H), 0.09 (s, 3H), 0.08 (s, 3H); **^{13}C NMR** (126 MHz, CDCl$_3$) δ 177.23, 73.58, 72.06, 37.58, 37.55, 35.24, 32.04, 29.65, 29.58, 25.86, 25.69, 25.46, 24.19, 22.77, 18.14, 14.19, -4.71, -5.12; **[α]$^{25}_{D}$** +19.6 (c = 0.27 in CHCl$_3$); **IR** (film) 3478 (N-H), 3300 (br O-H), 2927, 2856, 1682 (C=O), 1582, 1463, 1253, 1098, 908, 835, 778, 732, 669; **HRMS** Accurate mass (ES$^+$): Found 374.3101, $C_{20}H_{44}NO_3Si$ (M+H$^+$) requires 374.3090.

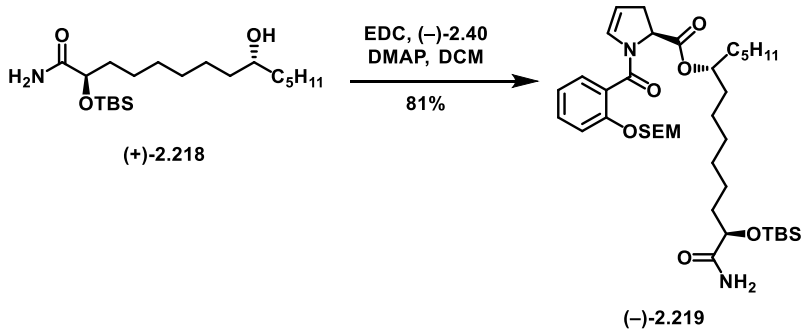

(6R,13R)-14-amino-13-((tert-butyldimethylsilyl)oxy)-14-oxotetradecan-6-yl (S)-1-(2-((2-(trimethylsilyl)ethoxy)methoxy)benzoyl)-2,3-dihydro-1H-pyrrole-2-carboxylate (–)-2.219. Following general procedure J; alcohol **(+)-2.218** (25 mg, 0.067 mmol) yielded the title compound as a clear oil (39 mg, 81% yield). **^{1}H NMR** (400 MHz, $CDCl_3$) δ 7.37 – 7.31 (m, 2H), 7.18 (d, *J* = 9.0 Hz, 1H), 7.02 (t, *J* = 7.4 Hz, 1H), 6.51 (s, 1H), 6.14 (d, *J* = 4.2 Hz, 1H), 5.51 – 5.42 (m, 1H), 5.21 (dd, *J* = 14.4, 7.1 Hz, 1H), 5.06 – 4.88 (m, 2H), 4.11 (t, *J* = 5.0 Hz, 1H), 3.77 – 3.68 (m, 1H), 3.11 (dd, *J* = 15.8, 12.9 Hz, 1H), 2.65 (d, *J* = 17.0 Hz, 1H), 1.78 – 1.69 (m, 1H), 1.66 – 1.51 (m, *J* = 12.0 Hz, 11H), 1.31 – 1.23 (m, 15H), 0.95 – 0.89 (m, 11H), 0.85 (t, *J* = 6.1 Hz, 3H), 0.07 (d, *J* = 5.7 Hz, 6H), -0.03 (s, *J* = 0.9 Hz, 9H) ; **^{13}C NMR** (126 MHz, $CDCl_3$) δ 177.00, 170.81, 165.01, 153.86, 131.23, 131.08, 129.03, 126.01, 121.99, 115.23, 108.36, 93.35, 75.58, 73.62, 66.63, 58.20, 35.17, 34.43, 34.12, 31.84, 29.84, 29.44, 25.88, 25.17, 25.03, 24.09, 22.67, 18.18, 18.16, 14.16, -1.26, -4.69, -5.11; **$[\alpha]^{25}_D$** -28.3 (c = 0.86 in $CHCl_3$); **IR** (film) 3219 (N-H), 2927, 2857, 1740 (C=O), 1652 (C=O), 1456, 1405, 1250, 1087, 983, 915, 835, 779, 730, 668; **HRMS** Accurate mass (ES^+): Found 741.4336, $C_{38}H_{66}N_2O_7Si_2Na$ ($M+Na^+$) requires 741.4306.

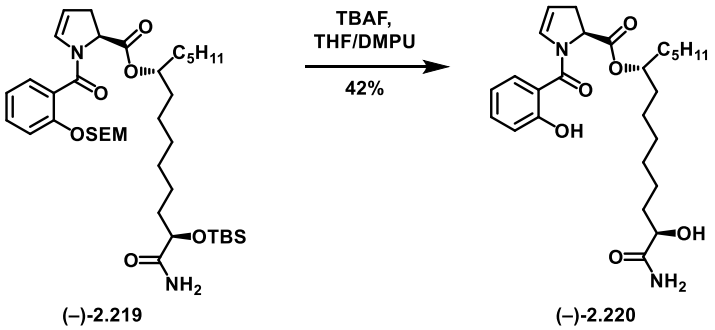

(6R,13R)-14-amino-13-hydroxy-14-oxotetradecan-6-yl (S)-1-(2-hydroxybenzoyl)-2,3-dihydro-1H-pyrrole-2-carboxylate (–)-2.220. Following general procedure L; silyl ether **(–)-2.219** (19 mg, 0.026 mmol) yielded the title compound as a clear oil (5 mg, 42% yield). **^{1}H NMR** (400 MHz, $CDCl_3$) δ 9.66 (s, 1H), 7.44 – 7.34 (m, 2H), 7.00 (s, *J* = 8.3 Hz, 1H), 6.90 (t, *J* = 7.5 Hz, 1H), 6.74 (s, 1H), 6.58 (s, 1H), 5.45 (s, 1H), 5.31 – 5.26 (m, 1H), 5.01 (dd, *J* = 11.2, 4.7 Hz, 2H), 4.04 (s, 1H), 3.40 (s, 1H), 3.20 – 3.07 (m, 1H), 2.70 (d, *J* = 15.0 Hz, 1H), 1.87 – 1.76 (m, *J* = 3.4 Hz, 1H), 1.73 – 1.48 (m, 11H), 1.47 – 1.21 (m, *J* = 43.7 Hz, 21H), 0.86 (t, *J* = 5.8 Hz, 3H); **^{13}C NMR** (100 MHz, $CDCl_3$) δ 176.92, 171.32, 167.46, 158.30, 133.56, 130.93, 128.39, 119.35, 118.04, 117.55, 110.98, 76.14, 71.81, 59.43, 34.68, 34.51, 34.36, 31.72, 29.85, 28.85, 28.63, 25.19, 24.60, 24.26, 22.63, 14.10.; **$[\alpha]^{25}_{D}$** -27.6 (c = 0.29 in $CHCl_3$); **IR** (film) 3338 (br O-H), 2924, 2855, 1734 (C=O), 1664 (C=O), 1616 (C=O), 1458, 1431, 1376, 1294, 1197, 1153, 1098, 1018, 858, 817, 756, 732, 654, 617; **HRMS** Accurate mass (ES^+): Found 497.2641, $C_{26}H_{38}N_2O_6Na$ ($M+Na^+$) requires 497.2628.

Chapter 3:

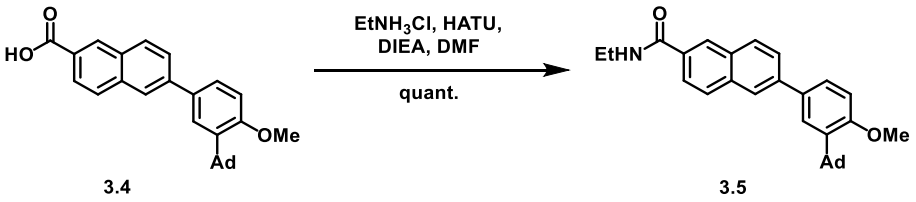

3.4 3.5

6-(3-(adamantan-1-yl)-4-methoxyphenyl)-N-ethyl-2-naphthamide (3.5). To a slurry of adapalene **3.4** (50 mg, 0.121 mmol) in DMF (3 mL) was added DIEA (0.13 mL, 0.726 mmol) followed by HATU (50.6 mg, 0.133 mmol) and $EtNH_3Cl$ (30 mg, 0.363 mmol) and the reaction was stirred at room temperature overnight. The reaction poured into water and quenched with sat. $NaHCO_3$, then extracted with CH_2Cl_2 3x. The combined organic layers were washed with water and brine, dried over Na_2SO_4, filtered, concentrated, and purified by prep TLC (neat EtOAc), yielding the title compound as a white solid (53 mg, quant.). **^{1}H NMR** (500 MHz, $CDCl_3$) δ 8.28 (s, 1H), 8.00 (s, 1H), 7.94 (dd, J = 13.3, 8.6 Hz, 2H), 7.83 (dd, J = 8.5, 1.7 Hz, 1H), 7.79 (dd, J = 8.5, 1.8 Hz, 1H), 7.59 (d, J = 2.4 Hz, 1H), 7.54 (dd, J = 8.4, 2.4 Hz, 1H), 7.00 (d, J = 8.5 Hz, 1H), 6.24 (br s, 1H), 3.91 (s, 3H), 3.58 (qd, J = 7.3, 5.9 Hz, 2H), 2.19 (s, 6H), 2.10 (s, 3H), 1.80 (s, 6H), 1.32 (t, J = 7.3 Hz, 3H); **^{13}C NMR** (125 MHz, $CDCl_3$) δ 167.64, 158.98, 140.85, 139.12, 135.23, 132.76, 131.65, 131.53, 129.36, 128.64, 127.15, 126.70, 126.08, 125.81, 124.86, 124.01, 112.24, 55.30, 40.75, 37.27, 35.20, 29.25, 15.13; **HRMS** Accurate mass (ES^+): Found 462.2404, $C_{30}H_{33}NO_2Na$ (M^+Na^+) requires 462.2409.

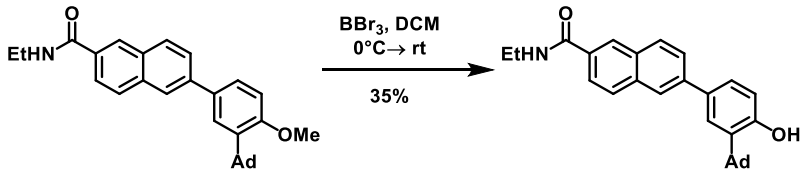

3.5 3.6

6-(3-(adamantan-1-yl)-4-hydroxyphenyl)-N-ethyl-2-naphthamide (3.6). To a solution of amide **3.5** (25 mg, 0.061 mmol) in CH_2Cl_2 (2 mL) at 0°C was added BBr_3 (1M in CH_2Cl_2, 0.12 mL, 0.122 mmol). The reaction was warmed to room temperature and stirred overnight. The reaction was cooled to 0 °C then

quenched with water and allowed to stir for 15 minutes, then extracted with EtOAc 3x. The combined organic layers were washed with water and brine, dried over Na_2SO_4, filtered, concentrated, and purified by HPLC, yielding the title compound as a white solid (5.3 mg, 35% yield). **^{1}H NMR** (500 MHz, $CDCl_3$) δ 8.29 (s, 1H), 8.06 (br s, 1H), 7.98 (s, 1H), 7.93 (dd, *J* = 12.3, 8.7 Hz, 2H), 7.82 (dd, *J* = 8.5, 1.8 Hz, 1H), 7.77 (dd, *J* = 8.5, 1.8 Hz, 1H), 7.58 (d, *J* = 2.3 Hz, 1H), 7.41 (dd, *J* = 8.1, 2.3 Hz, 1H), 6.81 (d, *J* = 8.1 Hz, 1H), 3.59 (qd, *J* = 7.3, 5.6 Hz, 2H), 2.22 (s, 6H), 2.12 (s, 3H), 1.81 (s, 6H), 1.32 (t, *J* = 7.3 Hz, 3H); **^{13}C NMR** (125 MHz, $CDCl_3$) δ 168.03, 154.86, 140.92, 137.04, 135.28, 133.01, 131.51, 131.41, 129.39, 128.71, 127.29, 126.74, 126.54, 125.81, 124.82, 123.94, 117.51, 40.70, 37.20, 37.06, 29.19, 15.08; **HRMS** Accurate mass (ES+): Found 448.2247, $C_{29}H_{31}NO_2Na$ (M+Na+) requires 448.2252.

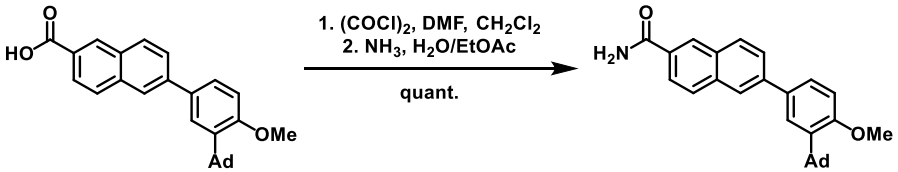

3.4 3.7

6-(3-(adamantan-1-yl)-4-methoxyphenyl)-2-naphthamide (3.7). To a solution of adapalene **3.4** (50 mg, 0.121 mmol) in CH_2Cl_2 (3 mL) and DMF (one drop, cat.) was added oxalyl chloride (2M in CH_2Cl_2, 0.15 mL, 0.30 mmol), and the reaction was stirred at room temperature 2 hours. The reaction was concentrated and dissolved in 8:1 EtOAc/NH_4OH (5 mL) and stirred at 0°C for 30 minutes. The reaction was diluted with EtOAc and water, and the aqueous layer was extracted with EtOAc 3x. The combined organic layers were washed with water and brine, dried over Na_2SO_4, filtered, and concentrated, yielding the title compound as a white solid (49 mg, quant.). **^{1}H NMR** (500 MHz, $CDCl_3$) δ 8.36 (s, 1H), 8.02 (s, 1H), 8.00 – 7.93 (m, 2H), 7.87 (dd, J = 8.5, 1.8 Hz, 1H), 7.81 (dd, J = 8.5, 1.8 Hz, 1H), 7.60 (d, J = 2.4 Hz, 1H), 7.55 (dd, J = 8.4, 2.4 Hz, 1H), 7.00 (d, J = 8.5 Hz, 1H), 3.91 (s, 3H), 2.19 (s, 6H), 2.11 (s, 3H), 1.80 (s, 6H); **^{13}C NMR** (125 MHz, $CDCl_3$) δ 170.04, 159.00, 141.20, 139.11, 135.53, 132.60, 131.39, 129.97, 129.49, 128.68, 128.09, 126.77, 126.03, 125.79, 124.79, 124.11, 112.22, 55.26, 40.69, 37.20, 29.19; **HRMS** Accurate mass (ES+): Found 434.2085, $C_{28}H_{29}NO_2Na$ (M+Na+) requires 434.2096.

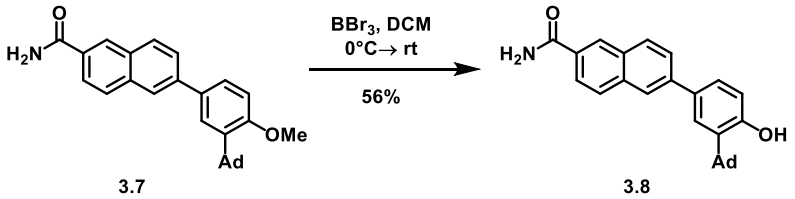

6-(3-(adamantan-1-yl)-4-hydroxyphenyl)-2-naphthamide (3.8). To a solution of amide **3.7** (25 mg, 0.061 mmol) in CH_2Cl_2 (2 mL) at 0°C was added BBr_3 (1M in CH_2Cl_2, 0.06 mL, 0.06 mmol), the reaction was warmed to room temperature and stirred overnight. The reaction was cooled to 0 °C and quenched with water and allowed to stir for 15 minutes, then extracted with EtOAc 3x. The combined organic layers were washed with water and brine, dried over Na_2SO_4, filtered, concentrated, and purified by HPLC, yielding the title compound as a white solid (13 mg, 56% yield). **^{1}H NMR** (500 MHz, DMSO) δ 9.68 (br s, 1H), 8.47 (s, 1H), 8.12 (d, J = 9.5 Hz, 2H), 8.02 (d, J = 8.6 Hz, 2H), 7.94 (dd, J = 8.6, 1.7 Hz, 1H), 7.84 (dd, J = 8.6, 1.8 Hz, 1H), 7.54 – 7.40 (m, 1H), 7.44 (br s, 1H) 6.92 (d, J = 8.2 Hz, 1H), 2.17 (s, 6H), 2.07 (s, 3H), 1.76 (s, 6H); **^{13}C NMR** (125 MHz, DMSO) δ 168.36, 156.84, 140.29, 136.44, 135.14, 131.45, 131.15, 130.47, 129.75, 128.28, 127.95, 126.13, 125.71, 125.52, 125.06, 123.99, 117.43, 37.06, 36.77, 28.83; **HRMS** Accurate mass (ES+): Found 398.2127, $C_{27}H_{28}NO_2$ (M+H+) requires 398.2120.

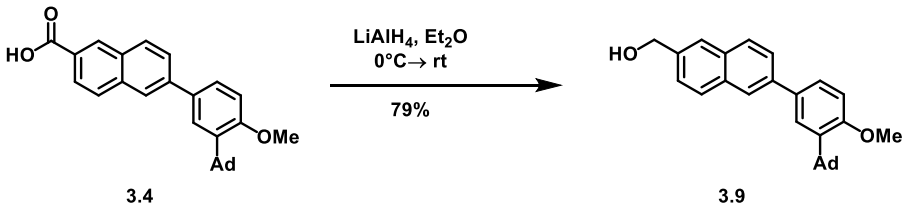

(6-(3-(adamantan-1-yl)-4-methoxyphenyl)naphthalen-2-yl)methanol (3.9). To a solution of lithium aluminum hydride (LAH) (5.05 mg, 0.133 mmol) in Et_2O (1 mL) at 0 °C was added adapalene **3.4** (50 mg, 0.121 mmol) in Et_2O (0.5 mL). The reaction was warmed to room temperature and stirred for 2 hours. The reaction was cooled to 0 °C and H_2O (1 mL) was added slowly followed by 1N NaOH (1 mL). The resulting slurry was filtered over Celite and washed with EtOAc. The aqueous layer was extracted with EtOAc 3x and the combined organics were washed with water and brine, dried over Na_2SO_4, filtered, and concentrated; yielding the title compound as a white solid (38 mg, 79% yield). **^{1}H NMR** (500 MHz, $CDCl_3$)

δ 7.98 (d, J = 1.1 Hz, 1H), 7.88 (t, J = 8.5 Hz, 2H), 7.82 (s, 1H), 7.74 (dd, J = 8.5, 1.8 Hz, 1H), 7.60 (d, J = 2.3 Hz, 1H), 7.53 (dd, J = 8.4, 2.3 Hz, 1H), 7.50 (dd, J = 8.4, 1.6 Hz, 1H), 6.99 (d, J = 8.4 Hz, 1H), 4.87 (s, 2H), 3.90 (s, 3H), 2.20 (s, 6H), 2.11 (s, 3H), 1.81 (s, 6H); **^{13}C NMR** (125 MHz, $CDCl_3$) δ 158.72, 139.19, 139.01, 138.09, 133.44, 133.20, 132.29, 128.64, 128.36, 126.17, 126.01, 125.70, 125.65, 125.40, 124.98, 112.22, 65.69, 55.31, 40.76, 37.28, 29.26; **HRMS** Accurate mass (ES+): Found 421.2141, $C_{28}H_{31}O_2Na$ (M+Na+) requires 421.2143.

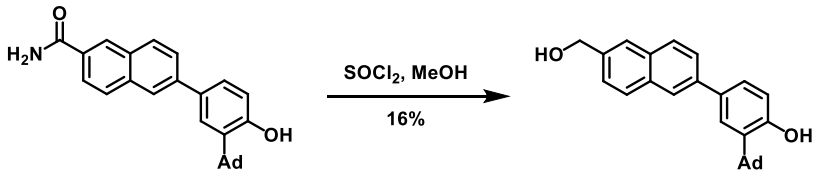

3.1 3.10

2-(adamantan-1-yl)-4-(6-(hydroxymethyl)naphthalen-2-yl)phenol (3.10). Lithium aluminum hydride (LAH) (44 mg, 1.154 mmol) was added to a solution of CD437, **3.1**, (230 mg, 0.577 mmol) in 2:1 Et_2O:THF (15 mL) at 0 °C. The reaction was warmed to room temperature and stirred for 2 hours. The reaction was cooled to 0 °C and H_2O (10 mL) was added slowly followed by 2M NaOH (10 mL). The resulting slurry was filtered over Celite and washed with EtOAc. The aqueous layer was extracted with EtOAc 3x and the combined organics were washed with water and brine, dried over Na_2SO_4, filtered, and concentrated; yielding the title compound as a white solid (217 mg, 98% yield). **^{1}H NMR** (500 MHz, DMSO) δ 8.03 (s, 1H), 7.90 (t, J = 8.9 Hz, 2H), 7.79 (s, 1H), 7.73 (dd, J = 8.5, 1.8 Hz, 1H), 7.47 – 7.38 (m, 3H), 6.96 (d, J = 8.2 Hz, 1H), 4.66 (s, 2H), 2.17 (s, 6H), 2.06 (s, 3H), 1.76 (s, 6H); **^{13}C NMR** (151 MHz, CDCl3) δ 154.33, 139.11, 138.11, 136.91, 133.67, 133.44, 132.30, 128.66, 128.39, 126.51, 126.14, 125.75, 125.69, 125.42, 124.97, 117.42, 65.73, 40.72, 37.20, 29.19; **HRMS** Accurate mass (ES+): Found 385.2177, $C_{27}H_{29}O_2$ (M+H+) requires 385.2168.

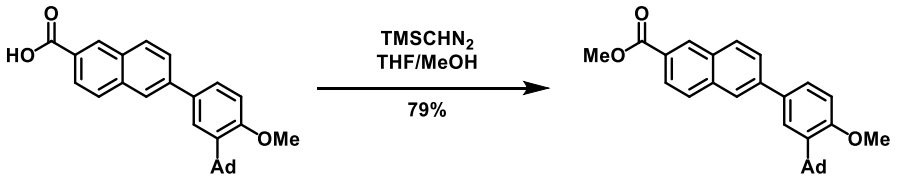

3.4 3.11

Methyl 6-(3-(adamantan-1-yl)-4-methoxyphenyl)-2-naphthoate (3.11). To a solution of adapalene **3.4** (50 mg, 0.121 mmol) in 4:1 THF/MeOH (0.4 mL) at 0 °C was added $TMSCHN_2$ (0.15 mL, 0.290 mmol) and the reaction was warmed to room temperature over 1 hour. The reaction mixture was concentrated, 1N HCl was added, and was extracted with EtOAc 3x. The combined organic layers were washed with water and brine, dried over Na_2SO_4, filtered, and concentrated; yielding the title compound as a white solid (41 mg, 79% yield). **^{1}H NMR** (500 MHz, $CDCl_3$) δ 8.61 (s, 1H), 8.07 (dd, J = 8.6, 1.7 Hz, 1H), 8.03 – 7.96 (m, 2H), 7.92 (d, J = 8.6 Hz, 1H), 7.80 (dd, J = 8.5, 1.8 Hz, 1H), 7.60 (d, J = 2.4 Hz, 1H), 7.55 (dd, J = 8.4, 2.4 Hz, 1H), 7.00 (d, J = 8.5 Hz, 1H), 3.99 (s, 3H), 3.91 (s, 3H), 2.19 (s, 6H), 2.10 (s, 3H), 1.80 (s, 6H); **^{13}C NMR** (125 MHz, $CDCl_3$) δ 167.44, 159.03, 141.51, 139.11, 136.06, 132.67, 131.35, 130.95, 129.82, 128.33, 127.02, 126.59, 126.09, 125.84, 125.68, 124.84, 112.21, 55.27, 52.31, 40.72, 37.25, 29.23; **HRMS** Accurate mass (ES+): Found 427.2268, $C_{29}H_{31}O_3$ (M+H+) requires 427.2273.

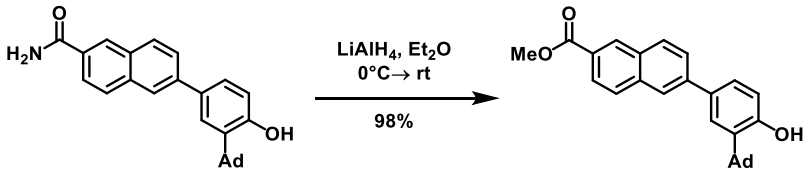

3.1 3.12

Methyl 6-(3-(adamantan-1-yl)-4-hydroxyphenyl)-2-naphthoate (3.12). To a solution of CD437 **3.1** (20 mg, 0.047 mmol) in MeOH (0.5 mL) was added $SOCl_2$ (0.01 mL, 0.12 mmol) at 0°C, the reaction was heated to reflux and stirred for 2 hours. The reaction was cooled to room temperature and concentrated. The yellow solid was purified by HPLC, yielding the title compound as a white solid (3.1 mg, 16% yield). **^{1}H NMR** (500 MHz, DMSO) δ 9.60 (s, 1H), 8.62 (s, 1H), 8.22 – 8.12 (m, 2H), 8.08 (d, *J* = 8.8 Hz, 1H), 7.97 (dd, *J* = 8.6, 1.7 Hz, 1H), 7.88 (dd, *J* = 8.6, 1.8 Hz, 1H), 7.55 – 7.46 (m, 2H), 6.92 (d, *J* = 8.2 Hz, 1H),

3.92 (s, 3H), 2.17 (s, 6H), 2.07 (s, 3H), 1.76 (s, 6H); **^{13}C NMR** (125 MHz, DMSO) δ 166.39, 156.55, 140.89, 136.09, 135.66, 130.68, 130.27, 129.91, 129.83, 128.50, 126.24, 126.06, 125.44, 125.26, 125.03, 123.65, 117.02, 52.19, 36.64, 36.37, 28.41; **HRMS** Accurate mass (ES+): Found 413.2115, $C_{28}H_{29}O_3$ (M+H+) requires 413.2117.

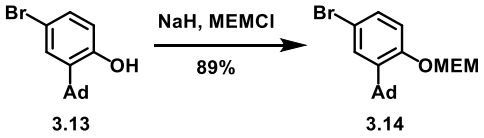

1-(5-bromo-2-((2-methoxyethoxy)methoxy)phenyl)adamantane (3.14). To a suspension of sodium hydride (60% in mineral oil, 53 mg, 1.33 mmol) in THF (3 mL) at 0 °C was added phenol **3.13** (spectra identical to known compound previously prepared by Liu, Z. & Xiang, J. Org. Process Res. Dev. 2006, 10, 285) (314 mg, 1.02 mmol) dissolved in THF (2 mL). The solution was warmed to room temperature and stirred for one hour, at which time MEMCl (0.19 mL, 1.64 mmol) was added dropwise, and the reaction was stirred for two hours at room temperature. The reaction was quenched with water, and extracted with EtOAc 3x. The combined organic layers were washed with water then brine, dried over Na_2SO_4, filtered, concentrated, and purified by column chromatography, yielding the title compound as a white solid (361 mg, 89% yield). **^{1}H NMR** (500 MHz, $CDCl_3$) δ 7.31 (d, J = 2.5 Hz, 1H), 7.23 (dd, J = 8.7, 2.5 Hz, 1H), 7.04 (d, J = 8.7 Hz, 1H), 5.28 (s, 2H), 3.87 – 3.79 (m, 2H), 3.59 – 3.56 (m, 2H), 3.39 (s, 3H), 2.06 (s, 9H), 1.76 (s, 6H); **^{13}C NMR** (125 MHz, $CDCl_3$) δ 155.68, 140.93, 129.95, 129.55, 116.49, 114.54, 93.51, 71.62, 67.91, 59.11, 40.52, 37.31, 37.02, 29.03; **HRMS** Accurate mass (ES+): Found 417.1036, $C_{20}H_{27}BrO_3Na$ (M+Na+) requires 417.1041.

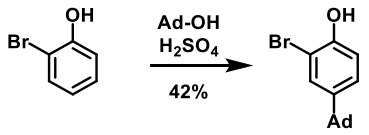

3.16 3.17

4-(adamantan-1-yl)-2-bromophenol (3.17). To a mixture of 2-bromophenol **3.16** (1.475g, 8.526 mmol) and 1-adamantol (1.298g, 8.526 mmol) in CH_2Cl_2 (4 mL) was added 5:1 AcOH:H_2SO_4 (3 mL), and the reaction was stirred at room temperature for 3 days. The reaction poured into water and quenched with sat. $NaHCO_3$, then extracted with CH_2Cl_2 3x. The combined organic layers were washed with water and brine, dried over Na_2SO_4, filtered, concentrated, and purified by column chromatography (loaded crude oil in hexanes, 0 → 2% EtOAc/hexanes), yielding the title compound as a white solid (1.100g, 42% yield). **^{1}H NMR** (500 MHz, $CDCl_3$) δ 7.41 (d, J = 2.3 Hz, 1H), 7.21 (dd, J = 8.5, 2.3 Hz, 1H), 6.98 – 6.95 (m, 1H), 5.34 (s, 1H), 2.08 (s, 3H), 1.85 (d, J = 2.6 Hz, 6H), 1.81 – 1.70 (m, 6H); **^{13}C NMR** (125 MHz, $CDCl_3$) δ 150.10, 145.54, 128.70, 125.83, 115.68, 110.16, 68.11, 43.40, 36.78, 35.83, 29.02, 25.74; **HRMS** Accurate mass (ES+): Found 307.0711, $C_{16}H_{20}BrO$ (M+H+) requires 307.0698.

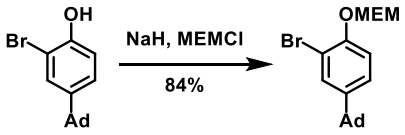

3.17 3.18

1-(3-bromo-4-((2-methoxyethoxy)methoxy)phenyl)adamantane (3.18). To a suspension of sodium hydride (60% in mineral oil, 258 mg, 6.453 mmol) in THF (5 mL) at 0 °C was added a solution of phenol **3.17** (1.525g, 4.964 mmol) in THF (3 mL) dropwise. The ice bath was removed, and the reaction was stirred at room temperature for 30 minutes, at which time MEMCl (0.91 mL, 7.942 mmol) was added. After 2 hours at room temperature, the reaction was quenched with water and extracted with EtOAc 3x. The combined organic layers were washed with brine, dried over Na_2SO_4, filtered, concentrated, and purified by column chromatography, yielding the title compound as a clear oil (1.650g, 84% yield). **^{1}H NMR** (500 MHz, $CDCl_3$) δ 7.50 (d, J = 2.3 Hz, 1H), 7.22 (dd, J = 8.6, 2.3 Hz, 1H), 7.13 (d, J = 8.7 Hz, 1H), 5.30 (d, J = 5.2 Hz, 2H), 3.89 – 3.85 (m, 2H), 3.59 – 3.55 (m, 2H), 3.37 (s, 3H), 2.08 (s, 3H), 1.85 (d, J = 2.3 Hz, 6H),

1.75 (dd, J = 26.7, 12.1 Hz, 6H); **^{13}C NMR** (125 MHz, $CDCl_3$) δ 151.53, 146.85, 130.11, 125.04, 116.05, 112.65, 94.33, 71.62, 68.02, 59.12, 43.28, 36.74, 35.84, 28.96; **HRMS** Accurate mass (ES+): Found 417.1058, $C_{20}H_{27}BrO_3Na$ (M+Na+) requires 417.1041.

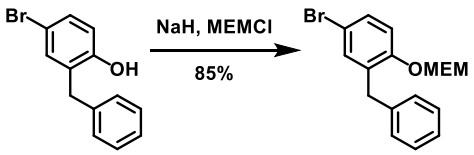

3.21 3.22

2-benzyl-4-bromo-1-((2-methoxyethoxy)methoxy)benzene (3.22). Phenol **3.21** (spectra identical to known compound previously prepared by Williams, A. B. & Hanson, R. N. Tetrahedron 2012, 68, 5406) (1.500g, 5.701 mmol) dissolved in THF (5 mL) was added via cannula to a suspension of NaH (60% in mineral oil, 296 mg, 7.411 mmol) in THF (15 mL) at 0 °C. The solution was warmed to room temperature and stirred for 30 minutes, after which time MEMCl (1.04 mL, 9.12 mmol) was added, and the reaction was stirred for 2 hours at room temperature. The reaction was quenched with water and extracted with EtOAc 3x. The combined organic layers were washed with brine, dried over Na_2SO_4, filtered, concentrated, and purified by column chromatography, yielding the title compound as a clear oil (1.70g, 85% yield). **^{1}H NMR** (500 MHz, $CDCl_3$) δ 7.32 - 7.27 (m, 3H), 7.25 (d, J = 2.5 Hz, 1H), 7.21 (t, J = 6.6 Hz, 3H), 7.04 (d, J = 8.7 Hz, 1H), 5.25 (s, 2H), 3.96 (s, 2H), 3.66 (dd, J = 5.5, 3.7 Hz, 2H), 3.49 (dd, J = 5.5, 3.8 Hz, 2H), 3.37 (s, 3H); **^{13}C NMR** (125 MHz, $CDCl_3$) δ 153.91, 139.93, 132.99, 132.38, 130.09, 128.68, 128.22, 125.94, 115.60, 113.87, 93.04, 71.34, 67.49, 58.77, 35.92; **HRMS** Accurate mass (ES+): Found 375.0382, $C_{17}H_{19}BrO_3Na$ (M+Na+) requires 375.0382.

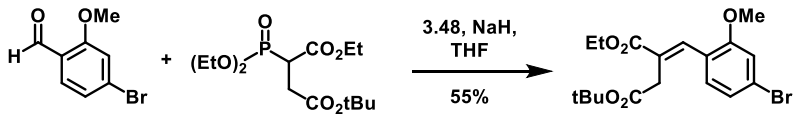

3.52 3.48 3.53

4-(tert-butyl) 1-ethyl (E)-2-(4-bromo-2-methoxybenzylidene)succinate (3.53). To a suspension of NaH (60% in mineral oil, 176 mg, 4.6 mmol) in THF (10 mL) at 0 °C was added phosphonate **3.48** (spectra

identical to known compound previously prepared by Owton, W. M.; Gallagher, P. T. & Juan-Montesinos, A. Synth. Commun. 1993, 23, 2119) (1.56g, 4.6 mmol), and the solution was warmed to room temperature and stirred for 1 hour. The solution was cooled back down to 0 °C and 4-bromo-2-methoxybenzaldehyde dissolved in THF (2 mL) was added dropwise. The resulting orange suspension was allowed to warm to room temperature and stirred overnight. The following day, the solvent was concentrated and diluted with EtOAc, then washed with water 3x and brine, dried over Na_2SO_4, filtered, concentrated, and purified by column chromatography, yielding the title compound as a clear oil (731 mg, 55% yield). **^{1}H NMR** (500 MHz, $CDCl_3$) δ 7.83 (s, 1H), 7.15 (dd, J = 8.1, 0.6 Hz, 1H), 7.10 (dd, J = 8.1, 1.7 Hz, 1H), 7.04 (d, J = 1.7 Hz, 1H), 4.27 (q, J = 7.1 Hz, 2H), 3.84 (s, 3H), 3.34 (d, J = 0.6 Hz, 2H), 1.46 (s, 9H), 1.33 (t, J = 7.1 Hz, 3H); **^{13}C NMR** (100 MHz, $CDCl_3$) δ 170.52, 167.38, 158.19, 136.60, 130.77, 127.51, 123.88, 123.65, 123.44, 114.42, 81.09, 61.16, 55.92, 35.37, 28.15, 14.40; **HRMS** Accurate mass (ES+): Found 365.0007, $C_{14}H_{15}BrO_5Na$ (M+Na+) requires 365.0001.

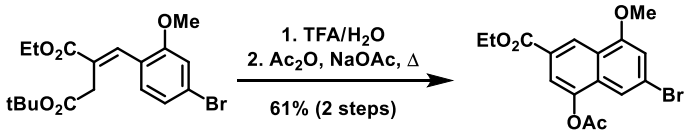

3.53 3.54

Ethyl 4-acetoxy-6-bromo-8-methoxy-2-naphthoate (3.54). Ester **3.53** (1.02g, 2.55 mmol) was dissolved in 9:1 TFA:H_2O (3 mL) and stirred at room temperature for 3.5 hours. The reaction was concentrated under reduced pressure and azeotropically dried twice with toluene. The crude oil was cooled to 0 °C and saturated $NaHCO_3$ was added (3 mL), then the mixture was acidified with 1M HCl (pH 1). The aqueous layer was extracted with EtOAc 3x, and the combined organic layers were washed with brine, dried over Na_2SO_4, filtered and concentrated, yielding the crude acid as a clear oil. The crude acid was dissolved in Ac_2O (13 mL) and sodium acetate (227 mg, 2.77 mmol) was added, and the mixture turned from pink to yellow. The reaction was refluxed for 2 hours, cooled to room temperature, and then poured into water. The yellow precipitate was filtered and washed with water. The solids were dissolved in CH_2Cl_2, washed with brine, and dried over Na_2SO_4, filtered and concentrated, yielding the title compound as a yellow solid (568 mg,

61% yield over two steps). **^{1}H NMR** (500 MHz, $CDCl_3$) δ 8.84 (dd, *J* = 1.5, 0.9 Hz, 1H), 7.86 (d, *J* = 1.6 Hz, 1H), 7.59 (dd, *J* = 1.5, 0.9 Hz, 1H), 6.97 (d, *J* = 1.6 Hz, 1H), 4.43 (q, *J* = 7.1 Hz, 1H), 4.03 (s, 1H), 2.48 (s, 1H), 1.43 (t, *J* = 7.1 Hz, 1H); **^{13}C NMR** (125 MHz, CDCl3) δ 169.12, 165.80, 157.05, 145.38, 130.60, 127.18, 124.77, 123.72, 123.23, 119.56, 115.85, 109.31, 61.41, 56.08, 21.01, 14.43; **HRMS** Accurate mass (ES+): Found 367.0162, $C_{16}H_{16}BrO_5$ (M+H+) requires 367.0181.

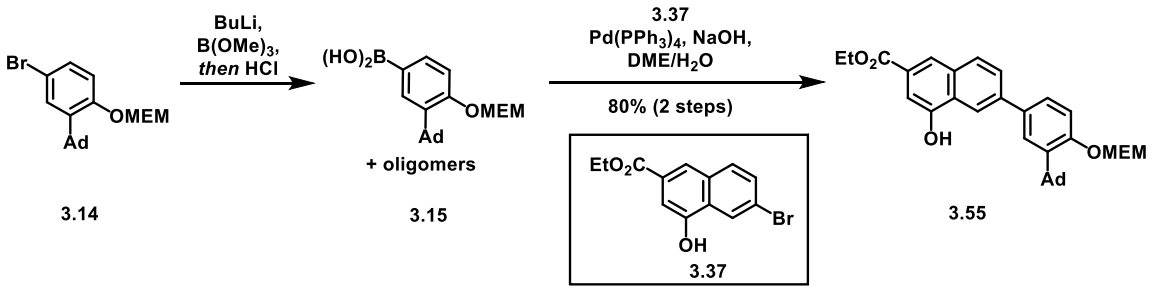

Ethyl 6-(3-(adamantan-1-yl)-4-((2-methoxyethoxy)methoxy)phenyl)-4-hydroxy-2-naphthoate (3.55). ***General procedure 3A:*** To a solution of bromide **3.14** (68 mg, 0.172 mmol) in THF (2 mL) at -78 °C was added *n*-BuLi (2.40 M in hexanes, 0.036 mL, 0.087 mmol) dropwise and then stirred for 15 minutes at -78 °C, over which time the reaction turned blue. $B(OMe)_3$ was then added dropwise, and the reaction stirred for an additional hour at -78 °C, then warmed to room temperature, over which time the reaction turned maroon. After one hour at room temperature, 0.1 M HCl was added (2 mL) and the reaction was stirred for an additional 30 minutes. Water was added, and the solution was extracted with EtOAc 3x. The combined organic layers were washed with brine, dried over Na_2SO_4, filtered, concentrated and purified by column chromatography (EtOAc/hexanes then MeOH/CH_2Cl_2). The intended boronic acid product also contained another similar compound, presumably a borate oligomer of the material (Rf = 0.75 in 5% MeOH/ 95% CH_2Cl_2, stains red in vanillin), both of which reacted in the following step. The boronic acid mixture was then dissolved in 9:1 DME/H_2O (2 mL), then naphthyl bromide **3.37** (spectra identical to known compound previously prepared by Tietze, L. F.; Panknin, O.; Major, F. & Krewer, B. Chem. Eur. J. 2008, 14, 2811) (53 mg, 0.143 mmol), and 1M NaOH (0.72 mL, 0.72 mmol) were added, then argon was bubbled through the mixture for 5 minutes. After degassing, $Pd(PPh_3)_4$ (5 mg, 0.004 mmol) was added, and the reaction was

heated to 75 °C for 4 hours, at which time another portion of 1M NaOH (0.72 mL, 0.72 mmol) was added, to ensure complete acetate hydrolysis. After 2 additional hours, the reaction was complete by TLC and **3.37** was consumed. Water and EtOAc were added, and the aqueous layer was extracted with EtOAc 3x. The combined organic layers were washed with brine, dried over Na_2SO_4, filtered, concentrated, and purified by column chromatography, yielding the title compound as a white foam (64 mg, 80% yield with respect to **3.37**). **^{1}H NMR** (500 MHz, $CDCl_3$) δ 8.40 (s, 1H), 8.21 (s, 1H), 7.95 (d, J = 8.6 Hz, 1H), 7.79 (dd, J = 8.5, 1.8 Hz, 1H), 7.65 – 7.60 (m, 2H), 7.53 (dd, J = 8.5, 2.3 Hz, 1H), 7.27 (d, J = 8.4 Hz, 1H), 6.64 (br s, 1H), 5.38 (s, 2H), 4.46 (q, J = 7.1 Hz, 2H), 3.95 – 3.88 (m, 2H), 3.69 – 3.62 (m, 2H), 3.44 (s, 3H), 2.19 (d, J = 2.0 Hz, 6H), 2.10 (s, 3H), 1.80 (s, 6H), 1.46 (t, J = 7.1 Hz, 3H); **^{13}C NMR** (125 MHz, $CDCl_3$) δ 167.41, 156.59, 152.38, 140.70, 139.06, 134.07, 132.71, 129.68, 127.39, 126.96, 126.23, 126.08, 123.35, 119.37, 115.19, 108.12, 93.51, 71.80, 67.97, 61.48, 59.21, 40.85, 37.40, 37.23, 29.23, 14.51; **HRMS** Accurate mass (ES+): Found 531.2758, $C_{33}H_{39}O_6$ (M+H+) requires 531.2747.

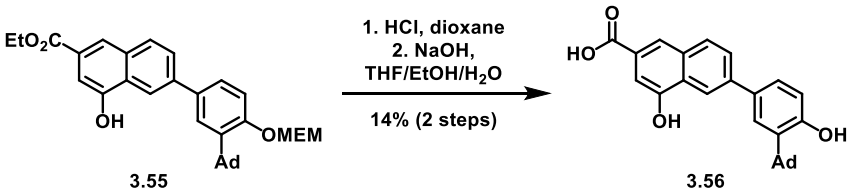

3.55 3.56

6-(3-(adamantan-1-yl)-4-hydroxyphenyl)-4-hydroxy-2-naphthoic acid (3.56). ***General procedure 3B:*** MEM ether **3.55** (20 mg, 0.038 mmol) was dissolved in 4M HCl in dioxane (2 mL) and the reaction was stirred at room temperature overnight. The reaction was quenched with water and extracted with EtOAc 3x. The combined organic layers were washed with brine, dried over Na_2SO_4, filtered, and concentrated. The crude intermediate was dissolved in 2:1 EtOH/THF (1.5 mL) and 1N NaOH was added (0.2 mL), the mixture was heated to 50°C and stirred overnight. The reaction was cooled to room temperature, acidified (pH 1) with 1M HCl and extracted with EtOAc 3x. The combined organic layers were washed with brine, dried over Na_2SO_4, filtered, concentrated, and purified by column chromatography (0→6% MeOH/0.1%AcOH/CH_2Cl_2) yielding the title compound as a white solid (2.1 mg, 14% over two steps). **^{1}H NMR** (500 MHz, CD_3CN) δ 8.33 (d, J = 1.9 Hz, 1H), 8.14 (s, 1H), 8.00 (d, J = 8.5 Hz, 1H), 7.84 (dd, J =

8.6, 1.9 Hz, 1H), 7.58 (d, J = 2.4 Hz, 1H), 7.47 (dd, J = 8.2, 2.4 Hz, 1H), 7.37 (d, J = 1.4 Hz, 1H), 6.88 (d, J = 8.2 Hz, 1H), 2.22 – 2.19 (m, 6H), 2.10 – 2.07 (m, 3H), 1.81 (t, J = 2.8 Hz, 6H); **^{13}C NMR** (100 MHz, CD_3CN) δ 167.87, 156.85, 153.83, 141.36, 137.78, 133.46, 132.88, 130.63, 128.30, 128.17, 127.45, 126.85, 126.61, 123.50, 119.26, 108.29, 41.05, 37.74, 30.04; **HRMS** Accurate mass (ES+): Found 415.1906, $C_{27}H_{27}O_4$ (M+H+) requires 415.1909.

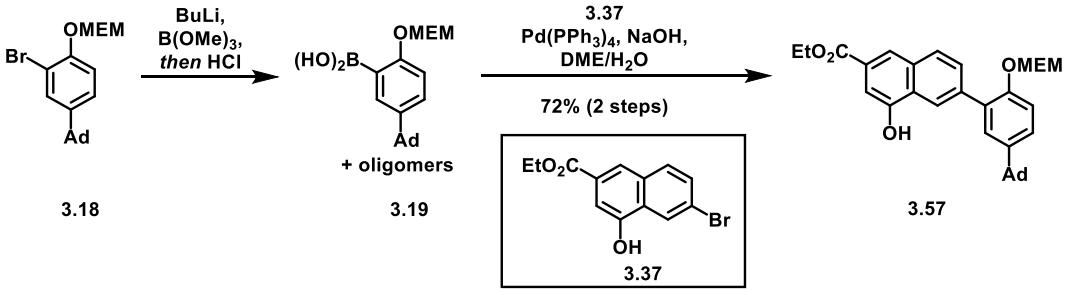

Ethyl 6-(5-(adamantan-1-yl)-2-((2-methoxyethoxy)methoxy)phenyl)-4-hydroxy-2-naphthoate (3.57). Following general procedure 3A (compound 3.55), bromide **3.18** (66 mg, 0.167 mmol) and naphthyl bromide **3.37** (47 mg, 0.139 mmol) yielded the title compound as a clear oil (53 mg, 72% yield with respect to **3.37**). **^{1}H NMR** (500 MHz, $CDCl_3$) δ 8.37 (s, 1H), 8.22 (s, 1H), 7.93 (d, J = 8.4 Hz, 1H), 7.75 (d, J = 8.2 Hz, 1H), 7.58 (s, 1H), 7.42 (s, 1H), 7.31 (t, J = 11.5 Hz, 1H), 7.23 (d, J = 8.6 Hz, 1H), 6.76 (br s, 1H), 5.22 (s, 2H), 4.46 (dd, J = 13.7, 6.7 Hz, 2H), 3.73 (s, 2H), 3.50 (s, 2H), 3.34 (s, 3H), 2.10 (s, 3H), 1.94 (s, 6H), 1.77 (q, J = 11.6 Hz, 6H), 1.46 (t, J = 7.0 Hz, 3H); **^{13}C NMR** (125 MHz, $CDCl_3$) δ 167.42, 152.23, 145.60, 138.77, 132.77, 131.05, 129.56, 128.60, 127.97, 127.64, 127.03, 125.61, 123.23, 122.38, 115.46, 108.00, 94.35, 71.70, 67.88, 61.49, 59.10, 43.45, 36.88, 35.90, 29.09, 14.51; **HRMS** Accurate mass (ES+): Found 553.2562, $C_{33}H_{38}O_6Na$ (M+Na+) requires 553.2566.

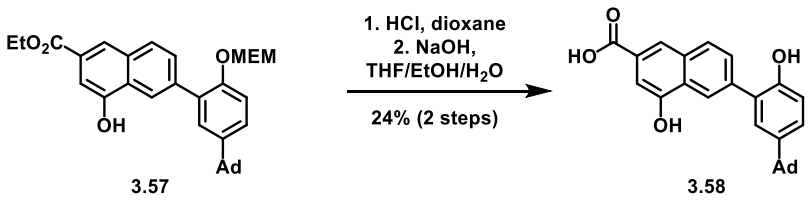

6-(5-(adamantan-1-yl)-2-hydroxyphenyl)-4-hydroxy-2-naphthoic acid (3.58). Following general procedure 3B (compound 3.56), MEM ether **3.57** (39 mg, .073 mmol) yielded the title compound as a yellow residue (7.2 mg, 24% yield over two steps). **^{1}H NMR** (500 MHz, CD_3CN) δ 8.31 (s, 1H), 8.17 (s, 1H), 7.98 (d, J = 8.5 Hz, 1H), 7.78 (dd, J = 8.5, 1.7 Hz, 1H), 7.40 – 7.35 (m, 2H), 7.24 (dd, J = 8.5, 2.5 Hz, 1H), 6.90 (d, J = 8.5 Hz, 1H), 1.97 – 1.95 (m, 6H), 1.93 – 1.90 (m, 3H), 1.81 – 1.75 (m, 6H); **^{13}C NMR** (125 MHz, CD_3CN) δ 172.64, 168.08, 153.93, 152.55, 144.70, 139.34, 133.62, 130.15, 129.69, 128.49, 128.44, 128.35, 127.93, 126.55, 123.48, 122.82, 116.84, 108.17, 44.04, 37.37, 30.04; **HRMS** Accurate mass (ES+): Found 415.1905, $C_{27}H_{27}O_4$ (M+H+) requires 415.1909.

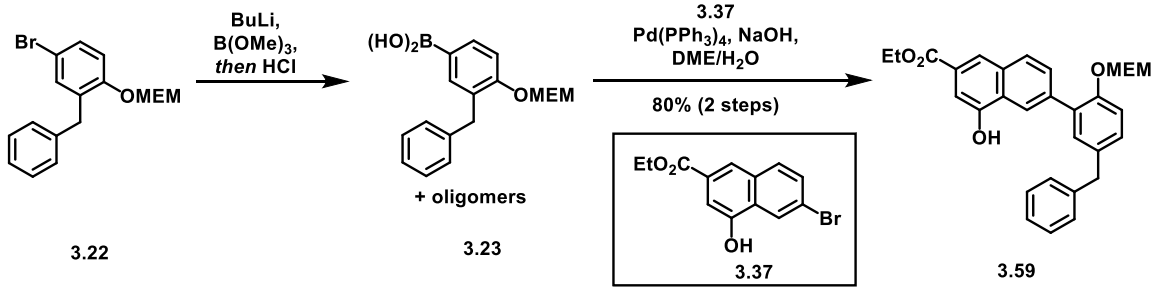

Ethyl 6-(3-benzyl-4-((2-methoxyethoxy)methoxy)phenyl)-4-hydroxy-2-naphthoate (3.59). Following general procedure 3A (compound 3.55), bromide **3.22** (40 mg, 0.114 mmol) and naphthyl bromide **3.37** (32 mg, 0.095 mmol) yielded the title compound as a clear oil (26 mg, 59% yield with respect to **3.55**). **^{1}H NMR** (400 MHz, $CDCl_3$) δ 8.35 (s, 1H), 8.20 (s, 1H), 7.93 (d, J = 8.5 Hz, 1H), 7.75 (dd, J = 8.5, 1.8 Hz, 1H), 7.60 – 7.54 (m, 2H), 7.48 (d, J = 1.2 Hz, 1H), 7.26 – 7.23 (m, 5H), 7.20 – 7.14 (m, 1H), 5.80 (br s, 1H), 5.30 (s, 2H), 4.43 (q, J = 7.1 Hz, 2H), 4.07 (s, 2H), 3.69 – 3.61 (m, 2H), 3.53 – 3.45 (m, 2H), 3.36 (s, 3H), 1.44 (t, J = 7.1 Hz, 3H); **^{13}C NMR** (125 MHz, $CDCl_3$) δ 167.48, 155.01, 152.52, 141.04, 139.89, 134.27, 132.74, 130.62, 129.92, 129.71, 128.90, 128.39, 127.45, 126.79, 126.70, 125.98, 123.20, 119.40,

114.45, 108.12, 93.20, 71.70, 67.67, 61.52, 59.12, 36.70, 29.84, 14.49; **HRMS** Accurate mass (ES+): Found 487.2126, $C_{30}H_{31}O_6$ (M+H+) requires 487.2121.

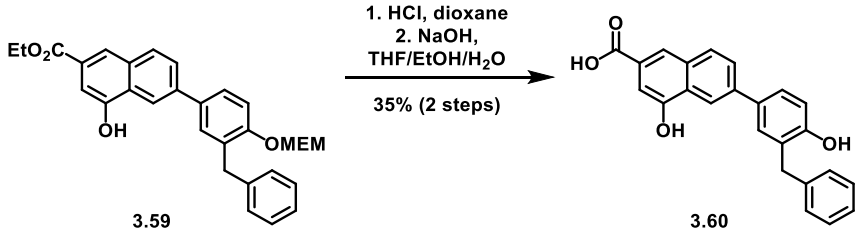

6-(3-benzyl-4-hydroxyphenyl)-4-hydroxy-2-naphthoic acid (3.60). Following general procedure 3B (compound 3.56), MEM ether **3.59** (25 mg, .055 mmol) yielded the title compound as a yellow residue (7.0 mg, 35% yield over two steps). **^{1}H NMR** (500 MHz, CD_3CN) δ 8.31 (s, 1H), 8.15 (d, J = 14.7 Hz, 1H), 8.01 – 7.93 (m, 1H), 7.83 – 7.77 (m, 1H), 7.58 (d, J = 1.9 Hz, 1H), 7.54 – 7.50 (m, 1H), 7.37 (s, 1H), 7.28 (q, J = 8.1 Hz, 4H), 7.18 (t, J = 6.9 Hz, 1H), 6.95 (d, J = 8.3 Hz, 1H), 4.02 (s, 2H); **^{13}C NMR** (125 MHz, CD_3CN) δ 172.55, 167.98, 155.76, 153.85, 142.27, 140.70, 133.53, 133.20, 130.65, 129.69, 129.46, 129.31, 128.27, 127.40, 127.29, 126.85, 123.49, 119.33, 116.72, 108.35, 36.52; **HRMS** Accurate mass (ES+): Found 393.1093, $C_{24}H_{18}O_4Na$ (M+Na+) requires 393.1103.

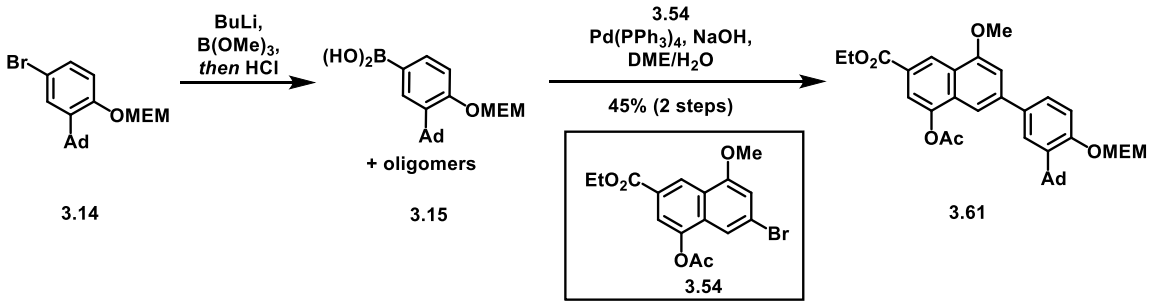

Ethyl 4-acetoxy-6-(3-(adamantan-1-yl)-4-((2-methoxyethoxy)methoxy)phenyl)-8-methoxy-2-naphthoate (3.61). Following general procedure 3A (compound 3.55), bromide **3.14** (43 mg, 0.109 mmol) and naphthyl bromide **3.54** (30 mg, 0.090 mmol) yielded the title compound as a clear oil (21 mg, 45% yield with respect to **3.54**). **^{1}H NMR** (500 MHz, $CDCl_3$) δ 8.92 (s, 1H), 7.86 (s, 1H), 7.53 (d, J = 8.4 Hz, 2H), 7.47 (d, J = 8.4 Hz, 1H), 7.29 (d, J = 8.4 Hz, 1H), 7.08 (s, 1H), 5.40 (s, 2H), 4.44 (q, J = 7.1 Hz, 2H),

4.10 (s, 3H), 3.94 – 3.86 (m, 2H), 3.67 – 3.60 (m, 2H), 3.42 (s, 3H), 2.47 (s, 3H), 2.19 (s, 6H), 2.11 (s, 3H), 1.81 (s, 6H), 1.45 (t, J = 7.1 Hz, 3H); **^{13}C NMR** (125 MHz, $CDCl_3$) δ 169.44, 166.29, 157.00, 156.80, 146.60, 143.00, 139.11, 134.51, 130.47, 126.45, 126.28, 126.18, 125.12, 123.43, 118.85, 115.16, 111.03, 105.42, 93.49, 71.74, 68.01, 61.31, 59.21, 55.94, 40.80, 37.39, 37.19, 29.82, 29.19, 21.11, 14.55; **HRMS** Accurate mass (ES+): Found 625.2781, $C_{36}H_{42}O_8Na$ (M+Na+) requires 625.2777.

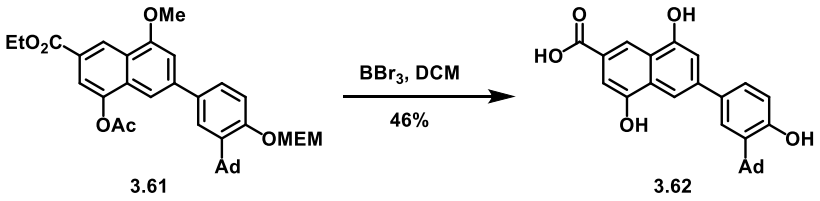

6-(3-(adamantan-1-yl)-4-hydroxyphenyl)-4,8-dihydroxy-2-naphthoic acid (3.62). ***General procedure 3C:*** To a solution of MEM ether **3.61** (18 mg, 0.03 mmol) dissolved in CH_2Cl_2 (2 mL) at -78 °C was added BBr_3 (1M in CH_2Cl_2, 0.24 mL, 0.24 mmol) dropwise, and the mixture was allowed to warm to room temperature and stir overnight. The reaction was quenched with water and extracted with EtOAc 3x. The combined organic layers were washed with brine, dried over Na_2SO_4, filtered, concentrated, and purified by column chromatography (0→6% MeOH/0.1%AcOH/DCM) yielding the title compound as an orange oil (7 mg, 46% yield). **^{1}H NMR** (400 MHz, CD_3CN) δ 8.37 (s, 1H), 7.85 (s, 1H), 7.55 (d, J = 2.2 Hz, 1H), 7.43 (dd, J = 8.3, 2.3 Hz, 1H), 7.34 (s, 1H), 7.23 (s, 1H), 6.87 (d, J = 8.1 Hz, 1H), 2.22 – 2.17 (m, 6H), 2.11 – 2.05 (m, 3H), 1.83 – 1.79 (m, 6H); **^{13}C NMR** (125 MHz, CD_3CN) δ 168.03, 156.86, 155.13, 153.73, 142.15, 137.68, 133.00, 129.59, 126.92, 126.69, 126.44, 124.74, 111.14, 109.72, 108.71, 41.07, 37.75, 30.07; **HRMS** Accurate mass (ES+): Found 431.1856, $C_{27}H_{27}O_5$ (M+H+) requires 431.1859.

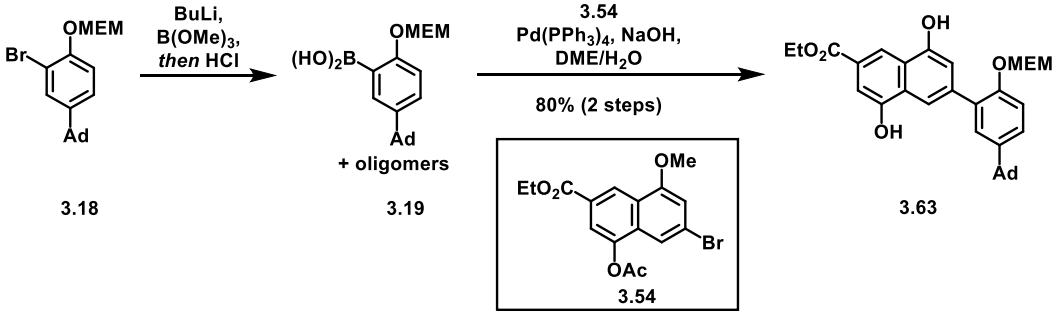

Ethyl 6-(5-(adamantan-1-yl)-2-((2-methoxyethoxy)methoxy)phenyl)-4-hydroxy-8-methoxy-2-naphthoate (3.63). Following general procedure 3A (compound 3.55), bromide **3.18** (68 mg, 0.172 mmol) and naphthyl bromide **3.54** (53 mg, 0.143 mmol) yielded the title compound as a white foam (64 mg, 80% yield with respect to **3.54**). **^{1}H NMR** (500 MHz, $CDCl_3$) δ 8.60 (s, 1H), 7.89 (s, 1H), 7.60 (s, 1H), 7.42 (d, J = 2.2 Hz, 1H), 7.33 (dd, J = 8.6, 2.1 Hz, 1H), 7.22 (d, J = 8.7 Hz, 1H), 7.10 (s, 1H), 6.49 (br s, 1H), 5.22 (s, 2H), 4.46 (q, J = 7.0 Hz, 2H), 4.03 (s, 3H), 3.75 – 3.70 (m, 2H), 3.52 – 3.48 (m, 2H), 3.34 (s, 3H), 2.10 (s, 3H), 1.94 (s, 6H), 1.77 (q, J = 12.2 Hz, 6H), 1.46 (t, J = 7.1 Hz, 3H); **^{13}C NMR** (125 MHz, $CDCl_3$) δ 167.74, 155.67, 152.48, 152.09, 145.57, 139.24, 131.66, 128.06, 127.79, 126.72, 125.54, 125.07, 117.40, 115.65, 114.67, 108.74, 107.83, 94.42, 71.65, 67.84, 61.41, 59.02, 55.73, 43.40, 36.84, 35.85, 29.05, 14.49; **HRMS** Accurate mass (ES+): Found 583.2653, $C_{34}H_{40}O_7Na$ (M+Na+) requires 583.2672.

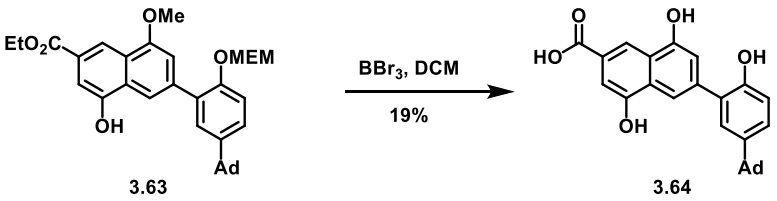

6-(5-(adamantan-1-yl)-2-hydroxyphenyl)-4,8-dihydroxy-2-naphthoic acid (3.64). Following general procedure 3C (compound 3.62), MEM ether **3.63** (19 mg, 0.034 mmol) yielded the title compound as an orange oil (2.8 mg, 19% yield). **^{1}H NMR** (500 MHz, CD_3CN) δ 8.40 (s, 1H), 7.80 (s, 1H), 7.74 (br s, 1H), 7.35 (s, 2H), 7.29 – 7.22 (m, 1H), 7.18 (s, 1H), 6.90 (d, J = 8.4 Hz, 1H), 6.74 (br s, 1H), 2.10 – 2.03 (m, 3H), 1.96 – 1.89 (m, 6H *overlaps with CD_3CN signal*), 1.83 – 1.75 (m, 6H); **^{13}C NMR** (125 MHz, CD_3CN) δ 168.06, 154.35, 153.77, 152.45, 144.59, 139.97, 129.19, 128.52, 128.12, 127.20, 126.50, 124.90, 117.85,

116.84, 114.63, 112.47, 108.54, 44.03, 37.35, 30.02; **HRMS** Accurate mass (ES+): Found 453.1673, $C_{27}H_{26}O_5Na$ (M+Na+) requires 453.1678.

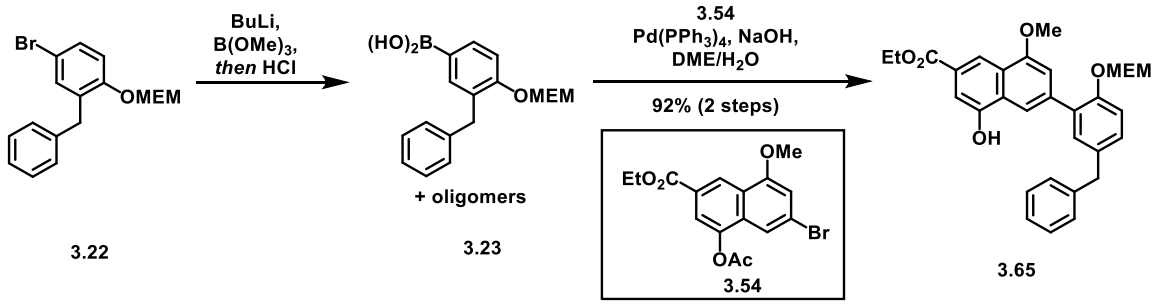

Ethyl 6-(3-benzyl-4-((2-methoxyethoxy)methoxy)phenyl)-4-hydroxy-8-methoxy-2-naphthoate (3.65). Following general procedure A (compound 3.55), bromide **3.22** (60 mg, 0.171 mmol) and naphthyl bromide **3.54** (50 mg, 0.136 mmol) yielded the title compound as a clear oil (66 mg, 92% yield with respect to **3.54**). **^{1}H NMR** (500 MHz, $CDCl_3$) δ 8.72 (s, 1H), 8.11 (s, 1H), 7.80 (s, 1H), 7.70 (s, 2H), 7.45 – 7.36 (m, 5H), 7.31 (s, 1H), 7.18 (s, 1H), 6.98 (br s, 1H), 5.44 (s, 2H), 4.61 (dd, J = 13.9, 6.8 Hz, 2H), 4.23 (s, 2H), 4.20 (s, 3H), 3.81 (s, 2H), 3.65 (s, 2H), 3.53 (s, 3H), 1.60 (t, J = 6.9 Hz, 3H); **^{13}C NMR** (125 MHz, $CDCl_3$) δ 167.73, 156.74, 154.97, 152.42, 141.03, 140.46, 134.80, 130.48, 129.92, 128.85, 128.34, 126.74, 126.54, 125.93, 125.04, 117.50, 114.33, 111.85, 108.96, 104.82, 93.14, 71.69, 67.62, 61.46, 59.08, 55.74, 36.69, 29.82, 14.50; **HRMS** Accurate mass (ES+): Found 517.2227, $C_{31}H_{33}O_7$ (M+H+) requires 517.2226.

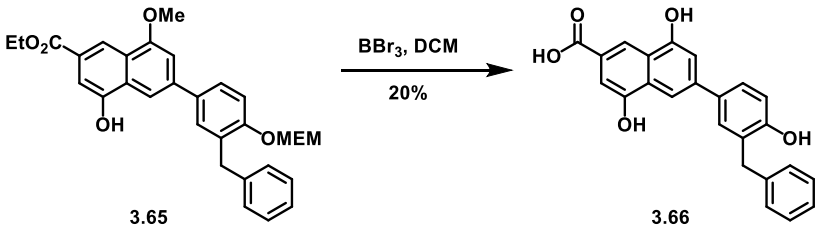

6-(3-benzyl-4-hydroxyphenyl)-4,8-dihydroxy-2-naphthoic acid (3.66). Following general procedure 3C (compound 3.62), MEM ether **3.65** (20 mg, 0.039 mmol) yielded the title compound as an orange oil (3.0 mg, 20% yield). **^{1}H NMR** (400 MHz, CD_3CN) δ 8.36 (s, 1H), 7.82 (s, 1H), 7.76 (br s, 1H), 7.52 (d, J = 2.4 Hz, 1H), 7.47 (dd, J = 8.3, 2.4 Hz, 1H), 7.34 (d, J = 1.4 Hz, 1H), 7.33 – 7.25 (m, 5H), 7.22 – 7.11 (m, 2H),

6.94 (d, J = 8.3 Hz, 1H), 4.02 (s, 2H); **^{13}C NMR** (125 MHz, CD_3CN) δ 168.08, 155.74, 155.12, 153.74, 142.28, 141.51, 133.36, 130.48, 129.67, 129.52, 129.30, 127.26, 127.02, 126.84, 124.79, 117.86, 116.62, 111.23, 109.59, 108.71, 36.48; **HRMS** Accurate mass (ES+): Found 387.1241, $C_{24}H_{19}O_5$ (M+H+) requires 387.1233.

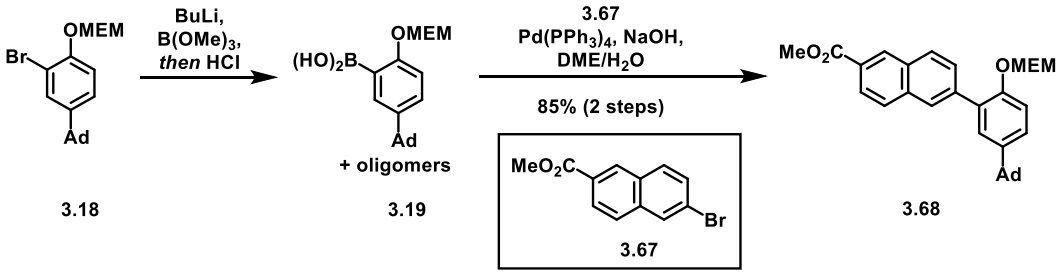

Methyl 6-(5-(adamantan-1-yl)-2-((2-methoxyethoxy)methoxy)phenyl)-2-naphthoate (3.68). Following general procedure 3A (compound 3.55), bromide **3.18** (31 mg, 0.079 mmol) and methyl 6-bromo-2-naphthoate **3.67** (21 mg, 0.079 mmol) yielded the title compound as a white foam (34 mg, 85% yield with respect to naphthyl bromide **3.67**). **^{1}H NMR** (500 MHz, $CDCl_3$) δ 8.63 (s, 1H), 8.07 (d, J = 8.6 Hz, 1H), 7.99 – 7.89 (m, 3H), 7.75 (d, J = 8.5 Hz, 1H), 7.40 (s, 1H), 7.34 (d, J = 8.6 Hz, 1H), 7.25 (d, J = 8.2 Hz, 1H), 5.21 (s, 2H), 3.99 (s, 3H), 3.72 – 3.65 (m, 2H), 3.49 – 3.42 (m, 2H), 3.32 (s, 3H), 2.10 (s, 3H), 1.95 (s, 6H), 1.77 (q, J = 12.2 Hz, 6H); **^{13}C NMR** (125 MHz, $CDCl_3$) δ 167.44, 152.34, 145.63, 139.61, 135.65, 131.47, 130.89, 130.71, 129.23, 128.68, 128.41, 127.99, 127.88, 127.31, 125.73, 125.46, 115.63, 94.46, 71.61, 67.82, 59.07, 52.32, 43.46, 36.87, 35.91, 29.07; **HRMS** Accurate mass (ES+): Found 523.2461, $C_{32}H_{36}O_5Na$ (M+Na+) requires 523.2460.

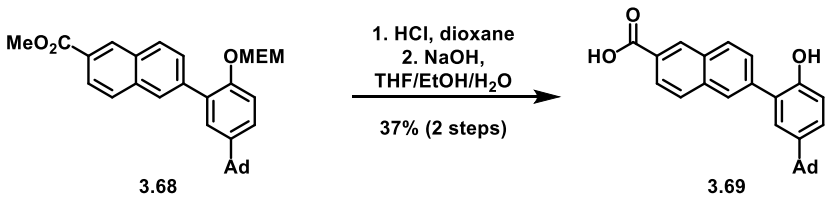

6-(5-(adamantan-1-yl)-2-hydroxyphenyl)-2-naphthoic acid (3.69). Following general procedure 3B (compound 3.56), MEM ether **3.68** (34 mg, 0.068 mmol) yielded the title compound as a white solid (10 mg, 37% yield over two steps). **^{1}H NMR** (500 MHz, DMSO) δ 13.06 (br s, 1H), 9.47 (br s, 1H), 8.60 (d, J = 0.7 Hz, 1H), 8.13 – 8.07 (m, 2H), 8.04 (d, J = 8.8 Hz, 1H), 7.97 (dd, J = 8.5, 1.6 Hz, 1H), 7.82 (dd, J = 8.5, 1.7 Hz, 1H), 7.32 (d, J = 2.5 Hz, 1H), 7.20 (dd, J = 8.5, 2.5 Hz, 1H), 6.93 (d, J = 8.5 Hz, 1H), 2.04 (s, 3H), 1.88 (d, J = 2.7 Hz, 6H), 1.72 (s, 6H); **^{13}C NMR** (100 MHz, DMSO) δ 167.56, 152.33, 142.08, 139.35, 135.05, 130.83, 130.18, 128.88, 128.46, 128.32, 127.73, 127.14, 126.89, 126.48, 125.35, 125.18, 115.82, 42.88, 36.23, 35.11, 28.41; **HRMS** Accurate mass (ES+): Found 399.1957, $C_{27}H_{27}O_3$ (M+H+) requires 399.1960.

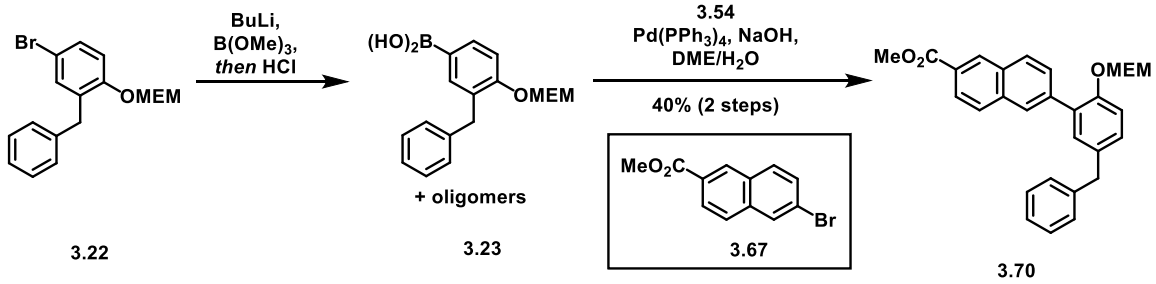

Methyl 6-(3-benzyl-4-((2-methoxyethoxy)methoxy)phenyl)-2-naphthoate (3.70). Following general procedure 3A (compound 3.55), bromide **3.22** (198 mg, 0.56 mmol) and methyl 6-bromo-2-naphthoate **3.67** (126 mg, 0.47 mmol) yielded the title compound as a white foam (86 mg, 40% yield with respect to naphthyl bromide **3.67**). **^{1}H NMR** (500 MHz, $CDCl_3$) δ 8.60 (s, 1H), 8.06 (dd, J = 8.6, 1.7 Hz, 1H), 7.98 - 7.97 (m, 2H), 7.90 (d, J = 8.7 Hz, 1H), 7.75 (dd, J = 8.5, 1.8 Hz, 1H), 7.56 (dd, J = 8.5, 2.4 Hz, 1H), 7.52 (d, J = 2.3 Hz, 1H), 7.30 – 7.24 (m, 5H), 7.20 – 7.16 (m, 1H), 5.32 (s, 2H), 4.08 (s, 2H), 3.99 (s, 3H), 3.70 – 3.65 (m, 2H), 3.52 – 3.47 (m, 2H), 3.37 (s, 3H); **^{13}C NMR** (125 MHz, $CDCl_3$) δ 167.33, 155.09, 140.88, 140.64,

135.94, 133.96, 131.42, 130.88, 130.76, 129.85, 129.79, 128.91, 128.40, 128.33, 127.15, 126.67, 126.35, 126.02, 125.71, 124.94, 114.47, 93.22, 71.64, 67.71, 59.10, 52.29, 36.59; **HRMS** Accurate mass (ES+): Found 457.2028, $C_{29}H_{29}O_5$ (M+H+) requires 457.2015.

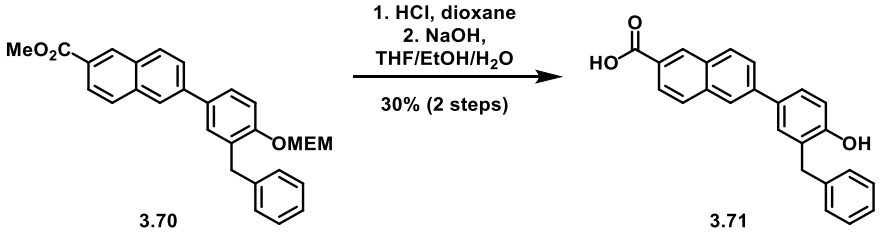

3.70 3.71

6-(3-benzyl-4-hydroxyphenyl)-2-naphthoic acid (3.71). Following general procedure 3B (compound 3.56), MEM ether **3.70** (78 mg, 0.17 mmol) yielded the title compound as a white solid (20 mg, 30% yield over two steps). **^{1}H NMR** (500 MHz, CD_3CN) δ 9.51 (br s, 1H), 8.60 (s, 1H), 8.11 (s, 1H), 8.06 (d, J = 8.7 Hz, 1H), 8.02 (dd, J = 8.6, 1.6 Hz, 1H), 7.97 (d, J = 8.6 Hz, 1H), 7.83 (dd, J = 8.6, 1.8 Hz, 1H), 7.61 (d, J = 2.4 Hz, 1H), 7.53 (dd, J = 8.3, 2.4 Hz, 1H), 7.33 – 7.25 (m, 4H), 7.20 – 7.13 (m, 2H), 6.96 (d, J = 8.3 Hz, 1H), 4.03 (s, 2H); **^{13}C NMR** (125 MHz, DMSO) δ 167.51, 155.48, 141.24, 139.95, 135.49, 130.83, 130.30, 130.27, 129.81, 129.29, 128.67, 128.25, 128.22, 128.15, 127.56, 126.14, 125.71, 125.55, 123.65, 115.79, 35.53; **HRMS** Accurate mass (ES+): Found 355.1331, $C_{24}H_{19}O_3$ (M+H+) requires 355.1334.

Appendix: NMR Spectra

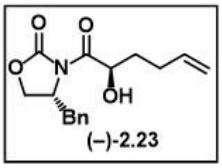
O
O
O
N
OH
Bn

(–)-2.23

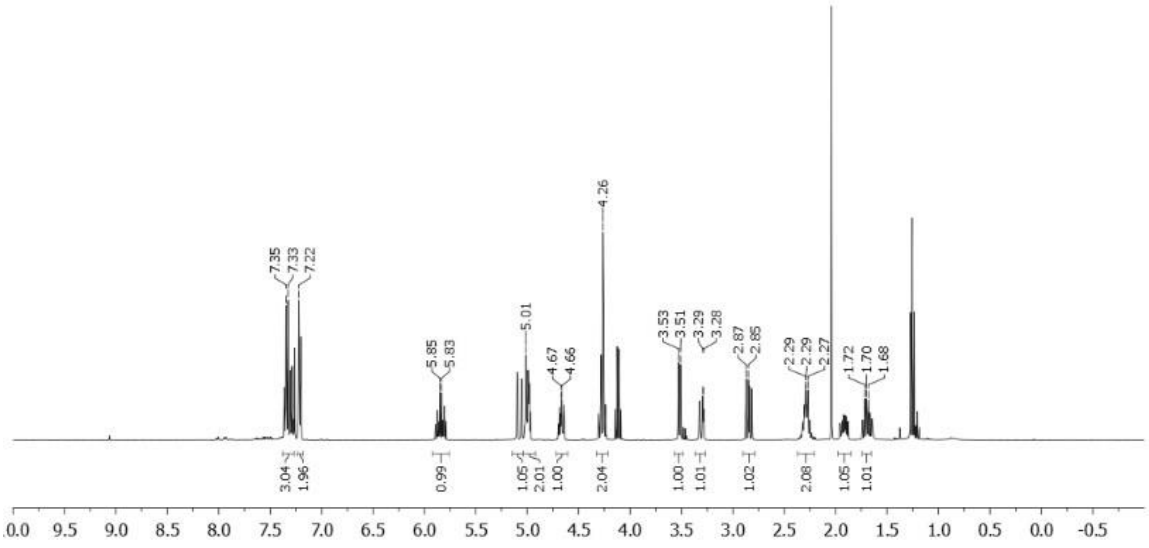
7.35
7.33
7.22
5.85
5.83
5.01
4.67
4.66
4.26
3.53
3.51
3.29
3.28
2.87
2.85
2.29
2.29
2.27
1.72
1.70
1.68
3.04
1.96
0.99
1.05
2.01
1.00
2.04
1.00
1.01
1.02
2.08
1.05
1.01

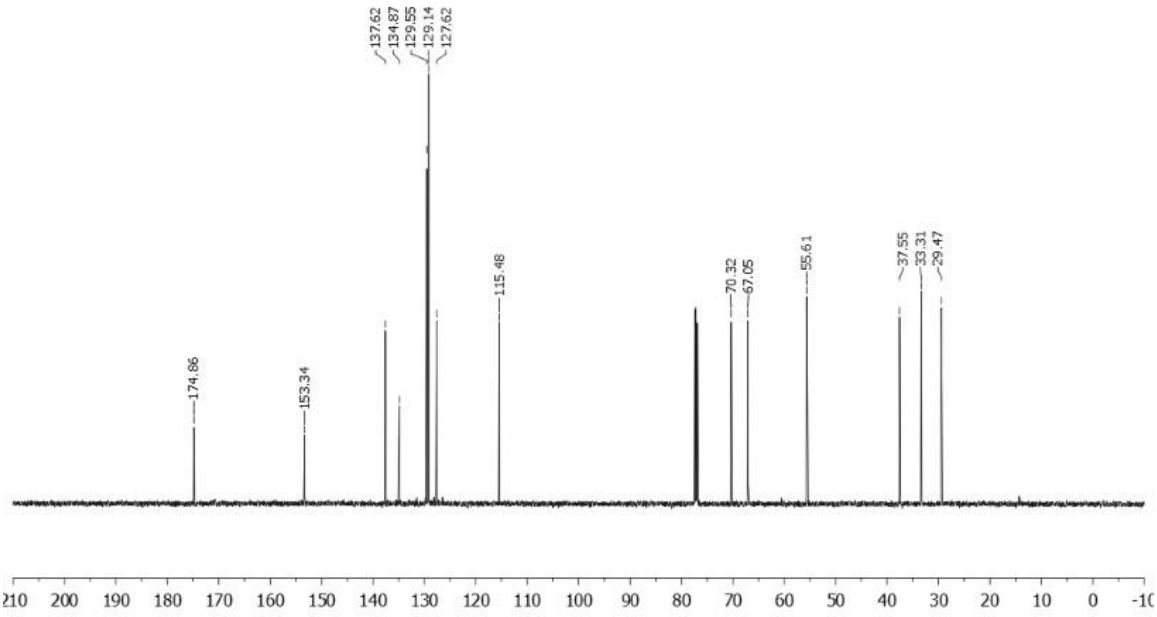
137.62
134.87
129.55
129.14
127.62
174.86
153.34
115.48
70.32
67.05
55.61
37.55
33.31
29.47

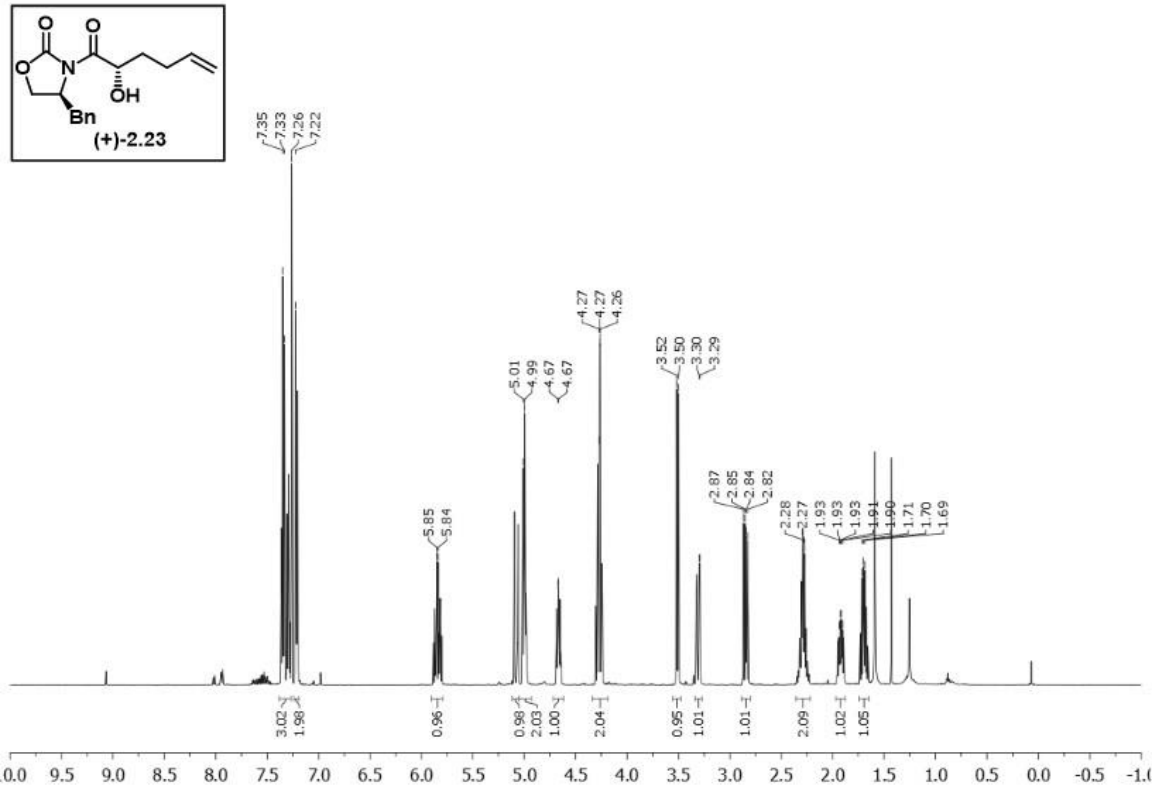
(+)-2.23
Bn
OH
7.35
7.33
7.26
7.22
5.85
5.84
5.01
4.99
4.67
4.67
4.27
4.27
4.26
3.52
3.50
3.30
3.29
2.87
2.85
2.84
2.82
2.28
2.27
1.93
1.93
1.93
1.91
1.90
1.71
1.70
1.69
3.02
1.98
0.96
0.98
2.03
1.00
2.04
0.95
1.01
1.01
2.09
1.02
1.05

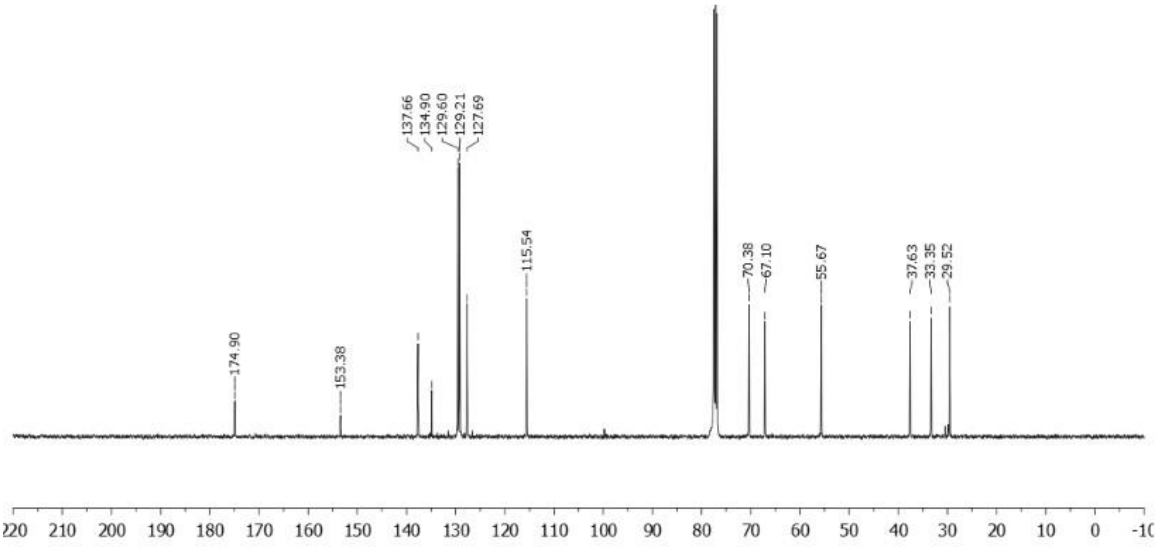
137.66
134.90
129.60
129.21
127.69
115.54
174.90
153.38
70.38
67.10
55.67
37.63
33.35
29.52

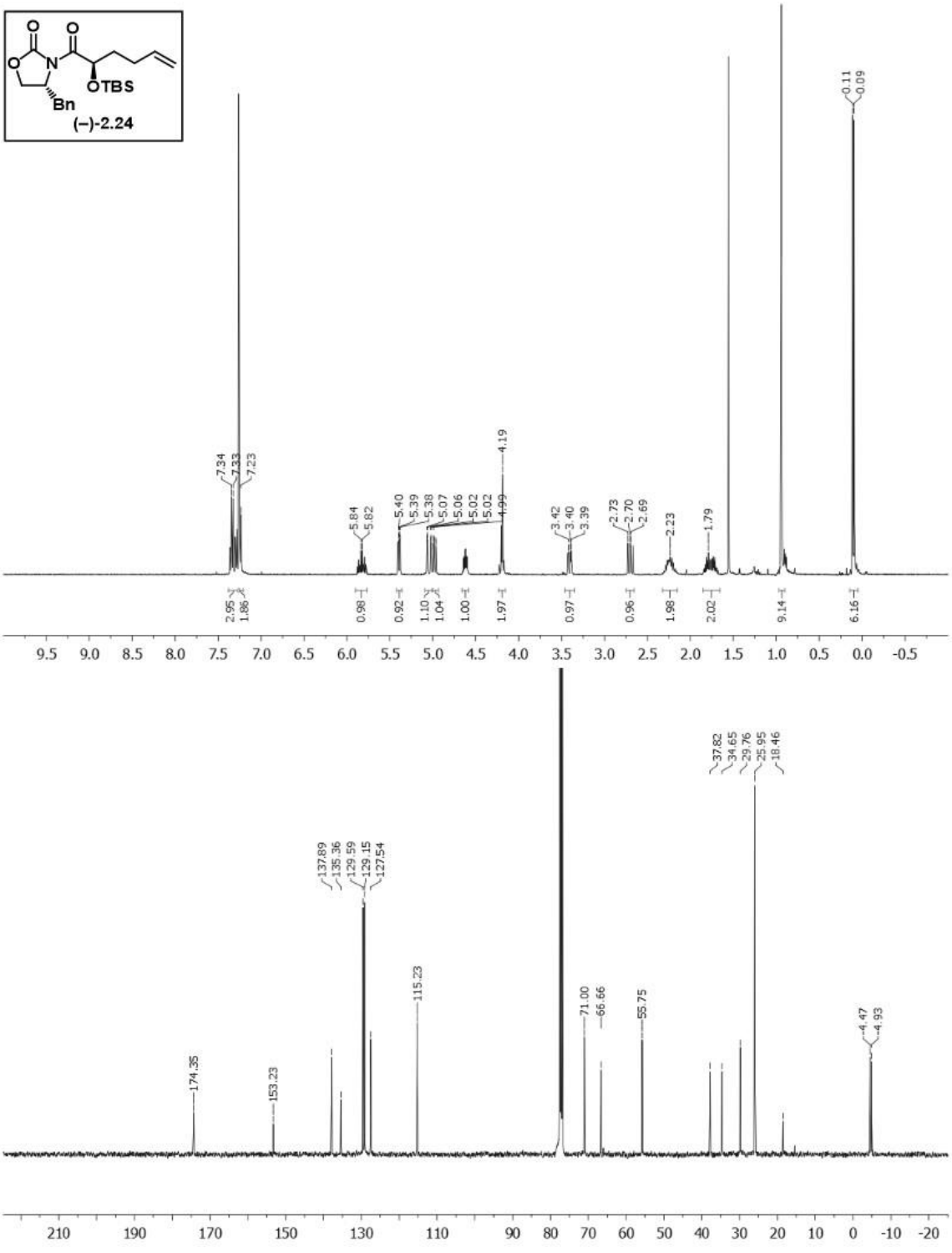
OTBS
Bn
(–)-2.24
7.34
7.33
7.23
5.84
5.82
5.40
5.39
5.38
5.07
5.06
5.02
5.02
4.99
4.19
3.42
3.40
3.39
2.73
2.70
2.69
2.23
1.79
0.11
0.09
2.95
1.88
0.98
0.92
1.10
1.04
1.00
1.97
0.97
0.96
1.98
2.02
9.14
6.16
137.89
135.36
129.59
129.15
127.54
115.23
174.35
153.23
71.00
66.66
55.75
37.82
34.65
29.76
25.95
18.46
4.47
4.93

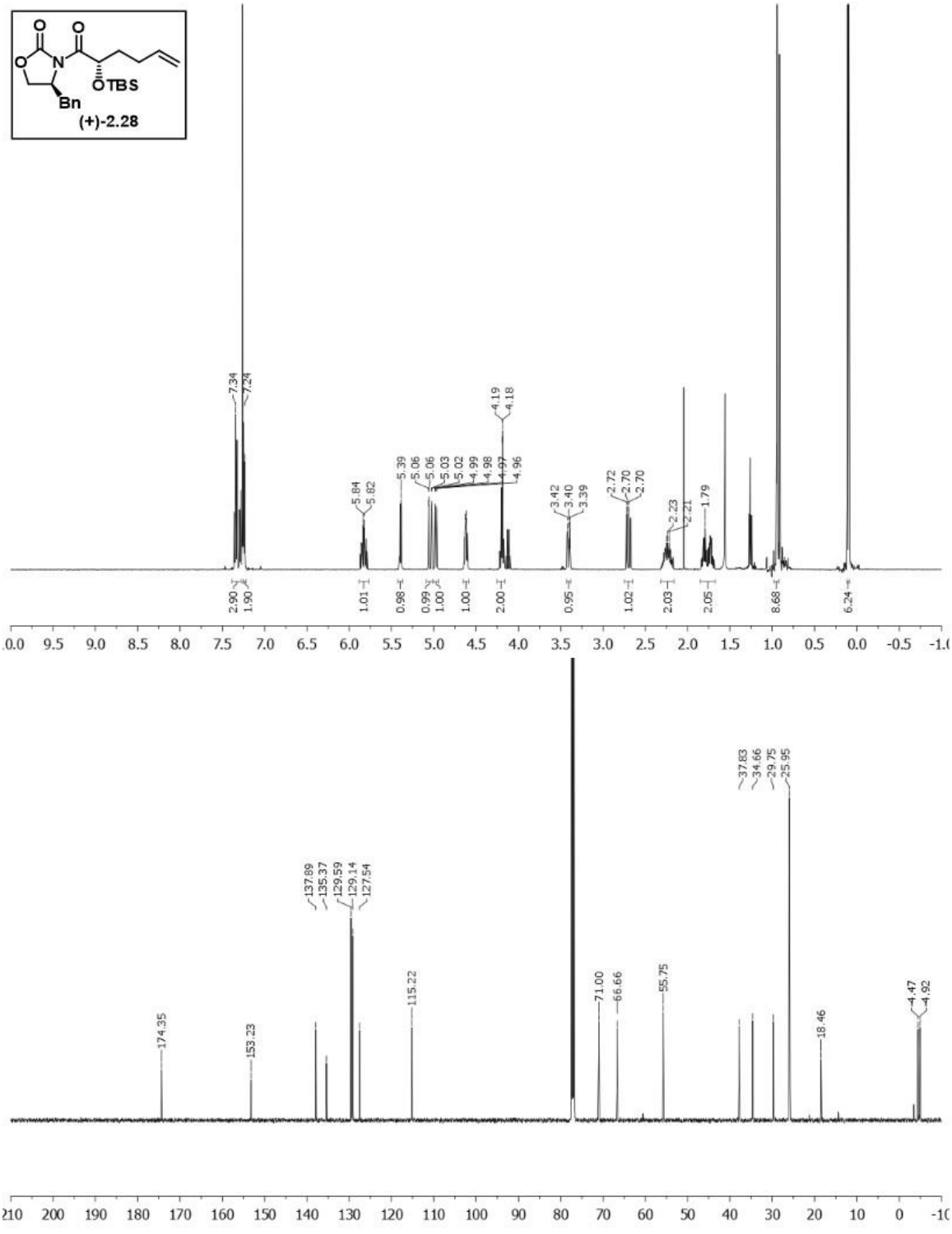
(+)-2.28
7.34
7.24
5.84
5.82
5.39
5.06
5.06
5.03
5.02
4.99
4.98
4.97
4.96
4.19
4.18
3.42
3.40
3.39
2.72
2.70
2.70
2.23
2.21
1.79
2.90
1.90
1.01
0.98
0.99
1.00
1.00
2.00
0.95
1.02
2.03
2.05
8.68
6.24
174.35
153.23
137.89
135.37
129.59
129.14
127.54
115.22
71.00
66.66
55.75
37.83
34.66
29.75
25.95
18.46
4.47
4.92

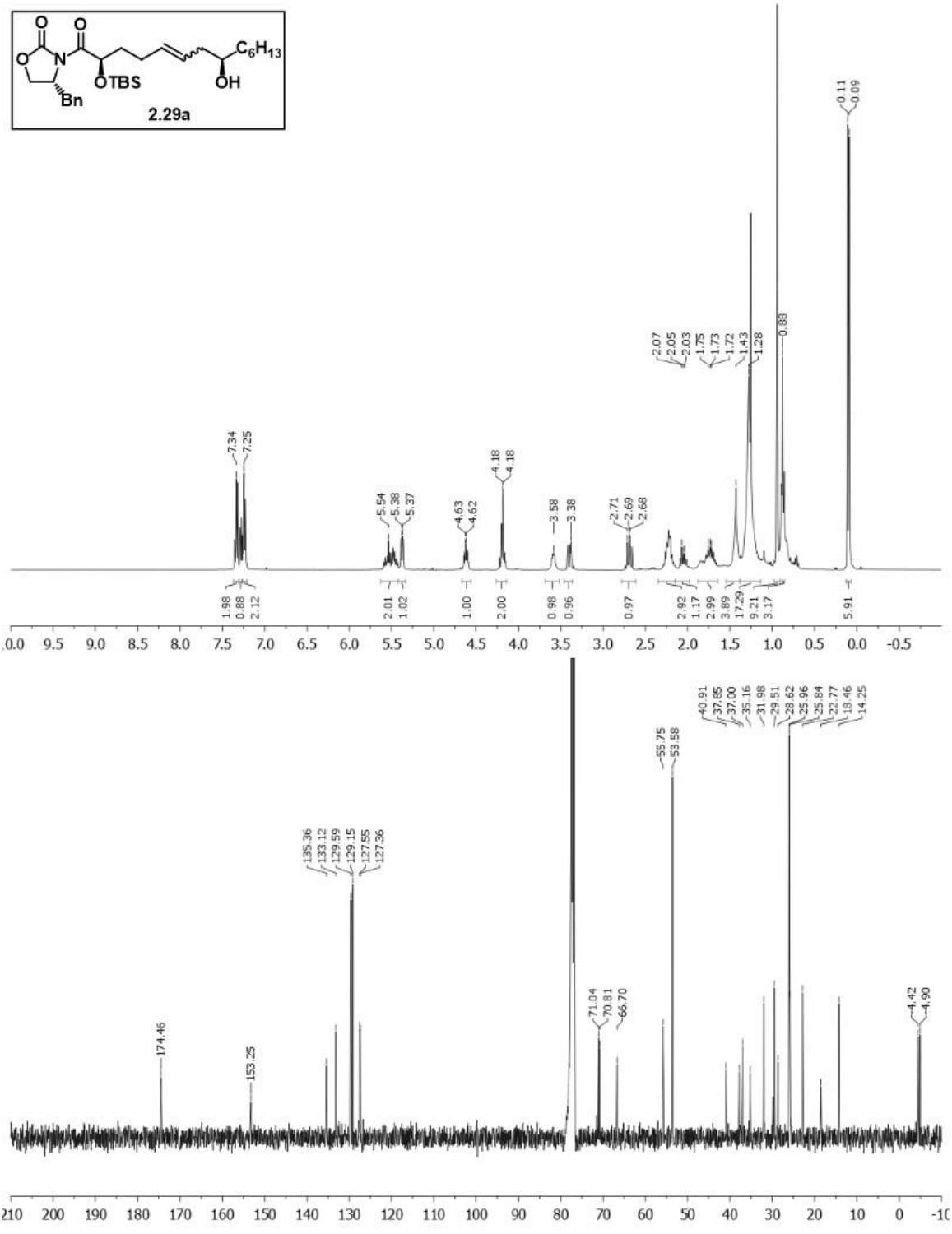
2.29a
7.34
7.25
5.54
5.38
5.37
4.63
4.62
4.18
4.18
3.58
3.38
2.71
2.69
2.68
2.07
2.05
2.03
1.75
1.73
1.72
1.43
1.28
0.88
0.11
0.09
135.36
133.12
129.59
129.15
127.55
127.36
174.46
153.25
71.04
70.81
66.70
55.75
53.58
40.91
37.85
37.00
35.16
31.98
29.51
28.62
25.96
25.84
22.77
18.46
14.25
4.42
4.90

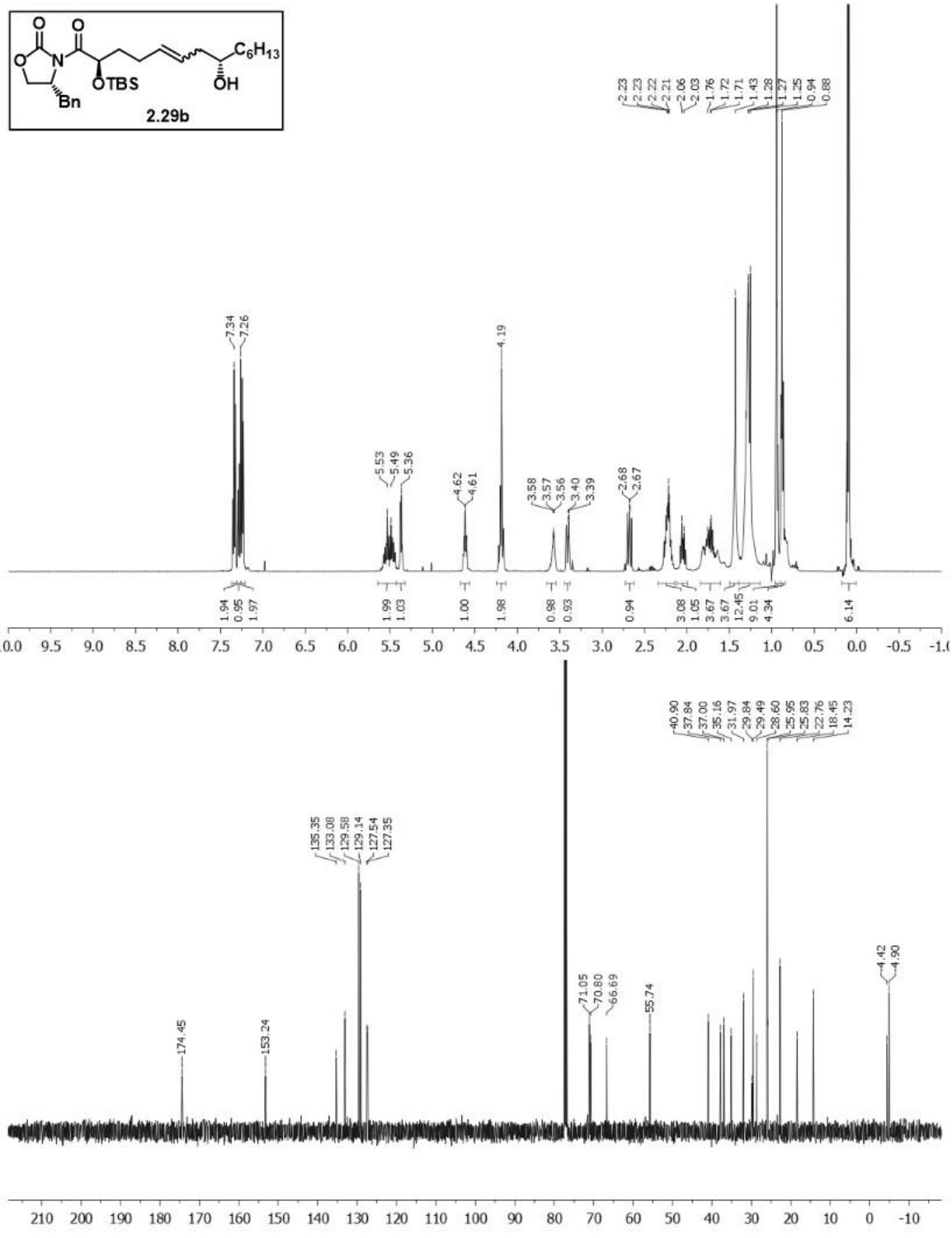
OTBS
OH
Bn
C_6H_{13}
2.29b
7.34
7.26
5.53
5.49
5.36
4.62
4.61
4.19
3.58
3.57
3.56
3.40
3.39
2.68
2.67
2.23
2.23
2.22
2.21
2.06
2.03
1.76
1.72
1.71
1.43
1.28
1.27
1.25
0.94
0.88
1.94
0.95
1.97
1.99
1.03
1.00
1.98
0.98
0.93
0.94
3.08
1.05
3.67
3.67
12.45
9.01
4.34
6.14
40.90
37.84
37.00
35.16
31.97
29.84
29.49
28.60
25.95
25.83
22.76
18.45
14.23
135.35
133.08
129.58
129.14
127.54
127.35
174.45
153.24
71.05
70.80
66.69
55.74
14.42
14.90

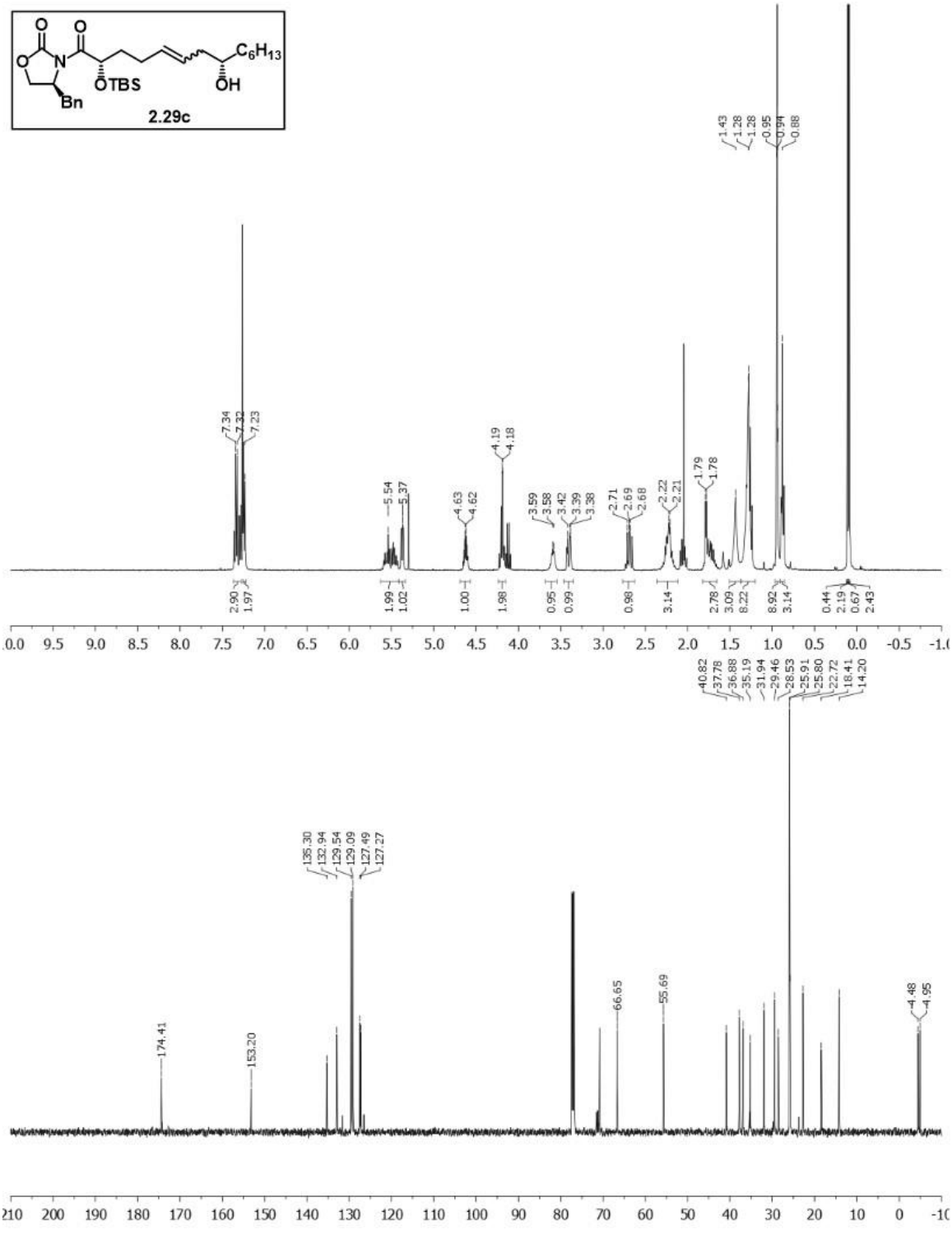
OTBS
OH
Bn
C_6H_{13}
2.29c

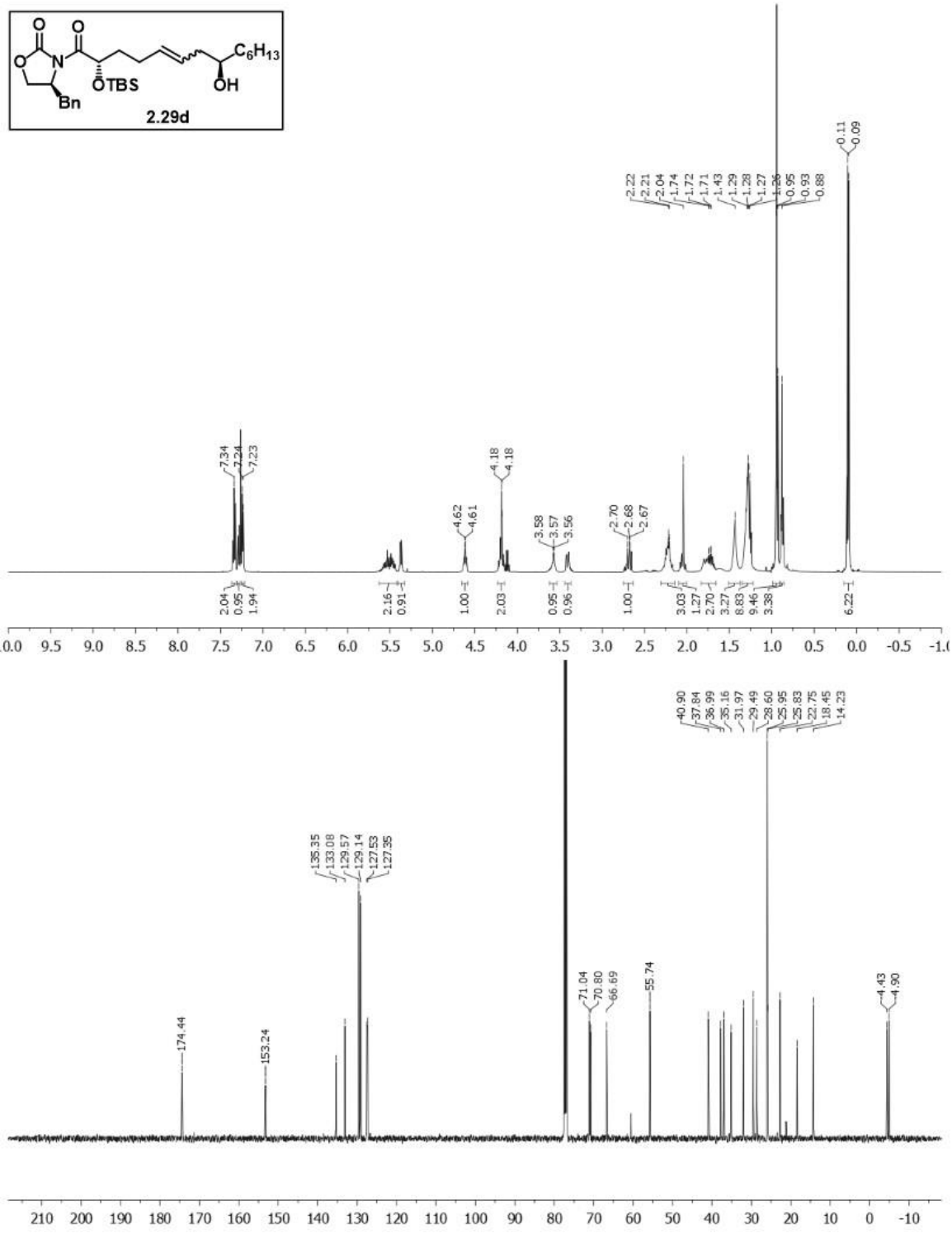
O
O
O
N
C6H13
OTBS
OH
Bn
2.29d
0.11
0.09
2.22
2.21
2.04
1.74
1.72
1.71
1.43
1.29
1.28
1.27
0.95
0.93
0.88
7.34
7.24
7.23
4.62
4.61
4.18
4.18
3.58
3.57
3.56
2.70
2.68
2.67
2.04
0.95
1.94
2.16
0.91
1.00
2.03
0.95
0.96
1.00
3.03
1.27
2.70
3.27
8.83
9.46
3.38
6.22
40.90
37.84
36.99
35.16
31.97
29.49
28.60
25.95
25.83
22.75
18.45
14.23
135.35
133.08
129.57
129.14
127.53
127.35
71.04
70.80
66.69
55.74
174.44
153.24
4.43
4.90

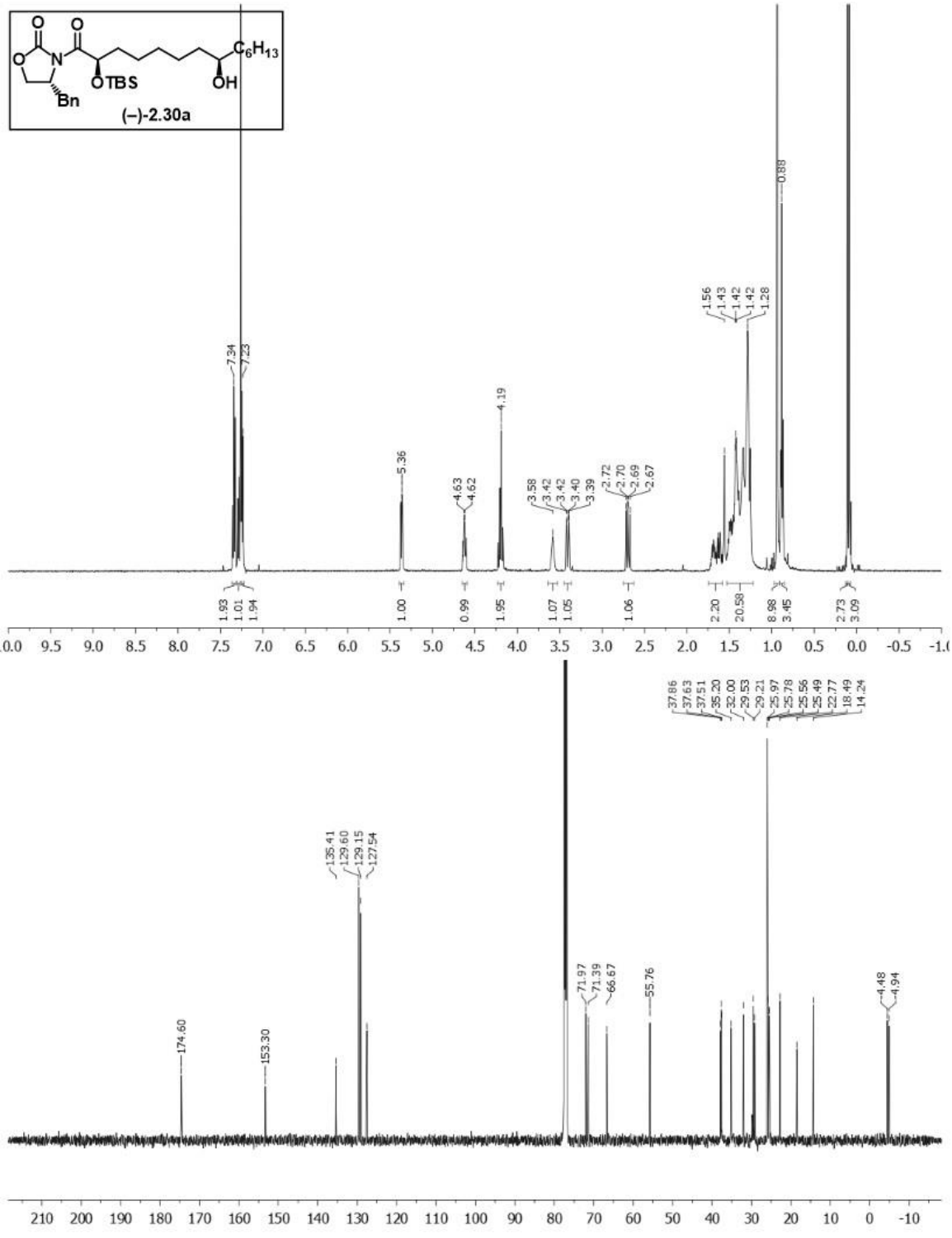
(–)-2.30a
7.34
7.23
5.36
4.63
4.62
4.19
3.58
3.42
3.42
3.40
3.39
2.72
2.70
2.69
2.67
1.56
1.43
1.42
1.42
1.28
0.88
1.93
1.01
1.94
1.00
0.99
1.95
1.07
1.05
1.06
2.20
20.58
8.98
3.45
2.73
3.09
37.86
37.63
37.51
35.20
32.00
29.53
29.21
25.97
25.78
25.56
25.49
22.77
18.49
14.24
135.41
129.60
129.15
127.54
174.60
153.30
71.97
71.39
66.67
55.76
4.48
-4.94

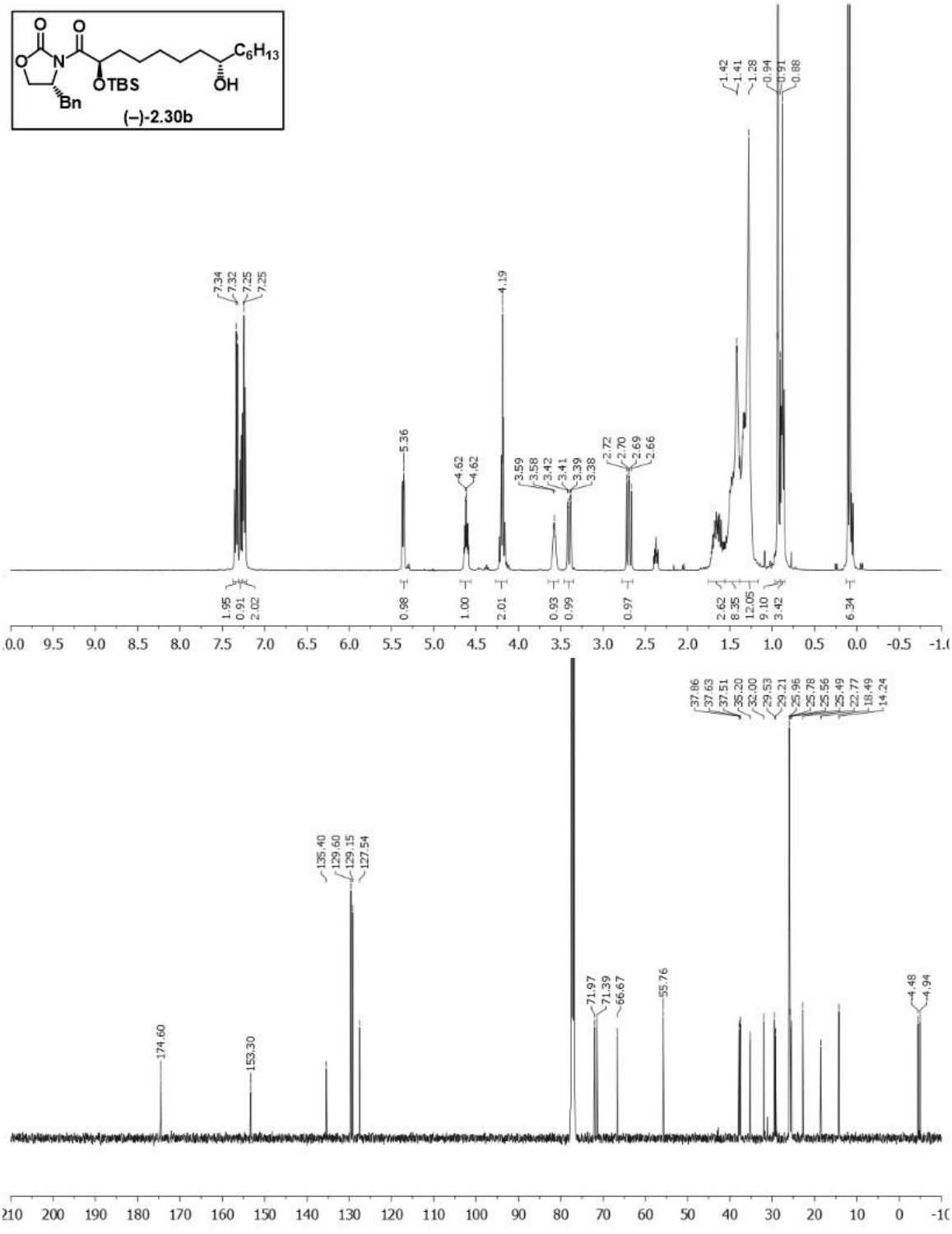
(–)-2.30b
OTBS
OH
Bn
C6H13
7.34
7.32
7.25
7.25
5.36
4.62
4.62
4.19
3.59
3.58
3.42
3.41
3.39
3.38
2.72
2.70
2.69
2.66
1.42
1.41
1.28
0.94
0.91
0.88
1.95
0.91
2.02
0.98
1.00
2.01
0.93
0.99
0.97
2.62
8.35
12.05
9.10
3.42
6.34
174.60
153.30
135.40
129.60
129.15
127.54
71.97
71.39
66.67
55.76
37.86
37.63
37.51
36.20
32.00
29.53
29.21
25.96
25.78
25.56
25.49
22.77
18.49
14.24
14.48
14.94

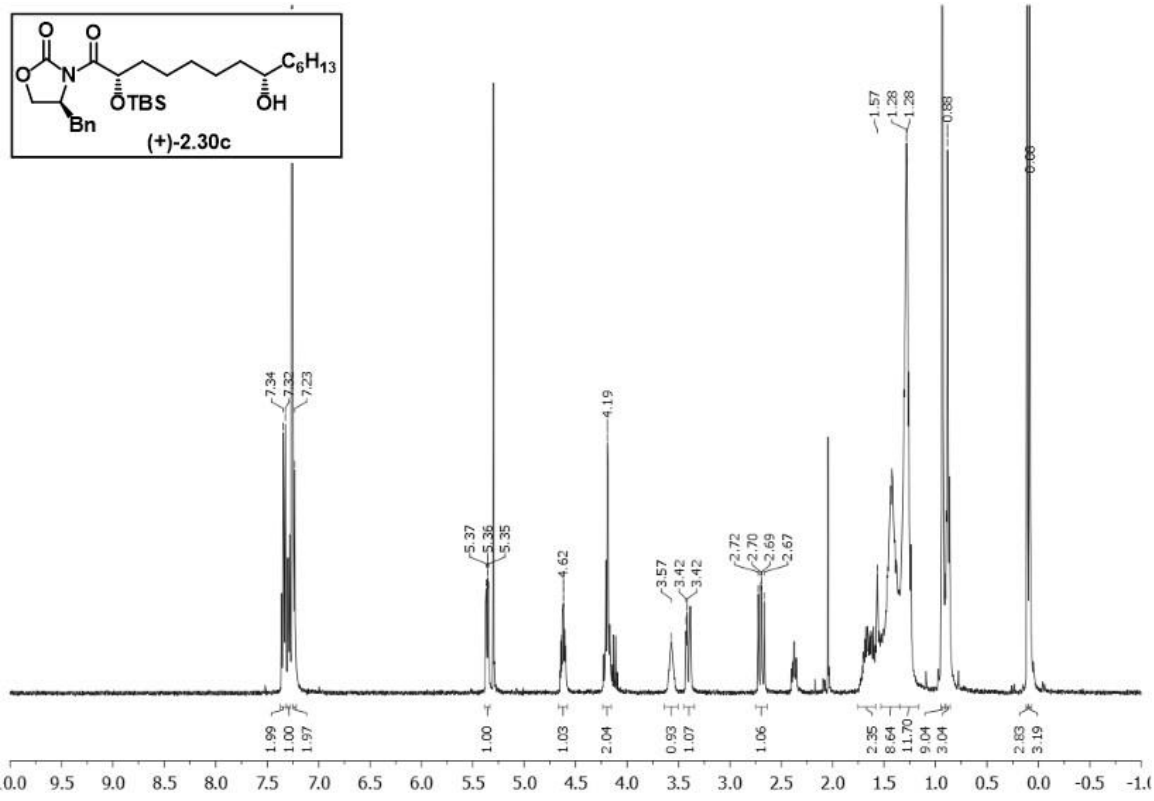
(+)-2.30c
7.34
7.32
7.23
5.37
5.36
5.35
4.62
4.19
3.57
3.42
3.42
2.72
2.70
2.69
2.67
1.57
1.28
1.28
0.88
0.00
1.99
1.00
1.97
1.00
1.03
2.04
0.93
1.07
1.06
2.35
8.64
11.70
9.04
3.04
2.83
3.19

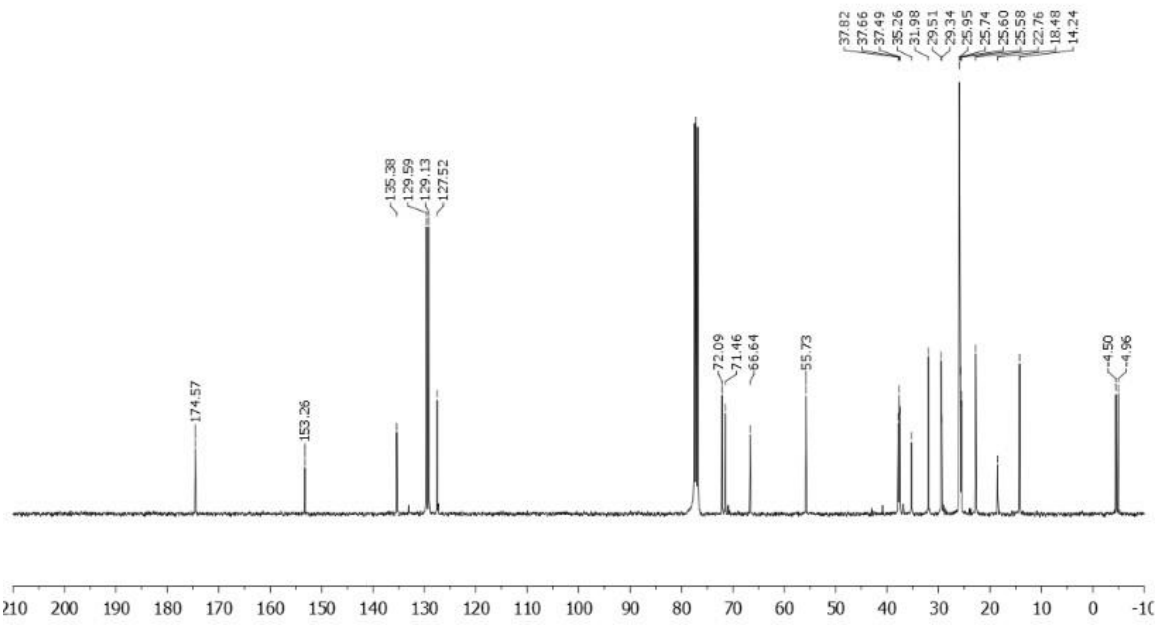
37.82
37.66
37.49
35.26
31.98
29.51
29.34
25.95
25.74
25.60
25.58
22.76
18.48
14.24
135.38
129.59
129.13
127.52
174.57
153.26
72.09
71.46
66.64
55.73
-4.50
-4.96

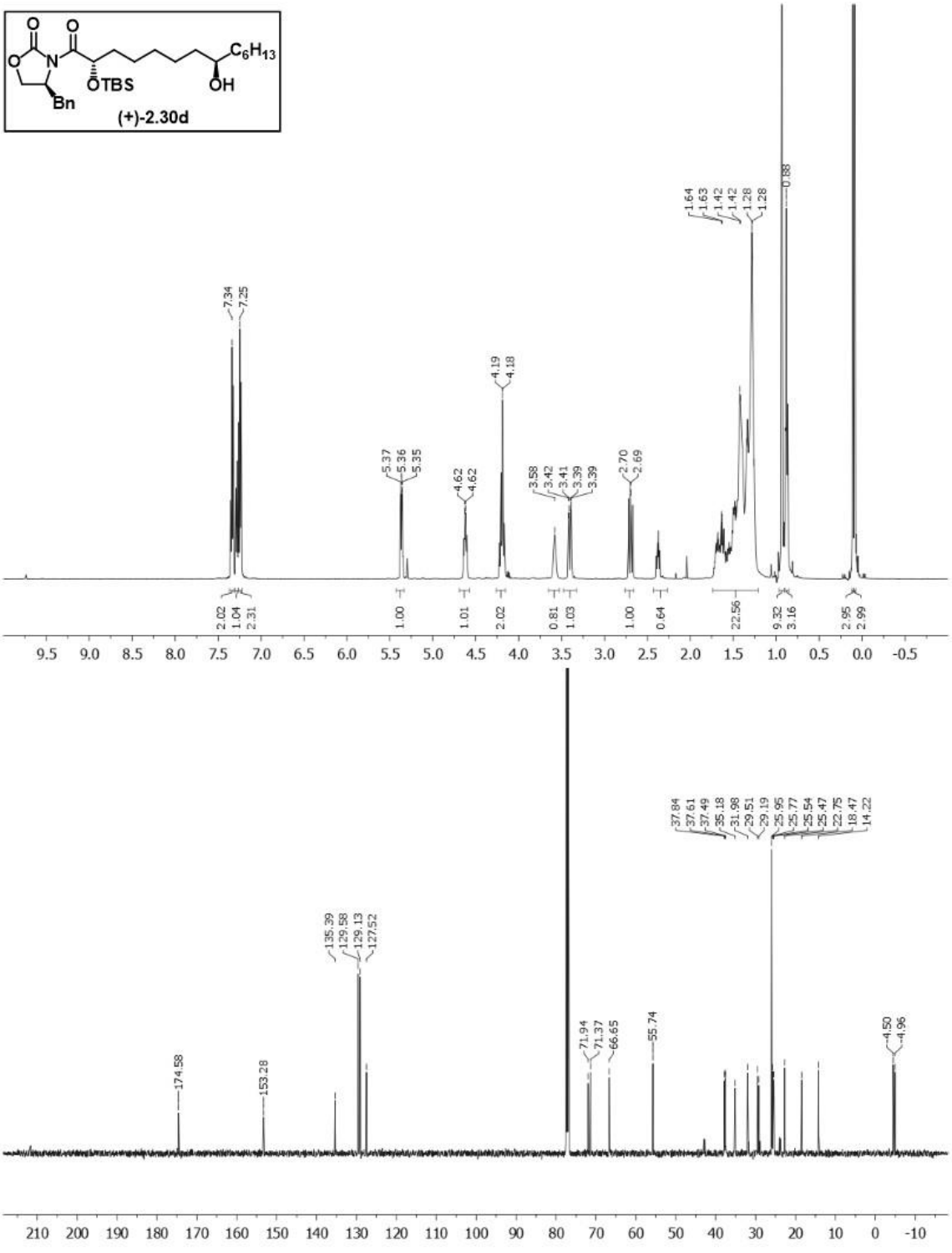
(+)-2.30d
OTBS
OH
Bn
C_6H_{13}
7.34
7.25
5.37
5.36
5.35
4.62
4.62
4.19
4.18
3.58
3.42
3.41
3.39
3.39
2.70
2.69
1.64
1.63
1.42
1.42
1.28
1.28
0.88
2.02
1.04
2.31
1.00
1.01
2.02
0.81
1.03
1.00
0.64
22.56
9.32
3.16
2.95
2.99
174.58
153.28
135.39
129.58
129.13
127.52
71.94
71.37
66.65
55.74
37.84
37.61
37.49
35.18
31.98
29.51
29.19
25.95
25.77
25.54
25.47
22.75
18.47
14.22
-4.50
-4.96

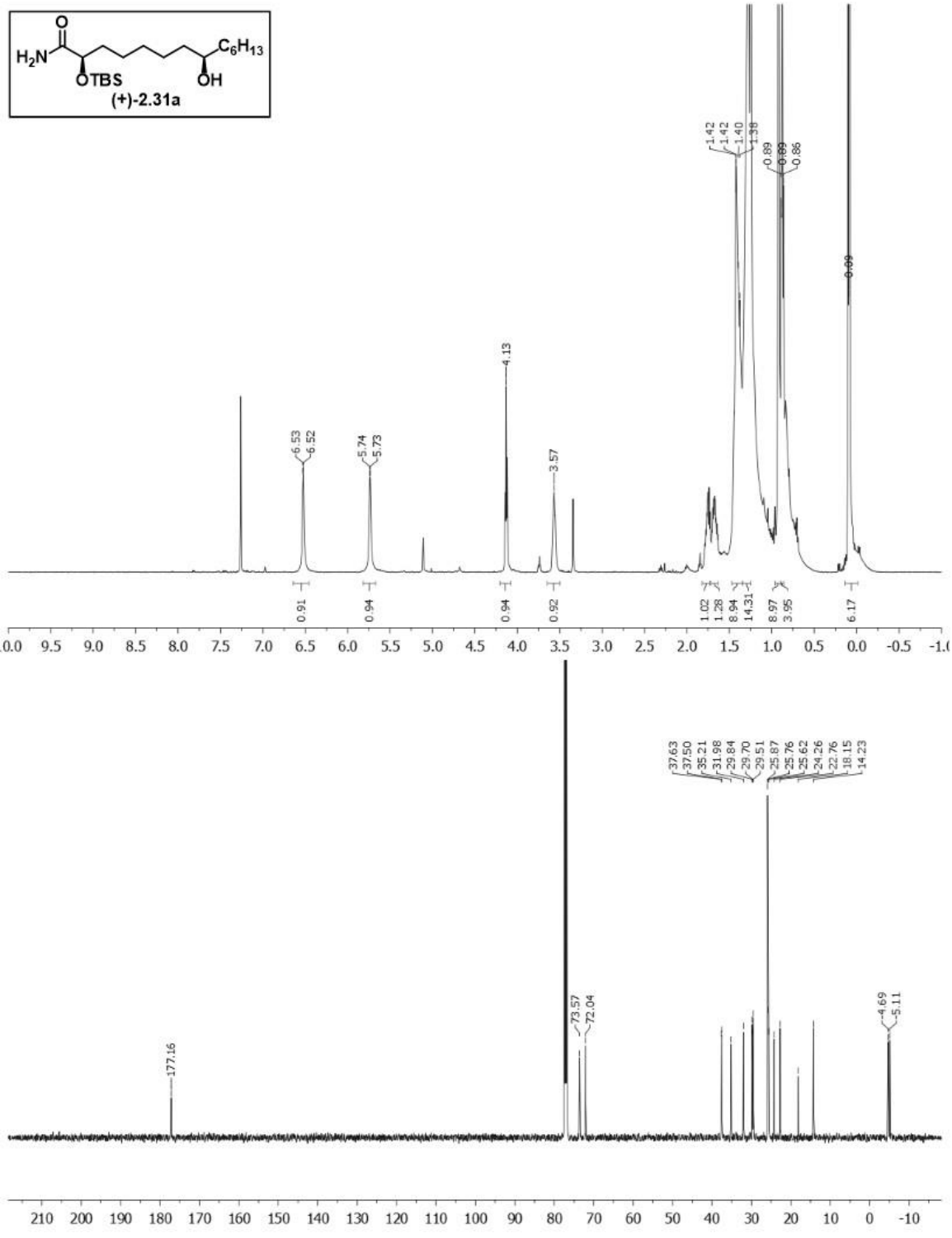
(+)-2.31a
6.53
6.52
5.74
5.73
4.13
3.57
1.42
1.42
1.40
1.38
0.89
0.89
0.86
0.09
0.91
0.94
0.94
0.92
1.02
1.28
8.94
14.31
8.97
3.95
6.17
177.16
73.57
72.04
37.63
37.50
35.21
31.98
29.84
29.70
29.51
25.87
25.76
25.62
24.26
22.76
18.15
14.23
4.69
-5.11

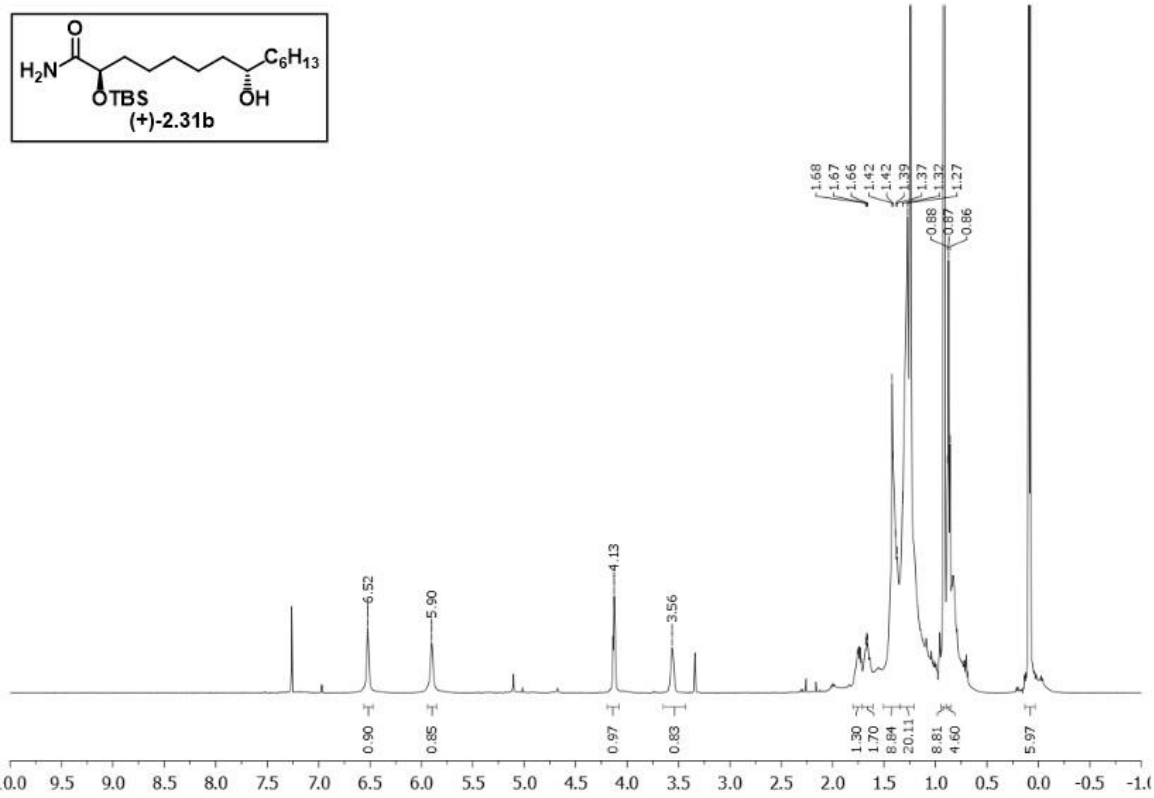
O
H2N
C6H13
OTBS
OH
(+)-2.31b
1.68
1.67
1.66
1.42
1.42
1.39
1.37
1.32
1.27
0.88
0.87
0.86
6.52
5.90
4.13
3.56
0.90
0.85
0.97
0.83
1.30
1.70
8.84
20.11
8.81
4.60
5.97

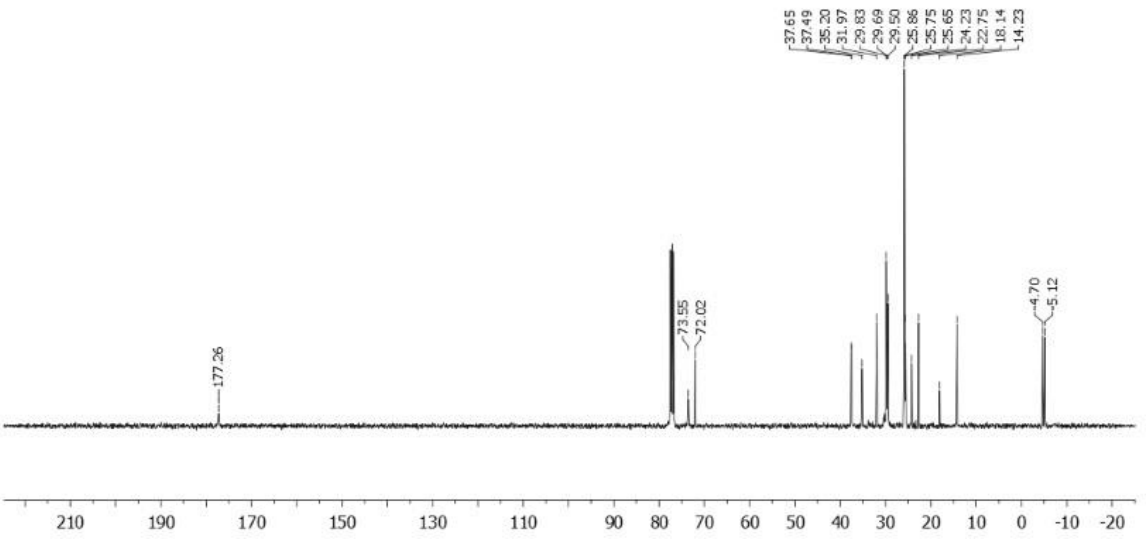
37.65
37.49
35.20
31.97
29.83
29.69
29.50
25.86
25.75
25.65
24.23
22.75
18.14
14.23
177.26
73.55
72.02
4.70
5.12

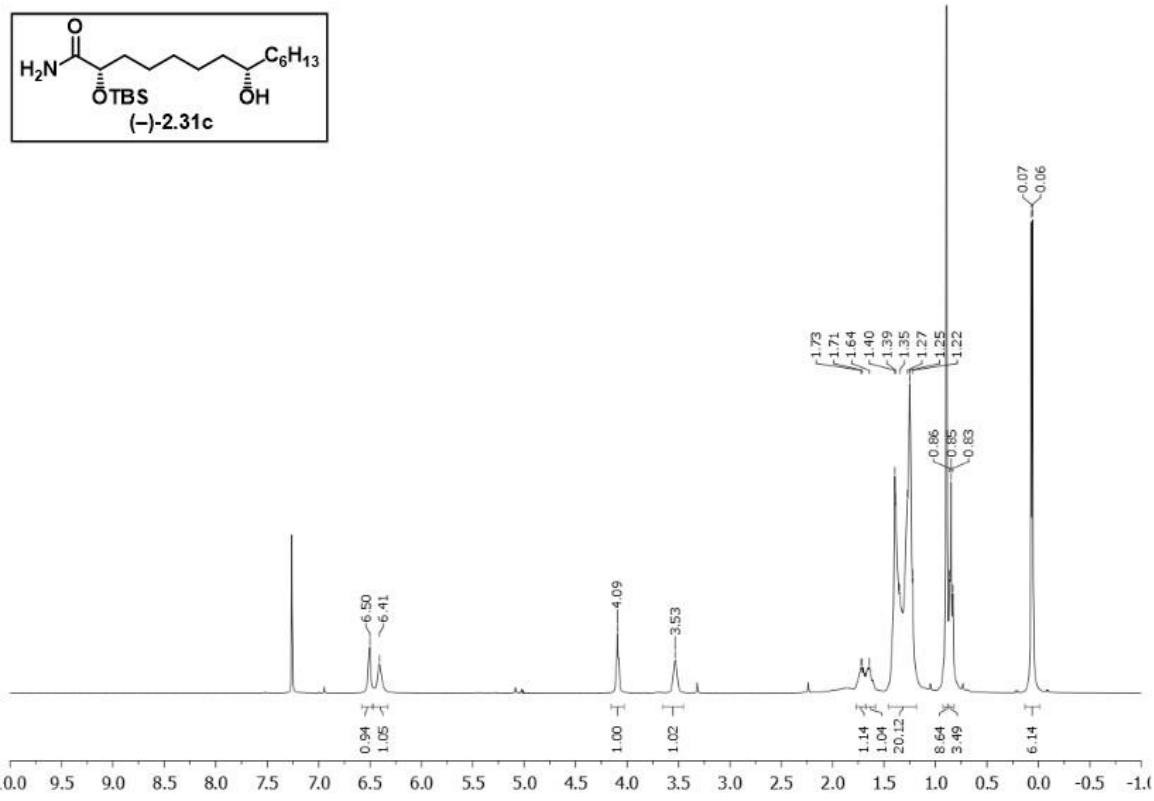
O
H2N
C6H13
OTBS
OH
(–)-2.31c
6.50
6.41
4.09
3.53
1.73
1.71
1.64
1.40
1.39
1.35
1.27
1.25
1.22
0.86
0.85
0.83
0.07
0.06
0.94
1.05
1.00
1.02
1.14
1.04
20.12
8.64
3.49
6.14

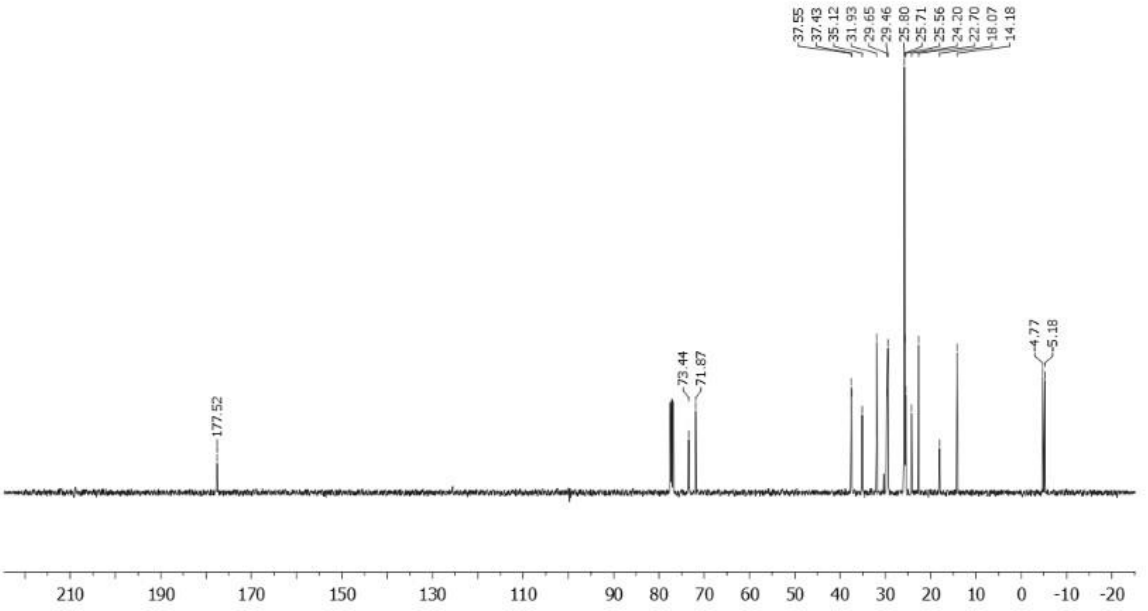
177.52
73.44
71.87
37.55
37.43
35.12
31.93
29.65
29.46
25.80
25.71
25.56
24.20
22.70
18.07
14.18
4.77
-5.18

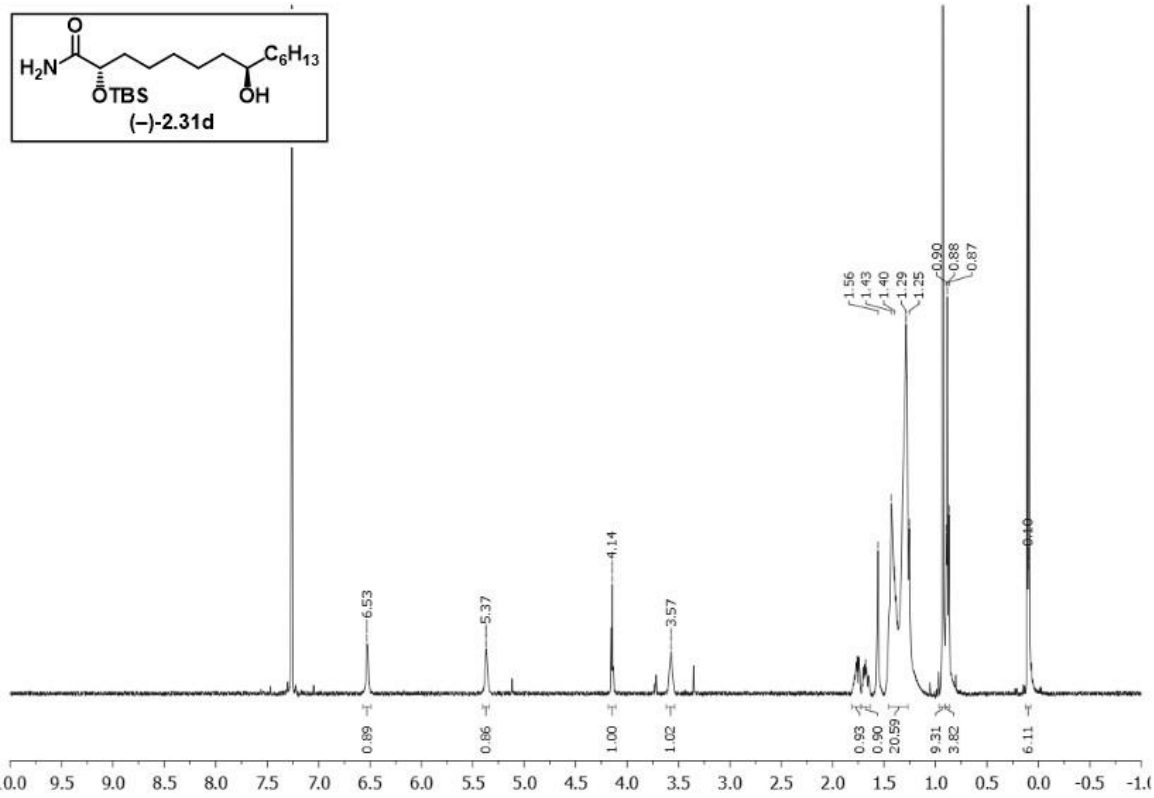
O
H2N
C6H13
OTBS
OH
(–)-2.31d
6.53
5.37
4.14
3.57
1.56
1.43
1.40
1.29
1.25
0.90
0.88
0.87
0.10
0.89
0.86
1.00
1.02
0.93
0.90
20.59
9.31
3.82
6.11

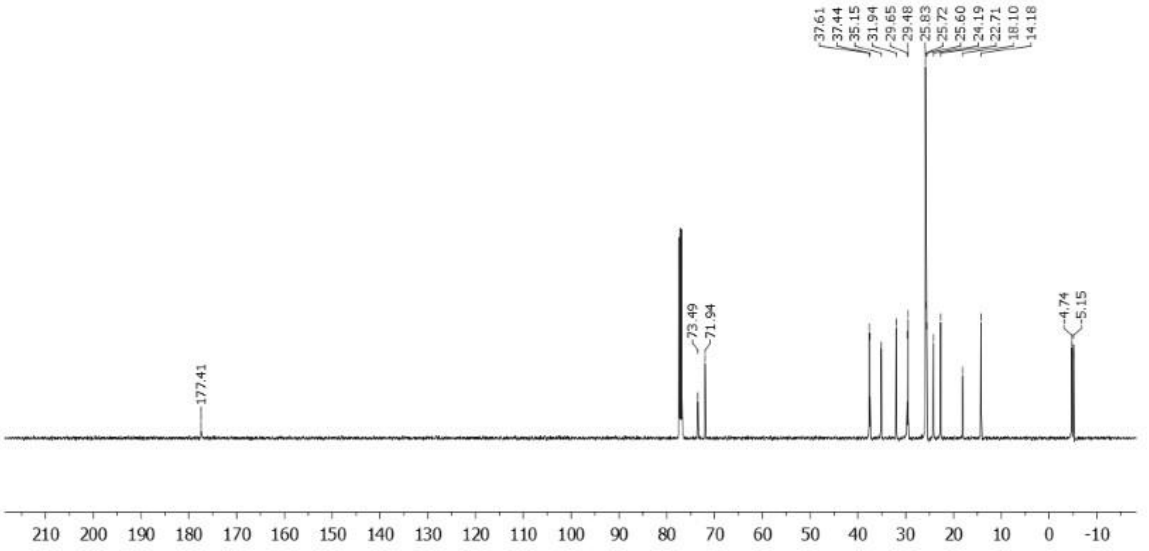
177.41
73.49
71.94
37.61
37.44
35.15
31.94
29.65
29.48
25.83
25.72
25.60
24.19
22.71
18.10
14.18
-4.74
-5.15

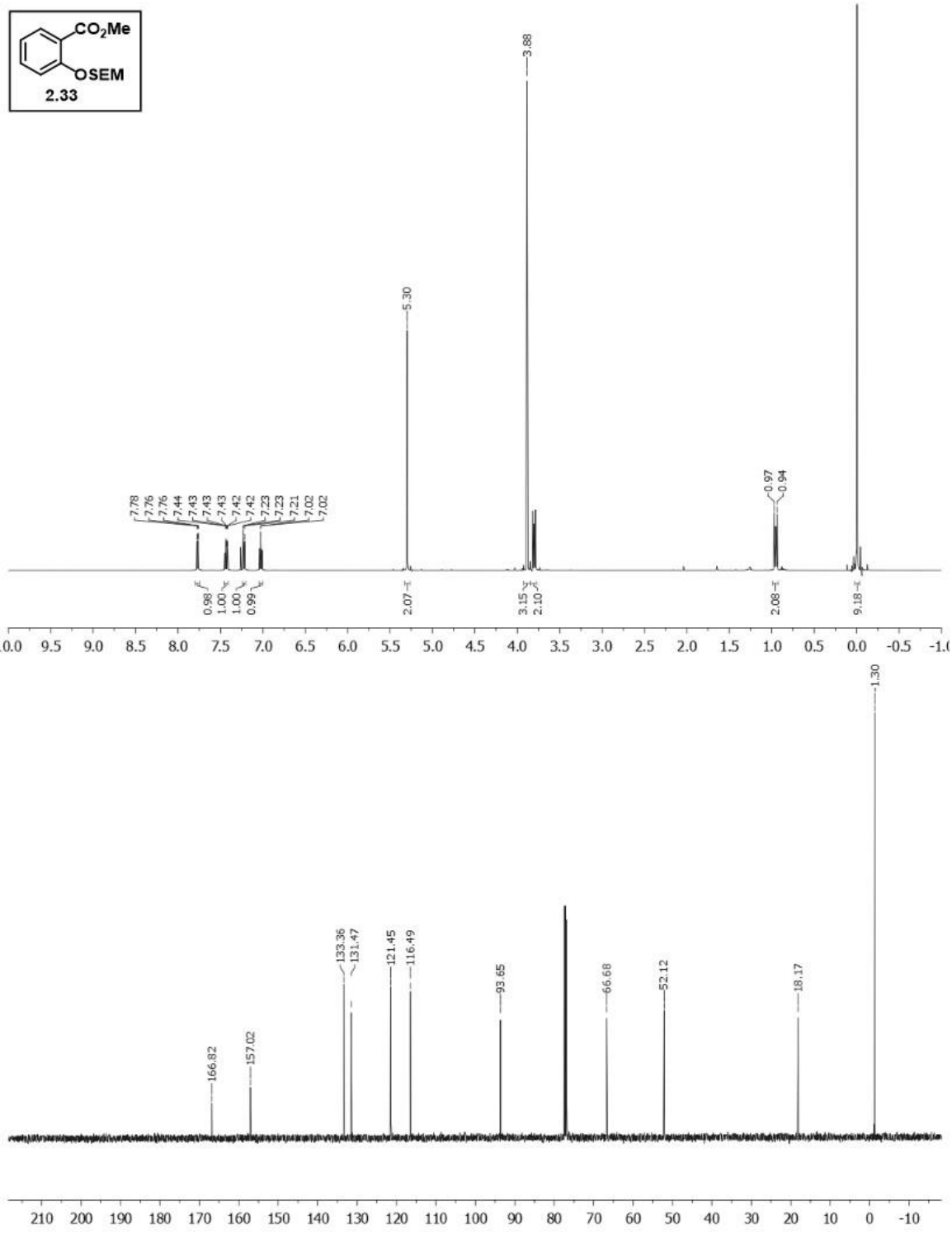
CO2Me
OSEM
2.33
7.78
7.76
7.75
7.44
7.43
7.43
7.43
7.42
7.42
7.23
7.23
7.21
7.02
7.02
5.30
3.88
0.97
0.94
0.98
1.00
1.00
0.99
2.07
3.15
2.10
2.08
9.18
1.30
166.82
157.02
133.36
131.47
121.45
116.49
93.65
66.68
52.12
18.17

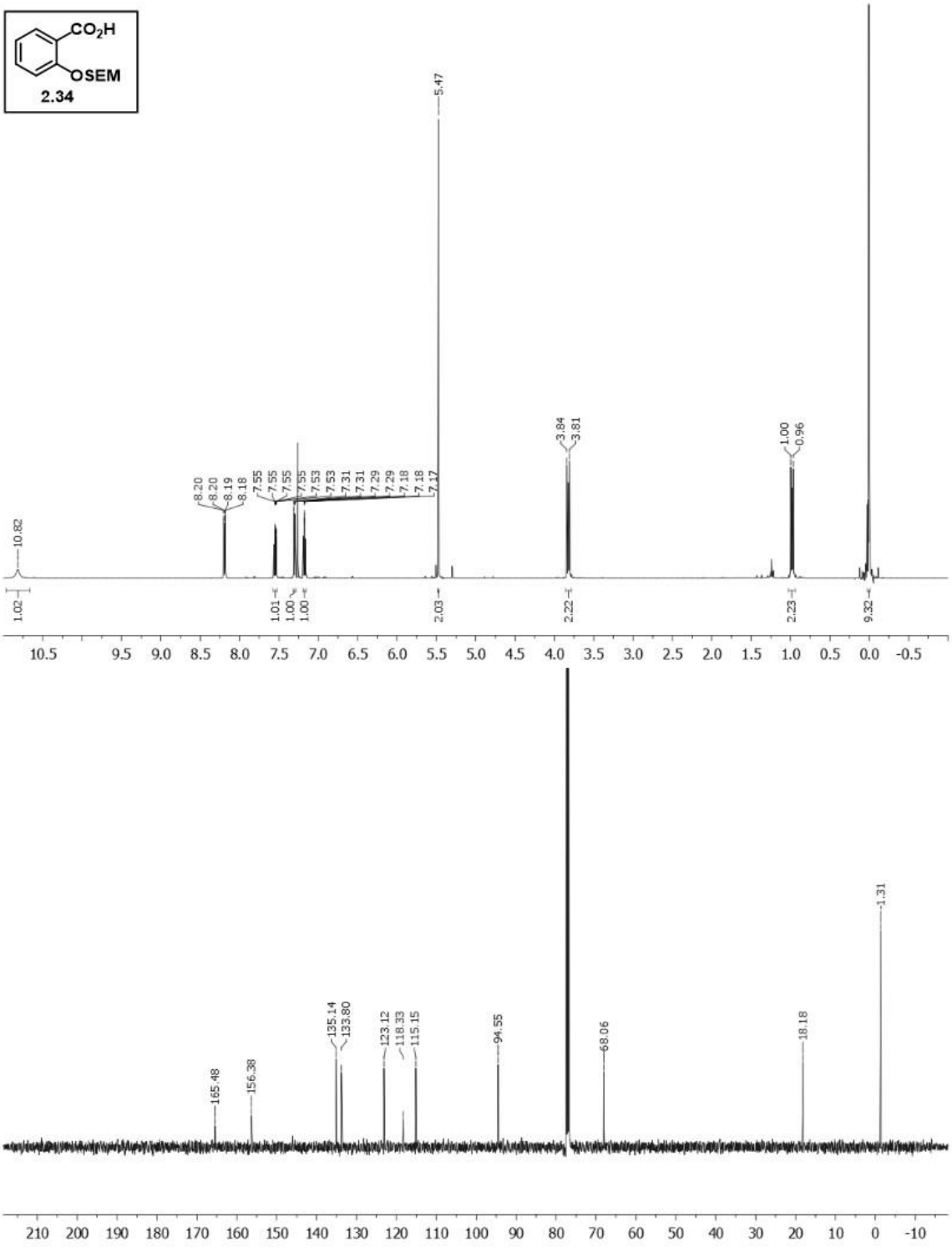
CO2H
OSEM
2.34
10.82
8.20
8.20
8.19
8.18
7.55
7.55
7.55
7.55
7.53
7.53
7.31
7.31
7.29
7.29
7.18
7.18
7.17
5.47
3.84
3.81
1.00
0.96
1.02
1.01
1.00
1.00
2.03
2.22
2.23
9.32
165.48
156.38
135.14
133.80
123.12
118.33
115.15
94.55
68.06
18.18
-1.31

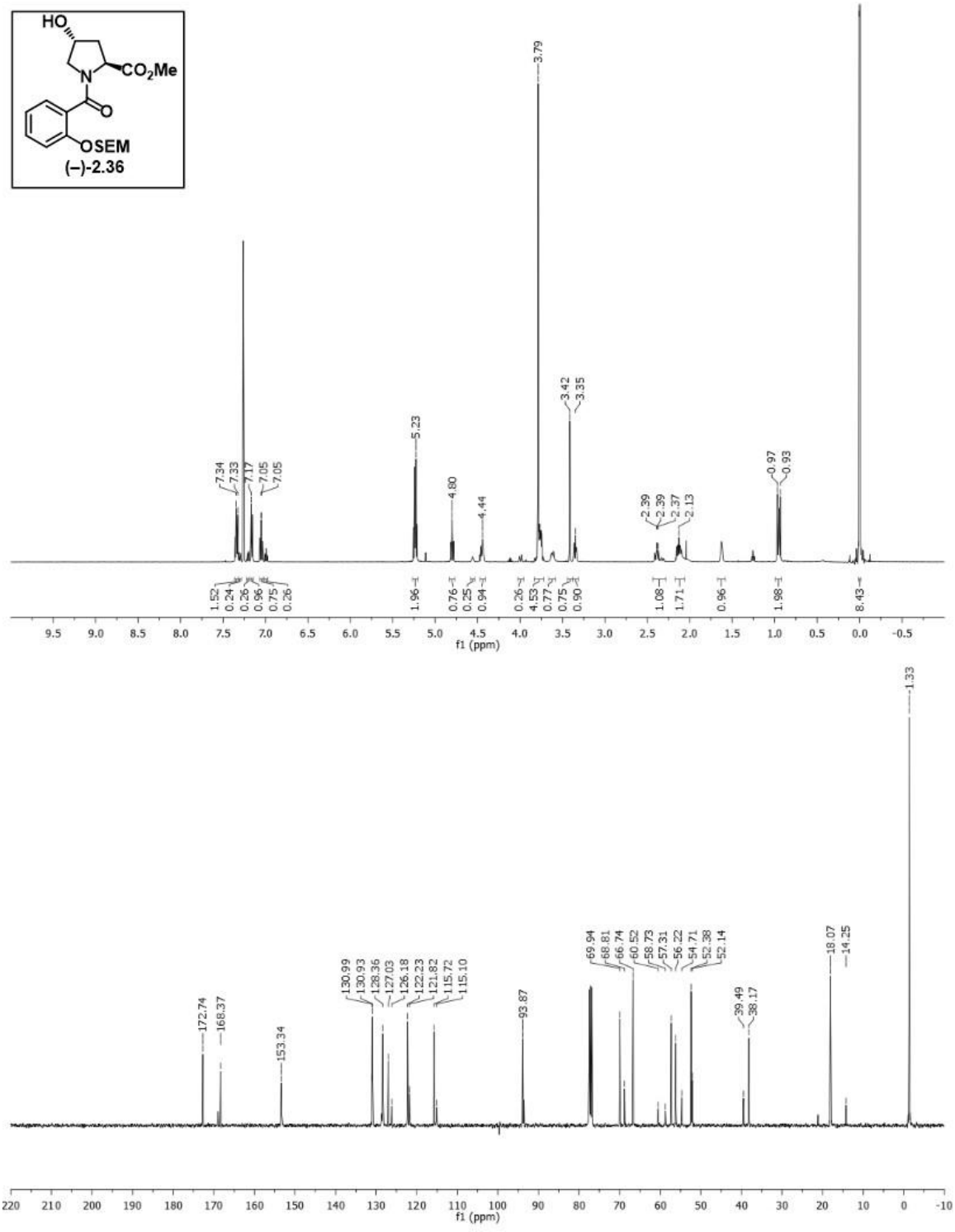
HO
CO2Me
N
O
OSEM
(–)-2.36
7.34
7.33
7.17
7.05
7.05
5.23
4.80
4.44
3.79
3.42
3.35
2.39
2.39
2.37
2.13
0.97
0.93
1.52
0.24
0.26
0.96
0.75
0.26
1.96
0.76
0.25
0.94
0.26
4.53
0.77
0.75
0.90
1.08
1.71
0.96
1.98
8.43
f1 (ppm)
1.33
172.74
168.37
153.34
130.99
130.93
128.36
127.03
126.18
122.23
121.82
115.72
115.10
93.87
69.94
68.81
66.74
60.52
58.73
57.31
56.22
54.71
52.38
52.14
39.49
38.17
18.07
14.25
f1 (ppm)

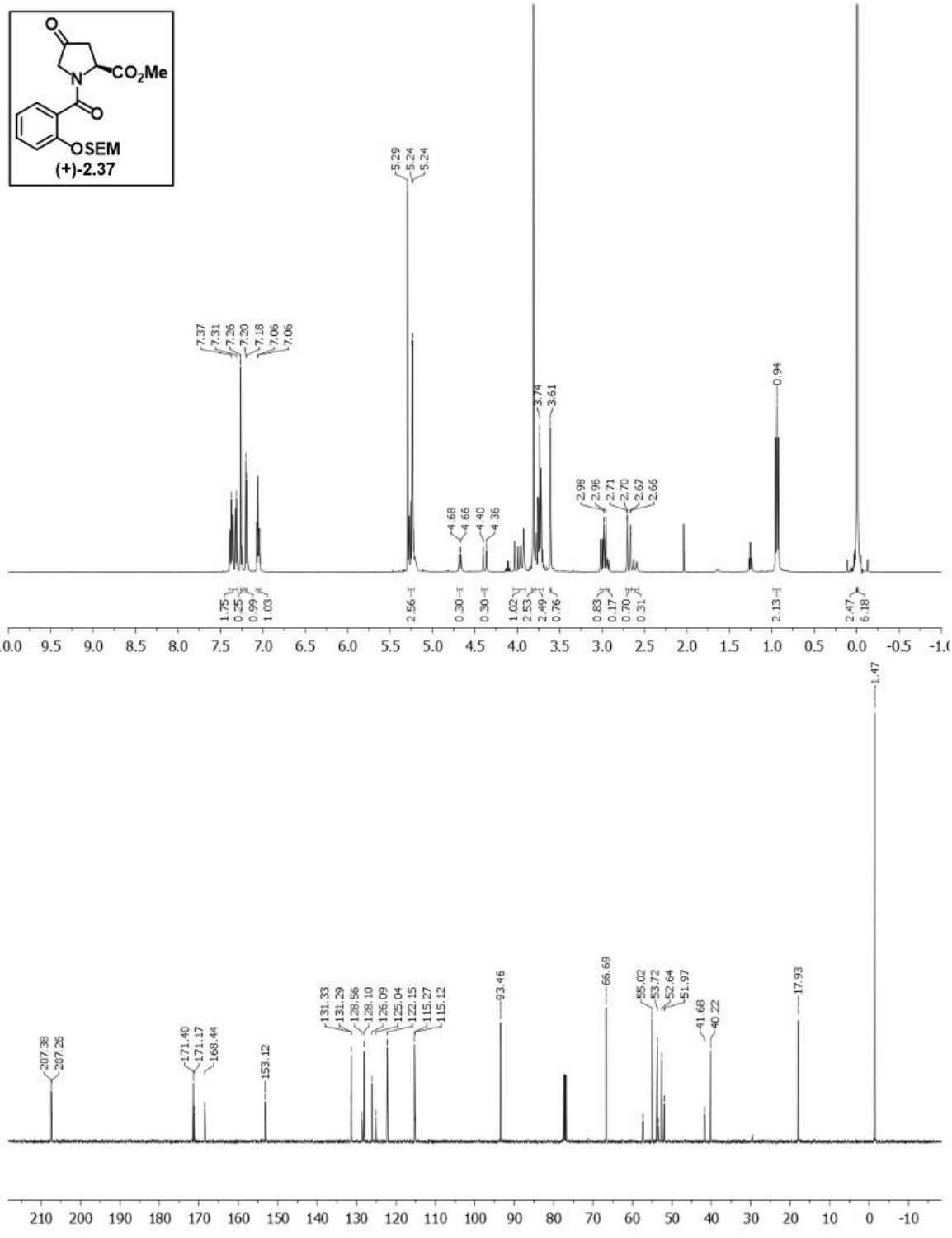
O
N
CO2Me
O
OSEM
(+)-2.37
7.37
7.31
7.26
7.20
7.18
7.06
7.06
5.29
5.24
5.24
4.68
4.66
4.40
4.36
3.74
3.61
2.98
2.96
2.71
2.70
2.67
2.66
0.94
1.75
0.25
0.99
1.03
2.56
0.30
0.30
1.02
2.53
2.49
0.76
0.83
0.17
0.70
0.31
2.13
2.47
6.18
1.47
207.38
207.26
171.40
171.17
168.44
153.12
131.33
131.29
128.56
128.10
126.09
125.04
122.15
115.27
115.12
93.46
66.69
55.02
53.72
52.64
51.97
41.68
40.22
17.93

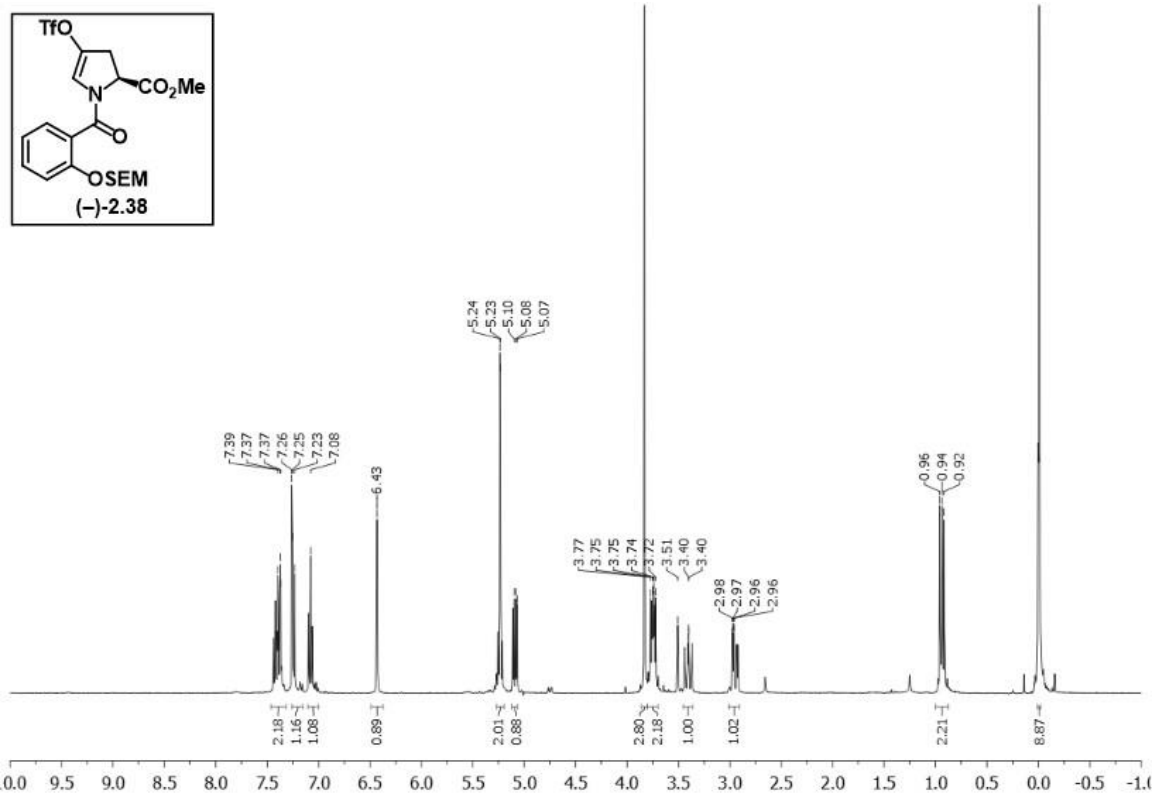
TfO
CO2Me
N
O
OSEM
(–)-2.38
7.39
7.37
7.37
7.26
7.25
7.23
7.08
6.43
5.24
5.23
5.10
5.08
5.07
3.77
3.75
3.75
3.74
3.72
3.51
3.40
3.40
2.98
2.97
2.96
2.96
0.96
0.94
0.92
2.18
1.16
1.08
0.89
2.01
0.88
2.80
2.18
1.00
1.02
2.21
8.87

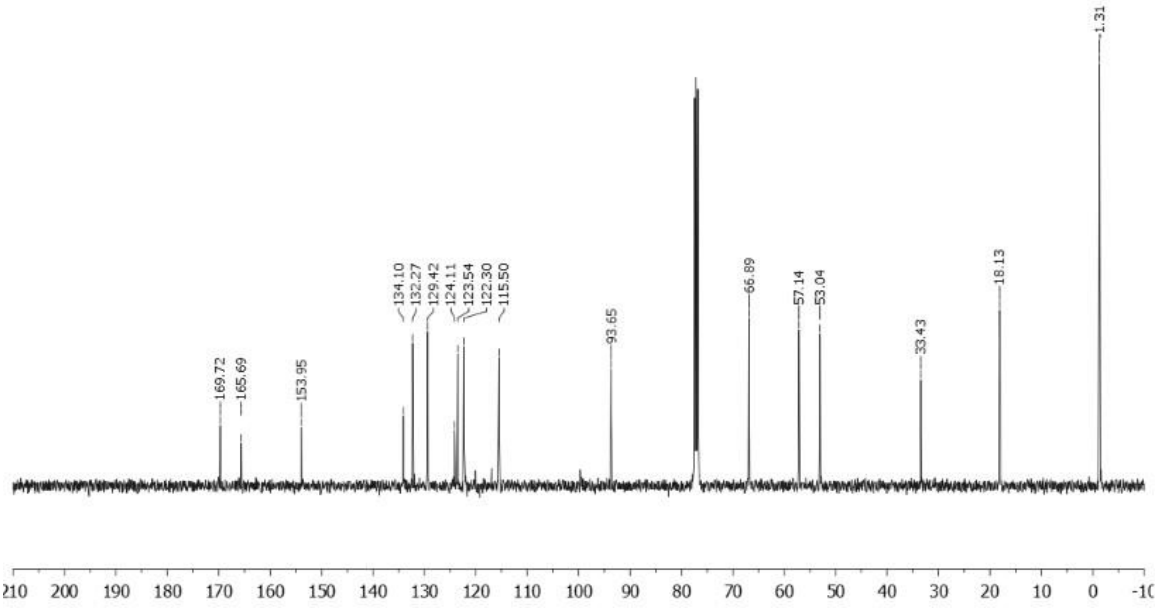
169.72
165.69
153.95
134.10
132.27
129.42
124.11
123.54
122.30
115.50
93.65
66.89
57.14
53.04
33.43
18.13
1.31

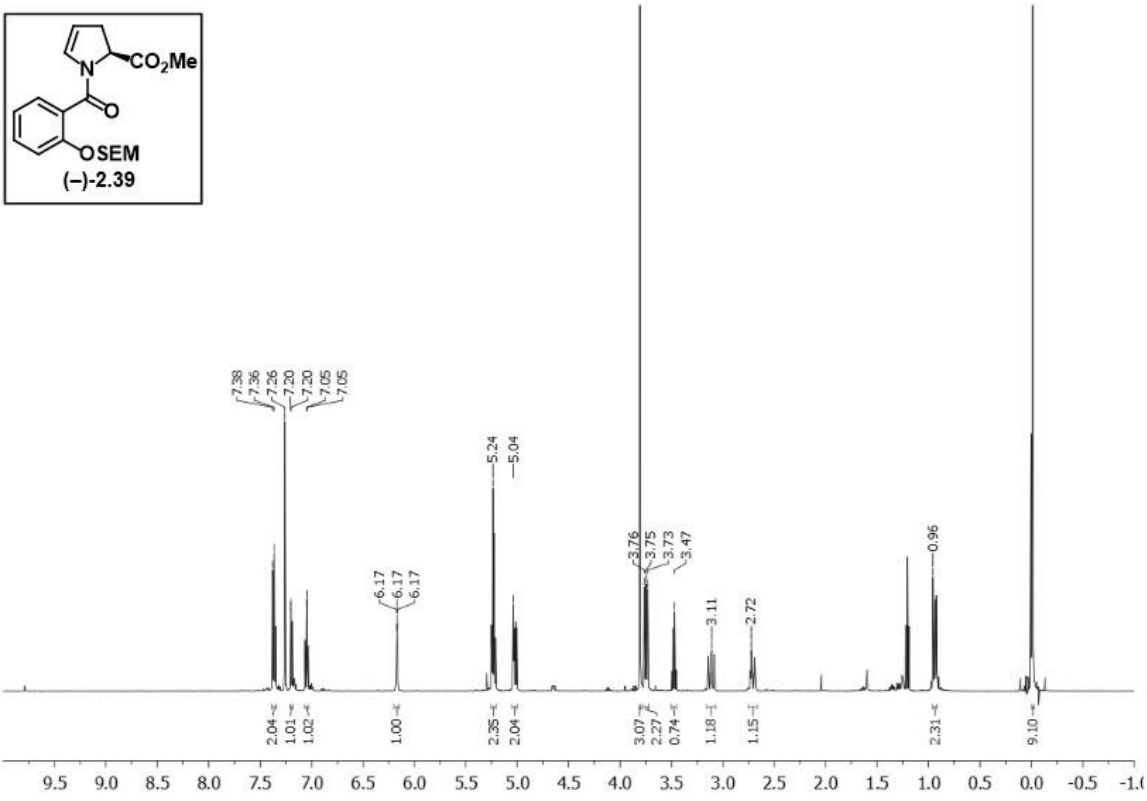
CO2Me
N
O
OSEM
(–)-2.39
7.38
7.36
7.26
7.20
7.20
7.05
7.05
6.17
6.17
6.17
5.24
5.04
3.76
3.75
3.73
3.47
3.11
2.72
0.96
2.04
1.01
1.02
1.00
2.35
2.04
3.07
2.27
0.74
1.18
1.15
2.31
9.10

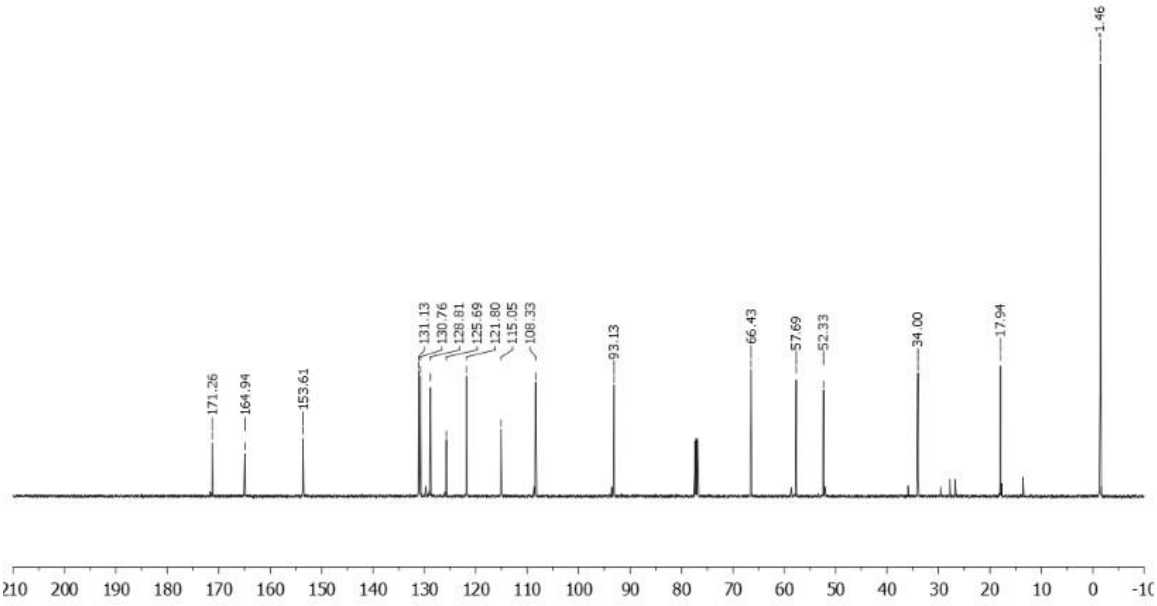
171.26
164.94
153.61
131.13
130.76
128.81
125.69
121.80
115.05
108.33
93.13
66.43
57.69
52.33
34.00
17.94
1.46

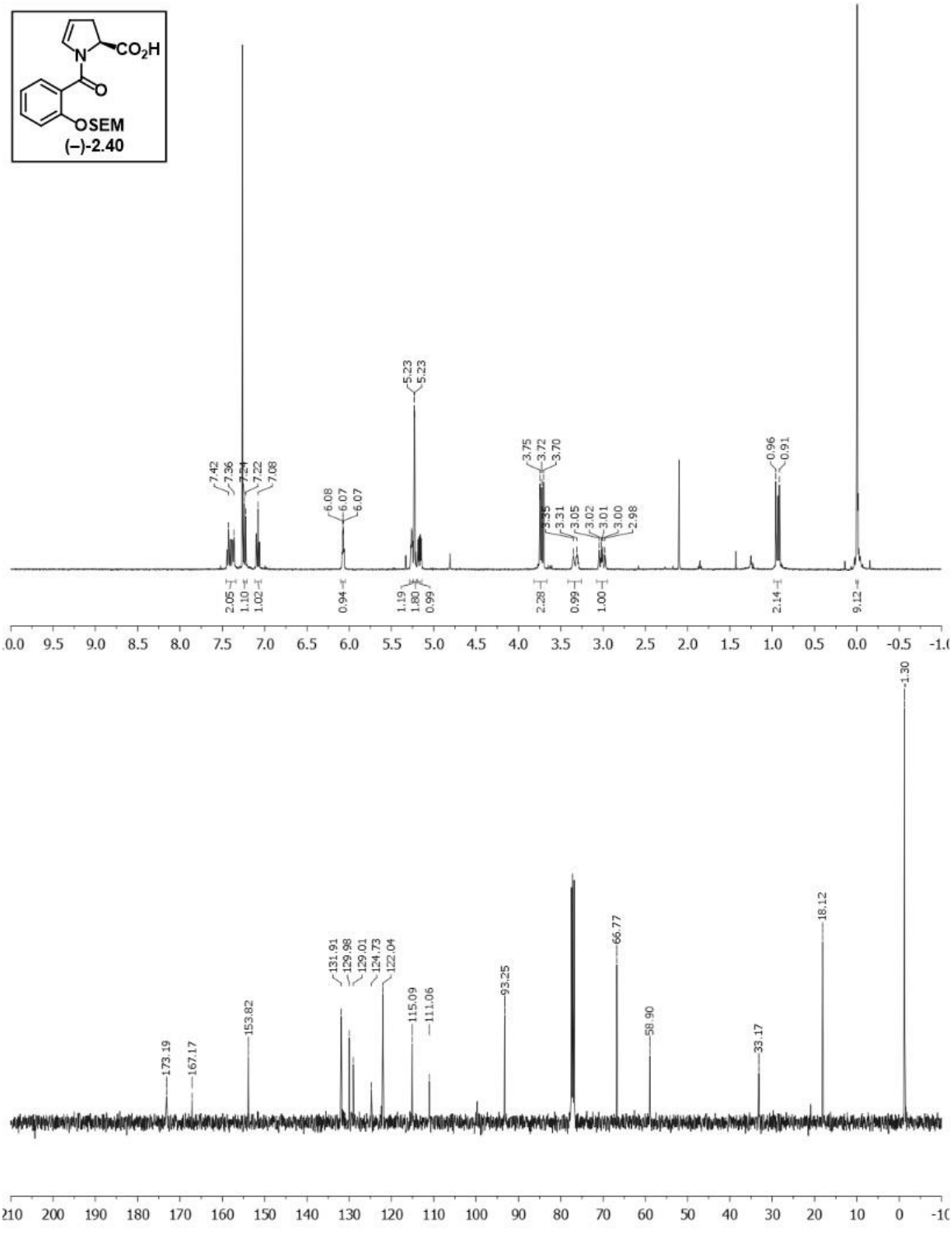
CO2H
N
O
OSEM
(–)-2.40
7.42
7.36
7.24
7.22
7.08
6.08
6.07
6.07
5.23
5.23
3.75
3.72
3.70
3.35
3.31
3.05
3.02
3.01
3.00
2.98
0.96
0.91
2.05
1.10
1.02
0.94
1.19
1.80
0.99
2.28
0.99
1.00
2.14
9.12
131.91
129.98
129.01
124.73
122.04
115.09
111.06
93.25
66.77
58.90
33.17
18.12
1.30
173.19
167.17
153.82

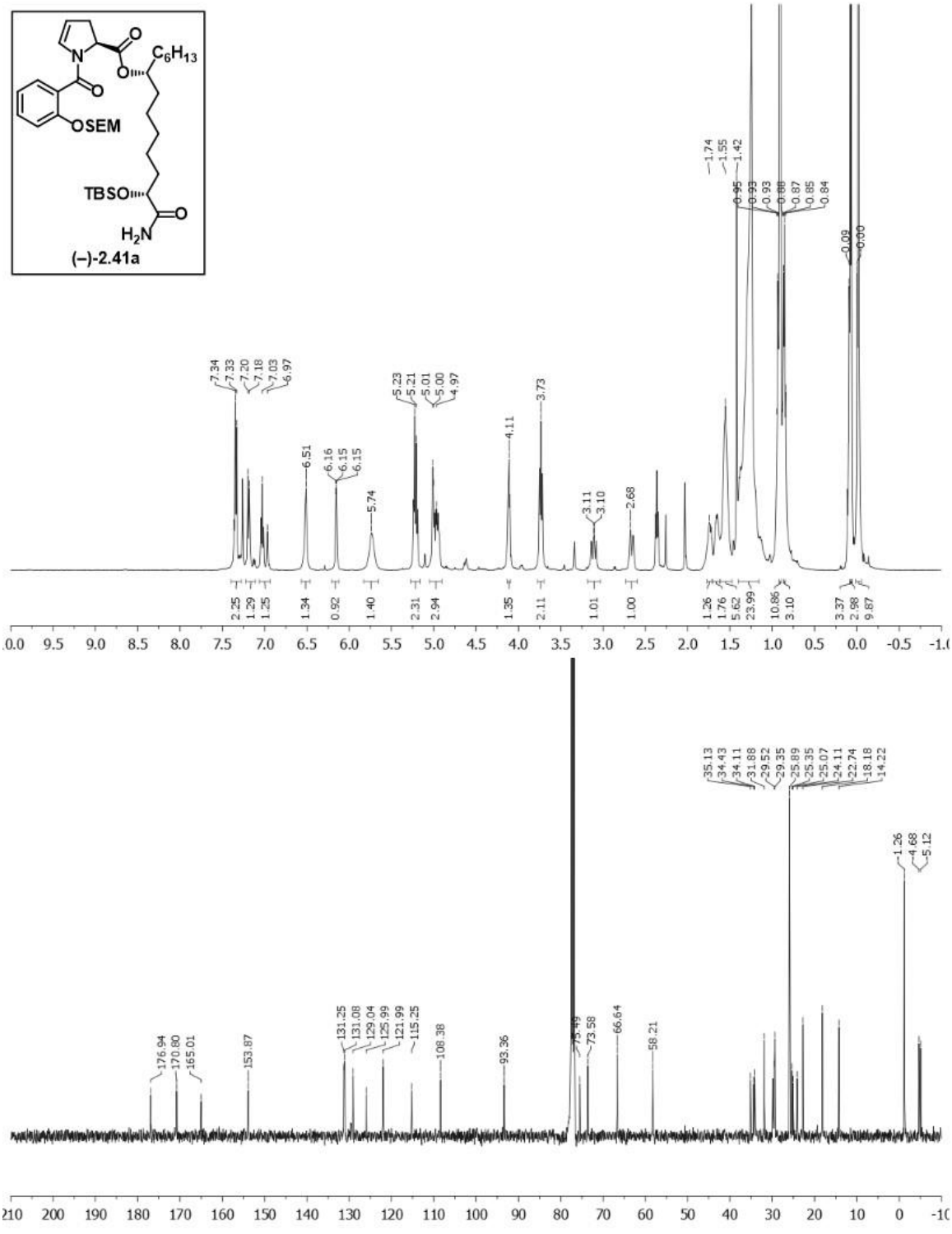
OSEM
TBSO
C_6H_{13}
H_2N
(–)-2.41a
7.34
7.33
7.20
7.18
7.03
6.97
6.51
6.16
6.15
6.15
5.74
5.23
5.21
5.01
5.00
4.97
4.11
3.73
3.11
3.10
2.68
1.74
1.55
1.42
0.95
0.93
0.93
0.88
0.87
0.85
0.84
0.09
0.00
2.25
1.29
1.25
1.34
0.92
1.40
2.31
2.94
1.35
2.11
1.01
1.00
1.26
1.76
5.62
23.99
10.86
3.10
3.37
2.98
9.87
176.94
170.80
165.01
153.87
131.25
131.08
129.04
125.99
121.99
115.25
108.38
93.36
73.58
66.64
58.21
35.13
34.43
34.11
31.88
29.52
29.35
25.89
25.35
25.07
24.11
22.74
18.18
14.22
1.26
4.68
5.12

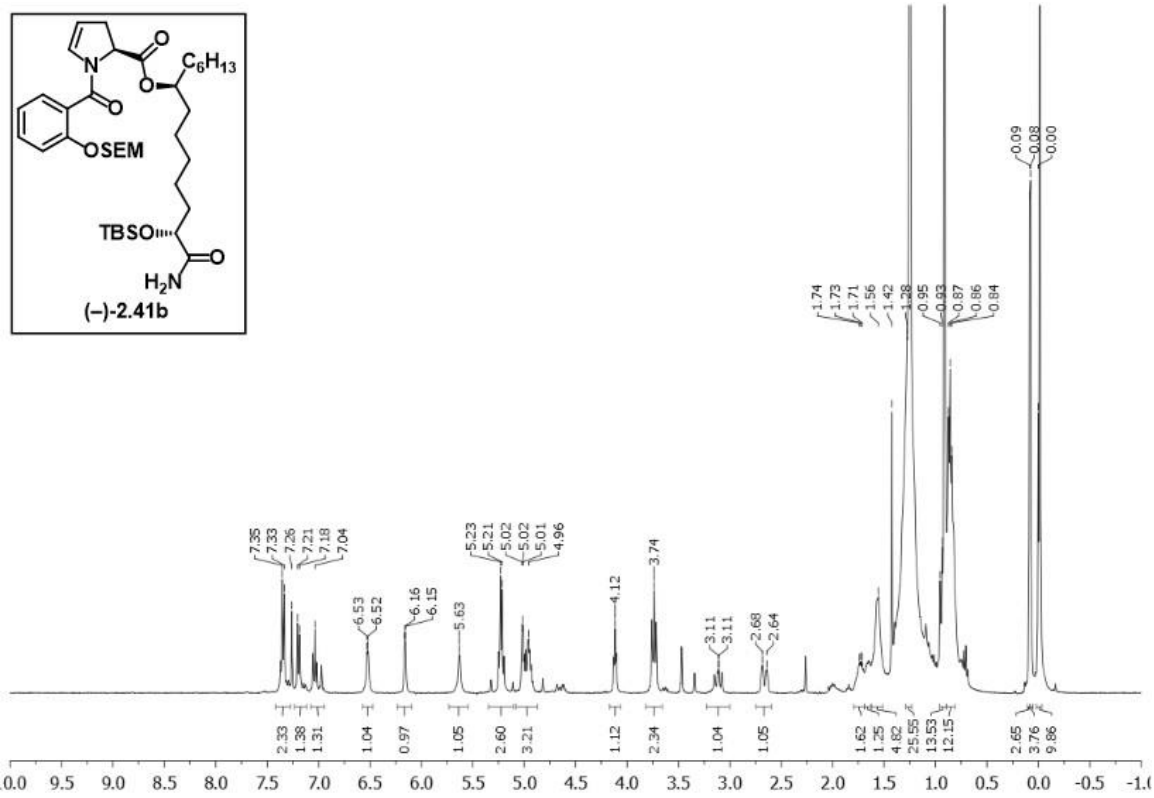
C6H13
OSEM
TBSO
H2N
(–)-2.41b

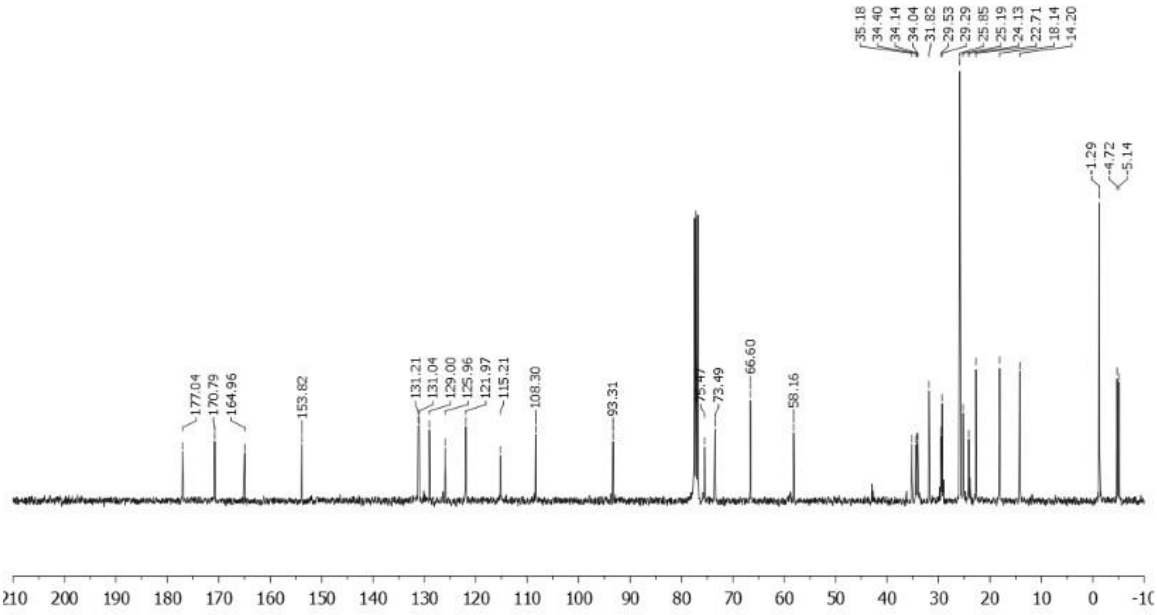

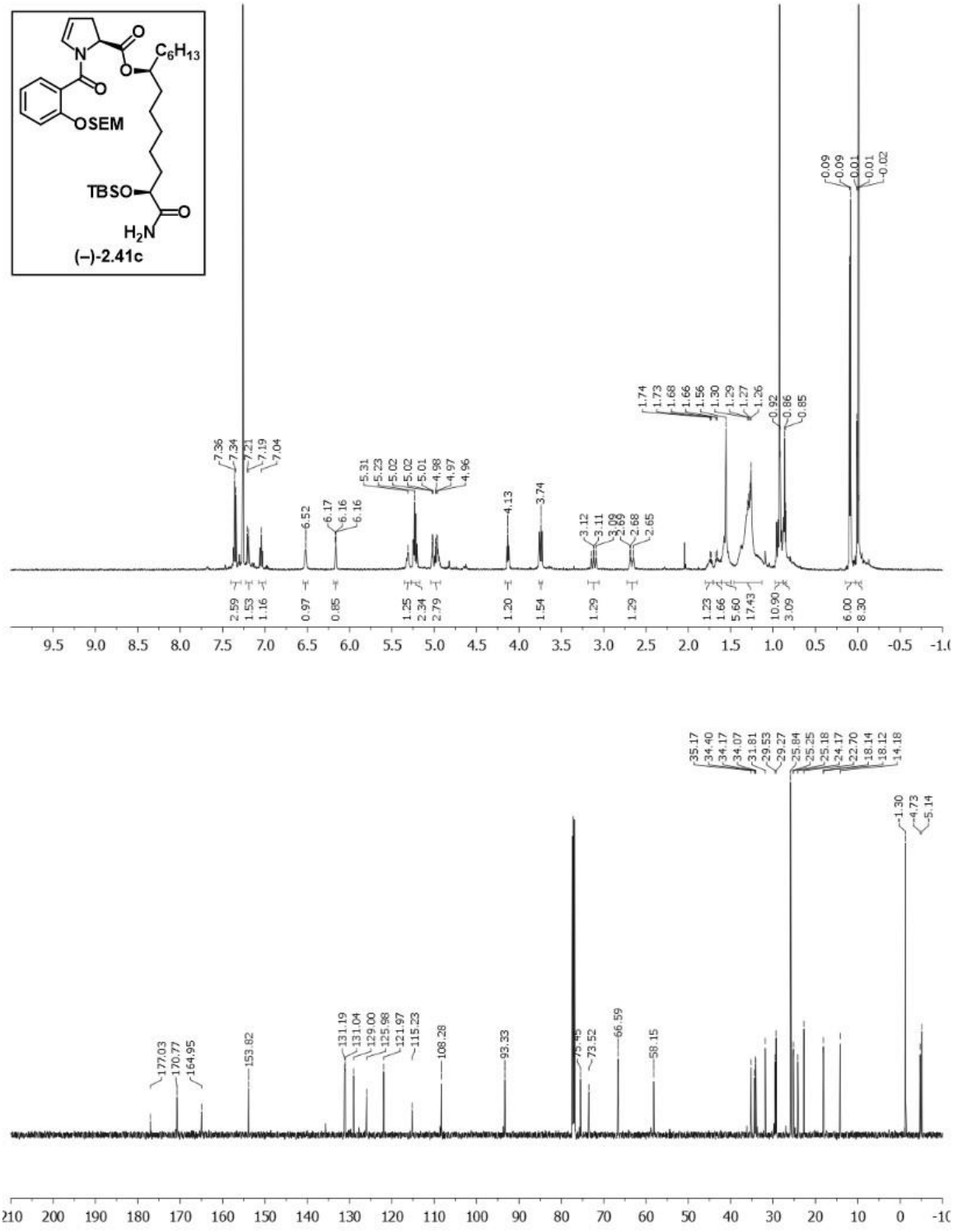
C6H13
OSEM
TBSO
H2N
(–)-2.41c

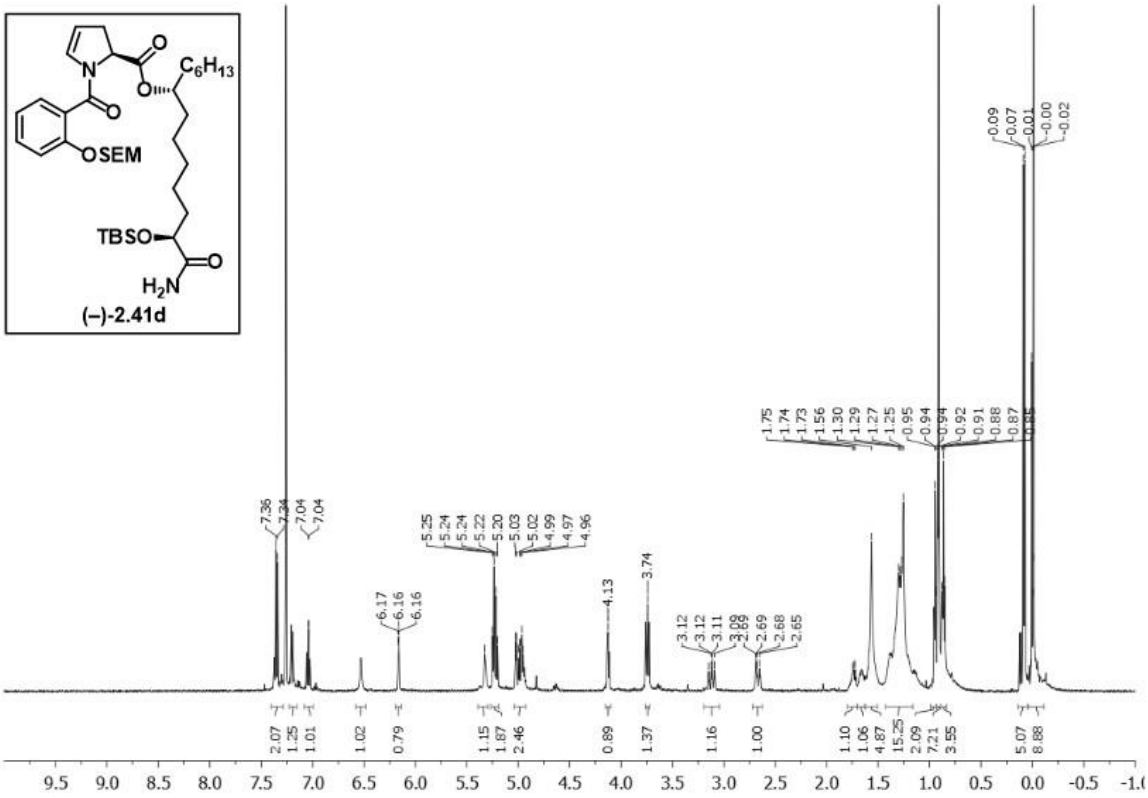
C6H13
OSEM
TBSO
H2N
(–)-2.41d

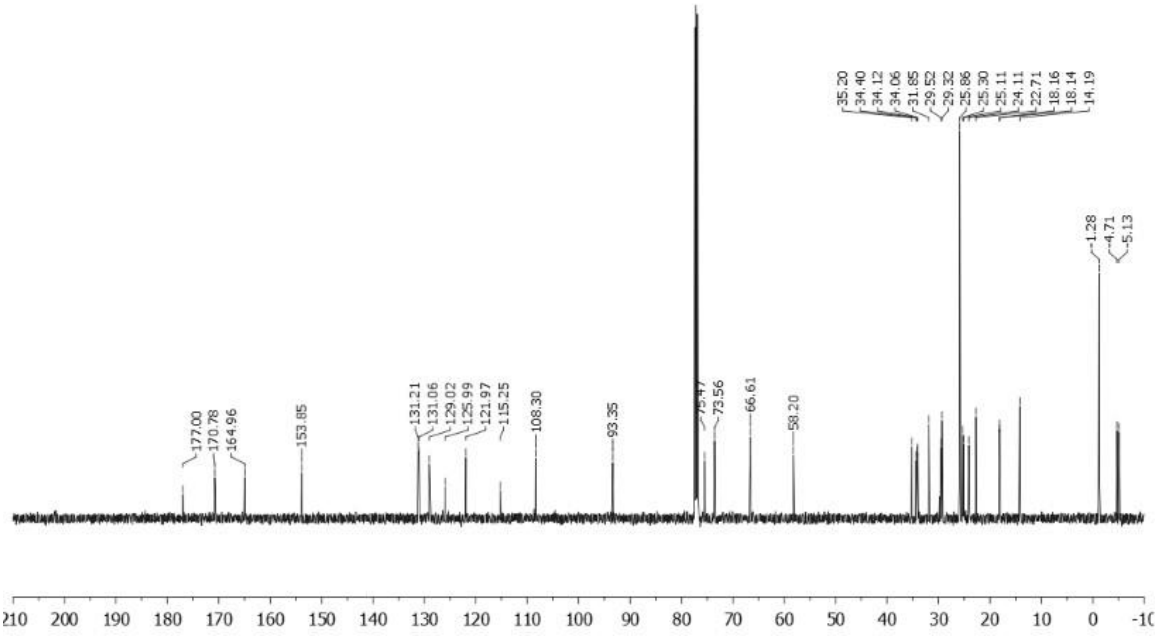

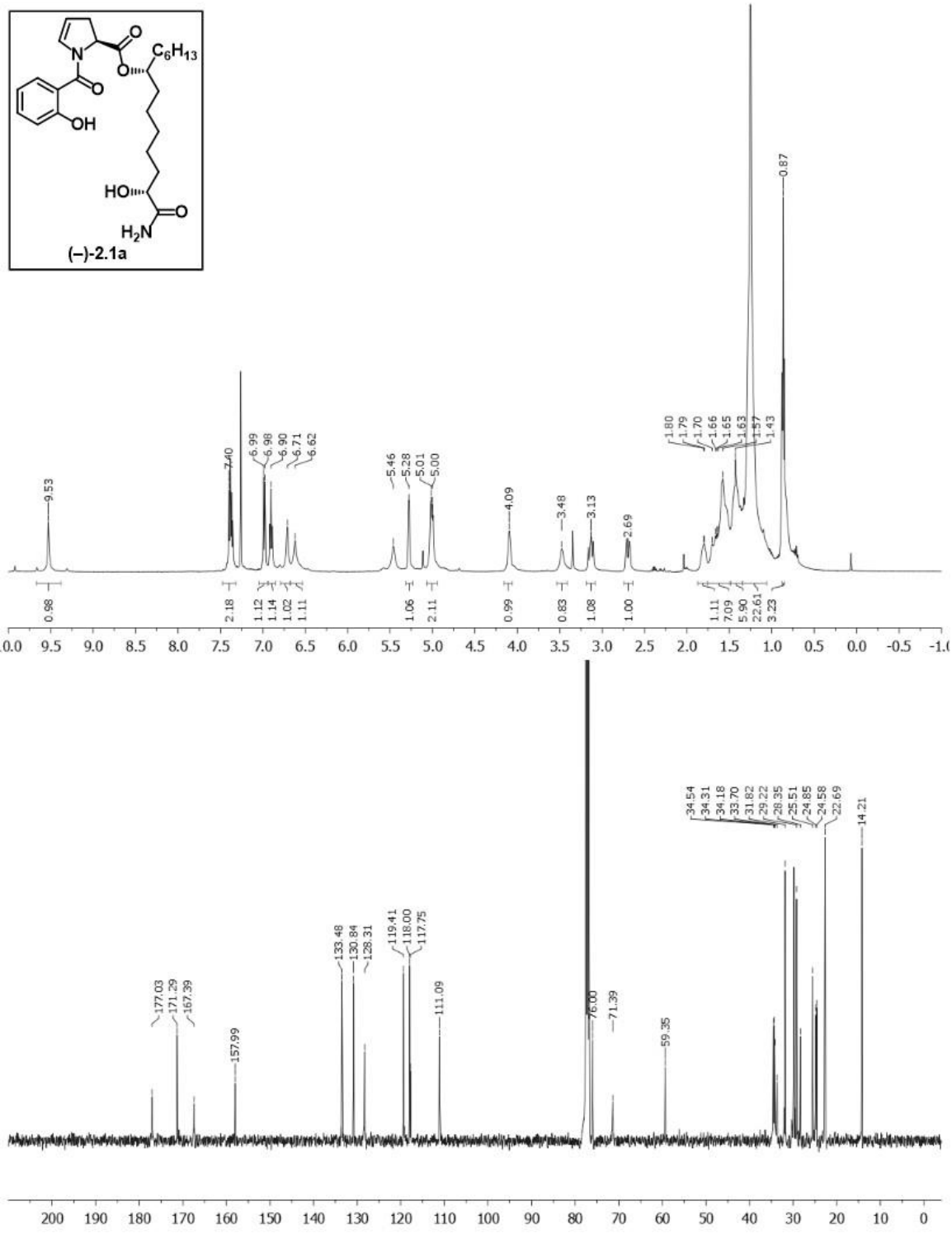
(–)-2.1a
9.53
7.40
6.99
6.98
6.90
6.71
6.62
5.46
5.28
5.01
5.00
4.09
3.48
3.13
2.69
1.80
1.79
1.70
1.66
1.65
1.63
1.57
1.43
0.87
0.98
2.18
1.12
1.14
1.02
1.11
1.06
2.11
0.99
0.83
1.08
1.00
1.11
7.09
5.90
22.61
3.23
177.03
171.29
167.39
157.99
133.48
130.84
128.31
119.41
118.00
117.75
111.09
76.00
71.39
59.35
34.54
34.31
34.18
33.70
31.82
29.22
28.35
25.51
24.85
24.58
22.69
14.21

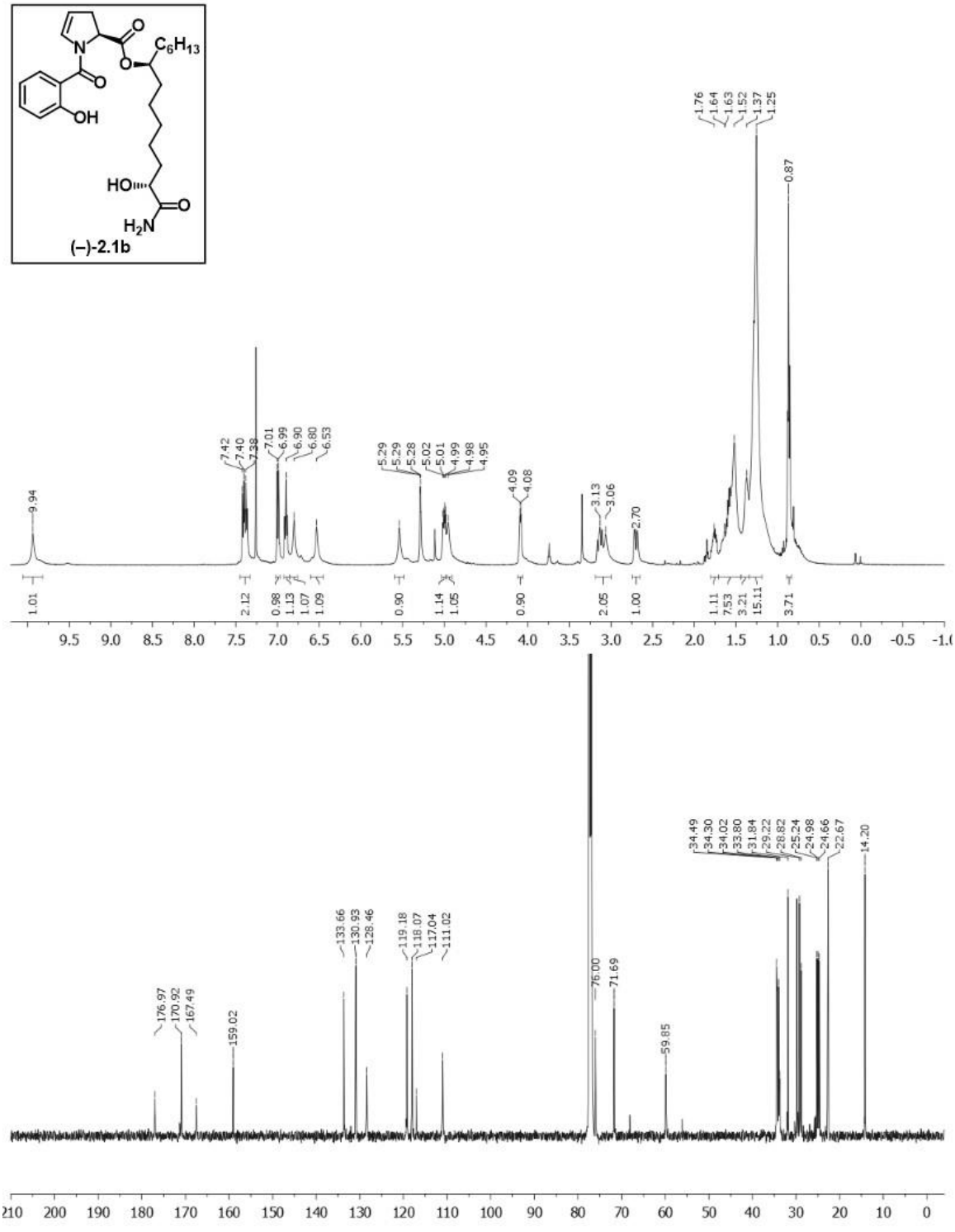
(–)-2.1b

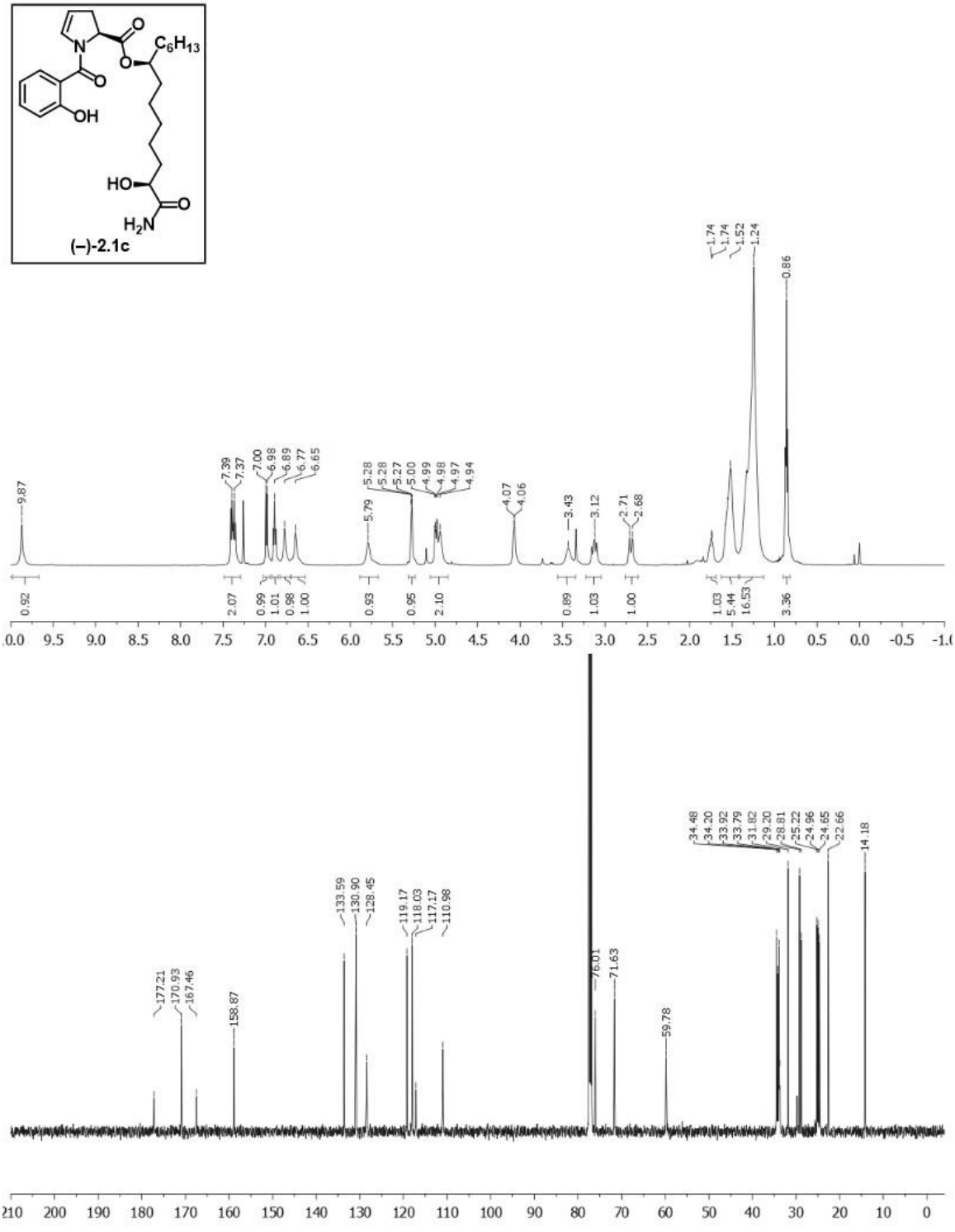
(–)-2.1c
9.87
7.39
7.37
7.00
6.98
6.89
6.77
6.65
5.79
5.28
5.28
5.27
5.00
4.99
4.98
4.97
4.94
4.07
4.06
3.43
3.12
2.71
2.68
1.74
1.74
1.52
1.24
0.86
177.21
170.93
167.46
158.87
133.59
130.90
128.45
119.17
118.03
117.17
110.98
76.01
71.63
59.78
34.48
34.20
33.92
33.79
31.82
29.20
28.81
25.22
24.96
24.65
22.66
14.18

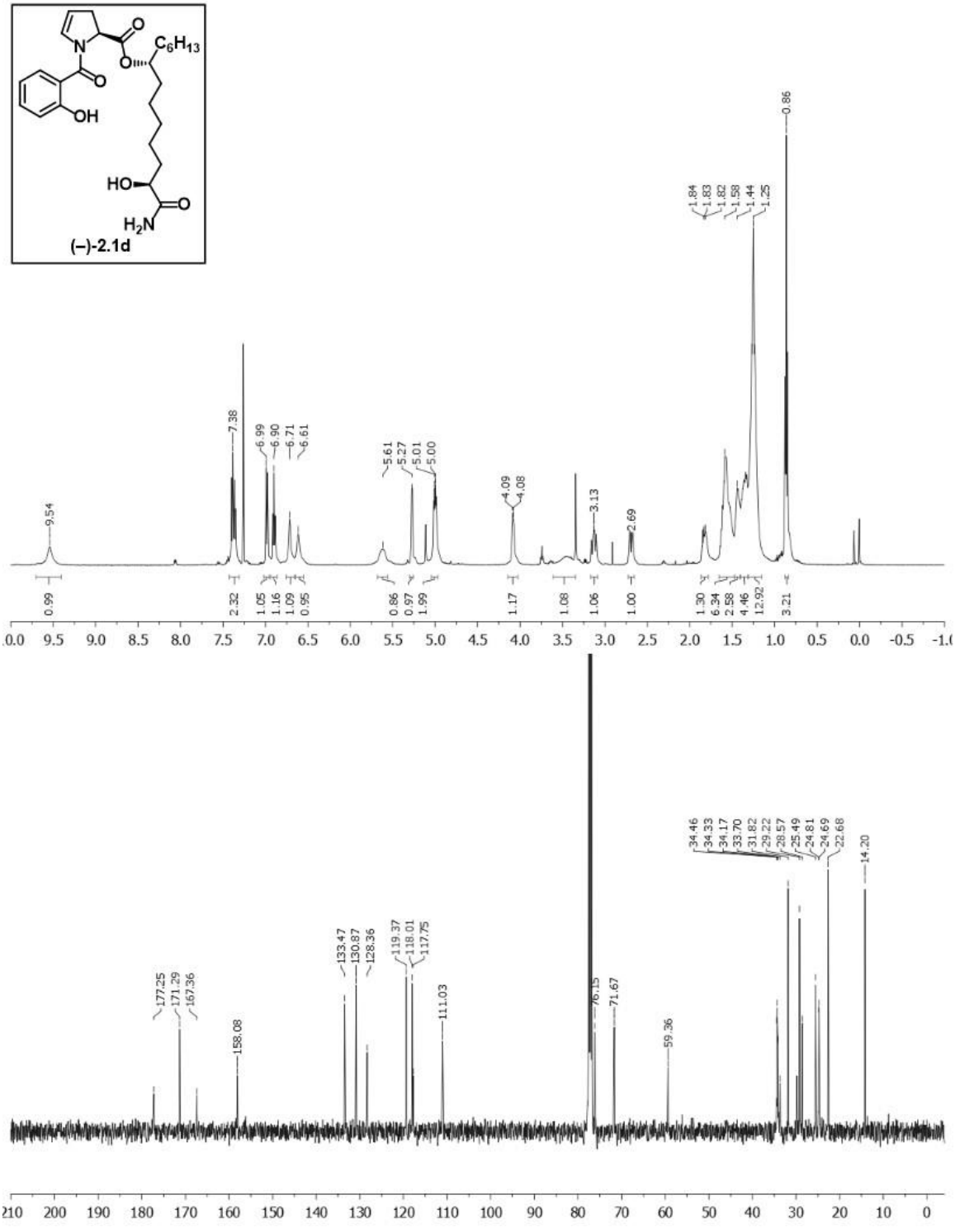
(–)-2.1d
9.54
7.38
6.99
6.90
6.71
6.61
5.61
5.27
5.01
5.00
4.09
4.08
3.13
2.69
1.84
1.83
1.82
1.58
1.44
1.25
0.86
177.25
171.29
167.36
158.08
133.47
130.87
128.36
119.37
118.01
117.75
111.03
76.15
71.67
59.36
34.46
34.33
34.17
33.70
31.82
29.22
28.57
25.49
24.81
24.69
22.68
14.20

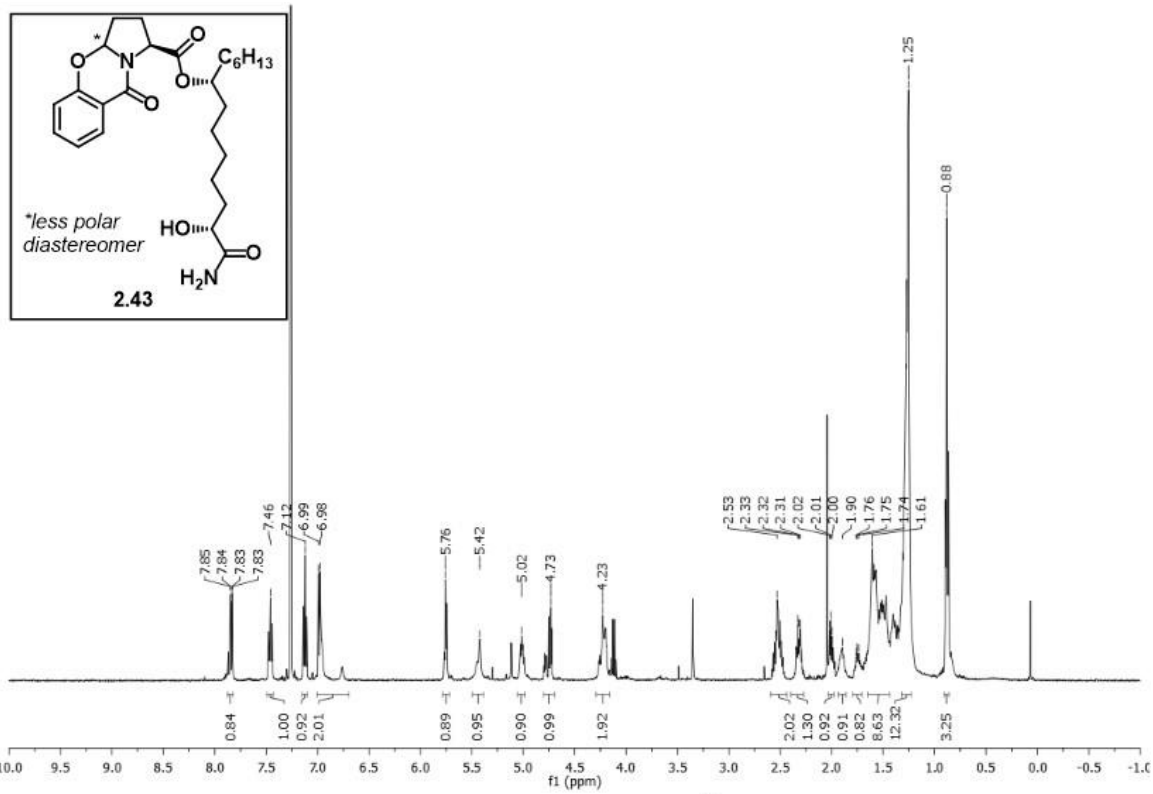
*less polar
diastereomer
2.43
f1 (ppm)

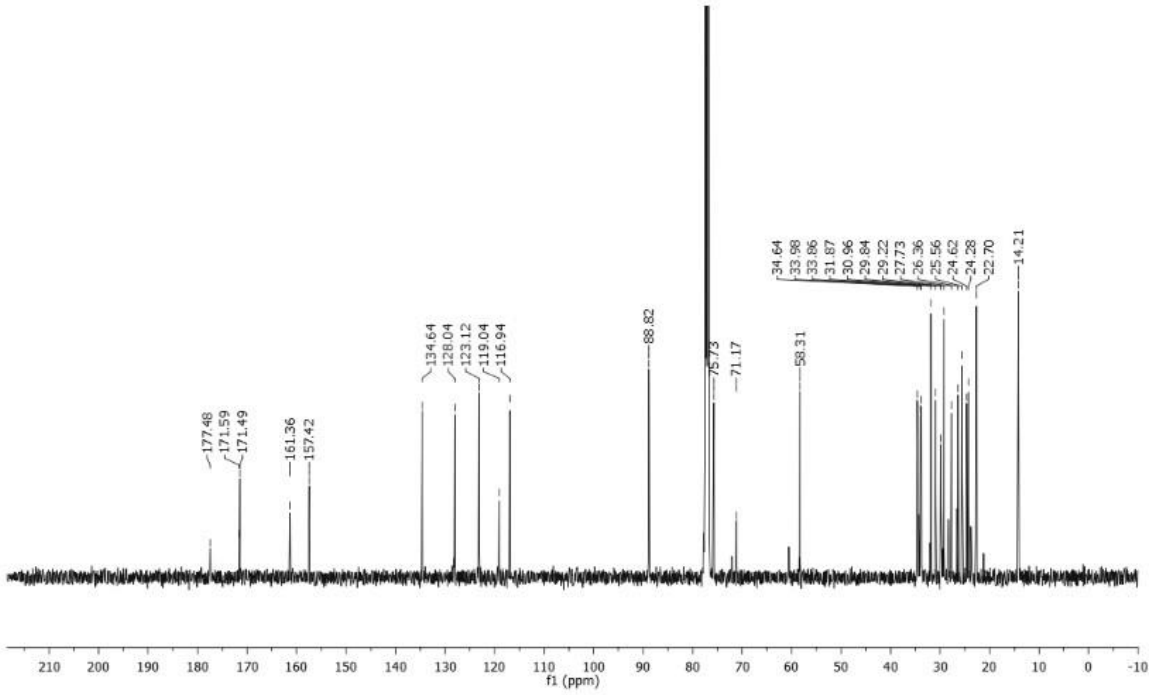
f1 (ppm)

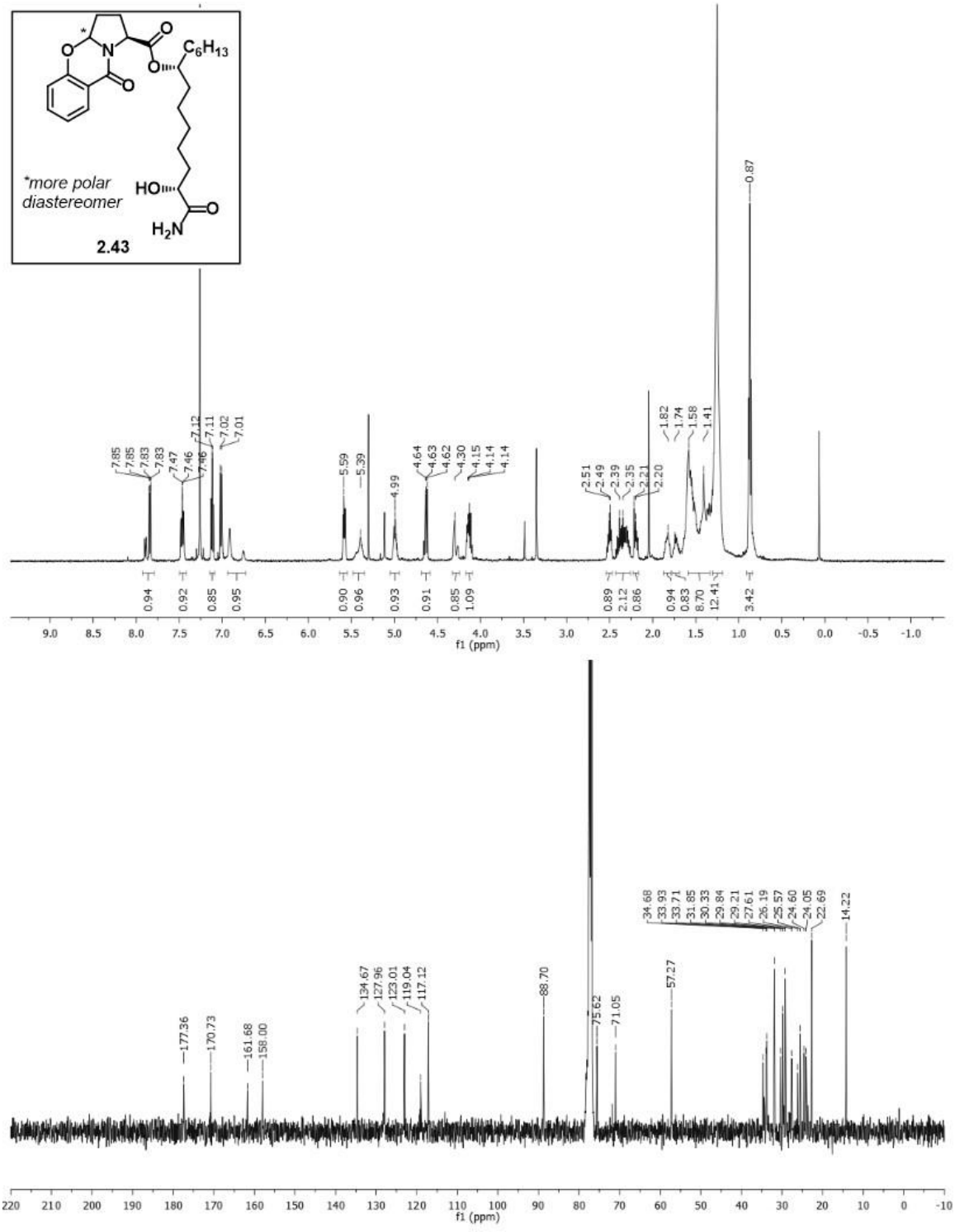
*more polar
diastereomer
2.43
f1 (ppm)
f1 (ppm)

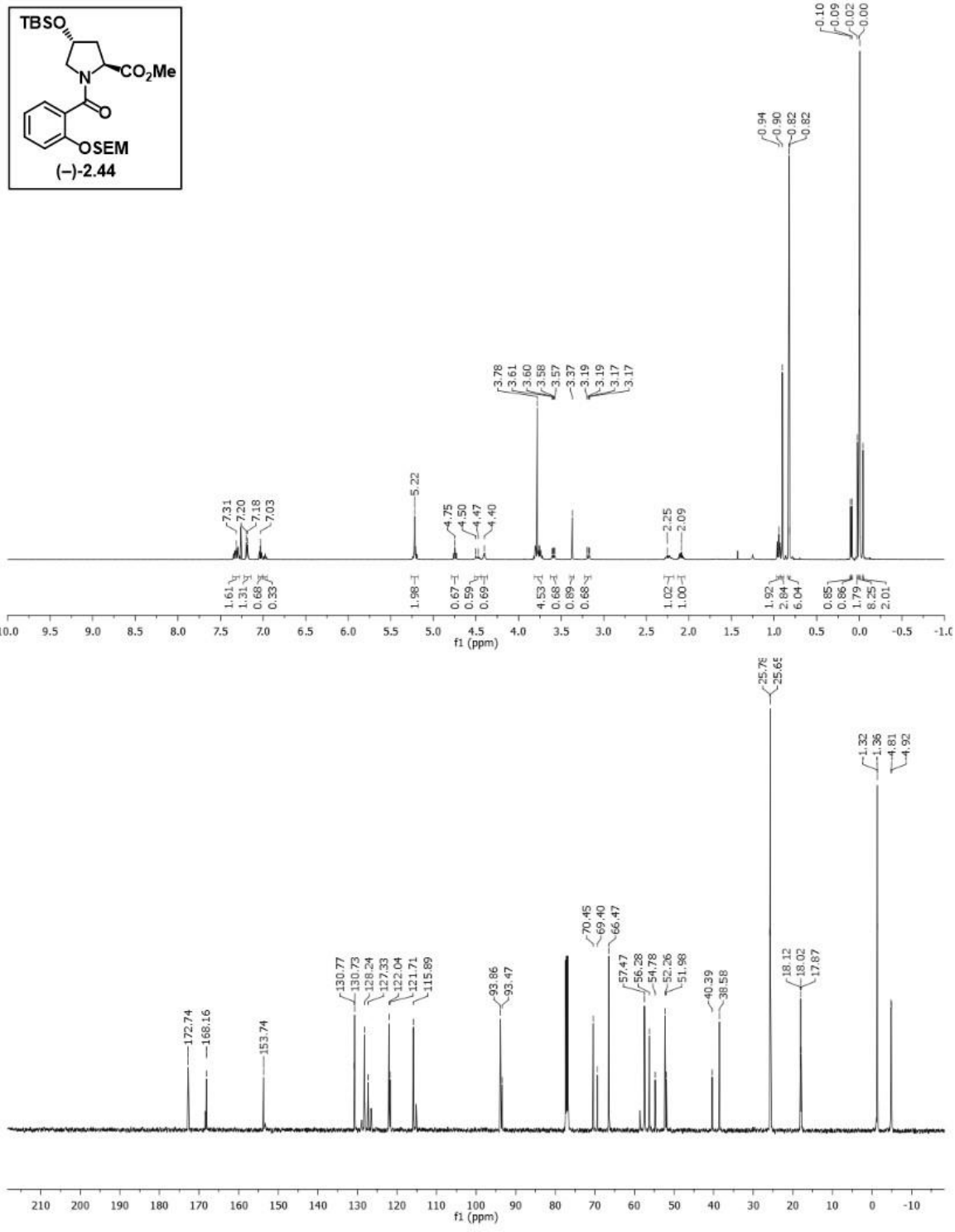
TBSO
CO2Me
N
O
OSEM
(–)-2.44
f1 (ppm)
f1 (ppm)

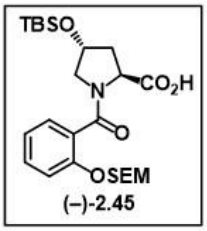
TBSO
CO2H
N
O
OSEM

(–)-2.45

0.03
0.01
0.06
0.93
0.91
0.82
7.38
7.31
7.29
7.23
7.21
7.05
5.22
4.87
4.36
3.75
3.48
3.47
3.24
2.48
2.20
1.03
1.18
1.18
1.21
1.08
2.32
1.05
1.07
1.02
1.04
1.00
1.23
3.36
9.38
2.94
9.38
3.10
f1 (ppm)

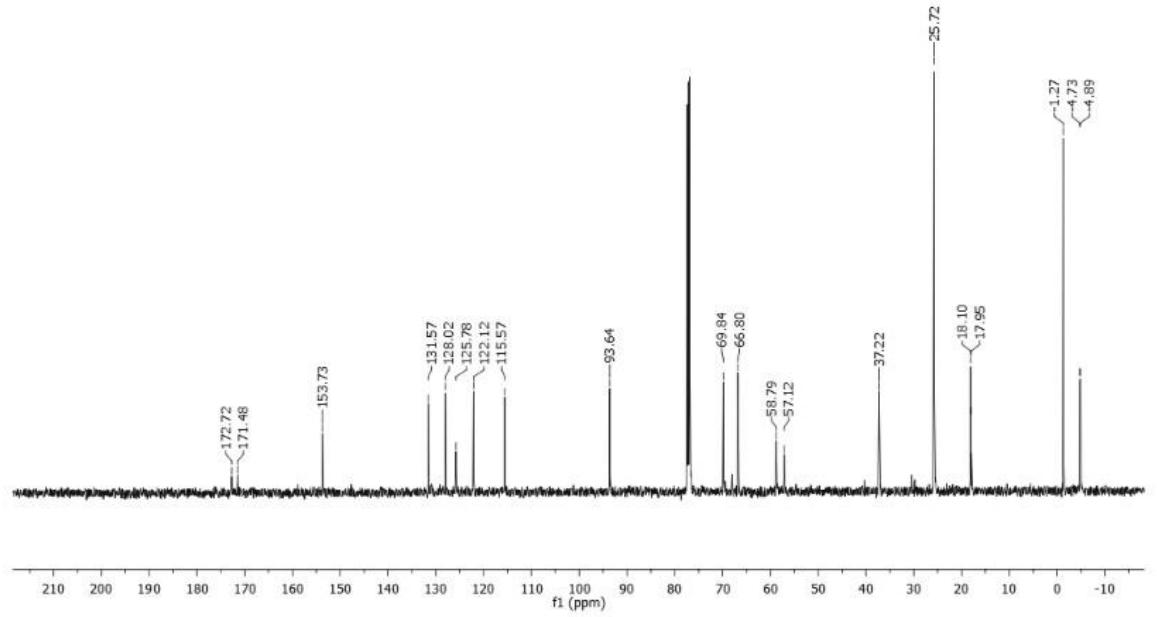
25.72
-1.27
-4.73
-4.89
172.72
171.48
153.73
131.57
128.02
125.78
122.12
115.57
93.64
69.84
66.80
58.79
57.12
37.22
18.10
17.95
f1 (ppm)

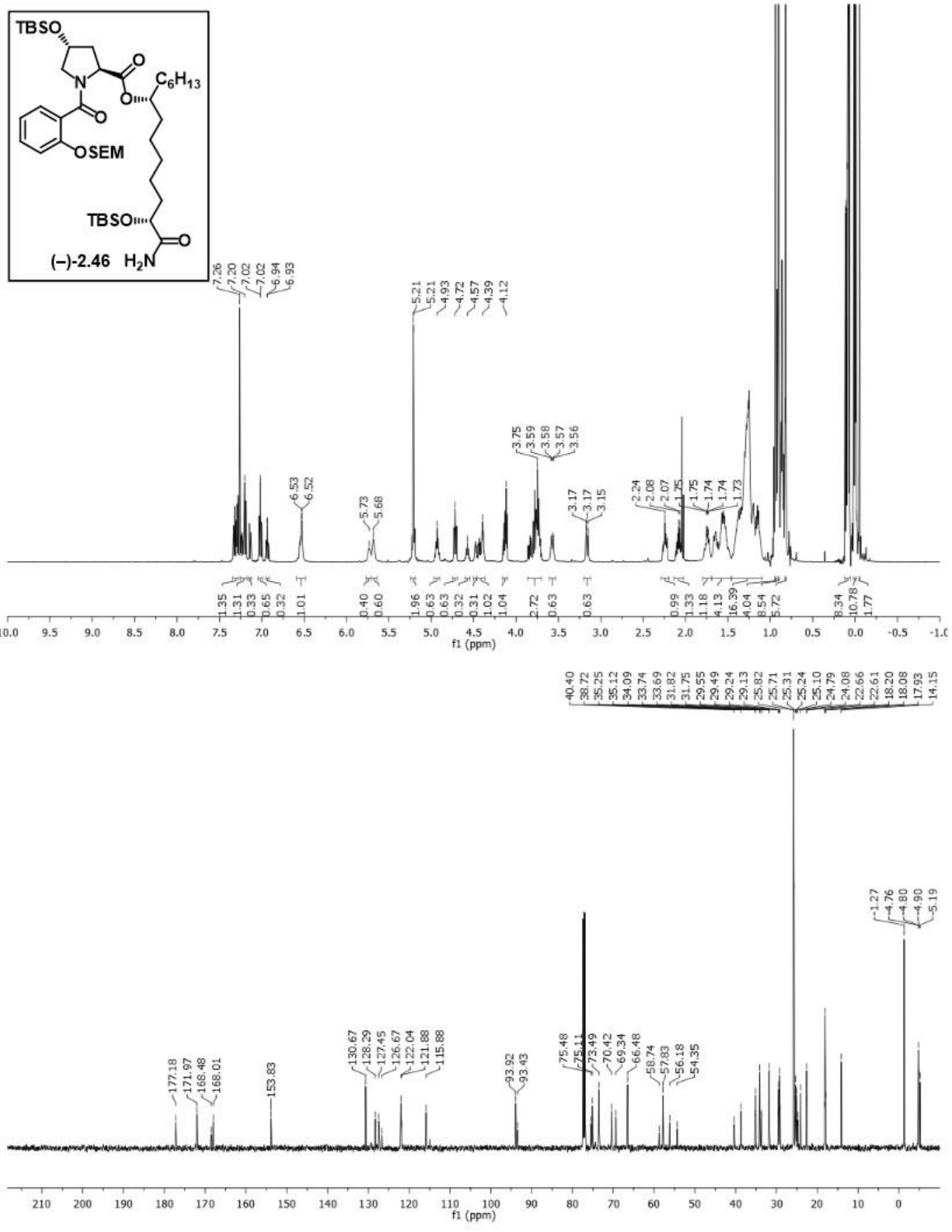
TBSO
N
O
O
C_6H_{13}
OSEM
TBSO
O
(–)-2.46 H_2N
f1 (ppm)
f1 (ppm)

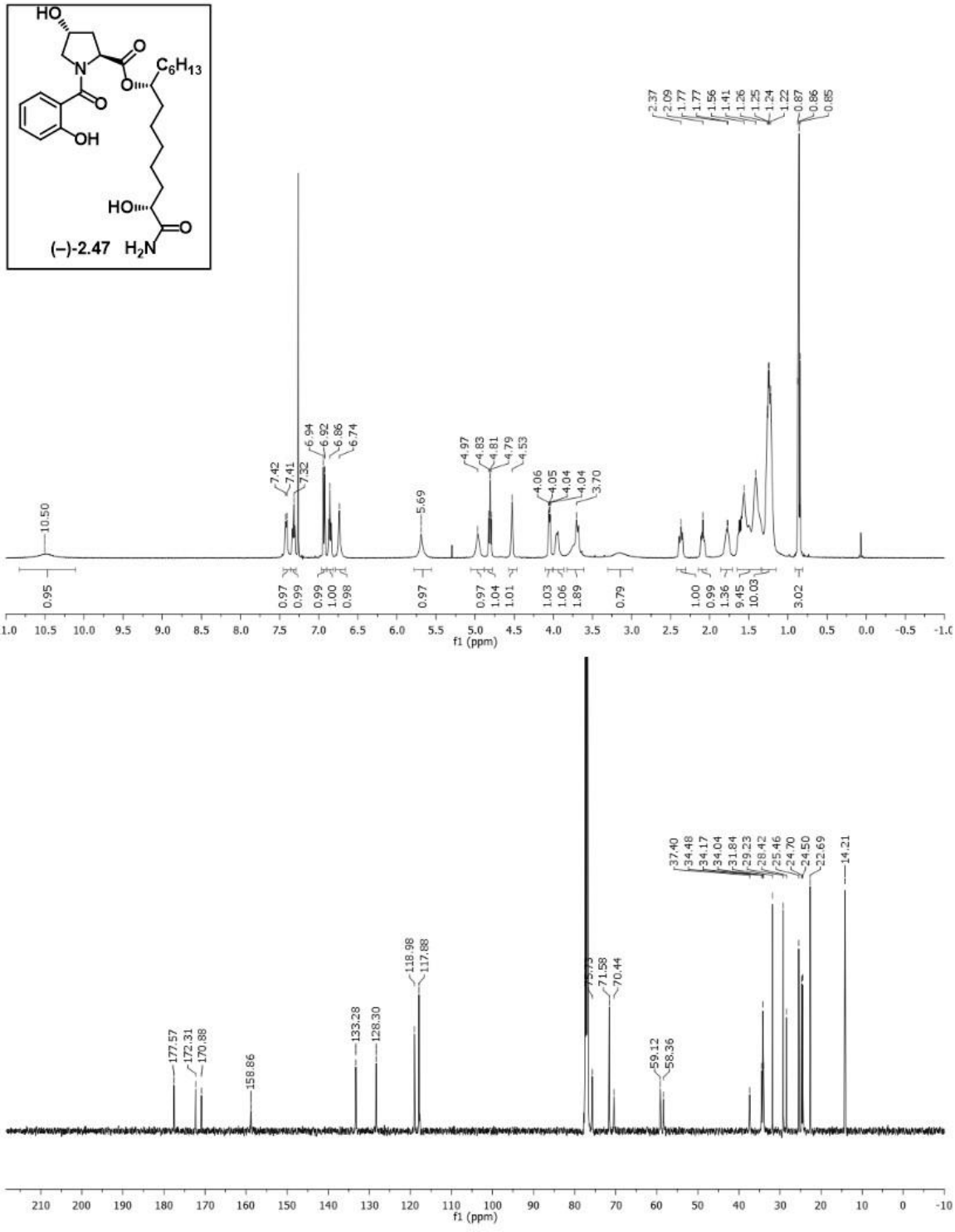
HO
O
N
O
C6H13
O
OH
HO
O
(–)-2.47 H2N
f1 (ppm)
f1 (ppm)

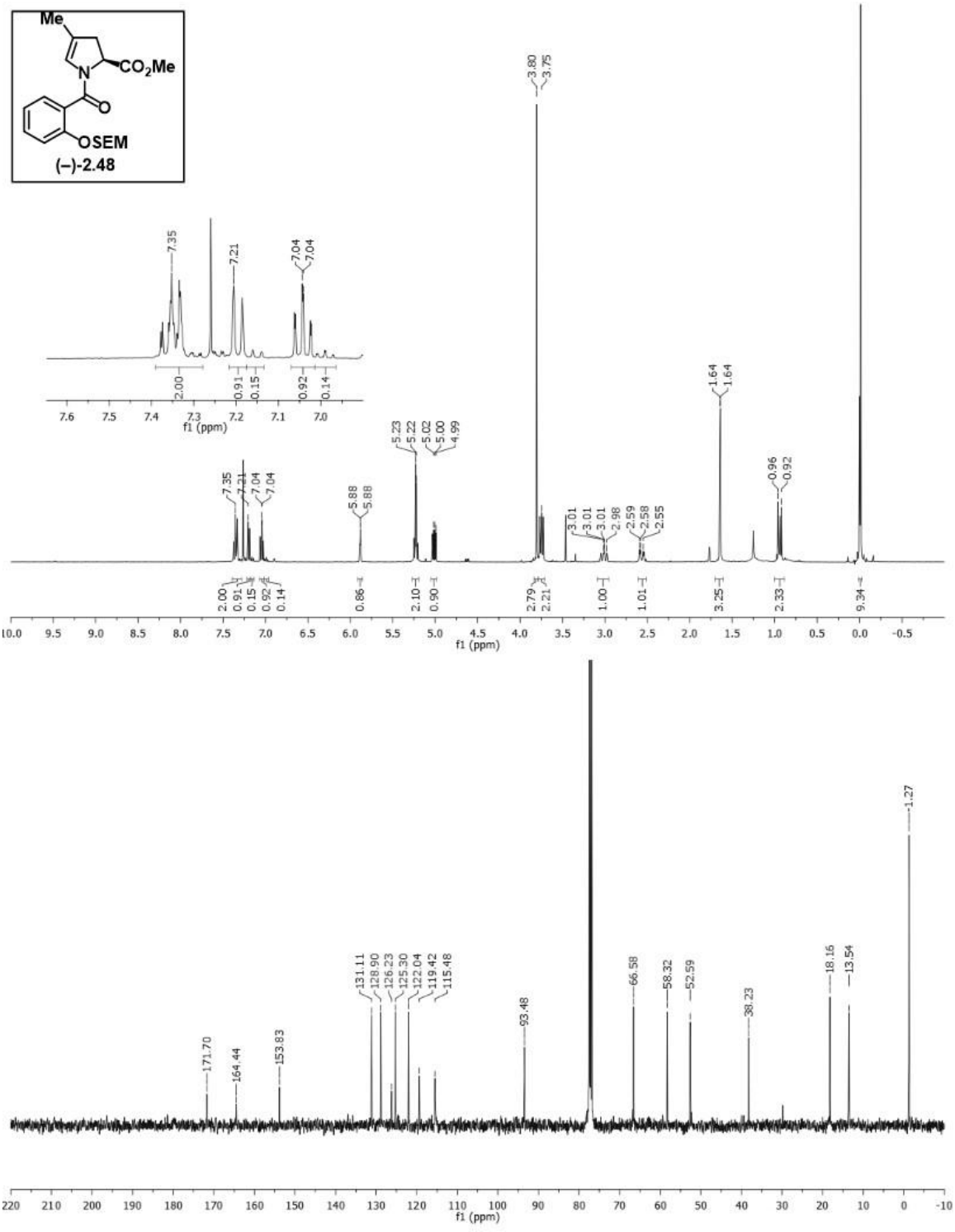
Me
CO2Me
N
O
OSEM
(–)-2.48
f1 (ppm)

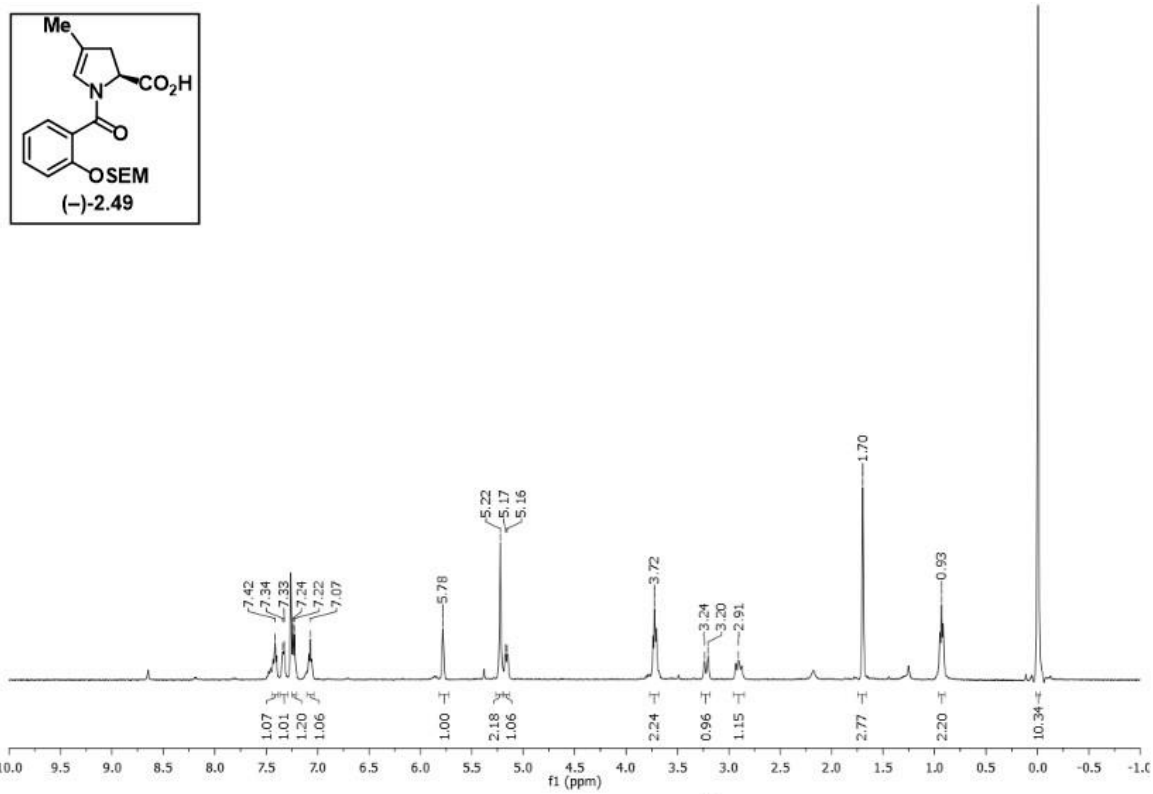
Me
CO2H
N
O
OSEM
(–)-2.49
7.42
7.34
7.33
7.24
7.22
7.07
5.78
5.22
5.17
5.16
3.72
3.24
3.20
2.91
1.70
0.93
1.07
1.01
1.20
1.06
1.00
2.18
1.06
2.24
0.96
1.15
2.77
2.20
10.34
f1 (ppm)

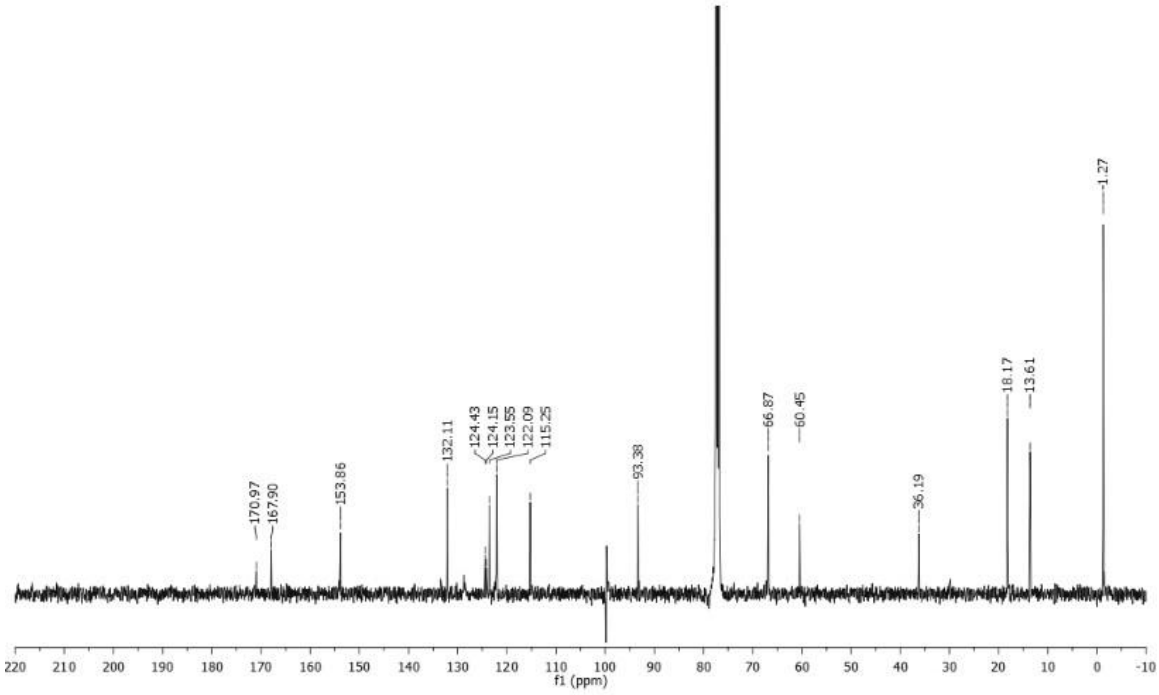
170.97
167.90
153.86
132.11
124.43
124.15
123.55
122.09
115.25
93.38
66.87
60.45
36.19
18.17
13.61
1.27
f1 (ppm)

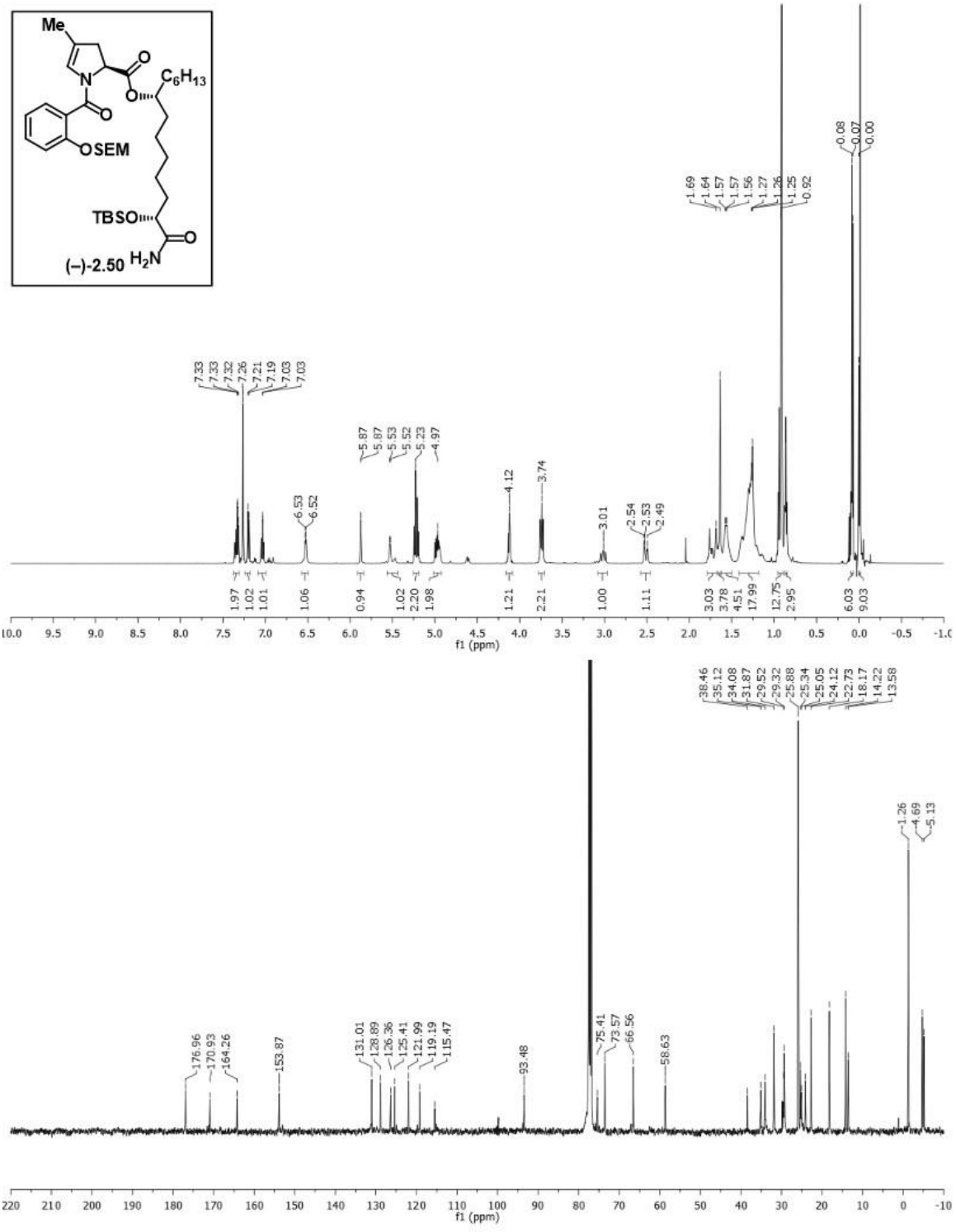
Me
C6H13
OSEM
TBSO
(–)-2.50 H2N
f1 (ppm)
f1 (ppm)

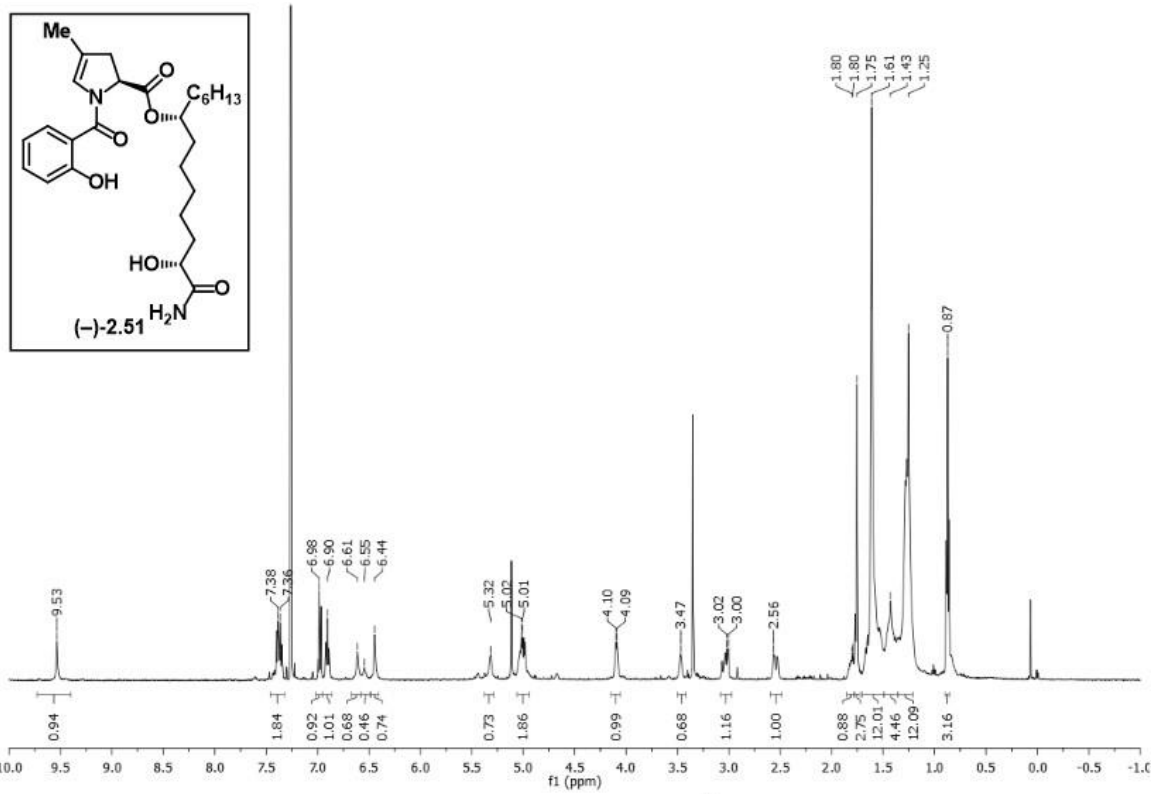
Me
O
N
O
C_6H_{13}
O
OH
HO
O
H_2N
(–)-2.51
9.53
7.38
7.36
6.98
6.90
6.61
6.55
6.44
5.32
5.02
5.01
4.10
4.09
3.47
3.02
3.00
2.56
1.80
1.80
1.75
1.61
1.43
1.25
0.87
0.94
1.84
0.92
1.01
0.68
0.46
0.74
0.73
1.86
0.99
0.68
1.16
1.00
0.88
2.75
12.01
4.46
12.09
3.16
f1 (ppm)

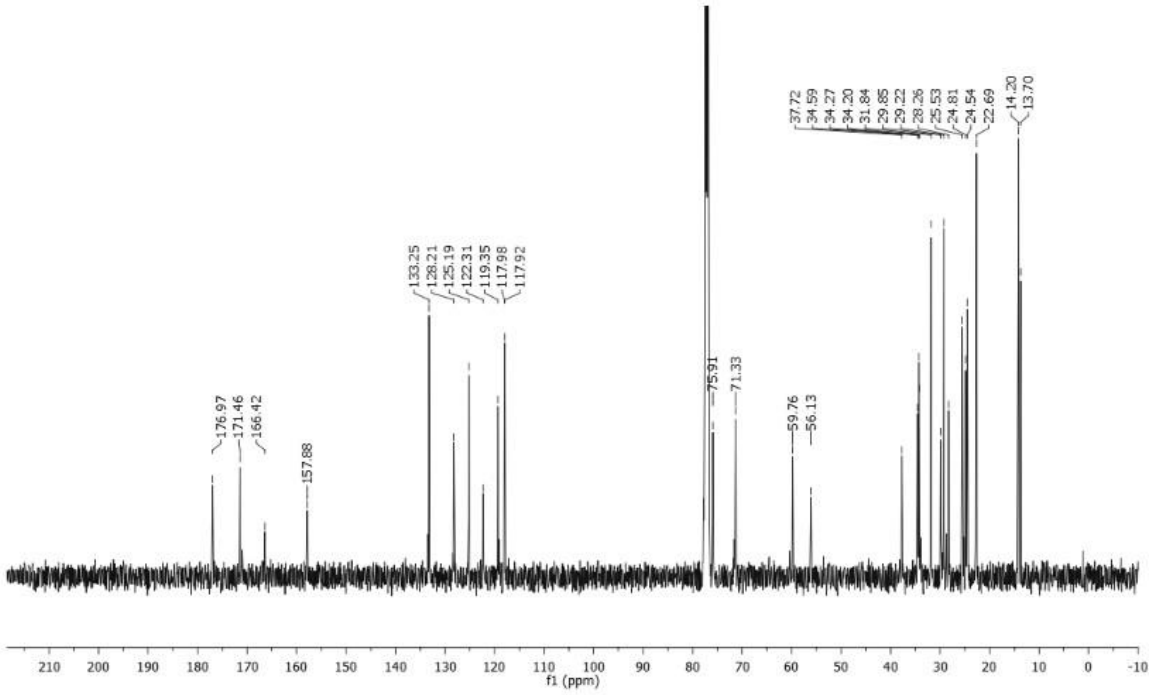
176.97
171.46
166.42
157.88
133.25
128.21
125.19
122.31
119.35
117.98
117.92
75.91
71.33
59.76
56.13
37.72
34.59
34.27
34.20
31.84
29.85
29.22
28.26
25.53
24.81
24.54
22.69
14.20
13.70
f1 (ppm)

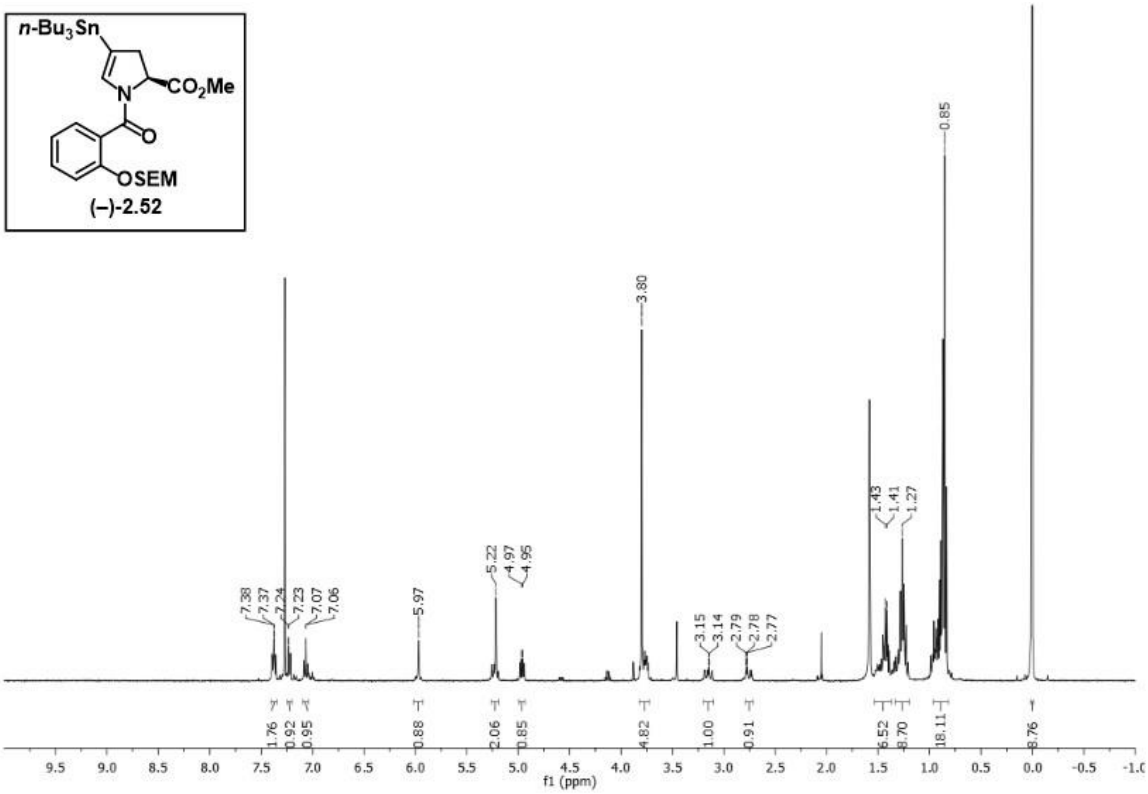
n-Bu3Sn
CO2Me
N
O
OSEM
(–)-2.52
7.38
7.37
7.24
7.23
7.07
7.06
5.97
5.22
4.97
4.95
3.80
3.15
3.14
2.79
2.78
2.77
1.43
1.41
1.27
0.85
1.76
0.92
0.95
0.88
2.06
0.85
4.82
1.00
0.91
6.52
8.70
18.11
8.76
f1 (ppm)

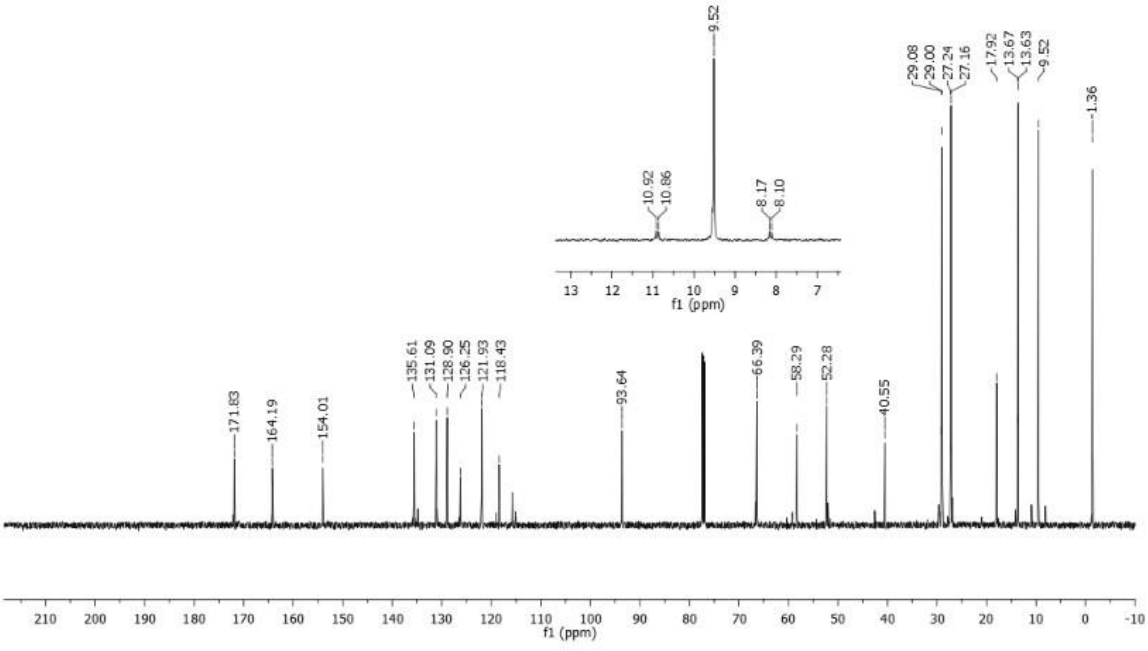
9.52
10.92
10.86
8.17
8.10
f1 (ppm)
29.08
29.00
27.24
27.16
17.92
13.67
13.63
9.52
1.36
171.83
164.19
154.01
135.61
131.09
128.90
126.25
121.93
118.43
93.64
66.39
58.29
52.28
40.55
f1 (ppm)

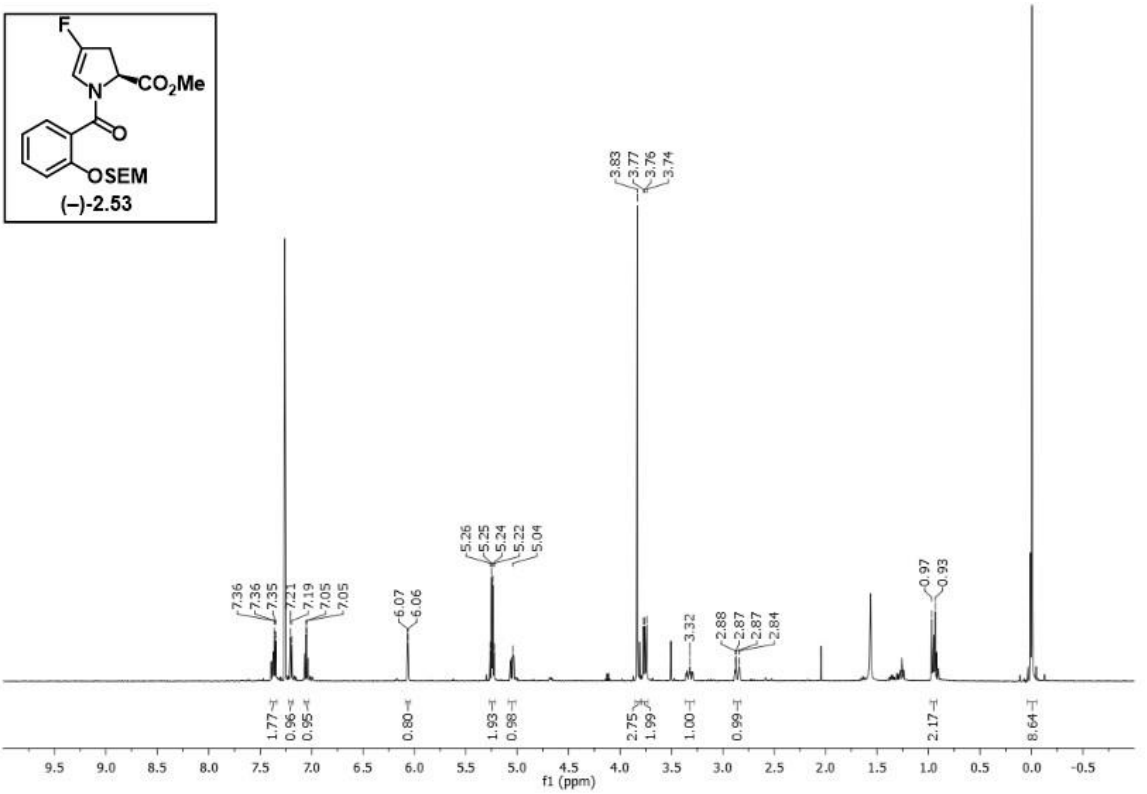
F
CO2Me
N
O
OSEM
(–)-2.53
7.36
7.36
7.35
7.21
7.19
7.05
7.05
6.07
6.06
5.26
5.25
5.24
5.22
5.04
3.83
3.77
3.76
3.74
3.32
2.88
2.87
2.87
2.84
0.97
0.93
1.77
0.96
0.95
0.80
1.93
0.98
2.75
1.99
1.00
0.99
2.17
8.64
f1 (ppm)

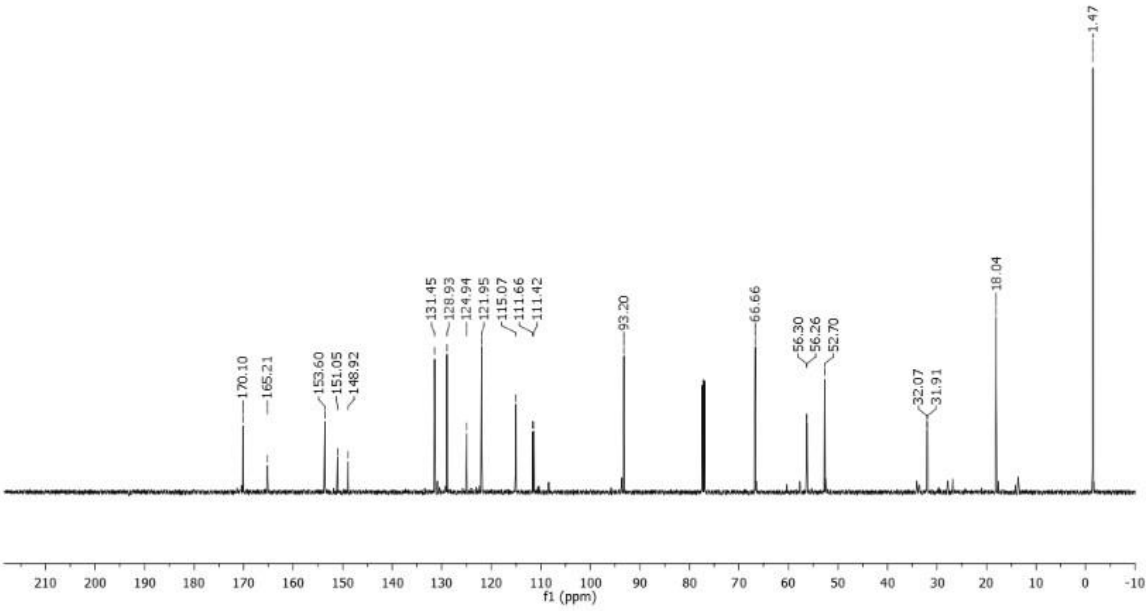
170.10
165.21
153.60
151.05
148.92
131.45
128.93
124.94
121.95
115.07
111.66
111.42
93.20
66.66
56.30
56.26
52.70
32.07
31.91
18.04
-1.47
f1 (ppm)

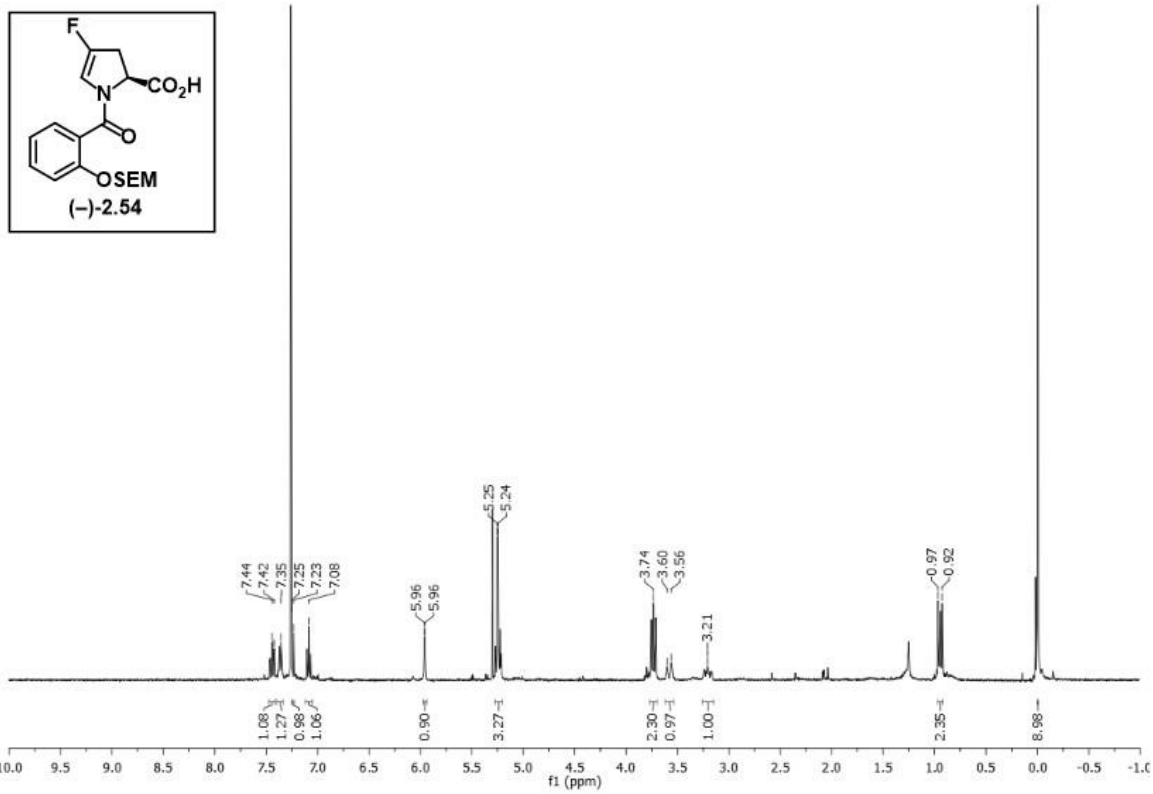
F
CO2H
N
O
OSEM
(–)-2.54
7.44
7.42
7.35
7.25
7.23
7.08
5.96
5.96
5.25
5.24
3.74
3.60
3.56
3.21
0.97
0.92
1.08
1.27
0.98
1.06
0.90
3.27
2.30
0.97
1.00
2.35
8.98
f1 (ppm)

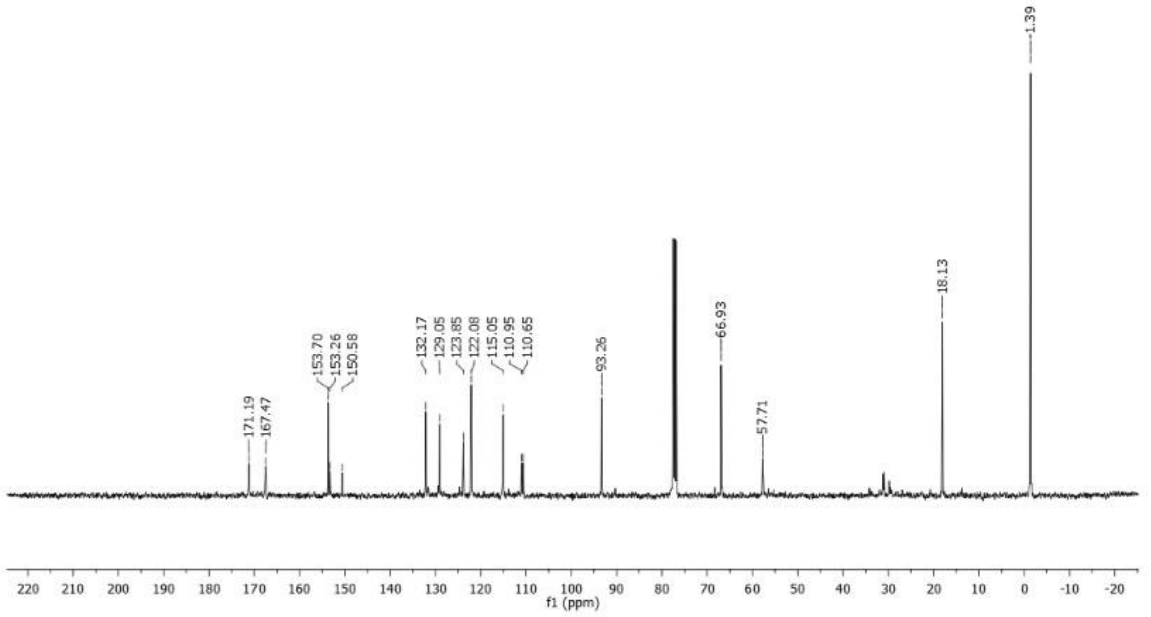
171.19
167.47
153.70
153.26
150.58
132.17
129.05
123.85
122.08
115.05
110.95
110.65
93.26
66.93
57.71
18.13
1.39
f1 (ppm)

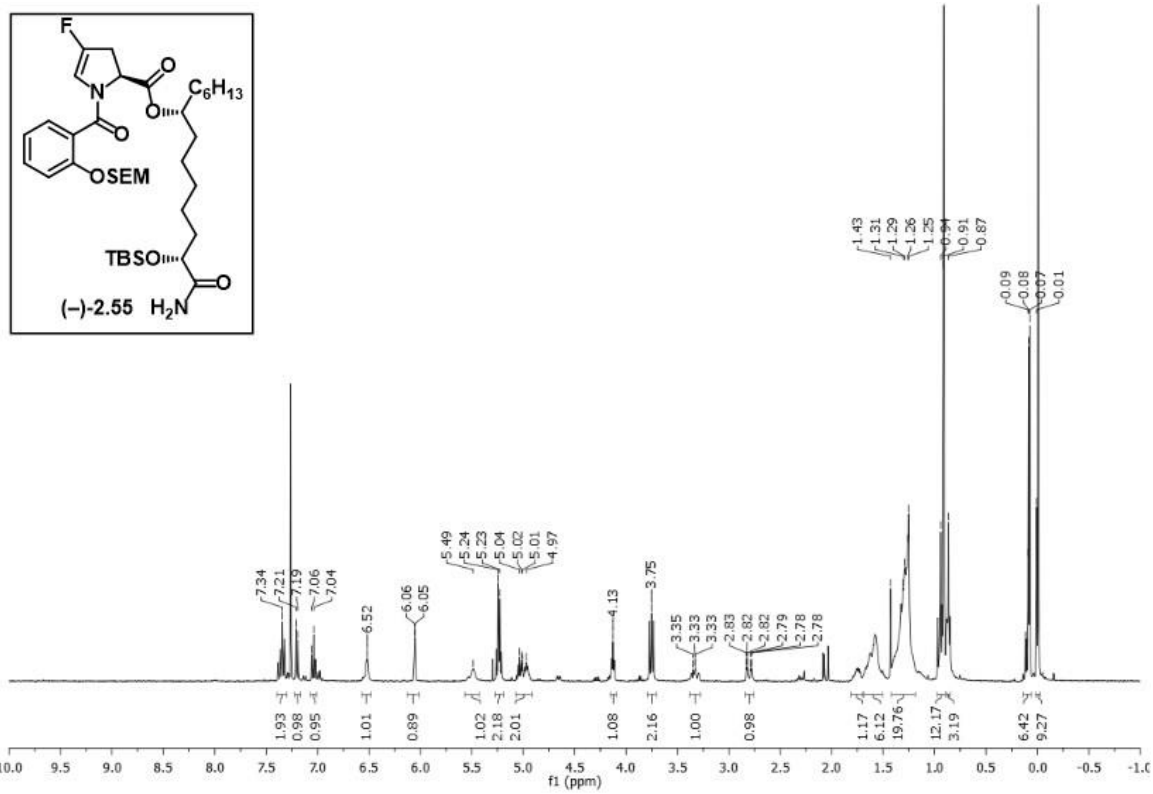
F
O
N
O
C6H13
O
OSEM
TBSO
O
(–)-2.55 H2N
1.43
1.31
1.29
1.26
1.25
0.91
0.87
0.09
0.08
0.07
0.01
7.34
7.21
7.19
7.06
7.04
6.52
6.06
6.05
5.49
5.24
5.23
5.04
5.02
5.01
4.97
4.13
3.75
3.35
3.33
3.33
2.83
2.82
2.82
2.79
2.78
2.78
1.93
0.98
0.95
1.01
0.89
1.02
2.18
2.01
1.08
2.16
1.00
0.98
1.17
6.12
19.76
12.17
3.19
6.42
9.27
f1 (ppm)

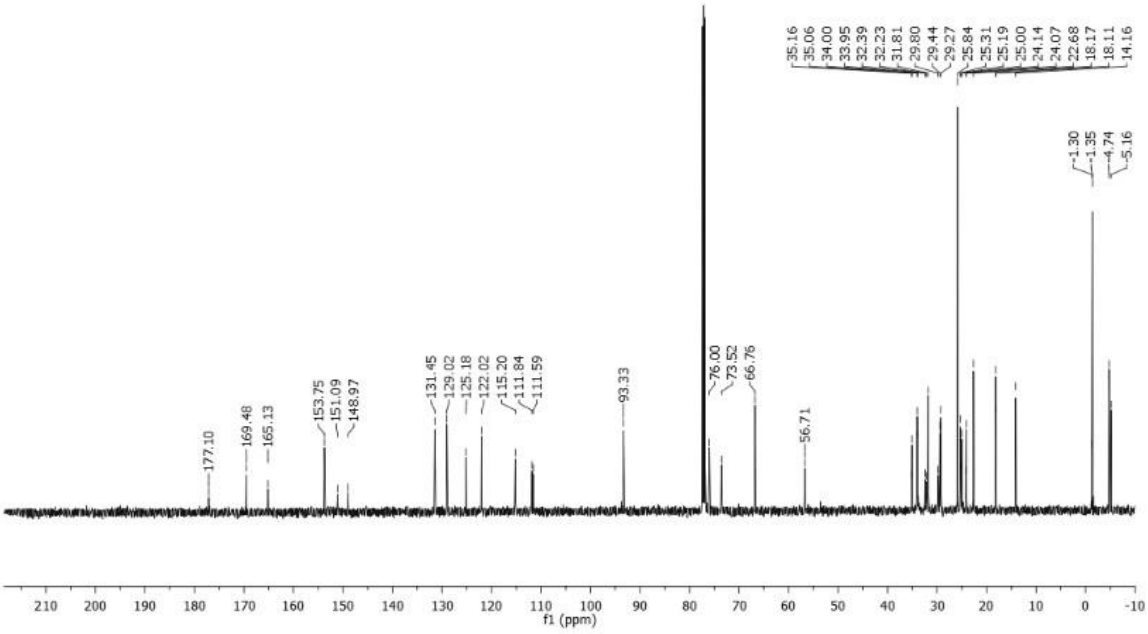
35.16
35.06
34.00
33.95
32.39
32.23
31.81
29.80
29.44
29.27
25.84
25.31
25.19
25.00
24.14
24.07
22.68
18.17
18.11
14.16
1.30
1.35
4.74
5.16
177.10
169.48
165.13
153.75
151.09
148.97
131.45
129.02
125.18
122.02
115.20
111.84
111.59
93.33
76.00
73.52
66.76
56.71
f1 (ppm)

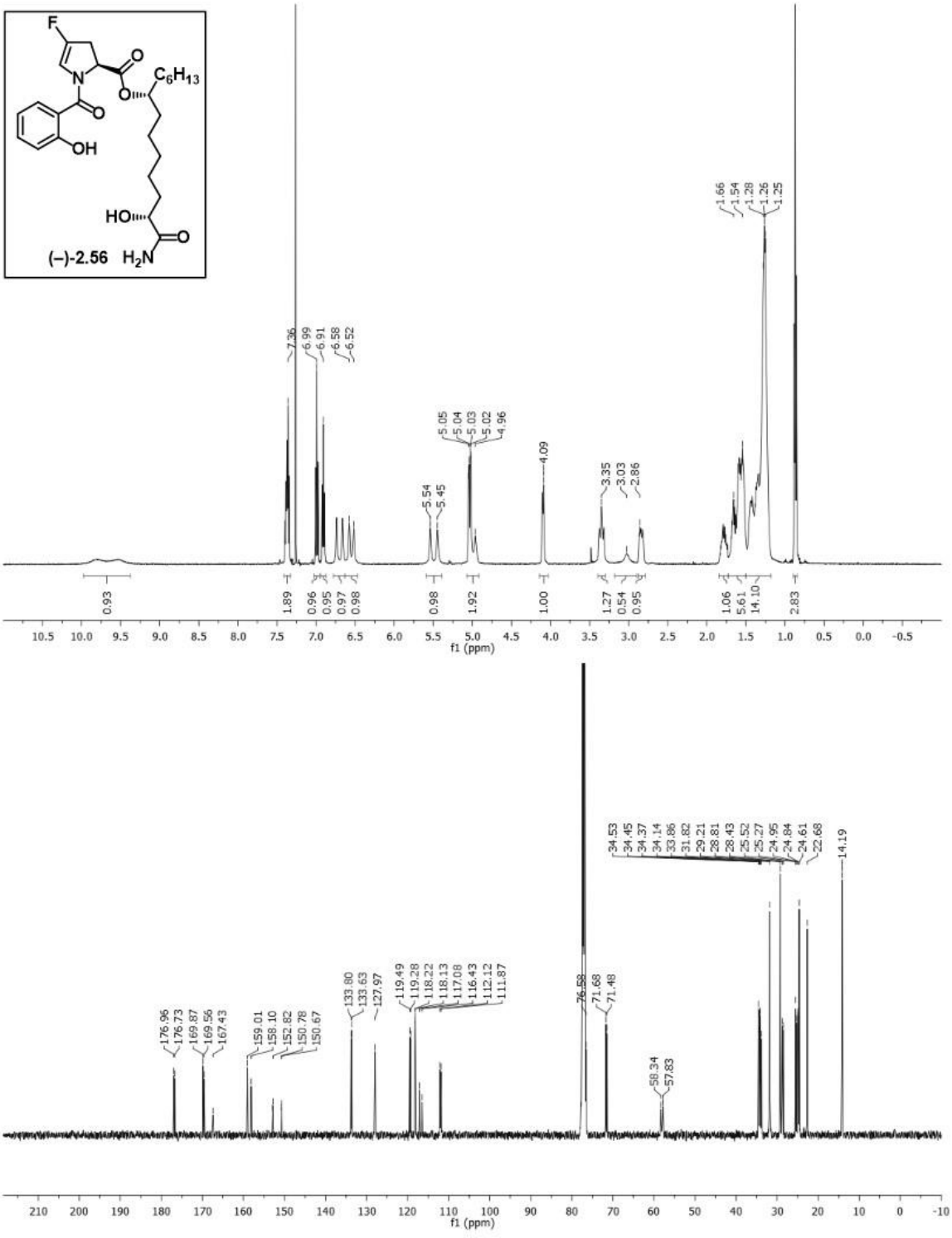
F
O
N
O
C6H13
O
OH
HO
O
(–)-2.56 H2N
7.36
6.99
6.91
6.58
6.52
5.54
5.45
5.05
5.04
5.03
5.02
4.96
4.09
3.35
3.03
2.86
1.66
1.54
1.28
1.26
1.25
0.93
1.89
0.96
0.95
0.97
0.98
0.98
1.92
1.00
1.27
0.54
0.95
1.06
5.61
14.10
2.83
f1 (ppm)
176.96
176.73
169.87
169.56
167.43
159.01
158.10
152.82
150.78
150.67
133.80
133.63
127.97
119.49
119.28
118.22
118.13
117.08
116.43
112.12
111.87
76.58
71.68
71.48
58.34
57.83
34.53
34.45
34.37
34.14
33.86
31.82
29.21
28.81
28.43
25.52
25.27
24.95
24.84
24.61
22.68
14.19
f1 (ppm)

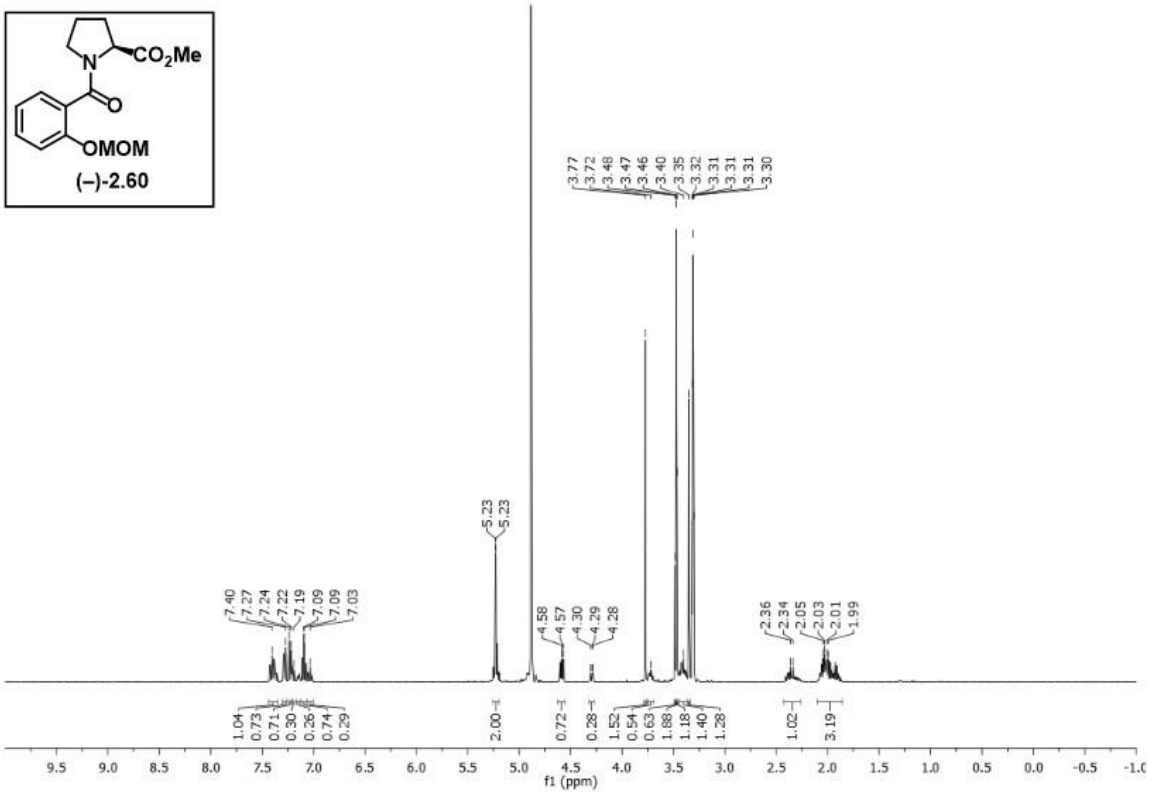
CO2Me
N
O
OMOM
(–)-2.60
7.40
7.27
7.24
7.22
7.19
7.09
7.09
7.03
5.23
5.23
4.58
4.57
4.30
4.29
4.28
3.77
3.72
3.48
3.47
3.46
3.40
3.35
3.32
3.31
3.31
3.31
3.30
2.36
2.34
2.05
2.03
2.01
1.99
1.04
0.73
0.71
0.30
0.26
0.74
0.29
2.00
0.72
0.28
1.52
0.54
0.63
1.88
1.18
1.40
1.28
1.02
3.19
f1 (ppm)

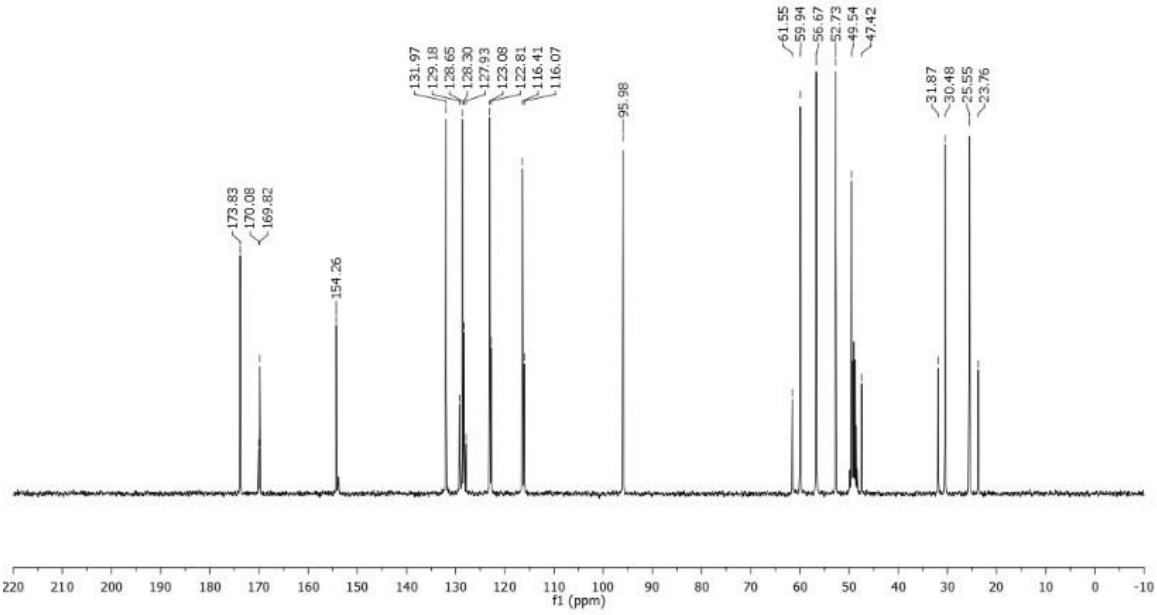
173.83
170.08
169.82
154.26
131.97
129.18
128.65
128.30
127.93
123.08
122.81
116.41
116.07
95.98
61.55
59.94
56.67
52.73
49.54
47.42
31.87
30.48
25.55
23.76
f1 (ppm)

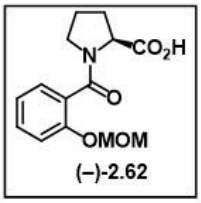
CO2H
N
O
OMOM

(–)-2.62

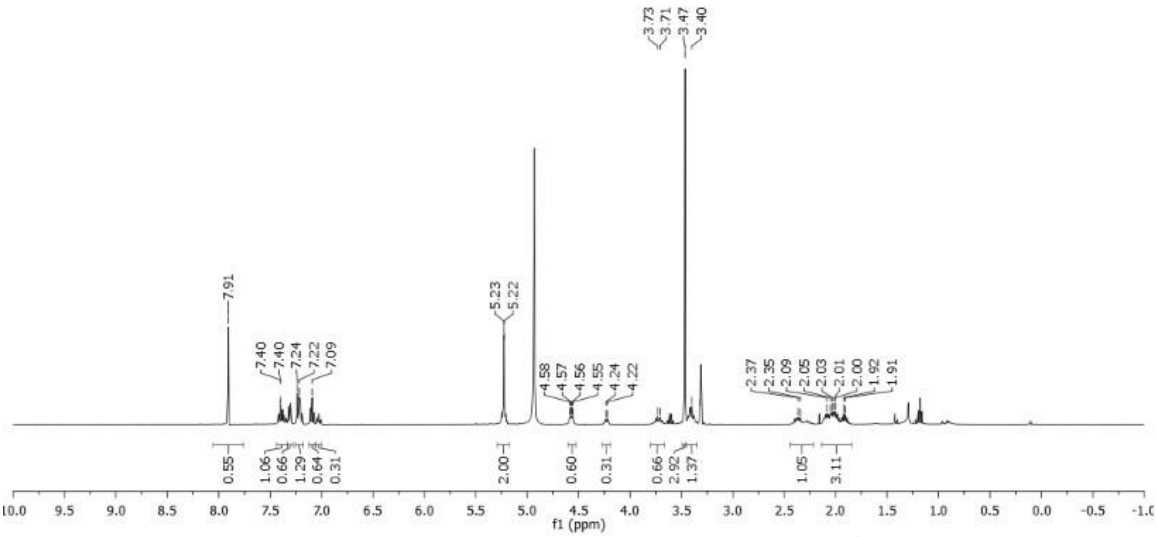
7.91
7.40
7.40
7.24
7.22
7.09
5.23
5.22
4.58
4.57
4.56
4.55
4.24
4.22
3.73
3.71
3.47
3.40
2.37
2.35
2.09
2.05
2.03
2.01
2.00
1.92
1.91
0.55
1.06
0.66
1.29
0.64
0.31
2.00
0.60
0.31
0.66
2.92
1.37
1.05
3.11
f1 (ppm)

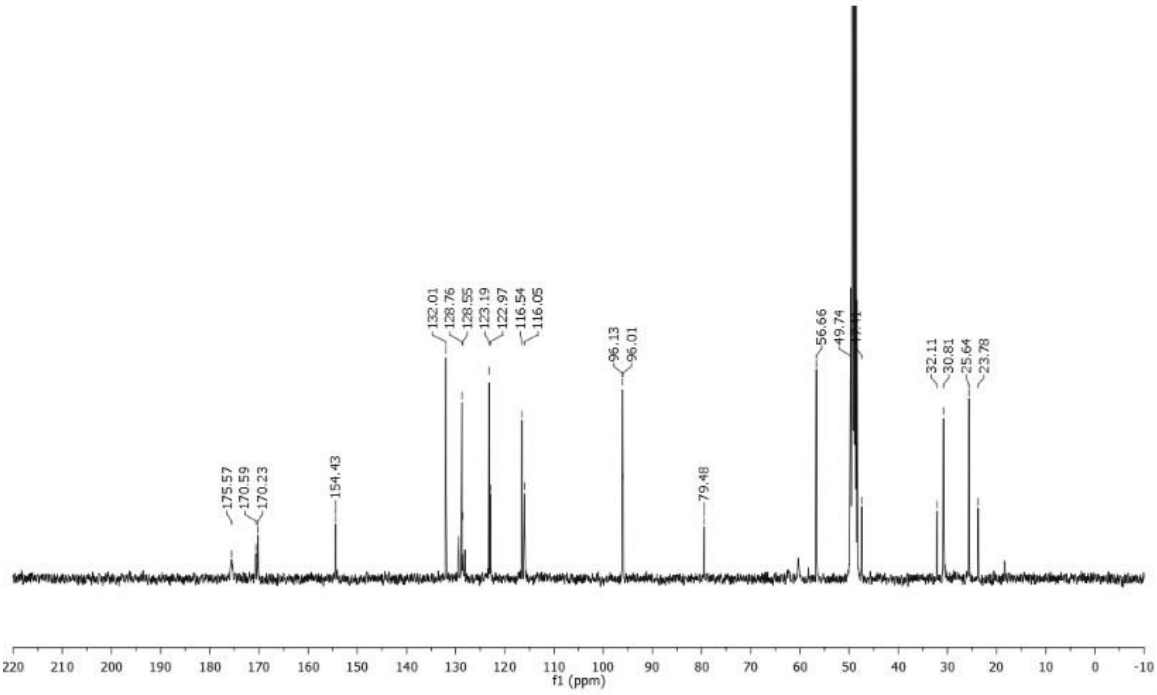
175.57
170.59
170.23
154.43
132.01
128.76
128.55
123.19
122.97
116.54
116.05
96.13
96.01
79.48
56.66
49.74
32.11
30.81
25.64
23.78
f1 (ppm)

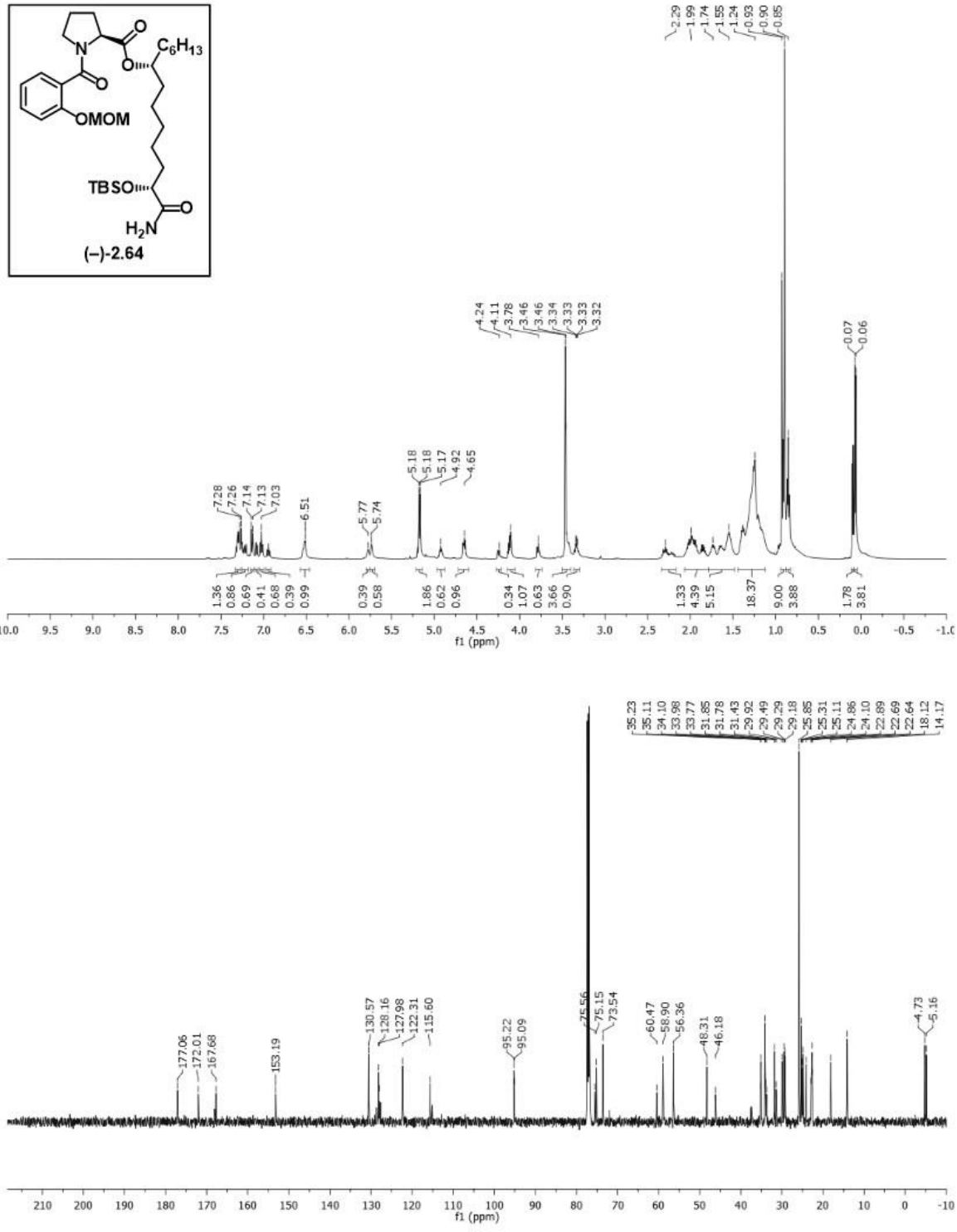
OMOM
TBSO
C_6H_{13}
H_2N
(–)-2.64
f1 (ppm)
f1 (ppm)

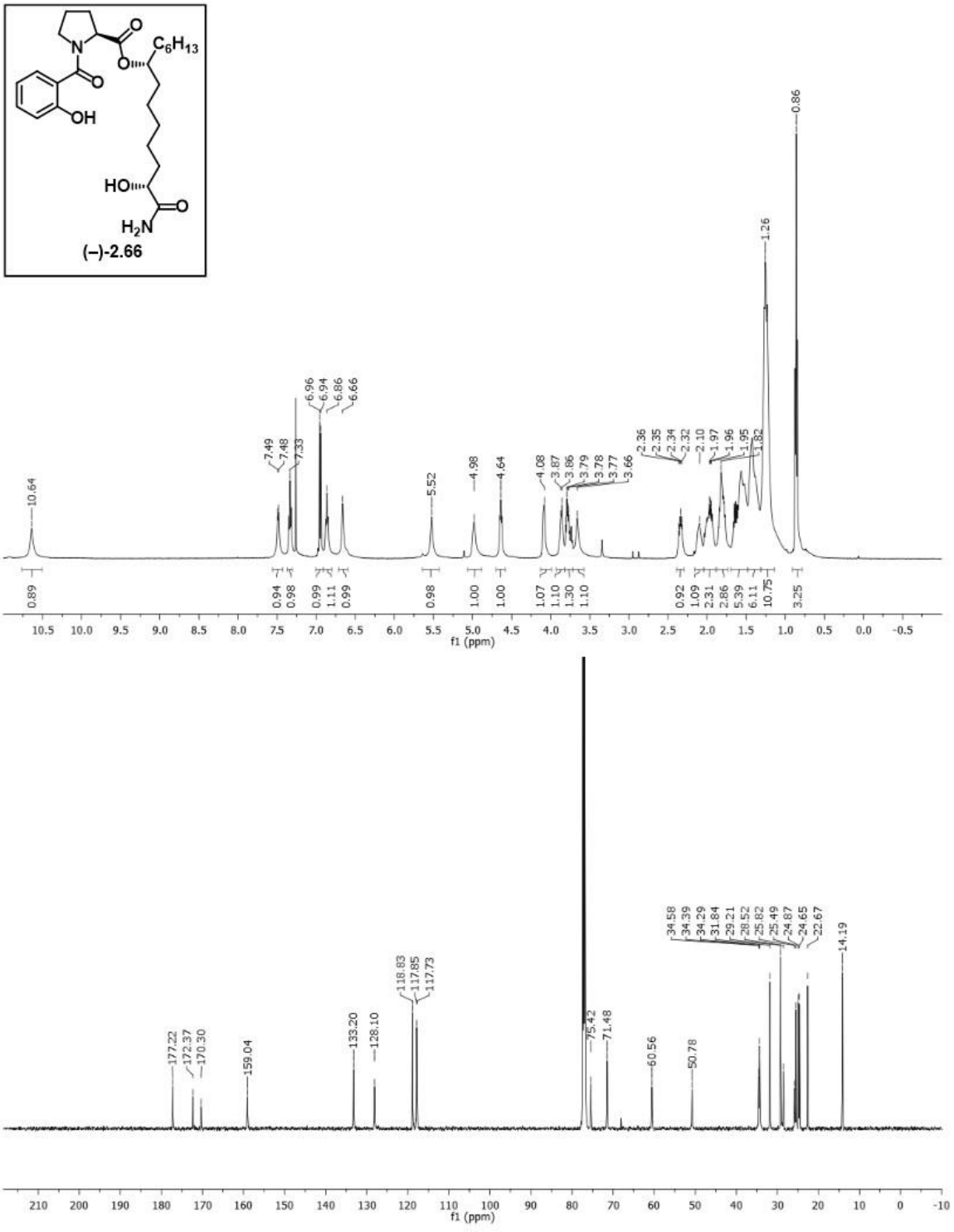
C6H13
OH
HO
H2N
(–)-2.66
f1 (ppm)
f1 (ppm)

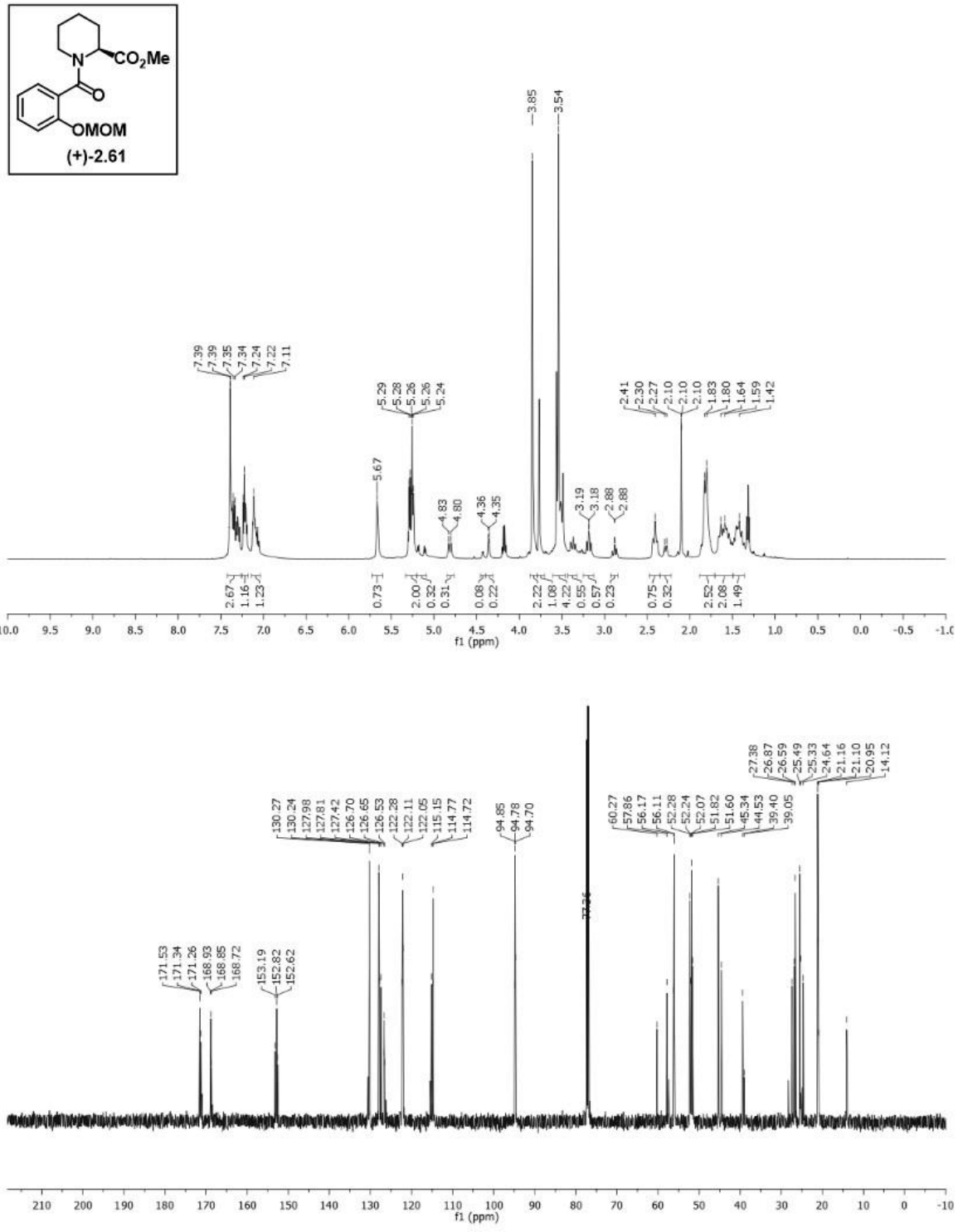
CO2Me
N
O
OMOM
(+)-2.61
f1 (ppm)
f1 (ppm)

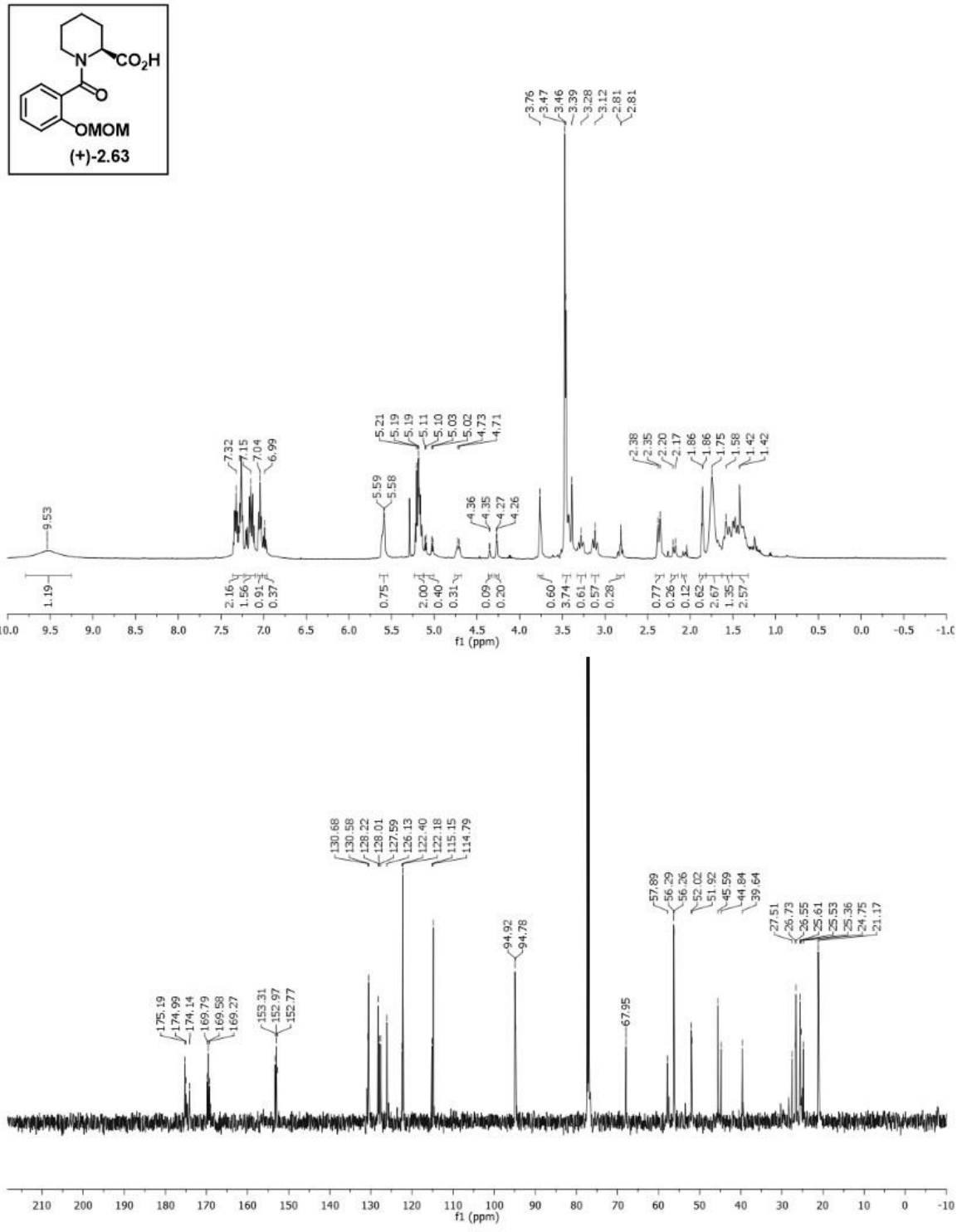
CO2H
N
O
OMOM
(+)-2.63
f1 (ppm)
f1 (ppm)

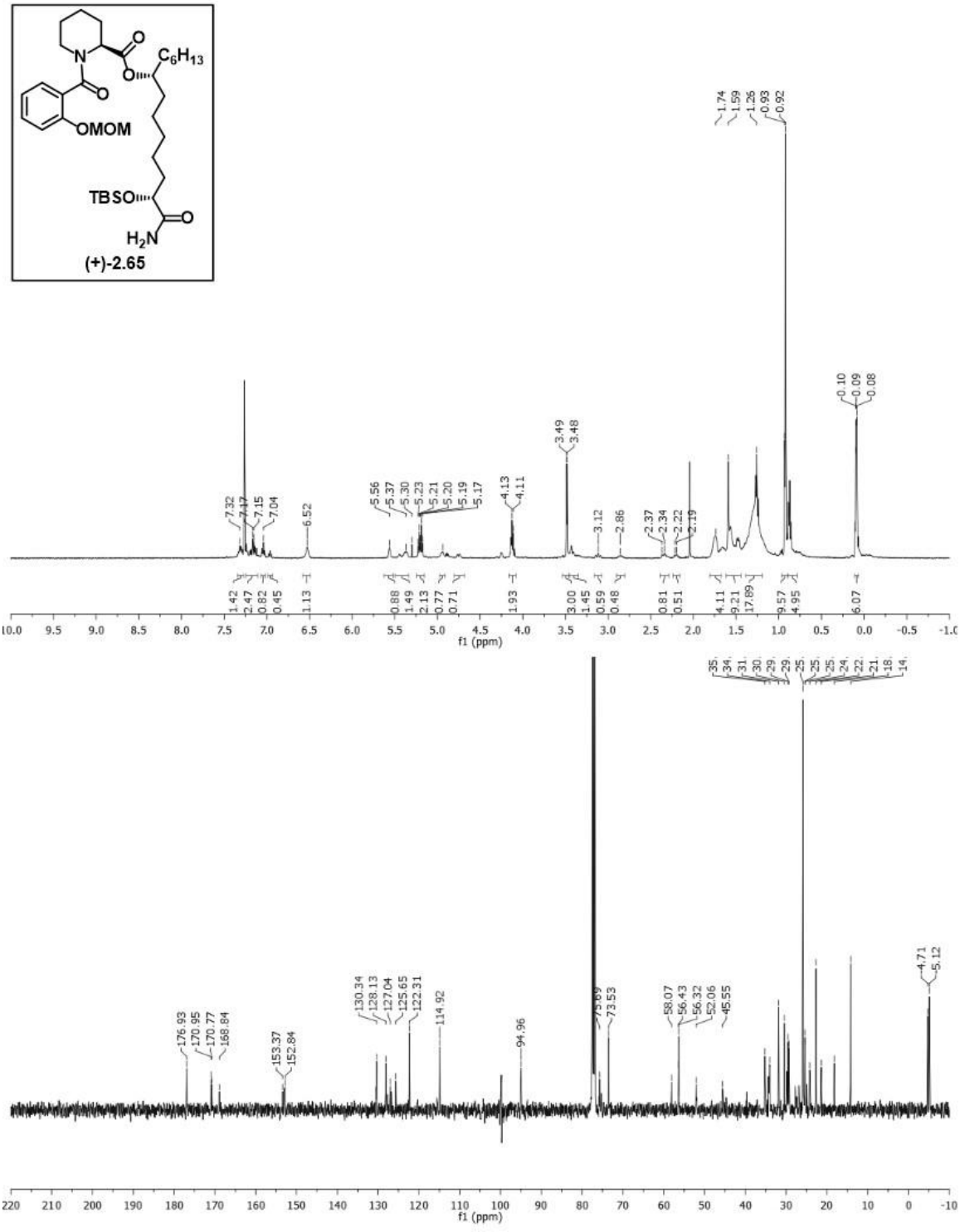
OMOM
TBSO
C_6H_{13}
H_2N
(+)-2.65
f1 (ppm)
f1 (ppm)

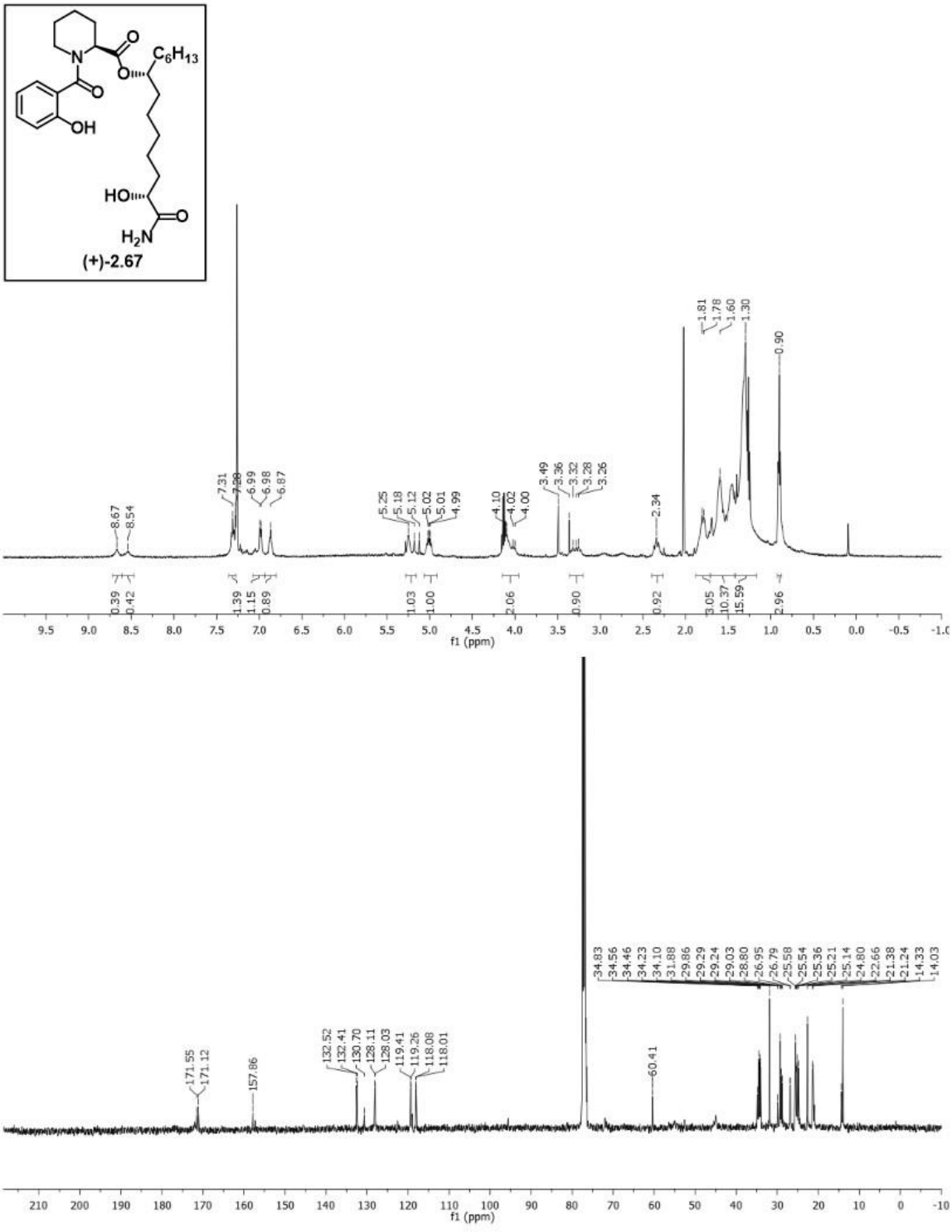
(+)-2.67
f1 (ppm)
f1 (ppm)

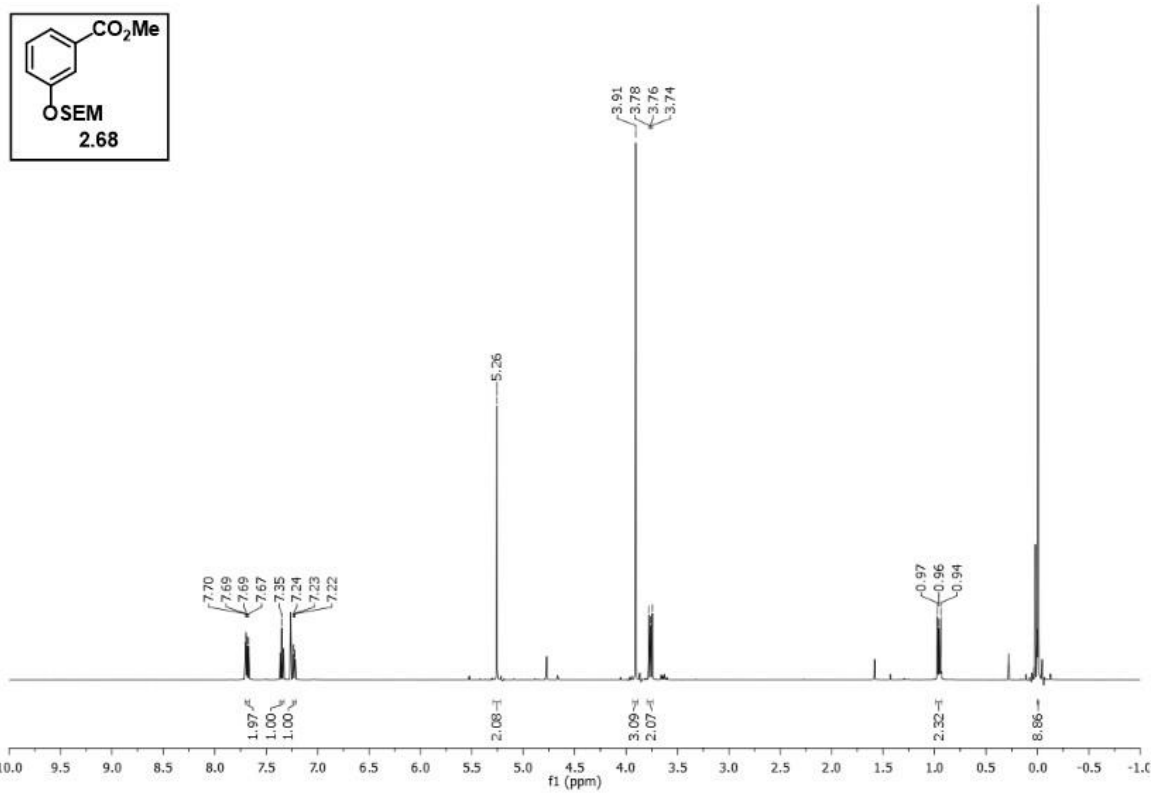
CO2Me
OSEM
2.68
7.70
7.69
7.69
7.67
7.35
7.24
7.23
7.22
5.26
3.91
3.78
3.76
3.74
0.97
0.96
0.94
1.97
1.00
1.00
2.08
3.09
2.07
2.32
8.86
f1 (ppm)

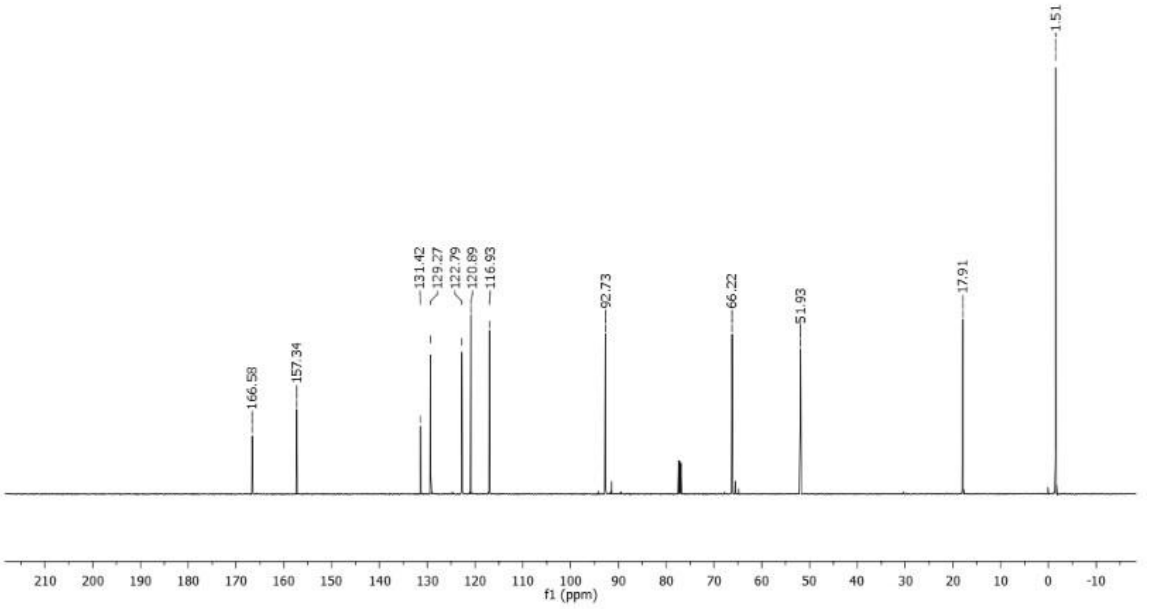
166.58
157.34
131.42
129.27
122.79
120.89
116.93
92.73
66.22
51.93
17.91
-1.51
f1 (ppm)

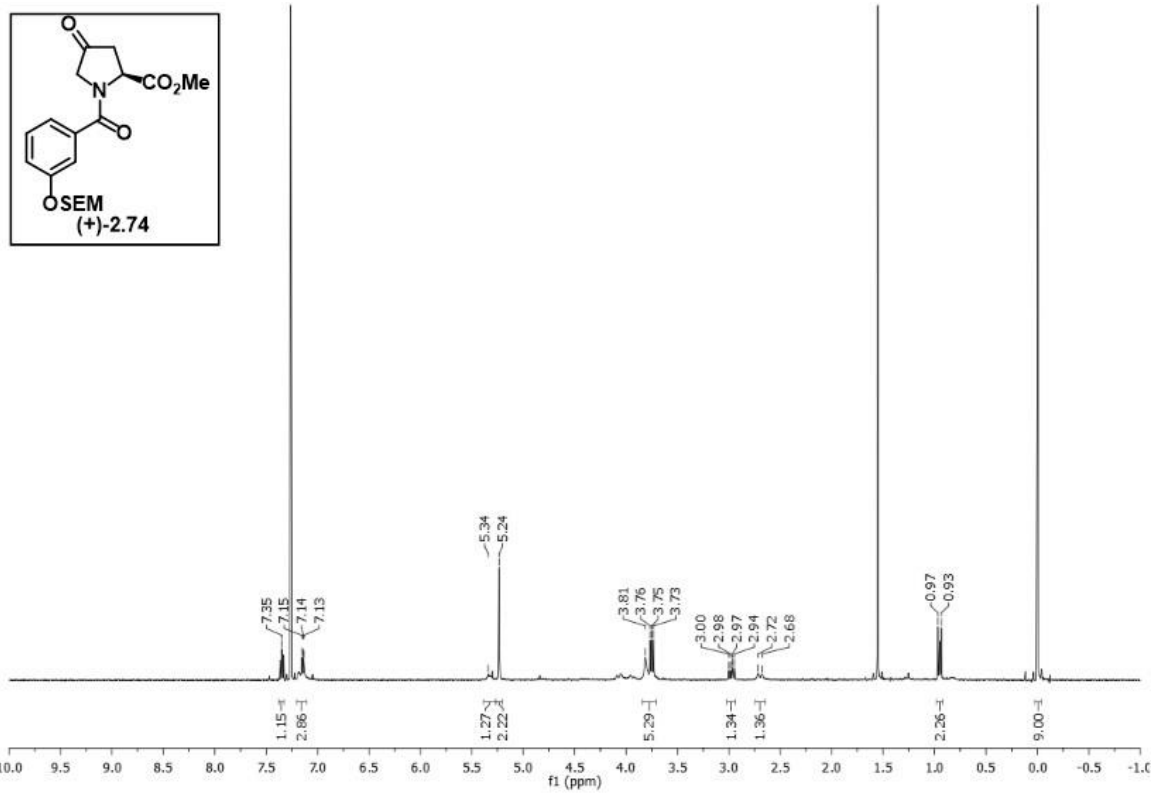
O
CO2Me
N
O
OSEM
(+)-2.74
7.35
7.15
7.14
7.13
5.34
5.24
3.81
3.76
3.75
3.73
3.00
2.98
2.97
2.94
2.72
2.68
0.97
0.93
1.15
2.86
1.27
2.22
5.29
1.34
1.36
2.26
9.00
f1 (ppm)

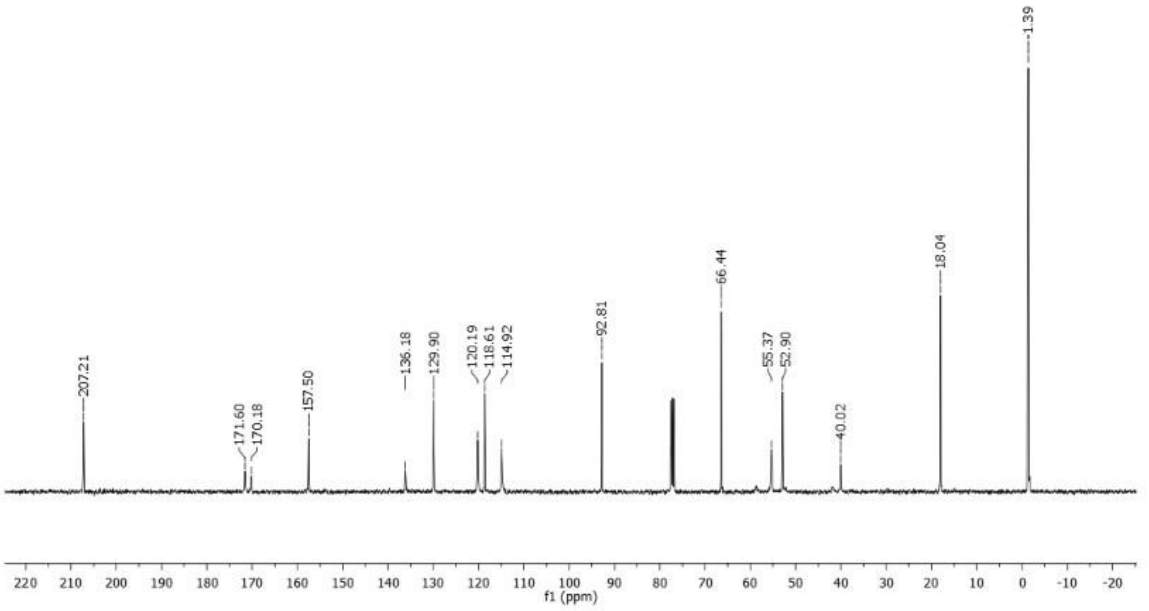
207.21
171.60
170.18
157.50
136.18
129.90
120.19
118.61
114.92
92.81
66.44
55.37
52.90
40.02
18.04
-1.39
f1 (ppm)

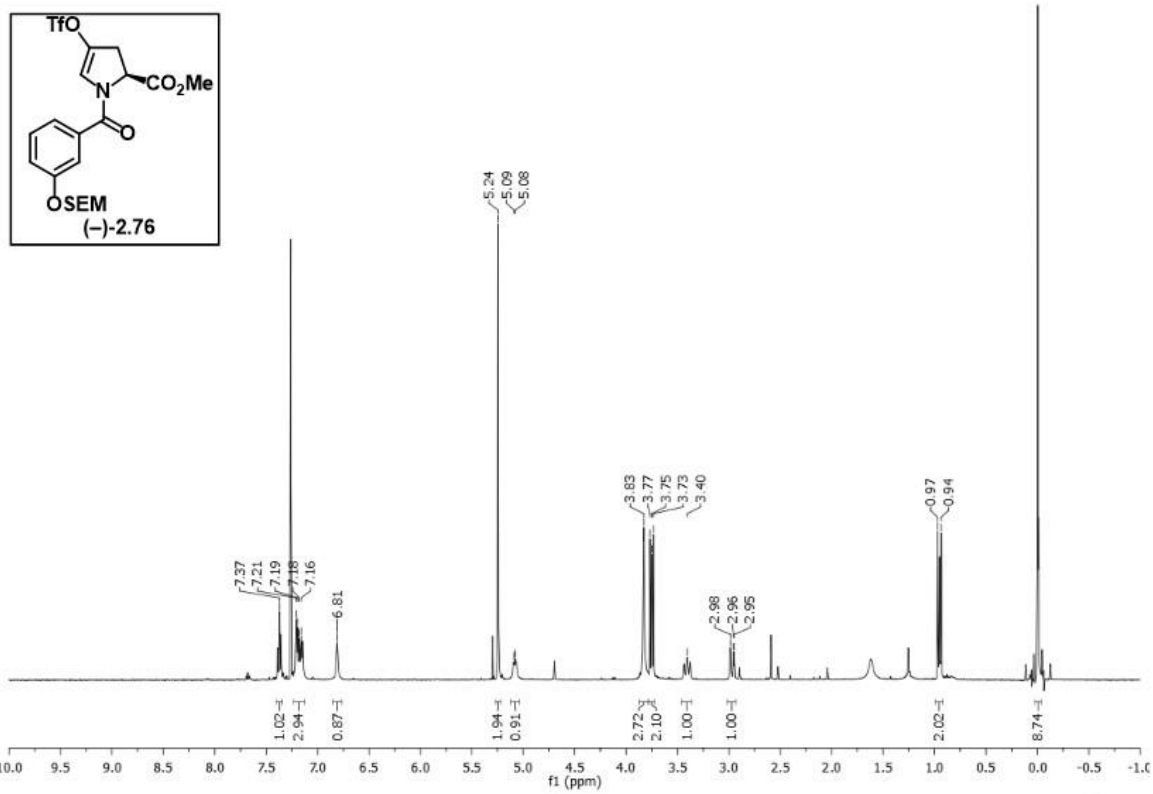
TfO
CO2Me
N
O
OSEM
(–)-2.76
5.24
5.09
5.08
7.37
7.21
7.19
7.18
7.16
6.81
3.83
3.77
3.75
3.73
3.40
2.98
2.96
2.95
0.97
0.94
1.02
2.94
0.87
1.94
0.91
2.72
2.10
1.00
1.00
2.02
8.74
f1 (ppm)

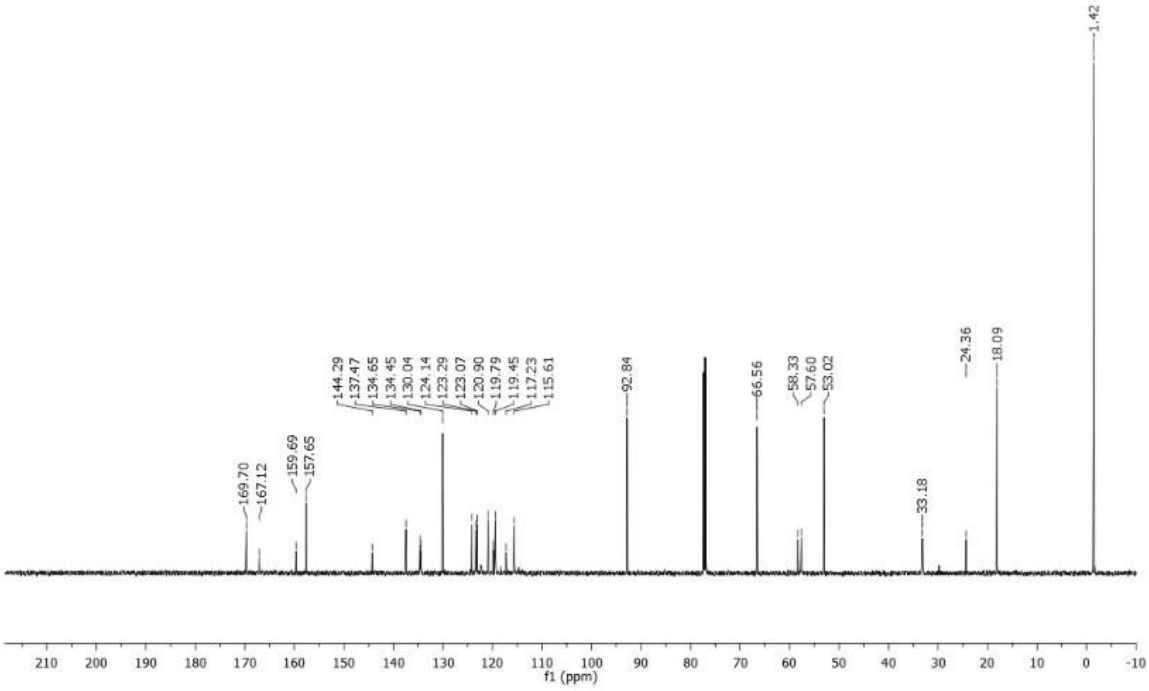
1.42
144.29
137.47
134.65
134.45
130.04
124.14
123.29
123.07
120.90
119.79
119.45
117.23
115.61
92.84
66.56
58.33
57.60
53.02
24.36
18.09
169.70
167.12
159.69
157.65
33.18
f1 (ppm)

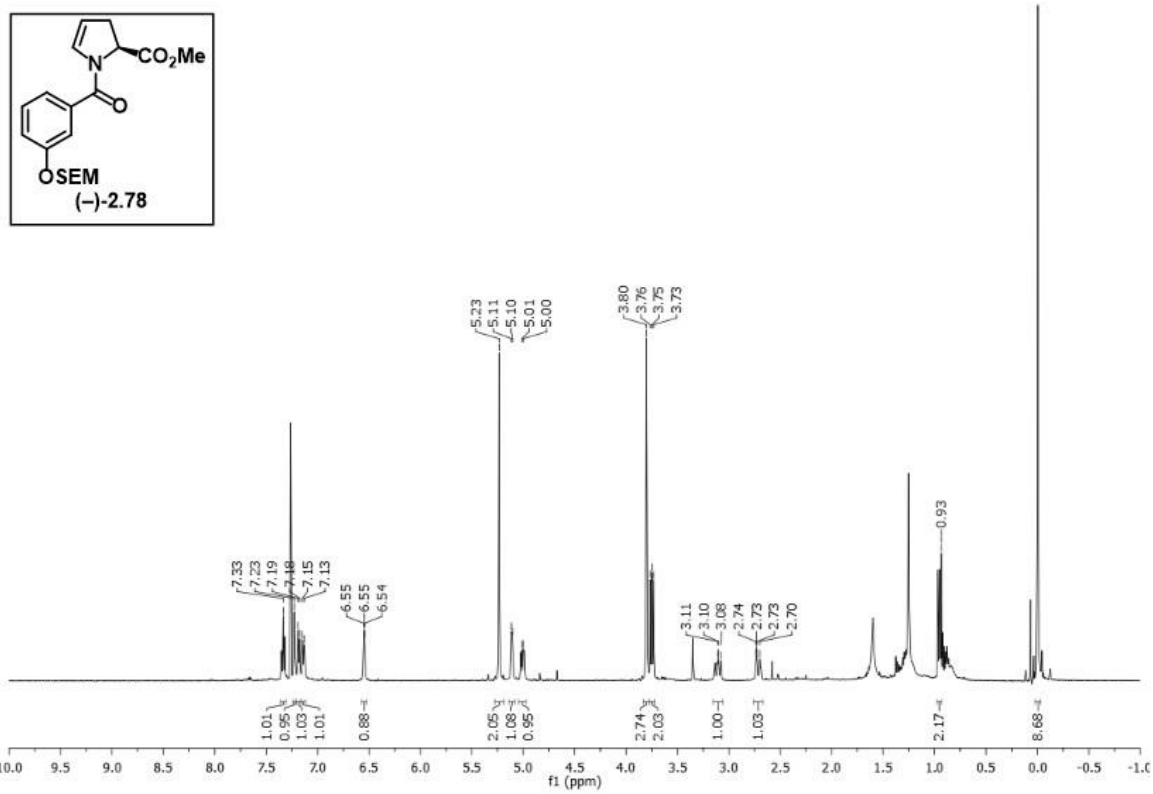
CO2Me
N
O
OSEM
(–)-2.78
7.33
7.23
7.19
7.18
7.15
7.13
6.55
6.55
6.54
5.23
5.11
5.10
5.01
5.00
3.80
3.76
3.75
3.73
3.11
3.10
3.08
2.74
2.73
2.73
2.70
0.93
1.01
0.95
1.03
1.01
0.88
2.05
1.08
0.95
2.74
2.03
1.00
1.03
2.17
8.68
f1 (ppm)

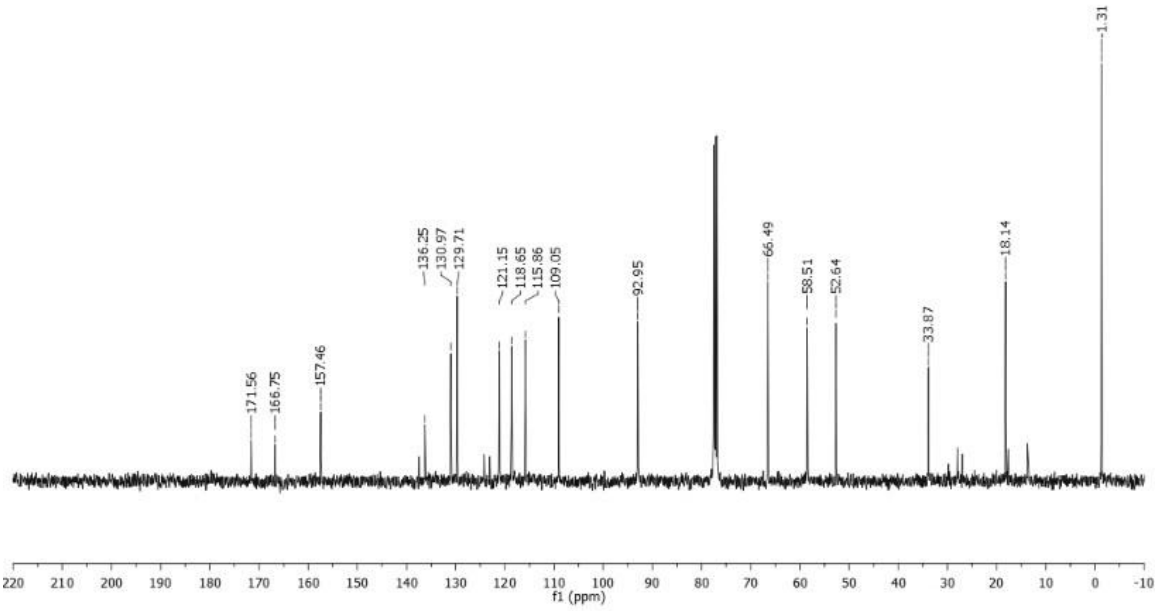
171.56
166.75
157.46
136.25
130.97
129.71
121.15
118.65
115.86
109.05
92.95
66.49
58.51
52.64
33.87
18.14
-1.31
f1 (ppm)

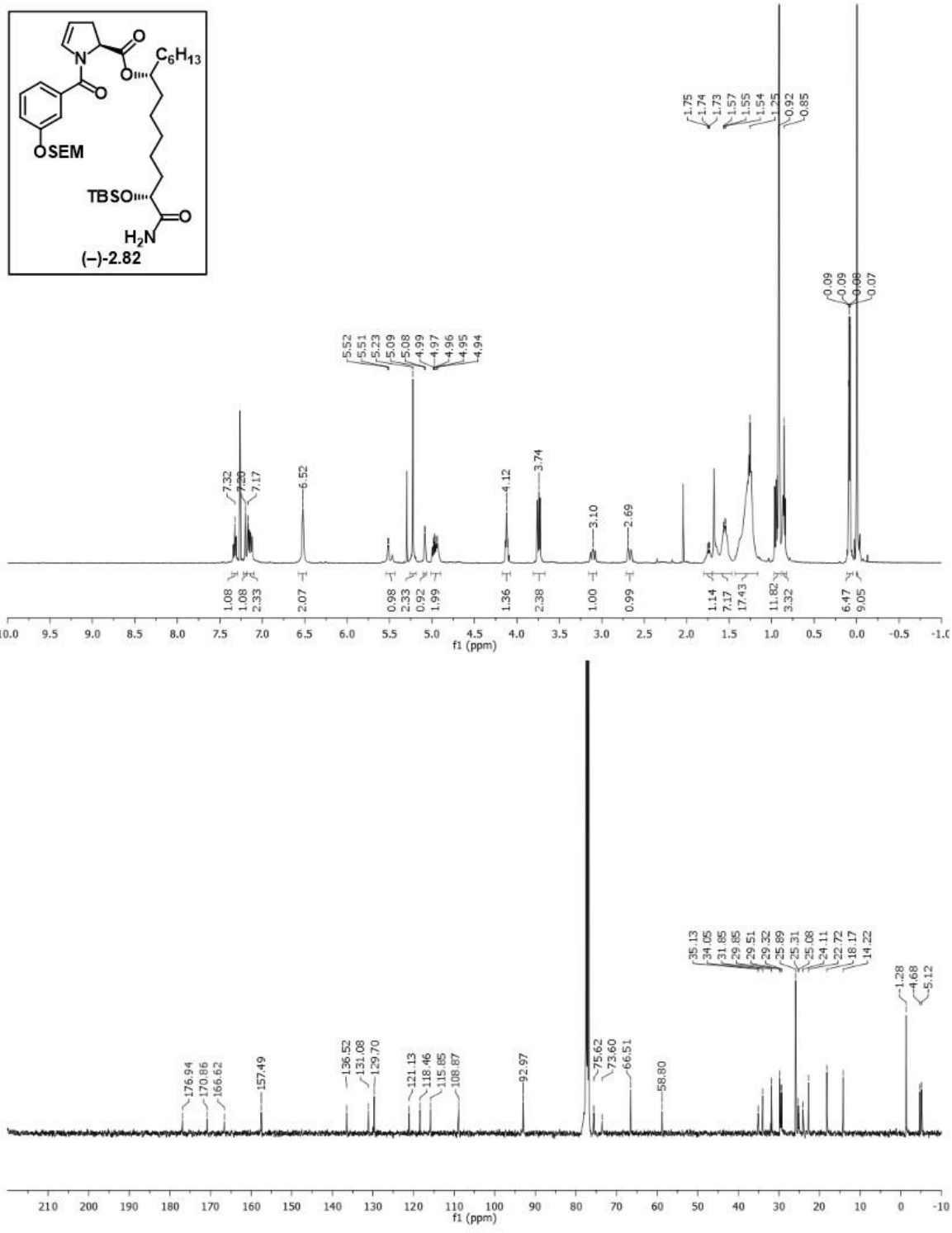
OSEM
TBSO
H_2N
C_6H_{13}
(–)-2.82
f1 (ppm)
f1 (ppm)

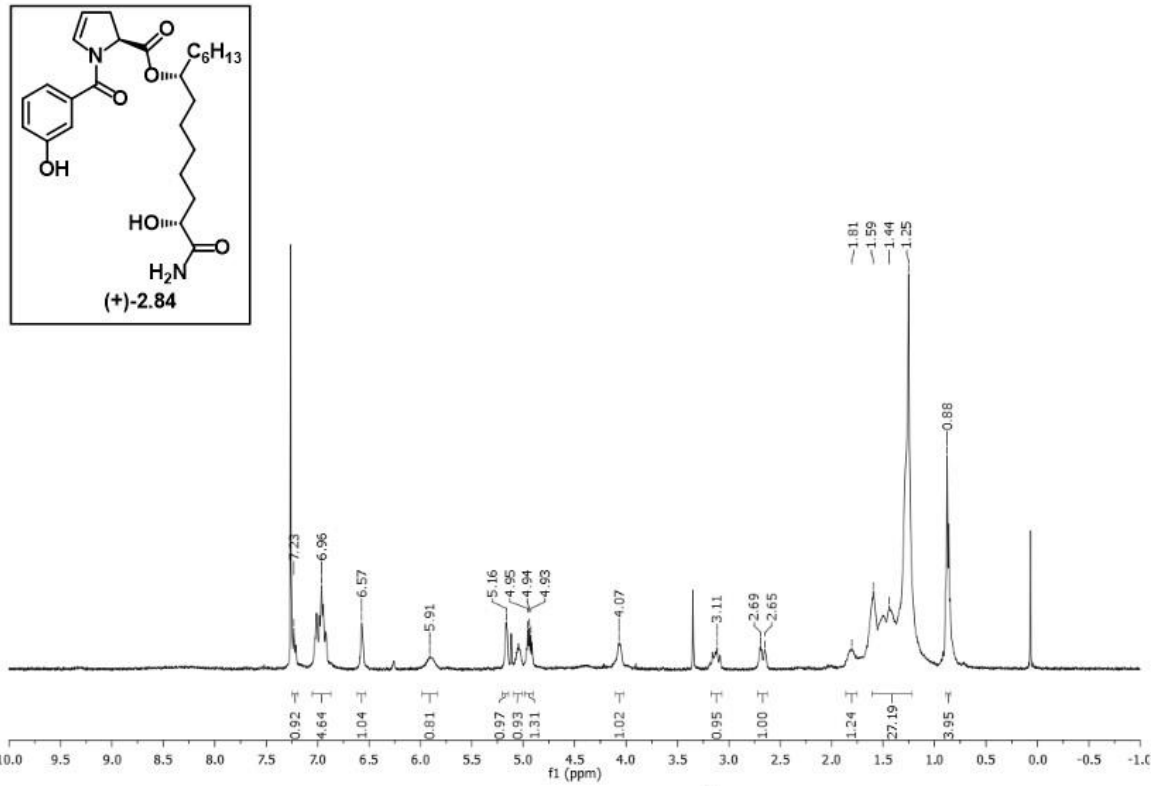
(+)-2.84
7.23
6.96
6.57
5.91
5.16
4.95
4.94
4.93
4.07
3.11
2.69
2.65
1.81
1.59
1.44
1.25
0.88
f1 (ppm)

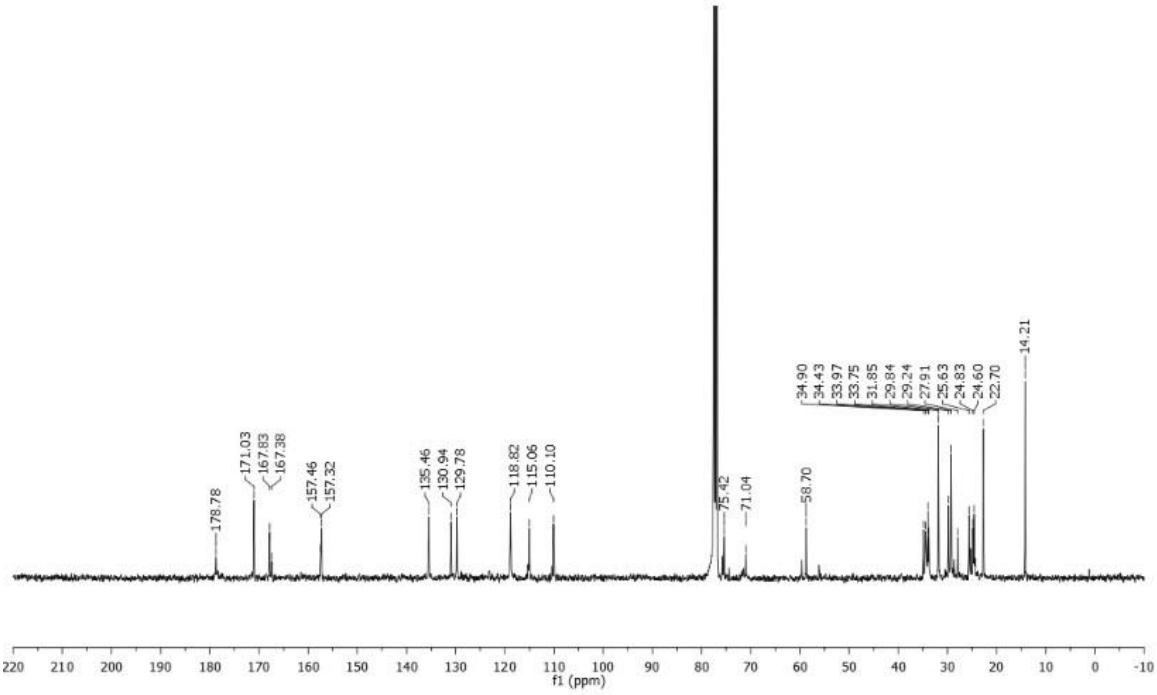
178.78
171.03
167.83
167.38
157.46
157.32
135.46
130.94
129.78
118.82
115.06
110.10
75.42
71.04
58.70
34.90
34.43
33.97
33.75
31.85
29.84
29.24
27.91
25.63
24.83
24.60
22.70
14.21
f1 (ppm)

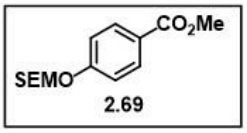
CO2Me
SEMO

2.69

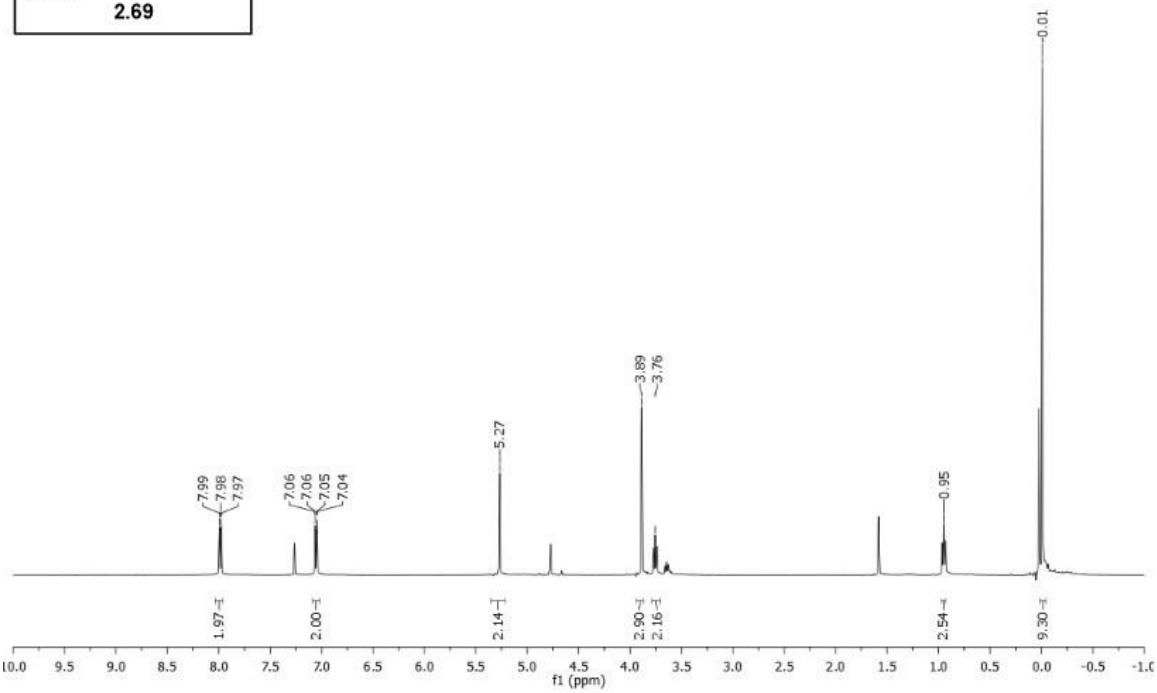
7.99
7.98
7.97
7.06
7.06
7.05
7.04
5.27
3.89
3.76
0.95
0.01
1.97
2.00
2.14
2.90
2.16
2.54
9.30
f1 (ppm)

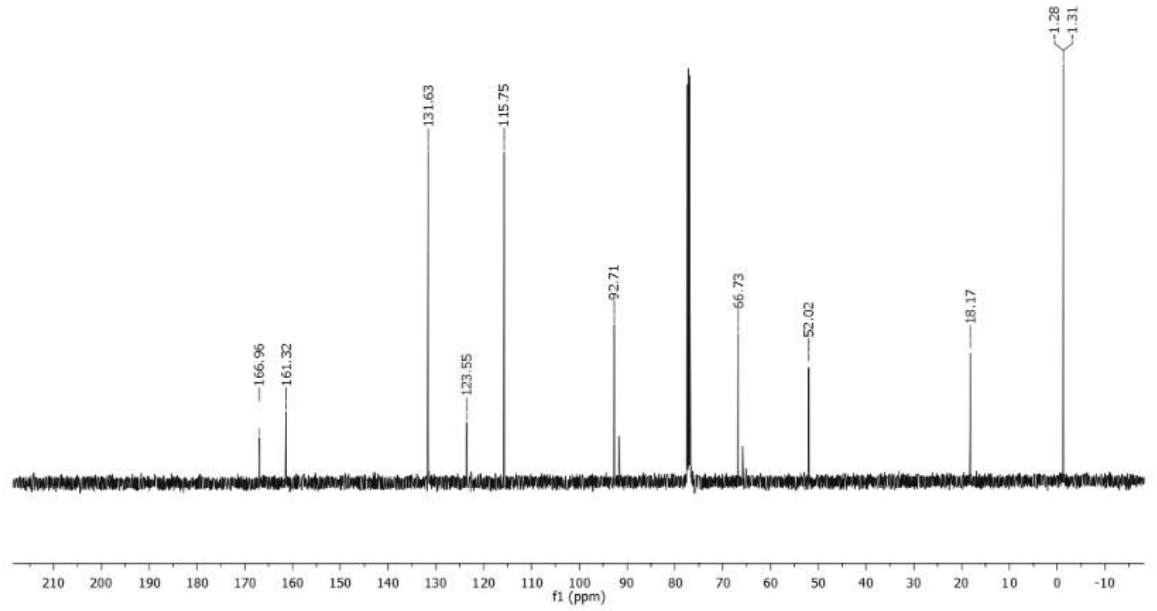
166.96
161.32
131.63
123.55
115.75
92.71
66.73
52.02
18.17
1.28
1.31
f1 (ppm)

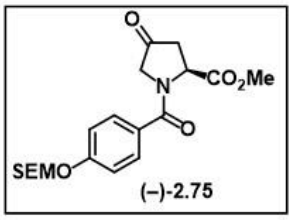
O
N
CO2Me
O
SEMO

(–)-2.75

0.00
7.49
7.08
7.06
5.25
3.77
3.73
2.95
2.93
2.71
2.70
0.97
0.93
1.88
1.82
1.96
5.05
1.00
1.03
1.97
9.08
f1 (ppm)

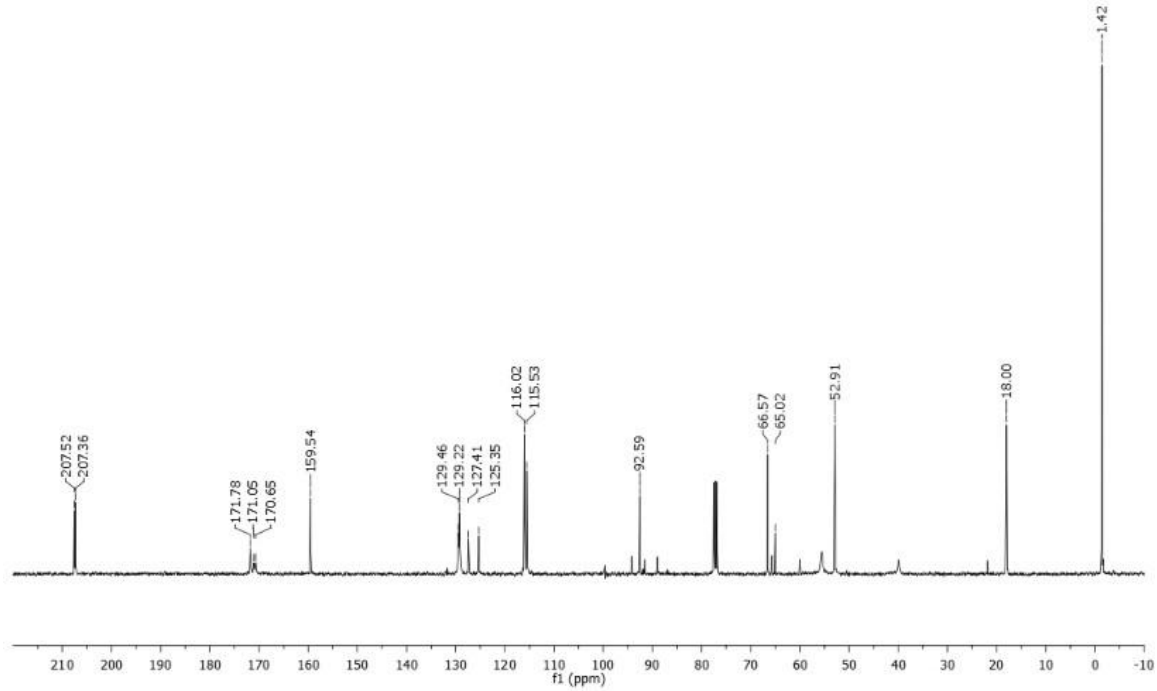
1.42
207.52
207.36
171.78
171.05
170.65
159.54
129.46
129.22
127.41
125.35
116.02
115.53
92.59
66.57
65.02
52.91
18.00
f1 (ppm)

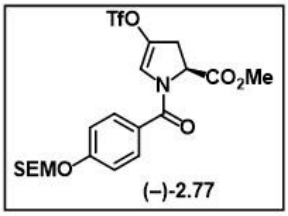
TfO
CO2Me
N
O
SEMO

(–)-2.77

7.53
7.51
7.11
7.09
6.87
5.27
5.08
5.07
3.82
3.78
3.76
3.74
3.40
2.98
2.96
0.98
0.95
0.93
0.00
2.00
2.08
0.95
2.01
0.95
2.85
2.22
1.02
1.00
2.03
9.04
f1 (ppm)

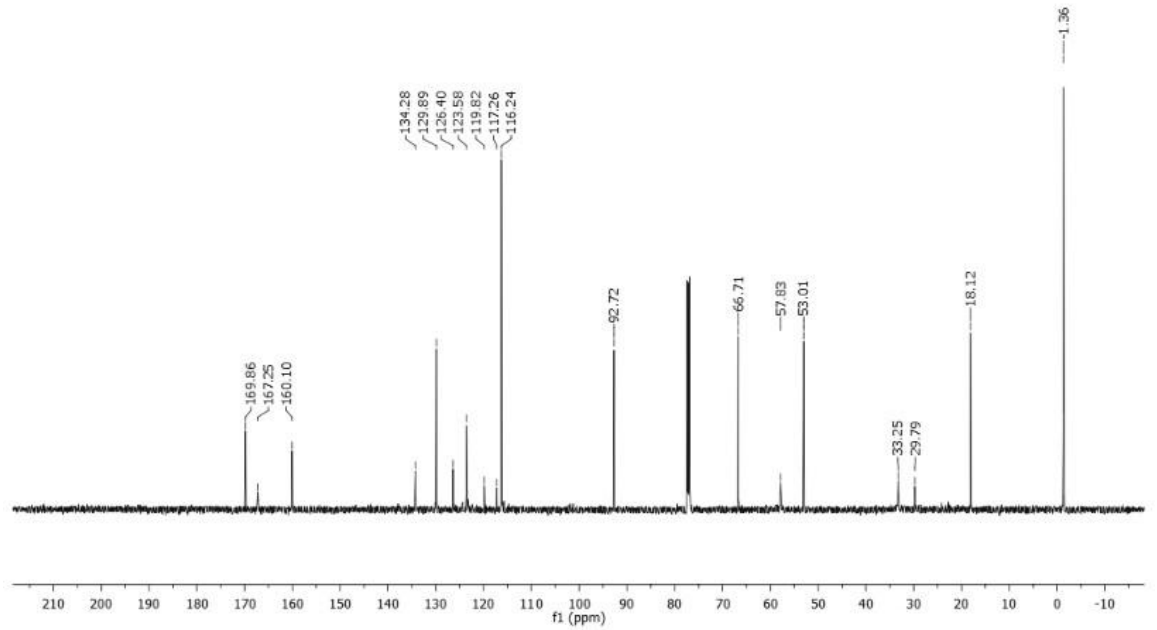
134.28
129.89
126.40
123.58
119.82
117.26
116.24
169.86
167.25
160.10
92.72
66.71
57.83
53.01
33.25
29.79
18.12
1.36
f1 (ppm)

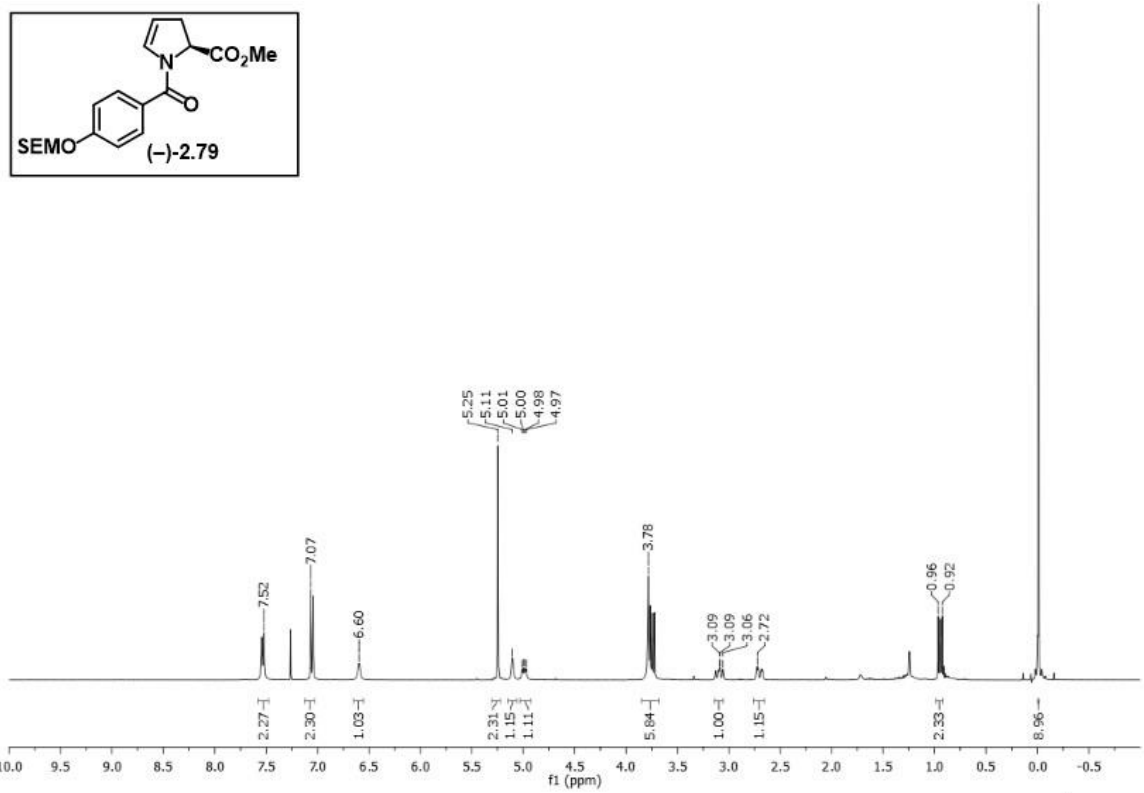
CO2Me
N
O
SEMO
(–)-2.79
5.25
5.11
5.01
5.00
4.98
4.97
7.52
7.07
6.60
3.78
3.09
3.09
3.06
2.72
0.96
0.92
2.27
2.30
1.03
2.31
1.15
1.11
5.84
1.00
1.15
2.33
8.96
f1 (ppm)

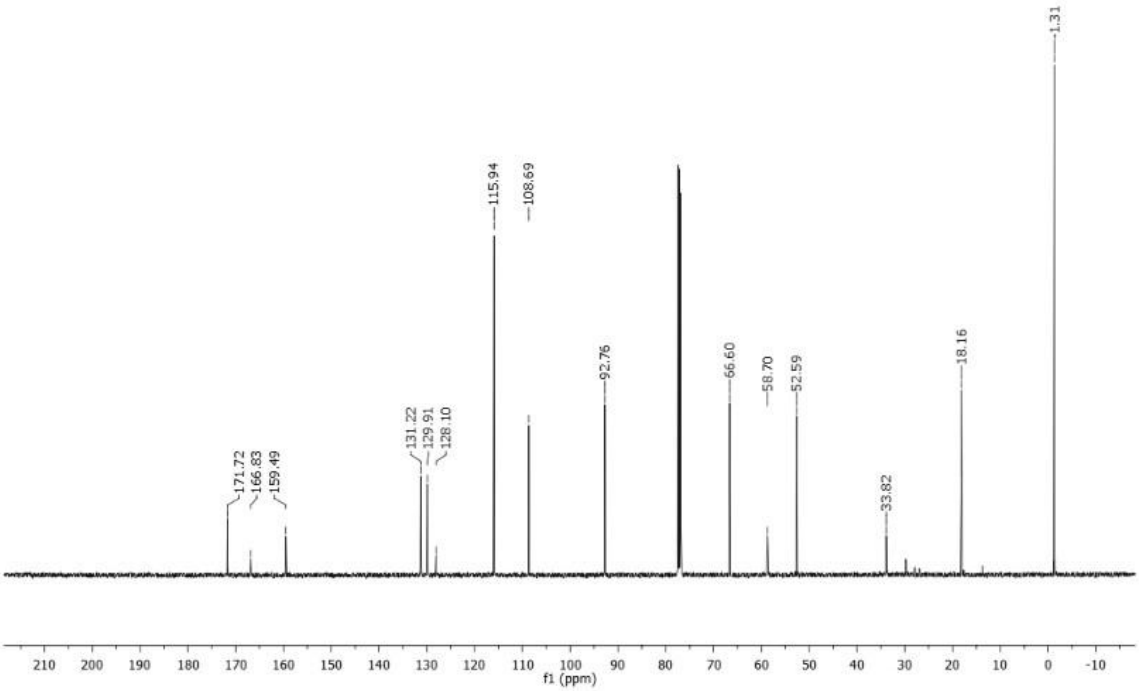
171.72
166.83
159.49
131.22
129.91
128.10
115.94
108.69
92.76
66.60
58.70
52.59
33.82
18.16
1.31
f1 (ppm)

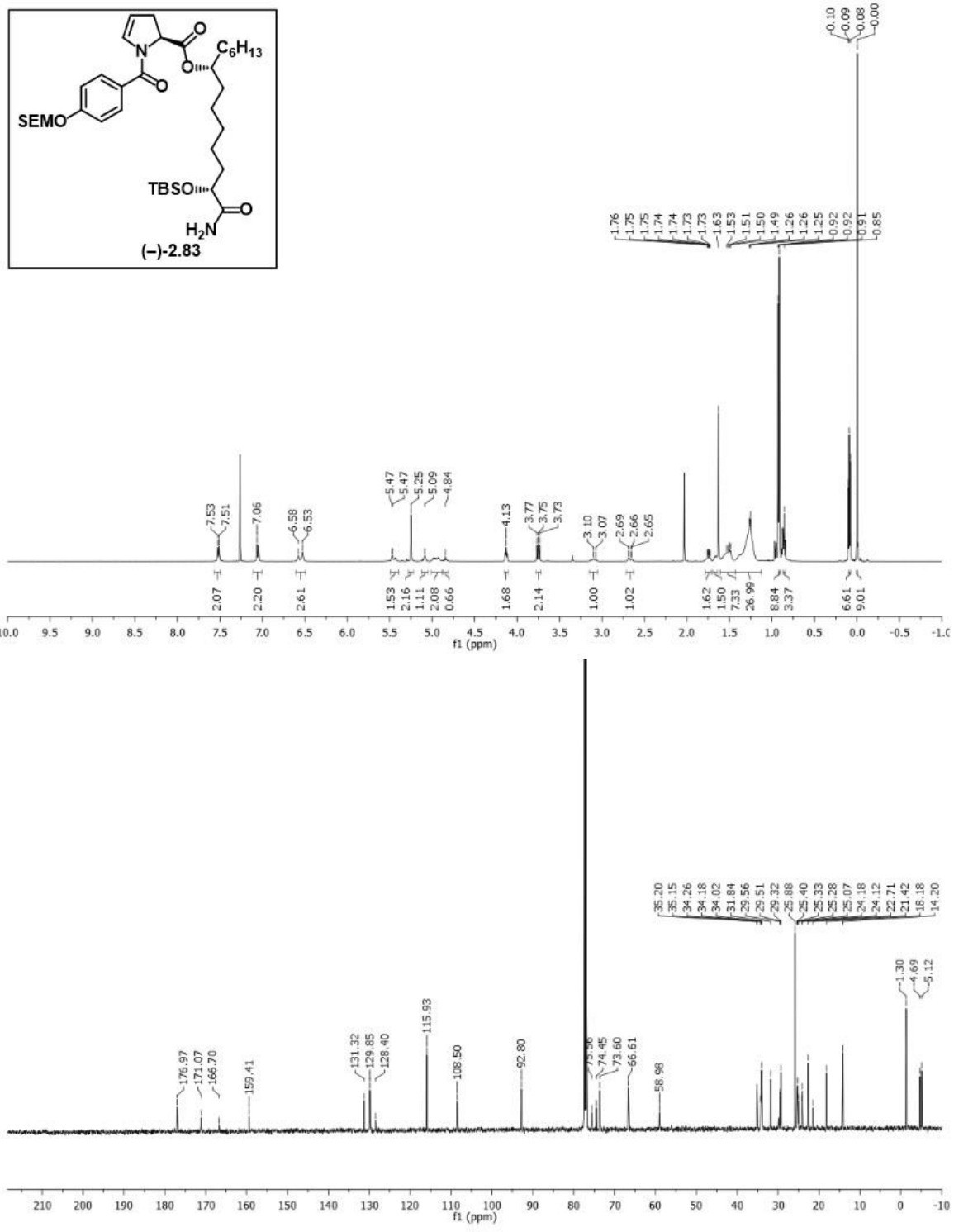
SEMO
TBSO
C_6H_{13}
H_2N
(–)-2.83
f1 (ppm)
f1 (ppm)

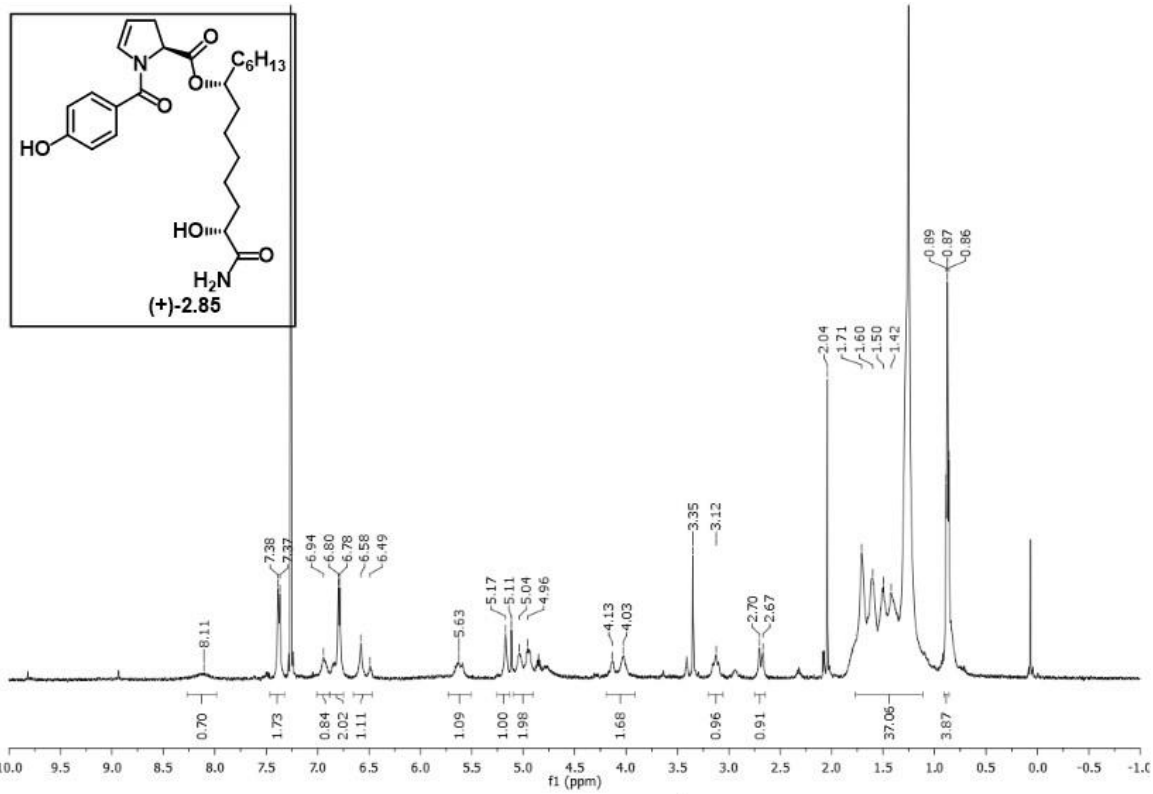
(+)-2.85
f1 (ppm)

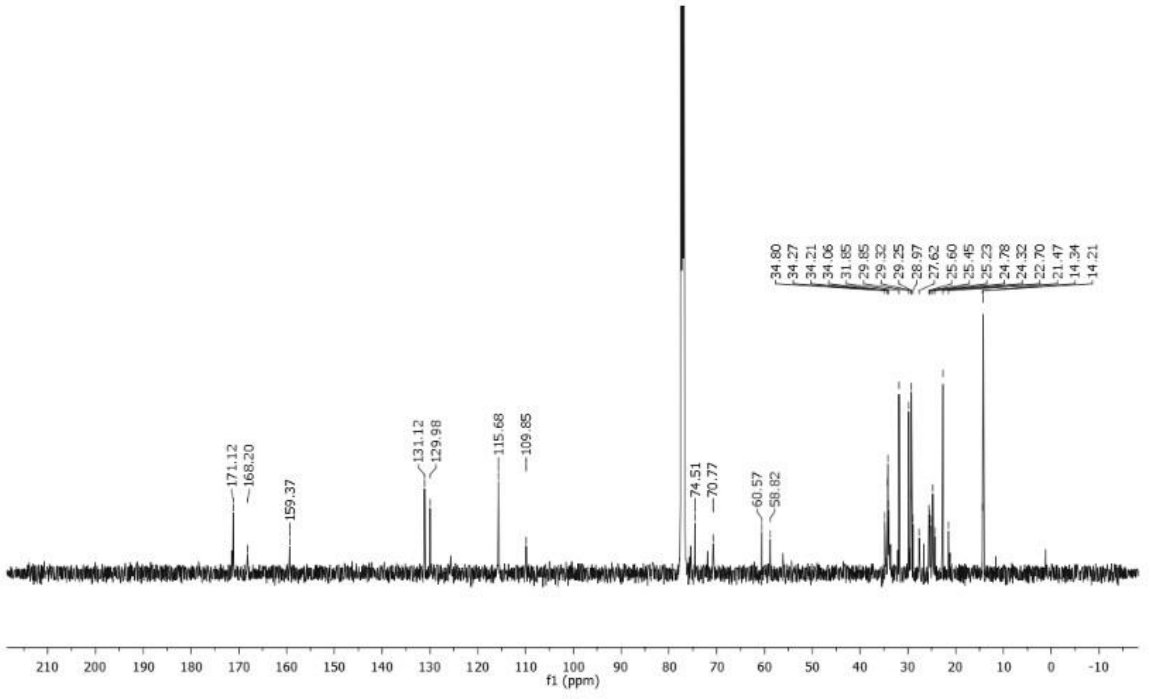
f1 (ppm)

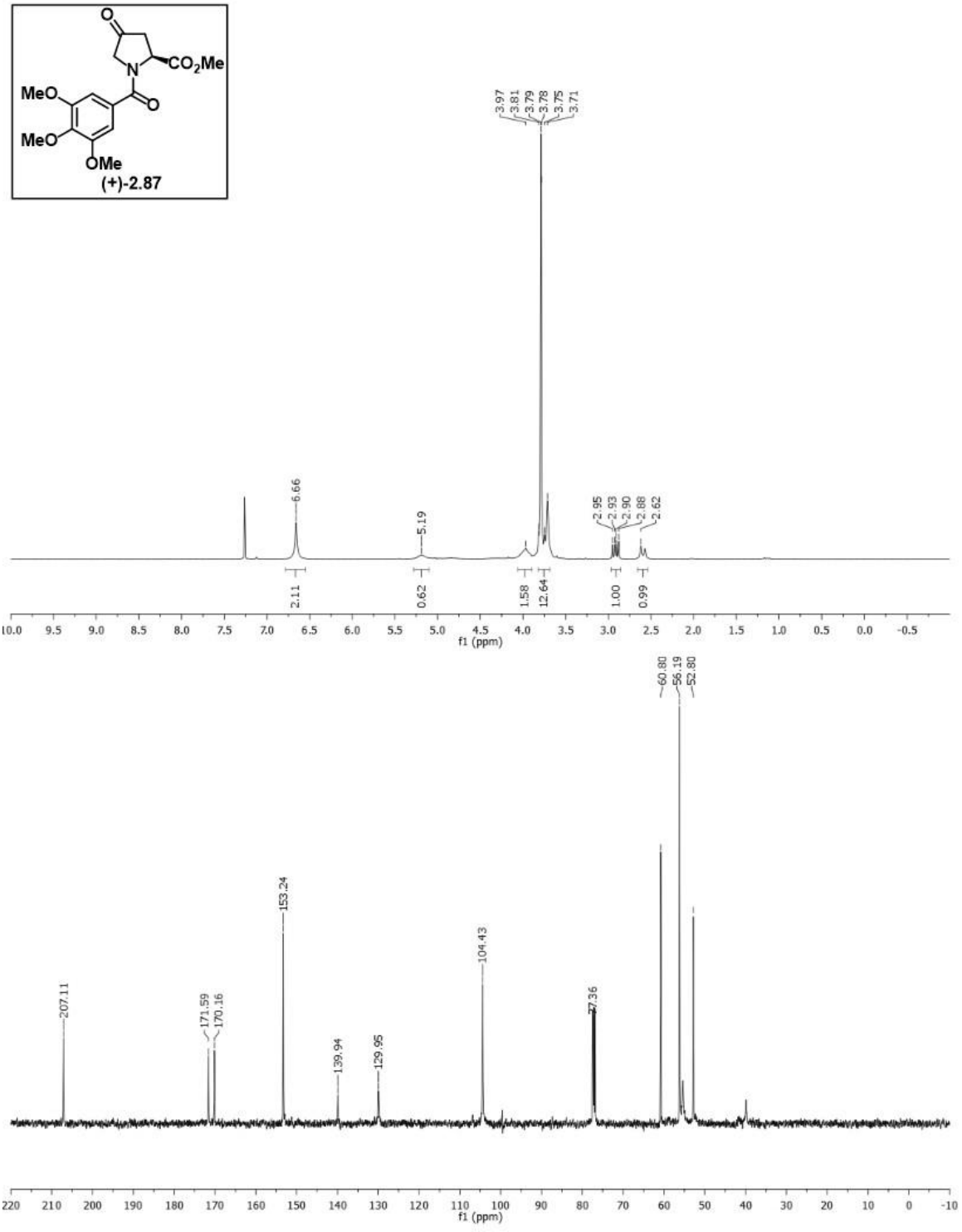
MeO
MeO
OMe
CO2Me
(+)-2.87
3.97
3.81
3.79
3.78
3.75
3.71
6.66
5.19
2.95
2.93
2.90
2.88
2.62
2.11
0.62
1.58
12.64
1.00
0.99
f1 (ppm)
60.80
56.19
52.80
207.11
171.59
170.16
153.24
139.94
129.95
104.43
27.36
f1 (ppm)

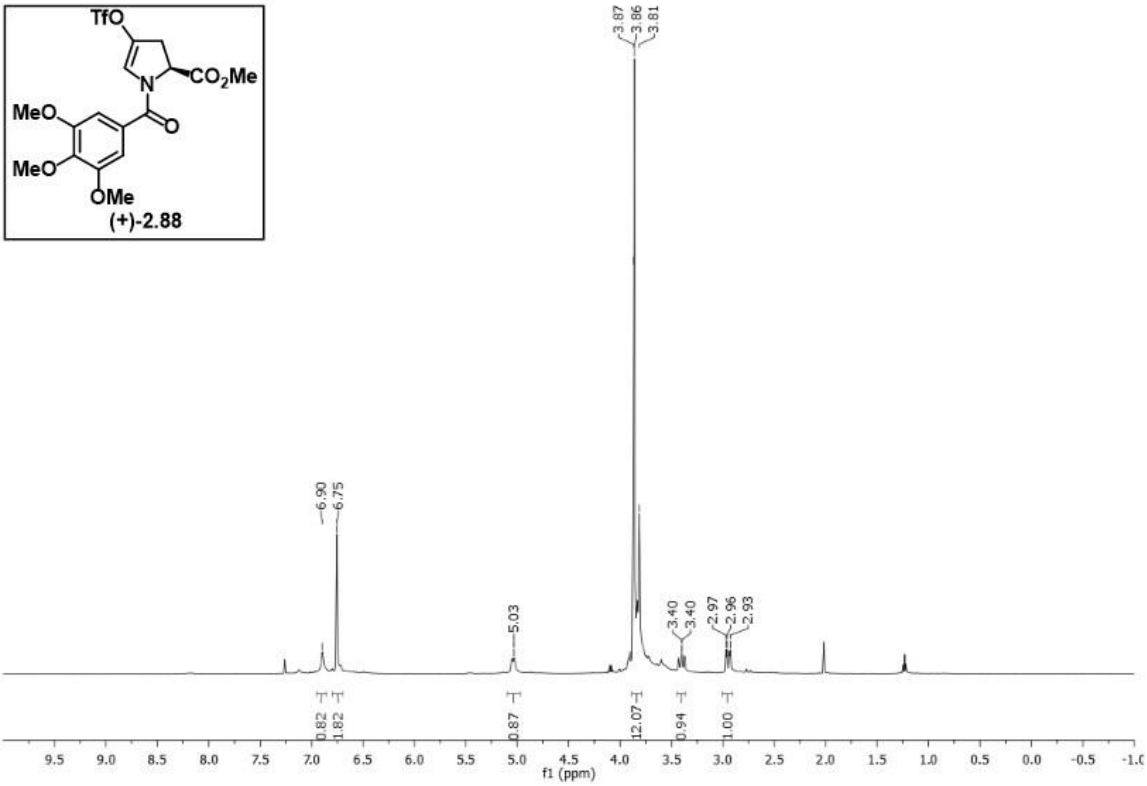
TfO
CO2Me
N
O
MeO
MeO
OMe
(+)-2.88
3.87
3.86
3.81
6.90
6.75
5.03
3.40
3.40
2.97
2.96
2.93
0.82
1.82
0.87
12.07
0.94
1.00
f1 (ppm)

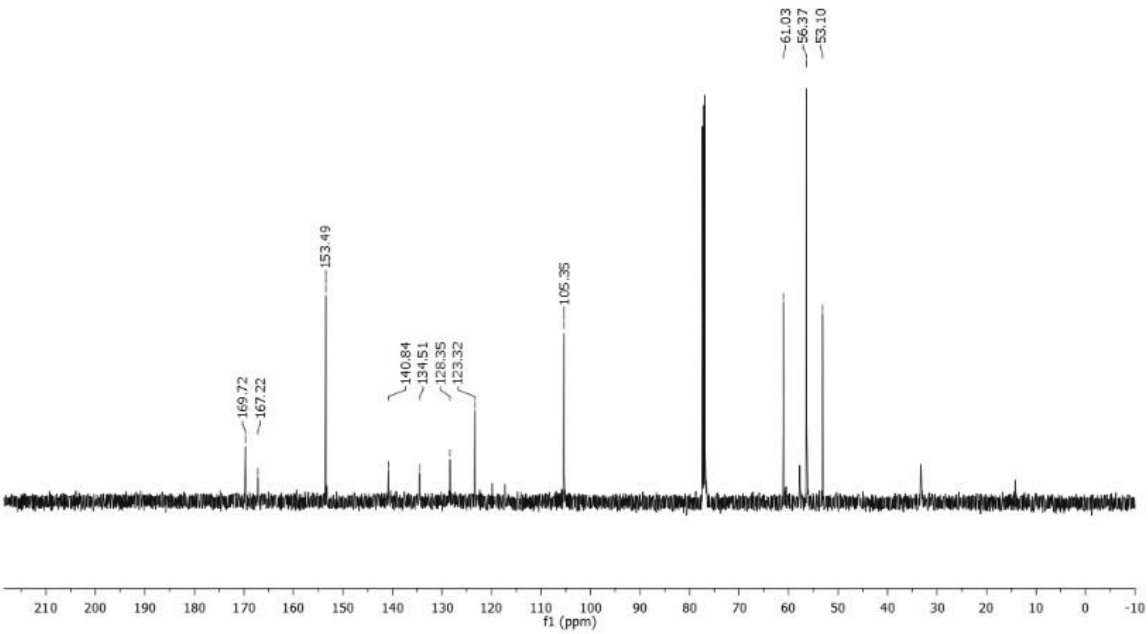
61.03
56.37
53.10
153.49
105.35
169.72
167.22
140.84
134.51
128.35
123.32
f1 (ppm)

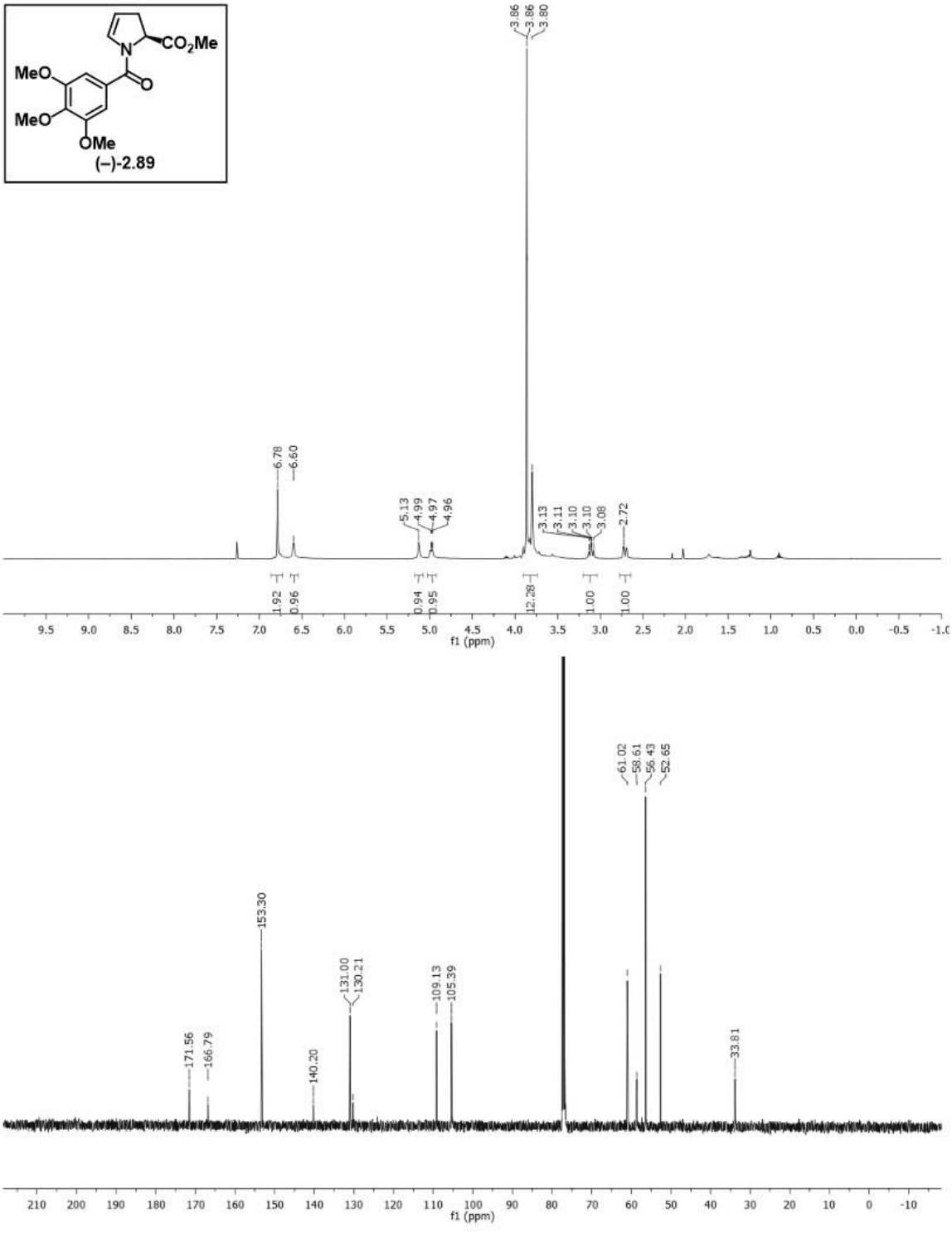
CO2Me
N
O
MeO
MeO
OMe
(–)-2.89
3.86
3.86
3.80
6.78
6.60
5.13
4.99
4.97
4.96
3.13
3.11
3.10
3.10
3.08
2.72
1.92
0.96
0.94
0.95
12.28
1.00
1.00
f1 (ppm)
61.02
58.61
56.43
52.65
153.30
131.00
130.21
109.13
105.39
171.56
166.79
140.20
33.81
f1 (ppm)

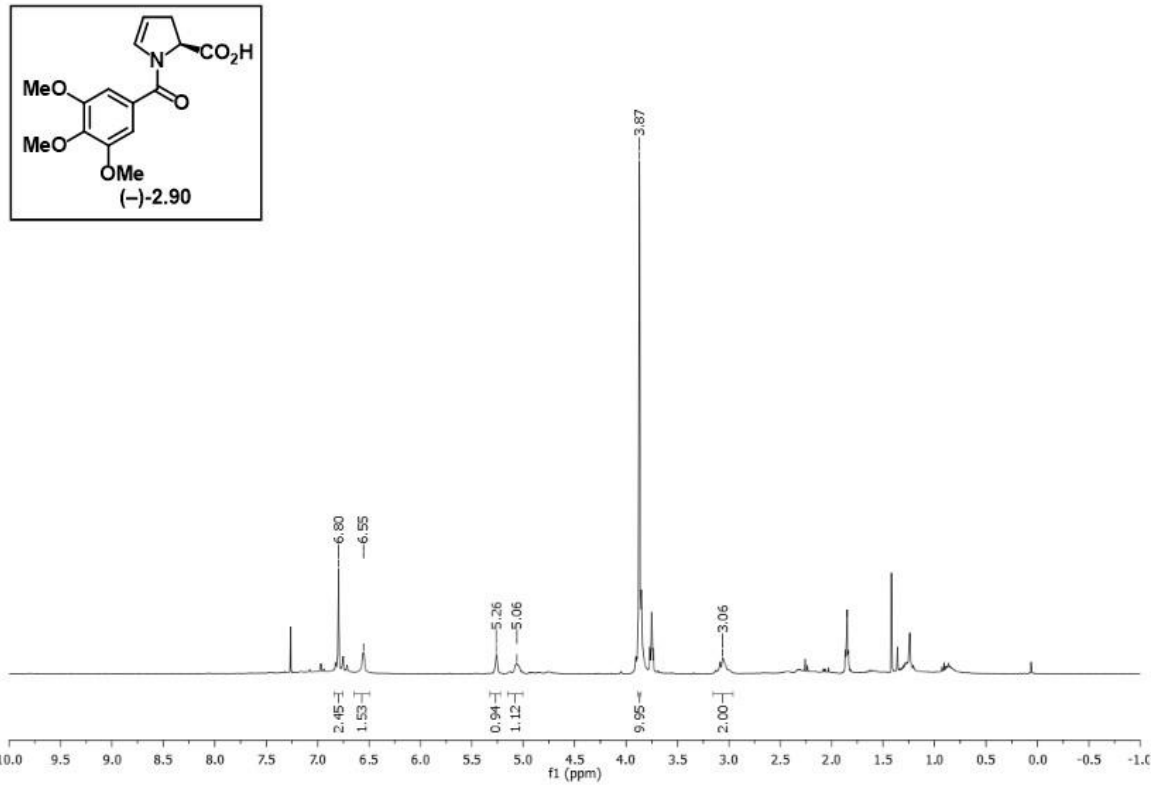
CO2H
N
O
MeO
MeO
OMe
(–)-2.90
3.87
6.80
6.55
5.26
5.06
3.06
2.45
1.53
0.94
1.12
9.95
2.00
f1 (ppm)

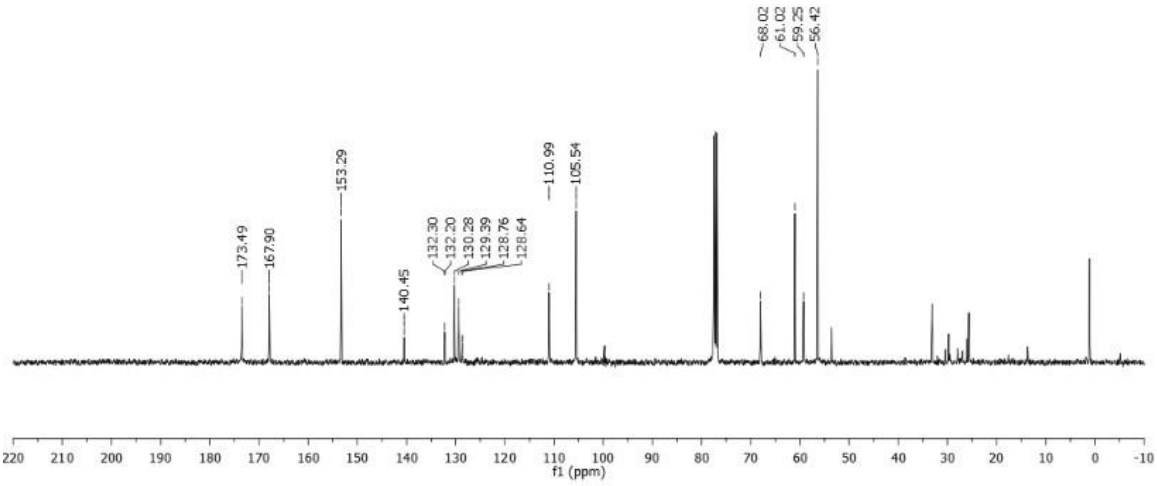
68.02
61.02
59.25
56.42
153.29
110.99
105.54
173.49
167.90
140.45
132.30
132.20
130.28
129.39
128.76
128.64
f1 (ppm)

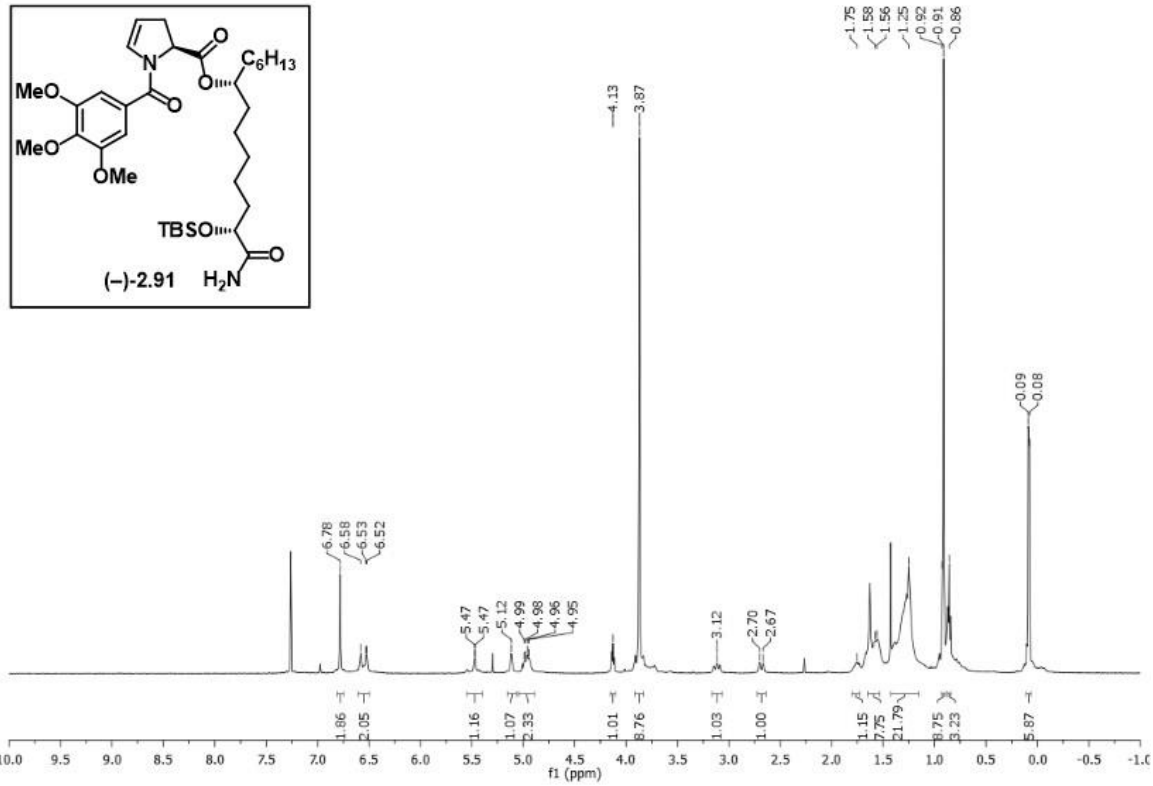
MeO
MeO
OMe
N
O
O
O
C6H13
TBSO
O
H2N
(–)-2.91
1.75
1.58
1.56
1.25
0.92
0.91
0.86
4.13
3.87
0.09
0.08
6.78
6.58
6.53
6.52
5.47
5.47
5.12
4.99
4.98
4.96
4.95
3.12
2.70
2.67
1.86
2.05
1.16
1.07
2.33
1.01
8.76
1.03
1.00
1.15
7.75
21.79
8.75
3.23
5.87
f1 (ppm)

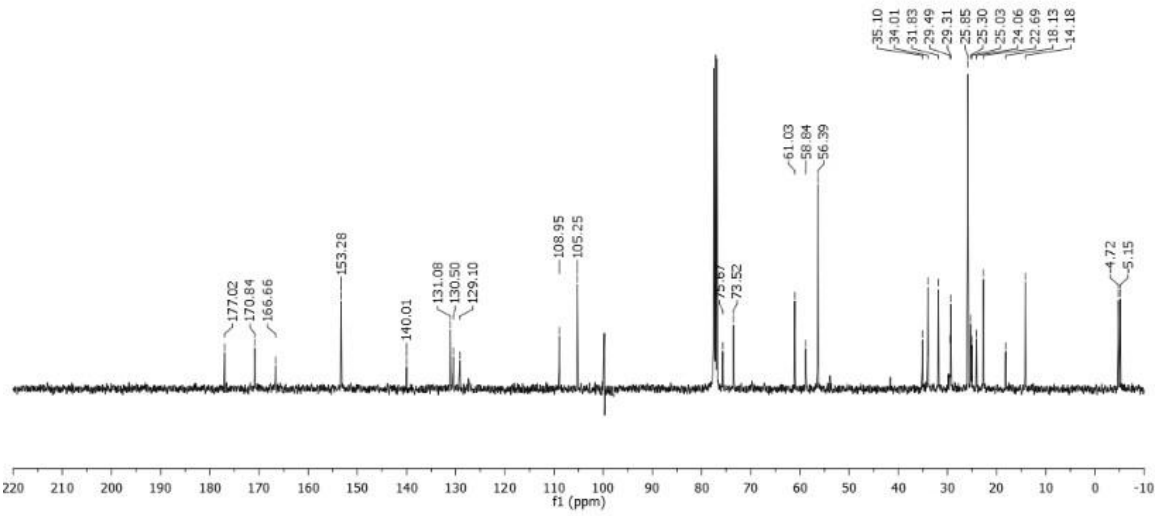
35.10
34.01
31.83
29.49
29.31
25.85
25.30
25.03
24.06
22.69
18.13
14.18
61.03
58.84
56.39
153.28
177.02
170.84
166.66
140.01
131.08
130.50
129.10
108.95
105.25
75.87
73.52
4.72
5.15
f1 (ppm)

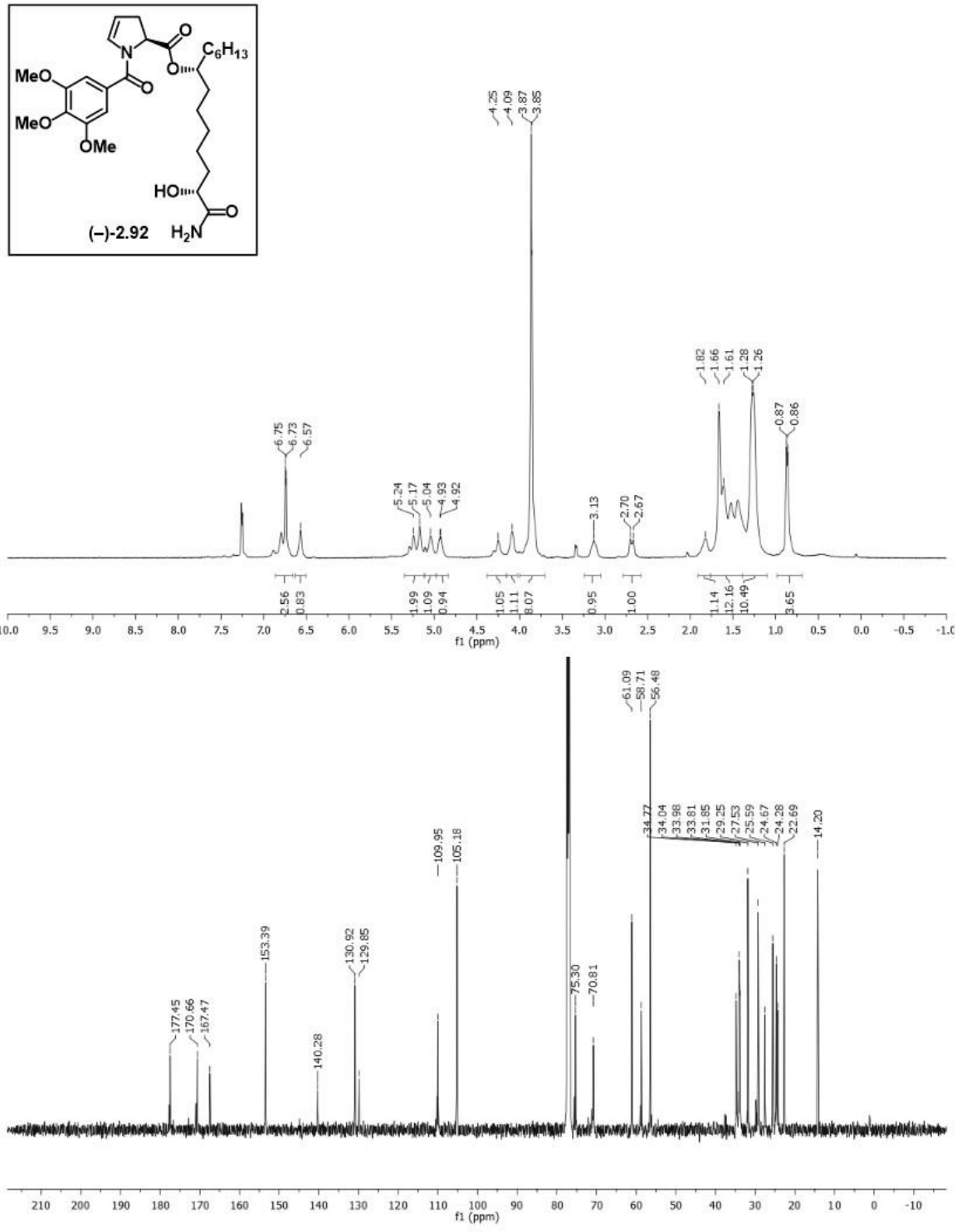
MeO
MeO
OMe
N
O
O
O
C6H13
HO
O
H2N
(–)-2.92
4.25
4.09
3.87
3.85
6.75
6.73
6.57
5.24
5.17
5.04
4.93
4.92
3.13
2.70
2.67
1.82
1.66
1.61
1.28
1.26
0.87
0.86
2.56
0.83
1.99
1.09
0.94
1.05
1.11
8.07
0.95
1.00
1.14
12.16
10.49
3.65
f1 (ppm)
61.09
58.71
56.48
34.77
34.04
33.98
33.81
31.85
29.25
27.53
25.59
24.67
24.28
22.69
14.20
109.95
105.18
153.39
130.92
129.85
140.28
177.45
170.66
167.47
75.30
70.81
f1 (ppm)

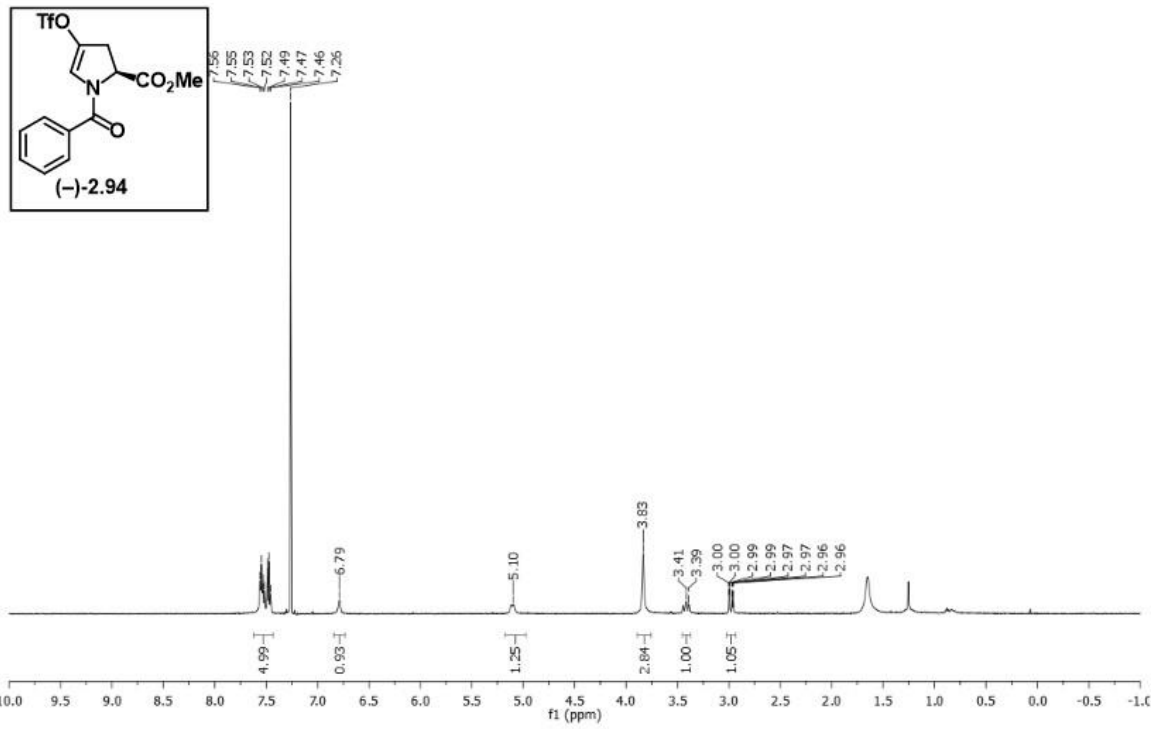
TfO
CO2Me
N
O
(–)-2.94
7.56
7.55
7.53
7.52
7.49
7.47
7.46
7.26
6.79
5.10
3.83
3.41
3.39
3.00
3.00
2.99
2.99
2.97
2.97
2.96
2.96
4.99
0.93
1.25
2.84
1.00
1.05
f1 (ppm)

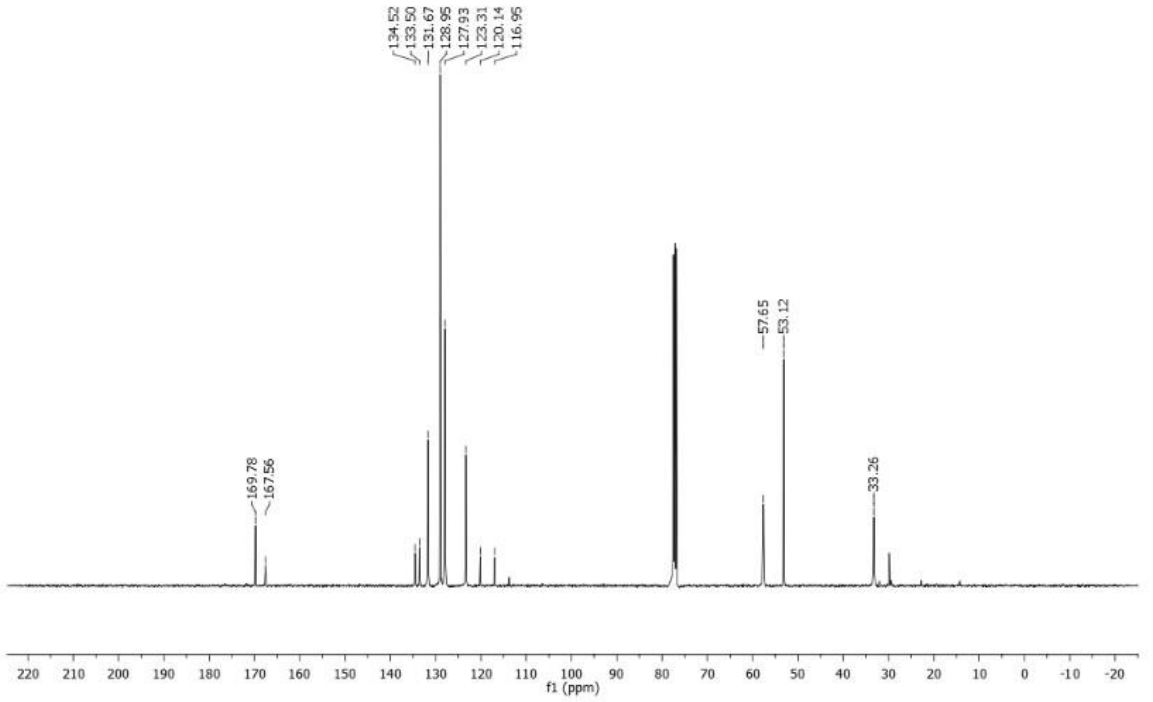
134.52
133.50
131.67
128.95
127.93
123.31
120.14
116.95
57.65
53.12
169.78
167.56
33.26
f1 (ppm)

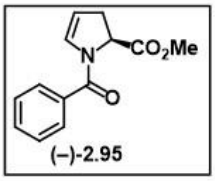
CO2Me
N
O

(–)-2.95

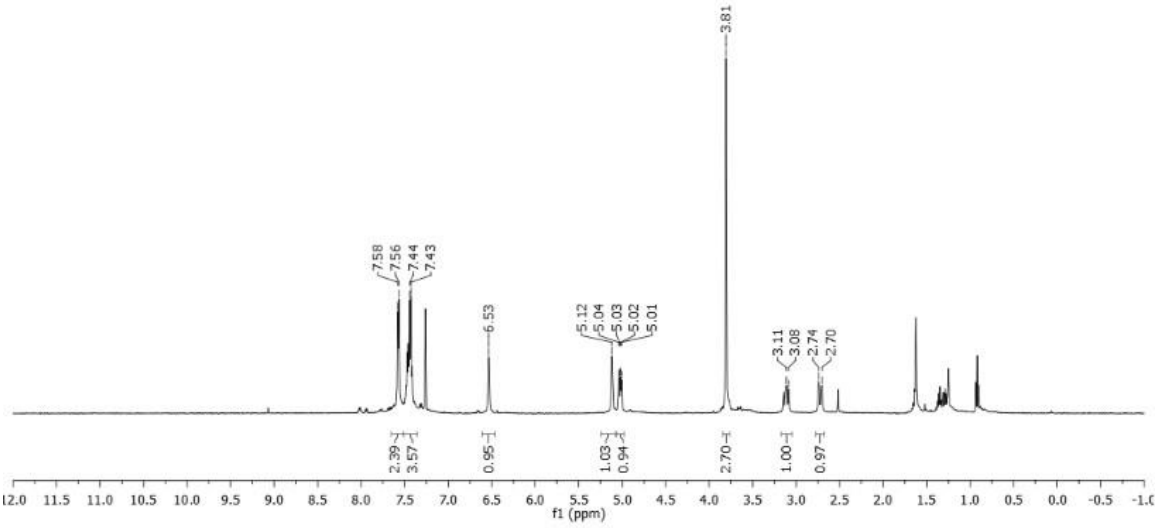
7.58
7.56
7.44
7.43
6.53
5.12
5.04
5.03
5.02
5.01
3.81
3.11
3.08
2.74
2.70
2.39
3.57
0.95
1.03
0.94
2.70
1.00
0.97
f1 (ppm)

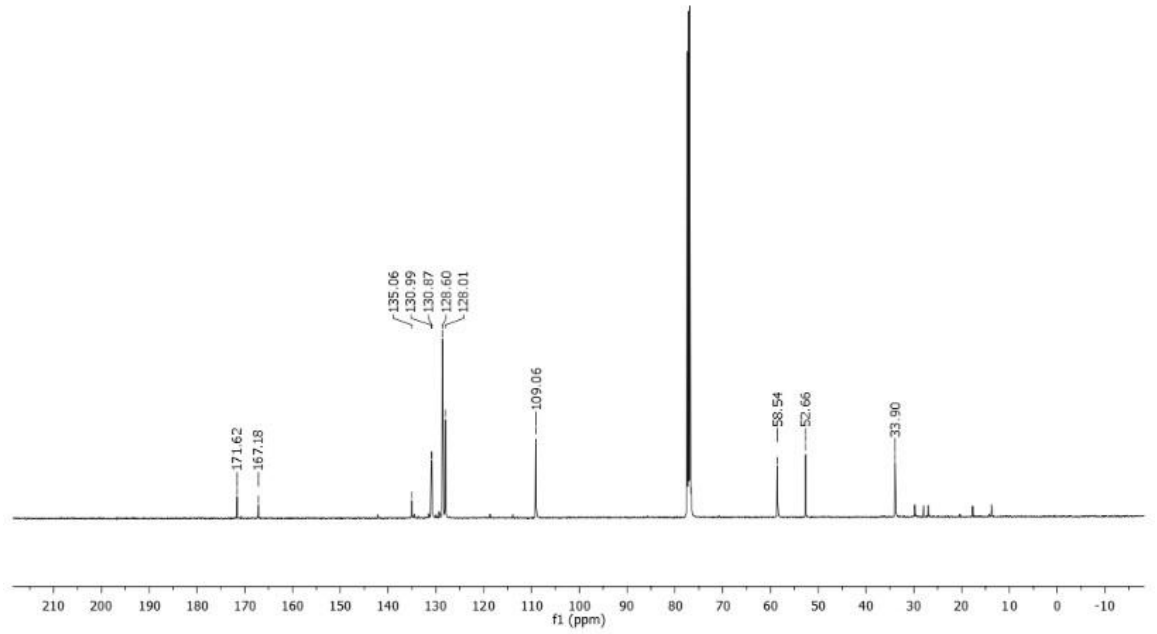
135.06
130.99
130.87
128.60
128.01
109.06
171.62
167.18
58.54
52.66
33.90
f1 (ppm)

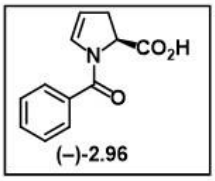
CO2H
N
O

(–)-2.96

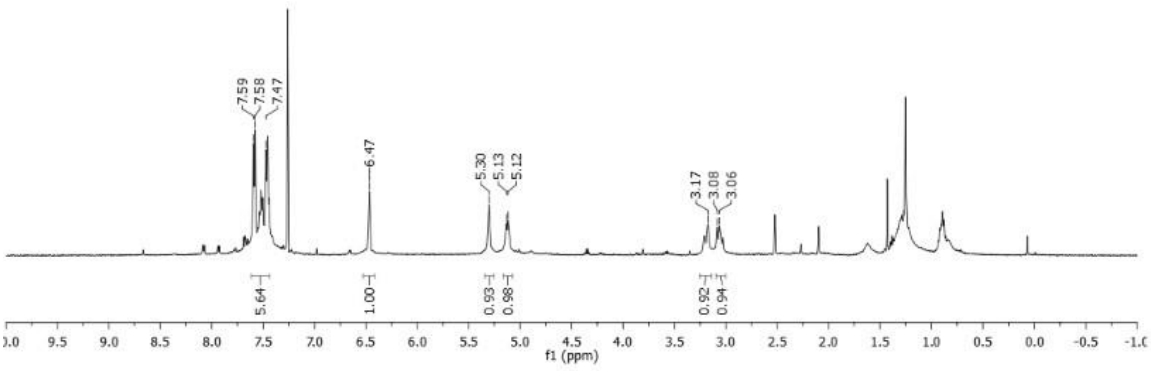
7.59
7.58
7.47
6.47
5.30
5.13
5.12
3.17
3.08
3.06
5.64
1.00
0.93
0.98
0.92
0.94
f1 (ppm)

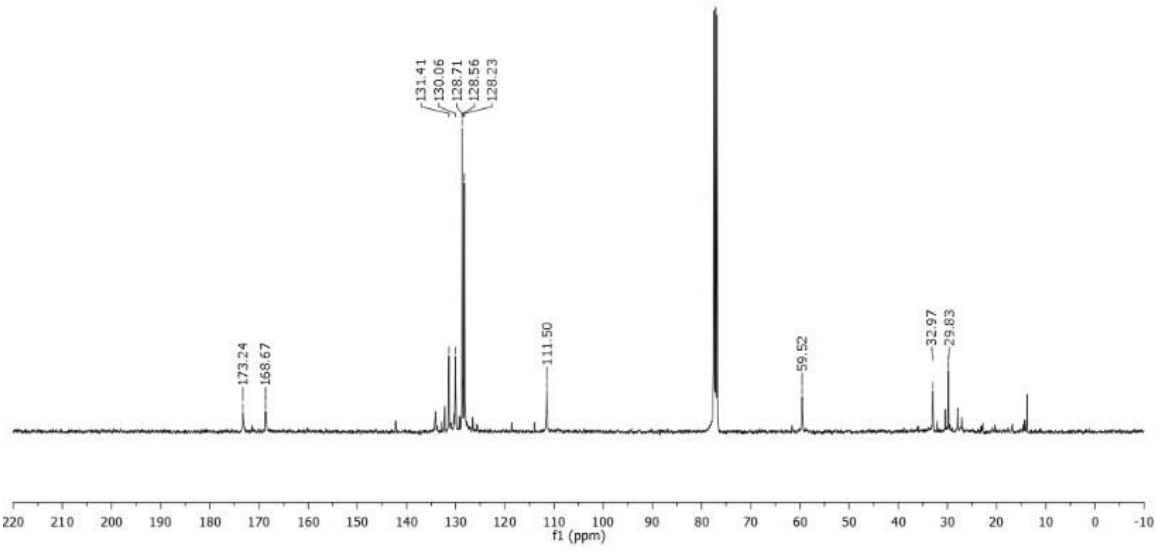
131.41
130.06
128.71
128.56
128.23
173.24
168.67
111.50
59.52
32.97
29.83
f1 (ppm)

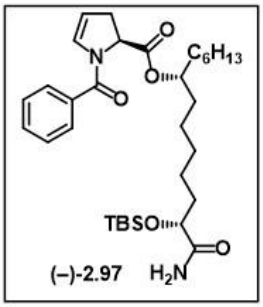
C6H13
TBSO
(–)-2.97
H2N

1.69
1.57
1.56
1.54
1.25
0.91
0.85
0.08
0.07
7.56
7.54
7.43
7.42
6.51
5.56
5.10
4.99
4.98
4.94
4.12
3.11
3.09
2.70
2.66
2.32
3.72
2.12
1.09
1.13
2.28
1.11
1.00
1.03
9.06
21.02
9.87
5.39
7.20
f1 (ppm)

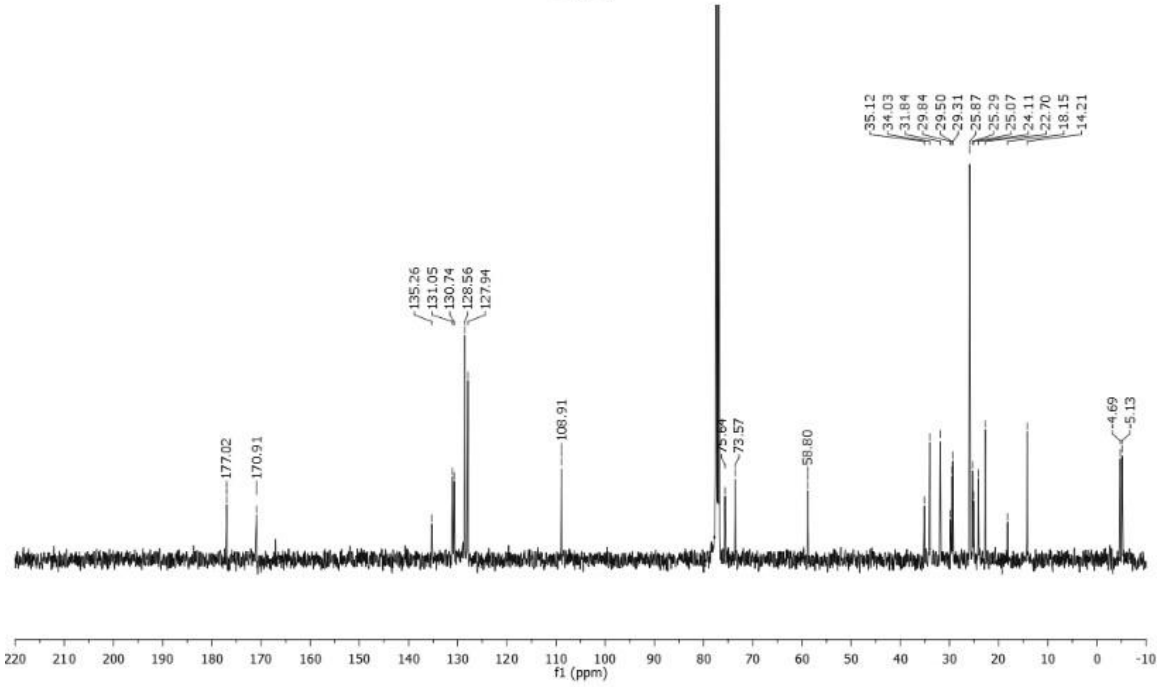
35.12
34.03
31.84
29.84
29.50
29.31
25.87
25.29
25.07
24.11
22.70
18.15
14.21
135.26
131.05
130.74
128.56
127.94
177.02
170.91
108.91
73.57
58.80
4.69
5.13
f1 (ppm)

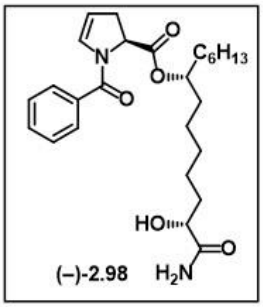
C_6H_{13}
HO
H_2N
(–)-2.98

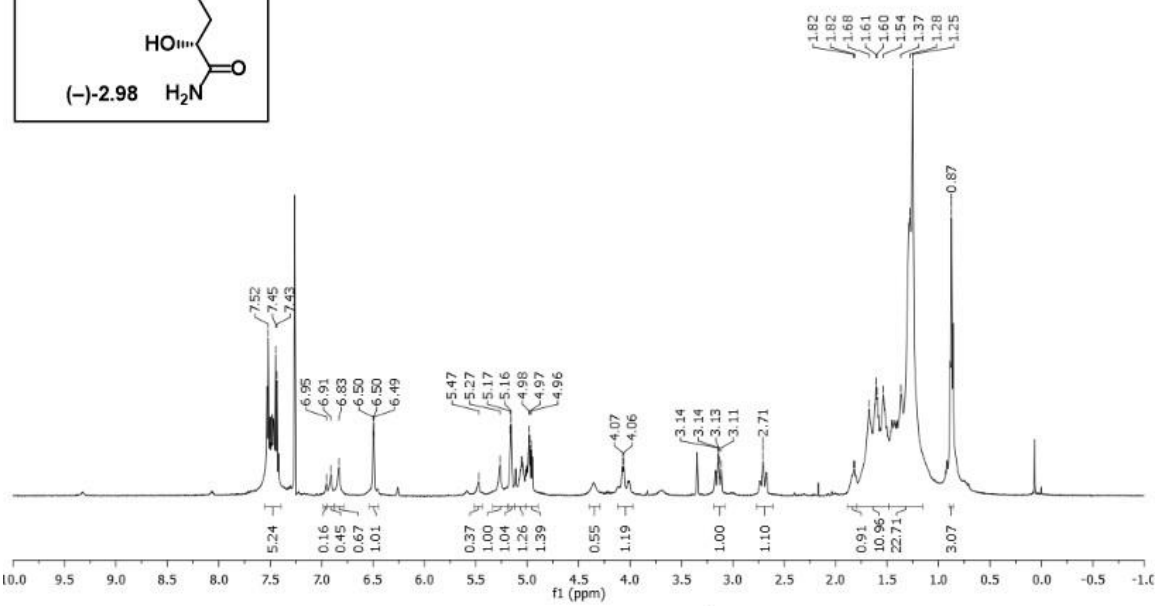
7.52
7.45
7.43
6.95
6.91
6.83
6.50
6.50
6.49
5.47
5.27
5.17
5.16
4.98
4.97
4.96
4.07
4.06
3.14
3.14
3.13
3.11
2.71
1.82
1.82
1.68
1.61
1.60
1.54
1.37
1.28
1.25
0.87
5.24
0.16
0.45
0.67
1.01
0.37
1.00
1.04
1.26
1.39
0.55
1.19
1.00
1.10
0.91
10.96
22.71
3.07
f1 (ppm)

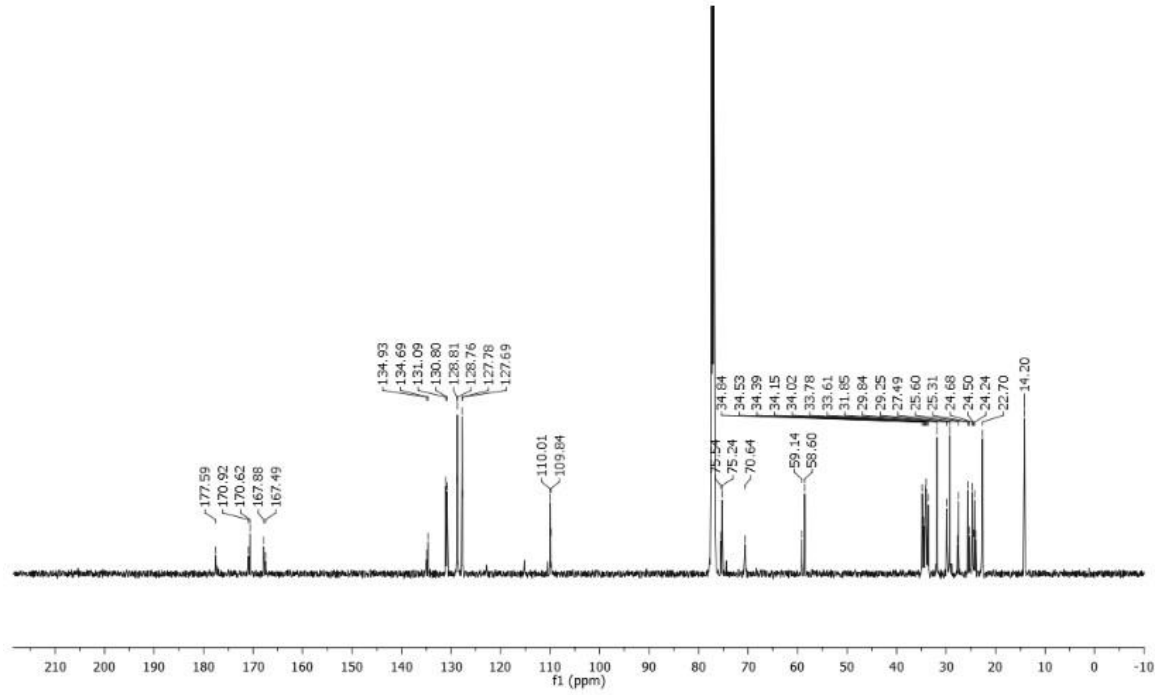
134.93
134.69
131.09
130.80
128.81
128.76
127.78
127.69
177.59
170.92
170.62
167.88
167.49
110.01
109.84
75.54
75.24
70.64
59.14
58.60
34.84
34.53
34.39
34.15
34.02
33.78
33.61
31.85
29.84
29.25
27.49
25.60
25.31
24.68
24.50
24.24
22.70
14.20
f1 (ppm)

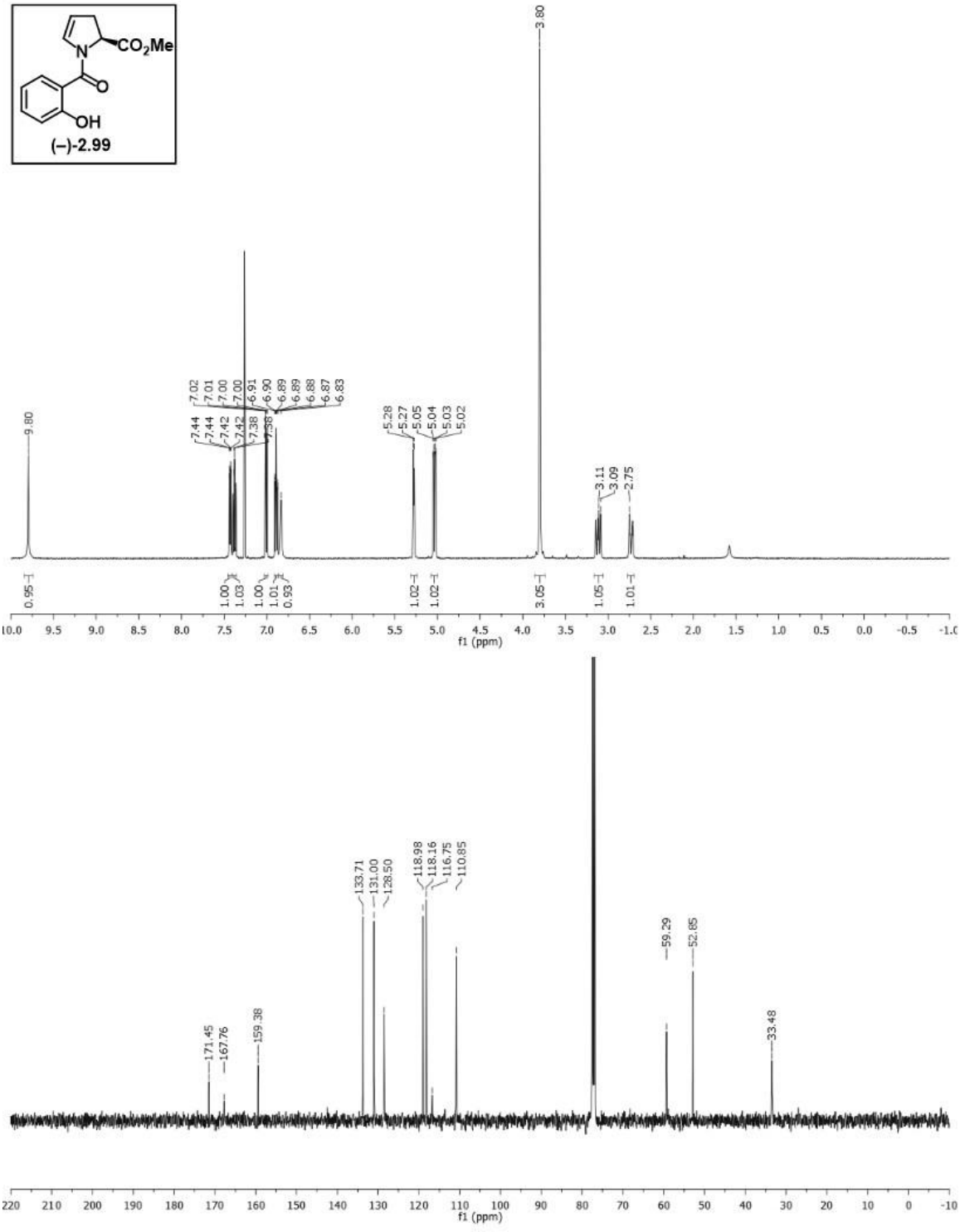
CO2Me
N
O
OH
(–)-2.99
9.80
7.44
7.44
7.42
7.42
7.38
7.38
7.02
7.01
7.00
7.00
6.91
6.90
6.89
6.89
6.88
6.87
6.83
5.28
5.27
5.05
5.04
5.03
5.02
3.80
3.11
3.09
2.75
0.95
1.00
1.03
1.00
1.01
0.93
1.02
1.02
3.05
1.05
1.01
f1 (ppm)
171.45
167.76
159.38
133.71
131.00
128.50
118.98
118.16
116.75
110.85
59.29
52.85
33.48
f1 (ppm)

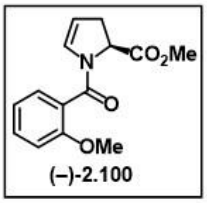
CO2Me
N
O
OMe

(–)-2.100

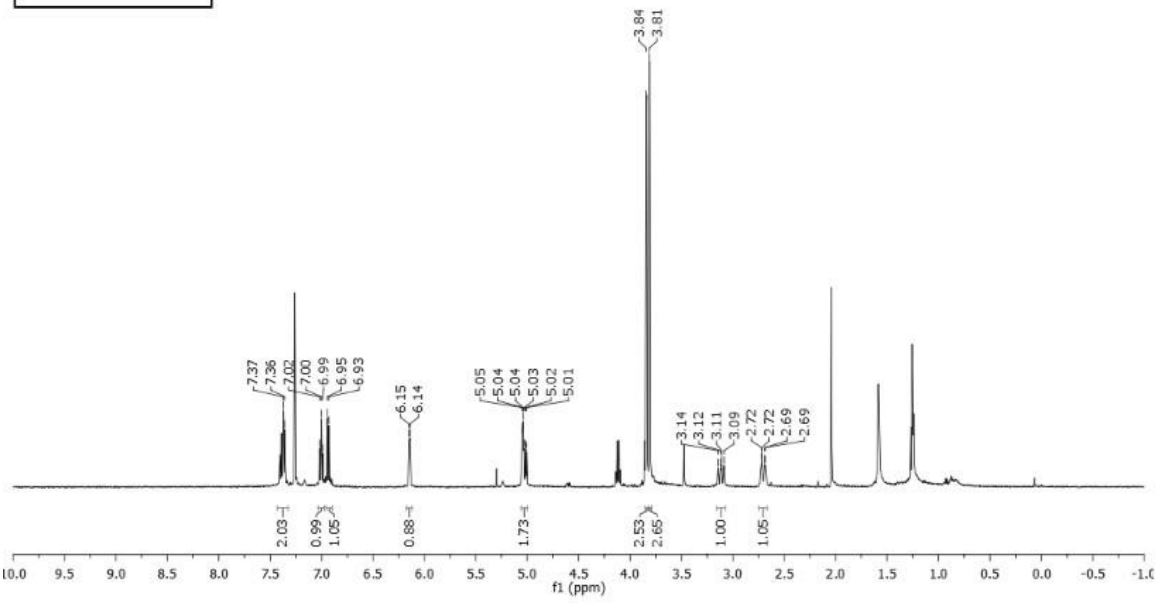
7.37
7.36
7.02
7.00
6.99
6.95
6.93
6.15
6.14
5.05
5.04
5.04
5.03
5.02
5.01
3.84
3.81
3.14
3.12
3.11
3.09
2.72
2.72
2.69
2.69
2.03
0.99
1.05
0.88
1.73
2.53
2.65
1.00
1.05
f1 (ppm)

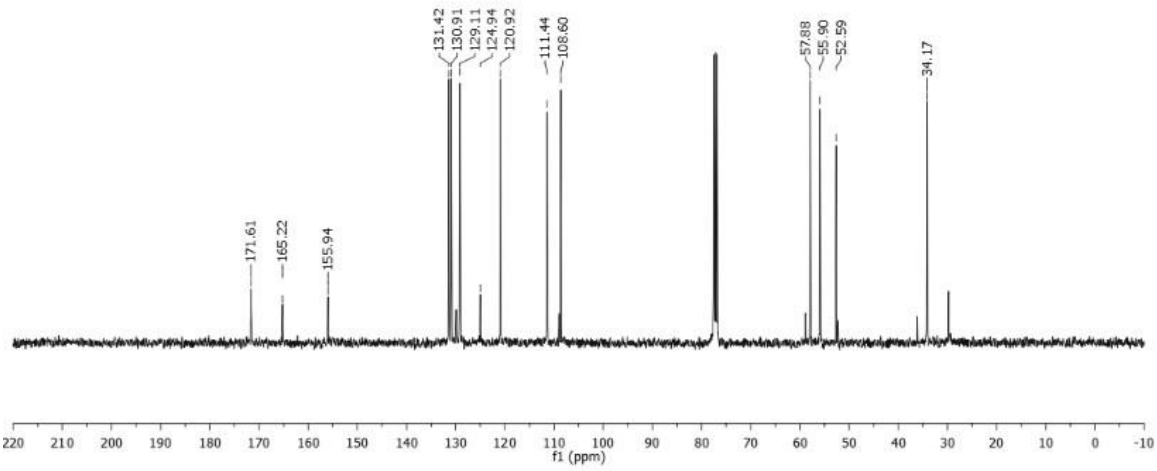
131.42
130.91
129.11
124.94
120.92
111.44
108.60
57.88
55.90
52.59
34.17
171.61
165.22
155.94
f1 (ppm)

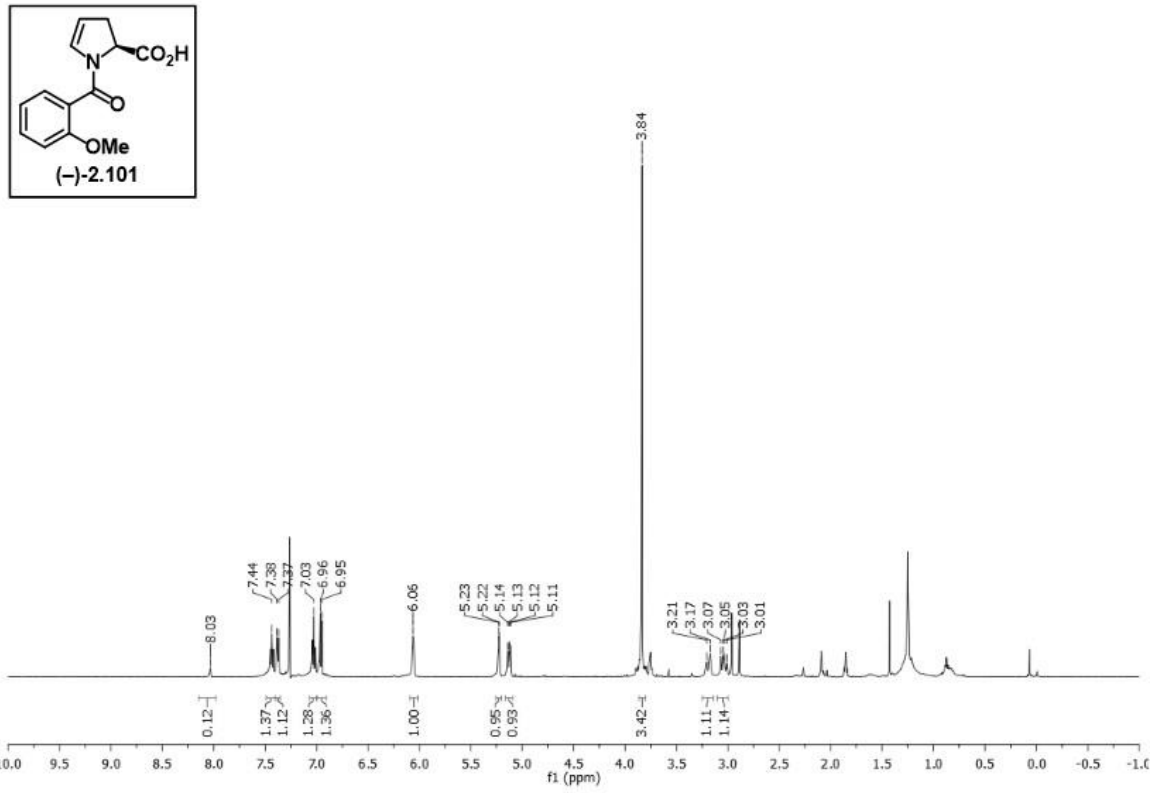
CO2H
N
O
OMe
(–)-2.101
8.03
7.44
7.38
7.37
7.03
6.96
6.95
6.06
5.23
5.22
5.14
5.13
5.12
5.11
3.84
3.21
3.17
3.07
3.05
3.03
3.01
0.12
1.37
1.12
1.28
1.36
1.00
0.95
0.93
3.42
1.11
1.14
f1 (ppm)

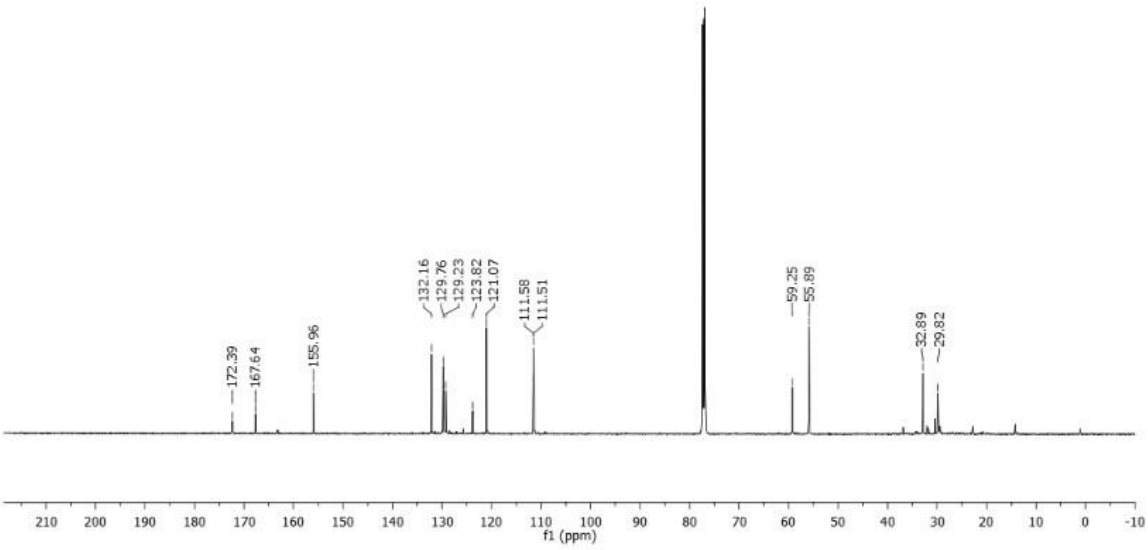
172.39
167.64
155.96
132.16
129.76
129.23
123.82
121.07
111.58
111.51
59.25
55.89
32.89
29.82
f1 (ppm)

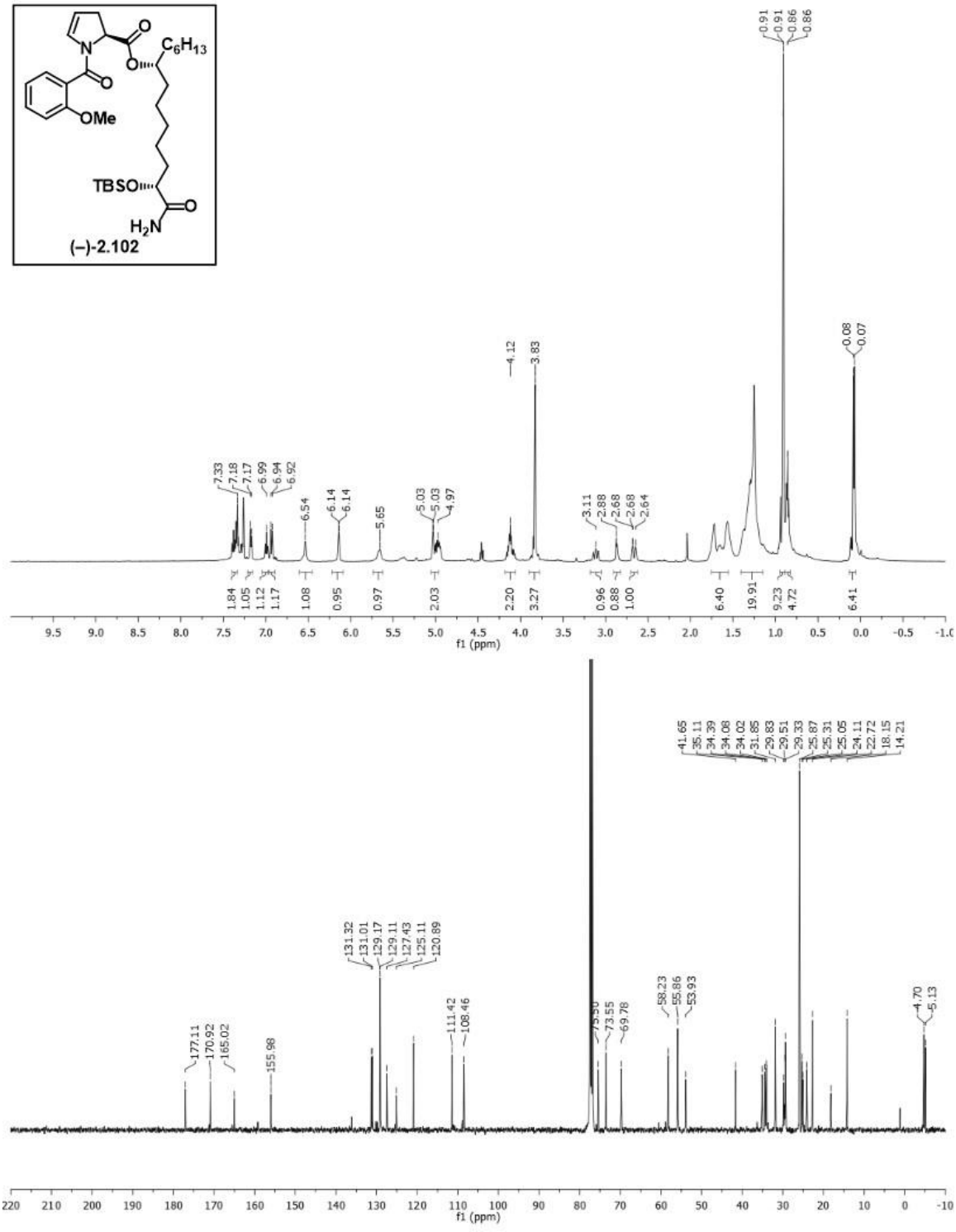
C6H13
OMe
TBSO
H2N
O
N
(–)-2.102
f1 (ppm)

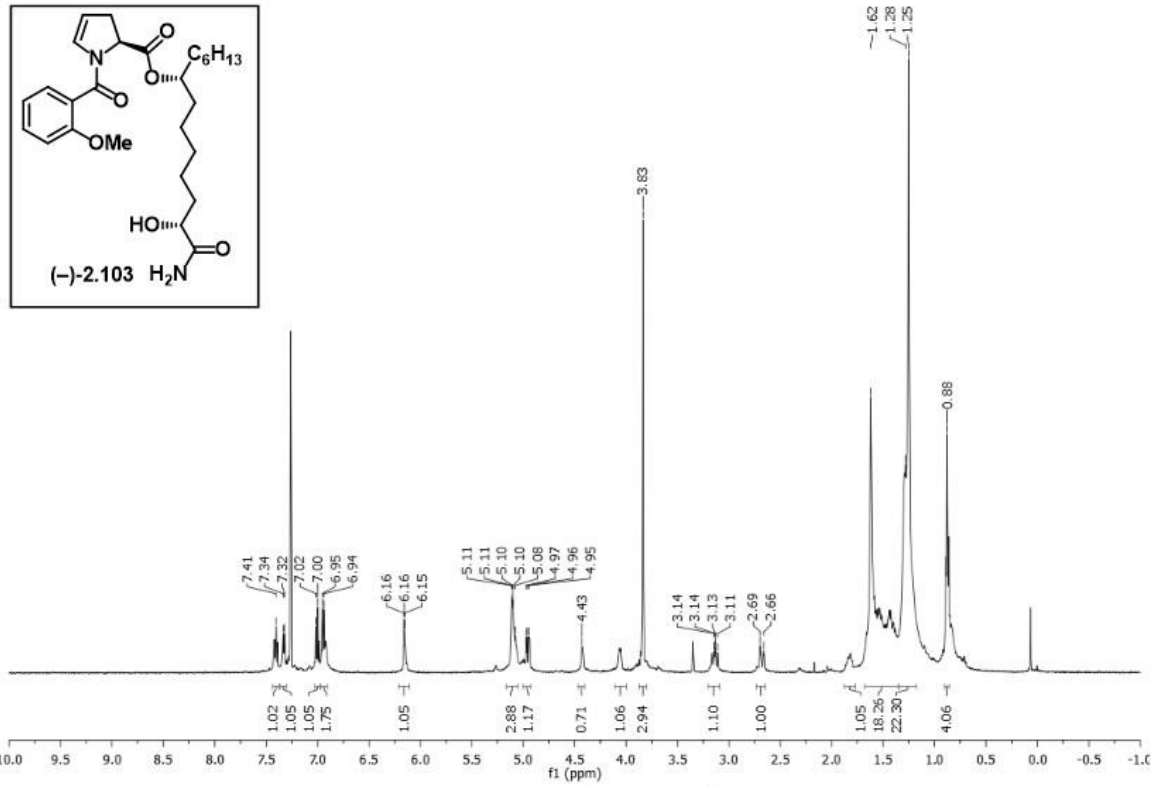
(–)-2.103

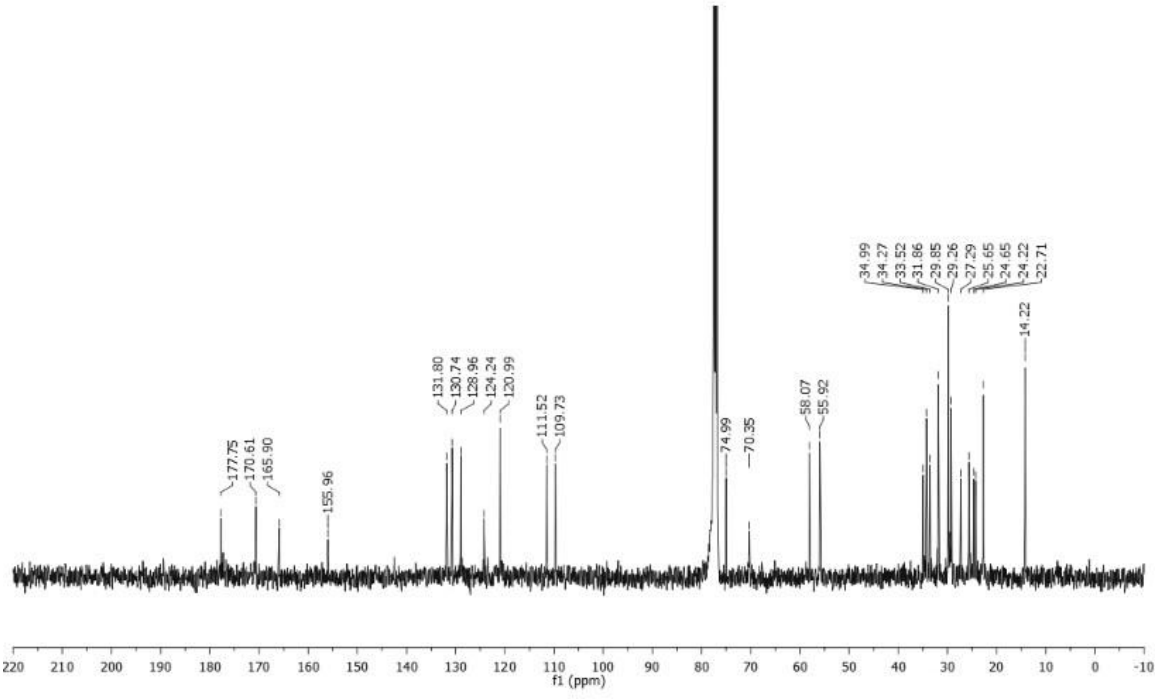
f1 (ppm)

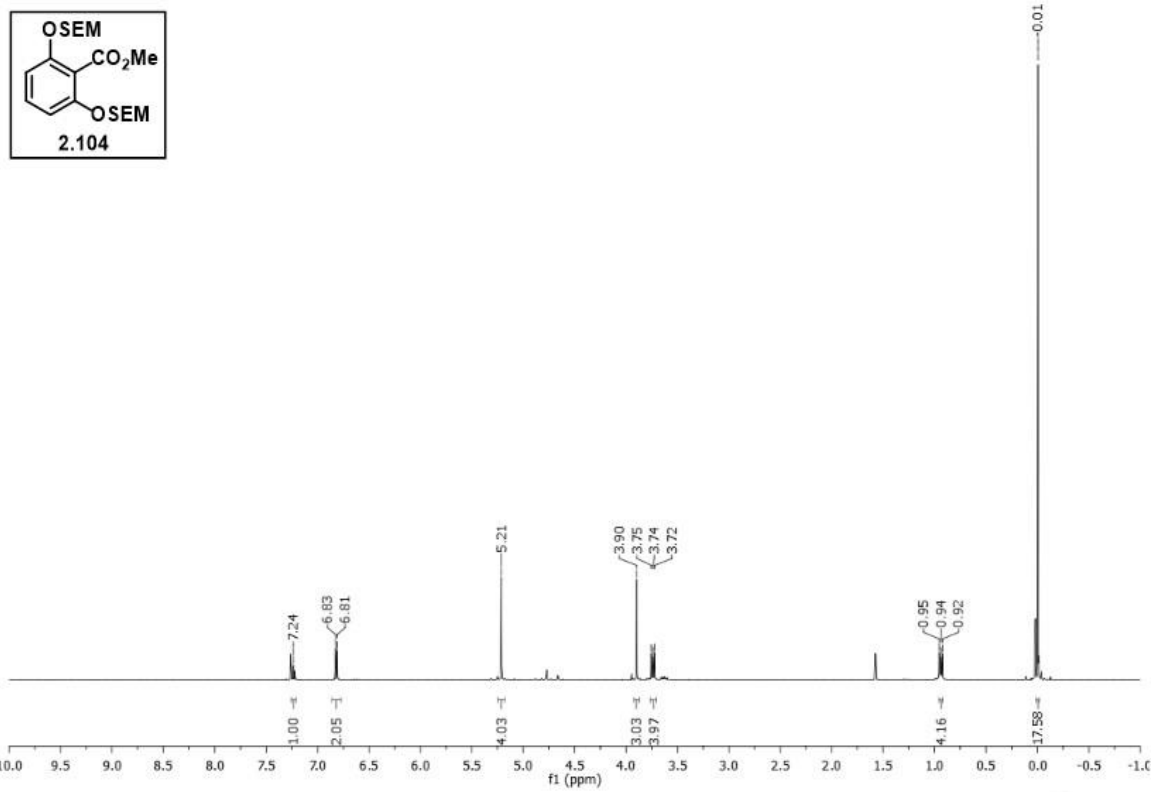
OSEM
CO2Me
OSEM
2.104
0.01
7.24
6.83
6.81
5.21
3.90
3.75
3.74
3.72
0.95
0.94
0.92
1.00
2.05
4.03
3.03
3.97
4.16
17.58
f1 (ppm)

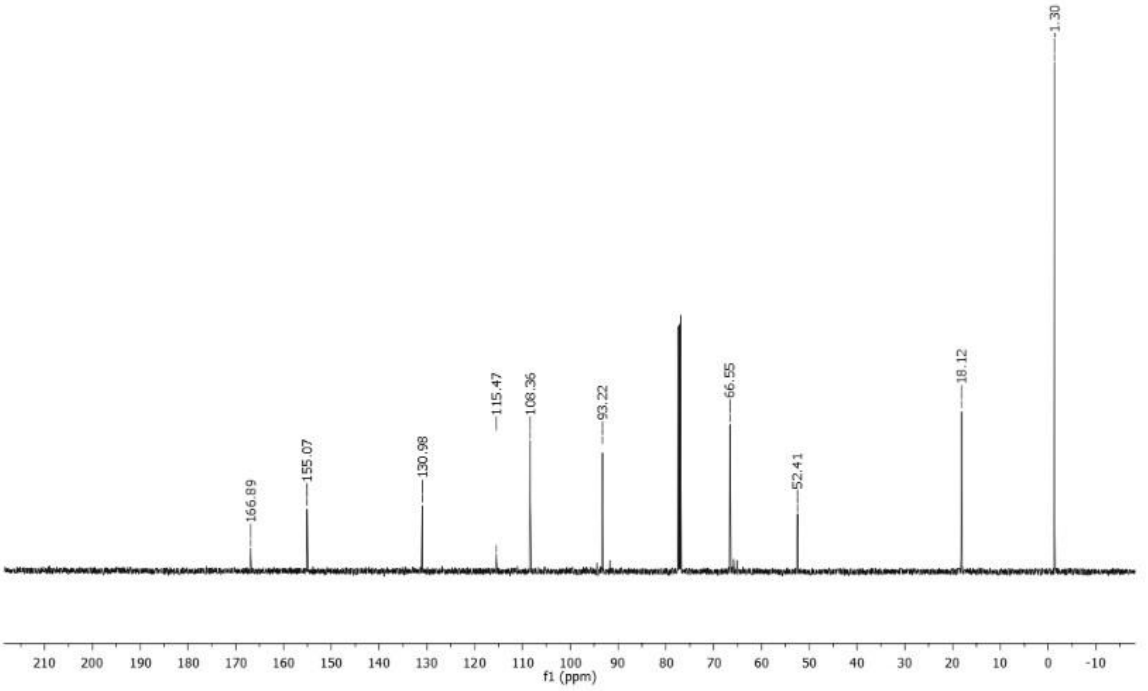
1.30
166.89
155.07
130.98
115.47
108.36
93.22
66.55
52.41
18.12
f1 (ppm)

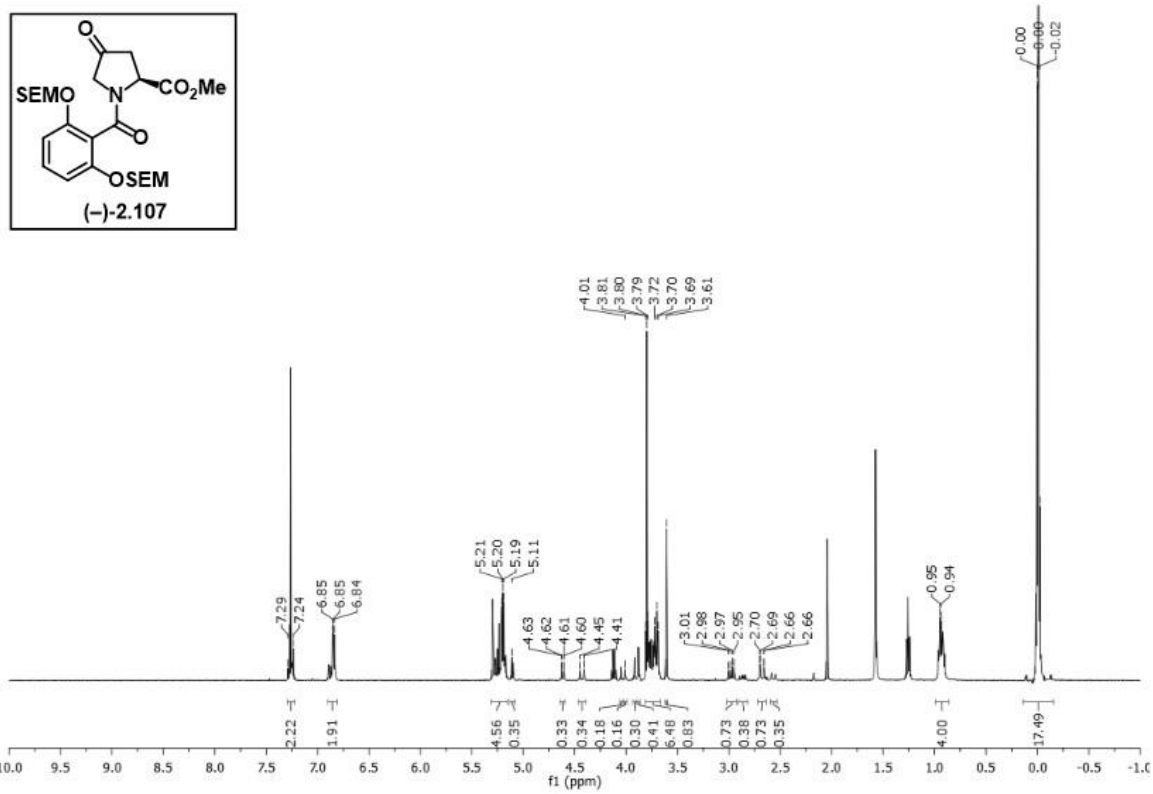
SEMO
N
CO2Me
O
OSEM
(–)-2.107
f1 (ppm)

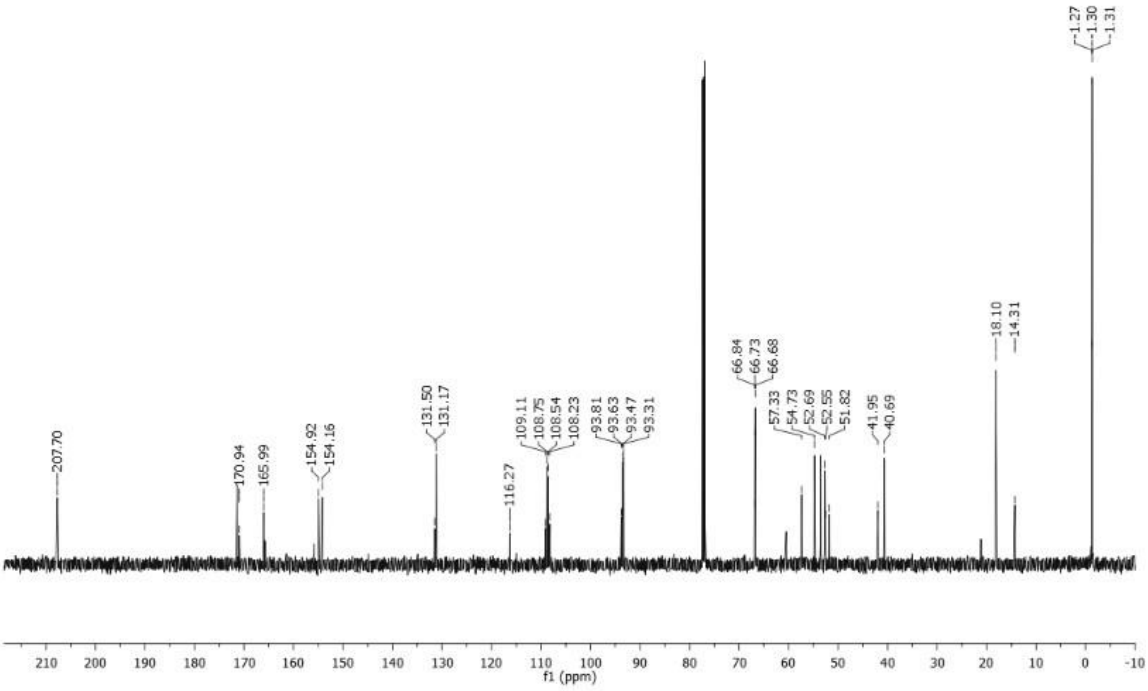
f1 (ppm)

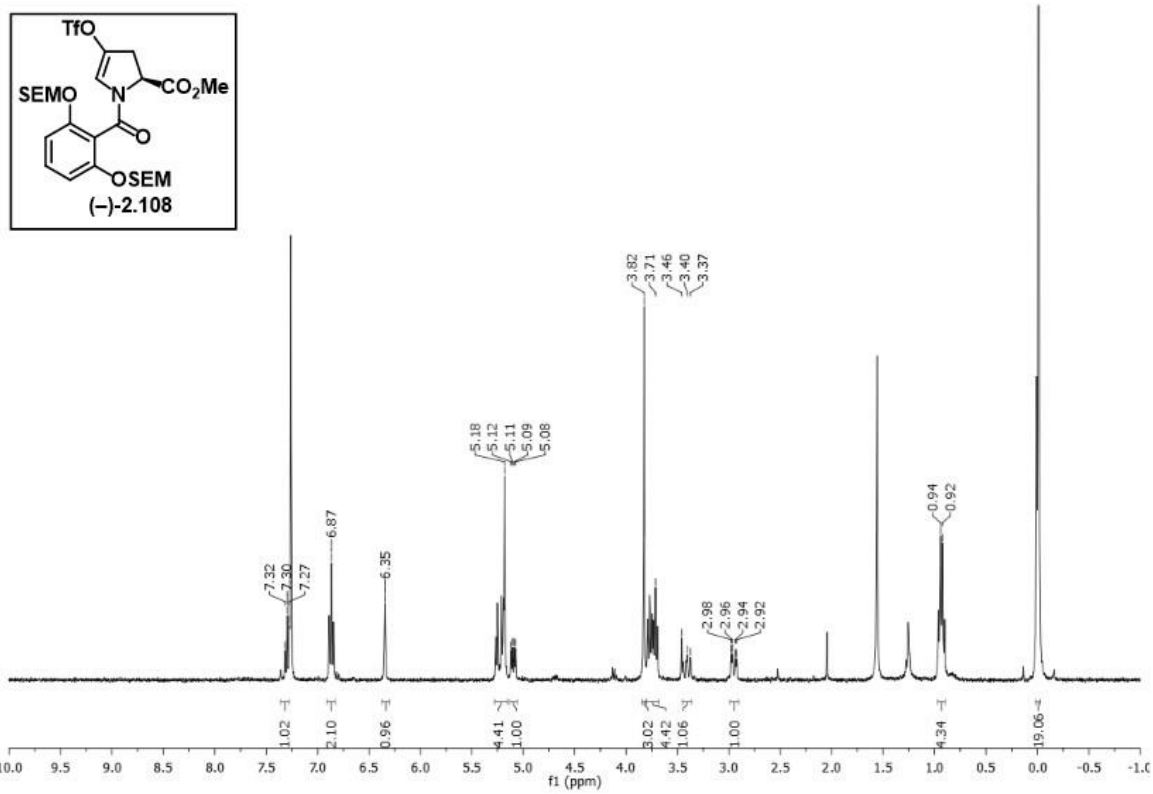
TfO
SEMO
N
CO2Me
O
OSEM
(–)-2.108
7.32
7.30
7.27
6.87
6.35
5.18
5.12
5.11
5.09
5.08
3.82
3.71
3.46
3.40
3.37
2.98
2.96
2.94
2.92
0.94
0.92
1.02
2.10
0.96
4.41
1.00
3.02
4.42
1.06
1.00
4.34
19.06
f1 (ppm)

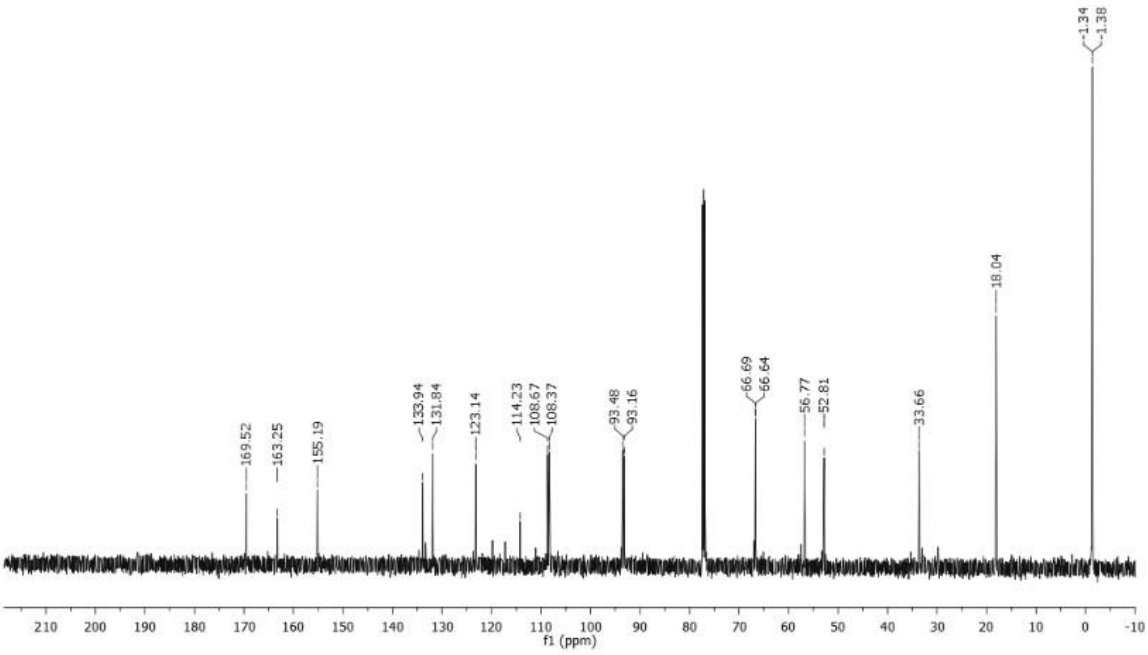
-1.34
-1.38
18.04
33.66
52.81
56.77
66.69
66.64
93.48
93.16
108.67
108.37
114.23
123.14
131.84
133.94
155.19
163.25
169.52
f1 (ppm)

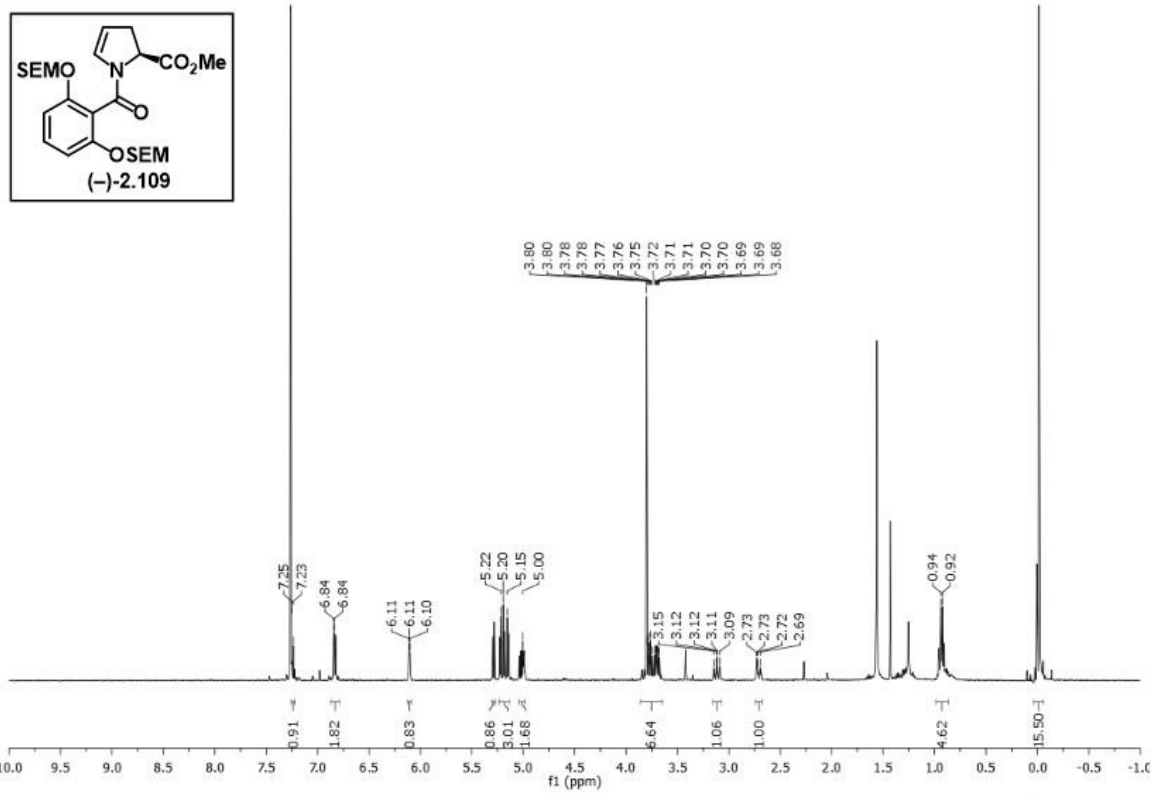
SEMO
N
CO2Me
O
OSEM
(–)-2.109
f1 (ppm)

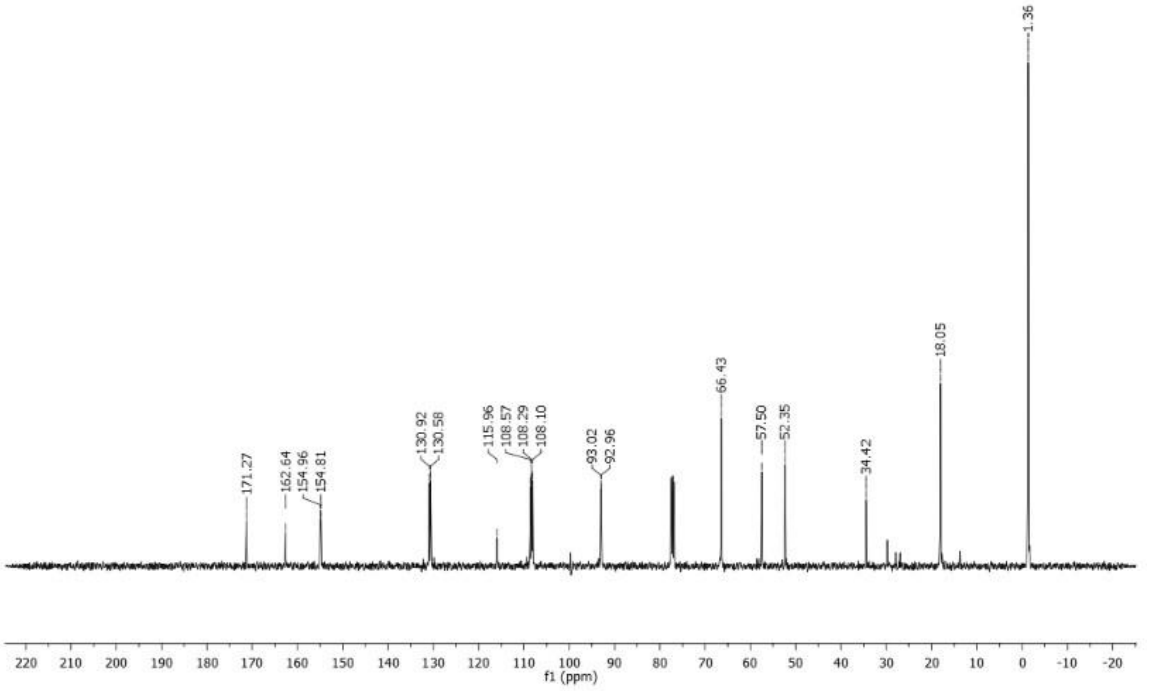
f1 (ppm)

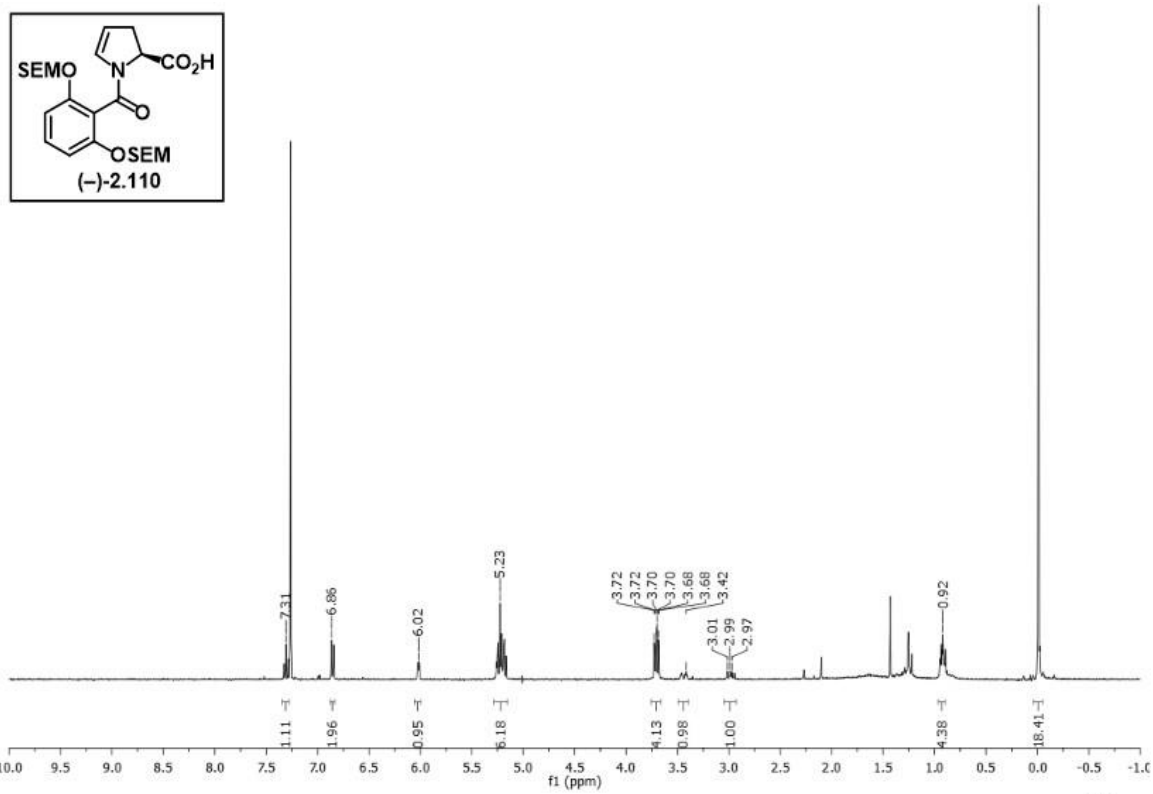
SEMO
N
CO2H
O
OSEM
(–)-2.110
7.31
6.86
6.02
5.23
3.72
3.72
3.70
3.70
3.68
3.68
3.42
3.01
2.99
2.97
0.92
1.11
1.96
0.95
6.18
4.13
0.98
1.00
4.38
18.41
f1 (ppm)

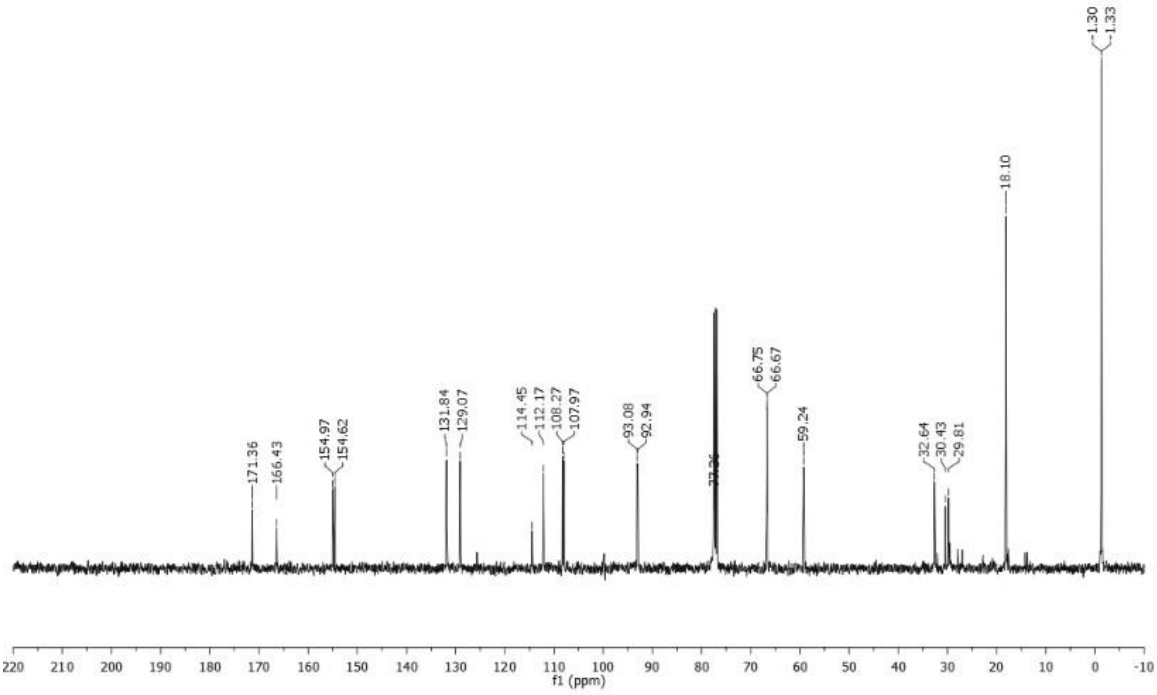
171.36
166.43
154.97
154.62
131.84
129.07
114.45
112.17
108.27
107.97
93.08
92.94
77.26
66.75
66.67
59.24
32.64
30.43
29.81
18.10
1.30
1.33
f1 (ppm)

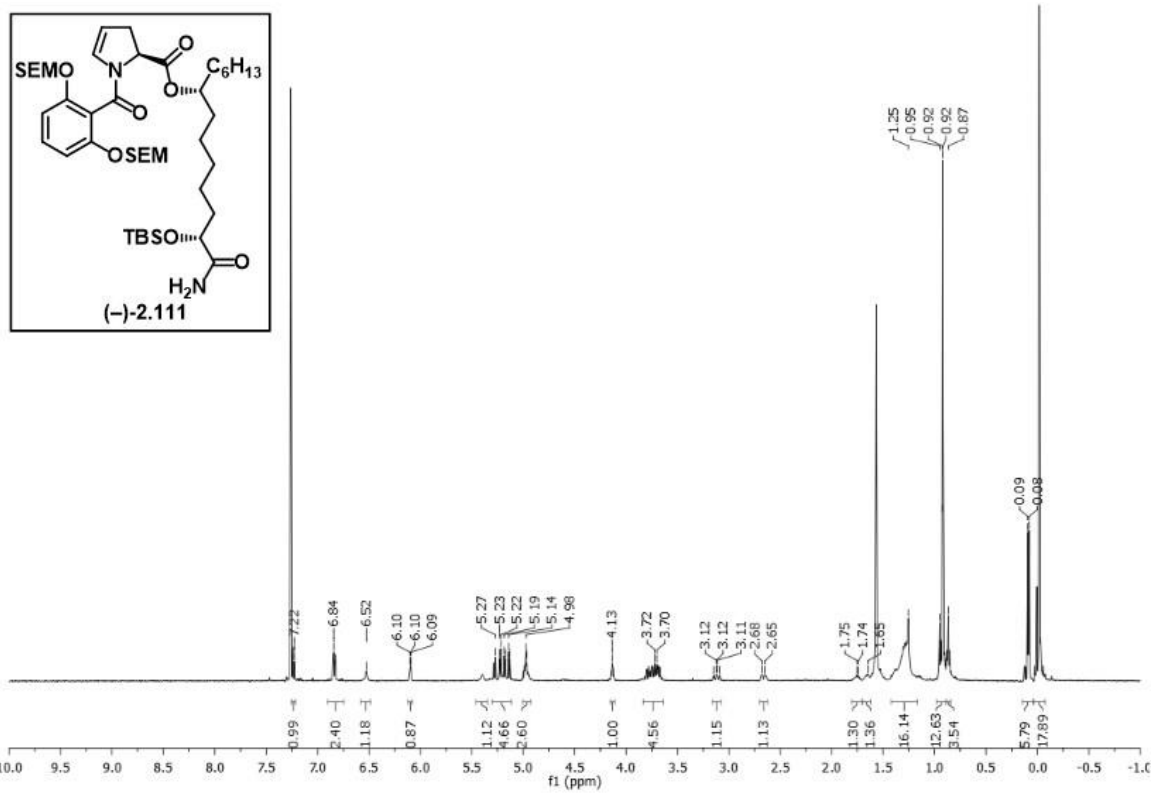
SEMO
OSEM
TBSO
C_6H_{13}
H_2N
(–)-2.111
f1 (ppm)

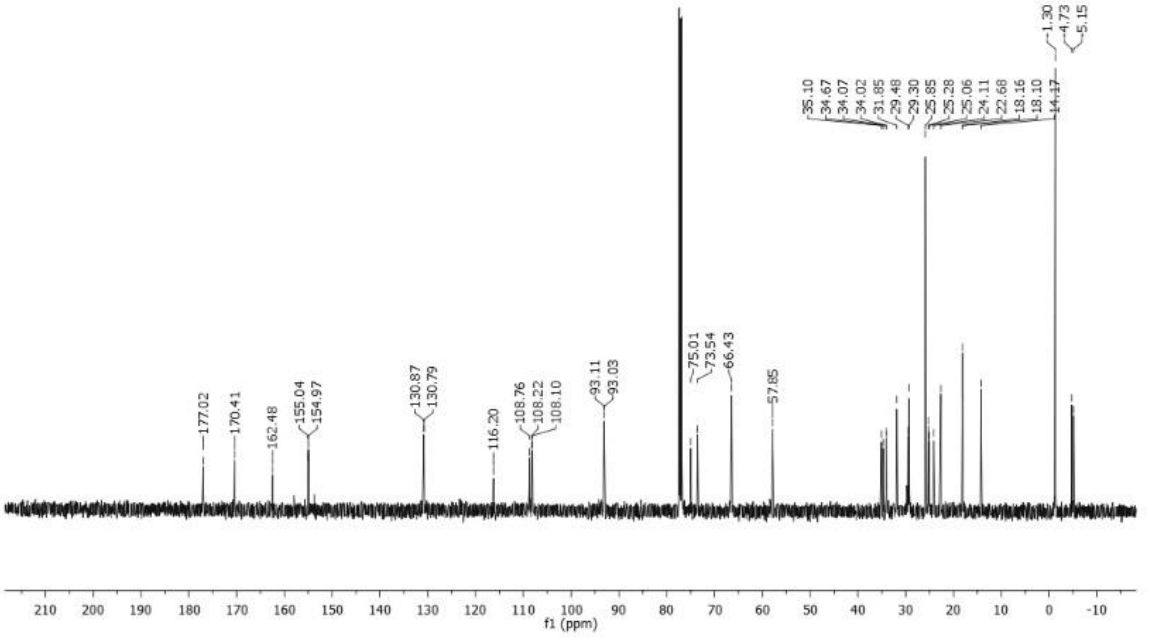
f1 (ppm)

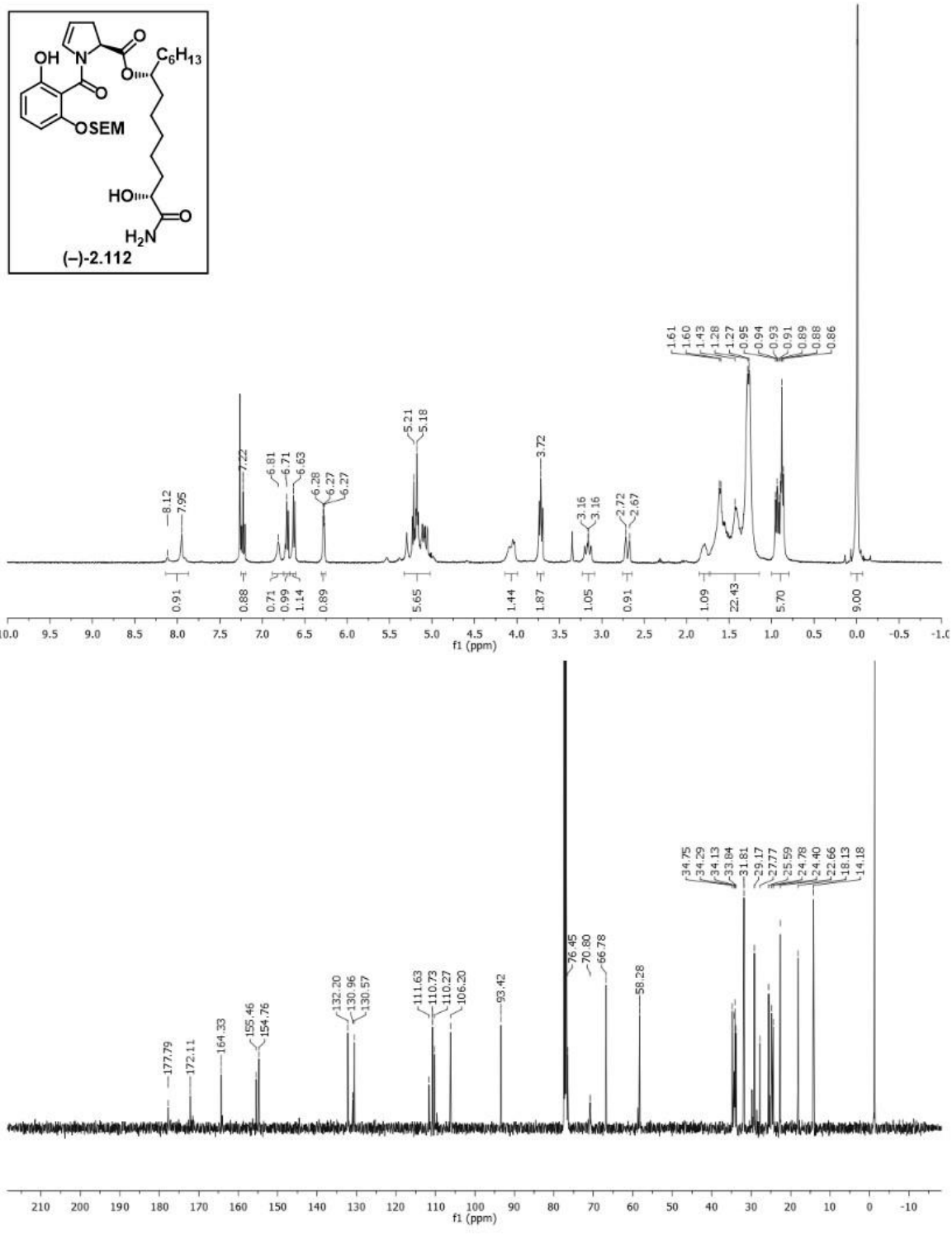
OH
N
O
O
C6H13
O
OSEM
HO
O
H2N
(–)-2.112
8.12
7.95
7.22
6.81
6.71
6.63
6.28
6.27
6.27
5.21
5.18
3.72
3.16
3.16
2.72
2.67
1.61
1.60
1.43
1.28
1.27
0.95
0.94
0.93
0.91
0.89
0.88
0.86
0.91
0.88
0.71
0.99
1.14
0.89
5.65
1.44
1.87
1.05
0.91
1.09
22.43
5.70
9.00
f1 (ppm)
177.79
172.11
164.33
155.46
154.76
132.20
130.96
130.57
111.63
110.73
110.27
106.20
93.42
76.45
70.80
66.78
58.28
34.75
34.29
34.13
33.84
31.81
29.17
27.77
25.59
24.78
24.40
22.66
18.13
14.18
f1 (ppm)

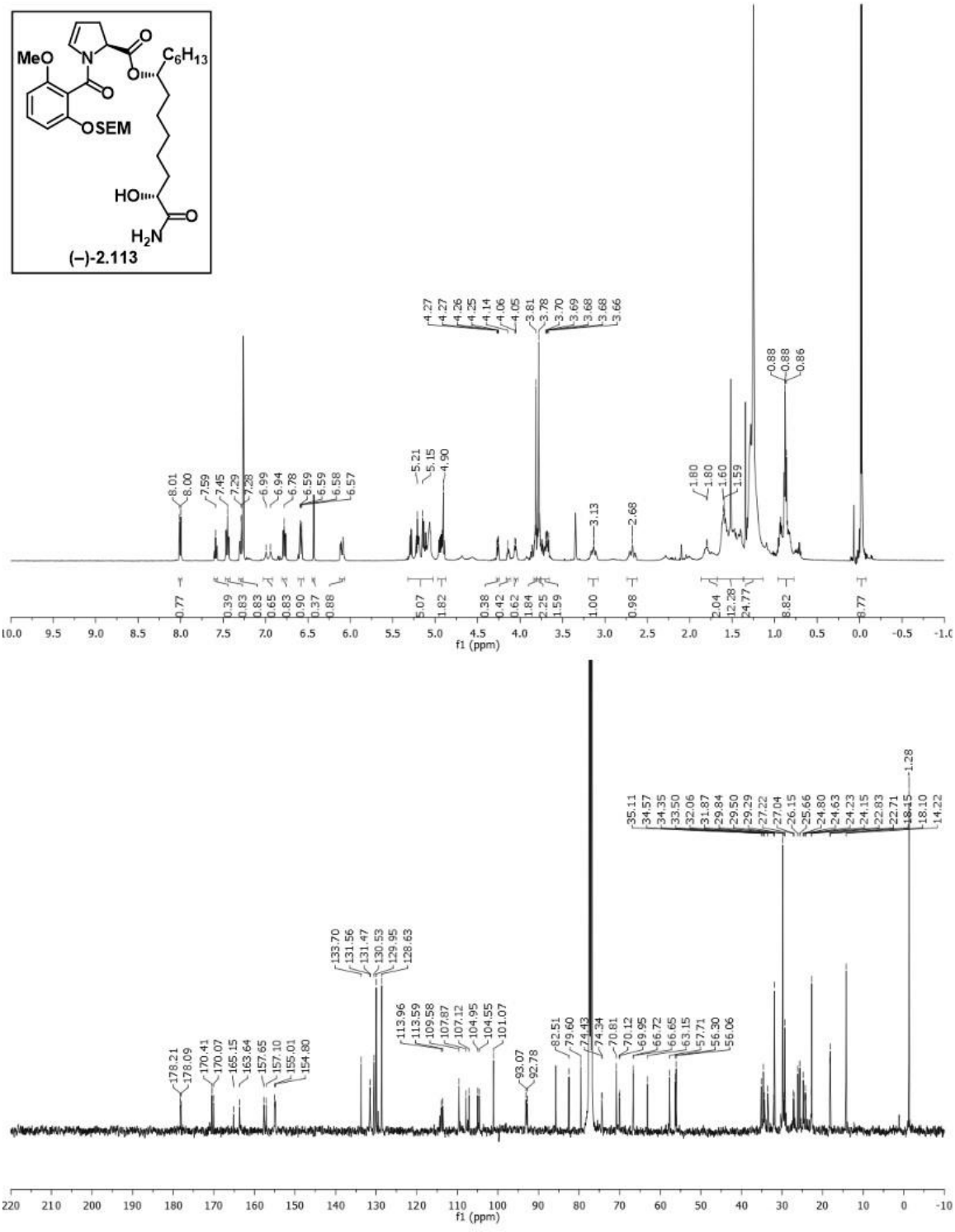
MeO
OSEM
HO
H2N
(–)-2.113
f1 (ppm)
f1 (ppm)

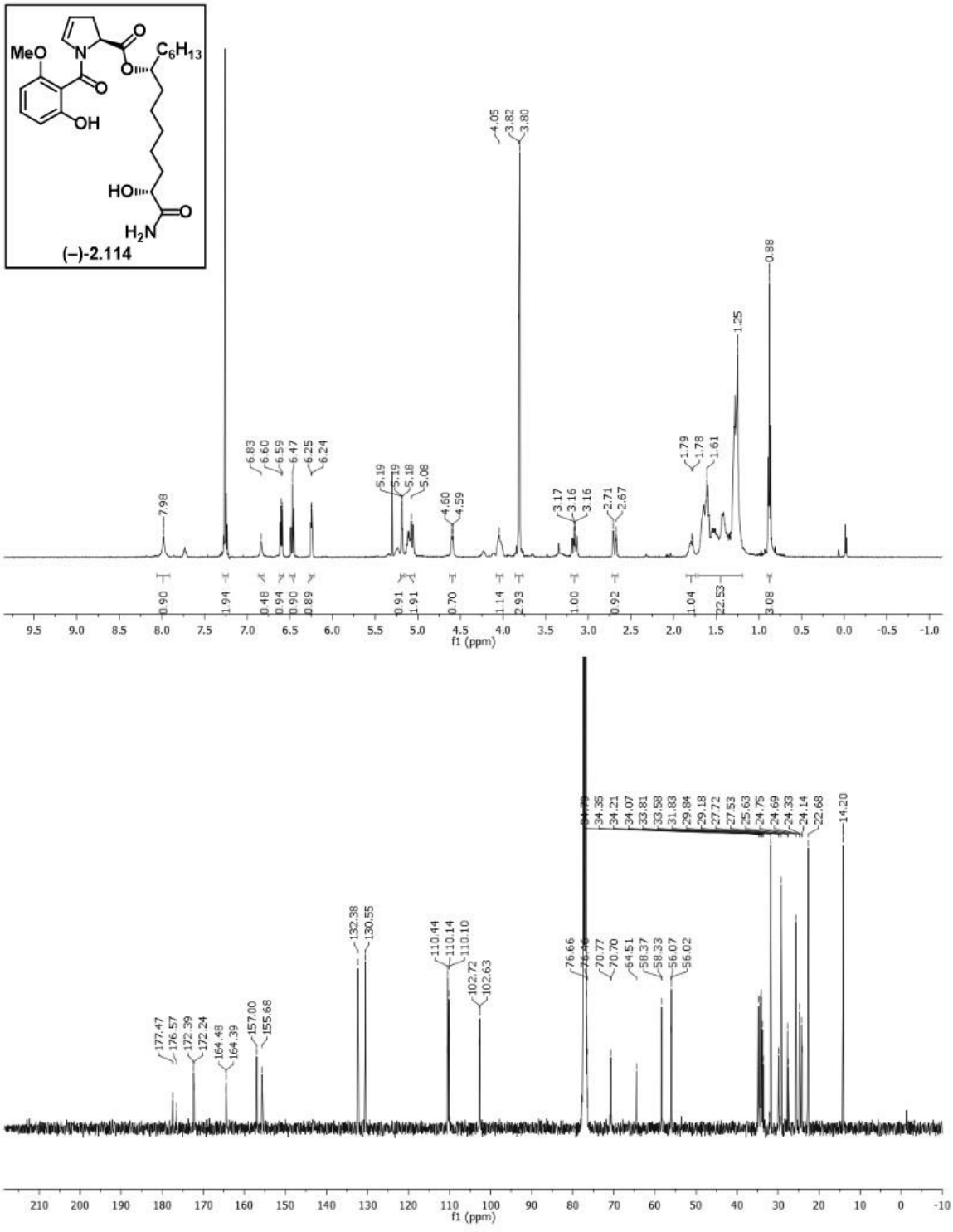
MeO
OH
HO
H2N
(–)-2.114
f1 (ppm)
f1 (ppm)

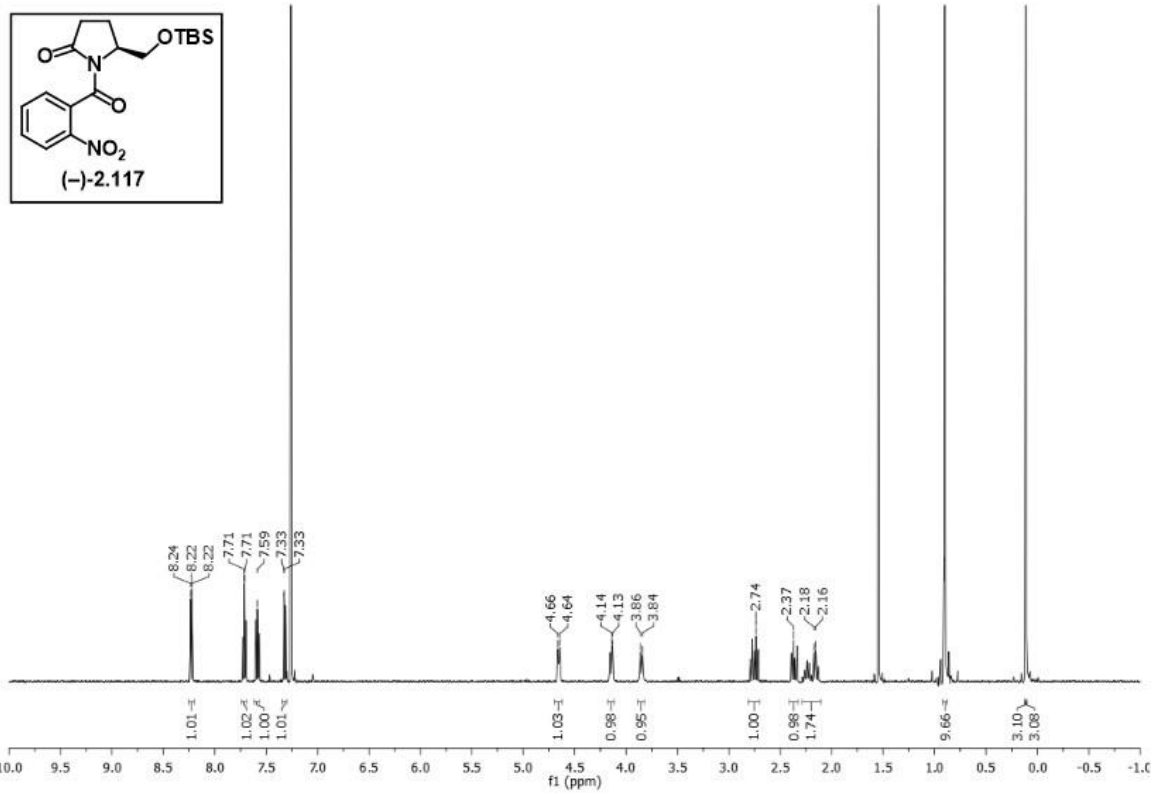
OTBS
O
N
O
NO2
(–)-2.117
8.24
8.22
8.22
7.71
7.71
7.59
7.33
7.33
4.66
4.64
4.14
4.13
3.86
3.84
2.74
2.37
2.18
2.16
1.01
1.02
1.00
1.01
1.03
0.98
0.95
1.00
0.98
1.74
9.66
3.10
3.08
f1 (ppm)

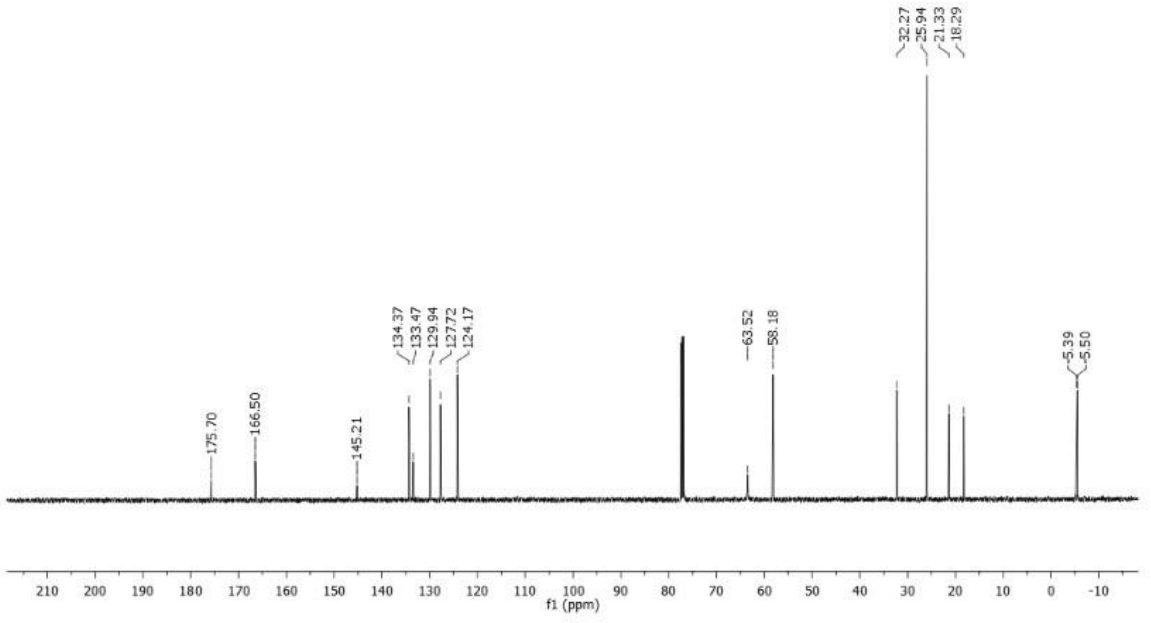
32.27
25.94
21.33
18.29
134.37
133.47
129.94
127.72
124.17
63.52
58.18
5.39
5.50
175.70
166.50
145.21
f1 (ppm)

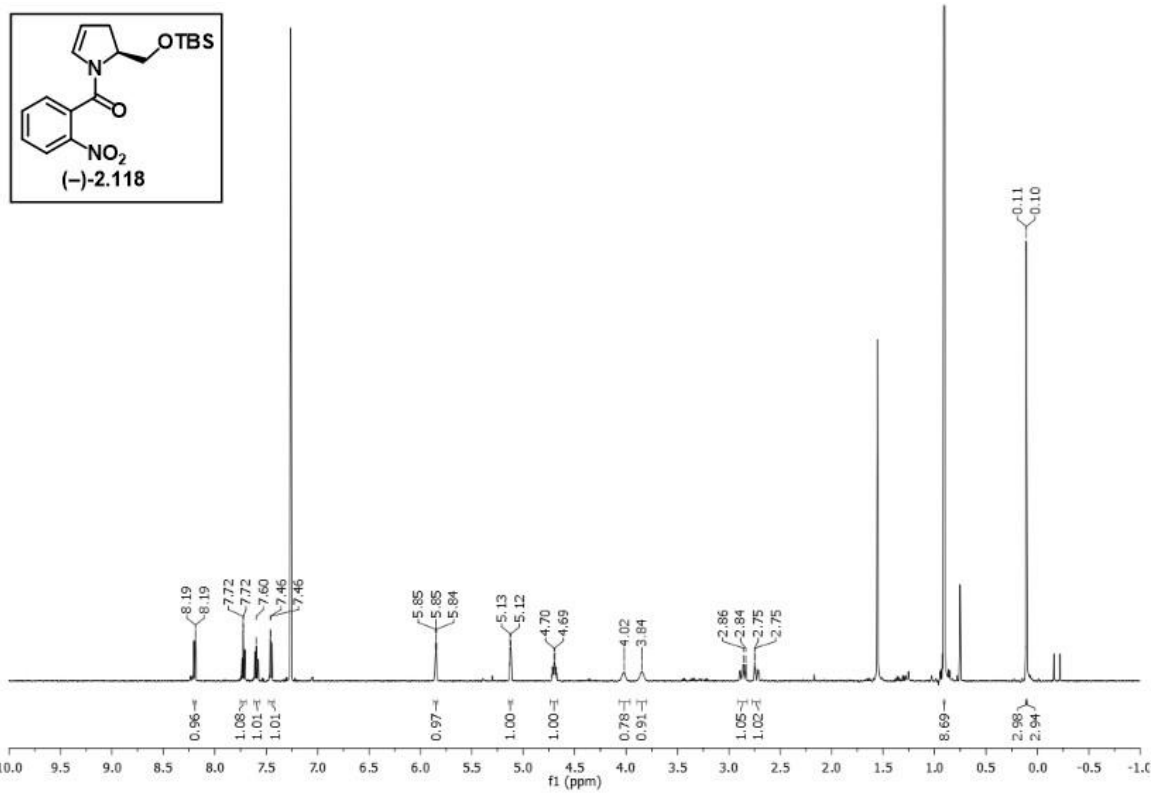
OTBS
N
O
NO2
(–)-2.118
8.19
8.19
7.72
7.72
7.60
7.46
7.46
5.85
5.85
5.84
5.13
5.12
4.70
4.69
4.02
3.84
2.86
2.84
2.75
2.75
0.11
0.10
0.96
1.08
1.01
1.01
0.97
1.00
1.00
0.78
0.91
1.05
1.02
8.69
2.98
2.94
f1 (ppm)

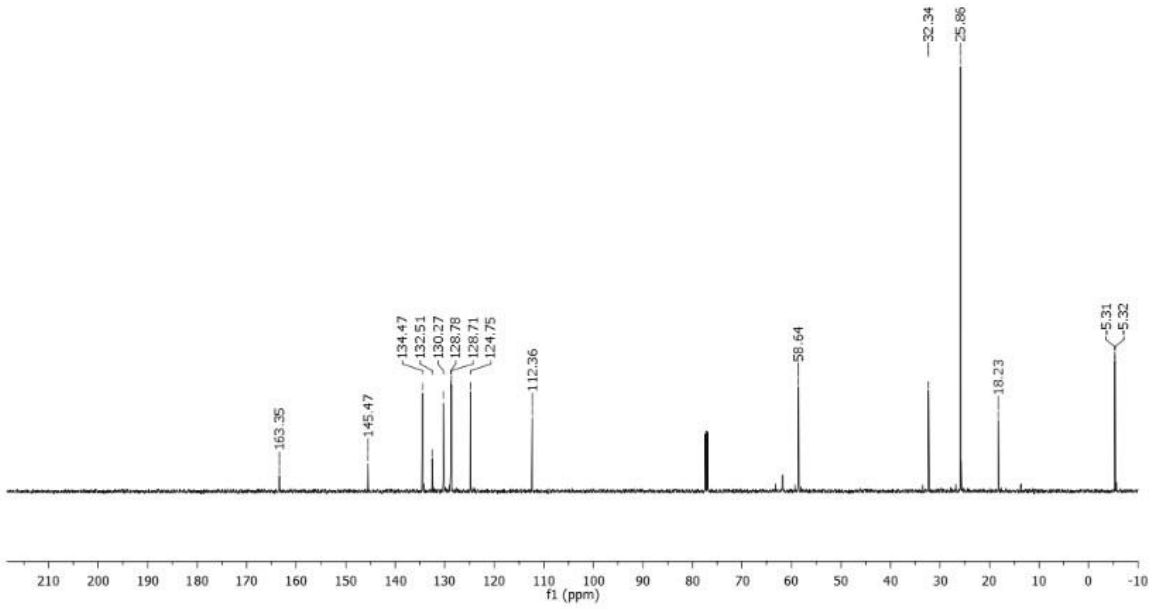
32.34
25.86
134.47
132.51
130.27
128.78
128.71
124.75
112.36
58.64
18.23
5.31
5.32
163.35
145.47
f1 (ppm)

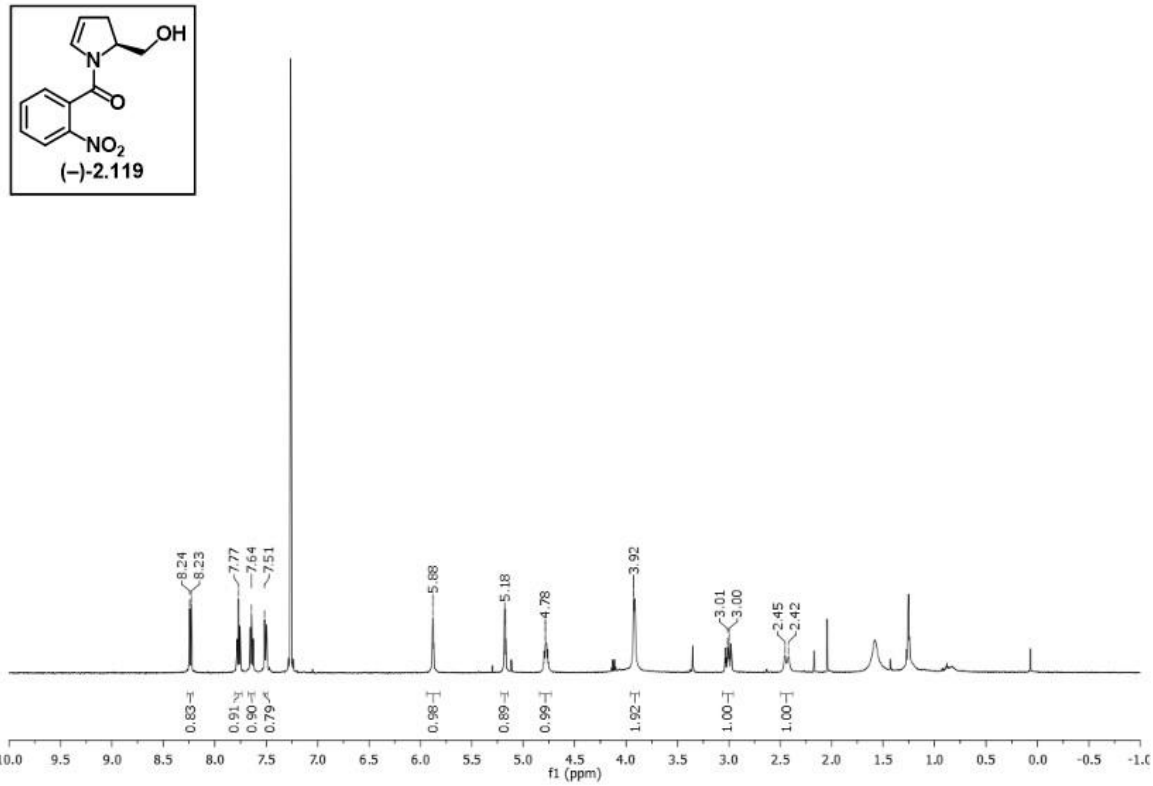
OH
N
O
NO2
(–)-2.119
8.24
8.23
7.77
7.64
7.51
5.88
5.18
4.78
3.92
3.01
3.00
2.45
2.42
0.83
0.91
0.90
0.79
0.98
0.89
0.99
1.92
1.00
1.00
f1 (ppm)

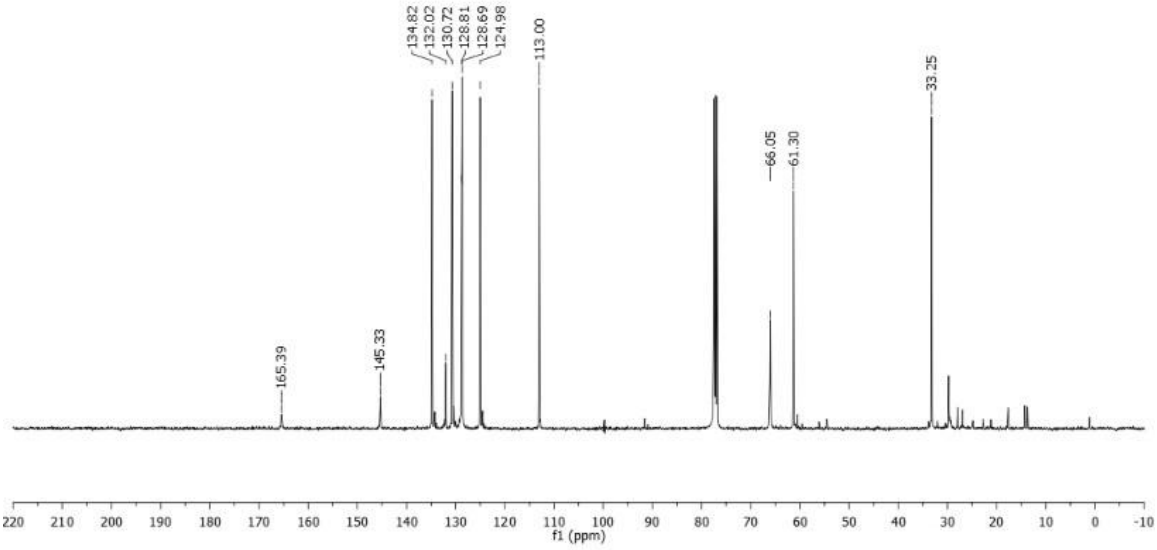
134.82
132.02
130.72
128.81
128.69
124.98
113.00
66.05
61.30
33.25
165.39
145.33
f1 (ppm)

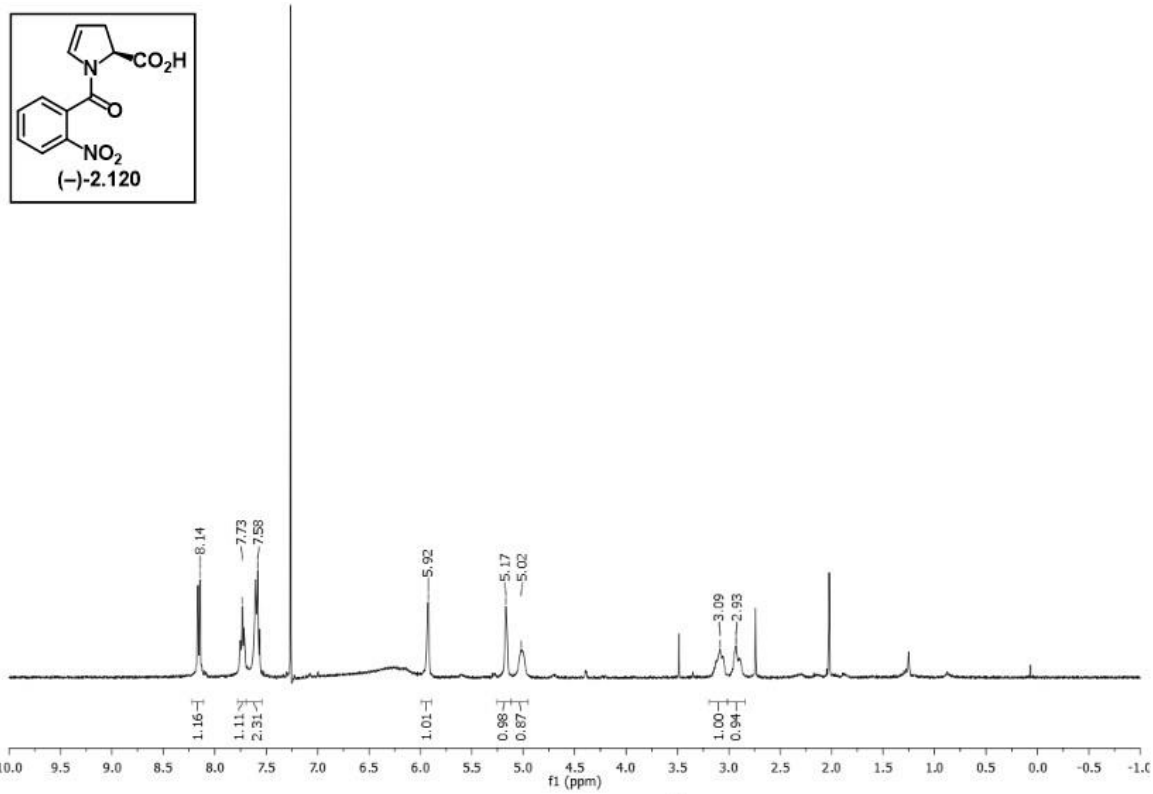
CO2H
N
O
NO2
(–)-2.120
8.14
7.73
7.58
5.92
5.17
5.02
3.09
2.93
1.16
1.11
2.31
1.01
0.98
0.87
1.00
0.94
f1 (ppm)

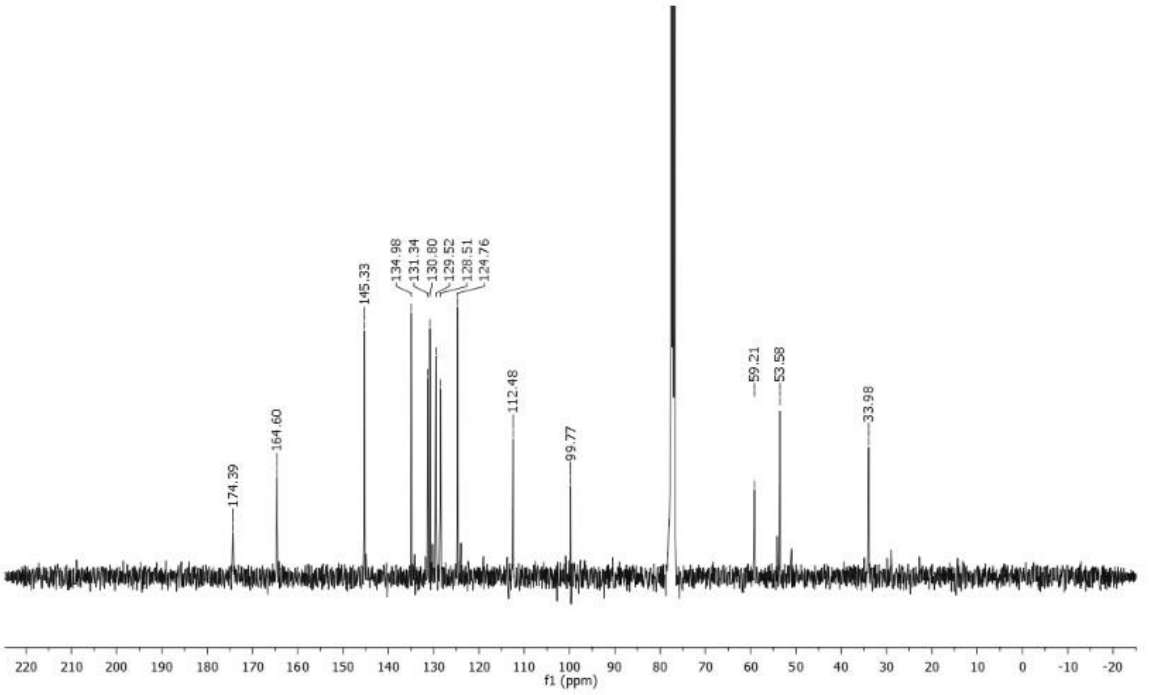
145.33
134.98
131.34
130.80
129.52
128.51
124.76
112.48
99.77
59.21
53.58
33.98
174.39
164.60
f1 (ppm)

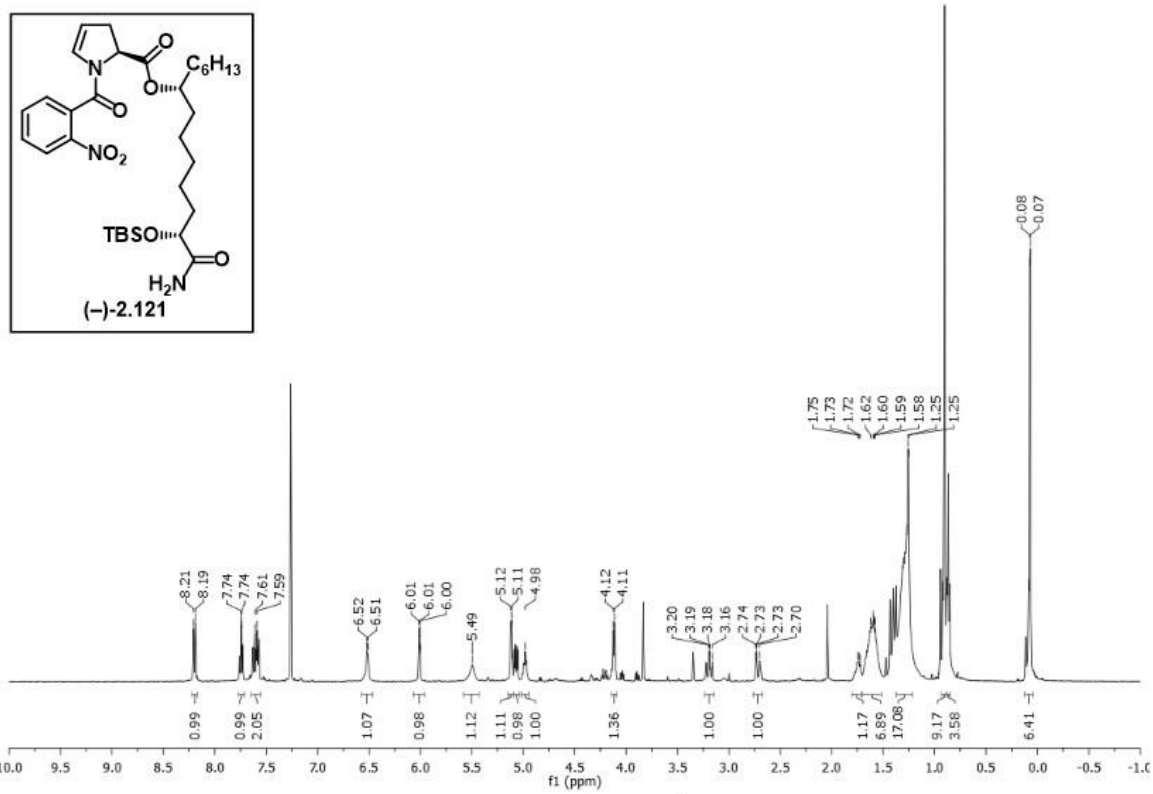
(–)-2.121

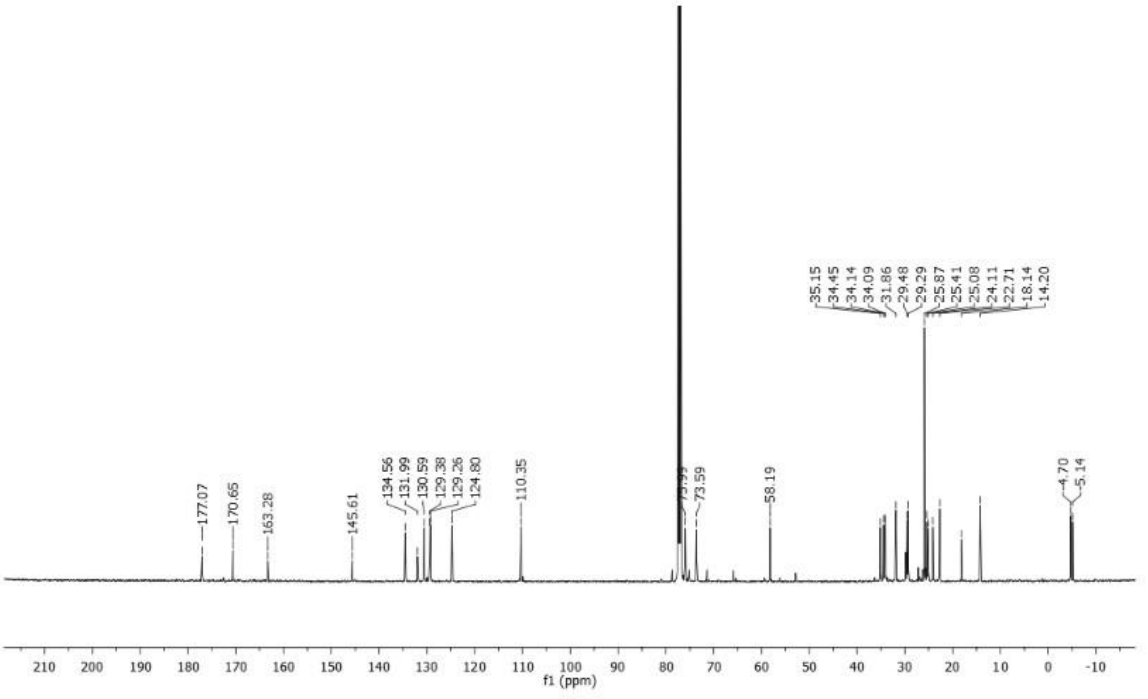

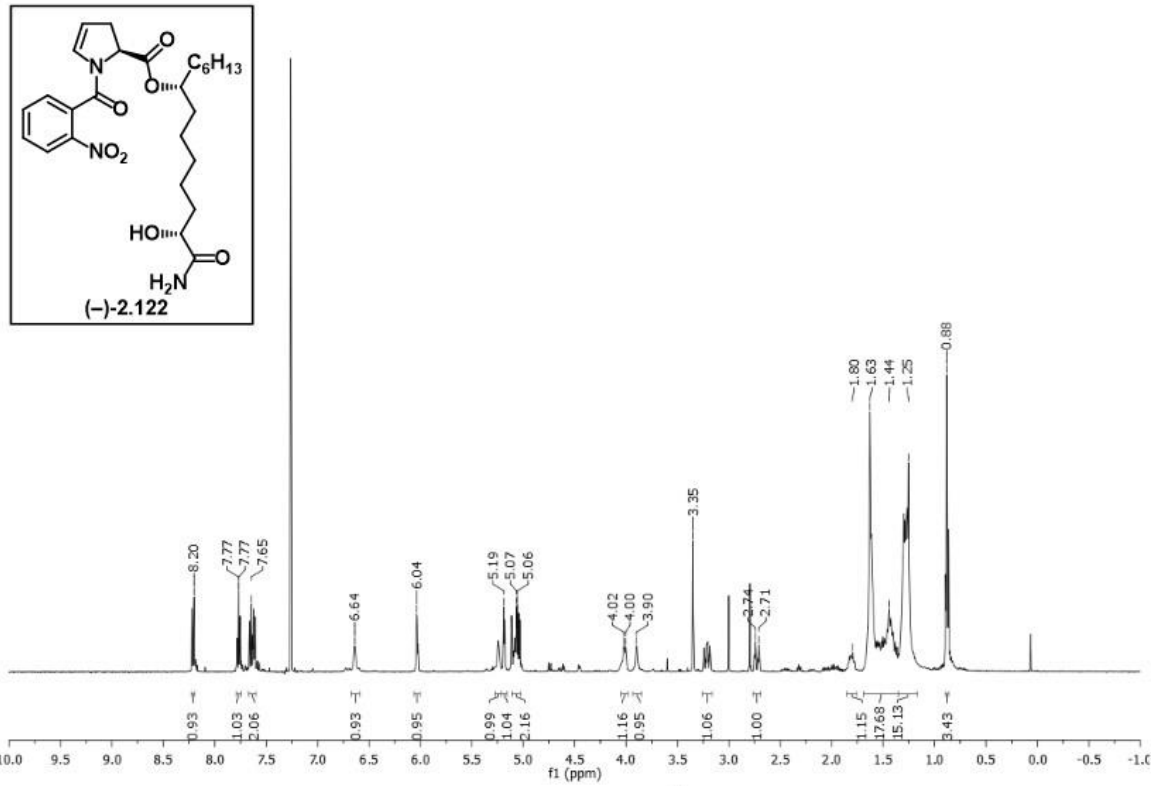
(–)-2.122
f1 (ppm)

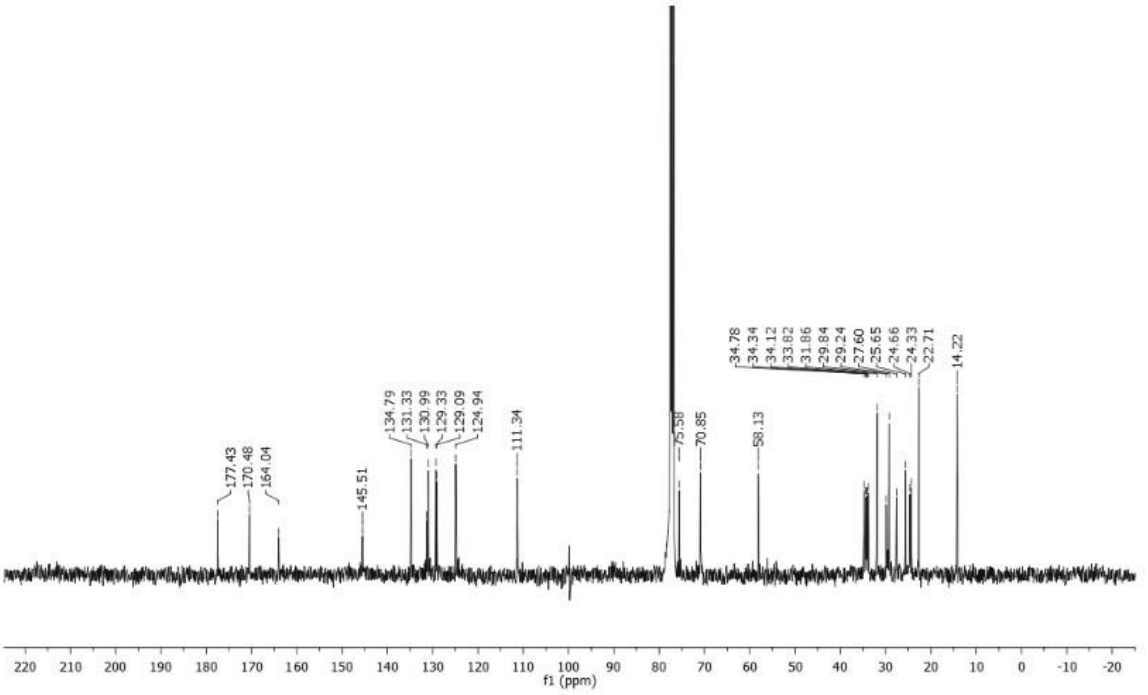
f1 (ppm)

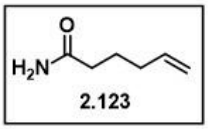
O
H2N

2.123

5.80
5.78
5.06
5.06
5.02
5.01
5.01
4.99
2.24
2.13
2.11
1.76
1.00
1.87
2.04
2.08
2.06
2.08
f1 (ppm)

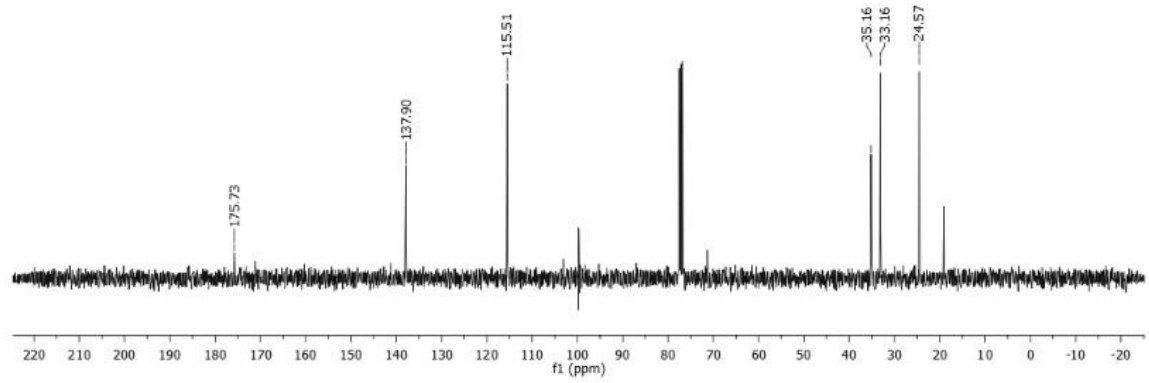
175.73
137.90
115.51
35.16
33.16
24.57
f1 (ppm)

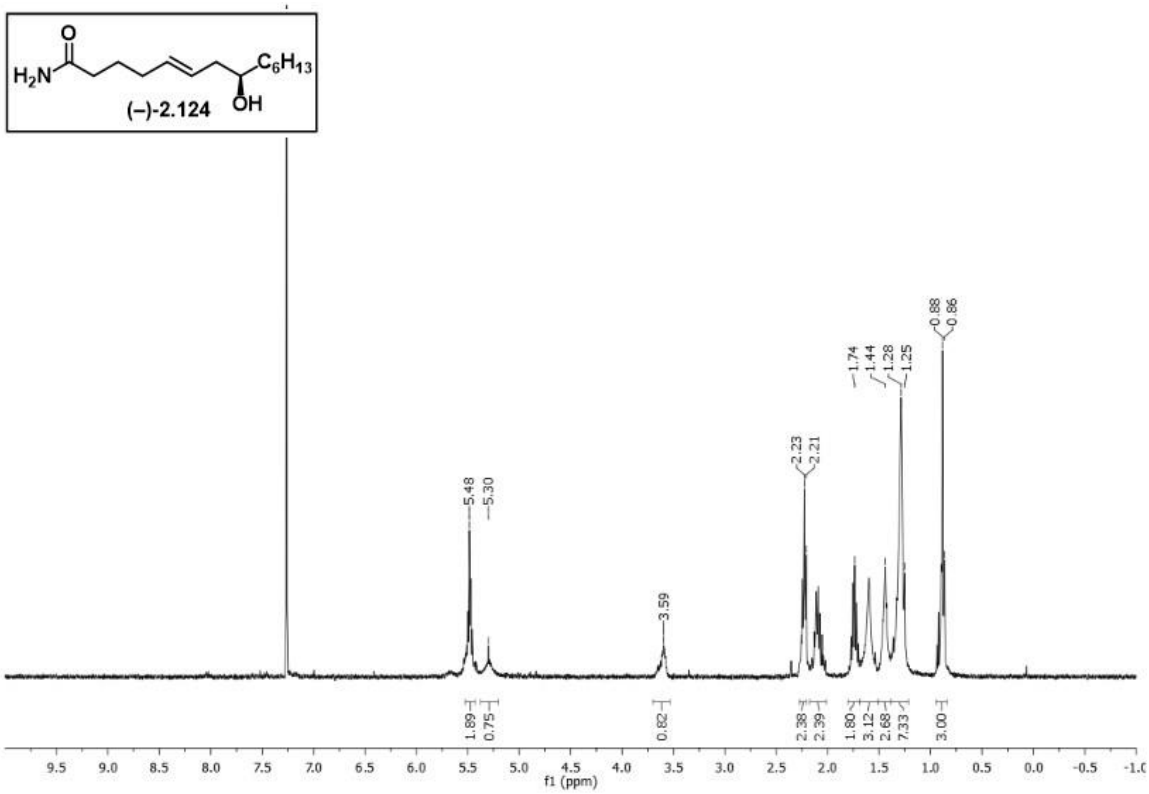
O
H2N
C6H13
OH
(–)-2.124
5.48
5.30
3.59
2.23
2.21
1.74
1.44
1.28
1.25
0.88
0.86
1.89
0.75
0.82
2.38
2.39
1.80
3.12
2.68
7.33
3.00
f1 (ppm)

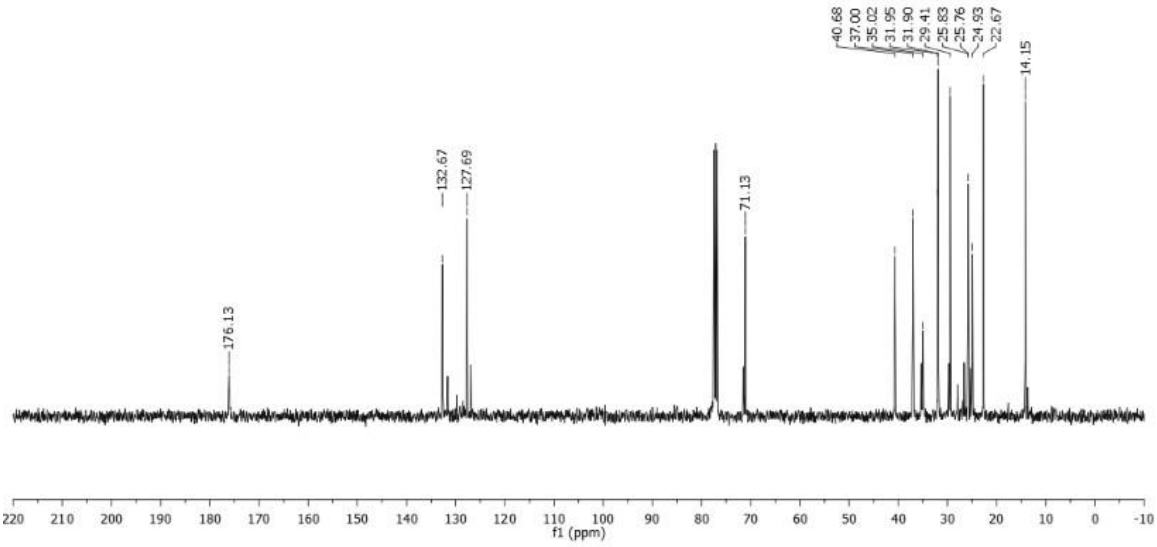
176.13
132.67
127.69
71.13
40.68
37.00
35.02
31.95
31.90
29.41
25.83
25.76
24.93
22.67
14.15
f1 (ppm)

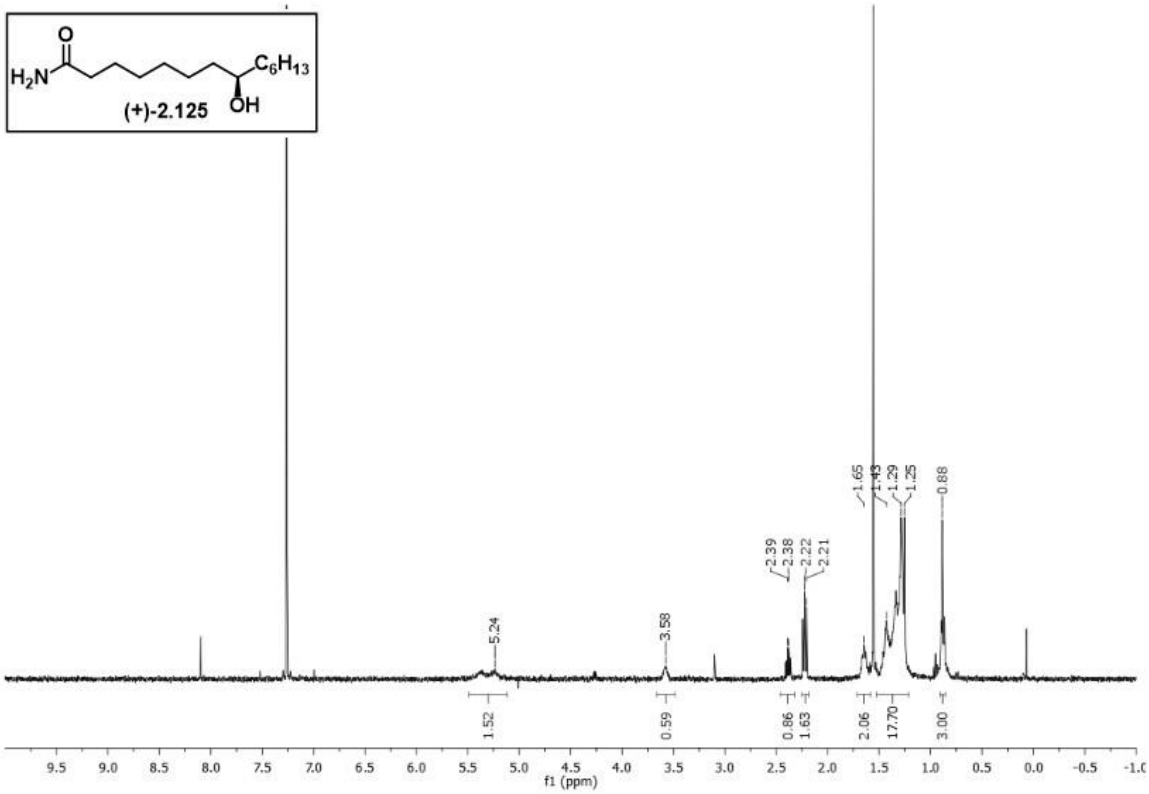
(+)-2.125
5.24
3.58
2.39
2.38
2.22
2.21
1.65
1.43
1.29
1.25
0.88
1.52
0.59
0.86
1.63
2.06
17.70
3.00
f1 (ppm)

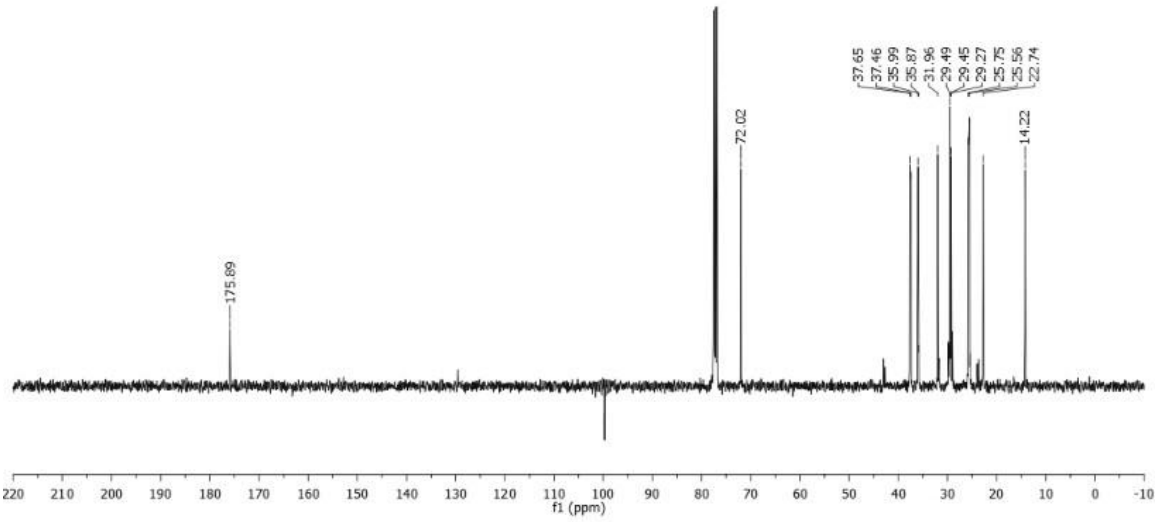
175.89
72.02
37.65
37.46
35.99
35.87
31.96
29.49
29.45
29.27
25.75
25.56
22.74
14.22
f1 (ppm)

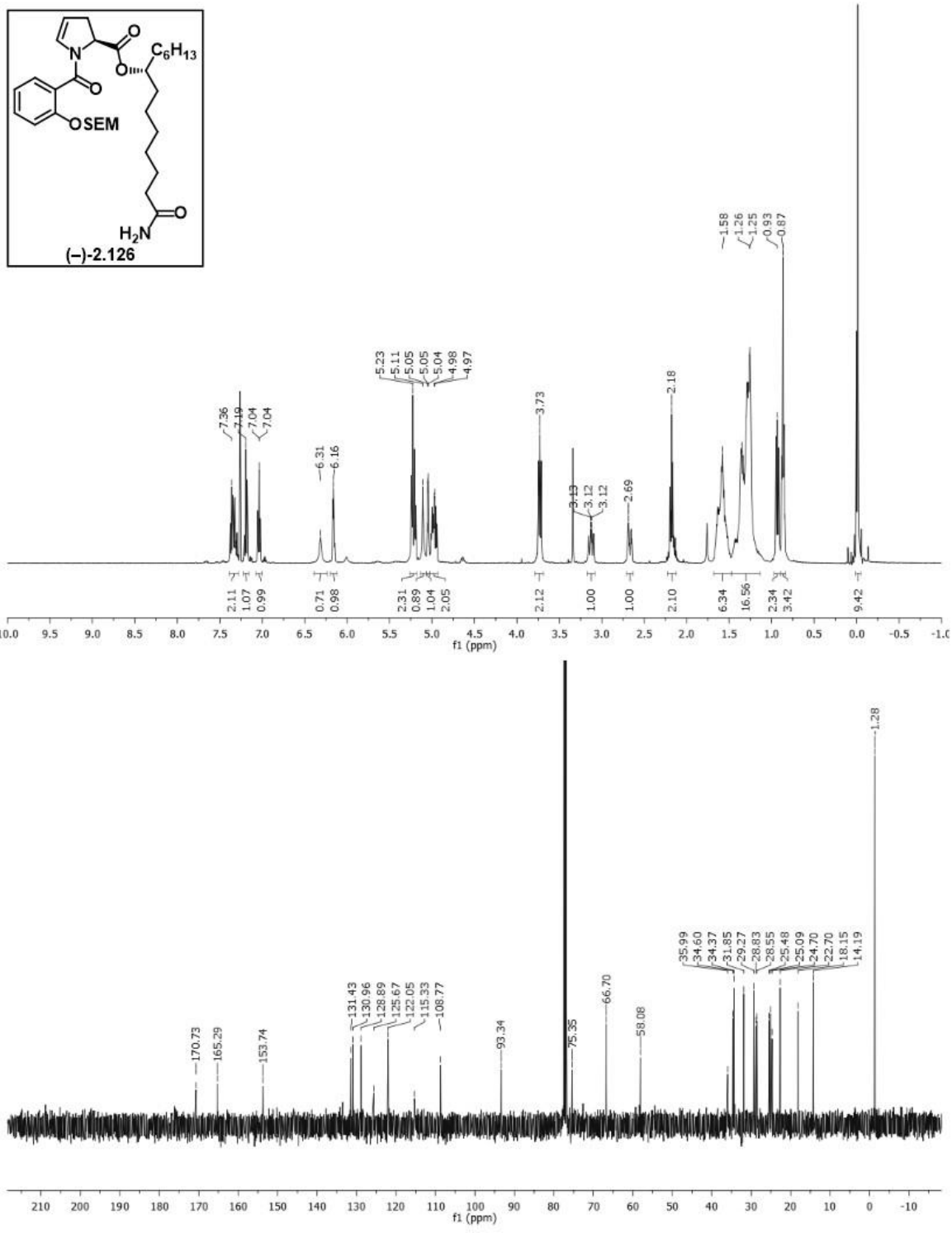
OSEM
C_6H_{13}
H_2N
(–)-2.126
f1 (ppm)
f1 (ppm)

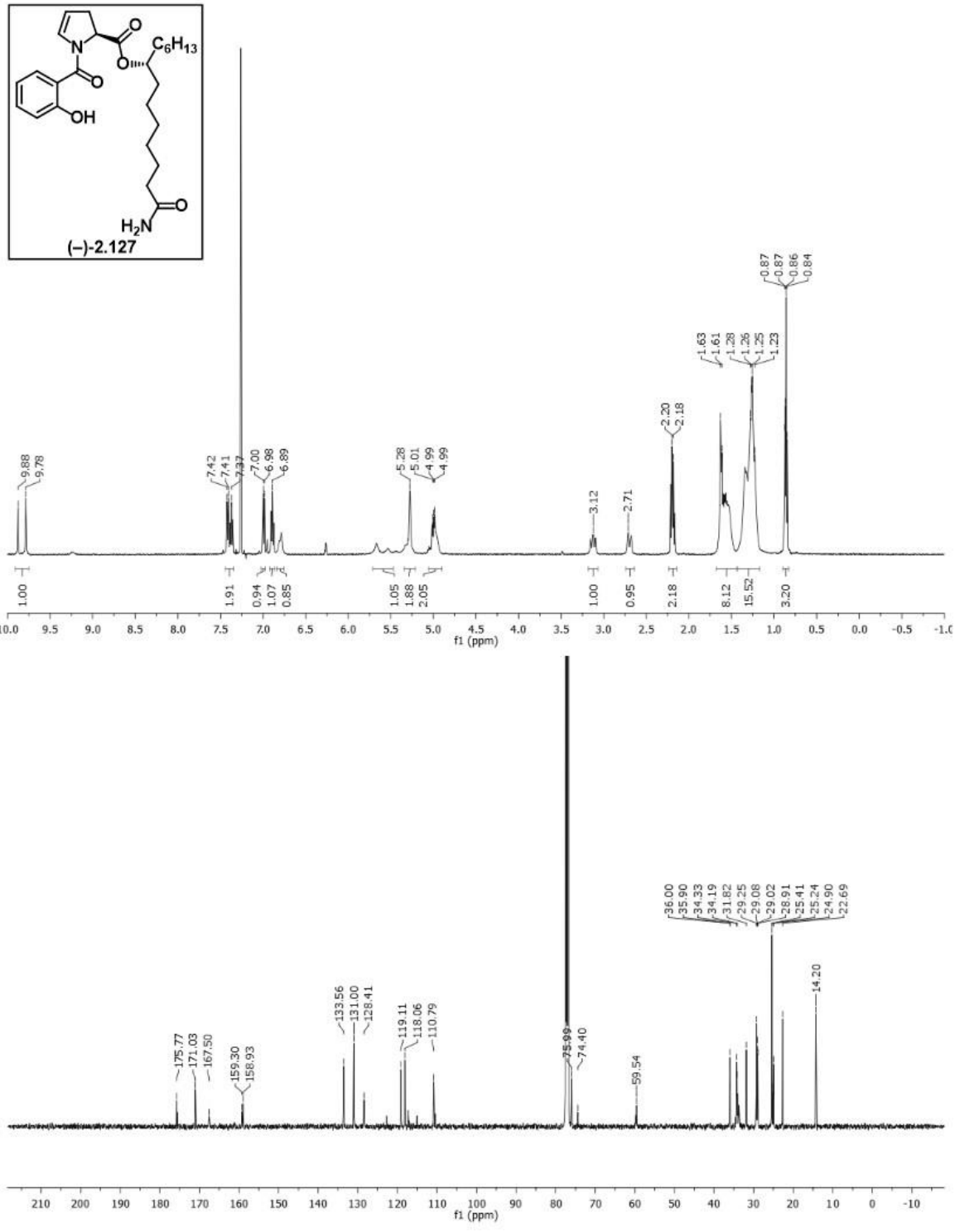
(–)-2.127
f1 (ppm)
f1 (ppm)

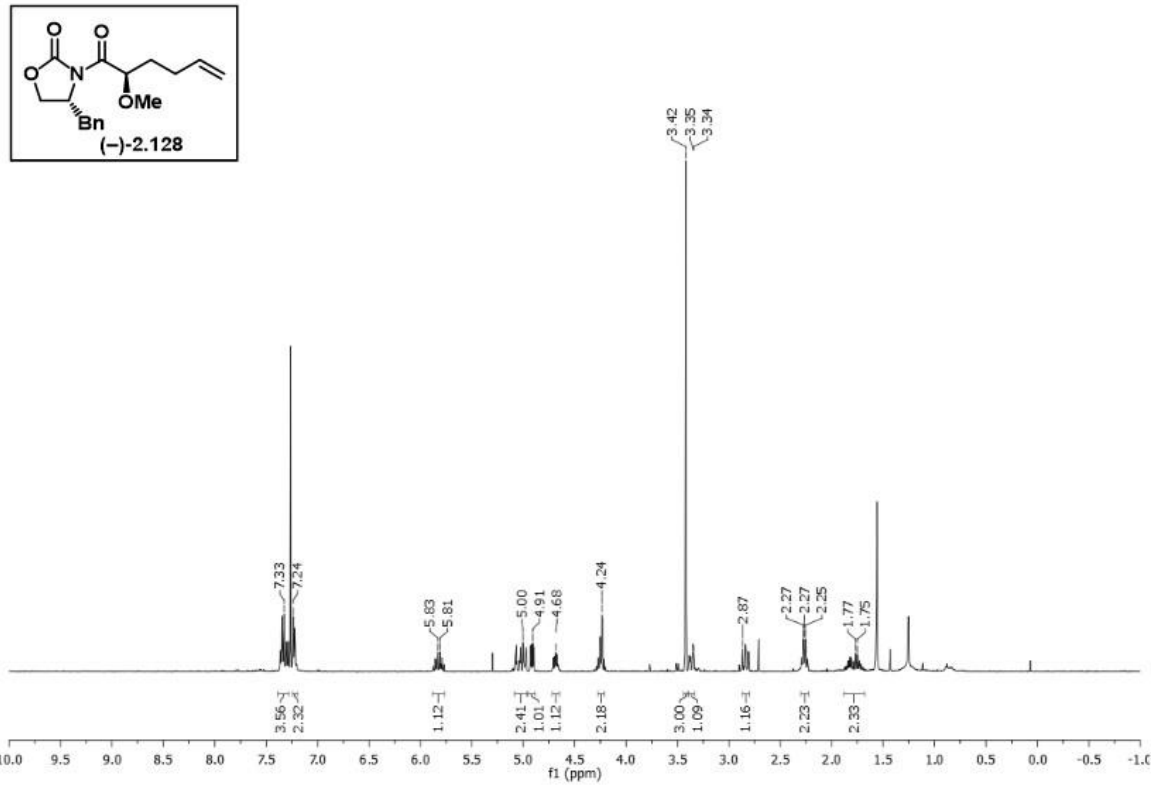
(–)-2.128
Bn
OMe
3.42
3.35
3.34
7.33
7.24
5.83
5.81
5.00
4.91
4.68
4.24
2.87
2.27
2.27
2.25
1.77
1.75
3.56
2.32
1.12
2.41
1.01
1.12
2.18
3.00
1.09
1.16
2.23
2.33
f1 (ppm)

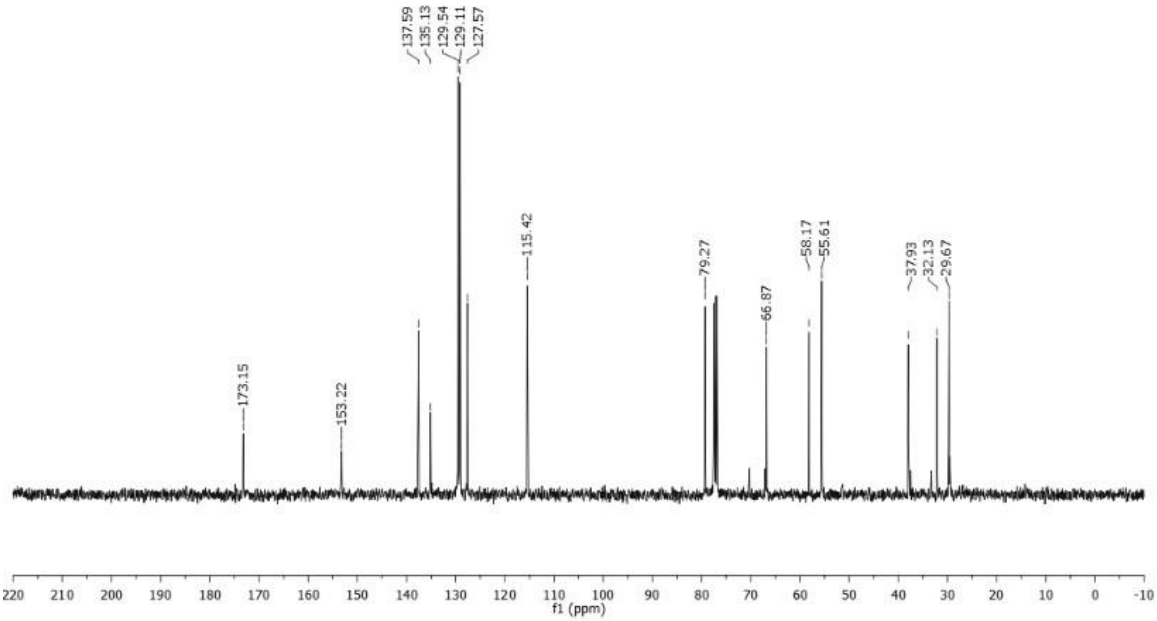
137.59
135.13
129.54
129.11
127.57
115.42
79.27
66.87
58.17
55.61
37.93
32.13
29.67
173.15
153.22
f1 (ppm)

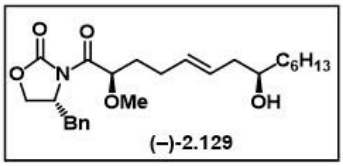
O
O
O
N
C_6H_{13}
OMe
OH
Bn

(–)-2.129

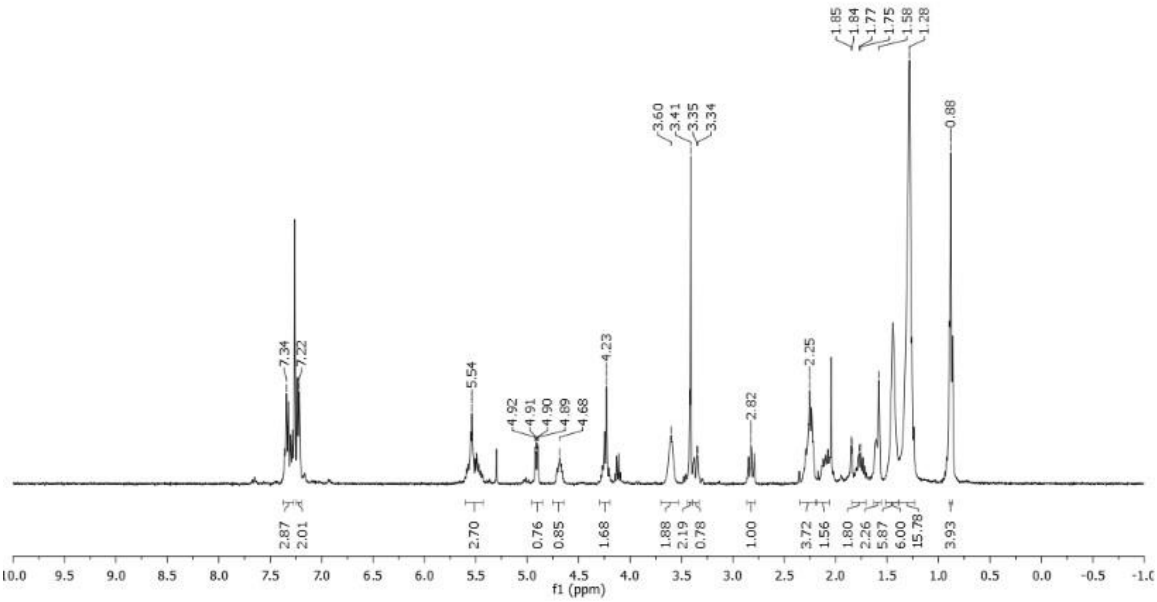
1.85
1.84
1.77
1.75
1.58
1.28
3.60
3.41
3.35
3.34
0.88
7.34
7.22
5.54
4.92
4.91
4.90
4.89
4.68
4.23
2.82
2.25
2.87
2.01
2.70
0.76
0.85
1.68
1.88
2.19
0.78
1.00
3.72
1.56
1.80
2.26
5.87
6.00
15.78
3.93
f1 (ppm)

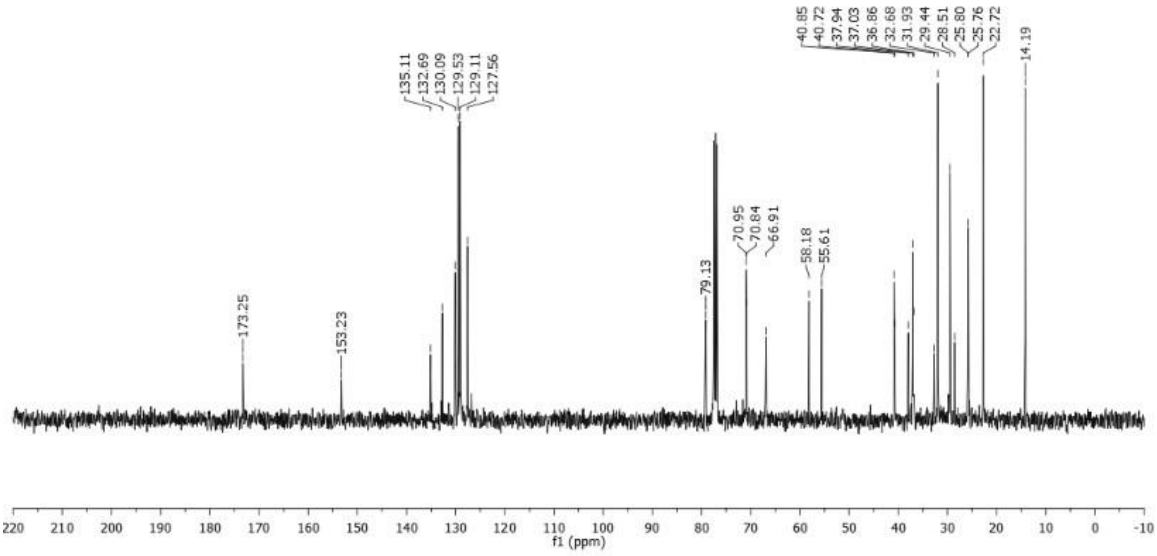
40.85
40.72
37.94
37.03
36.86
32.68
31.93
29.44
28.51
25.80
25.76
22.72
14.19
135.11
132.69
130.09
129.53
129.11
127.56
70.95
70.84
66.91
58.18
55.61
79.13
173.25
153.23
f1 (ppm)

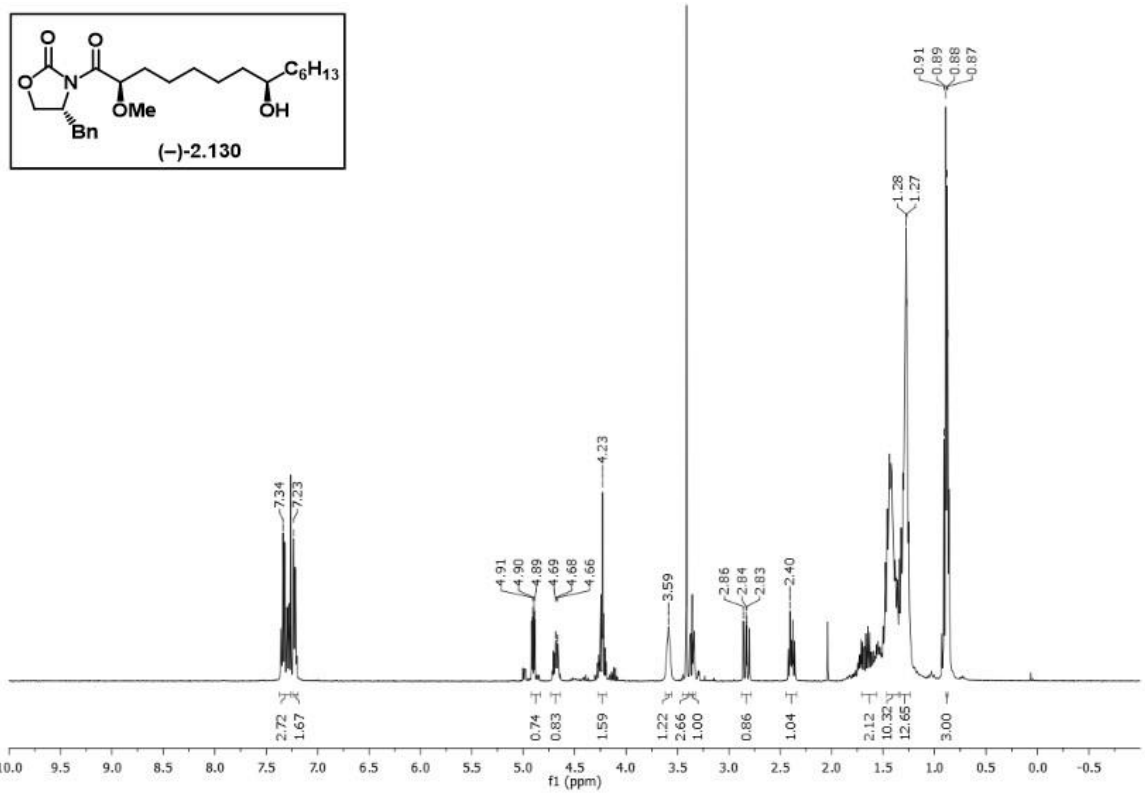
(–)-2.130
7.34
7.23
4.91
4.90
4.89
4.69
4.68
4.66
4.23
3.59
2.86
2.84
2.83
2.40
1.28
1.27
0.91
0.89
0.88
0.87
2.72
1.67
0.74
0.83
1.59
1.22
2.66
1.00
0.86
1.04
2.12
10.32
12.65
3.00
f1 (ppm)

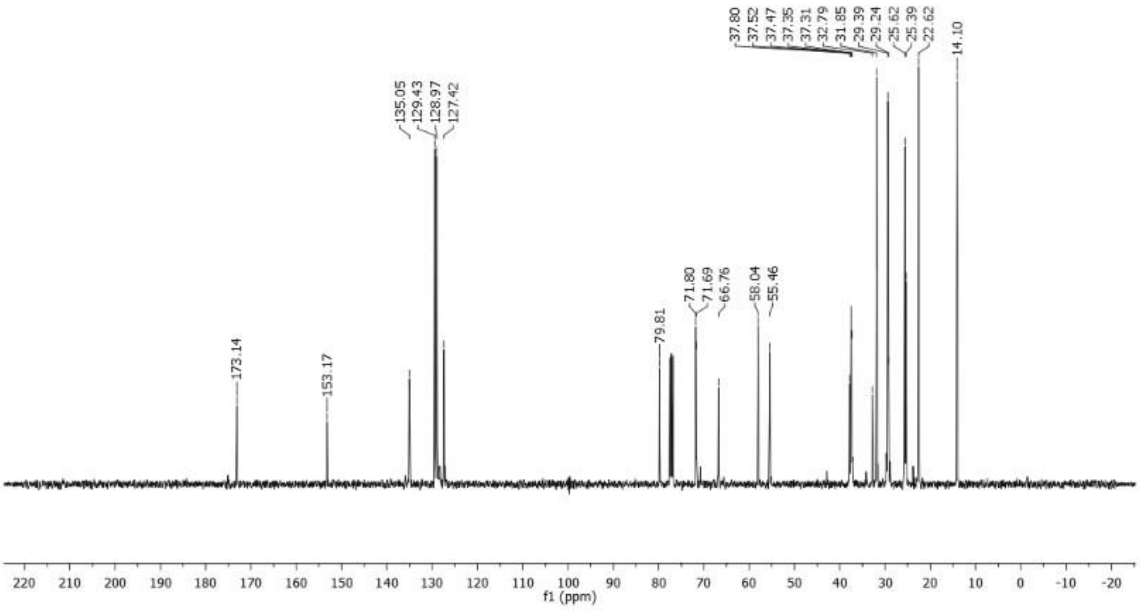
173.14
153.17
135.05
129.43
128.97
127.42
79.81
71.80
71.69
66.76
58.04
55.46
37.80
37.52
37.47
37.35
37.31
32.79
31.85
29.39
29.24
25.62
25.39
22.62
14.10
f1 (ppm)

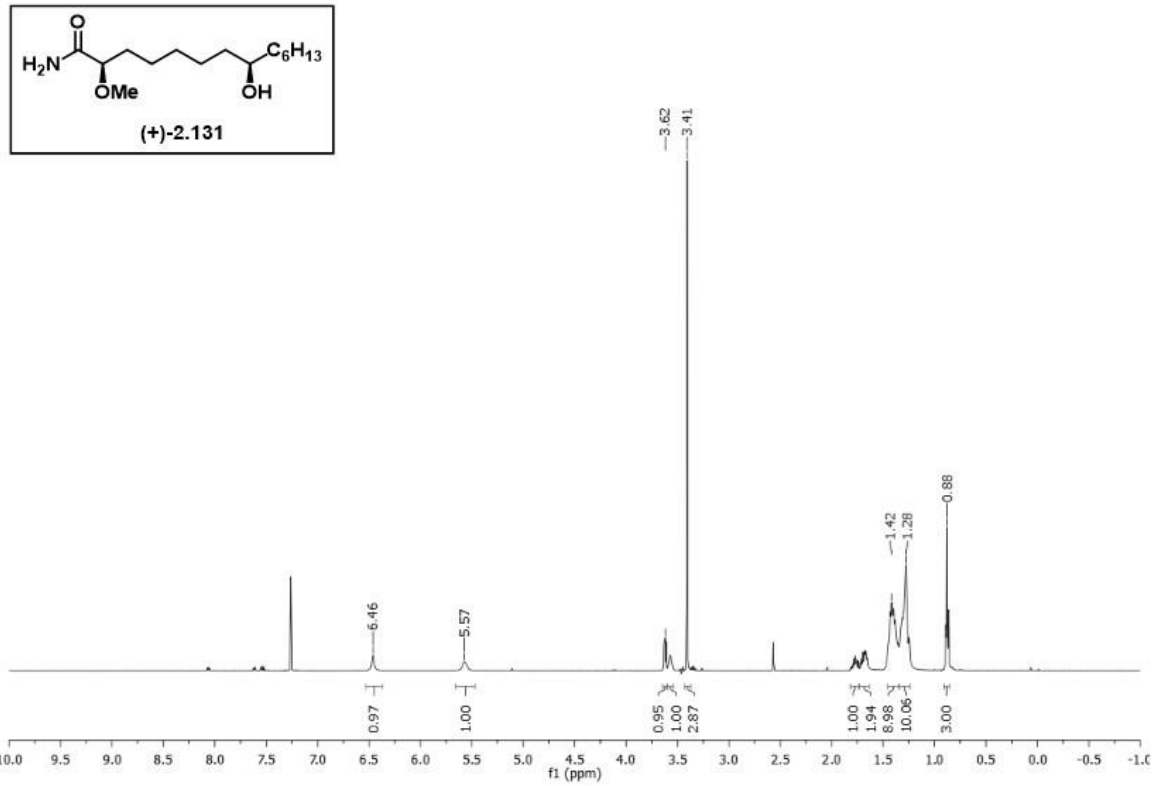
O
H2N
C6H13
OMe
OH
(+)-2.131
3.62
3.41
6.46
5.57
1.42
1.28
0.88
0.97
1.00
0.95
1.00
2.87
1.00
1.94
8.98
10.06
3.00
f1 (ppm)

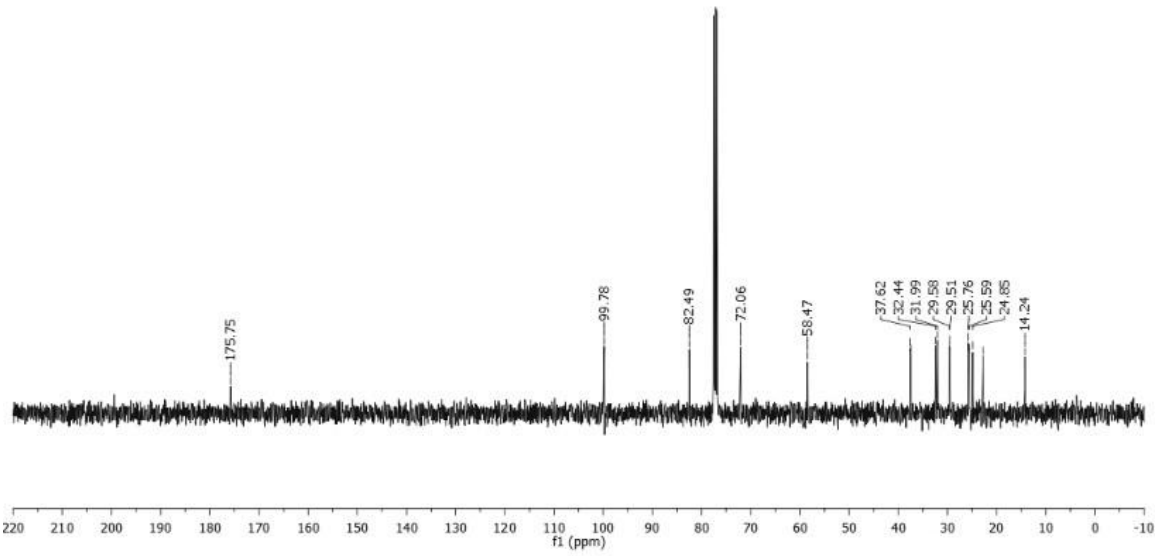
175.75
99.78
82.49
72.06
58.47
37.62
32.44
31.99
29.58
29.51
25.76
25.59
24.85
14.24
f1 (ppm)

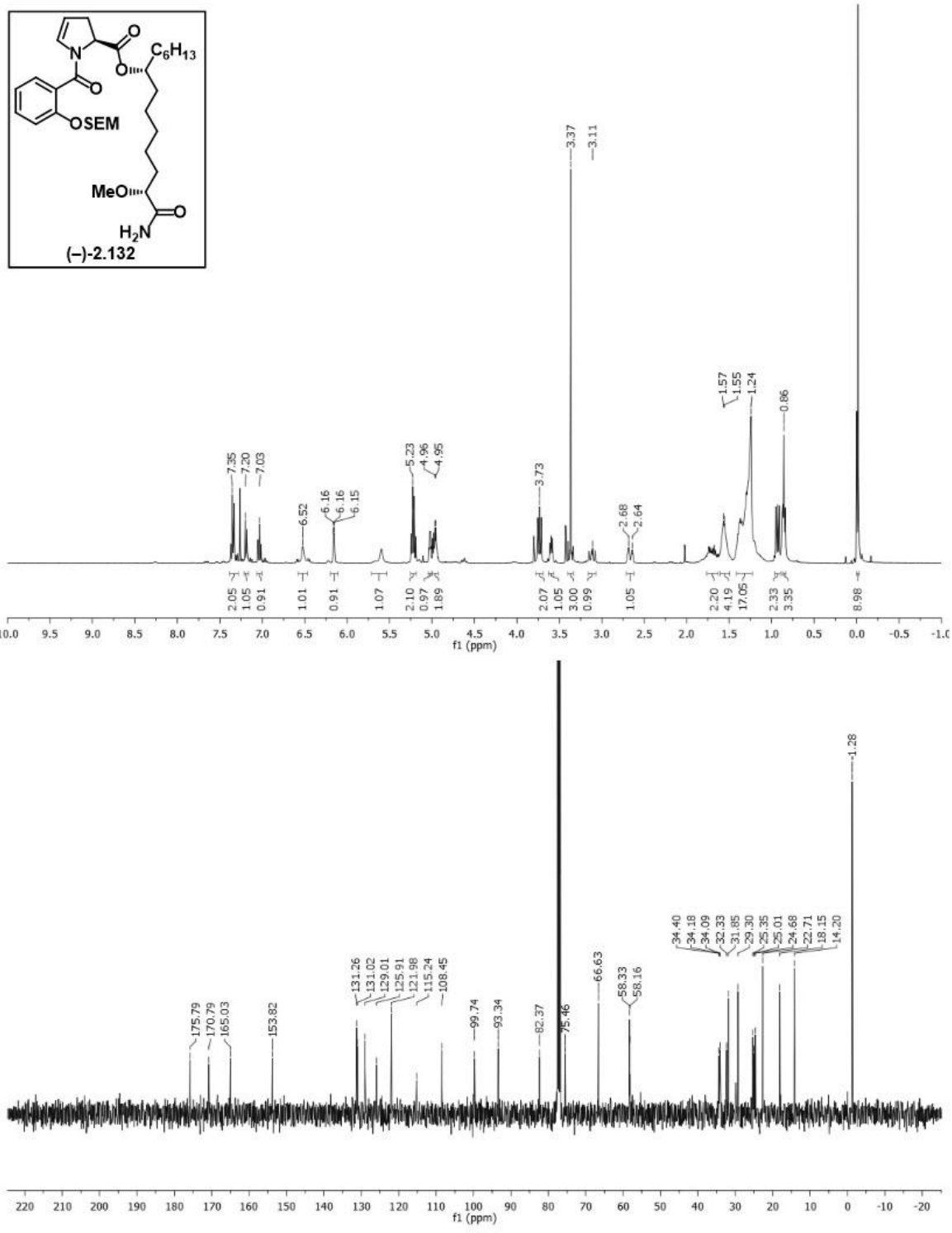
OSEM
MeO
C_6H_{13}
H_2N
(–)-2.132
f1 (ppm)
f1 (ppm)

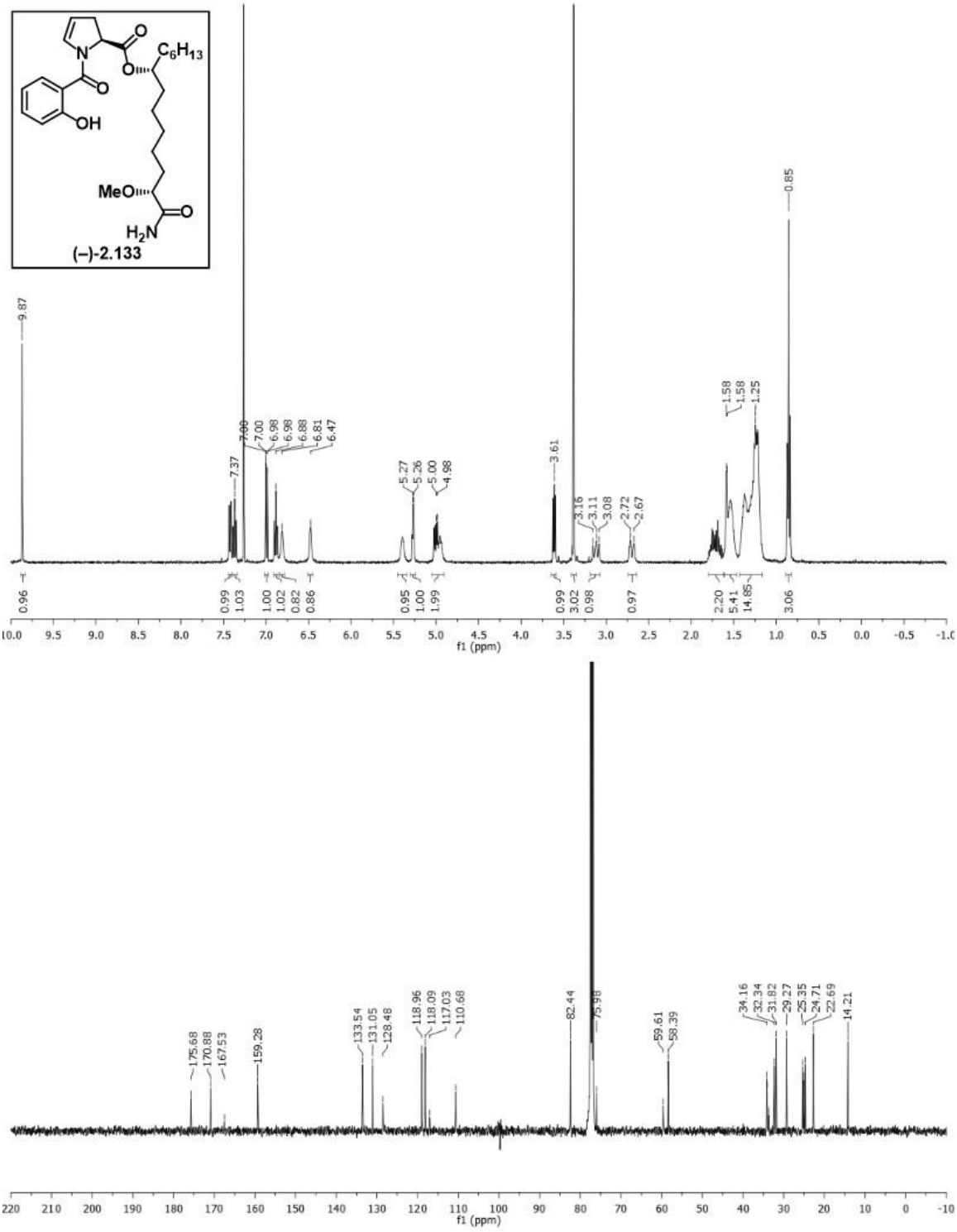
(–)-2.133
f1 (ppm)
f1 (ppm)

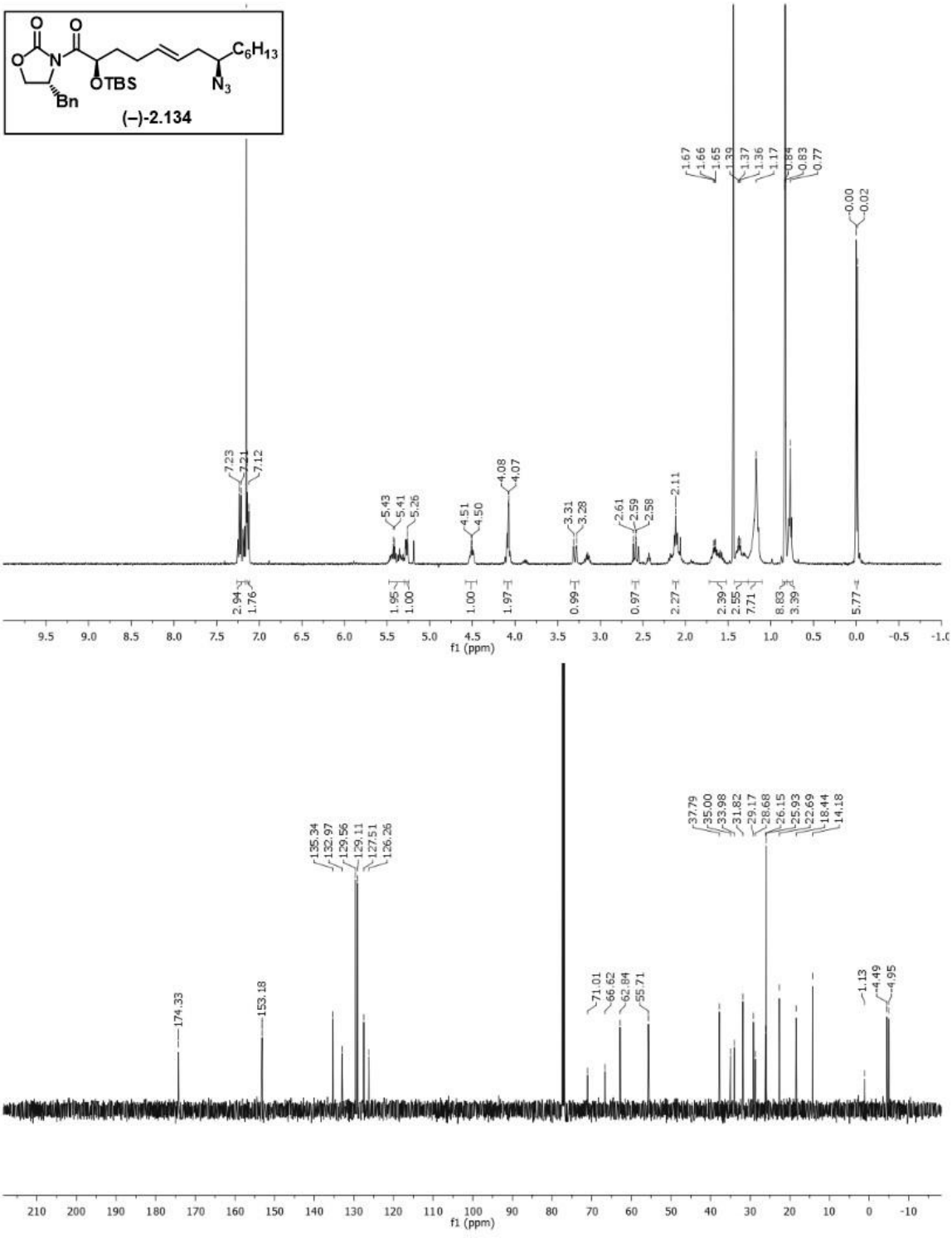
(–)-2.134
f1 (ppm)
f1 (ppm)

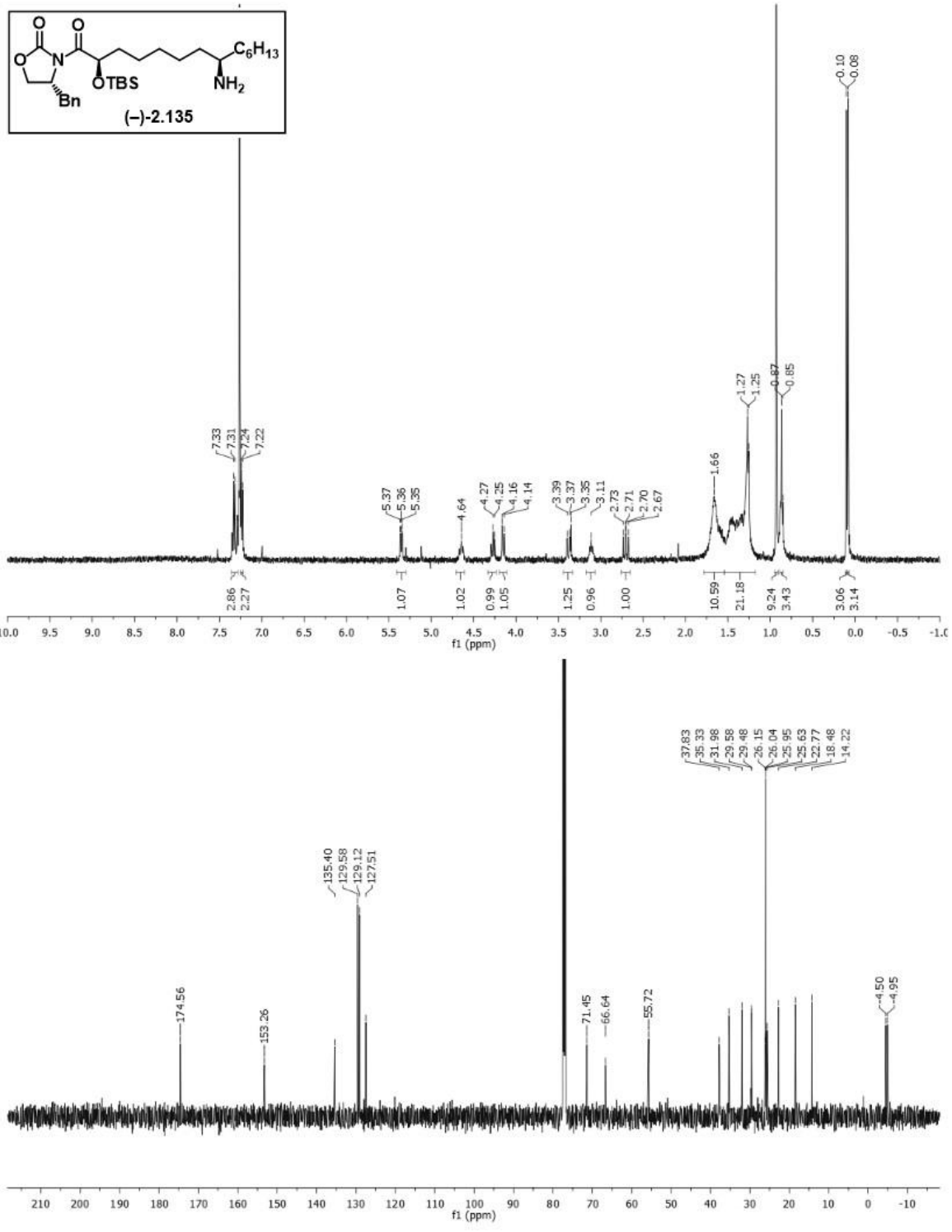
(–)-2.135
f1 (ppm)
f1 (ppm)

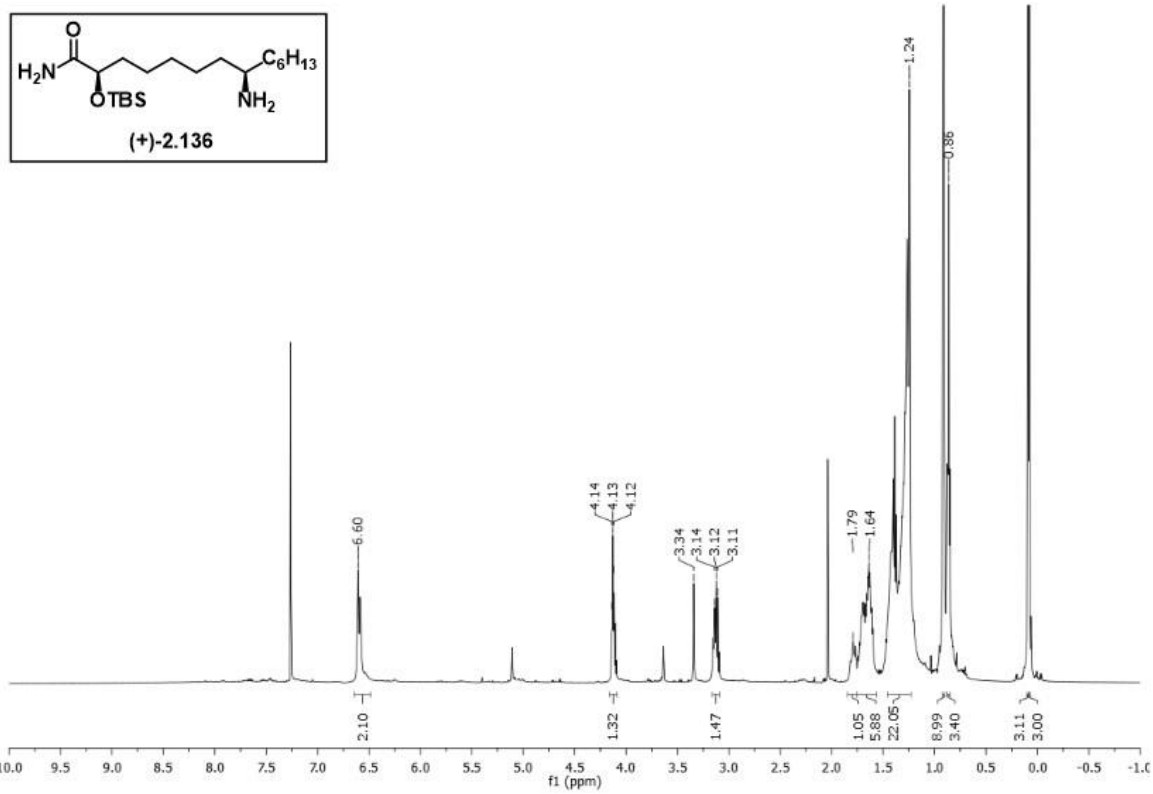
(+)-2.136
6.60
4.14
4.13
4.12
3.34
3.14
3.12
3.11
1.79
1.64
1.24
0.86
2.10
1.32
1.47
1.05
5.88
22.05
8.99
3.40
3.11
3.00
f1 (ppm)

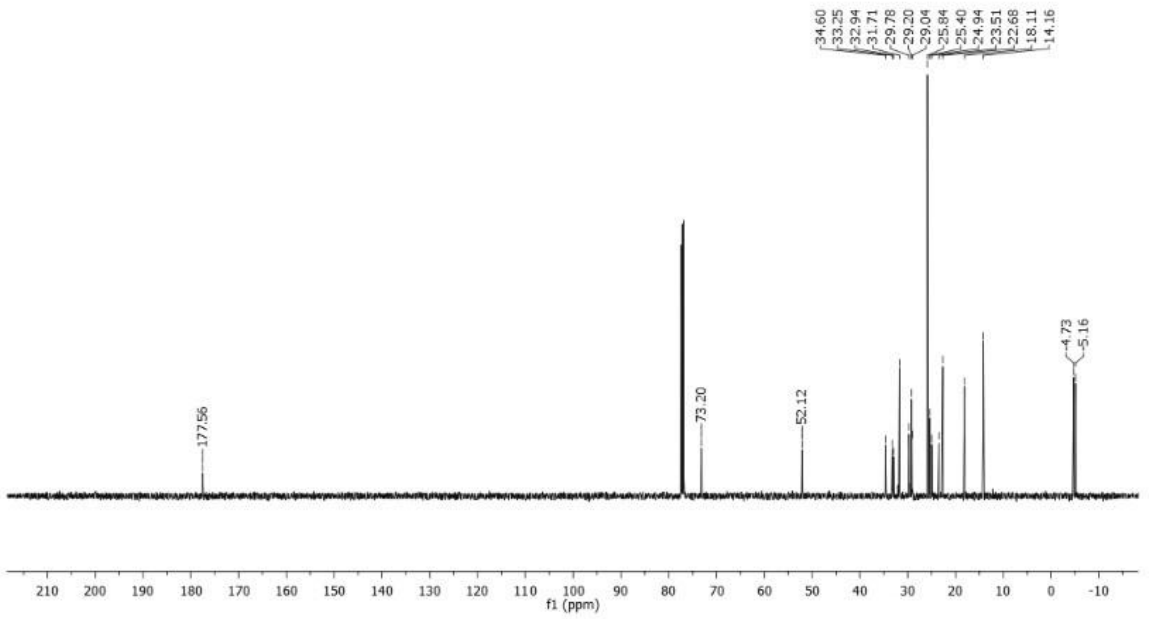
177.56
73.20
52.12
34.60
33.25
32.94
31.71
29.78
29.20
29.04
25.84
25.40
24.94
23.51
22.68
18.11
14.16
-4.73
-5.16
f1 (ppm)

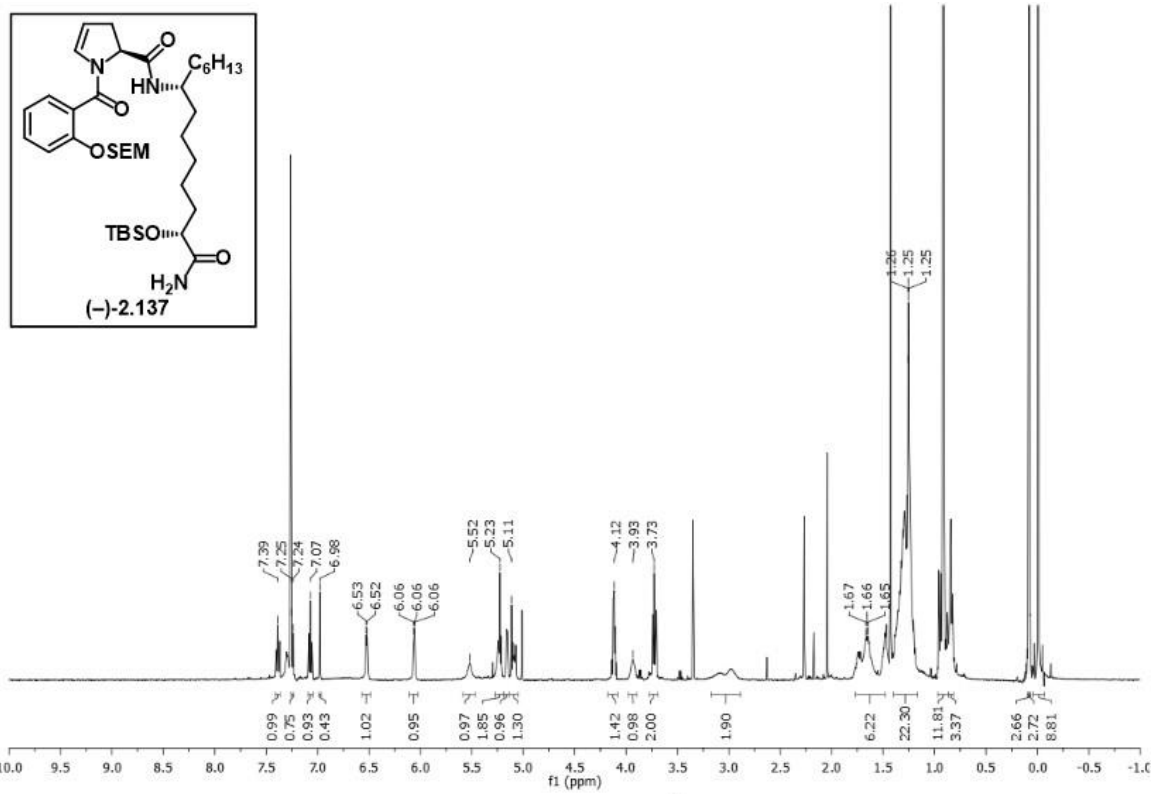
OSEM
TBSO
HN
C6H13
H2N
(–)-2.137
7.39
7.25
7.24
7.07
6.98
6.53
6.52
6.06
6.06
6.06
5.52
5.23
5.11
4.12
3.93
3.73
1.67
1.66
1.65
1.26
1.25
1.25
0.99
0.75
0.93
0.43
1.02
0.95
0.97
1.85
0.96
1.30
1.42
0.98
2.00
1.90
6.22
22.30
11.81
3.37
2.66
2.72
8.81
f1 (ppm)

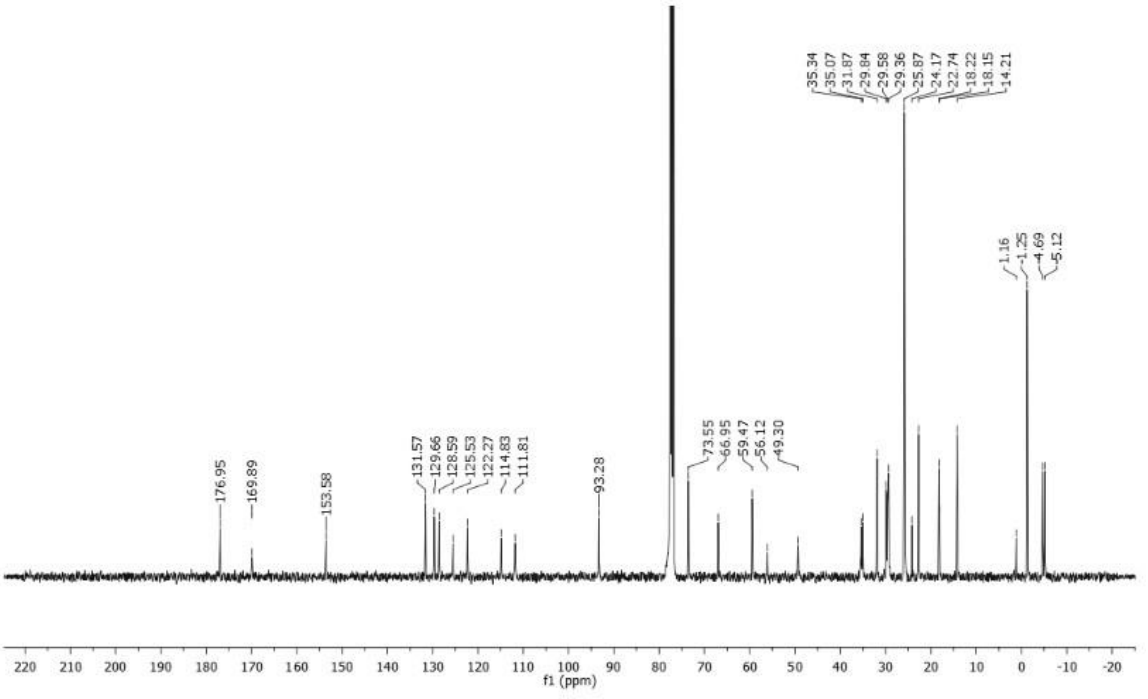
35.34
35.07
31.87
29.84
29.58
29.36
25.87
24.17
22.74
18.22
18.15
14.21
1.16
1.25
4.69
5.12
176.95
169.89
153.58
131.57
129.66
128.59
125.53
122.27
114.83
111.81
93.28
73.55
66.95
59.47
56.12
49.30
f1 (ppm)

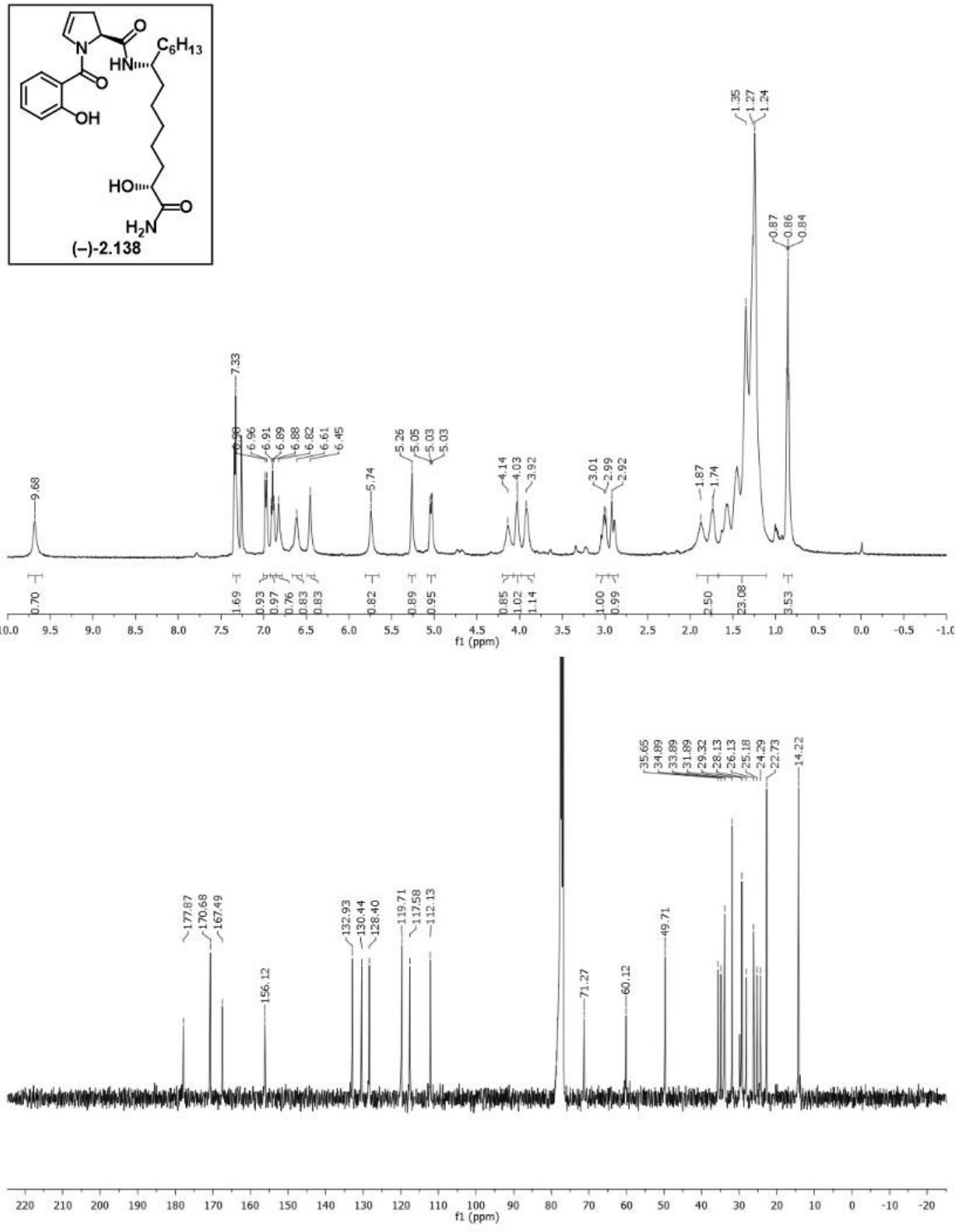
(–)-2.138
f1 (ppm)
f1 (ppm)

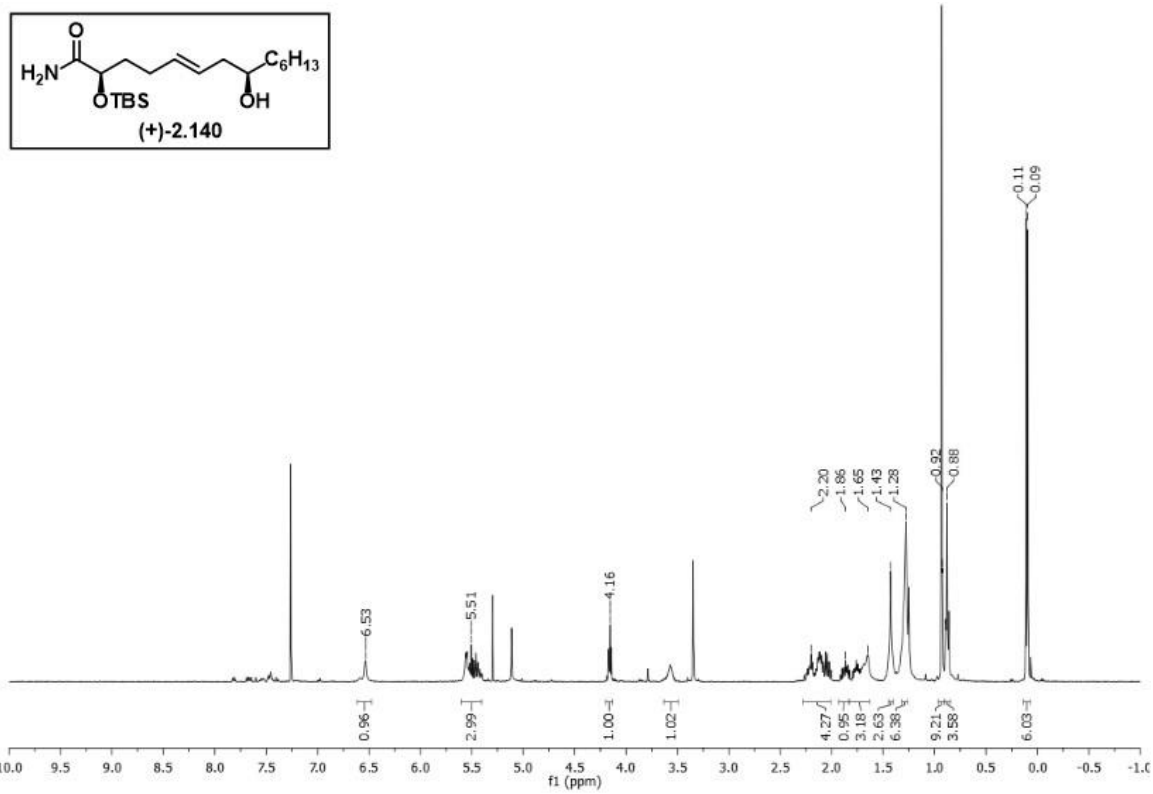
O
H2N
C6H13
OTBS
OH
(+)-2.140
0.11
0.09
2.20
1.86
1.65
1.43
1.28
0.92
0.88
6.53
5.51
4.16
0.96
2.99
1.00
1.02
4.27
0.95
3.18
2.63
6.38
9.21
3.58
6.03
f1 (ppm)

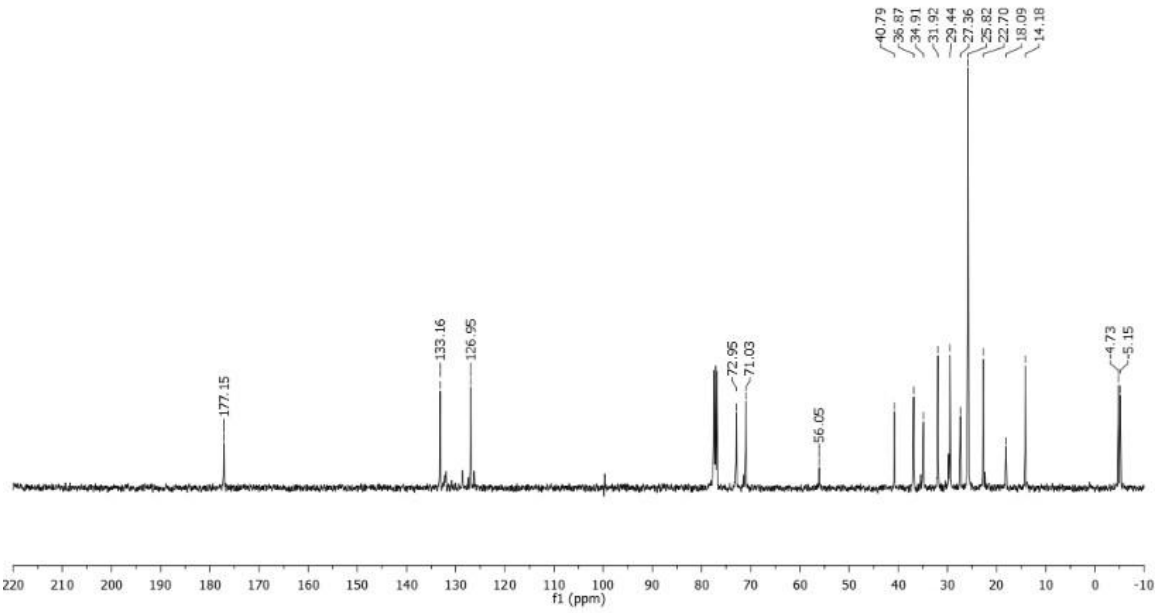
40.79
36.87
34.91
31.92
29.44
27.36
25.82
22.70
18.09
14.18
177.15
133.16
126.95
72.95
71.03
56.05
4.73
5.15
f1 (ppm)

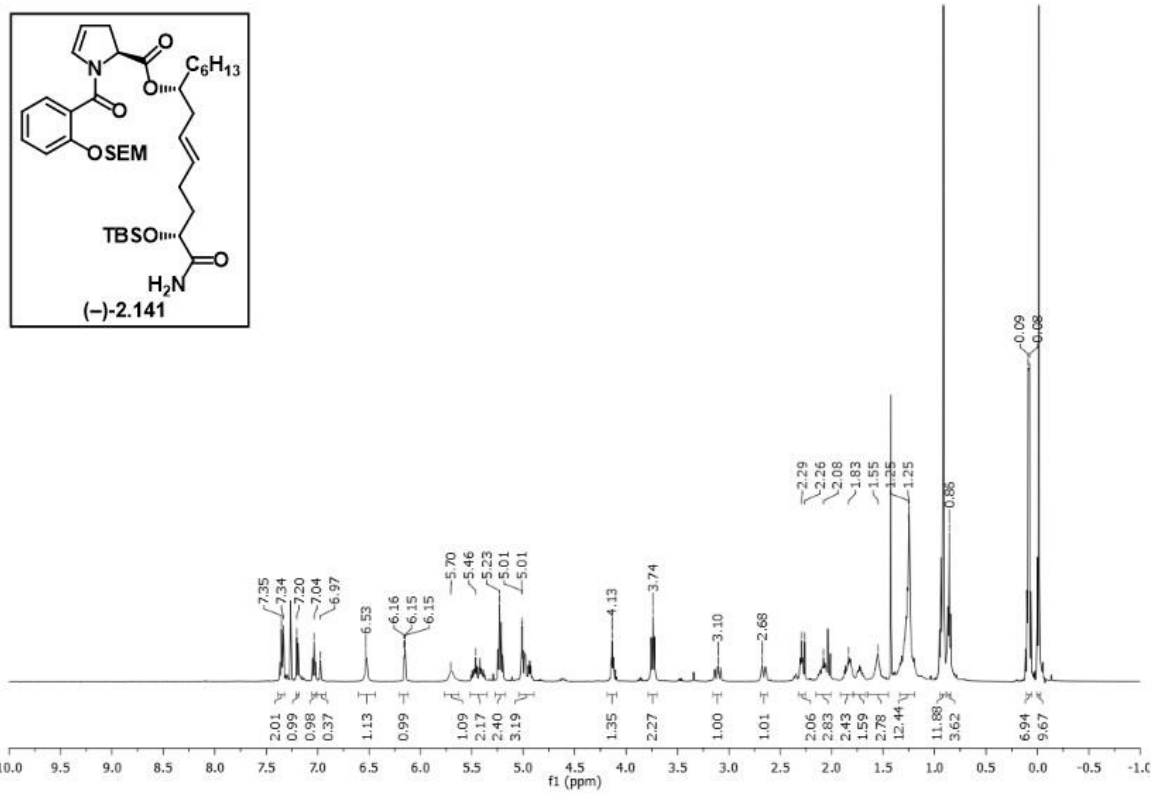
C6H13
OSEM
TBSO
H2N
(–)-2.141
7.35
7.34
7.20
7.04
6.97
6.53
6.16
6.15
6.15
5.70
5.46
5.23
5.01
5.01
4.13
3.74
3.10
2.68
2.29
2.26
2.08
1.83
1.55
1.25
1.25
0.86
0.09
0.08
2.01
0.99
0.98
0.37
1.13
0.99
1.09
2.17
2.40
3.19
1.35
2.27
1.00
1.01
2.06
2.83
2.43
1.59
2.78
12.44
11.88
3.62
6.94
9.67
f1 (ppm)

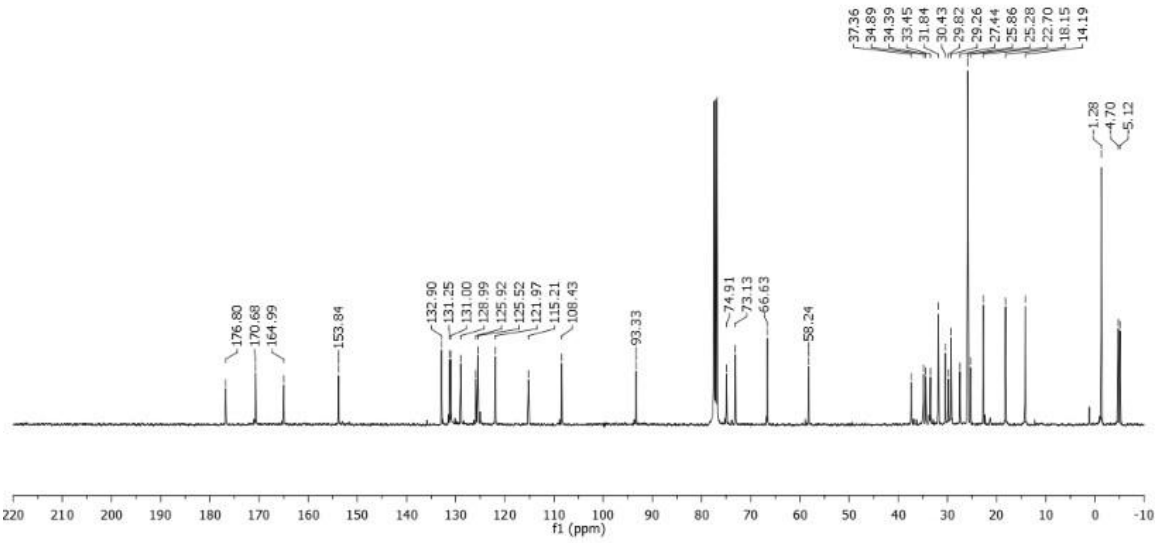
176.80
170.68
164.99
153.84
132.90
131.25
131.00
128.99
125.92
125.52
121.97
115.21
108.43
93.33
74.91
73.13
66.63
58.24
37.36
34.89
34.39
33.45
31.84
30.43
29.82
29.26
27.44
25.86
25.28
22.70
18.15
14.19
1.28
4.70
5.12
f1 (ppm)

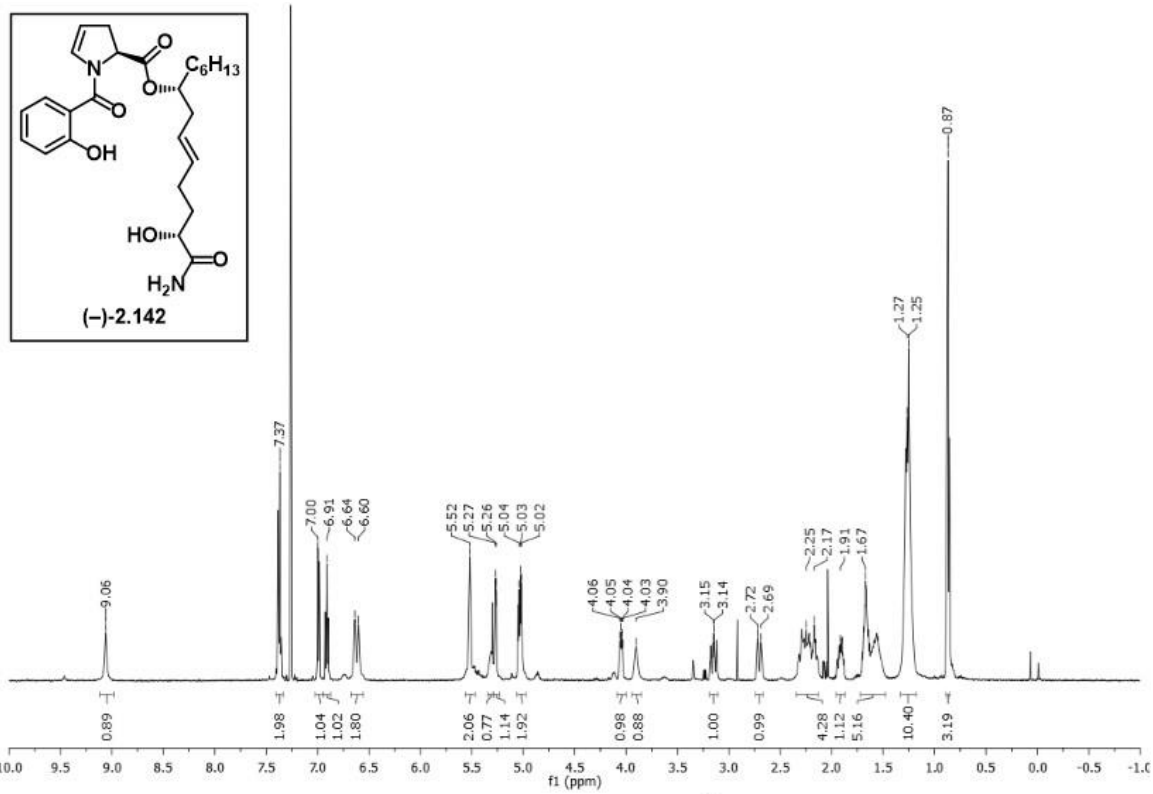
(–)-2.142
9.06
7.37
7.00
6.91
6.64
6.60
5.52
5.27
5.26
5.04
5.03
5.02
4.06
4.05
4.04
4.03
3.90
3.15
3.14
2.72
2.69
2.25
2.17
1.91
1.67
1.27
1.25
0.87
f1 (ppm)

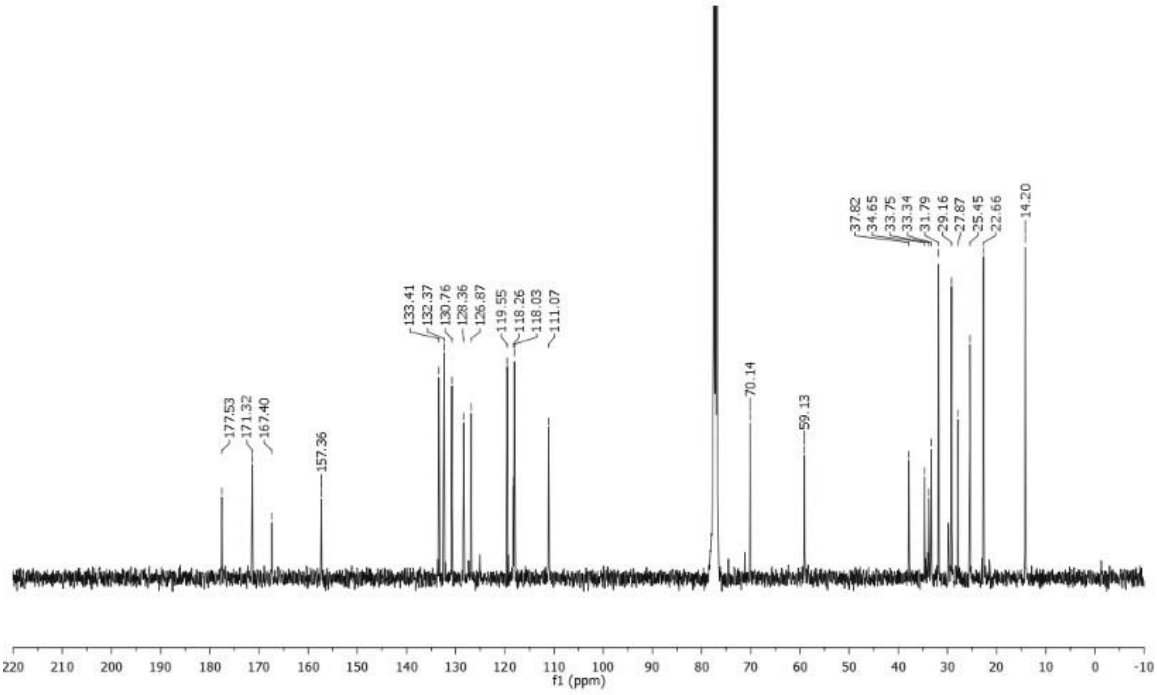
177.53
171.32
167.40
157.36
133.41
132.37
130.76
128.36
126.87
119.55
118.26
118.03
111.07
70.14
59.13
37.82
34.65
33.75
33.34
31.79
29.16
27.87
25.45
22.66
14.20
f1 (ppm)

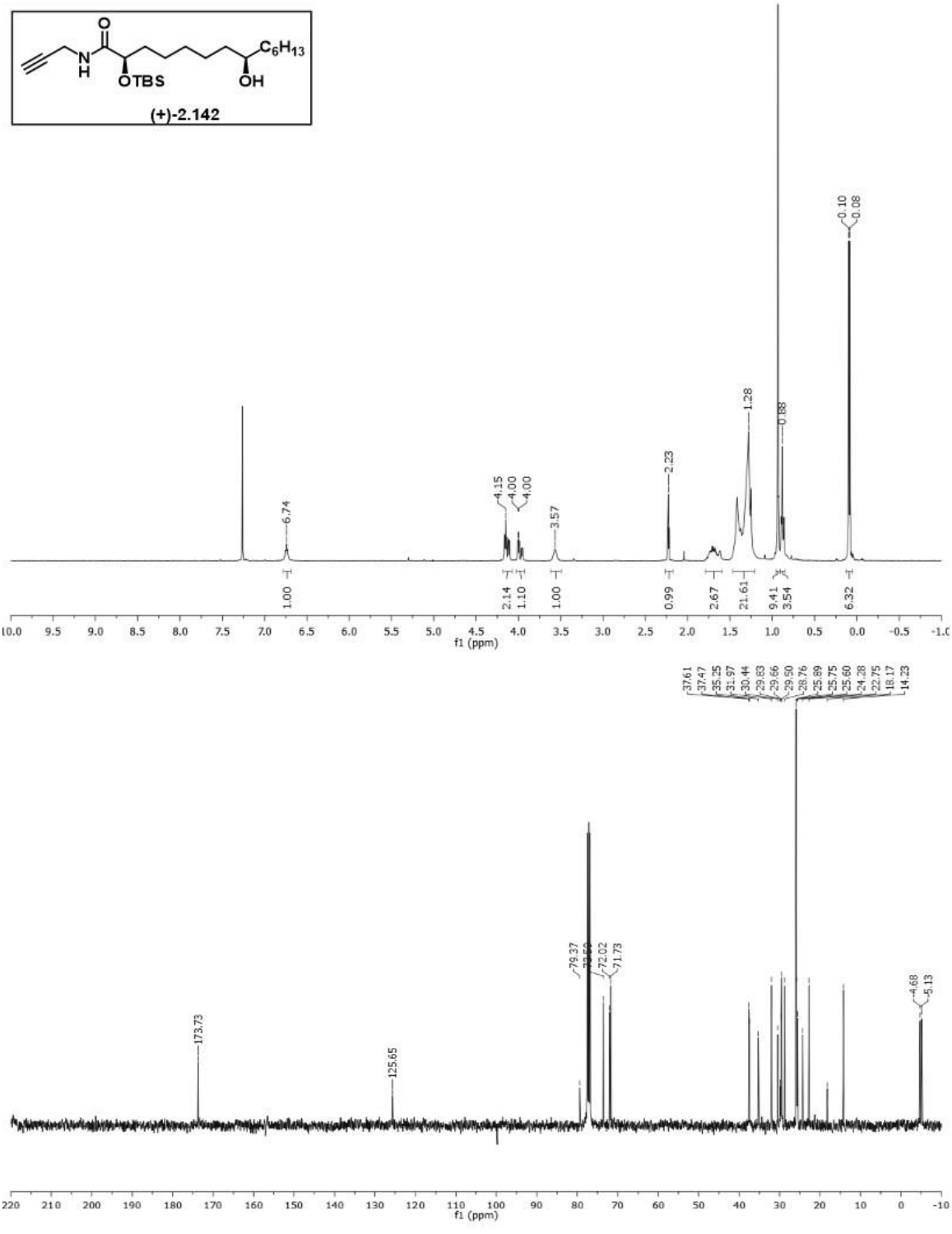
(+)-2.142
f1 (ppm)
f1 (ppm)

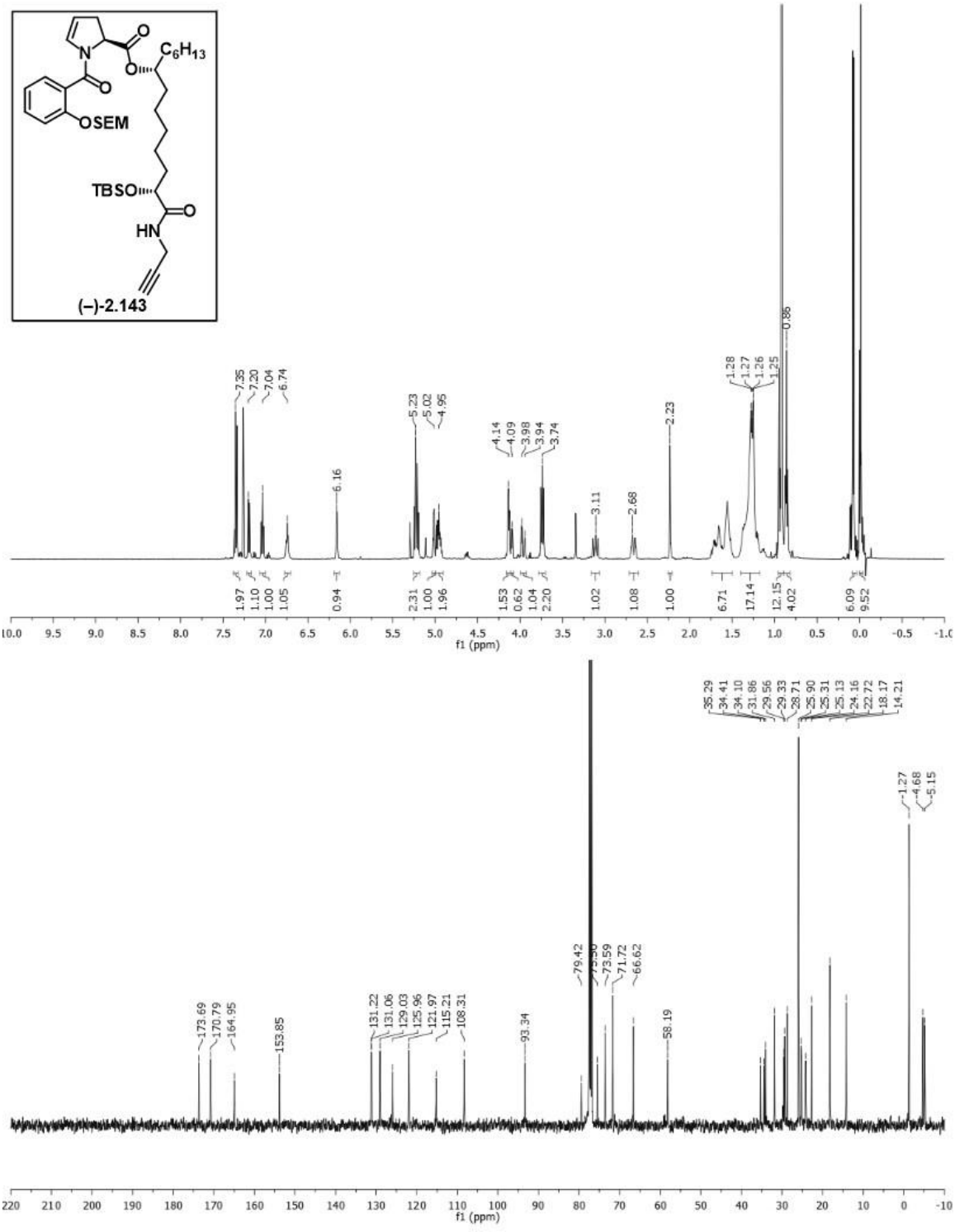
C6H13
OSEM
TBSO
HN
(–)-2.143
7.35
7.20
7.04
6.74
6.16
5.23
5.02
4.95
4.14
4.09
3.98
3.94
3.74
3.11
2.68
2.23
1.28
1.27
1.26
1.25
0.86
f1 (ppm)
35.29
34.41
34.10
31.86
29.56
29.33
28.71
25.90
25.31
25.13
24.16
22.72
18.17
14.21
-1.27
-4.68
-5.15
173.69
170.79
164.95
153.85
131.22
131.06
129.03
125.96
121.97
115.21
108.31
93.34
79.42
73.59
71.72
66.62
58.19
f1 (ppm)

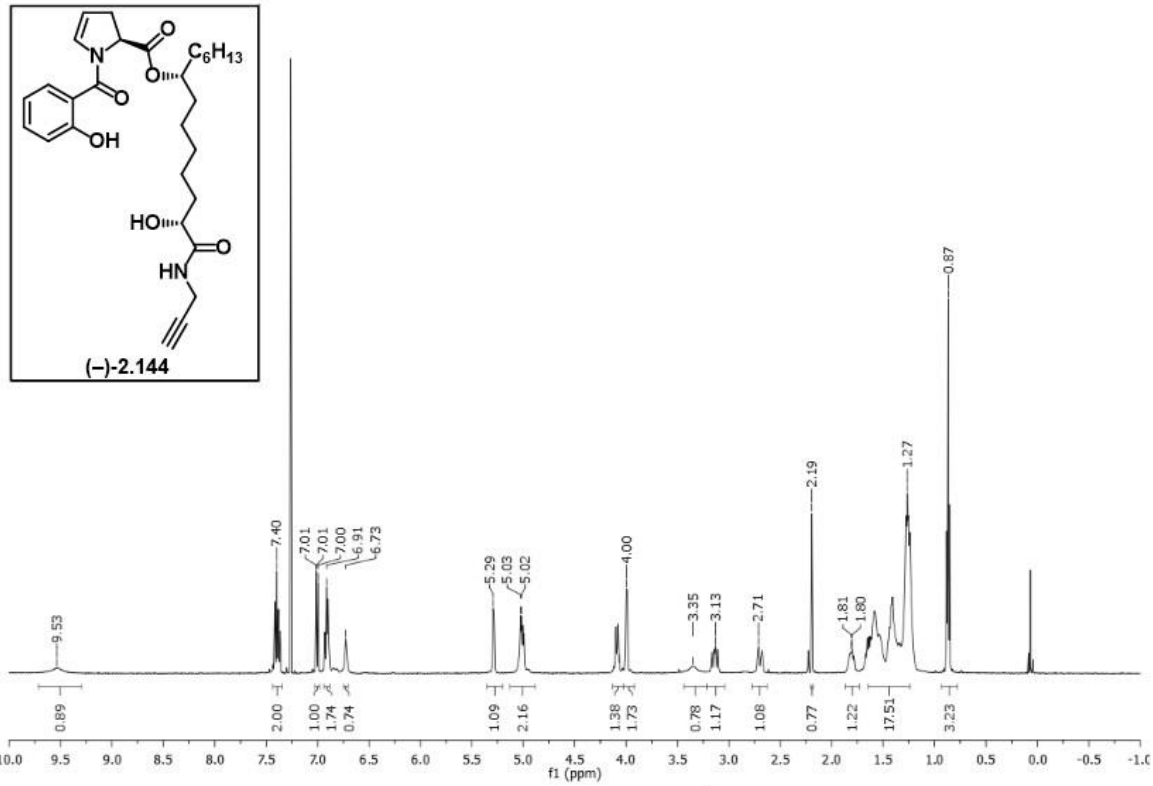
(–)-2.144
f1 (ppm)

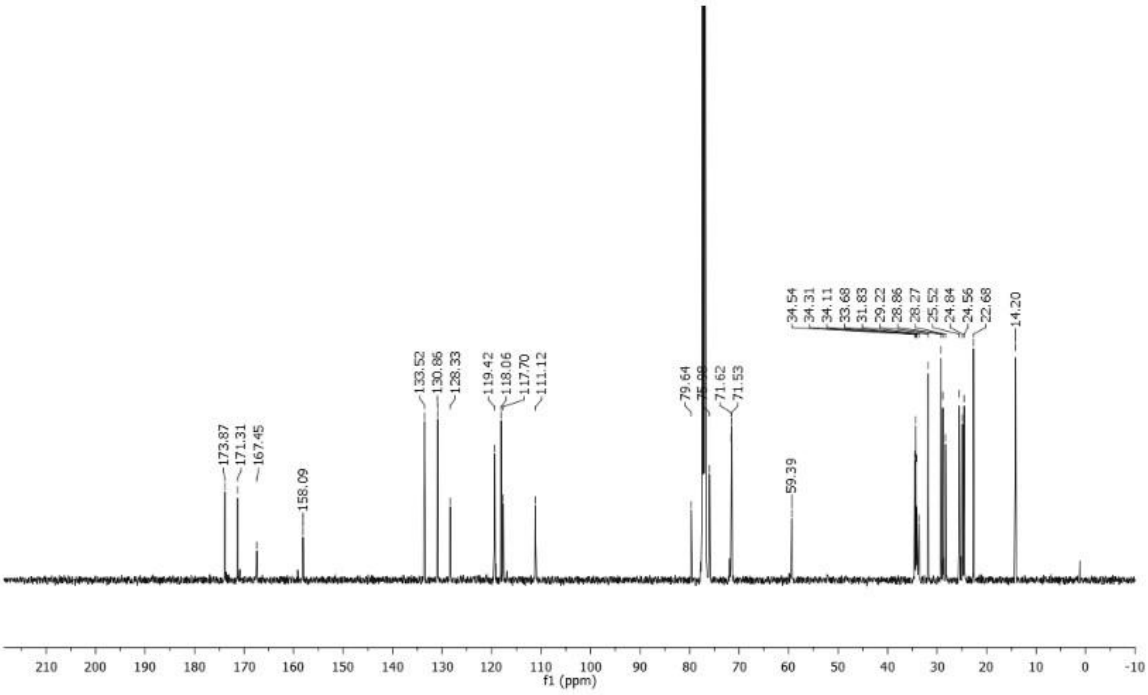
f1 (ppm)

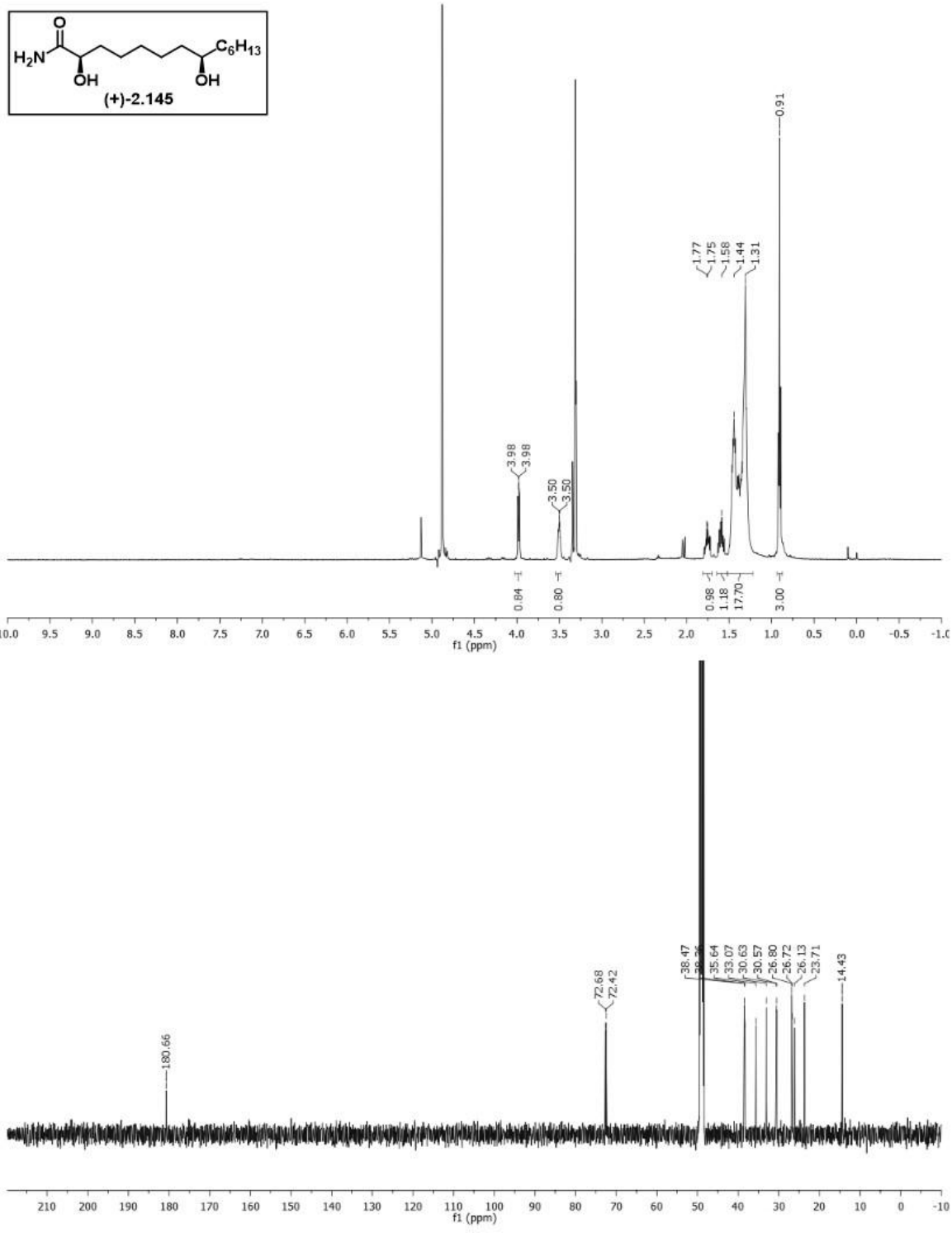
(+)-2.145
3.98
3.98
3.50
3.50
1.77
1.75
1.58
1.44
1.31
0.91
0.84
0.80
0.98
1.18
17.70
3.00
f1 (ppm)
180.66
72.68
72.42
38.47
35.64
33.07
30.63
30.57
26.80
26.72
26.13
23.71
14.43
f1 (ppm)

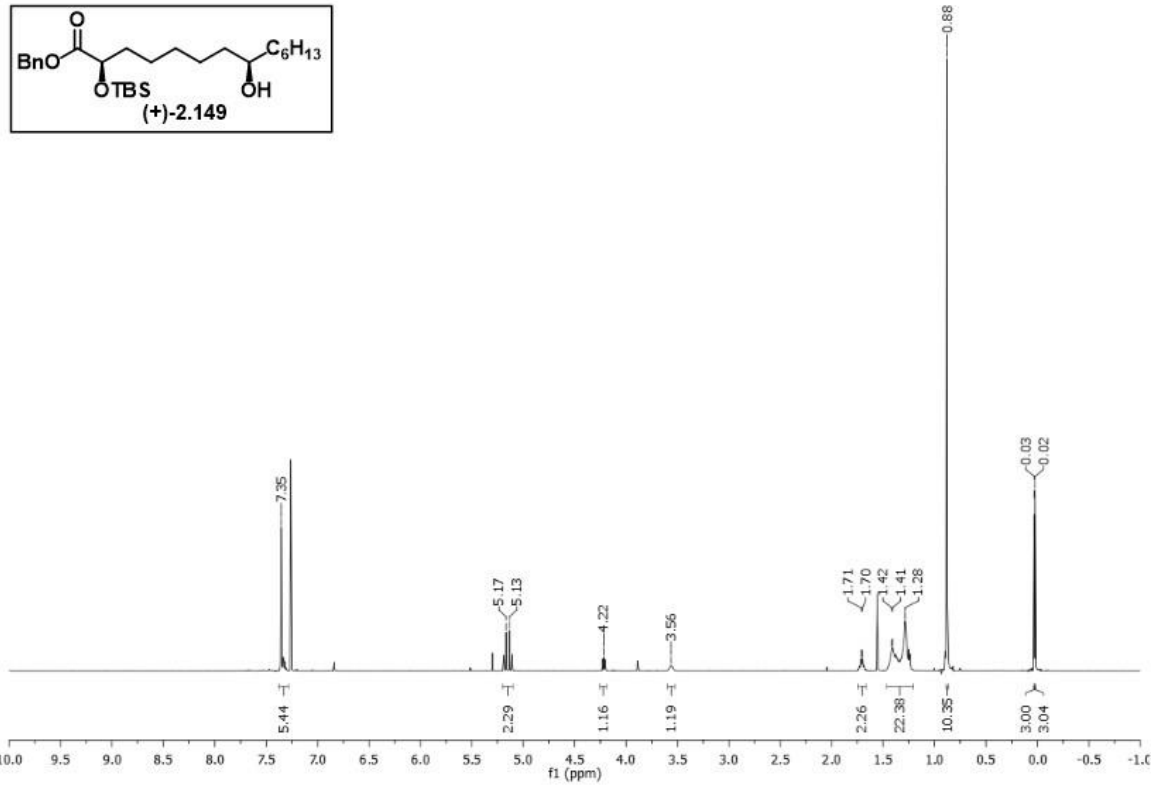
BnO
O
OTBS
OH
C6H13
(+)-2.149
7.35
5.17
5.13
4.22
3.56
1.71
1.70
1.42
1.41
1.28
0.88
0.03
0.02
5.44
2.29
1.16
1.19
2.26
22.38
10.35
3.00
3.04
f1 (ppm)

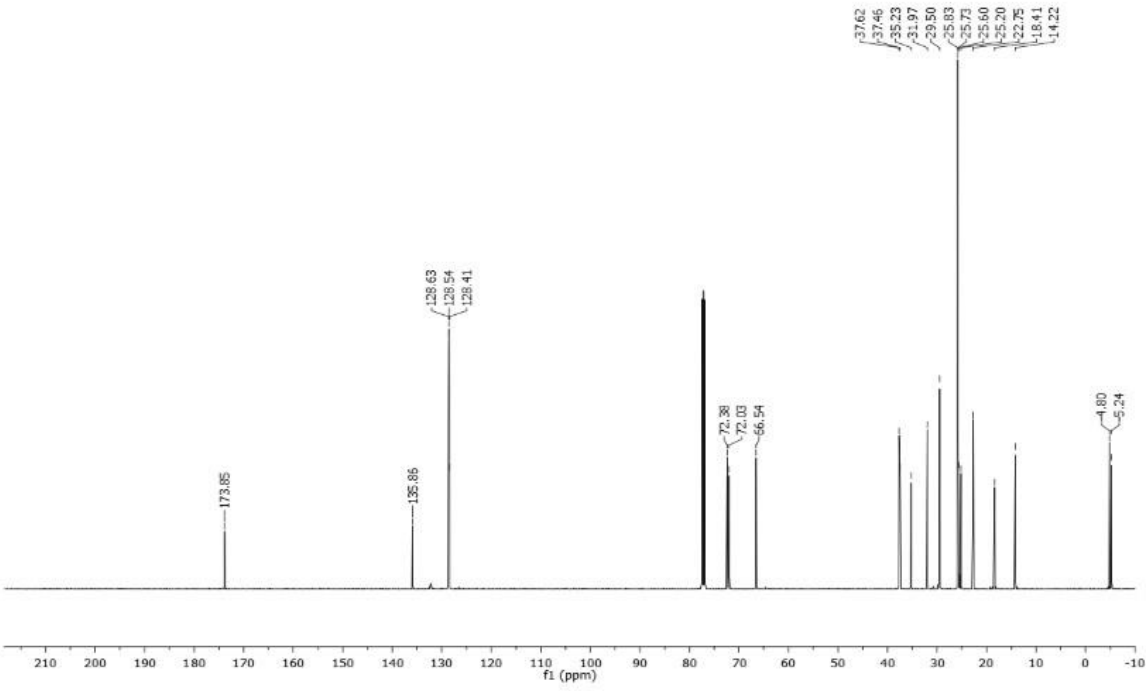
37.62
37.46
35.23
31.97
29.50
25.83
25.73
25.60
25.20
22.75
18.41
14.22
128.63
128.54
128.41
173.85
135.86
72.38
72.03
66.54
4.80
5.24
f1 (ppm)

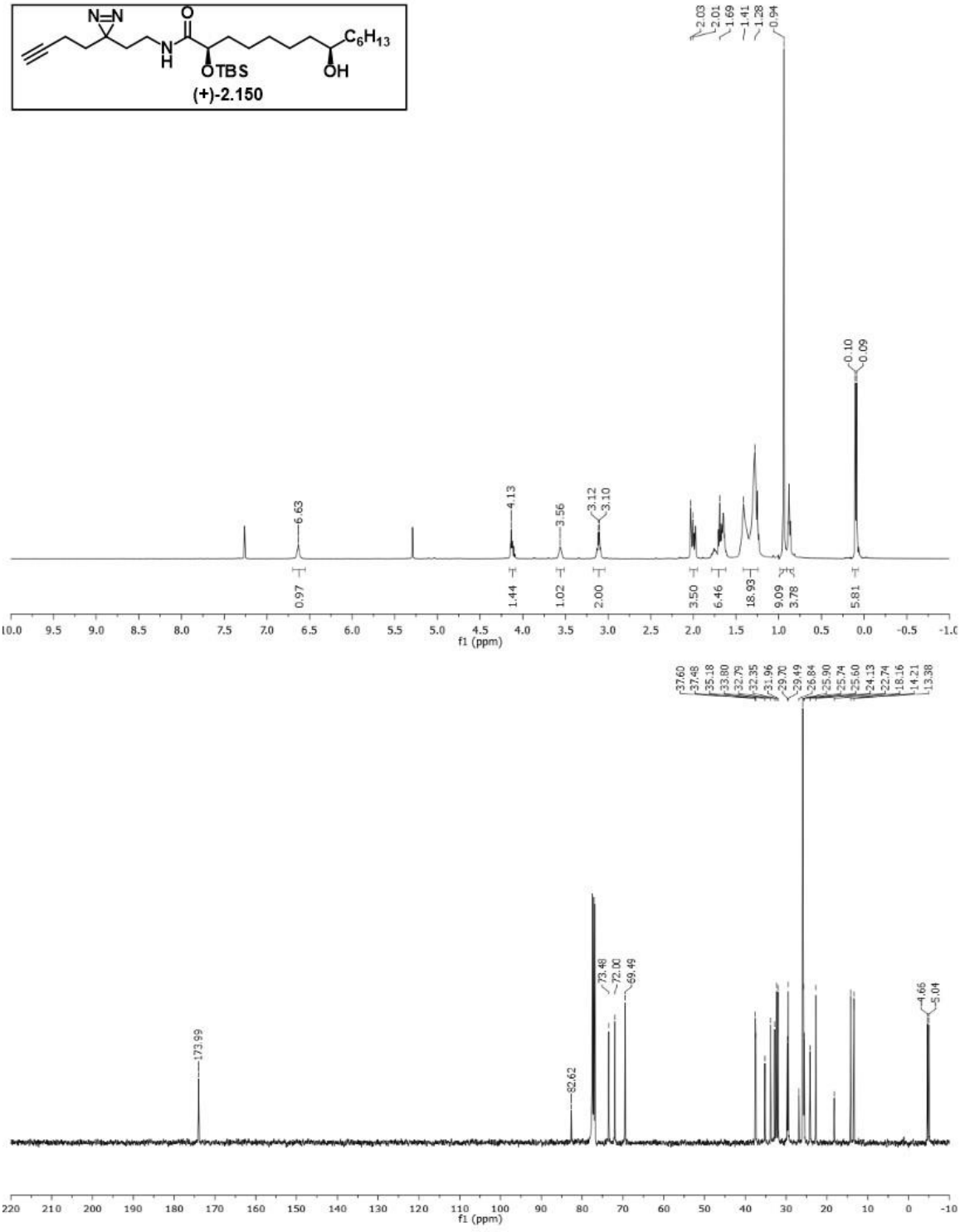
N=N
O
N
H
OTBS
OH
C6H13
(+)-2.150
f1 (ppm)

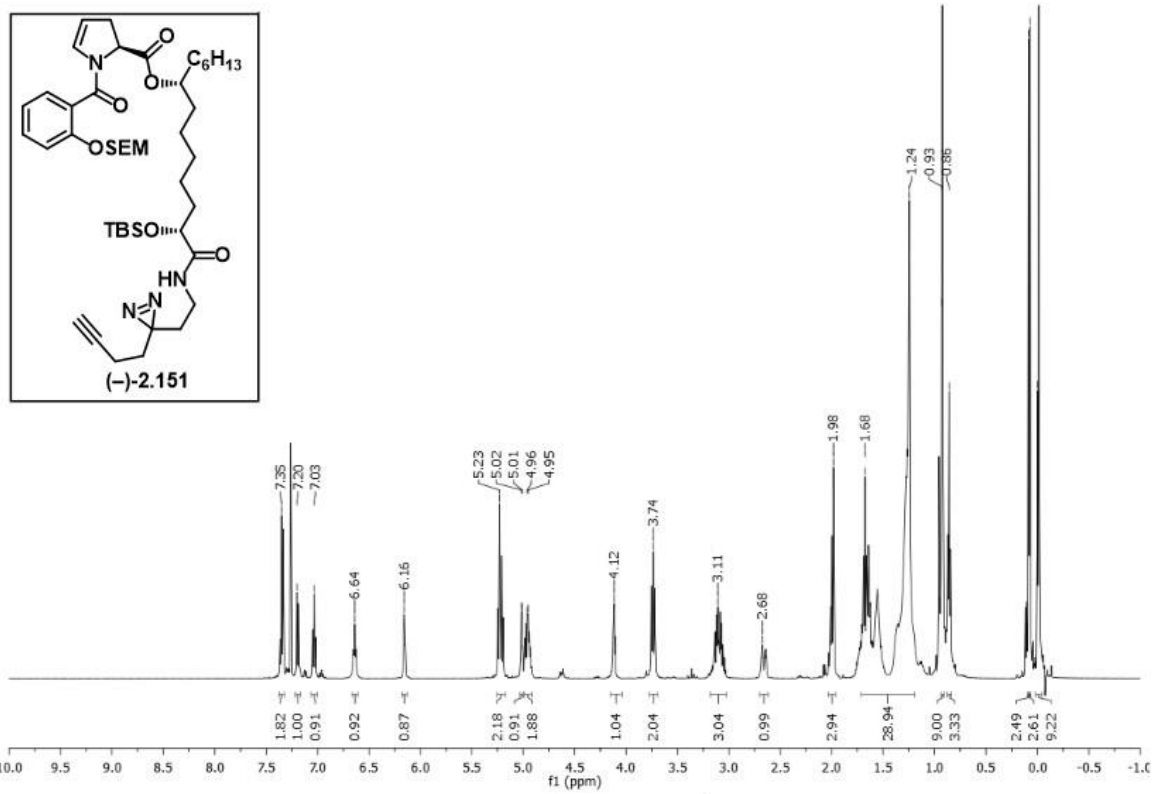
(–)-2.151
OSEM
TBSO
HN
7.35
7.20
7.03
6.64
6.16
5.23
5.02
5.01
4.96
4.95
4.12
3.74
3.11
2.68
1.98
1.68
1.24
0.93
0.86
f1 (ppm)

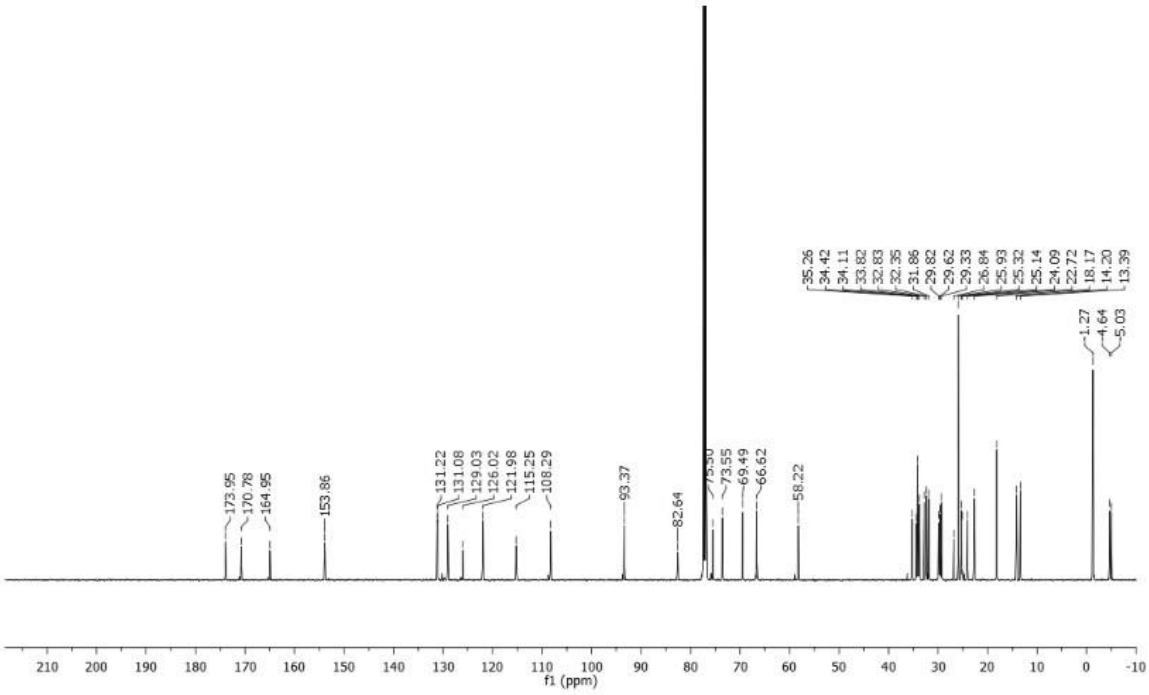
173.95
170.78
164.95
153.86
131.22
131.08
129.03
126.02
121.98
115.25
108.29
93.37
82.64
73.55
69.49
66.62
58.22
35.26
34.42
34.11
33.82
32.83
32.35
31.86
29.82
29.62
29.33
26.84
25.93
25.32
25.14
24.09
22.72
18.17
14.20
13.39
1.27
4.64
5.03
f1 (ppm)

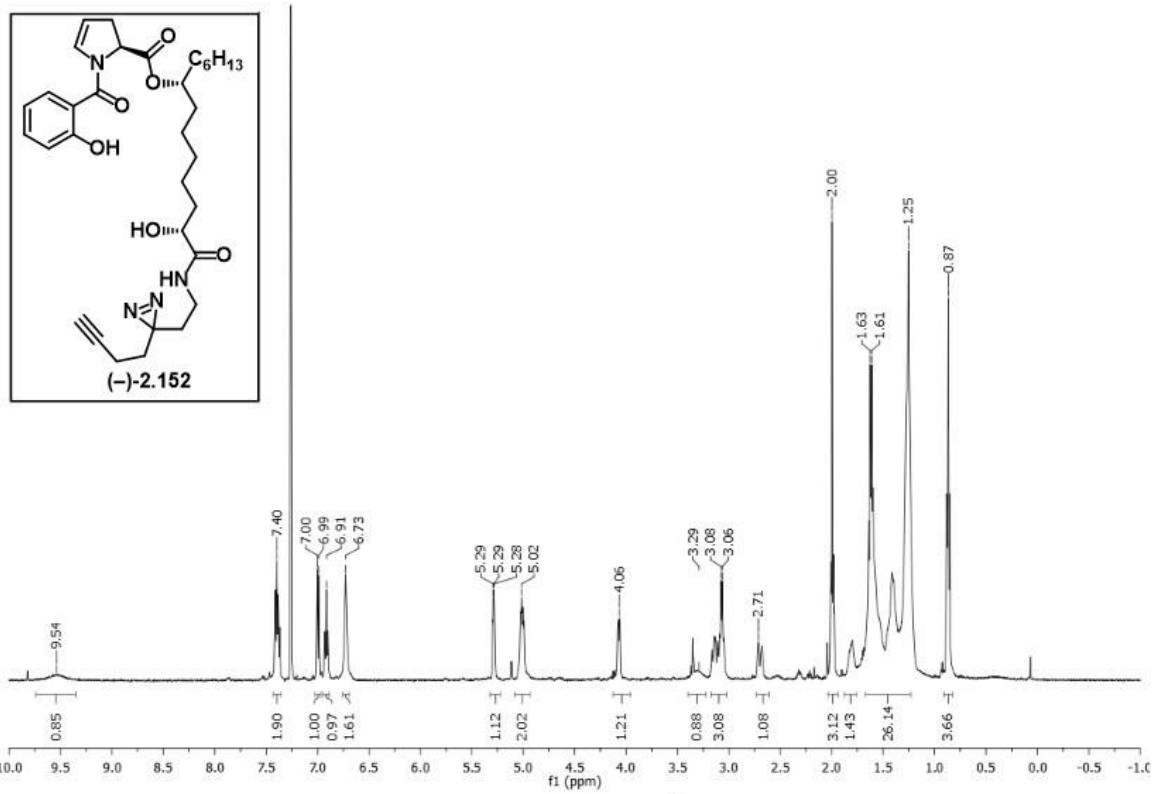
(–)-2.152
9.54
7.40
7.00
6.99
6.91
6.73
5.29
5.29
5.28
5.02
4.06
3.29
3.08
3.06
2.71
2.00
1.63
1.61
1.25
0.87
0.85
1.90
1.00
0.97
1.61
1.12
2.02
1.21
0.88
3.08
1.08
3.12
1.43
26.14
3.66
f1 (ppm)

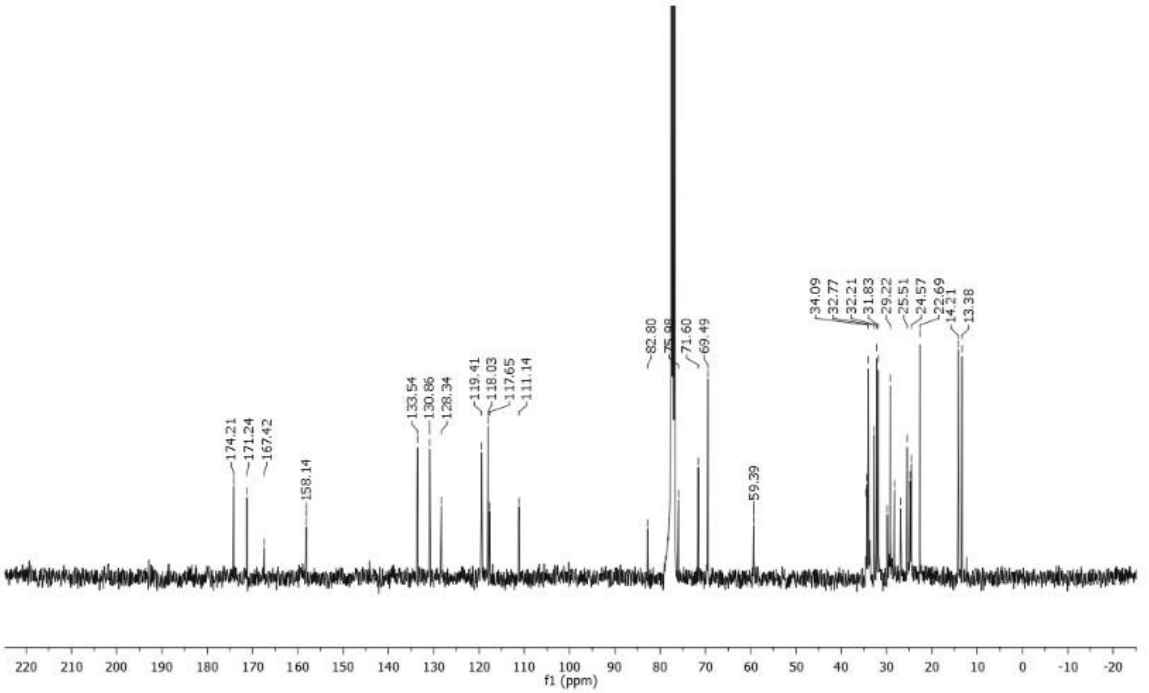
174.21
171.24
167.42
158.14
133.54
130.86
128.34
119.41
118.03
117.65
111.14
82.80
71.60
69.49
59.39
34.09
32.77
32.21
31.83
29.22
25.51
24.57
22.69
14.21
13.38
f1 (ppm)

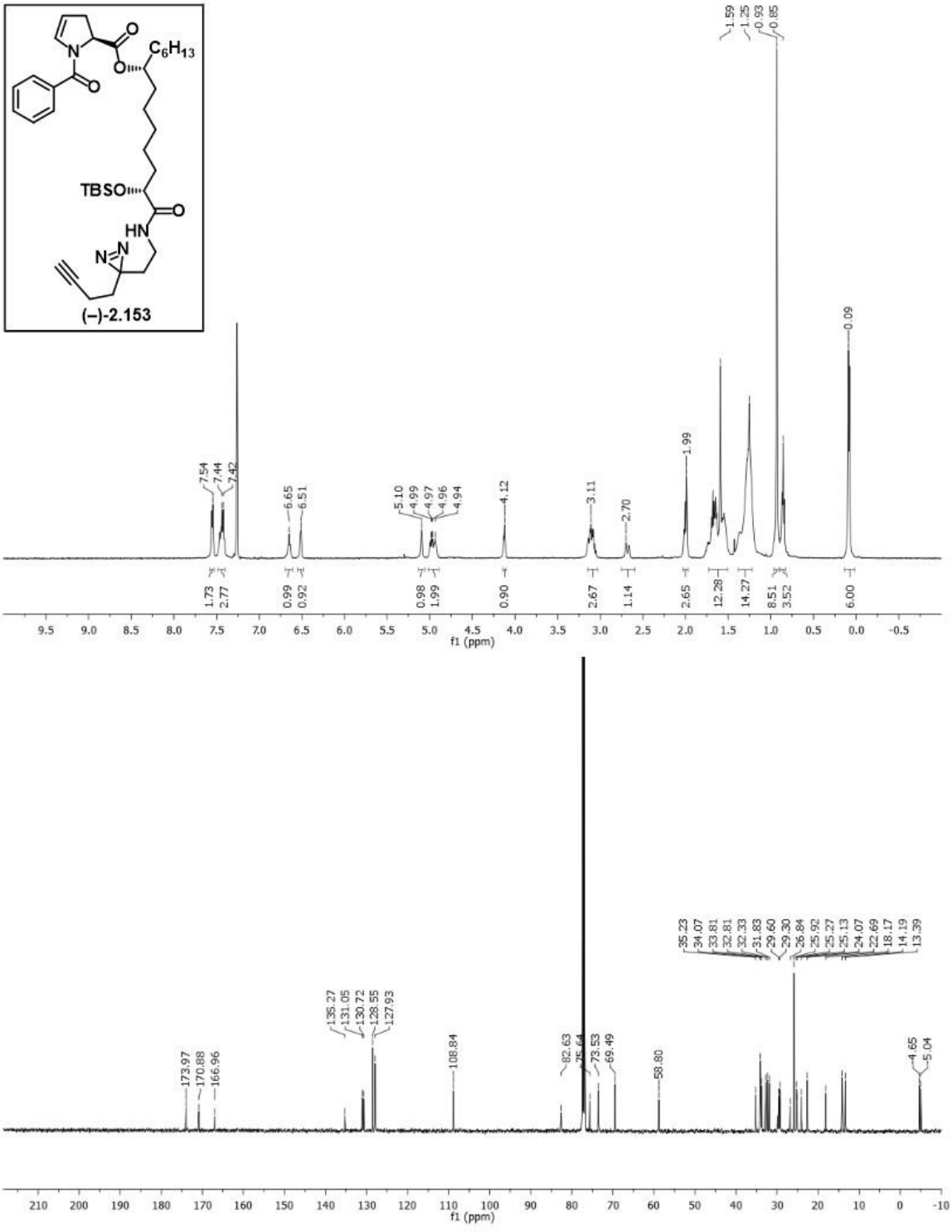
(–)-2.153
f1 (ppm)
f1 (ppm)

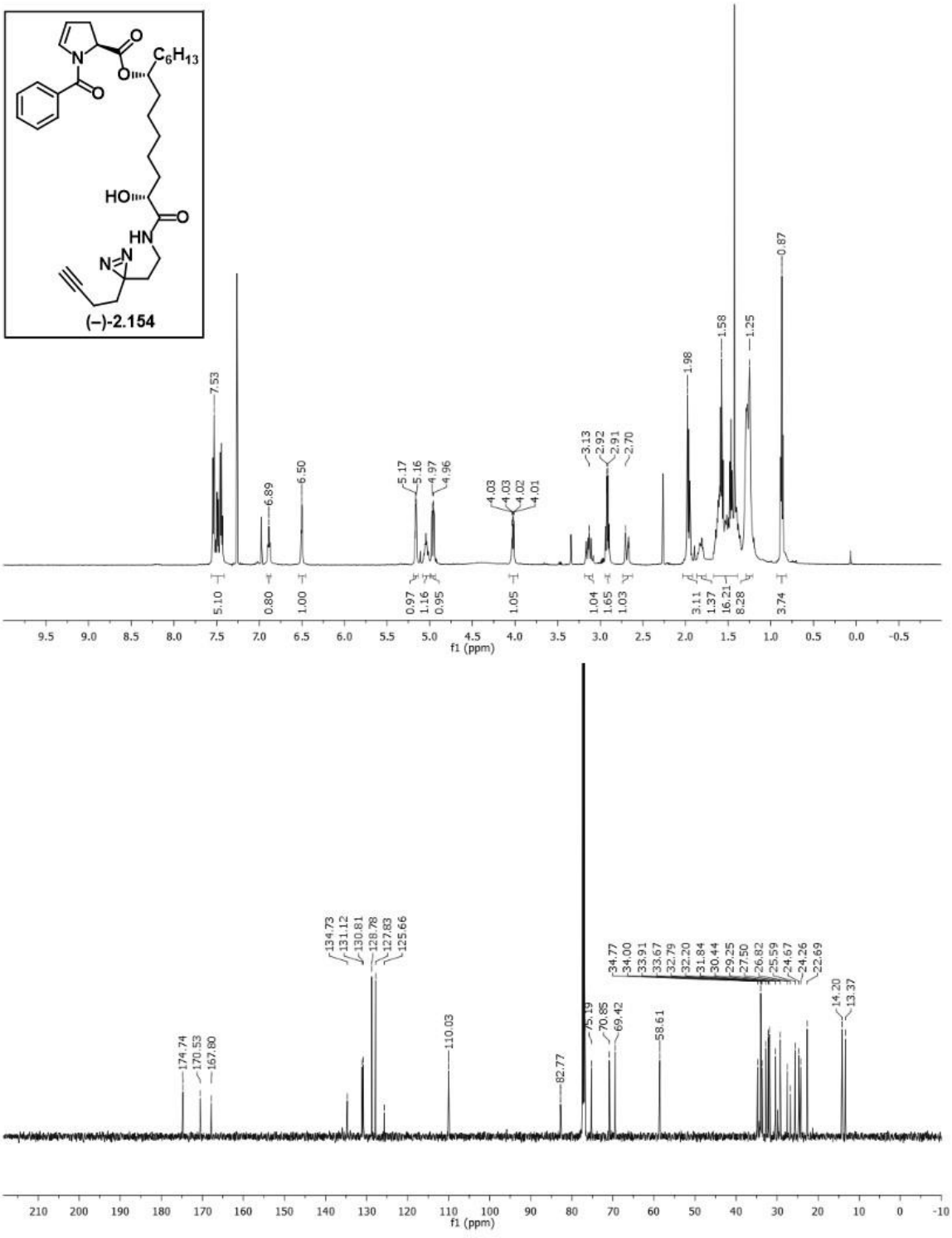
(–)-2.154
7.53
6.89
6.50
5.17
5.16
4.97
4.96
4.03
4.03
4.02
4.01
3.13
2.92
2.91
2.70
1.98
1.58
1.25
0.87
5.10
0.80
1.00
0.97
1.16
0.95
1.05
1.04
1.65
1.03
3.11
1.37
16.21
8.28
3.74
f1 (ppm)
174.74
170.53
167.80
134.73
131.12
130.81
128.78
127.83
125.66
110.03
82.77
75.19
70.85
69.42
58.61
34.77
34.00
33.91
33.67
32.79
32.20
31.84
30.44
29.25
27.50
26.82
25.59
24.67
24.26
22.69
14.20
13.37
f1 (ppm)

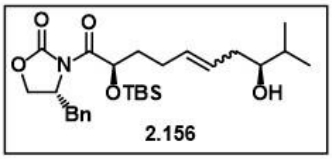

2.156

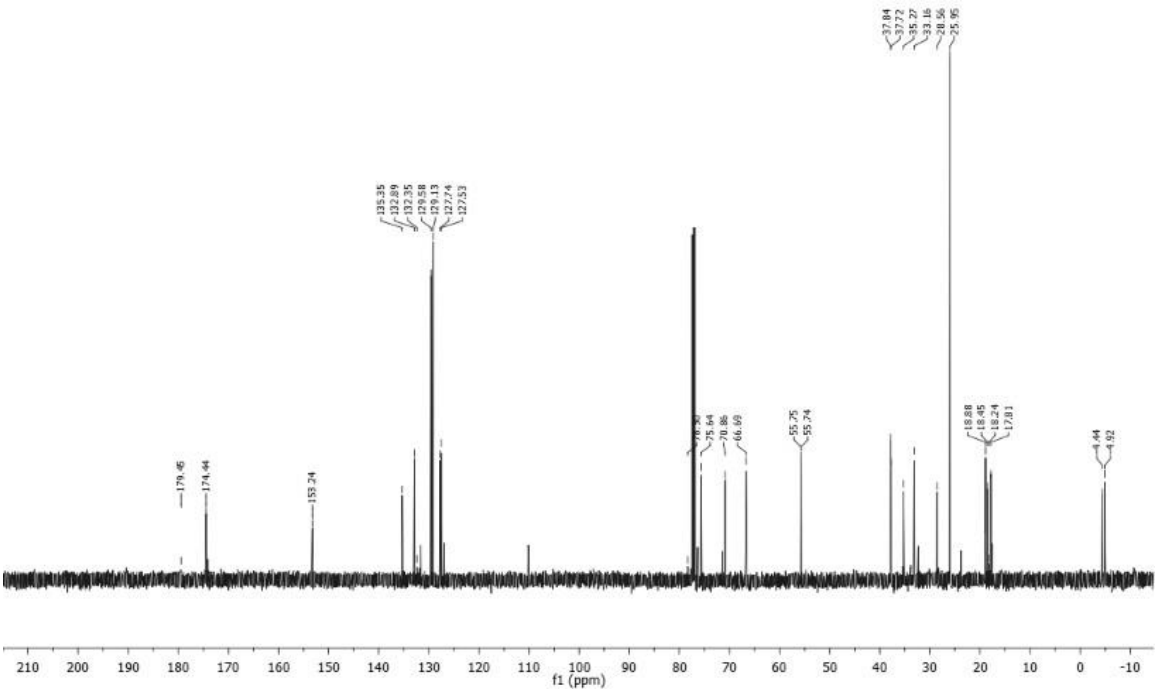

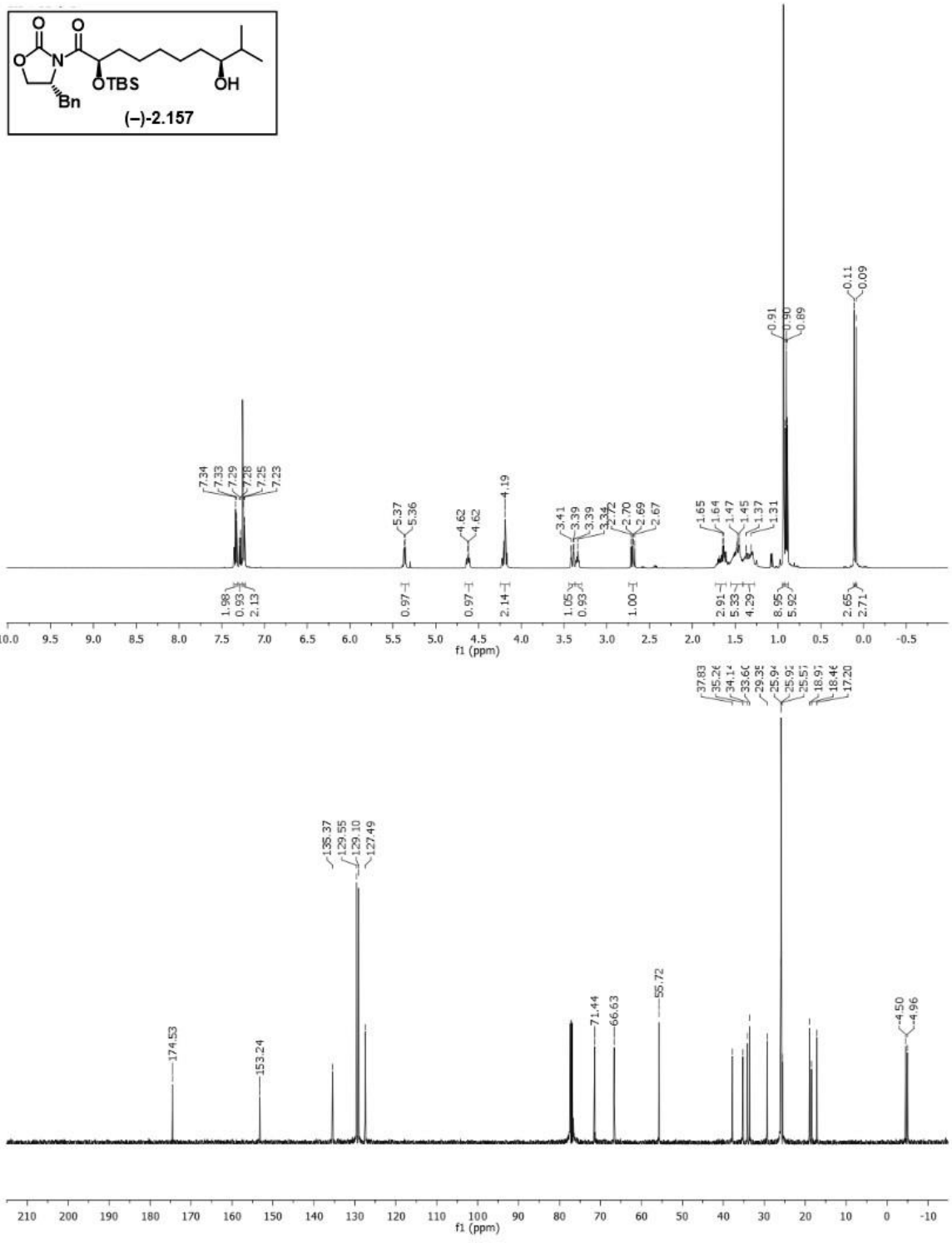
OTBS
OH
Bn
(–)-2.157
f1 (ppm)
f1 (ppm)

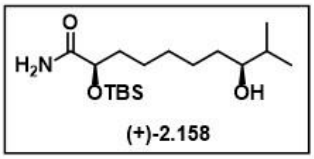
O
H2N
OTBS
OH

(+)-2.158

0.91
0.91
0.90
0.89
0.89
0.88
0.09
0.08
6.52
6.51
5.94
5.93
4.13
4.12
4.11
3.33
1.74
1.63
1.45
1.33
1.08
1.07
1.00
1.08
1.13
2.09
3.14
5.01
8.39
6.26
2.69
2.62
f1 (ppm)

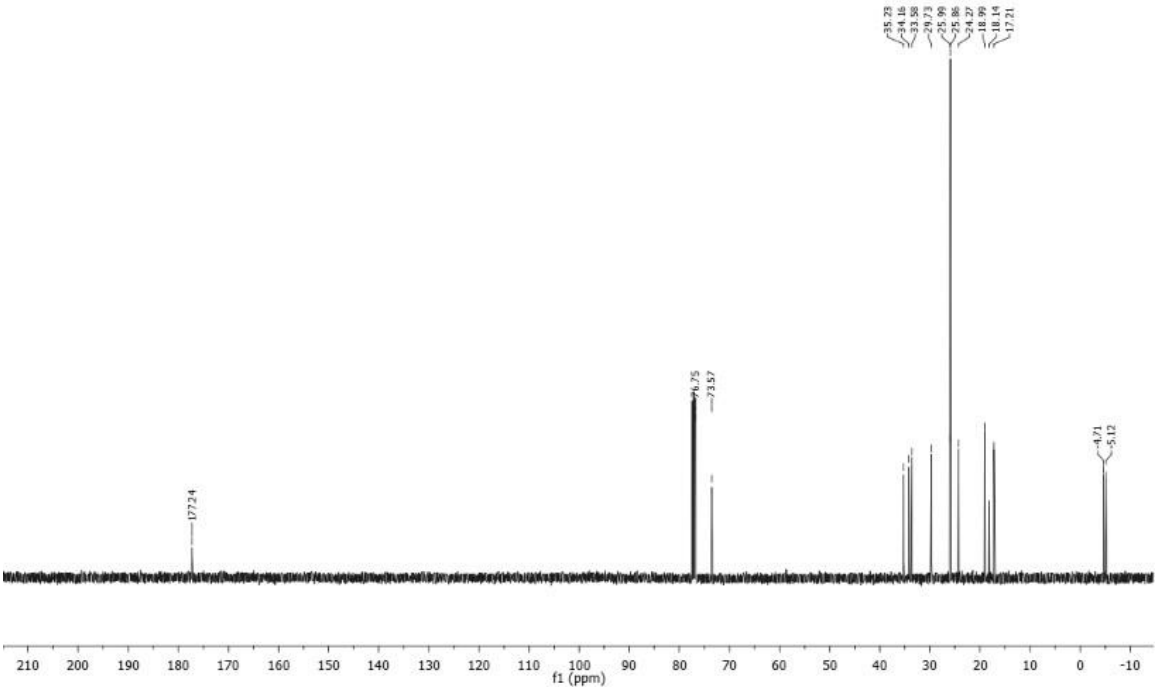
35.23
34.16
33.58
29.73
25.99
25.86
24.27
18.99
18.14
17.21
76.75
73.57
17724
4.71
5.12
f1 (ppm)

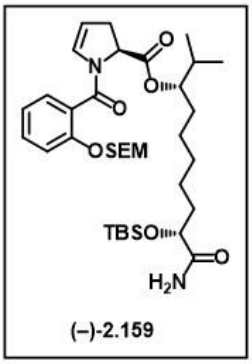

(–)-2.159

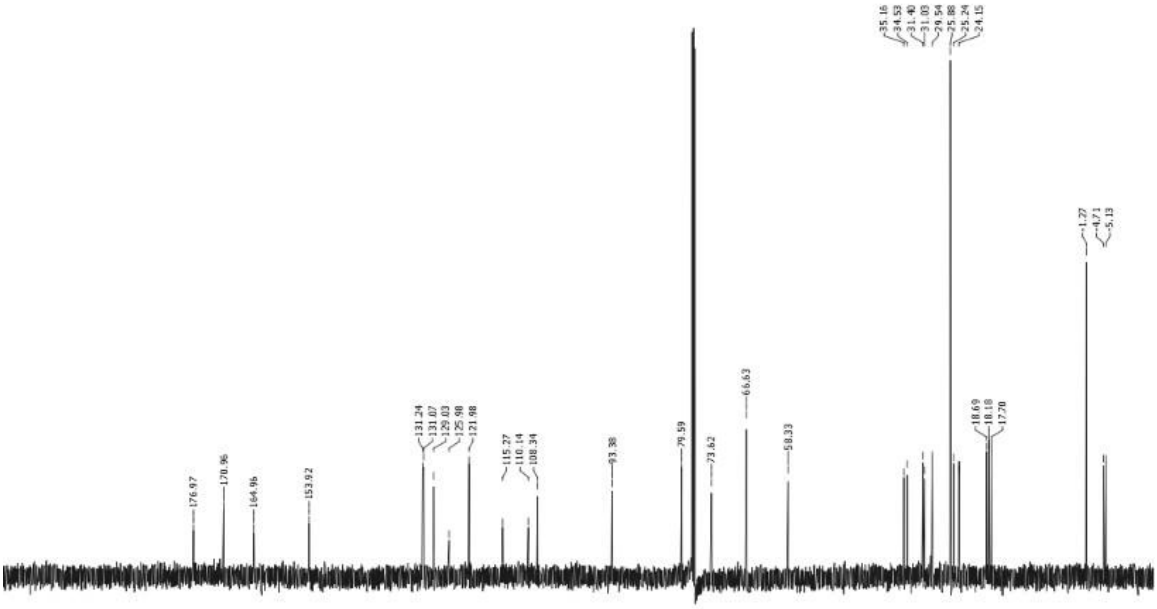

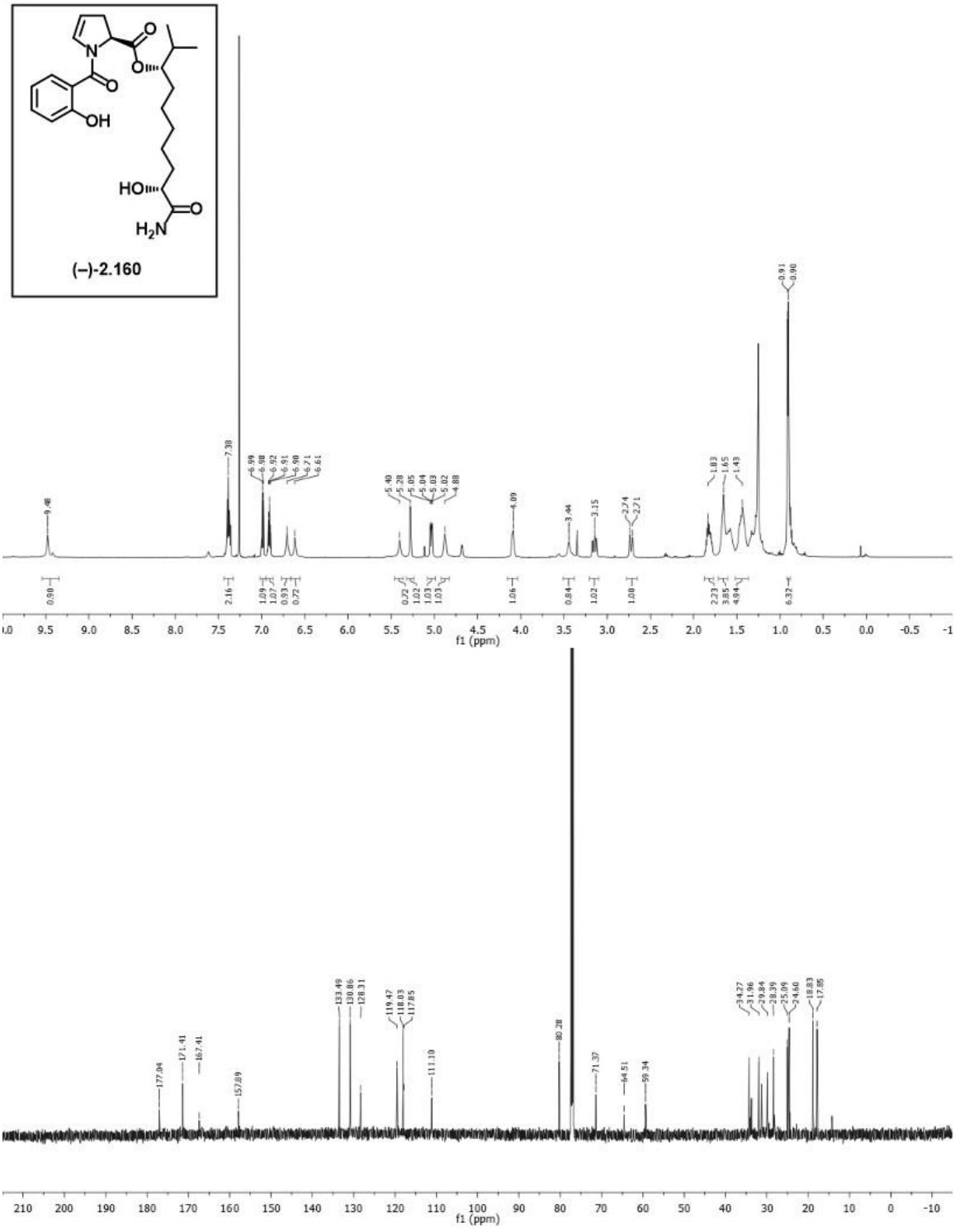
(–)-2.160
f1 (ppm)
f1 (ppm)

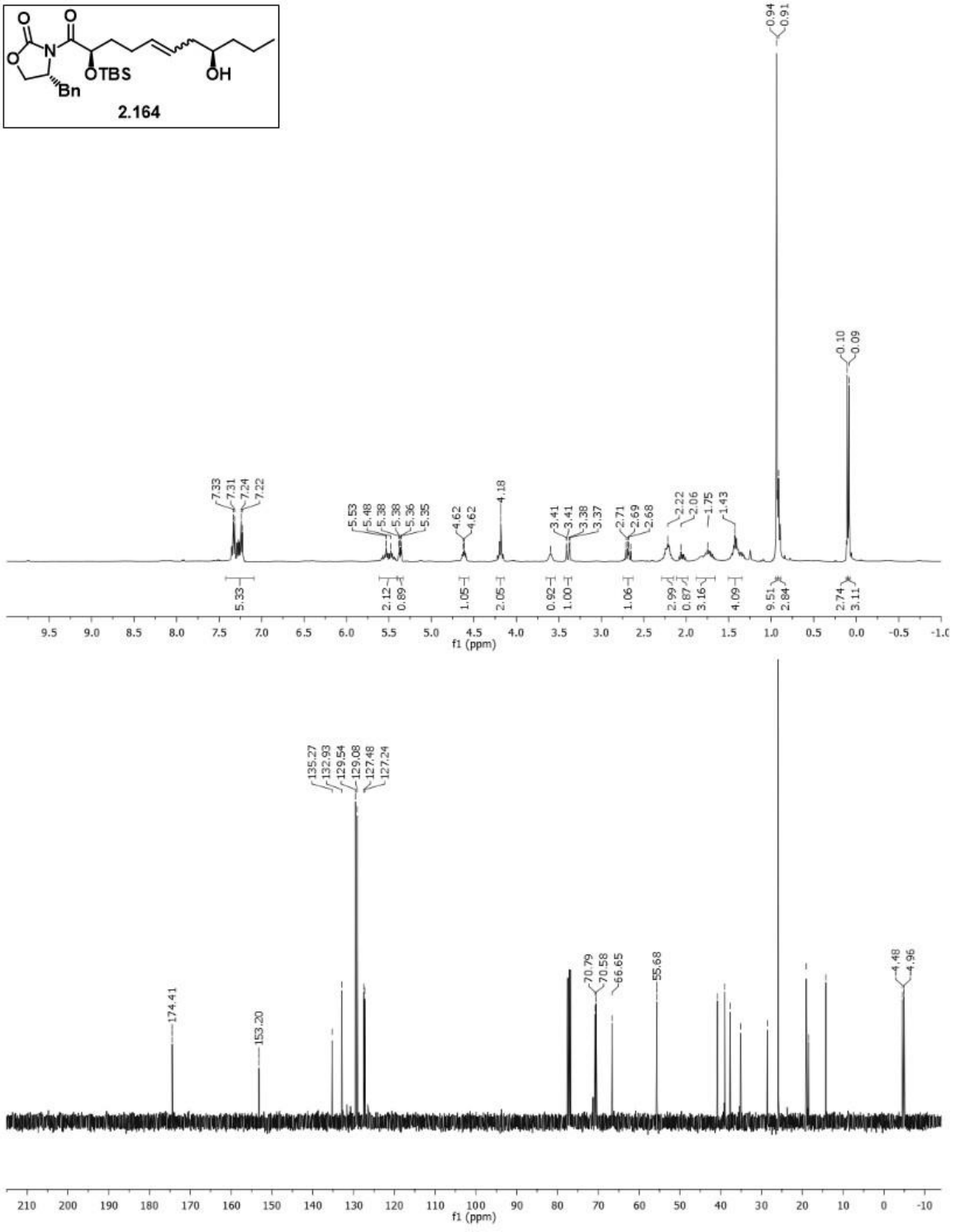
OTBS
OH
Bn
2.164
f1 (ppm)
f1 (ppm)

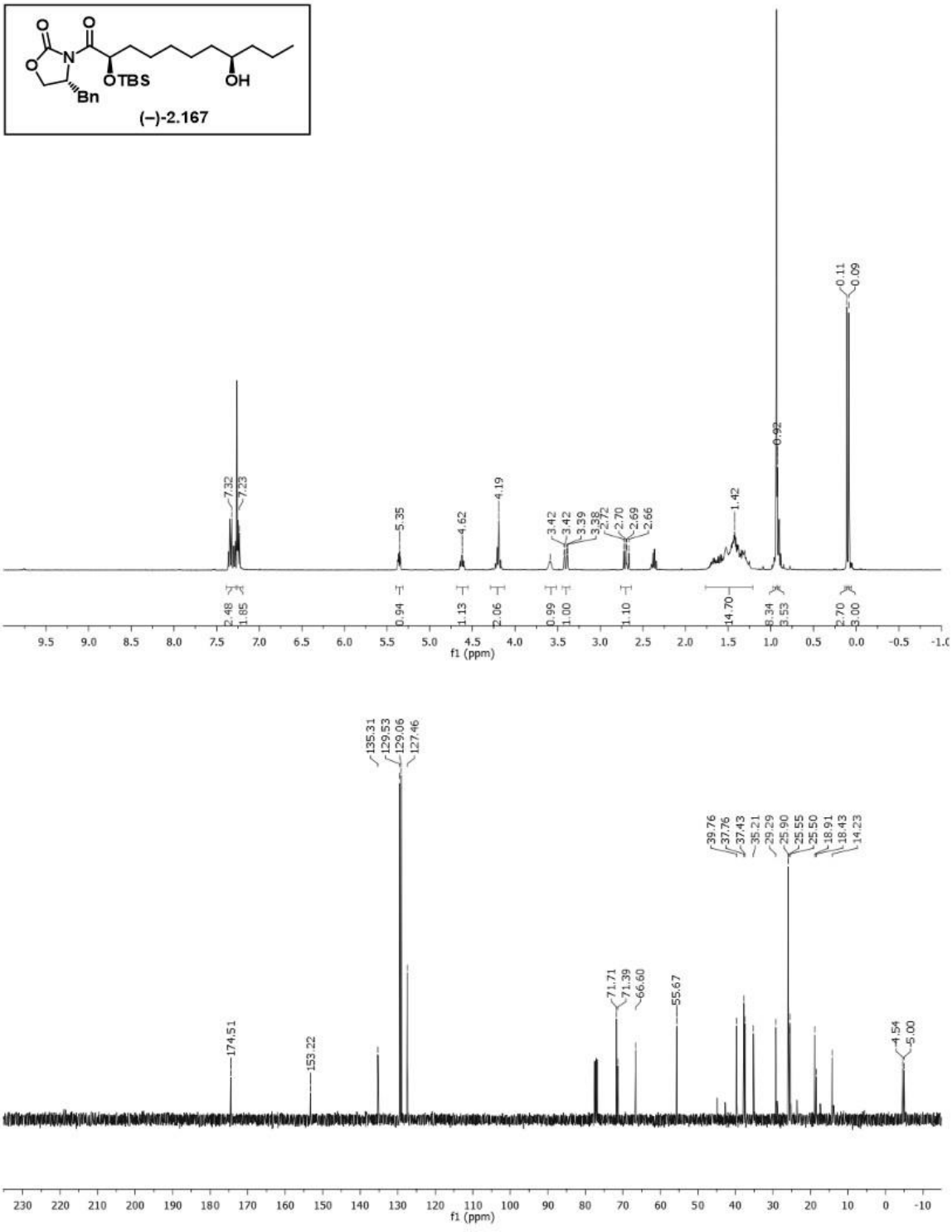
OTBS
OH
Bn
(–)-2.167
f1 (ppm)
f1 (ppm)

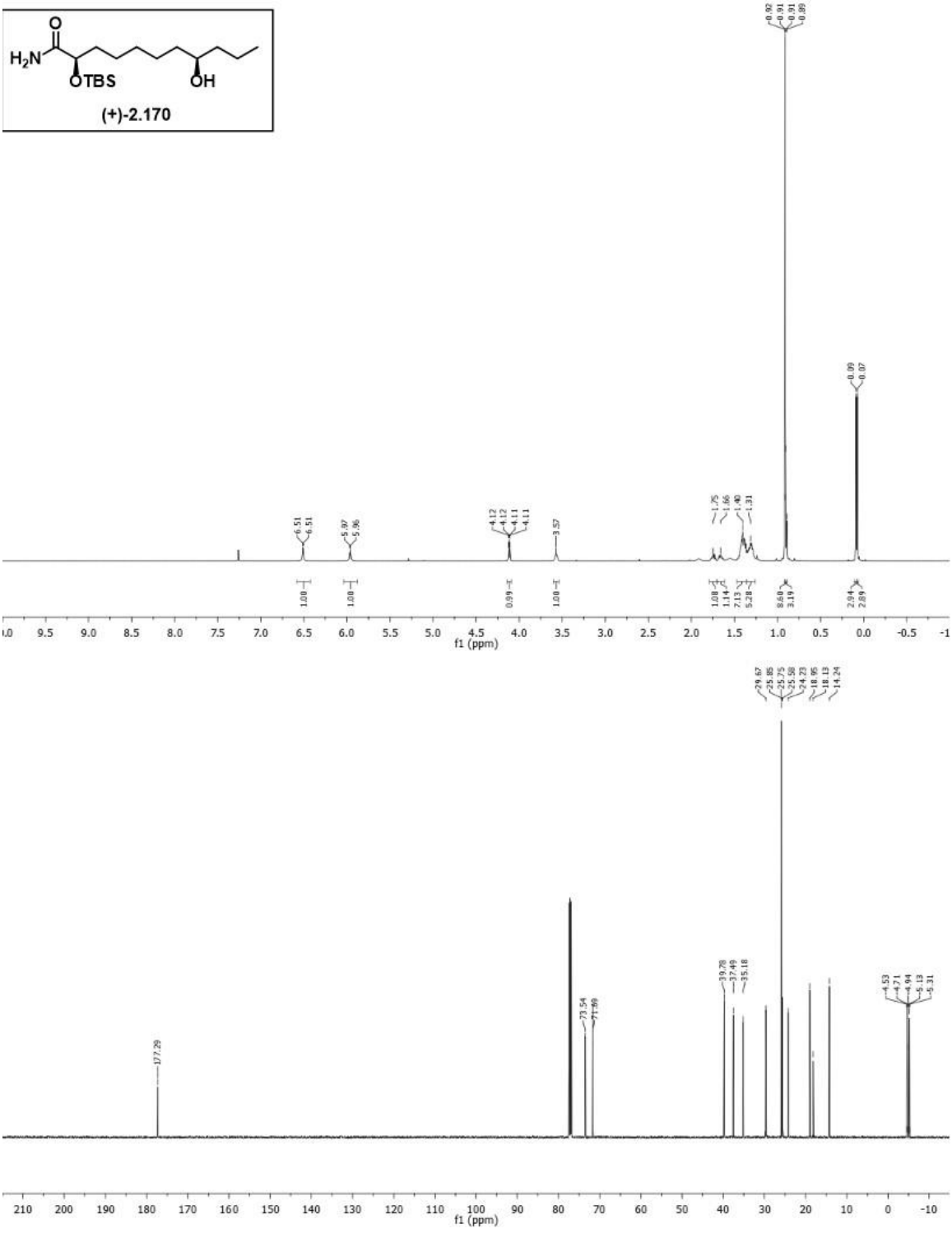
H2N
O
OTBS
OH
(+)-2.170
f1 (ppm)
f1 (ppm)

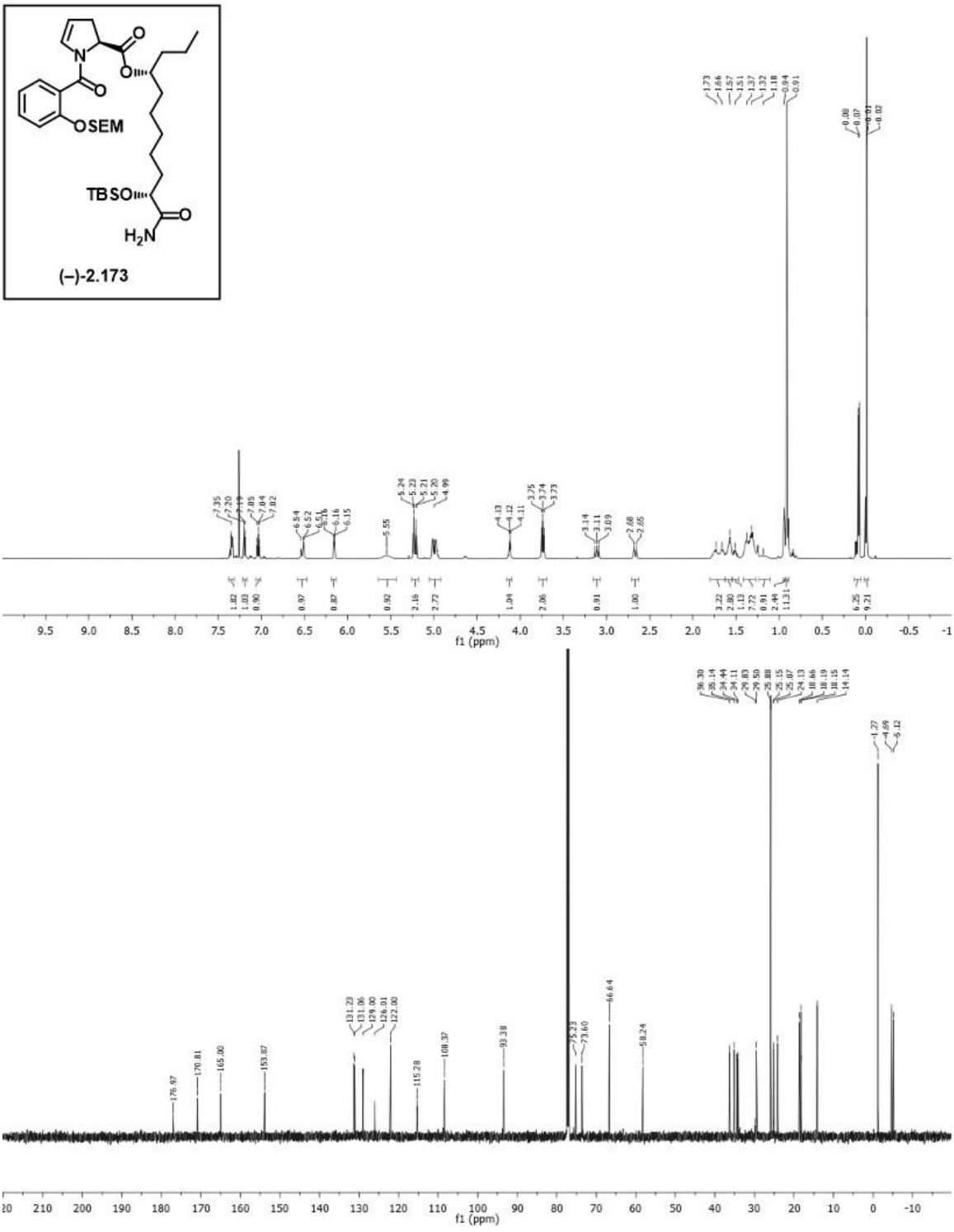
OSEM
TBSO
H_2N
(–)-2.173
f1 (ppm)
f1 (ppm)

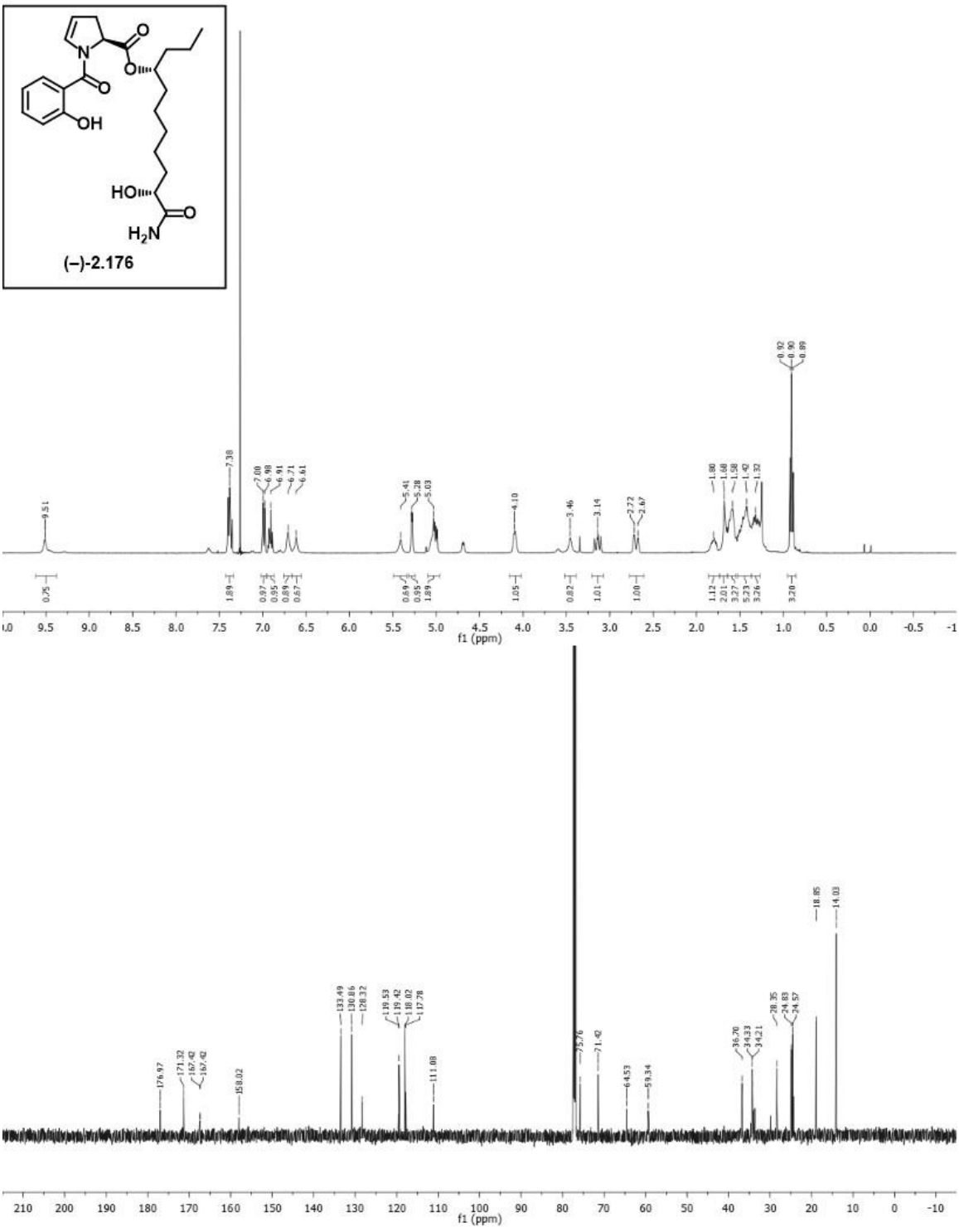
(–)-2.176
f1 (ppm)
f1 (ppm)

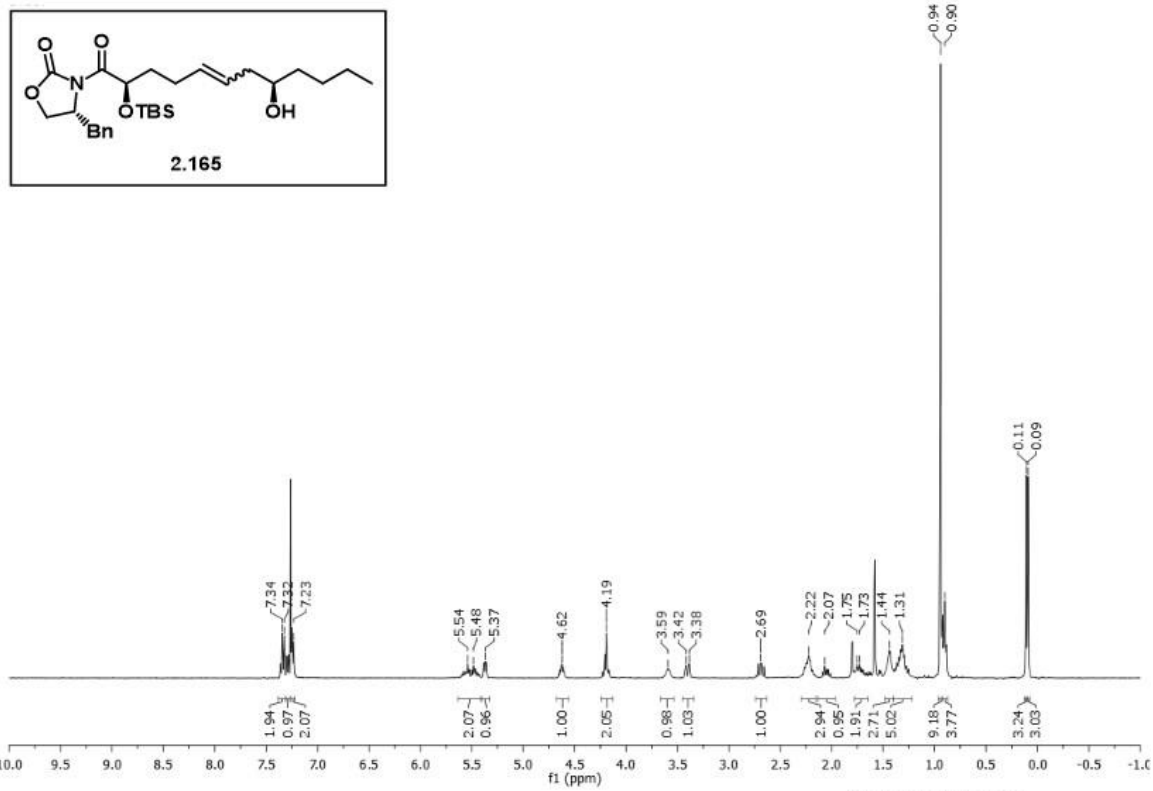
OTBS
OH
Bn
2.165
f1 (ppm)

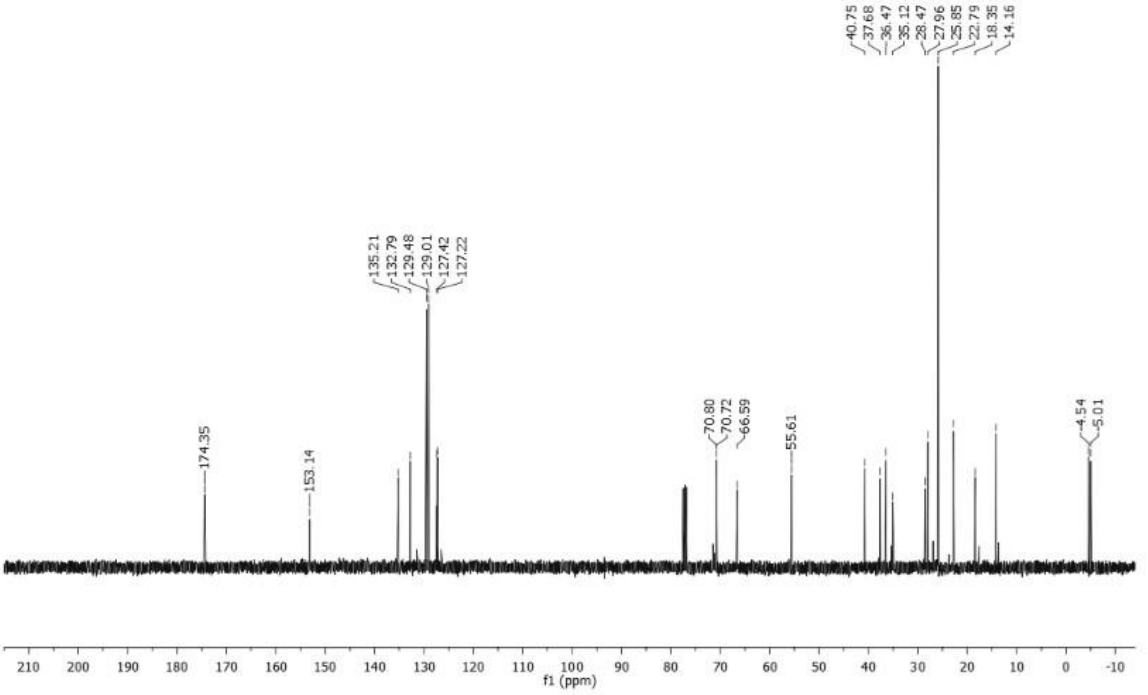
f1 (ppm)

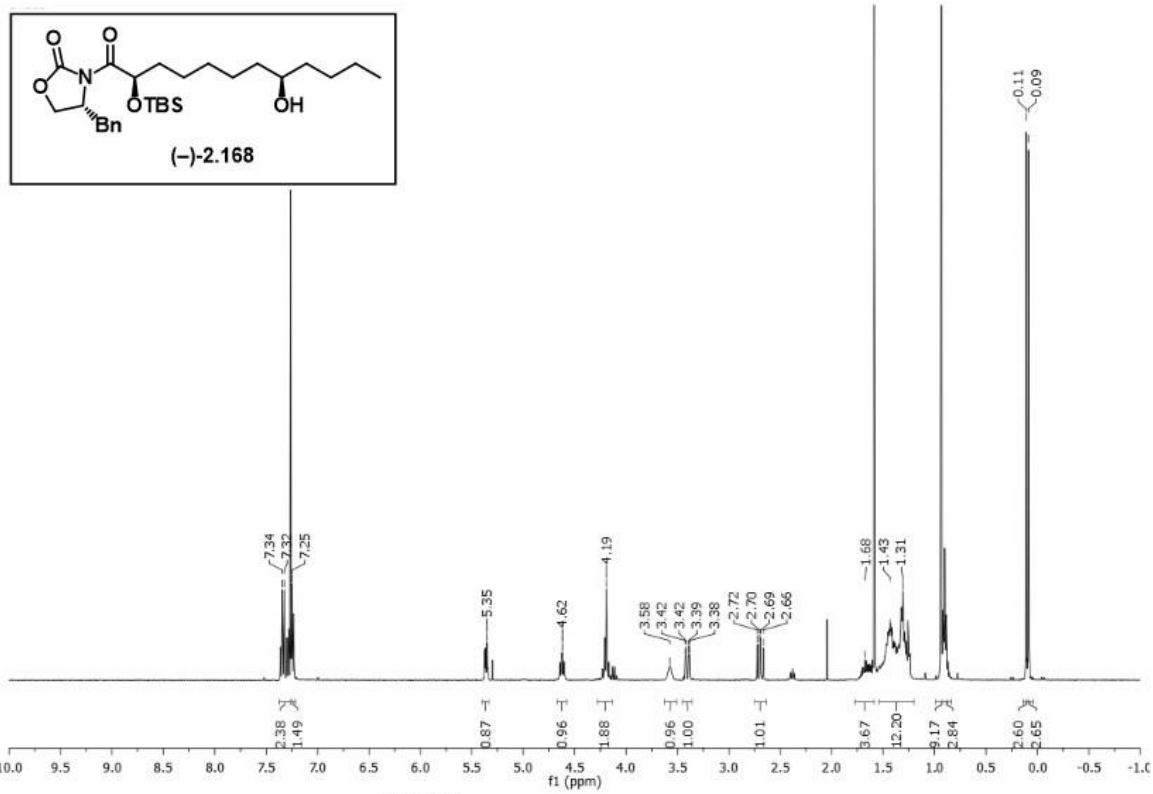
OTBS
OH
Bn
(–)-2.168
f1 (ppm)

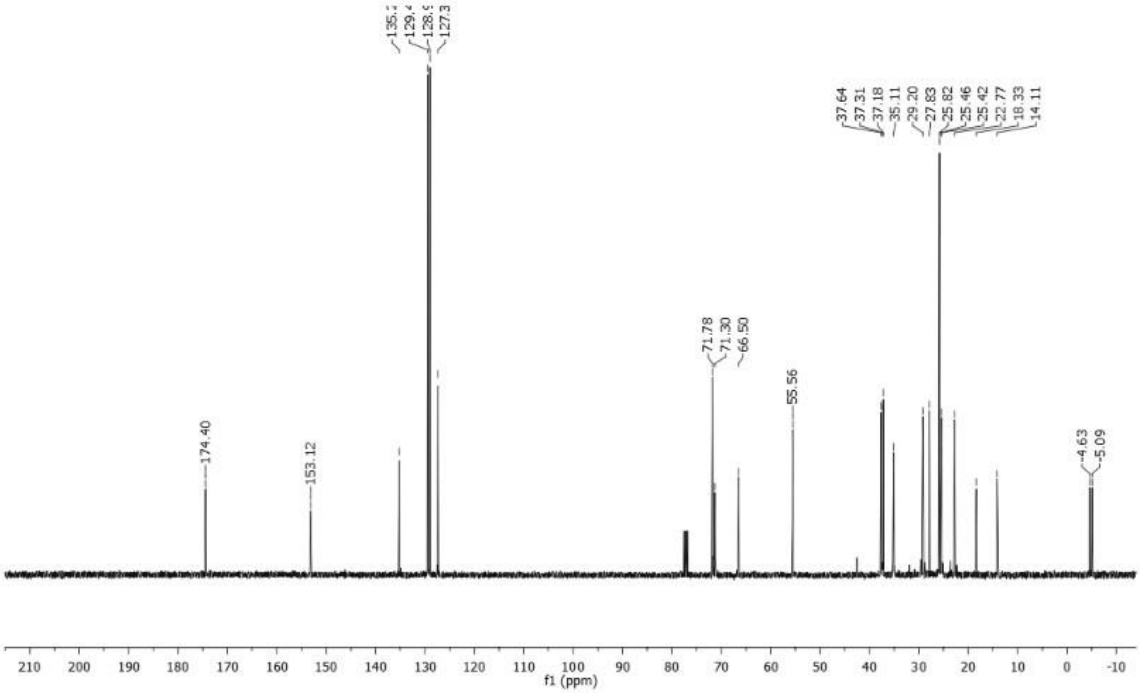
f1 (ppm)

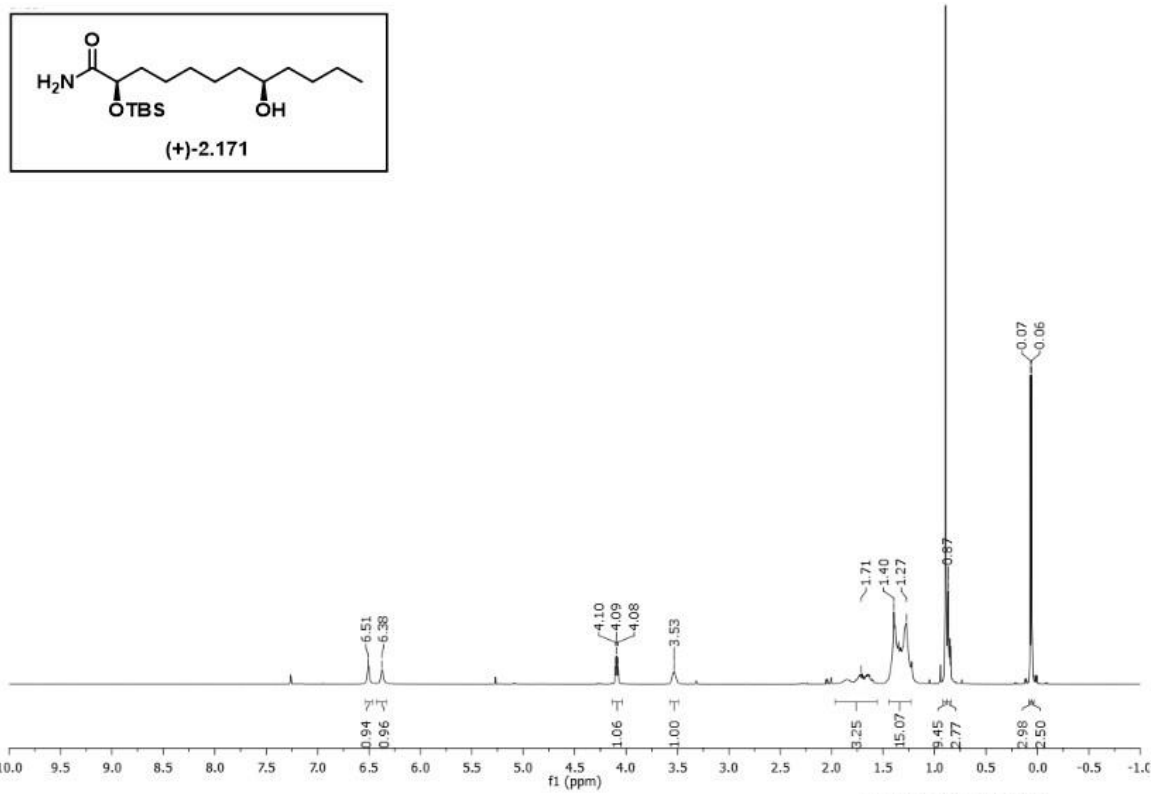
O
H2N
OTBS
OH
(+)-2.171
6.51
6.38
4.10
4.09
4.08
3.53
1.71
1.40
1.27
0.87
0.07
0.06
0.94
0.96
1.06
1.00
3.25
15.07
9.45
2.77
2.98
2.50
f1 (ppm)

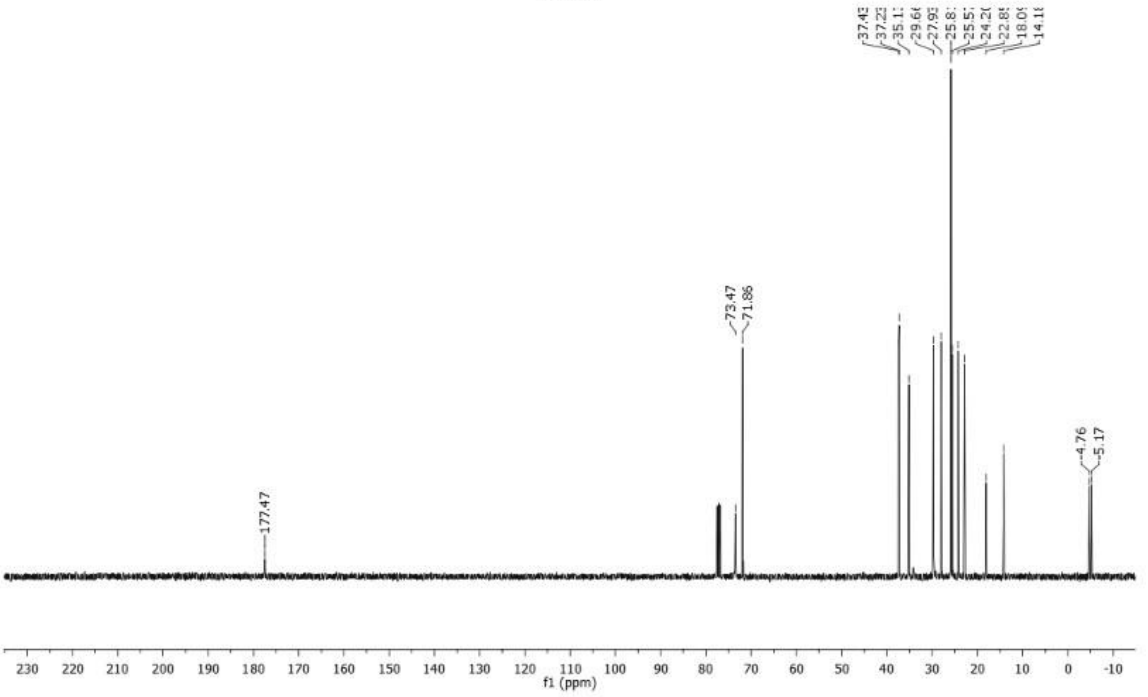
177.47
73.47
71.86
4.76
5.17
f1 (ppm)

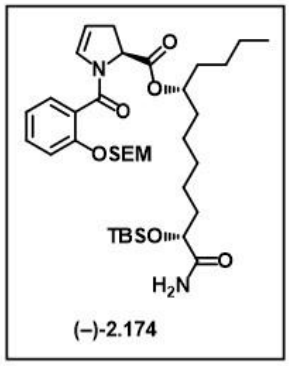
OSEM
TBSO
H_2N
(–)-2.174

f1 (ppm)

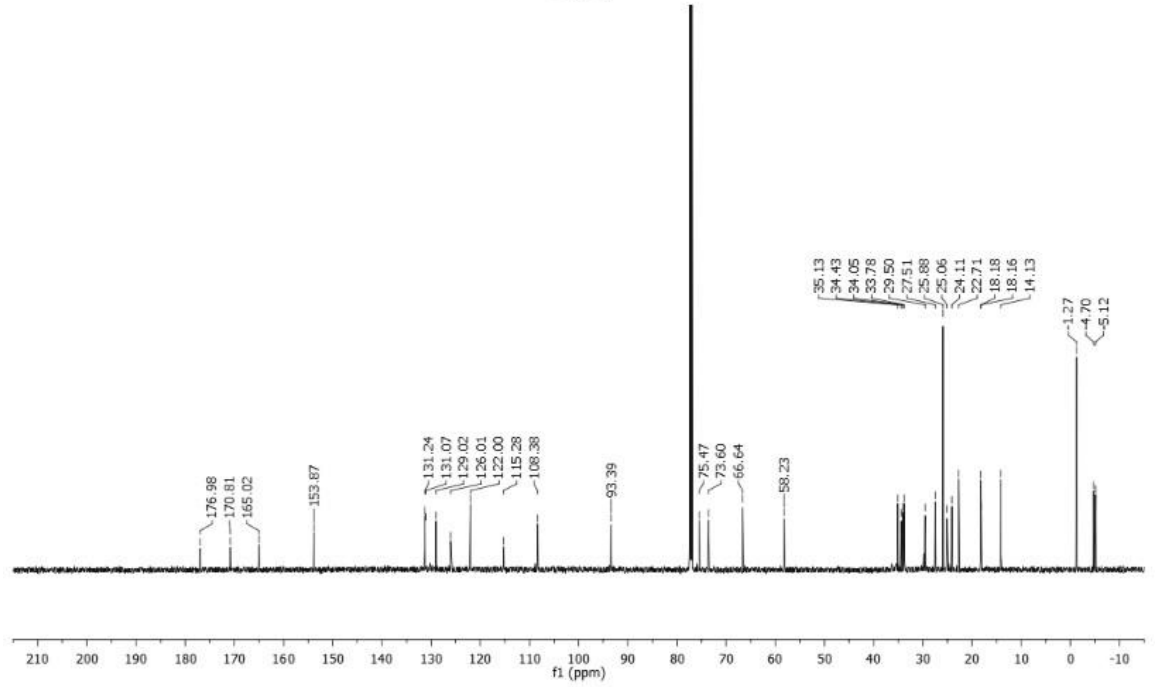
f1 (ppm)

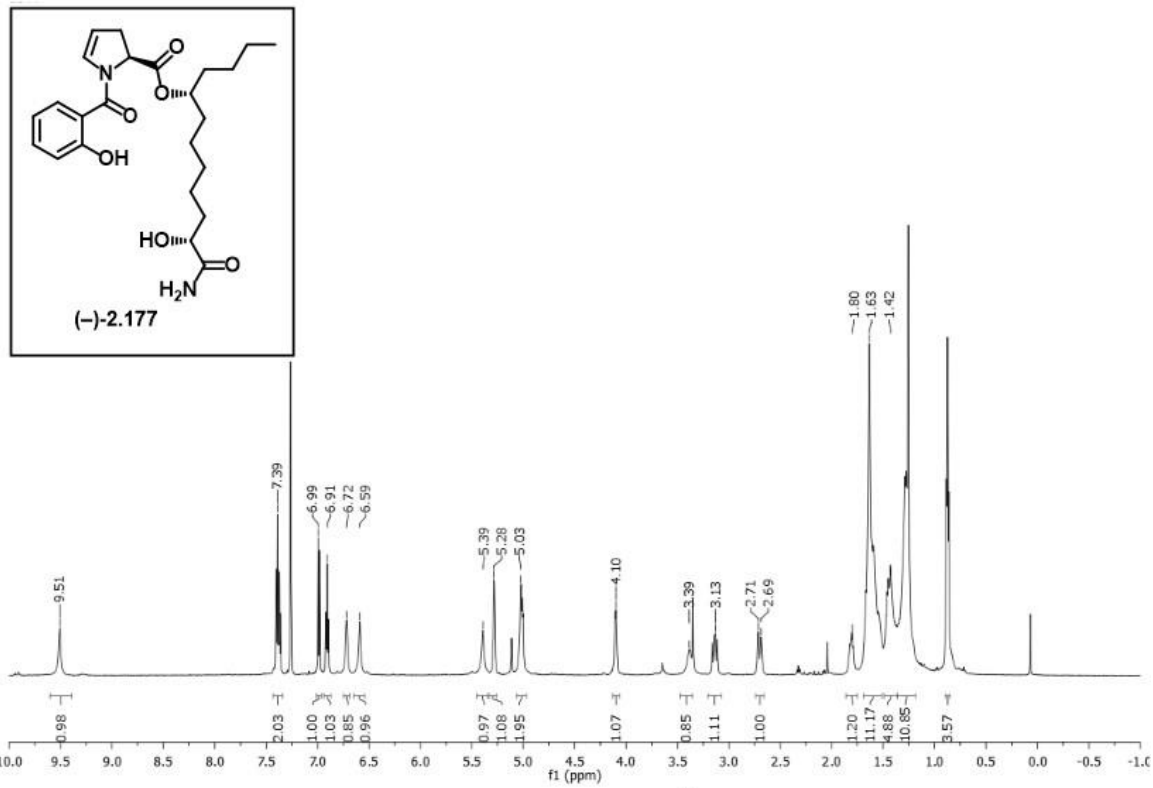
(–)-2.177
9.51
7.39
6.99
6.91
6.72
6.59
5.39
5.28
5.03
4.10
3.39
3.13
2.71
2.69
1.80
1.63
1.42
f1 (ppm)

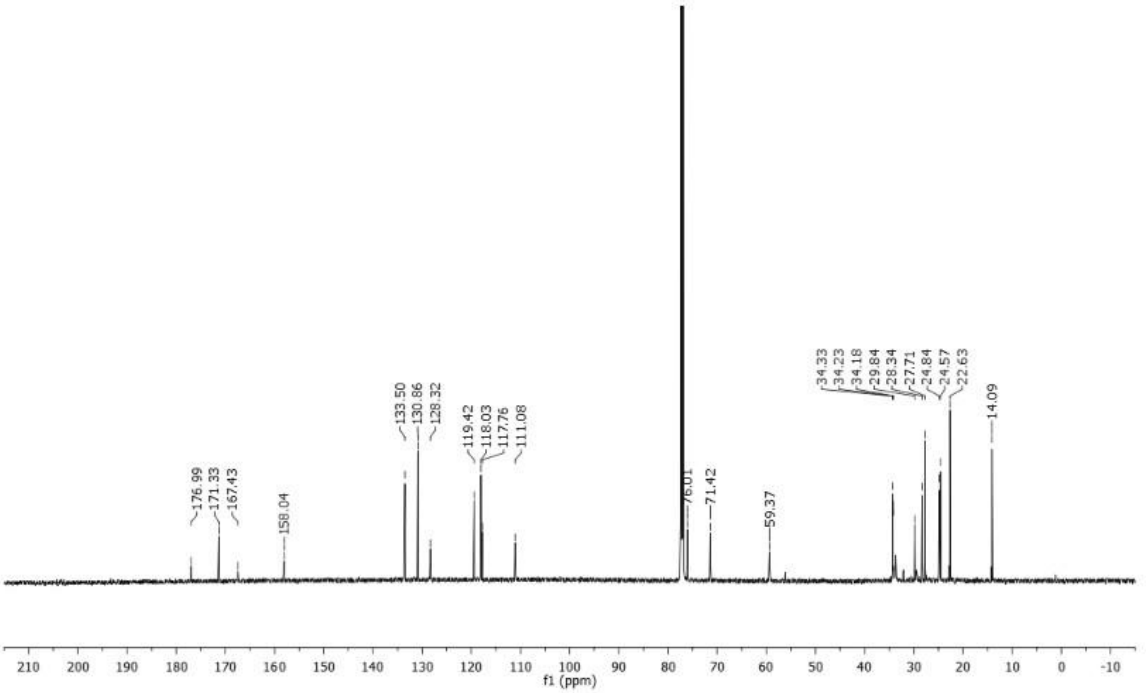
176.99
171.33
167.43
158.04
133.50
130.86
128.32
119.42
118.03
117.76
111.08
76.01
71.42
59.37
34.33
34.23
34.18
29.84
28.34
27.71
24.84
24.57
22.63
14.09
f1 (ppm)

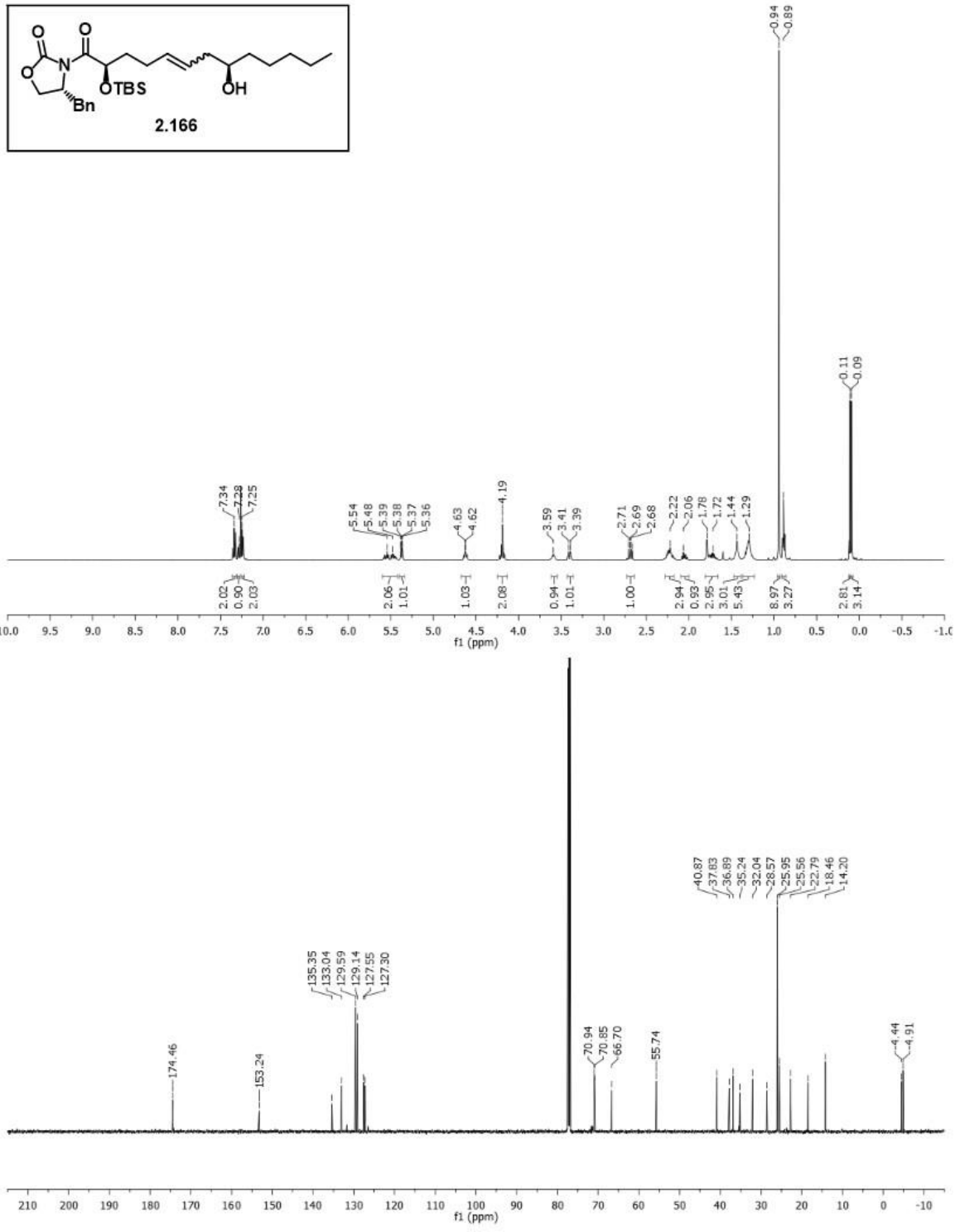
OTBS
OH
Bn
2.166
f1 (ppm)
f1 (ppm)

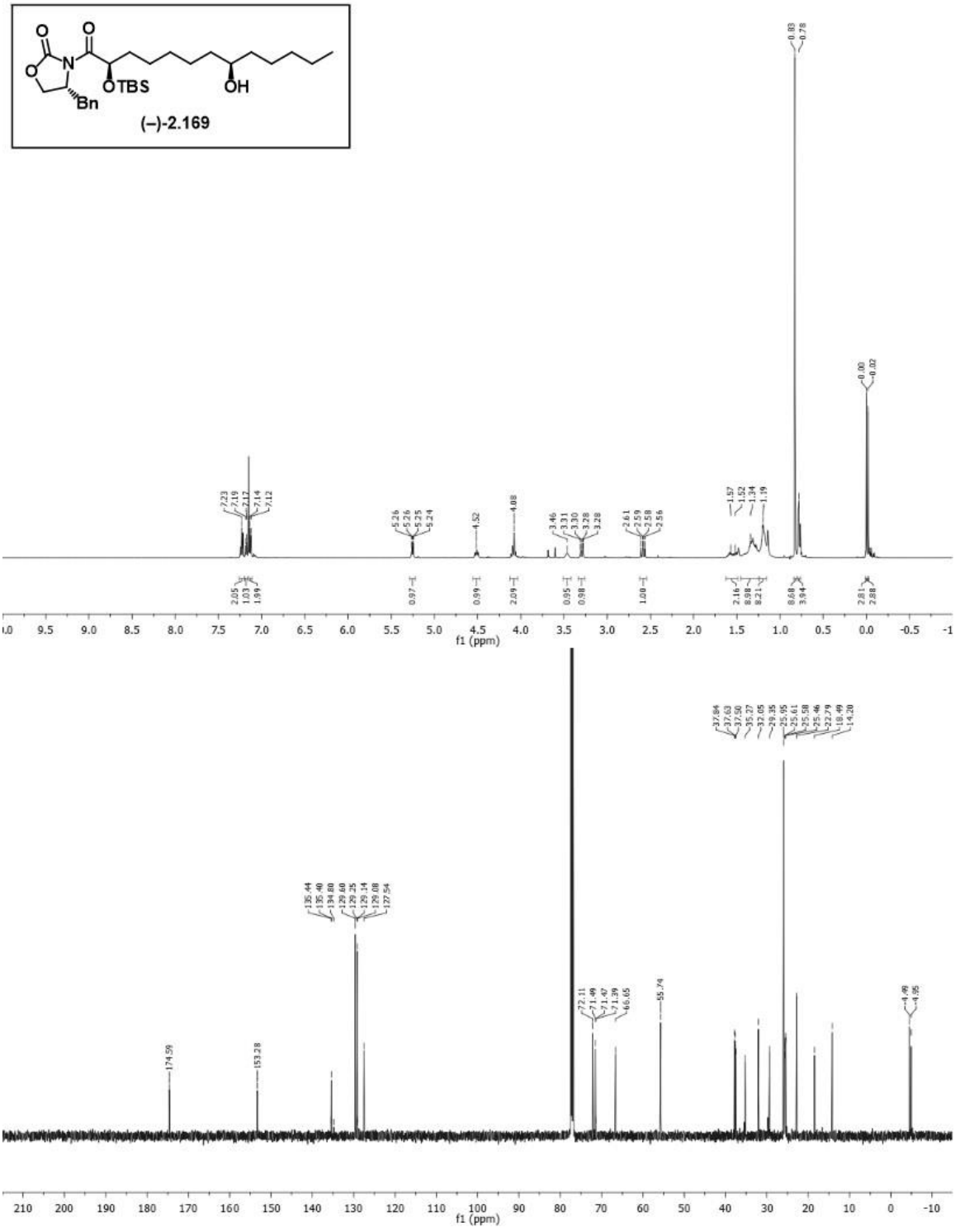
OTBS
OH
Bn
(–)-2.169
f1 (ppm)
f1 (ppm)

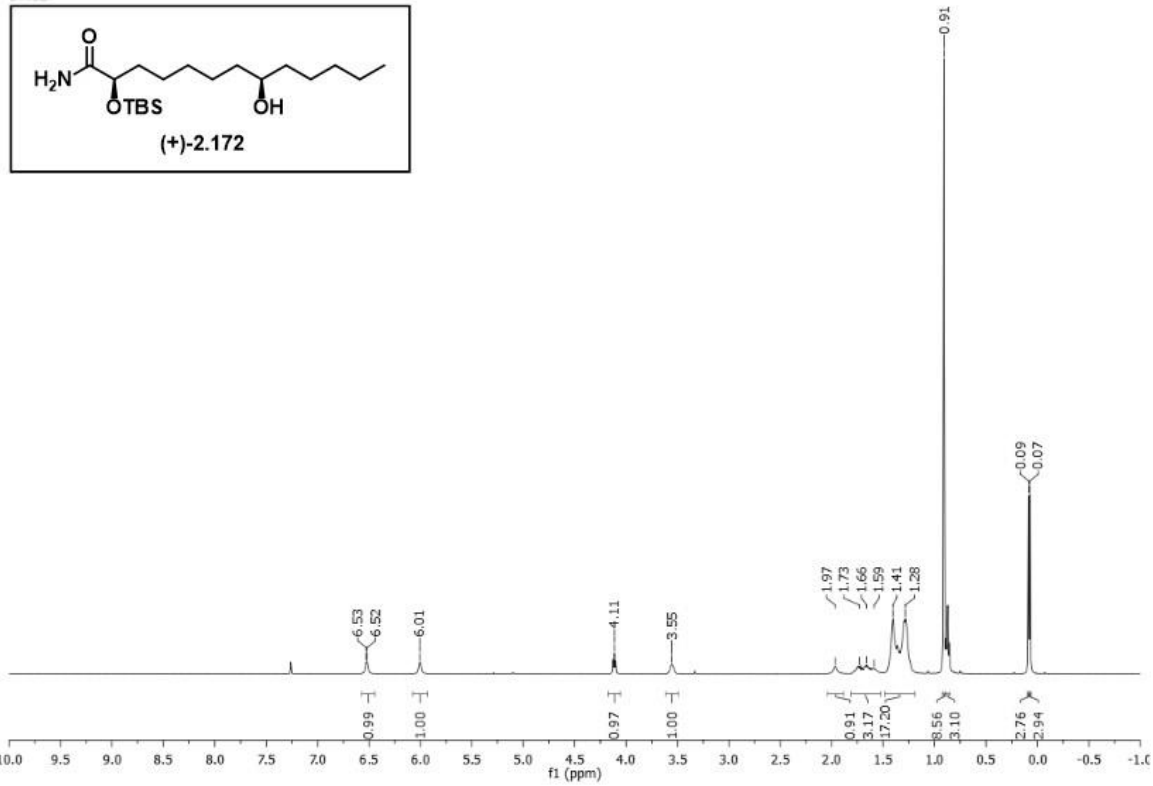
O
H2N
OTBS
OH
(+)-2.172
0.91
0.09
0.07
1.97
1.73
1.66
1.59
1.41
1.28
6.53
6.52
6.01
4.11
3.55
0.99
1.00
0.97
1.00
0.91
3.17
17.20
8.56
3.10
2.76
2.94
f1 (ppm)

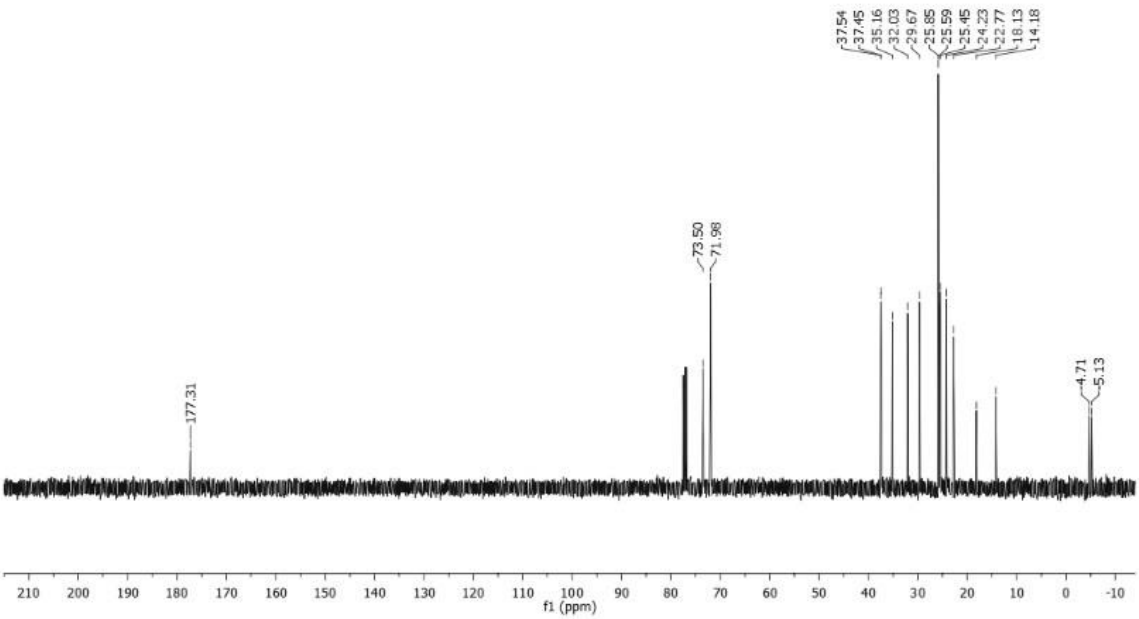
37.54
37.45
35.16
32.03
29.67
25.85
25.59
25.45
24.23
22.77
18.13
14.18
73.50
71.98
177.31
4.71
5.13
f1 (ppm)

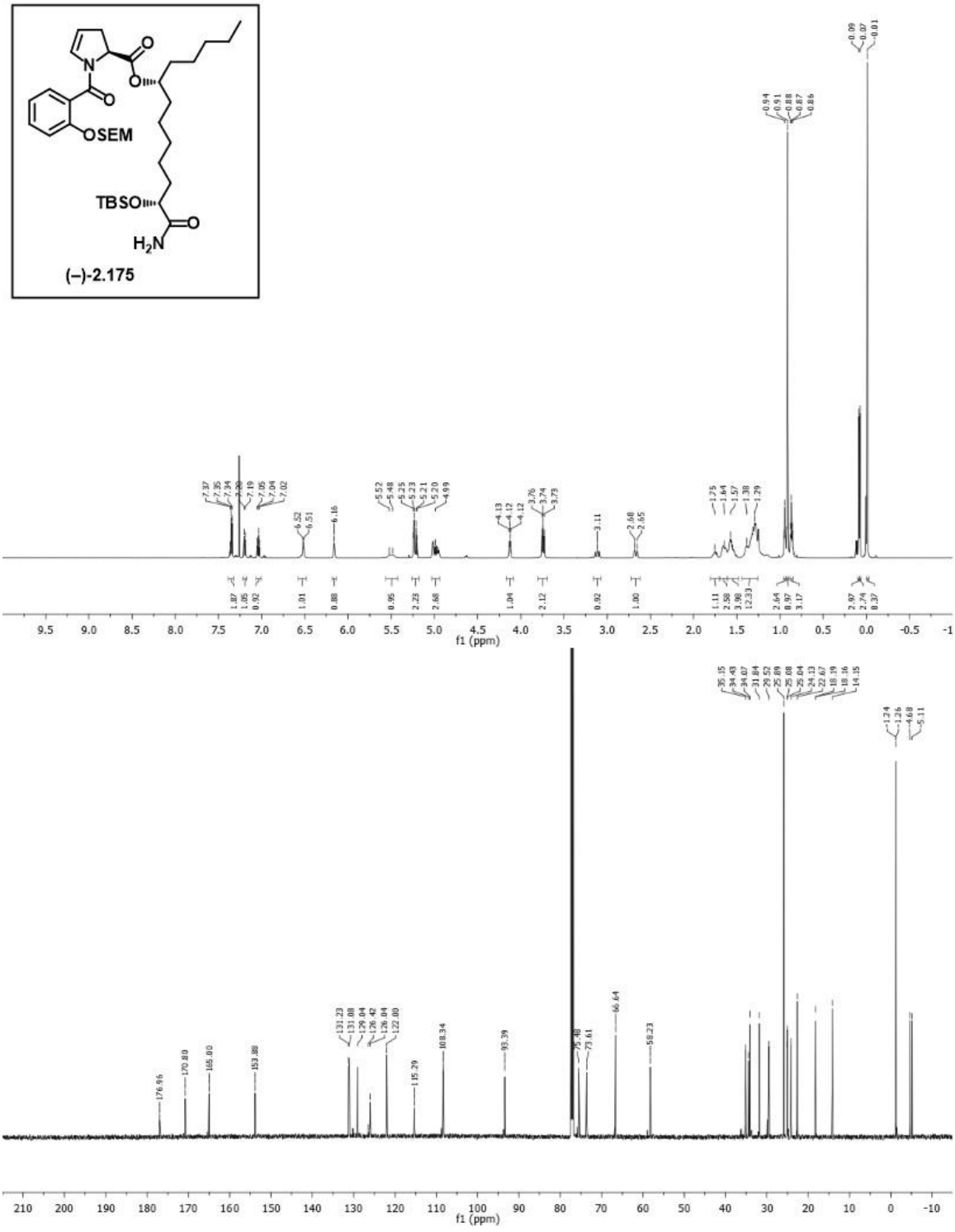
OSEM
TBSO
H_2N
(–)-2.175
f1 (ppm)
f1 (ppm)

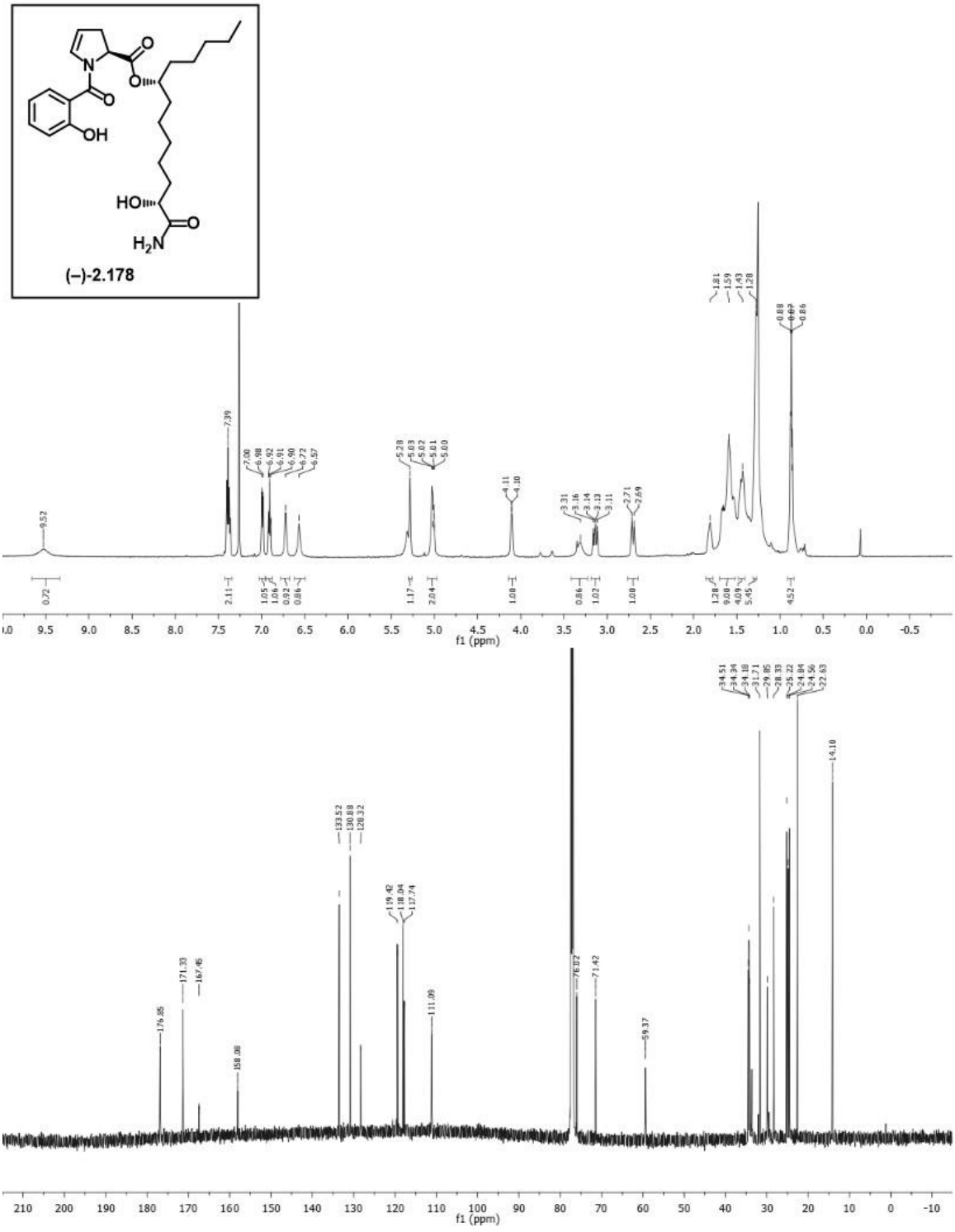
(–)-2.178
f1 (ppm)
f1 (ppm)

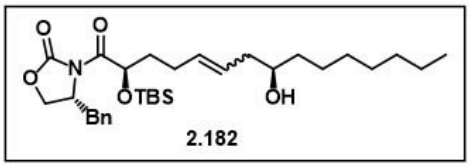
O
O
N
O
OTBS
OH
Bn

2.182

1.72
1.43
1.28
0.94
0.88
0.11
0.09
7.34
7.25
5.54
5.48
5.37
4.62
4.19
3.59
3.39
2.71
2.68
2.22
2.06
2.02
0.90
1.92
2.11
1.03
1.03
2.02
1.02
0.98
1.00
3.34
0.90
3.15
3.12
10.11
9.15
3.52
2.71
2.94
f1 (ppm)

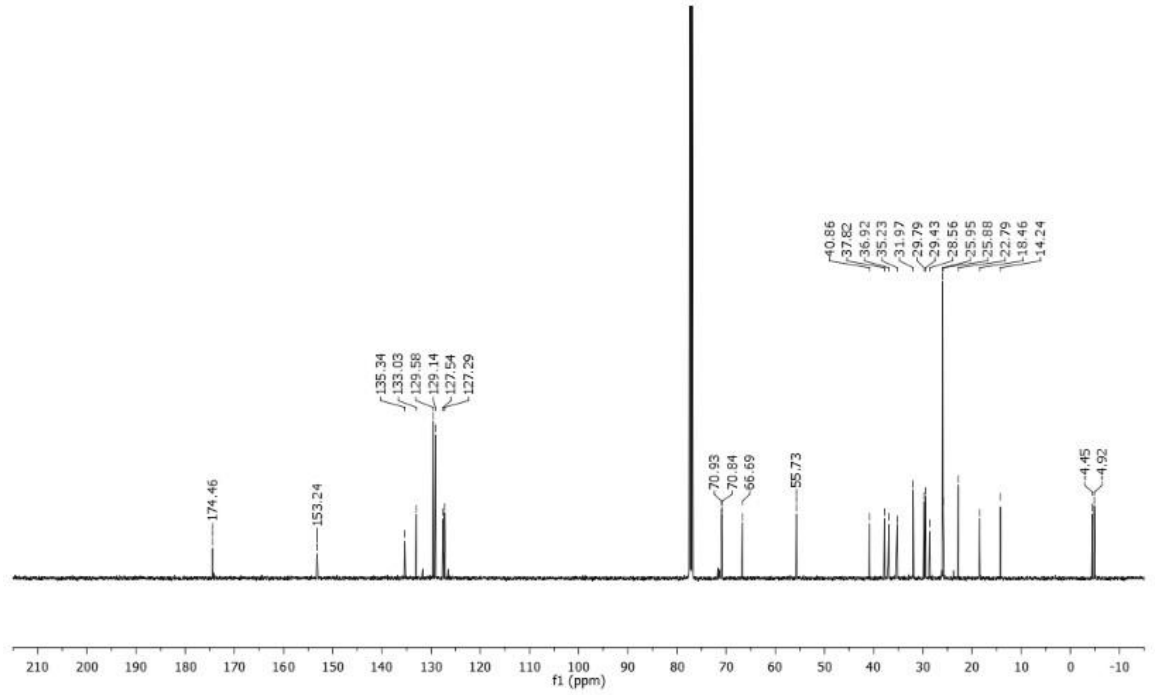
40.86
37.82
36.92
35.23
31.97
29.79
29.43
28.56
25.95
25.88
22.79
18.46
14.24
135.34
133.03
129.58
129.14
127.54
127.29
174.46
153.24
70.93
70.84
66.69
55.73
14.45
14.92
f1 (ppm)

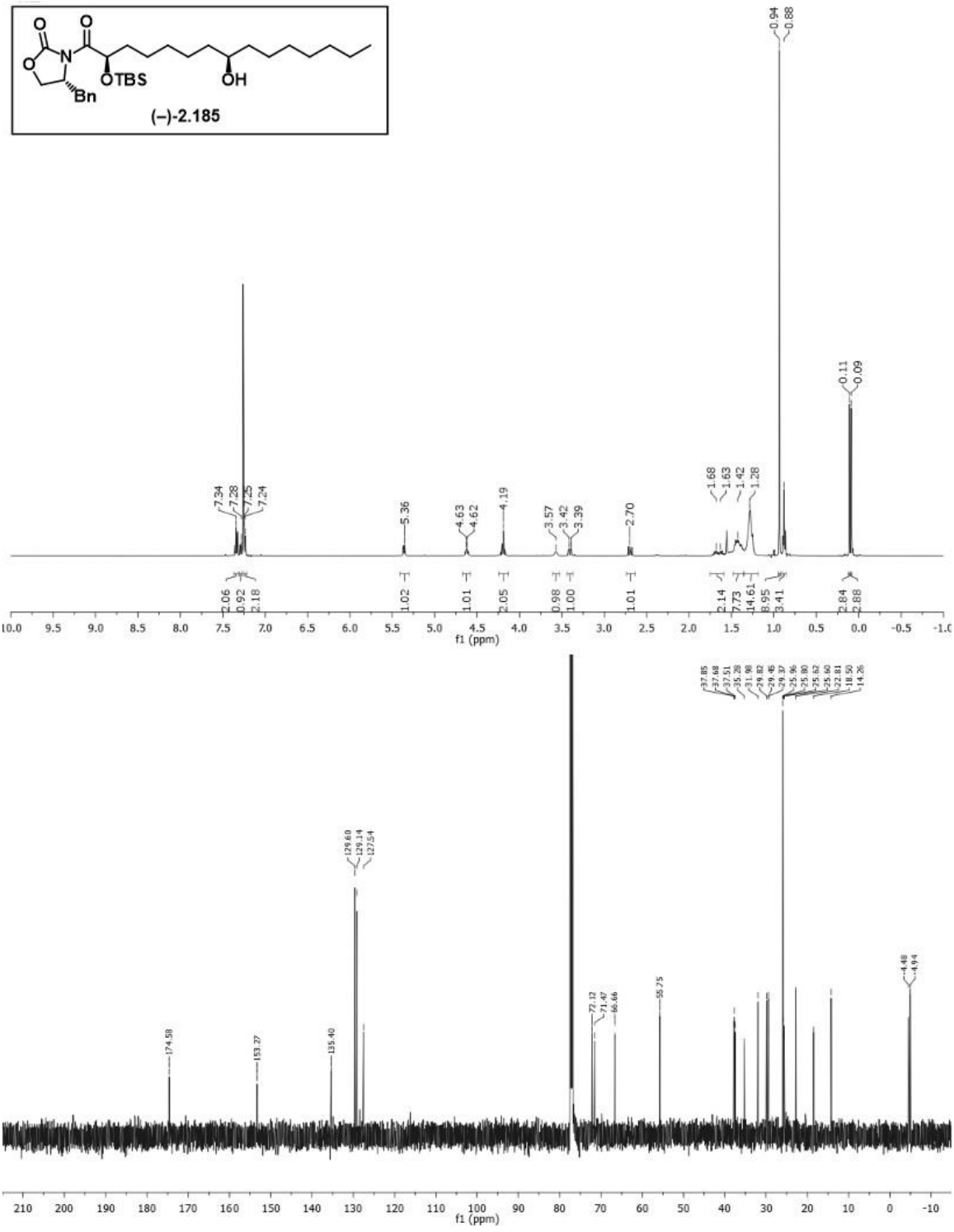
OTBS
OH
Bn
(–)-2.185
f1 (ppm)
f1 (ppm)

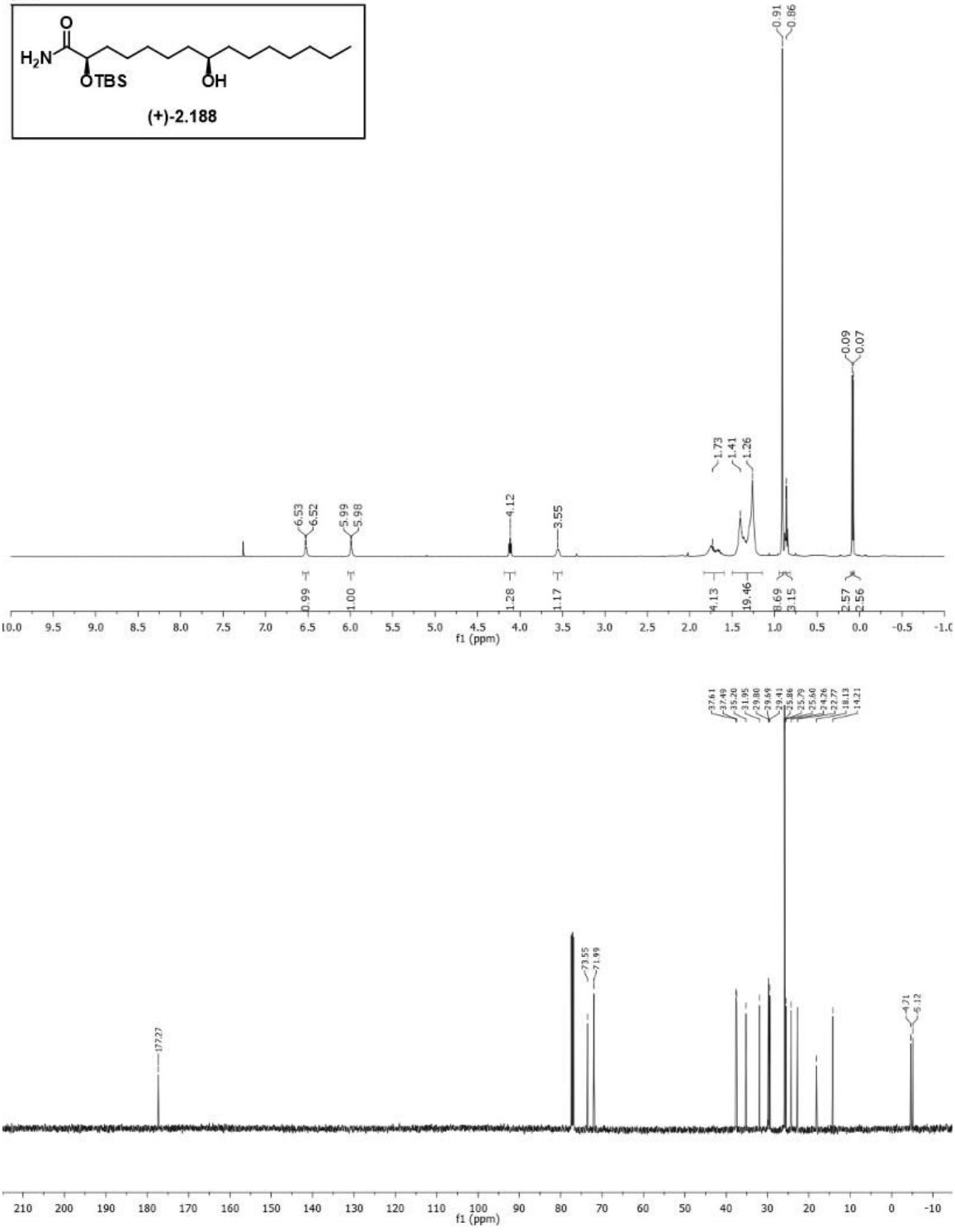
(+)-2.188
f1 (ppm)
f1 (ppm)

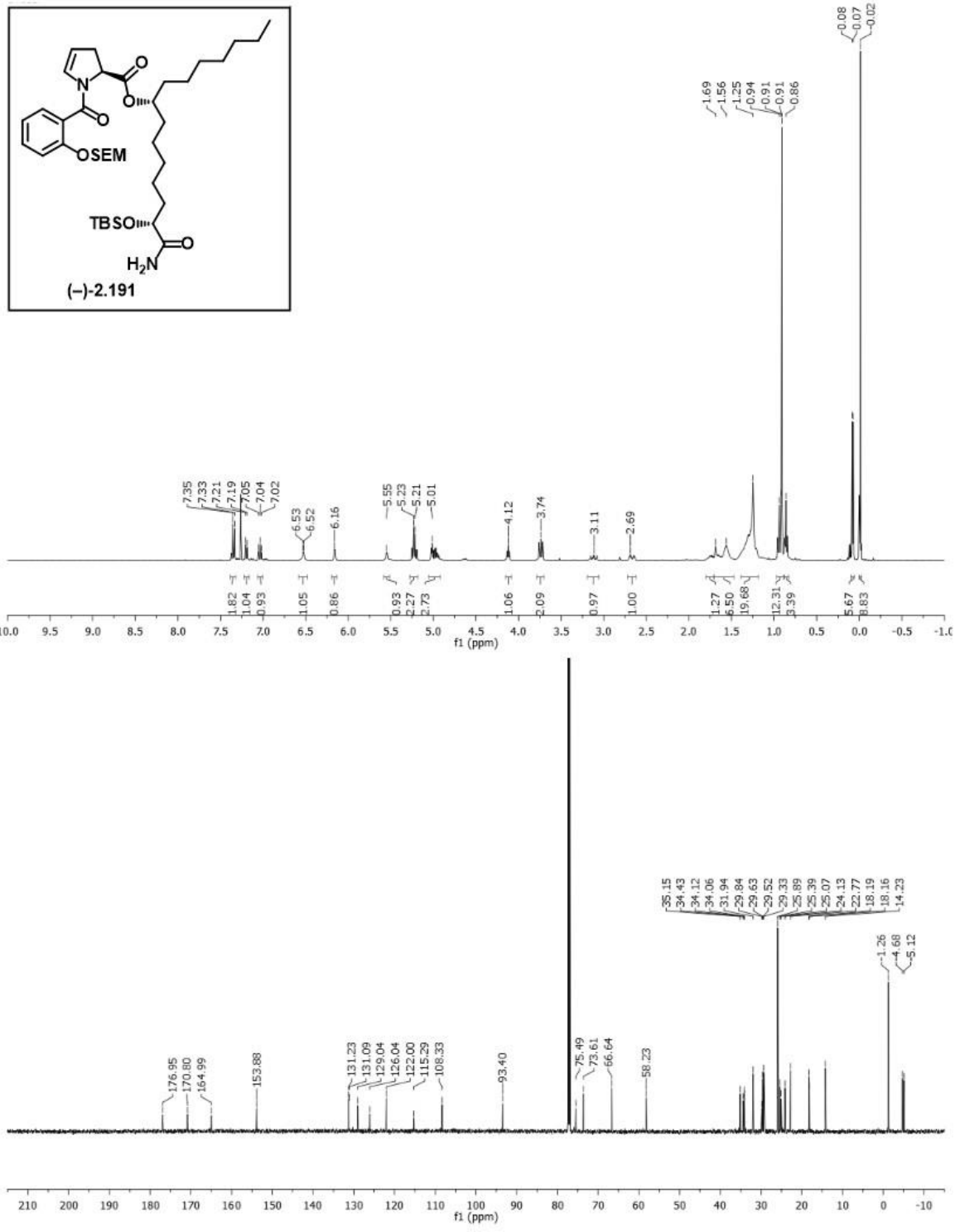
OSEM
TBSO
H_2N
(–)-2.191
f1 (ppm)
f1 (ppm)

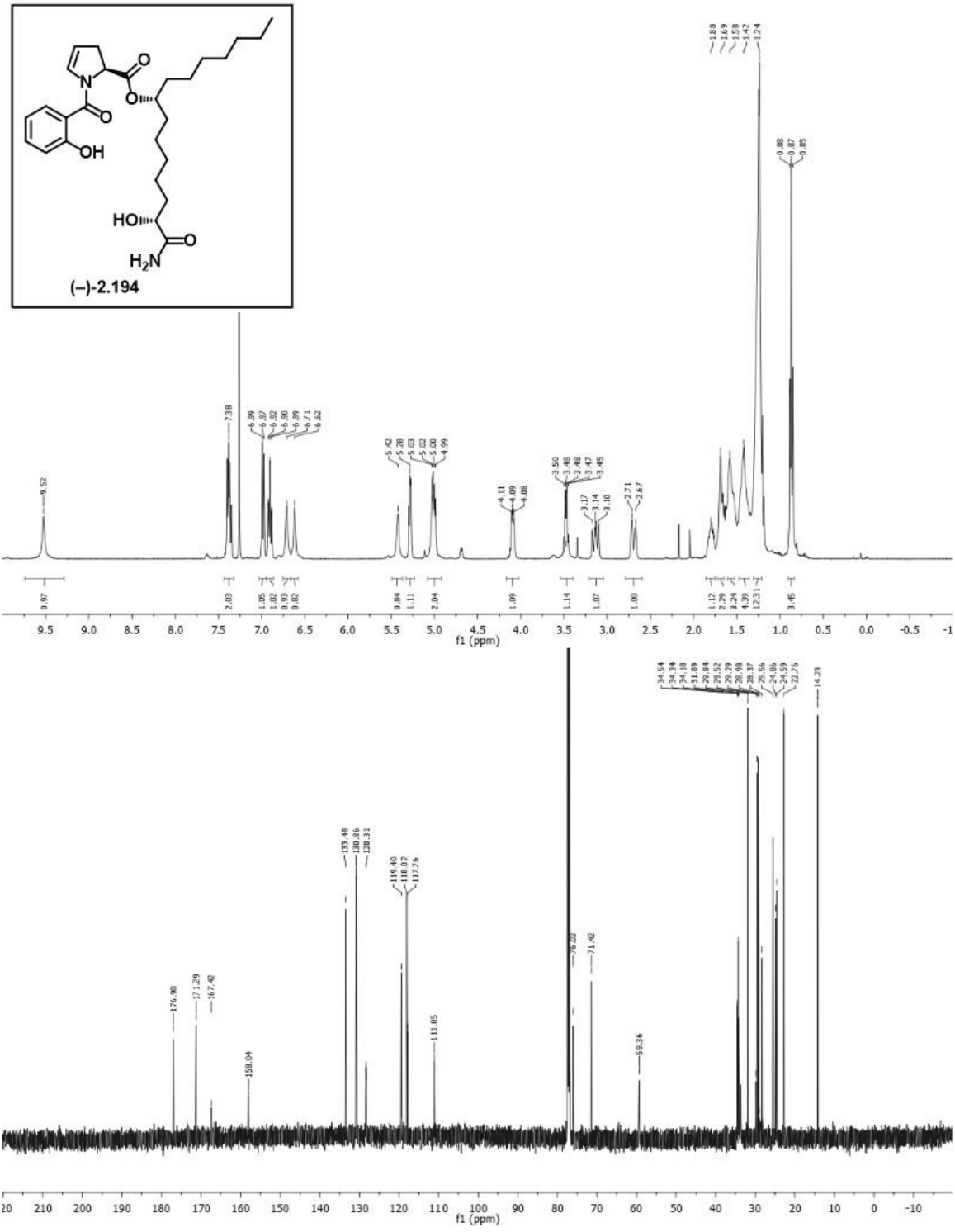
(–)-2.194
f1 (ppm)
f1 (ppm)

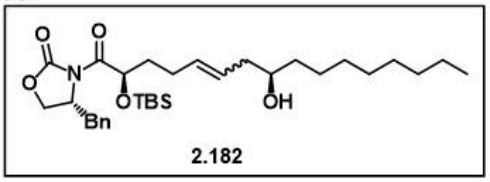
O
O
N
O
OTBS
OH
Bn

2.182

2.23
2.06
2.03
1.73
1.66
1.43
1.27
0.95
0.94
0.87
0.11
0.09
7.34
7.32
7.23
5.54
5.48
5.37
4.63
4.62
4.19
3.58
3.42
3.42
3.39
3.38
2.69
2.91
1.83
2.01
0.98
0.96
2.10
1.00
1.00
0.96
3.12
0.85
5.08
3.17
13.13
9.28
3.40
2.58
2.62
f1 (ppm)

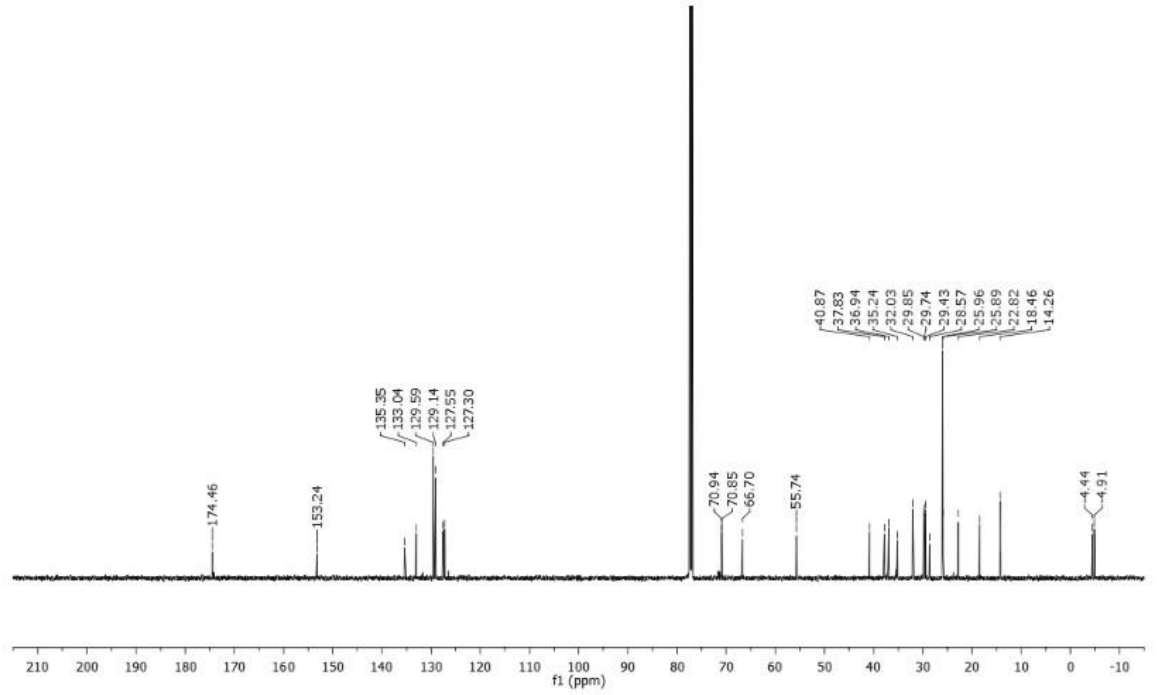
40.87
37.83
36.94
35.24
32.03
29.85
29.74
29.43
28.57
25.96
25.89
22.82
18.46
14.26
135.35
133.04
129.59
129.14
127.55
127.30
174.46
153.24
70.94
70.85
66.70
55.74
4.44
4.91
f1 (ppm)

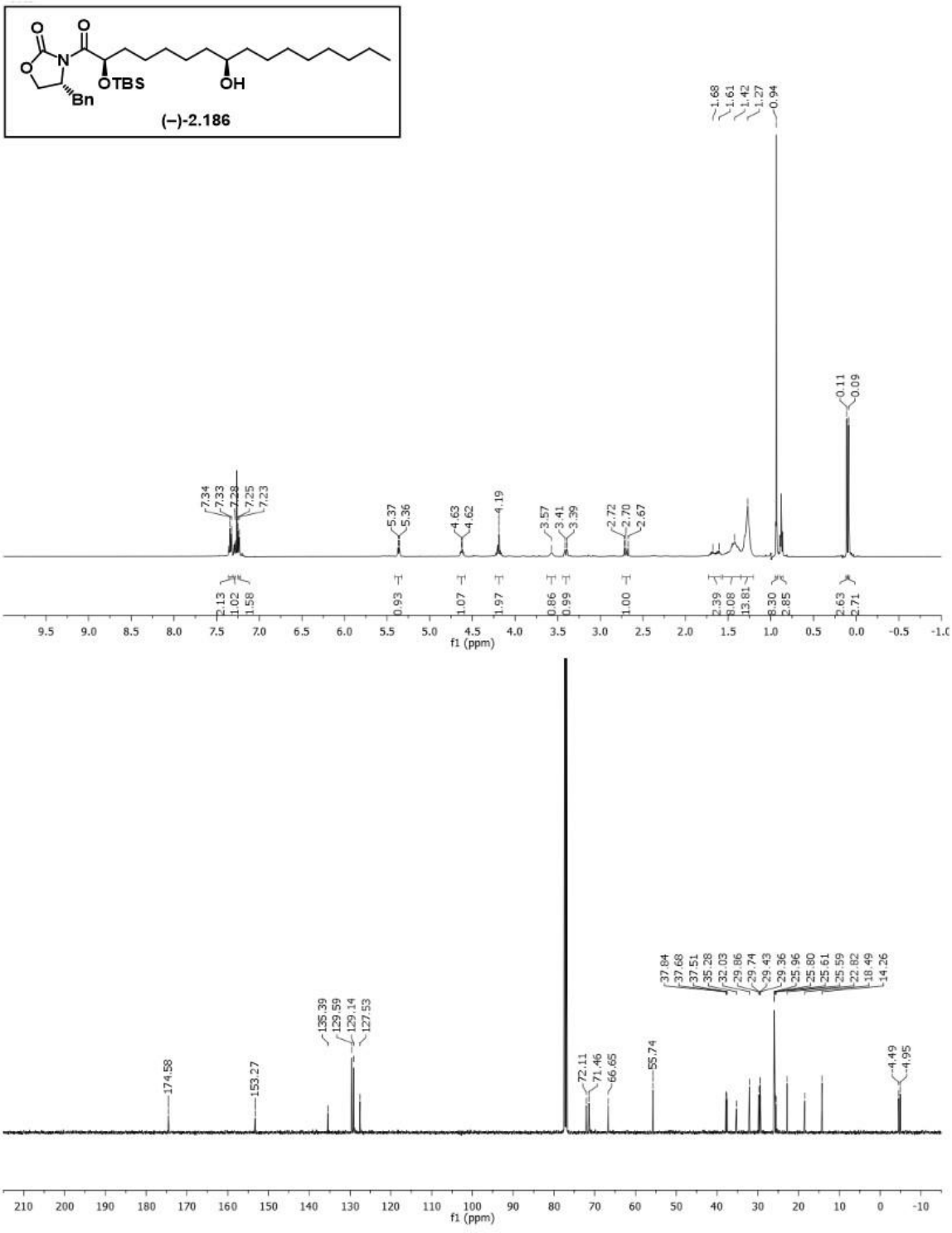
OTBS
OH
Bn
(–)-2.186
f1 (ppm)
f1 (ppm)

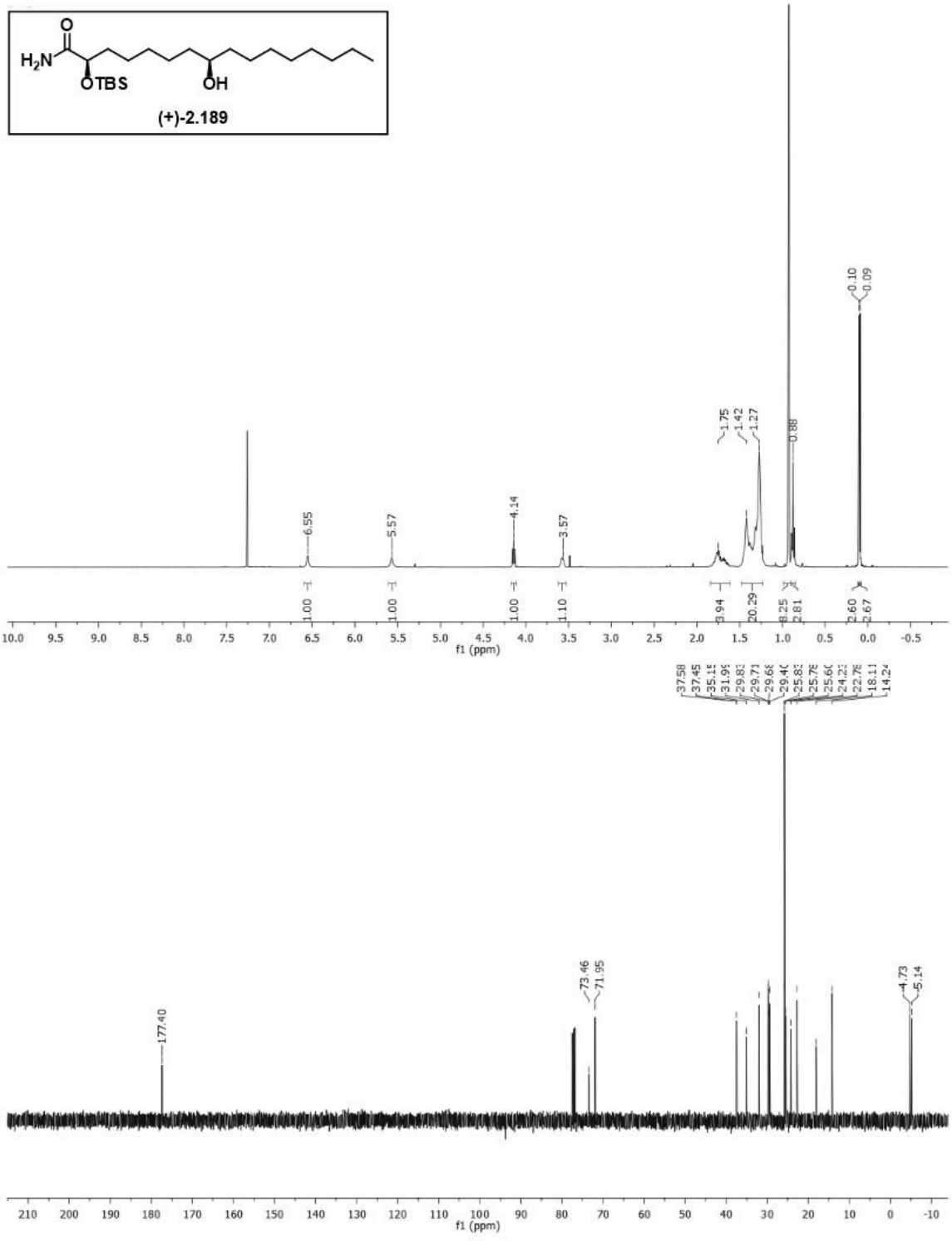
O
H2N
OTBS
OH
(+)-2.189
6.55
5.57
4.14
3.57
1.75
1.42
1.27
0.88
0.10
0.09
1.00
1.00
1.00
1.10
8.94
20.29
8.25
2.81
2.60
2.67
f1 (ppm)
177.40
73.46
71.95
14.73
14.14
f1 (ppm)

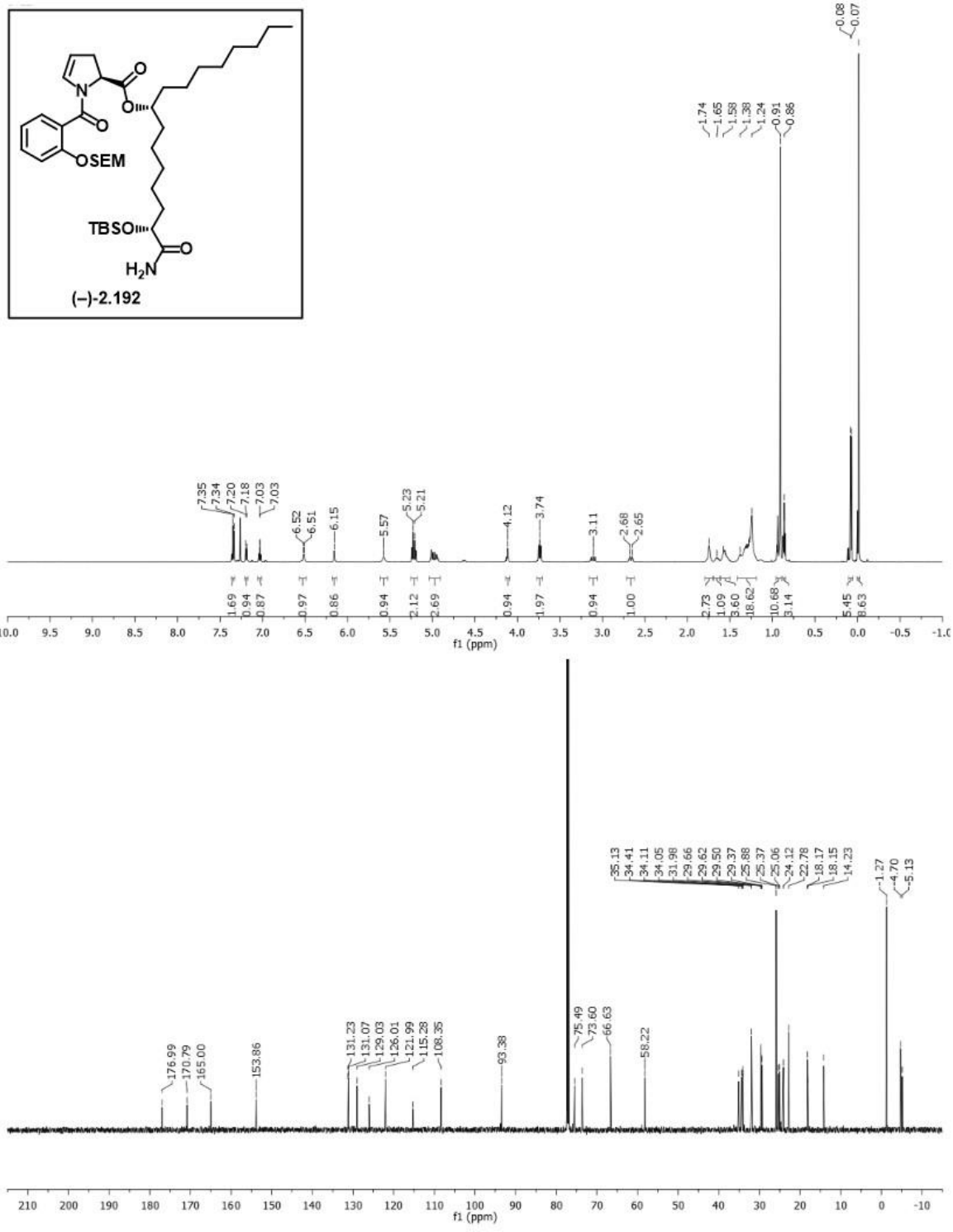
OSEM
TBSO
H_2N
(–)-2.192
f1 (ppm)
f1 (ppm)

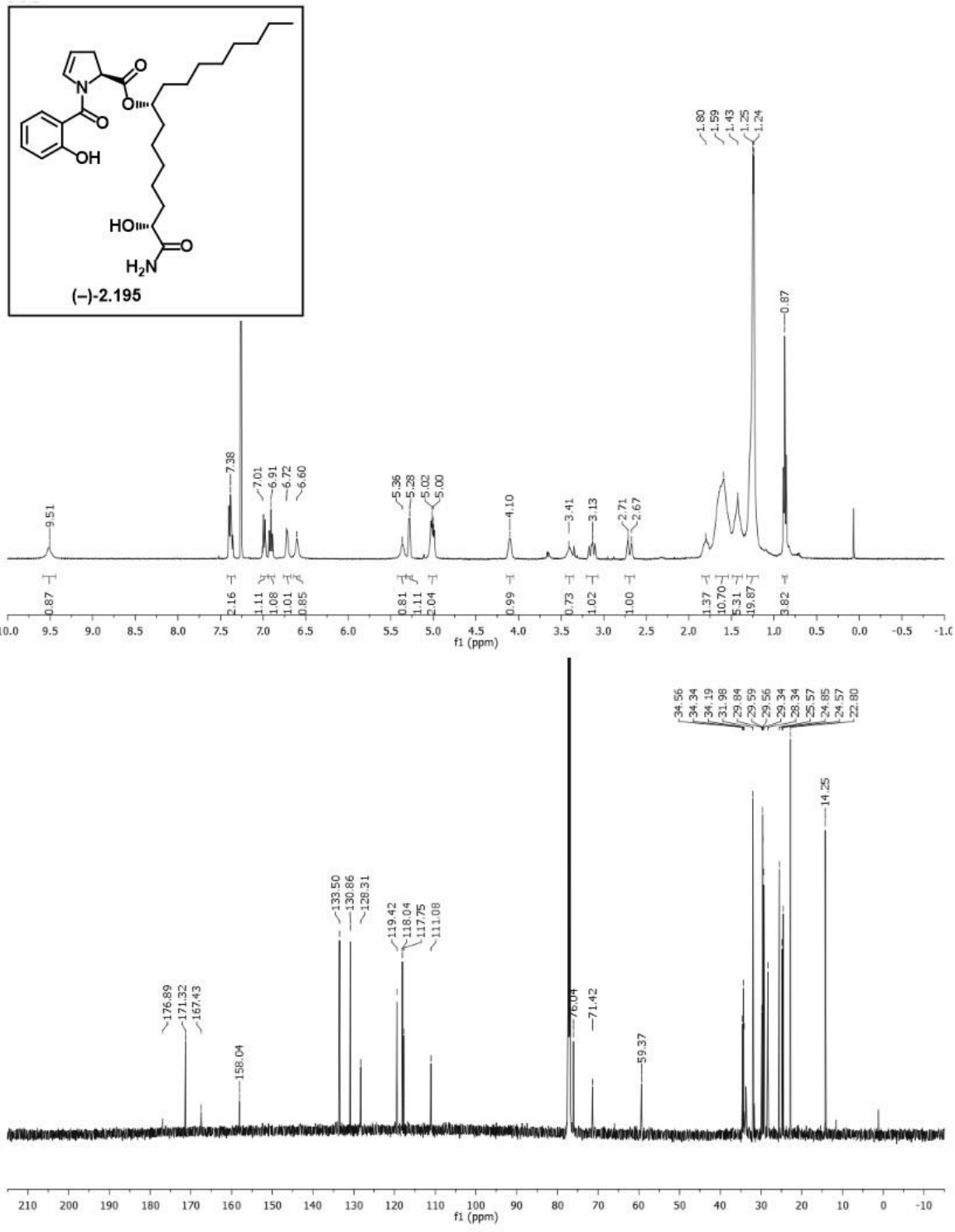
(–)-2.195
f1 (ppm)
f1 (ppm)

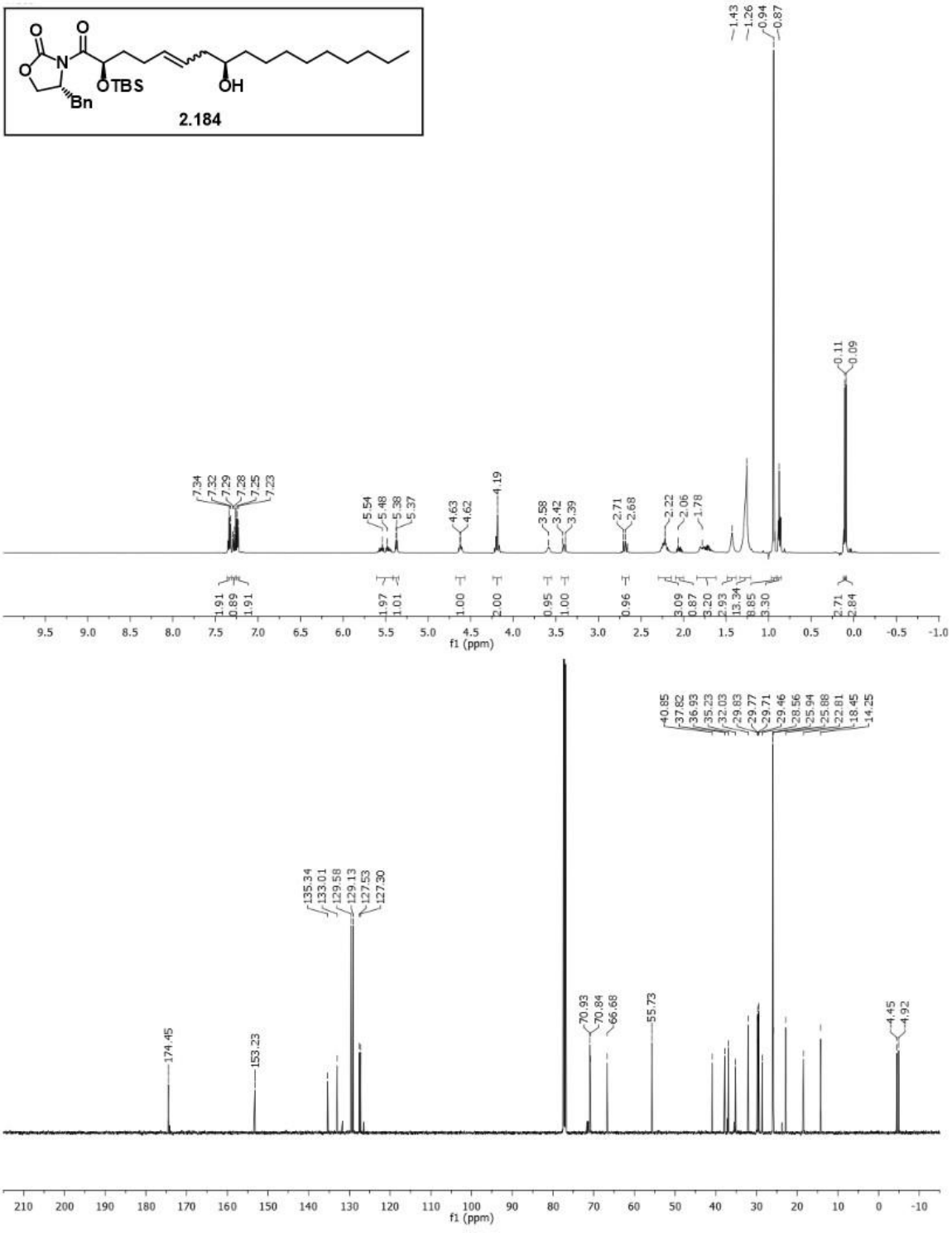
2.184
OTBS
OH
Bn
1.43
1.26
0.94
0.87
0.11
0.09
7.34
7.32
7.29
7.28
7.25
7.23
5.54
5.48
5.38
5.37
4.63
4.62
4.19
3.58
3.42
3.39
2.71
2.68
2.22
2.06
1.78
1.91
0.89
1.91
1.97
1.01
1.00
2.00
0.95
1.00
0.96
3.09
0.87
3.20
2.93
13.34
8.85
3.30
2.71
2.84
f1 (ppm)
40.85
37.82
36.93
35.23
32.03
29.83
29.77
29.71
29.46
28.56
25.94
25.88
22.81
18.45
14.25
135.34
133.01
129.58
129.13
127.53
127.30
174.45
153.23
70.93
70.84
66.68
55.73
14.45
14.92
f1 (ppm)

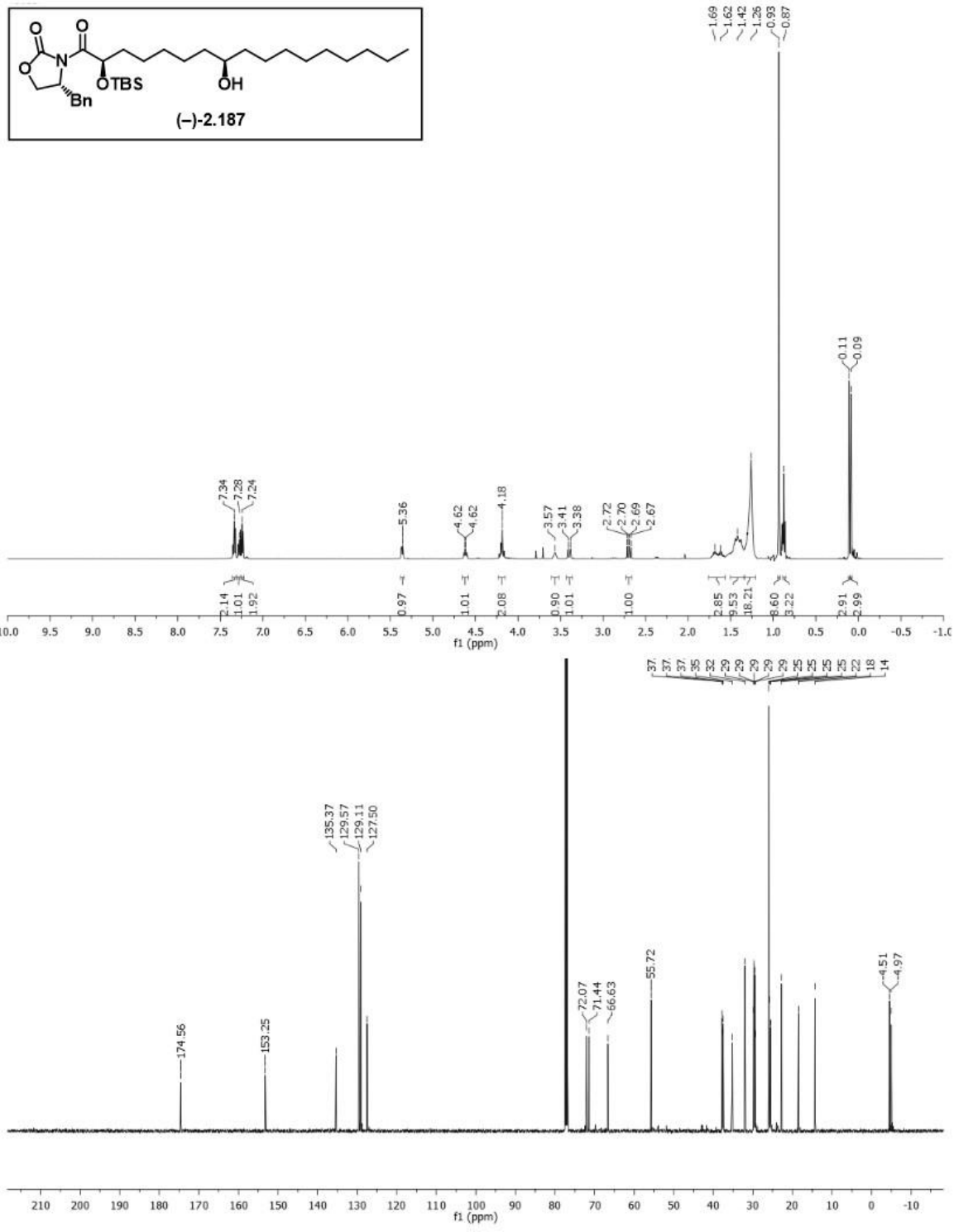
OTBS
OH
Bn
(–)-2.187
f1 (ppm)
f1 (ppm)

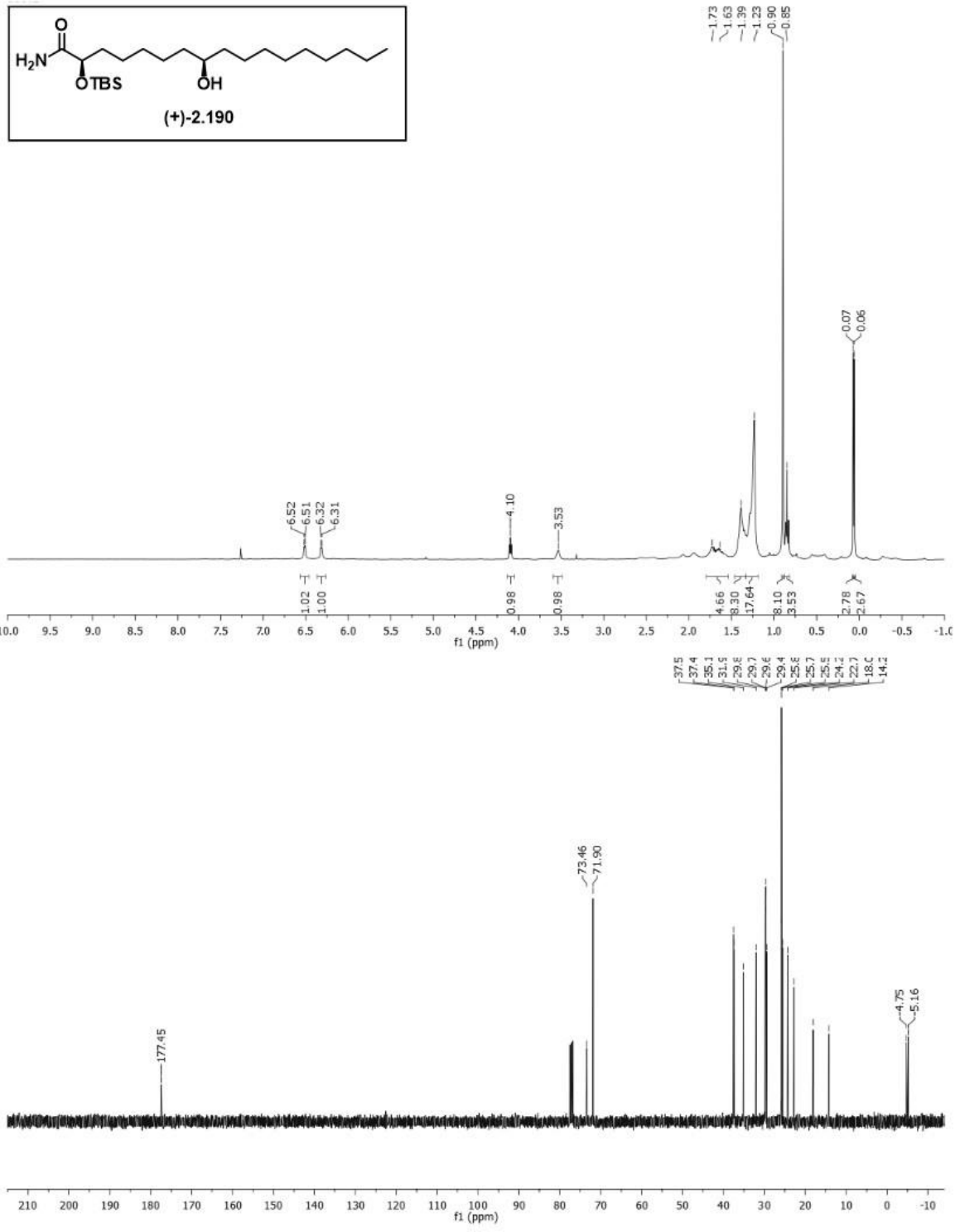
(+)-2.190
f1 (ppm)
f1 (ppm)

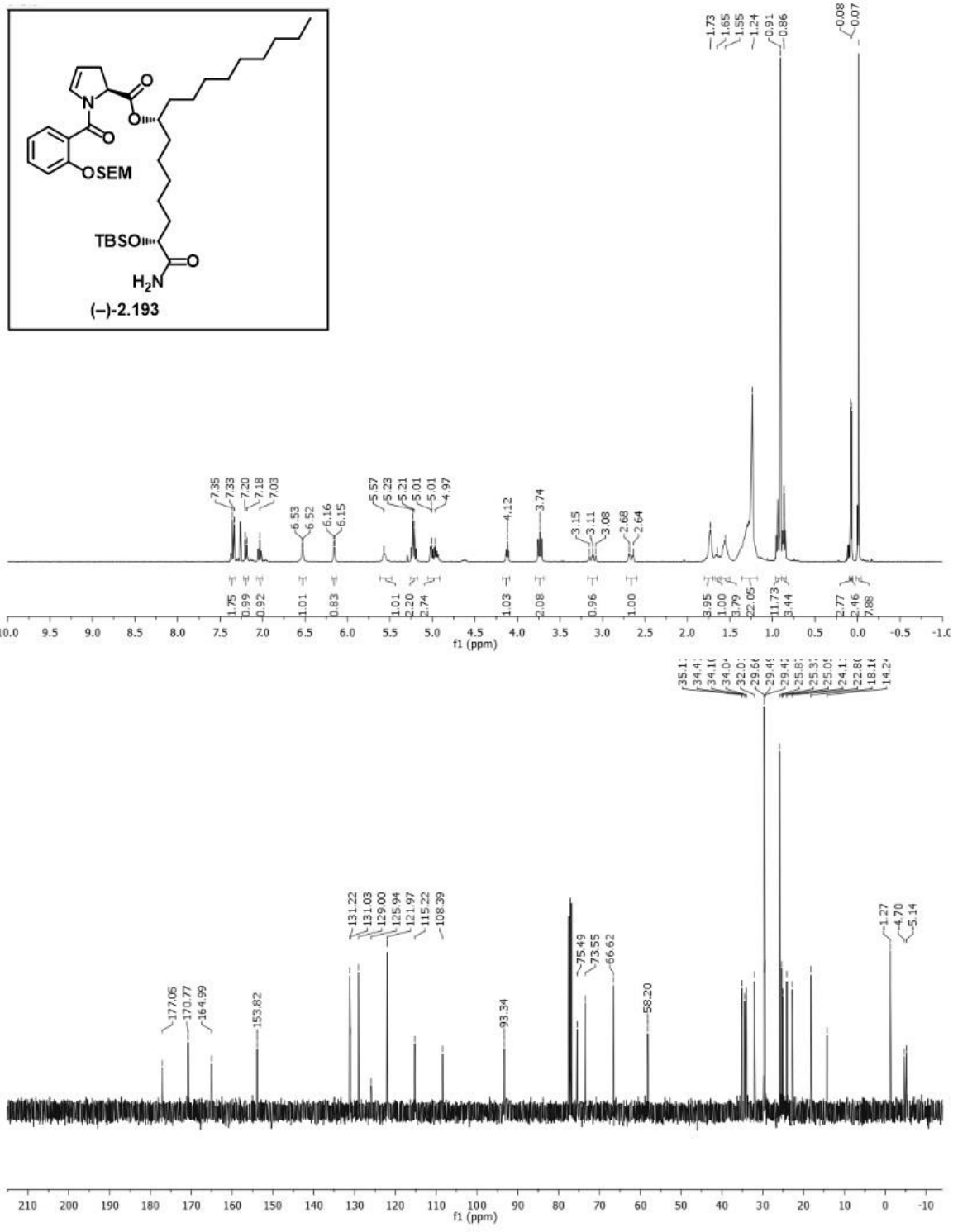
OSEM
TBSO
H2N
(–)-2.193
f1 (ppm)
f1 (ppm)

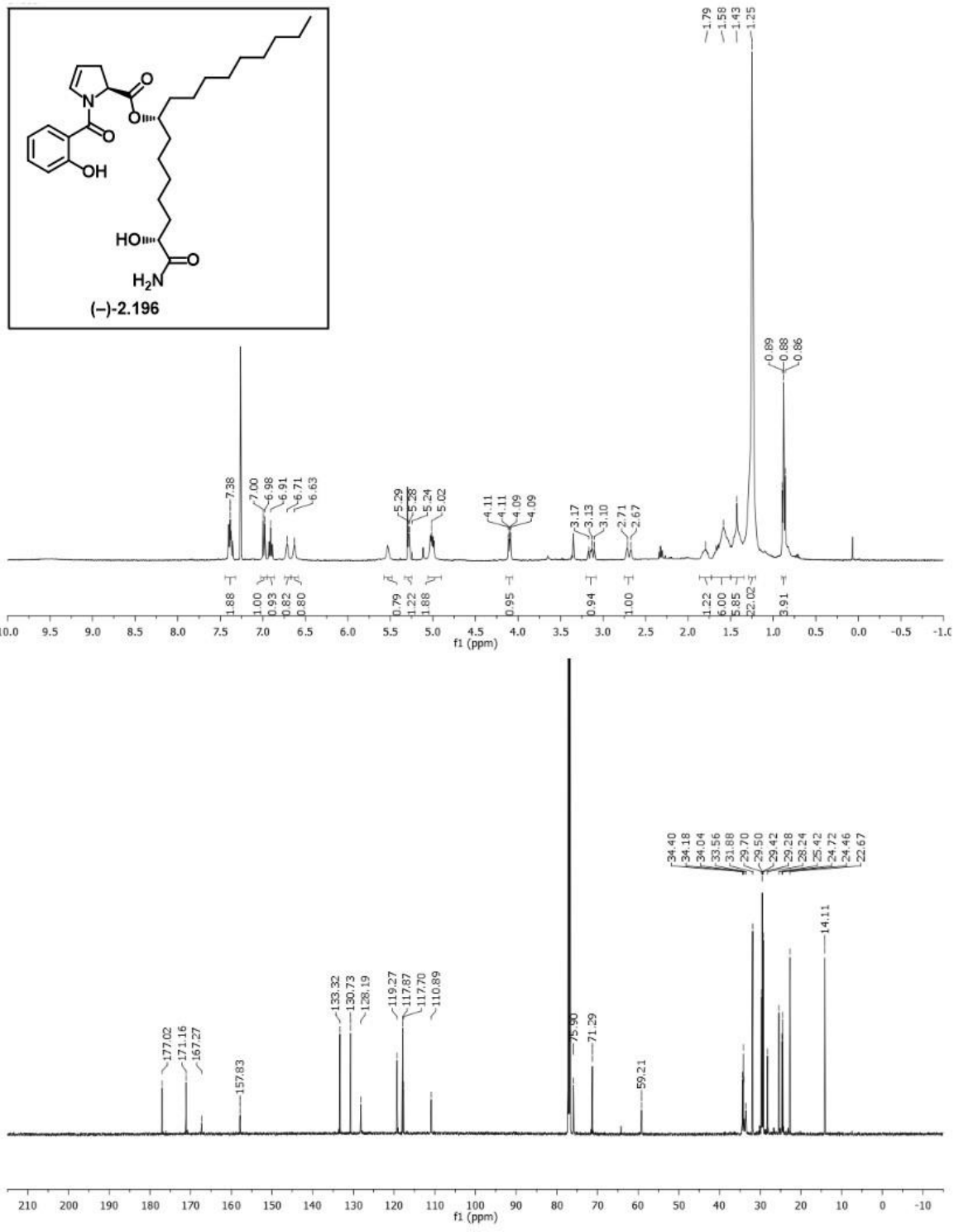
(–)-2.196
f1 (ppm)
f1 (ppm)

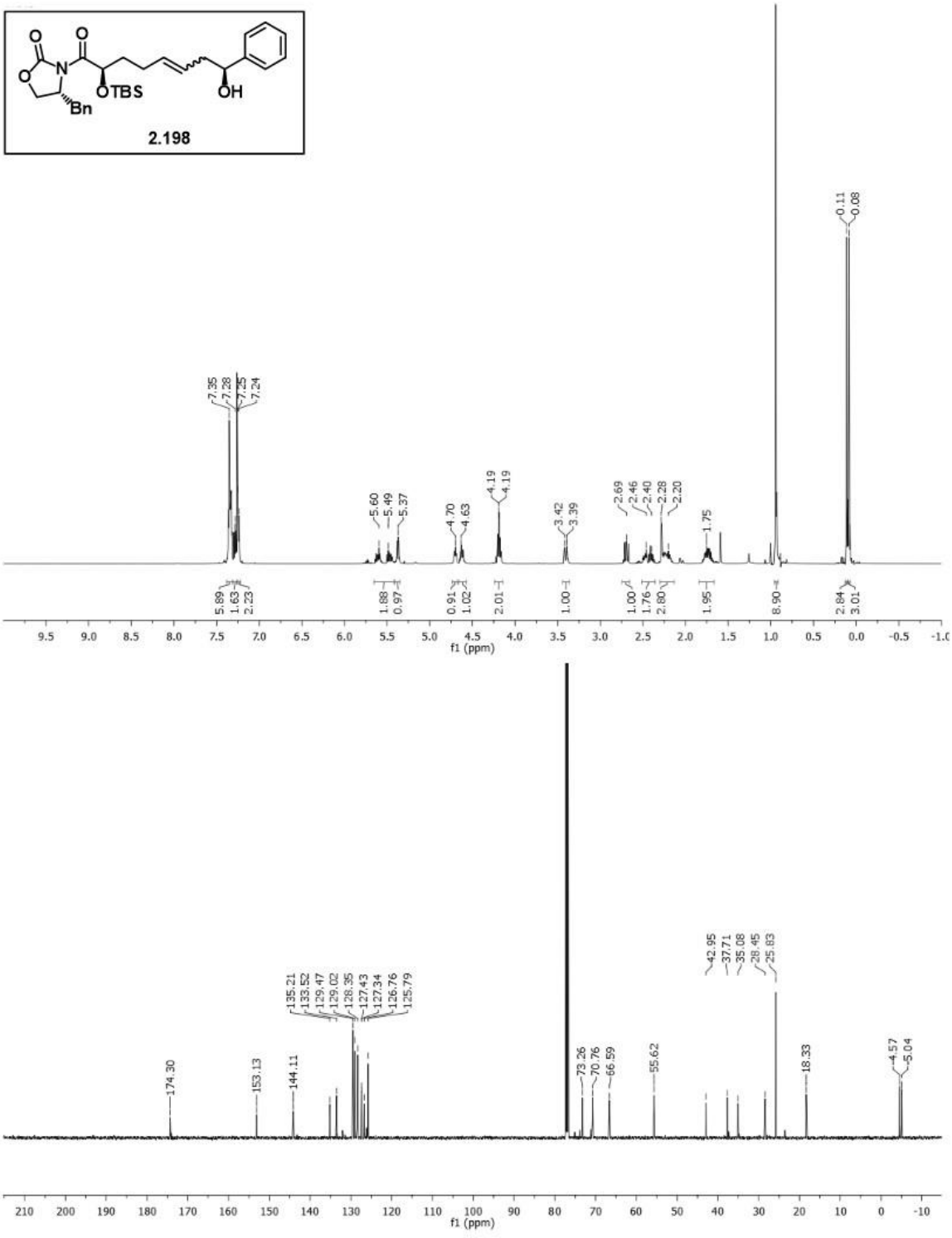
2.198
7.35
7.28
7.25
7.24
5.60
5.49
5.37
4.70
4.63
4.19
4.19
3.42
3.39
2.69
2.46
2.40
2.28
2.20
1.75
0.11
0.08
5.89
1.63
2.23
1.88
0.97
0.91
1.02
2.01
1.00
1.00
1.76
2.80
1.95
8.90
2.84
3.01
f1 (ppm)
174.30
153.13
144.11
135.21
133.52
129.47
129.02
128.35
127.43
127.34
126.76
125.79
73.26
70.76
66.59
55.62
42.95
37.71
35.08
28.45
25.83
18.33
4.57
5.04
f1 (ppm)

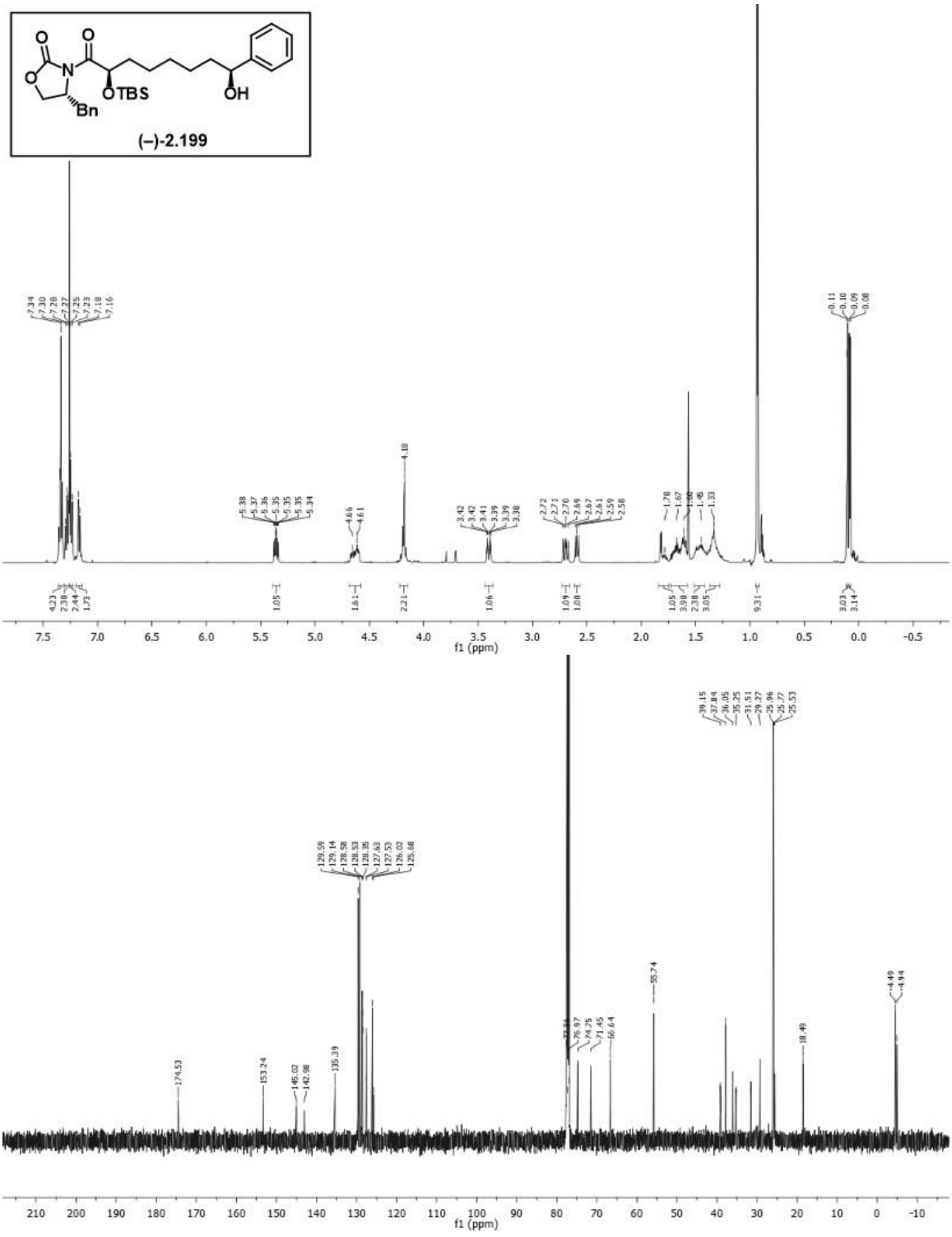
(–)-2.199
f1 (ppm)
f1 (ppm)

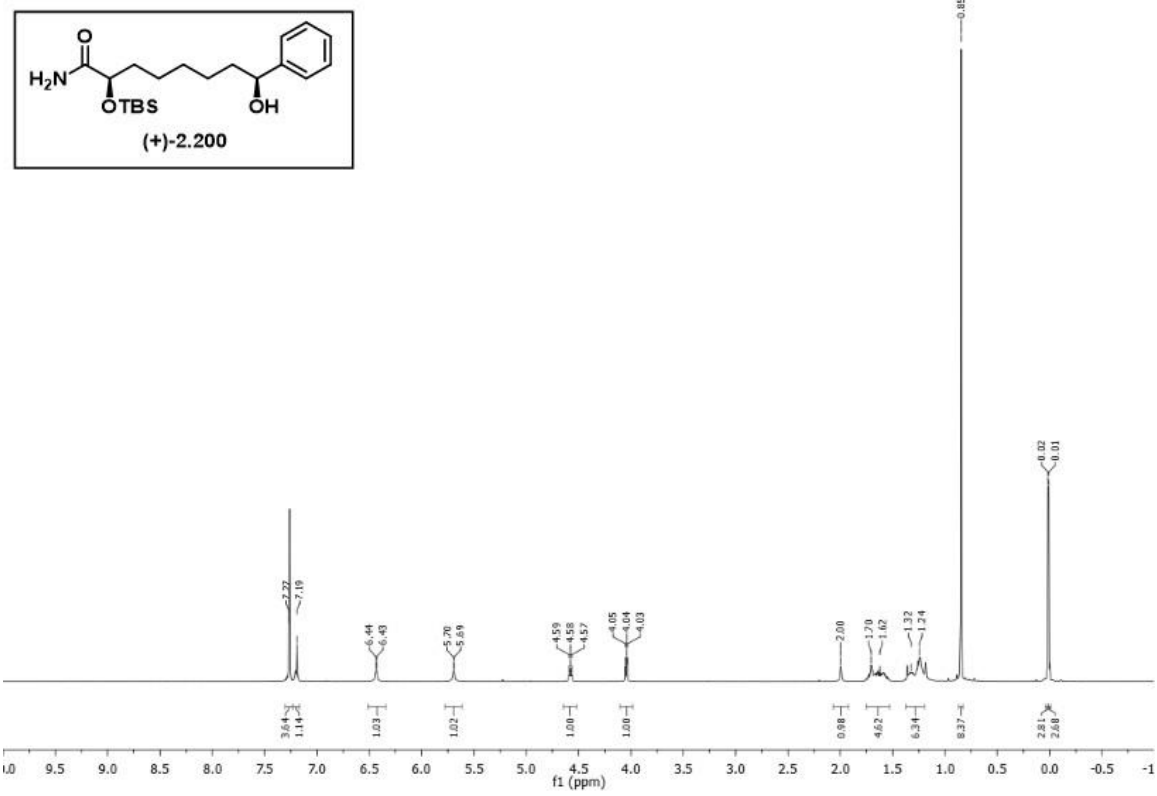
O
H2N
OTBS
OH
(+)-2.200
f1 (ppm)

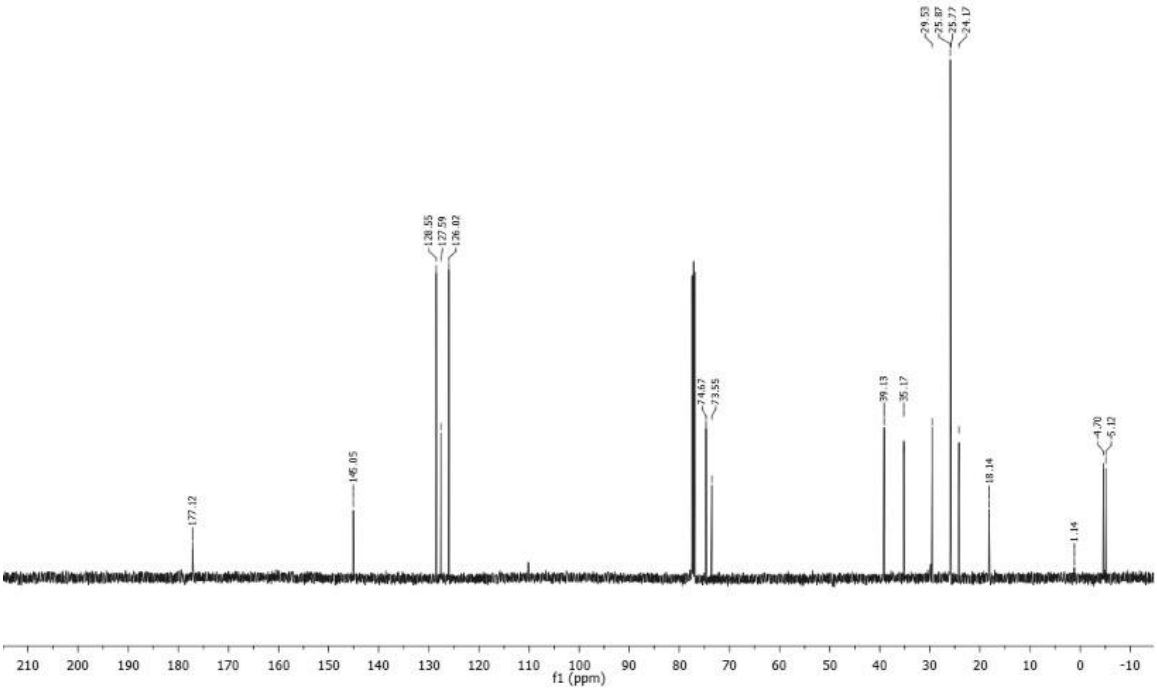
f1 (ppm)

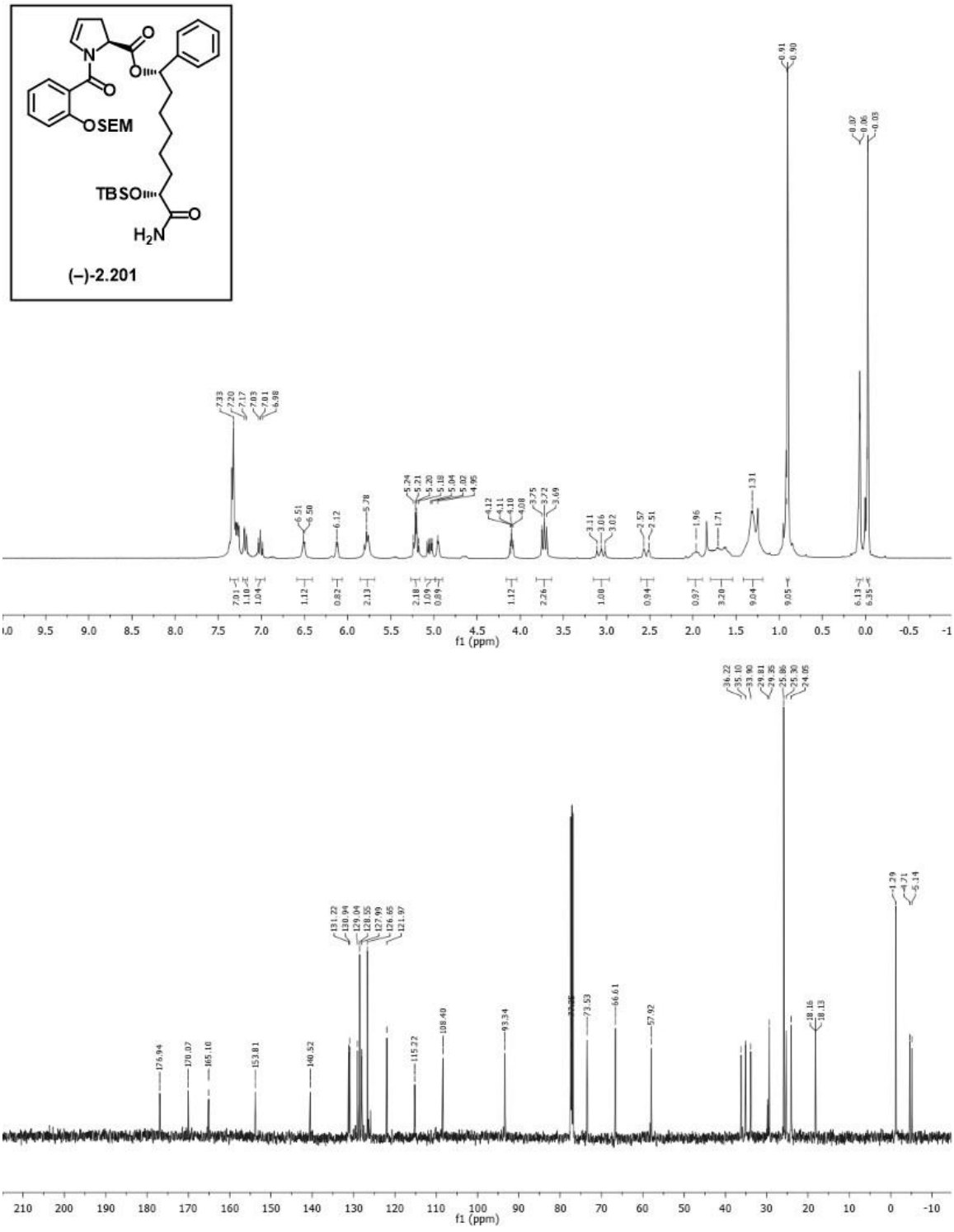
OSEM
TBSO
H_2N
(–)-2.201
f1 (ppm)
f1 (ppm)

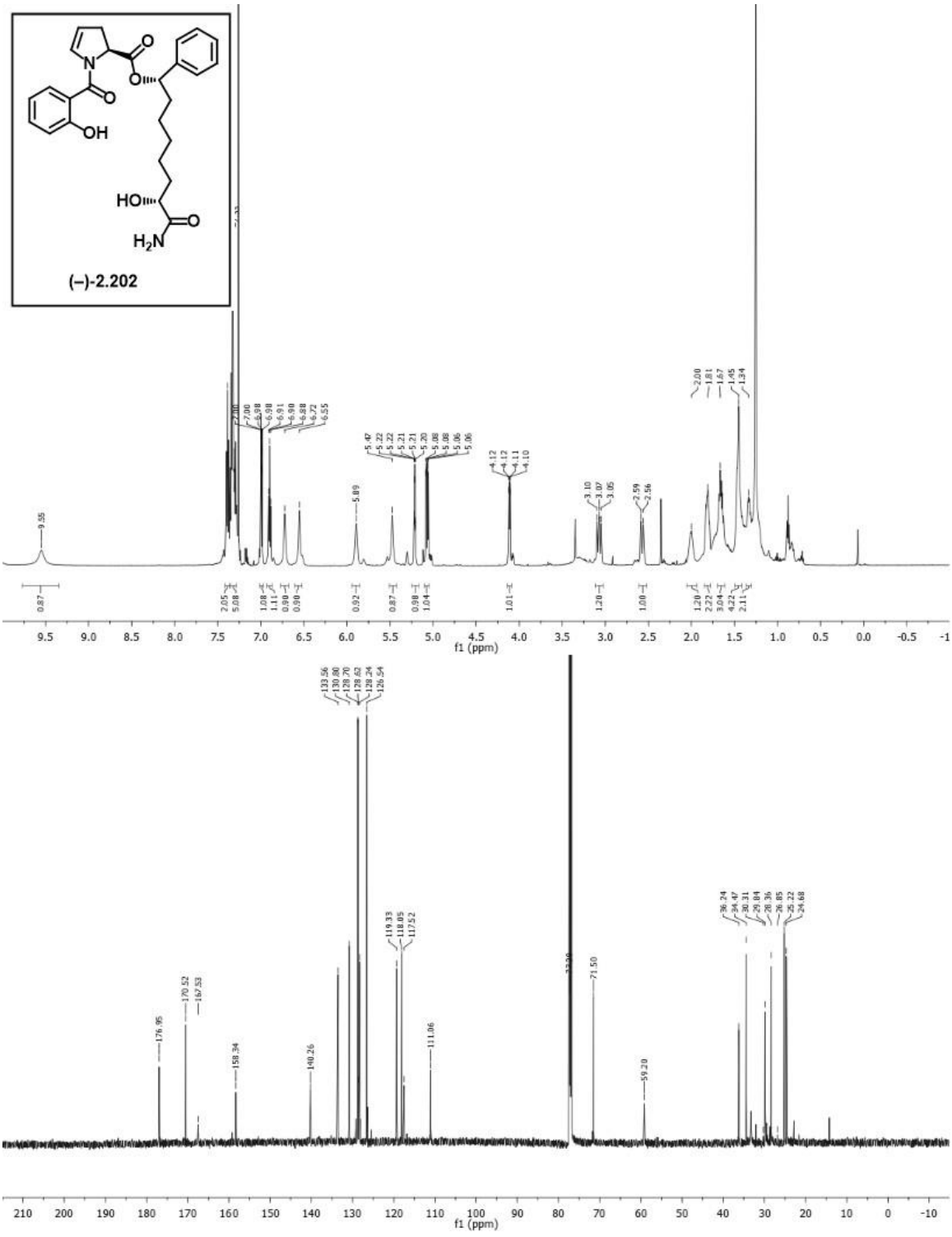
(–)-2.202
f1 (ppm)
f1 (ppm)

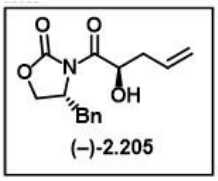
O
O
N
O
OH
Bn

(–)-2.205

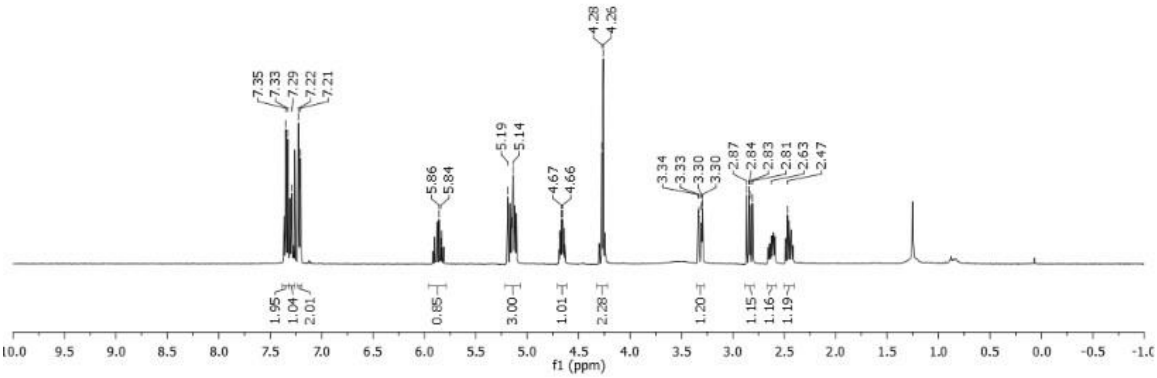
7.35
7.33
7.29
7.22
7.21
5.86
5.84
5.19
5.14
4.67
4.66
4.28
4.26
3.34
3.33
3.30
3.30
2.87
2.84
2.83
2.81
2.63
2.47
1.95
1.04
2.01
0.85
3.00
1.01
2.28
1.20
1.15
1.16
1.19
f1 (ppm)

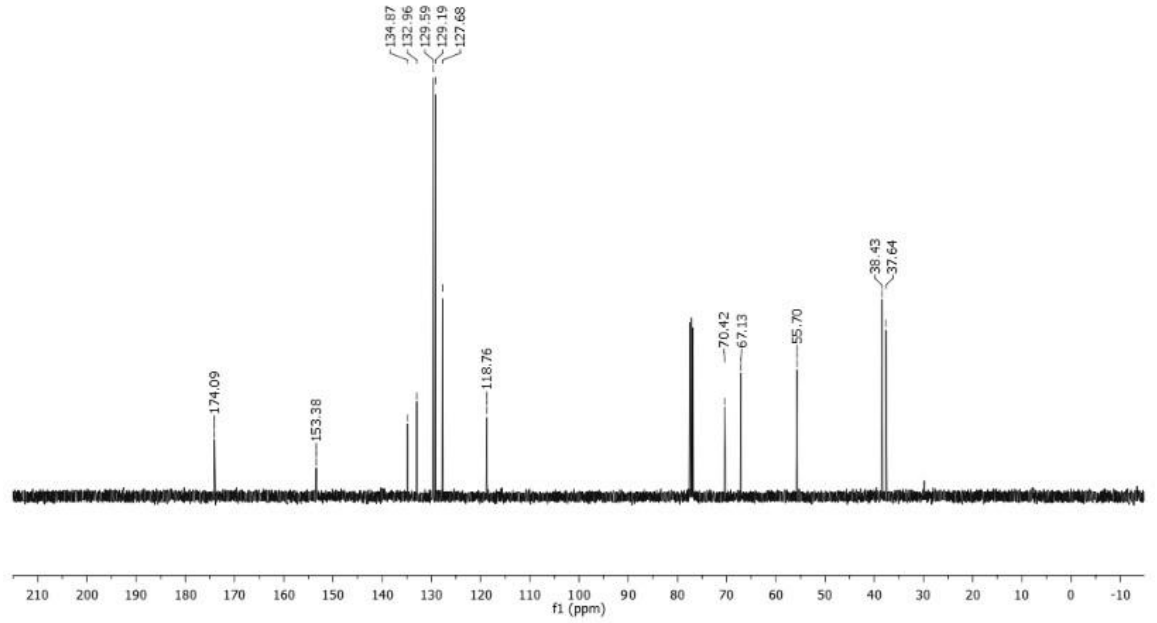
134.87
132.96
129.59
129.19
127.68
174.09
153.38
118.76
70.42
67.13
55.70
38.43
37.64
f1 (ppm)

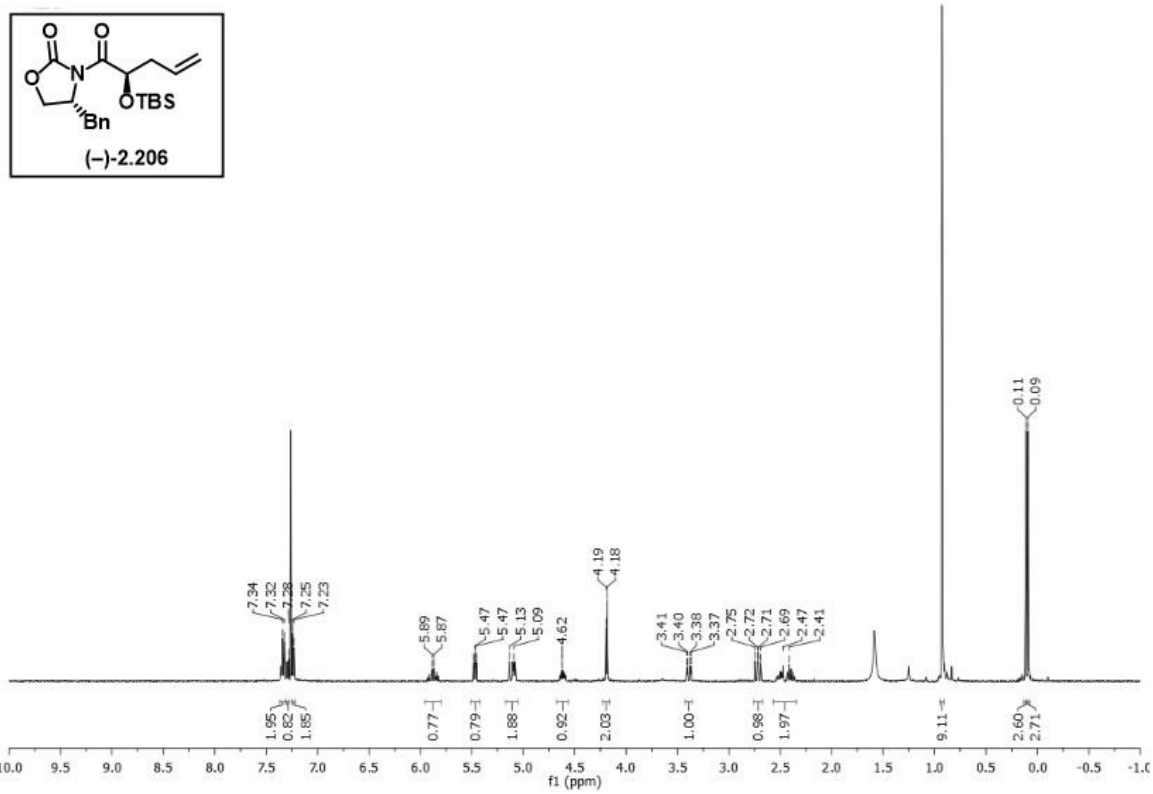
(–)-2.206
7.34
7.32
7.28
7.25
7.23
5.89
5.87
5.47
5.47
5.13
5.09
4.62
4.19
4.18
3.41
3.40
3.38
3.37
2.75
2.72
2.71
2.69
2.47
2.41
0.11
0.09
f1 (ppm)

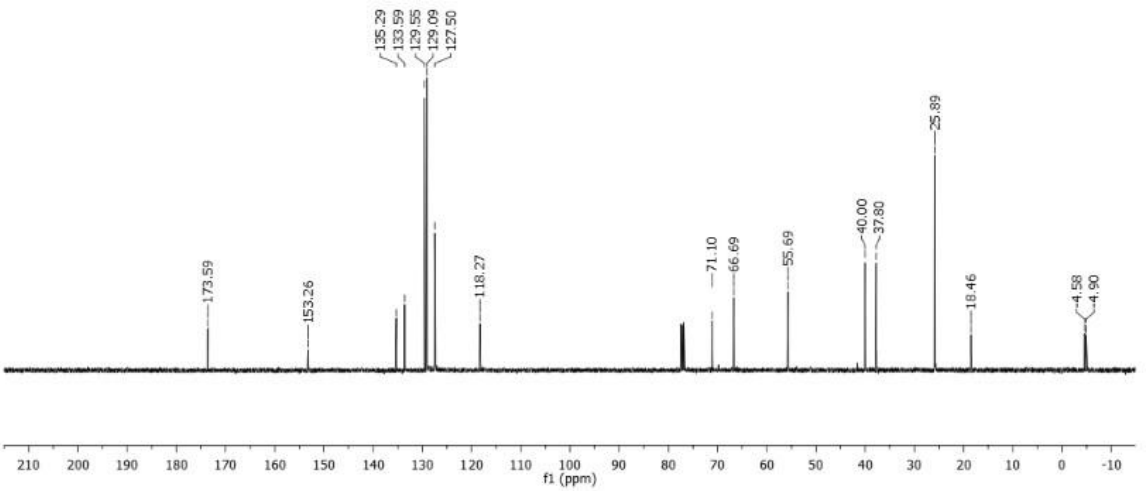
135.29
133.59
129.55
129.09
127.50
173.59
153.26
118.27
71.10
66.69
55.69
40.00
37.80
25.89
18.46
4.58
4.90
f1 (ppm)

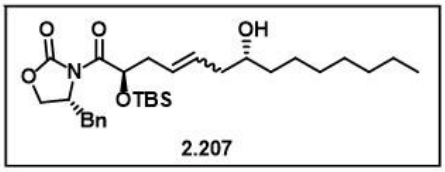

2.207

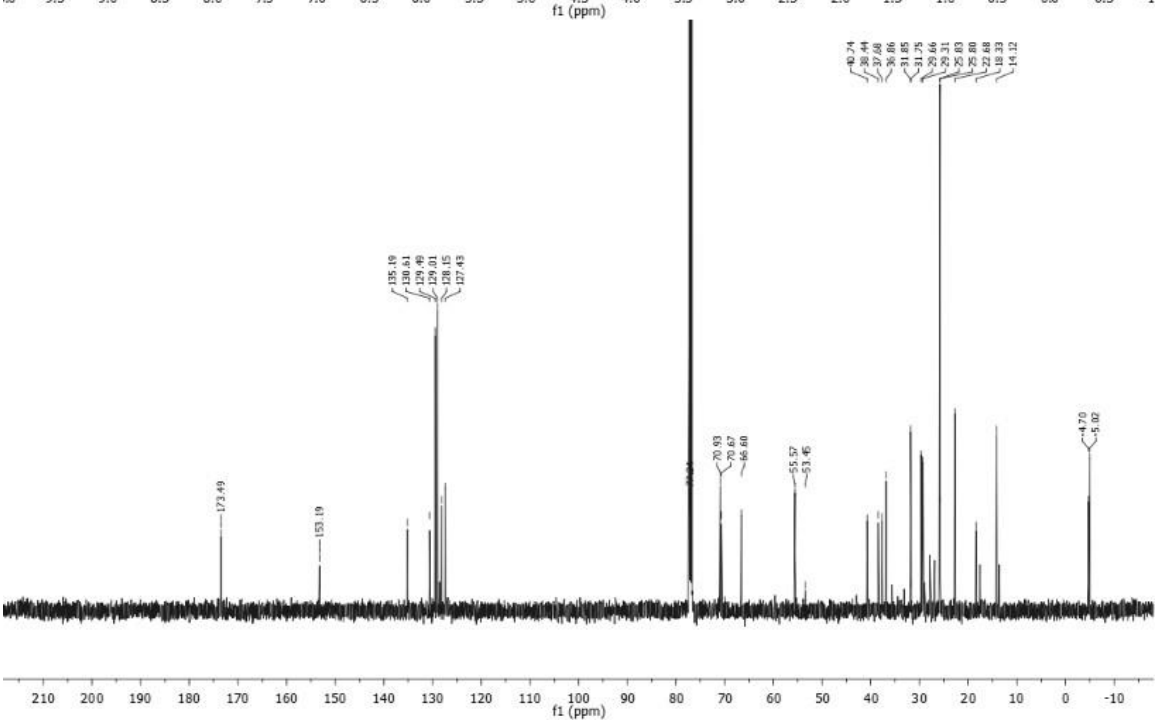

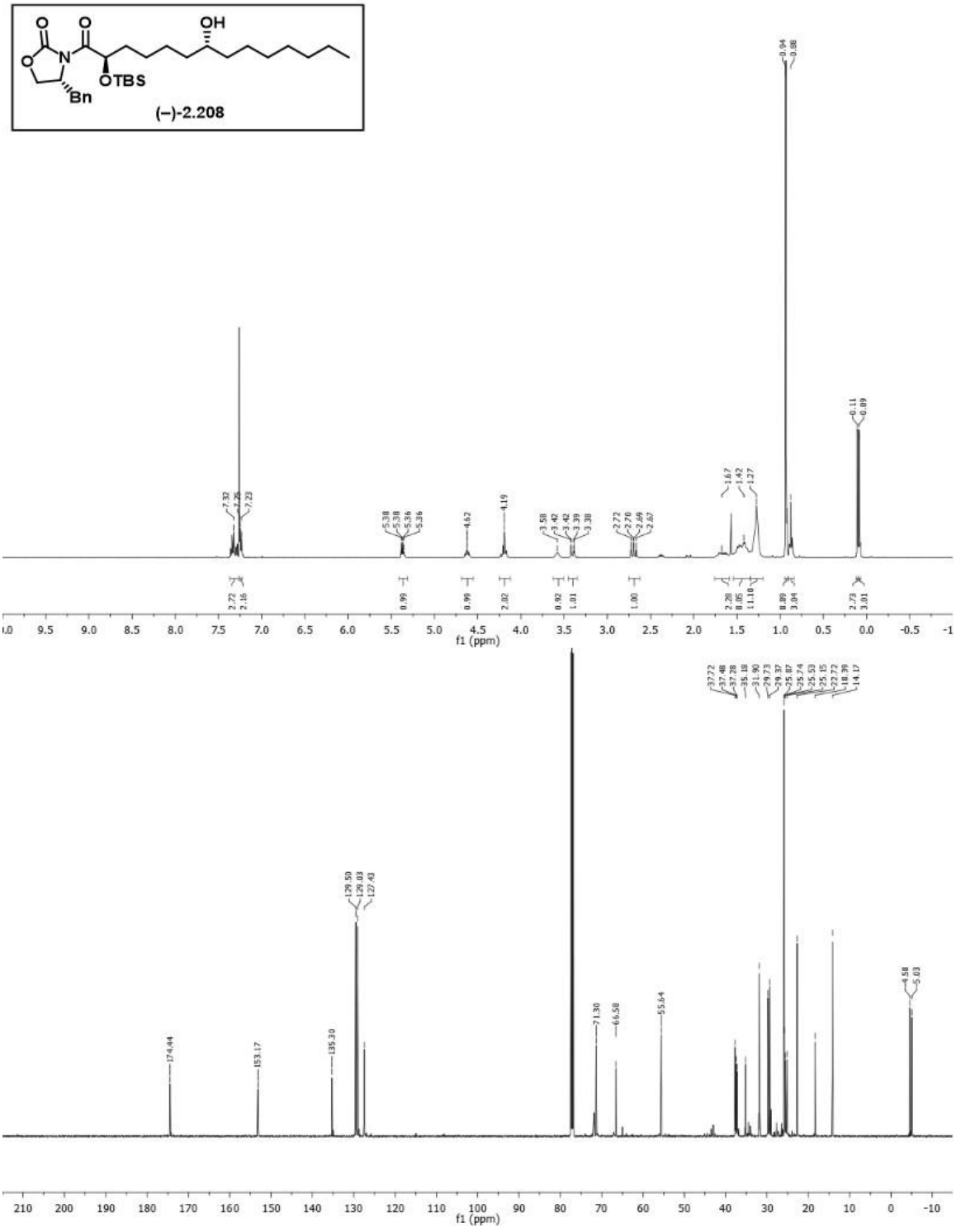
OH
O
O
N
O
OTBS
Bn
(–)-2.208
f1 (ppm)
f1 (ppm)

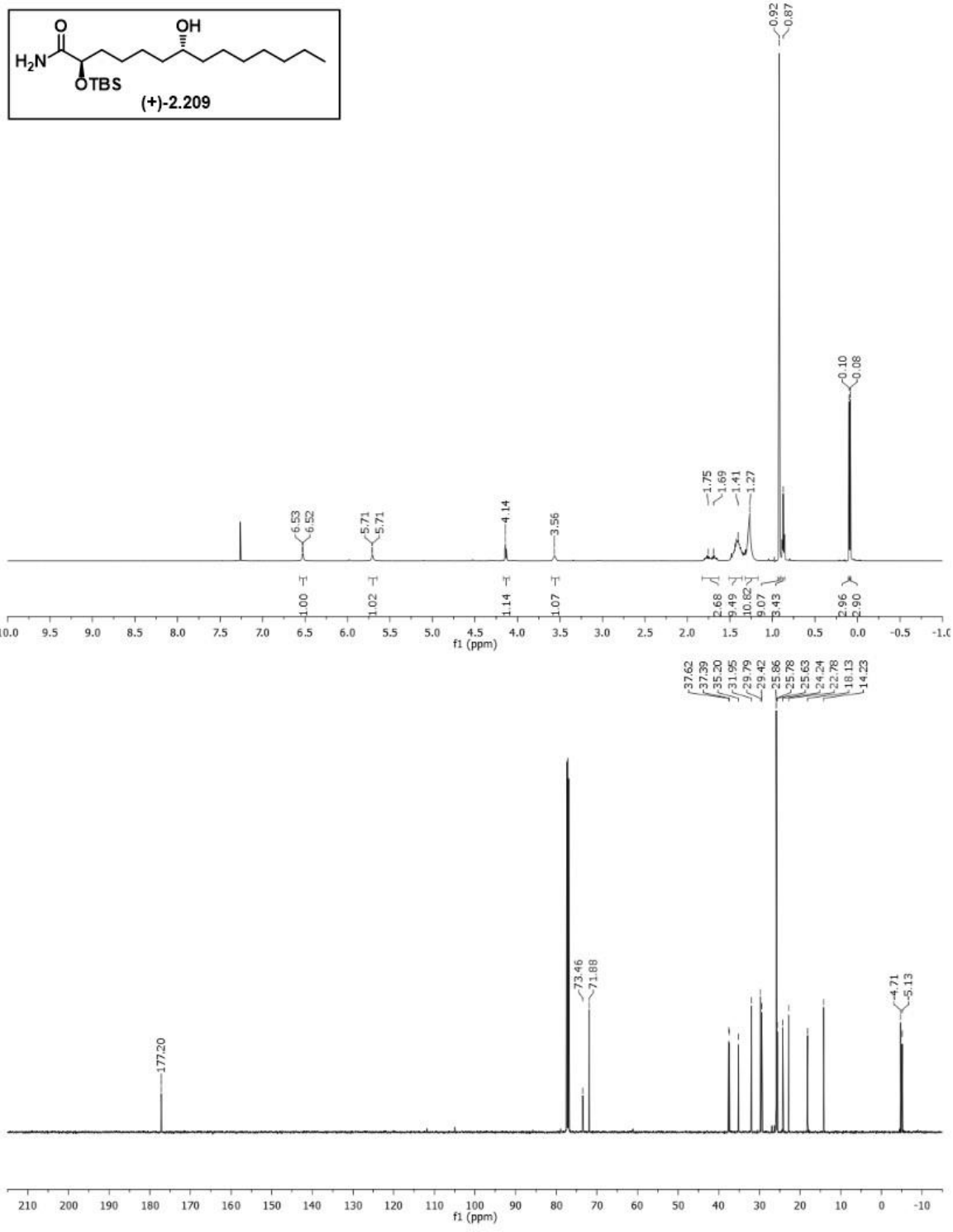
O
OH
H2N
OTBS
(+)-2.209
0.92
0.87
0.10
0.08
1.75
1.69
1.41
1.27
6.53
6.52
5.71
5.71
4.14
3.56
1.00
1.02
1.14
1.07
2.68
9.49
10.82
9.07
3.43
2.96
2.90
f1 (ppm)
37.62
37.39
35.20
31.95
29.79
29.42
25.86
25.78
25.63
24.24
22.78
18.13
14.23
73.46
71.88
177.20
4.71
5.13
f1 (ppm)

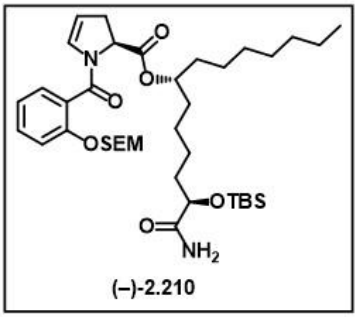

(–)-2.210

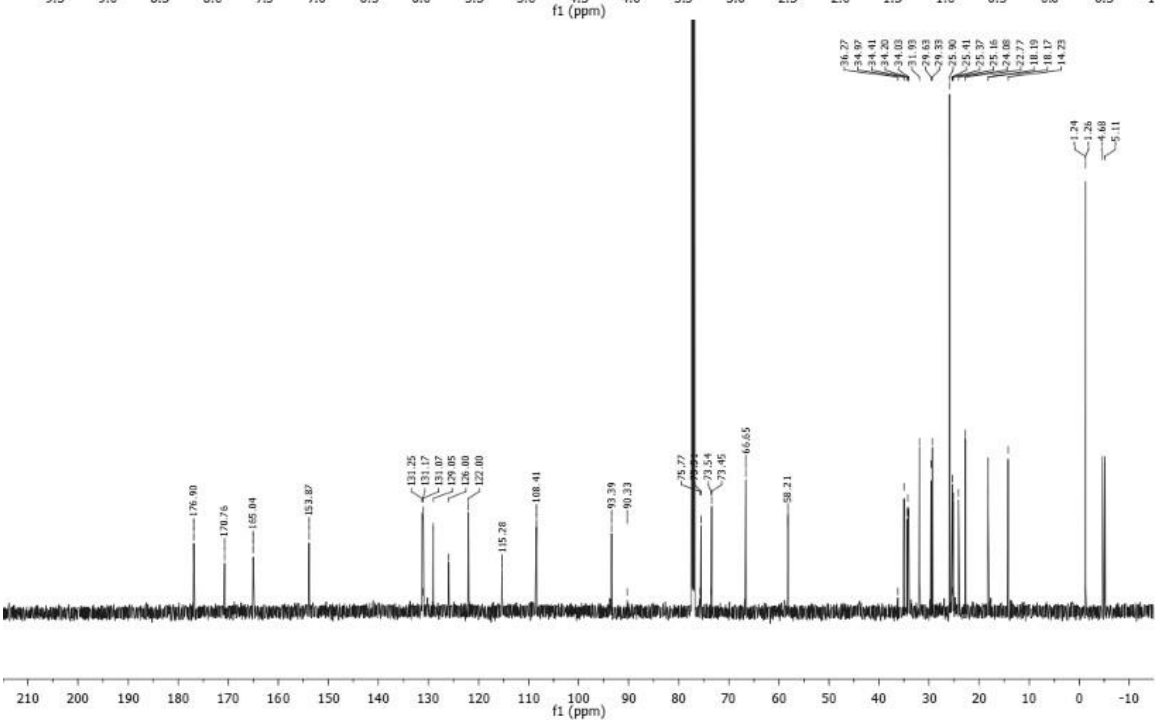

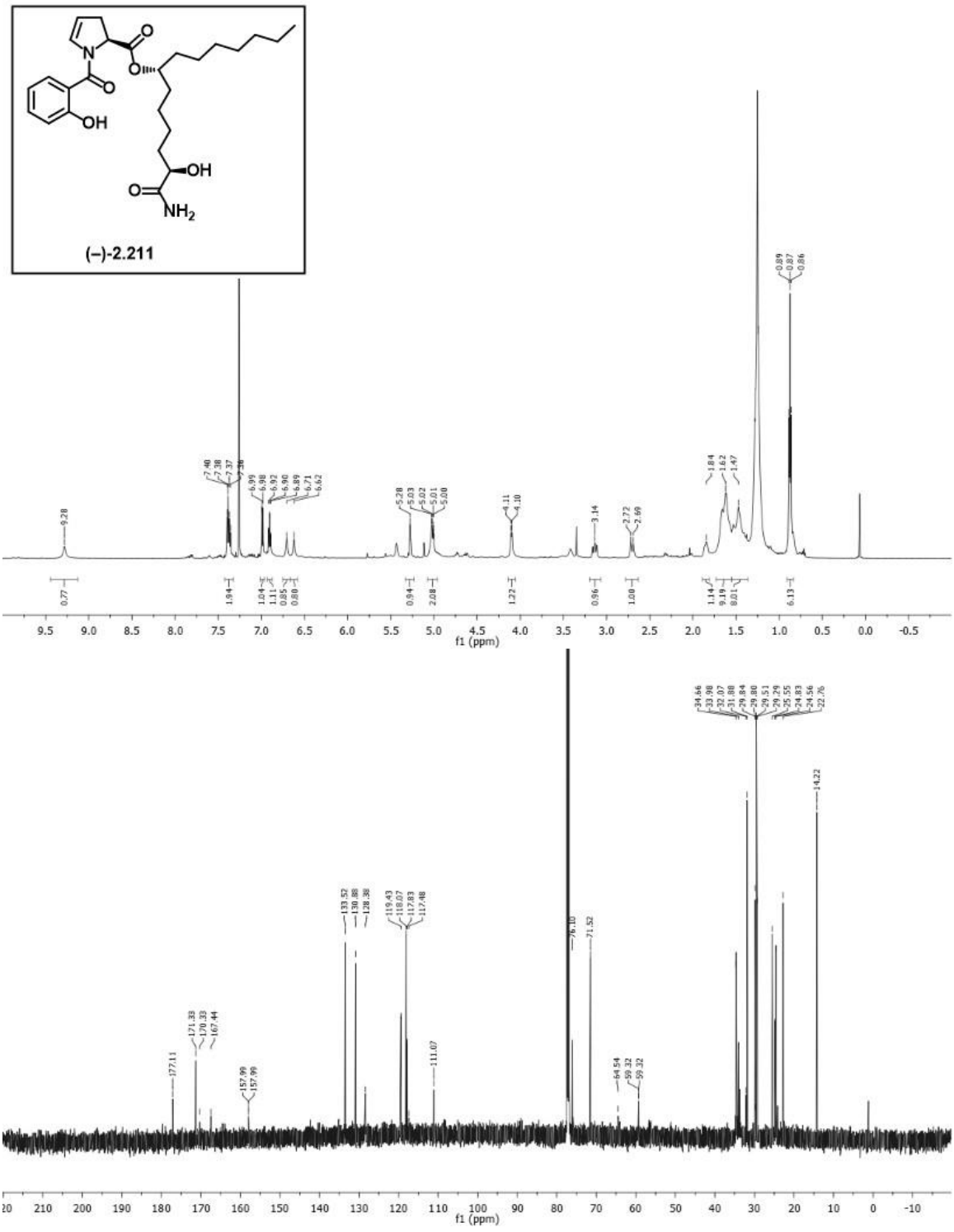
(–)-2.211
f1 (ppm)
f1 (ppm)

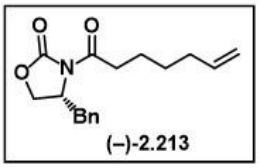
O
O
O
N
Bn

(–)-2.213

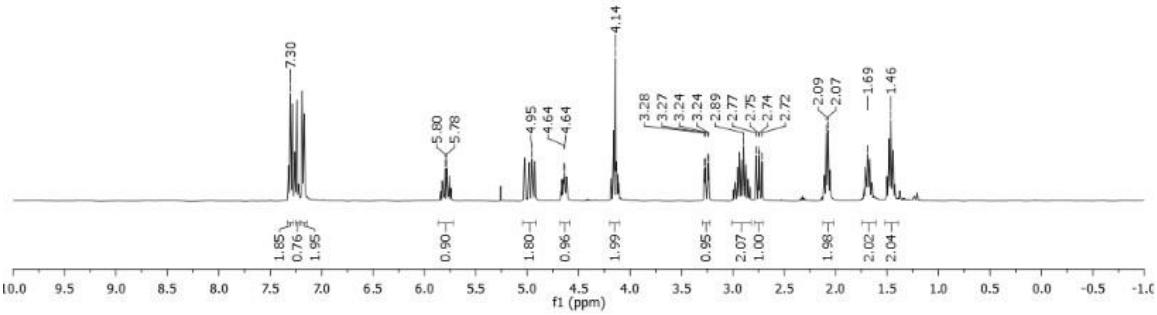
7.30
5.80
5.78
4.95
4.64
4.64
4.14
3.28
3.27
3.24
3.24
2.89
2.77
2.75
2.74
2.72
2.09
2.07
1.69
1.46
1.85
0.76
1.95
0.90
1.80
0.96
1.99
0.95
2.07
1.00
1.98
2.02
2.04
f1 (ppm)

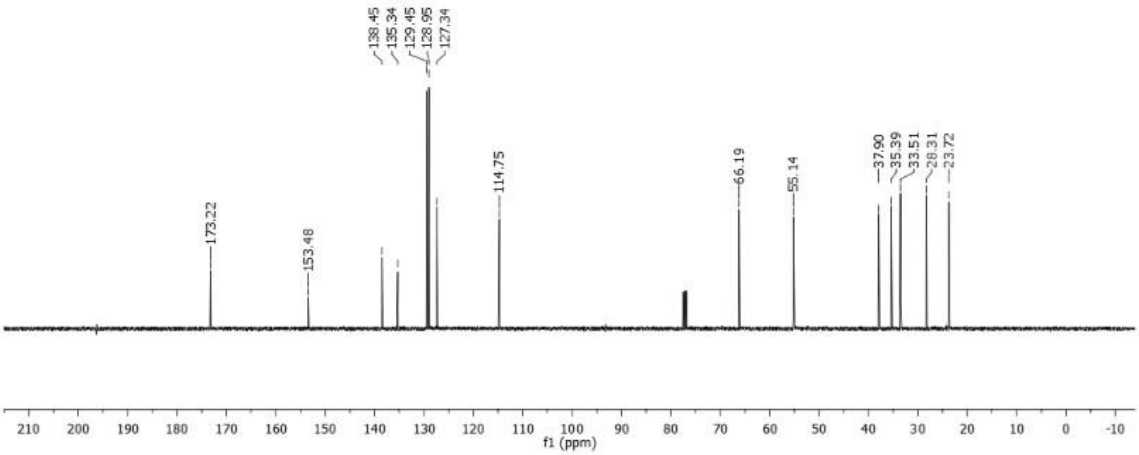
138.45
135.34
129.45
128.95
127.34
173.22
153.48
114.75
66.19
55.14
37.90
35.39
33.51
28.31
23.72
f1 (ppm)

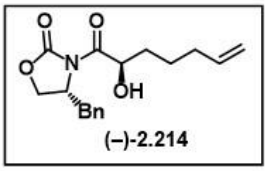
O
O
N
O
OH
Bn

(–)-2.214

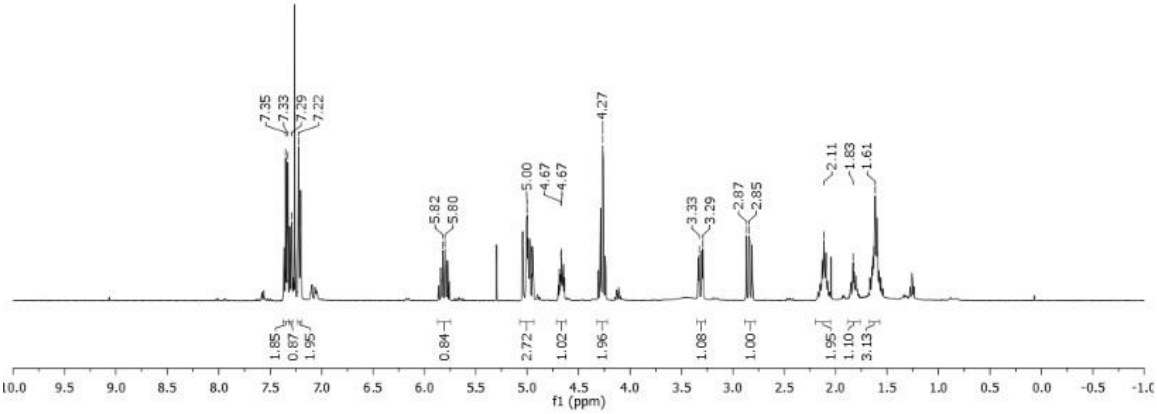
7.35
7.33
7.29
7.22
5.82
5.80
5.00
4.67
4.67
4.27
3.33
3.29
2.87
2.85
2.11
1.83
1.61
1.85
0.87
1.95
0.84
2.72
1.02
1.96
1.08
1.00
1.95
1.10
3.13
f1 (ppm)

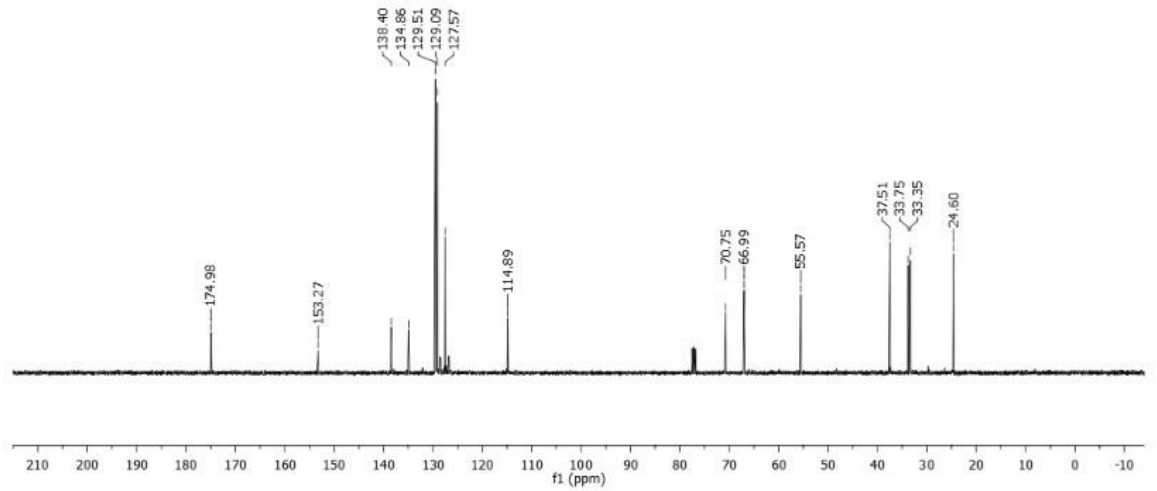
138.40
134.86
129.51
129.09
127.57
174.98
153.27
114.89
70.75
66.99
55.57
37.51
33.75
33.35
24.60
f1 (ppm)

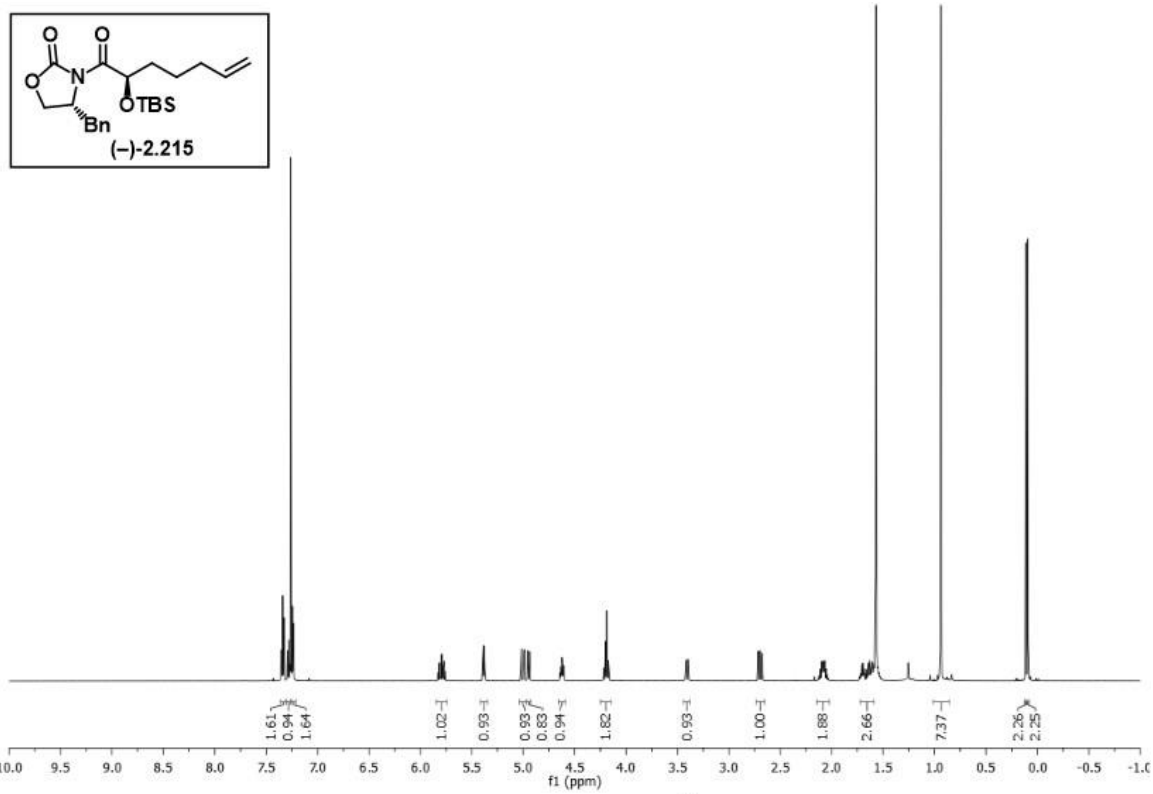
OTBS
Bn
(–)-2.215
1.61
0.94
1.64
1.02
0.93
0.93
0.83
0.94
1.82
0.93
1.00
1.88
2.66
7.37
2.26
2.25
f1 (ppm)

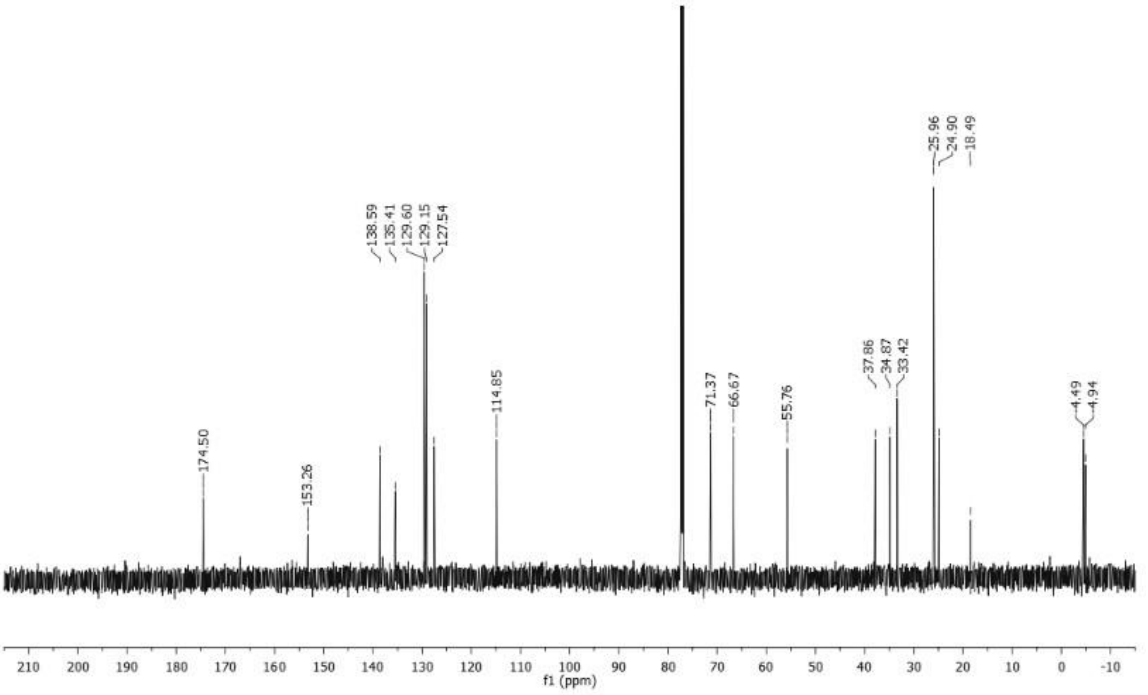
138.59
135.41
129.60
129.15
127.54
114.85
174.50
153.26
71.37
66.67
55.76
37.86
34.87
33.42
25.96
24.90
18.49
4.49
4.94
f1 (ppm)

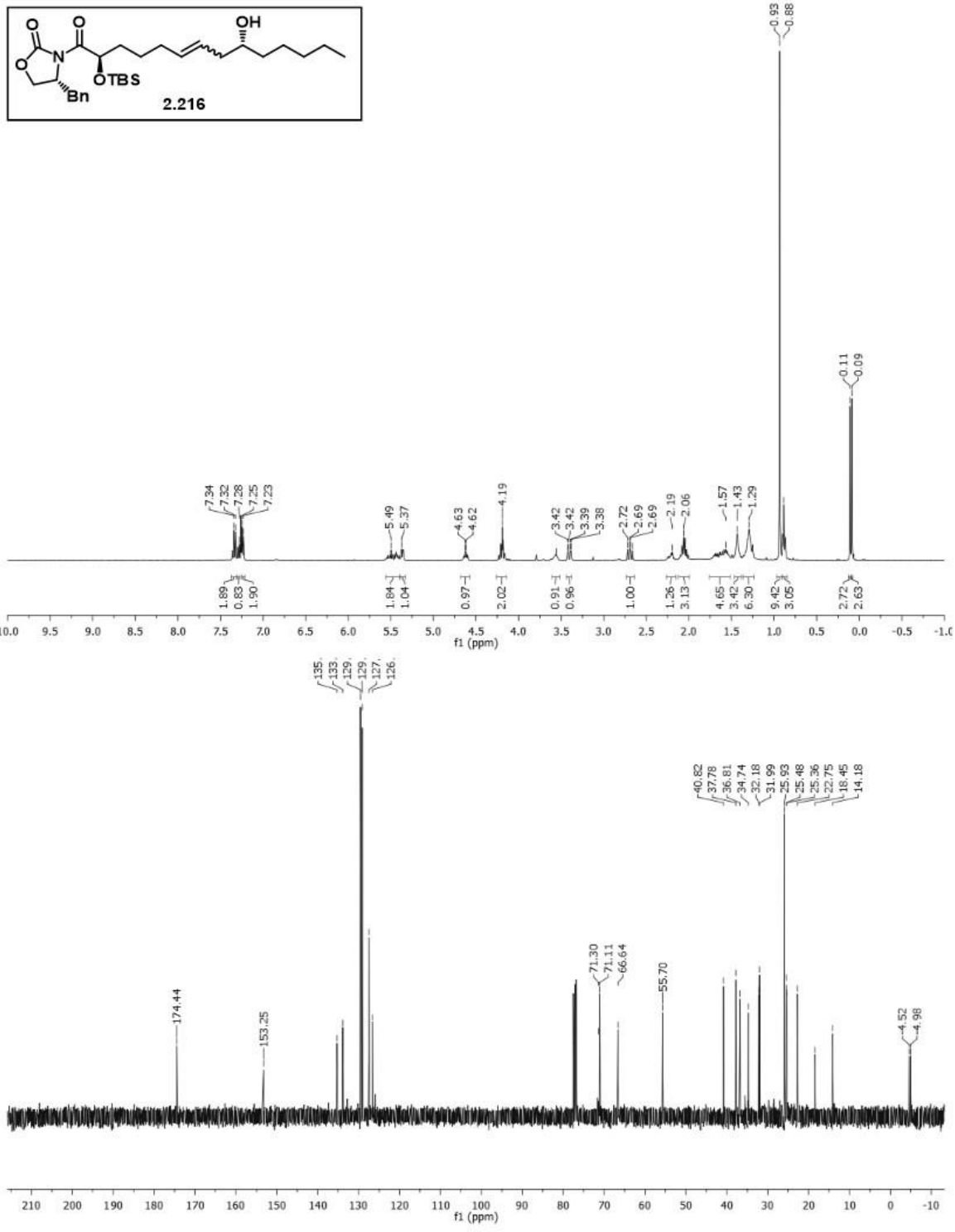
OH
O
O
N
O
OTBS
Bn
2.216
f1 (ppm)
f1 (ppm)

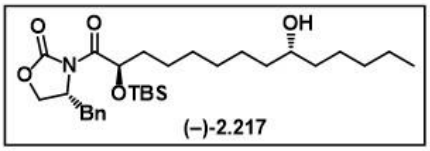
O
O
N
O
OH
OTBS
Bn

(–)-2.217

0.93
0.11
0.09
1.67
1.59
1.42
1.30
7.34
7.32
7.25
7.23
5.37
5.35
4.63
4.62
4.19
3.42
3.42
3.39
3.38
2.72
2.70
2.69
2.66
2.74
1.85
0.98
0.99
2.05
0.96
1.04
1.00
9.41
7.28
11.18
9.23
3.21
2.77
2.67
f1 (ppm)

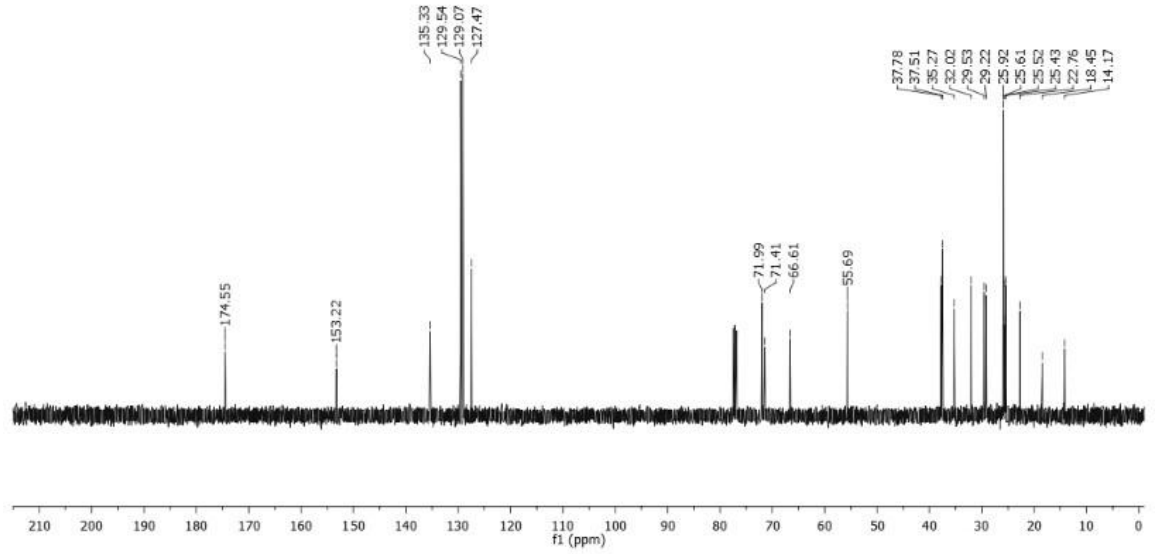
135.33
129.54
129.07
127.47
37.78
37.51
35.27
32.02
29.53
29.22
25.92
25.61
25.52
25.43
22.76
18.45
14.17
174.55
153.22
71.99
71.41
66.61
55.69
f1 (ppm)

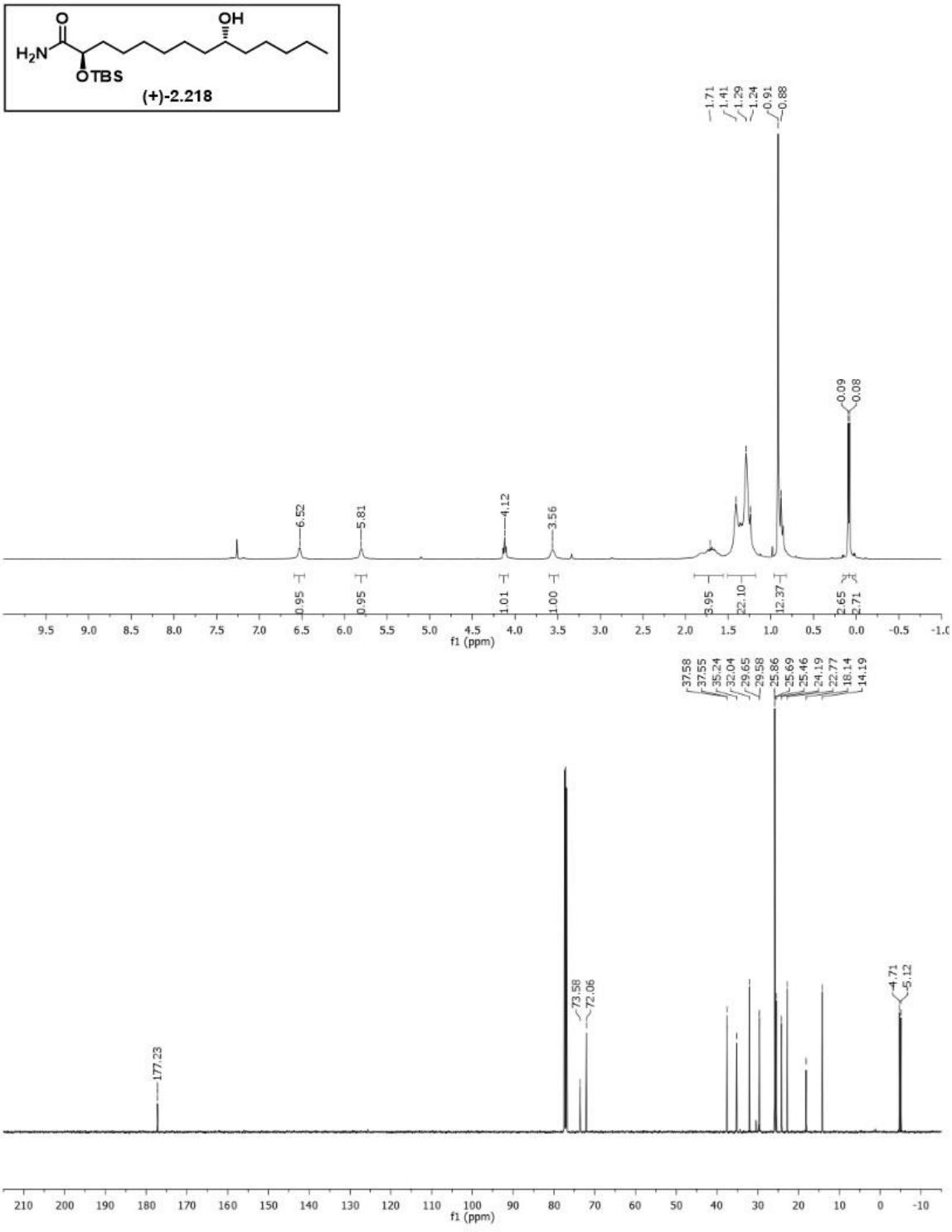
O
OH
H2N
OTBS
(+)-2.218
1.71
1.41
1.29
1.24
0.91
0.88
0.09
0.08
6.52
5.81
4.12
3.56
0.95
0.95
1.01
1.00
3.95
22.10
12.37
2.65
2.71
f1 (ppm)
37.58
37.55
35.24
32.04
29.65
29.58
25.86
25.69
25.46
24.19
22.77
18.14
14.19
177.23
73.58
72.06
14.71
15.12
f1 (ppm)

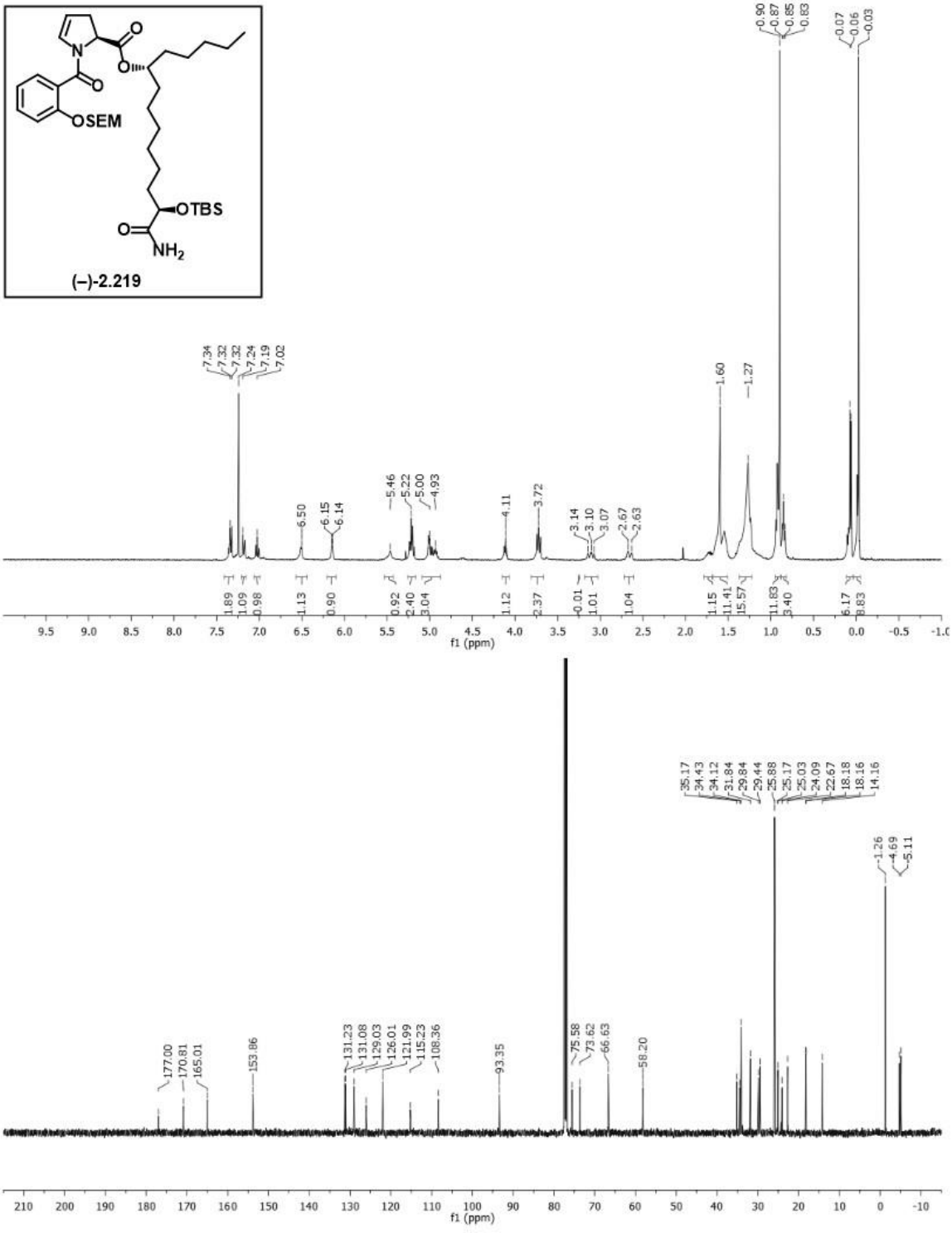
OSEM
OTBS
NH2
(–)-2.219
f1 (ppm)
f1 (ppm)

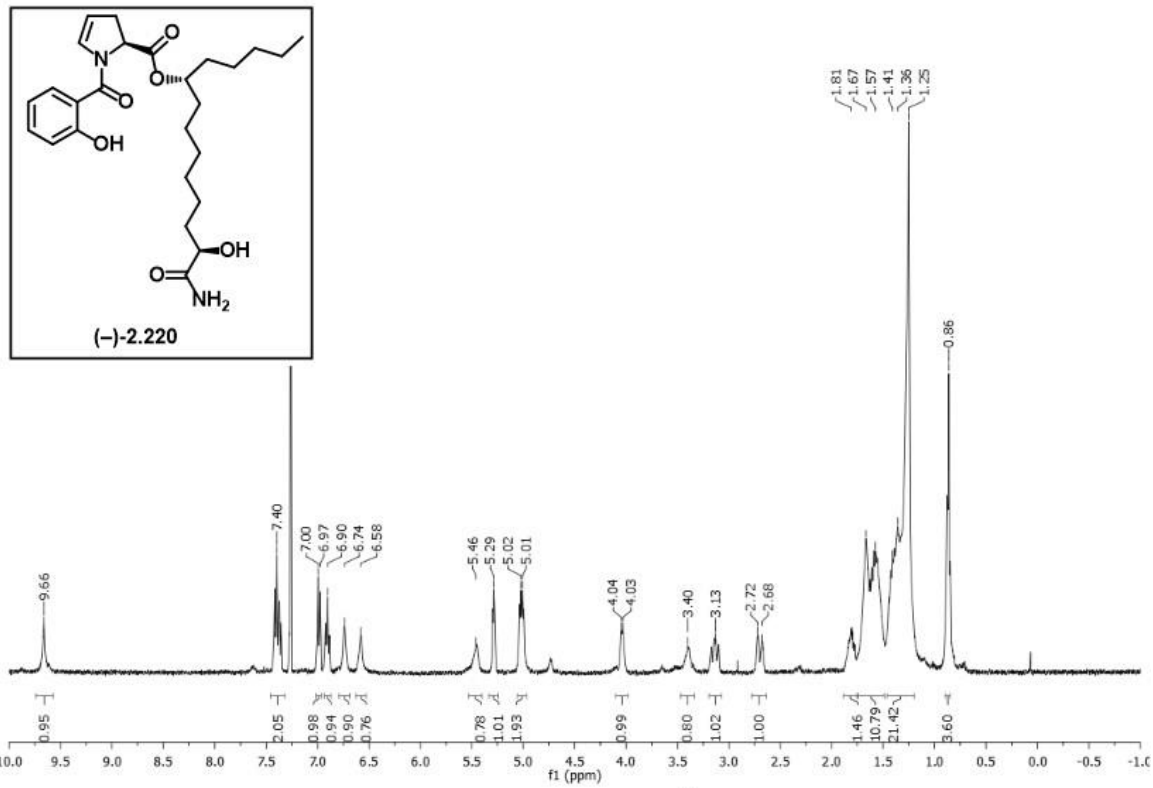
(–)-2.220
OH
O
N
O
O
OH
O
NH2
9.66
7.40
7.00
6.97
6.90
6.74
6.58
5.46
5.29
5.02
5.01
4.04
4.03
3.40
3.13
2.72
2.68
1.81
1.67
1.57
1.41
1.36
1.25
0.86
f1 (ppm)

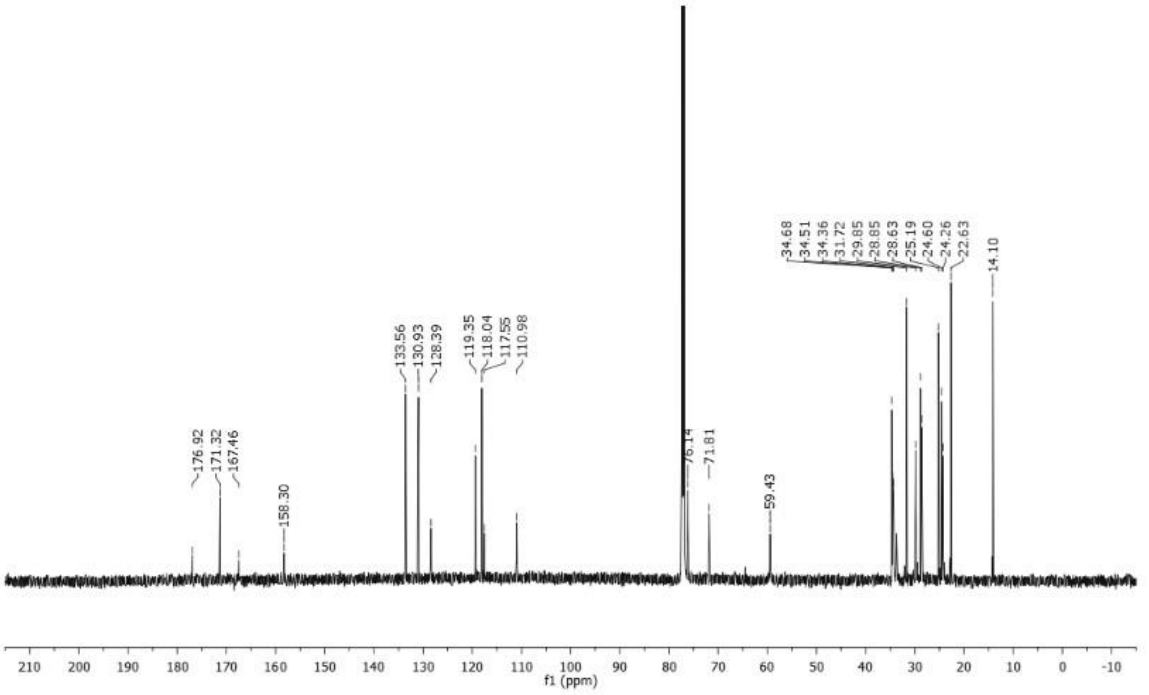
176.92
171.32
167.46
158.30
133.56
130.93
128.39
119.35
118.04
117.55
110.98
76.14
71.81
59.43
34.68
34.51
34.36
31.72
29.85
28.85
28.63
25.19
24.60
24.26
22.63
14.10
f1 (ppm)

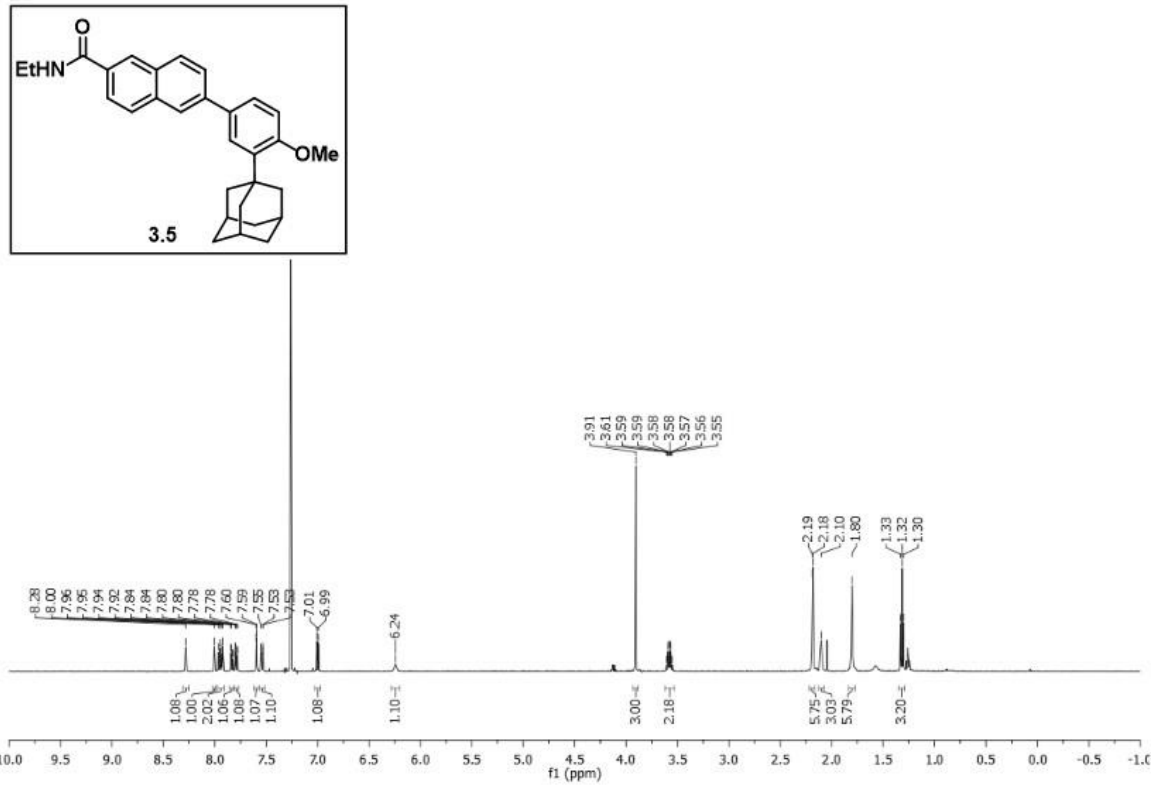
EtHN
O
OMe
3.5
8.28
8.00
7.96
7.95
7.94
7.92
7.84
7.84
7.80
7.80
7.78
7.78
7.60
7.59
7.55
7.53
7.53
7.01
6.99
6.24
3.91
3.61
3.59
3.59
3.59
3.58
3.58
3.57
3.56
3.55
2.19
2.18
2.10
1.80
1.33
1.32
1.30
1.08
1.00
2.02
1.06
1.08
1.07
1.10
1.08
1.10
3.00
2.18
5.75
3.03
5.79
3.20
f1 (ppm)

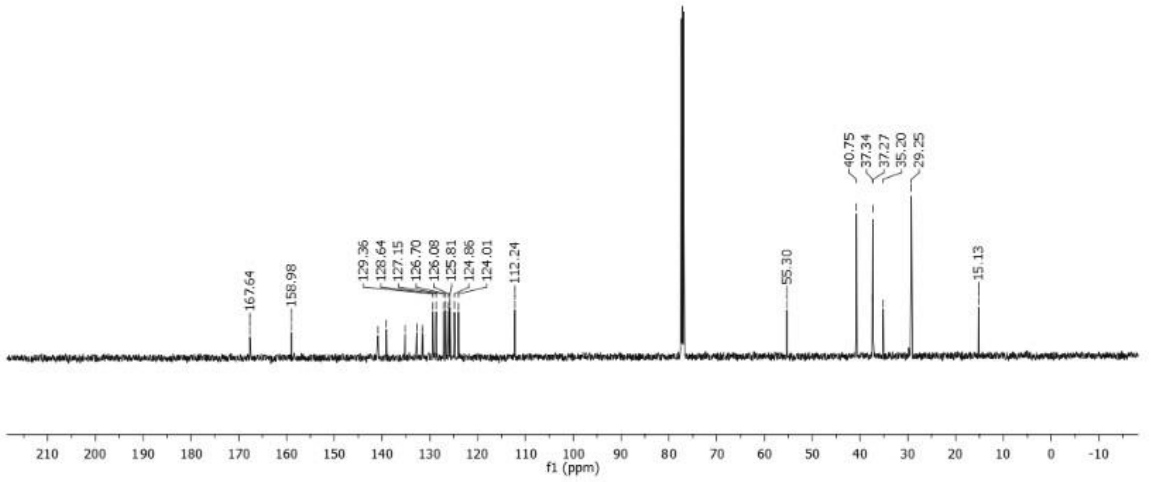
167.64
158.98
129.36
128.64
127.15
126.70
126.08
125.81
124.86
124.01
112.24
55.30
40.75
37.34
37.27
35.20
29.25
15.13
f1 (ppm)

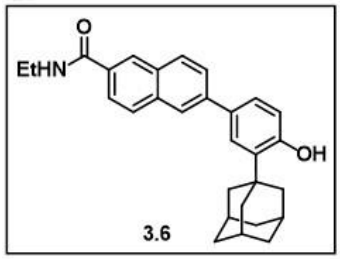
O
EtHN
OH
3.6

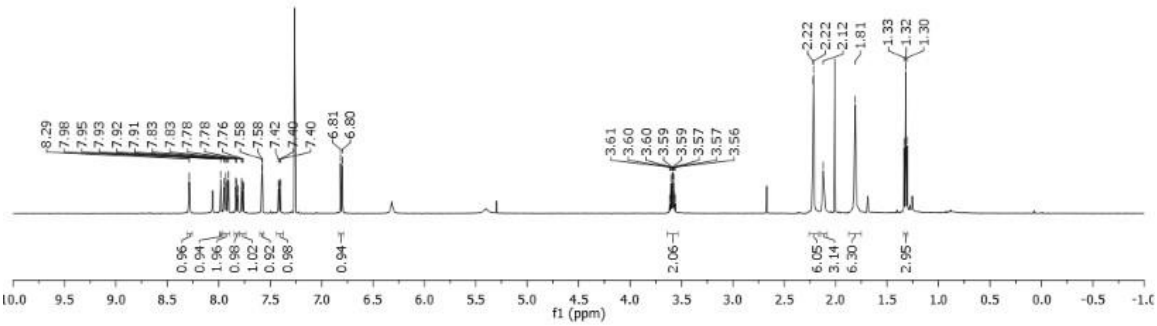
8.29
7.98
7.95
7.93
7.92
7.91
7.83
7.78
7.78
7.76
7.58
7.58
7.42
7.40
7.40
6.81
6.80
3.61
3.60
3.60
3.59
3.59
3.57
3.57
3.56
2.22
2.22
2.12
1.81
1.33
1.32
1.30
0.96
0.94
1.96
0.98
1.02
0.92
0.98
0.94
2.06
6.05
3.14
6.30
2.95
f1 (ppm)

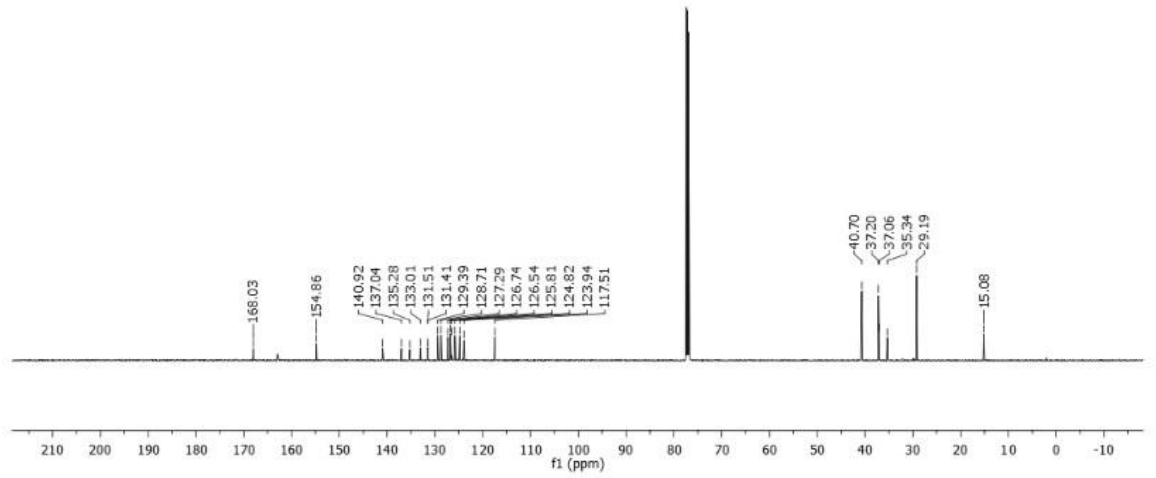
168.03
154.86
140.92
137.04
135.28
133.01
131.51
131.41
129.39
128.71
127.29
126.74
126.54
125.81
124.82
123.94
117.51
40.70
37.20
37.06
35.34
29.19
15.08
f1 (ppm)

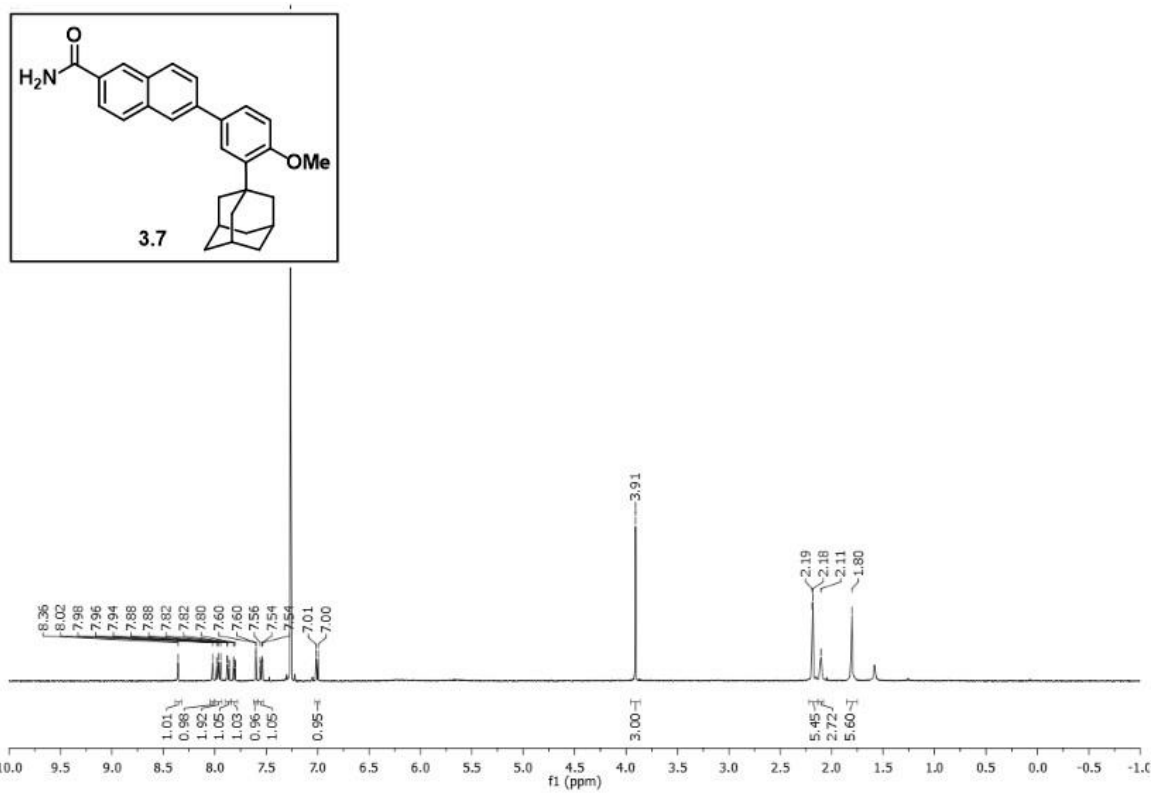
H2N
O
OMe
3.7
8.36
8.02
7.98
7.96
7.94
7.88
7.88
7.82
7.82
7.80
7.60
7.60
7.56
7.54
7.54
7.01
7.00
3.91
2.19
2.18
2.11
1.80
1.01
0.98
1.92
1.05
1.03
0.96
1.05
0.95
3.00
5.45
2.72
5.60
f1 (ppm)

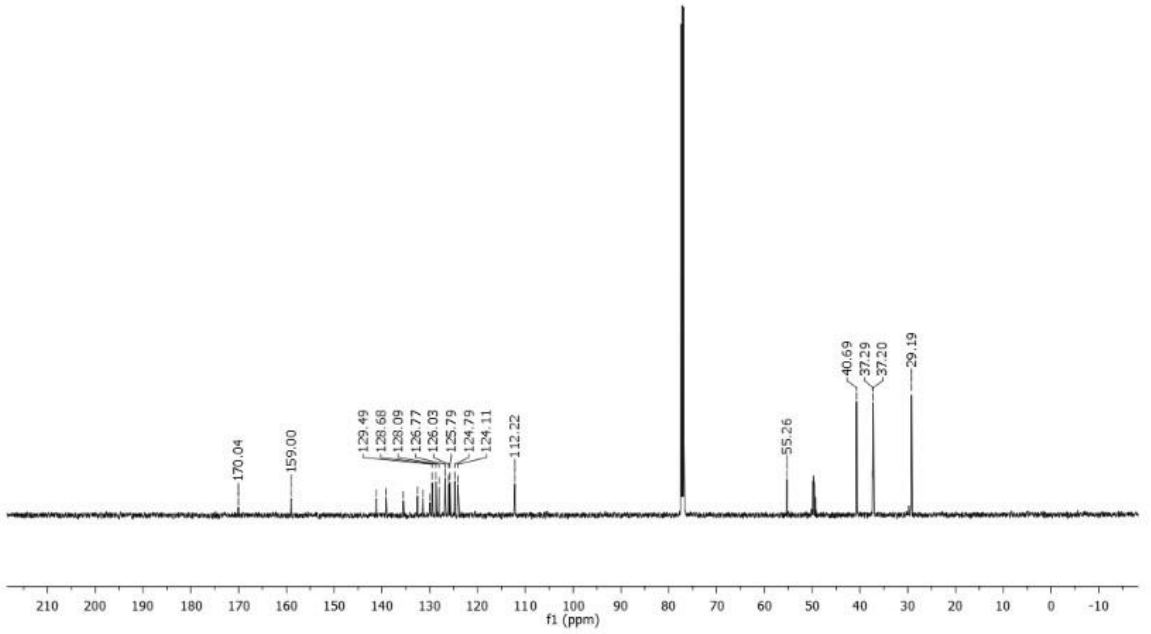
170.04
159.00
129.49
128.68
128.09
126.77
126.03
125.79
124.79
124.11
112.22
55.26
40.69
37.29
37.20
29.19
f1 (ppm)

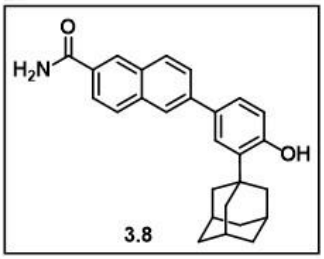
O
H2N
OH
3.8

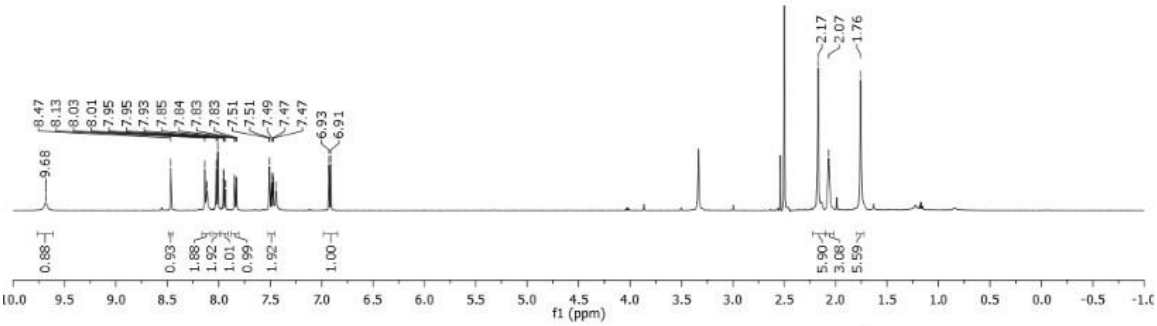
8.47
8.13
8.03
8.01
7.95
7.95
7.93
7.85
7.84
7.83
7.83
7.51
7.51
7.49
7.47
7.47
6.93
6.91
9.68
2.17
2.07
1.76
0.88
0.93
1.88
1.92
1.01
0.99
1.92
1.00
5.90
3.08
5.59
f1 (ppm)

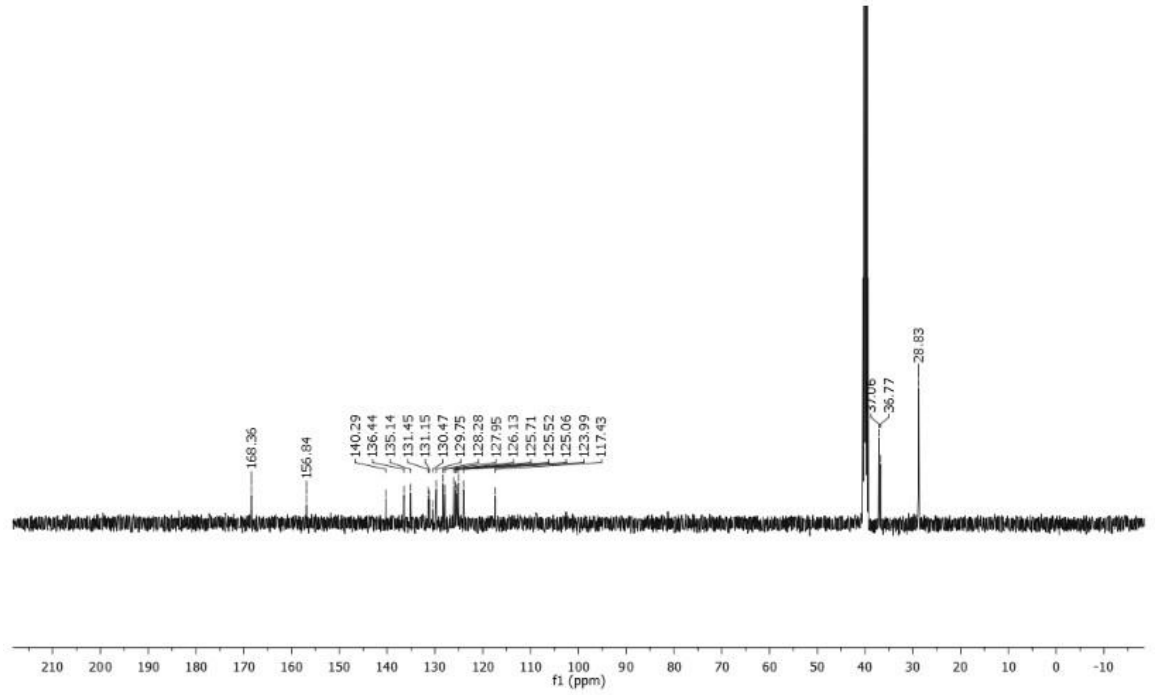
168.36
156.84
140.29
136.44
135.14
131.45
131.15
130.47
129.75
128.28
127.95
126.13
125.71
125.52
125.06
123.99
117.43
37.06
36.77
28.83
f1 (ppm)

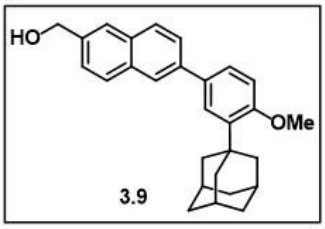
HO
OMe
3.9

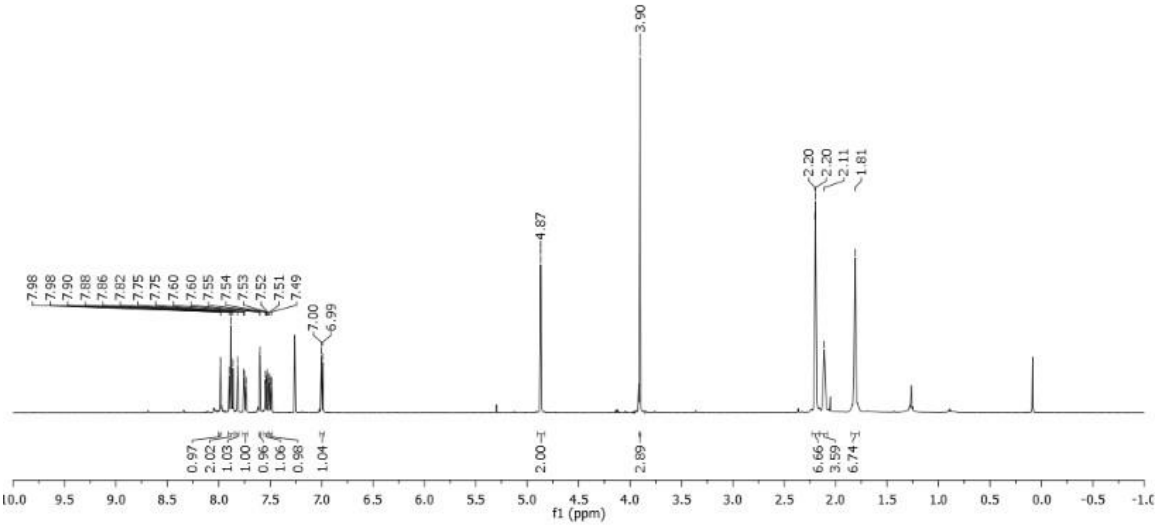
7.98
7.98
7.90
7.88
7.86
7.82
7.75
7.75
7.60
7.60
7.55
7.54
7.53
7.52
7.51
7.49
7.00
6.99
4.87
3.90
2.20
2.20
2.11
1.81
0.97
2.02
1.03
1.00
0.96
1.06
0.98
1.04
2.00
2.89
6.66
3.59
6.74
f1 (ppm)

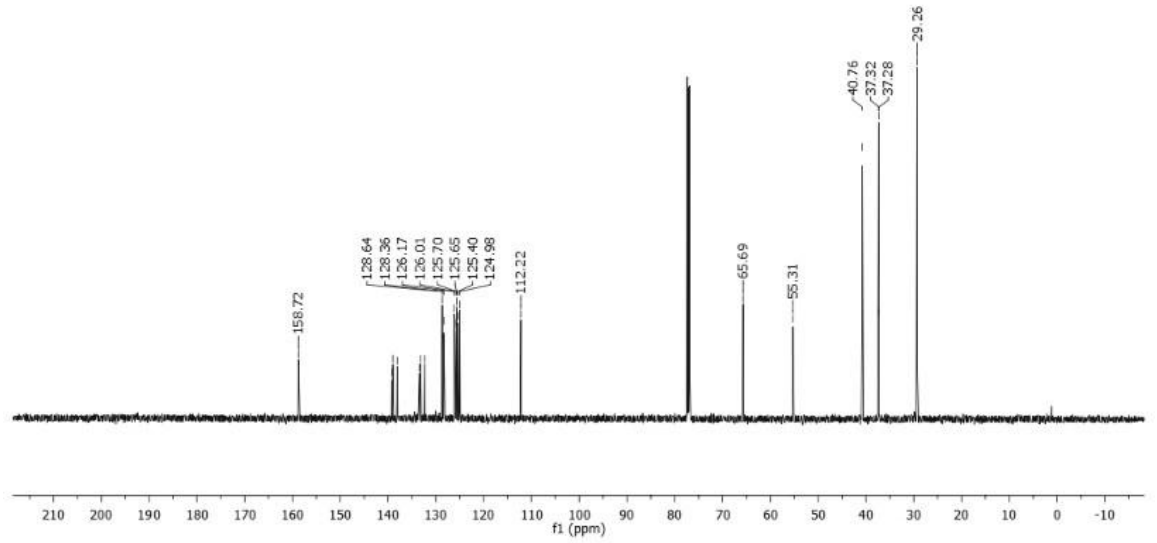
158.72
128.64
128.36
126.17
126.01
125.70
125.65
125.40
124.98
112.22
65.69
55.31
40.76
37.32
37.28
29.26
f1 (ppm)

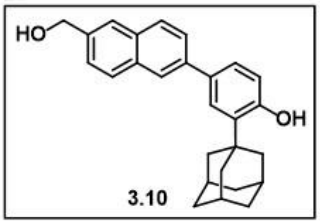
HO
OH
3.10

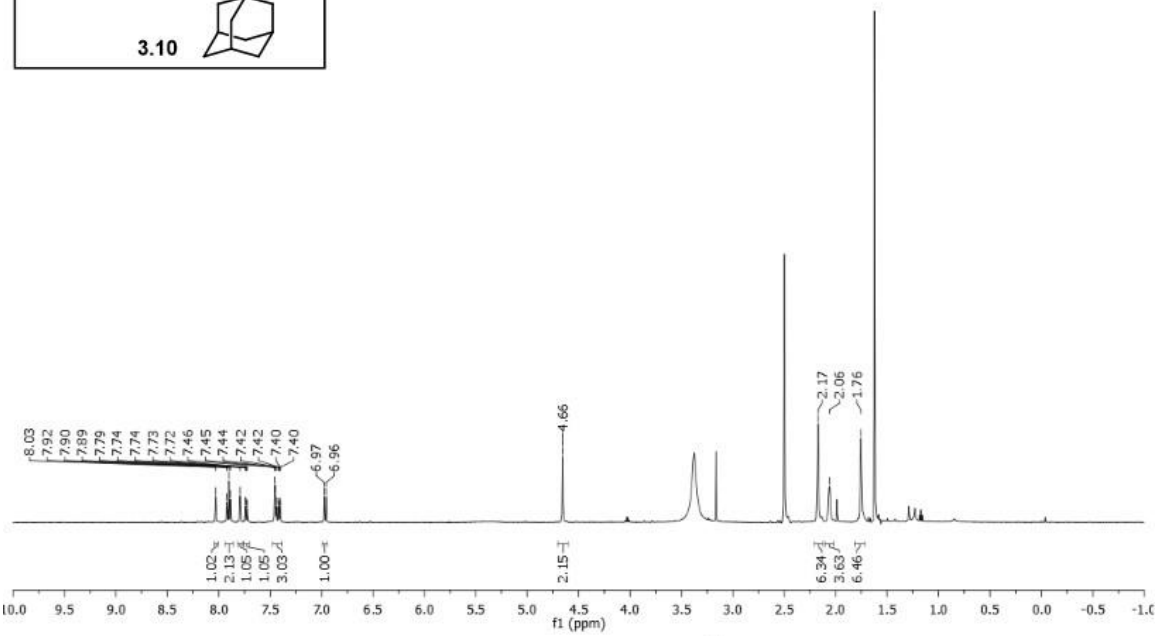
8.03
7.92
7.90
7.89
7.79
7.74
7.74
7.73
7.72
7.46
7.45
7.44
7.42
7.42
7.40
7.40
6.97
6.96
4.66
2.17
2.06
1.76
1.02
2.13
1.05
1.05
3.03
1.00
2.15
6.34
3.63
6.46
f1 (ppm)

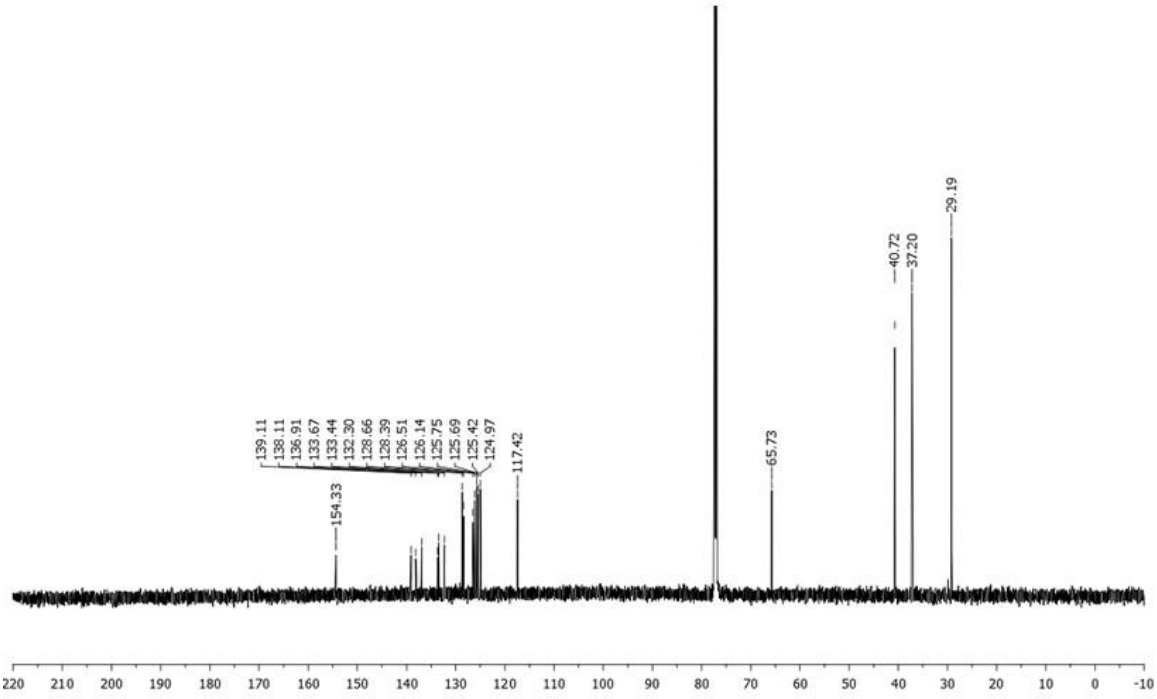
139.11
138.11
136.91
133.67
133.44
132.30
128.66
128.39
126.51
126.14
125.75
125.69
125.42
124.97
117.42
154.33
65.73
40.72
37.20
29.19

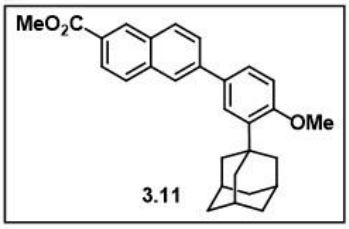
MeO2C
OMe
3.11

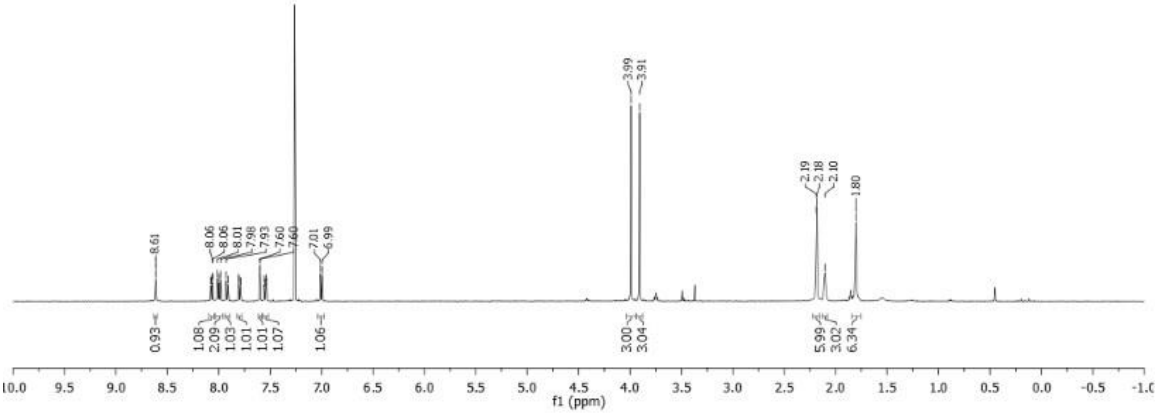
8.61
8.06
8.06
8.01
7.98
7.93
7.60
7.60
7.01
6.99
3.99
3.91
2.19
2.18
2.10
1.80
0.93
1.08
2.09
1.03
1.01
1.01
1.07
1.06
3.00
3.04
5.99
3.02
6.34
f1 (ppm)

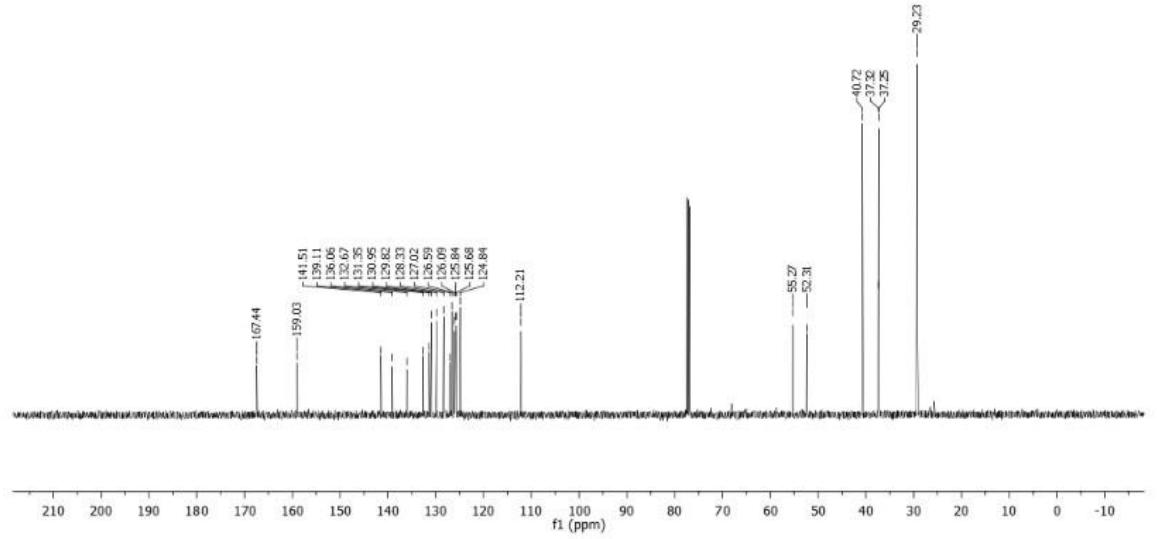
167.44
159.03
141.51
139.11
136.06
132.67
131.35
130.95
129.82
128.33
127.02
126.59
126.09
125.84
125.68
124.84
112.21
55.27
52.31
40.72
37.32
37.25
29.23
f1 (ppm)

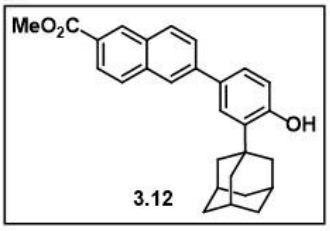
MeO2C
OH

3.12

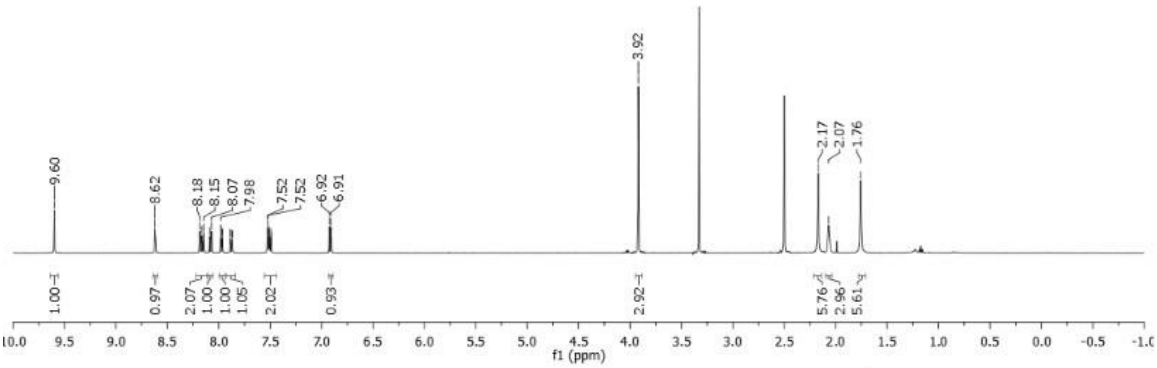
9.60
8.62
8.18
8.15
8.07
7.98
7.52
7.52
6.92
6.91
3.92
2.17
2.07
1.76
1.00
0.97
2.07
1.00
1.00
1.05
2.02
0.93
2.92
5.76
2.96
5.61
f1 (ppm)

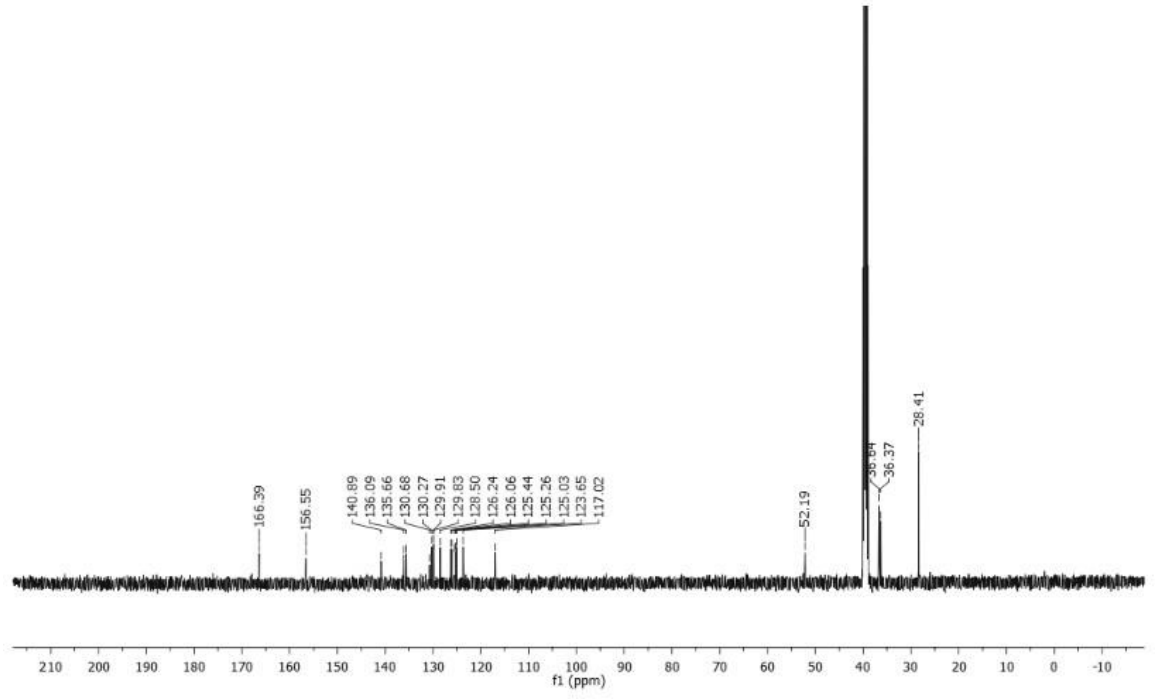
166.39
156.55
140.89
136.09
135.66
130.68
130.27
129.91
129.83
128.50
126.24
126.06
125.44
125.26
125.03
123.65
117.02
52.19
38.64
36.37
28.41
f1 (ppm)

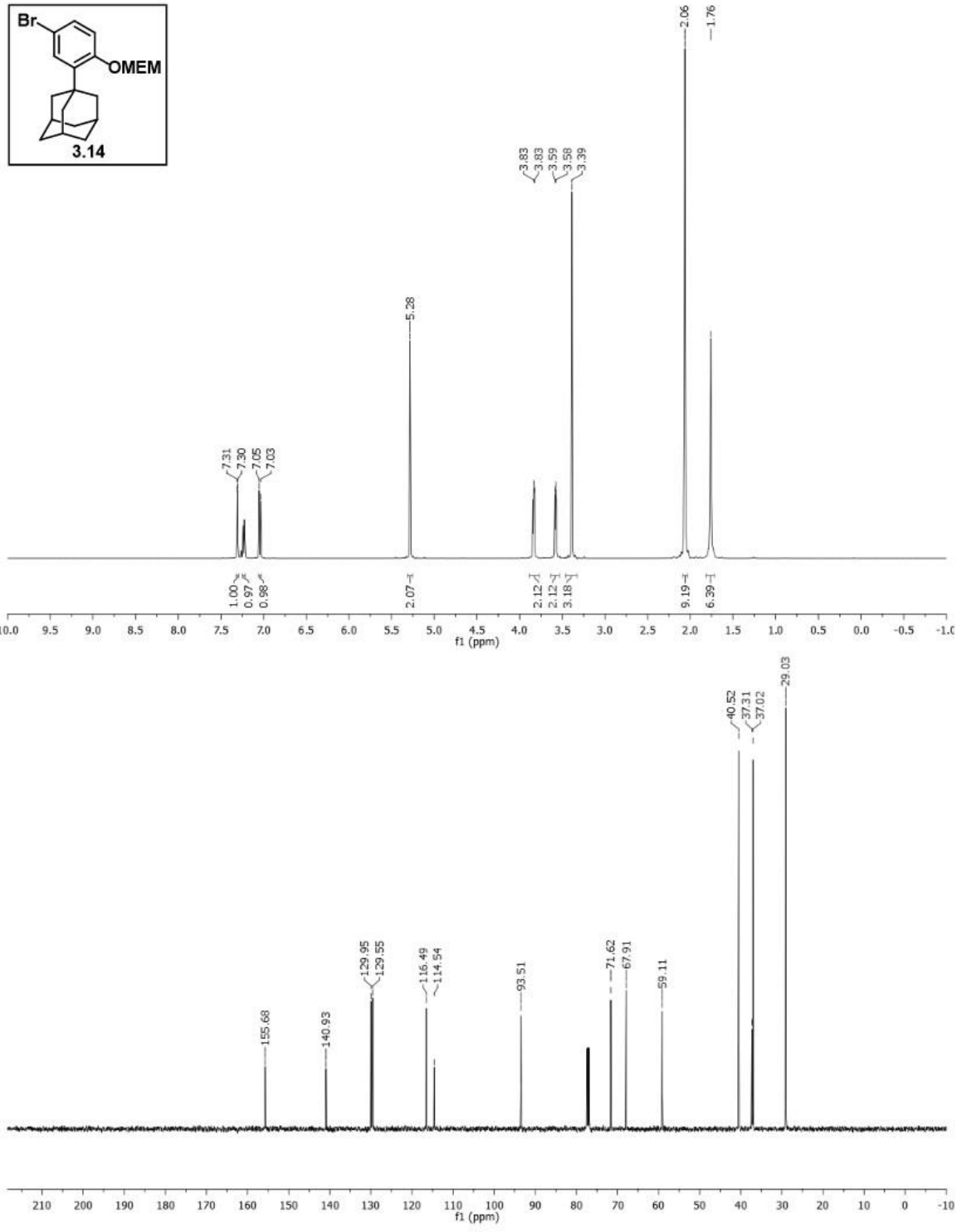
Br
OMEM
3.14
2.06
1.76
3.83
3.83
3.59
3.58
3.39
5.28
7.31
7.30
7.05
7.03
1.00
0.97
0.98
2.07
2.12
2.12
3.18
9.19
6.39
f1 (ppm)
40.52
37.31
37.02
29.03
155.68
140.93
129.95
129.55
116.49
114.54
93.51
71.62
67.91
59.11
f1 (ppm)

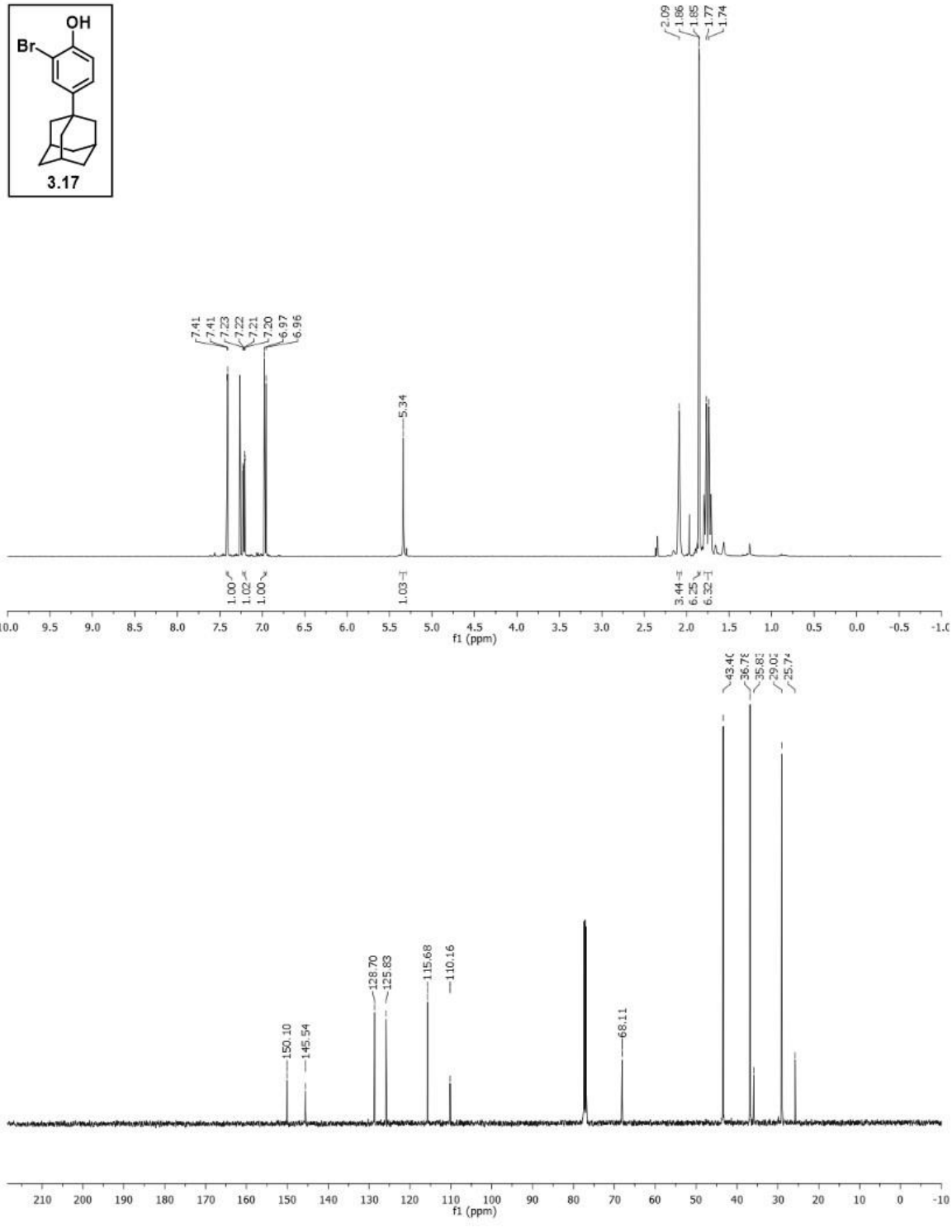
OH
Br
3.17
7.41
7.41
7.23
7.22
7.21
7.20
6.97
6.96
5.34
2.09
1.86
1.85
1.77
1.74
1.00
1.02
1.00
1.03
3.44
6.25
6.32
f1 (ppm)
150.10
145.54
128.70
125.83
115.68
110.16
68.11
f1 (ppm)

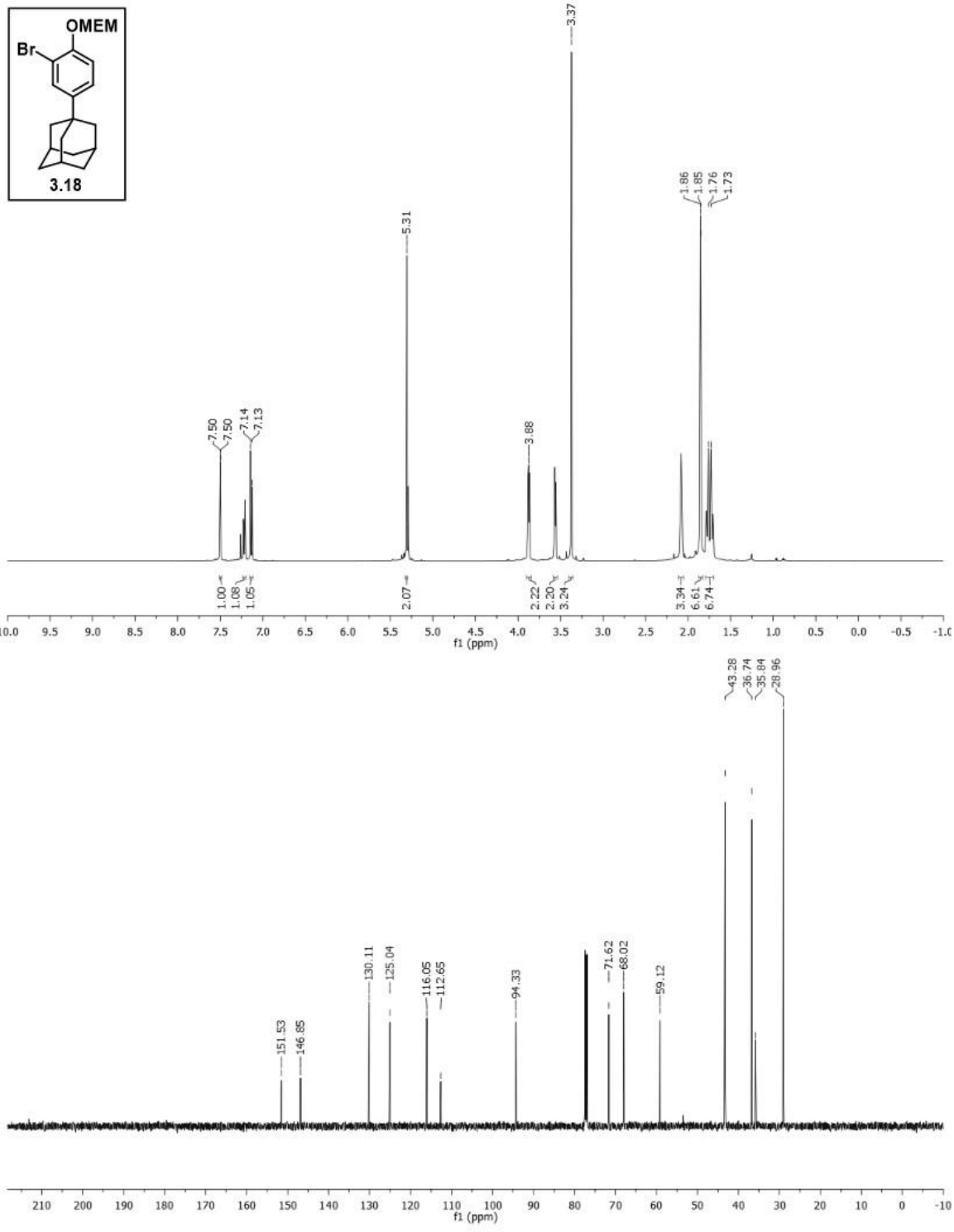
OMEM
Br
3.18
7.50
7.50
7.14
7.13
5.31
3.88
3.37
1.86
1.85
1.76
1.73
1.00
1.08
1.05
2.07
2.22
2.20
3.24
3.34
6.61
6.74
f1 (ppm)
43.28
36.74
35.84
28.96
151.53
146.85
130.11
125.04
116.05
112.65
94.33
71.62
68.02
59.12
f1 (ppm)

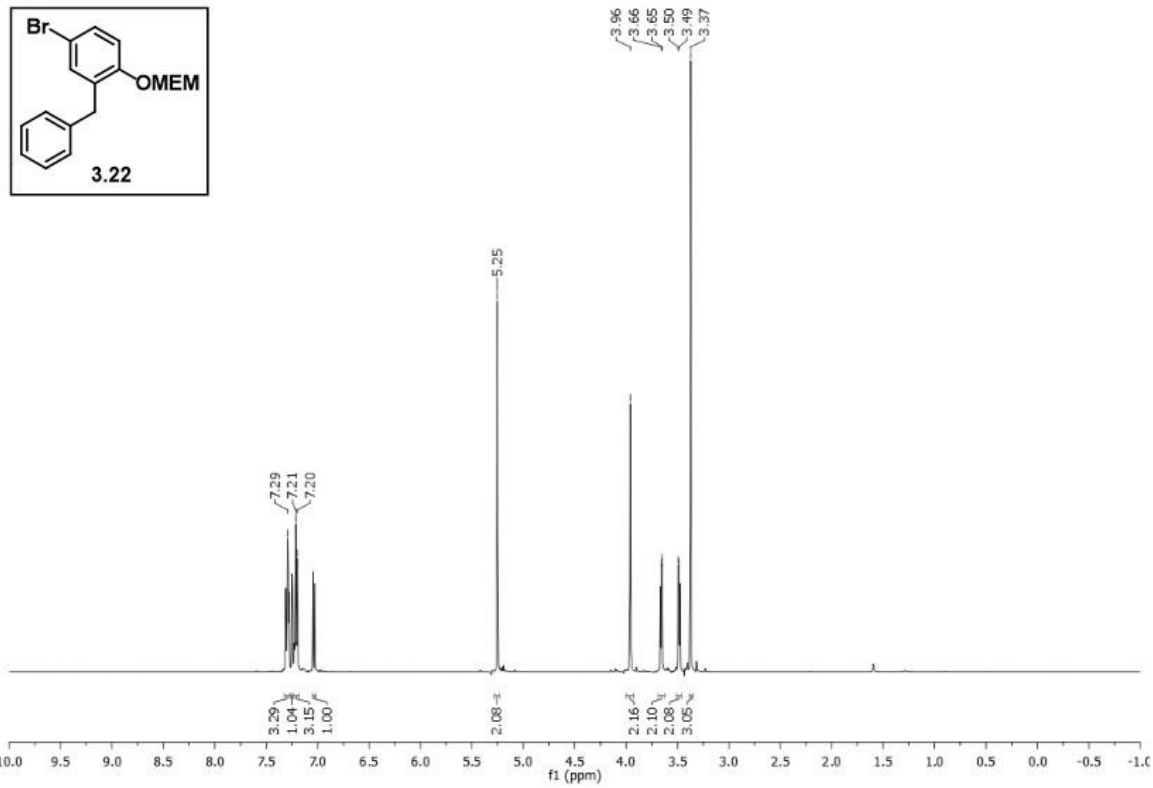
Br
OMEM
3.22
3.96
3.66
3.65
3.50
3.49
3.37
5.25
7.29
7.21
7.20
3.29
1.04
3.15
1.00
2.08
2.16
2.10
2.08
3.05
f1 (ppm)

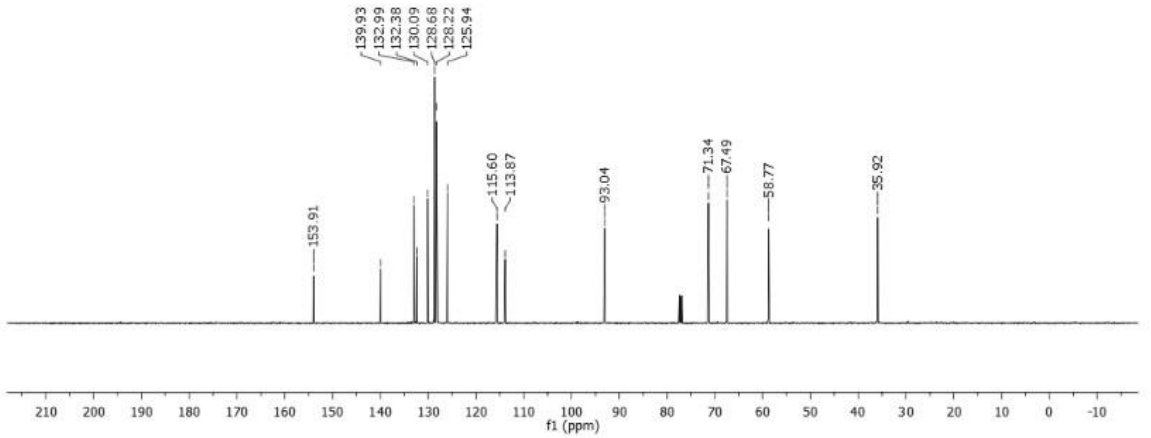
139.93
132.99
132.38
130.09
128.68
128.22
125.94
153.91
115.60
113.87
93.04
71.34
67.49
58.77
35.92
f1 (ppm)

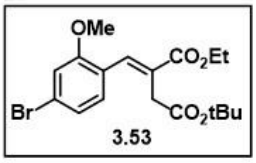
OMe
CO2Et
Br
CO2tBu
3.53

1.46
1.35
1.33
1.32
3.84
3.34
3.34
4.29
4.28
4.26
4.25
7.83
7.16
7.16
7.15
7.14
7.11
7.11
7.10
7.09
7.04
7.03
0.95
0.96
0.96
1.02
2.00
2.84
1.90
8.97
3.09
f1 (ppm)

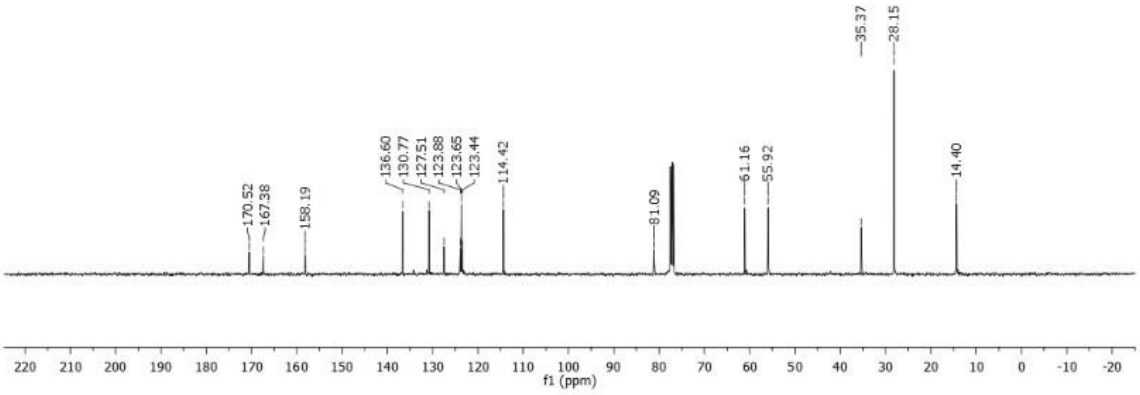
35.37
28.15
136.60
130.77
127.51
123.88
123.65
123.44
114.42
81.09
61.16
55.92
14.40
170.52
167.38
158.19
f1 (ppm)

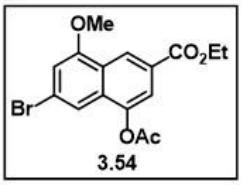
OMe
CO2Et
Br
OAc

3.54

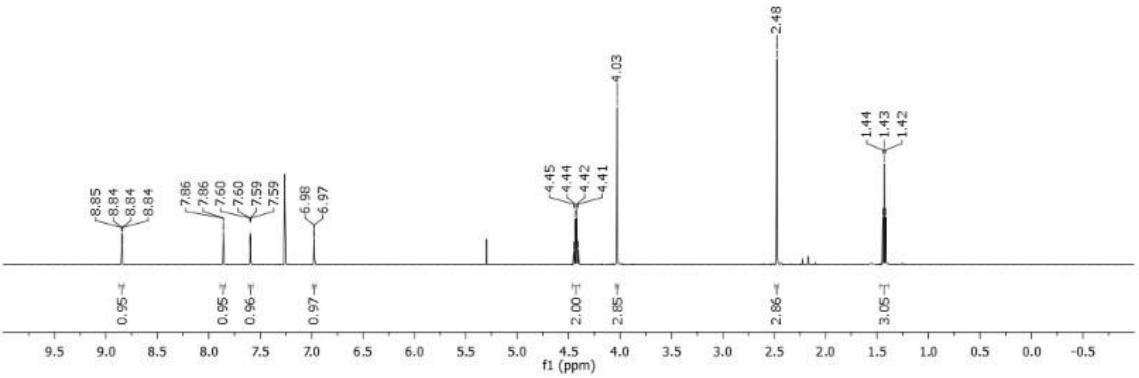
8.85
8.84
8.84
8.84
7.86
7.86
7.60
7.60
7.59
7.59
7.59
6.98
6.97
4.45
4.44
4.42
4.41
4.03
2.48
1.44
1.43
1.42
0.95
0.95
0.96
0.97
2.00
2.85
2.86
3.05
f1 (ppm)

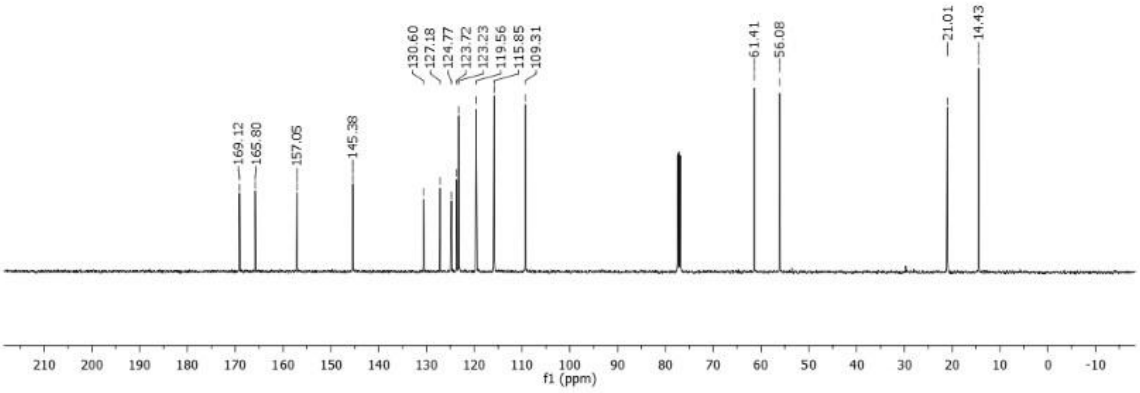
169.12
165.80
157.05
145.38
130.60
127.18
124.77
123.72
123.23
119.56
115.85
109.31
61.41
56.08
21.01
14.43
f1 (ppm)

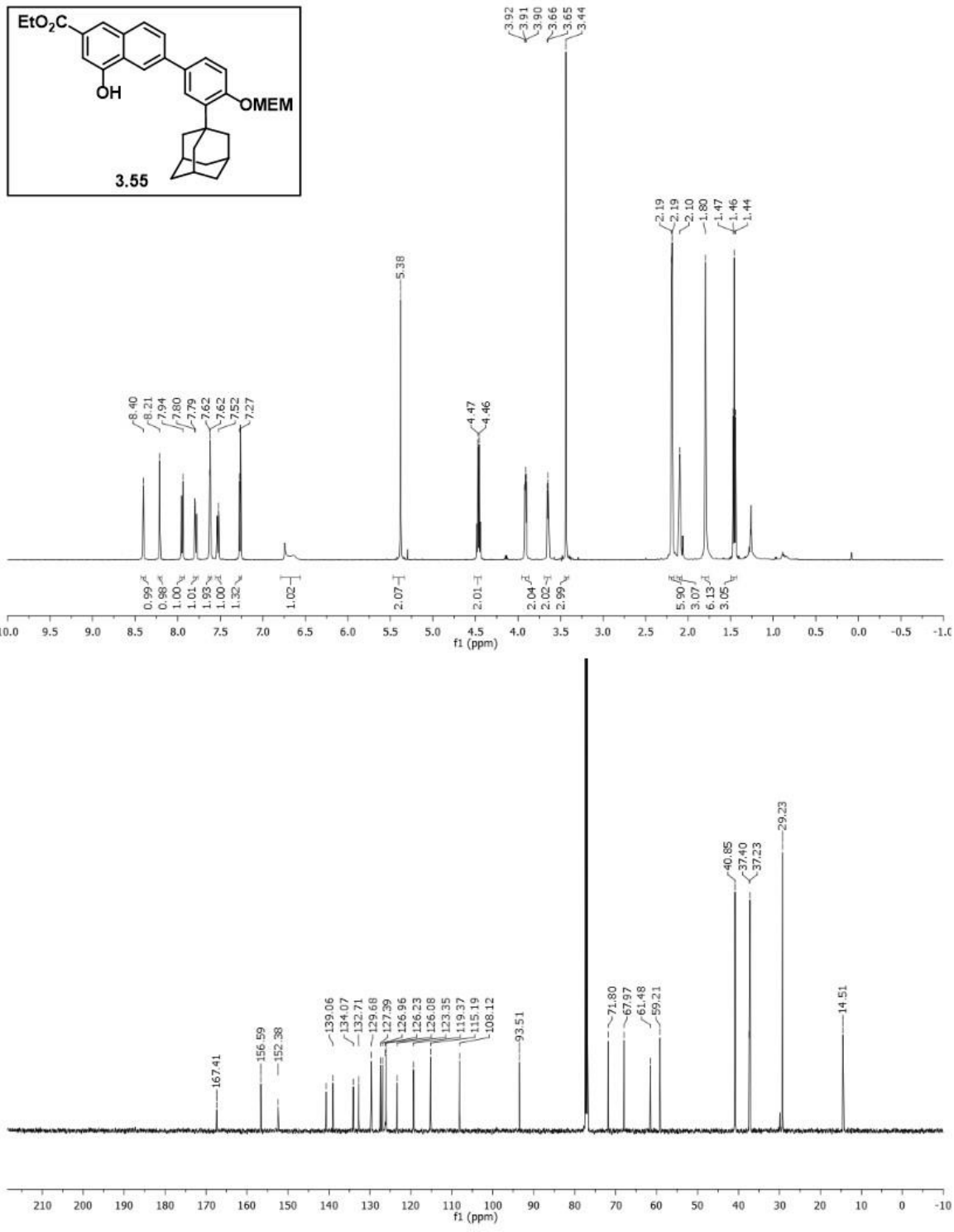
EtO2C
OH
OMEM
3.55
f1 (ppm)
f1 (ppm)

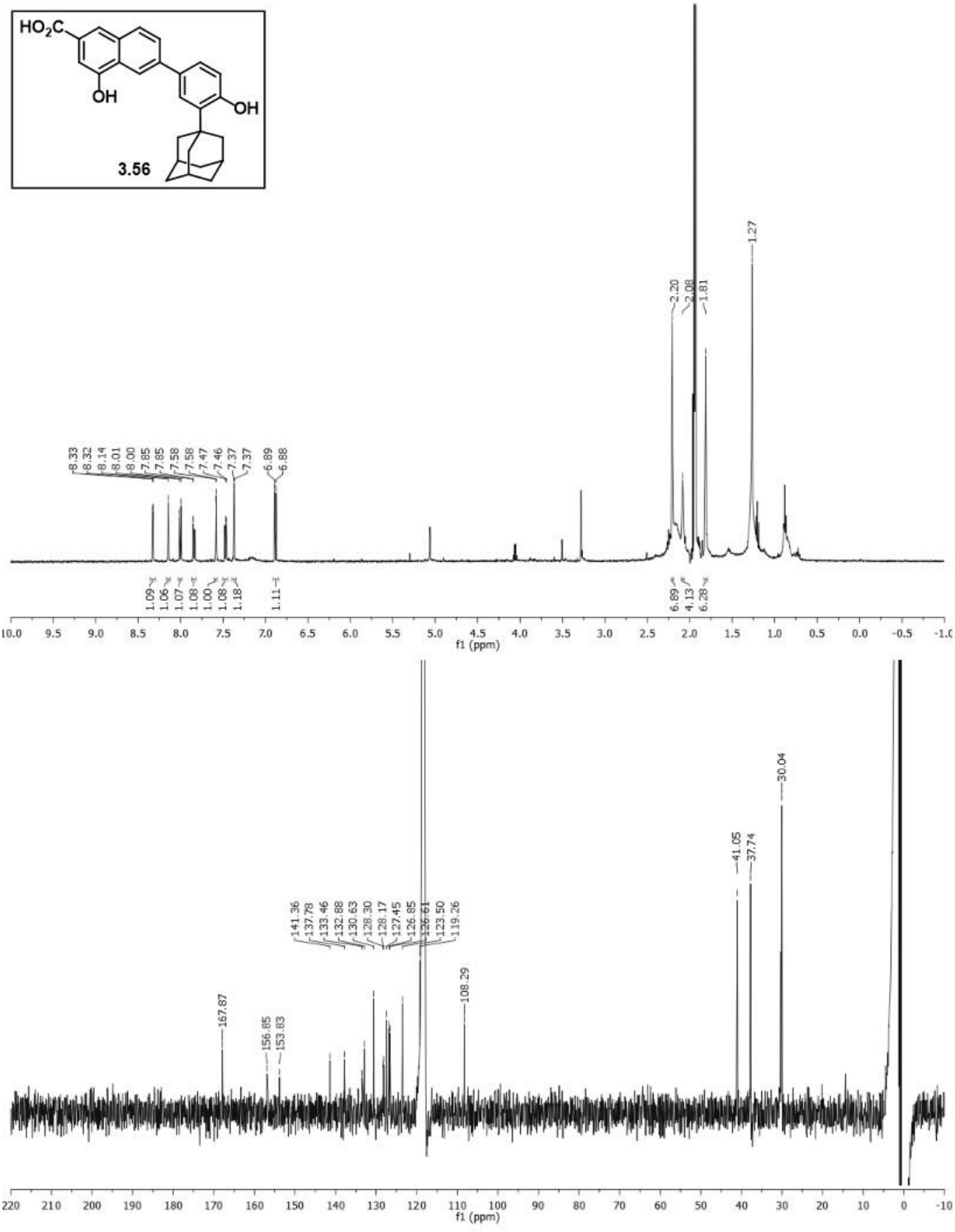
HO2C
OH
OH
3.56
8.33
8.32
8.14
8.01
8.00
7.85
7.85
7.58
7.58
7.47
7.46
7.37
7.37
6.89
6.88
2.20
2.08
1.81
1.27
1.09
1.06
1.07
1.08
1.00
1.08
1.18
1.11
6.89
4.13
6.28
f1 (ppm)
141.36
137.78
133.46
132.88
130.63
128.30
128.17
127.45
126.85
126.61
123.50
119.26
108.29
167.87
156.85
153.83
41.05
37.74
30.04
f1 (ppm)

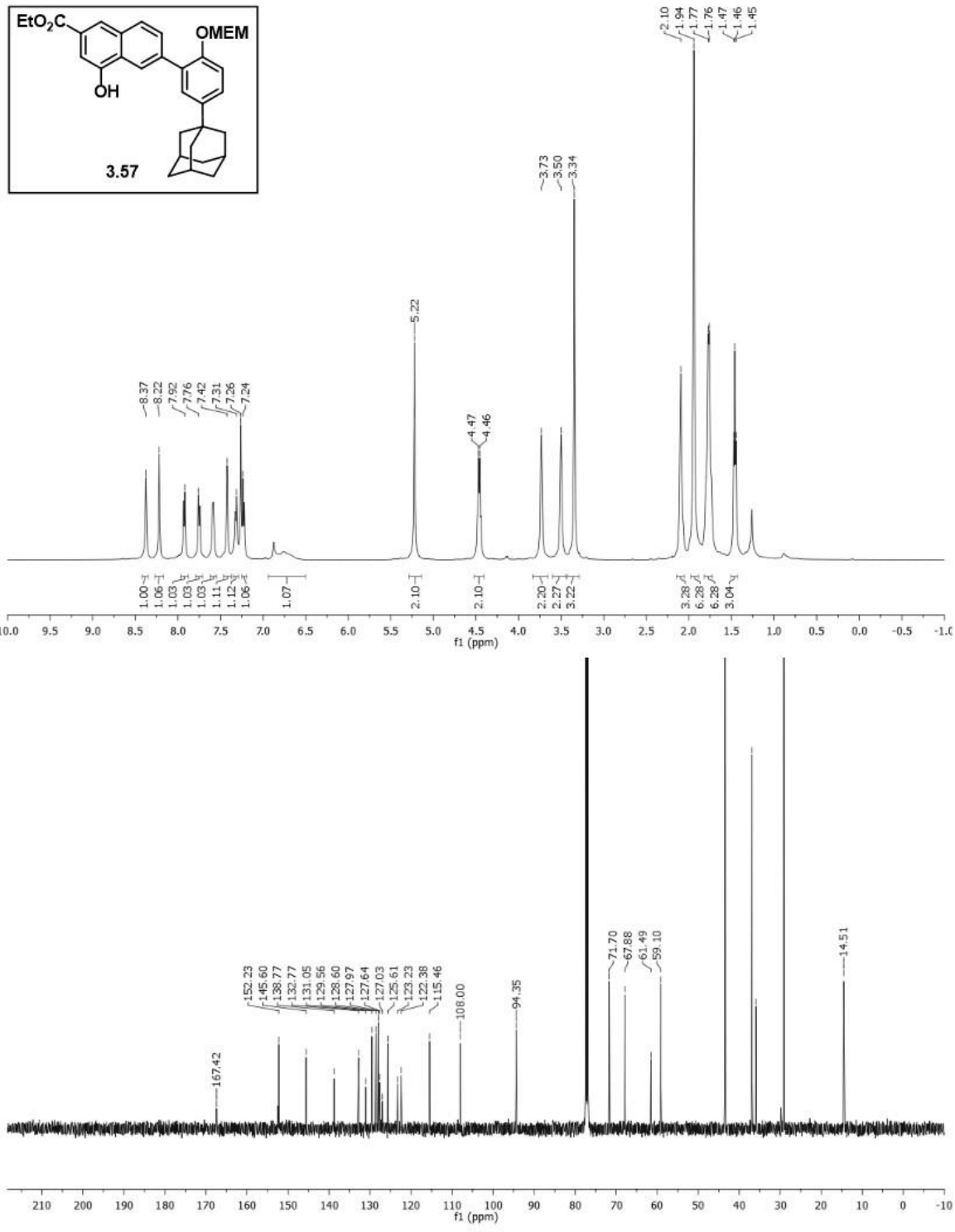
EtO2C
OMEM
OH
3.57
8.37
8.22
7.92
7.76
7.42
7.31
7.26
7.24
5.22
4.47
4.46
3.73
3.50
3.34
2.10
1.94
1.77
1.76
1.47
1.46
1.45
1.00
1.06
1.03
1.03
1.03
1.11
1.12
1.06
1.07
2.10
2.10
2.20
2.27
3.22
3.28
6.28
6.28
3.04
f1 (ppm)
152.23
145.60
138.77
132.77
131.05
129.56
128.60
127.97
127.64
127.03
125.61
123.23
122.38
115.46
108.00
94.35
71.70
67.88
61.49
59.10
14.51
167.42
f1 (ppm)

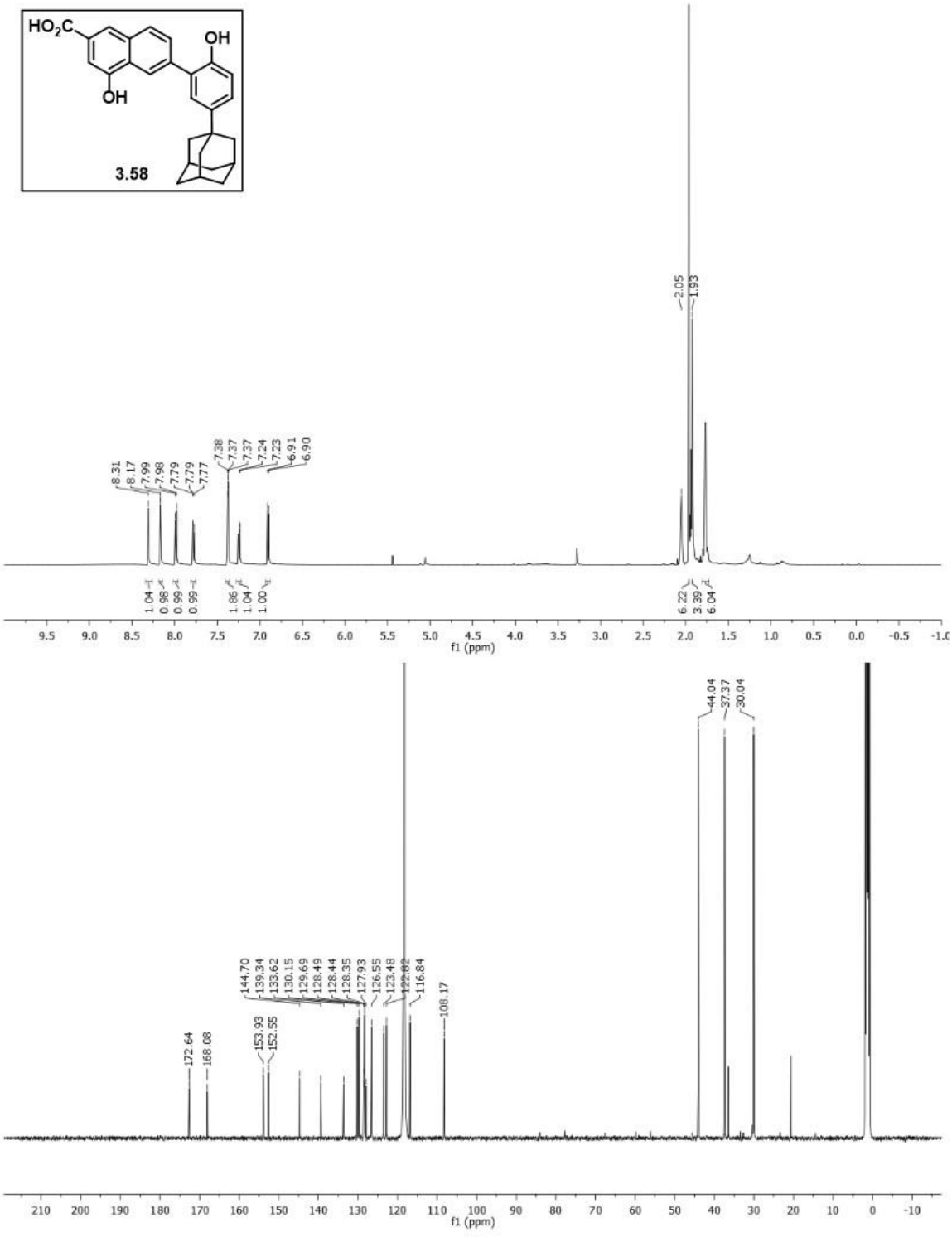
HO2C
OH
OH
3.58
8.31
8.17
7.99
7.98
7.79
7.79
7.77
7.38
7.37
7.37
7.24
7.23
6.91
6.90
2.05
1.93
1.04
0.98
0.99
0.99
1.86
1.04
1.00
6.22
3.39
6.04
f1 (ppm)
172.64
168.08
153.93
152.55
144.70
139.34
133.62
130.15
129.69
128.49
128.44
128.35
127.93
126.55
123.48
122.82
116.84
108.17
44.04
37.37
30.04
f1 (ppm)

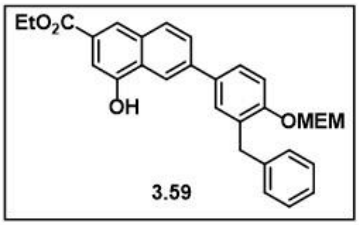
EtO2C
OH
OMEM

3.59

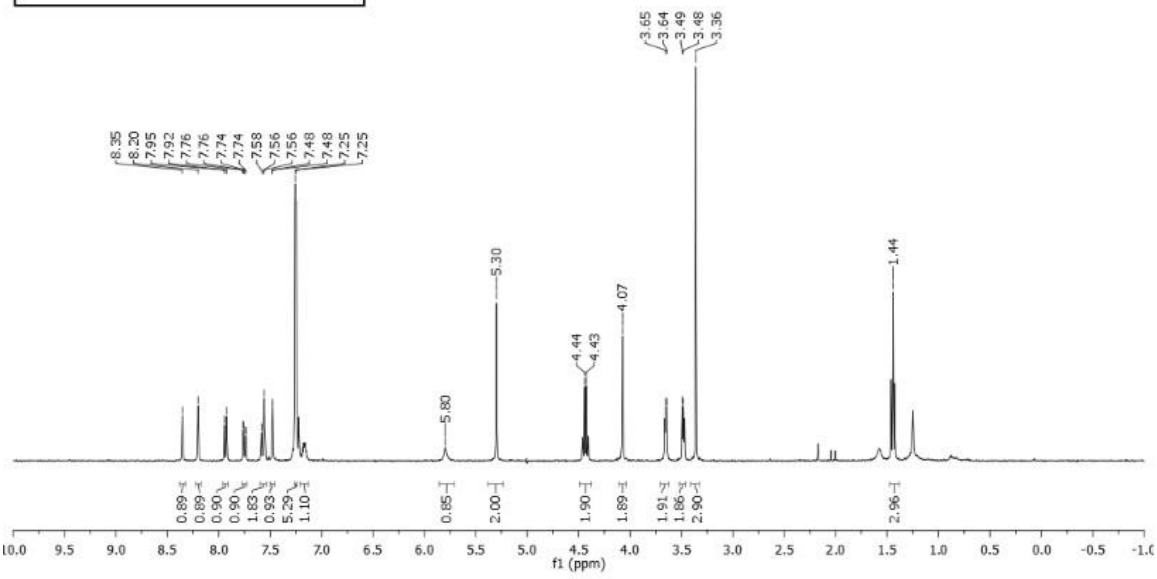
8.35
8.20
7.95
7.92
7.76
7.76
7.74
7.74
7.58
7.56
7.56
7.48
7.48
7.25
7.25
5.80
5.30
4.44
4.43
4.07
3.65
3.64
3.49
3.48
3.36
1.44
0.89
0.89
0.90
0.90
1.83
0.93
5.29
1.10
0.85
2.00
1.90
1.89
1.91
1.86
2.90
2.96
f1 (ppm)

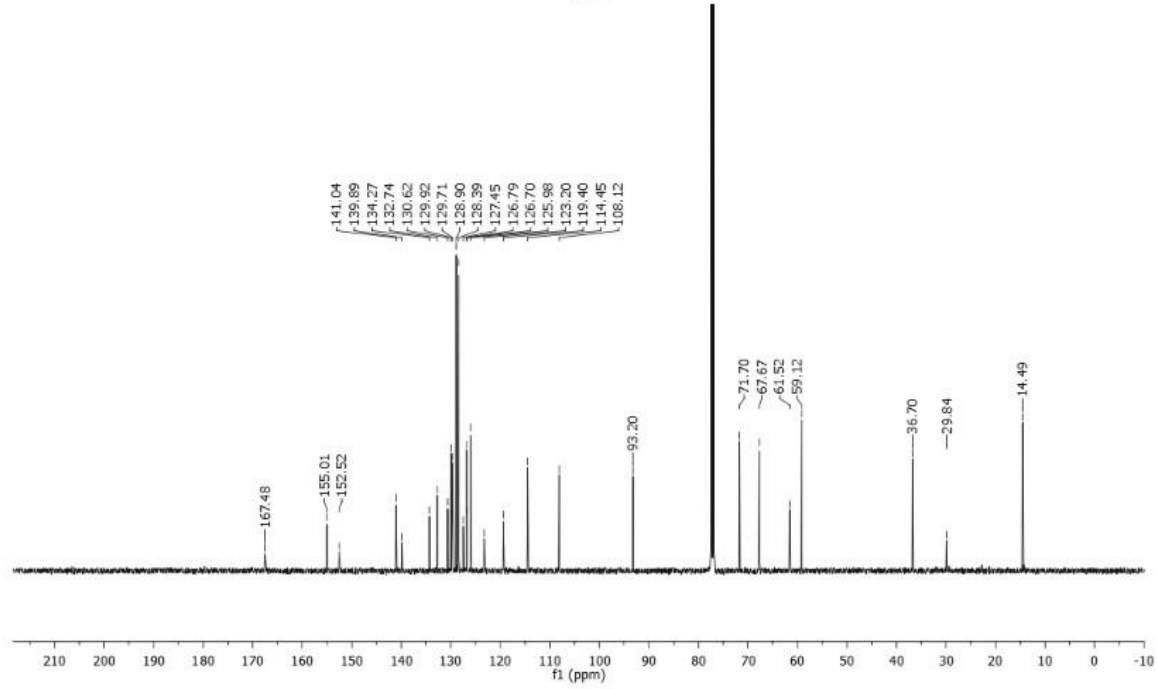
141.04
139.89
134.27
132.74
130.62
129.92
129.71
128.90
128.39
127.45
126.79
126.70
125.98
123.20
119.40
114.45
108.12
167.48
155.01
152.52
93.20
71.70
67.67
61.52
59.12
36.70
29.84
14.49
f1 (ppm)

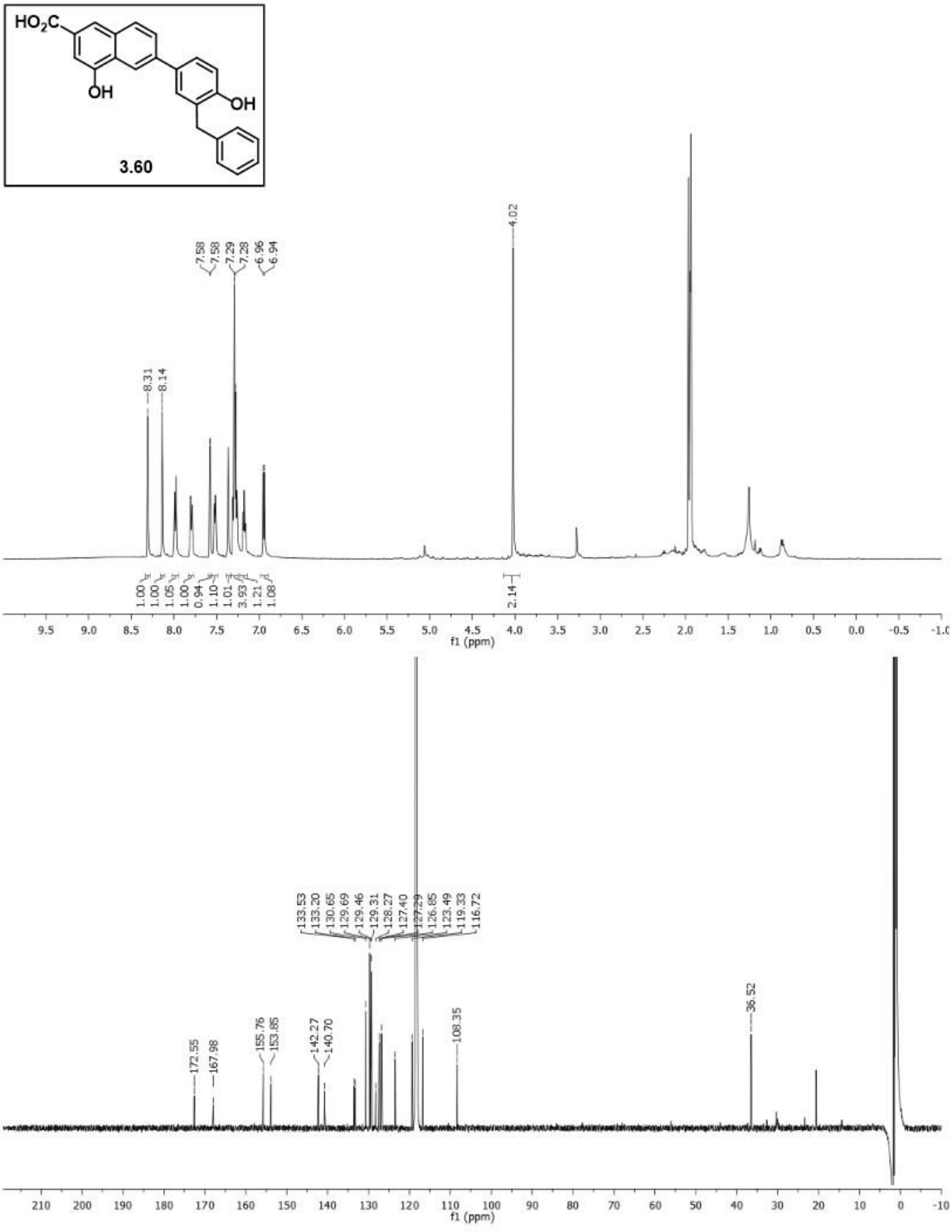
HO2C
OH
OH
3.60
8.31
8.14
7.58
7.58
7.29
7.28
6.96
6.94
4.02
1.00
1.00
1.05
1.00
0.94
1.10
1.01
3.93
1.21
1.08
2.14
f1 (ppm)
133.53
133.20
130.65
129.69
129.46
129.31
128.27
127.40
127.29
126.85
123.49
119.33
116.72
172.55
167.98
155.76
153.85
142.27
140.70
108.35
36.52
f1 (ppm)

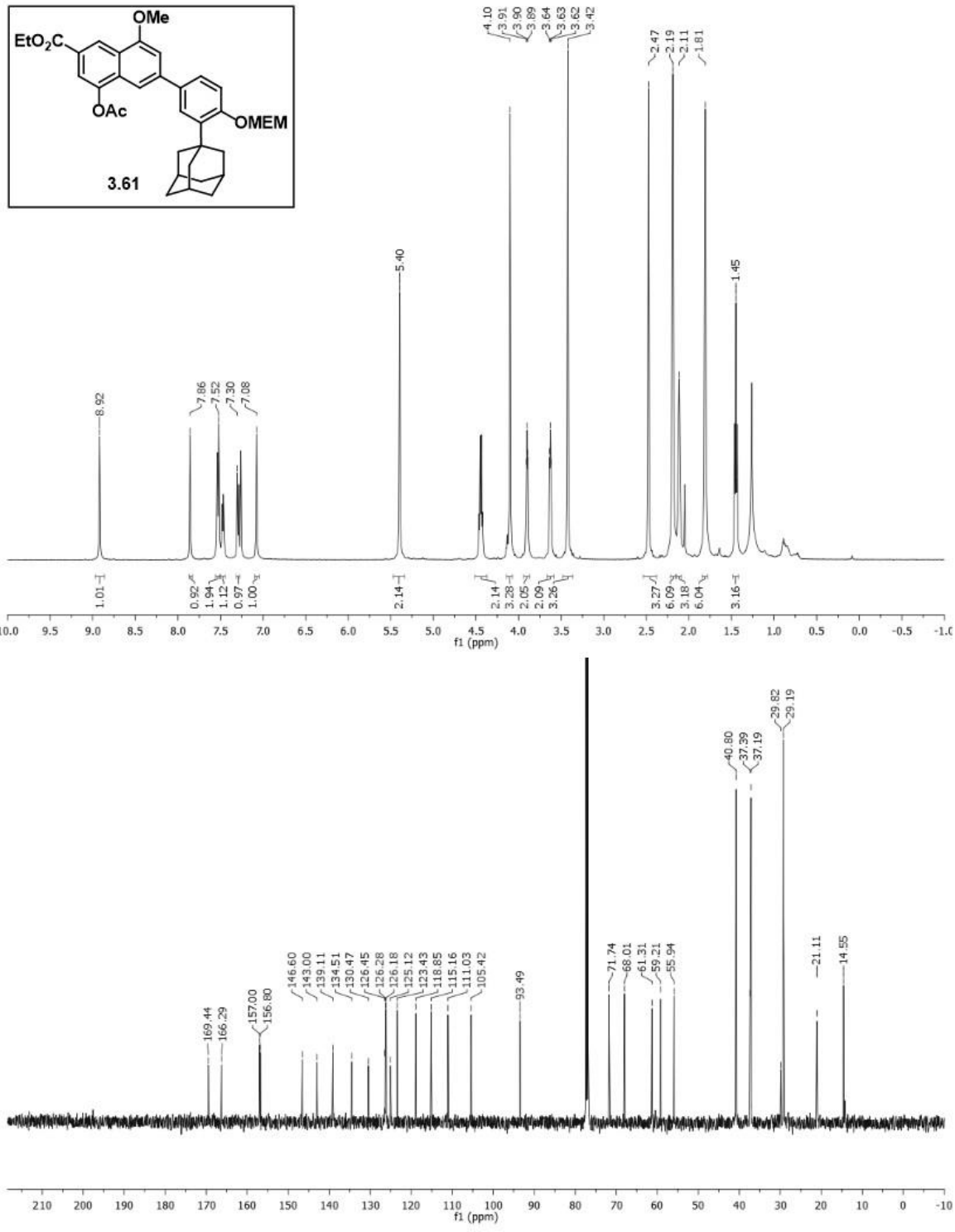
OMe
EtO2C
OAc
OMEM
3.61
f1 (ppm)
f1 (ppm)

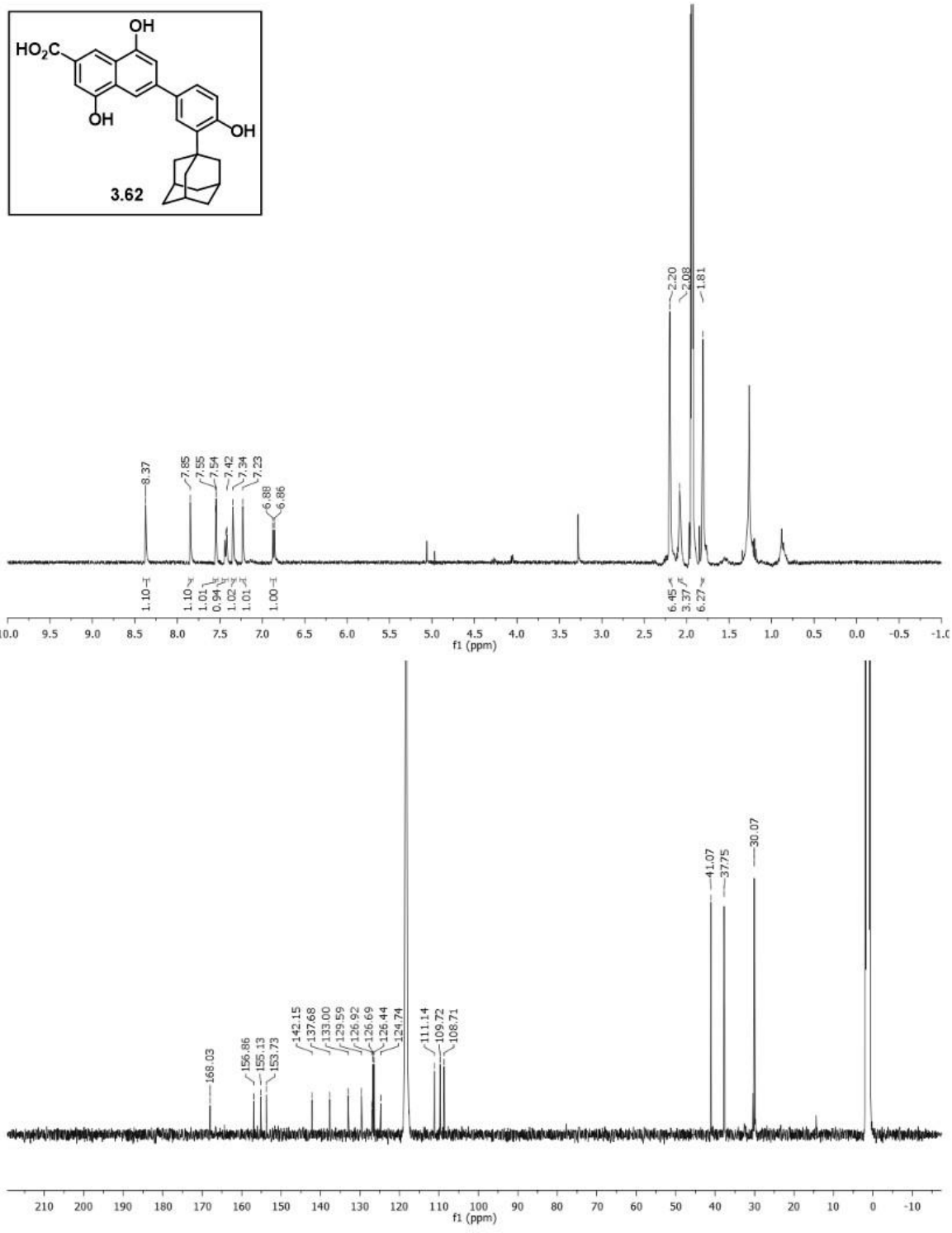
OH
HO2C
OH
OH
3.62
8.37
7.85
7.55
7.54
7.42
7.34
7.23
6.88
6.86
2.20
2.08
1.81
1.10
1.10
1.01
0.94
1.02
1.01
1.00
6.45
3.37
6.27
f1 (ppm)
168.03
156.86
155.13
153.73
142.15
137.68
133.00
129.59
126.92
126.69
126.44
124.74
111.14
109.72
108.71
41.07
37.75
30.07
f1 (ppm)

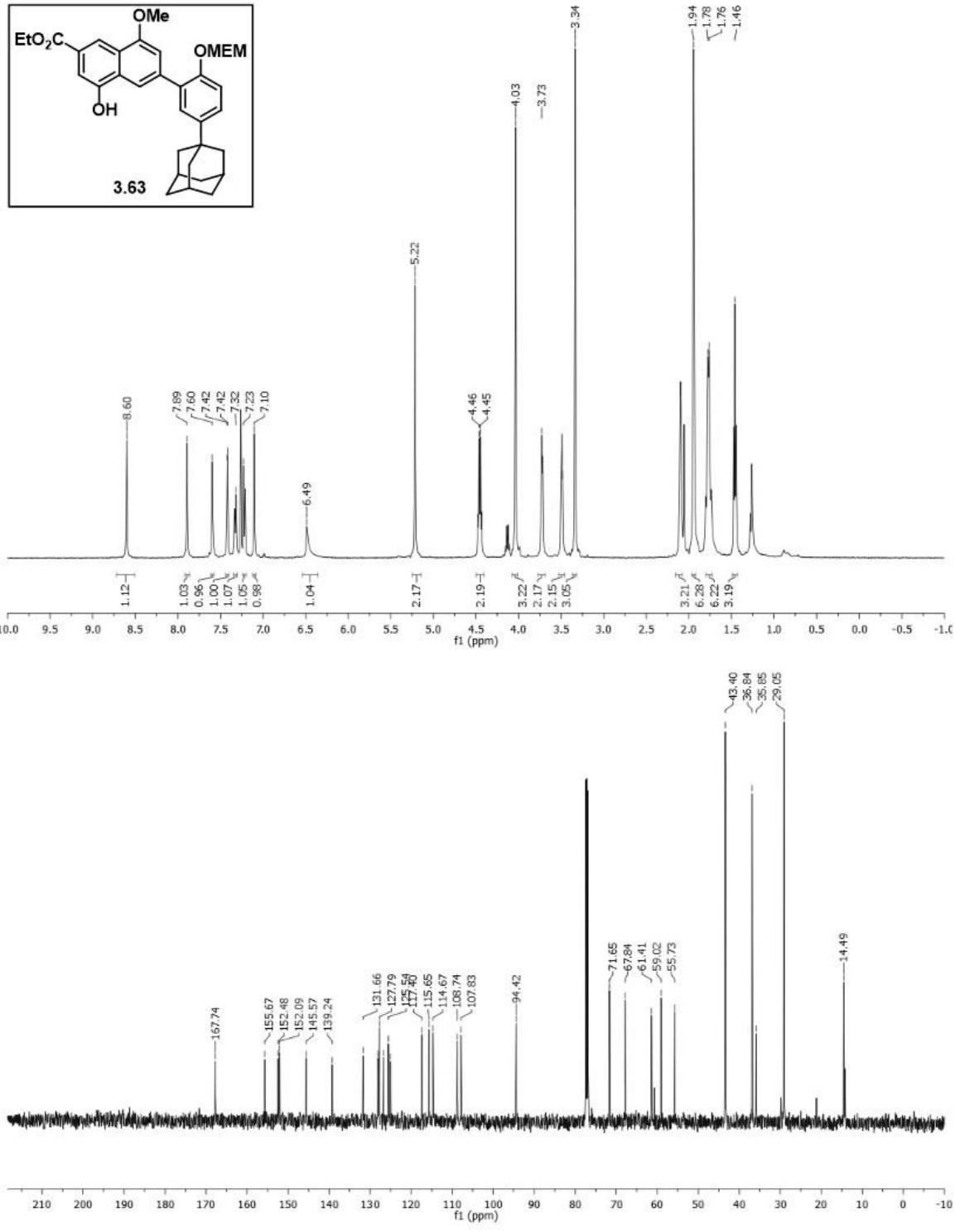
OMe
EtO2C
OMEM
OH
3.63
8.60
7.89
7.60
7.42
7.42
7.32
7.23
7.10
6.49
5.22
4.46
4.45
4.03
3.73
3.34
1.94
1.78
1.76
1.46
1.12
1.03
0.96
1.00
1.07
1.05
0.98
1.04
2.17
2.19
3.22
2.17
2.15
3.05
3.21
6.28
6.22
3.19
f1 (ppm)
167.74
155.67
152.48
152.09
145.57
139.24
131.66
127.79
125.54
117.40
115.65
114.67
108.74
107.83
94.42
71.65
67.84
61.41
59.02
55.73
43.40
36.84
35.85
29.05
14.49
f1 (ppm)

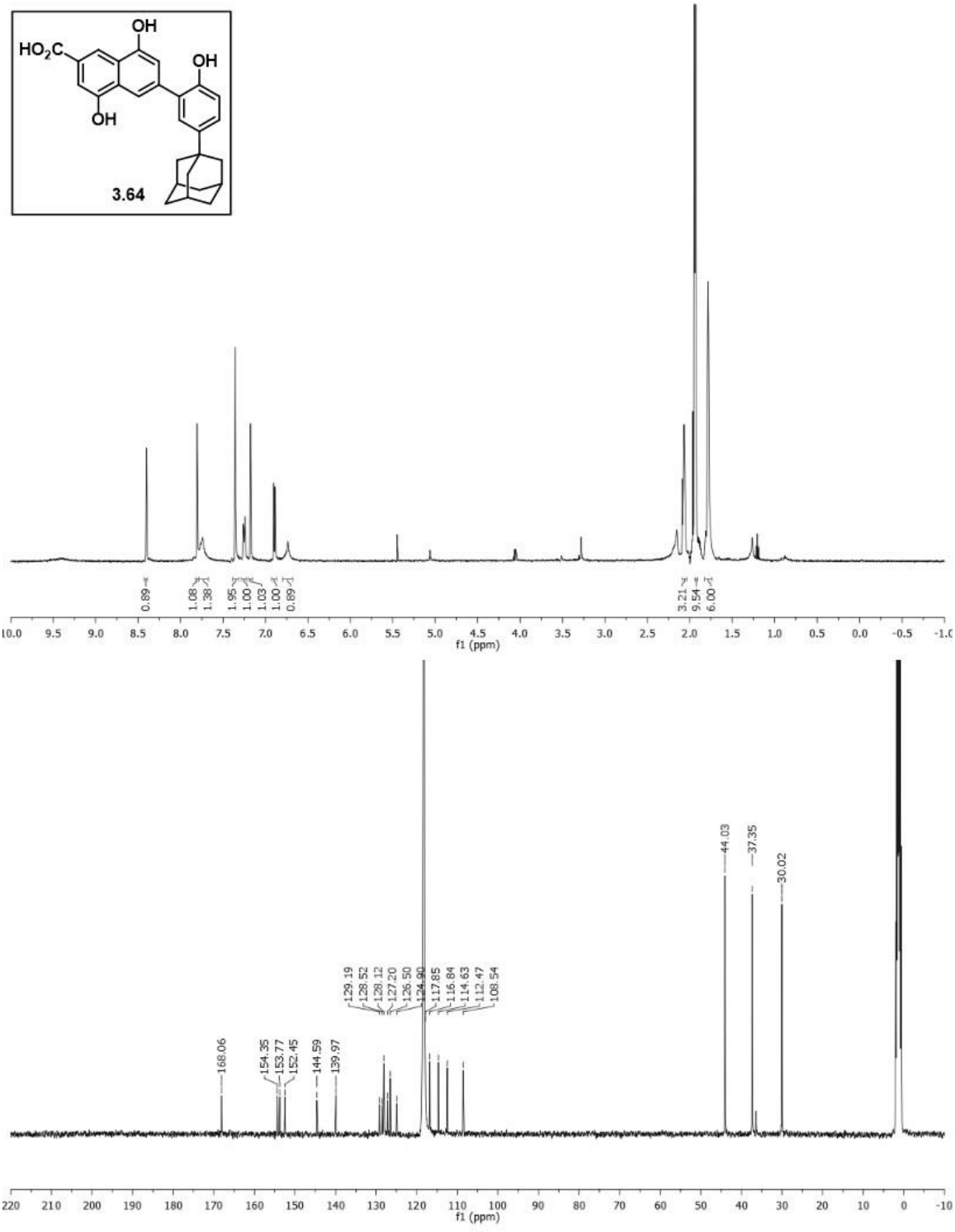
OH
HO2C
OH
OH
3.64
0.89
1.08
1.38
1.95
1.00
1.03
1.00
0.89
3.21
9.54
6.00
f1 (ppm)
168.06
154.35
153.77
152.45
144.59
139.97
129.19
128.52
128.12
127.20
126.50
124.90
117.85
116.84
114.63
112.47
108.54
44.03
37.35
30.02
f1 (ppm)

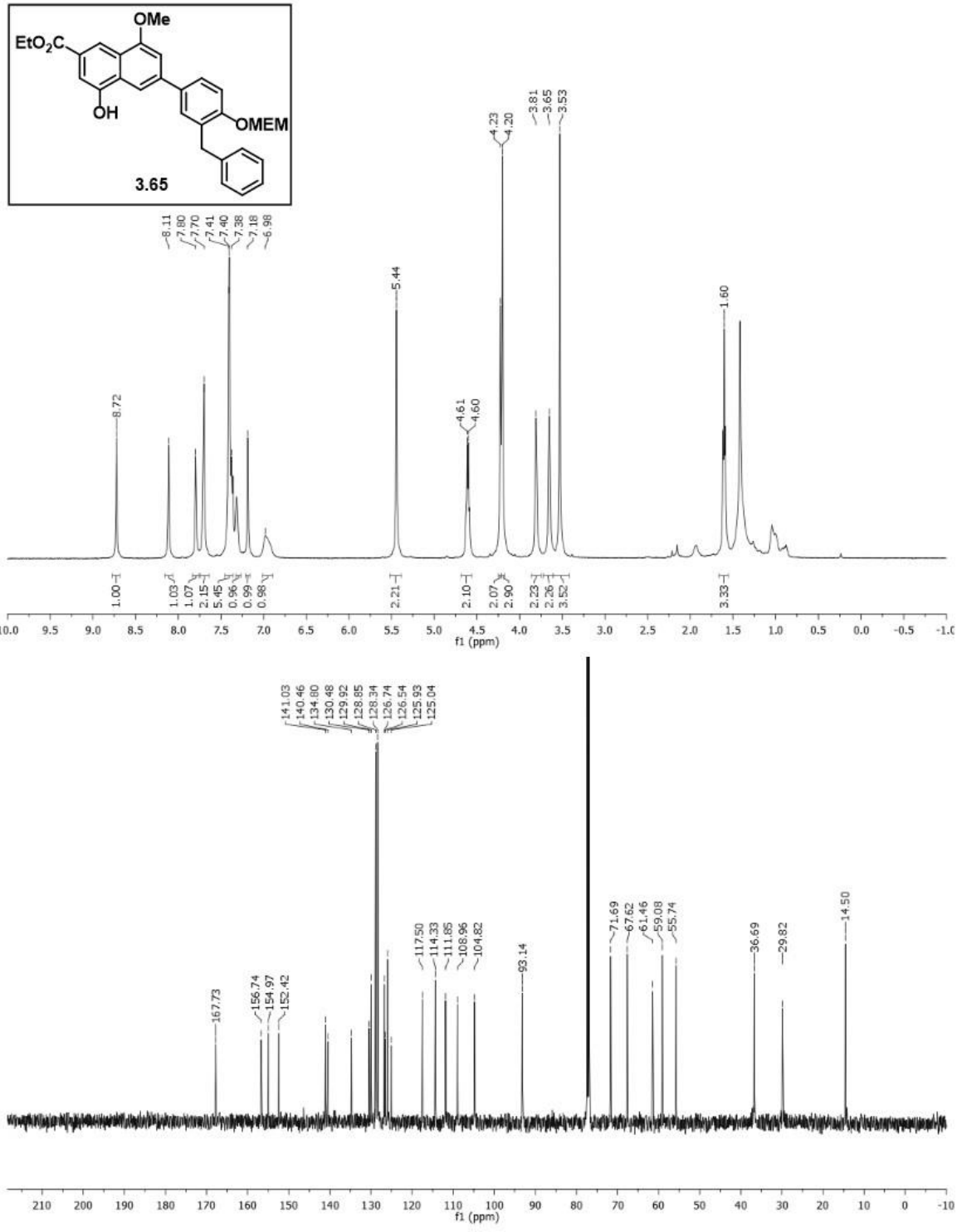
OMe
EtO2C
OH
OMEM
3.65
8.72
8.11
7.80
7.70
7.41
7.40
7.38
7.18
6.98
5.44
4.61
4.60
4.23
4.20
3.81
3.65
3.53
1.60
1.00
1.03
1.07
2.15
5.45
0.96
0.99
0.98
2.21
2.10
2.07
2.90
2.23
2.26
3.52
3.33
f1 (ppm)
167.73
156.74
154.97
152.42
141.03
140.46
134.80
130.48
129.92
128.85
128.34
126.74
126.54
125.93
125.04
117.50
114.33
111.85
108.96
104.82
93.14
71.69
67.62
61.46
59.08
55.74
36.69
29.82
14.50
f1 (ppm)

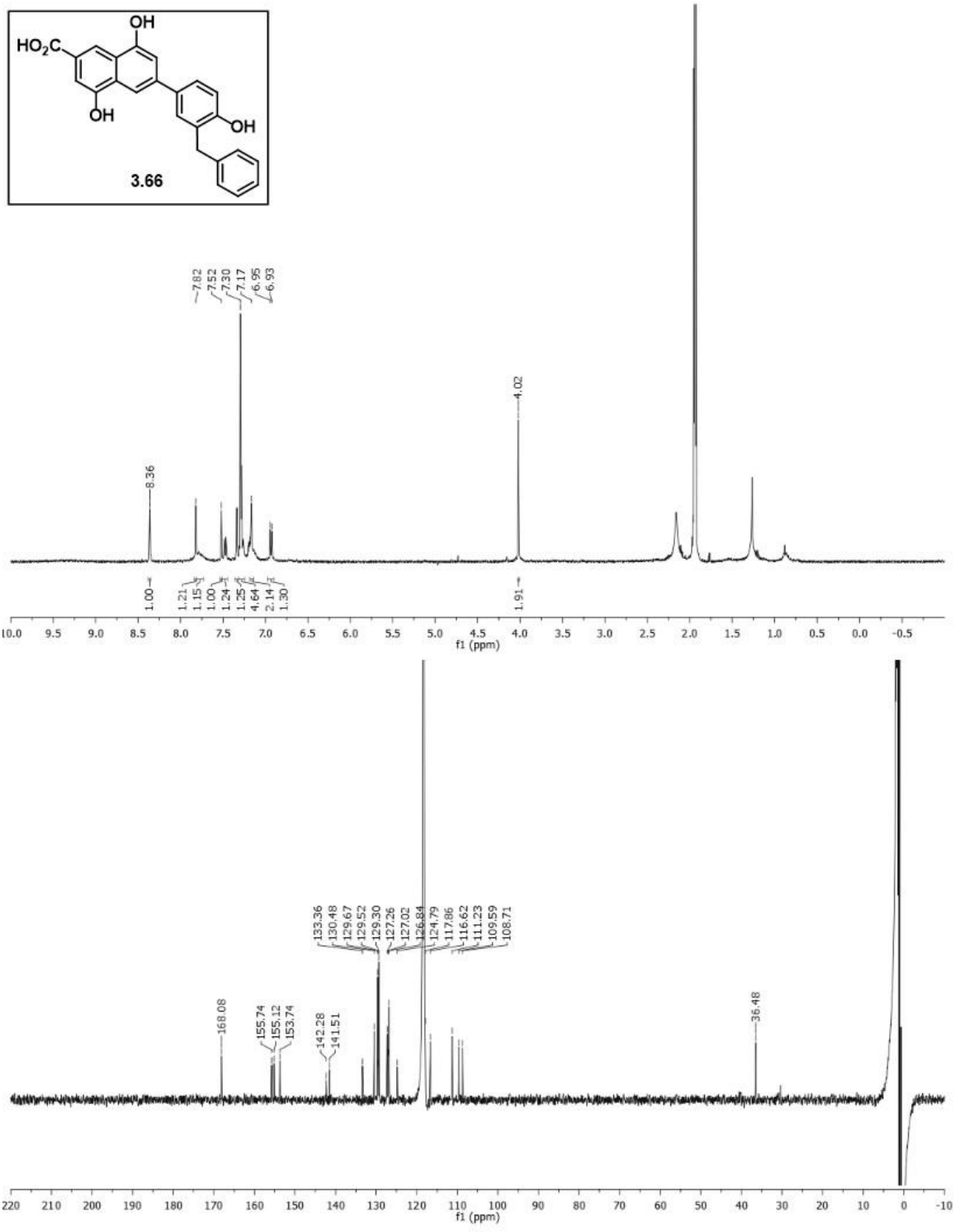
OH
HO2C
OH
OH
3.66
7.82
7.52
7.30
7.17
6.95
6.93
4.02
8.36
1.00
1.21
1.15
1.00
1.24
1.25
4.64
2.14
1.30
1.91
f1 (ppm)
133.36
130.48
129.67
129.52
129.30
127.26
127.02
126.84
124.79
117.86
116.62
111.23
109.59
108.71
168.08
155.74
155.12
153.74
142.28
141.51
36.48
f1 (ppm)

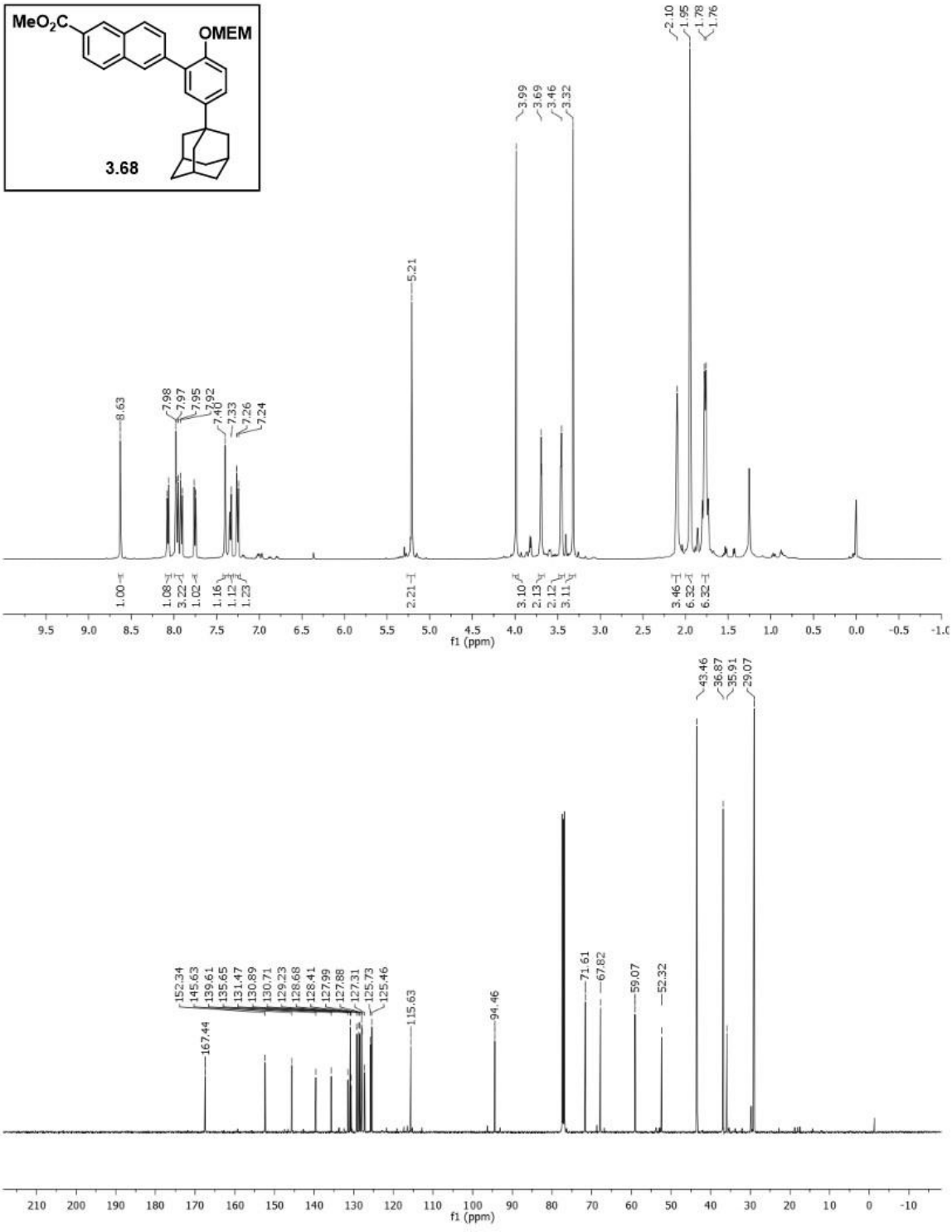
MeO2C
OMEM
3.68
8.63
7.98
7.97
7.95
7.92
7.40
7.33
7.26
7.24
5.21
3.99
3.69
3.46
3.32
2.10
1.95
1.78
1.76
1.00
1.08
3.22
1.02
1.16
1.12
1.23
2.21
3.10
2.13
2.12
3.11
3.46
6.32
6.32
f1 (ppm)
152.34
145.63
139.61
135.65
131.47
130.89
130.71
129.23
128.68
128.41
127.99
127.88
127.31
125.73
125.46
167.44
115.63
94.46
71.61
67.82
59.07
52.32
43.46
36.87
35.91
29.07
f1 (ppm)

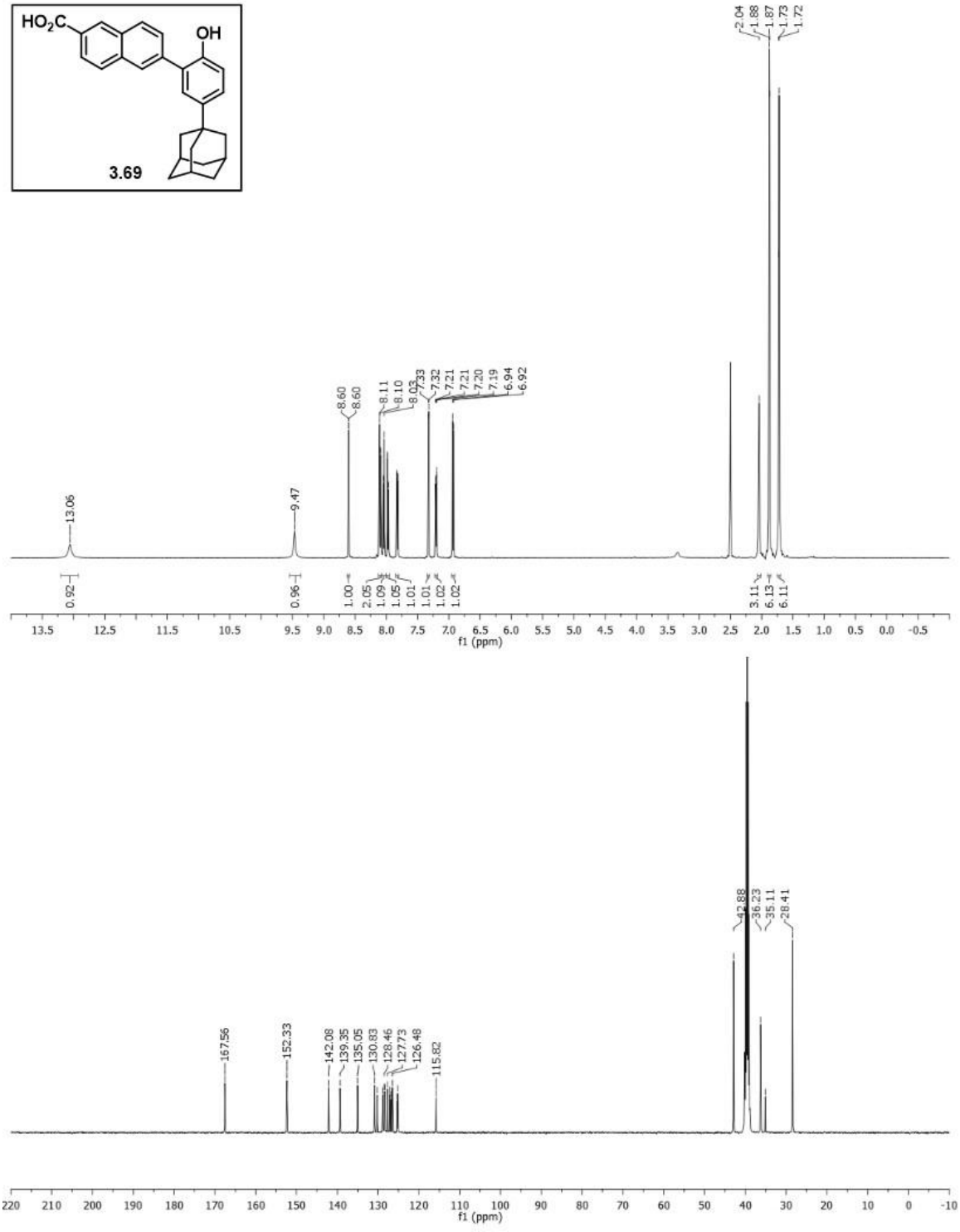
HO2C
OH
3.69
13.06
9.47
8.60
8.60
8.11
8.10
8.02
7.33
7.32
7.21
7.21
7.20
7.19
6.94
6.92
2.04
1.88
1.87
1.73
1.72
0.92
0.96
1.00
2.05
1.09
1.05
1.01
1.01
1.02
1.02
3.11
6.13
6.11
f1 (ppm)
167.56
152.33
142.08
139.35
135.05
130.83
128.46
127.73
126.48
115.82
42.88
36.23
35.11
28.41
f1 (ppm)

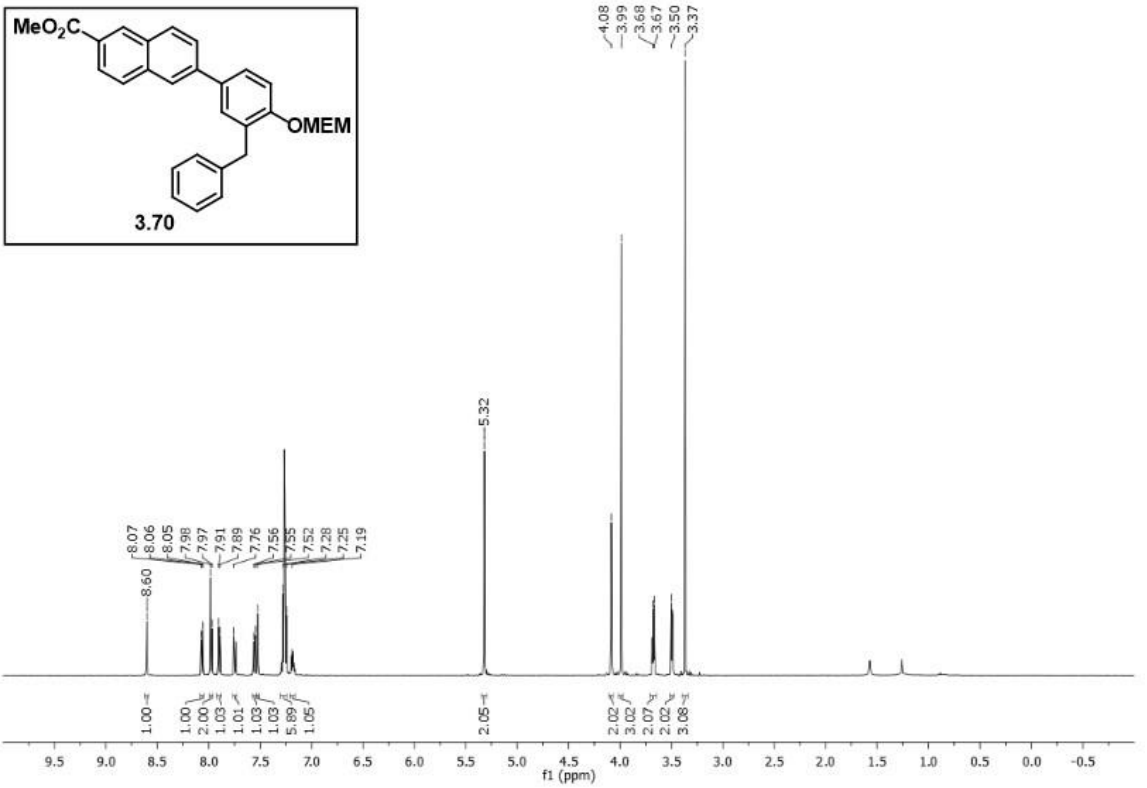
MeO2C
OMEM
3.70
4.08
3.99
3.68
3.67
3.50
3.37
5.32
8.07
8.06
8.05
7.98
7.97
7.91
7.89
7.76
7.56
7.55
7.52
7.28
7.25
7.19
8.60
1.00
1.00
2.00
1.03
1.01
1.03
1.03
5.89
1.05
2.05
2.02
3.02
2.07
2.02
3.08
f1 (ppm)

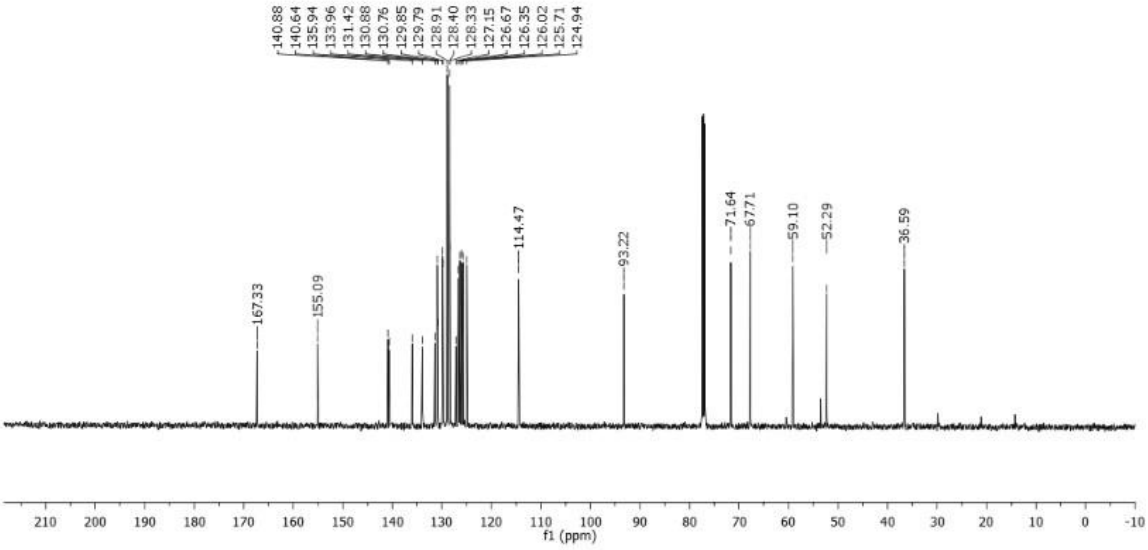
140.88
140.64
135.94
133.96
131.42
130.88
130.76
129.85
129.79
128.91
128.40
128.33
127.15
126.67
126.35
126.02
125.71
124.94
167.33
155.09
114.47
93.22
71.64
67.71
59.10
52.29
36.59
f1 (ppm)

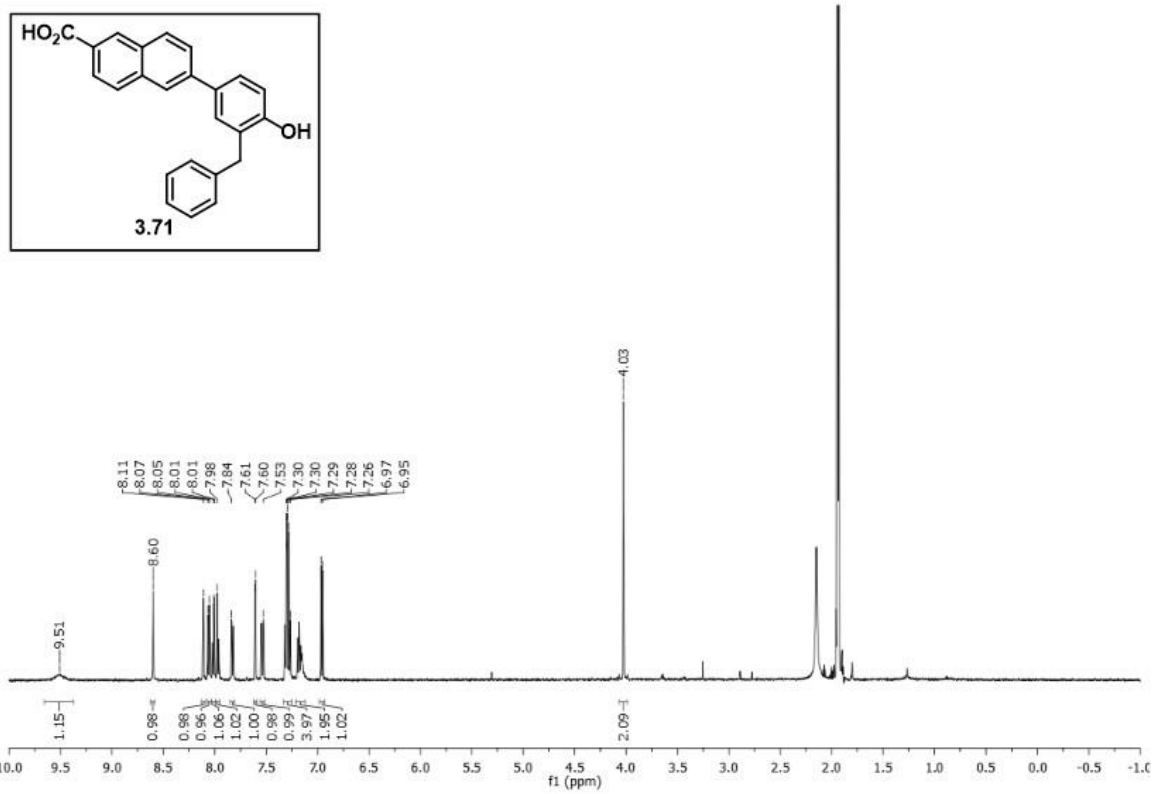
HO2C
OH
3.71
8.11
8.07
8.05
8.01
8.01
7.98
7.84
7.61
7.60
7.53
7.30
7.30
7.29
7.28
7.26
6.97
6.95
9.51
8.60
4.03
1.15
0.98
0.98
0.96
1.06
1.02
1.00
0.98
0.99
3.97
1.95
1.02
2.09
f1 (ppm)

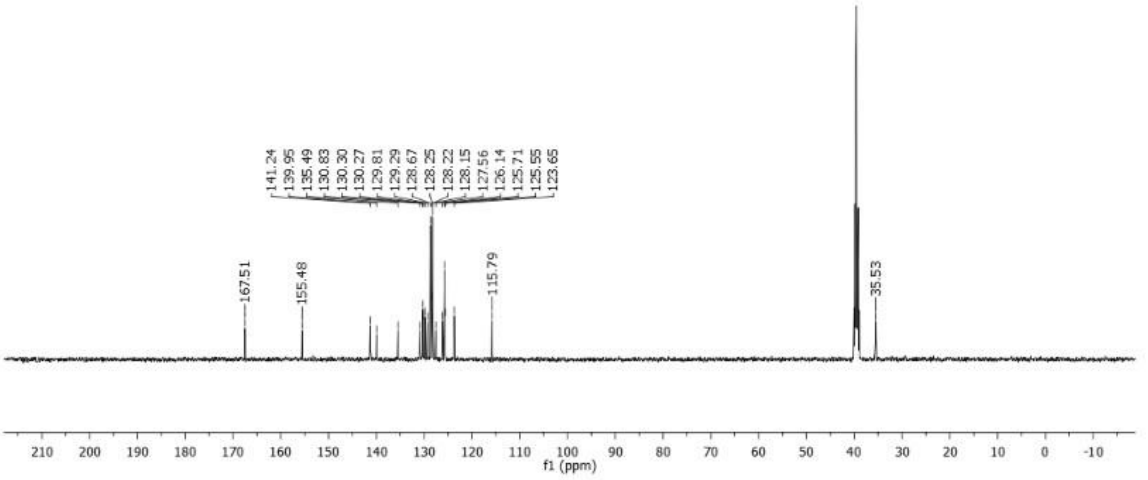
141.24
139.95
135.49
130.83
130.30
130.27
129.81
129.29
128.67
128.25
128.22
128.15
127.56
126.14
125.71
125.55
123.65
167.51
155.48
115.79
35.53
f1 (ppm)